British Journal of Pharmacology

October 1993

Volume 110 Number 2 pages 507–924

Br. J. Pharmacol. (1993), 110, 507–517

FOURTEENTH GADDUM MEMORIAL LECTURE

UNIVERSITY OF CAMBRIDGE

JANUARY 1993

A current view of tamoxifen for the treatment and prevention of breast cancer

V. Craig Jordan

Department of Human Oncology, University of Wisconsin, Comprehensive Cancer Center, Madison, WI 57392, U.S.A.

Keywords: Tamoxifen; antioestrogen; breast cancer; prevention; oestrogen receptors

Introduction

Tamoxifen (ICI 46,474 Nolvadex) is a non-steroidal antioestrogen (Harper & Walpole, 1966) with antifertility properties in rats and mice (Harper & Walpole, 1967a,b). The compound was shown to have efficacy in the treatment of advanced breast cancer (Cole *et al.*, 1971; Ward, 1973), but it is the low incidence of side effects and the continuing conversation between laboratory and the clinic that has guided the strategic application of tamoxifen, for the therapy of all stages of breast cancer. Indeed, tamoxifen is now being evaluated as a preventive agent in women at risk of breast cancer (Powles *et al.*, 1989; Fisher, 1992).

In the laboratory, tamoxifen prevents the induction (Jordan, 1974; 1976) and growth (Jordan & Dowse, 1976; Jordan & Jaspan, 1976) of carcinogen-induced rat mammary tumours. However if tamoxifen is administered daily after the carcinogenic insult is delivered to rats, the induction of tumours is prevented as long as the drug is administered (Jordan, 1978; Jordan *et al.*, 1979). If therapy is stopped, tumours reappear (Jordan & Allen, 1980; Gottardis & Jordan, 1987). Tamoxifen is now considered to be both a tumoristatic and tumoricidal agent so that a strategy of long term treatment (up to 5 years or indefinitely) after mastectomy has become accepted as a reasonable therapeutic approach (Jordan, 1983; 1990).

It is not the purpose of this lecture to review the development and complex pharmacology of antioestrogens; this has been done elsewhere (Jordan, 1984; 1988; Jordan & Murphy, 1990; Lerner & Jordan, 1990), rather it is to provide an up to date evaluation of the current mode of action of antioestrogens, their applications and the problems for future treatment strategies. Most importantly I will point out areas that need to be developed to clarify toxicological issues.

Basic molecular mechanism of action

Oestrogen action is mediated through the nuclear oestrogen receptor in oestrogen target tissues (uterus, vagina and some breast cancers) (Jensen & Jacobson, 1962; Gorski *et al.*, 1968; Welshon *et al.*, 1984). It has been known for a century that oestrogen withdrawal causes the regression of some breast cancers (Beatson, 1896; Boyd, 1900) but the measurement of oestrogen receptors in tumours to predict which will respond to endocrine ablation (Jensen *et al.*, 1971; McGuire *et al.*, 1975) revolutionized breast cancer therapy and provided a target for therapeutic intervention. Tamoxifen is a competitive inhibitor of oestrogen binding at the oestrogen receptor (Skidmore *et al.*, 1972; Jordan & Koerner, 1975; Jordan & Prestwich, 1977) and blocks oestrogen action in breast cancer cells which contain receptors.

Within the cell, both oestrogen- and antioestrogen-oestrogen receptor complexes can bind to response-enhancer elements and both cause a similar alteration in chromatin structure (Pham *et al.*, 1991) but the antioestrogen-oestrogen receptor DNA complexes are transcriptionally nonproductive (Green, 1990). The precise molecular mechanism is at present obscure, but studies in yeast transfected with mutant oestrogen receptors indicate that the antagonistic effects of antioestrogens arise from a synergistic interaction of transactivating functions (TAF) of one and two sites on the oestrogen receptor protein (Pham *et al.*, 1992) and not simply from an inactivation of TAF-2 as previously thought (Berry *et al.*, 1990).

An important aspect of recent progress in understanding antioestrogen action in breast cancer is the use of clinical specimens before and after tamoxifen therapy to confirm studies conducted in the laboratory during the past decade. Oestrogen causes an increase in the growth factors transforming growth factor (TGF) α that can stimulate tumour growth through an autocrine loop using the epidermal growth factor receptor (Figure 1). It is also possible that TGF α can aid tumour cell survival by promoting angiogenesis (Schrieber *et al.*, 1986). Tamoxifen therapy causes an up regulation of the level of oestrogen receptors (Noguchi *et al.*, 1993a) but a decrease in tumour concentrations of TGF α (Noguchi *et al.*, 1993b) which might be partly responsible for stopping tumour growth. However, regulation of TGF α might also have an important impact on tumour cell survival. Recent studies (Gagliardi & Collins, 1993) have shown that antioestrogens can inhibit angiogenesis in laboratory models; an action that could explain the sustained survival advantage (up to 10 years) observed after limited (two years) adjuvant tamoxifen therapy (Early Breast Cancer Trials Collaborative Group, 1992).

Another aspect of tumour growth control by tamoxifen is the influence on endocrine and paracrine growth regulators (Figure 2). Tamoxifen increases sex hormone binding globulin (SHBG) levels in postmenopausal patients which in turn lowers the amount of free-oestradiol that is present in the serum (Rose *et al.*, 1992). Similarly, tamoxifen reduces the circulating level of insulin-like growth factor 1 (IGF1) (Pollak *et al.*, 1992), a growth factor that is known to

stimulate the growth of breast tumour cells *in vitro*. Indeed tamoxifen reduces the production of IGF-1 in normal tissues (Huynh *et al.*, 1993) so it is possible that metastatic spread would be reduced if there was a reduction in supportive paracrine growth factor that was needed for tumour cell survival. The other piece of the tumour cell mosaic is the role played by the inhibitory growth factor TGF β (Figure 1). The peptide is made in oestrogen receptor positive breast cancer cells in response to tamoxifen (Knabbe *et al.*, 1987) but in the laboratory, TGF β will inhibit the growth of oestrogen receptor negative cells (Arteaga *et al.*, 1988). These observations lead to the view that TGF β produced in oestrogen receptor positive cells could influence the growth of adjacent oestrogen receptors negative cells. However, the recent finding that tumour stromal cells can also produce TGF β in the laboratory (Colletta *et al.*, 1990) and in response to tamoxifen therapy (Butta *et al.*, 1992) provides compelling evidence that a complex intercellular conversation occurs to regulate growth.

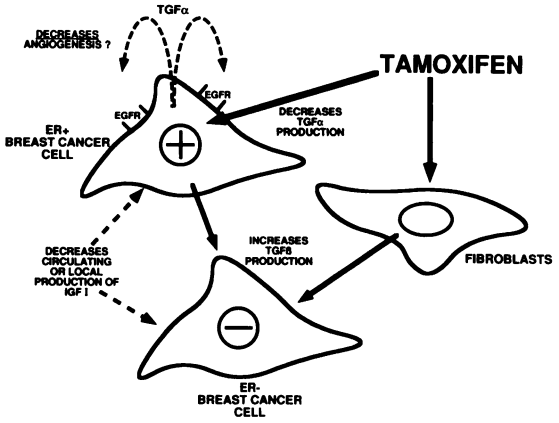

Figure 1 The potential mode of action of tamoxifen to control the growth of oestrogen receptor positive (+) and negative (−) breast cancer cells within a tumour. Tamoxifen can decrease the production of transforming growth factor (TGF) α in oestrogen receptor-positive cells that could reduce angiogenesis and can decrease cell replication by reducing activation of epidermal growth factor receptors (EGFR). The inhibitor growth factor, TGF β, produced both oestrogen receptor-positive cells and fibroblasts, can inhibit the growth of oestrogen receptor negative cells. Insulin-like growth factor (IGF-1), a stimulatory growth factor is reduced by tamoxifen therapy.

Although the oestrogen receptor mediated mechanism might be the most important in the breast tumour, the fact that tamoxifen can provide significant survival advantages in breast cancer patients with oestrogen receptor-poor tumours (Early Breast Cancer Trials Collaborative Group, 1992) has raised the possibility that all postmenopausal women with a diagnosis of breast cancer should receive tamoxifen maintenance (Jordan, 1993). The multiple mechanisms of action of tamoxifen (Figures 1 and 2) that can potentially control tumour growth provides compelling evidence to support the clinical view that all menopausal patients can benefit from tamoxifen.

Pharmacology of tamoxifen

Tamoxifen displays an interesting spectrum of agonist and antagonist actions in different tissues and in different species. This pharmacology has been reviewed (Furr & Jordan, 1984; Jordan, 1984; Jordan & Murphy, 1990) but several recent

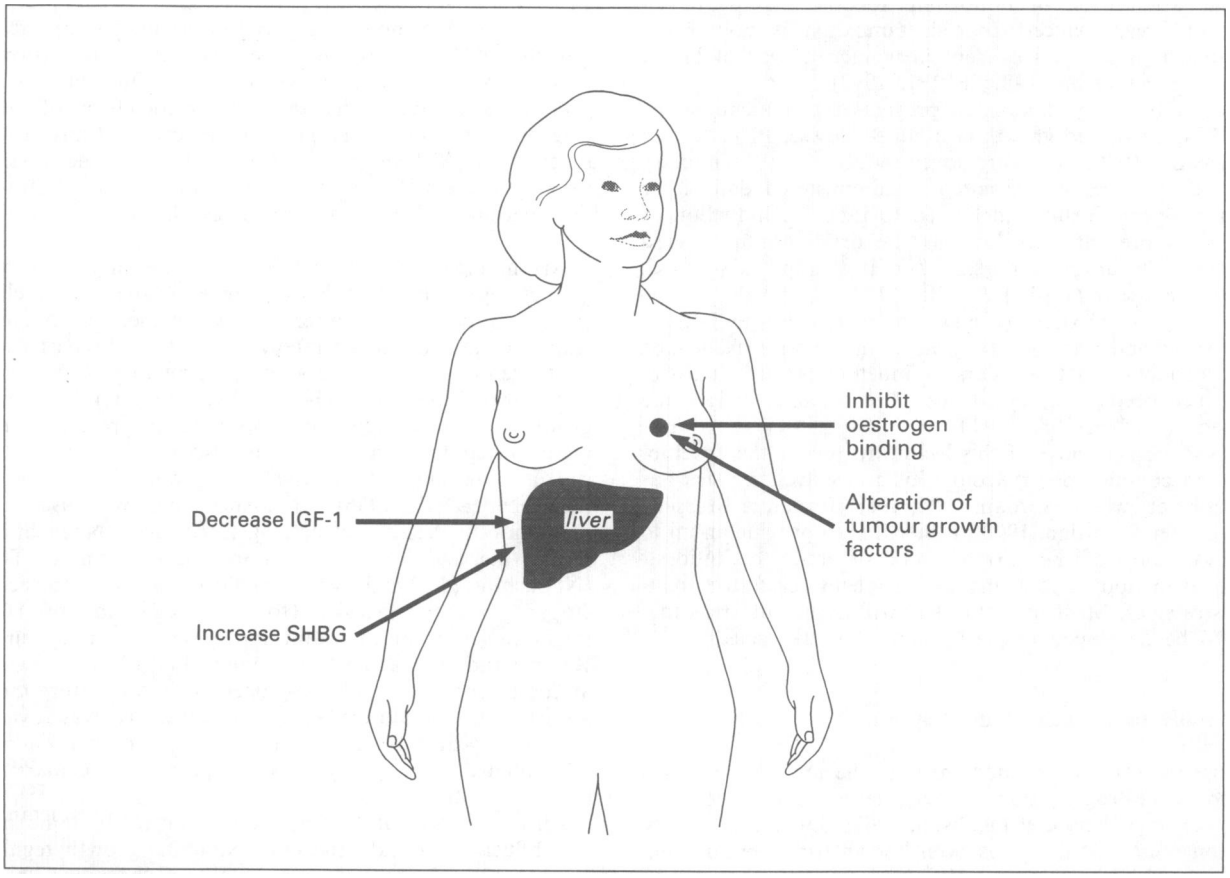

Figure 2 An overview of the actions of tamoxifen in controlling breast cancer growth. Tamoxifen will inhibit oestrogen binding to tumour oestrogen receptors and alter the regulation of growth factors in the tumour (see Figure 1). The circulating level of insulin-like growth factor (IGF-1) is reduced and in postmenopausal patients, tamoxifen increases the circulating level of sex hormone binding globulin (SHBG). As a result, the level of free versus SHBG bound oestradiol is reduced in the tamoxifen-treated patient.

laboratory findings have implications for the clinical applications of tamoxifen. The wide acceptance of tamoxifen as a breast cancer therapy coupled with its potential as a preventive in normal women has re-focused attention on laboratory studies that could have long term consequences for patients.

In short term laboratory assays, tamoxifen is usually classified as an oestrogen in the mouse, and partial antagonist in rats and man. At present there is no adequate explanation for the species differences in pharmacology. Numerous studies have been completed to determine whether different metabolites are present in different species (Lyman & Jordan, 1985; Langan-Fahey *et al.*, 1990; Robinson *et al.*, 1991). However, the studies have only demonstrated increased production of 4-hydroxytamoxifen in the mouse (Robinson *et al.*, 1991). This metabolite has high binding affinity for the oestrogen receptor (Jordan *et al.*, 1977) but does not display exceptional oestrogenicity in mouse assays (Jordan *et al.*, 1978). In fact the view that tamoxifen is an oestrogen in the mouse might be an over simplification, because the sustained administration of tamoxifen to ovariectomized mice results in the uterus becoming refractory to oestrogen administration (Jordan *et al.*, 1990). It appears that the uterus initially responds to tamoxifen as an oestrogen but the longer tamoxifen administration is continued, uterine weight decreases back to untreated values.

The pharmacology of tamoxifen is extremely complex and appears not only to be species- but also tissue- and duration of administration-specific. This pharmacology has yet to be resolved; nevertheless, the necessity of determining the mechanism of actions of tamoxifen in various tissues to explain its agonist and antagonist actions is becoming essential. Obviously the safety of a medicine is of paramount importance so laboratory test systems are established to discover any potential toxicities that might have important consequences for the deployment of a drug. Unfortunately it may become difficult to determine what is a clinically relevant toxicological result from the laboratory in the light of extensive clinical experience.

A current concern is the potential of tamoxifen to produce liver tumours because the laboratory and clinical information is divergent. Tamoxifen has 4.5 million women years of experience and by and large the toxicology monitoring has revealed few serious side effects. At present there are no reports of increases in the incidence of hepatocellular carcinoma at the 10 mg tamoxifen twice daily dose, although two cases of hepatocellular carcinoma have been noted with the use of 20 mg tamoxifen twice daily. In contrast, tamoxifen is known to form DNA adducts in the rat liver and to cause rat liver tumours (Dragan *et al.*, 1991; Han & Liehr, 1992; White *et al.*, 1992; Williams *et al.*, 1993). These data in the laboratory cannot be ignored because they represent important information about the pharmacology of tamoxifen. Indeed the research effect must be intensified in the laboratory to determine the mechanism for the carcinogenic effect of tamoxifen. It may be found that the phenomenon is species-specific and does not occur to a significant extent in man. However the comparative study will yield valuable comparative toxicities and an insight into the mechanism of toxicity. One explanation for the carcinogenic action of tamoxifen in the rat liver may be as an oestrogenic tumour promoter. It is known that oestradiol and synthetic oestrogens are powerful promoters of rat liver carcinogenesis but the administration of contraceptive oestrogens and oestrogen replacement therapy in patients has not demonstrated an increased incidence of liver tumours that restricts clinical usage.

Overall the toxicology of tamoxifen has proved to be a controversial issue and the adverse publicity has become extremely troublesome for the hundreds of thousands of women who benefit from the drug. Fortunately the benefit of tamoxifen as an anticancer agent can be quantitated and has been the subject of a recent overview analysis of controlled clinical trials.

An overview of adjuvant tamoxifen therapy

The effectiveness of adjuvant tamoxifen in both node positive (tumour spread to lymph nodes) and node negative breast cancer has recently been established in an overview analysis (Early Breast Cancer Trials Collaborative Group, 1992). The review included 30,000 women in randomized trials of tamoxifen. Highly significant reductions in the annual rates of recurrence and death are produced (25% for recurrence and 17% for mortality) and tamoxifen reduced the risk of developing a contralateral breast cancer by 39%. Most interestingly, the differences in survival produced by two years of tamoxifen therapy was larger at 10 years than at 5 years. However, as was predicted by the laboratory data (Jordan, 1983), the duration of adjuvant therapy was important for controlling recurrence and improving mortality. Women who received only one year of tamoxifen had a worse prognosis than those receiving more than two years of tamoxifen. Node negative women had a similar benefit from tamoxifen monotherapy whether they were above or below the age of 50. In contrast, the node positive women had more benefit from tamoxifen containing regimens if they were postmenopausal and less benefit if they were premenopausal. This, in part, could be because the node positive breast cancer patients also received combination chemotherapy which is known to cause ovarian ablation (Rose & Davis, 1977). It is therefore possible that the benefit to be gained from this form of 'endocrine therapy' i.e. chemical *oophorectory*, is optimal and tamoxifen can add little further benefit. It is perhaps pertinent to point out that the overview analysis found that ovarian ablation below the age of 50 decreases mortality (25%) to a similar extent as polychemotherapy (16%).

Finally, there has been much controversy about the role of the oestrogen receptor in predicting response to tamoxifen therapy. In the United States tamoxifen is approved as an adjuvant therapy for all postmenopausal patients with node positive disease but an increased level of oestrogen receptor might improve the chances of a beneficial response. The overview analysis found that oestrogen receptor-poor postmenopausal patients (<10 fmol mg^{-1} cytosol protein) had a 16% reduction in annual odds of recurrence. The situation improves if the oestrogen receptor is >10 fmol mg^{-1} cytosol protein; the reduction in the annual odds of recurrence is 36% for women over 50 years of age.

These statistical studies have established the worth of adjuvant tamoxifen to aid survival and placed a valuable therapeutic agent in the hands of the medical community. This success has resulted in an extension of adjuvant tamoxifen therapy and a careful evaluation of the potential side effects of long term adjunct tamoxifen therapy.

Long term tamoxifen therapy

During the 1970's, several clinical trials organizations decided to select a conservative course of one year of adjuvant therapy. This decision was, however, based upon a number of reasonable concerns. Patients with advanced disease usually respond to tamoxifen for one year and it was expected that oestrogen receptor negative disease would be encouraged to grow prematurely during adjuvant therapy. If this occurred, then the physician would have already used a valuable palliative drug and would have only combination chemotherapy to slow the relentless growth of recurrent disease. The argument produced an intuitive reluctance to use long term tamoxifen therapy because it would lead to premature drug resistance: longer might not be better.

Finally, there were sincere concerns about the side effects of adjuvant therapy and the ethical issues of treating node negative patients who might never have recurrent disease. Few women in the mid 1970's had received extended therapy with tamoxifen, so that long-term side effects were largely

unknown. The majority of tamoxifen-treated patients had received only about two years of treatment for advanced disease before drug resistance occurred. Potential side effects of thrombosis, osteoporosis, and so on were only of secondary importance. The use of tamoxifen in the disease-free patients would change that perspective.

The first evaluation of long-term tamoxifen therapy in node positive breast cancer patients was initiated in 1977 at the University of Wisconsin Comprehensive Cancer Center. This pilot study was to determine whether patients could tolerate five years of adjuvant tamoxifen therapy and whether changes in the metabolism of the drug would occur during long-term treatment. No unusual side effects of tamoxifen were noted, and blood levels of tamoxifen and its metabolites N-desmethyltamoxifen and metabolite Y remained stable throughout the five years of treatment (Tormey & Jordan, 1984; Tormey *et al.*, 1987). Although this study was not a randomized trial, those patients who are receiving long-term tamoxifen therapy continue to make excellent progress and many patients have been taking the drug for more than 15 years. We have recently reported (Langan-Fahey *et al.*, 1990) that tamoxifen does not produce metabolic tolerance during 10 years of administration.

The clinical data from the pilot study in Wisconsin and the DMBA rat mammary carcinoma data (Jordan, 1983) were used to support randomized Eastern Cooperative Oncology Group trials EST 4181 and 5181. An early analysis of both EST 4181 (Falkson *et al.*, 1990) and EST 5181 (Tormey *et al.*, 1992) which compares short term with long term tamoxifen (both with combination chemotherapy) has demonstrated an increase in disease-free survival with long-term tamoxifen therapy. In fact, the five year tamoxifen arm has now gone through a second randomization either to stop the tamoxifen or to continue the antioestrogen indefinitely.

The National Surgical Adjuvant Breast and Bowel Project (NSABP) has conducted a registration study of two years of combination chemotherapy plus tamoxifen and compared the result with the same regimen but with an additional year of tamoxifen (Fisher *et al.*, 1987). Overall, the NSABP investigators conclude that three years of tamoxifen is superior to two years of tamoxifen. Most importantly, there is now a belief that tamoxifen alone may be optimal adjuvant therapy for postmenopausal patients. However, this point is controversial as tamoxifen is clearly effective in postmenopausal but such high numbers are needed to discern any small additional advantages in survival by adding chemotherapy. Be that as it may, even if modest differences are detected in survival, or even disease-free survival, this apparent advantage does not take into account the decrease in the quality of life experienced by the recipient of combination chemotherapy. The NSABP has demonstrated a survival advantage for patients receiving an adriamycin containing regimen with tamoxifen compared with tamoxifen alone (Fisher *et al.*, 1990). In contrast, a report from Italy has demonstrated that the addition of combination chemotherapy to long term tamoxifen (5 years) therapy does not seem to improve significantly the clear cut effectiveness of tamoxifen alone to prevent occurrence in oestrogen receptor and node positive disease (Boccardo *et al.*, 1990).

Although the two year adjuvant tamoxifen study that was conducted by the Nolvadex Adjuvant Trials Organization (NATO) was the first to demonstrate a survival advantage for women with tamoxifen alone (Nolvadex Adjuvant Trial Organization, 1985) current clinical trials are all evaluating a longer duration of therapy. The Scottish trial has evaluated five years of tamoxifen versus treatment and has demonstrated a survival advantage for patients who take 10 mg b.i.d. tamoxifen (Breast Cancer Trials Committee, 1987). The Scottish trial is particularly interesting because it addresses the question of whether to administer tamoxifen early as an adjuvant or save the drug until recurrence. This comparison was possible because most patients (92%) in the control arm received tamoxifen at recurrence. Early concerns that long-term adjuvant tamoxifen would result in premature drug reistance are unjustified as the patients have a survival advantage on the adjuvant tamoxifen arm.

Finally the NSABP landmark study B14 to evaluate adjuvant tamoxifen therapy in oestrogen receptor positive, node negative patients (Fisher *et al.*, 1989) has demonstrated advantages for both pre- and postmenopausal patients. The patients were initially randomized to placebo or tamoxifen (10 mg bi.d.) for five years but now the tamoxifen treatment arm is being randomized either to stop tamoxifen or to continue for another five years.

All of the long term tamoxifen clinical trials have led to a general trend for extended tamoxifen therapy in general practice. This broad use of tamoxifen in women who are either disease free or indeed may never have a recurrence has mandated the re-evaluation of the toxicology and side effects of therapy.

Additional benefits of tamoxifen therapy

In the mid 1980's, concerns were raised about the wisdom of treating women chronically with an antioestrogen. Oestrogen is beneficial to women to maintain bone density and to maintain a favourable lipid profile and protect against coronary heart disease. However tamoxifen exhibits numerous oestrogen-like effects in postmenopausal women (Furr & Jordan, 1984). It was believed that these partial agonist actions of tamoxifen could translate into beneficial effects to maintain bone density and to prevent coronary heart disease. At present there are several encouraging studies that indicate the possible merit of long term tamoxifen therapy.

Tamoxifen does not cause any reduction in bone density (Love *et al.*, 1988; Fentiman *et al.*, 1989; Powles *et al.*, 1990; Kalef-Ezra *et al.*, 1992) and in two clinical trials postmenopausal patients receiving tamoxifen experienced a beneficial effect on bone density compared to patients receiving no endocrine treatment (Love *et al.*, 1992a; Turken *et al.*, 1989). However, no comparisons have been made between the ability of tamoxifen or exogenous oestrogens to maintain bone in postmenopausal women. Nevertheless, since women with breast cancer are a group of patients that is uniformly ineligible for postmenopausal oestrogen replacement therapy, any bone preserving effect produced by tamoxifen is an added benefit to its antitumour actions.

Furthermore patients treated with tamoxifen also experience significant reductions in total serum cholesterol, low-density lipoprotein cholesterol and apolipoprotein B levels (Powles *et al.*, 1989; Love *et al.*, 1990; 1991a). The other interesting observation is that the high density lipoprotein cholesterol either increases or is unchanged but total serum cholesterol is reduced relative to baseline i.e. if the patient has a higher than normal baseline cholesterol there is a greater percentage decrease than a patient with a low baseline cholesterol value (Love *et al.*, 1991a). These effects of lipids are usually associated with reductions in the risk of cardiovascular disease and in one study, a significant reduction in the incidence of fatal myocardial infarction was observed in the tamoxifen-treated group compared to controls (McDonald & Stewart, 1991).

Overall, the oestrogenic activity of tamoxifen could produce a profound effect to support physiological functions in women and help to prevent the development of osteoporosis and coronary heart disease. However the oestrogenicity may also cause deleterious side effects that must be carefully monitored in patients.

Side effects related to the ostrogenicity of tamoxifen

There are several anecdotal reports (Nevasaari *et al.*, 1978; Hendrick & Subraminian, 1980; Lipton *et al.*, 1984) of

thromboembolic events occurring in association with tamoxifen therapy. However, detailed studies documenting statistically significant increases in thromboembolic disorders during long term tamoxifen monotherapy are lacking. Venous and arterial thombosis does occur more frequently in patients receiving chemotherapy and tamoxifen (Saphner *et al.*, 1991), so it might be prudent to monitor this parameter. Tamoxifen has been associated with decreased levels of antithrombin III (Jordan *et al.*, 1987; Love *et al.*, 1992b) but these are not clinically significant reductions, except possibly in the case of a patient with a previous history of a clotting disorder. It is however important to point out that tamoxifen alters the blood transport of the coumarin type anticoagulants (Ritchie & Grant, 1984; Tenni *et al.*, 1989) so special care must be taken to ensure the appropriate types and levels of medication.

Considerable interest is currently focused on the risks of developing endometrial carcinoma during long-term tamoxifen therapy. However, the relationship between tamoxifen and endometrial carcinoma remains controversial. Interestingly, though, tamoxifen has been used as a treatment for endometrial carcinoma (Broens *et al.*, 1980; Swenerton, 1980; Bonte *et al.*, 1981). The antioestrogenic action of tamoxifen dominates in this pharmacological application. However, recent evidence from both the laboratory and clinic indicate that tamoxifen can act as a growth promoter for occult endometrial carcinoma. In the athymic mouse model, oestrogen receptor-positive human endometrial carcinoma will grow in response to tamoxifen (Satyaswaroop *et al.*, 1984). Indeed in animals co-transplanted with human endometrial tumours and breast tumours, tamoxifen will prevent the oestrogen stimulated growth of the breast tumours but enhance the growth of the endometrial tumours (Gottardis *et al.*, 1988). This observation heightened awareness about the possibility that tamoxifen could encourage the development of endometrial carcinoma during breast cancer therapy.

Tamoxifen has now been implicated in the development of endometrial tumours in patients. In one study, with accrual of over 1 800 postmenopausal women who received either tamoxifen or placebo after primary surgery for breast cancer, 13 patients in the tamoxifen-treated group compared to two in the placebo-treated group developed endometrial cancer (Fornander *et al.*, 1989). This study also showed that the incidence of endometrial cancer was correlated with the duration of tamoxifen. Women who received tamoxifen for five years were at greater risk for developing endometrial carcinoma. However, the women in the study all received tamoxifen 20 mg b.i.d. which is twice the dose normally prescribed in the United States. There are other reports of endometrial carcinoma with high dose tamoxifen treatment (Hardell, 1988; Atlante *et al.*, 1990; Magriples *et al.*, 1993) but interest is currently focused on the epidemiology of endometrial cancer at the standard dose regimen of 20 mg daily. In a study conducted by the Southwest Oncology Group, four of the 641 patients treated for one year with tamoxifen developed endometrial cancer, compared to no cases of endometrial cancer in the 325 patients treated with adjuvant chemotherapy (Sunderland & Osborne, 1991). Similarly in a study by Anderson and colleagues (1991) of one year of adjuvant tamoxifen there was a trend toward an increased risk of developing endometrial carcinoma. Unfortunately in neither report was any clinical information given. However, in a recent review of the published information (Nayfield *et al.*, 1991) (Table 1), the incidence data only translates to an extra four women per thousand who take tamoxifen who will develop endometrial carcinoma. In fact the difference becomes insignificant if high dose tamoxifen-treated patients are excluded. It has been suggested (Gusberg, 1990) that careful patient monitoring, using serial endometrial biopsies, may be an appropriate screening technique. Unfortunately, this approach may not be acceptable to patients. Careful patient monitoring and endometrial biopsies *when* the patient experiences unexplained spotting or bleeding may be the most appropriate. Surgical intervention may then become necessary.

The strategy of targeting individuals on tamoxifen who experience symptoms rather than screening the whole treatment population may have merit by analogy with oestrogen based hormone replacement therapy in postmenopausal women. Horowitz & Feinstein (1986) argue that the observed increase in endometrial carcinoma attributed to oestrogens (and presumably we can also suggest tamoxifen) may be due to increased detection of lesions that would otherwise remain as silent tumours. They support this conjecture by reporting that the incidence of 'silent' endometrial cancers diagnosed at autopsy is roughly three times the incidence in the living population. It is possible that the partial agonist action of tamoxifen could act on silent tumours and any resultant abnormal bleeding would bring about an increased detection rate. Indeed this may be beneficial to the patient. The probability of surviving five years after a diagnosis of endometrial carcinoma is 0.89 for previous oestrogen users but only 0.53 for non-users (Schwartzbaum *et al.*, 1987). One interpretation of these data is that oestrogen promotes the early detection of occult tumours by causing abnormal bleeding before the development of metastases. Early detection may be the best strategy for the patient rather than the slow growth of silent disease.

It is also important for the gynaecologiest to appreciate that tamoxifen has been associated with endometriosis, endocervical and endometrial polyps (Ford *et al.*, 1988; Neven *et al.*, 1989; Nuovo *et al.*, 1989; DeMuylder *et al.*, 1991; Corley *et al.*, 1992). As a result, any bleeding that occurs does not automatically mean the patient has endometrial carcinoma.

Despite concerns about the development of the endometrial carcinoma during long term tamoxifen therapy for breast cancer there is insufficient evidence to deny a woman tamoxifen treatment. The benefits far outweigh the risks and regular gynaecological examinations will provide adequate safeguards for both the physicians and the patient.

Overall the past decade has established the effectiveness of tamoxifen as a valuable therapeutic agent. The proven antitumour actions of tamoxifen and the low incidence of side effects have increased enthusiasm to evaluate the role of tamoxifen to prevent breast cancer in high risk women. The concept is a direct result of a sound laboratory rationale and broad clinical experience.

The biological basis for prevention

During the past two decades a growing body of literature on the prevention of mammary cancer in rodents has been used to support the clinical use of tamoxifen to prevent breast. However it was Lacassagne (1936) who predicted that a therapeutic intervention could be developed that would 'prevent or antagonize the congestion of oestrogen in the breast'. Unfortunately, at that time no therapeutic agent was

Table 1 Cumulative frequency of uterine cancers during adjuvant tamoxifen therapy

Trial	*Tamoxifen-treated cancers* (n)	*Control cancers* (n)
Copenhagen	2 (164)	0 (153)
ECOG	1 (91)	1 (90)
NATO	0 (564)	0 (567)
NSABP	2 (1419)	0 (1428)
Scottish	4 (661)	2 (651)
Stockholm	13 (931)	2 (915)
Toronto-Edmonton	0 (198)	1 (202)
Total	0.5%	0.1%

Adapted from Nayfield *et al.* (1991).

available and all his predictions were based upon the known effect of early oophorectomy in preventing the development of mammary cancer in high incidence strains of mice.

The animal studies with tamoxifen have been undertaken for two reasons. First, to establish the efficiency of tamoxifen in well-described models of carcinogenesis and second to discover whether tamoxifen would always be an inhibitor or whether the drug could exacerbate tumorigenesis. Two animal model systems have been used extensively: the carcinogen-induced rat mammary carcinoma model and mouse mammary tumour virus (MMTV) infected strains.

The mammary carcinogens DMBA (Huggins *et al.*, 1961) and NMU (Gullino *et al.*, 1975) induce tumours in young female rats. The timing of the carcinogenic insult is very important because as the animals age they become resistant to mammary carcinogens. Tumorigenesis does not occur in oophorectomized animals and the sooner oophorectomy is performed after the carcinogenic insult the more effective it is in preventing the development of tumours (Dao, 1962). The administration of tamoxifen to carcinogen-treated rats prevents the initiation of carcinogenesis and animals remain tumour-free (Jordan, 1976; Turcot-Lemay & Kelley, 1980).

The short term administration of tamoxifen at different times after the carcinogenic insult is effective in reducing the number of tumours that develop (Jordan *et al.*, 1979; Jordan & Allen, 1980; Wilson *et al.*, 1982) although most animals develop at least one tumour after therapy is stopped. In contrast, continuous therapy that is started one month after the administration of carcinogens completely inhibits the appearance of mammary tumours (Jordan, 1983; Gottardis & Jordan, 1987). Under these circumstances, tamoxifen is preventing promotion and is suppressing the appearance of occult disease.

Consideration of the use of tamoxifen in mouse models was delayed because the pharmacology of tamoxifen in the mouse was initially thought to be very different from the rat. Tamoxifen is oestrogenic in short term tests in oophorectomized (Harper & Walpole, 1967b) and immature mice (Terenius, 1971). However, the finding that long-term therapy renders the oophorectomized mouse vagina (Jordan, 1975) and athymic mouse uterus (Gottardis & Jordan, 1988) refractory to oestrogenic stimuli prompted a reconsideration of the value of tamoxifen as a preventive in mouse mammary tumour models. Tumorigenesis is ovarian-dependent in the MMTV model (Lathrop & Loeb, 1916). However, unless the animals are ovariectomized just after weaning about 50% of the animals produce tumours. In contrast the sustained administration of tamoxifen prevents mammary tumorigenesis in 90% of the animals; a result that is superior to ovariectomy (Jordan *et al.*, 1991).

Although the animal studies are encouraging, the most compelling evidence that tamoxifen can be an effective preventive comes from an analysis of adjuvant clinical trials. The incidence of contralateral breast cancer is estimated as 8/1 000 women annually (Chaudary *et al.*, 1984) and it was possible that the tumoristatic action of tamoxifen could reduce second primary breast cancers. Cuzick & Baum (1985) were the first to note that tamoxifen prevented the appearance of secondary breast cancers. A review of published clinical trials which involve nearly 5 000 women per arm, shows a one third reduction of contralateral breast cancer with tamoxifen treatment (Table 2). Similarly the overview analysis of randomized clinical trial (EBCTC 1992) with 9 000 women per group showed a rate of developing primary breast cancers in control of 2% but 1.3% in tamoxifen-treated groups. Since the timing of initiation in human breast cancer is unknown, tamoxifen will be given to target populations to suppress and hopefully reverse the promotional effects of oestrogen during carcinogenesis.

Table 2 Comparison of contralateral breast cancer rates for tamoxifen-treated versus placebo-treated women with early-stage breast cancer

Clinical trial	*Rate for tamoxifen-treated women*	*Rate for control-treated women*
Copenhagen	1.8%	2.6%
ECOG 1178	1.1%	3.3%
Stockholm	1.9%	3.5%
Toronto-Edmonton	1.5%	1.5%
Scottish	1.4%	1.8%
CRC	0.7%	1.9%
NATO	2.7%	3.0%
NSABP-14	1.6%	2.2%
Average	1.6%	2.4%

Adapted from Nayfield *et al.* (1991).

Current tamoxifen prevention trials

Unlike the laboratory models of mammary tumorigenesis where all animals develop tumours and the efficacy of tamoxifen is readily demonstrated, it is difficult to target the appropriate population of women at risk for breast cancer. Numerous risk factors have been identified (Table 3) but these have been reviewed elsewhere (Morrow, 1992; Morrow & Jordan, 1992). However, because the incidence of breast cancer is so small in the general population, it is essential to recruit women volunteers with a high risk profile to be able to evaluate the worth of tamoxifen. It is essential to design a double blind trial, but the large numbers of volunteers required and the long time period necessary to obtain a statistically significant results mandates an enormous clinical trials effort, data management, and compliance monitoring.

There are currently three clinical trials recruiting women to test the worth of tamoxifen to prevent breast cancer. The first trial was begun at the Royal Marsden Hospital in 1986 (Powles *et al.*, 1989; 1990). At present about 2 000 women are randomized to receive either tamoxifen 20 mg daily or placebo for five years. High risk women, for the purposes of this study, are defined as those with at least one first degree relative who developed breast cancer under age 40, or bilateral cancer at any age, or at least two first degree relatives with breast cancer at any age. Risk factors other than family history are not considered. The age range of study participants is from 30 to 66 with a mean age of 48 years. At 12 months an 83% compliance rate was noted for women in the tamoxifen arm which by two years had decrease to approximately 70%. This study is designed as a feasibility trial with the ultimate goal being a large scale multi-centre trial. In March 1992 the Medical Research Council (MRC) of Great Britain voted to restrict entry to the multi-centre trial to women over the age of 40 with a four fold or greater relative risk of breast cancer. The current estimate for the risk of the recruited population is 3.8. Concerns over the induction of liver tumours in rats by tamoxifen was cited by the MRC as the major reason for restricting entry into the study (Anonymous, 1992). The trial is, however, now (July, 1993) approved by the department of health and is actively recruiting 15,000 women.

Table 3 Estimates of increase in the risks of a woman developing breast cancer if she has individual risk factors

	Increase in relative risk
Mother or sister with breast cancer	1.5–3.0
Mother plus sister	4.6
Nulliparous woman	1.4
First pregnancy >30	2–5
Atypical hyperplasia	4.4
Lobular carcinoma *in situ* (LCIS)	6.9–12

Adapted from Morrow (1992).

A second study, again randomizing participants to treatment with tamoxifen, 20 mg daily or placebo, opened in the United States in May, 1992. This study, administered by the NSABP with National Cancer Institute funding, has an accrual goal of 16 000 women over the next two years. Those eligible for entry into the study include any woman over the age of 60, or women between the ages of 35 and 59 whose five year risk of developing breast cancer, as predicted by the Gail model (Gail *et al.*, 1989) equals that of a 60 year old woman. Any woman over age 35 with a diagnosis of lobular carcinoma *in situ* (LCIS) treated by biopsy alone is eligible for study entry. In the absence of LCIS, the risk factors for entry vary with age so that a 35 year old woman must have a relative risk of 5.07 while a 45 year old woman's relative risk must be 1.79 to be eligible for study entry. Treatment will continue for a minimum of five years.

Finally, in Italy, the Milan Cancer Institute has initiated a five year study of tamoxifen (20 mg daily) versus placebo for five years in hysterectomized women over the age of 45 years. The aim is to avoid any complications with either pregnancy or endometrial carcinoma. The group will recruit 20 000 volunteers for the study.

For the first time, the clinical trials community is in the process of evaluating a therapy to prevent breast cancer. However, the majority of women recruited to the trials will not develop breast cancer although they will experience symptoms and side effects related to the pharmacology of tamoxifen. The evaluation of the toxicology of tamoxifen in the trials is extremely important not only to determine the therapeutic value of the intervention but also to assess whether compliance can be maintained by the study population. Extra attention is being paid to acute and chronic toxicities.

Table 4 Percentage of patients with acute adverse side effects from tamoxifen

Fatigue*	5–70%
Vasomotor instability (hot flushes)	17–67%
Insomnia	0–54%
Headache	9–37%
Depression	1–33%
Altered menses – (amenorrhoea, oligomenorrhoea, menstrual disorders, vaginal discharge, vaginal bleeding)	1–31%
Pain (bone or musculoskeletal)	2–30%
Fluid retention (oedema)	2–25%
Nausea	3–21%
Anorexia	1–16%
Leukopaenia	1–15%
Skin rash	4–13%
Vomiting	1–12%
Diarrhoea	8–10%
Ovarian cysts	3–5%
Constipation	2–4%
Weight gain	4%
Hypercalcaemia	3–4%
Abdominal cramps	1–3%
Thrombocytopaenia	1–2%
Phlebitis	<1%
Dizziness, light-headedness	<1%

*Shown are the range of the percentages of tamoxifen-treated patients reporting side effects (Pritchard *et al.*, 1980; Ingle *et al.*, 1981; NATO, 1983; 1985; Cummings *et al.*, 1985; Buchanan *et al.*, 1986; Love, 1988; Powles *et al.*, 1989; Fisher *et al.*, 1989; Paterson *et al.*, 1990; Love *et al.*, 1991b).

Side effects of tamoxifen therapy

The side effects of tamoxifen are related to its differential oestrogenic and antioestrogenic properties at various target tissues. Several studies (Ingle *et al.*, 1981; Fisher *et al.*, 1989; Pritchard *et al.*, 1980; Nolvadex Adjuvant Trial Organization, 1983; 1985; Cummings *et al.*, 1985; Buchanan *et al.*, 1986; Love, 1988; Powles *et al.*, 1989; Paterson *et al.*, 1990; Love *et al.*, 1991b) have compared the incidence of side effects observed in patients treated with tamoxifen with those in an alternate therapy or given a placebo. The range of the percentage incidence of side effects during tamoxifen therapy are illustrated in Table 4. Interestingly the only adverse side effect consistently reported by patients receiving tamoxifen that was significantly greater than placebo was hot flushes. All of the other side effects occurred with a similar incidence in the placebo arm. This illustrates how important it is to have placebo controlled trials and good support services for prevention studies. Gynaecological symptoms can become troublesome and must be a focus for attention in premenopausal women recruited into prevention studies. Patients experience leukorrhoea, endometrial hyperplasia (Gal *et al.*, 1991; Neven *et al.*, 1990), polyps (Corley *et al.*, 1992) and one recent case report describes the rapid growth of a leiomyoma in a patient receiving tamoxifen (Dilts *et al.*, 1992). Although some premenopausal women become amenorrhoeic during tamoxifen therapy, most continue to have normal or mildly altered menstrual cycles. These women should be considered to be at risk for pregnancy and indeed tamoxifen is known to induce ovulation in sub fertile women (Furr & Jordan, 1984). Although there are no reports of teratogenicity in response to tamoxifen, the drug should not be prescribed to the pregnant patient. The endocrinological effects of tamoxifen in pre- and postmenopausal women are summarized in Figure 3. Tamoxifen induces ovarian steroidogenesis (Groom & Griffiths, 1976; Jordan *et al.*, 1991) elevating serum oestradiol levels to as high as 2500 pg ml^{-1} in premenopausal women (Manni & Pearson, 1980; Jordan *et al.*, 1991). Chronically elevated oestrogen levels normally cause decrease follicle stimulating hormone (FSH) and leutinizing hormone (LH) production. Treatment with tamoxifen might be expected to elevate gonadotropin levels by blocking negative feedback. However, FSH and LH levels remain largely unchanged which indicates that tamoxifen may act directly on the ovary to increase steroidogenesis, and the balance between its agonist and antagonist activities maintains pituitary gonadotropin secretions at normal levels in the face of elevated serum oestradiol. It is unclear whether or not hypersecretion from the ovary will result in an increased pathology, but tamoxifen has been associated with an increased incidence of fibroid ovaries and ovarian cysts (Powles *et al.*, 1989).

A recent concern is the increasing reports of ophthalmic problems. Triphenylethylenes, including tamoxifen and clomiphene can cause cataracts in rats (Furr & Jordan, 1984). The difficulty in assessing the anecdotal reports is the fact that the incidence of problems is not being assessed in large treatment or placebo groups. Case reports of retinopathy (Kaiser-Kupfer & Lippman, 1978; Kaiser-Kupfer *et al.*, 1981; Vinding & Nielsen, 1983; Griffiths, 1987; Bentley *et al.*, 1992), optic neuritis (Pubesgaard & Von Byben, 1986) and keratopathy (Kaiser-Kupfer & Lippman, 1978) have been reported in patients receiving tamoxifen. Retinopathy was initially reported in patients receiving very high doses of tamoxifen, but recent reports suggest retinopathy can also occur at the usual low dose of 20 mg/day (Griffiths, 1987; Gerner, 1989; Pavlidis *et al.*, 1992).

Two prospective studies have demonstrated no adverse ocular effects associated with low dose tamoxifen therapy (Beck & Mills, 1979; Longstaff *et al.*, 1989) whereas a recent prospective study has demonstrated reversible ocular toxicity, macular degeneration, associated with low dose tamoxifen therapy (Pavlidis *et al.*, 1992). Patients with macular degeneration are not candidates for recruitment to the NSABP prevention trial. Clearly new studies to evaluate the visual acuity and ocular changes in pre-existing tamoxifen

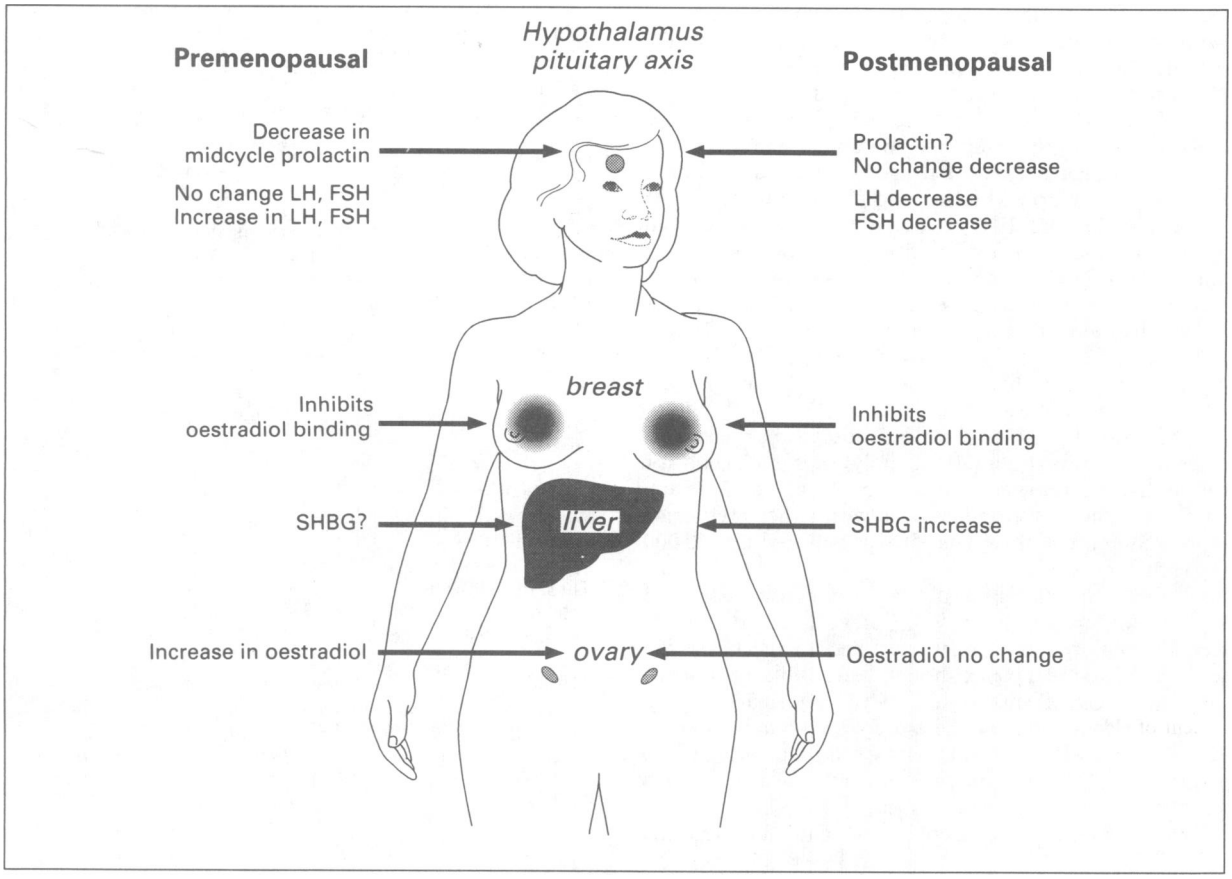

Figure 3 The endocrine effects of tamoxifen in pre- and postmenopausal patients.

versus placebo clinical trials are essential to reassure the clinical community.

Summary and conclusions

Tamoxifen has been found to be a safe and effective treatment for all stages of breast cancer. Long term tamoxifen therapy is associated with some rare, but potentially serious, side effects so patients should be carefully monitored. However, long term tamoxifen therapy is also associated with a number of physiological benefits over and above its tumouristatic action. These benefits include a decrease in the development of contralateral breast cancer, the maintenance of bone density in postmenopausal women and a decrease in cardiovascular disease.

The successful application of tamoxifen to treat breast cancer has increased enthusiasm to test its worth to prevent breast cancer. Although there are individual requests by patients for tamoxifen to prevent breast cancer, individual treatment is inappropriate. Tamoxifen can only be adequately evaluated as a preventive in randomized, double-blind clinical trials. These trials are in place and physicians should encourage women to participate and establish a new therapeutic option as rapidly as possible.

References

ANDERSON, M., STORM, H.H. & MOURIDSEN, H.T. (1991). Incidence of new primary cancer after adjuvant tamoxifen therapy and radiotherapy for early breast cancer. *J. Natl. Cancer Inst.*, **83**, 1013–1017.

ANONYMOUS (1992). Tamoxifen trial controversy. *Lancet*, **339**, 735.

ARTEAGA, C.L., TANDON, A.K., VON HOFF, D.D. & OSBORNE, C.K. (1988). Transforming growth factor β potential autocrine growth inhibitor of estrogen receptor negative breast cancer cells. *Cancer Res.*, **48**, 3898–3904.

ATLANTE, G., POZZI, M., VINCENZONI, C. & VOCATURO, G. (1990). Four case reports presenting new acquisitions on the association between breast and endometrial carcinoma. *Gynec. Oncol.*, **37**, 378–380.

BEATSON, G.T. (1896). On the treatment of inoperable cases of carcinoma of the mamma: suggestions for a new method of treatment with illustrative cases. *Lancet*, **ii**, 104–107; 162–167.

BECK, M. & MILLS, P.V. (1979). Ocular assessment of patients treated with tamoxifen. *Cancer Treat. Rep.*, **63**, 1833–1834.

BENTLEY, C.R., DAVIS, G. & ACLIMANDOS, W.A. (1992). Tamoxifen retinopathy: a rare but serious complication. *Br. Med. J.*, **304**, 495–496.

BERRY, M., METZGER, D. & CHAMBON, P. (1990). Role of the two activating domains of the oestrogen receptor in the cell-type and promoter-context dependent agonist activity of the antioestrogen 4-hydoxytamoxifen. *EMBO J.*, **9**, 2811–2818.

BOCCARDO, F., RUBOYOTTI, A., BRUZZI, P., CAPPELLINI,M., ISOLA, G., NENCI, I., PIFFANELLI, A., SCONNI, A., SISMONDI, P., SANTI, L., GENTA, F., SACCANI, F., SASSI, M., MALACANE, P., DONATI, D., FARRIS, A., CASTAGNETTA, L., DICARLO, A.M., TRAINA, A., GALLETTO, L., SMERIER, F. & BUZZI, F. (1990). Chemotherapy versus tamoxifen versus chemotherapy plus tamoxifen in node positive, estrogen receptor positive breast cancer patients: results of a multicentric Italian study. *J. Clin. Oncol.*, **8**, 1310–1320.

BONTE, J., IDE, P., BILLIET, G. & WYNANTS, P. (1981). Tamoxifen as a possible chemotherapeutic agent in endometrial adenocarcinoma. *Gynec. Oncol.*, **II**, 140–141.

BOYD, S. (1900). On oophorectomy in cancer of the breast. *Br. Med. J.*, **2**, 1161–1167.

BREAST CANCER TRIALS COMMITTEE, SCOTTISH TRIALS OFFICE (1987). Adjuvant tamoxifen in the management of operable breast cancer: the Scottish Trial. *Lancet*, **ii**, 171–175.

BROENS, J., MOURIDSEN, H.T. & SOERENSEN, H.M. (1980). Tamoxifen in advanced endometrial carcinoma. *Cancer Chemother. Pharmacol.*, **4**, 213.

BUCHANAN, R.B., BLAMEY, R.W., DURRENT, K.R., HOWELL, A., PATERSON, A.G., PREECE, P.E., SMITH, D.C., WILLIAMS, C.J. & WILSON, R.G. (1986). A randomized comparison of tamoxifen with surgical oophorectomy in premenopausal patients with advanced breast cancer. *J. Clin. Oncol.*, **4**, 1326–1330.

BUTTA, A., MACLENNAN, K., FLANDERS, K.C., SACKS, N.P.M., SMITH, I., MCKINNA, A., DOWSETT, M., WAKEFIELD, L.M., SPORN, M.B., BAUM, M. & COLLETTA, A.A. (1992). Induction of transforming growth factor β in human breast cancer *in vivo* following tamoxifen treatment. *Cancer Res.*, **52**, 4261–4264.

CHAUDARY, M.A., MILLIS, R.R., HOSKINS, E.O., HALDO, M. & BULBROOK, R.D. (1984). Bilateral primary breast cancer: a prospective study of disease incidence. *Br. J. Surg.*, **71**, 711–714.

COLE, M.P., JONES, C.T.A. & TODD, I.D.H. (1971). A new antioestrogenic agent in late breast cancer: an early clinical appraisal of ICI 46, 474. *Br. J. Cancer*, **25**, 270–275.

COLLETTA, A.A., WAKEFIELD, L.M., HOWELL, F.V., VAN ROOZENDAAL, K.E., DANIELPOUR, D., EBBS, S.R., SPORN, M.B. & BAUM, M. (1990). Antioestrogens induce the secretion of active transforming growth factor beta from human fetal fibroblasts. *Br. J. Cancer*, **62**, 405–409.

CORLEY, D., ROWE, J., CURTIS, M.T., HOGAN, W.M., NOUMOFF, J.S. & LIVOLSI, V.A. (1992). Postmenopausal bleeding from unusual endometrial polyps in women in chronic tamoxifen therapy. *Gynecol.*, **79**, 111–116.

CUMMINGS, F.J., GRAY, R., DAVIS, T.E., TORMEY, D.C., HARRIS, J.E., FALKSON, G.G. & ARSENEAU, J. (1985). Adjuvant tamoxifen treatment of elderly women with stage II breast cancer. A double blind comparison with placebos. *Am. Int. Med.*, **103**, 324–329.

CUZICK, J. & BAUM, M. (1985). Tamoxifen and contralateral breast cancer. *Lancet*, **ii**, 282.

DAO, T.L. (1962). The role of ovarian hormones in initiating the induction of mammary cancer in rats by polynuclear hydrocarbons. *Cancer Res.*, **22**, 973–981.

DEMUYLDER, X., NEVEN, P., DESOMER, M., VAN BELLE, Y., VANDERICK, G. & DEMUYLDER, E. (1991). Endometrial lesions in patients undergoing tamoxifen therapy. *Int. J. Gynecol. Obstet.*, **36**, 127–130.

DILTS, P.V., HOPKINS, M.P., CHANG, A.E. & CODY, R.L. (1992). Rapid growth of leiomyoma in patients receiving tamoxifen. *Am. J. Obst. Gynecol.*, **1663**, 167–168.

DRAGAN, Y.P., XU, Y.D. & PITOT, H.C. (1991). Tumor promotion as a target for estrogen/antiestrogen effects in rat hepatocarcinogenesis. *Prev. Med.*, **20**, 15–26.

EARLY BREAST CANCER TRIALS COLLABORATIVE GROUP (1992). Systemic treatment of early breast cancer by hormonal cytotoxic and immune therapy: 133 randomized trials involving 331,000 recurrences and 24,000 deaths among 75,000 women. *Lancet*, **339**, 1–15.

FALKSON, H.C., GRAY, R., WOLBERG, W.H., GILCHRIST, K.W., HARRIS, J.F., TORMEY, D.C. & FALKSON, G. (1990). Adjuvant trial of 12 cycles of CMFPT followed by observation at continuous tamoxifen versus four cycles of CMFPT in postmenopausal women with breast cancer. An Eastern Cooperative Oncology Group Phase III study. *J. Clin. Oncol.*, **8**, 599–607.

FENTIMAN, I.S., CALEFFI, M., RODIN, A., MURBY, B. & FOGELMAN, I. (1989). Bone mineral content of women receiving tamoxifen for mastalgia. *Br. J. Cancer*, **60**, 262–264.

FISHER, B. (1992). The evolution of paradigms for the management of breast cancer: a personal perspective. *Cancer Res.*, **52**, 2371–2382.

FISHER, B., BROWN, A., WOLMARK, N. and other members of the NSABP (1987). Prolonging tamoxifen therapy for primary breast cancer. *Am. J. Int. Med.*, **106**, 649–654.

FISHER, B., COSTANTINO, J., REDMOND, C., POISSAN, R., BOWMAN, D., COUTURE, J., DIMITROV, N.V., WOLMARK, N., WICKSHAM, D.C., FISHER, E.R., MARGOLESE, R.D., SUTHERLAND, C., GLAS, A., FOSTER, R. & CAPLAN, R. (1989). A randomized clinical trial evaluating tamoxifen in the treatment of patients with node-positive breast cancer who have estrogen receptor-positive tumors. *N. Engl. J. Med.*, **320**, 429–484.

FISHER, B., REDMOND, C., LAGAULT-POISSAN, S., DIMITROV, N.V. & BROWN, A.M. (1990). Post operative chemotherapy and tamoxifen compared with tamoxifen alone in the treatment of positive-node breast cancer patients aged 50 years and older with tumours responsive to tamoxifen. Results from NSABP study B16. *J. Clin. Oncol.*, **8**, 1005–1018.

FORD, M.R., TURNER, M.J., WOOD, C. & SOUTHERN, W.P. (1988). Endometriosis developing during tamoxifen therapy. *Am. J. Obstet. Gynecol.*, **158**, 1119.

FORNANDER, T., RUTQVIST, L.E., CEDERMARK, B., GLAS, U., MATTSSON, A., SILJVERSWARD, C., SKOOG, L., SOMELL, A., THEVE, T., WILKING, N., ASKERGREN, J. & HJALMER, M.L. (1989). Adjuvant tamoxifen in early breast cancer: occurrence of new primary cancers. *Lancet*, **i**, 117–120.

FURR, B.J.A. & JORDAN, V.C. (1984). The pharmacology and clinical use of tamoxifen. *Pharmacol. Ther.*, **25**, 127–205.

GAGLIARDI, A. & COLLINS, D.C. (1993). Inhibition of angiogenesis by antiestrogens. *Cancer Res.*, **53**, 533–535.

GAIL, M.H., BRINTON, L.A., BYAR, D.P., CORLE, D.K., GREEN, S.B., SHIRO, C. & MULVIHILL, J.J. (1989). Projecting individualized probabilities of developing breast cancer for white females who are being examined annually. *J. Natl. Cancer Inst.*, **81**, 1879–1886.

GAL, D., KOPEL, S., BASHEVKIN, M., LEBOWICS, J., LEV, R. & TANCER, M.L. (1991). Oncogenic potential of tamoxifen or endometria of postmenopausal women with breast cancer – a preliminary report. *Gynecol. Oncol.*, **42**, 120–123.

GERNER, E.W. (1989). Ocular toxicity of tamoxifen. *Int. Ophthamol.*, **21**, 420–423.

GORSKI, J., TOFT, D., SHYAMALA, G., SMITH, D.M. & NOTIDES, A. (1968). Hormone receptors: studies on the interaction of estrogen with the uterus. *Recent Prog. Horm. Res.*, **24**, 45–80.

GOTTARDIS, M.M. & JORDAN, V.C. (1987). The antitumor actions of keoxifene and tamoxifen in the N-nitrosomethylurea-induced rat mammary carcinoma model. *Cancer Res.*, **47**, 4020–4024.

GOTTARDIS, M.M. & JORDAN, V.C. (1988). Development of tamoxifen-stimulated growth of MCF-7 tumors in athymic mice after long-term antiestrogen administrations. *Cancer Res.*, **48**, 5183–5187.

GOTTARDIS, M.M., ROBINSON, S.P., SATYASWAROOP, P.G. & JORDAN, V.C. (1988). Contrasting actions of tamoxifen on endometrial and breast tumor growth in the athymic mouse. *Cancer Res.*, **48**, 812–815.

GREEN, S. (1990). Modulations of oestrogen receptor activity by oestrogens and antioestrogens. *J. Steroid. Biochem. Mol. Biol.*, **37**, 747–751.

GRIFFITHS, M.F. (1987). Tamoxifen retinopathy in low dosage. *Am. J. Ophthamol.*, **104**, 185–186.

GROOM, G.V. & GRIFFITHS, K. (1976). Effect of the antioestrogen tamoxifen on plasma levels of luteinizing hormone, follicle-stimulating hormone, prolactic, oestradiol and progesterone in normal premenopausal women. *J. Endocrinol.*, **70**, 421–428.

GULLINO, P.M., PETTIGREW, H.M. & GRANTHAM, F.H. (1975) N-Nitrosomethylurea as mammary gland carcinogen in rats. *J. Natl. Cancer Inst.*, **54**, 401–414.

GUSBERG, S.B. (1990). Tamoxifen for breast cancer: associated endometrial cancer. *Cancer*, **65**, 1463–1464.

HAN, X. & LIEHR, J.G. (1992). Induction of covalent DNA adducts in rodents by tamoxifen. *Cancer Res.*, **52**, 1360–1363.

HARDELL, L. (1988). Tamoxifen as risk factor for carcinoma of corpus uteri. *Lancet*, **ii**, 563.

HARPER, M.J.K. & WALPOLE, A.L. (1966). Contrasting endocrine activities of *cis* and *trans* isomers in a series of substituted triphenylethylenes. *Nature*, **212**, 87.

HARPER, M.J.K. & WALPOLE, A.L. (1967a). Mode of action of ICI 46, 474 in preventing implantations in rats. *J. Endocrinol.*, **37**, 83–92.

HARPER, M.J.K. & WALPOLE, A.L. (1967b). A new derivative of triphenylethylene: effect on implantations and mode of action in rats. *J. Reprod. Fertil.*, **13**, 101–119.

HENDRICK, A. & SUBRAMANIAN, V.P. (1980). Tamoxifen and thrombo-embolism. *J. Am. Med. Ass.*, **243**, 514–515.

HOROWITZ, R.I. & FEINSTEIN, A.R. (1986). Estrogens and endometrial cancer. Responses to arguments and current status of an epidemiologic controversy. *Am. J. Med.*, **81**, 503–507.

HUGGINS, C., GRAND, L.C. & BRILLANTES, F.P. (1961) Mammary cancer induced by a single feeding of polynuclear hydrocarbons and its suppression. *Nature*, **189**, 204–207.

HUYNY, H.T., TETENESE, E., WALLACE, L. & POLLAK, M. (1993). *In vivo* inhibitions of insulin-like growth factor 1 gene expression by tamoxifen. *Cancer Res.*, **53**, 1727–1730.

INGLE, J.N., AHMANN, D.L., GREEN, S.J., EDMONSON, J.H., BISEL, H.F., KROLS, L.K., NICHOLS, W.C., CREAGON, E.T., HAHN, R.G., RUBIN, J. & KRYTAK, S. (1981). Randomize clinical trial of diethylstilberol versus tamoxifen in postmenopausal women with advanced breast cancer. *N. Engl. J. Med.*, **304**, 16–21.

JENSEN, E.V., BLOCK, G.E., SMITH, S., KYSER, K. & DESOMBRE, E.R. (1971). Estrogen receptors and breast cancer response to adrenalectory. In *Prediction of Response in Cancer Therapy* ed. Hall, T.C. *Natl. Cancer Inst. Mongr.*, **34**, 55–70.

JENSEN, E.V. & JACOBSON, H.I. (1962). Basic guides to the mechanism of estrogen action. *Recent Prog. Hor. Res.*, **18**, 387–414.

JORDAN, V.C. (1974). Antitumour activity of the antioestrogen ICI 46, 474 (tamoxifen) in the dimethyl-benzanthracene (DMBA)-induced rat mammary carcinoma model. *J. Steroid Biochem.*, **5**, 354.

JORDAN, V.C. (1975). Prolonged antioestrogenic activity of ICI 46, 474 in the ovariectomized mouse. *J. Reprod. Fertil.*, **52**, 251–258.

JORDAN, V.C. (1976). Effect of tamoxifen (ICI 46, 474) on initiation and growth of DMBA-induced rat mammary carcinomata. *Eur. J. Cancer*, **12**, 419–424.

JORDAN, V.C. (1978). Use of the DMBA-induced rat mammary carcinoma system for the evaluation of tamoxifen treatment as a potential adjuvant therapy. *Rev. Endocrine Rel. Cancer*, October Supplement, 49–55.

JORDAN, V.C. (1983). Laboratory studies to develop general principles for the adjuvant treatment of breast cancer with antiestrogens: problems and potential for future clinical applications. *Breast Cancer Res. Treat.*, **3** (suppl), S73–86.

JORDAN, V.C. (1984). Biochemical pharmacology of antiestrogen action. *Pharmacol. Rev.*, **36**, 245–276.

JORDAN, V.C. (1988). The development of tamoxifen for breast cancer therapy: a tribute to the late Arthur L. Walpole. *Breast Cancer Res. Treat.*, **11**, 197–209.

JORDAN, V.C. (1990). Long-term adjuvant tamoxifen therapy for breast cancer. *Breast Cancer Res. Treat.*, **15**, 125–136.

JORDAN, V.C. (1993). Should all postmenopausal women with a diagnosis of breast cancer receive tamoxifen? *Postgrad. Gen. Surgery*, (in press).

JORDAN, V.C. & ALLEN, K.E. (1980). Evaluation of the antitumour activity of the nonsteroidal antioestrogen monohydroxytamoxifen in the DMBA-induced rat mammary carcinoma model. *Eur. J. Cancer*, **16**, 239–251.

JORDAN, V.C., COLLINS, M.M., ROWSBY, L. & PRESTWICH, G. (1977). A monohydroxylated metabolite of tamoxifen with potent antioestrogenic activity. *J. Endocrinol.*, **75**, 305–316.

JORDAN, V.C., DIX, C.J. & ALLEN, K.E. (1979). The effectiveness of long-term treatment in a laboratory model for adjuvant hormone therapy of breast cancer. In *Adjuvant Therapy for Cancer*, II, ed. Solomon, L.E. & Jones, L.E. pp. 19–26. New York: Grune & Stratton.

JORDAN, V.C., DIX, C.J., NAYLOR, K.E., PRESTWICH, G. & ROWSBY, L. (1978). Non-steroidal antiestrogens: their biological effects and potential mechanisms of action. *J. Toxicol. Environ. Health*, **4**, 364–390.

JORDAN, V.C. & DOWSE, L.J. (1976). Tamoxifen as an antitumour agent: effect on oestrogen binding. *J. Endocrinol.*, **68**, 297–303.

JORDAN, V.C., FRITZ, N.F., LANGAN-FAHEY, S., THOMPSON, M. & TORMEY, D.C. (1991). Alteration of endocrine parameters in premenopausal women with breast cancer during long term adjuvant therapy with tamoxifen as a single agent. *J. Natl. Cancer Inst.*, **83**, 1488–1491.

JORDAN, V.C., FRITZ, N.F. & TORMEY, D.C. (1987). Long-term adjuvant therapy with tamoxifen: effects on sex hormone binding globulin and antithrombin III. *Cancer Res.*, **47**, 4517–4519.

JORDAN, V.C. & JASPAN, T. (1976). Tamoxifen as an antitumour agent: oestrogen binding as a predictive test for tumour response. *J. Endocrinol.*, **68**, 453–460.

JORDAN, V.C. & KOERNER, S. (1975). Tamoxifen (ICI 46, 474) and the human carcinoma 8S oestrogen receptor. *Eur. J. Cancer*, **11**, 205–206.

JORDAN, V.C., LABABIDI, M.K. & LANGAN-FAHEY, S.M. (1991). Suppression of mouse mammary tumorigenesis by long-term tamoxifen therapy. *J. Natl. Cancer Inst.*, **83**, 492–496.

JORDAN, V.C., LABABIDI, M..K. & MIRECKI, D.M. (1990). The antiestrogenic and antitumor properties of prolonged tamoxifen therapy in C3H/OUJ mice. *Eur. J. Cancer*, **26**, 718–721.

JORDAN, V.C. & MURPHY, C.S. (1990). Endocrine pharmacology of antiestrogens as antitumor agents. *Endocrine Rev.*, **11**, 578–610.

JORDAN, V.C. & PRESTWICH, G. (1977). Binding of [^{3}H] tamoxifen in rat uterine cytosols. A comparison of swinging bucket and vertical tube rotor sucrose density gradient analysis. *Mol. Cell. Endocrinol.*, **8**, 179–188.

KAISER-KUPFER, M.I., KUPFER, C. & RODRIGUEZ, M.M. (1981). Tamoxifen retinopathy: a clinicopathologic report. *Ophthalmology*, **88**, 89–93.

KAISER, KUPFER, M.I. & LIPPMAN, M.E. (1978). Tamoxifen retinopathy. *Cancer Treat. Rep.*, **62**, 315–320.

KALEF-EZRA, J., GLAVOS, D., KLOUVAS, G., HATZIBONSTANTINOU, J., KARANTARAS, A., SIAMOPOULOS, K.C. & PAVLIDES, N. (1992). New evidence that tamoxifen does not induce osteoporosis: a nuclear activation analysis and absorptiometry study. *Br. J. Radiol.*, **65**, 417–420.

KNABBE, C., LIPPMAN, M.E., WAKEFIELD, L.M., FLANDERS, K.C., KASID, A., DERYNCK, R. & DICKSON, R.B. (1987). Evidence that transforming growth factor β is a hormonally regulated negative growth factor in human breast cancer cells. *Cell*, **48**, 417–428.

LACASSAGNE, A. (1936). Hormonal pathogenesis of adenocarcinoma of the breast. *Am. J. Cancer*, **14**, 217–225.

LANGAN-FAHEY, S.M., TORMEY, D.C. & JORDAN, V.C. (1990). Tamoxifen metabolites in patients or long-term adjuvant therapy for breast cancer. *Eur. J. Cancer*, **26**, 883–888.

LATHROP, A.E.C. & LOEB, L. (1916). Further investigations on the origins of tumors in mice III. Or the part played by internal secretions in the spontaneous development of tumors. *J. Cancer Res.*, **1**, 1–16.

LERNER, L.J. & JORDAN, V.C. (1990). Development of antiestrogens and their use in breast cancer. Eighth Cain Memorial Award Lecture. *Cancer Res.*, **50**, 4177–4189.

LIPTON, A., HARVEY, H.A. & HAMILTON, R.W. (1984). Venous thrombosis as a side effect of tamoxifen treatment. *Cancer Treat. Rep.*, **68**, 882–889.

LONGSTAFF, S., SIGURDSSON, H., O'KEEF, M., OGSTAN, S. & PREECE, P. (1989). A controlled study of the ocular effects of tamoxifen in conventional dosage in the treatment of breast cancer. *Eur. J. Cancer*, **25**, 1805–1808.

LOVE, R.R. (1988). The Wisconsin tamoxifen study: toxicity in node negative postmenopausal women. *Cancer Invest.*, **6**, 601–605.

LOVE, R.R., CAMERON, L., CORNELL, B.L. & LEVENTHAL, H. (1991b). Symptoms associated with tamoxifen treatment in postmenopausal women. *Arch. Inv. Med.*, **151**, 1842–1847.

LOVE, R.R., MAZESS, R.B., BARDEN, H.S., EPSTEIN, S., NEWCOMB, P.A., JORDAN, V.C., CARBONE, P.P. & DEMETS, D.L. (1992a). Effects of tamoxifen on bone mineral density in postmenopausal women with breast cancer. *N. Engl. J. Med.*, **326**, 852–856.

LOVE, R.R., MAZESS, R.B., TORMEY, D.C., BARDEN, H.S., NEWCOMB, P.A. & JORDAN, V.C. (1988). Bone mineral density in women with breast cancer treated with adjuvant tamoxifen for at least 2 years. *Breast Cancer Res. Treat.*, **12**, 297–302.

LOVE, R.R., NEWCOMB, P.A., WEIBE, D.A., SURAWICZ, T.S., JORDAN, V.C., CARBONE, P.P. & DEMETS, D.L. (1990). Effects of tamoxifen therapy on lipid and lipoprotein levels in postmenopausal patients with node-negative breast cancer. *J. Natl. Cancer Inst.*, **82**, 1327–1332.

LOVE, R.R., SURAWICZ, T.S. & WILLIAMS, E.C. (1992b). Antithrombin III level, fibrinogen level and platelet count changes with adjuvant tamoxifen therapy. *Arch. Int. Med.*, **152**, 317–320.

LOVE, R.R., WEIBE, D.A., NEWCOMB, P.A., CAMERON, L., LEVENTHAL, H., JORDAN, V.C., FEYZI, J. & DEMETS, D.L. (1991a). Effects of tamoxifen on cardiovascular risk factors in postmenopausal women. *Ann. Int. Med.*, **115**, 860–864.

LYMAN, S.D. & JORDAN, V.C. (1985). Metabolism of tamoxifen and its uterotrophic activity. *Biochem. Pharmacol.*, **34**, 2787–2794.

MAGRIPLES, U., NAFTOLIN, F., SCHWARTZ, P.E. & CARCANGIUM, M.L. (1993). High grade endometrial carcinoma in tamoxifen treated breast cancer patients. *J. Clin. Oncol.*, **11**, 485–490.

MANNI, A. & PEARSON, O.H. (1980). Antiestrogen-induced remissions in premenopausal women with stage IV breast cancer: effects on ovarian function. *Cancer Treat. Rep.*, **64**, 779–785.

MCDONALD, C.C. & STEWART, H.J. (1991). Fatal myocardial infarction in the Scottish adjuvant tamoxifen trial. The Scottish Breast Cancer Committee. *Br. Med. J.*, **303**, 435–437.

MCGUIRE, W.L., CARBONE, P.P. & VOLLMER, E.P. (ed) (1975). *Estrogen Receptors in Human Breast Cancer*. New York: Raven Press.

MORROW, M. (1992). Pre-cancerous breast lesions: implication for breast cancer prevention trials. *Int. J. Rad. Oncol. Biol. Physiol.*, **23**, 1071–1078.

MORROW, M. & JORDAN, V.C. (1992). Prospects for the prevention of breast cancer. In *Breast Disease Updates*. ed. Harris, J.R. & Lippincott, J.P. Vol. 1, pp. 1–12. Philadelphia, Healthcare Co.

NAYFIELD, S.G., KARP, J.E., FORD, L.G., DORR, F.A. & KRAMER, B.S. (1991). Potential role of tamoxifen in prevention of breast cancer. *J. Natl. Cancer Inst.*, **83**, 1450–1459.

NEVASAARI, K., HEIKKINEN, M. & TASKINEN, P.J. (1978). Tamoxifen and thrombosis. *Lancet*, **ii**, 946–947.

NEVEN, P., DE MUYLDER, X., VAN BELLE, Y., VANDERICK, G. & DEMUYLDER, E. (1989). Tamoxifen and the uterus and endometrium. *Lancet*, **i**, 375–376.

NOGUCHI, S., MOTOMURA, K., INAJI, H., IMAOKA, S. & KOYAMA, H. (1993a). Up regulation of estrogen receptor by tamoxifen inhuman breast cancer. *Cancer*, **71**, 1268–1272.

NOGUCHI, S., MOTOMURA, K., INAJI, H., IMAOKA, S. & KOYAMA, H. (1993b). Down regulation of transforming growth factor alpha by tamoxifen in human breast cancer. *Cancer*, **72**, 131–136.

NOLVADEX ADJUVANT TRIAL ORGANIZATION (1983). Controlled trial of tamoxifen as adjunct agent in the management of early breast cancer. Interim analysis at four years by Nolvadex Adjuvant Trial Organization. *Lancet*, **i**, 257–261.

NOLVADEX ADJUVANT TRIAL ORGANIZATION (1985). Controlled trial of tamoxifen as a single adjuvant agent in the management of early breast cancer. *Lancet*, **i**, 836–840.

NUOVO, M.A., NUOVO, G.J., MCCAFFREY, R.M., LEVINE, R.U., BARON, B. & WINKLER, B. (1989). Endometrial polyps in postmenopausal patients reviewing tamoxifen. *Int. J. Gynecol. Pathol.*, **8**, 125–131.

PATERSON, A.H., HANSON, J., PRITCHARD, K.I., SANSREGRET, E., DOHROURGE, S., MCDERMOT, R.S., KINE, S., WHITE, D.F., TRUDEAU, M., STEWARD, D.J. & UNGAR, W. (1990). Comparison of antiestrogen and progestin therapy for initial treatment and consequences of their combination for second-line treatment of recurrent breast cancer. *Sem. Oncol.*, **17**, 52–62.

PAVLIDIS, N.A., PETRIS, C., BRIASSOULIS, E., KLOUVAS, G., PSILOS, C., REMPOPIS, J. & PETROUTSOS, G. (1992). Clear evidence that long-term, low dose tamoxifen treatment can induce ocular toxicity. *Cancer*, **69**, 2961–2964.

PHAM, T.A., ELLISTON, J.F., NAWAZ, Z., MCDONNELL, D.P., TSAI, M.-J. & O'MALLEY, B.W. (1991). Antiestrogens can establish nonproductive receptor complexes and alters chromatin structure at target enhancers. *Proc. Natl. Acad. Sci. U.S.A.*, **88**, 3125–3129.

PHAM, T.A., HWUNG, Y.-P., SANTISO-MERE, D., MCDONNELL, D.P. & O'MALLEY, B.W. (1992). Ligand-dependent and -independent function of the transactivation regions of the human estrogen receptor in yeast. *Mol. Endocrinol.*, **6**, 1043–1052.

POLLAK, M.N., HUYNH, H.T. & LEFEBVRE, S.P. (1992). Tamoxifen reduces serum insulin-like growth factor 1 (IGF-1). *Breast Cancer Res. Treat.*, **22**, 91–95.

POWLES, T.J., HARDY, J.R., ASHLEY, S.E., FARRINGTON, G.H., COSGROVE, D., DAVEY, J.R., DORSETT, M., MCKINNA, J.A., WASH, A.G., SENNETT, H.D., TILLYER, C.R. & TRELEAVEN, J.G. (1989). A pilot trial to evaluate the acute toxicology and feasibility of tamoxifen for prevention of breast cancer. *Br. J. Cancer*, **60**, 126–131.

POWLES, T.J., TILLYER, C.R., JONES, A.L., ASHLEY, S.E., TRELEAVEN, J., DAVEY, J.B. & MCKINNA, J.A. (1990). Prevention of breast cancer with tamoxifen – an update on the Royal Marsden Hospital Pilot Program. *Eur. J. Cancer*, **26**, 680–684.

PRITCHARD, K.I., THOMSON, D.B., MYERS, R.E., SUTHERLAND, D.J., MOBBS, B.G. & MEAKINS, J.W. (1980). Tamoxifen therapy in premenopausal patients with metastatic breast cancer. *Cancer Treat. Rep.*, **64**, 787–796.

PUBESGAARD, T. & VON EYBEN, F.E. (1986). Bilateral optic neuritis evolved during tamoxifen treatment. *Cancer*, **58**, 383–386.

RITCHIE, L.D. & GRANT, S.M. (1989). Tamoxifen-warfain interaction: the Aberdeen hospital drug file. *Br. Med. J.*, **298**, 1253.

ROBINSON, S.P., LANGAN-FAHEY, S.M., JOHNSON, D.A. & JORDAN, V.C. (1991). Metabolites, pharmacodynamics, and pharmacokinetics of tamoxifen in rats and mice compared to the breast cancer patient. *Drug Met. Disp.*, **19**, 36–43.

ROSE, D.P., CHLEBOWSKI, R.T., CONNOLLY, J.M., JONES, L.A. & WYNDER, E.L. (1992). Effects of tamoxifen adjuvant therapy and a low-fat diet or serum binding proteins and estradiol bioavailability in postmenopausal breast cancer patients. *Cancer Res.*, **52**, 5386–5390.

ROSE, D.P. & DAVIS, T.E. (1977). Ovarian function in patients receiving adjuvant chemotherapy for breast cancer. *Lancet*, **i**, 1174–1176.

SAPHNER, T., TORMEY, D.C. & GRAY, R. (1991). Venous and arterial thrombosis in patients who received adjuvant therapy for breast cancer. *J. Clin. Oncol.*, **9**, 286–294.

SATYASWAROOP, P.G., ZAINO, R.J. & MORTEL, R. (1984). Estrogen-like effects of tamoxifen on human endometrial carcinoma transplanted into nude mice. *Cancer Res.*, **44**, 4006–4010.

SCHREIBER, A.R., WINKLER, M.E. & DERYNCK, R. (1986). Transforming growth factor alpha: a more potent angiogenic mediator than epidermal growth factor. *Science*, **232**, 1250–1252.

SCHWARTZBAUM, J.A., HILKA, B.S., FOWLER, W.C., KAUFMAN, D.G. & HOBERMAN, D. (1987). The influence of exogenous estrogen use on survival after diagnosis of endometrial cancer. *Am. J. Epid.*, **126**, 851–860.

SKIDMORE, J.R., WALPOLE, A.L. & WOODBURN, J. (1972). Effect of some triphenylethylenes on oestradiol binding *in vitro* to macromolecules from uterus and anterior pituitary. *J. Endocrinol.*, **52**, 289–298.

SUNDERLAND, M.C. & OSBORNE, C.K. (1991). Tamoxifen in premenopausal patients with metastatic breast cancer: a review. *J. Clin. Oncol.*, **9**, 1283–1297.

SWENERTON, K.D. (1980). Treatment of advanced endometrial carcinoma with tamoxifen. *Cancer Treat. Rep.*, **64**, 805–811.

TENNI, P., LALICH, D.L. & BYRNE, M.J. (1989). Life threatening interaction between tamoxifen and warfarin. *Br. Med. J.*, **298**, 93.

TERENIUS, L. (1971). Structure activity relationships of antiestrogens with regard to interaction with 17β oestradiol in the mouse uterus and vagina. *Acta Endocrinol.*, **66**, 431–447.

TORMEY, D.C., GRAY, R., ABELOFF, M.D., ROSEMAN, D.L., GILCHRIST, K.W., BARYLAB, E.J., STOTT, P. & FALKSON, G. (1992). Adjuvant therapy with a doxirubicin regimen and long term tamoxifen in premenopausal breast cancer patients. an Eastern Cooperative Oncology Group Trial. *J. Clin. Oncol.*, **10**, 1848–1856.

TORMEY, D.C. & JORDAN, V.C. (1984). Long-term adjuvant therapy in node positive breast cancer – a metabolic and pilot clinical study. *Breast Cancer Res. Treat.*, **4**, 297–302.

TORMEY, D.C., RASMUSSEN, P. & JORDAN, V.C. (1987). Update on long-term tamoxifen study. *Breast Cancer Res. Treat.*, **9**, 157–158.

TURCOT-LEMAY, L. & KELLEY, P.A. (1980). Characterization of estradiol, progesterone and prolactin receptors in N-nitrosomethyurea-induced mammary tumors and effects of antiestrogen treatment on the development and growth of these tumors. *Cancer Res.*, **40**, 3232–3240.

TURKEN, S., SIRIS, E., SELDIN, D., FLASTER, E., HYMAN, G. & LINDSAY, R. (1989). Effect of tamoxifen on spinal bone density in women with breast cancer. *J. Natl. Cancer Inst.*, **81**, 1086–1088.

VINDING, T. & NIELSEN, N.V. (1983). Retinopathy caused by treatment with tamoxifen in low dosages. *Act. Ophthalmologica*, **61**, 45–50.

WARD, H.W.C. (1973). Antioestrogenic therapy for breast cancer: a trial of tamoxifen at two dose levels. *Br. Med. J.*, **i**, 13–14.

WELSHON, S.W.V., LIEBERMAN, M.E. & GORSKI, J. (1984). Nuclear localization of unoccupied oestrogen receptors: cytochalasin enucleation of GH3 cells. *Nature*, **307**, 747–749.

WHITE, I.N.H., DEMATTEIS, F., DAVIS, A., SMITH, L.L., CROFTON-SLEIGH, C., VENITT, S., HEWER, A. & PHILLIPS, D.H. (1992). Genotoxic potential of tamoxifen and analogues in female Fischer F344/n rats, DBA/d and C578L/6 mice and in human MCL-5 cells. *Carcinogenesis*, **13**, 2197–2203.

WILLIAMS, G.M., IATROPOULOS, M.J., DJORDJEVIC, M.V. & KALTENBERG, O.P. (1993). The triphenylethylene drug tamoxifen is a strong liver carcinogen in the rat. *Carcinogenesis*, **14**, 315–317.

WILSON, A.J., TEHRANI, F. & BAUM, M. (1982). Adjuvant tamoxifen therapy for early breast cancer: an experimental study with reference to oestrogen and progesterone receptors. *Br. J. Surgery*, **69**, 121–125.

(Received July 1, 1993)

Br. J. Pharmacol. (1993), **110**, 519–520

SPECIAL REPORT

PAF activation of a voltage-gated R-type Ca^{2+} channel in human and canine aortic endothelial cells

[1]Ghassan Bkaily, †Pedro D'Orléans-Juste, Radha Naik, Jacqueline Pérodin, *Jana Stankova, ‡Elias Abdulnour & *Marek Rola-Pleszczynski

Departments of Physiology and Biophysics, †Pharmacology, *Immunology and ‡Surgery, Faculty of Medicine, University of Sherbrooke, Sherbrooke, Québec, Canada J1H 5N4

By the use of fura-2 and digital imaging techniques, $[K]_o$ depolarization or PAF (10^{-9} M) were shown to induce a sustained increase of $[Ca]_i$ in human or canine single aortic vascular endothelial cells (VEC) that was insensitive to nifedipine but sensitive to (−)-PN200-110 or to lowering of $[Ca]_o$. The PAF-induced effect on $[Ca]_i$ was blocked by the PAF receptor antagonist, WEB2170. Our results suggest that $[K]_o$ depolarization and PAF increase $[Ca]_i$ via the activation of R-type Ca^{2+} channels.

Keywords: Endothelial cells; Ca^{2+} channel; PAF; calcium blockers; calcium

Introduction A sustained increase of intracellular free calcium ($[Ca]_i$) in vascular endothelial cells (VEC) after stimulation by diverse vasoactive agents is dependent on Ca^{2+} influx (Sturek *et al.*, 1991). However, the ionic channels responsible for this sustained increase of $[Ca]_i$ are not known (Takeda & Klepper, 1990). The difficulty in identifying the Ca^{2+} channel type that is responsible for the sustained increase of $[Ca]_i$ in VEC has been attributed to damage of these cells during enzymatic dispersion and/or to the use of long term culture preparations (Sturek *et al.*, 1991). Recently, in our laboratory, we have reported the presence of a new type of Ca^{2+} channel (R-type), in several cell types, that is responsible for the sustained increase of $[Ca]_i$ (Bkaily, 1991; Bkaily *et al.*, 1991; 1992).

The present study was undertaken in order to verify if the voltage-dependent steady-state R-type Ca^{2+} channel exists in VEC and if platelet-activating factor (1-*O*-alkyl-2-acetyl-sn-glycero-3-phosphocholine; PAF)-induced stimulation of $[Ca]_i$ (Bregestovski & Ryan, 1989) is mediated via activation of this type of channel.

Methods VEC were isolated as single cells from the luminal surface of human and adult mongrel dog aortae by use of 0.1% trypsin solution as previously described for vascular endothelial cells (Sturek *et al.*, 1991); the single cells were left to attach (within 1 h) to a glass cover slip that fitted a bath chamber (1 ml) of 20 mm diameter (Bkaily *et al.*, 1992). The work was performed in accordance with the requirements of the institutional review committee for the use of human material. The technique used to load the VEC with fura-2 and the Ca^{2+} measurement technique in single cells using an Imagescan microfluorometer (Photo Technology International Inc., Princeton, NJ, U.S.A.) are identical to those previously described for vascular smooth muscle cells (Bkaily *et al.*, 1992).

Freshly isolated VEC were superfused (5 ml min^{-1}) with Tyrode solution containing (in mM) either: NaCl 130, KCl 5, $CaCl_2$ 2, HEPES 10 and glucose 10 or NaCl 105, KCl 30, $CaCl_2$ 2, HEPES 10 and glucose 10. The solutions were buffered to pH 7.4 with Tris base and the osmolarity was adjusted with sucrose to 310 mOsm (Advanced DigiMatic Osmometer 3DII, Massachusetts, U.S.A.). The dual L- (Striessnig *et al.*, 1986) and R-type (Bkaily *et al.*, 1992) Ca^{2+} channel blocker (−)-isradipine (PN200-110) was obtained from Sandoz Canada Inc. PAF was obtained from Bachem (U.S.A.) and WEB2170 (3-[4-(2-chlorophenyl)-9-methyl-6H-thieno[3,2-f][1,2,4]triazolo-[4,3-a][1,4]-diazepin-2-yl]-1-(4-morpholimyl)-1-propanone; Casals-Stenzel, 1987) was a generous gift of H. Heuer (Boehringer-Ingelheim, Germany). The fura-2AM was purchased from Molecular Probes Inc. (Eugene, OR, U.S.A.) and all other substances were purchased from Sigma (St Louis, MI, U.S.A.).

Data used in the text and figures are expressed as means ± s.e.mean of *n* different observations. Statistical comparisons between controls and each experimental interaction were made by paired Student's *t* test. *P* values of <0.05 were considered to be statistically significant. All experiments were carried out at 28°C.

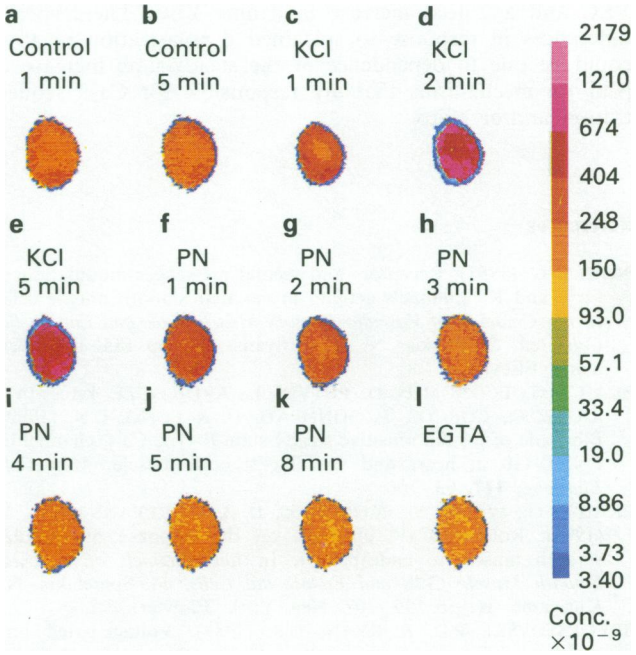

Figure 1 Blockade of the sustained increase of $[Ca]_i$ induced with high $[K]_o$ by PN200-110 in human aortic vascular endothelial cells. (a–b) control (5 mM $[K]_o$) digital colour image maps of basal steady state free $[Ca]_i$ at 1 min (170 nM) and 5 min (170 nM) recording. (c) Increase in $[Ca]_i$ taken at 1 min (280 nM) in presence of high $[K]_o$ (30 mM). (d–e) Sustained increase in $[Ca]_i$ taken at 2 min (d, 560 nM) and 5 min (e, 560 nM) in presence of high $[K]_o$. (f–k) Superfusion with high $[K]_o$ containing 10^{-7} M PN200-110 rapidly (f, at 1 min, 262 nM) and progressively blocked the sustained increase of $[Ca]_i$ induced with high $[K]_o$. Addition of 30 mM EGTA did not further decrease the $[Ca]_i$ (156 nM).

[1] Author for correspondence.

Results The basal level of $[Ca]_i$ of human and canine VEC in normal K^+ (5 mM) solution was 135 ± 24 nM ($n = 12$) 154 ± 27 nM ($n = 12$) respectively. Sustained depolarization with 30 mM KCl induced (within 1 min) a steady-state increase of $[Ca]_i$ in both human (from 132 ± 21 to 506 ± 63 nM, $n = 5$) and canine (from 156 ± 21 to 281 ± 33 nM, $n = 5$) VEC that was, as in vascular smooth muscle cells (VSMC) (Bkaily *et al.*, 1992), insensitive to the L-type Ca^{2+} blocker nifedipine (Figure 2) but sensitive to the dual Ca^{2+} L- and R-type blocker PN200-110 (Figure 1, an example out of 8 experiments and Figure 2) and to the Ca^{2+} chelator EGTA (Figure 2). As for high $[K]_o$, superfusion with a Tyrode solution containing 10^{-9} M PAF induced (within 1 min) a sustained increase of $[Ca]_i$ of both human and canine VEC (Figure 2) that was insensitive to nifedipine (10^{-5} M) but significantly decreased by PN200-110 (10^{-7} M). The remaining increase of $[Ca]_i$ was completely blocked by 30 mM EGTA (Figure 2). The PAF-receptor antagonist, WEB2170 (10^{-5} M) significantly decreased the PAF-induced sustained increase of $[Ca]_i$ (Figure 2).

Discussion Our study demonstrates that the mean basal resting $[Ca]_i$ in human and canine aortic VEC is similar, and comparable to values obtained in endothelial cells from bovine aorta (Sturek *et al.*, 1991) and human umbilical cords (Jacob *et al.*, 1988). Our results show that a voltage-sensitive Ca^{2+} channel does exist in VEC and that this channel is similar to the nifedipine-insensitive and PN200-110-sensitive R-type Ca^{2+} channel described in heart and vascular smooth muscle cells in response to endothelin-1 and insulin (Bkaily *et al.*, 1991; 1992). This channel in human and canine VEC seems also to be responsive to PAF. Since the PAF receptor antagonist, WEB2170, reversed the effect of PAF, it may suggest that the effect of PAF on the R-type Ca^{2+} channel is mediated via a receptor-dependent mechanism which remains to be determined. Our results also show that high $[K]_o$ or PAF induced a 4 fold increase of steady-state $[Ca]_i$, in human VEC and a 2 fold increase in canine VEC. These species differences in response to sustained depolarization or PAF could be due to dependence of the steady-state increase of $[Ca]_i$ on mechanisms that are responsible for Ca^{2+} sequestration and/or efflux.

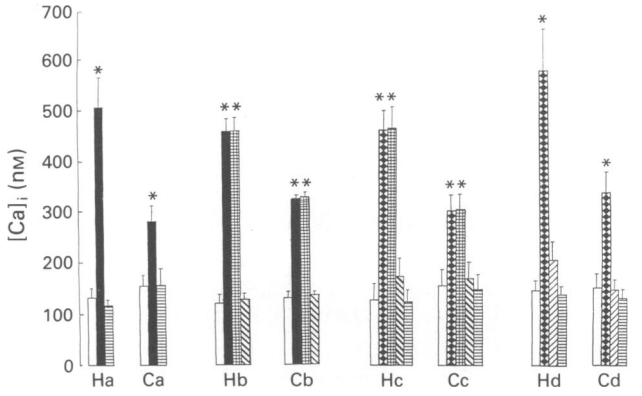

Figure 2 High $[K]_o$ (30 mM) depolarization (■) and PAF (10^{-9} M, ▩)-induced a sustained increase of $[Ca]_i$ in both human (H) and canine (C) vascular endothelial cells that was completely blocked by 30 mM EGTA (▤) (a, c and d). The high $[K]_o$- or PAF-induced sustained increase of $[Ca]_i$ in both preparations is insensitive to 10^{-5} M nifedipine (▦) but sensitive to 10^{-7} M PN200-110 (▨) (Hb, c and Cb, c) and the PAF receptor antagonist, WEB2170 (10^{-5} M, ▨) (Hd and Cd for PAF only; effects against high $[K]_o$ are not shown). The control steady-state $[Ca]_i$ basal level is □. The number of experiments (n) in Ha, Ca, Hb, Cb, Hc, Cc, Hd and Cd are respectively 5, 5, 4, 4, 3 4, 4, and 3. $^*P < 0.01$ compared to control values only. Substances were added sequentially at intervals of approximately 7 min in the order indicated.

We suggest that the presence of an R-type Ca^{2+} channel that could be gated by voltage or a receptor in VEC may play an important role in excitation-secretion coupling mechanisms in the VEC and subsequent release of vasoactive factors such as endothelium-derived relaxing factor and endothelin-1.

The authors would like to acknowledge the financial support of the Medical Research Council of Canada and the Fonds de Recherche en Santé du Québec, the technical assistance of G.B. Bkaily Jr. and the secretarial assistance of Mrs C. Ducharme.

References

BKAILY, G. (1991). Receptors and second messenger modulation of Ca^{2+} and K^+ channels activity in vascular smooth muscle cells. In *Ion Channels of Vascular Smooth Muscle Cells and Endothelial Cells*. ed. Sperelakis, N. & Kuriyama, H. pp. 185–198. New York: Elsevier.

BKAILY, G., ECONOMOS, D., POTVIN, L., ARDILOUZE, J.-L., MARRIOTT, C., CORCOS, J., BONNEAU, D. & FONG, C.N. (1992). Blockade of insulin sensitive steady-state R-type Ca^{2+} channel by PN200-110 in heart and vascular smooth muscle. *Mol. Cell. Biochem.*, **117**, 93–106.

BKAILY, G., WANG, S., ECONOMOS, D. & D'ORLEANS-JUSTE, P. (1991). Role of Ca^{2+} channels on the response of vascular smooth muscle to endothelin-1. In *Ion Channels of Vascular Smooth Muscle Cells and Endothelial Cells*. ed. Sperelakis, N., Kuriyama, H. pp. 199–207. New York: Elsevier.

BREGESTOVSKI, P.D. & RYAN, U.S. (1989). Voltage-gated and receptor-mediated ionic currents in the membrane of endothelial cells. *J. Mol. Cell. Cardiol.*, **21**, (Suppl. I), 103–108.

CASALS-STENZEL, J. (1987). Triazolodiazepines are potent antagonists of platelet-activating factor (PAF) *in vitro* and *in vivo*. *Arch. Pharmacol.*, **335**, 351–356.

JACOB, R., MERRITT, J.E., HALLAM, T.J. & RINK, T.J. (1988). Repetitive spikes in cytoplasmic calcium evoked by histamine in human endothelial cells. *Nature*, **335**, 40–45.

STRIESSNIG, J., MOOSBURGER, K., GOLL, A., FERRY, D.R. & GLOSSMANN, H. (1986). Stereoselective photoaffinity labelling of the purified 1,4-dihydropyridine receptor of the voltage-dependent calcium channel. *Eur. J. Biochem.*, **161**, 603–609.

STUREK, M., SMITH, P. & STEHNO-BITTEL, L. (1991). In vitro models of vascular endothelial cell calcium regulation. In *Ions Channels of Vascular Smooth Muscle Cells and Endothelial Cells*. ed. Sperelakis, N. & Kuriyama, H. pp. 349–364. New York: Elsevier.

TAKEDA, K. & KLEPPER, M. (1990). Voltage-dependent and agonist-activated ionic currents in vascular endothelial cells: a review. *Blood Vessels*, **27**, 169–183.

(Received May 4, 1993
Accepted June 14, 1993)

Br. J. Pharmacol. (1993), **110**, 521–530

Nitric oxide synthase in pig lower urinary tract: immunohistochemistry, NADPH diaphorase histochemistry and functional effects

Katarina Persson, *Per Alm, †Kjell Johansson, Bengt Larsson & [1]Karl-Erik Andersson

Departments of Clinical Pharmacology, *Pathology and †Zoology, Lund University, Lund, Sweden

1 The distribution and colocalization of nitric oxide synthase (NOS)-like immunoreactivity and NADPH diaphorase activity in the pig lower urinary tract were investigated by immunohistochemical and histochemical staining techniques. Functional *in vitro* studies were performed to correlate the presence of NOS-immunoreactivity/NADPH diaphorase staining with smooth muscle responses involving the L-arginine/nitric oxide (NO) pathway.

2 NOS-immunoreactivity and NADPH diaphorase activity were expressed in nerve trunks and fine nerve fibres in and/or around muscular bundles in the detrusor, trigone and urethra. Thin nerve fibres that dispersed within the muscle bundles were mainly found in the urethral/trigonal area, whereas such fibres were less common in the detrusor.

3 Almost all neuronal structures that were NOS-immunolabelled were also stained for NADPH diaphorase. In contrast, the urothelium, which was intensively stained by the NADPH diaphorase technique, remained unstained by immunohistochemistry.

4 Electrical field stimulation of pig isolated trigonal and urethral preparations induced relaxations, which were inhibited by tetrodotoxin (1 μM) and N^G-nitro-L-arginine (L-NOARG, 10 μM).

5 L-Arginine (1 mM), but not D-arginine, inhibited (25–30%) electrically evoked detrusor contractions. This inhibition was reversed by L-NOARG (0.1 mM). L-Arginine did not inhibit detrusor contractions in the presence of scopolamine (1 μM) and had no direct smooth muscle effects *per se*.

6 Acetylcholine (1 nM–10 μM) caused concentration-dependent relaxations of noradrenaline-induced contractions in pig vesical arteries. Removal of the endothelium practically abolished the acetylcholine-induced relaxation. Pretreatment with L-NOARG (0.1 mM and 0.3 mM) caused a rightward shift of the concentration-response curves to acetylcholine, but the maximal relaxation obtained was significantly reduced (to 65 ± 12%; $n = 6$; $P < 0.05$) only at 0.3 mM L-NOARG.

7 In vessel segments contracted with K^+ (60 mM), acetylcholine induced concentration-dependent relaxations. When the vessels were incubated with 0.3 mM L-NOARG and then contracted with K^+ (60 mM) all relaxant responses to acetylcholine were abolished.

8 The presence of NO synthesizing enzyme in nerve fibres and the pharmacological evidence for NO-mediated relaxation of the trigone and urethra suggest that NO or a NO-related substance may have a role in inhibitory neurotransmission in these regions. In the detrusor, the presence of NO-synthesizing enzyme in nerves can be demonstrated, but its functional importance is unclear. NO, as well as other endothelium-derived factors seem to be involved in the endothelium-dependent acetylcholine-induced relaxation of pig vesical arteries.

Keywords: Nitric oxide; nitric oxide synthase; immunohistochemistry; NADPH diaphorase; urinary tract; N^G-nitro-L-arginine

Introduction

Much evidence has been produced showing that nitric oxide (NO) plays a major role in the non-adrenergic, non-cholinergic (NANC) inhibitory response in the urethra, bladder neck and trigone from various species (Garcia-Pascual *et al.*, 1991; Dokita *et al.*, 1991; Andersson *et al.*, 1991; 1992; Persson & Andersson, 1992; Persson *et al.*, 1992; Thornbury *et al.*, 1992). The relaxation induced by electrical stimulation is totally or partially abolished by enzymatic blockade of NO production by use of analogues of L-arginine, the natural substrate for NO synthase (NOS). Furthermore, in these studies NO and NO-donors (e.g. sodium nitroprusside and SIN-1) were shown to have postjunctional effects producing smooth muscle relaxations more effectively in the trigone and urethra than in the detrusor (Persson & Andersson, 1992; Persson *et al.*, 1992). Thus, while it seems that NO is released from nerves and acts like a neurotransmitter in the bladder outlet, the possible role of NO in the detrusor is still uncertain. A mechanism for detrusor relaxation mediated by release of NO, not from nerves, but from the smooth muscle itself, has been suggested (James *et al.*, 1991).

NO is synthesized from L-arginine by two main classes of synthase: a constitutive form that is present in the brain, endothelial cells and peripheral nerves, and an inducible form that can be induced in macrophages, endothelial cells and vascular smooth muscle cells by endotoxin and cytokines (e.g. Moncada, 1992). The constitutive NOS has been purified from rat cerebellum and antibodies raised against the enzyme have been used to determine the localization of NOS (Bredt *et al.*, 1990). By means of immunohistochemistry major populations of NOS positive nerves have been demonstrated throughout the peripheral nervous system in, e.g., the gastrointestinal tract (Bredt *et al.*, 1990; Ward *et al.*, 1992b; Young *et al.*, 1992; Saffrey *et al.*, 1992; Alm *et al.*, 1993), the urogenital tract (Burnett *et al.*, 1992; Sheng *et al.*, 1992; Alm *et al.*, 1993) and perivascular nerve fibres (Kummer *et al.*, 1992). The distribution of nerves staining for NOS does not seem to be associated with any particular neurotransmitter system, although some NOS immunolabelled nerves in the

[1] Author for correspondence at: Department of Clinical Pharmacology, Lund University Hospital, 221 85 Lund, Sweden.

brain also express somatostatin, neuropeptide Y (NPY) and choline acetyltransferase (Dawson *et al.*, 1991), and in the intestine, VIP (Ward *et al.*, 1992b). However, extensive colocalization has recently been reported between NOS immunopositive nerves and nerves stained histochemically by the NADPH diaphorase method (Dawson *et al.*, 1991; Hope *et al.*, 1991; Alm *et al.*, 1993).

In an attempt to obtain highly specific antisera against neuronal NOS, we have immunized rabbits with fragments of the C- and N-terminal parts of the NOS sequence (Alm *et al.*, 1993), described from rat cerebellum (Bredt *et al.*, 1991). Antibodies raised against the two fragments visualized immunoreactive nerve structures in, e.g., the rat intestine, adrenal glands and penile erectile tissue. No immunoreactive staining was found in the endothelium, suggesting that these fragments of the NOS enzyme may be used for specific localization of neuronal NOS (Alm *et al.*, 1993).

The aim of the present study was to establish the distribution of NOS containing nerves, as studied by immunohistochemistry and NADPH diaphorase histochemistry, in the pig lower urinary tract. In addition, functional *in vitro* studies were performed in order to evaluate whether the presence of NOS immunoreactivity/NADPH diaphorase staining correlates with smooth muscle responses involving the L-arginine/NO pathway.

Methods

The bladder and urethra from female pigs were removed in a slaughterhouse shortly after the animals had been killed. The tissue was transported to the laboratory in cold Krebs solution (for composition, see below). The bladder and urethra were opened longitudinally and tissue pieces from the detrusor, trigone, urethra and vesical arteries were prepared. The specimens used for morphological studies were fixed for 3–4 h in an ice-cold freshly prepared solution of 4% formaldehyde in phosphate buffered saline (PBS, pH 7.4) and then rinsed in 15% sucrose in PBS (for 2–3 days). The tissue pieces were frozen at −40°C in isopentane and stored at −70°C.

NADPH diaphorase histochemistry

Tissue demonstration of NADPH diaphorase activity was performed by incubating tissue sections with 1 mM β-NADPH and 0.5 mM nitro blue tetrazolium dissolved in 50 mM Tris/HCl buffer (pH 8.0) containing 0.2% Triton X-100 for 30–120 min at 37°C. After rinsing in PBS the sections were mounted in Kaiser's glycerol gelatin. In some sections β-NADPH was excluded, or exchanged for 1 mM α-NADPH or 1 mM β-NADP. Various other methods were also used to study the specificity of the β-NADPH diaphorase reaction. The heat-stability was checked by preincubating some sections at 77°C for 5 min. Other pretreatments included incubation with 0.1 mM N^G-nitro-L-arginine (L-NOARG) at room temperature for 40 min, 0.1 mM dicoumarol, or 1 and 5 mM L-canavanine for 60 min, or incubation with 1 mM 5,5'-dithio-*bis*(2-nitrobenzoic acid) (DTNB) for 90 min. All substances used for preincubation were also present during the NADPH diaphorase activity reaction, except DTNB, which was present only at the preincubation.

The NADPH diaphorase activity obtained by the various procedures was judged subjectively.

NOS immunohistochemistry

Tissue sections, cut at a thickness of 9 μm, were air-dried for 15 min and then incubated in PBS containing 0.2% Triton X-100 for 2 h. Incubation took place overnight at room temperature in an antiserum, raised in rabbits against a 15-amino acid C-terminal fragment of NOS, diluted 1:1280 (Alm *et al.*, 1993) in PBS containing 0.2% Triton X-100. After rinsing in PBS the sections were incubated with FITC, (diluted 1:80 in PBS) for 90 min, followed by rinsing in PBS. The sections were then mounted in buffered PBS/glycerol containing *p*-phenylenediamine to prevent fluorescence fading (Johnson & Araujo, 1981) and investigated in a fluorescence microscope. The immunoreactivity was documented by microphotography, after which the cover-slips were carefully detached from the slides and subsequently rinsed overnight in PBS. Tissue demonstration of NADPH diaphorase activity was then undertaken in the same section. As cross-reaction to other proteins sharing amino acid sequences with the synthesized products cannot be excluded, the immunoreactive products were referred to as NOS-like immunoreactive (NOS-IR). Details and characterization of the antiserum are described elsewhere (Alm *et al.*, 1993).

In control experiments, sections were incubated in the absence of the primary antiserum or with antiserum absorbed with the soluble, purified homogenate from rat cerebellum (Knowles *et al.*, 1989).

Functional studies

Recording of mechanical activity The preparations were transferred to 2.5 or 5 ml organ baths containing Krebs solution maintained at 37°C by a thermoregulated water circuit. The Krebs solution was bubbled with a mixture of 95% O_2 and 5% CO_2, maintaining pH at 7.4. The strips were mounted between two L-shaped hooks by means of silk ligatures. One of the hooks was connected to a Grass Instrument FT03C force-displacement transducer for registration of isometric tension and the other was attached to a movable unit. By varying the distance between the hooks the tension could be adjusted. The transducer output was recorded on a Grass Polygraph model 7D or E. During an equilibration period of 45–60 min, the preparations were stretched until a stable tension was obtained.

When subjected to electrical field stimulation (EFS), the preparations were mounted between two parallel platinum electrodes in the organ baths. Transmural stimulation of nerves was performed using a Grass S48 or S88 stimulator delivering single square wave pulses (duration 0.8 ms) at supramaximum voltage. The polarity of the electrodes was reversed after each pulse by means of a polarity-changing unit. The train duration was 5 s and the stimulation interval 120 s.

Tissue preparations and experimental procedures The preparations were investigated on the same day as the tissue was obtained, or stored for 24 h at 4°C in Krebs solution before investigation. There was no difference in the response to drugs between preparations investigated on the first day and those studied the day after.

Detrusor: Preparations (1 × 2 × 5 mm), stripped of mucosa, were prepared from the anterior wall of the detrusor. The tension of the preparations was adjusted during the equilibration period to a final level of 4–6 mN. After the equilibration period, each experiment was started by exposing the detrusor preparations to a K^+ (124 mM) Krebs solution (for composition, see below), until two reproducible contractions (difference $<10\%$) had been obtained. The following investigations were performed: (1) The supramaximum voltage was determined individually for the detrusor preparations at 20 Hz, then electrically-induced contractions were recorded at 10, 20 or 40 Hz. At least three consecutive reproducible contractions (difference $<10\%$) were required before the different drugs (L-arginine, D-arginine, L-NOARG, SIN-1, propranolol, isoprenaline or scopolamine) were added to the baths. (2) Concentration-response relations for carbachol (10 nM–0.1 mM) with or without preincubation with L-arginine (1 mM), L-NOARG (0.1 mM) or SIN-1 (0.1 mM). (3) Responses of L-arginine (1 mM) and SIN-1 (0.1 mM) in precontracted (carbachol 10 μM) muscle strips.

Urethra and trigone: Smooth muscle strips (1 × 2 × 5 mm), stripped of mucosa, were prepared from the trigone and urethra. The urethral strips were cut transversely from the proximal part of the urethra. The trigone strips were taken in an oblique direction from the internal urethral orifice towards one of the ureteric orifices. The tension of the urethral and trigonal strips was adjusted during the equilibration period to 4–8 mN. Trigonal strips were initially exposed to a K^+ (124 mM)-Krebs according to the procedure previously described for the detrusor. Responses to EFS in urethral and trigonal preparations were studied after precontraction of the strips, to a stable level, with noradrenaline (10 μM). First, the supramaximum voltage was determined individually for each strip at 8 Hz. This frequency has previously been shown to cause maximal relaxation of the pig urethra and trigone (Persson & Andersson, 1992). Thereafter, relaxant responses at 8 Hz were studied in the presence or absence of L-NOARG (10 μM) and TTX (1 μM). SIN-1 (0.1 mM) was added to the baths at the end of the experiment followed by determination of baseline level by changing the bath medium to a Ca^{2+} free solution.

Vesical arteries: Extramural arteries (inner diameter = 250–400 μm) supplying the detrusor were taken from the fascia adjacent to the lateral surface of the bladder, 2–4 cm before entering the bladder wall. The vessels were then dissected free from surrounding tissue under a microscope and cut into 1–2 mm long ring segments. After mounting, the vessels were stretched stepwise during the equilibration period to a stable tension of 2–4 mN. Each experiment was started by exposing the vessels to a K^+ (124 mM)-Krebs solution. At least two reproducible contractions (difference $<10\%$) were required before the experiments were begun: (1) The vessel segments were precontracted with a submaximal concentration of noradrenaline (50–80% of the initial K^+ (124 mM)-induced contraction). The noradrenaline concentration (0.5–6 μM) was chosen individually for each segment since this ensured that the precontracted level was the same, relative to K^+, in all experiments. Separate experiments, with different levels of noradrenaline-induced tension, showed that when the tension was higher than 80% of K^+, the relaxation to acetylcholine was impaired. (2) The presence of an intact endothelium was confirmed in each preparation by addition of acetylcholine (1 μM), and only vessels exhibiting $>80\%$ relaxation of the noradrenaline-induced tension were accepted for relaxation studies. (3) To study the endothelium-dependent relaxation, the endothelium was removed by allowing carbogen gas to flow through the lumen for 2–3 min. Loss of relaxant response to acetylcholine (1 μM) was considered to indicate endothelium removal. (4) The effects of L-NOARG (0.1 mM–0.3 mM) and indomethacin (1 μM) on acetylcholine-induced relaxations were examined by adding the drugs either during a noradrenaline-induced contraction or before the contraction. In all cases the drugs were in contact with the vessels over a period of at least 15 min before concentration-response curves for acetylcholine were constructed. (5) In some experiments the vessels were pretreated with phentolamine (1 μM) and indomethacin (1 μM) and contracted with 60 mM K^+ in the presence or absence of 0.3 mM L-NOARG. Concentration-response curves to acetylcholine or SIN-1 were then obtained. (6) Relaxant responses to exogenous NO (acidified $NaNO_2$ (pH 2), as described by Furchgott *et al.*, 1988) and SIN-1 were recorded in vessels without endothelium. Separate experiments showed that the vehicle (H_2O, pH 2), in equivalent volumes, had no relaxing effect *per se*.

Drugs and solutions

The following drugs were used: (−)-noradrenaline hydrochloride, carbamylcholine chloride, acetylcholine chloride, isoprenaline hydrochloride, nitro blue tetrazolium, propranolol hydrochloride, tetrodotoxin, scopolamine hydrochloride, N^G-nitro-L-arginine (L-NOARG), L-arginine hydrochloride, D-arginine hydrochloride, β-NADPH, tris(hydroxymethyl) aminomethane (Tris), 5,5′-dithio-*bis*-(2-nitrobenzoic acid) (DTNB), L-canavanine, dicoumarol, (Sigma Chemical Company, St Louis, MO, U.S.A.), indomethacin (Confortid, Dumex, Copenhagen, Denmark), phentolamine methane sulphonate (Ciba-Geigy, Basel, Switzerland), Triton X-100, *p*-phenylenediamine, Kaiser's glycerol gelatin, ethyleneglycol *bis* (β-aminoethylether)-N,N′-tetraacetic acid (EGTA) (Merck, Darmstadt, Germany), FITC (fluorescein isothiocyanate)-conjugated swine antirabbit immunoglobulins (Dakopatts, Stockholm, Sweden), SIN-1 (3-morpholino-sydnonimine hydrochloride) was a gift from Dr Kunstmann, Cassella AG, Germany. Stock solutions were prepared and then stored at − 70°C. Subsequent dilutions of the drugs were made with 0.9% NaCl, and when appropriate, 1 μM ascorbic acid was added as an antioxidant. The reported concentrations are the calculated final concentrations in the bath solution.

The Krebs solution used had the following composition (mM): NaCl 119, KCl 4.6, $CaCl_2$ 1.5, $MgCl_2$ 1.2, $NaHCO_3$ 15, NaH_2PO_4 1.2, glucose 11. K^+-Krebs solutions (60 and 124 mM) were prepared by replacing NaCl with equimolar amounts of KCl. Ca^{2+}-free medium was prepared by omitting Ca^{2+} from the normal Krebs solution and adding 0.1 mM EGTA.

Analysis of data

The relaxant effects of EFS and drugs were normalized and have been expressed as percentage reduction in tension. In urethral and trigonal strips, baseline level was defined as the tension reached after exposing the strips to Ca^{2+}-free medium. The effect of drugs on electrically induced detrusor contractions are expressed as percentage change of control contractions obtained before drug administration. The − log IC_{50} values (the negative logarithm of the drug concentration producing 50% of the maximum relaxation obtained) were determined graphically for each curve by linear interpolation. *P* values were determined by an unpaired Student's *t* test (two-tailed) corrected for multiple comparisons by Bonferroni's method, and considered significant if lower than 0.05. *n* denotes the number of preparations and *N* the number of animals. When the number of preparations and animals is the same, only *n* is given. Results are given as mean values ± s.e.mean.

Results

NADPH diaphorase histochemistry

NADPH diaphorase positive varicose nerve fibres of various thickness, and coarse nerve branches, were found in and/or around muscular bundles in the detrusor, trigone and urethra (Figure 1). In general, the nerve fibres in the trigone and urethra were much thinner and more dispersed within the muscular tissue than in the detrusor. In the outer parts of the smooth musculature and the surrounding connective tissue, some NADPH diaphorase positive nerve cells in ganglionic structures could be seen. In the urothelium of all tissues, the NADPH diaphorase reaction was found to be particularly strong. Frequently, NADPH diaphorase positive nerve fibres could be seen around arteries, but only rarely around veins. A positive NADPH diaphorase reaction was found in the endothelium of some arteries. Arteries that displayed a positive endothelial and/or perivascular NADPH diaphorase activity were often seen in the lamina propria and in the outer parts of the smooth musculature. No NADPH diaphorase activity was seen in the endothelium of veins. In segments of the extramural vesical artery, located in the fascia adjacent to the lateral surface of the detrusor, NADPH diaphorase positive staining was found in thin nerve fibres surrounding the vessels and in the endothelium.

In the detrusor and trigone, the specificity of the NADPH

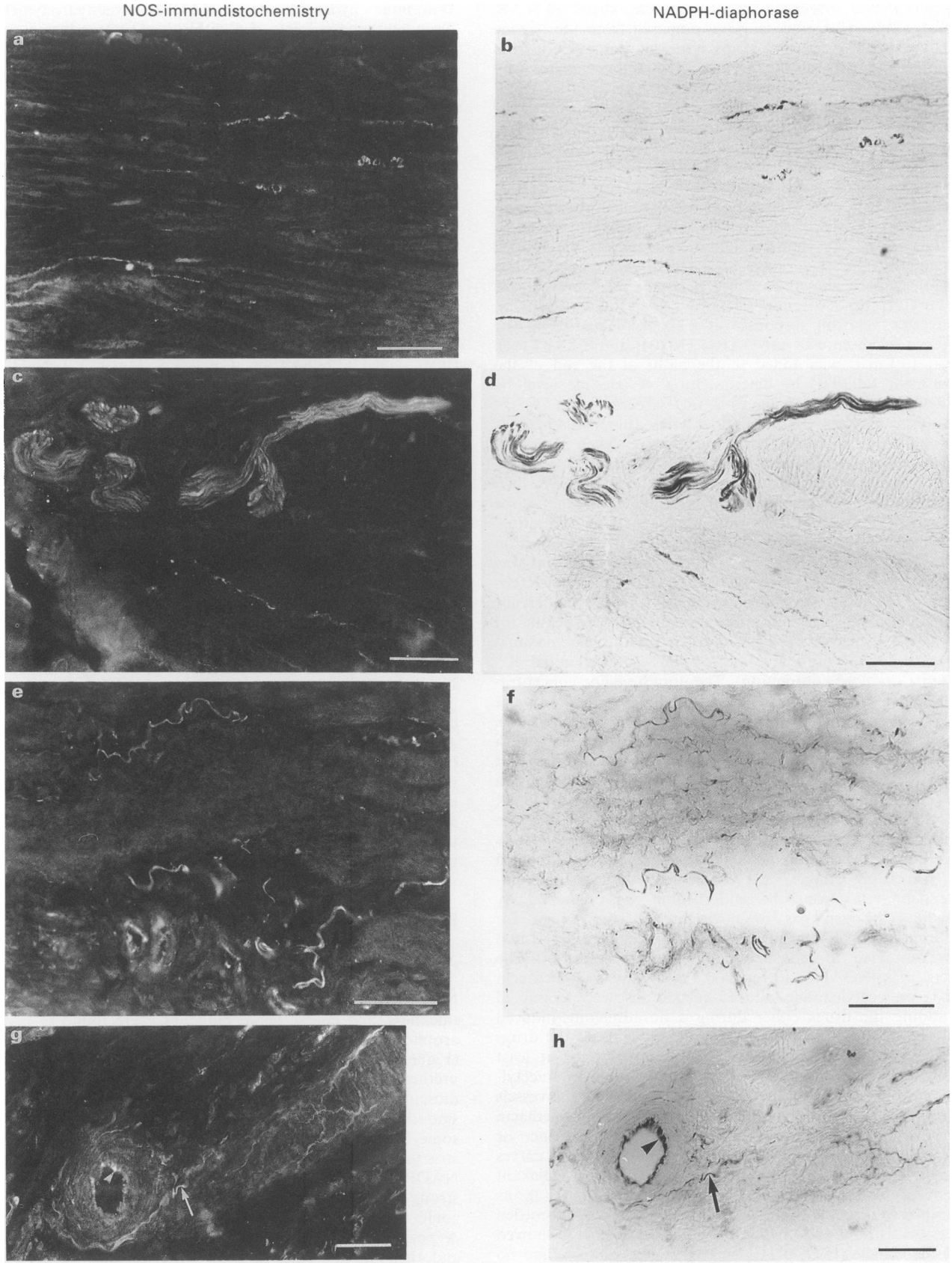

Figure 1 Microphotographs showing the distribution and colocalization of nitric oxide synthase (NOS)-like immunoreactivity and NADPH diaphorase activity in tissue sections of the pig lower urinary tract. The sections were processed for NOS immunohistochemistry (a, c, e, g) and subsequently for NADPH diaphorase (b, d, f, h). (a–d) Immunohistochemical localization of NOS, showing thin nerve fibres (a) and coarse nerve trunks (c) in the smooth muscle layer of the detrusor. Almost identical staining was observed using the NADPH diaphorase technique (b, d). (e, f) Sections of urethral tissue showing thin NOS-immunolabelled nerve fibres dispersed within the smooth muscle layer (e). Almost all NOS-immunolabelled nerve fibres were also stained for NADPH diaphorase (f). (g, h) Intramural vessel in the trigone area surrounded by numerous NOS-immunoreactive (g) and NADPH diaphorase positive (h) nerve fibres (arrows). The endothelium of the vessel (arrowheads) is strongly positive for NADPH diaphorase activity, while inconsistent staining is demonstrated by immunohistochemistry. (Scale bar = 50 μm).

diaphorase reaction was studied by various procedures. The neuronal and endothelial NADPH diaphorase reaction was abolished, or virtually abolished, by heat and DTNB, or if β-NADPH was excluded or substituted with α-NADPH. When β-NADP was used instead of β-NADPH, nearly all structures in the tissue reacted strongly and nerves could not be separated from other structures in the tissue. L-NOARG, dicoumarol, and L-canavanine were essentially without effect on the NADPH diaphorase reaction. A NADPH diaphorase reaction in the urothelium could still be observed if β-NADPH was substituted with α-NADPH or in the presence of L-canavanine, dicoumarol or L-NOARG, or if the sections were pretreated with DTNB.

NOS immunohistochemistry

NOS-IR nerve fibres in the pig lower urinary tract were mainly distributed in the smooth muscle layers of the detrusor, trigone and urethra regions (Figure 1). A gradient in the density of immunolabelled fibres was discernible, showing the highest density of NOS-IR fibres in the urethra and the lowest in the detrusor. The NOS antiserum labelled different types of neuronal structures, ranging from coarse trunks to delicate fibres, throughout all regions. Coarse nerve trunks with NOS-IR fibres were observed mainly in the adventitia but also in the muscle layers. Finer nerve trunks consisting of NOS-IR fibres were observed in the connective tissue between the smooth muscle bundles. In addition, delicate immunolabelled fibres coursed along and dispersed within the smooth muscle bundles. Thin NOS-IR fibres could be found in the lamina propria of all regions, mostly in the vicinity of vessels. However, no immunolabelling could be observed in the urothelium.

The NOS antiserum labelled vessels localized in the lamina propria, intramurally and close to the adventitia in all regions. Labelling occurred in the endothelial lining of vessels in the lamina propria, and in perivascular varicose fibres innervating them. Likewise, intramural vessels in all regions were surrounded by thin NOS-IR nerves, that formed plexi around the vessels. NOS-IR labelling also seemed to be confined to the endothelial lining of some intramural vessels, but vessels without both NOS-IR perivascular labelling and endothelium staining were observed. Perivascular fibres around the extramural vesical artery displayed NOS-IR labelling. Thin, delicate fibres as well as nerve trunks were present in the tunica adventitia and occasionally the former penetrated superficially in the tunica media. The endothelium was also stained.

In sections where the antiserum was absorbed with antigen extracted from rat cerebellum, immunoreactivity of neuronal structures was abolished. However, immunoreactivity was still observed in the endothelium of vessels. No staining of neuronal structures or endothelium was found when the primary antiserum was omitted.

Correlation between NADPH diaphorase staining and NOS immunoreactivity

NADPH diaphorase staining in the lower urinary tract showed both similarities and differences with the NOS immunohistochemistry. Thus, the distribution of fibres in the smooth musculature obtained with the NADPH-diaphorase technique was almost identical to that revealed with NOS immunohistochemistry (Figure 1). However, the fibres were sometimes better visualized with the NOS antiserum than after NADPH diaphorase staining. In addition, the gradient with highest density of stained fibres in the urethra was also revealed with the NADPH-diaphorase staining. In contrast to the NADPH diaphorase technique, no labelling was observed in the urothelium with NOS immunohistochemistry. Moreover, the endothelium of vessels was more frequently stained using the NADPH diaphorase technique than immunohistochemistry (Figure 1g, h).

Functional studies

Detrusor EFS of pig detrusor strips at 10, 20 and 40 Hz produced phasic contractions. Separate experiments showed that these frequencies corresponded to approximately 30, 70 and 100% of the maximal response induced by EFS. Detrusor preparations were treated with L-NOARG (1 μM–0.1 mM), added cumulatively to the bath, and the contractile response to EFS at 10, 20 and 40 Hz studied. L-NOARG (10 μM) increased the contractions by a maximum of 12 ± 2% at 10 Hz, 12 ± 5% at 20 Hz, and 3 ± 4% at 40 Hz ($n = 6$ for all; data not shown). Compared to time-matched control preparations, running in parallel, these increases were not statistically significant.

In the presence of L-arginine (1 mM), contractions induced by EFS at 10, 20 and 40 Hz were reduced by 28 ± 3%, 30 ± 2%, and 25 ± 4% ($n = 6$ for all), respectively (Figure 2). This action of L-arginine was inhibited ($P < 0.01$) by 0.1 mM L-NOARG (Figure 2). D-Arginine (1 mM; $n = 4$) was without effect on EFS-induced detrusor contractions (Figure 3). Propranolol (1 μM) had no effect *per se*, and did not affect the L-arginine-induced decrease in contractile response (26 ± 2% at 20 Hz; $n = 6$ after propranolol pretreatment; Figure 3). On the other hand, in the presence of scopolamine (1 μM), L-arginine had no effect ($n = 6$) on electrically evoked (20 Hz) detrusor contractions (Figure 3). The scopolamine- and L-arginine resistant part of the contraction amounted to 12 ± 4% ($n = 6$). The NO-donor SIN-1 (1 μM–0.3 mM) had only minor effects on electrically evoked (20 Hz) detrusor contractions (8 ± 3% reduction at 0.1 mM, $n = 5$). Isoprenaline (1 nM–10 μM) caused concentration-dependent inhibition of the EFS-induced detrusor contractions (20 Hz), that amounted to 52 ± 11% ($n = 5$) at 10 μM.

Concentration-response curves to carbachol (10 nM–0.1 mM) were unaffected by pretreatment with L-arginine (1 mM, $n = 5$), L-NOARG (0.1 mM; $n = 4$) or SIN-1 (0.1 mM; $n = 5$). L-Arginine (1 mM) had no influence on tension when applied to preparations precontracted by carbachol (10 μM; $n = 6$), whereas SIN-1 (0.1 mM) in the same protocol reduced the tension by 40 ± 5% ($n = 6$; data not shown).

Urethra and trigone EFS of urethral and trigonal strips at 8 Hz produced pure relaxant responses. All responses were practically abolished by TTX (1 μM), verifying that they were nerve-mediated (Figure 4a). The relaxations amounted to 47 ± 5% ($n = 7$, $N = 4$) and 49 ± 6% ($n = 8$, $N = 5$), for urethral and trigonal preparations, respectively. Addition of L-NOARG (10 μM) to urethral and trigonal preparations

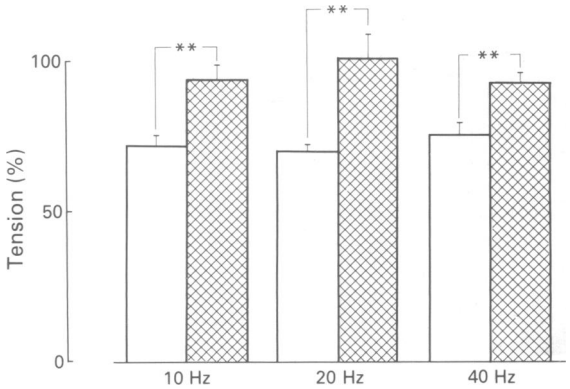

Figure 2 Effect of L-arginine on contractions induced by electrical field stimulation at 10, 20 and 40 Hz in pig isolated detrusor smooth muscle preparations. Open columns indicate the response to L-arginine (1 mM) and cross-hatched columns the response to L-arginine after pretreatment with N^G-nitro-L-arginine (L-NOARG, 0.1 mM). Results are expressed as a percentage of the contractions before drug treatment and given as mean ± s.e.mean ($n = 6$). $^{**}P < 0.01$.

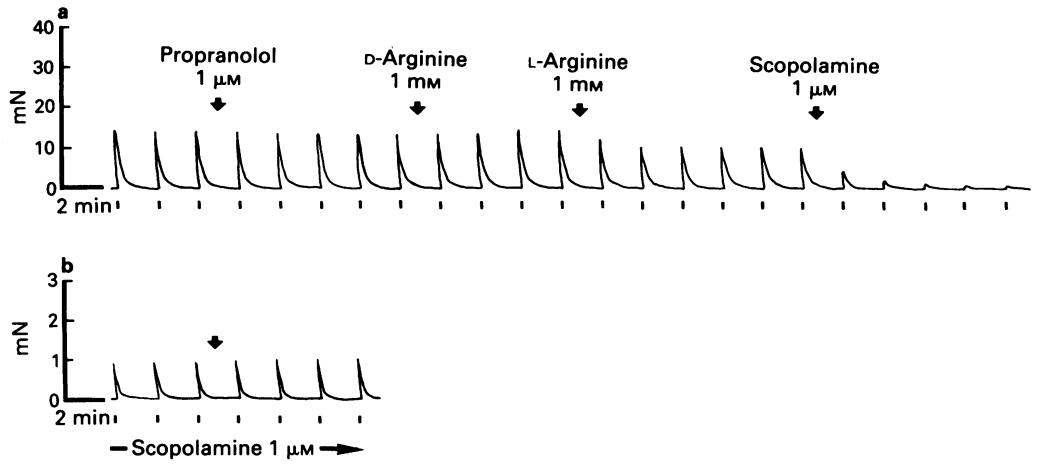

Figure 3 Recordings of contractions evoked by electrical field stimulation at 20 Hz in pig isolated detrusor smooth muscle preparations. In (a) is shown the effect of L-arginine (1 mM) and in (b) the lack of effect in the presence of scopolamine (1 μM). Bars indicate time of stimulation (supramaximum voltage, 0.8 ms pulses, 5 s train duration).

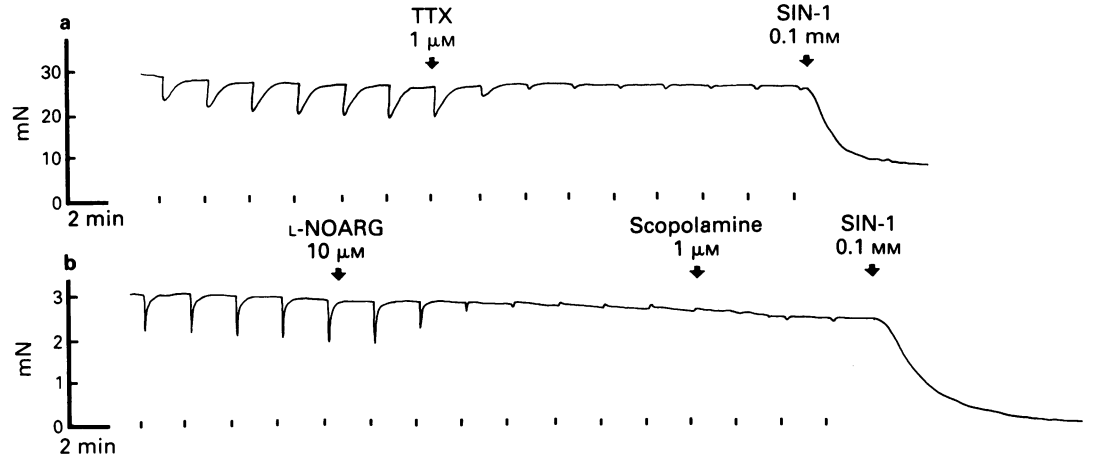

Figure 4 Recordings of relaxations evoked by electrical field stimulation at 8 Hz in (a) the pig isolated trigone and (b) the pig isolated urethra demonstrating the response to tetrodotoxin (TTX; 1 μM) and N^G-nitro-L-arginine (L-NOARG, 10 μM) in noradrenaline-contracted preparations. The NO-donor 3-morpholino-sydnonimine (SIN-1, 0.1 mM) was applied at the end of the experiment. Baseline level was defined as the level reached after exposing the strips to Ca^{2+}-free solution. Bars indicate time of stimulation (supramaximum voltage, 0.8 ms pulses, 5 s train duration).

stimulated by EFS resulted in a marked decrease in the relaxant response with time. Maximal inhibition was reached within 10–15 min and in some preparations the response changed into a contraction (Figure 4b). Scopolamine (1 μM) reversed these contractions to a weak relaxation (Figure 4b). SIN-1 (0.1 mM) produced pronounced relaxations of both urethral (88 ± 2%, $n = 7$, $N = 4$) and trigonal strips (84 ± 3%, $n = 8$, $N = 5$) (Figure 4).

Vesical arteries Acetylcholine (1 nM–10 μM) caused concentration-dependent relaxations of noradrenaline-induced contractions in pig vesical arteries. A maximum relaxation of 97 ± 1% ($n = 16$) was obtained with acetylcholine 10 μM, and the $-\log IC_{50}$ value was 7.1 ± 0.1. The maximum relaxation (93 ± 3%, $n = 6$) and the $-\log IC_{50}$ value (7.1 ± 0.1) were not affected by preincubation with indomethacin (1 μM) (Figure 5). Removal of the endothelium practically abolished the acetylcholine-induced relaxation, since maximum relaxation was reduced to 4.7 ± 1.9% ($n = 8$, $P < 0.001$) (Figure 5). Pretreatment with L-NOARG (0.1 mM and 0.3 mM) caused a rightward shift of the concentration-response curves, but $-\log IC_{50}$ values were not calculated since no defined maxima were obtained. The maximal relaxations obtained amounted to 88 ± 6% ($n = 6$) and 65 ± 12% ($n = 6$, $P <$ 0.05) of the noradrenaline-induced contraction after pretreatment with L-NOARG, 0.1 mM and 0.3 mM, respectively (Figure 5).

In vessel segments contracted with 60 mM K^+ (contraction level: 54 ± 4%, $n = 10$, $N = 5$, of the initial K^+ 124 mM response), acetylcholine induced concentration-dependent relaxations (Figure 6). The relaxation obtained at 10 μM amounted to 65 ± 9% in K^+ (60 mM)-contracted vessels (compared to 97 ± 1% in noradrenaline-contracted vessels). When the vessels were incubated with 0.3 mM L-NOARG and then contracted with K^+ 60 mM (contraction level: 100 ± 2%, $n = 10$, $N = 5$ of the initial K^+ 124 mM response) all relaxant responses to acetylcholine were abolished (Figure 6). In contrast, SIN-1 produced relaxations of K^+ 60 mM contracted vessels both in the absence and presence of L-NOARG (data not shown). In arteries where the tension was raised with K^+ (124 mM), acetylcholine (1 μM) reduced the tension by 24 ± 2% ($n = 6$).

Addition of L-NOARG (0.1 mM) to vessel segments at baseline caused a small, approximately 3–4%, increase in tension. On the other hand, if L-NOARG (0.1 mM) was applied on top of a noradrenaline-induced contraction, it resulted in a pronounced increase in tension (26 ± 4%, $n = 12$). No increase in tension was seen when L-NOARG

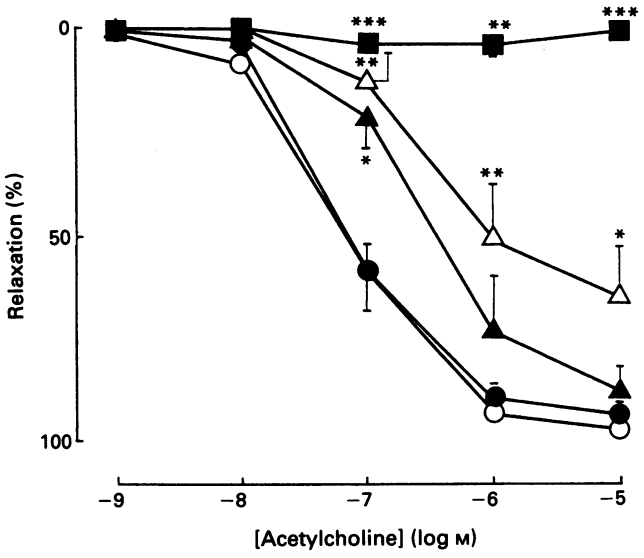

Figure 5 Relaxation of pig isolated vesical arteries induced by acetylcholine in controls (○) or in the presence of 1 μM indomethacin (●), 0.1 mM N^G-nitro-L-arginine (L-NOARG, ▲), 0.3 mM L-NOARG (△) or in vessels without endothelium (■). Results are expressed as percentage relaxation of the noradrenaline-induced tension and given as mean ± s.e.mean ($n = 6-16$). $*P<0.05$; $**P<0.01$; $***P<0.001$.

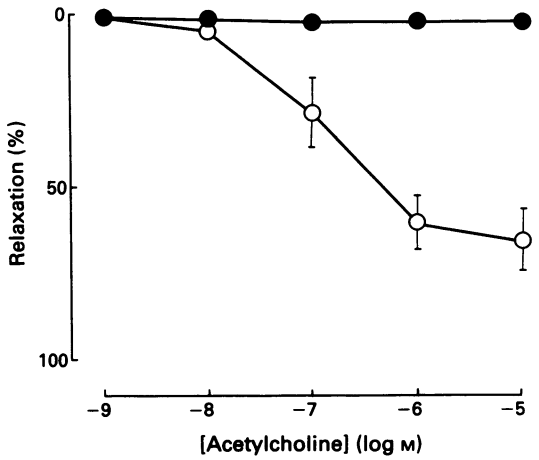

Figure 6 Relaxation of pig isolated vesical arteries induced by acetylcholine in K^+ (60 mM)-contracted preparations in the absence (○) or presence of N^G-nitro-L-arginine (L-NOARG, 0.3 mM) (●). The vessels were pretreated with phentolamine (1 μM) and indomethacin (1 μM) for 30 min. Results are expressed as percentage relaxation of the K^+ (60 mM)-induced tension and given as mean ± s.e.mean ($n = 5$).

(0.1 mM) was administered to vessels without endothelium ($n = 7$).

Noradrenaline-contracted pig vesical arteries without endothelium responded to increasing concentrations of SIN-1 and NO (present in acidified solution of $NaNO_2$) with concentration-dependent relaxations. SIN-1 (10 μM) relaxed the vessels by 96 ± 3% ($n = 6$) and NO (1 mM) by 97 ± 2% ($n = 6$; data not shown).

Discussion

The present study demonstrates that NOS-IR and NADPH diaphorase activity are expressed in nerve trunks and fine nerve fibres throughout the pig lower urinary tract. NOS-IR and NADPH diaphorase staining were present in neuronal structures both within and/or around smooth muscle bundles in the detrusor, trigone and urethra. Thin nerve fibres that dispersed within the muscle bundles were mainly found in the urethral/trigonal area, whereas such fibres were less common in the detrusor area. In previous studies, the involvement of NO as an inhibitory NANC-transmitter has been based mainly on the fact that relaxant responses to EFS of nerves in the urethra, bladder neck and trigone were inhibited by NOS-inhibitors and that exogenous NO mimicked the response to NANC-nerve stimulation (Garcia-Pascual *et al.*, 1991; Dokita *et al.*, 1991; Andersson *et al.*, 1991; 1992; Persson & Andersson, 1992; Persson *et al.*, 1992; Thornbury *et al.*, 1992). Furthermore, relaxations of the rabbit urethra in response to sodium nitroprusside (Morita *et al.*, 1992) and electrical stimulation (Persson & Andersson, 1993) seem to be associated with increases in smooth muscle content of cyclic GMP. Measurement of NOS activity in the rat urogenital tract, by monitoring the conversion of [^{3}H]-arginine to [^{3}H]-citrulline, revealed a high catalytic activity in the bladder neck and urethra (Burnett *et al.*, 1992). By localization of the enzyme involved in the synthesis of NO, morphological evidence for the assumption that NO may act as a neurotransmitter in the lower urinary tract now exists, strengthening the hypothesis of a role for NO in this tissue. The morphological findings in the present study, demonstrating that the detrusor region expresses a low density of thin NOS-IR/NADPH diaphorase stained fibres compared to the outlet region, are consistent with previous functional findings that NO may serve as a NANC inhibitory neurotransmitter mainly in the outlet region (Persson & Andersson, 1992; Persson *et al.*, 1992).

The observation that NADPH diaphorase histochemistry can be used to identify neuronal NOS (Hope *et al.*, 1991; Dawson *et al.*, 1991) has resulted in several reports about the distribution of NADPH diaphorase positive nerves in peripheral tissues, including the lower urinary tract (Larsson *et al.*, 1992; Keast, 1992; McNeill *et al.*, 1992; Grozdanovic *et al.*, 1992). In the rat urinary tract, NADPH diaphorase positive staining was observed in the urethra, close to the urothelium (Keast, 1992) and in the bladder base (McNeill *et al.*, 1992). Conflicting results have been reported concerning the NADPH diaphorase staining of the detrusor of different species. No staining could be identified in the rat detrusor by Keast (1992), but McNeill *et al.* (1992) and Grozdanovic *et al.* (1992) found staining in the rat and mouse detrusor, respectively.

In this and a previous study (Larsson *et al.*, 1992), the specificity of the NADPH diaphorase staining in the pig lower urinary tract was examined. L-NOARG, in a concentration sufficient to inhibit the enzyme functionally, caused no reduction in NADPH diaphorase staining. This suggests that the portion of the NOS enzyme that yields the NADPH diaphorase staining is not identical to, and does not interact with, the site of NO production. The marked increase in staining using β-NADP most probably reflects non-specific staining by other enzymes with diaphorase activity (Hope & Vincent, 1989). Dicoumarol, reported to inhibit some non-specific diaphorase staining (Ernster *et al.*, 1962), and L-canavanine, known to inhibit the inducible form of NOS (Iyengar *et al.*, 1987), were without effect on the NADPH diaphorase reaction found in this study. However, DTNB and α-NADPH abolished the NADPH diaphorase activity in nerves and in the endothelium, but not in the urothelium. Thus, the neuronal and endothelial NADPH diaphorase activity, suggested to indicate NOS (Dawson *et al.*, 1991; Hope *et al.*, 1991), exhibited characteristics different from the activity found in the urothelium.

Immunohistochemistry and NADPH-diaphorase histochemistry performed on the same preparations in the pig lower urinary tract, revealed an extensive colocalization of the two markers in all regions. However, the urothelium of all regions was intensively stained by the NADPH dia-

phorase technique, whereas no immunolabelling of the urothelium could be observed. The reason for this may be, as discussed above, that the NADPH diaphorase technique stains additional enzymes besides NOS, or that NADPH diaphorase staining of the urothelium represents an isoform of NOS not readily detectable with our antiserum The antiserum used in this study, raised against a fragment of the rat cerebellar NOS, has been shown to be selective for neuronal compared to endothelial NOS in rat tissue (Alm *et al.*, 1993). This was not the case with antisera raised against the whole enzyme (Bredt *et al.*, 1990; Schmidt *et al.*, 1992). In tissues from pig lower urinary tract, the present antiserum stained besides neuronal structures, also the endothelium of some vessels. Thus, it seems that our rat neuronal NOS antiserum recognizes a protein in the pig endothelium that is similar, but not identical to the neuronal one; possibly endothelial NOS.

Activation of inhibitory nerves to the detrusor might be one factor, behind the largely unknown mechanism, by which the detrusor muscle relaxes to promote urine storage (e.g. De Groat & Kawatani, 1985). In the stomach, NO has been suggested to have a function as a mediator of adaptive relaxation to accommodate food and fluid (Desai *et al.*, 1991). Likewise, a neurogenic inhibition involving NO release would theoretically be a possible factor for bladder relaxation during filling. However, a role for NO in detrusor relaxation has been questioned (Persson & Andersson, 1992; Persson *et al.*, 1992), due to difficulties in demonstrating relaxant responses upon nerve stimulation, and because the potency of NO-related agonists was low in the detrusor. In the present study, NOS-IR nerves were demonstrated in the pig detrusor muscle, although not as pronounced as in the outlet region, which indeed suggests that NO is present in neuronal structures in the detrusor. Even if NO does not seem to act as a neurotransmitter causing direct smooth muscle relaxation of the detrusor smooth muscle, it is possible that the L-arginine/NO system modulates the bladder tone by other mechanisms. L-Arginine was found to be without postjunctional effects on the detrusor muscle, but caused a small inhibition of the electrically evoked detrusor contractions that was reversed by L-NOARG. This may be explained by L-arginine stimulating neuronal NOS to yield an increased NO production. NO production, in turn, may be initiated by contractile activation. However, the NO production in the absence of exogenous L-arginine was apparently not sufficient to depress significantly the electrically induced contractions.

L-Arginine had no effect after muscarinic receptor blockade, indicating that the effect of L-arginine was restricted to cholinergic neurotransmission. Thus, available information suggests that the effect of L-arginine on the cholinergic neurotransmission in the pig detrusor may be due to either functional antagonism at the smooth muscle level, or to prejunctional inhibition of acetylcholine release. It has been suggested that the L-arginine/NO pathway affects cholinergic neurotransmission in guinea-pig trachea at the level of the smooth muscle or via a pre-junctional inhibition of acetylcholine release (Belvisi *et al.*, 1991). However, recent studies found no evidence for an affect on acetylcholine release either in guinea-pig trachea or human airway smooth muscle (Brave *et al.*, 1991; Ward *et al.*, 1992a), suggesting that functional antagonism accounts for the inhibitory action of NO rather than attenuation of transmitter release. However, it cannot be excluded that L-arginine *per se* and/or NO caused a release of an unknown substance, which in turn modulated the cholinergic response.

Smooth muscle cells have been suggested as a possible source of NO formation in the human detrusor muscle (James *et al.*, 1991) as well as in the gastrointestinal tract (Grider *et al.*, 1992). An inducible form of NOS has been demonstrated in vascular smooth muscle cells (Rees *et al.*, 1990) but the physiological relevance of an inducible enzyme, involved in immunological responses, for normal detrusor relaxation seems limited. On the other hand, if smooth muscle cells express a constitutive form of NOS it must be different from the neuronal and endothelial NOS since in this study no labelling of the musculature could be detected with markers for the constitutive enzyme.

Interestingly, retrograde axonal tracing has recently been performed to examine the origin of NADPH diaphorase positive nerves in the rat bladder (McNeill *et al.*, 1992). Numerous NADPH diaphorase positive nerves were present in the major pelvic ganglia and the (T_{13}–L_2, L_6 and S_1) dorsal root ganglia, but not in the inferior mesenteric ganglia. This indicates that if NO contributes to the function in the detrusor, it is most likely through the parasympathetic and/or sensory nervous system. Colocalization studies of NOS, choline acetyltransferase and various peptides are currently being carried out, and may help to elucidate whether some portion of the peripheral nervous system in the lower urinary tract uses NO as a cotransmitter.

Urodynamic studies have revealed a decrease in urethral pressure, in normal micturition, 5–15 s before the detrusor contracts (Scott *et al.*, 1964; Tanagho & Miller, 1970; Low, 1977). Whether this reflects an involvement of a NANC-transmitter reducing the urethral tone is not known. Several histological studies (e.g. Gu *et al.*, 1984; Crowe & Burnstock, 1989) have demonstrated a rich occurrence of NANC-nerves in the bladder outlet region, in support of activation of NANC-inhibitory nerves as a possible mechanism for urethral relaxation. In the present study, histological evidence was provided that nerves coursing through the smooth muscle bundles in the pig urethra and trigone contained the enzyme producing the inhibitory substance NO. In addition, the fact that transient relaxant responses induced by electrical stimulation of pig urethral and trigonal preparations were practically abolished by inhibition of NOS, suggests that NO might have a functional role in urethral relaxation. However, NANC-relaxations evoked at high frequencies in the dog urethra do not seem to be mediated by NO (Hashimoto *et al.*, 1993), implying that at least two neurogenic responses are involved in dog urethral relaxation.

In the unanaesthetized rat, intra-arterial administration of a NOS-inhibitor caused bladder hyperactivity and decreased bladder capacity (Persson *et al.*, 1992). The mechanisms behind bladder hyperactivity are not known, but changes in afferent and/or efferent activity due to lack of inhibitory substances in either the detrusor or the outlet region might be one possible mechanism (Gu *et al.*, 1983; Chapple *et al.*, 1992). Since the NO innervation was found to be particularly well developed in the outlet region, it seems reasonable to assume that the observed bladder hyperactivity evoked by inhibition of NOS, was caused by functional disturbance in this region. In agreement with this, it has been suggested that bladder hyperactivity may be initiated from the bladder outlet region, rather than from the detrusor muscle itself (Hindmarsh *et al.*, 1983; Low *et al.*, 1989). In the present study, L-arginine was found to have an inhibitory effect on the cholinergic neurotransmission in the pig detrusor. This was not found in the rat detrusor (Persson *et al.*, 1992). Despite this, it cannot be excluded that the bladder hyperactivity observed in the rat was due to a lack of inhibitory mechanisms modulating the efferent neurotransmission in the detrusor.

The majority of the vessels throughout the pig detrusor, trigone and urethra were supplied by fine plexus of NOS-IR fibres. Moreover, labelling of the endothelium was seen in some, although not all vessels. It is known that acetylcholine produces relaxations of vessels entirely dependent on the presence of endothelium (Furchgott & Zawadzki, 1980) by release of an endothelium-derived relaxing factor (EDRF) identified as NO (Palmer *et al.*, 1987). The endothelium-dependent acetylcholine-induced relaxation of the pig vesical artery was only partially inhibited by the NOS-inhibitor, L-NOARG. This indicates that NO, provided that the NO formation is completely blocked by L-NOARG, is not the only endothelium-derived factor activated in response to

acetylcholine. Indomethacin had no effect on the relaxation, excluding contribution of a cyclo-oxygenase product. Vascular smooth muscle cells are able to relax upon hyperpolarization and an endothelium-derived hyperpolarizing factor (EDHF) has been postulated (e.g. Taylor & Weston, 1988). If the L-NOARG-resistant, acetylcholine-induced relaxation of the pig vesical artery is mediated by EDHF, an inhibition would be expected if the vessels are pretreated with L-NOARG and contracted with a potassium solution high enough to counteract the effect of EDHF (Nagao & Vanhoutte, 1992). This was also found and indicates that the overall relaxant response to acetylcholine in the pig vesical artery is determined by a combined effect of NO release and possible activation of a hyperpolarizing factor. It was further shown that L-NOARG, in endothelium-intact preparations, caused a marked increase in tension of preconstricted vessels. This was not found in vessels at resting level, suggesting that in vessel segments maintained under active tone, NO generation occurs continuously.

Neuronally-mediated vasorelaxations in e.g. bovine penile artery (Liu *et al.*, 1991) and dog, bovine and monkey cerebral arteries (Toda & Okamura, 1990; Gonzalez & Estrada, 1991) have been reported to be blocked by NOS-inhibitors. In preliminary experiments, long-lasting relaxations evoked by EFS were recorded in the pig vesical artery. However, the responses were unaffected by tetrodotoxin (TTX) and L-NOARG, which raises questions about the origin of the relaxations.

The physiological role of neuronal and endothelial NO-mediated vasodilatation in the bladder can only be speculated upon. The urinary bladder wall frequently undergoes changes in wall tension during filling, which may be sufficient to affect the blood flow. If the blood flow decreases during filling of the bladder (Dunn, 1974; Siroky *et al.*, 1990) an activation of vasodilator mechanisms has to take place in order to supply oxygen to the detrusor muscle. There is evidence from e.g. the guinea-pig coronary vasculature (Park *et al.*, 1992) and rabbit pulmonary circulation (Persson *et al.*, 1990) that hypoxia stimulates the release of NO. This may be the case also in bladder vessels.

In conclusion, the data obtained by immunohistochemistry and NADPH diaphorase staining suggest that NOS is localized in nerve fibres throughout the pig lower urinary tract and predominantly in the outflow region. This is consistent with functional data showing NANC nerve-mediated relaxation, involving the L-arginine/NO pathway, in trigonal and urethral smooth muscle preparations. In the detrusor, the presence of NO-synthesizing enzymes in nerves can be demonstrated, but its functional importance is unclear. NO, as well as other endothelium-derived factors seems to be involved in the endothelium-dependent acetylcholine-induced relaxation of pig vesical arteries.

This work was supported by the Swedish Medical Research Council (grant no 6837) and by the Medical Faculty, University of Lund, Sweden.

References

ALM, P., LARSSON, B., EKBLAD, E., SUNDLER, F. & ANDERSSON, K.-E. (1993). Immunohistochemical localization of peripheral nitric oxide synthase containing-nerves using antibodies raised against synthesized C- and N-terminal fragments of a cloned enzyme from rat brain. *Acta Physiol. Scand.*, (in press).

ANDERSSON, K.-E., GARCIA PASCUAL, A., FORMAN, A. & TØTTRUP, A. (1991). Non-adrenergic, non-cholinergic nerve-mediated relaxation of rabbit urethra is caused by nitric oxide. *Acta Physiol. Scand.*, **141**, 133–134.

ANDERSSON, K.-E., GARCIA PASCUAL, A., PERSSON, K., FORMAN, A. & TØTTRUP, A. (1992). Electrically-induced, nerve-mediated relaxation of rabbit urethra involves nitric oxide. *J. Urol.*, **147**, 253–259.

BELVISI, M.G., STRETTON, D. & BARNES, P.J. (1991). Nitric oxide as an endogenous modulator of cholinergic neurotransmission in guinea-pig airways. *Eur. J. Pharmacol.*, **198**, 219–221.

BRAVE, S.R., HOBBS, A.J., GIBSON, A. & TUCKER, J.F. (1991). The influence of L-N^G-nitroarginine on field stimulation induced contractions and acetylcholine release in guinea-pig isolated tracheal smooth muscle. *Biochem. Biophys. Res. Commun.*, **179**, 1017–1022.

BREDT, D.S., HWANG, P.M., GLATT, C., LOWENSTEIN, C. & SNYDER, S.H. (1991). Cloned and expressed nitric oxide synthase structurally resembles cytochrome P-450 reductase. *Nature*, **351**, 714–718.

BREDT, D.S., HWANG, P.M. & SNYDER, S.H. (1990). Localization of nitric oxide synthase indicating a neural role for nitric oxide. *Nature*, **347**, 768–770.

BURNETT, A.L., LOWENSTEIN, C.J., BREDT, D.S., CHANG, T.S.K. & SNYDER, S.H. (1992). Nitric oxide: a physiologic mediator of penile erection. *Science*, **257**, 401–403.

CHAPPLE, C.R., MILNER, P., MOSS, H.E. & BURNSTOCK, G. (1992). Loss of sensory neuropeptides in the obstructed human bladder. *Br. J. Urol.*, **70**, 373–381.

CROWE, R. & BURNSTOCK, G. (1989). A histochemical and immunohistochemical study of the autonomic innervation of the lower urinary tract of the female pig. Is the pig a good model for the human bladder and urethra? *J. Urol.*, **141**, 414–422.

DAWSON, T.M., BREDT, D.S., FOTUHI, M., HWANG, P.M. & SNYDER, S.H. (1991) Nitric oxide synthase and neuronal NADPH diaphorase are identical in brain and peripheral tissues. *Proc. Natl. Acad. Sci. U.S.A.*, **88**, 7797–7801.

DE GROAT, W.C. & KAWATANI, M. (1985). Neural control of the urinary bladder: possible relationship between peptidergic inhibitory mechanisms and detrusor instability. *Neurourol. Urodyn.*, **4**, 285–300.

DESAI, K.M., SESSA, W.C. & VANE, J.R. (1991). Involvement of nitric oxide in the reflex relaxation of the stomach to accommodate food or fluid. *Nature*, **351**, 477–479.

DOKITA, S., MORGAN, W.R., WHEELER, M.A., YOSHIDA, M., LATIFPOUR, J. & WEISS, R.M. (1991). N^G-nitro-L-arginine inhibits non-adrenergic, non-cholinergic relaxation in rabbit urethral smooth muscle. *Life Sci.*, **48**, 2429–2436.

DUNN, M. (1974). A study of the bladder blood flow during distension in rabbits. *Br. J. Urol.*, **46**, 67–72.

ERNSTER, L., DANIELSON, L. & LJUNGGREN, M. (1962). DT-diaphorase. Purification from the soluble fraction of rat liver cytoplasm and properties. *Biochim. Biophys. Acta*, **58**, 171–200.

FURCHGOTT, R.F. & ZAWADZKI, J.V. (1980). The obligatory role of endothelial cells in the relaxation of arterial smooth muscle by acetylcholine. *Nature*, **288**, 373–376.

FURCHGOTT, R.F., KHAN, M.T., JOTHIANANDAN, D. & KHAN, A.S. (1988). Evidence that the endothelium-derived relaxing factor of rabbit aorta is nitric oxide. In *Vascular Neuroeffector Mechanisms*. ed. Bevan, J.A., Majewski, H., Maxwell, R.A. & Story, D.F. pp. 77–84. Oxford: IRL Press.

GARCIA-PASCUAL, A., COSTA, G., GARCIA-SACRISTAN, A. & ANDERSSON, K.-E. (1991). Relaxation of sheep urethral muscle induced by electrical stimulation of nerves: involvement of nitric oxide. *Acta Physiol. Scand.*, **141**, 531–539.

GONZALEZ, C. & ESTRADA, C. (1991). Nitric oxide mediates the neurogenic vasodilation of bovine cerebral arteries. *J. Cereb. Blood Flow Metab.*, **11**, 366–370.

GRIDER, J.R., MURTHY, K.S., JIN, J.-G. & MAKHLOUF, G.M. (1992). Stimulation of nitric oxide from muscle cells by VIP: prejunctional enhancement of VIP release. *Am. J. Physiol.*, **262**, G774–G778.

GROZDANOVIC, Z., BAUMGARTEN, H.G. & BRÜNING, G. (1992). Histochemistry of NADPH-diaphorase, a marker for neuronal nitric oxide synthase, in the peripheral autonomic nervous system of the mouse. *Neuroscience*, **48**, 225–235.

GU, J.,M BLANK, M.A., HUANG, W.M., ISLAM, K.N., MCGREGOR, G.P., CHRISTOFIDES, N., ALLEN, J.M., BLOOM, S.R. & POLAK, J.M. (1984). Peptide-containing nerves in human urinary bladder. *Urology*, **24**, 353–357.

GU, J., RESTORICK, J.M., BLANK, M.A., HUANG, W.M., POLAK, J.M., BLOOM, S.R. & MUNDY, A.R. (1983). Vasoactive intestinal polypeptide in the normal and unstable bladder. *Br. J. Urol.*, **55**, 645–647.

HASHIMOTO, S., KIGOSHI, S. & MURAMATSU, I. (1983). Nitric oxide-dependent and -independent neurogenic relaxation of isolated dog urethra. *Eur. J. Pharmacol.*, **231**, 209–214.

HOPE, B.T. & VINCENT, S.R. (1989). Histochemical characterization of neuronal NADPH-diaphorase. *J. Histochem. Cytochem.*, **37**, 653–661.

HOPE, B.T., MICHAEL, G.J., KNIGGE, K.M. & VINCENT, S.R. (1991). Neuronal NADPH diaphorase is a nitric oxide synthase. *Proc. Natl. Acad. Sci. U.S.A.*, **88**, 2811–2814.

HINDMARSH, J.R., GOSLING, P.T. & DEANE, A.M. (1983). Bladder instability. Is the primary defect in the urethra? *Br. J. Urol.*, **55**, 648–651.

IYENGAR, R., STUEHR, D.J. & MARLETTA, M.A. (1987). Macrophage synthesis of nitrite, nitrate and N-nitrosamines: precursors and role of the respiratory burst. *Proc. Natl. Acad. Sci. U.S.A.*, **84**, 6369–6373.

JAMES, M.J., BIRMINGHAM, A.T. & BATES, C.P. (1991). Relaxation of human isolated detrusor strips in response to electrical field stimulation: a possible role for nitric oxide in the human bladder. *J. Urol.*, **145**, 307A (abstract 380).

JOHNSON, G.D. & ARAUJO, G.M. (1981). A simple method of reducing the fading of immunofluorescence during microscopy. *J. Immunol. Methods*, **43**, 349–350.

KEAST, J.R. (1992). A possible neural source of nitric oxide in the rat penis. *Neurosci. Lett.*, **143**, 69–73.

KNOWLES, R.G., PALACIOS, M., PALMER, R.M.J. & MONCADA, S. (1989). Formation of nitric oxide from L-arginine in the central nervous system: a transduction mechanism for stimulation of the soluble guanylate cyclase. *Proc. Natl. Acad. Sci. U.S.A.*, **86**, 5159–5162.

KUMMER, W., FISCHER, A., MUNDEL, P., MAYER, B., HOBA, B., PHILIPPIN, B. & PREISSLER, U. (1992). Nitric oxide synthase in VIP-containing vasodilator nerve fibres in the guinea-pig. *Neuroreport*, **3**, 653–655.

LARSSON, B., ALM, P., PERSSON, K. & ANDERSSON, K.-E. (1992). Studies on the localization of some neurotransmitters, nerve markers, and NADPH diaphorase activity in tissues from the pig lower urinary tract. *Neurourol. Urodyn.*, **11**, 444–445.

LOW, J.A. (1977). Urethral behaviour during the involuntary detrusor contraction. *Am. J. Obstet. Gynecol.*, **128**, 32–39.

LOW, J.A., ARMSTRONG, J.B. & MAUGER, G.M. (1989). The unstable urethra in the female. *Obstet. Gynecol.*, **74**, 69–74.

LIU, X., GILLESPIE, J.S., GIBSON, I.F. & MARTIN, W. (1991). Effects of N^G-substituted analogues of L-arginine on NANC relaxation of the rat anococcygeus and bovine retractor penis and the bovine penile artery. *Br. J. Pharmacol.*, **104**, 53–58.

MCNEILL, D.L., TRAUGH, N.E., VAIDYA, A.M., HUA, H.T. & PAPKA, R.E. (1992). Origin and distribution of NADPH-diaphorase-positive neurons and fibers innervating the urinary bladder of the rat. *Neurosci. Lett.*, **147**, 33–36.

MONCADA, S. (1992). The L-arginine:nitric oxide pathway. The 1991 Ulf von Euler Lecture. *Acta Physiol. Scand.*, **145**, 201–227.

MORITA, T., TSUJII, T. & DOKITA, S. (1992). Regional difference in functional roles of cAMP and cGMP in lower urinary tract smooth muscle contractility. *Urol. Int.*, **49**, 191–195.

NAGAO, T. & VANHOUTTE, P.M. (1992). Hyperpolarization as a mechanism for endothelium-dependent relaxations in the porcine coronary artery. *J. Physiol.*, **445**, 355–367.

PALMER, R.M.J., FERRIGE, A.G. & MONCADA, S. (1987). Nitric oxide release accounts for the biological activity of endothelium-derived relaxing factor. *Nature*, **327**, 524–526.

PARK, K.H., RUBIN, L.E., GROSS, S.S. & LEVI, R. (1992). Nitric oxide is a mediator of hypoxic coronary vasodilatation. Relation to adenosine and cyclooxygenase-derived metabolites. *Circ. Res.*, **71**, 992–1001.

PERSSON, K. & ANDERSSON, K.-E. (1992). Nitric oxide and relaxation of pig lower urinary tract. *Br. J. Pharmacol.*, **106**, 416–422.

PERSSON, K. & ANDERSSON, K.-E. (1993). Nerve-mediated relaxation of the rabbit isolated urethra is associated with an increase in the smooth muscle content of cGMP. *J. Urol.*, **149**, 386A (abstract 695).

PERSSON, K., IGAWA, Y., MATTIASSON, A. & ANDERSSON, K.-E. (1992). Effects of inhibition of the L-arginine/nitric oxide pathway in the rat lower urinary tract *in vivo* and *in vitro*. *Br. J. Pharmacol.*, **107**, 178–184.

PERSSON, M.G., GUSTAFSSON, L.E., WIKLUND, N.P., MONCADA, S. & HEDQUIST, P. (1990). Endogenous nitric oxide as a probable modulator of pulmonary circulation and hypoxic pressor response in vivo. *Acta Physiol. Scand.*, **140**, 449–457.

REES, D., CELLEK, S., PALMER, R.M.M.J. & MONCADA, S. (1990). Dexamethasone prevents the induction by endotoxin of a nitric oxide synthase and the associated effects on the vascular tone. An insight into endotoxin shock. *Biochem. Biophys. Res. Commun.*, **173**, 541–547.

SAFFREY, M.J., HASSALL, C.J.S., HOYLE, C.H.V., BELAI, A., MOSS, J., SCHMIDT, H.H.H.W., FÖRSTERMANN, U.G., MURAD, F. & BURNSTOCK, G. (1992). Colocalization of nitric oxide synthase and NADPH-diaphorase in cultured myenteric neurones. *Neuroreport.*, **3**, 333–336.

SCHMIDT, H.H.H.W., GAGNE, G.D., NAKANE, M., POLLOCK, J.S., MILLER, M.F. & MURAD, F (1992). Mapping of neural nitric oxide synthase in the rat suggests frequent co-localization with NADPH diaphorase but not with soluble guanylyl cyclase, and novel paraneural functions for nitrinergic signal transduction. *J. Histochem. Cytochem.*, **40**, 1439–1456.

SCOTT, F.B., QUESADA, E.M. & CARDUS, D. (1964). Studies on the dynamics of micturition: observations on healthy men. *J. Urol.*, **92**, 455–463.

SHENG, H., SCHMIDT, H.H.H.W., NAKANE, M., MITCHELL, J.A., POLLOCK, J.S., FÖRSTERMANN, U. & MURAD, F. (1992). Characterization and localization of nitric oxide synthase in non-adrenergic non-cholinergic nerves from bovine retractor penis muscles. *Br. J. Pharmacol.*, **106**, 768–773.

SIROKY, M.B., NEHRA, A., VARDI, Y. & KRANE, R.J. (1990). Vesical blood flow: effect of hydrodistension and nerve stimulation. *Neurourol. Urodynam.*, **9**, 360–362.

TANAGHO, E.A. & MILLER, E.R. (1970). Initiation of voiding. *Br. J. Urol.*, **42**, 175–183.

TAYLOR, S.G. & WESTON, A.H. (1988). Endothelium-derived hyperpolarizing factor: a new endogenous inhibitor from the vascular endothelium. *Trends Pharmacol. Sci.*, **9**, 272–274.

THORNBURY, K.D., HOLLYWOOD, M.A. & MCHALE, N.G. (1992). Mediation by nitric oxide of neurogenic relaxation of the urinary bladder neck muscle in sheep. *J. Physiol.*, **451**, 133–144.

TODA, N. & OKAMURA, T. (1990). Mechanism underlying the response to vasodilator nerve stimulation in isolated dog and monkey cerebral arteries. *Am. J. Physiol.*, **259**, H1511–H1517.

WARD, J.K., FOX, A.J., MIURA, M., TADJIKARIMI, S., YACOUB, M.H., BARNES, P.J. & BELVISI, M.G. (1992a). Modulation of cholinergic neurotransmission by nitric oxide in human airway smooth muscle. *Br. J. Pharmacol.*, **107**, 85P.

WARD, S.M., XUE, C., SHUTTLEWORTH, C.W., BREDT, D.S., SNYDER, S.H. & SANDERS, K.M. (1992b). NADPH diaphorase and nitric oxide synthase colocalization in enteric neurons of canine proximal colon. *Am. J. Physiol.*, **263**, G277–G284.

YOUNG, H.M., FURNESS, J.B., SHUTTLEWORTH, C.W.R., BREDT, D.S. & SNYDER, S.H. (1992). Co-localization of nitric oxide synthase immunoreactivity and NADPH diaphorase staining in neurons of guinea-pig intestine. *Histochemistry*, **97**, 375–378.

(Received April 6, 1993
Revised June 8, 1993
Accepted June 10, 1993)

Br. J. Pharmacol. (1993), **110**, 531–538

Differential Class III and glibenclamide effects on action potential duration in guinea-pig papillary muscle during normoxia and hypoxia/ischaemia

[1]I. MacKenzie, V.L. Saville & J.F. Waterfall

Roche Research Centre, PO Box 8, Welwyn Garden City, Hertfordshire AL7 3AY

1 Microelectrode recording techniques were used to study the effects of several potassium channel blockers which are considered to be Class III antiarrhythmic compounds. The effects of (+)-sotalol, UK-66,914, UK-68,798 and E-4031 on action potential duration (APD) were determined in guinea-pig isolated papillary muscles. The compounds were evaluated under normoxic or hypoxic/ischaemic conditions at 36.5°C and compared to glibenclamide, which is considered to be a blocker of ATP-dependent potassium channels. Prolongation of action potential duration at 90% repolarization (APD_{90}) was taken as an indirect measure of potassium channel blockade.

2 Under normoxic conditions, the Class III compounds prolonged APD in a concentration-dependent manner. According to EC_{15} values, the order of potency of the Class III compounds was found to be UK-68,798 > E-4031 > UK-66,914 > (+)-sotalol. Glibenclamide did not significantly prolong APD_{90} under normoxic conditions.

3 Perfusion with an experimental hypoxic or ischaemic bathing solution produced qualitatively similar effects on action potentials. Over a period of 20–25 min in either of the experimental solutions, there was a small decrease in action potential amplitude (APA) and a prominent shortening of APD. The ischaemic solution also depolarized the resting membrane potential by about 15 mV.

4 (+)-Sotalol and UK-66,914 did not reverse the shortening of APD induced by perfusion with hypoxic Krebs solution. High concentrations of glibenclamide (10 μM) and UK-68,798 (30 and 60 μM) partially reversed the hypoxia-shortened APD. Glibenclamide was more potent and exhibited a greater time-dependent action than UK-68,798.

5 During experimental ischaemia, the Class III compound E-4031 (10 μM, $n = 7$) produced small, but significant, increases in the APD_{90} (11 ± 3 ms after 20 min) which were not clearly time-dependent (14 ± 4 ms after 30 min). UK-68,798 (10 μM) also produced a small, but insignificant, increase in APD_{90} (12 ± 6 ms at 20 min, $n = 4$). Higher concentrations of UK-68,798 (30 and 60 μM, $n = 4$) did not produce a consistently significant increase in APD_{90} during ischaemia: significance was only attained after 20 min in the presence of 60 μM UK-68,798 (24 ± 12 ms). However, in marked contrast to the effects of the Class III compounds, glibenclamide (10 μM) produced large time-dependent increases in ischaemic APD_{90} (34 ± 11 ms at 7 min, $n = 9$) which were significant 15 min or more after drug addition (52 ± 12 ms at 20 min, $n = 7$; 74 ± 5 ms at 30 min, $n = 6$).

6 The present microelectrode data suggest that blockers of ATP-dependent potassium channels, such as glibenclamide, might prove to be more effective than Class III compounds against ischaemia-induced shortening of cardiac action potentials.

Keywords: Antiarrhythmic drugs; ATP-dependent potassium channels; Class III drugs; glibenclamide; guinea-pig papillary muscle

Introduction

One of the principal causes of sudden death in the western world is the onset of lethal ventricular arrhythmias which follow myocardial ischaemia where partial membrane depolarization, a shortened action potential duration and impaired conduction velocity set up re-entrant arrhythmias (Janse & Wit, 1989). There has been much discussion as to the most appropriate form of therapy for these ischaemic arrhythmias since the sodium channel blockers flecainide and encainide increased mortality in a population of patients which had previous myocardial infarction (CAST Investigators, 1989). Therefore, attention has recently turned to the modulation of other ion channel subtypes, particularly potassium channels, for an antiarrhythmic compound which prolongs action potential duration in the ischaemic myocardium.

Vaughan Williams (1970) originally termed compounds which selectively prolonged action duration as Class III agents. Subsequently, these drugs were believed to prolong action potential repolarization by blockade of a delayed rectifier (Carmeliet, 1985), a low-conductance potassium channel which is both voltage- and time-dependent (Giles & Shibata, 1985; Matsuura *et al.*, 1987; Shibasaki, 1987). Early Class III compounds in clinical use are typified by sotalol (Antonaccio & Gomoll, 1988; Nademanee & Singh, 1990). More recently, there have been other highly potent sotalol derivatives (such as UK-66,914, UK-68,798 and E-4031) which, under normoxic conditions, prolong ventricular action potential duration and refractoriness in electrophysiological studies (Tande *et al.*, 1990; Gwilt *et al.*, 1991a,b). These Class III drugs also prolong refractoriness in some *in vivo* models (Gwilt *et al.*, 1989; 1991b) and, additionally, exhibit antiarrhythmic effects in other *in vivo* models of prior myocardial infarction (Katoh *et al.*, 1990; Lynch *et al.*, 1990; Zuanetti & Corr, 1991).

An ATP-dependent outward potassium conductance is activated in cardiac myocytes by a reduction in intracellular ATP concentration (Noma, 1983), which can be produced either by attenuation of the glycolytic pathway (e.g. by hypoxia), or by use of metabolic inhibitors (Trube &

[1]Author for correspondence.

Hescheler, 1984; Weiss & Lamp, 1989). Promotion of this ATP-dependent potassium current by hypoxia or metabolic inhibition results in a shorter action potential duration (Kodama *et al.*, 1984; Fosset *et al.*, 1988). Thus, blockers of ATP-dependent potassium channels which could selectively prolong APD in metabolically compromised tissue represent a potential drug target with a pathophysiological relevance in myocardial ischaemia. Blockers of cardiac ATP-dependent potassium channels are typified by sulphonylureas such as glibenclamide (Fosset *et al.*, 1988). Glibenclamide also has a therapeutic effect on insulin secretion associated with its blocking action on pancreatic ATP-dependent potassium channels (Zünkler *et al.*, 1988). However, some of the differences in the biophysical and pharmacological properties of cardiac and pancreatic ATP-dependent potassium channels could be exploited to yield novel cardioselective compounds.

The present work has investigated the effects of the Class III compounds (+)-sotalol, UK-66,914 (N-[4-[1-Hydroxy-2-[4-(4-pyridyl)-1-piper = azinyl] ethyl] phenyl] methanesulphonamide), UK-68,798 (N-[4-[2-[N-methyl-[2-[4-(methylsulphonamido) = phenoxy]ethyl]amino]ethyl]phenyl]methanesulphonamide) and E-4031 (N-[4-[1-[2-(6-Methyl-2-pyridyl)ethyl]-4-piperidinyl = carbonyl]phenyl]methanesulphonamide dihydrochloride) on action potential duration in guinea-pig isolated papillary muscle under normoxic conditions. Maximally effective concentrations were determined and the compounds additionally tested under hypoxic or ischaemic conditions. These drug profiles were then compared with those of glibenclamide.

Some of this work has been communicated in preliminary form (MacKenzie *et al.*, 1990; Saville *et al.*, 1991).

Methods

Electrophysiological recording

Guinea-pigs (300–550 *g*) underwent cervical dislocation, or were stunned and exsanguinated. The heart was quickly removed and a papillary muscle (generally from the right ventricle) with attached piece of ventricular wall was pinned out in a tissue bath (2 ml, flow rate of 6 ml min^{-1}) containing oxygenated Krebs solution at 36.5°C. The preparations were stimulated at a frequency of 1 Hz (2 ms pulse width, threshold voltage plus 50%) by bipolar platinum electrodes placed against the preparation. After an initial stabilization period (1–1.5 h), action potentials were recorded from the papillary muscle using microelectrode recording techniques. Data were displayed on a digital oscilloscope (Gould 1604) where waveforms were overlaid and output as necessary. Figure 2 was taken from a chart recording (Gould 3400, pen frequency-response of 30–50 Hz) and other experiments used a DAT tape recorder (Biologic) in conjunction with a high-frequency recorder (Gould TA4000, with 10 kHz).

The temporal characteristics of the action potentials were recorded semi-automatically, at regular time intervals, from prolonged impalements of a single cell in the preparation. The effects of drugs on these steady-state determinations were then evaluated at fixed time points. The action potential duration at 90% repolarization (APD_{90}) from maximal amplitude (APA) was aken as an indirect measure of potassium channel activity. Drugs which prolonged the APD_{90} without effects on the action potential upstroke velocity (V_{max}) were considered to be potassium channel blocking agents. Action potential duration at 30 and 50% repolarization (APD_{30} and APD_{50}, respectively) was also routinely measured. The effects of Class III compounds on the APD_{90} were quantified by establishing concentration-response curves using a 7 min time cycle. This time cycle was chosen because preliminary experiments with the reference compound (+)-sotalol had shown that there was no further increase in the APD_{90} with extended exposure. Due to difficulty in completely washing out the effects of the compounds, only one agent was studied in each preparation. From these experiments, EC_{15} values were determined (i.e. the concentration of compound which prolonged the APD_{90} by 15%) and used to establish the relative potencies of the Class III compounds. An EC_{15} value was chosen for two reasons: firstly, because the prolongation induced by some compounds did not consistently exceed 20 or 25% and, secondly, because the errors associated with this value were small.

Illustrations show a continuous recording from a single cell in a preparation. Mean data (± s.e.mean) were compared by Student's paired *t* test where appropriate with $P < 0.05$ considered statistically significant.

Bathing solutions and drugs

The Krebs solution was of the following ionic composition (mM): Na^+ 149.1, K^+ 5.4, Mg^{2+} 1.2, Ca^{2+} 2.0, Cl^- 144.2, HCO_3^- 15.5, $H_2PO_4^-$ 1.2 and glucose 11. This 'normoxic' Krebs had a pH of 7.3 and was gassed by 95% O_2/5% CO_2. The 'hypoxic' Krebs solution was of the same composition as that above, except that it was glucose-free and gassed by 95% N_2/5% O_2 to reduce substantially the oxygen tension in the solution (Po_2 in bath 150 mmHg, by Corning 168 analyser). The 'ischaemic' Krebs solution was also glucose-free but the potassium concentration and pH were changed to simulate some of the changes measured in the *in vivo* myocardium during ischaemia (see Gettes, 1986). The ischaemic bathing solution was of the following composition (mM): Na^+ 137.3, K^+ 9.2, Mg^{2+} 1.2, Ca^{2+} 2.0, Cl^- 143.7, HCO_3^- 8.0, $H_2PO_4^-$ 1.2 and glucose 0. The ischaemic bathing solution was gassed with 55% O_2/40% N_2/5% CO_2 to produce a less severe change in oxygen tension (Po_2 in bath 200 mmHg), and had a pH of 6.9.

Glibenclamide was obtained from Sigma. The Class III agents were synthesized in the Cardiovascular Chemistry Department at Roche Products Ltd. E-4031 was made up as a stock solution in distilled water and (+)-sotalol was dissolved initially in ethanol. Other drugs were dissolved in dimethylsulphoxide (DMSO), to a maximal solvent concentration of 0.5%, which had no effects on action potential configuration.

Results

Action potentials under normoxic conditions

Action potentials were usually recorded from preparations maintained for 2–4 h after equilibration. Within any experiment, a sample of cells tested in the absence of drugs generally exhibited action potentials of similar amplitude (mean APA was 113 ± 1 mV, $n = 22$) and duration. Between preparations, however, the duration of the action potential repolarization was quite variable (range 85–180 ms, mean APD_{90} 130.5 ± 3.2 ms, $n = 68$). The average action potential upstroke velocity (V_{max}) was 215 ± 14 mVs^{-1} ($n = 18$) with an average APD_{30} and APD_{50} of 74.6 ± 6.3 ms and 99.3 ± 7.2 ms ($n = 22$), respectively. In any given preparation, once the time-course and amplitude of the action potentials had attained a steady-state level (usually 10–15 min after impalement), the effects of drugs on the action potential parameters were measured.

Prolongation of normoxic action potentials

The order of potency of the Class III compounds in this study, as determined using EC_{15} values (see Methods) obtained from concentration-response relationships (Figure 1), was UK-68,798 > E-4031 > UK-66,914 > (+)-sotalol.

The mean EC_{15} values together with their 95% confidence limits were calculated as 0.92 (0.18–4.68) μM ($n = 3$) for UK-68,798, 2.25 (1.48–3.41) μM ($n = 7$) for E-4031, 3.37

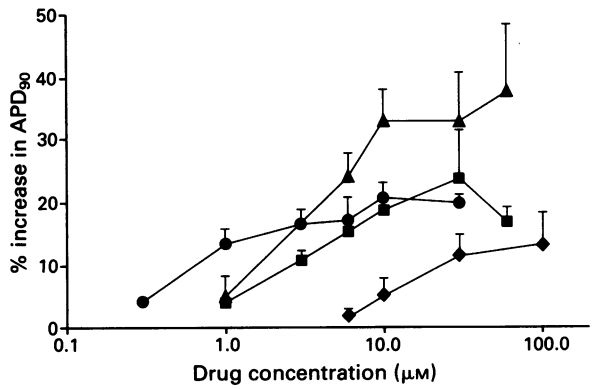

Figure 1 Concentration-dependent effects of UK-68,798 (●), E-4031 (▲), UK-66,914 (■) and (+)-sotalol (◆) on action potential duration recorded from guinea-pig papillary muscles under normoxic conditions and measured at 90% repolarization (APD_{90}). See text for details.

(2.08–5.45) μM ($n = 4$) for UK-66,914 and 29.8 (1.28–691) μM ($n = 3$) for (+)-sotalol. The mean maximal increase in APD_{90} obtained with a 10 μM concentration of each compound was 20.6 ± 3.1% for UK-68,798 ($n = 3$, control APD_{90} = 159.5 ± 2.0), 33.0 ± 4.7% for E-4031 ($n = 7$, control APD_{90} = 95.0 ± 11.9), 18.5 ± 4.7% for UK-66,914 ($n = 5$, control APD_{90} = 136.5 ± 8.7) and 5.9 ± 3.0% for (+)-sotalol ($n = 6$, control APD_{90} = 132.8 ± 6.8). These agents prolonged the APD at 30, 50 and 90% repolarization. The percentage increase in APD_{90} for a Class III compound was larger than corresponding increases in either APD_{30} or APD_{50} (for example 10 μM UK-68,798 prolonged the APD_{90} by 20.6 ± 3.1%, the APD_{50} by 17.7 ± 3.5% and the APD_{30} by 8.6 ± 2.5%, $n = 3$). These drugs prolonged repolarization without any significant reduction in the V_{max}. These observations confirm the reported Class III profiles of these compounds.

In contrast to the Class III compounds described above, the ATP-dependent potassium channel blocker, glibenclamide (10 μM for up to 30 min) did not significantly prolong APD_{90} under normoxic conditions. The values for APD_{90}, in the presence of 10 μM glibenclamide, over a 30 min incubation period were as follows: control = 146.6 ± 6.3 ms, 7 min glibenclamide 145.2 ± 6.7 ms, 15 min glibenclamide 151.4 ± 5.6 ms, 20 min glibenclamide 152.7 ± 5.3 ms, 25 min glibenclamide 152.6 ± 5.8 ms and 30 min glibenclamide 151.8 ± 7.7 ms ($n = 5$).

Effect of drugs under hypoxic conditions

When the Krebs bathing solution was exchanged for the 'hypoxic' bathing solution (see Methods), there was a small but consistent reduction in the APA of a few millivolts and a marked reduction in the APD_{90}. These changes attained a near steady-state after 20–25 min. Thereafter, drugs were added during continued hypoxia to assess whether they had any effect on action potential configuration.

A high concentration of the Class III compound (+)-sotalol (30 μM) had no effect on the APD_{90} under hypoxic conditions (Figure 2a), which contrasted with its Class III activity under normoxic conditions (Figure 1). The more potent Class III compounds, UK-66,914 and UK-68,798, were used in another series of experiments at concentrations which were maximal for their Class III effects. UK-66,914 (30 μM) had no effect under hypoxic conditions (Figure 2b). However, UK-68,798 (30 μM) had some effect on the hypoxia-shortened APD (Figure 3). There was a small increase in the mean APD_{90} produced by 30 μM UK-68,798 which was significant only after 15 min (the hypoxic APD_{90} was increased by 22 ± 5.5 ms, $n = 3$) and this increase did not become larger with time (23 ± 11 ms, $n = 3$, after 20 min). At a higher concentration (60 μM UK-68,798, $n = 3$) there was no significant increase in APD_{90}.

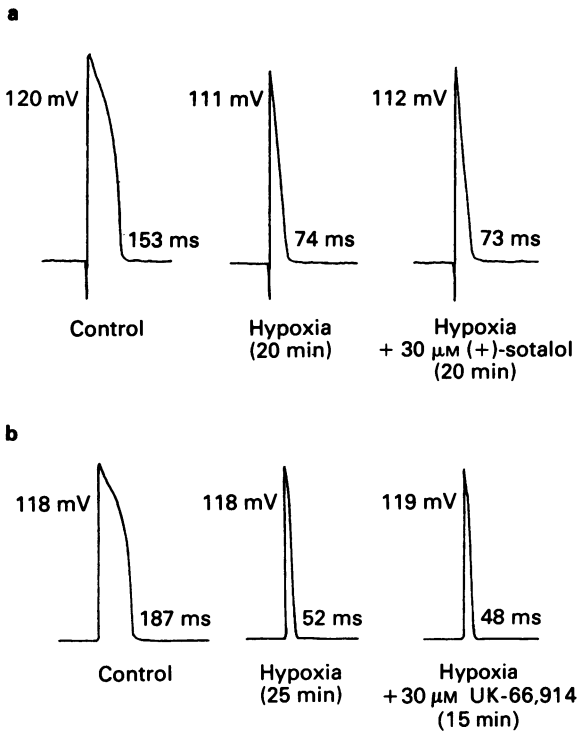

Figure 2 Lack of effect of (a) (+)-sotalol (30 μM) and (b) UK-66,914 (30 μM) during hypoxic conditions. Action potentials were recorded initially under normoxic conditions (controls) and then progressively shortened under hypoxic conditions until they attained a steady-state. The subsequent addition of (a) (+)-sotalol or (b) UK-66,914 did not prolong the hypoxic APD_{90} in these experiments. (In this and subsequent figures of this type, the hypoxic action potential illustrated was measured at the annotated time after the onset of hypoxia. The APD_{90} had then reached a steady-state and drugs were subsequently added to the hypoxic solution for the times shown below these drug-treated responses). There was no apparent effect of hypoxia on resting membrane potential in these experiments.

The ATP-dependent potassium channel blocking agent glibenclamide also prolonged the hypoxia-shortened APD_{90}. The threshold concentration for this effect was about 10 μM. One striking feature of the action of glibenclamide was its clear latency (around 10–15 min) before an initial effect was apparent (compare the insignificant increase of 4 ± 2.1 ms at 7 min, $n = 7$, with that of 28 ± 7.3 ms at 15 min, $n = 6$, significant at $P < 0.01$). Thereafter, the effect of glibenclamide at a fixed concentration (generally 10 μM in these studies) progressively increased as the period of drug incubation was extended (Figure 4). A significant ($P < 0.01$) net increase in the APD_{90} of 50 ± 9.6 ms ($n = 4$) was observed after 20 min exposure to 10 μM glibenclamide.

Effect of drugs under ischaemic conditions

Although the experimental hypoxia methodology is often used in cardiac electrophysiological studies, we also used an alternative experimental stimulus which would better simulate some of the ionic and chemical changes which arise within the myocardium during ischaemia. A simulated ischaemic bathing solution (see Methods) was used to shorten the APD, probably by activating ATP-dependent potassium channels. The ability of compounds to reverse the shortening effect of ischaemia on the APD was then assessed.

The 'ischaemic' bathing solution prolonged qualitatively similar effects on action potential configuration to those seen with the 'hypoxic' solution. There was a small decrease in the APA and a pronounced shortening of the APD_{90}, both of which reached a steady-state after about 20 min (Figures 5

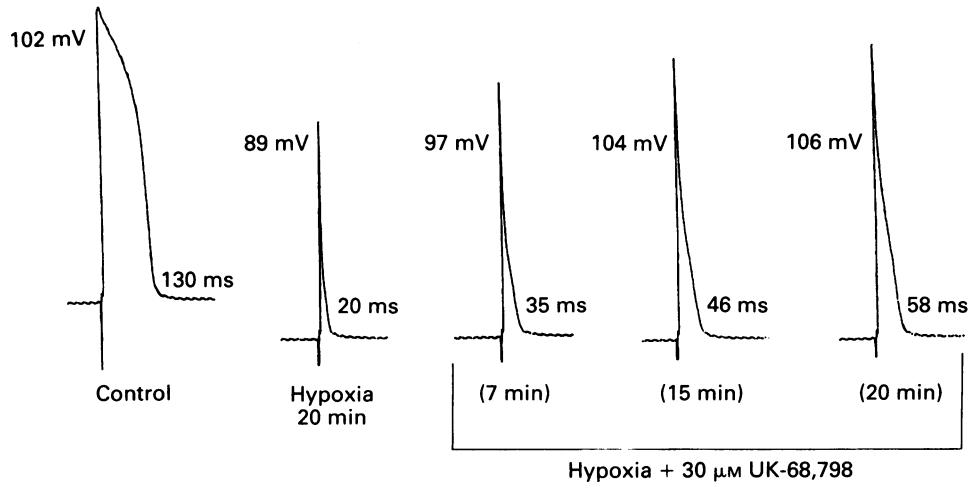

Figure 3 The effect of UK-68,798 on the APD_{90} recorded from a guinea-pig papillary muscle following exposure to the hypoxic bathing solution. There was a significant reduction in the APD_{90} after 20 min experimental hypoxia. UK-68,798 (30 μM) elicited a small increase in APD_{90} (see text). In this recording, there was some instability in the resting membrane potential as the hypoxic solution entered the bath. This quickly restabilized, at the lower level shown, and remained constant for the rest of the experiment.

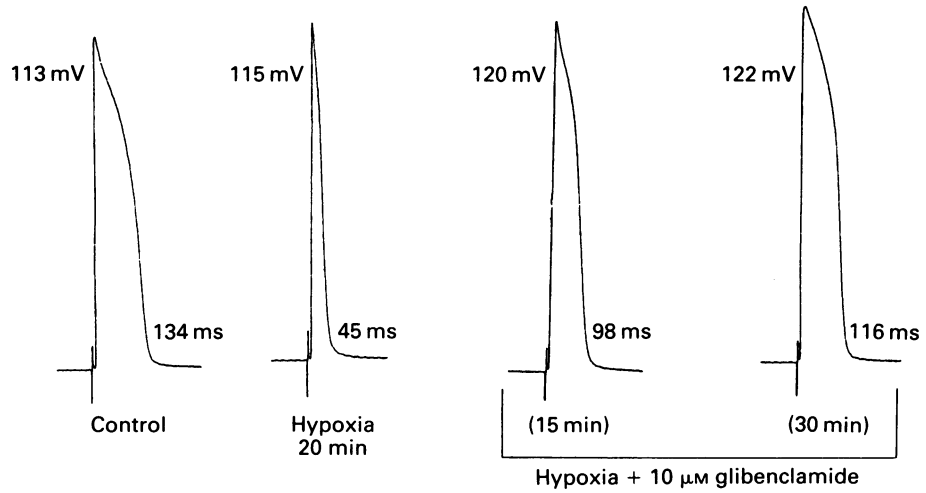

Figure 4 The effect of glibenclamide (10 μM) on hypoxia-induced shortening of APD_{90} in guinea-pig papillary muscle. There was a latency of 10–15 min following the infusion of glibenclamide before an increase in the APD_{90} was observed. Thereafter, glibenclamide progressively increased the duration of the hypoxic APD_{90} as its period of incubation was extended.

and 6). The following data demonstrate the stability of the response under ischaemic conditions and shows that DMSO (the solvent used to dissolve some of the drugs) had no effect on APD_{90}. The control APD_{90} was 137.8 ± 8.5 ms, after 20 min ischaemia it was reduced to 63.8 ± 18.8 ms and in the presence of 0.1% DMSO the APD_{90} values obtained over time were 66.0 ± 17.7 ms (7 min), 65.8 ± 18.2 ms (15 min), 66.7 ± 15.3 ms (20 min), 66.7 ± 15.1 ms (25 min) and 67.6 ± 15.8 ms (30 min) ($n = 4$ in all cases). In most experiments, test drugs were added after 20 min of ischaemia, although a few preparations required a further 5 min for APD_{90} readings to attain steady-state. One marked difference between the use of hypoxic and ischaemic bathing solutions was the depolarization of the cell membrane potential (by about 15 mV) which occurred with the ischaemic bathing solution. The depolarization preceded the shortening of the APD_{90} by several minutes, and was presumably a consequence of the elevated extracellular K^+ (9.2 mM) in the ischaemic solution.

The aim of this series of experiments was to obtain more quantitative data about the effects of high (near-maximally effective) concentrations of E-4031 and UK-68,798, which were the two most potent Class III compounds previously studied under normoxic conditions. As far as we are aware, this is the first time that these Class III drugs have been compared with glibenclamide under ischaemic conditons for their effects on APD. Neither E-4031 (10 μM, Figure 5a) nor UK-68,798 (10, 30 and 60 μM, Figure 5b) produced substantial reversal of the ischaemia-induced shortening of the action potential. E-4031 (10 μM, $n = 7$) produced a net mean increase of 7 ± 3 ms (at 7 min), 11 ± 3 ms (at 20 min) and 14 ± 4 ms (at 30 min); these small increases in the APD_{90} after 20 and 30 min were significant (Figures 5a and 6a). UK-68,798 (10 μM, $n = 4$) produced net increases in the APD_{90} (Figure 5b) similar to those observed with the same concentration of E-4031 (see above data) with increases of 7 ± 4 ms (at 7 min) and 12 ± 6 ms (at 20 min). Even with higher concentrations of UK-68,798 (30 and 60 μM, $n = 4$), a significant net increase in APD_{90} was only attained after 20 min in the presence of 60 μM UK-68,798, when the increase was 24 ± 12 ms (Figures 5b and 6b).

Glibenclamide prolonged ischaemic action potentials in a similar manner to that described above for the hypoxic solu-

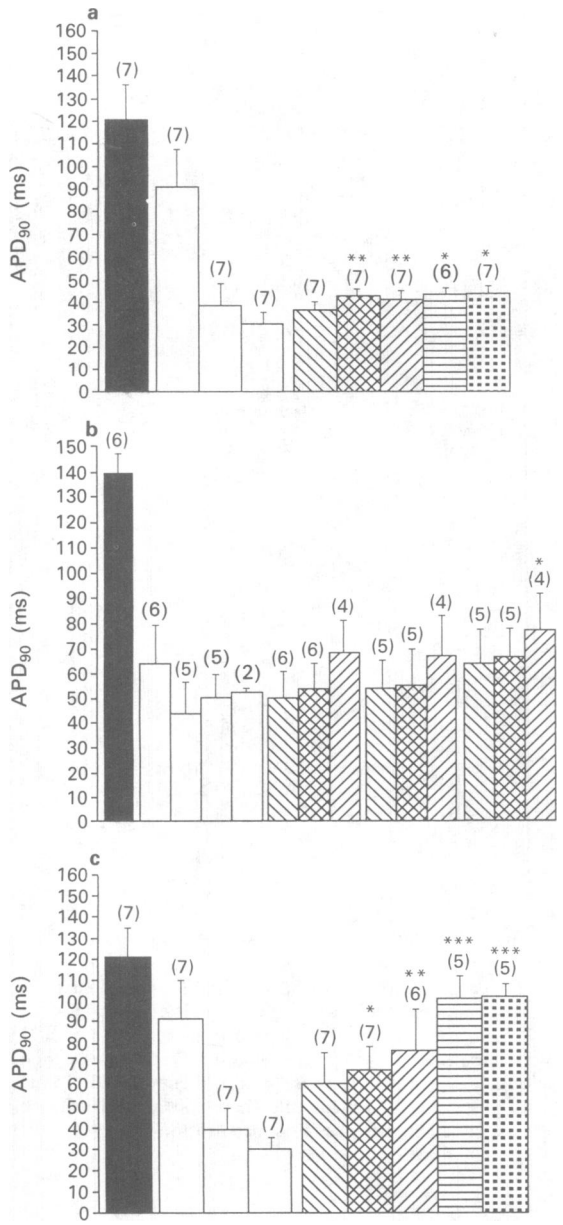

Figure 5 Comparison of the effects of (a) E-4031 (10 μM), (b) UK-68,798 (10, 30 and 60 μM) and (c) glibenclamide (10 μM) on APD_{90} recorded from guinea-pig papillary muscles under conditions of experimental ischaemia (see Methods). The APD_{90} recorded under ischaemic conditions (open columns show measurements after 7, 15, and 20 min of ischaemia, respectively) was smaller than a corresponding control value (solid column). Once the action potentials under ischaemic conditions had attained a steady-state a test drug was added (hatched columns for times indicated). (a) E-4031 produced a small, but significant, increase in the ischaemic APD_{90} after 15 min or more (shaded columns show data 7, 15, 20, 25 and 30 min after drug treatment, respectively). (b) UK-68,798 was studied at three concentrations (10 μM [left hand group of shaded columns], 30 μM [central group of shaded columns] and 60 μM [right hand group of shaded columns]) and changes in APD_{90} were measured after 7, 15 and 20 min. There were small increases in APD_{90} which were only significant at the highest concentration used (60 μM for 20 min). (c) Glibenclamide induced larger increases in APD_{90} during ischaemia which was clearly a time-dependent effect (columns represent measurements made 7, 15, 20, 25 and 30 min after drug addition, respectively). The time-dependent action of glibenclamide contrasts with the effects of E-4031 and UK-68,798. Asterisks represent significant increases in the ischaemic APD_{90} (measured after 20 min ischaemia) by drug treatment: $*P < 0.05$; $**P < 0.01$; $***P < 0.001$.

tion. The threshold concentration for glibenclamide was about 6 μM and it exhibited a pronounced and progressive time-dependent action (Figure 5c and see Figure 4, in hypoxia). Glibenclamide (10 μM) produced net increases in the ischaemic APD_{90} of 34 ± 11 ms (at 7 min, $n = 9$), 52 ± 12 ms (at 20 min, $n = 7$) and 74 ± 5 ms (at 30 min, $n = 6$). These increases in the APD_{90} were significant 15 min or more after drug addition (Figures 5c and 6a) and were larger than those observed with either E-4031 or UK-68,798 (see above data). Despite prolonged exposure to glibenclamide, ischaemic action potentials were incompletely restored to their control (pre-ischaemic) values. For example, after 30 min of glibenclamide treatment (10 μM), there was $85 \pm 8\%$ ($n = 6$) restoration of the APD_{90}.

Discussion

In the present experiments, the electrophysiological effects of several Class III compounds have been studied under either normoxic conditions or conditions designed to simulate experimental hypoxia or myocardial ischaemia. The Class III compounds evaluated here exhibited different pharmacological profiles in comparison to the ATP-dependent potassium channel blocking agent, glibenclamide. Under normoxic conditions, the Class III compounds prolonged the intracellularly recorded APD, whereas glibenclamide had no significant effect. In contrast, during hypoxia, the ability of both (+)-sotalol and another more potent methanesulphonamide, UK-66,914, to prolong APD was lost whereas glibenclamide significantly prolonged the shortened action potentials. Similarly, during experimental ischaemia, a near-threshold (10 μM) concentration of glibenclamide produced larger increases in the APD_{90} than did high concentrations of E-4031 or UK-68,798. This is particularly pertinent since UK-68,798 is the most potent Class III compound studied to date. In addition, this is the first time that the effects of glibenclamide on APD have been compared with those of E-4031 and UK-68,798 during simulated ischaemia.

Effect of Class III compounds during normoxia and ischaemia

The present data agree with the earlier characterization of the compounds studied ((+)-sotalol, UK-66,914, UK-68,798 and E-4031) as Class III agents (Carmeliet, 1985; Sawada *et al.*, 1988; Tande *et al.*, 1990; Gwilt *et al.*, 1991a,b) since they prolonged the APD_{90} without any changes in the V_{max}, although there was generally a small increase in the APA of a few millivolts. The threshold concentrations for Class III effects in this study were similar to those obtained in other tests used within our laboratory (for example, changes in the refractory period, Cooper, Lad & MacKenzie, unpublished observations), although they are at variance with other studies which have shown that UK-66,914 and UK-68,798 are about 30 times more potent than the present data. For example, in experiments which used similar experimental conditions (36–37°C and a stimulation frequency of 1 Hz) UK-68,798 and UK-66,914 elicited threshold increases in the canine ventricular muscle APD at $\geqslant 5$ nM and $\geqslant 0.1$ μM, respectively (Gwilt *et al.*, 1991a,b). In addition, Tande *et al.* (1991) used continuous microelectrode recordings from guinea-pig papillary muscles (32°C and 1 Hz) to show that $\geqslant 10$ nM UK-68,798 prolonged the APD.

Although some differences in methodology are apparent between the present microelectrode work and that of other groups (for example, slight differences in bathing solution composition, cell sampling technique or experimental temperature), the differences in threshold potency between the present data and that from other studies cannot be fully explained. Like Tande *et al.* (1991), we studied action potential parameters from prolonged recordings of a single, representative, cell within the preparation in the absence and

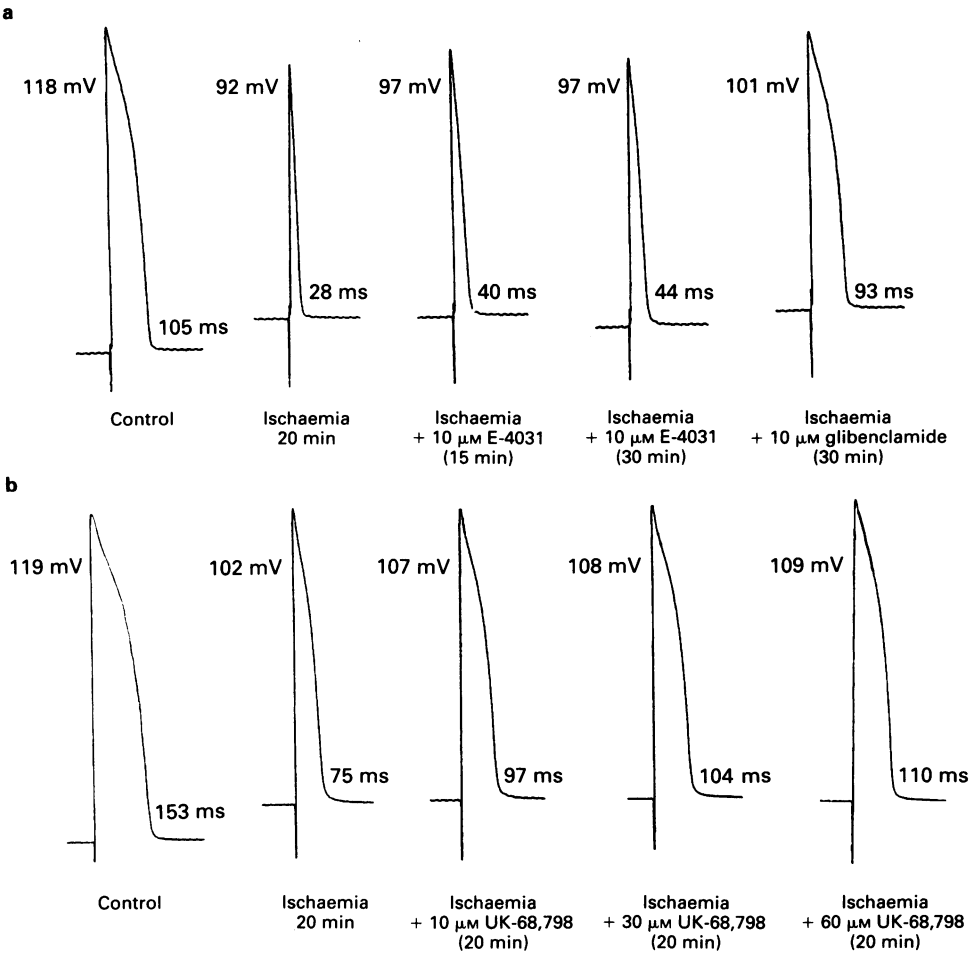

Figure 6 The effect of (a) E-4031 (10 μM) followed by glibenclamide (10 μM) and (b) UK-68,798 (10, 30 and 60 μM) on ischaemia-induced shortening of APD_{90} in guinea-pig papillary muscle. (a) In this cell, there was only a small effect of E-4031, which showed no time-dependency, over a 30 min period (see Figure 5a for quantified data). After 30 min treatment with E-4031, this drug was removed from the ischaemic bathing solution and replaced with glibenclamide (10 μM for 30 min). During this period, glibenclamide induced a prominent and characteristic time-dependent prolongation of APD_{90}. There was a latency of 10–15 min following the infusion of glibenclamide before an increase in the APD_{90} was observed. (b) In this cell, there was a small effect of UK-68,798 which was more prominent at the lowest concentration used (10 μM); further increases in concentration (30 and 60 μM) produced comparatively small increases in APD_{90} (see Figure 5b for quantified data).

presence of drugs, rather than use a serial sampling technique. This is because we wanted to use each cell as its own control to study the effect of several drug concentrations, measured at predetermined time-points, once the cell had completely resealed after impalement. The action potential parameters usually attained a steady-state 10–15 min after impalement. Although Tande *et al.* used a 40 min exposure period for each concentration of Class III agent, they also saw significant effects of lower concentrations within 10 min (which was similar to the 7 min time cycle adopted here).

Our rank order of potency, with UK-68,798 as the most potent of these compounds, is in good agreement with the literature. An EC_{15} value was used only as an indicator of potency – it did not, however, take into account the different maximal responses to the Class III compounds. The newer methanesulphonamide derivatives produced a larger maximal prolongation of APD_{90} than (+)-sotalol, suggesting their greater efficacy or a slightly different mechanism of action. (+)-Sotalol was used in these experiments because the (+)-stereoisomer has less activity as a β-adrenoceptor blocking agent compared to the (−)-stereoisomer (Woosley *et al.*, 1990).

Several questions could not be addressed using data from the present microelectrode experiments. Firstly, which potassium channel(s) is (are) associated with the drug-induced Class III effects under normoxic conditions? We can speculate about some possibilities based upon voltage-clamp data from guinea-pig isolated myocytes. Under normoxic conditions, time- and voltage-dependent potassium currents and their associated tail currents are mediated by different mechanisms (Sanguinetti & Jurkiewicz, 1990; Wettwer, 1990). It has also been suggested that there are two components of this 'delayed rectifier' current which exhibit differential drug sensitivity to the Class III compounds E-4031 and (+)-sotalol (Sanguinetti & Jurkiewicz, 1990). This interpretation differs from the more established view that Class III compounds act only on the time- and voltage-dependent currents or their tails (often collectively described as the 'delayed rectifier' or I_K). Secondly, how was the slight prolongation of the APD_{90} produced by Class III drugs during experimental hypoxia or ischaemia? This could have arisen from incomplete block of a single component of outward current. Alternatively, the high concentrations of Class III agents used could have had a small effect on other potassium channel subtypes, or they could have promoted some inward current which might explain some of the small increases in APA which we see during ischaemia or hypoxia.

The implications of the present experiments are that Class III compounds may have limited effects against ischaemic arrhythmias in some experimental or clinical settings. Cobbe (1988) reviewed available evidence which suggested that Class III compounds largely lost their ability to prolong action

potential duration in abnormal (hypoxic or ischaemic) myocardium. Much of the experimental support for this suggestion (see Cobbe, 1988) relied on observations made with sotalol, but the limited effects of the newer and more potent Class III compounds studied in the present microelectrode experiments endorse these views. Additionally, recent *in vivo* data suggest that these newer Class III compounds do not provide significant protection against the lethal ischaemic arrhythmias which follow coronary artery occlusion in the anaesthetized cat, even at relatively high doses (Lad & MacKenzie, 1991). However, E-4031 has been reported to have antagonistic effects towards chronic ischaemic arrhythmias *in vivo* in canine post-infarction models (Katoh *et al.*, 1990; Lynch *et al.*, 1990). This could be due to either its primary Class III effect in the normoxic myocardium, rather than an effect on ATP-dependent potassium channels, or even some other effect *in vivo*.

Effect of glibenclamide under hypoxic/ischaemic conditions

Under hypoxic or ischaemic conditions, ATP-dependent potassium channels are activated by falls in the intracellular ATP concentration and the cardiac action potential is shortened as a result of the promotion of a time-independent outward K^+ current (Noma, 1983; Fosset *et al.*, 1988). When such a low intracellular ATP concentration was produced by internal perfusion of guinea-pig cardiac myocytes, glibenclamide (20–50 nM) prolonged the shortened APD and also reduced the opening probability of the ATP-dependent single channels (Fosset *et al.*, 1988). In the present work, the electrophysiological consequences of hypoxia (shortening of APD and small reduction in APA) were largely the same as those following ischaemia, with the exception that the elevated potassium concentration in the ischaemic bathing solution elicited an additional partial membrane depolarization, and these effects were largely antagonized by the subsequent addition of glibenclamide. The significant effect of glibenclamide on APD under hypoxic or ischaemic conditions contrasted with its lack of effect under normoxic conditions. Glibenclamide antagonized the effects of ischaemia at a slightly lower threshold concentration (about 6 μM) than under hypoxic conditions (about 10 μM) but the effects of the drug were qualitatively similar. The incomplete restoration of ischaemic APD to control values by glibenclamide (approximately 85% at 10 μM) could either be interpreted as a substantial but partial block of ATP-dependent potassium channels by glibenclamide, or could indicate the presence of other minor components of potassium current activated during ischaemia.

Numerous investigators have shown that glibenclamide **pre**treatment has antagonistic effects in isolated cardiac muscle (usually at micromolar concentrations) against subsequent events elicited by metabolic inhibition or experimental hypoxia/ischaemia. Nakaya *et al.* (1991) showed that 60 min pretreatment of guinea-pig isolated papillary muscle with 10 μM glibenclamide partially prevented the subsequent shortening effects of experimental hypoxia or metabolic inhibition on APD; this effect of glibenclamide was maximal at 20 μM. In the present work, continuous microelectrode recordings of action potentials have extended these observations. For the first time, our recordings from cardiac muscle under normoxic and, subsequently hypoxic or ischaemic conditions, have highlighted a time-dependent component of the action of glibenclamide. This effect was apparent 7–10 min after the additon of glibenclamide during ischaemia (or hypoxia) and was significant and progressive after 15 min or more. This might have implications for experiments where long periods of pretreatment with glibenclamide are studied.

The time-dependent action of glibenclamide raises some questions as to the precise site and mechanism of action of this drug. Although glibenclamide and other sulphonylureas have high-affinity binding sites typified by low K_d values (with potent compounds having activity in the nanomolar range, see Fosset *et al.*, 1988), the precise relationship between the concentrations required for binding at these sites and those required for their pharmacological effects in cardiac tissue (usually in the micromolar range or higher) have yet to be determined for a wide range of compounds. In guinea-pig myocytes, in the presence of low intracellular ATP concentrations, glibenclamide has been shown to have a potent action (20–50 nM) on both APD and single ATP-dependent potassium channels (Fosset *et al.*, 1988). However, other groups have found that much higher concentrations of glibenclamide are required to modify either hypoxic/ischaemic APD (Nakaya *et al.*, 1991 and present work), ATP-dependent potassium current from whole-cell recordings of guinea-pig myocytes during metabolic inhibition (Venkatesh *et al.*, 1991), or single-channel recordings from inside-out membrane patches (Venkatesh *et al.*, 1991) or open-cell patches (Nakaya *et al.*, 1991). Sulphonylureas have a comparatively short latency of action at single channels in heart (Nakaya *et al.*, 1991; Venkatesh *et al.*, 1991) and pancreas (Belles *et al.*, 1987) and a slower time-course in whole-cell experiments (Belles *et al.*, 1987) so this might have implications for the present microelectrode study. Perhaps, in addition to an immediate action on channels in isolated membrane patches, glibenclamide has some delayed effect on membrane conductance associated with slower second-messenger systems or by some metabolic pathway compartmentalised within the cardiac cells. These second messenger systems might be better preserved by use of microelectrode techniques.

While physicochemical properties of sulphonylureas may contribute to components of their biological activity in pancreatic β-cells (Zünkler *et al.*, 1989), it is at present unclear to what extent these factors come into play in myocardial tissue. Since sulphonylureas are generally more potent in electrophysiological terms in pancreatic tissue compared to cardiac muscle (Trube *et al.*, 1986; Belles *et al.*, 1987), ATP-dependent potassium channel blockers with greater cardioselectivity would obviously be desirable for the management of some ischaemic cardiac rhythm disturbances.

Conclusion

Class III agents clearly have an important role to play in the management of certain atrial and ventricular rhythm disturbances in normoxic situations, whereas glibenclamide would be ineffective. In a pro-arrhythmic ischaemic environment, a compound with a glibenclamide-like profile (showing decreased dispersion of refractoriness) would probably be more effective than a Class III agent. Indeed, the Class III agent might still prolong APD in normoxic tissue and exacerbate the dispersion in refractoriness between normoxic and ischaemic tissue. However, a more complete understanding of the functional effects of glibenclamide against ischaemic arrhythmias is desirable in a wider range of species *in vivo* before ATP-dependent potassium channel blockers can be used clinically in the treatment of lethal ventricular arrhythmias which arise after acute myocardial ischaemia.

The Class III compounds were prepared for us by our colleagues in the Cardiovascular Chemistry Department and we are particularly grateful to M.G. Carr, R.M. Dunsdon, D.N., Hurst, Dr P.S. Jones and Dr P.B. Kay for their assistance. We would also like to thank David Adams, Sara Cooper, Nagin Lad and Ian Lightbown for their comments and Helen Searle for her help in the preparation of this manuscript.

References

ANTONACCIO, M.J. & GOMOLL, A.W. (1988). Sotalol-pharmacological and antiarrhythmic effects. *Cardiovasc. Drug Rev.*, **6**, 239–263.

BELLES, B., HESCHELER, J. & TRUBE, G. (1987). Changes of membrane currents in cardiac cells induced by long whole-cell recordings and tolbutamide. *Pflügers Arch.*, **409**, 582–588.

CARMELIET, E. (1985). Electrophysiologic and voltage clamp analysis of the effects of sotalol on isolated cardiac muscle and Purkinje fibers. *J. Pharmacol. Exp. Ther.*, **232**, 817–825.

CAST INVESTIGATORS (1989). Preliminary report: effect of encainide and flecainide on mortality in a randomized trial of arrhythmia suppression after myocardial infarction. *New Engl. J. Med.*, **321**, 406–412.

COBBE, S.M. (1988). Editorial: modification of class III antiarrhythmic activity in abnormal myocardium. *Cardiovasc. Res.*, **22**, 847–854.

FOSSET, M., DE WEILLE, J.R., GREEN, R.D., SCHMID-ANTOMARCHI, H. & LAZDUNSKI, M. (1988). Antidiabetic sulphonylureas control action potential properties in heart cells via high affinity receptors that are linked to ATP-dependent K^+ channels. *J. Biol. Chem.*, **263**, 7933–7936.

GETTES, L.S. (1986). Effect of ischemia on cardiac electrophysiology. In *The Heart and Cardiovascular System*, ed. Fozzard, H.A., Haber, E., Jennings, R.B., Katz, A.M. & Morgan, H.E. pp. 1317–1341. New York: Raven Press.

GILES, W.R. & SHIBATA, E.F. (1985). Voltage clamp of bull-frog cardiac pace-maker cells: a quantitative analysis of potassium currents. *J. Physiol.*, **368**, 265–292.

GWILT, M., ARROWSMITH, J.E., BLACKBURN, K.J., BURGES, R.A., CROSS, P.E., DALRYMPLE, H.W. & HIGGINS, A.J. (1991a). UK-68,798: a novel, potent and highly selective class III antiarrhythmic agent which blocks potassium channels in cardiac cells. *J. Pharmacol. Exp. Ther.*, **256**, 318–324.

GWILT, M., DALRYMPLE, H.W., BURGES, R.A., BLACKBURN, K.J., DICKINSON, R.P., CROSS, P.E. & HIGGINS, A.J. (1991b). Electrophysiologic properties of UK-66,914, a novel class III antiarrhythmic agent. *J. Cardiovasc. Pharmacol.*, **17**, 376–385.

GWILT, M., SOLCA, A.M., BURGES, R.A., BLACKBURN, K.J. & HIGGINS, A.J. (1989). Antifibrillatory action and haemodynamic properties of UK-68,798, a new class III antiarrhythmic agent, in anaesthetised dogs. *J. Mol. Cell. Cardiol.*, **21**, (Supp. II), S.11.

JANSE, M.J. & WIT, A.L. (1989). Electrophysiological mechanisms of ventricular arrhythmias resulting from myocardial ischemia and infarction. *Physiol. Rev.*, **69**, 1049–1169.

KATOH, H., OGAWA, S., FURUNO, I., SATO, Y., YOH, S., SAEKI, K. & NAKAMURA, Y. (1990). Electrophysiologic effects of E-4031, a Class III antiarrhythmic agent, on re-entrant ventricular arrhythmias in a canine 7-day-old myocardial infarction model. *J. Pharmacol. Exp. Ther.*, **253**, 1077–1082.

KODAMA, I., WILDE, A., JANSE, M.J., DURRER, D. & YAMADA, K. (1984). Combined effects of hypoxia, hyperkalemia and acidosis on membrane action potential and excitability of guinea-pig ventricular muscle. *J. Mol. Cell. Cardiol.*, **16**, 247–259.

LAD, N. & MACKENZIE, I. (1991). Limited effect of Class III agents against acute ischaemic arrhythmias in anaesthetised cats. *J. Mol. Cell. Cardiol.*, **23**, (suppl. V), S.38.

LYNCH, J.J., HEANEY, L.A., WALLACE, A.A. GEHRET, J.R., SELNICK, H.G. & STEIN, R.B. (1990). Suppression of lethal ischemic ventricular arrhythmias by the class III agent E4031 in a canine model of previous myocardial infarction. *J. Cardiovasc. Pharmacol.*, **15**, 764–775.

MACKENZIE, I., WATERFALL, J.F., JONES, P.S. & DUNSDON, R.M. (1990). Comparison of class III antiarrhythmics and glibenclamide on action potentials from guinea pig papillary muscle under normoxic and hypoxic conditions. *Br. J. Pharmacol.*, **100**, 320P.

MATSUURA, H., EHARA, T. & IMOTO, Y. (1987). An analysis of the delayed outward current in single ventricular cells of the guinea-pig. *Pflügers Arch.*, **410**, 596–603.

NADEMANEE, K. & SINGH, B.N. (1990). Effects of sotalol on ventricular tachycardia and fibrillation produced by programmed electrical stimulation: comparison with other antiarrhythmic agents. *Am. J. Cardiol.*, **65**, 53A–57A.

NAKAYA, H., TAKEDA, Y., TOHSE, N. & KANNO, M. (1991). Effects of ATP-sensitive K^+ channel blockers on the action potential shortening in hypoxic and ischaemic myocardium. *Br. J. Pharmacol.*, **103**, 1019–1026.

NOMA, A. (1983). ATP regulated potassium channels in cardiac muscle. *Nature*, **305**, 147–148.

SANGUINETTI, M.C. & JURKIEWICZ, N.K. (1990). Two components of delayed rectifier K^+ current. Differential sensitivity to block by Class III antiarrhythmic compounds. *J. Gen. Physiol.*, **96**, 195–215.

SANGUINETTI, M.C., SCOTT, A.L., ZINGARO, G.J. & SIEGL, P.K.S. (1988). BRL 34915 (cromakalim) activates ATP-sensitive K^+ current in cardiac muscle. *Proc. Natl. Acad. Sci. U.S.A.*, **85**, 8360–8364.

SAVILLE, V.L., MACKENZIE, I., CARR, M.G. & KAY, P.B. (1991). Glibenclamide, but not the Class III compounds E-4031, prolongs ischaemic action potentials in guinea-pig papillary muscle. *Br. J. Pharmacol.*, **104**, 21P.

SAWADA, K., NOMOTO, K.-I. & HIRAOKA, M. (1988). Effects of a novel class 3 antiarrhythmic agent, E-4031, on ventricular arrhythmias. *Jpn. Circ. J.*, **52**, 919–920.

SHIBASAKI, T. (1987). Conductance and kinetics of delayed rectifier potassium channels in nodal cells of the rabbit heart. *J. Physiol.*, **387**, 227–250.

TANDE, P.M., BJØRNSTAD, H., YANG, T. & REFSUM, H. (1990). Rate-dependent class III antiarrhythmic action, negative chronotropy, and positive inotropy of a novel I_k blocking drug, UK-68,798: potent in guinea pig but no effect in rat myocardium. *J. Cardiovasc. Pharmacol.*, **16**, 401–410.

TRUBE, G. & HESCHELER, J. (1984). Inward-rectifying channels in isolated patches of the heart cell membrane: ATP-dependence and comparison with cell-attached patches. *Pflügers Arch.*, **401**, 178–184.

TRUBE, G., RORSMAN, P. & OHNO-SHOSAKU, T. (1986). Opposite effects of tolbutamide and diazoxide on the ATP-dependent K^+ channel in mouse pancreatic β-cells. *Pflügers Arch.*, **407**, 493–499.

VAUGHAN WILLIAMS, E.M. (1970). The classification of antiarrhythmic drugs. In *Symposium on Cardiac Arrhythmias*, ed. Sandoe, E., Flensted-Jensen, E. & Olesen, K.H. pp. 449–472. Sodertalje: AB Astra.

VENKATESH, N., LAMP, S.T. & WEISS, J.N. (1991). Sulfonylureas, ATP-sensitive K^+ channels, and cellular K^+ loss during hypoxia, ischemia, and metabolic inhibition in mammalian ventricle. *Circ. Res.*, **69**, 623–637.

WEISS, J.M. & LAMP, S.T. (1989). Cardiac ATP-sensitive K^+ channels. Evidence for preferential regulation by glycolysis. *J. Gen. Physiol.*, **94**, 911–935.

WETTWER, E. (1990). The antiarrhythmic agent E-4031 prolongs action potentials in guinea-pig cardiomyocytes by the inhibition of an ionic current different from the delayed rectifier (I_k). *Naunyn-Schmied. Arch. Pharmacol.*, **341**, R53.

WOOSLEY, R.L., BARBEY, J.T., WANG, T. & FUNCK-BRENTANO, C. (1990). Concentration/response relations for the multiple antiarrhythmic actions of sotalol. *Am. J. Cardiol.*, **65**, 22A–27A.

ZUANETTI, G. & CORR, P.B. (1991). Antiarrhythmic efficacy of a new class III agent, UK-68,798, during chronic myocardial infarction: evaluation using three-dimensional mapping. *J. Pharmacol. Exp. Ther.*, **256**, 325–334.

ZÜNKLER, B.J., LENZEN, S., MÄNNER, K., PANTEN, U. & TRUBE, G. (1988). Concentration-dependent effects of tolbutamide, meglitinide, glipizide, glibenclamide and diazoxide on ATP-regulated K^+ currents in pancreatic β-cells. *Pflügers Arch.*, **337**, 225–230.

ZÜNKLER, B.J., TRUBE, G. & PANTEN, U. (1981). How do sulfonylureas approach their receptor in the β-cell membrane? *Naunyn-Schmied. Arch. Pharmacol.*, **340**, 328–332.

(Received April 19, 1993
Revised May 17, 1993
Accepted May 21, 1993)

Br. J. Pharmacol. (1993), **110**, 539–547

Characteristics of the binding of [^{3}H]-GR32191 to the thromboxane (TP-) receptor of human platelets

[1]Roma A. Armstrong, [2,]*P.P.A. Humphrey & *P. Lumley

Department of Pharmacology, University of Edinburgh Medical School, 1 George Square, Edinburgh EH8 9JZ and *Department of Cardiovascular and Respiratory Pharmacology, Glaxo Group Research Ltd., Park Road, Ware, Herts SG12 0DP

1 The interaction of the specific thromboxane (TP-) receptor blocking drug, [^{3}H]-GR32191 with human intact platelets and platelet membranes has been investigated *in vitro*.

2 On intact platelets, association of specific [^{3}H]-GR32191 binding at 37°C was biphasic, with an initial rapid component and a slower secondary phase. Dissociation experiments indicated displacement from two sites with $t_{\frac{1}{2}}$ values of 8.1 and 65.6 minutes. K_d values derived from the kinetic rate constants for the rapid onset/offset and slow onset/offset phases were 0.4 and 0.5 nM respectively.

3 Competition binding of [^{3}H]-GR32191 and GR32191 on intact platelets gave an IC_{50} of 2.3 nM. Scatchard analysis indicated a single class of binding site with a K_d of 2.2 nM. Further analysis of the data yielded a Hill slope of -1.0 again indicating an interaction at a single binding site. Saturation binding experiments gave a similar estimate of the K_d value for [^{3}H]-GR32191 to that obtained from competition binding experiments. A possible explanation for the biphasic interaction of the GR32191 in intact platelets may lie in restriction of its access to and egress from a population of TP-receptors.

4 In platelet membranes at 37°C, specific [^{3}H]-GR32191 binding was complete within 5 min with a calculated association rate constant of 3.2×10^8 M^{-1} min^{-1}. Dissociation of [^{3}H]-GR32191 was relatively slow, with measurable specific binding persisting for >40 min. Analysis of these data yielded a $t_{\frac{1}{2}}$ of 17.7 min and a dissociation rate constant of 0.04 min^{-1} and indicated dissociation from a single site. The $t_{\frac{1}{2}}$ for dissociation appeared to be related to the contact time of platelet membranes with [^{3}H]-GR32191. Derivation of a K_d from the kinetic rate constants gave a value of 0.13 nM.

5 Competition binding of [^{3}H]-GR32191 and GR32191 to platelet membranes gave an IC_{50} value of 3.5 nM. Scatchard analysis of these data indicated a single binding site with a K_d of 2.1 nM. Saturation binding experiments with [^{3}H]-GR32191 yielded similar IC_{50} and K_d values to those from competition experiments.

6 In further competition binding experiments, the TP-receptor agonists U-46619, STA_2, EP171 and 9,11-azo PGH_2 and antagonists SQ29,548, BM 13.177 and EP092 all competed with specific [^{3}H]-GR32191 binding on intact platelets and, where determined, on platelet membranes. All compounds fully displaced specific [^{3}H]-GR32191 binding. However, where tested, the IC_{50} values for a particular compound were always greater when [^{3}H]-GR32191 was the radioligand than when [^{3}H]-SQ29,548 was used. At the concentrations used in these studies (2 and 5 nM respectively), platelets appeared to bind approximately twice as much [^{3}H]-GR32191 as [^{3}H]-SQ29,548.

7 In conclusion, the interaction of [^{3}H]-GR32191 with human intact platelets was complex but the data were consistent with an action at a single class of binding site; from competition experiments this appears to be the functional TP-receptor. The interaction of the drug with this binding site is, however, characterized by a slow dissociation. This characteristic was confirmed in studies with platelet membranes and does not therefore appear to be an artefact of diffusion. Estimates of the K_d of the drug differed depending on the method of determination. Because of the slow dissociation of [^{3}H]-GR32191, those relying upon equilibrium of the radioligand with competing agent may be unreliable. The rate of dissociation also appeared to be related to the contact time of drug with receptor. An explanation for this phenomenon may lie in the ability of GR32191 to induce a change in the conformational state or location of the human platelet TP-receptor.

Keywords: Human platelet; thromboxane A_2 receptor blocking drug; radioligand binding; thromboxane A_2 receptor

Introduction

Thromboxane (Tx) A_2 is a potent platelet aggregatory and vasoconstrictor agent which has been implicated in the pathophysiology of occlusive vascular disease (FitzGerald *et al.*, 1987). To exert its effects, TxA_2 appears to act at a specific receptor which has been termed a TP-receptor (Coleman *et al.*, 1984). GR32191 is a potent and specific TP-receptor blocking drug which prevents human platelet aggregation and contraction of vascular smooth muscle induced by TxA_2 and its mimetics (Lumley *et al.*, 1989; Hornby *et al.*, 1989). The interaction of GR32191 with the human platelet TP-receptor has been supported by its ability to compete for binding with the TP-receptor radioligand [^{125}I]-PTAOH, the K_i for inhibition of binding being in close agreement with the K_d value obtained from functional studies (Lawrence *et al.*, 1988). However, in these functional studies, GR32191 appeared to antagonize U-46619-induced platelet aggregation in an non-competitive manner, with slopes of the Schild plot being significantly greater than unity (Lumley *et al.*, 1989). In addition, the attainment of the peak aggregatory response to U-46619 was slowed in the presence of GR32191. At concentrations approximately 10–30 times greater than the estimated pA_2 value, an unsurmountable antagonism of U-46619-in-

[1] Author for correspondence.
[2] Present address: Glaxo Inst. Applied Pharmacology, Dept. Pharmacology, University of Cambridge, Tennis Court Road, Cambridge CB2 1QJ.

duced platelet aggregation was seen. This profile of GR32191 appeared unique to platelets since the antagonism of U-46619-induced contraction of vascular smooth muscle was competitive and surmountable (Lumley *et al.*, 1989).

The aim of the present study was therefore to investigate the binding of GR32191 to the human platelet. To achieve this, [^{3}H]-GR32191 was prepared and binding investigated both in intact platelets and in a platelet membrane preparation. For comparison with results observed with [^{3}H]-GR 32191, binding studies were also performed with [^{3}H]-SQ 29,548 (Hedberg *et al.*, 1988). This TP-receptor blocking drug potently antagonizes U-46619-induced human platelet aggregation (Lumley *et al.*, 1989). However, unlike GR32191, the antagonism produced by SQ29,548 appears to be competitive, with slopes of the Schild regression not significantly different from unity (Lumley, unpublished). In addition no marked slowing of the aggregatory response to U-46619 is observed in the presence of SQ29,548. In binding studies [^{3}H]-SQ29,548 associates and dissociates rapidly from human platelets and appears to represent a relatively uncomplicated radioligand for studying the platelet TP-receptor (Hedberg *et al.*, 1988).

Methods

Preparation of human platelet and platelet membrane suspensions

Human blood (180 ml) was withdrawn from the ante-cubital vein and mixed with 36 ml acid-citrate-dextrose solution (see Drugs used) before centrifugation at 250 *g* for 20 min to give platelet-rich plasma (PRP). Following addition of prostacyclic (30 nM) the PRP was further centrifuged at 450 *g* for 20 min to give a platelet pellet. For intact platelet studies the pellet was resuspended in 15 ml of assay buffer. For membrane studies, platelet pellets were frozen at − 20°C, thawed, resuspended in assay buffer and the suspension homogenized on ice in a Ystral homogenizer.

Radioligand assay

Each assay tube contained 360 µl buffer, [^{3}H]-GR32191 (final concentration of 2 nM added in 10 µl), 50 µl buffer or test compound and 80 µl of intact platelets or platelet membrane suspension.

Association experiments To determine the association rate of [^{3}H]-GR32191, platelets or platelet membranes were incubated with 2 nM of the radioligand at 37°C for various periods of time. Incubation was terminated by the addition of 3 ml of ice-cold assay buffer and rapid filtration under suction through Whatman GF/B glass fibre filters using a Brandell cell harvester. Filters were rinsed three times with 3 ml of ice-cold buffer, placed in counting vials containing 3 ml of scintillant and counted in a scintillation counter.

Dissociation experiments Association of 2 nM [^{3}H]-GR32191 with whole platelets or platelet membranes was achieved by incubation at 37°C for 30 min before dissociation was initiated by the addition of 5 µM unlabelled GR32191. Samples were incubated at 37°C for various lengths of time after the addition of unlabelled GR32191 before the reaction was stopped as above. In some experiments the dissociation of [^{3}H]-SQ29,548 (5 nM) was determined in the same way.

Competition experiments Drugs tested for competition with [^{3}H]-GR32191 binding were added either to platelet membranes or intact platelets in concentrations ranging from 0.1 nM to 10 µM simultaneously with 2 nM [^{3}H]-GR32191 and incubated for 30 min at 37°C before termination of the reaction as above. When aggregatory agonists were studied, 4 nM cicaprost (Sturzebecher *et al.*, 1986) was included to prevent platelet aggregation. Inhibition experiments using [^{3}H]-SQ29,548 were carried out as for GR32191, except that the concentration of radioligand used was 5 nM.

Saturation experiments Increasing concentrations of [^{3}H]-GR32191 (2–50 nM) were incubated for 30 min at 37°C with either intact platelets or membranes before terminating the reaction.

Non-specific binding (NSB) In all experiments described above, NSB was determined at either each or selected time points by co-incubating 5 µM GR32191 with samples containing 2 nM [^{3}H]-GR32191. In some experiments on intact platelets, EP092 (5 µM) was used instead of GR32191.

Analysis of data

All analyses were performed only on data (counts min^{-1}, c.p.m.) expressed as specific binding utilising published methods/programmes (see Barlow, 1983).

Association/dissociation Association of [^{3}H]-GR32191 with both intact platelets and platelet membranes was analysed by linear regression of $\log_{10}$ bound [^{3}H]-GR32191 at equilibrium (B_{eq}; c.p.m.) divided by B_{eq} minus the amount bound at any given time (B_t) against time, using a computerised least-squares fit to a straight line ('Linefit'). K_{obs} was determined from the slope of the regression × 2.303 and the association rate constant (k_{+1}) determined as

$$k_{+1} = \frac{K_{obs} - k_{-1}}{[L]}$$

where k_{-1} and [L] are the dissociation rate constant and the radioligand concentration respectively.

The dissociation rate constant (k_{-1}) was determined using the data from each individual dissociation curve by a least-squares fit of bound [^{3}H]-GR32191 (B) to time ('Expofit') according to the equation $B = B_o e^{-kt}$ where B_o is the c.p.m. prior to addition of excess GR32191 ('time zero') and $k = k_{-1}$. The time to half dissociation ($t_{\frac{1}{2}}$) was calculated from the k_{-1} value as:

$$t_{\frac{1}{2}} = \frac{0.693}{k_{-1}}$$

With some data (see Figure 3), points lay consistently above or below the fitted line suggesting that a two phase dissociation process may be involved. In these instances data were fitted to $B = B_o[e^{-k1t} + e^{-k2t}]$ using the programme 'Doublexp' which yielded two rate constants.

Competition studies IC_{50} values were determined from competition studies by analysing specifically bound [^{3}H]-GR 32191 (c.p.m.) versus concentration of competing agent using 'Polyfit' (Barlow, 1991).

Saturation binding K_d values were determined from saturation binding data using a direct fit to a hyperbola using 'Hypmic'.

Scatchard analysis K_d was determined from Scatchard analysis which was performed on data from both competition and saturation experiments. A plot of bound (fmol/assay tube) divided by free (nM) [^{3}H]-GR32191 versus bound [^{3}H]-GR32191 (fmol/assay tube) was analysed by linear regression ('Linefit'). The negative reciprocal of the slope of the line was equivalent to K_d. Competition data were also analysed using a Hill plot of the data according to the equation, log $B/B_{max} - B$ vs log [L] ('Inhibition') with a B_{max} estimated from the Scatchard plot of the same data.

For all graphical presentations of data, the linear regression programme 'Linefit' was used to obtain the line of best fit.

Drugs used

The assay buffer (pH 7.4) had the following composition (mM); NaCl 100, glucose 5, Tris HCl 50 and contained indomethacin (1 μM). Acid citrate-dextrose solution was prepared by dissolving disodium hydrogen citrate (2 g) and glucose (3 g) in 120 ml of distilled water. All reagents were Analar grade and obtained from BDH. Prostacyclin (PGI_2) sodium salt (Schering A.G.) was prepared as a 50 μg ml^{-1} stock solution in 50 mM Tris-HCl, pH 9.0; dilutions were prepared in saline. Cicaprost (ZK96480, Schering) was dissolved in saline to give a stock solution of 50 μg ml^{-1}. Indomethacin (Sigma) was prepared as a 10 mM solution in absolute ethanol; dilutions were prepared in saline. [^{3}H]-GR32191 hydrochloride salt (specific activity 48.3 Ci mmol^{-1}; >96% pure) was tritiated at Amersham and incorporated two tritium atoms in the alkyl carboxyclic acid chain of the GR32191 molecule (Figure 1) and was supplied as a 50 μM solution in ethanol. Dilutions were prepared in the assay buffer to give a final concentration of ethanol of 0.04% v/v in each assay tube. GR32191 (1α-(6'-carboxyhex-3'2-enyl)-2β-(N-piperidino)-3α-hydroxy-5α-(4''-biphenylylmethoxy)-cyclopentane; hydrochloride salt, Glaxo Group Research) was prepared as an 2.0 mg ml^{-1} solution in saline. U-46619 (11α, 9α-epoxymethano PGH_2, Upjohn Diagnostics) was prepared as its sodium salt by dissolving in approximately 1% w/v $NaHCO_3$ in saline. Dilutions of these drugs were prepared using the assay buffer. [^{3}H]-SQ29,548 (2α-(6'-carboxyhex-2'z-enyl)-3α-(1'-(N-(phenylcarbamoyl)-hydrazino) methyl)-7-oxabicyclo [2,2,1] heptane, specific activity 30–60 Ci mmol^{-1}) was purchased from NEN. EP171 ((rac) 9α,11α-epoxy-10a-homo-16-p-fluorophenoxy-w-tetranor-15S-hydroxy-prosta-SZ, 13E-dienoic acid) and EP092 ((rac) 9α,11α-ethano-1-methyl-13 (N-phenyl thio-carbamoyl) hydrazono-w-heptanor-prosta-SZ-enoic acid) were synthesized in the Department of Pharmacology, Edinburgh University whilst the following were obtained as indicated; 9,11-azo PGH_2 (Upjohn), STA_2 (11a-carba-9,11-thia TXA_2, Ono), BM 13.177 (4-[2-[[(4-chlorophenyl) sulphonyl]amino] ethyl] benzeneacetic acid, Glaxo), SQ29,548 Squibb. Stock solutions of the prostanoids (5–10 mg ml^{-1}) were prepared in ethanol and stored at −20°C. Aqueous solutions were obtained by adding the calculated molar equivalent of NaOH, evaporating to dryness and dissolving the residue in warm saline. Further dilutions were prepared in assay buffer. PGI_2, cicaprost, U-46619 and GR32191 stock solutions were stored at −20°C between experiments. All drugs were stored on ice during an experiment.

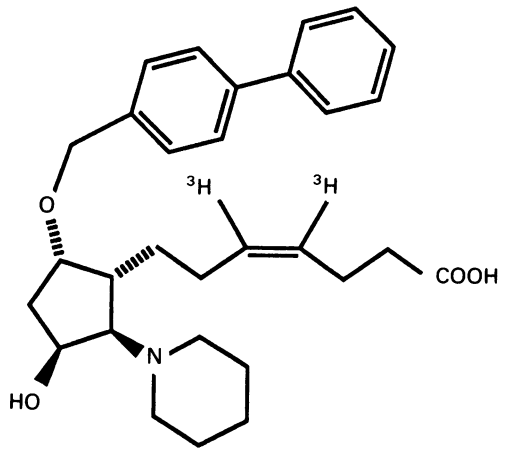

Figure 1 The chemical structure of [^{3}H]-GR32191.

Results

Intact platelets

The rate of association of [^{3}H]-GR32191 to intact platelets at 37°C was slow and complex. Although 80% of binding was

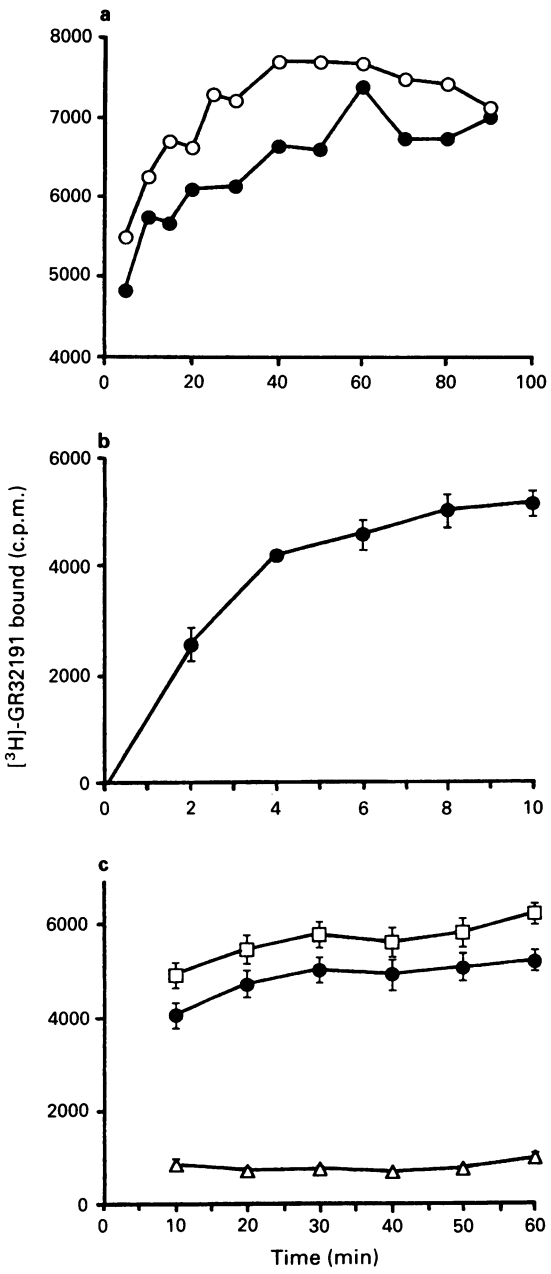

Figure 2 The onset of [^{3}H]-GR32191 (2 nM) binding to human intact platelets at 37°C. (a) Individual preliminary experiments showing total binding assessed over 90 min indicate an initial rapid (approximately 80% of maximum) phase of binding over 10 min followed by a more prolonged phase. In (b) and (c), the fast onset (0–10 min) and slower onset (10–60 min) specific binding phases are shown from separate series of experiments ($n = 4$ and 13 respectively). These data were analysed separately to obtain k_{+1} values using mean B_{eq} values, calculated from individual experiments, of 10 min for the slow component and 53 min for the fast component. Specific binding (●) was determined at total binding (□) minus non specific binding (NSB) (△), the latter being determined in the presence of 5 μM unlabelled GR32191. In (b), NSB was determined at 10 min whereas in (c) it was assessed routinely at virtually all time points to allow for an accurate assessment of the slow binding component. At time points where NSB was not determined, specific binding was calculated from an average value of NSB from adjacent time points. In (c), specific binding at 10 min was significantly less than binding at 30, 40, 50 and 60 min ($P < 0.05$, Student's t test).

Table 1 Association and dissociation rate constants and affinity constants for the interaction of [^{3}H]-GR32191 with human platelets and platelet membranes *in vitro*

			Intact platelets			
Measured variables	*Platelet membranes*	n	*Fast component*	n	*Slow component*	n
Association rate constant (k_{+1}) ($\times 10^8$ M^{-1} min^{-1})	3.2 ± 0.8	(4)	1.9 ± 0.3[a]	(4)	0.19 ± 0.0004[b]	(13)
k_{obs}	0.69 ± 0.16	(4)	0.46 ± 0.05[a]	(4)	0.05 ± 0.01[b]	(13)
Dissociation rate constant (k_{-1}) (min^{-1})	0.044 ± 0.004	(8)	0.093 ± 0.015	(4)	0.011 ± 0.001	(4)
$t_{\frac{1}{2}}$ (min)	17.7 ± 2.8	(8)	8.1 ± 1.5	(4)	65.6 ± 8.8	(4)
K_d (nM) c	2.1 ± 0.2	(8)		2.2 ± 0.1[e]	(4)	
d	1.8 ± 0.1	(4)		2.8 ± 0.03[e]	(6)	

[a]For calculation of k_{obs}, B_{eq} value taken at 10 min.
[b]For calculation of k_{obs}, B_{eq} value taken between 30–60 min (mean, 53 ± 3 min).
K_d was derived from [c] competition experiments between 2 nM [^{3}H]-GR32191 and increasing concentration of GR32191 and [d] saturation binding experiments using [^{3}H]-GR32191. [e]K_d measured on intact platelets for both fast and slow sites together.

complete within 10 min, equilibration of a slower component required 30–60 min. Figure 2a shows data from two preliminary experiments. Because of this complex profile, the fast component (0–10 min) and slow component (10–60 min) were analysed separately, with parallel comprehensive analysis of NSB in the case of the latter (Figures 2b and c). Values for k_{obs} and k_{+1} for the two components are shown in Table 1.

Initial experiments to examine the dissociation of [^{3}H]-GR32191 from intact platelets, indicated displacement from two sites. The best fit of the data from an initial series of experiments is shown in Figure 3a. Experiments were repeated (Figure 3b; $n = 4$), the log plot of these data being curvilinear (Figure 3c). Each individual dissociation curve was analysed separately by 'Doublexp' to derive $t_{\frac{1}{2}}$ and k_{-1} values for the fast and slow offset components separately (Table 1).

In some experiments in intact platelets the TP-receptor blocking drug, EP092 (5 μM; K_d 10 nM; Jones *et al.*, 1984), was used to determine the NSB of [^{3}H]-GR32191 for comparison with the value obtained with GR32191 itself (5 μM). In these experiments no significant difference was observed in the two determinations of NSB, with mean ($n = 4$) values of 876 ± 42 and 756 ± 85 c.p.m. being obtained with EP092 and GR32191 respectively.

Scatchard analysis of [^{3}H]-GR32191 binding in intact platelets was determined by two methods. Firstly, intact platelets were incubated with 2 nM [^{3}H]-GR32191 at 37°C for 30 min simultaneously with increasing concentrations of unlabelled GR32191. The mean competition curve is shown in Figure 4a and the mean IC_{50} for unlabelled GR32191 from individual experiments was 2.3 ± 0.1 nM ($n = 4$). Scatchard analysis of each experiment gave a straight line (mean $r = 0.90 \pm 0.05$) suggesting a single class of binding site with a K_d of 2.2 ± 0.1 nM (Figure 4b). Because of the suggestion of two binding sites from the dissociation experiments in intact platelets, data was also analysed by 'Inhibition'. Analysis of the data gave a Hill slope of − 1.0 ± 0.08 also suggesting the existence of one class of binding site. In the second method, intact platelets were incubated at 37°C for 30 min with increasing concentrations of [^{3}H]-GR32191. The individual saturation curves (data not shown) gave a mean K_d of 2.3 ± 0.2 nM ($n = 6$). Transformation of these data into Scatchard plots gave straight lines (mean $r = 0.91 \pm 0.02$), again indicating one class of binding site with a mean K_d of 2.8 ± 0.3 nM. The K_d values obtained by division of the measured kinetic rate constants (k_{-1}/k_{+1}) obtained with intact platelets for the fast onset/offset and slow onset/offset components were 0.5 nM and 0.4 nM respectively. This was some 5 fold lower than the K_d values obtained from both Scatchard analysis and functional experiments (1.7 ± 0.2 nM) of GR32191 antagonism of U-46619-induced human platelet aggregation (Lumley *et al.*, 1989).

Platelet membranes

Figure 5a shows the association binding of 2 nM [^{3}H]-GR32191 to platelet membranes. At 37°C, binding was virtually complete within 5 min and plateaued at this level for up to 20 min. The plot of log $B_{eq}/B_{eq} - B_t$ versus time (Figure 5b) for individual experiments gave a mean (± s.e.mean, $n = 4$) k_{obs} of 0.69 ± 0.16 and k_{+1} of 3.2 ± 0.8 × 10^8 M^{-1} min^{-1}. After incubation of 2 nM [^{3}H]-GR32191 with platelet membranes for 30 min at 37°C, addition of 5 μM unlabelled GR32191 reversed specific binding, but this dissociation was very slow (Figure 5c). Even 40 min after the addition of unlabelled GR32191, binding of [^{3}H]-GR32191 had not returned to the level of non-specific binding. Figure 5d shows the mean plot of the log bound ligand against time which yields a straight line consistent with dissociation from one site. Each individual dissociation curve was analysed separately and gave a mean ($n = 8$) $t_{\frac{1}{2}}$ value of 17.7 ± 2.8 min and dissociation rate constant k_{-1} value of 0.044 ± 0.004 min^{-1}. To investigate the possibility that the rate of dissociation of GR32191 from the platelet TP-receptor was related to the contact time, dissociation experiments were carried out using platelet membranes pre-incubated with 2 nM [^{3}H]-GR32191 for 5–10 and 15–20 min. The mean ($n = 5$–6) $t_{\frac{1}{2}}$ values obtained at these times were 8.5 ± 0.2 and 12.3 ± 1.7 min, respectively.

Scatchard analysis of binding of [^{3}H]-GR32191 to platelet membranes was determined, as for intact platelets, by two different methods. The mean IC_{50} for competition between unlabelled GR32191 and 2 nM [^{3}H]-GR32191 was 3.5 ± 0.2 nM ($n = 8$) (Figure 6a). When these data were transformed into Scatchard plots (Figure 6b), straight lines (mean $r = 0.93 \pm 0.01$) were obtained indicating one class of binding site with a mean K_d of 2.1 ± 0.2 nM. Increasing concentrations of [^{3}H]-GR32191 gave saturation binding curves (data not shown) with a mean K_d value of 1.6 ± 0.2 nM ($n = 4$). Again the Scatchard plots were straight lines (mean $r = 0.93 \pm 0.02$) indicating one class of binding site with a K_d of 1.8 ± 0.1 nM. These values again correlate well with the K_d value from functional studies. However, the K_d value obtained by division of the measured mean kinetic rate constants (k_{-1}/k_{+1}) was 0.14 nM and is therefore lower than the K_d value obtained from either Scatchard analysis or functional studies.

Competition experiments

The IC_{50} values for competition between either 2 nM [^{3}H]-GR32191 or 5 nM [^{3}H]-SQ29,548 and a range of TP-receptor agonists and antagonists for binding to intact human platelets and, where tested, to platelet membranes is shown in Table 2. SQ-29,548 is a TP-receptor antagonist with a reported K_d of 5 nM (Hedberg *et al.*, 1988). The drug dis-

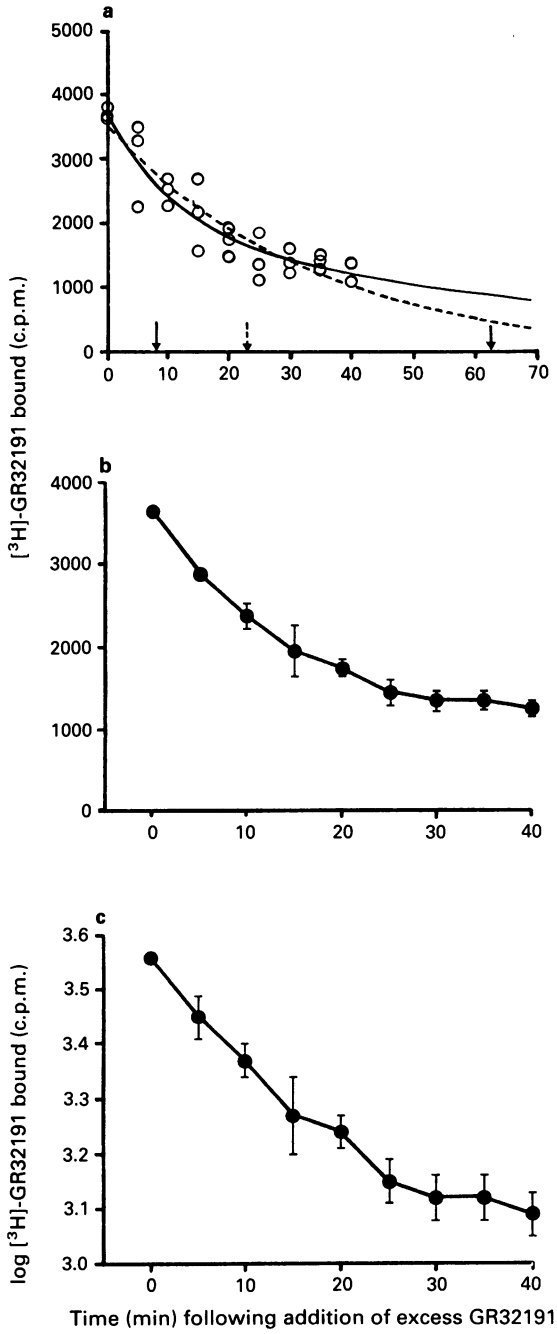

Figure 3 The dissociation of specific [3H]-GR32191 binding from human intact platelets at 37°C. Platelets were pre-incubated with 2 nM [3H]-GR32191 for 30 min at which time dissociation was instigated by the addition of 5 μM unlabelled GR32191 (time 0). In (a), dissociation data from a series ($n = 3$) of experiments has been fitted either to a single exponential (broken line) or to the equation $B = B_0[e^{-k_1 t} + e^{-k_2 t}]$ (solid line). Note that the scatter of data about the solid line is uniform compared with that around the broken line (and has a reduced standard deviation). The half times for the single exponential (broken arrow) and for the two phase dissociation (solid arrows) are indicated on the abscissa scale. In the experiments depicted in (b), each point represents the mean ± s.e.mean of 4 determinations. In all experiments in (a) and (b), determinations of control binding and nonspecific binding (NSB) were performed at the beginning ('0' min) and end ('40' min) of each experiment and showed that these values did not significantly change over this period. Mean ($n = 7$) control values of 5262 ± 37 and 5461 ± 158 c.p.m. and NSB values of 970 ± 53 and 826 ± 58 c.p.m. were obtained at the two times respectively. In (c), the log plot of the dissociation data is curvilinear and $t_{\frac{1}{2}}$ and k_{-1} values for a fast and slow component were determined from individual experiments by computer analysis (see text and Table 1).

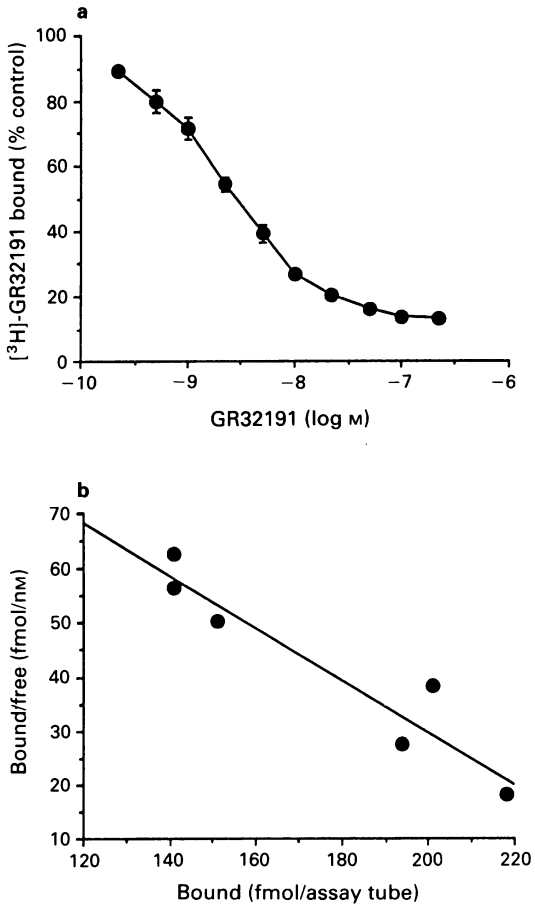

Figure 4 (a) Competition binding between 2 nM [3H]-GR32191 and unlabelled GR32191 in intact platelets. Each point represents the mean ± s.e.mean of 4 determinations. (b) Scatchard plot of the data in (a).

sociates from the TP receptor of human platelets very rapidly. For example, on intact platelets at 37°C it had a measured mean ($n = 3$) $t_{\frac{1}{2}}$ of 1.7 ± 0.14 min (this study). It was a consistent finding in these paired inhibition experiments that, at 2 and 5 nM respectively, the specific binding of [3H]-GR32191 to intact platelets was approximately twice that of [3H]-SQ29,548 (8065 ± 365 versus 3205 ± 296 c.p.m., $n = 16$). Scatchard analysis of a paired saturation binding experiment, performed in quadruplicate on a single preparation of platelet membranes, gave a K_d of 1.7 nM and an x intercept of 97.3 fmol for [3H]-GR32191 and values of 4.6 nM and 56.9 fmol for [3H]-SQ29,548. A part of these differences in binding of the two radioligands appeared to be accounted for by a difference in their specific activities (see Drugs used). The mean ($n = 4$, total counts added for each radioligand, 43991 ± 10760 c.p.m. for 2 nM [3H]-GR32191 and 78116 ± 5956 c.p.m. for 5 nM [3H]-SQ29,548, supported this view. Competition curves for U46619, EP171, STA_2 and SQ29,548 are shown in Figure 7. For all TP-receptor agonists and antagonists tested, the radioligand binding curves obtained with [3H]-GR32191 for the TP agonists lie to the right of those found using [3H]-SQ29,548 (Table 2 and Figure 7). However, all compounds tested were able to displace fully all specific [3H]-GR32191 and [3H]-SQ29,548 binding.

Discussion

The antagonism of TP-receptor-mediated human platelet aggregation by GR32191 is characterized by a slowing of the aggregatory response to agonist, suppression of its maximum effect and Schild regression slopes of greater than unity

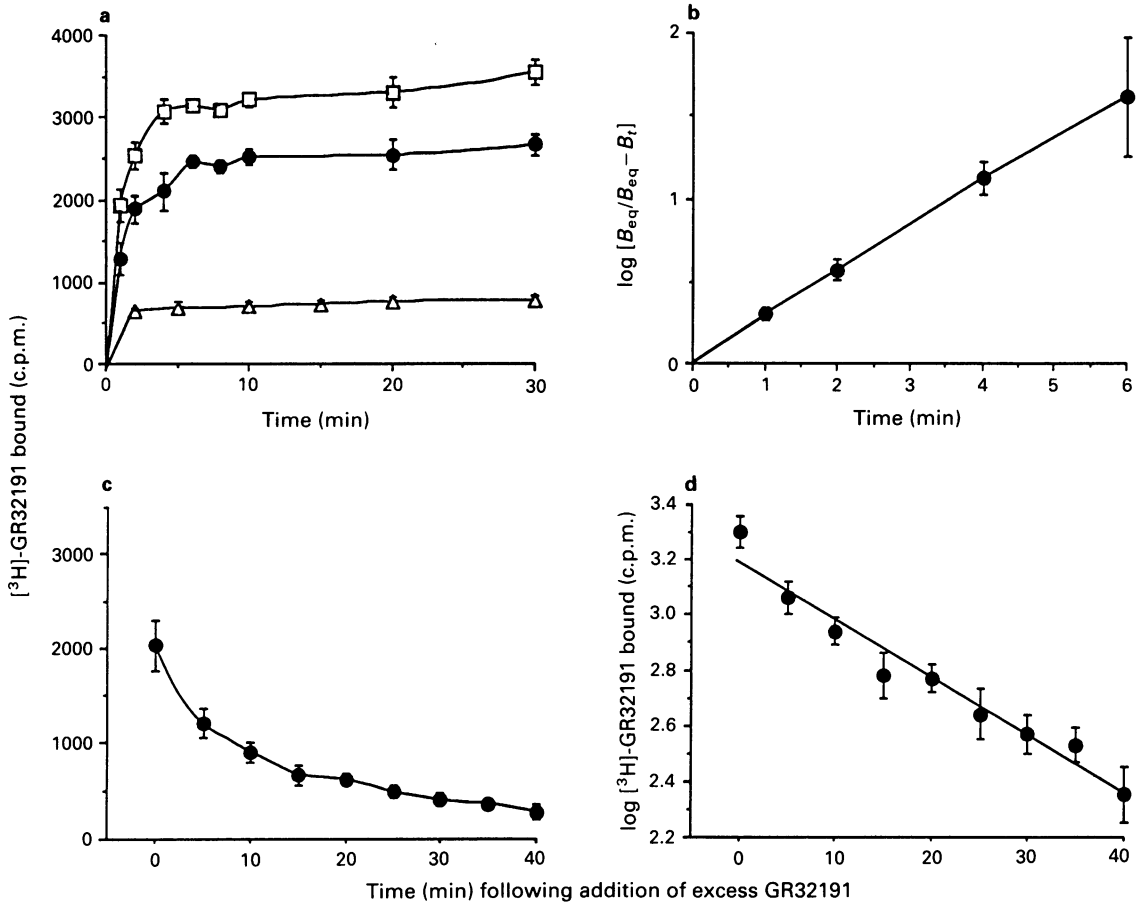

Figure 5 Onset (a and b) and dissociation (c and d) of specific [^{3}H]-GR32191 (2 nM) binding to human platelet membranes at 37°C. (a) Specific binding (●) was determined as total binding (□) minus nonspecific binding (NSB) △) the latter being determined in the presence of 5 μM unlabelled GR32191. NBS was not determined at each time point (see legend to Figure 2). Each point represents the mean ± s.e.mean of 4 determinations. (b) Log transformation of the specific binding data from experiments shown in (a). K_{obs} and association rate constant (k_{+1}) values quoted in text were derived from similar plots from individual experiments. In (c), membranes were pre-incubated with 2 nM [^{3}H]-GR32191 for 30 min at 37°C and then dissociation instigated by the addition of 5 μM unlabelled GR32191 (time 0). Specific binding data (i.e. total binding minus NSB) (●) are shown, each point representing the mean ± s.e.mean of 8 determinations. Determinations of control binding and NSB were performed at the beginning (0 min) and end (40 min) of each experiment and showed that these values did not change significantly over this period. Mean ($n = 8$) control values of 2298 ± 220 and 2371 ± 250 c.p.m. and NSB values of 643 ± 95 and 673 ± 79 c.p.m. were obtained at the two times respectively. (d) Log transformation of dissociation data from the individual experiments from (c). The slope of the plot gives the dissociation rate constant k_{-1}.

(Lumley *et al.*, 1989). In addition, the drug has a duration of action upon platelets in man, which far exceeds its detection in plasma (Thomas & Lumley, 1990). The present study has examined *in vitro*, the binding characteristics of GR32191 to the human platelet TP-receptor in an attempt to explain some of these phenomena. For this purpose [^{3}H]-GR32191 was synthesized, the resultant radioligand possessing high specific activity. The specific [^{3}H]-GR32191 binding studied appeared to occur with the platelet TP-receptor since it was fully prevented by a range of TP-receptor agonists and antagonists. In the present study, the interaction of [^{3}H]-GR32191 with both intact platelets and platelet membranes was investigated.

In intact platelets a complex picture emerged, with both association and dissociation of [^{3}H]-GR32191 occurring in two distinct phases. With association, although 80% of binding was complete within 10 min at 37°C, equilibration of a slower component required 30–60 min. Similarly, following a 30 min incubation, dissociation $t_{\frac{1}{2}}$ values of approximately 8 and 66 min were observed for the two phases. These data could be taken as evidence for [^{3}H]-GR32191 interacting at two sites. However, calculation of K_d values from the kinetic rate constants for the fast onset/offset and slow onset/offset phases yielded very similar values. In support of this, Scatchard analysis of competition and saturation binding data with [^{3}H]-GR32191 in intact platelets appeared to indicate binding of the drug at a single site. Takahara and colleagues (1990) have also studied the binding of [^{3}H]-GR32191 to human intact platelets. Association of the drug appeared to occur at a single site, whereas dissociation was biphasic and best described by a two site model. The slow dissociation component seen with [^{3}H]-GR32191 was more pronounced that that seen in the present study, possibly a reflection of the higher concentration of drug used (10 nM versus 2 nM in the two studies respectively).

One possible explanation for the association/dissociation profile observed in intact platelets with [^{3}H]-GR32191 in both the present study and that of Takahara and associates is that, in addition to binding to TP-receptors on the platelet surface, the drug also undergoes binding to an identical but 'internalised' TP-receptor. Being a zwitterion, GR32191 is highly charged at neutral pH and this would be expected to slow its passage, in both directions, across biological membranes so explaining the slow onset and offset. Studies with [^{3}H]-SQ29,548 also indicated the possible existence of such an internalised pool of receptors (Hedberg *et al.*, 1988). An alternative explanation is that a proportion of the TP-receptor population, with which the drug interacts, may become internalised. The latter hypothesis is supported by data *in vivo* in man where GR32191 treatment appears to

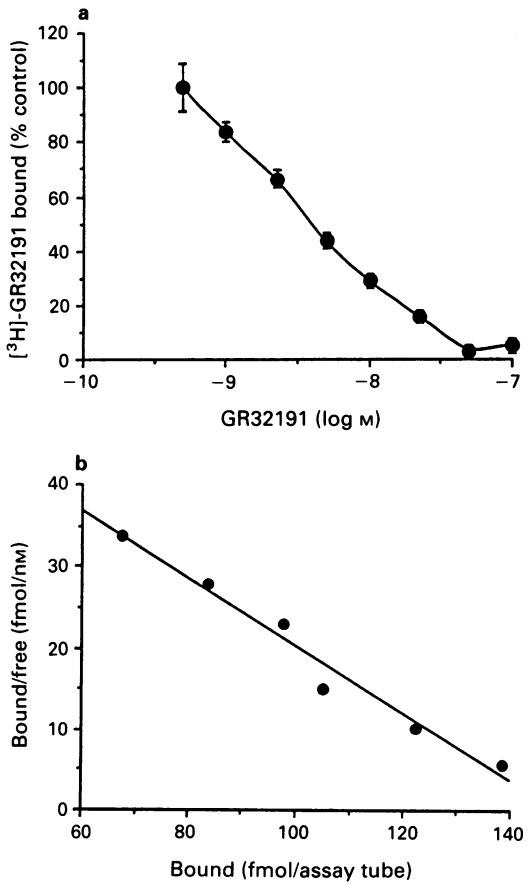

Figure 6 (a) Competition binding between 2 nM [^{3}H]-GR32191 and unlabelled GR32191 in platelet membranes. In (a) each point represents the mean ± s.e.mean of 8 determinations. (b) Scatchard plot of the data in (a).

result in a reduction of platelet TP-receptor density (see below) (Takahara *et al.*, 1990, Armstrong *et al.*, 1990). We are not aware of a similar biphasic association/dissociation profile being reported with other antagonists, although it is well established in studies on β-adrenoceptors that internalisation of the receptor occurs upon exposure to agonist which then results in a reduced access, and therefore binding, with certain ligands (Harden, 1983).

In the simpler membrane preparation, where potential artefacts arising from internalisation of receptors and diffusion of drugs are minimized, the onset of [^{3}H]-GR32191 binding was relatively rapid, reaching equilibrium at 37°C within 5 min. In contrast, the rate of dissociation following a 30 min incubation was slow at 37°C, with measurable specific binding persisting for greater than 40 min with a $t_{\frac{1}{2}}$ value of 17.7 min. This dissociation $t_{\frac{1}{2}}$ was directly related to the contact time of the drug, being 8.5 min with incubations of 5–10 min and 12.3 min with incubations of 15–20 min. Analysis of both association and dissociation data for [^{3}H]-GR32191 indicated interaction of the drug with a single site. From competition binding and saturation binding experiments with membranes, mean K_d values of approximately 2 nM were obtained. Scatchard analysis of these data also indicated interaction at a single binding site. In addition, the K_d values obtained agree closely with the corresponding value (1.7 nM) determined from functional studies on human platelets (Lumley *et al.*, 1989).

A feature of the present study on both membranes and intact platelets was that the K_d value determined from the kinetic rate constants, k_{+1} and k_{-1}, was lower than that determined from Scatchard analysis of both competition and saturation data and from functional experiments. Clearly, K_d values determined by all of these methods should theoretically be the same. However, the slow dissociation of the drug from platelets would suggest that, in some situations (see below) true equilibrium of a competing agent with the platelet TP-receptor may not occur, the so-called 'hemi-equilibrium' state (see Rang, 1966). Thus, the K_d value determined from experiments assumed to be at equilibrium, such as competition and functional studies may be unreliable, whereas those derived from kinetic experiments may be the more accurate.

Table 2 IC_{50} values for competition between [^{3}H]-GR32191 or [^{3}H]-SQ29,548 and a range of TP-receptor agonists and antagonists for binding to human intact platelets

	IC_{50} (nM)	
	[^{3}H]-GR32191	*[^{3}H]-SQ29,548*
TP-agonists		
U-46619	947 ± 134	220 ± 21
	1220 ± 150[a]	
STA_2	205 ± 39	87 ± 19
	420 ± 80[a]	
EP171	23.3 ± 2.0	5.4 ± 0.8
9,11-azo PGH_2	314.9 ± 15.6	NT
TP antagonists		
GR32191	2.3 ± 0.12	1.2 ± 0.12
SQ29,548	17.5 ± 2.1	5.7 ± 0.2
BM13.177	13,400 ± 1,200	NT
EP092	226.5 ± 22.5	NT

Values are the mean (± s.e.mean) from 4 experiments. For each drug, individual IC_{50} values for the two radioligands were obtained from paired experiments using blood from the same individual. NT = not tested.
[a]Value, obtained on human platelet membranes.

The present study points towards interaction of specifically bound [^{3}H]-GR32191 with a single site on human platelets. As mentioned, from competition experiments with a range of TP-receptor agonists and antagonists, specific [^{3}H]-GR32191 binding appeared to occur with the platelet TP-receptor. In paired experiments the ability of the same range of compounds to compete with [^{3}H]-SQ29,548 for binding was also studied. In general the IC_{50} values obtained with this range of compounds using [^{3}H]-SQ29,548, agree with those reported by others for it and other TP-receptor radioligands such as [^{3}H]-U-46619 and [^{125}I]-PTA-OH with values (range) for U-46619 of 9–125 nM, STA_2 27–220 nM, EP171 2.9 nM and SQ29,548 8–25 nM (Mais *et al.*, 1985; Kattelman *et al.*, 1986; Narumiya *et al.*, 1986; Liel *et al.*, 1987; Hedberg *et al.*, 1988; Lawrence *et al.*, 1988; Jones *et al.*, 1989). In contrast, IC_{50} values obtained with [^{3}H]-GR32191 for any given ligand were always greater than those obtained with [^{3}H]-SQ29,548 despite the fact that all compounds were able to displace fully both radioligands. In addition, at the radioligand concentrations used in these studies, platelets appeared to bind approximately twice as much [^{3}H]-GR32191 as they did [^{3}H]-SQ 29,548. Nevertheless, SQ29,548 was able to displace fully all the [^{3}H]-GR32191 specific binding.

The radioligands were used at concentrations (2 and 5 nM respectively), close to their K_d values determined from functional studies or Scatchard analysis of competition data. In addition both compounds possessed similar specific activities. However, as indicated above, the 'true' K_d value for GR 32191 may be closer to the value of 0.5 nM derived kinetically. Thus in terms of receptor occupancy, 2 nM [^{3}H]-GR 32191 would produce a disproportionately greater amount of binding than 5 nM [^{3}H]-SQ29,548 and would therefore require correspondingly greater concentrations of competing ligand to displace it. The K_i values for U-46619, STA_2, EP171 and GR32191, determined from the experiments using [^{3}H]-SQ29,548, were 117, 46.3, 2.9 and 0.64 nM respectively. Normally in the Cheng-Prusoff equation, the K_d of the radioligand is known whereas the K_i of the competing ligand is unknown. However, by utilising the above [^{3}H]-SQ29,548-derived K_i values in the Cheng-Prusoff equation, applied to

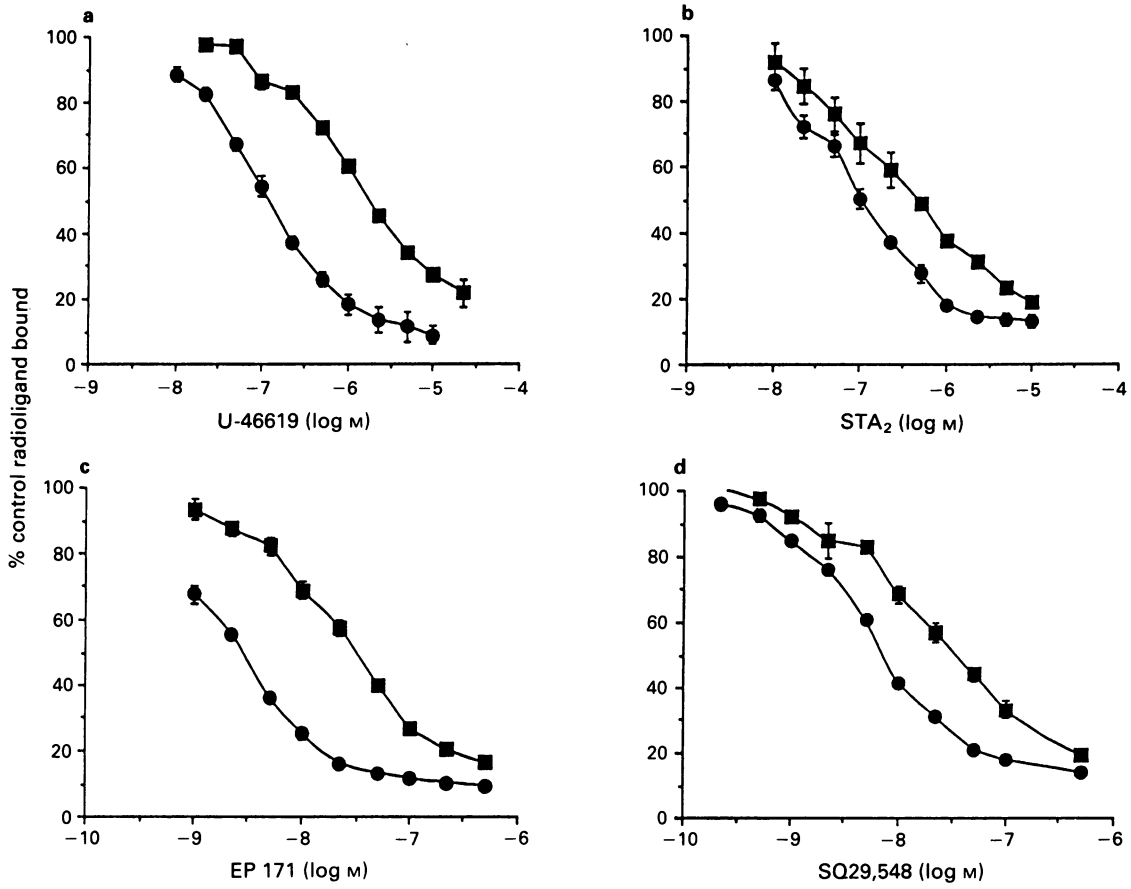

Figure 7 Competition between 2 nM [^{3}H]-GR32191 (■) or 5 nM [^{3}H]-SQ29,548 (●) and (a) U46619, (b) STA_2 (c) EP171, and (d) SQ29,548 for binding to intact platelets. For each compound, inhibition experiments were performed using both radioligands in the same preparation of platelets to allow for direct comparison of results. Results are mean ± s.e.mean of 4 determinations.

the corresponding data for each compound using [^{3}H]-GR 32191 as the radioligand, the K_d of [^{3}H]-GR32191 can be calculated as the unknown. From this exercise, K_d values for [^{3}H]-GR32191 of 0.3–0.8 (mean 0.5) nM are derived which are lower than those derived from Scatchard analysis or from functional studies and closer to the values derived from the kinetic constants.

The slow dissociation of [^{3}H]-GR32191 seen in the present study could explain the *in vitro* profile seen with the drug on platelets (slowing of aggregation, suppression of agonist maxima, Schild regression slopes greater than unity) (Lumley *et al.*, 1989; Hornby *et al.*, 1989). In the presence of a slowly dissociating antagonist, an agonist can only readily equilibrate with unoccupied receptors, the so-called 'hemi-equilibrium' state (see Rang, 1966). Equilibration of the agonist with antagonist-occupied receptors will be slower and be dictated by the dissociation rate of the complex. If the agonist requires only low occupancy to achieve a given response, then the response measured may not show any deviation from that predicted by a competitive model. However, when the agonist occupancy required for the given response is high, a slowing of the response will ensue, even in the presence of relatively small amounts of antagonist. With higher concentrations of antagonist, an agonist response may not occur at all, either because the biological response is not observed for long enough or, deactivation or desensitization processes in the cell nullify the slowly rising activation. In the case of platelet aggregation, it has been calculated that U-46619 requires approximately 40% receptor occupancy to achieve a full effect (Armstrong *et al.*, 1985). With this level of occupancy required by the agonist and in the presence of a slowly dissociating antagonist such as GR32191, a hemi-equilibrium state would be anticipated with consequential slowing of the response and suppression of the maxima.

Interestingly, in platelets, a maximum shape change response to U-46619 requires only 5% receptor occupancy (Armstrong *et al.*, 1985) indicating that this response is better coupled than is aggregation. In the case of the shape change, parallel rightward displacements of the U-46619 concentration-effect curve are observed in the presence of concentrations of GR32191 which suppress the aggregation responses to the same agonist (Lumley, unpublished). In this context, it is interesting to note that an apparent 'resistance' of U-46619-induced shape change to suppression by GR32191 compared with aggregation has been cited as evidence for these responses being mediated by different TP-receptors (Takahara *et al.*, 1990). In the latter study, platelets were exposed to GR32191 and then washed to remove the reversibly bound drug, U-46619-induced aggregation, phosphoinositide hydrolysis and 5-hydroxytryptamine secretion were inhibited, yet shape change and elevation of cytosolic Ca^{2+} induced by the agonist were not. However, in these studies, only a single, high concentration of U-46619 was used (1 μM). This would produce a supramaximal effect upon shape change but a sub- or just-maximal effect upon aggregation. It is quite feasible, therefore, that following exposure to GR32191 complete inhibition of aggregation could be observed whereas shape change, whilst being significantly antagonized, would appear to be unaffected because of the supra-maximal stimulus used. Construction of full concentration-effect curves for shape change and aggregation might resolve this question. However, it would seem premature at this stage to invoke the existence of two TP-receptor populations in human platelets.

The same *in vitro* functional profile on platelets, to that seen with GR32191, has been observed with other structurally-related compounds such as AH23848 (Brittain *et al.*, 1985). The slow dissociation of [^{3}H]-GR32191 from human platelet TP-receptors would not appear to be simply a function of its high potency since [^{3}H]-SQ29,548, which is of

similar potency (K_d = 5 nM), dissociates rapidly from human platelet membranes with a $t_{\frac{1}{2}}$ of 1.7 min at 37°C (this study). Furthermore, whilst SQ29,548 potently antagonizes TP-receptor agonist-induced aggregation of human platelets, no slowing of the aggregatory response, depression of the agonist maxima nor high slopes of the Schild regression is observed (Takahara *et al.*, 1990; Lumley, unpublished data). It is also interesting to note that, in contrast to platelets, on vascular smooth muscle GR32191 behaves as a fully surmountable and competitive TP-receptor blocking drug (Lumley *et al.*, 1989). This, like the shape change response of platelets described above, could reflect a better coupling of TP-receptor stimulation in vascular smooth muscle and therefore a less pronounced hemi-equilibrium phenomenon in this tissue.

It is also likely that slow dissociation of GR32191 from the platelet TP-receptor also, in part, accounts for its long duration *in vivo* in man following termination of oral dosing (Thomas & Lumley, 1990). However, such a mechanism alone seems unlikely to explain a duration in excess of 4 days seen in such studies (Thomas & Lumley, 1990; Takahara *et al.*, 1990). It is possible that the nature of the GR32191 binding changes with time, the binding being stronger the longer the drug is in contact with the TP-receptor. As mentioned above, the dissociation $t_{\frac{1}{2}}$ of [^{3}H]-GR32191 from platelet membranes appeared to be directly related to the initial contact time of the drug. In a further recent study (Armstrong *et al.*, 1990), we have presented evidence that prolonged incubation of human platelets with GR32191 *in vitro* or 'exposure' to the drug *in vivo* leads to a reduction in the density of platelet TP-receptors. Takahara and colleagues (1990) have also demonstrated a similar phenomenon, with suppression of platelet aggregation in patients receiving GR 32191 being more closely correlated with a reduction in TP-receptor density than with plasma drug levels. The mechanism of this reduction in receptor number is, as yet, unknown.

In summary, the present study indicates that GR32191 interacts with a single site on human platelets which has the characteristics of the TP-receptor. In platelet membranes the interaction of the drug with the receptor is characterized by a slow dissociation which is directly related to contact time. In intact platelets the association and dissociation profile of GR32191 are more protracted, possibly due to interaction of the drug with 'internalised' receptors. Because of this complex profile, estimation of a true K_d value for the compound is difficult. The characteristics of the interaction of GR32191 with the human platelet TP-receptor probably explain its profile of action *in vitro* and may go some way to explaining its long duration following administration to man.

We wish to thank Dr Ian Fellows (Chemical Development, GGR) for assistance with supplies of [^{3}H]-GR32191, Dr Mike Sumner and Dr Anton Michel (Pharmacology Division, GGR) and Dr Harry Olverman (Dept. Pharmacology, Edinburgh University) for helpful criticism and discussion and Dr Dick Barlow for help and advice on data fitting.

References

ARMSTRONG, R.A., HUMPHREY, P.P.A. & LUMLEY, P. (1993). Reduction in the number of thromboxane receptors on human platelets after exposure to GR32191. *Br. J. Pharmacol.*, **110**, 548–552.

ARMSTRONG, R.A., JONES, R.L., PEESAPATI, V., WILL, S.G. & WILSON, N.H. (1985). Competitive antagonism at thromboxane receptors in human platelets. *Br. J. Pharmacol.*, **84**, 595–607.

ARMSTRONG, R.A., LUMLEY, P. & HUMPHREY, P.P.A. (1990). Reduction in the number of thromboxane receptor (B_{max}) on human platelets after exposure to GR32191. *Br. J. Pharmacol.*, **99**, 113P.

BARLOW, R.B. (1983). *Biodata Handling with Microcomputers*. Cambridge, England: Elsevier.

BARLOW, R.B. (1991). *Foundation of Pharmacology*. Cerberus Printing.

BRITTAIN, R.T., BOUTAL, L., CARTER, M.C., COLEMAN, R.A., COLLINGTON, E.W., GEISOW, H.P., HALLETT, P., HORNBY, E.J., HUMPHREY, P.P.A., JACK, D., KENNEDY, I., LUMLEY, P., MCCABE, P.J., SKIDMORE, I.F., THOMAS, M. & WALLIS, C.J. (1985). AH23848: a thromboxane receptor-blocking drug that can clarify the pathophysiological role of thromboxane A_2. *Circulation*, **72**, 1208–1218.

COLEMAN, R.A., HUMPHREY, P.P.A., KENNEDY, I. & LUMLEY, P. (1984). Prostanoid receptors – the development of a working classification. *Trends Pharmacol. Sci.*, **5**, 303–306.

FITZGERALD, G.A., HEALY, C. & DAUGHERTY, J. (1987). Thromboxane A_2 biosynthesis in human disease. *Fed. Proc.*, **46**, 154–158.

HARDEN, T.K. (1983). Agonist-induced desensitization of the β-adrenergic receptor-linked adenylate cyclase. *Pharmacol. Rev.*, **35**, 5–32.

HEDBERG, A., HALL, S.E., OGLETREE, M.L., HARRIS, D.N. & LIU, E.C.-K. (1988). Characterisation of [5,6-^{3}H] SQ29,548 as a high affinity radioligand binding to thromboxane A_2/Prostaglandin H_2-receptors in human platelets. *J. Pharmacol. Exp. Ther.*, **245**, 786–792.

HORNBY, E.J., FOSTER, M.R., MCCABE, P.J. & STRATTON, L.E. (1989). The inhibitory effect of GR32191, a thromboxane receptor blocking drug, on human platelet aggregation, adhesion and secretion. *Thromb. Haemostas.*, **61**, 429–436.

JONES, R.L., WILSON, N.H., ARMSTRONG, R.A. & DONG, Y.J. (1984). Receptors for thromboxane and prostaglandins. *Proc. 9th Intl. Congr. Pharmacol.* (IUPHAR), **2**, 293–301.

JONES, R.L., WILSON, N.H. & LAWRENCE, R.A. (1989). EP171: a high affinity thromboxane A_2-mimetic, the actions of which are slowly reversed by receptor blockade. *Br. J. Pharmacol.*, **96**, 875–887.

KATTELMAN, E.J., VENTON, D.L. & LE BRETON, G.C. (1986). Characterisation of U46619 binding in unactivated intact human platelets and determination of binding site affinities of four TXA_2/PGH_2 receptor antagonists (13-APA, BM 13.177, ONO 3708 and SQ29,548). *Thromb. Res.*, **41**, 471–481.

LAWRENCE, R.A., JONES, R.L., WILSON, N.H. & LUMLEY, P. (1988). Thromboxane receptor agonists and antagonists: radioligand displacement and pharmacological activity on human platelets. *Br. J. Pharmacol,*. **95**, 680P.

LIEL, N., MAIS, D.E. & MALUSHKA, P.V. (1987). Binding of a thromboxane A_2/Prostaglandin H_2 against [^{3}H] U46619 to washed human platlets. *Prostaglandins*, **33**, 789–797.

LUMLEY, P., WHITE, B.P. & HUMPHREY, P.P.A. (1989). GR32191, a highly potent and specific thromboxane A_2 receptor blocking drug on platelets and vascular and airways smooth muscle *in vitro*. *Br. J. Pharmacol.*, **97**, 783–794.

MAIS, D.E., BURCH, R.M., SAUSSY, D.L., KOCHER, P.J. & HALUSHKA, P.V. (1985). Binding of a thromboxane A_2/Prostaglandin H_2 receptor antagonist to washed human platelets. *J. Pharmacol. Exp. Ther.*, **235**, 729–734.

NARUMIYA, S., OKUMA, M. & USHIKUBNI, F. (1986). Binding of a radioligand 13-azapine thromboxane antagonist to platelets: correlation with anti-aggregatory activity in different species. *Br. J. Pharmacol.*, **88**, 323–331.

RANG, H.P. (1966). The kinetics of action of acetylcholine antagonists in smooth muscle. *Proc. R. Soc.*, **164**, 488–510.

STURZEBECHER, S., HABEREY, M., MULLER, B., SCHILLINGER, E., SCHRODER, G., SKUBALLA, W., STOCK, G., VORBRUGGEN, H. & WITT, W. (1986). Pharmacological profile of a novel carbacyclin derivative with high metabolic stability and oral activity in the rat. *Prostaglandins*, **31**, 95–109.

TAKAHARA, K., MURRAY, R., FITZGERALD, G.A. & FITZGERALD, D.J. (1990). The response to thromboxane A_2 analogues in human platelets. *J. Biol. Chem.*, **265**, 6836–6844.

THOMAS, M. & LUMLEY, P. (1990). A preliminary assessment of a novel thromboxane A_2 receptor blocking drug GR32191 in healthy subjects. *Circulation*, **81** (Suppl. I), I-53–I-58.

(Received April 14, 1993
Accepted May 26, 1993)

Br. J. Pharmacol. (1993), **110**, 548–552

Reduction in the number of thromboxane receptors on human platelets after exposure to GR32191

[1]Roma A. Armstrong, [2,]*P.P.A. Humphrey & *P. Lumley

Department of Pharmacology, University of Edinburgh Medical School, 1 George Square, Edinburgh EH8 9JZ and *Division of Pharmacology, Glaxo Group Research Ltd., Park Road, Ware, Herts SG12 0DP

1 Exposure of human resuspended platelets *in vitro* for 30 min to the potent thromboxane A_2 (TP)-receptor blocking drug GR32191, followed by its removal by dilution-dissociation, reduced the degree of subsequent binding to 2 nM [^{3}H]-GR32191 by almost 50%. Exposure for longer periods (60 min) led to a further reduction. However, no change in the K_d of the radioligand was observed.

2 This effect of GR32191 could not be explained by persistent binding of drug to platelets since a dilution-dissociation stage, designed to remove all drug, was included prior to measurement of binding.

3 Using an alternative TP-receptor radioligand, [^{3}H]-SQ29,548, to monitor receptor number, a reduction in B_{max} was observed after GR32191 pre-treatment; the K_d value of the radioligand remained unchanged.

4 The effect was not a common property of TP-receptor blocking drugs since pre-exposure of platelets *in vitro* for 30 min to BM13.177 or SQ29,548 did not produce a fall in subsequent B_{max} to [^{3}H]-SQ29,548.

5 While the mechanism behind this apparent down-regulation of platelet TP-receptor is unknown, it may explain the long duration of action of GR32191 upon platelets in man which persists in the absence of detectable drug in the plasma.

Keywords: Human platelet; thromboxane A_2 receptor blocking drug; radioligand binding; receptor down-regulation; thromboxane A_2 receptor

Introduction

GR32191 is a high affinity thromboxane A_2 (TP)-receptor antagonist which has an exceptionally long duration of action in man (Thomas & Lumley, 1990). Oral dosing with GR32191 produces a cumulative antagonism of platelet aggregation *ex vivo* induced by the thromboxane (Tx)A_2-mimetic U46619, which is not accompanied by a parallel increase in plasma levels of the drug. In addition, upon termination of dosing, the antagonism of platelet aggregation persists for between 3–5 days (Thomas & Lumley, 1990). In contrast, repeat dosing with the TP-receptor blocking drug BM 13.177 is not associated with such phenomena (Patscheke *et al.*, 1986) indicating that it is not a common feature of this class of drugs.

Binding of [^{3}H]-GR32191 to intact human platelets *in vitro* is characterized by a slow dissociation from the platelet TP-receptor (Armstrong *et al.*, 1993). In keeping with this, the *in vitro* TP-receptor blocking profile of the drug upon human platelets is characterized by a slowing of the aggregatory response to agonists such as U-46619 and an unsurmountable antagonism at high concentrations (Lumley *et al.*, 1989). This may reflect the lack of the equilibrium between agonist, such as U-46619, and receptor in the presence of GR32191. However, it is difficult to envisage how the slow dissociation of GR32191 from the TP-receptor can fully explain its long duration in man.

The present study was therefore undertaken to determine whether some other phenomenon contributes to the profile of GR32191 in man. To this end we have examined whether exposure of platelets *in vitro* to GR32191 followed by its removal, affects the subsequent binding of TP-receptor ligands.

[1] Author for correspondence.
[2] Present address: Glaxo Inst. Applied Pharmacology, Dept. Pharmacology, University of Cambridge, Tennis Court Road, Cambridge CB2 1QJ.

Methods

Preparation of human platelet suspensions

Human blood (180 ml) was withdrawn from an ante-cubital vein and mixed with 36 ml acid-citrate-dextrose (ACD) solution (see Drugs used). Samples were centrifuged at 250 *g* for 20 min to give platelet-rich plasma. This was treated with 30 nM prostacyclin then further centrifuged at 450 *g* for 20 min to give a platelet pellet.

Validation of dilution-dissociation procedure

Platelet pellets were resuspended in 4.4 ml assay buffer (see Drugs used). Four 1 ml aliquots were dispensed and incubated with either 100 µl of saline or 1, 10 or 100 nM [^{3}H]-GR32191 (final concentration) at 37°C for 30 min. The same concentrations of [^{3}H]-GR32191 were also added to 1 ml aliquots of buffer and duplicate 100 µl samples withdrawn and added to 10 ml scintillant for scintillation counting ('control' count). Preincubation of platelets with saline or [^{3}H]-GR32191 was terminated by the addition of 100 ml assay buffer. After further incubation for 3 h at 37°C, the platelet suspensions were centrifuged and the platelet pellets resuspended in 1 ml aliquots of buffer. Duplicate 100 µl samples were withdrawn and added to 10 ml scintillant as above.

Pre-incubation with GR32191, SQ29,548 or BM13.177 in vitro

Platelet pellets were resuspended in 4.4 ml assay buffer. Four 1 ml aliquots were dispensed and incubated with either 100 µl saline or 1, 10 or 100 nM unlabelled GR32191 at 37°C for 30 or 60 min. In a further series of experiments platelets were exposed for 30 min to either 5 µM SQ29,548, 500 µM BM 13.177, 100 nM GR32191 or saline. In both series, this incubation was followed by dilution with 100 ml of assay buffer and further incubation for 3 h at 37°C to ensure complete dissociation of the drug from the TP-receptor. Samples were centrifuged at 450 *g* for 20 min and the platelet pellets

resuspended in assay buffer (2.5 ml) for the radioligand binding assay described below.

Determination of competition curve for [^{3}H]-GR32191

In platelets exposed to GR32191 (or SQ29,548 or BM 13.177), competition curves between [^{3}H]-GR32191 (2 nM) and increasing concentrations of GR32191 were determined. For these experiments, each assay tube contained 360 µl buffer, 10 µl [^{3}H]-GR32191 (final concentration 2 nM), 50 µl buffer or unlabelled GR32191 (0.1 nM–1 µM), and finally 80 µl of the platelet suspension to initiate binding. Incubation at 37°C for 30 min was terminated by the addition of 3 ml ice-cold assay buffer and rapid filtration under suction through Whatman GF/B glass fibre filters using a Brandell cell harvester. Filters were rinsed three times with 3 ml ice-cold assay buffer, then suspended in scintillation fluid and counted in a scintillation counter.

In some platelets exposed to GR32191 (or SQ29,548 or BM 13.177), saturation binding experiments were performed using [^{3}H]-SQ29,548 and maximal, TP-receptor binding (B_{max}) determined from Scatchard analysis of the data. Each assay tube contained 360 µl buffer, 10 µl [^{3}H]-SQ29,548 (1–30 nM), 50 µl buffer or 50 µl unlabelled GR32191 (50 µM, for determination of non-specific binding) and 80 µl platelet suspension. Incubations and separation of bound and free radioligand were carried out as above.

Analysis of binding data

Data from competition binding experiments were expressed as IC_{50} values (Armstrong *et al.*, 1993). For Scatchard analysis, data were plotted as bound/free radioligand vs bound radioligand. The line of best fit was obtained by the method of least squares using a computer programme 'Linefit' (Barlow, 1983). B_{max} and K_d values (the intercept with the abscissa scale and the negative reciprocal of the slope of the line respectively) as well as the correlation coefficient r were also determined with this programme. Data were expressed either as individual values or arithmetic mean values ± s.e.mean.

Drugs used

Trisodium citrate, aspirin and U-46619 solutions were prepared as previously reported (Lumley *et al.*, 1989). Details of the preparation and sources of acid-citrate-dextrose, the assay buffer and all other drugs used as described in the preceding paper (Armstrong *et al.*, 1993).

Results

Validation of dilution-dissociation procedure

The time (t) chosen for the dilution-dissociation procedure was determined from the formula for drug elimination, $M_t = M_0\ 2^{-t/t_{\frac{1}{2}}}$ (Bowman & Rand, 1980) where M_t is the concentration of drug bound at time t, M_0 is the starting concentration and $t_{\frac{1}{2}}$ is the half-time of dissociation of the drug. For GR32191, dissociation from intact platelets appears to occur in two phases with mean $t_{\frac{1}{2}}$ values at 37°C of 8.1 and 65.6 min (Armstrong *et al.*, 1993). To obtain at least 92.5% dissociation of [^{3}H]-GR32191 following a 100 fold dilution a time of 3 h at 37°C was chosen. To ensure that this degree of dissociation occurred in practice, 1 ml aliquots of resuspended platelets were incubated for 30 min at 37°C with 1, 10 or 100 nM [^{3}H]-GR32191. This was followed by the dilution-dissociation procedure and the residual radioactivity in the samples measured by scintillation counting. The mean ($n = 2$) control counts were 4543, 38608 and 422970 c.p.m. at the three concentrations of [^{3}H]-GR32191 respectively. Following dilution-dissociation, the remaining mean background-subtracted counts in 100 µl samples of the platelet suspensions were 0, 146 and 608 for 1, 10 and 100 nM of the radioligand respectively, representing 0, 0.38 and 0.14% of the initial radioactivity added. If a 'worst case' situation is assumed and all of this [^{3}H]-GR32191 was bound to platelet TP-receptors then this would represent only 1.8% receptor occupancy (assuming 2.4×10^8 platelets in a 100 µl sample and 2000 TP-receptors per platelet (Armstrong *et al.*, 1983b; Mais *et al.*, 1985; Kattelman *et al.*, 1986)).

Exposure of platelets to GR32191

Pre-incubation of human platelets with 10 or 100 nM GR32191 for 30 min followed by dilution-dissociation resulted in a reduction in the subsequent mean (± s.e.mean, $n = 4$) binding of 2 nM [^{3}H]-GR32191 of 19 ± 9% and 47 ± 8% respectively compared with saline-treated control (Figure 1). However, pre-incubation for 30 min with 1 nM GR32191 did not lead to any significant reduction in binding compared with control platelets. A 60 min pre-incubation with 1, 10 and 100 nM GR32191 produced a greater reduction in binding of radiolabelled drug of 38 ± 14 ($n = 4$), 35 ± 6 ($n = 4$) and 53% ($n = 3$) respectively (Figure 1). No effect on the IC_{50} for GR32191 was observed at any of the time points. For example, mean values of 1.3 ± 0.4 and 2.8 ± 0.4 nM at 30 min and 3.0 ± 0.4 and 2.2 ± 0.7 at 60 min following exposure to 10 and 100 nM GR32191 respectively were comparable to a control value (saline for 30 min) of 1.4 ± 0.3 nM. The reduction in [^{3}H]-GR32191 binding was seen only with GR32191; pre-incubation of platelets with other TP-receptor blocking drugs such as BM 13.177 (500 µM) or SQ29548 (5 µM) for 30 min did not significantly reduce subsequent [^{3}H]-GR32191

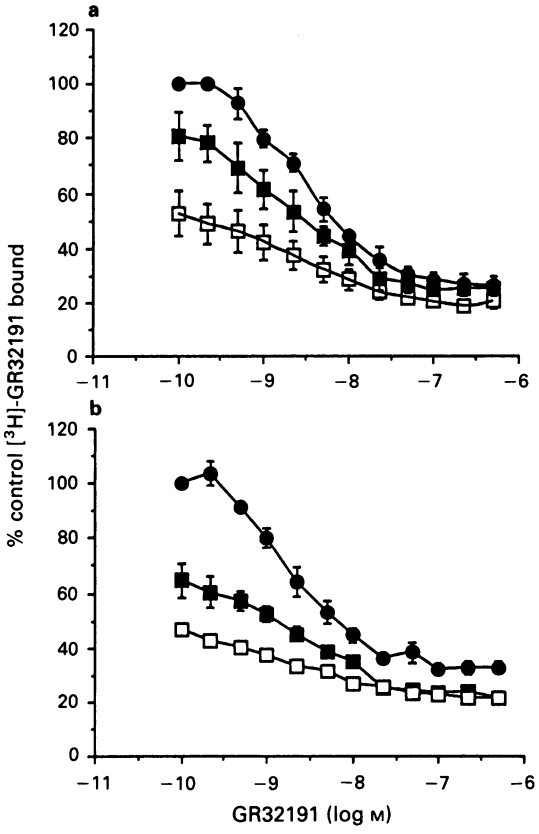

Figure 1 The inhibition of total [^{3}H]-GR32191 (2 nM) binding by increasing concentrations of GR32191 in human platelets *in vitro* pre-exposed for (a) 30 min, or (b) 60 min to saline (●), 10 nM (■) or 100 nM (□) GR32191 followed by its removal by dilution-dissociation. Curves are the mean from 3–4 experiments (± s.e.mean shown where $n = 4$).

Table 1 Determination by Scatchard analysis of the TP-receptor B_{max} and K_d for [^{3}H]-SQ29,548 on human platelets pre-exposed *in vitro* to various TP-receptor blocking drugs (individual data are shown)

Pre-incubation	*Concentration* (μM)	K_d (nM)	B_{max} (% saline-treated)
Saline	–	1.9, 2.1, 1.9	100, 100, 100
GR32191	0.1	2.0, 3.2, 2.8	49, 19, 59
SQ29,548	5.0	2.7, 5.6, 3.2	108, 113, 92
BM13.177	500	1.6, 5.3, 1.7	107, 125, 109

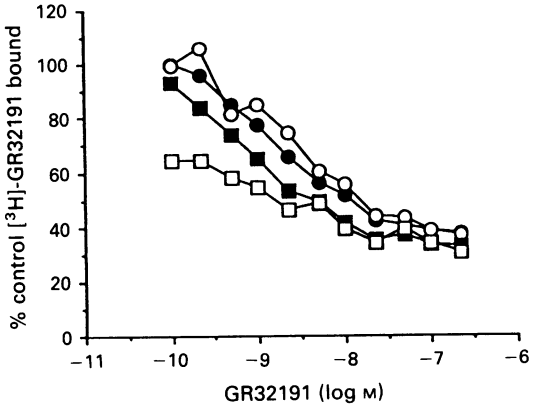

Figure 2 The inhibition of total [^{3}H]-GR32191 (2 nM) binding by increasing concentrations of GR32191 *in vitro* in human platelets pre-exposed for 30 min to BM 13.177 (500 μM, ○), SQ29,548 (5 μM, ■), GR32191 (100 nM, □) or saline (●) followed by their removal by dilution-dissociation. Curves are the mean from 2–3 experiments.

binding (Figure 2). However, in these experiments GR32191 (100 nM) reduced 2 nM [^{3}H]-GR32191 binding by 35% (n = 2) (Figure 2).

To test whether the reduction in binding was in some way a result of using [^{3}H]-GR32191 as the radioligand, B_{max} was determined by Scatchard analysis using another TP-receptor radioligand, [^{3}H]-SQ29,548 (Hedberg *et al.*, 1988) (1–30 nM). With this radioligand, platelets pre-exposed for 30 min to GR32191 (100 nM) showed a mean reduction in B_{max} of 58% (n = 3; Table 1). However, platelets exposed to SQ29,548 (5 μM) or BM13.177 (500 μM) exhibited no reduction in [^{3}H]-SQ29,548 binding (Table 1). In addition, none of the pre-treatments affected the estimated K_d for [^{3}H]-SQ 29,548 (Table 1).

Discussion

Pre-incubation of platelets with GR32191 *in vitro* resulted in an apparent fall in TP-receptor number which was dependent both on the concentration of GR32191 and the length of pre-incubation time. The reduction in receptor number was observed in platelets pre-exposed to GR32191 whether estimated from subsequent competition experiments between GR32191 and [^{3}H]-GR32191 or as a B_{max} value by Scatchard analysis of saturation binding experiments using [^{3}H]-SQ 29,548. In contrast such a phenomenon was not seen when platelets were pre-exposed to other TP-receptor blocking drugs such as SQ29,548 or BM 13.177.

GR32191 is a highly potent TP-receptor blocking drug on human platelets with a K_d value of approximately 2 nM derived from functional experiments in resuspended platelets (antagonism of U-46619-induced aggregation) (Lumley *et al.*, 1989) and a K_d value of 0.5–2 nM determined from radioligand binding studies utilizing [^{3}H]-GR32191, [^{3}H]-SQ29,548 or [^{125}I]-PTA-OH (Lawrence, 1989; Armstrong *et al.*, 1993). The antagonism produced by GR32191 on human platelets against TP-receptor agonists such as U-46619 is characterized by a slowing of the aggregatory response, an insurmountable antagonism at high concentrations and slopes of the Schild regression significantly greater than unity (Lumley *et al.*, 1989). In previous studies, [^{3}H]-GR32191 has been shown to have a rapid onset but a very slow dissociation from human platelets (Armstrong *et al.*, 1993). Thus in this respect it differs from other TP-receptor antagonists of similar high affinity, such as SQ29,548 (K_d approximately 5 nM; this study; Hedberg *et al.*, 1988). Using intact human platelets incubated with [^{3}H]-GR32191 for 30 min at 37°C, an apparent dissociation from two sites was detected, one with a mean $t_{\frac{1}{2}}$ of 8 min and the other with a $t_{\frac{1}{2}}$ of 66 min (Armstrong *et al.*, 1993). Bearing in mind that these dissociation experiments were carried out at 37°C, these dissociation rates are slow. For example, in experiments carried out at 25°C, SQ29,548 dissociates from the human platelet TP-receptor with a $t_{\frac{1}{2}}$ of 10 min (Hedberg *et al.*, 1988). At 37°C dissociation would be expected to be too rapid to measure accurately. The reason for the slow dissociation of GR32191 is, however, not known.

It is possible, therefore, that this reduction of the number of TP-receptors by GR32191 is a result of its persistent occupation of TP-receptors. In a recently reported study, Takahara and colleagues (1990) found that in human platelets exposed to 1 μM GR32191 followed by washing, a 26% reduction in subsequent [^{3}H]-SQ29,548 binding occurred. These authors found persistent binding of [^{3}H]-GR32191. For example, in platelets exposed to 10 nM [^{3}H]-GR32191 for 30 min followed by exposure to excess (10 μM) unlabelled drug, a residual 40–50% binding was present at 4 h. Further, in platelets exposed to 100 nM [^{3}H]-GR32191 and then washed three times, a high degree (43%) of specific binding remained. However, in the present *in vitro* study, persistent binding of GR32191 would not appear to explain readily the reduction in TP-receptor B_{max} since we were careful to establish conditions where near maximal dissociation of the drug from platelets had taken place. Thus, in platelets which had been exposed *in vitro* for 30 min to 100 nM [^{3}H]-GR32191, the highest concentration used, 3 h of dilution-dissociation resulted in only 0.14% of the initial radioactivity being associated with platelets. In terms of TP-receptor occupancy, this would represent less than 2% which is too little to account for the fall in B_{max} of 47% observed following 30 min incubation with 100 nM GR32191. Thus in the present *in vitro* experiments it would appear unlikely that the reduction in B_{max} was due to a persistent (or irreversible) binding of GR32191 to the TP-receptor and an alternative explanation must therefore be sought. The difference between our results and those of Takahara and colleagues (1990) is difficult to explain, although it is possible that the three washes of platelets which they used is not equivalent to the 3 h of dilution-dissociation used in the present study.

As mentioned above, in a previous study (Armstrong *et al.*, 1993), we described the characteristics of slow association and dissociation for [^{3}H]-GR32191 on platelets which were particularly marked in intact cells. One question arising out of the present study is whether the phenomenon of apparent receptor down-regulation may have also occurred during the above study and if so, what would have been the consequences of this. In the present study, 1 nM GR32191 for 30 min failed to produce a reduction in subsequent [^{3}H]-

GR32191 binding whereas 1 nM for 60 min did. In our previous study virtually all experiments were conducted with 2 nM GR32191, also over a 30 min period. However, we can only speculate as to whether any reduction in available TP-receptors occurred with this protocol. In membranes, association of [^{3}H]-GR32191 was relatively rapid and would not be anticipated to have been affected by any reduction in TP-receptors of the time-scale described in the present study. However, in intact platelets, the associaton of [^{3}H]-GR32191 was slower and experiments were continued for up to 60 min. If, therefore, a reduction in TP-receptors was occurring, this might serve to hasten or self-limit the association of the drug with the available receptor pool. However, it would not be predicted to alter the fundamental observation of a slow association. In contrast, in dissociation experiments with [^{3}H]-GR32191, a 30 min incubation period with 2 nM [^{3}H]-GR32191 was followed by exposure of platelets to 5 μM GR32191 for 40 min whilst dissociation was measured. In this situation, some reduction in receptors would be predicted to have occurred. If the reduction in receptor number represents internalization (see below), then some of the [^{3}H]-GR32191-receptor complex may have undergone such a process. Thus, the 'dissociation' of the radioligand from this internalised complex might be protracted, especially in intact platelets. Indeed, we found that the dissociation $t_{\frac{1}{2}}$ in intact plateletes was very much longer than in membranes, where any effect of 'internalization' would not be expected to be so marked. In summary, whether the phenomenon of reduction in available receptors was the sole reason for the slow association/dissociation observed with GR32191 in platelets is difficult to say. The fact that these characteristics were observed in membranes as well as intact platelets may, however, indicate a more fundamental property of the drug.

One further interesting question, is whether or not this phenomenon of TP-receptor down-regulation occurs following oral dosing with GR32191 in man? If this were the case, it may explain the long duration of action of the drug in the absence of measurable plasma concentrations after the cessation of dosing (Thomas & Lumley, 1990). We have previously reported results of a study in volunteers who ingested 20 mg GR32191 twice daily for 7 days (Armstrong *et al.*, 1990). In this study B_{max} was measured both during and after cessation of dosing, in both unmanipulated platelets and those subjected to the same dilution-dissociation procedure used in the present study. An apparent reduction in TP-receptor B_{max} was seen which reached a peak after the last dose of drug and returned to control 84 h after the final dose. The time course of the reduction in B_{max} also correlated with antagonism of U-46619-induced platelet aggregation (unpublished observation). However, the reduction in B_{max} was most clearly seen in platelets, not subjected to the dilution-dissociation procedure may therefore have simply reflected residual binding of GR32191. In samples subjected to the dilution-dissociation, the reduction in TP-receptor B_{max} was less dramatic and was variable between subjects. Thus, whilst supporting the *in vitro* findings, these preliminary *in vivo* data must be viewed with caution. They do, however, warrant further investigation.

What therefore is the mechanism for the apparent TP-receptor down regulation produced by GR32191 *in vitro*? It is generally accepted that chronic exposure of a tissue to an agonist leads to a down-regulation of receptors, whilst exposure to a pure receptor blocking drug leads to an up-regulation. In the case of human platelets, the TP-receptor has been shown, by various groups, to be down-regulated by prolonged exposure to a TP-receptor agonist (Armstrong *et al.*, 1983a; Liel *et al.*, 1988; Murray & Fitzgerald, 1989). This down-regulation appears to be similar to that reported for the β-adrenoceptor (Harden, 1983). Thus, prolonged stimulation of the TP-receptor by an agonist first appears to lead to its uncoupling from the G protein followed either by a 'sequestration' from the membrane surface or conversion to a form which cannot bind ligands (Murray & Fitzgerald, 1989). The uncoupling (desensitization) phase occurs rapidly, within 30 min of exposure to U-46619, whereas the sequestration phase only occurs with more prolonged (24 h) exposure (Murray & Fitzgerald, 1989). The possibility that regulation of platelet TP-receptor density also occurs *in vivo* through endogenous TxA_2 has been suggested from studies with aspirin. Thus in the monkey, a single dose of aspirin of 10 mg kg^{-1}, an effective inhibitory dose, was found to produce a 100% increase in the number of [^{125}I]-PTA-OH binding sites on platelet membranes (Hedberg & Liu, 1986).

Both these *in vitro* and *in vivo* data therefore indicate that platelet TP-receptor density can be readily regulated by agonists. However, such a mechanism is unlikely to account for the effect seen with GR32191 since it does not possess any TP-receptor agonist activity. For example, up to concentrations of 10 μM, GR32191 failed to induce any TP-receptor stimulated effects *in vitro* either on human platelets (induction of shape change; Lumley *et al.*, 1989) or on dog saphenous vein or *in vivo* in the anaesthetized guinea-pig (Lumley *et al.*, 1988), test systems which have previously been shown to be highly sensitive to TP-receptor agonists and partial agonists (Armstrong *et al.*, 1985; Humphrey *et al.*, 1986; Lumley *et al.*, 1989).

As mentioned, the predicted effect of a receptor blocking drug upon receptor density would be an up-regulation. The observed effect of down-regulation of TP-receptors by a pure receptor blocking drug would therefore appear contrary to theory. However, there are interesting precedents. In ligand binding studies on human lymphocytes, exposure either *in vitro* or *in vivo* to the β-adrenoceptor blocking drug, tertatolol led to a rapid loss in receptor density (De Blasi *et al.*, 1986). Interestingly, the drug has two properties which are very similar to those of GR32191. Firstly, the compound displays a biphasic dissociation curve from mouse S49 lymphocytes with an initial rapid dissociation followed by a much slower second phase (Struyker Boudier & Abbott, 1989). However, a persistent binding of drug to the receptor was ruled out as a mechanism for the phenomenon observed (De Blasi *et al.*, 1986). Further, the effects of tertatolol upon heart rate in man persist for at least 48 h at which time no drug is detectable in plasma (De Blasi *et al.*, 1986). The β-adrenoceptor down-regulating effect of tertalolol is also shared by bopindolol and timolol but not by other β-adrenoceptor antagonists (Struyker Boudier & Abbott, 1989). Further evidence of receptor down-regulation has also been obtained in the rat with an antagonist to arginine vasopressin (see Lutz *et al.*, 1991). However, the possibility of agonist activity of the compound does not appear to have been fully ruled out. Finally, in a preliminary report, Gresele *et al.* (1991) have reported reduction in TP-receptor number in human platelets following prolonged incubation with both SQ29,548 and BM 13.177. Significant reductions in B_{max} occurred after a 3 h exposure of platelets to the drugs, a maximal effect of approximately 30% being observed following 20 h exposure. The time scale of this effect is, however, in marked contrast to that of GR32191. Furthermore, chronic dosing of BM 13.177 in man did not result in any 'accumulation' of the TP-receptor blockade as was seen with GR32191 (Patscheke *et al.*, 1986). This seems to suggest a different mechanism in the reduction in TP-receptor B_{max} *in vitro* reported by Gresele and colleagues.

In summary GR32191 appears to reduce the number (B_{max}) of TP-receptors upon human platelets available for interaction with radioligands. If the phenomenon, which appears to be unique for GR32191, also occurs *in vivo*, it may explain the prolonged action of the drug in man, which persists when no drug is detectable in the plasma (Thomas & Lumley, 1990).

We would like to thank Dr Ian Fellows for help with supplies of [^{3}H]-GR32191.

References

ARMSTRONG, R.A., HUMPHREY, P.P.A. & LUMLEY, P. (1993). Characteristics of [^{3}H]-GR32191 binding to the thromboxane (TP) receptor of human platelets. *Br. J. Pharmacol.*, **110**, 539–547.

ARMSTRONG, R.A., JONES, R.L., PEESAPATI, V., WILL, S.G. & WILSON, N.H. (1985). Competitive antagonism at thromboxane receptors in human platelets. *Br. J. Pharmacol.*, **84**, 595–607.

ARMSTRONG, R.A., JONES, R.L. & WILSON, N.H. (1983a). The effect of thromboxane antagonism on aggregation and release in human platelets. *Br. J. Pharmacol.*, **78**, 159P.

ARMSTRONG, R.A., JONES, R.L. & WILSON, N.H. (1983b). Ligand binding to thromboxane receptors on human platelets: correlation with biological activity. *Br. J. Pharmacol.*, **79**, 953–964.

ARMSTRONG, R.A., LUMLEY, P. & HUMPHREY, P.P.A. (1990). Reduction in the number of thromboxane receptors (B_{max}) on human platelets after exposure to GR32191. *Br. J. Pharmacol.*, **99**, 113P.

BARLOW, R.B. (1983). *Biodata Handling with Microcomputers*. Cambridge, England: Elsevier-Biosoft.

BOWMAN, W.C. & RAND, M.J. (1980). Absorption, distribution, excretion and metabolism of drugs. In *Textbook of Pharmacology*, 2nd edition. pp. 40–46. Oxford: Blackwell Scientific Publication.

DE BLASI, A., LIPARTITI, M., PIRONE, F., ROCHAT, C., PROST, J.-F. & GARATTINI, S. (1986). Reduction of beta-adrenergic receptors by tertatolol: an additional mechanism for beta-adrenergic blockade. *Clin. Pharmacol.*, **39**, 245–254.

GRESELE, P., ZHOU, D.Y., BOSCHETTI, E. & NENCI, G.G. (1991). Loss of thromboxane receptor (TR) sites without impairment of the functional response to thromboxane in human platelets (Plts) exposed to TR antagonists. *Thromb. Haemost.*, **65**, (abstract 1614) 1144.

HARDEN, T.K. (1983). Agonist-induced desensitisation of the β-adrenergic receptor-linked adenylate cyclase. *Pharmacol. Rev.*, **35**, 5–32.

HEDBERG, A., HALL, S.E., OLGETREE, M.L., HARRIS, D.N. & LIU, E.C.K. (1988). Characterisation of [5,6-^{3}H] SQ29,548 as a high affinity radioligand, binding to thromboxane A_2/prostaglandin H_2-receptors in human platelets. *J. Pharmacol. Exp. Ther.*, **245**, 786–792.

HEDBERG, A. & LIU, E.C.K. (1986). Regulation of thromboxane A_2 receptor density, studied by specific binding of [^{125}I]-p-0H-SQ28,668 in platelet membranes from man and monkey. *Acta Pharmacol. Toxicol.*, **59**, Suppl. V, 49.

HUMPHREY, P.P.A., LUMLEY, P. & WHITE, B.P. (1986). The agonist action of AH23848 at guinea-pig vascular and airway smooth muscle TP-receptors in vivo. *Br. J. Pharmacol.*, **89**, 820P.

KATTELMAN, E.J., VENTON, D.L. & LE BRETON, G.C. (1986). Characterization of U46619 binding in unactivated, intact human platelets and determination of binding site affinities of four TXA_2/PGH_2 receptor antagonists (13-APA, BM 13.177, ONO 3708 and SQ 29,548). *Thromb. Res.*, **41**, 471–481.

LAWRENCE, R.A. (1989). Investigation into subtypes of the prostacyclin and prostaglandin E receptor present in smooth muscle. *Ph.D. Thesis. University of Edinburgh.*

LIEL, N., MAIS, D.E. & HALUSHKA, P.V. (1988). Desensitization of platelet thromboxane A_2/prostaglandin H_2 receptor by the mimetic U-46619. *J. Pharmacol. Exp. Ther.*, **247**, 1133–1138.

LUMLEY, P., SEAGER, K. & WHITE, B.P. (1988). The TP-receptor blocking drugs GR32191 and BM13.177 have a differential profile of action on vascular smooth muscle. *Br. J. Pharmacol.*, **95**, 685P.

LUMLEY, P., WHITE, B.P. & HUMPHREY, P.P.A. (1989). GR32191, a highly potent and specific thromboxane A_2 receptor blocking drug on platelets and vascular and airways smooth muscle *in vitro*. *Br. J. Pharmacol.*, **97**, 783–794.

LUTZ, W., SALISBURY, J.L. & KUMAR, R. (1991). Vasopressin receptor-mediated endocytosis: current view. *Am. J. Physiol.*, **261**, F1–F13.

MAIS, D.E., BURCH, R.M., SAUSSY, D.L., KOCHEL, P.J. & HALUSHKA, P.V. (1985). Binding of a thromboxane A_2/prostaglandin H_2 receptor antagonist to washed human platelets. *J. Pharmacol. Exp. Ther.*, **235**, 729–734.

MURRAY, R. & FITZGERALD, G.A. (1989). Regulation of thromboxane receptor activation in human platelets. *Proc. Natl. Acad. Sci. U.S.A.*, **86**, 124–128.

PATSCHEKE, H., STAIGER, C., NEUGEBAUER, G., KAUFMANN, B., STREIN, K., ENDELE, R. & STEGMEIER, K. (1986). The pharmacokinetic and pharmacodynamic profiles of the thromboxane A-2 receptor blocker BM13.177. *Clin. Pharmacol. Ther.*, **39**, 145–150.

STRUYKER BOUDIER, H. & ABBOTT, A. (1989). Novel antihypertensive drug reveals unexpected complexities in β-adrenoceptor pharmacology. *Trends Pharmacol. Sci.*, **10**, 469–471.

TAKAHARA, K., MURRAY, R., FITZGERALD, G.A. & FITZGERALD, D.J. (1990). The response to thromboxane A_2 analogues in human platelets. Discrimination of two binding sites linked to distinct effector systems. *J. Biol. Chem.*, **265**, 6836–6844.

THOMAS, M. & LUMLEY, P. (1990). A preliminary assessment of a novel thromboxane A_2 receptor blocking drug GR32191 in healthy subjects. *Circulation*, **81**, Suppl I, I-53–I-58.

(Received April 14, 1993
Accepted May 26, 1993)

Br. J. Pharmacol. (1993), **110**, 553–558

Production by R-α-methylhistamine of a histamine H_3 receptor-mediated decrease in basal vascular resistance in guinea-pigs

Robbie L. McLeod, Sheldon B. Gertner & [1]*John A. Hey

Department of Pharmacology and Toxicology, New Jersey Medical School-UMDNJ Newark, NJ and *Department of Allergy, Schering-Plough Research Institute, Kenilworth, NJ 07033, U.S.A.

1 The effect of the selective histamine H_3 receptor agonist, **R**-α-methylhistamine given intravenously (10–100 μg kg^{-1}) was examined on baseline total peripheral resistance (TPR), and cardiovascular haemodynamics in bilaterally vagotomized, anaesthetized guinea-pigs.

2 **R**-α-methylhistamine produced a dose-dependent hypotension and fall in TPR at 30 and 100 μg kg^{-1}. A decrease in heart rate (HR) was observed at a dose of 100 μg kg^{-1}. **R**-α-methylhistamine (10–100 μg kg^{-1}) also produced a dose-dependent fall in rate pressure product (RPP). There was no effect on cardiac output (CO) or stroke volume (SV) at these doses.

3 Histamine H_1 and H_2 blockade in animals pretreated with a combination of chlorpheniramine (0.3 mg kg^{-1}) and cimetidine (3.0 mg kg^{-1}) did not alter the haemodynamic actions of **R**-α-methylhistamine (100 μg kg^{-1}, i.v.). Pretreatment with the selective H_3 antagonist, thioperamide (1 mg kg^{-1}), completely blocked the action of **R**-α-methylhistamine on haemodynamic parameters.

4 To study the mechanism of action of **R**-α-methylhistamine, the vasodilator hydralazine (1 mg kg^{-1}, i.v.) was used. Hydralazine lowered BP, TRP and RPP in guinea-pigs pretreated with ipratropium (50 μg kg^{-1}, i.v.). Hydralazine had no effect on HR, SV or CO.

5 **R**-α-methylhistamine (100 μg kg^{-1}) did not affect the vasopressor action and increases in TPR produced by adrenaline (1 and 3 μg kg^{-1}). On the other hand, the vasodilator hydralazine (1 mg kg^{-1}, i.v.) inhibited the effects of adrenaline (3 μg kg^{-1}) on TPR and RPP. The effect of both doses of adrenaline on BP were attenuated by hydralazine. Therefore, the inhibitory effects of **R**-α-methylhistamine are not mediated through a direct action on vascular smooth muscle.

6 In adrenalectomized guinea-pigs, **R**-α-methylhistamine (100 μg kg^{-1}) produced a drop in BP and HR. There was no difference between the effects of **R**-α-methylhistamine on blood pressure and heart rate in adrenalectomized and non-adrenalectomized guinea-pigs.

7 These results show that activation of peripheral H_3 receptors lowers basal BP, HR and TPR, most likely by a peripheral prejunctional mechanism. The fall in BP and TPR is probably due to a decrease in noradrenaline release from sympathetic effector nerves innervating the resistance blood vessels.

Keywords: Histamine H_3 receptors; **R**-α-methylhistamine; haemodynamics; cardiac output; total peripheral resistance; presynaptic inhibition; sympathetic neurotransmission; adrenalectomy; thioperamide

Introduction

Histamine is an ubiquitous biogenic amine that affects a diverse array of physiological and behavioural responses in animals and man. The majority of the peripheral and central effects of histamine on cardiovascular function have been classically associated with histamine (H_1) and/or histamine (H_2) receptor stimulation (Klein & Gertner, 1981; Satoh & Inuli, 1984; Toda, 1986; Tsuru *et al.*, 1987; Poulakos & Gertner, 1989). A third histamine receptor (H_3) has been identified by Arrang *et al.* (1983, 1985) on presynaptic histaminergic nerve terminals within the brain. This receptor has been shown to be pharmacologically distinct from H_1 and H_2 receptors. Activation of H_3 receptors inhibits histamine release and synthesis from histaminergic neurones (Arrang *et al.*, 1988; Timmerman *et al.*, 1990). Furthermore, stimulation of central H_3 receptors has also been shown to inhibit the release of other CNS neurotransmitters such as 5-hydroxytryptamine (Schlicker *et al.*, 1988) and more recently acetylcholine (Clapham & Kilpatrick, 1992). In the peripheral autonomic system, Ishikawa & Sperelakis (1987) showed H_3 receptor activation depresses sympathetic extrajunctional potentials by a prejunctional mechanism.

The introduction of two pharmacological tools (Arrang *et al.*, 1987), **R**-α-methylhistamine, a selective H_3 chiral agonist, and thioperamide, a competitive H_3 antagonist, has made it possible to explore the physiological role of H_3 receptors in central and peripheral cardiovascular regulation. Recent studies have shown that H_3 receptor activation in the CNS elicits responses that are different from those resulting from activation of peripheral H_3 receptors. For example, intracerebroventricular injections of **R**-α-methylhistamine given to conscious guinea-pigs produce an increase in vagal tone resulting in a bradycardia and hypotension (McLeod *et al.*, 1991). However, in the periphery, i.v. **R**-α-methylhistamine produced a dose-dependent depression of electrically induced sympathetic adrenergically mediated responses in the cat (Koss & Hey, 1992), rat (Malinowska & Schlicker, 1991) and the guinea-pig (Hey *et al.*, 1992a). In all of the above mentioned studies the effects of **R**-α-methylhistamine were reversed by the H_3 antagonist, thioperamide, but not by the H_2 antagonist, cimetidine or by the H_1 antagonist, chlorpheniramine. Further confirmation of these findings has been provided by *in vitro* studies showing that H_3 activation by **R**-α-methylhistamine produced a dose-dependent prejunctional inhibition of the sympathetic inotropic responses to electrical stimulation in guinea-pig isolated atria (Lou *et al.*, 1991).

To date, studies examining the role of the H_3 receptors on autonomic cardiovascular function have done so in electrically driven systems. The purpose of the present study was to investigate the role of H_3 receptors in the regulation of basal

[1] Author for correspondence at: Department of Allergy, Schering Plough Research Institute, 2015 Galloping Hill Road, Kenilworth, NJ 07033, U.S.A.

cardiovascular function and characterize the haemodynamic consequences of H_3 activation in the anaesthetized guinea-pig.

Methods

Animal preparation

Male Hartley guinea-pigs (425–600 g, Charles River, Bloomington, MA, U.S.A.) were anaesthetized with α-chloralose (125 mg kg^{-1}, i.p.). The left common carotid artery and the right jugular vein were cannulated with PE-50 tubing for measurement of blood pressure and i.v. administration of drugs. Both the left and right vagus were cut at the cervical level to eliminate vagal contribution to the heart. A catheter (PE-200) was placed in the trachea and animals were mechanically-ventilated (v = 4 ml, f = 45 breaths min^{-1}) with room air using a rodent respirator. Since the chest was open, animals were paralyzed with gallamine triethiodide (2 mg kg^{-1}, i.v.). Blood pressure and heart rates were derived from the arterial pulse pressure connected to a pressure transducer. Physiological parameters were recorded on a Hewlett Packard polygraph. Adrenalectomized male guinea-pigs (400–500 g) were obtained from Charles River, Bloomington, MA, U.S.A.

Determination of cardiac output

The animal was placed in a left lateral recumbent position. The chest was shaved and cleaned with 70% ethanol. The muscles of the chest were blunt dissected away to reveal the intercostal tissue. A thoracotomy was performed by making an incision through the third right intercostal space. The ribs were retracted and the lung gently pushed aside. The ascending aorta was dissected free and a perivascular 3S transonic flow probe (Transonic Systems Inc., Ithaca, NY, U.S.A.) was placed around the vessel. The signal from the transonic flow probe was directed into a small animal blood flow meter (Model T206, Transonic Systems Inc.). Cardiac output tracing was recorded on a polygraph.

Pharmacological studies

To study the dose-response characteristics of **R**-α-methylhistamine, blood pressure (BP), heart rate (HR), cardiac output (CO), total peripheral resistance (TPR), stroke volume (SV) and rate pressure product (RPP = systolic blood pressure × heart rate) were measured. The rate pressure product (RPP) is an index of myocardial oxygen demand (Holmberg *et al.*, 1971; Kitamura *et al.*, 1972; Foltin & Fischman, 1992). The effects of **R**-α-methylhistamine (10–100 μg kg^{-1}, i.v.) on these haemodynamic parameters were determined ($n = 8–10$ animals per group) for a period from 10 min before the drug until 30 min post-drug administration.

To determine the specific histamine receptor type involved in the haemodynamic responses to **R**-α-methylhistamine, these effects were evaluated in the presence of either thioperamide (1.0 mg kg^{-1}, i.v.), or a combination of cimetidine (3.0 mg kg^{-1}, i.v.) and chlorpheniramine (0.3 mg kg^{-1}, i.v.). In each experiment **R**-α-methylhistamine (100 μg kg^{-1}, i.v.) was administered 10 min after the pretreatment drug ($n = 4–9$ animals per group).

The haemodynamic effects of **R**-α-methylhistamine (100 μg kg^{-1}, i.v.) were compared to the effects of the direct vasodilator, hydralazine (1 mg kg^{-1}, i.v.) in intact guinea-pigs. Animals were pretreated with ipratropium (50 μg kg^{-1}, i.v.) to block parasympathetic effects on the heart. Animals were then given vehicle, **R**-α-methylhistamine or hydralazine. The dose of hydralazine chosen (1 mg kg^{-1}) produced a fall in BP similar to that produced by **R**-α-methylhistamine (100 μg kg^{-1}).

To determine whether a direct vascular smooth muscle action contributes to the effects of **R**-α-methylhistamine (100 μg kg^{-1}, i.v.), the vasopressor and haemodynamic effects of adrenaline (1 and 3 μg kg^{-1}, i.v.) were evaluated before and 5 min after treatment with the direct vasodilator, hydralazine (1 mg kg^{-1}, i.v.) or **R**-α-methylhistamine (100 μg kg^{-1}, i.v.).

The possible relationship between adrenal catecholamines and the cardiovascular actions of i.v. **R**-α-methylhistamine was also studied. **R**-α-methylhistamine was given to adrenalectomized bilaterally vagotomized, anaesthetized guinea-pigs. The effects of **R**-α-methylhistamine on TPR and cardiovascular haemodynamics were compared with its effects in non-adrenalectomized guinea-pigs.

Drugs

α-Chloralose, hydralazine, chlorpheniramine maleate, cimetidine and ipratropium bromide were purchased from Sigma Chemical Co. (St. Louis, MO, U.S.A.). **R**-α-methylhistamine and thioperamide maleate was purchased from Research Biochemical Incorporated (Natick, MA, U.S.A.). Cimetidine was dissolved in a 5% dextrose, 5% glycol and water (w/v solution). All other drugs were dissolved in physiological saline (0.9%). Drug doses refer to their respective free base.

Statistics

Mean arterial blood pressure was mathematically derived from the arterial pulse pressure using the relationship pulse pressure divided by three plus diastolic blood pressure. TPR and SV were calculated from the equations [BP/CO] and [CO/HR] respectively. Values represent the mean ± s.e.mean. Statistical significance was evaluated by a one way analysis of variance (ANOVA) in conjunction with Dunnett's two tailed t test. Statistical significance was set at $P < 0.05$.

Results

Figure 1 illustrates the hypotensive actions of **R**-α-methylhistamine (10–100 μg kg^{-1}, i.v.) in anaesthetized guinea-pigs. The maximum hypotensive effect of **R**-α-methylhistamine was observed at 5 min. Only the highest dose of **R**-α-methylhistamine (100 μg kg^{-1}) produced a significant bradycardia. Baseline haemodynamic values for the **R**-α-methylhistamine-treated (10–100 μg kg^{-1}) groups were not different from the vehicle group. Baseline (BP) values were 40 ± 2 mmHg for the saline group and 43 ± 4, 42 ± 2 and 39 ± 5 for animals given **R**-α-methylhistamine (10, 30 and 100 μg kg^{-1}, i.v.) respectively. Baseline (HR) values were 245 ± 8, 242 ± 6, 245 ± 8 and 231 ± 10 beats min^{-1} for vehicle and **R**-α-methylhistamine groups (10, 30 and 100 μg kg^{-1}) respectively. Total peripheral resistance (TPR) was decreased at 30 and 100 μg kg^{-1} of **R**-α-methylhistamine (Figure 1). TPR baseline values for the control group were 0.88 ± 0.06 mmHg min^{-1} ml^{-1}. **R**-α-methylhistamine (10–100 μg kg^{-1}) baseline TPR values were 0.78 ± 0.08, 0.88 ± 0.09 and 1.2 ± 0.02. Rate pressure product (RPP) was decreased with all doses of **R**-α-methylhistamine. **R**-α-methylhistamine however, did not alter cardiac output (CO) or stroke volume (SV) in these animals (Table 1).

The histamine H_3 antagonist, thioperamide (1 mg kg^{-1}, i.v.), antagonized the actions of **R**-α-methylhistamine (100 μg kg^{-1}) on BP, HR, TPR and RPP (Figure 2). These values were not different from animals given saline vehicle. The combination of histamine H_1 and H_2 receptor blockade with cimetidine (3.0 mg kg^{-1}) and chlorpheniramine (0.3 mg kg^{-1}) did not alter the haemodynamic actions of **R**-α-methylhistamine (100 μg kg^{-1}). The BP, HR, TPR and RPP effects of **R**-α-methylhistamine in the presence of H_1 and H_2 blockade and in animals given **R**-α-methylhistamine were not different from each other. Both of these groups however, were different from the saline group.

Figure 3 illustrates the effects of **R**-α-methylhistamine (100 μg kg^{-1}) and hydralazine (1 mg kg^{-1}, i.v.) on BP, HR, TPR and RPP in intact guinea-pigs pretreated with the muscarinic antagonist, ipratropium (50 μg kg^{-1}, i.v.). Ipratropium was used in these studies to allow cardiovascular reflexes to remain intact. The response to i.v. **R**-α-methylhistamine in the ipratropium-treated group was identical to the response obtained in vagotomized animals. This dose of ipratropium has been shown to block vagal input to the heart (McLeod *et al.*, 1991). Baseline haemodynamic values between the groups were not different (data not shown). Both **R**-α-methylhistamine and hydralazine produced similar falls in BP, TPR and RPP. Only **R**-α-methylhistamine lowered HR. Neither drug altered CO or SV. Table 2 shows that **R**-α-methylhistamine (100 μg kg^{-1}) had no effect on the haemodynamic actions of exogenous adrenaline (1 and 3 μg kg^{-1}, i.v.). Hydralazine (1 mg kg^{-1}, i.v.)-attenuated the effects of adrenaline on BP, TPR and RPP.

In the adrenalectomized guinea-pig, **R**-α-methylhistamine (100 μg kg^{-1}, i.v.) lowered BP, TPR, HR and RPP (Figure 4). There was no difference in the haemodynamic effects of **R**-α-methylhistamine (100 μg kg^{-1}, i.v.) in adrenalectomized and non-adrenalectomized guinea-pigs. Baseline haemodynamic values for adrenalectomized and non-adrenalectomized guinea-pigs were not different. Baseline BP values were 37 ± 2 mmHg for adrenalectomized guinea-pigs and 43 ± 2 mmHg for non-adrenalectomized animals given **R**-α-methylhistamine. Basal HR and TPR were 245 ± 10 beats min^{-1} and 1.03 ± 0.06 ml min^{-1} mmHg^{-1} for adrenalectomized guinea-pigs, and 246 ± 13 beats min^{-1} and 0.95 ± 0.10 ml min^{-1} mmHg^{-1} for non-adrenalectomized guinea-pigs.

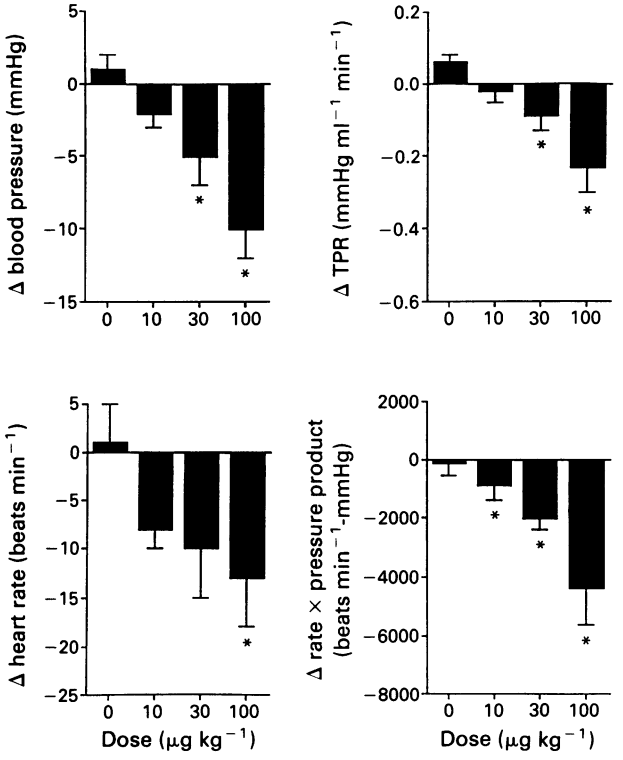

Figure 1 Figure illustrating dose-dependent inhibitory effect of **R**-α-methylhistamine on cardiovascular haemodynamic parameters. The effects (ΔBP, ΔTPR ΔHR and ΔRPP) of **R**-α-methylhistamine (10–100 μg kg^{-1}, i.v.) are shown at 5 min. Each column represents the mean ± s.e. mean (n = 8–10 per group). The data were analyzed by one-way ANOVA in conjunction with Dunnett's t test. *P<0.05 compared to saline vehicle.

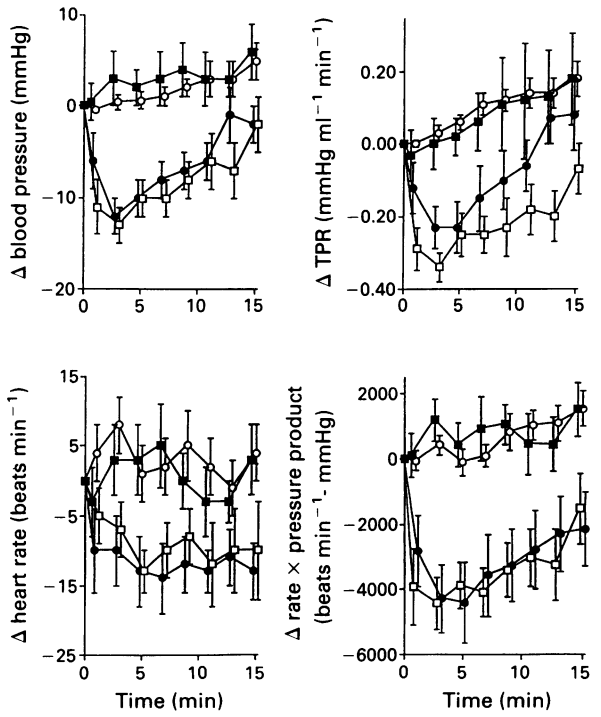

Figure 2 Haemodynamic effects of **R**-α-methylhistamine in the presence of H_1, H_2 and H_3 blockade. Figure displays the ΔBP, ΔTPR, ΔHR and ΔRPP responses of i.v. saline vehicle (○, n = 20), **R**-α-methylhistamine (100 μg kg^{-1}, i.v., n = 9) given alone (●), **R**-α-methylhistamine in animals pretreated with thioperamide (1 mg kg^{-1}, i.v.; ■, n = 4) or in animals pretreated with a combination of chlorpheniramine (0.3 mg kg^{-1}, i.v.) and cimetidine (3.0 mg kg^{-1}; □, n = 6). **R**-α-methylhistamine alone and in animals pretreated with a combination of cimetidine and chlorpheniramine lowered BP, TPR, HR and RPP compared to saline vehicle and the thioperamide pretreated group. Haemodynamic values of animals pretreated with thioperamide were not different from the saline control group. Each point represents the mean ± s.e.mean. The data were analyzed by one-way ANOVA in conjunction with Dunnett's t test; statistical significance was set at P<0.05.

Table 1 Effect of **R**-α-methylhistamine (100 μg kg^{-1}, i.v.) on cardiac output and stroke volume

		Δ *Cardiac output* (ml min^{-1})		
	Baseline	3 min	5 min	15 min
Vehicle	44.0 ± 1.8	−0.5 ± 0.4	−1.9 ± 0.7	−2.7 ± 0.8
R-α-methylhistamine	40.8 ± 4.6	−3.8 ± 1.3	−2.7 ± 1.1	−4.4 ± 1.8
		Δ *Stroke volume* (ml beat^{-1})		
	Baseline	3 min	5 min	15 min
Vehicle	0.19 ± 0.01	−0.01 ± 0.004	−0.01 ± 0.004	−0.02 ± 0.01
R-α-methylhistamine	0.18 ± 0.02	−0.01 ± 0.01	−0.00 ± 0.01	−0.01 ± 0.01

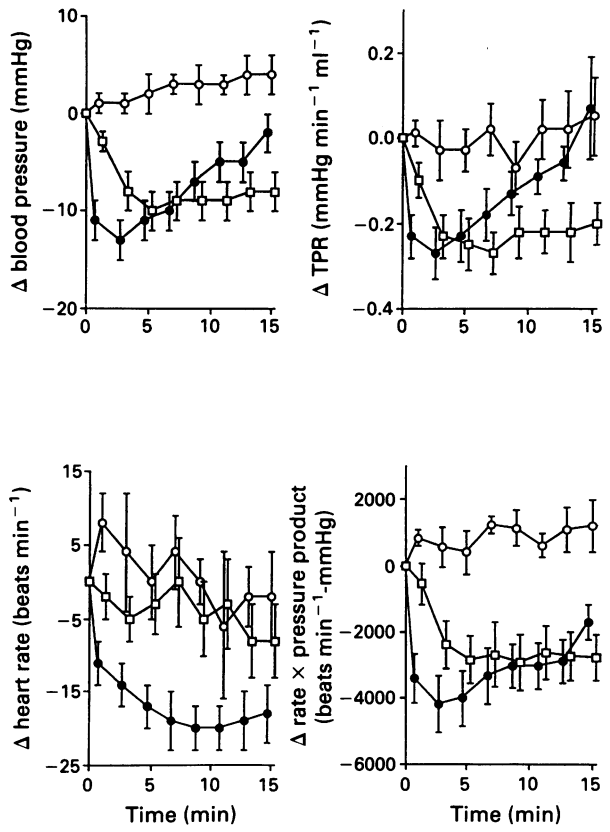

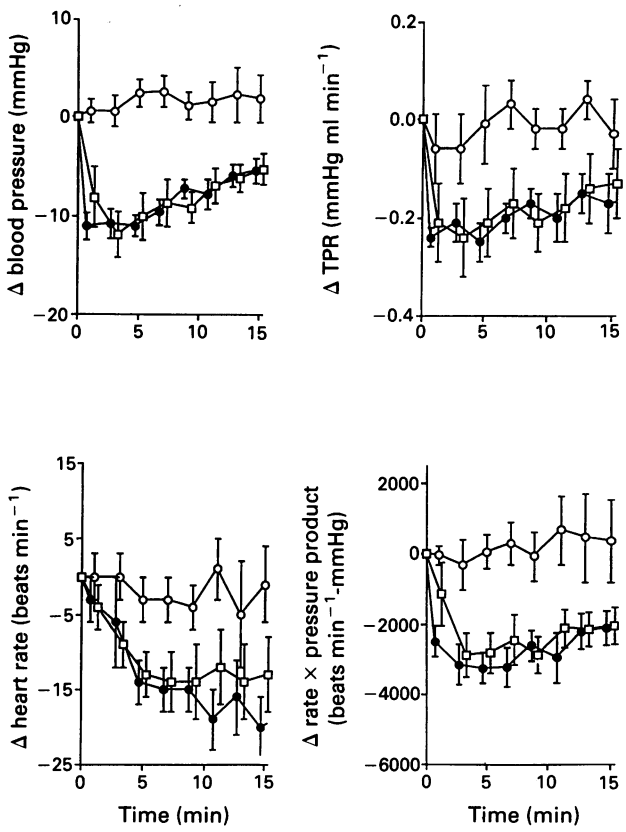

Figure 3 Comparative profile of haemodynamic effects of **R**-α-methylhistamine and hydralazine. Figure displays the ΔBP, ΔTPR, ΔHR and ΔRPP responses of saline vehicle (○), **R**-α-methylhistamine (100 μg kg^{-1}, i.v., ●) and hydralazine (1.0 mg kg^{-1}, i.v.; □) in intact guinea-pigs pretreated with the muscarinic antagonist, ipratropium (50 μg kg^{-1}, i.v.). Both **R**-α-methylhistamine and hydralazine lowered BP, TPR and RPP compared to the saline group. Note that only **R**-α-methylhistamine lowered HR. Each point represents the mean ± s.e.mean ($n = 6$–8 per group). The data were analysed by one-way ANOVA in conjunction with Dunnett's t test; statistical significance was set at $P < 0.05$.

Figure 4 Haemodynamic effects of **R**-α-methylhistamine in the adrenalectomized guinea-pig. Figure displays the ΔBP, ΔTPR, ΔHR and ΔRPP responses of i.v. saline vehicle (○), **R**-α-methylhistamine (100 μg kg^{-1}, i.v.; ●) in adrenalectomized guinea-pigs and **R**-α-methylhistamine (100 μg kg^{-1}, i.v.; □) in non-adrenalectomized guinea pigs. **R**-α-methylhistamine lowered BP, TPR, HR and RPP in both non-adrenalectomized and adrenalectomized guinea pigs. There was no difference in the haemodynamic responses to **R**-α-methylhistamine between these two groups. Each point represents the mean ± s.e.mean ($n = 6$–8 per group). The data were analyzed by one-way ANOVA in conjunction with Dunnett's t test; statistical significance was set at $P < 0.05$.

Table 2 Effect of adrenaline before and after treatment with **R**-α-methylhistamine (100 μg kg^{-1}, i.v.) and hydralazine (1 mg kg^{-1}, i.v.)

	Adrenaline 1 μg kg		*Adrenaline* 3 μg kg	
	Δ *mean blood pressure* (mmHg)		Δ *mean blood pressure* (mmHg)	
	Before	*After*	*Before*	*After*
Saline	28 ± 5	30 ± 3	46 ± 6	44 ± 5
R-α-methylhistamine	33 ± 6	28 ± 2	47 ± 5	54 ± 4
Hydralazine	25 ± 4	13 ± 3*	44 ± 2	24 ± 4*
	Δ *TPR* (mmHg ml^{-1} min^{-1})		Δ *TPR* (mmHg ml^{-1} min^{-1})	
	Before	*After*	*Before*	*After*
Saline	0.58 ± 0.20	0.67 ± 0.11	0.91 ± 0.18	1.12 ± 0.28
R-α-methylhistamine	0.59 ± 0.19	0.54 ± 0.09	0.65 ± 0.17	1.00 ± 0.05
Hydralazine	0.63 ± 0.18	0.33 ± 0.09	1.02 ± 0.22	0.47 ± 0.06*
	Δ *heart rate* (beats min^{-1})		Δ *heart rate* (beats min^{-1})	
	Before	*After*	*Before*	*After*
Saline	29 ± 11	16 ± 9	34 ± 16	33 ± 14
R-α-methylhistamine	22 ± 6	20 ± 4	28 ± 7	16 ± 7
Hydralazine	15 ± 7	12 ± 5	23 ± 7	18 ± 5
	Δ *RPP* (beats min^{-1} mmHg^{-1})		Δ *RPP* (beats min^{-1} mmHg^{-1})	
	Before	*After*	*Before*	*After*
Saline	10134 ± 1687	8813 ± 1614	18890 ± 3563	13521 ± 2021
R-α-methylhistamine	10605 ± 1520	9040 ± 1082	16660 ± 2649	16435 ± 1684
Hydralazine	6233 ± 1228	3433 ± 1029	12425 ± 1286	6054 ± 1311*

TPR: total peripheral resistance. RPP: rate pressure product.
*$P < 0.05$.

Discussion

The present study indicates that prejunctional H_3 activation with i.v. **R**-α-methylhistamine produces a decrease in mean basal blood pressure and heart rate. This fall in mean blood pressure is probably the result of a decrease in sympathetic tone to resistance vessels. This is based on the finding that **R**-α-methylhistamine produced a fall in total peripheral resistance without a fall in cardiac output. These vascular effects are not likely to be the result of direct smooth muscle dilatation because **R**-α-methylhistamine does not reverse the cardiopressor effects of a direct agonist, adrenaline (Hey *et al.*, 1992a). We have presented findings that **R**-α-methylhistamine does not alter the effects of adrenaline on vascular resistance and cardiovascular haemodynamics. In contrast, the vasodilator, hydralazine, inhibited the vasopressor actions of adrenaline indicating that these two drugs lowered blood pressure by different mechanisms.

It has been proposed that activation of preganglionic H_3 receptors inhibits ganglionic neurotransmission (Tamura *et al.*, 1988; Christian & Weinreich, 1992). Thus the inhibitory effect on the cardiovascular system may be due in part to inhibition of adrenal catecholamines. In adrenalectomized guinea-pigs however, the haemodynamic profile of **R**-α-methylhistamine is not differnt from that in non-adrenalectomized guinea-pigs. The results from the present study, therefore do not rule out the possibility that part of the action of **R**-α-methylhistamine may involve an inhibitory effect on sympathetic ganglionic neurotransmission. The present findings are consistent with studies by Koss & Hey (1992) who showed that **R**-α-methylhistamine acts at postganglionic prejunctional H_3 receptors.

R-α-methylhistamine has been shown to cross the blood brain barrier (Garbarg *et al.*, 1989; Oishi *et al.*, 1989). Furthermore, we have demonstrated that i.c.v. **R**-α-methylhistamine elicits bradycardia and hypotension by activation of CNS vagal pathways (McLeod *et al.*, 1991). However, in the current study, it is unlikely that vagal enhancement due to central H_3 activation is involved in the bradycardic and hypotensive effects of i.v. **R**-α-methylhistamine because both vagi were cut at the cervical level to inhibit parasympathetic effects on the heart. The present findings show that **R**-α-methylhistamine lowered basal heart rate and vascular resistance by activation of peripheral prejunctional H_3 receptors.

R-α-methylhistamine also has H_1 agonist properties at doses greater than 0.3 mg kg^{-1}, i.v. (Hey *et al.*, 1992b). The dose of **R**-α-methylhistamine used in this study is below the threshold dose that has been demonstrated to produce H_1 effects in the anaesthetized guinea-pig. Additional proof that the inhibitory actions of **R**-α-methylhistamine are solely mediated through H_3 receptors is provided by the observation that only thioperamide, a selective H_3 antagonist with neglible effect on H_1 and H_2 receptors, blocked the haemodynamic actions of **R**-α-methylhistamine. Blockade of H_1 and H_2 receptors did not alter the haemodynamic actions of **R**-α-methylhistamine indicating a lack of H_1 or H_2 involvement. Furthermore, it is not likely that histamine H_1 receptors play a role in the inhibitory actions of **R**-α-methylhistamine because it has been shown that H_1 receptor activation elicits a stimulatory action on ganglionic sympathetic neural traffic that is not observed in our studies (Christian *et al.*, 1989; Christian & Weinreich, 1992).

Evidence is emerging to suggest important species variations in the pharmacological responses to H_3 activation. In the present study **R**-α-methylhistamine had prominent effects on basal cardiovascular function of the guinea-pig. In contrast, in the rat i.v. **R**-α-methylhistamine does not lower basal BP and HR with doses as high as 10 mg kg^{-1} i.v. (unpublished observations). However in an electrically driven system, **R**-α-methylhistamine inhibits neurogenically induced hypertensive responses in the pithed rat (Malinowska & Schlicher, 1991). The differences in the pharmacological responses to H_3 activation may not be unexpected because it is well known that the responses to histamine on the cardiovascular system vary greatly among species (Levi *et al.*, 1982). The physiological implications for autonomic function remain to be elucidated further.

In summary, the results presented here demonstrate that the H_3 agonist **R**-α-methylhistamine given by systemic i.v. route lowers blood pressure, total peripheral resistance, heart rate and rate pressure product in the anaesthetized guinea-pig. It is concluded that the hypotension is produced by prejunctional activation of H_3 receptors located on sympathetic neurones. Activation of these receptors probably acts to inhibit noradrenaline release from sympathetic effector nerves to resistance vessels, resulting in a decrease of total peripheral resistance.

We thank Drs R.W. Egan, W. Kreutner and R.W. Chapman, Schering-Plough Research Institute, Kenilworth, N.J. for their useful discussions and review of this manuscript.

References

ARRANG, J.-M., GARBARG, M. & SCHWARTZ, J.-C. (1983). Auto-inhibition of brain histamine release mediated by a novel class (H_3) of histamine receptor. *Nature*, **302**, 832–837.

ARRANG, J.-M., GARBARG, M. & SCHWARTZ J.-C. (1985). Autoregulation of histamine release in brain by presynaptic H_3-receptors. *Neurosci.*, **15**, 553–562.

ARRANG, J.-M., GARBARG, M., LANCELOT, J.C., LECOMTE, J.M., POLLARD, H., ROBBA, M., SCHUNACK, W. & SCHWARTZ, J.-C. (1987). Highly potent and selective ligands for histamine H_3-receptors. *Nature*, **327**, 117–123.

ARRANG, J.-M., DEVAUX, B., CHODKIEWICZ, J.P. & SCHWARTZ, J.-C. (1988). H_3-receptors control histamine release in human brain. *J. Neurochem.*, **51**, 105–108.

CHRISTIAN, E.P., UNDEM, B.J. & WEINREICH, D. (1989). Endogenous histamine excites neurones in the guinea-pig superior cervical ganglion *in vitro*. *J. Physiol.*, **409**, 297–312.

CHRISTIAN, E.P. & WEINREICH, D. (1992). Presynaptic histamine H_1 and H_3 receptors modulate sympathetic ganglionic synaptic transmission in the guinea-pig. *J. Physiol.*, **457**, 407–430.

CLAPHAM, J. & KILPATRICK, G.J. (1992). Histamine H_3 receptors modulated the release of [^{3}H]-acetylcholine from slices of rat entorhinal cortex: evidence for the possible existence of H_3 receptor subtypes. *Br. J. Pharmacol.*, **107**, 919–923.

FOLTIN, R.W. & FISCHMAN, M.W. (1992). The cardiovascular and subjective effects of intravenous cocaine and morphine combinations in humans. *J. Pharmacol. Exp. Ther.*, **261**, 623–631.

GARBARG, M., TRUNG TRONG, M.D., GROS, C. & SCHWARTZ, J.C. (1989). Effects of histamine H_3-receptor ligands on various biochemical indices of histaminegic neuron activity in the rat brain. *Eur. J. Pharmacol.*, **164**, 1–11.

HEY, J.A., DEL PRADO, M., EGAN, R., KREUTNER, W. & CHAPMAN, R.W. (1992a). Inhibition of sympathetic hypertensive responses in the guinea-pig by prejunctional H_3-receptors. *Br. J. Pharmacol.*, **107**, 347–351.

HEY, J.A., DEL PRADO, M., EGAN, R., KREUTNER, W. & CHAPMAN, R.W. (1992b). R-*alpha*-methylhistamine augments neural, cholinergic bronchospasm in guinea pigs by histamine H_1-receptor activation. *Eur. J. Pharmacol.*, **211**, 421–426.

HOLMBERG, S., SERZYSKO, W. & VARNAUKAS, E. (1971). Coronary circulation during heavy exercise in control subjects and patients with coronary heart disease. *Acta Med. Scand.*, **190**, 465–480.

ISHIKAWA, S. & SPERELAKIS, N. (1987). A novel class (H_3) of histamine receptor on perivascular nerve terminals. *Nature*, **327**, 152–160.

KITAMURA, K., JORGENSEN, C.R., GOBEL, F.L., TAYLOR, H.L. & WANG, Y. (1972). Hemodynamic correlates of myocardial oxygen consumption during upright exercise. *J. Appl. Physiol.*, **32,** 516–522.

KLEIN, M.C. & GERTNER, S.B. (1981). Evidence for a role of endogenous histamine in central cardiovascular regulation: inhibition of histamine-N-methyltransferase by SKF 91488. *J. Pharmacol. Exp. Ther.*, **216,** 315–320.

KOSS, M.C. & HEY, J.A. (1992). Activation of histamine H_3 receptors produces presynaptic inhibition of neurally evoked cat nictitating membrane responses in vivo. *Naunyn-Schmied. Arch. Pharmacol.*, **346,** 208–212.

LEVI, R., OWEN, D.A.A. & TRZECIAKOWSKI, J. (1982). Actions of histamine on the heart and vasculature. In *Pharmacology of Histamine Receptors.* ed. Ganellin, C.R. & Parsons, M.E. pp. 236–297. Bristol: John Wright & Sons.

LOU, X.L., TAN, Y.H. & SHENG, B.H. (1991). Histamine H_3-receptors inhibit sympathetic neurotransmission in guinea pig myocardium. *Eur. J. Pharmacol.*, **204,** 311–314.

MALINOWSKA, B. & SCHLICKER, E. (1991). H_3 receptor-mediated inhibiton of neurogenic vasopressor response in pithed rats. *Eur. J. Pharmacol.*, **205,** 307–310.

McLEOD, R.L., GERTNER, S.B. & HEY, J.A. (1991). Central H_3 modulation of vagal tone and blood pressure in the conscious guinea-pig. *Eur. J. Pharmacol.*, **209,** 214–142.

OISHI, R., ITOH, Y., NISHIBORI, M. & SAEKI, K. (1989). Effects of the histamine H_3-agonist (R)-*alpha*-methylhistamine and the antagonist thioperamide on histamine metabolism in the mouse and rat brain. *J. Neurochem.*, **52,** 1388–1392.

POULAKOS, J.J. & GERTNER, S.B. (1989). Studies on the cardiovascular actions of central histamine H_1 and H_2 receptors. *J. Pharmacol. Exp. Ther.*, **250,** 500–505.

SATOH, H. & INUI, J. (1984). Endothelial cell-dependent relaxation and contraction induced by histamine in isolated guinea-pig pulmonary artery. *Eur. J. Pharmacol.*, **97,** 321–324.

SCHLICKER, E., BETZ, R. & GOTHERT, M. (1988). Histamine H_3 receptor-mediated inhibition of serotonin release in the rat brain cortex. *Naunyn-Schmied. Arch. Pharmacol.*, **337,** 588–590.

TAMURA, K., PALMER, J.M. & WOOD, J.D. (1988). Presynaptic inhibition produced by histamine at nicotinic synapse in enteric ganglia. *Neurosci.*, **25,** 171–179.

TIMMERMAN, H. (1990). Histamine H_3 ligand, just pharmacological tools or potential therapeutic agents? *J. Med. Chem.*, **33,** 4–11.

TODA, N. (1986). Mechanism of histamine-induced relaxation in isolated monkey and dog coronary arteries. *J. Pharmacol. Exp. Ther.*, **239,** 529–535.

TSURU, H., KOHNO, S., IWATA, M. & SHIGEI, T. (1987). Characterization of histamine receptors in isolated rabbit veins. *J. Pharmacol. Exp. Ther.*, **243,** 696–702.

(Received March 29 1993
Revised May 18, 1993
Accepted May 20, 1993)

Br. J. Pharmacol. (1993), **110**, 559–564

Prejunctional modulation of the nitrergic innervation of the canine ileocolonic junction via potassium channels

Joris G. De Man, Guy E. Boeckxstaens, Paul P. Pelckmans, Benedicte Y. De Winter, Arnold G. Herman & Yvan M. Van Maercke

Divisions of Gastroenterology and Pharmacology, Faculty of Medicine, University of Antwerp (UIA), Universiteitsplein 1, B-2610 Wilrijk, Belgium

1 The effects of different K^+ channel blockers were studied on nitric oxide (NO)-mediated non-adrenergic non-cholinergic (NANC) relaxations in the canine ileocolonic junction.

2 The non-selective blockers of K^+ channels, 4-aminopyridine (4-AP) and tetraethylammonium (TEA) and the blocker of large conductance Ca^{2+}-activated K^+ channels, charybdotoxin, potently enhanced the NANC relaxations induced by low frequency stimulation. The blocker of small conductance Ca^{2+}-activated K^+ channels, apamin, had no effect on electrically-induced NANC relaxations.

3 NANC nerve-mediated relaxations induced by adenosine 5'-triphosphate (ATP), acetylcholine (ACh) and γ-aminobutyric acid (GABA) were significantly enhanced by 4-AP and charybdotoxin but not by apamin. TEA significantly enhanced the NANC relaxations in response to GABA and ATP while that in response to ACh was abolished.

4 None of the K^+ channel blockers had an effect on the dose-response curve to NO, on the noradrenaline-induced contraction or on the relaxation to nitroglycerine (GTN).

5 From these results we conclude that inhibition of prejunctional K^+ channels increases the nitrergic relaxations induced by electrical and chemical receptor stimulation of NANC nerves and thus suggests a regulatory role for these prejunctional K^+ channels in the release of NO from NANC nerves in the canine ileocolonic junction.

Keywords: Electrical stimulation; ileocolonic junction; K^+ channels; nitric oxide; non-adrenergic non-cholinergic; presynaptic modulation

Introduction

Evidence is accumulating confirming the role of nitric oxide (NO) as the inhibitory non-adrenergic non-cholinergic (NANC) neurotransmitter in the gastrointestinal tract (for review see Sanders & Ward, 1992; Stark & Szurzewsky, 1992). In the canine ileocolonic junction (ICJ) we showed that NANC nerve-mediated relaxations induced by electrical pulses, adenosine 5'-triphosphate (ATP), acetylcholine (ACh) and γ-aminobutyric acid (GABA) are mediated by NO (Boeckxstaens *et al.*, 1990a; 1991a). Furthermore, using a bioassay cascade, we actually demonstrated the release of a NO-related substance in response to electrical and nicotinic receptor stimulation (Bult *et al.*, 1990; Boeckxstaens *et al.*, 1991b). Recently, we also illustrated Ca^{2+}-dependency (De Man *et al.*, 1992) and α_2-adrenoceptor-mediated modulation (Boeckxstaens *et al.*, 1993) of the release of NO in the canine ICJ. These findings, together with the knowledge that other putative NANC neurotransmitters such as ATP and vasoactive intestinal polypeptide have been excluded (Boeckxstaens *et al.*, 1990b,c), make the canine ICJ a good model to study the nitrergic innervation.

Release of neurotransmitters is known to be modulated by activation of specific prejunctional receptors (Westfall & Martin, 1991). At present, it is thought that prejunctional inhibition of neurotransmitter release results from receptor-mediated regulation of ion channels in the nerve terminal. Prejunctional Ca^{2+} channels which are responsible for the Ca^{2+} influx that triggers neurotransmitter release, might be directly regulated by a prejunctional receptor (Miller, 1990). Neurones also possess a great variety of K^+ channels that are involved in many aspects of neuronal function, including prejunctional modulation of neurotransmission (Belardetti & Siegelbaum, 1988; Miller, 1990). Blockade of different types of K^+ channels has a profound effect on the stimulated release of neurotransmitters from various tissues. In rabbit vas deferens, cat spleen and rat portal vein, the non-specific K^+ channel blockers 4-aminopyridine (4-AP) and tetraethylammonium (TEA) potentiated the release of noradrenaline upon nerve stimulation (Johns *et al.*, 1976; Kirkepar *et al.*, 1977; Kirkepar & Prat, 1978; Leander *et al.*, 1977). Charybdotoxin, a blocker of large conductance Ca^{2+}-activated K^+ channels, and 4-AP both increased the nerve-evoked endplate potentials and the amplitude of the endplate current in the frog neuromuscular junction (Molgo *et al.*, 1977; Robitaille & Charlton, 1992). Also in the frog neuromuscular junction, TEA and 4-AP were shown to cause a massive increase in acetylcholine release upon electrotonic depolarization of nerve endings (Katz & Miledi, 1969; Lundh & Thesleff, 1977). Prejunctional modulation of neurotransmitter release by K^+ channels is not confined to adrenergic and cholinergic neurotransmission, as it was reported that TEA and 4-AP also affect NANC neurotransmission (Gillespie & Tilmisany, 1976; Jury *et al.*, 1985). However, the effect of K^+ channel blockers on the nitrergic neurotransmission has not yet been studied. Therefore, this study was designed to evaluate the involvement of prejunctional K^+ channels in the nitrergic neurotransmission of the canine ICJ by evaluating the effect of K^+ channel blockers on the relaxations induced by electrical and chemical receptor stimulation of the NANC nerves.

Methods

Tissue preparation

Mongrel dogs of either sex (body weight 10–30 kg) were anaesthetized with sodium pentobarbitone (30 mg kg^{-1}, i.v.) and a laparotomy was performed. A gut segment, 3 cm

[1] Author for correspondence.

above and 5 cm below the ileocolonic junction (ICJ) was resected and cut open longitudinally. After rinsing and cleaning the resected segment, the mucosa was removed by means of sharp dissection (Pelckmans *et al.*, 1989). Circular muscle strips (approximately 10 mm in length and 3 mm wide) were cut, mounted between two platinum ring electrodes and placed in organ baths (25 ml) filled with a modified Krebs-Ringer solution (in mM: NaCl 118.3, KCl 4.7, $MgSO_4$ 1.2, KH_2PO_4 1.2, $CaCl_2$ 2.5, $NaHCO_3$ 25, CaEDTA 0.026 and glucose 11.1). The solution was maintained at 37°C and continuously aerated with a mixture of 95% O_2 and 5% CO_2. The muscle strips were connected to a strain gauge transducer (Statham UC2) for continuous measurement of isometric tension. The muscle strips were brought to their optimal point of length-tension relationship as described earlier (Pelckmans *et al.*, 1989). Electrical pulses (rectangular waves, 60 mA, 9 V, 2–16 Hz, 1–2 ms) were delivered by a GRASS-stimulator and a direct current amplifier in stimuli trains of 10 s. All muscle strips were allowed to equilibrate for at least 45 min before experimentation.

Experimental protocols

All experiments were performed on a noradrenaline (NA, 30 μM)-induced contraction and in the presence of atropine (1 μM). After each NA-induced contraction, the muscle strips were washed at least three times every 5 min. The effects of the non-selective K^+ channel blockers, 4-aminopyridine (4-AP, 3–30 μM) and tetraethylammonium (TEA, 0.1–1 mM) and of charybdotoxin (ChTx, 0.1–0.2 μg ml^{-1}) and apamin (1–2 μM), were studied on the concentration-response curves to NO (0.3–30 μM) and on the NANC relaxations induced by electrical stimulation (ES, 2–16 Hz, 1–2 ms), ATP (100 μM), acetylcholine (30 μM) and GABA (30 μM) and on the relaxations induced by nitroglycerine (1 μM).

Statistical analysis and presentation of results

The results are expressed as percentage decrease of the NA-induced contraction of the muscle strip of the canine ICJ. Values are shown as mean ± s.e.mean for the number of dogs indicated and statistical significance ($P<0.05$) was determined by Student's two tailed t test for paired or unpaired observation.

Drugs

The following drugs were used: acetylcholine chloride, adenosine 5'-triphosphate; γ-aminobutyric acid, 4-aminopyridine, apamin, charybdotoxin, 1,1-dimethyl-4-phenylpiperazinium iodide, tetraethylammonium chloride (Sigma Chemical Co, St. Louis, MO, U.S.A.); atropine sulphate (Federa, Brussels, Belgium); nitroglycerin (Merck, Darmstadt, Germany); noradrenaline hydrogentartrate (Fluka AG, Buchs SG, Switzerland).

All drugs were administered as aqueous solutions. Noradrenaline was dissolved in 0.57 mM ascorbic acid. All solutions were prepared on the day of experimentation. Charybdotoxin, which was used as the crude venom of *Leiurus quinquestriatus* (Miller *et al.*, 1985), and apamin were stored in small amounts in stock-vials at − 20°C. The solutions of NO were prepared as described by Kelm *et al.* (1988).

Results

Effect of K^+ channel blockers on the basal tension and NA-induced contraction

Neither the basal tension of the canine ICJ nor the contraction induced by NA (30 μM), was affected by the K^+ channel blockers 4-AP (3–30 μM), TEA (0.1–1 μM), charybdotoxin (0.1–0.2 μg ml^{-1}) or apamin (1–2 μM) (results not shown). However, raising the concentrations of TEA above 3 mM or of charybdotoxin above 0.4 μg ml^{-1} evoked a rise in basal tone, rhythmic contractions and unstable NA-induced contractions. Therefore the effect of these K^+ channel blockers was not tested at or above these concentrations.

Effect of K^+ channel blockers on the nitrergic relaxations induced by electrical stimulation (ES)

The NANC relaxations induced by ES (2 and 4 Hz, 1 ms) were significantly and concentration-dependently enhanced

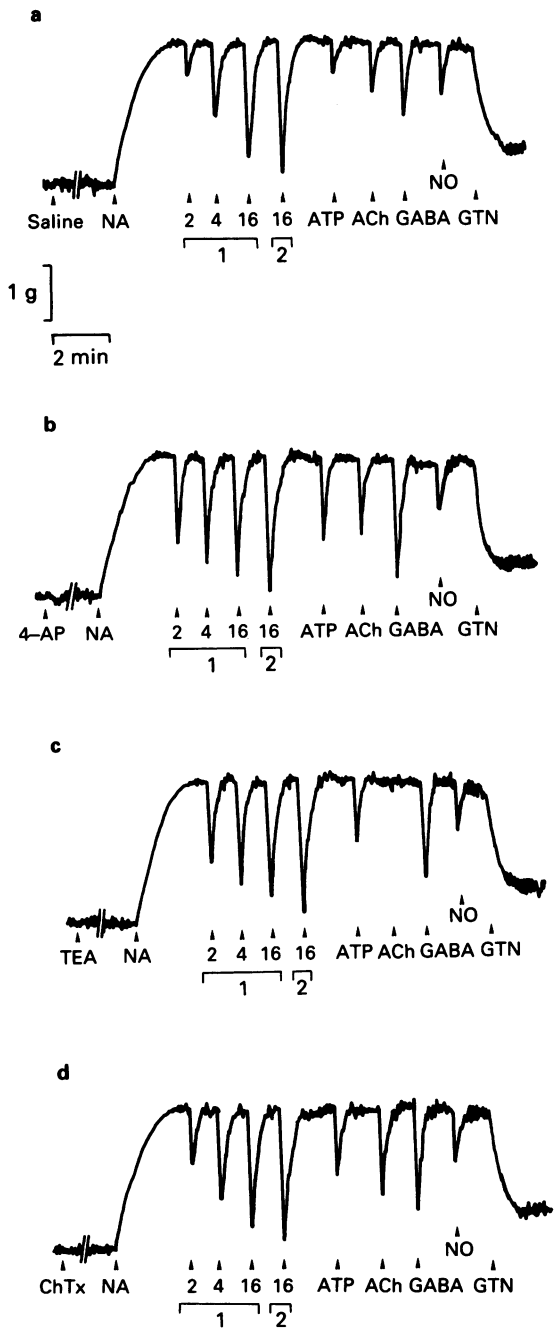

Figure 1 Typical tracing of a circular muscle strip of the canine ileocolonic junction (contracted with noradrenaline, NA) showing the relaxations to electrical stimulation (2–16 Hz, 1–2 ms), adenosine 5'-triphosphate (ATP, 100 μM), acetylcholine (ACh, 30 μM), γ-aminobutyric acid (GABA, 30 μM), NO (1 μM) and nitroglycerin (GTN, 1 μM) in control experiments (a) and in the presence of (b) 4-aminopyridine (30 μM), (c) tetraethylammonium (1 mM) and (d) charybdotoxin (ChTx, 0.2 μg ml^{-1}). Similar results were obtained in at least 5 other experiments. Tracing breaks represent 15 min of tissue equilibration.

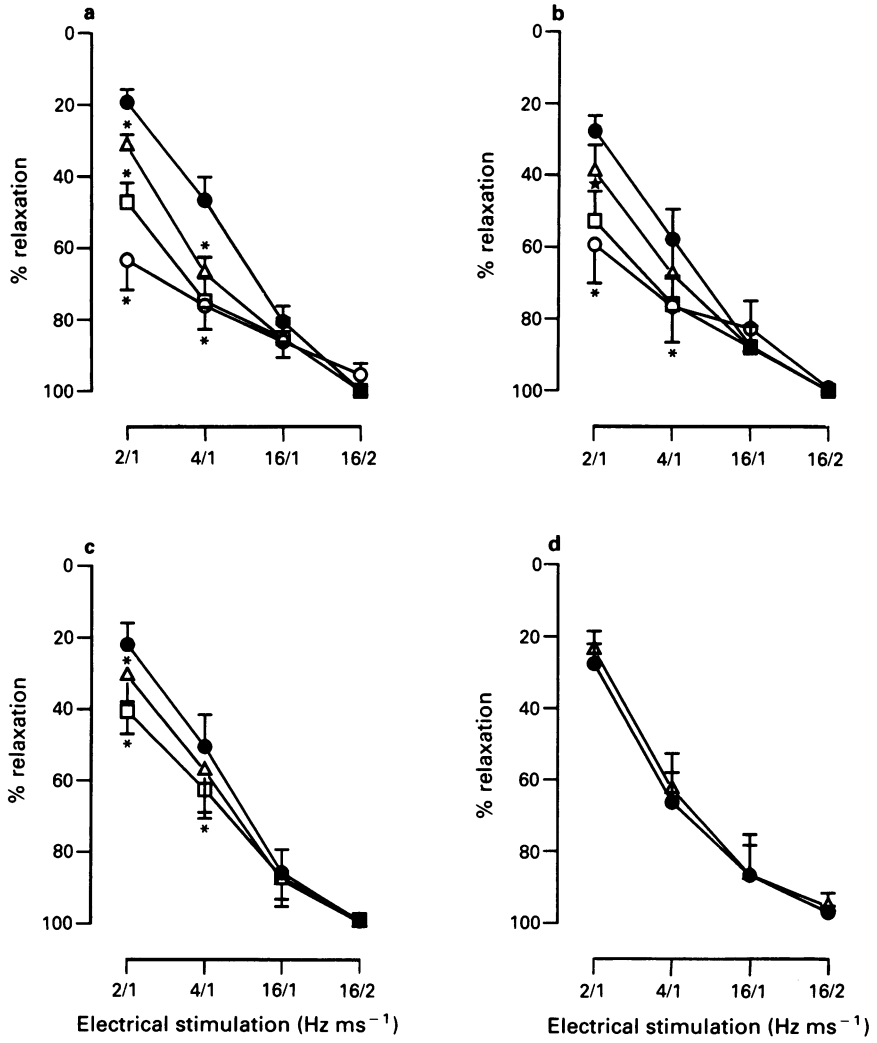

Figure 2 Frequency-response curves showing the effect of (a) 4-aminopyridine (Δ, 3 μM; □, 10 μM; ○, 30 μM), (b) tetraethylammonium (Δ, 0.1 mM; □, 0.3 mM; ○, 1 mM), (c) charybdotoxin (Δ, 0.1 μg ml^{-1}; □, 0.2 μg ml^{-1}) and (d) apamin (Δ, 2 μM) on the NANC relaxations induced by electrical stimulation (●, 2–16 Hz, 1–2 ms). Results are shown as mean ± s.e.mean for $n = 6$ experiments and expressed as percentage decrease of the noradrenaline-induced contraction. *$P < 0.05$, significantly different from control value, Student's t test for paired observations.

by 4-AP (3–30 μM), TEA (0.3–1 mM) and charybdotoxin (0.2 μg ml^{-1}), but not by apamin (1–2 μM) (Figures 1 and 2). The potentiating effect of 4-AP, TEA and charybdotoxin was most pronounced on relaxations induced by lower frequency stimulation: for 2 Hz, 1 ms the NANC relaxations were enhanced from 20 ± 3% to 64 ± 8% by 4-AP (30 μM), from 27 ± 4% to 60 ± 10% by TEA (1 mM) and from 22 ± 6% to 41 ± 6% by charybdotoxin (0.2 μg ml^{-1}) for $n = 6$ (Figures 1 and 2).

Effect of K^+ channel blockers on the nitrergic relaxations induced b y ATP, ACh and GABA

As previously described (Boeckxstaens *et al.*, 1990a; 1991a), ATP, ACh and GABA induced concentration-dependent and tetrodotoxin-sensitive NANC relaxations which are mediated by NO. 4-AP (30 μM) and charybdotoxin (0.2 μg ml^{-1}) both significantly enhanced the NANC relaxations induced by ATP (100 μM), ACh (30 μM) and GABA (30 μM). TEA at higher concentrations (1 mM) significantly potentiated the relaxations to ATP and GABA whereas TEA in all concentration ranges used (0.1–1 mM) almost completely abolished the relaxation to ACh (Figures 1 and 3). Apamin (1–2 μM) had no effect on these NANC relaxations (Figure 3).

Effect of K^+ channel blockers on the relaxations induced by GTN or NO

Both GTN (1 μM) and NO (0.3–30 μM) relaxed the circular muscle strips of the canine ICJ. None of the K^+ channel blockers used, had an effect on the relaxations induced by GTN (1 μM) (Figure 1) or NO (0.3–30 μM) (Figure 4).

Discussion

The multiplicity of K^+ channels and a lack of specific drugs to block or open these channels, has been a major problem in the understanding of K^+ channels and their involvement in physiological processes. Aminopyridines and tetraethylammonium (TEA) have been used as non-specific K^+ channel blockers for several decades. With the discovery of selective toxins like charybdotoxin and apamin, it has become clear that K^+ channels indeed play an important role in the regulation of neuronal transmission (Belardetti & Siegelbaum, 1988; Miller, 1990). Blockers of K^+ channels have been shown to enhance potently neurotransmitter release from adrenergic and cholinergic nerves in various tissues (see Introduction). In the present study, we demonstrated a

potentiating prejunctional effect of these agents on NO-mediated NANC relaxations and therefore suggest a modulatory role of prejunctional K^+ channels in nitrergic neurotransmission.

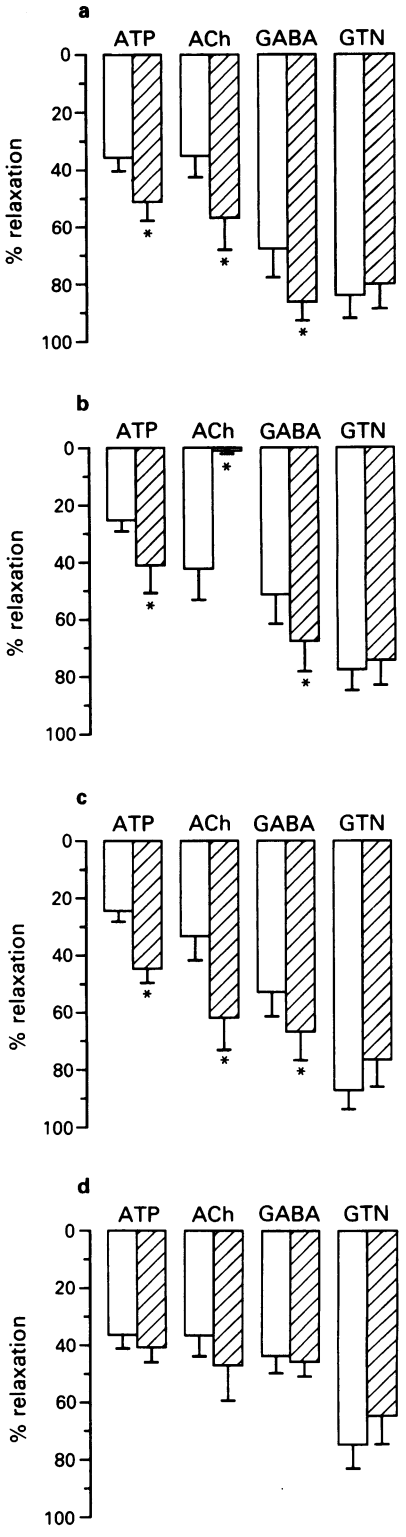

Figure 3 Effect of (a) 4-aminopyridine (30 μM, hatched columns), (b) tetraethylammonium (1 mM, hatched columns), (c) charybdotoxin (0.2 μg ml^{-1}, hatched columns) and (d) apamin (2 μM, hatched columns) on the NANC relaxations induced by ATP (100 μM), acetylcholine (ACh, 30 μM) and γ-aminobutyric acid (GABA, 30 μM) and on the relaxations to nitroglycerin (GTN, 1 μM) (all open columns). Results are shown as mean ± s.e.mean for $n = 5$ experiments at least and expressed as percentage decrease of the noradrenaline-induced contraction. $^*P < 0.05$, significantly different from control value, Student's t test for paired observations.

The non-selective K^+ channel blockers, 4-AP and TEA and the blocker of large and intermediate conductance Ca^{2+}-activated K^+ channels charybdotoxin, significantly enhanced the electrically- and receptor-induced NANC relaxations, which were previously demonstrated to be mediated by NO (Boeckxstaens *et al.*, 1990; 1991a; Bult *et al.*, 1990). The effects of 4-AP, TEA and charybdotoxin were of prejunctional origin since the relaxations to NO and nitroglycerin, or the contractions to NA were not affected by these blockers. The latter results suggest that postjunctional K^+ channels, which are undoubtedly present in gut smooth muscle (Szurszewsky, 1978; Barajas-Lopez & Huizinga, 1988) are not involved in mediating NANC relaxations in the canine ICJ.

The potentiating effects of 4-AP, TEA and charybdotoxin on the electrically-induced NANC relaxations, were most pronounced at lower frequency stimulations. This is in accordance with other studies (Gillespie & Tilmisany, 1976; Johns *et al.*, 1976; Kirkepar *et al.*, 1977) and is typical for the competitive nature of these blockers: higher frequency stimulation induces a larger K^+-efflux that overcomes the effect of the K^+ channel blockers. The underlying mechanism, responsible for the increased neurotransmitter release induced by K^+ channel blockers, is believed to result from their effect on the depolarization phase of the action potential, which is generally associated with a K^+ efflux from the nerve terminal (for review see Rudy, 1988). As shown for TEA and charybdotoxin, this action results in an increase in the duration of the prejunctional action potential (Augustine, 1990; Morita & Barrett, 1990). Consequently, the enduring Ca^{2+} influx into the nerve terminals leads to enhanced neurotransmitter release.

Although it has been reported that apamin, which selectively blocks small conductance Ca^{2+}-activated K^+ channels, reduces the amplitude of the fast hyperpolarization phase of the inhibitory junction potentials (i.j.p.) in the canine ICJ (Ward *et al.*, 1992), it had no effect on the NANC relaxations. The explanation for this discrepancy still has to be elucidated; however, these findings might suggest that the fast component of the i.j.p. is of rather minor importance to the mechanical response in the canine ICJ.

The influence of K^+ channel blockers on the NO release is further confirmed by their effect on the NANC-relaxations induced by ATP, ACh and GABA. 4-AP and charybdotoxin but not apamin enhanced these relaxations without affecting those to NO, indeed confirming their prejunctional potentiating effect on the NO release. Relaxations induced by electrical stimulation were increased to a greater extent than relaxations of comparable amplitude resulting from receptor stimulation, which might suggest activation of different K^+ channels by different stimuli. Alternatively, this might suggest that the receptor-mediated pathway involves intracellular mechanisms which are independent of K^+ channels. In contrast to 4-AP and charybdotoxin, TEA almost abolished the relaxation to ACh. This blockade might result from an antagonistic effect of TEA at the nicotinic receptor on the NANC nerve as both TEA and ACh include in their molecular structure a quaternary ammonium group, which represents one of the two binding sites of the nicotinic receptor (Popot & Changeux, 1984). In confirmation of this hypothesis, we found that the NANC relaxations induced by the nicotinic agonist 1,1-dimethyl-4-phenylpiperazinium (DMPP) were also blocked by TEA (results not shown).

As activation or inhibition of neuronal K^+ channels modulates the amount of neurotransmitter released, K^+ channels may represent a substrate for prejunctional modulation. This is supported by the finding that the prejunctional inhibition of neurotransmitter release via opiate and α_2-adrenoceptors is accompanied by an enhanced K^+ conductance (Rezvani *et al.*, 1983; Bauer, 1985). Furthermore, Morita & North (1981) suggested the involvement of Ca^{2+}-sensitive K^+ channels in the α_2-adrenoceptor activation of neurones in the myenteric plexus of the guinea-pig ileum. Recently, we demonstrated that activation of presynaptic

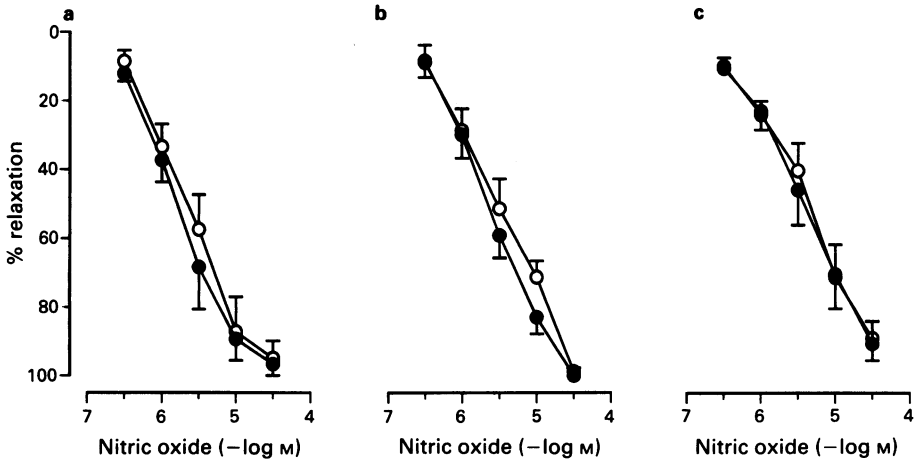

Figure 4 Concentration-response curves showing the effect of (a) 4-aminopyridine (○, 30 μM), (b) tetraethylammonium (○, 1 mM) and (c) charybdotoxin (○, 0.2 μg ml^{-1}) on the relaxations in response to NO (●, 0.3–30 μM). Results are shown as mean ± s.e.mean for $n = 4$ experiments and expressed as percentage decrease of the noradrenaline-induced contraction.

α_2-adrenoceptors in the canine ICJ inhibits the nitrergic relaxations induced by ES, suggesting prejunctional regulation of NO release via α_2-adrenoceptors (Boeckxstaens *et al.*, 1993). Whether there is a relationship between this α_2-adrenoceptor-regulated inhibition and the presence of the prejunctional K^+ channels described here remains to be investigated.

In conclusion, we here demonstrate that blockers of K^+ channels induce a significant enhancement of electrically- and chemically-induced NANC relaxations without affecting the postjunctional response to NO, thereby providing evidence for the involvement of prejunctional K^+ channels in the prejunctional modulation of the nitrergic NANC innervation of the canine ICJ.

This work was supported by the Belgian Fund for Medical Research (Grant 3.0014.90). The authors are grateful to Mrs L. Van de Noort for typing the manuscript and to F.H. Jordaens for his technical assistance.

References

AUGUSTINE, G.J. (1990). Regulation of transmitter release at the squid giant synapse by presynaptic delayed rectifier potassium current. *J. Physiol.*, **431**, 343–364.

BAUER, V. (1985). Effects of 3,4-diaminopyridine and tetraethylammonium on the pre- and post-junctional α-adrenoceptor mediated inhibitory actions of noradrenaline in the guinea-pig ileum. *Br. J. Pharmacol.*, **85**, 171–177.

BARAJAS-LOPEZ, C. & HUIZINGA, J.D. (1988). Heterogeneity in spontaneous and tetraethylammonium induced activity in dog colon circular muscle. *Pflügers Arch.*, **412**, 203–210.

BELARDETTI, F. & SIEGELBAUM, S.A. (1988). Up- and down-modulation of single K^+ channel function by distinct second messengers. *Trends Neurosci.*, **11**, 232–239.

BOECKXSTAENS, G.E., DE MAN, J.G., PELCKMANS, P.A., HERMAN, A.G. & VAN MAERCKE, Y.M. (1993). α_2-Adrenoceptor-mediated modulation of the nitrergic innervation of the canine isolated ileocolonic junction. *Br. J. Pharmacol.*, (in press).

BOECKXSTAENS, G.E., PELCKMANS, P.A., BULT, H., DE MAN, J.G., HERMAN, A.G. & VAN MAERCKE, Y.M. (1990a). Non-adrenergic non-cholinergic relaxation mediated by nitric oxide in the canine ileocolonic junction. *Eur. J. Pharmacol.*, **190**, 239–246.

BOECKXSTAENS, G.E., PELCKMANS, P.A., BULT, H., DE MAN, J.G., HERMAN, A.G. & VAN MAERCKE, Y.M. (1991a). Evidence for nitric oxide as mediator of non-adrenergic non-cholinergic relaxations induced by ATP and GABA in the canine gut. *Br. J. Pharmacol.*, **102**, 434–438.

BOECKXSTAENS, G.E., PELCKMANS, P.A., RAMPART, M., VERBEUREN, T.J., HERMAN, A.G. & VAN MAERCKE, Y.M. (1990b). Evidence against ATP being the inhibitory transmitter released by nonadrenergic noncholinergic nerves in the canine ileocolonic junction. *J. Pharmacol. Exp. Ther.*, **254**, 659–663.

BOECKXSTAENS, G.E., PELCKMANS, P.A., RAMPART, M., VERBEUREN, T.J., HERMAN, A.G. & VAN MAERCKE, Y.M. (1990c). Non-adrenergic non-cholinergic mechanisms in the ileocolonic junction. *Arch. Int. Pharmacodyn. Ther.*, **303**, 270–281.

BOECKXSTAENS, G.E., PELCKMANS, P.A., RUYTJENS, I.F., BULT, H., DE MAN, J.G., HERMAN, A.G. & VAN MAERCKE, Y.M. (1991b). Bioassay of nitric oxide released upon stimulation of non-adrenergic non-cholinergic nerves in the canine ileocolonic junction. *Br. J. Pharmacol.*, **103**, 1085–1091.

BULT, H., BOECKXSTAENS, G.E., PELCKMANS, P.A., JORDAENS, F.H., VAN MAERCKE, Y.M. & HERMAN, A.G. (1990). Nitric oxide as an inhibitory non-adrenergic non-cholinergic neurotransmitter. *Nature*, **345**, 346–347.

DE MAN, J.G., BOECKXSTAENS, G.E., PELCKMANS, P.A., HERMAN, A.G. & VAN MAERCKE, Y.M. (1992). Nitric oxide release from non-adrenergic non-cholinergic nerves in the canine ileocolonic junction is calcium dependent. *J. Gastrointest. Motil.*, **4**, 216.

GILLESPIE, J.S. & TILMISANY, A.K. (1976). The action of tetraethylammonium chloride on the response of the rat anococcygeus muscle to motor and inhibitory nerve stimulation and to some drugs. *Br. J. Pharmacol.*, **58**, 47–55.

JOHNS, A., GOLKO, D.S., LAUZON, P.A. & PATON, D.M. (1976). The potentiating effects of 4-aminopyridine on adrenergic transmission in the rabbit vas deferens. *Eur. J. Pharmacol.*, **38**, 71–78.

JURY, J., JAGER, L.P. & DANIEL, E.E. (1985). Unusual potassium channels mediate non-adrenergic non-cholinergic nerve-mediated inhibition in opossum esophagus. *Can. J. Physiol. Pharmacol.*, **63**, 107–112.

KATZ, B. & MILEDI, R. (1969). Spontaneous and evoked activity of motor nerve endings in calcium ringer. *J. Physiol.*, **203**, 689–706.

KELM, M., FEELISCH, M., SPAHR, R., PIPER, H.M., NOACK, E. & SCHRADER, J. (1988). Quantitative and kinetic characterization of nitric oxide and EDRF released from cultured endothelial cells. *Biochem. Biophys. Res. Commun.*, **154**, 236–244.

KIRKEPAR, M., KIRKEPAR, S.M. & PRAT, J.C. (1977). Effect of 4-aminopyridine on release of noradrenaline from the perfused cat spleen by nerve stimulation. *J. Physiol.*, **272**, 517–528.

KIRKEPAR, S.M. & PRAT, J.C. (1978). Effect of tetraethylammonium on noradrenaline release from cat spleen treated with tetrodotoxin. *Nature*, **276**, 623–624.

LEANDER, S., ARNER, A. & JOHANSSON, B. (1977). Effects of 4-aminopyridine on mechanical activity and noradrenaline release in the rat portal vein in vitro. *Eur. J. Pharmacol.*, **46**, 351–361.

LUNDH, H. & THESLEFF, S. (1977). The mode of action of 4-aminopyridine and guanidine on transmitter release from motor nerve terminals. *Eur. J. Pharmacol.*, **42**, 411–412.

MILLER, C., MOCZYDLOWSKI, E., LATORRE, R. & PHILLIPS, M. (1985). Charybdotoxin, a protein inhibitor of single Ca^{++} activated K^+ channels from mammalian skeletal muscle. *Nature*, **313**, 316–318.

MILLER, R.J. (1990). Receptor-mediated regulation of calcium channels and neurotransmitter release. *FASEB J.*, **4**, 3291–3299.

MOLGO, J., LEMEIGNAN, M. & LECHAT, P. (1977). Effects of 4-aminopyridine at the frog neuromuscular junction. *J. Pharmacol. Exp. Ther.*, **203**, 653–663.

MORITA, K. & BARRETT, E.F. (1990). Evidence for two calcium-dependent potassium conductances in lizard motor nerve terminals. *J. Neurosci.*, **10**, 2614–2625.

MORITA, K. & NORTH, R.A. (1981). Clonidine activates membrane potassium conductance in myenteric neurones. *Br. J. Pharmacol.*, **74**, 419–428.

PELCKMANS, P.A., BOECKXSTAENS, G.E., VAN MAERCKE, Y.M., HERMAN, A.G. & VERBEUREN, T.J. (1989). Acetylcholine is an indirect inhibitory transmitter in the canine ileocolonic junction. *Eur. J. Pharmacol.*, **170**, 235–242.

POPOT, J. & CHANGEUX, J. (1984). Nicotinic receptor of acetylcholine: structure of an oligomeric integral membrane protein. *Physiol. Rev.*, **64**, 1162–1239.

REZVANI, A., HUIDOBRO-TORO, J.P. & WAY, E.L. (1983). Effect of 4-aminopyridine and verapamil on the inhibitory action of normorphine on the guinea pig ileum. *Eur. J. Pharmacol.*, **86**, 111–115.

ROBITAILLE, R. & CHARLTON, M.P. (1992). Presynaptic calcium signals and transmitter release are modulated by calcium-activated potassium channels. *J. Neurosci.*, **12**, 297–305.

RUDY, B. (1988). Diversity and ubiquity of K channels. *Neurosci.*, **25**, 729–749.

SANDERS, K.M. & WARD, S.M. (1992). Nitric oxide as a mediator of non adrenergic non cholinergic neurotransmission. *Am. J. Physiol.*, **262**, G379–392.

STARK, M.E. & SZURSZEWSKI, J.H. (1992). Role of nitric oxide in gastrointestinal and hepatitic function and disease. *Gastroenterology*, **103**, 1928–1949.

SZURSZEWSKI, J.H. (1978). A study of the canine gastric action potential in the presence of tetraethylammonium chloride. *J. Physiol.*, **277**, 91–102.

WARD, S.M., MCKEEN, E.S. & SANDERS, K.M. (1992). Role of nitric oxide in non-adrenergic non-cholinergic inhibitory junction potentials in canine ileocolonic sphincter. *Br. J. Pharmacol.*, **105**, 776–782.

WESTFALL, T.C. & MARTIN, J.R. (1991). Presynaptic receptors in the peripheral and central nervous system. In *Presynaptic Regulation of Neurotransmitter Release: a Handbook*. ed. Feigenbaum, J. & Hanani, M. vol. 1. pp. 311–370. London: Freund Publishing House.

(Received March 22, 1993
Revised May 17, 1993
Accepted May 21, 1993)

Br. J. Pharmacol. (1993), **110**, 565–572

Cyclopiazonic acid, an inhibitor of Ca^{2+}-ATPase in sarcoplasmic reticulum, increases excitability in ileal smooth muscle

Yoshiaki Uyama, [1]Yuji Imaizumi & Minoru Watanabe

Department Chemical Pharmacology, Faculty of Pharmaceutical Sciences, Nagoya City University, 3-1 Tanabedori, Mizuhoku, Nagoya 467, Japan

1 Effects of cyclopiazonic acid (CPA), a specific inhibitor of Ca^{2+}-ATPase in endo- and sarcoplasmic reticulum (ER/SR), on contractile responses, cytosolic Ca^{2+} concentration and spontaneous electrical activity were examined in ileal longitudinal smooth muscle strips.

2 After intracellular stored Ca^{2+} in intact ileal strips was depleted by application of 25 mM caffeine in Ca^{2+}-free solution, Ca^{2+}-loading was performed in the absence or presence of 10 μM CPA in a standard solution containing 2.2 mM Ca^{2+}. Subsequent application of caffeine in Ca^{2+}-free solution induced a phasic contraction which was significantly smaller in the strip pretreated with CPA than that in the control.

3 Spontaneous and 20 mM K^+-induced contractions in the presence of 1 μM atropine were markedly enhanced by 1–30 μM CPA, whereas that induced by 80 mM K^+ was not. The magnitude of repetitive transient elevation of cytosolic Ca^{2+} concentration ($[Ca^{2+}]_i$) and concomitant phasic contractions were markedly enhanced by CPA. The effects were abolished by 10 μM verapamil and restored by 10 μM Bay K 8644.

4 Application of 10 μM CPA depolarized the cell by about 5 mV, decreased the action potential (AP) afterhyperpolarization and markedly increased the frequency of spontaneous AP. These effects were mimicked by 100 nM charybdotoxin.

5 The rate of decay of $[Ca^{2+}]_i$ and tension after the bathing solution was changed from one containing 140 mM K^+ and 2.2 mM Ca^{2+} to one containing 5.9 mM K^+ and 0 mM Ca^{2+} was significantly slowed when 10 μM CPA was added to the latter solution.

6 These results indicate that CPA enhances ileal smooth muscle excitability and increases Ca^{2+}-influx through voltage-dependent Ca^{2+} channels. The effect may be consistent with the hypothesis that CPA-induced decrease in stored Ca due to Ca-pump inhibition reduces the Ca^{2+}-dependent K^+ current and indirectly enhances Ca^{2+}-influx through membrane activity resulting from the increased excitability. Direct evidence for the regulation of Ca^{2+} channel activity by intracellular Ca storage sites was not obtained in the present study.

Keywords: Cyclopiazonic acid; smooth muscle; Ca-pump; Ca^{2+}-ATPase; sarcoplasmic reticulum; Ca^{2+}-dependent K^+ current; Ca current; guinea-pig ileum; skinned fibre

Introduction

Cyclopiazonic acid (CPA), a mycotoxin from *Aspergillus* and *Penicillium*, has been described as a highly selective inhibitor of Ca^{2+}-ATPase in skeletal, cardiac and smooth muscle sarcoplasmic reticulum (SR) (Goeger & Riley, 1989; Seidler *et al.*, 1989) and inhibits Ca^{2+}-uptake of SR in skeletal muscle (Goeger *et al.*, 1988; Kurebayasi & Ogawa, 1991). Recently, we showed that CPA is a selective and reversible inhibitor of ATP-dependent Ca^{2+}-uptake of SR/ER in the skinned fibre of ileal smooth muscle (Uyama *et al.*, 1992). Moreover, it has been suggested that CPA can inhibit Ca^{2+}-ATPase in intact preparations of aorta (Deng & Kwan, 1991), trachea (Bourreau *et al.*, 1991) and mesenteric artery (Low *et al.*, 1992).

In intact smooth muscle tissue preparations, however, the effects of CPA on the contractile responses to various types of stimulation are complicated and not always consistent between different smooth muscles. This may be due to differences in characteristics of intracellular Ca-storage sites and also of Ca^{2+}-influx and -extrusion through the plasma membrane during stimulation. In addition, the function of intracellular Ca storage sites as one of the important regulatory factors of membrane ionic currents (Ohya *et al.*, 1987; Wong, 1991) has not been taken into consideration. The effects of CPA in intact preparations have been examined in electrically quiescent muscles which do not show spontaneous myogenic activity (Deng & Kwan, 1991; Bourreau *et al.*, 1991; Low *et al.*, 1992).

In a previous paper, we showed that application of CPA selectively inhibits Ca^{2+}-dependent K^+-current ($I_{K\text{-}Ca}$) in single smooth muscle cells of guinea-pig ileum and urinary bladder (Suzuki *et al.*, 1992). Activity of single large conductance Ca^{2+}-dependent K^+ channels (BK channels) are not affected by 10 μM CPA. The inhibition of $I_{K\text{-}Ca}$ may be attributable to the suppression of SR/ER Ca^{2+}-ATPase, which presumably results in a marked decrease in releasable Ca in storage sites. The large transient $I_{K\text{-}Ca}$ upon depolarization in these cells is induced by Ca-release from ryanodine-sensitive Ca storage sites (Sakai *et al.*, 1988), which is triggered by Ca^{2+}-influx through voltage-dependent Ca^{2+} channels (Ohya *et al.*, 1987; Kitamura *et al.*, 1989) via Ca^{2+}-induced Ca^{2+} release mechanisms (Suzuki *et al.*, 1992; Ganitkevich & Isenberg, 1992), which it has been suggested do not have a functional role in skinned fibres (Iino, 1989). This current may be responsible for action potential (AP) repolarization and afterhyperpolarization (AHP) (Mitra & Morad, 1985; Ohya *et al.*, 1987; Watanabe *et al.*, 1989; Wong, 1991). Moreover, $I_{K\text{-}Ca}$ significantly contributes to the regulation not only of APs, but also of the resting membrane potential (Hu *et al.*, 1989) and muscle tone (Brayden & Nelson, 1992) in some kinds of smooth muscle cells. The inhibition of $I_{K\text{-}Ca}$, therefore, may depolarize the cell membrane, increase AP

[1] Author for correspondence.

duration, decrease AHP and possibly increase spontaneous spike generation and membrane excitability of smooth muscle cells.

Based upon these results, it can be speculated that the decrease in $I_{K\text{-}Ca}$ by CPA may result in an increase in membrane excitability and, therefore, spontaneous spike generation. It is, however, not clear whether spontaneous contractile activity is increased or decreased under conditions where stored Ca is significantly decreased by CPA. The present study was undertaken to examine how CPA affects electrical activity, $[Ca^{2+}]_i$ concentration and mechanical activity in an intact tissue preparation of ileal longitudinal muscle.

Methods

Male Hartley guinea-pigs, weighing about 200 g, were killed by a blow on the head. The terminal portion of the ileum was isolated.

Intact preparation and tension measurement

Longitudinal muscle strips (2–3 mm wide and 10 mm long) were dissected from the ileum in Krebs solution (see Solutions) at room temperature. The muscle strip was mounted horizontally on a silicon rubber sheet at the bottom of an organ bath which had a volume of 0.3 ml and was filled with modified Krebs solution or HEPES buffered salt solution. The solutions were continuously bubbled with 95% O_2:5% CO_2 or 100% O_2, respectively. Temperature was maintained at 36 ± 1°C except where mentioned in figure legends. Contractile responses were measured isometrically with a strain gauge transducer and recorded on a pen-recorder.

Skinned fibre preparation

Skinning of ileal longitudinal strips was performed as described previously (Uyama *et al.*, 1992). In brief, strips were incubated with 60 μM β-escin in a solution of pCa 6.0 (Kobayashi *et al.*, 1989; Kitazawa & Somlyo, 1990). After skinning, the solution was changed to a relaxing solution containing 2 mM EGTA (R2G). Contractile responses to caffeine were tested in a relaxing solution containing 0.1 mM EGTA (R0.1G). Experiments were performed at room temperature (22 ± 1°C). Calmodulin was not added except when mentioned.

Measurement of membrane potential

The conventional glass microelectrode technique was used to measure the membrane potential of smooth muscle cells in ileal longitudinal muscle strips. A strip was prepared in the same manner as the intact preparations for tension measurement and was pinned firmly to the silicon rubber at the bottom of a chamber which had volume of about 0.3 ml. The strip was perfused with modified Krebs solution at rate of 10 ml min^{-1} and kept at 35 ± 1°C. Glass microelectrodes having a resistance of 40–60 Mohm when filled with 3 M KCl were inserted into smooth muscle cells from the outside of the strip. Electrical signals were amplified (Nihon Koden MEZ-8101), monitored on a storage oscilloscope (Nihon Koden, VC10) and recorded on a pen recorder and a video tape via a PCM recorder (Sony PCM-501ES; modified to obtain frequency response from d.c. to 20 kHz). Records on the video tape were replayed and stored on the hard disk of a computer (IBM-AT) after A-D conversion and analysed on the computer as described previously (Imaizumi *et al.*, 1990).

Simultaneous measurement of cytosolic Ca^{2+} concentration ($[Ca^{2+}]_i$) and contraction

Longitudinal strips of guinea-pig ileum were isolated and were treated with 5 μM acetoxymethyl ester of Fura-2 (Fura-2/AM) for 4–6 h at room temperature in 4 ml HEPES-buffer solution in a dark place. A non-cytotoxic detergent, pulronic F-127 (0.02–0.04%), was added to the loading solution to increase the solubility of Fura-2/AM. A Fura-2-loaded strip was mounted horizontally in a chamber which had volume of approximately 1.2 ml and continuously superfused at 12 ml min^{-1} with a HEPES buffered solution oxygenated by 100% O_2. The temperature of the solution was maintained at 35 ± 1°C. Fura-2-Ca^{2+} signals were measured simultaneously with muscle contractions as described by Ozaki *et al.* (1987). Muscle strips were illuminated alternately at the excitation wavelengths (340 nm and 380 nm). The amounts of 500 nm fluorescence induced by 340 nm excitation (F340) and by 380 nm excitation (F380) were measured with a fluorimeter (CAF-100, JASCO). The ratio of F340 and F380 was used as an indicator of $[Ca^{2+}]_i$, taking the ratio in resting state as 0% and that in 80 mM K^+-stimulated state as 100%.

Solutions

The composition of Krebs solution was (in mM): NaCl 112.0, KCl 4.7, $CaCl_2$ 2.2, $MgCl_2$ 1.2, $NaHCO_3$ 25.0, KH_2PO_4 1.2 and glucose 14.0. The composition of the physiological salt HEPES-buffer solution was (in mM): NaCl 137.0, KCl 5.9, $CaCl_2$ 2.2, $MgCl_2$ 1.2, glucose 14.0 and HEPES 10.0. The pH was adjusted to 7.4 with NaOH. A high K^+ solution was prepared by replacing NaCl with equimolar KCl. A Ca^{2+}-free solution was prepared by removing $CaCl_2$ and added 0.1 mM EGTA to the HEPES buffered solution. The composition of R2G was (in mM): K-propionate 130, $MgCl_2$ 4.0, adenosine triphosphate (ATP)-2Na 4.0, creatine phosphate 10, NaN_3 10, Tris 20.0 and EGTA 2.0. Solutions containing 0.1 or 0.5 mM EGTA (R0.1G and R0.5G) were prepared by reducing the EGTA concentration in R2G from 2.0 to 0.1 or 0.5 mM, respectively. The approximate pCa of R0.1G was calculated to be 7.2, assuming the contamination of Ca^{2+} to be 15 μM. The pH was adjusted to 6.8 with maleic acid. Solutions of pCa 6.3 and 6.0 were prepared by using a Ca^{2+}-EGTA buffer of 3 mM EGTA and corresponding Ca^{2+}.

Drugs

Cyclopiazonic acid (CPA) and β-escin was obtained from Sigma Ltd. Pulronic F-127 was from Calbiochem. Ltd. EGTA and Fura-2/AM were from Dojin. Caffeine, acetylcholine and atropine were from Wako Junyaku. Charybdotoxin was from Peptide Institute, Inc. Bay K 8644 (methyl 1,4 dihydro-2,6-dimethyl-3-nitro-4-(2-trifluoromethyl phenyl)-pyridine-5-carboxylate) was obtained from Bayer, Japan.

Statistics

Pooled data are expressed as mean ± s.e.mean. Statistical significance was examined with a paired or unpaired Student's t test and is indicated by $*P<0.05$; $**P<0.01$ and $***P<0.001$.

Results

First, we determined whether CPA applied to intact ileal longitudinal strips can inhibit Ca^{2+}-uptake by intracellular storage sites as it does in skinned preparations (Uyama *et al.*, 1992). Figure 1 shows the effects of CPA on 25 mM caffeine-induced contraction in intact strips. To reduce spontaneous contractions, experiments were performed at room temperature (20–22°C). After the strip was loaded with Ca^{2+} in a HEPES buffered solution containing 2.2 mM Ca^{2+} (Ca^{2+}-loading or Ca^{2+}-uptake, see Methods, not shown in Figure 1a), 25 mM caffeine was applied twice in a Ca^{2+}-free solution (Figure 1a(i)). The second application of caffeine did not elicit a response, implying that Ca in storage sites may be almost depleted after the first application. The Ca^{2+}-load and

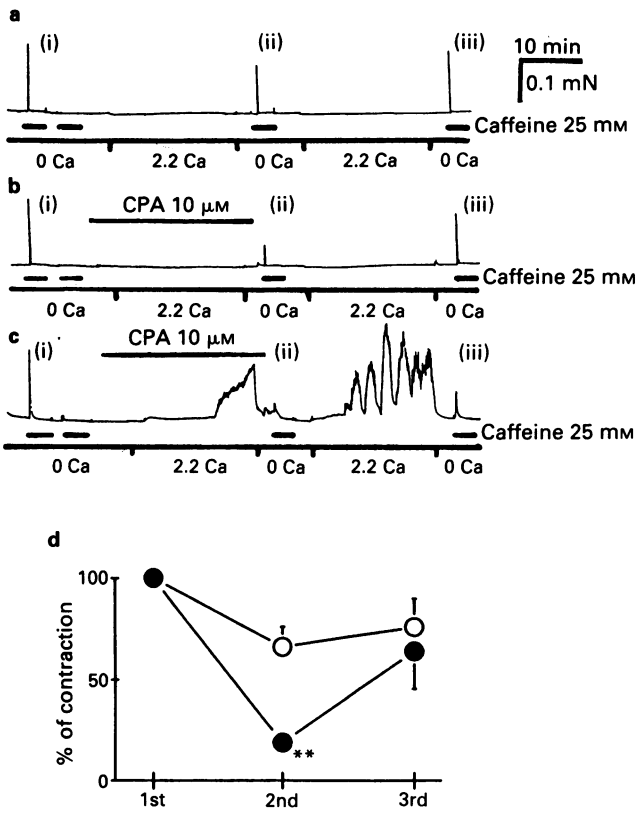

Figure 1 Effects of cyclopiazonic acid (CPA) on 25 mM caffeine-induced contraction in intact ileal smooth muscle strips. Experiments were performed at 21 ± 1°C to depress spontaneous contractions. After Ca^{2+}-loading in a HEPES buffered solution containing 2.2 mM Ca^{2+} (not shown), 25 mM caffeine was applied twice in a Ca^{2+}-free solution (i). Note that the second application of caffeine induced no response. Thereafter, Ca^{2+}-loading was performed in the absence (a) or the presence of 10 μM CPA (b,c) in a solution containing 2.2 mM Ca^{2+}. The subsequent response to caffeine was inhibited, when the Ca^{2+}-loading was performed in the presence of CPA (b(ii) and c(ii)). The contractile response to caffeine recovered substantially in the third trial as shown in (b(iii)) and (c(iii)). Application of 10 μM CPA to the solution containing 2.2 mM Ca^{2+} did not change the muscle tone in most preparations examined as shown in (b). In about 30% of preparations, however, CPA itself increased the muscle tone and induced repetitive phasic spontaneous contractions (c). This effect of CPA was occasionally irreversible. Summarized data shown in (d) are from preparations in which CPA itself did not induce contractions and indicate that 10 μM CPA significantly reduced caffeine-induced contraction in a reversible manner: (○) control response; (●) 2nd response measured after treatment with 10 μM CPA. $n = 6$.

subsequent Ca^{2+} release by caffeine was repeated three times (Figure 1(i), (ii) and (iii)) in each preparation. In the second trial, Ca^{2+}-loading was performed in the absence or presence of 10 μM CPA. Addition of 10 μM CPA in a Ca^{2+}-free solution did not change the muscle tone. The change in solution from Ca^{2+}-free solution to Ca^{2+}-containing solution in the presence of CPA did not alter muscle tone in 70% of preparations but induced tonic or phasic contraction in the other preparations. Such a contraction during Ca^{2+}-loading was not observed in the control. In strips where Ca^{2+}-loading was performed in the presence of 10 μM CPA, the subsequent contraction induced by caffeine was significantly smaller (Figure 1b, c and d). In the third trial, application of caffeine elicited substantial responses in all preparations. In strips where CPA *per se* induced contraction during Ca^{2+}-loading (Figure 1c (ii)), spontaneous phasic contractions were often observed during Ca^{2+} loading in the third trial (c).

Summarized data in Figure 1d show that the caffeine-induced contraction was significantly reduced when the preceding Ca^{2+}-loading was performed in the presence of 10 μM CPA. It is clear that 10 μM CPA reversibly reduced Ca^{2+}-uptake of storage sites in intact ileal smooth muscle strips, at least under these conditions (at room temperature and without spontaneous contractions). The results obtained from preparations which showed substantial contractions during Ca^{2+}-loading in the presence of CPA were not included in Figure 1d. When the temperature was kept at 36 ± 1°C, spontaneous contraction was observed during Ca^{2+}-loading in every preparation. Similar results with much larger variance were obtained at this temperature using the same experimental procedure (not shown). The Ca^{2+}-uptake was also significantly decreased by 10 μM CPA at 36°C ($P < 0.05$; not shown). Caffeine-induced contractions in a Ca^{2+}-free solution were, however, much smaller than the spontaneous contractions in Ca^{2+} containing solution even in the control at 36°C (not shown).

In previous work (Uyama *et al.*, 1992), caffeine- and inositol 1,4,5-trisphosphate (IP_3)-induced Ca^{2+} release in skinned fibres were not affected by the presence of 1 μM CPA. Since higher concentrations of CPA were used in the present study, the effects of 10 μM CPA on Ca^{2+} release itself were re-examined in skinned preparations (Figure 2). After skinning, application of pCa 6.3 solution evoked a control contractile response (Figure 2a). This procedure also resulted in Ca^{2+}-loading. Subsequent application of 25 mM caffeine in a relaxing solution (R0.1G) induced a transient contraction. A second application of 25 mM caffeine in R0.1G elicited either a small or no response. The pair of contractions induced by pCa 6.3 and 25 mM caffeine was repeated three times in each preparation (three trials) at an interval of approximately 30 min. In Figure 2b, 10 μM CPA was applied about 2 min after the change in solution to R0.1G. The application of 10 μM CPA elicited a small phasic contraction in all prepara-

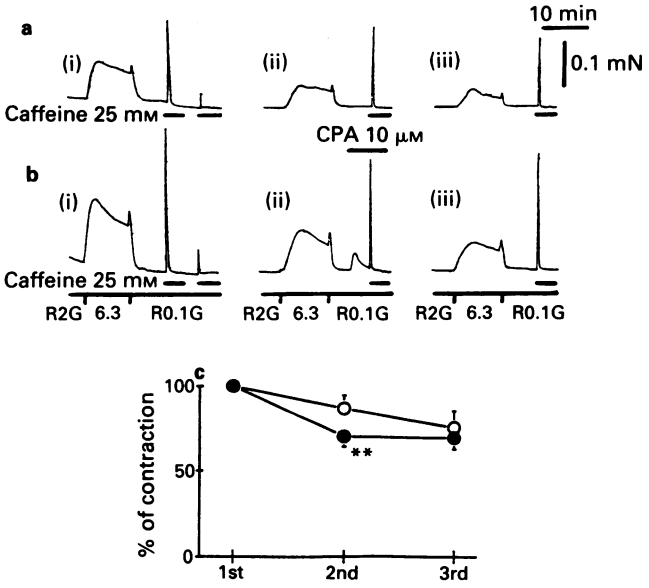

Figure 2 Effects of 10 μM cyclopiazonic acid (CPA) on 25 mM caffeine-induced contractions in skinned preparations. Skinned strips were contracted by changing R2G to a pCa 6.3 solution as indicated below (b). This was also a Ca^{2+} loading period. Caffeine (25 mM) was added twice as indicated by bars in R0.1G solution (a(i) and b(i)). Note that the second response to caffeine was very small. Ca^{2+} loading and subsequent Ca^{2+} release by caffeine were repeated three times (three trials; (i), (ii) and (iii)). The amplitude of the responses to caffeine decreased progressively even in the control (a). In b(ii) (in the second trial), 10 μM CPA was added to R0.1G solution after Ca^{2+} loading. Application of CPA induced a small phasic contraction. The subsequent caffeine-induced contraction in the presence of CPA was smaller than in the control, whereas the response recovered substantially in the third trial (b(iii)). (c) Shows the summarized data indicating that caffeine-induced Ca^{2+} release was slightly but significantly reduced in the presence of 10 μM CPA: (○) control response; (●) 2nd response measured after treatment with 10 μM CPA. $n = 4$.

tions examined ($n = 4$). When the relaxing solution containing higher concentrations of EGTA (R2G or R0.5G), CPA did not induce the small phasic contraction. The subsequent application of caffeine in R0.1G induced a response which was slightly smaller than that in the control. The effect of 10 μM CPA was removed by washout (Figure 2b). Summarized data shown in Figure 2c indicate that the caffeine-induced contraction in skinned preparations was slightly but significantly reduced in the presence of 10 μM CPA. The decrease was, however, too small to explain the large decrease in caffeine-induced Ca^{2+}-release by CPA in intact strips shown in Figure 1, implying that it was mainly due to inhibition of Ca^{2+}-uptake.

The effects of CPA on spontaneous and 20 mM K^+-induced contractions were examined at 36°C in the presence of 1 μM atropine. Figure 3 shows that CPA at concentrations higher than 1 μM enhanced the amplitude of spontaneous contraction at 36°C. High concentrations of CPA (>3 μM) also increased the muscle tone. The frequency of spontaneous contraction varied widely from preparation to preparation (0.2–5.0 contractions min^{-1}). CPA (1–30 μM) increased the frequency in all preparations examined ($n = 26$). Initial phasic and following sustained contractions were induced by 20 mM K^+ in the presence of 1 μM atropine (Figure 3a). Repetitive small phasic contractions were superimposed on the tonic contraction. A potassium concentration of 20 mM was chosen, since all the contractile responses to 20 mM K^+ were almost abolished by 1 μM nicardipine, suggesting that the responses were evoked by Ca^{2+} influx through voltage-dependent Ca^{2+} channels. The initial phasic contractions induced by 20 mM K^+ were enhanced by CPA in a concentration range of 1–10 μM. The enhancement was rather less at higher concentrations (>10 μM) (Figure 3b). The CPA concentration giving a half maximum effect (EC_{50}) was approximately 3 μM. The effect of CPA on 80 mM K^+-induced contraction was also examined (Figure 4). Although there was a tendency for the peak amplitide of the 80 mM K^+-induced contraction to be enhanced by 10 μM CPA, the enhancement was not statistically significant (Figure 4b, $P > 0.05$). The steady phase was not affected by 10 μM CPA ($P > 0.05$).

The effects of CPA on resting membrane potential and electrical activity were examined with conventional microelectrodes in longitudinal smooth muscle strips at 35°C in the presence of 1 μM atropine (Figure 5a). Application of 10 μM CPA slightly depolarized the cell membrane from -48.6 ± 1.2 mV ($n = 34$) to -44.7 ± 1.3 mV ($n = 22$, $P < 0.05$ vs. the control). The depolarization started after a short delay of about 20–80 s, gradually developed and reached a steady level within 3 min. Although the AP frequency in the control varied widely from preparation to preparation and also depended upon how stretched the preparation was, it was in a range of 0.2–20 APs min^{-1}. A burst of several APs often occurred. After application of 10 μM CPA, the AP frequency markedly increased with the depolarization in all preparations examined ($n = 13$, $P < 0.01$) to higher than 0.5 Hz in 10 preparations out of 18, although it varied with time. Another important finding was that both peak amplitude and 50% duration of AP afterhyperpolarization (AHP) were decreased after application of 10 μM CPA (Figure 5a(ii) and (iii)). Spontaneous APs and the effects of CPA were not affected by 1 μM TTX, 0.3 μM phentolamine and 0.3 μM propranolol.

These CPA-induced effects on membrane potential were mimicked by application of 30–100 nM charybdotoxin (ChTX). The cells were depolarized by about 5 mV (-43.2 ± 1.3 mV, $n = 28$, $P < 0.05$) within 20 s of the application of 100 nM charybdotoxin (ChTX). Concomitantly, the AP fre-

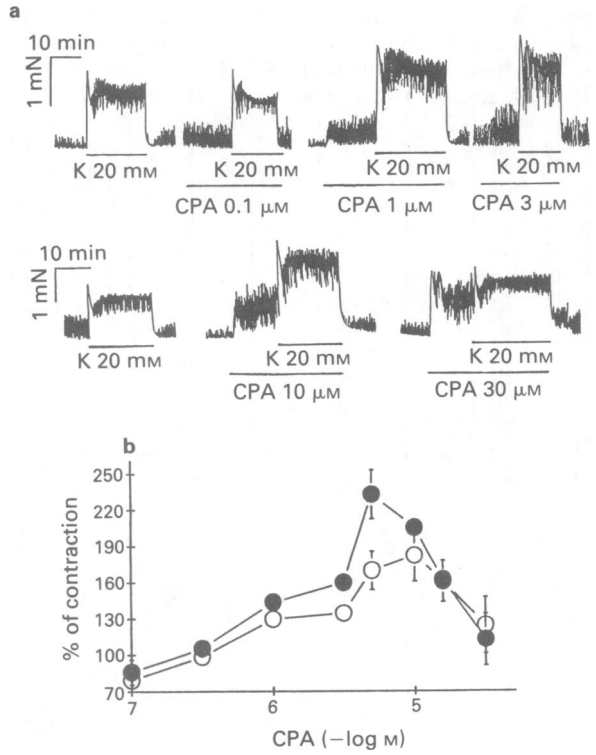

Figure 3 Effects of cyclopiazonic acid (CPA) on 20 mM K^+-induced contraction in intact ileal longitudinal smooth muscle strips at 36 ± 1°C. (a) Typical recordings of 20 mM K^+-induced contractions in the absence or presence of 0.1, 1, 3, 10 or 30 μM CPA. All experiments were performed in the presence of 1 μM atropine. CPA was added 15 min prior to the application of 20 nM K^+-solution. (b) Summarized data of the amplitude of phasic and sustained components of 20 mM K^+-induced contractions are shown by (○) and (●) respectively. Those in the control (in the absence of CPA) were taken as 100%. The amplitude of the sustained component was measured at the mean level of repetitive phasic contractions from the resting tone 10 min after the application of 20 mM K^+ solution. The number of observations was four except at 1 μM CPA where it was seven. The amplitude of both initial phasic and following sustained components was significantly larger than 100% at CPA concentrations in the range of 1 and 20 μM.

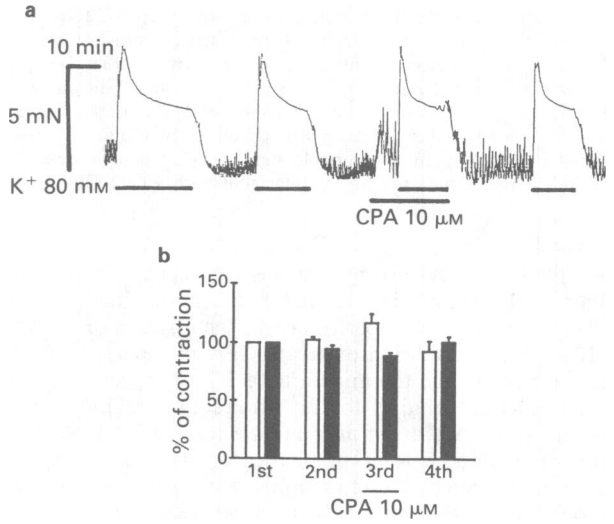

Figure 4 Effects of 10 μM cyclopiazonic acid (CPA) on 80 mM K^+-induced contractions: 80 mM K^+ solution was applied four times. In the third trial, CPA was added 10 min prior to the application of 80 mM K^+. All experiments were performed in the presence of 1 μM atropine at 36 ± 1°C. (b) Summarized data of the amplitude of 80 mM K^+-induced contractions at the peak (phasic component; open columns) and at 15 min from the application of 80 mM K^+ (sustained component; solid columns): $n = 5$. No statistically significant difference was found between the data in the first trial and those in the second, third or fourth trial for each component, respectively.

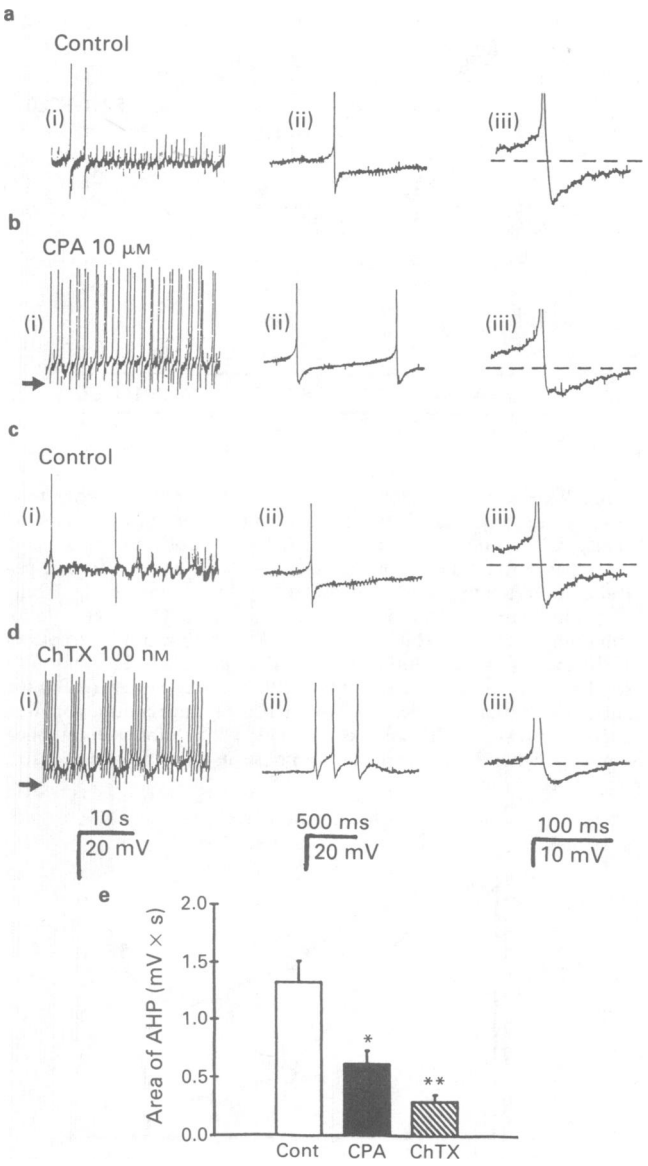

Figure 5 Effects of cyclopiazonic acid (CPA) (b) and charybdotoxin (ChTX) (d) on electrical activity in ileal longitudinal smooth muscle strips. Membrane potentials were measured with conventional glass microelectrodes in the presence of 1 μM atropine at 35°C. (a) and (b) show recordings from a smooth muscle cell before and about 5 min after the application of 10 μM CPA, respectively; (c) and (d) show recordings from a smooth muscle cell before and about 3 min after the application of 100 nM ChTX, respectively. Traces in (ii) and (iii) show faster recordings of parts of (i). The broken lines in (iii) indicate the level of the membrane potential just before the depolarization triggering an action potential. The arrows in (b(i)) and (d(i)) indicate the resting membrane potential before the application of CPA or ChTX. Note that action potential frequency was markedly increased and AHP was substantially decreased in the presence of 10 μM CPA (b) or 100 nM ChTX (d). The AHP from the level indicated by the broken line was integrated on the computer and shown as the area of AHP in (e). The AHP areas were obtained from over 10 APs in each preparation before and after application of CPA or ChTX and averaged, respectively. Shown are the average of pooled data from 4–8 preparations. The area of AHP was significantly decreased by 10 μM CPA or 100 nM ChTX.

quency and AHP amplitude markedly increased and decreased, respectively, as shown in Figure 5d. To evaluate the effects of CPA and ChTX on AHP, AHP was integrated as the area from the level of the membrane potential just before the rapid depolarization which triggered a burst of APs. The summarized data indicate that the area of AHP was significantly decreased by 10 μM CPA and more extensively by 100 nM ChTX (Figure 5e).

To confirm that the increase in spontaneous contractions and muscle tone by CPA was preceded by an increase in $[Ca^{2+}]_i$, changes in $[Ca^{2+}]_i$ were monitored at 35°C in intact strips, which were loaded with the fluorescent Ca^{2+}-indicator, Fura-2/AM. Application of 3 μM CPA, in the presence of 1 μM atropine, markedly enhanced the phasic increases in $[Ca^{2+}]_i$ (Figure 6a(i)). Concomitantly, phasic contractions were greatly enhanced (Figure 6a(ii)). The increase in $[Ca^{2+}]_i$ changes and phasic contractions by CPA were blocked by 1–10 μM verapamil (Figure 6a) or 10 mM EGTA (not shown) and recovered on further addition of 1–10 μM Bay K 8644 (Figure 6a). Similar results were obtained in five preparations out of five. When a slight increase in basal $[Ca^{2+}]_i$ and muscle tone was observed on application of 3 μM CPA in addition to the enhancement of repetitive phasic changes, it was abolished by addition of 10 μM verapamil or 10 mM EGTA ($n = 2$). Application of 100 nM ChTX showed similar effects: enhancement of spontaneous phasic increase in $[Ca^{2+}]_i$ and contractions (Figure 6b).

Although these effects of CPA on spontaneous electrical and mechanical activities may be consistent with inhibition of SR/ER Ca^{2+}-ATPase by CPA, a line of direct evidence was required to conclude that 10 μM CPA substantially reduced Ca^{2+}-uptake at 36°C. Figure 7 shows the effect of CPA on the decay time course of $[Ca^{2+}]_i$ and contraction after $[K^+]_o$ was decreased from 80 to 5.9 mM. The $[Ca^{2+}]_o$ was changed from 2.2 mM to nominally Ca-free (with 0.1 mM EGTA) at the same time. The rate of decay of $[Ca^{2+}]_i$ was markedly slowed when the Ca-free solution contained 10 μM CPA. After 5 min from the decrease in $[K^+]_o$, 100 μM acetylcholine (ACh) was applied to estimate the amount of stored Ca^{2+}.

Summarized data are shown in Figure 8. During the decay for 5 min, the relative $[Ca^{2+}]_i$ and force were significantly larger in the presence of 10 μM CPA. Since 30 μM CPA had similar potency (not shown), 10 μM CPA appeared to be almost maximally effective. It is worth noting that the increase in relative $[Ca^{2+}]_i$ and force by ACh was smaller in the presence of CPA and that the final levels of $[Ca^{2+}]_i$ in the presence of ACh were similar in the control and CPA-treated preparations.

Discussion

The present study was focused on the possibility that electrical and mechanical activities are enhanced in ileal smooth muscle, when Ca^{2+}-uptake by intracellular storage sites is significantly reduced by CPA. The results clearly show that spontaneous APs, repetitive phasic increase in $[Ca^{2+}]_i$ and concomitant phasic contractions were markedly enhanced by 1–10 μM CPA. Since the ileal longitudinal strips were prepared free from interstitial cells of Cajal and the circular muscle layer, the APs observed in the presence of atropine are myogenic from longitudinal smooth muscle cells. Phasic and tonic contractions induced by 20 mM K^+ were markedly enhanced by CPA. These results strongly suggest that Ca^{2+}-influx through voltage-dependent Ca^{2+} channels is enhanced by CPA, and may be consistent with the observation that thapsigargin, another inhibitor of SR/ER Ca^{2+}-ATPase, increases the amplitude of the spontaneous mechanical activity in rat portal vein (Mikkelsen *et al.*, 1992).

Direct evidence indicating that the increase in Ca^{2+}-influx by CPA is attributable to the inhibition of Ca^{2+}-ATPase in intracellular Ca storage sites is difficult to obtain in multicellular preparations. However, a line of indirect evidence shown in the present and previous studies strongly suggests that CPA significantly reduces $I_{K\text{-}Ca}$ by inhibition of Ca^{2+}-uptake of storage sites and consequently increases Ca^{2+}-influx in intact ileal longitudinal smooth muscle.

First, CPA slightly depolarized the cell membrane, reduced AHP and increased AP frequency in a similar manner to

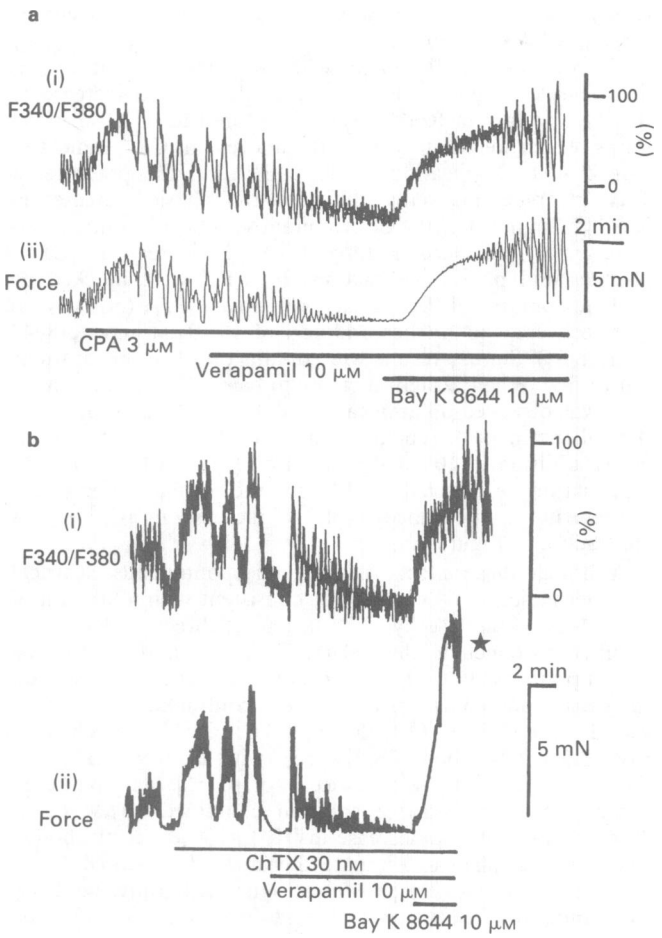

Figure 6 Effects of cyclopiazonic acid (CPA, a) and charybdotoxin (ChTX, b) on changes in $[Ca^{2+}]_i$ in a strip loaded with Fura-2/AM. $[Ca^{2+}]_i$ signals are shown as the ratio of amplitude of 500 nm fluorescence elicited by 340 and 380 nm excitation. (a) Application of 3 μM CPA induced a slow phasic increase in $[Ca^{2+}]_i$ and enhanced repetitive fast transients of $[Ca^{2+}]_i$, which corresponded to a slow phasic increase in the muscle tone and large spontaneous contractions, respectively. (b) Application of 30 nM ChTX immediately enhanced the spontaneous $[Ca^{2+}]_i$ changes and contractions. These changes were abolished by addition of 10 μM verapamil and recovered on further addition of 10 μM Bay K 8644. The asterisk in (b(ii)) indicates that the contraction after the addition of Bay K 8644 was out of scale in this preparation.

ChTX. Corresponding to the significant decrease in AHP, the $I_{K\text{-}Ca}$ activated by depolarization in single cells was very selectively blocked by 10 μM CPA (Suzuki *et al.*, 1992) or 100 nM ChTX (Uyama, unpublished observation). ChTX directly blocked single BK channel current (Brayden & Nelson, 1992) but CPA did not (Suzuki *et al.*, 1992). The same phenomena including changes in resting membrane potential, AP frequency and AHP in tissue preparations and $I_{K\text{-}Ca}$ inhibition in single cells by quinidine have been reported in ileal circular smooth muscle of the guinea-pig (Nakao *et al.*, 1986). The AP falling phase and AHP are mainly due to $I_{K\text{-}Ca}$ activation, which is susceptible to quinidine but not apamin. In rat sympathetic neurones, it has been shown that CPA reduces the ryanodine-sensitive component of AHP and facilitates repetitive AP generation (Kawai & Watanabe, 1989; Ishii *et al.*, 1992).

Second, 10 μM CPA inhibited Ca^{2+}-uptake of intracellular storage sites in intact ileal strips at 22°C. The inhibition of caffeine-induced contraction by CPA is mainly due to inhibition of Ca^{2+}-loading of the storage sites but not due to the direct change in Ca^{2+} release. Although 10 μM CPA slightly reduced caffeine-induced Ca^{2+} release in skinned preparations, it is probably due to the preceding small Ca^{2+} release

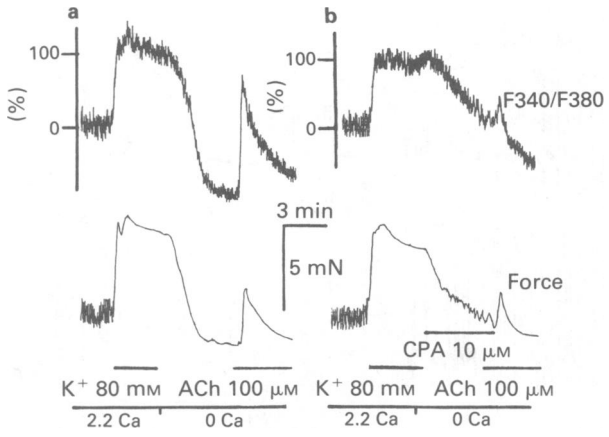

Figure 7 Effects of cyclopiazonic acid (CPA) on the decay time-course of elevated $[Ca^{2+}]_i$ and evoked contraction during washout of 80 mM K^+ solution in Fura-2 loaded ileal smooth muscle at 35°C. upper and lower traces show changes in $[Ca^{2+}]_i$ and tension, respectively. After treatment with 80 mM K^+ solution containing 2.2 mM Ca^{2+} for 4 min, the solution was changed to a Ca^{2+}-free solution containing 0.1 mM EGTA and 5.9 mM K^+ as shown at the bottom. In (b) the Ca^{2+}-free solution contained 10 μM CPA. Five min after the change to the Ca^{2+}-free solution, 100 μM actylcholine (ACh) was added. Note that the decay of both $[Ca^{2+}]_i$ and contraction were markedly slowed in the presence of 10 μM CPA. Subsequent application of ACh induced a smaller response in the CPA-treated strip than in the control.

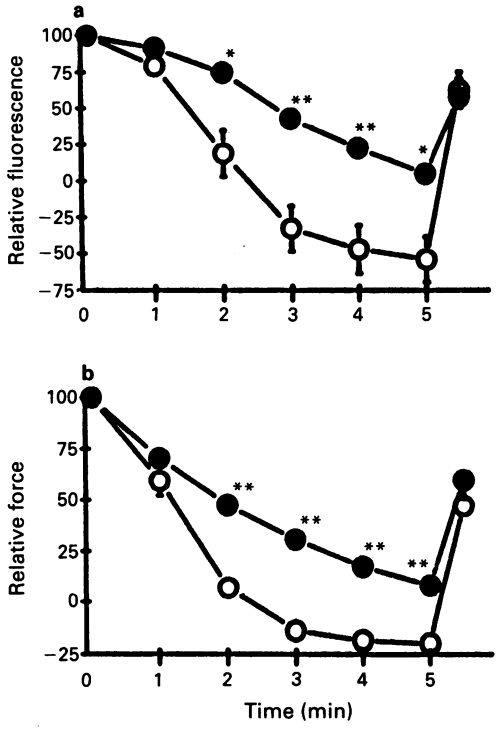

Figure 8 Summarized data of effects of 10 μM cyclopiazonic acid (CPA) on the decay time-courses of 80 mM K^+-induced high $[Ca^{2+}]_i$ and contraction. These results were obtained from experiments such as that shown in Figure 7. The time of the solution change to the Ca^{2+}-free solution was taken as 0 min. The resting and high K^+-stimulated levels of signals were taken as 0 and 100%, respectively. (a) The time-course of relative amplitude of fluorescence ($[Ca^{2+}]_i$). (b) The time-course of relative force: mean values in the absence (○) ($n = 6$) or presence (●) of 10 μM CPA ($n = 3$), are shown. In the presence of 10 μM CPA, the decay of both signals (between 2 to 5 min) was significantly slowed by CPA. Note that the peak levels of $[Ca^{2+}]_i$ and contraction induced by 100 μM acetylcholine (ACh, applied after 5 min in Ca^{2+}-free solution) in the presence of CPA were not significantly different from those in the control.

by CPA itself, which slightly reduced the amount of stored Ca. It has been suggested that Ca in storage sites is spontaneously released and is retaken up by Ca-pumps in several types of cells (Thastrup *et al.*, 1990; Stehno-Bittel & Sturek, 1992; Chen *et al.*, 1992). Ca-pump inhibition may allow accumulation of spontaneously released Ca^{2+} and result in a small contraction.

Third, the decay of high $[Ca^{2+}]_i$ and contraction induced by 80 mM K^+ after washout with Ca^{2+}-free solution containing 5.9 mM K^+ was significantly slowed by CPA. Since plasmalemmal Ca^{2+}-ATPase is not affected by CPA (Seidler *et al.*, 1989), Ca^{2+}-extrusion from the cell by the Ca-pump would not be directly affected by CPA. Effects of CPA on Ca^{2+}-extrusion by Na^+-Ca^{2+} exchange have not been clarified. Under those conditions, however, the subsequent application of ACh induces smaller Ca^{2+} release in preparations treated with CPA than in the control. A combination of these findings gives additional evidence that CPA also significantly reduced Ca^{2+}-uptake by storage sites at 35°C.

Fourth, the EC_{50} of CPA for the enhancement of 20 mM K^+-induced contraction was approximately 3 μM and close to the IC_{50} for the inhibition of $I_{K\text{-}Ca}$ (~3 μM, Suzuki *et al.*, 1992). Although the EC_{50} is about 5 times higher than the IC_{50} for the inhibition of Ca^{2+}-uptake in skinned fibres (0.6 μM; Uyama *et al.*, 1992), the difference is rather small considering the diffusion barrier of the plasma membrane.

The mechanisms of CPA-induced increase in Ca^{2+}-influx, however, may not be as simple as those of the ChTX-induced increase. The initial transient Ca release from storage sites after the application of 10 μM CPA may activate not only $I_{K\text{-}Ca}$ but also other Ca^{2+} dependent currents: Cl^- current or non-selective cationic current, as has been reported for caffeine or agonists (Amédée *et al.*, 1990; Janssen & Sims, 1992). The subsequent depolarization was small but sustained and may result from suppression of spontaneous transient outward currents (Suzuki *et al.*, 1992) which are elicited by activation of BK channels by spontaneous Ca release from local storage sites (Benham & Bolton, 1986) and possibly contribute, in part, to the resting membrane potential (Hu *et al.*, 1989; Brayden & Nelson, 1992). The CPA-induced decrease in AHP is due to the selective inhibition of $I_{K\text{-}Ca}$ (Suzuki *et al.*, 1992) which also has been reported for thapsigargin in urinary bladder smooth muscle cells (Ganitkevich & Isenberg, 1992). The decrease in resting membrane potential and AHP by CPA may be responsible for the marked increase in frequency of spontaneous APs. It is, however, likely that the increase in AP frequency caused by CPA may itself result in a further decrease in Ca store size and, thereby, AHP. Moreover, the combination of the increase in Ca^{2+}-influx and the inhibition of Ca^{2+}-uptake by CPA raised $[Ca^{2+}]_i$ and may partly compensate the decreased $I_{K\text{-}Ca}$. It may be the reason why the decrease in AHP by CPA was smaller than that induced by ChTX in tissue preparations.

It should be mentioned that the BK channel activity is regulated by $[Ca^{2+}]_i$ near the inner mouth of the channels and, therefore, may well be affected by Ca storage sites localized just beneath the cell membrane. Activation of BK channels by Ca^{2+} release from storage sites can often be observed in cell free patches (Xiong *et al.*, 1992). The activation of $I_{K\text{-}Ca}$ by Ca^{2+}-influx upon depolarization may be greatly amplified by the large increase in local $[Ca^{2+}]_i$ via Ca^{2+}-induced Ca^{2+} release from the storage sites (Suzuki *et al.*, 1992; Ganitkevich & Isenberg, 1992). On the other hand, the $[Ca^{2+}]_i$ measured by Fura-2 signals show averaged changes in $[Ca^{2+}]_i$ of the whole cytoplasm. The increase in Ca^{2+}-influx directly results in elevation of Fura-2 or Indo-1 signal (Becker *et al.*, 1989) but may not result in the increase in $I_{K\text{-}Ca}$, if releasable Ca in storage sites is substantially reduced by CPA. Such dissociation between $[Ca^{2+}]_i$ detected by Indo-1 or Fura-2 and $I_{K\text{-}Ca}$ has been suggested in smooth muscle cells (Bittel & Sturek, 1992; Ganitkevich & Isenberg, 1992).

It has been reported that Ca^{2+}-entry through the plasma membrane depends upon the filling state of the ER/SR (Putney, 1986, 1990; Missiaen *et al.*, 1990; Dolor *et al.*, 1992; Byron *et al.*, 1992). CPA and thapsigargin deplete intracellular stored Ca^{2+} and activate an influx pathway for divalent cations (Takemura *et al.*, 1989, 1991; Demaurex *et al.*, 1992). It has been suggested that some Ca^{2+}-storage sites may couple with DHP-sensitive Ca^{2+}-channels in the plasma membrane in smooth muscle cells (Bourreau *et al.*, 1991; Low *et al.*, 1992; Xuan *et al.*, 1992) as well as in other types of cells (Hoth & Penner, 1992). The present results are not opposed to this hypothesis. When $I_{K\text{-}Ca}$ is decreased and AP frequency is increased by CPA, Ca^{2+}-influx through Ca^{2+} channels must be markedly increased even when Ca^{2+} channel properties *per se* are not changed.

The tonic contraction induced by 80 mM K^+ was not significantly enhanced by CPA in the present study, while 50 mM K^+-induced contraction in aorta and mesenteric artery of the rat was enhanced by thapsigargin (Shima & Blaustein, 1992). When I_{Ca} was measured under whole-cell clamp, 10 μM CPA did not affect I_{Ca} (Suzuki *et al.*, 1992). Under these conditions, 5 mM EGTA in the pipette solution may remove stored Ca. It has been reported that a high concentration of CPA inhibits Ca^{2+}-influx pathways in rat thymic lymphocytes (Mason *et al.*, 1991). Based on these observations, it is suggested that the enhancement of Ca^{2+}-influx through voltage-dependent Ca^{2+} channels in ileal longitudinal smooth muscle is an indirect effect of CPA. The possibility that the activity of Ca^{2+} channels on the cell membrane is directly regulated by the amount of Ca in storage sites is, however, interesting and remains to be examined more exactly in smooth muscle cells.

In conclusion, CPA applied from outside the cell in intact ileal smooth muscle can reduce Ca^{2+}-uptake of intracellular Ca storage sites via the inhibition of Ca^{2+}-ATPase. The decrease in stored Ca by CPA may increase Ca^{2+}-influx. The decrease in $I_{K\text{-}Ca}$ may be one of the major causes. Of importance is the fact that inhibition of Ca^{2+}-uptake of intracellular storage sites by CPA in intact strips was partly reversible, as shown in single smooth muscle cells and skinned fibres.

Y.I. was supported by a Grant-in-Aid for Scientific Research from the Japanese Ministry of Education, Science and Culture.

References

AMÉDÉE, T., BENHAM, C.D., BOLTON, T.B., BYRNE, N.G. & LARGE, W.A. (1990). Potassium, chloride and non-selective cation conductances opened by noradrenaline in rabbit ear artery cells. *J. Physiol.*, **423**, 551–568.

BECKER, P.L., SINGER, J.J., WALSH, J.V. Jr. & FAY, F.S. (1989). Regulation of calcium concentration in voltage clamped smooth muscle cells. *Science*, **244**, 211–214.

BENHAM, C.D. & BOLTON, T.B. (1986). Spontaneous transient outward currents in single visceral and vascular smooth muscle cells of the rabbit. *J. Physiol.*, **281**, 385–406.

BITTEL, L.S. & STUREK, M. (1992). Spontaneous sarcoplasmic reticulum calcium release and extrusion from bovine, not porcine coronary artery smooth muscle. *J. Physiol.*, **451**, 49–78.

BOURREAU, J.P., ABELA, A.P., KWAN, C.Y. & DANIEL, E.E. (1991). Acetylcholine Ca^{2+} stores refilling directly involves a dihydropyridine-sensitive channel in dog trachea. *Am. J. Physiol.*, **261**, C497–C505.

BRAYDEN, J.E. & NELSON, M.T. (1992). Regulation of arterial tone by activation of calcium-dependent potassium channels. *Science*, **256**, 532–535.

BYRON, K.L., BABNIGG, G. & VILLEREAL, M.L. (1992). Bradykinin-induced Ca^{2+} entry, release, and refilling of intracellular Ca^{2+} store; relationships revealed by image analysis of individual human fibroblasts. *Am. J. Physiol.*, **267**, 108–118.

CHEN, Q., CANNELL, M. & VAN BREEMAN, C. (1992). The superficial buffer barrier in vascular smooth muscle. *Can. J. Physiol. Pharmacol.*, **70**, 509–514.

DEMAUREX, M., LEW, D.P. & KRAUSE, K.H. (1992). Cyclopiazonic acid depletes intracellular Ca^{2+}-stores and activates an influx pathway for divalent cations in HL-60 cells. *J. Biol. Chem.*, **267**, 2318–2324.

DENG, H.W. & KWAN, C.Y. (1991). Cyclopiazonic acid is a sarcoplasmic reticulum Ca^{2+}-pump inhibitor of rat aortic muscle. *Acta Pharmacol. Sinica*, **12**, 53–58.

DOLOR, R.J., HURWITZ, L.M., MIRZA, Z., STRAUSS, H.C. & WHORTON, A.R. (1992). Regulation of extracelluar calcium entry in endothelial cells: role of intracellular calcium pool. *Am. J. Physiol.*, **262**, C171–C181.

GANITKEVICH, V.Y. & ISENBERG, G. (1992). Contribution of Ca^{2+}-induced Ca^{2+} release to the $[Ca^{2+}]_i$ transients in myocytes from guinea-pig urinary bladder. *J. Physiol.*, **458**, 119–137.

GOEGER, D.E. & RILEY, R.T. (1989). Interaction of cyclopiazonic acid with rat skeletal muscle sarcoplasmic reticulum vesicles. Effects on Ca^{2+} binding and Ca^{2+} permeability. *Biochem. Pharmacol.*, **38**, 3995–4003.

GOEGER, D.E., RILEY, R.T., DORNER, J.W. & COLE, R.J. (1988). Cyclopiazonic acid inhibition of the Ca^{2+}-transport ATPase in rat skeletal muscle sarcoplasmic reticulum vesicles. *Biochem. Pharmacol.*, **37**, 978–981.

HOTH, M. & PENNER, R. (1992). Depletion of intracellular calcium stores activates a calcium current in mast cells. *Nature*, **355**, 353–355.

HU, S.L., YAMAMOTO, Y. & KAO, C.Y. (1989). The Ca^{2+}-activated K^+ channel and its functional roles in smooth muscle cells of guinea pig taenia coli. *J. Gen. Physiol.*, **94**, 833–847.

ISHII, Y., KAWAI, T. & WATANBE, M. (1992). Inhibitory effects of cyclopiazonic acid on the spike after-hyperpolarization in rat sympathetic neurons. *Jpn. J. Pharmacol.*, **58**, 451–456.

IINO, M. (1989). Calcium-induced calcium release mechanism in guinea pig taenia caeci. *J. Gen. Physiol.*, **94**, 363–383.

IMAIZUMI, Y., MURAKI, K. & WATANABE, M. (1990). Characteristics of transient outward currents in single smooth muscle cells from the ureter of the guinea-pig. *J. Physiol.*, **427**, 301–324.

JANSSEN, L. & SIMS, S. (1992). Acetylcholine activates non-selective cation and chloride conductances in canine and guinea-pig tracheal myocytes. *J. Physiol.*, **453**, 197–218.

KAWAI, T. & WATANABE, M. (1989). Effects of ryanodine on the spike afterhyperpolarization in sympathetic neurones of the rat superior cervical ganglion. *Pflügers Arch.*, **413**, 470–475.

KITAMURA, K., SAKAI, T., KAJIOKA, S. & KURIYAMA, H. (1989). Activation of the Ca dependent K channel by Ca released from the sarcoplasmic reticulum of mammalian smooth muscles. *Biomed. Biochim. Acta*, **48**, S364–369.

KITAZAWA, T. & SOMLYO, A.P. (1990). Desensitization and muscarinic re-sensitization of force and myosin light chain phosphorylation to cytoplasmic Ca^{2+} in smooth muscle. *Biochem. Biophys. Res. Commun.*, **172**, 1291–1297.

KOBAYASHI, S., KITAZAWA, T., SOMLYO, A.V. & SOMLYO, A.P. (1989). Cytosolic heparin inhibits muscarinic and alpha-adrenergic Ca2+-release in smooth muscle. *J. Biol. Chem.*, **264**, 17997–18004.

KUREBAYASHI, N. & OGAWA, Y. (1991). Discrimination of Ca2+-ATPase activity of sarcoplasmic reticulum from actomyosin-type ATPase activity of myofibrils in skinned mammalian skeletal muscle fibres: distinct effects of cyclopiazonic acid on the two ATPase activities. *J. Muscle Res. Cell Motil.*, **12**, 355–365.

LOW, A.M., KWAN, C.Y. & DANIEL, E.E. (1992). Evidence for two types of internal Ca^{2+}-stores in canine mesenteric artery with different refilling mechanisms. *Am. J. Physiol.*, **262**, H31–H37.

MASON, M.J., GARCIA-RODRIGUEZ, C. & GRINSTEIN, S. (1991). Coupling between intracellular Ca^{2+}-store and the Ca^{2+} permeability of plasma membrane. *J. Biol. Chem.*, **266**, 20856–20862.

MIKKELSEN, E.O., POULSEN, S.H. & CHRISTENSEN, S.B. (1992). Comparison of the effects of thapsigargin and Bay K 8644 on spontaneous mechanical activity in rat portal vein and contractile responses of rat cardiac muscle. *Pharmacol. Toxicol.*, **70**, 152–156.

MISSIAEN, L., DECLERCK, I., DROOGMANS, G., PLESSER, L., SMEDT, H.D., RAEYMAREKERS, L. & CASTEELS, R. (1990). Agonist-dependent Ca^{2+} and Mn^{2+} entry dependent on state of filling of Ca^{2+} stores in aortic smooth muscle cells of the rat. *J. Physiol.*, **427**, 171–186.

MITRA, R. & MORAD, M. (1985). Ca^{2+} and Ca^{2+}-activated K^+ currents in mammalian gastric smooth muscle cells. *Science*, **229**, 269–272.

NAKAO, K., INOUE, R., YAMANAKA, K. & KITAMURA, K. (1986). Actions of quinidine and apamin on after-hyperpolarization of the spike in circular smooth muscle cells of the guinea-pig ileum. *Naunyn-Schmied. Arch. Pharmacol.*, **334**, 508–513.

OHYA, Y., KITAMURA, K. & KURIYAMA, H. (1987). Cellular calcium regulates outward currents in rabbit intestinal smooth muscle cell. *Am. J. Physiol.*, **252**, C401–C410.

OZAKI, H., SATO, K., SATO, T., & KARAKI, H. (1987). Simultaneous recording of calcium signals and mechanical activity using fluorescent dye fura-2 in isolated strips of vascular smooth muscle. *Jpn. J. Pharmacol.*, **45**, 429–433.

PUTNEY, J.W. Jr. (1986). A model for receptor-regulated calcium entry. *Cell Calcium*, **7**, 1–12.

PUTNEY, J.W. Jr. (1990). Capasitative calcium entry revisited. *Cell Calcium*, **11**, 611–624.

SAKAI, T., TERADA, K., KITAMURA, K. & KURIYAMA, H. (1988). Ryanodine inhibits the Ca-dependent K current after depletion of Ca stored in smooth muscle cells of the rabbit ileal longitudinal muscle. *Br. J. Pharmacol.*, **95**, 1089–1100.

SEIDLER, N.W., JONA, I., VEGH, M. & MARTONOSI, A. (1989). Cyclopiazonic acid is a specific inhibition of the Ca^{2+}-ATPase of sarcoplasmic reticulum. *J. Biol. Chem.*, **264**, 17816–17823.

SHIMA, H. & BLAUSTEIN, M.P. (1992). Modulation of evoked contraction in rat arteries by ryanodine, thapsigargin and cyclopiazonic acid. *Circ. Res.*, **70**, 968–977.

STEHNO-BITTEL, L. & STUREK, M. (1992). Spontaneous sarcoplasmic reticulum calcium release and extrusion from bovine, not porcine, coronary artery smooth muscle. *J. Physiol.*, **451**, 49–78.

SUZUKI, M., MURAKI, K., IMAIZUMI, Y. & WATANABE, M. (1992). Cyclopiazonic acid, an inhibitor of sarcoplasmic reticulum Ca^{2+}-pump, reduces Ca^{2+}-dependent K^+ current in smooth muscle cells. *Br. J. Pharmacol.*, **107**, 134–140.

TAKEMURA, H., HUGHES, A.R., THATRUP, O. & PUTNEY Jr, J.W. (1989). Activation of calcium entry by the tumor promoter thapsigargin in parotid acinar cells. *J. Biol. Chem.*, **264**, 12266–12271.

TAKEMURA, H., OHSHIKA, H., YOKOSAWA, N., OGUMA, K. & THASTRUP, O. (1991). The thapsigargin sensitive intracellular Ca^{2+}-pool is more important in plasma membrane Ca^{2+}-entry than the IP_3-sensitive intracellular Ca^{2+}-pool in neuronal cell lines. *Biochem. Biophys. Res. Commun.*, **180**, 1518–1526.

THASTRUP, O., CULLEN, P.J., DROBAK, B.K., HANLEY, M.R. & DAWSON, A.P. (1990). Thapsigargin, a tumor promoter, discharges intracellular Ca^{2+} store by specific inhibition of the endoplasmic reticulum. *Proc. Natl. Acad. Sci. U.S.A.*, **87**, 2466–2470.

UYAMA, Y., IMAIZUMI, Y. & WATANABE, M. (1992). Effects of cyclopiazonic acid, a novel Ca^{2+}-ATPase inhibitor, on contractile respones in skinned ileal smooth muscle. *Br. J. Pharmacol.*, **106**, 208–214.

WATANABE, M., IMAIZUMI, Y., MURAKI, K. & TAKEDA, M. (1989). A comparative study about voltage-dependent Ca currents in smooth muscle cells isolated from several tissues. In: *Calcium Protein Signaling*. ed. Hidaka, H. pp. 119–128. New York: Plenum Press.

WONG, B. (1991). Ionic conductances in dissociated smooth muscle cells. *Proc. Soc. Exp. Biol. Med.*, **197**, 125–134.

XIONG, Z., KITAMURA, K. & KURIYAMA, H. (1992). Evidence for contribution of Ca^{2+} storage sites on unitary K^+ channel currents in inside-out membrane of rabbit portal vein. *Pflügers Arch.*, **420**, 112–114.

XUAN, YU-T., WANG, OU-LI & WHORTON, A.R. (1992). Thapsigargin stimulates Ca^{2+} entry in vascular smooth muscle cells: nicardipine-sensitive and -insensitive pathways. *Am. J. Physiol.*, **262**, C1258–C1265.

(Received January 4, 1993
Revised May 25, 1993
Accepted June 1, 1993)

Br. J. Pharmacol. (1993), **110**, 573–582

K channel activation by nucleotide diphosphates and its inhibition by glibenclamide in vascular smooth muscle cells

[1]D.J. Beech, H. Zhang, K. Nakao & [2]T.B. Bolton

Department of Pharmacology and Clinical Pharmacology, St. George's Hospital Medical School, London SW17 0RE

1 Whole-cell and inside-out patch recordings were made from single smooth muscle cells that had been isolated enzymatically and mechanically from the rabbit portal vein.

2 In whole-cells the inclusion in the recording pipette solution of nucleotide diphosphates (NDPs), but not tri- or monophosphates, induced a K-current that developed gradually over 5 to 15 min. Intracellular 1 mM guanosine 5'-diphosphate (GDP) induced a slowly developing outward K-current at − 37 mV that reached a maximum on average of 72 ± 4 pA ($n = 40$). Half maximal effect was estimated to occur with about 0.2 mM GDP. Except for ADP, other NDPs had comparable effects. At 0.1 mM, ADP was equivalent to GDP but at higher concentration ADP was less effective. ADP induced its maximum effect at 1 mM but had almost no effect at 10 mM.

3 In 14% of inside-out patches exposed to 1 mM GDP at the intracellular surface, characteristic K channel activity was observed which showed long (> 1 s) bursts of openings separated by longer closed periods. The current-voltage relationship for the channel was linear in a 60 mM:130 mM K-gradient and the unitary conductance was 24 pS.

4 Glibenclamide applied via the extracellular solution was found to be a potent inhibitor of GDP-induced K-current ($I_{K(GDP)}$) in the whole-cell. The K_d was 25 nM and the inhibition was fully reversible on wash-out.

5 $I_{K(GDP)}$ was not evoked if Mg ions were absent from the pipette solution. In contrast the omission of extracellular Mg ions had no effect on outward or inward $I_{K(GDP)}$.

6 Inclusion of 1 mM ATP in the recording pipette solution reduced $I_{K(GDP)}$ and also attenuated its decline during long (25 min) recordings.

7 When perforated-patch whole-cell recording was used, metabolic poisoning with cyanide and 2-deoxy-D-glucose induced a glibenclamide-sensitive K-current. This current was not observed when conventional whole-cell recording was used. Possible reasons for this difference are discussed.

8 These K channels appear similar to ATP-sensitive K channels but we refer to them as nucleotide diphosphate-dependent K channels (K_{NDP}) to emphasise what seems to be a primary role for nucleotide diphosphates in their regulation.

Keywords: Smooth muscle; ATP-sensitive K channel; glibenclamide

Introduction

Potassium channels that are inhibited by adenosine 5'-triphosphate (ATP) acting at the cytoplasmic side of the plasma membrane were first observed in cardiac muscle (Noma, 1983). ATP was subsequently found to inhibit K channels in other types of cell (reviewed by Ashcroft & Ashcroft, 1990) and the common theme of ATP-sensitivity has led to a grouping of the channels under the name ATP-sensitive K channels, or K_{ATP}. The name implies a particular significance of ATP but other intracellular factors such as pH, Ca, Mg, nucleotide diphosphates, pyridine nucleotides, adenosine 3':5'-cyclic monophosphate (cyclic AMP) and GTP-binding proteins can also modulate K_{ATP} to varying degrees in different cells (reviewed by Ashcroft & Ashcroft, 1990; Davies *et al.*, 1991). The antidiabetic sulphonylureas (e.g. tolbutamide and glibenclamide) inhibit K_{ATP} and the K channel opener (KCO) drugs (e.g. diazoxide, pinacidil and cromakalim) activate K_{ATP} in some cells (reviewed by Ashcroft & Ashcroft, 1990; 1992; Nichols & Lederer, 1991; Lazdunski *et al.*, 1992).

Although K_{ATP} were not found in smooth muscle when single channel and whole-cell patch-clamp recordings were first introduced (reviewed by Tomita, 1988; Bolton & Beech, 1992) the observation that the smooth muscle relaxant effects of KCOs, an emerging class of drugs (reviewed by Robertson & Steinberg, 1990; Weston & Edwards, 1992), were inhibited by glibenclamide (Quast & Cook, 1989) suggested that K_{ATP} might after all exist in smooth muscle. On the basis that K_{ATP} characteristically open simply in the absence of ATP several attempts were made to identify K_{ATP} in smooth muscle by depleting $[ATP]_i$ in single cells or by forming inside-out patches into ATP-free solution. Glibenclamide-sensitive K-current or hyperpolarization has been observed in single cells expected to be depleted of $[ATP]_i$, suggesting the presence of K_{ATP} (Clapp & Gurney, 1992; Silberberg & van Breemen, 1992; Noack *et al.*, 1992). Single K channel activity has been observed in the absence of $[ATP]_i$ in patches and in some studies clear inhibition by $[ATP]_i$ has been seen (Standen *et al.*, 1989). The channels are infrequently observed, however, and have widely varying properties (see Discussion). Thus it is unclear whether there are different types of K_{ATP} in smooth muscle or if other factors have led to an apparent heterogeneity in experiments so far described.

This study was prompted by our own inability to observe ATP-sensitive K-currents in either whole-cells or isolated patches from smooth muscle cells (Nakao & Bolton, 1991) and by the results of Kajioka *et al.* (1991) which suggested that K channels which did not open simply in the absence of $[ATP]_i$ could be activated by guanosine diphosphate (GDP), but only if pinacidil was present. It is significant that GDP, and other nucleotide diphosphates (NDPs), activate the K_{ATP} of other cell types but in the absence of a KCO drug (Dunne

[1] Present address: Department of Pharmacology, The University of Leeds, Leeds, LS2 9JT.
[2] Author for correspondence.

& Petersen, 1986; Tung & Kurachi, 1991; Allard & Lazdunski, 1992). We decided to investigate the action of NDPs on smooth muscle at both whole-cell and single channel levels and in doing so we have developed a working hypothesis where K_{ATP}-like channels in smooth muscle do not open simply in the absence of intracellular ATP but depend on the presence of a NDP at the intracellular surface of the membrane. Inability of the channels to open in the absence of $[ATP]_i$ does not exclude them from the K_{ATP} class but we refer to the channels as K_{NDP} to avoid a seemingly undue emphasis on the action of ATP and to recognise the particularly critical role of NDPs in the control of these smooth muscle K channels.

Methods

Single smooth muscle cells were isolated from the rabbit portal vein by a method similar to that previously described (Beech & Bolton, 1989), except the enzymatic incubation medium included collagenase (1 mg ml^{-1}; Sigma type XI) with papain (4 mg ml^{-1}; Sigma; no dithiothreitol added) and the solution was magnesium-free. Cells were stored at 4°C in a quasi-physiological medium containing Ca and Mg (both at 0.2 mM).

Patch-clamp recordings (Hamill *et al.*, 1981) were made from cells within 10 h of the isolation procedure. All recordings were made at room temperature (20–24°C). The patch-clamp amplifier was either an Axopatch-1D (Axon Instr.) or an RK300 (Biologic). Patch pipettes were made from borosilicate glass (Clark Electromedical or Plowden & Thompson); they had resistance of 2 to 4 MΩ after fire-polishing, and were coated with Sylgard (Dow Corning) for single channel recordings. Data were either stored on FM-tape (Racal) or captured directly to a 386 PC after digitization (CED interface and software). All whole-cell current records were filtered at 500 Hz (Bessel) and single channel records as described in the legend of Figure 4. Capacity currents were partially cancelled in the whole-cell recordings.

When the effects of different pipette solutions were compared in whole-cell experiments we carried out a series of experiments where the pipette solutions were used in strict rotation or we observed the effect of 1 mM GDP (with Mg) to evaluate the responsiveness of the cells on a given day. All averages are expressed as mean ± s.e.mean and *t* tests were used to assess statistical significance. The input resistance was monitored in whole-cell experiments by square or ramp hyperpolarizing commands. The series resistance was estimated by the rate of decay of the capacity current after an instantaneous step in the command voltage and was estimated to be < 10 MΩ in all experiments. Junction potentials between path and pipette solutions were measured using a 3 M KCl reference electrode and were < 3 mV; correction for these potentials was not made. The volume of the bath was 150 µl and the flow rate through it about 2 ml min^{-1}. The start of the application of substances is indicated in the figures as the time when the solution reservoirs were switched and complete exchange of the bath was not until about 30 s later. In all figures, except Figure 9b, zero time is when recording in whole-cell mode began.

All solutions (Table 1) were titrated to the specified pH using the hydroxide of the dominant cation. The total K concentration in solution Y with 1 mM GDP added and after titration to pH 7.4 with KOH was 171 mM and the final osmolarity was measured as 290 M Osmol. Nucleotides were added as the Na-salt (2.5 mM Na for 1 mM GDP) and the solution was titrated to pH 7.4, filtered (pore size 0.2 µm; Whatman) and frozen in aliquots at − 20°C. For the inside-out patch experiments 1 mM GDP was added to the bath solution by dilution immediately prior to the application from a 100 mM stock solution of Na-GDP dissolved in bath solution which had been titrated to pH 7.4 and frozen at − 20°C. Nystatin was prepared as a 5 mg ml^{-1} stock in methanol and used at final concentration of 100 µg ml^{-1}. Glibenclamide was prepared as 10 mM stock solution in dimethylsulphoxide (DMSO). The final concentration of DMSO was 0.2% for 20 µM glibenclamide and less for other concentrations. These dilutions of DMSO had no effect on $I_{K(NDP)}$.

The following were used: ADP (adenosine diphosphate), GDP (guanosine diphosphate), TDP (thymidine diphosphate), UDP (uridine diphosphate), IDP (inosine diphosphate), CDP (cytidine diphosphate), GMP (guanosine monophosphate), GTP (guanosine triphosphate), ATP (adenosine triphosphate), AMP (adenosine monophosphate), EGTA (ethylglycol-*bis*-(β-aminoethyl)-N,N,N′,N′-tetraacetic acid), EDTA (ethylenediaminetetraacetic acid), BAPTA (*bis*-(*o*-aminophenoxy)-ethane-N,N,N′,N′-tetraacetic acid) and HEPES (N-2-hydroxyethylpiperazine-N′-2-ethanesulphonic acid). Most salts were from BDH and other chemicals from Sigma.

Results

Outward current induced by purine and pyrimidine diphosphates (NDPs)

We have concentrated on a search for K channels at a membrane potential of − 37 mV and thus have assumed that they can open near the resting potential. The experimental design was to compare whole-cell recordings under voltage-clamp with or without a nucleotide in the recording pipette solution and determine if current was either induced or inhibited. Pipette solution X or Y included 5 mM EGTA or 10 mM BAPTA respectively and 20 mM HEPES and so it is expected that intracellular Ca and H ions were strongly buffered.

Figure 1 shows membrane current recorded from 12 cells under the same conditions except for the inclusion of different nucleotides in the pipette solution. All cells were voltage-clamped at − 37 mV, about 50 mV positive of the K equilibrium potential (E_K), and averages for all of these recordings are shown in Figure 2. With no nucleotide present the current record usually remained constant at a level within a few picoamperes of zero current, suggesting that K-current did not develop. This result is surprising if it is assumed that K_{ATP} in smooth muscle behave as they do in cardiac muscle and open simply when $[ATP]_i$ decreases (reviewed by Nichols & Lederer, 1991), which is to be expected as endogenous $[ATP]_i$ and substrates for metabolism diffused into the pipette solution (see Discussion). However, also on the basis of results on the cardiac K_{ATP}, it might be that $[ATP]_i$ in the cells was already so low that the channels were dephos-

Table 1 Composition of solutions

Solution	*NaCl*	*KCl*	*$CaCl_2$*	*$MgCl_2$*	*HEPES*	*Glucose*	*EGTA*	*BAPTA*	*pH*
A (bath)	130	5	1.7	1.2	10	10	0	0	7.4
B (bath)	126	6	1.7	1.2	10.5	14	0	0	7.2
X (pipette)	0	130	0	2	20	0	5	0	7.4
Y (pipette)	0	110	0	2	20	0	0	10	7.4
Z (pipette)	0	134	0	1.2	10.5	14	3	0	7.2
E (bath or pipette)	80	60	1.7	1.2	10	10	0	0	7.4
I (bath or pipette)	9	117	0	3	18	0	9	0	7.4

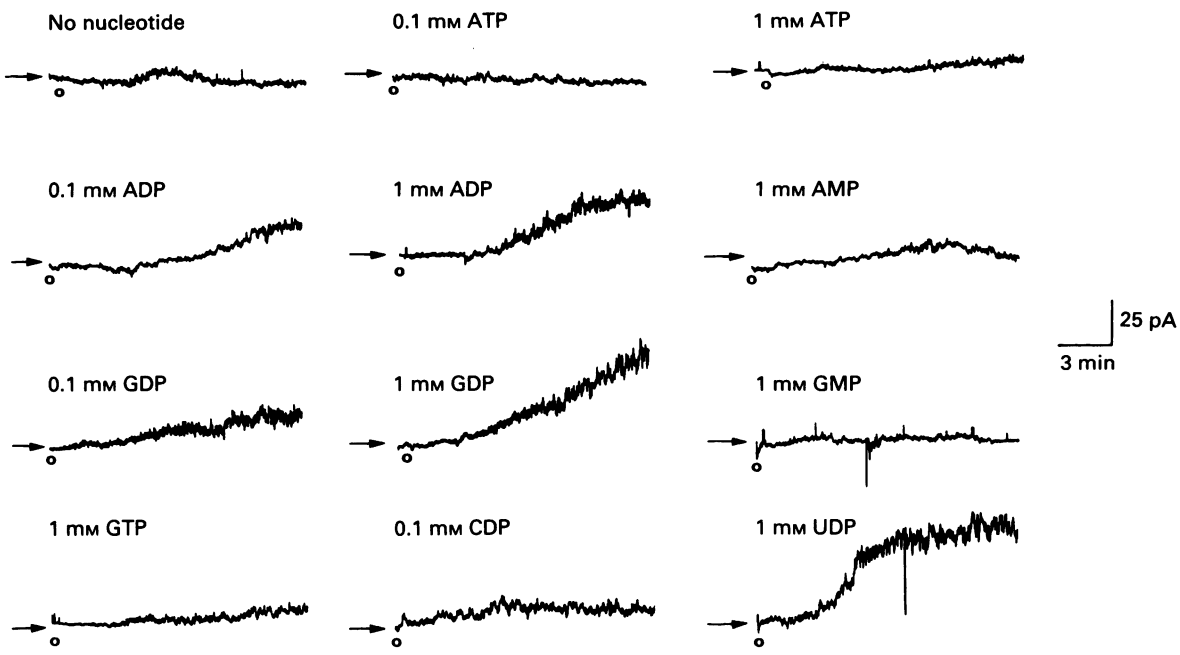

Figure 1 Effects of intracellular nucleotides on membrane current in whole-cells at a holding potential of − 37 mV. The cells were smooth muscle cells isolated from the rabbit portal vein and each recording was from a separate cell. The cell-attached patch was formed, − 37 mV applied to the pipette and then the patch was ruptured to provide access of the whole-cell (time marked as 0). Pipette solution X was used with nucleotides included as indicated and the external solution was A. The arrows mark the position of zero current.

phorylated and thus closed. This explanation was investigated by including 0.1 mM ATP in the pipette which is sufficient to phosphorylate K_{ATP} but not block them completely (Noma & Shibasaki, 1985; Ashcroft & Ashcroft, 1990). Again no appreciable outward current was evoked, the average current was 0.7 ± 0.7 pA ($n = 3$; an example is shown in Figure 1).

The current recordings were strikingly different when a NDP was present in the pipette (Figures 1 and 2). GDP (1 mM), for example, induced a slowly developing outward current that reached a maximum, on average, of 72 ± 4 pA ($n = 40$) after 5 to 15 min. Half maximal effect was estimated to occur with 0.2 mM GDP in the pipette (Figure 2a). ADP was equivalent to GDP at 0.1 mM but was less effective at higher concentrations (Figure 2a). ADP evoked its maximum effect at 1 mM but had almost no effect at 10 mM. Figure 2b shows averages for a series of experiments where the actions of nucleotides were compared in strict rotation to avoid complications of cell-to-cell variation. (This was clearly important because in these experiments the K-current amplitudes were on average less than those observed in other sets of experiments.) ATP (1 mM), GTP (1 mM), AMP (1 mM) or GMP (1 mM) in the pipette did not induce any appreciable outward current (Figures 1 and 2). All NDPs tested induced appreciable outward current and all appeared equally effective at 1 mM except for ADP. Our experiments investigated the effects of NDPs at 0.1 mM and 14–15 min after starting the whole-cell recording outward current at − 37 mV averaged: 8.6 ± 2.8 pA (IDP, $n = 4$); 8.0 ± 2.2 pA (CDP, $n = 4$); 16.0 ± 5.8 pA (TDP, $n = 3$); 6.2 ± 2.8 pA (UDP, $n = 4$). These outward currents were not significantly different from controls (one-tail test, $P > 0.05$).

Figure 3 shows the evidence that the outward current induced by GDP was a K-current. Firstly, raising the external K concentration from 5 mM (E_K − 88 mV) to 60 mM (E_K − 26 mV) changed the current at a holding potential of − 37 mV from outward to inward. Secondly, ramp voltage changes from − 37 mV and − 107 mV in 5 mM external K gave a reversal potential for the GDP-induced current of − 82 mV (Figure 3b), close to the calculated E_K. The reversal potential in 60 mM K was not determined.

Single channel recordings

Single channel studies were carried out to investigate further if GDP did open K channels and to observe the properties of the channels. When inside-out patches were formed into zero-Ca EGTA solution in the absence of a nucleotide at the inner surface of the patch, no distinct channel activity was seen in 64 patches held at − 80 mV (an example is shown in Figure 4a). This observation contrasts with that found in the heart where K_{ATP} open readily when patches are excised into ATP-free solution (Kakei *et al.*, 1985; Tung & Kurachi, 1991). However, in 14% of patches (15 out of 109) the application of a solution containing 1 mM GDP to the inner surface of the patch induced characteristic channel activity which showed long bursts of openings (many seconds) separated by even longer closed periods (Figure 4a). Channel activity at various voltages is shown in Figure 4b. It was noticed that in the open-state, current fluctuations were more pronounced when the current direction was inward. This effect resembled that observed for the cardiac K_{ATP} which may reflect a dependence of gating on ion flux (Zilberter *et al.*, 1988), but this phenomenon was not investigated in detail. In cell-attached patches this K channel was only rarely observed (a brief opening occurred in 2 out of 152 recordings). The current-voltage relationship was linear and reversed at − 20 mV (E_K − 19.5 mV), suggesting K ions were the charge carrier (Figure 4b, and Beech *et al.*, 1993). The mean unitary current was 1.5 ± 0.2 pA (13 patches) at − 80 mV, giving a conductance of 24 pS in the 60 mM: 130 mM K-gradient.

Inhibition of GDP-induced K-current $I_{K(GDP)}$ by glibenclamide

Glibenclamide inhibits K_{ATP} in pancreatic β-cells in the nanomolar concentration range and may be a specific inhibitor of this class of channel in several cell types (Ashcroft & Ashcroft, 1992). Figure 5a shows that bath application of glibenclamide did inhibit $I_{K(GDP)}$ in portal vein smooth muscle cells at very low concentrations; 50 nM glibenclamide in the bath solution caused the outward current to decline

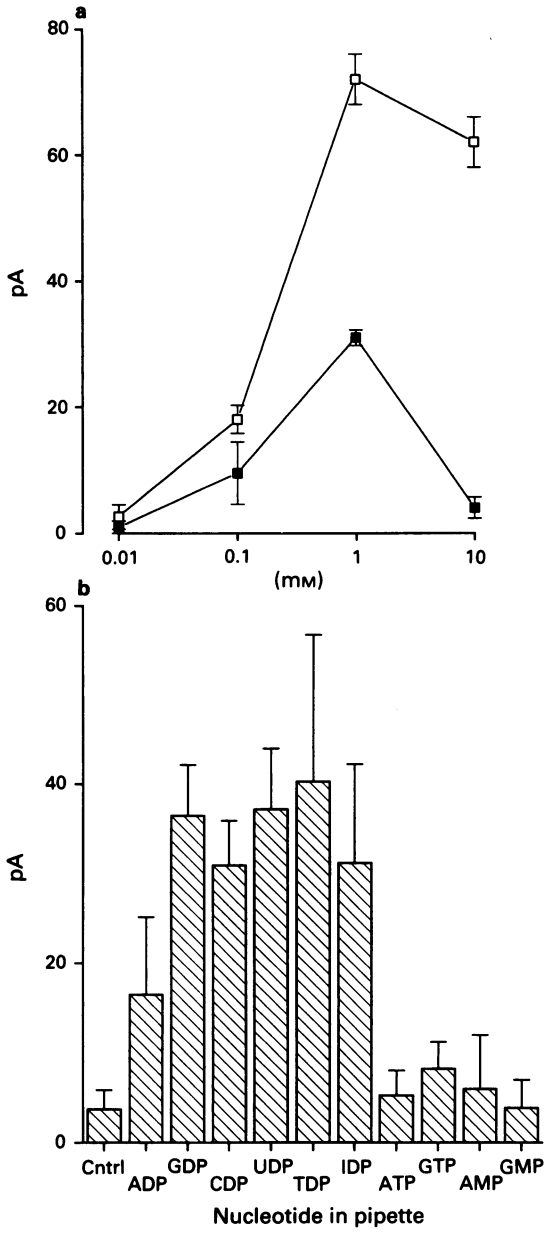

Figure 2 Averages (mean ± s.e.mean) for the outward current occurring in whole-cells loaded with different nucleotides and held at − 37 mV. The outward current was measured 14–15 min after break-through to the whole-cell mode and was defined as that which was blocked by 5 μM glibenclamide (see Figure 5): measurement of net outward current gave a similar result. (a) Concentration-response curves for the peak effects (glibenclamide-sensitive outward current at − 37 mV) of GDP (□) or ADP (■) in the pipette solution ($n = 4$–6). The pipette solution was X or Y (no difference was evident) and the bath solution was A. (b) The pipette solution X and bath solution A were used. The pipette solution included 1 mM of: ADP ($n = 4$); GDP ($n = 4$); TDP ($n = 3$); UDP ($n = 4$); IDP ($n = 4$); CDP ($n = 4$); GMP ($n = 4$); GTP ($n = 4$); ATP ($n = 4$); AMP ($n = 4$); control (no nucleotide, $n = 6$). The current amplitudes with GDP, TDP, UDP, IDP and CDP in the pipette were significantly different from the control at $P < 0.05$ and using a two-tailed test, the current amplitudes in cells held with ADP, ATP, GTP, AMP and GMP were not significantly different from control group.

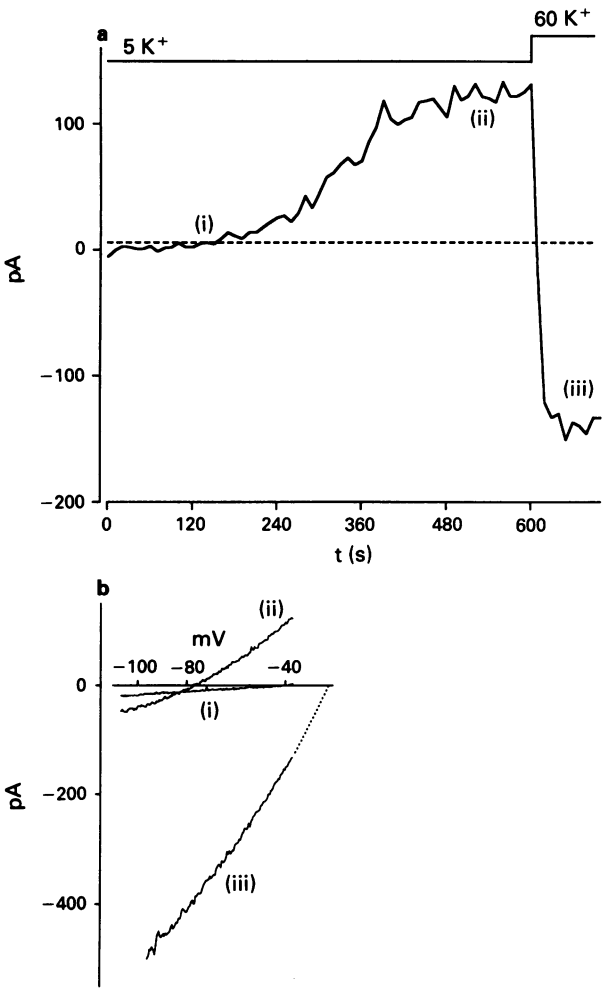

Figure 3 The outward current induced by GDP is a K-current. (a) Whole-cell recording of current at − 37 mV when the pipette solution Y contained 1 mM GDP. The bath solution was A initially and then the external [K] was raised as indicated (solution E). (b) Current in response to linear ramp (80 ms duration) changes in membrane voltage from the holding potential of − 37 mV to − 107 mV: (i) an average of 3 current records captured at 10 s intervals starting 1.3 min after break-through to the whole-cell mode; (ii) a single current record taken 9.5 min after break-through. Current records (i) and (ii) intersected at − 82 mV. Assuming a − 3 mV junction potential the reversal potential for the GDP-induced current was − 85 mV (calculated E_K was − 88 mV). Record (iii) was in 60 mM $[K]_o$ and the extrapolation (dotted line) is the Goldman-Hodgkin-Katz current equation.

from 62 pA to 34 pA and raising the concentration to 5 μM reduced the current to about zero (− 3 pA). At 20 μM glibenclamide had no further effect and wash-out of glibenclamide from the bath allowed a recovery of the current to 58 pA. When nucleotides were omitted from the pipette, glibenclamide had only small effects on membrane current (Figure 2b). A concentration-response curve is shown in Figure 5b for glibenclamide inhibition of $I_{K(GDP)}$. The Hill equation was fitted by eye with a slope of 1 and the IC_{50} (K_d) was 25 nM.

Dependence on Mg ions

Although the work of Kajioka *et al.* (1991) suggested that GDP opened K channels in the absence of Mg ions we investigated this possibility because the action of NDPs on K_{ATP} in other types of cell does require Mg ions (e.g. Tung & Kurachi, 1991) and because quite low concentrations of Mg are required for the activity of some enzymes (Sun *et al.*, 1990).

Three 1 mM GDP-containing pipette solutions were compared alternately in different cells: (Ya) included 3 mM Mg; (Yb) included 4 mM Mg and 2 mM EDTA; (Yc) had no Mg added and included 2 mM EDTA. All solutions contained 10 mM BAPTA and no added Ca. Figure 6a shows typical recordings for pipette solutions Yb and Yc, and Figure 6b

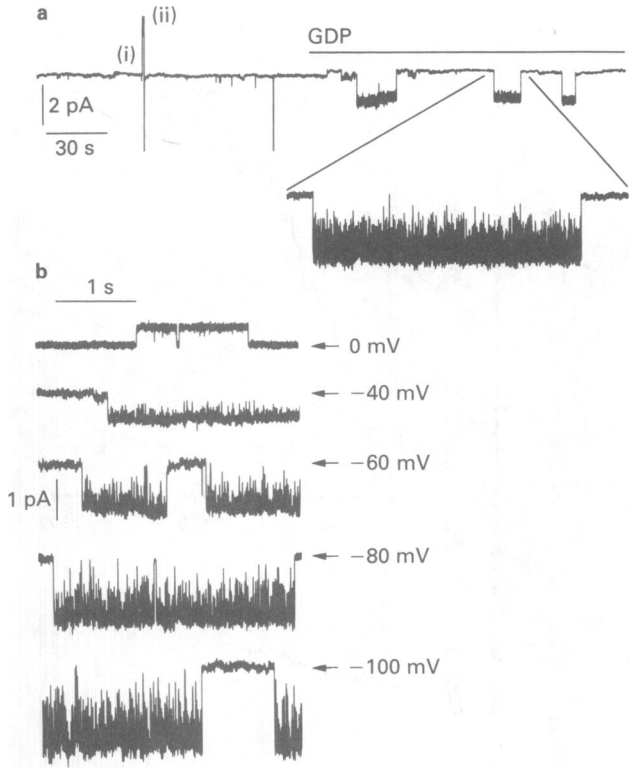

Figure 4 Inside-out patch recordings showing K channels activated by GDP. (a) A continuous recording of current in a patch held at − 80 mV with solution E in the pipette and solution I in the bath. Initially the patch was cell-attached and then it was excised (i) into the ATP- and GDP-free solution and brief test voltage steps applied to 0, 80 and 0 mV (ii) to test for activity of large Ca-activated K-channels and confirm the patch was inside-out. GDP (1 mM) was applied via the bath solution as indicated and 3 long bursts of channel openings were observed. The continuous trace was recorded on FM-tape (3.75 in s^{-1}) with a 0.5 kHz low-pass filter (− 3 dB, 4-pole Bessel) and filtered for presentation at 50 Hz. The expanded segment was amplified 2 times and filtered again at 0.5 kHz. (b) In a different patch, the GDP-activated channel at 0, − 40, − 60, − 80, − 100 mV. The current level when the channel was not open is marked with arrows. A plot of unitary current amplitude against voltage (not shown, but see the following paper) showed that the current reversed at − 20 mV, suggesting the channels were K-selective. The unitary conductance of the channel was 24 pS.

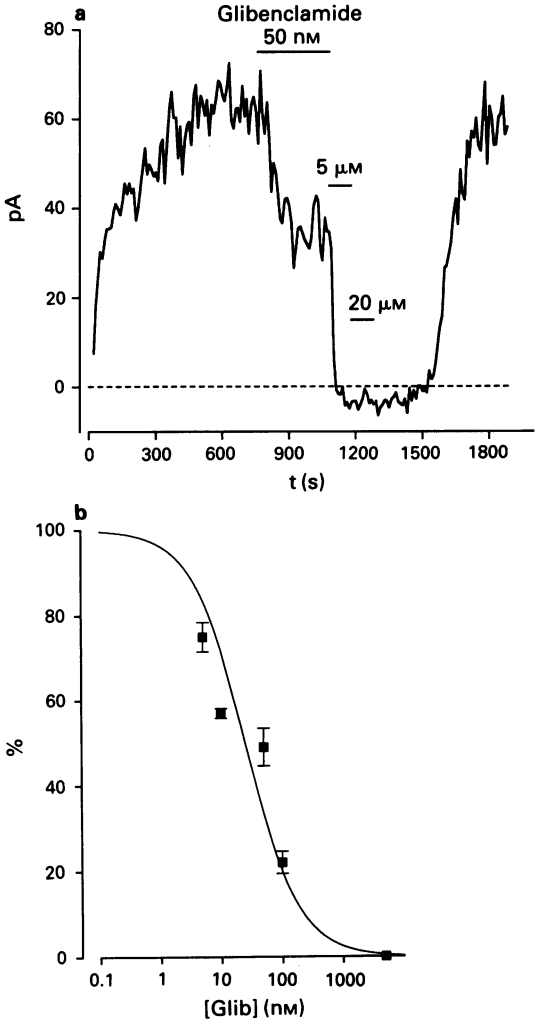

Figure 5 Inhibition of $I_{K(GDP)}$ by glibenclamide. (a) Plot of membrane current sampled every 10 s at − 37 mV. GDP (10 mM) was in the pipette solution X. Application of glibenclamide (50 nM, then 5 and 20 μM) inhibited $I_{K(GDP)}$ and after returning to glibenclamide-free solution current returned. Ramp voltage changes (as in Figure 3b) were used to measure the reversal potential of the glibenclamide-sensitive current and it was found to be close to − 80 mV (not shown) and thus close to E_K. (b) Plot of the mean (± s.e.mean; $n = 3$–16) percentage of $I_{K(GDP)}$ remaining in the presence of various concentrations of glibenclamide. The smooth function is the Hill equation with slope 1 and mid-point 25 nM (fitted by least squares method).

shows the averages for all of the experiments. It seemed that Mg ions were required for $I_{K(GDP)}$ and that EDTA did not have a blocking action when Mg ions were present in excess. In contrast, external Mg ions seemed of no importance for $I_{K(GDP)}$. Figure 7a shows that $I_{K(GDP)}$ occurred normally in the absence of Mg from the bath solution and that addition of Mg ions did not block the current. Mg ions were also unimportant when $I_{K(GDP)}$ was inward and thus more likely to be affected by an external cation (Figure 7b).

Effects of intracellular ATP

Although the K channels we observed did not open simply in the absence of $[ATP]_i$ in inside-out patches, which contrasts with the observations made on K_{ATP} for example in the heart (Kakei *et al.*, 1985), we looked for an effect of $[ATP]_i$ when the channels were opened by GDP in the whole-cell. To investigate if an effect of ATP might occur because Mg was chelated (the pK for Mg binding to ATP is near 4; Sillen & Martell, 1964), three pipette solutions were compared alternately: (YA) 2 mM Mg and 1 mM GDP; (YB) 3 mM Mg and 1 mM GDP; (YC) 3 mM Mg, 1 mM GDP and 1 mM ATP. This experimental design relies on the assumption that 1 mM ATP reduces free Mg ions from 3 mM to not less than 2 mM and considers principally the effect of Mg-ATP. *In vivo*, $[Mg]_i$ may be lower than in our experiments, perhaps 0.3 mM (Nakayama & Tomita, 1991), and so more of the ATP may be free. In cardiac and skeletal muscle cells K_{ATP} channels are roughly equally susceptible to inhibition by free ATP and Mg-ATP but in pancreatic β-cells free ATP seems a more potent inhibitor (Ashcroft & Ashcroft, 1990).

Figure 8 shows typical experiments with the YB and YC pipette solutions. Both outward (5 mM external K) and inward (60 mM external K) $I_{K(GDP)}$ were measured in the absence and presence of 5 μM glibenclamide. $I_{K(GDP)}$ measured about 10 min after starting the whole-cell recording was less when ATP was in the pipette and the averages suggested $I_{K(GDP)}$ was reduced by 64% (Figure 8c). Reducing Mg from 3 to 2 mM (in the absence of ATP) did not affect the amplitude of outward $I_{K(GDP)}$ (100 ± 18 pA to 94 ± 9 pA; $n = 4$ and 5 respectively) or inward $I_{K(GDP)}$ (122 ± 8 pA to 127 ± 12 pA; $n = 4$ and 5 respectively). It was noted that $I_{K(GDP)}$ declined

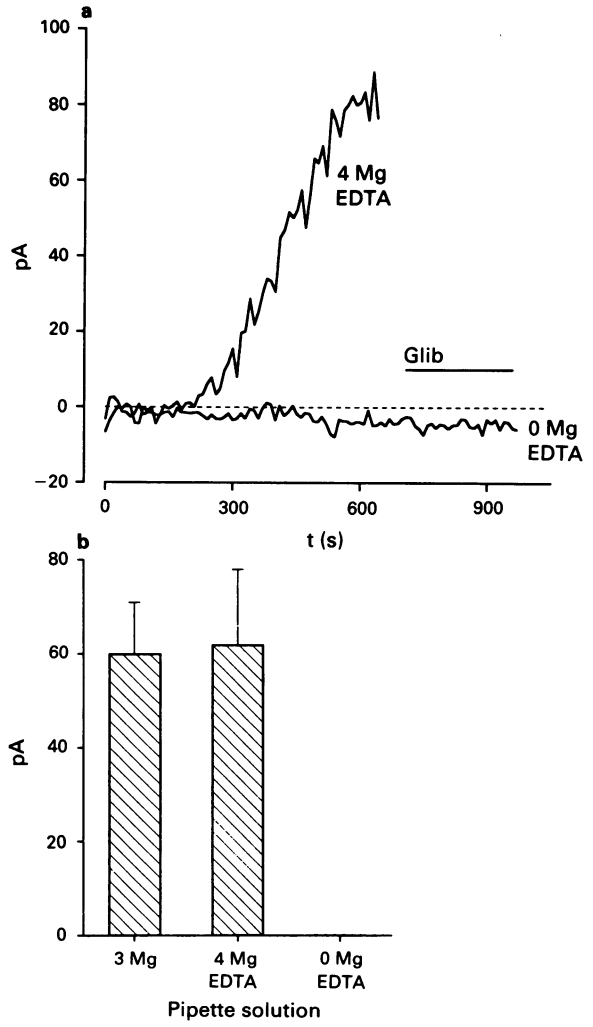

Figure 6 Dependence of $I_{K(GDP)}$ on intracellular Mg ions. Whole-cell current was sampled every 10 s at a holding potential of − 37 mV. The bath solution was A and the pipette solution Y with: (Ya) 1 mM GDP plus 1 mM extra $MgCl_2$ (total Mg = 3 mM); (Yb) 2 mM extra $MgCl_2$ and 2 mM EDTA; (Yc) 2 mM EDTA and with $MgCl_2$ omitted. (a), An experiment with pipette solution Yb compared with one using solution Yc. Glibenclamide (5 μM) was bath-applied as indicated. (b) Means (± s.e.mean, $n = 4-5$) for the three pipette solutions.

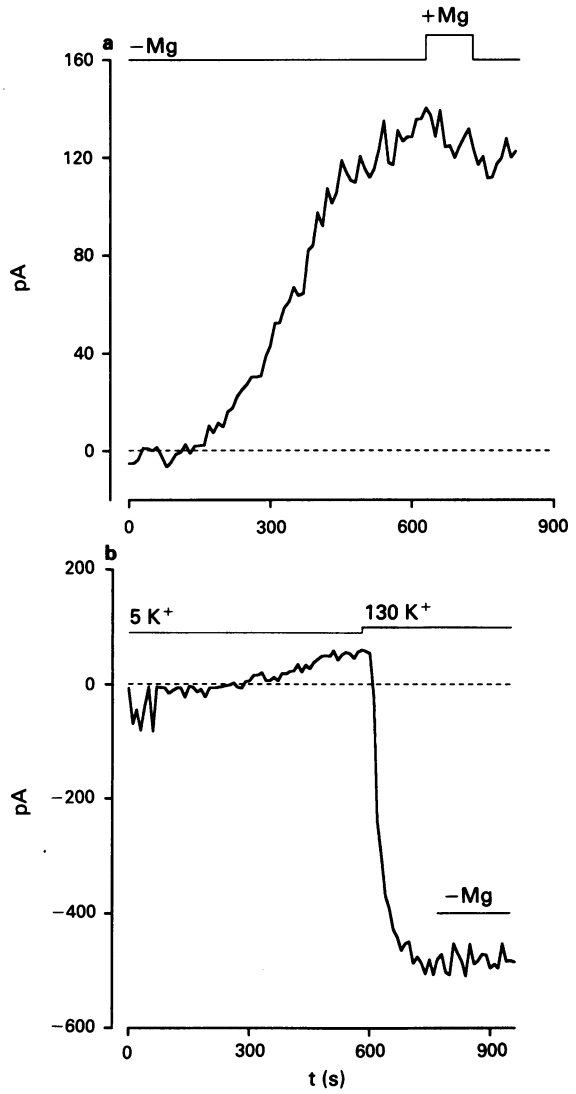

Figure 7 Dependence of $I_{K(GDP)}$ on external Mg ions (Mg was present in the pipette solution). (a) Whole-cell current sampled every 10 s at a holding potential of − 37 mV. Pipette solution Y contained 1 mM GDP plus 1 mM extra Mg (total Mg = 3 mM). Initially Mg was omitted from the bath solution A and then at 10 min $MgCl_2$ (1.2 mM) was added as indicated. (b) Holding current sampled every 10 s at − 37 mV. Pipette solution Y contained 1 mM GDP plus 1 mM extra Mg. The recording was initiated in the presence of 1.2 mM in bath solution A and then the external K concentration was raised from 5 mM to 130 mM (KCl replaced NaCl in solution A) to produce an inward current through the GDP-activated K channels. The same solution but without Mg ions was then applied and no change in current occurred. In all of these experiments Mg ions were simply omitted from the bath solution and EDTA was not included.

slowly after reaching a maximum in long (25 min) whole-cell recordings without ATP in the pipette solution but that with ATP present $I_{K(GDP)}$, although smaller, was better maintained (Figure 8a and b). Measured 25 min into the whole-cell recording $I_{K(GDP)}$ was 45.0 ± 5.6 pA ($n = 4$) for pipette solution YB and 53.3 ± 7.9 pA ($n = 4$) for pipette solution YC ($[K]_o$ was 5 mM).

Metabolic poisoning

In all of the experiments described so far glucose was present in the extracellular solution. Although the cells were expected to be able to produce ATP in this condition their ability to maintain a normal level may have been reduced when the whole-cell pipette solution contained a low concentration of ATP or no ATP (see Discussion). In an attempt to determine if production of ATP inside the cell was of consequence we removed glucose from the bath solution and replaced it with 2-deoxy-D-glucose (2-DG) to prevent glycolysis and added cyanide (CN) to inhibit aerobic metabolism.

Figure 9a shows a whole-cell recording where the pipette solution contained no NDP. This pipette solution had little effect on the holding current at − 37 mV and the subsequent removal of glucose and application of 10 mM 2-DG and 5 mM CN also did not alter the holding current. Separate experiments were carried out to compare the input resistance of cells under severe metabolic deprivation (a), or with a very high concentration of intracellular ATP (b). The conditions were: (a) pretreatment for more than 30 min with 6 mM CN and 14 mM 2-DG in the bath solution and recording with a pipette solution containing 14 mM 2-DG; (b) incubation of cells in 14 mM glucose and recording with a pipette solution containing 14 mM glucose and 10 mM Mg-ATP. Under condition (a) the input resistance was 3.18 ± 0.18 GΩ ($n = 9$) and under condition (b) it was 3.21 ± 0.23 GΩ ($n = 5$). In some cells under condition (a) 10 mM caged-ATP was included in the pipette solution (see Methods in the following

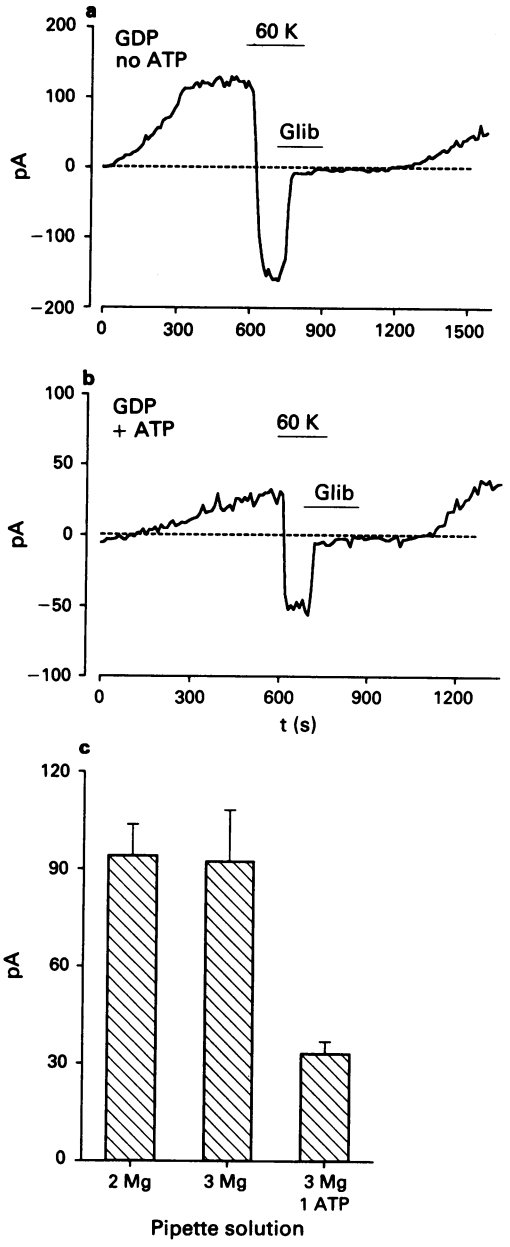

Figure 8 Effects of $[ATP]_i$ on $I_{K(GDP)}$. Whole-cell current was sampled every 10 s at − 37 mV with 1 mM GDP in pipette solution Y. (a) The pipette solution had added a total of 3 mM $MgCl_2$. The external K concentration was raised from 5 mM (solution A) to 60 mM (solution E) and 5 μM glibenclamide was applied in the bath as indicated. (b) The same experimental procotol was used as in (a) but the pipette solution included 1 mM Na-ATP in addition to the 1 mM GDP and 3 mM $MgCl_2$. (c) Averages (mean ± s.e.mean; $n = 5$) for a series of experiments on cells held at − 37 mV for 10 min with 1 mM GDP in the pipette plus: (YA) 2 mM Mg; (YB) 3 mM Mg; (YC) 3 mM Mg and 1 mM Na-ATP. Outward current recorded with pipette solution YC was significantly less than that recorded with pipette solution YA ($P < 0.01$, two-tailed test). Inward $I_{K(GDP)}$ (60 mM external K) was also inhibited by ATP: with pipette solution (YB) the current was − 122.3 ± 7.8 pA ($n = 4$) and with pipette solution (YC) it was − 47.5 ± 3.9 pA ($n = 4$).

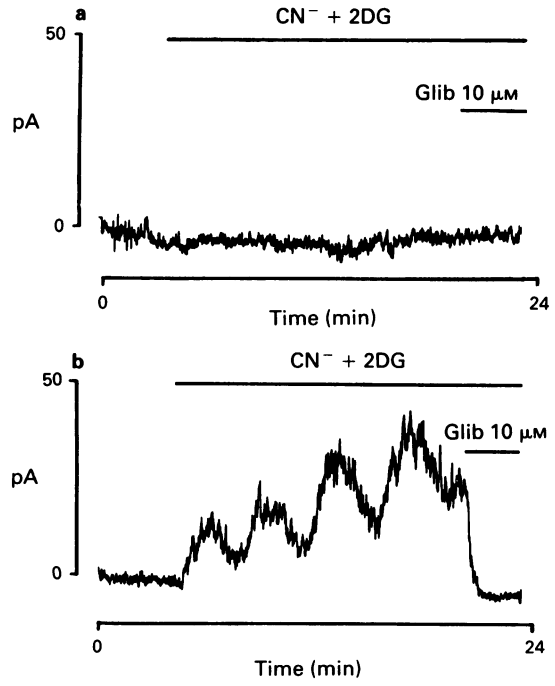

Figure 9 Effects of metabolic poisoning on membrane current. (a) A conventional whole-cell recording of membrane current at − 37 mV. Pipette solution X was used without a nucleotide and initially 10 mM glucose was present in the bath (solution A). As indicated, the bath solution was changed so that glucose was absent and 2 mM cyanide and 5 mM 2-deoxy-D-glucose were included. No outward current occurred and glibenclamide had no effect. (b) A nystatin-mode whole-cell recording at a holding potential of − 37 mV. As indicated, the bath solution was changed so that glucose was absent and 2 mM cyanide and 5 mM 2-deoxy-D-glucose were included. An undulating outward current developed that was inhibited by 10 μM glibenclamide.

paper for details). A standard pulse of u.v.-light from a xenon flash lamp was estimated to release about 1 mM free ATP from the caged precursor but the flash had no effect on membrane current in cells loaded with caged-ATP ($n = 4$; not shown).

In contrast, metabolic poisoning in perforated-patch whole-cell recordings (Horn & Marty, 1988) did affect membrane current. Figure 9b shows a typical perforated-patch whole-cell recording where there was no change in holding current in the presence of glucose but removal of glucose and the application of 2-DG and CN caused a pronounced outward current that undulated slowly. Bath application of 10 μM glibenclamide abolished this current. The same procedure induced a similar outward current in all 7 cells studied. Glibenclamide (100 nM) was applied to 3 of these cells and it was observed that the undulations ceased and that the current level was reduced to a steady level; 10 μM glibenclamide reduced the outward current further to near zero current. Although it proved difficult to quantify the effect of glibenclamide in these perforated-patch whole-cell recordings it seemed that the 2-DG/CN-induced current showed a sensitivity to glibenclamide that was similar to that of $I_{K(GDP)}$ recorded in the conventional whole-cell (Figure 5b), suggesting that K_{NDP} carried both currents.

Discussion

We have observed a class of small conductance K channels (K_{NDP}) that opened when NDPs were present with Mg ions at the intracellular surface of the plasma membrane of smooth muscle cells. K-current through K_{NDP} in the whole-cell was found to be sensitive to inhibition by nanomolar glibenclamide. It is our working hypothesis that NDPs are a crucial regulator of these channels and that ATP effects are only of consequence once NDPs have opened the channel. Although K_{NDP} did not open simply in the absence of $[ATP]_i$ in other regards they showed several similarities to the ATP-sensitive K channels (K_{ATP}) of other cell types.

The interpretation of our whole-cell experiments depends partly on the changes which might be supposed to occur in

the intracellular ATP concentration. We describe here our working hypothesis for the changes and absolute values of $[ATP]_i$ in whole-cells which is firstly consistent with our inside-out patch experiments that suggested K channels did not open simply in the absence of ATP, and secondly explains the observation that metabolic poisoning did not affect membrane current during conventional whole-cell recording. We cannot be certain of the total concentration of ATP in the cell or of the concentration close to a channel but we estimate here what the reasonable limits for $[ATP]_i$ might have been. We know that smooth muscle cells in the intact tissue have an $[ATP]_i$ in the region of 3 to 5 mM (van Breemen *et al.*, 1975; Ishida & Paul, 1990) and so the value in an isolated cell maintained in glucose may be similar and certainly more than 1 mM. Therefore, after breakthrough to the whole-cell recording mode without ATP in the pipette solution, $[ATP]_i$ may decline from 1 mM as ATP and some substrates for metabolism diffuse into the pipette. That $[ATP]_i$ was < 1 mM 10 min into a whole-cell recording was suggested by the observation that 1 mM ATP in the pipette solution inhibited $I_{K(GDP)}$ at this time (Figure 8). Therefore, we estimate that $[ATP]_i$ may have been between 1 and 100 μM after 10 min of whole-cell recording. Metabolic poisoning would cause $[ATP]_i$ to decline further and initially $[NDP]_i$ to increase relative to $[ATP]_i$. The maximum rise of $[NDP]_i$ relative to $[ATP]_i$ on metabolic poisoning is uncertain but $[NDP]_i$ could rise to 15% of $[ATP]_i$ (Ishida & Paul, 1990). On this basis, in our whole-cell recordings $[NDP]_i$ would not become more than 15 μM and $I_{K(NDP)}$ would be small or insignificant (Figure 2a). In perforated-patch whole-cell recordings $[ATP]_i$ would not decline as a result of diffusion into the pipette and metabolic poisoning might cause NDPs to rise to 150 μM or more and so induce $I_{K(NDP)}$. Silberberg & van Breemen (1992) also observed glibenclamide-sensitive K-current in response to metabolic poisoning of mesenteric artery smooth muscle cells from which recordings were made by the perforated-patch whole-cell method. Our result is similar except we observed undulations in the K-current, the mechanism of which is being investigated. The physiological significance of ATP effects on K_{NDP} is uncertain. The slope of the concentration-inhibition curve for Mg-ATP against K_{NDP} seems likely to be in the millimolar range (Figure 8) and so it might be that slight changes in the normal ATP concentration (3–5 mM) will have important effects on K_{NDP} channel activity if it has already been induced by a NDP. However, because $[ATP]_i$ tends to be quite resistant to change (van Breemen *et al.*, 1975) it might be that $[ATP]_i$ is relatively unimportant for regulation and instead it is changes in $[NDP]_i$ in the threshold region for channel activation that are of most significance. The latter interpretation also seems to be favoured by Pfründer *et al.* (1993) after a recent study on guinea-pig portal vein smooth muscle cells.

The K_{ATP} of cardiac muscle exhibit a high opening probability when patches are excised into ATP-free solution and a large K-current is induced in whole-cells when $[ATP]_i$ is depleted (Kakei *et al.*, 1985; Noma & Shibasaki, 1985). These effects did not occur in our recordings from smooth muscle or in those of others (Robertson *et al.*, 1992; Kamouchi *et al.*, 1993). With reference to work on other cell types it might be suggested that this difference occurred because K_{NDP} became dephosphorylated particularly quickly when $[ATP]_i$ was low. (Dephosphorylation is the proposed mechanism for 'run-down' of K_{ATP} which occurs over several minutes in inside-out patch excised from cardiac muscle in the absence of ATP.) However, we argue that the smooth muscle channels are closed in the absence of ATP not because they are dephosphorylated but because this is the state the channels adopt unless an agonist (e.g. GDP) is present. This is not only a simpler interpretation of our data but one that is supported by two key observations: (a) K channels did not open even within a few milliseconds after an inside-out patch was formed and patches formed in 10 μM ATP did not reveal channel activity (not shown); (b) whole-cell experiments with 100 μM ATP and no GDP in the pipette did not reveal K-current (Figure 1) and yet this concentration of ATP was not expected to inhibit $I_{K(GDP)}$ strongly (Figure 8) and is known to be sufficient for phosphorylation of K_{ATP} (Ashcroft & Ashcroft, 1990) so K_{ATP} channels should open.

Clapp & Gurney (1991) and Noack *et al.* (1992) have attempted to deplete $[ATP]_i$ in smooth muscle cells during whole-cell recording and have found evidence for glibenclamide-sensitive K-current or hyperpolarization. Although these experiments were on different smooth muscles from the one we used and so the channel properties may be different it is possible to interpret their data using our hypothesis for the control of K_{NDP}. Clapp & Gurney (1991) recorded from pulmonary artery smooth muscle cells with 11 mM glucose in the external solution and compared the effects of pipette solutions with and without ATP (1–3 mM) on membrane potential. When ATP was omitted the cells were more hyperpolarized and 1 μM glibenclamide depolarized them on average by 15 mV. We calculate that 3 pA of glibenclamide-sensitive K-current would have occurred at −40 mV and find it plausible that residual NDPs in the cell or GDP formed from the GTP (see Kajioka *et al.*, 1991) loaded into the cell from the whole-cell pipette (0.5 mM GTP was present) could have been enough to induce $I_{K(GDP)}$. Working on rat portal vein smooth muscle Noack *et al.* (1992) found a transient outward current (I_{met}) in some whole-cells held at −50 mV in the absence of ATP and metabolic substrates. A small transient outward current resembling I_{met} occurred in some of our whole-cell recordings from rabbit portal vein smooth muscle cells without nucleotide in the pipette (in the 9 cells in which it occurred its maximum amplitude was 10 ± 11 pA at 6 min after break-through to the whole-cell; Figure 1). In guinea-pig portal vein smooth muscle cells, the absence of metabolic substrates and of ATP in the pipette did not induce glibenclamide-sensitive outward current (Pfründer *et al.*, 1993). I_{met} in rat portal vein smooth muscle was inhibited by 1 μM but not 100 nM glibenclamide (Noack *et al.*, 1992). An explanation for I_{met} could be that $[NDP]_i$ was high before break-through to the whole-cell because the cells were already metabolically compromised and the transient time-course of I_{met} might have reflected complex changes in intracellular K, ATP, ADP and other NDPs. Dephosphorylation of the K channels underlying I_{met} seems unlikely, however, because the decline in I_{met} was unaffected by 18.7 μM ATP in the pipette. A comparison between rat and rabbit portal veins should be made cautiously because the underlying channels may be different (Kajioka *et al.*, 1990; 1991; see below).

The single channel observations suggest ATP-sensitive K channels in smooth muscle can be divided into 3 groups: (i) large conductance channels; (ii) small conductance channels opening without NDPs; (iii) small conductance channels that require NDPs. (i) Standen *et al.* (1989) observed 135 pS K channels (60 mM:120 mM K-gradient) in inside-out patches from mesenteric artery smooth muscle cells. These channels were clearly inhibited by ATP with an IC_{50} of 50–300 μM and were Ca- and voltage-insensitive. They were not demonstrated to be sensitive to glibenclamide in the absence of cromakalim. Similar K channels from the aorta have been observed in lipid bilayers (Kovacs & Nelson, 1991). The K channels observed by Lorenz *et al.* (1992) were also of large conductance but they were activated by depolarization and were inhibited by 1 μM glibenclamide. (ii) Kajioka *et al.* (1990) observed 10 pS K channel activity (6 mM:138 mM K-gradient) in outside-out and inside-out patches from rat portal vein smooth muscle cells. NDPs and glibenclamide were not tested but the channel opened in the absence of $[ATP]_i$ if 1 μM Ca_i was present and this activity could then be inhibited by 5 mM Na-ATP_i but not by Mg-ATP_i. These channels appear similar to those observed by Wakatsuki *et al.* (1992) in patches from cultured coronary artery smooth muscle cells ($[Ca]_o$ 0.1 mM), which were inhibited by 30 μM glibenclamide.

(iii) Kajioka *et al.* (1991) and Kamouchi *et al.* (1993) observed a Ca- and voltage-insensitive 15 pS K channel (6 mM:140 mM K-gradient) in cell-attached and inside-out patches from rabbit portal vein smooth muscle cells. This channel only opened when >3 μM pinacidil (or LP-805) was present and was inhibited completely by 100 μM glibenclamide. Even in the presence of pinacidil the channel activity disappeared on forming an inside-out patch and or an open-cell patch into ATP-free solution and could not be reactivated by 1 mM Mg-ATP_i. However, the channels were clearly activated in inside-out patches (pinacidil present) if 1 mM GDP_i was applied. Subsequent application of Na-ATP_i inhibited the channels potently (IC_{50} 29 μM), despite the presence of pinacidil (cf. Fan *et al.*, 1990); Mg-ATP was found to be a less effective inhibitor, producing about 65% inhibition at 1 mM.

The small conductance GDP-dependent K channel we observed seems most similar to that described by Kajioka *et al.* (1991). However, there are a number of differences in properties between the whole-cell K-currents we observed and those of the single K channel currents studied by Kajioka *et al.* (1991), viz: ADP evoked whole-cell current in our experiments but not channel openings in theirs; our GDP-induced current required Mg ions but their K channel activity did not; GDP alone evoked whole-cell current or single channel activity in our experiments but single channel opening was seen in theirs only when pinacidil was also present, our GDP-evoked currents were shown to be 1000 times more sensitive than theirs to glibenclamide. The explanations for these differences are not clear but they may be due to differences between the whole-cell and isolated patch recording modes and reflect difficulties experienced in detecting the channels in patches and then studying their regulation in detail. Nevertheless, our results and those of Kajioka *et al.* (1991) and of Kamouchi *et al.* (1993) support the conclusion that the K_{ATP}-like channels of these smooth muscle cells do not open simply in the absence of ATP and that the reason for this absence of activity is not because the channels have become dephosphorylated but because they adopt the closed state unless NDPs are present.

Physiological roles for K_{NDP} channels are indicated by the action of glibenclamide. On the assumption that low concentrations of glibenclamide (we suggest <1 μM) specifically inhibit K_{NDP} channels it seems that the channels may underlie some of the effects on smooth muscle of hypoxia (Daut *et al.*, 1990; Lydrup & Hellstrand, 1991), endothelium-derived hyperpolarizing factor (Brayden, 1990), nitric oxide (Garland & MacPherson, 1992) and peptide neurotransmitters (Nelson *et al.*, 1990). The effects of metabolic poisoning or deprivation on electrical activity in smooth muscle appear complex, perhaps because many membrane proteins are affected by changes in nucleotide levels. In the rat portal vein glucose-removal caused a small depolarization but if cyanide was applied in addition there was a pronounced hyperpolarization (Ekmeharg, 1989). The significance of K_{NDP} channels will need to be addressed carefully and in the context of other membrane effects in a given smooth muscle type. Pharmacologically the identification of K_{NDP} could be important if the channels are the target for the hyperpolarizing action of KCO drugs (see the following paper, Beech *et al.*, 1993). In addition, however, it is not inconceivable that as the properties of K_{NDP} channels are better understood and their role more clearly defined that a wider therapeutic potential will be realised for selective inhibitors and activators of these channels.

The work was supported by the Wellcome Trust, the MRC and the World Health Organization.

References

ALLARD, B. & LAZDUNSKI, M. (1992). Nucleotide diphosphates activate the ATP-sensitive potassium channel in mouse skeletal muscle. *Pflügers Arch.*, **422**, 185–192.

ASHCROFT, S.J.H. & ASHCROFT, F.M. (1990). Properties and functions of ATP-sensitive K-channels. *Cell. Signal.*, **2**, 197–214.

ASHCROFT, S.J.H. & ASHCROFT, F.M. (1992). The sulphonylurea receptor. *Biochim. Biophys. Act.*, **1175**, 45–59.

BEECH, D.J. & BOLTON, T.B. (1989). Properties of the cromakalim-induced potassium conductance in smooth muscle cells isolated from the rabbit portal vein. *Br. J. Pharmacol.*, **98**, 851–864.

BEECH, D.J., ZHANG., H., NAKAO, K. & BOLTON, T.B. (1993). Single channel and whole-cell K-currents evoked by levcromakalim in smooth muscle cells from the rabbit portal vein. *Br. J. Pharmacol.*, **110**, 583–590.

BOLTON, T.B. & BEECH, D.J. (1992). Smooth muscle potassium channels: their electrophysiology and function. In *Potassium Channel Modulators: Pharmacological, Molecular and Clinical Aspects.* ed. Weston, A.H. & Hamilton, T.C. Chapter 7, pp. 144–180. Oxford: Blackwell Scientific Publications).

BRAYDEN, J.E. (1990). Membrane hyperpolarization is a mechanism of endothelium-dependent cerebral vasodilation. *Am. J. Physiol.*, **259**, H668–H673.

CLAPP, L.H. & GURNEY, A.M. (1992). ATP-sensitive K^+ channels regulate resting potential of pulmonary arterial smooth muscle cells. *Am. J. Physiol.*, **262**, H916–H920.

DAUT, J., MAIER-RUDOLPH, W., VON BECKERATH, N., MEHRKE, G., GÜNTHER, K. & GOEDEL-MEINEN, L. (1990). Hypoxic dilation of coronary arteries is mediated by ATP-sensitive potassium channels. *Science*, **247**, 1341–1344.

DAVIES, N.W., STANDEN, N.B. & STANFIELD, P.R. (1991). ATP-dependent potassium channels of muscle cells: their properties, regulation, and possible functions. *J. Bioeng. Biomembr.*, **23**, 509–535.

DUNNE, M.J. & PETERSEN, O.H. (1986). Intracellular ADP activates K^+ channels that are inhibited by ATP in an insulin-secreting cell line. *FEBS Lett.*, **208**, 59–62.

EKMEHARG, B.L. (1989). Electrical and mechanical responses to inhibition of cell respiration in vascular smooth muscle of the rat portal vein. *Acta Physiol. Scand.*, **137**, 41–51.

FAN, Z., NAKAYAMA, K. & HIRAOKA, M. (1990). Multiple actions of pinacidil on adenosine triphosphate-sensitive potassium channels in guinea-pig ventricular myocytes. *J. Physiol.*, **430**, 273–295.

GARLAND, C.J. & MCPHERSON, G.A. (1992). Evidence that nitric oxide does not mediate the hyperpolarization and relaxation to acetylcholine in the rat small mesenteric artery. *Br. J. Pharmacol.*, **105**, 429–435.

HAMILL, O.P., MARTY, E., NEHER, B., SAKMANN, B. & SIGWORTH, F.J. (1981). Improved patch-clamp techniques for the high-resolution current recording from cells and cell-free membrane patches. *Pflügers Arch.*, **391**, 85–100.

HORN, R. & MARTY, A. (1988). Muscarinic activation of ionic currents measured by a new whole-cell recording method. *J. Gen. Physiol.*, **92**, 145–159.

ISHIDA, Y. & PAUL, R.J. (1990). Effects of hypoxia on high-energy phosphagen content, energy metabolism and isometric force in guinea-pig taenia caeci. *J. Physiol.*, **424**, 41–56.

KAJIOKA, S., KITAMURA, K. & KURIYAMA, H. (1991). Guanosine diphosphate activates an adenosine 5'-triphosphate-sensitive K^+ channels in the rabbit portal vein. *J. Physiol.*, **444**, 397–418.

KAJIOKA, S., OIKE, M. & KITAMURA, K. (1990). Nicorandil opens a calcium-dependent potassium channel in smooth muscle cells of the rat portal vein. *J. Pharmacol. Exp. Ther.*, **254**, 905–913.

KAKEI, M., NOMA, A. & SHIBASAKI, T. (1985). Properties of adenosine-triphosphate-regulated potassium channels in guinea-pig ventricular cells. *J. Physiol.*, **363**, 441–462.

KAMOUCHI, M., KAJIOKA, S., SAKAI, T., KITAMURA, K. & KURIYAMA, H. (1993). A target K^+ channel for the LP-805-induced hyperpolarization in smooth muscle cells of the rabbit portal vein. *Naunyn-Schmied. Arch. Pharmacol.*, **347**, 329–335.

KOVACS, R.J. & NELSON, M.T. (1991). ATP-sensitive K^+ channels from aortic smooth muscle incorporated into planar bilayers. *Am. J. Physiol.*, **261**, H604–H609.

LAZDUNSKI, M., BERNARDI, H. DE WEILLE, J.R., MOURRE, C. & FOSSET, M. (1992). Agonists and antagonists of ATP-sensitive potassium channels. *Adv. Nephrol.*, **21**, 195–202.

LORENZ, J.N., SCHNERMANN, J., BROSIUS, F.C., BRIGGS, J.P. & FURSPAN, P.B. (1992). Intracellular ATP can regulate afferent arteriolar tone via ATP-sensitive K^+ channels in the rabbit. *J. Clin. Invest.*, **90**, 733–740.

LYDRUP, M.-L. & HELLSTRAND, P. (1991). Metabolic correlates to pacemaker activity in the smooth muscle of guinea-pig mesotubarium. *Acta Physiol. Scand.*, **141**, 263–272.

NAKAO, K. & BOLTON, T.B. (1991). Cromakalim-induced potassium currents in single dispersed smooth muscle cells of rabbit artery and vein. *Br. J. Pharmacol.*, **102**, 155P.

NAKAYAMA, S. & TOMITA, T. (1991). Regulation of intracellular free magnesium concentration in the taenia of the guinea-pig caecum. *J. Physiol.*, **435**, 559–572.

NELSON, M.T., HUANG, Y., BRAYDEN, J.E., HESCHELER, J. & STANDEN, N.B. (1990). Arterial dilations in response to calcitonin gene-related peptide involve activation of K^+ channels. *Nature*, **344**, 770–773.

NICHOLS, C.G. & LEDERER, W.J. (1991). Adenosine triphosphate-sensitive potassium channels in the cardiovascular system. *Am. J. Physiol.*, **261**, H1675–H1686.

NOACK, TH., EDWARDS, G., DEITMER, P. & WESTON, A.H. (1992). Potassium channel modulation in rat portal vein by ATP depletion: a comparison with the effects of levcromakalim (BRL 38227). *Br. J. Pharmacol.*, **107**, 945–955.

NOMA, A. (1983). ATP-regulated K^+ channels in cardiac muscle. *Nature*, **305**, 147–148.

NOMA, A. & SHIBASAKI, T. (1985). Membrane current through adenosine-triphosphate-regulated potassium channels in guinea-pig ventricular cells. *J. Physiol.*, **363**, 463–480.

PFRÜNDER, D., ANGHELESCU, I. & KREYE, V.A.W. (1993). Intracellular ADP activates ATP-sensitive K^+ channels in vascular smooth muscle cells of the guinea-pig portal vein. *Pflügers Arch.*, **423**, 149–151.

QUAST, U. & COOK, N.S. (1989). In vitro and in vivo comparison of two K^+ channel openers, diazoxide and cromakalim, and their inhibition by glibenclamide. *J. Pharmacol. Exp. Ther.*, **250**, 261–271.

ROBERTSON, B.E., CORRY, P.R., NYE, P.C.G. & KOZLOWSKI, R.Z. (1992). Ca^{2+} and Mg-ATP activated potassium channels from rat pulmonary artery. *Pflügers Arch.*, **421**, 94–96.

ROBERTSON, D.W. & STEINBERG, M.I. (1990). Potassium channel modulators: scientific applications and therapeutic promise. *J. Med. Chem.*, **33**, 1529–1541.

SILBERBERG, S.D. & VAN BREEMEN, C. (1992). A potassium current activated by lemakalim and metabolic inhibition in rabbit mesenteric artery. *Pflügers Arch.*, **420**, 118–120.

SILLEN, L.G. & MARTELL, A.E. (1964). Section I (p. 652). In *Stability Constants of Metal-Ion Complexes*. London: The Chemical Society.

STANDEN, N.B., QUAYLE, J.M., DAVIES, N.W., BRAYDEN, J.E., HUANG, Y. & NELSON, M.T. (1989). Hyperpolarizing vasodilators activate ATP-sensitive K^+ channels in arterial smooth muscle. *Science*, **245**, 177–180.

SUN, H.T., YOSHIDA, Y. & IMAI, S. (1990). A Ca^{2+}-activated, Mg^{2+}-dependent ATPase with high affinities for both Ca^{2+} and Mg^{2+} in vascular smooth muscle microsomes: comparison with plasma membrane Ca^{2+}-pump ATPase. *J. Biochem.*, **108**, 730–760.

TOMITA, T. (1988). Ionic channels in smooth muscle studied with patch-clamp methods. *Jpn. J. Physiol.*, **38**, 1–18.

TUNG, R.T. & KURACHI, Y. (1991). On the mechanism of nucleotide diphosphate activation of the ATP-sensitive K^+ channel in ventricular cell of guinea-pig. *J. Physiol.*, **437**, 239–256.

VAN BREEMEN, C., WUYTACK, F. & CASTEELS, R. (1975). Stimulation of ^{45}Ca efflux from smooth muscle cells by metabolic inhibition and high K depolarization. *Pflügers Arch.*, **359**, 183–196.

WAKATSUKI, T., NAKAYA, Y. & INOUE, I. (1992). Vasopressin modulates K^+-channel activities of cultured smooth muscle cells from porcine coronary artery. *Am. J. Physiol.*, **263**, H491–H496.

WESTON, A.H. & EDWARDS, G. (1992). Recent progress in potassium channel opener pharmacology. *Biochem. Pharmacol.*, **43**, 47–54.

ZILBERTER, Y., BURNASHEV, N., PAPIN, A., PORTNOV, V. & KHODOROV, B. (1988). Gating kinetics of ATP-sensitive single potassium channels in myocardial cells depends on electromotive force. *Pflügers Arch.*, **411**, 584–589.

(Received March 18, 1993
Revised June 21, 1993
Accepted June 23, 1993)

Br. J. Pharmacol. (1993), **110**, 583–590

Single channel and whole-cell K-currents evoked by levcromakalim in smooth muscle cells from the rabbit portal vein

[1]D.J. Beech, H. Zhang, K. Nakao & [2]T.B. Bolton

Department of Pharmacology and Clinical Pharmacology, St. George's Hospital Medical School, London, SW17 0RE

1 Single channel and whole-cell current recordings were made from single smooth muscle cells isolated from the rabbit portal vein.

2 Application of 10 μM levcromakalim ((−)-Ckm) to single cells held with pipettes containing 1 mM GDP induced a K-current ($I_{K(Ckm)}$) which occurred in addition to the current caused by GDP alone ($I_{K(GDP)}$) and averaged 135 pA at − 37 mV. We have investigated whether the same K channels underlie the GDP- and Ckm-induced K-currents.

3 If 1 mM GDP was in the pipette but Mg ions were omitted the effect of GDP was absent and $I_{K(Ckm)}$ averaged only 10 pA, suggesting that the action of (−)-Ckm was Mg-dependent.

4 Intracellular ATP was not observed to have much effect on $I_{K(-Ckm)}$. Loading of cells with 10 mM ATP from the recording pipette had no significant effect and flash photolysis of caged-ATP loaded into cells from the pipette, estimated to release about 1 mM free ATP, also had no effect on $I_{K(-Ckm)}$.

5 Bath-applied glibenclamide inhibited $I_{K(-Ckm)}$ with an IC_{50} of 200 nM, a value 8 times higher than that found for inhibition of $I_{K(GDP)}$. The delayed rectifier K-current ($I_{K(DR)}$) was also inhibited by glibenclamide but at higher concentrations (IC_{50} 100 μM). Bath-applied tetraethylammonium ions (TEA) inhibited $I_{K(-Ckm)}$ and $I_{K(GDP)}$ to the same extent (IC_{50} about 7 mM).

6 In inside-out patch recordings (−)-Ckm (10 μM) applied to the intracellular surface of the membrane potentiated the opening of K channels already stimulated by 1 mM GDP and all of the channel activity was abolished by 10 μM glibenclamide. The unitary conductance of the channels was 24 pS in a 60 mM:130 mM K-gradient.

7 We suggest that (−)-Ckm may hyperpolarize and relax smooth muscle cells by opening K_{NDP}, a class of small conductance K channels that are related to the ATP-sensitive K channels seen in other tissues.

Keywords: Smooth muscle; levcromakalim; K channel

Introduction

K channel openers (KCOs) are a new class of drugs with a variety of different structures that have in common the ability to open K channels. They are particularly potent relaxants of smooth muscle and are of promise for the treatment of diseases such as asthma, essential hypertension and urinary incontinence (reviewed by Robertson & Steinberg, 1990). A major mechanism underlying the relaxant effects of KCOs appears to be the opening K channels in the cell membrane which leads to membrane hyperpolarization (reviewed by Edwards *et al.*, 1992). The target K channel and the mechanism of its activation are the subjects of this study.

There is good evidence that KCOs open ATP-sensitive K channels (K_{ATP}) in cardiac muscle but the target K channel in smooth muscle is less clear. Both small and large conductance ATP-sensitive K channels (Standen *et al.*, 1989; Wakatsuki *et al.*, 1992), large conductance Ca-activated K channels (BK_{Ca}) (Klöckner *et al.*, 1989; Carl *et al.*, 1992) and delayed rectifier K channels (K_{DR}) (Beech & Bolton, 1989a) have been suggested as targets for the action of KCOs. It is surprising that there is so much inconsistency in the literature regarding the properties of the target K channels and although KCOs appear to open several types of K channel in isolated patches of membrane it is uncertain whether the effects occur in the intact cell or whole tissue. For example, the KCO cromakalim has often been found to stimulate BK_{Ca} in patches and yet its action on the whole tissue is not blocked by tetraethylammonium (< 1 mM) or charybdotoxin but is inhibited by 4-aminopyridine, a pharmacology that is inconsistent with a role for BK_{Ca} (Beech & Bolton, 1989a; Strong *et al.*, 1989). In addition, data from noise analysis suggest the K channels underlying the whole-cell current are of small conductance (Beech & Bolton, 1989a; Noack *et al.*, 1992a; Langton *et al.*, 1992), thus implying that large conductance channels do not open in response to KCOs in the intact cell.

Our previous data on the action of the KCO cromakalim (Ckm; BRL 34915) in rabbit portal vein smooth muscle cells suggested that a population of small conductance K channels were opened in single cells (Beech & Bolton, 1989a). The whole-cell K-current showed only minor voltage-dependence and had a pharmacology distinct from that of BK_{Ca}. A comparison of the Ckm-induced K-current with other K-currents in the same cells indicated most similarity with the delayed rectifier and so we developed a working hypothesis where Ckm caused a proportion of K_{DR} to shift into a voltage-independent gating mode so that they were open at the resting potential. However, although ATP-sensitive K-current was not noticed in these recordings from portal vein smooth muscle cells we have now identified a new K-current in the same cells which is activated by nucleotide diphosphates (NDPs) acting intracellularly (Beech *et al.*, 1993). The channels carrying this K-current are also of small conductance and they appear related to the K_{ATP} seen in other tissues. We refer to these channels as K_{NDP} to indicate the importance of NDPs in their activation and the failure of a reduction in $[ATP]_i$ alone to open them. In the light of this

[1] Present address: Department of Pharmacology, The University of Leeds, Leeds, LS2 9JT.
[2] Author for correspondence.

finding we have reinvestigated the action of Ckm, to see if K_{NDP} are the site of action of this drug. In this study we have mostly used the active enantiomer of Ckm, levcromakalim ((−)-Ckm; BRL 38227).

Methods

Methodology for the isolation of single smooth muscle cells from the rabbit portal vein, experimental procedures and the composition of solutions were the same as those described in the preceding paper (Table 1). Flash photolysis was performed with a xenon flash lamp (Hitech). Flash pulses (1 ms duration) were transmitted through a UG-11 filter. The efficiency of flash-induced hydrolysis was estimated by placing a 20 µl drop of pipette solution containing 0.5 mM NPE-caged-ATP on a cover-slip in place of a cell. High performance liquid chromatography (h.p.l.c.) was kindly carried out by S.A. Prestwich to determine the percentage conversion. A single flash (100 V) converted about 10% of the NPE-caged-ATP and a smaller flash (50 V) converted about 4%. NPE caged-ATP (adenosine 5'-triphosphate, P^3-1-(2-nitrophenyl)-ethyl-ester) and NPE-caged IP_3 (D-*myo*-inositol 1,4,5-trisphosphate, $P^{4(5)}$-1-(2-nitrophenyl)-ethyl ester) were from Calbiochem. (−)-Ckm and glibenclamide were prepared as 10 mM stock solutions in dimethylsulphoxide (DMSO). The final concentration of DMSO was 0.2% for 20 µM (−)-Ckm or glibenclamide and less for other concentrations. These dilutions of DMSO had no effect on $I_{K(NDP)}$ or $I_{K(-Ckm)}$. Levcromakalim ((−)-Ckm, BRL 38227) was a gift from Dr T. Hamilton (SKB).

Results

Whole-cell K-currents induced by intracellular GDP ($I_{K(GDP)}$) and bath-applied (−)-Ckm ($I_{K(-Ckm)}$)

Whole-cell recordings were made from rabbit portal vein smooth muscle cells. Figure 1a shows a recording where an outward current of 88 pA developed at a holding potential of − 37 mV when GDP was included in the pipette solution. Once the response to GDP had reached a maximum, (−)-Ckm (10 µM) was bath-applied and an additional outward current was observed which reached a maximum of 167 pA (in addition to the GDP-induced current) and then declined while (−)-Ckm was still present; on average the additional current was 135 ± 16 pA ($n = 22$) at its peak. The currents induced by GDP and by (−)-Ckm reversed close to the calculated E_K, suggesting they were both carried mostly by K ions (Figure 1b; the total K concentration in the pipette was 171 mM, making E_K − 88 mV). Figure 1c shows a recording of membrane current at − 77 mV when the external [K] was 60 mM (E_K − 26 mV). This condition was expected to increase the amplitude of the K-currents and the associated noise because the driving force on K was greater and because the conductance of K channels normally increases when the external [K] is raised in this range. A slowly undulating noise was associated with the GDP-induced current but the application of (−)-Ckm, although increasing the current by over 4 times, did not increase the noise further. This may indicate

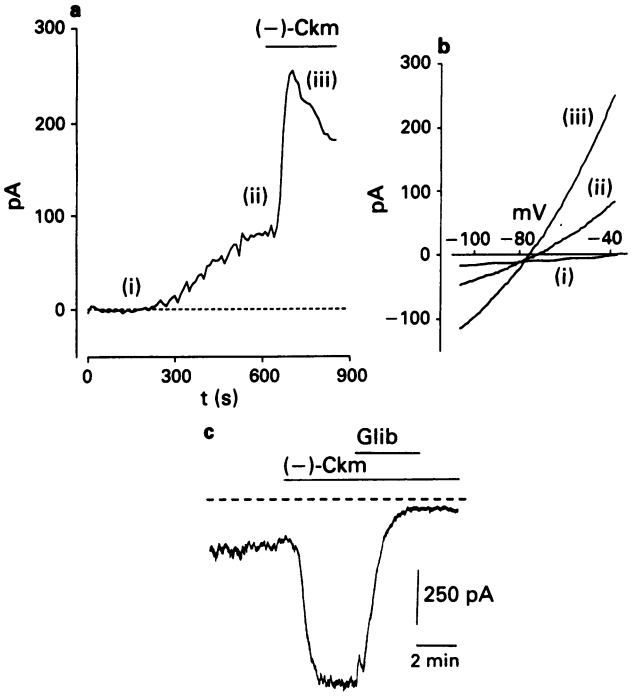

Figure 1 Levcromakalim ((−)-Ckm) and GDP_i activate a similar K-current in single smooth muscle cells isolated from the rabbit portal vein. (a) Whole-cell current sampled every 10 s at a holding potential of − 37 mV. Pipette solution Y was used with 1 mM GDP, 2 mM EDTA and 2 mM $MgCl_2$ added. The extracellular solution was A. (−)-Ckm (10 µM) was bath-applied 10 min after starting the whole-cell recording. (b) From the same cell as described in (a), currents (each a mean of 3) in response to ramp changes in voltage from the holding potential of − 37 mV to − 107 mV: (i) about 2 min after break-through to the whole-cell; (ii) when the maximum $I_{K(GDP)}$ was observed; (iii) at the peak of the response to (−)-Ckm. (c) Whole-cell current at − 77 mV in a cell bathed in solution E (60 mM K). The recording is shown from 7 min after break-through to the whole-cell mode; 1 mM GDP was present in the pipette and (−)-Ckm (10 µM) and glibenclamide (Glib, 10 µM) were applied via the bath solution was indicated. Broken lines mark zero current.

that the K channels opened by (−)-Ckm were not of a larger conductance than K_{NDP} channels (24 pS in these solutions; see preceding paper). Noise analysis was not carried out, however, because a low frequency noise component (<0.05 Hz) necessitated that long constant recordings of current be obtained and both $I_{K(GDP)}$ and $I_{K(-Ckm)}$ declined over long periods.

Effects of (−)-Ckm on single K_{NDP} channels

To investigate further whether (−)-Ckm and GDP caused K-current by opening the same K channel we recorded from isolated inside-out patches in the presence of 1 mM GDP at the intracellular surface. (−)-Ckm (10 µM) was applied to 10

Table 1 Composition of solutions

Solution	*NaCl*	*KCl*	*$CaCl_2$*	*$MgCl_2$*	*HEPES*	*Glucose*	*EGTA*	*BAPTA*	*pH*
A (bath)	130	5	1.7	1.2	10	10	0	0	7.4
B (bath)	126	6	1.7	1.2	10.5	14	0	0	7.2
X (pipette)	0	130	0	2	20	0	5	0	7.4
Y (pipette)	0	110	0	2	20	0	0	10	7.4
Z (pipette)	0	134	0	1.2	10.5	14	3	0	7.2
E (bath or pipette)	80	60	1.7	1.2	10	10	0	0	7.4
I (bath or pipette)	9	117	0	3	18	0	9	0	7.4

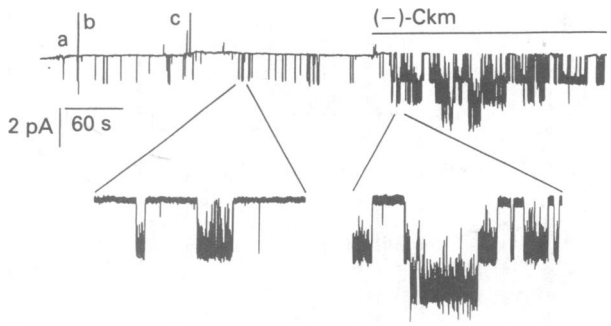

Figure 2 Stimulation of GDP-dependent K channels (K_{NDP}) in an inside-out patch by levcromakalim ((−)-Ckm). Solution E was in the pipette and solution I in the bath: 1 mM GDP was present in the bath solution from the beginning of the recording. The patch was initially cell-attached and then the inside-out patch was formed at (a) by pulling the pipette away from the cell. The holding voltage was − 80 mV except for a brief period (b) when activity of large conductance Ca-activated K-channels was looked for by depolarizing to 0, 80, 0 mV. This test revealed activity of these large channels only at 80 mV, as expected in this condition and confirmed that the patch was inside-out. Once the inside-out patch was formed, intermittent unitary current steps of about 1.5 pA occurred and there was conspicuous noise during the openings. At (c) the 1 mM GDP solution was exchanged for a new solution of 1 mM GDP but no noticeable effect occurred. (−)-Ckm (10 μM) was bath-applied as indicated and a large increase in channel activity occurred which declined slightly in the continued presence of (−)-Ckm. The continuous trace was recorded on FM-tape (3.75 in s^{-1}) with a 0.5 kHz low-pass filter (− 3 dB, 4-pole Bessel) and filtered for presentation at 50 Hz. The expanded sections of trace (amplified 2 times and filtered at 0.5 kHz) before and in the presence of (−)-Ckm showed that the channel had the same unitary size and characteristics in both cases. (−)-Ckm increased the channel activity and on occasions as many as 3 channels were open simultaneously.

patches held at − 80 mV in which K_{NDP} were observed; in 4 of these channel activity ceased before (−)-Ckm was applied and (−)-Ckm had no effect, in the remaining 6 patches (−)-Ckm increased channel activity. In 6 patches 10 μM (−)-Ckm was applied using the same protocol except in the absence of GDP and no channel openings were observed. The clearest response we observed to (−)-Ckm is shown in Figure 2. The patch was excised into 1 mM GDP and inward unitary currents of 1.5 pA were observed at the holding potential of − 80 mV when K_{NDP} opened. Subsequent application of (−)-Ckm caused a marked increase in channel activity and occasionally 3 channels were open simultaneously. The sections of current record on a faster time base show that the characteristics of the channels opened by (−)-Ckm were similar to those of K_{NDP}.

Figure 3a shows that the unitary current-voltage relationship was linear for the channel activated in the presence of (−)-Ckm plus GDP and that the relationship was similar for the channel activated by GDP alone. Channel activity induced by (−)-Ckm and GDP was rapidly abolished by 10 μM glibenclamide applied to the intracellular surface of the patch and partial recovery occurred on wash-out (Figure 3b). These experiments suggested that the channel opened by GDP was also the one stimulated by (−)-Ckm. An estimate of the mean effect of GDP and GDP plus (−)-Ckm was calculated (Figure 3c) and this indicated that the probability of opening increased from 0.03 (GDP only) to 0.17 (GDP plus (−)-Ckm). On the basis that the average channel density in a patch was 0.2 and the ratio of cell:patch surface area was 10000:1 the whole-cell currents at − 80 mV resulting from the channel activity would be − 90 pA (GDP only) and − 510 pA (GDP plus (−)-Ckm). These values are close to those actually recorded under the same ionic and voltage conditions in the whole-cell (e.g. Figure 1c).

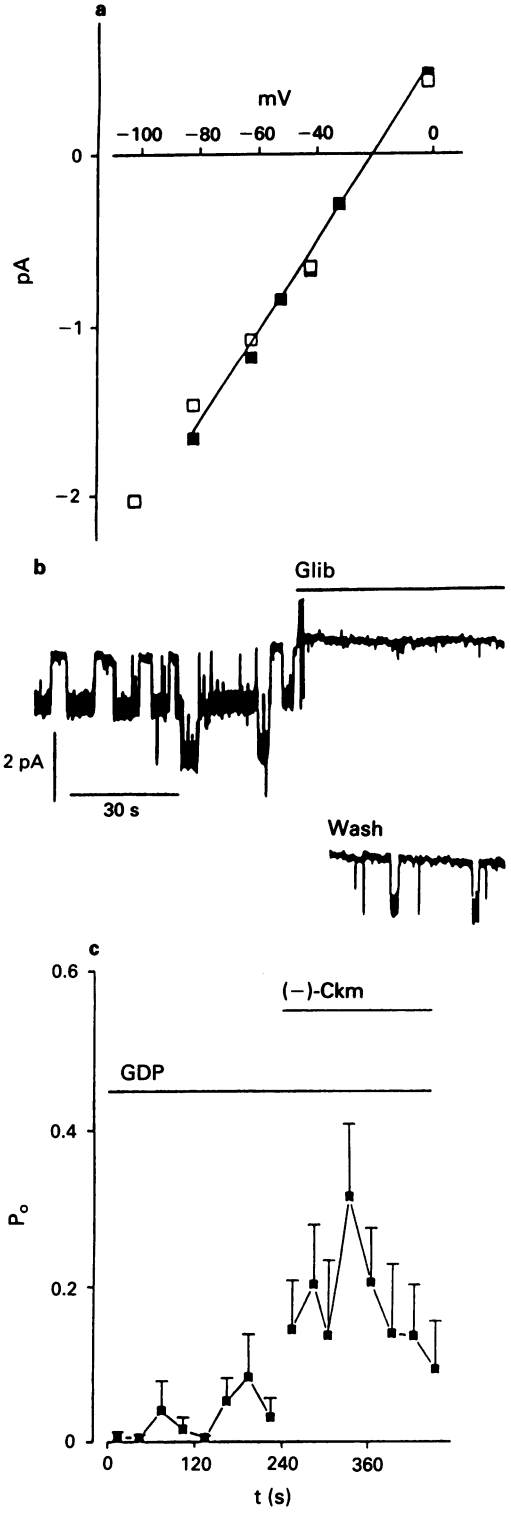

Figure 3 GDP- and levcromakalim ((−)-Ckm)-activated K channels in inside-out patches. Solution E was in the pipette and solution I in the bath. (a) Unitary current-voltage relationship in the presence of 1 mM GDP (□) and in a different patch in the presence of 1 mM GDP and 10 μM (−)-Ckm (■). Unitary current was measured by constructing amplitude histograms for the closed and open state current levels. (b) K channel activity in a patch held at − 80 mV in the presence of 1 mM GDP and 10 μM (−)-Ckm in the bath. Glibenclamide (10 μM) was applied with GDP and (−)-Ckm via the bath solution as indicated. Wash out of glibenclamide allowed partial recovery of channel activity; the section of current record marked 'wash' started 1 min after glibenclamide was washed from the bath. (c) Estimated channel opening probability before and during 10 μM (−)-Ckm, averaged for 6 patches (mean ± s.e.mean). The calculation assumed the maximum number of unitary current levels observed in a patch to be equal to the number of channels in the patch and ignored the fluctuations in the open-state current.

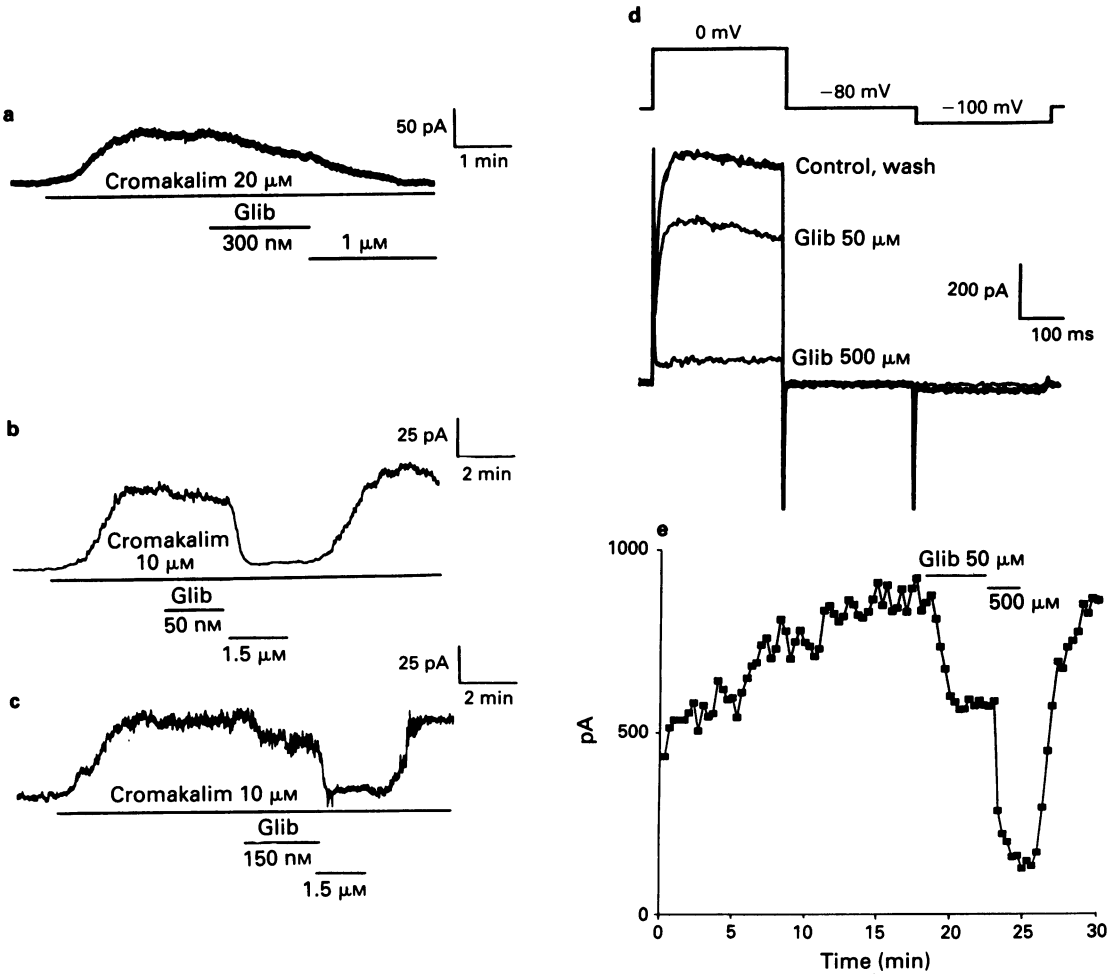

Figure 4 Inhibition of $I_{K(-Ckm)}$ and $I_{K(DR)}$ by glibenclamide. (a) Current in a conventional whole-cell recording at − 40 mV with pipette solution Z and bath solution B. Cromakalim (Ckm, 20 μM) and then 300 nM and 1 μM glibenclamide (Glib) with Ckm were bath-applied as marked. (b and c) Current during a perforated-patch whole-cell recording using pipette solution X and bath solution A. (−)-Ckm (20 μM) and glibenclamide with (−)-Ckm were bath-applied as marked. (d) Conventional whole-cell recording with pipette solution X and bath solution was A. The holding potential was − 80 mV and 0.5 s-test voltage steps were applied every 20 s to 0 mV (to elicit $I_{K(DR)}$) and to − 100 mV (to assess leak current). Currents are shown for the control, in 50 and 500 μM glibenclamide and after wash-out of glibenclamide. (e) For the experiment described in (d) a plot of current amplitude at the end of each test step to 0 mV. 'Leak' current (which was very small compared with $I_{K(DR)}$) was estimated from the inward current elicited by stepping from − 80 mV to − 100 mV each time after stepping to 0 mV. This current was scaled linearly and added to the current elicited by stepping to 0 mV. Glibenclamide was bath-applied as indicated.

Actions of glibenclamide and tetraethylammonium (TEA)

The data presented in Figures 1 to 3 suggest that (−)-Ckm acted on K_{NDP} to produce K-current in the whole-cell. To test this hypothesis further we investigated the actions of glibenclamide, a potent inhibitor of K_{NDP} (see preceding paper), and TEA which, although a blocker of many K channels (Rudy, 1988), can be helpful for the classification of K channels when IC_{50} values are measured (Bolton & Beech, 1992).

Figure 4a shows current induced by Ckm in the conventional whole-cell. Bath-applied 300 nM glibenclamide inhibited the current by 37% and 1 μM caused a decline to the pre-Ckm level. The whole-cell experiments were, however, often complicated by a decline of $I_{K(Ckm)}$ in the absence of glibenclamide and so further experiments were carried out in which perforated-patch whole-cell recording was used (Horn & Marty, 1988) where the Ckm-response was better maintained. Two experiments are shown (Figure 4b and c), in both of which 1.5 μM glibenclamide caused complete inhibition of $I_{K(-Ckm)}$: 50 nM glibenclamide reduced $I_{K(-Ckm)}$ by 18% in one cell and 150 nM glibenclamide reduced $I_{K(-Ckm)}$ by 33% in another. Wash-out of glibenclamide allowed full recovery (sometimes with post-wash potentiation) of $I_{K(-Ckm)}$. For comparison, the effect of glibenclamide on the outward current elicited by depolarization from − 80 mV to 0 mV was studied without GDP in the pipette solution. This current is mostly the delayed rectifier current ($I_{K(DR)}$) under these conditions (Beech & Bolton, 1989b). Figure 4d shows an experiment where glibenclamide (50 μM) caused a 29% reduction of $I_{K(DR)}$ and 500 μM caused a 90% reduction. Recovery of current was good on wash-out of glibenclamide (Figure 4e). The averages for these and other experiments are shown in Figure 5. An IC_{50} of 200 nM was indicated for glibenclamide-induced inhibition of $I_{K(-Ckm)}$, similar to that found for glibenclamide-induced inhibition of Ckm-induced ^{86}Rb-efflux from a segment of rat portal vein (Quast & Cook, 1989). The IC_{50} for inhibition of $I_{K(DR)}$ was relatively high at 100 μM. Delayed rectifier type K-current was also inhibited by glibenclamide in the neuroblastoma cell line SH-SY5Y (Reeve *et al.*, 1992) and in hippocampal neurones (Crépel *et al.*, 1992).

At 7 mM, TEA inhibited the K-current induced by GDP (1 mM) by 47 ± 4% ($n = 3$) and K-current induced by GDP and (−)-Ckm together by 46 ± 6% ($n = 3$). This blocking action of TEA agrees well with the IC_{50} of 7 mM previously

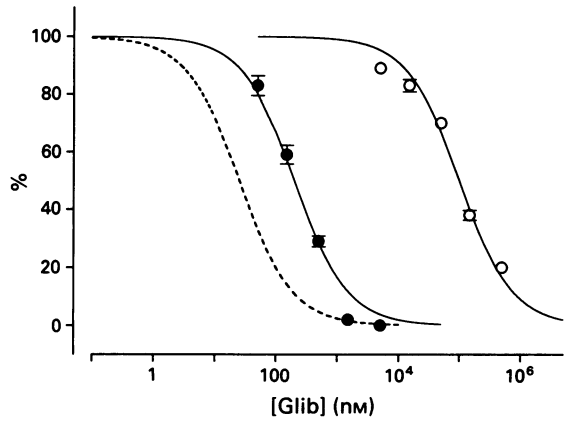

Figure 5 Comparison of concentration-inhibition curves for glibenclamide effects on: K-current induced by 10 μM levcromakalim ((−)-Ckm) in perforated-patch whole-cells ($I_{K(-Ckm)}$, ●); delayed rectifier K-current in conventional whole-cells ($I_{K(DR)}$, ○); and GDP-induced K-current in conventional whole-cells (broken line; from Beech *et al.*, 1993). The data points are mean ± s.e.mean ($n = 3-14$); when the error bars are not shown they are smaller than the symbol. The smooth lines are Hill equations fitted by the method of least squares with a slope of 1. The estimated K_d values are: 200 nM, $I_{K(Ckm)}$; 100 μM, $I_{K(DR)}$; 25 nM, $I_{K(GDP)}$. The ordinate scale is the % of the control current remaining in the presence of glibenclamide.

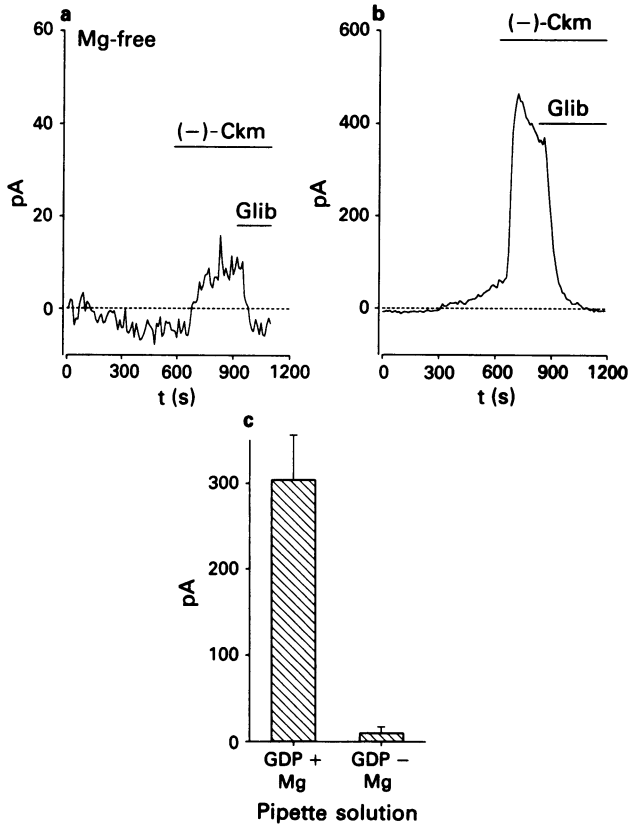

Figure 6 Dependence of $I_{K(-Ckm)}$ on Mg ions. (a) Whole-cell current sampled every 10 s at − 37 mV with pipette solution Y plus 2 mM EDTA, 1 mM GDP and Mg ions omitted (GDP-Mg). Levcromakalim ((−)-Ckm) 10 μM and 10 μM glibenclamide (Glib) were bath-applied as marked. (b) Whole-cell current sampled every 10 s at − 37 mV with pipette solution Y plus 2 mM EDTA, 2 mM $MgCl_2$ (total Mg = 4 mM) and 1 mM GDP (GDP + Mg). (−)-Ckm 10 μM and 10 μM glibenclamide were bath-applied as marked. (c) Averages (mean ± s.e.mean) for the whole-cell current induced by bath-applied 10 μM (−)-Ckm at − 37 mV with the two pipette solutions: GDP + Mg ($n = 4$) and GDP − Mg ($n = 7$).

found for TEA against current induced by (±)-Ckm (BRL 34915) in these cells (Beech & Bolton, 1989a).

Dependence of $I_{K(-Ckm)}$ *on Mg ions*

We have found that the action of GDP to induce K-current requires intracellular Mg ions (Beech *et al.*, 1993) and so for comparison we investigated if the action of (−)-Ckm might also require Mg ions. This possibility was investigated in experiments where Mg ions were omitted from the pipette solution (Figure 6a and c). In experiments where 1 mM GDP was included in the pipette but Mg ions were omitted (EDTA was included to chelate residual Mg ions) it was found that GDP had no effect and 10 μM (−)-Ckm had much less effect; (−)-Ckm produced a slowly developing outward current of 10 ± 7 pA at − 37 mV and this current was inhibited by glibenclamide. In contrast, when the EDTA was saturated with excess Mg ions, GDP and (−)-Ckm produced normal glibenclamide-sensitive responses (Figure 6b and c). These observations suggest that the responses to GDP and to (−)-Ckm (GDP in the pipette) depend absolutely on the presence of intracellular Mg ions.

Effects of $[ATP]_i$ *on* $I_{K(-Ckm)}$

It is commonly suggested that (−)-Ckm and other KCOs act on K_{ATP} in smooth muscle but evidence is lacking that KCO effects can be inhibited by $[ATP]_i$, even at very high concentrations. Therefore, we have investigated the effects of $[ATP]_i$ on $I_{K(-Ckm)}$.

The first experimental design was to compare the effects of Ckm on cells when $[ATP]_i$ was expected to be very low or very high. Cells were either incubated for 30 min prior to recording with 6 mM cyanide and 14 mM 2-deoxy-D-glucose (2-DG) in the external solution and recordings made with a pipette solution containing 14 mM 2-DG and no glucose, or they were maintained in 14 mM glucose and the recording pipette containing 14 mM glucose plus 10 mM Na-ATP or 10 mM Mg-ATP. At a holding potential of − 40 mV, bath-application of 20 μM Ckm induced an outward current of 59.9 ± 11.3 pA ($n = 22$) in the cells treated with cyanide and 2-DG, and 37.2 ± 5.2 pA ($n = 14$) and 32.7 ± 8.9 pA ($n = 11$)

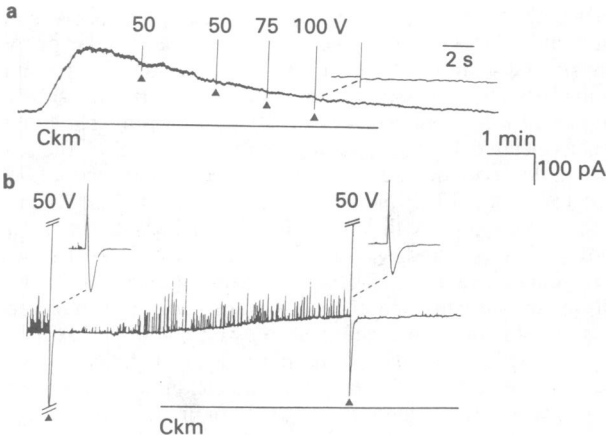

Figure 7 Lack of effect of flash photolysis of intracellular caged-ATP on $I_{K(Ckm)}$. Whole-cell current was recorded at a holding potential of − 40 mV in both experiments and pipette solution Z and bath solution B were used. (a) The pipette solution contained 10 mM NPE-caged-ATP and 3 mM EGTA without ATP or glucose. Once outward current had been induced by 20 μM levcromakalim single flash pulses were applied (50, 50, 75, 100 V). The inset current record is on an expanded time-scale. (b) The pipette solution contained 100 μM NPE-caged-IP_3, 1 mM ATP and 0.05 mM EGTA. A single flash pulse (50 V) was applied in the absence and presence of 20 μM Ckm. The upper two traces are shown on an expanded time-scale and with different current sensitivities.

in the cells loaded with Na-ATP or Mg-ATP respectively. These $I_{K(Ckm)}$ were not significantly different although there was some indication that $I_{K(Ckm)}$ was less when $[ATP]_i$ was high.

Figure 7 shows a different approach to investigating effects of $[ATP]_i$. A cell was loaded with NPE-caged-ATP (10 mM in the pipette solution) and a brief flash of u.v. light was applied to the cell from a xenon flash lamp. The maximum flash (100 V) was estimated to release about 1 mM free ATP (see Methods) but no obvious effect on $I_{K(Ckm)}$ was observed (Figure 7a). Figure 7b shows a control experiment where the pipette solution contained 100 μM NPE-caged-IP_3 instead of the NPE-caged-ATP. A flash (50 V) caused rapid transient outward and inward currents at a holding potential of −40 mV as well as a prolonged reduction in the brief outward currents that were occurring spontaneously. The experiments of Komori & Bolton (1991) suggest that these effects occur because free IP_3 was generated inside the cell which then released Ca from intracellular stores causing the opening of Ca-activated K channels and Cl channels. The result serves here as an indication of the effectiveness of the technique. Although NPE-caged-ATP inhibits cardiac K_{ATP} prior to flash, the inhibition is not complete and flash does cause a further reduction in K-current (Nichols *et al.*, 1990). A different 'cage' on the ATP (4,5-dimethoxy-2-nitrophenyl-ethyl-ester) does not prevent the inhibitory action in the dark (Nichols *et al.*, 1990; Ammälä *et al.*, 1991). Thus, although these caged-ATPs are not well-suited to the study of K_{ATP}, flash photolysis does increase the free ATP and sensitivity to released ATP can be detected (see Clapp & Gurney, 1992). Our results suggested that $I_{K(Ckm)}$ was not sensitive to intracellular ATP in the region of 1 mM.

Discussion

We have investigated the characteristics of K-currents induced by (−)-Ckm, a KCO, at whole-cell and single channel levels in vascular smooth muscle cells. Similarities were apparent between the actions of (−)-Ckm and intracellular GDP and the results point towards the conclusion that (−)-Ckm acted to potentiate the activity of K channels normally opened by GDP or other NDPs.

Evidence in favour of (−)-Ckm inducing hyperpolarization via an action on K_{NDP} is: (i) in inside-out patches (−)-Ckm stimulated the activity of K channels that had similar properties to K_{NDP} and the effect of (−)-Ckm on the channels seemed sufficient to explain the whole-cell current; (ii) in the whole-cell noise associated with $I_{K(-Ckm)}$ was not greater than that associated with $I_{K(GDP)}$, suggesting a channel of the same or smaller conductance (see also Beech & Bolton, 1989a; Langton *et al.*, 1992; Noack *et al.*, 1992a); (iii) TEA blocked $I_{K(-Ckm)}$ and $I_{K(GDP)}$ with similar IC_{50}s; (iv) 1 μM glibenclamide abolished $I_{K(-Ckm)}$ and $I_{K(GDP)}$; (v) Kajioka *et al.* (1991) showed that pinacidil (a KCO) opened a small conductance K channel in cell-attached patches on rabbit portal vein smooth muscle cells and these channels showed some similarities to K_{NDP} (see preceding paper). Evidence against the K_{NDP} hypothesis is weaker: (i) the IC_{50} for glibenclamide inhibition of $I_{K(-Ckm)}$ was 8 times higher than that for inhibition of $I_{K(GDP)}$; (ii) (−)-Ckm induced a large K-current when GDP had already produced its maximum effect (i.e. one effect did not prevent the other): (iii) $[ATP]_i$ did reduce $I_{K(GDP)}$ but inhibition of $I_{K(-Ckm)}$ was difficult to demonstrate. If (−)-Ckm does open K_{NDP} it remains to be explained why these differences should exist. It is possible that GDP_i enhanced the sensitivity of K_{NDP} to glibenclamide, perhaps via a mechanism similar to that suggested for the action of tolbutamide on the β-cell K_{ATP} (Schwanstecher *et al.*, 1992). Pinacidil has been found to reduce the sensitivity of cardiac K_{ATP} to $[ATP]_i$ (Fan *et al.*, 1990). A similar effect might make $I_{K(-Ckm)}$ particularly resistant to $[ATP]_i$. These possibilities will need to be investigated.

Our previous working hypothesis was that Ckm acted to shift a proportion of delayed rectifier K channels (K_{DR}) to a voltage-independent state and that glibenclamide inhibited this effect by acting as an antagonist at the Ckm receptor (Beech & Bolton, 1989a). This view was favoured by evidence that: (i) 4-aminopyridine and phencyclidine inhibited $I_{K(DR)}$ and $I_{K(Ckm)}$ at similar concentrations; (ii) the noises associated with $I_{K(DR)}$ and $I_{K(Ckm)}$ were both small and suggestive of a small conductance for the underlying channels; (iii) $I_{K(DR)}$ was reduced when $I_{K(Ckm)}$ developed (see also Okabe *et al.*, 1990; Noack *et al.*, 1992a); we suggested this effect occurred as a result of K_{DR} channels shifting to a voltage-independent state so that fewer were available for opening by depolarization; drug-induced shifts in channel gating have also been proposed for the action of disulphonic stilbene derivatives (e.g. SITS) on squid axon delayed rectifier K channels (Inoue, 1986) and veratridine on voltage-gated Na channels (Leibowitz *et al.*, 1986); (iv) glibenclamide inhibited relaxation induced by Ckm in a manner that appeared competitive (Quast & Cook, 1989), which allows the interpretation that glibenclamide prevented an action of Ckm on K_{DR} channels simply by inhibiting binding of Ckm at its receptor rather than the alternative hypothesis where glibenclamide inhibits the K channels directly.

Although the evidence in favour of an exclusive action of (−)-Ckm on K_{NDP} is compelling, it is difficult to rule out the K_{DR} hypothesis. However, we can now say that the IC_{50} for glibenclamide inhibition of $I_{K(DR)}$ was 500 times higher than that for $I_{K(-Ckm)}$ and that recovery of $I_{K(DR)}$ from block by glibenclamide was fast in comparison to the recovery of $I_{K(-Ckm)}$. In addition, Russell *et al.* (1992) found that (−)-Ckm could induce K-current without reducing $I_{K(DR)}$ in rabbit portal vein, and Noack *et al.* (1992a) found no effect of 1 μM glibenclamide on the inhibition of a $I_{K(DR)}$-like current (designated I_{TO}) by (−)-Ckm in rat portal vein. Therefore, K_{DR} and K_{NDP} may be separate populations of K channels but with some similarities with regard to unitary conductance, opening characteristics and pharmacology. It is tempting to speculate that K_{DR} channels might be sensitive to higher concentrations of Ckm on the basis that they are sensitive to higher concentrations of glibenclamide. Indeed, it has recently been suggested that the sulphonylurea receptor could be associated with channels other than K_{ATP}, such as K_{DR}-like channels or the CFTR chloride channel (Ashcroft & Ashcroft, 1992). There is evidence that nicorandil (a KCO that also has nitrate-like properties) can open small conductance K channels that are not K_{NDP} in smooth muscle cells from the rat portal vein (Kajioka *et al.*, 1990) and porcine coronary artery (Wakatsuki *et al.*, 1992). The K channel in porcine coronary artery may also be activated by SITS (Inoue *et al.*, 1989). Similar small conductance K channels have been observed to be stimulated occasionally by Ckm in some patches from the rabbit portal vein held at depolarized potentials (Nakao & Bolton, 1991). The relationship between these small channels and K_{NDP} and their significance in whole-cells has yet to be established.

Some single channel studies have suggested that Ckm opens large conductance K channels in smooth muscle (Standen *et al.*, 1989; Kovacs & Nelson, 1991; Lorenz *et al.*, 1992). Although the channels have a conductance close to that of the BK_{Ca} channels, which can also be activated by cromakalim in patches (e.g. Klöckner *et al.*, 1989), and they may show similar voltage-dependence (Lorenz *et al.*, 1992) they are not Ca-dependent, are inhibited by intracellular ATP (BK_{Ca} are not; Klöckner & Isenberg, 1992; Silberberg & van Breemen, 1992) and have a distinct pharmacology. Therefore, there is evidence that Ckm can act on a population of large conductance K channels but there is no evidence that these channels are opened by Ckm in the whole-cell and noise analysis suggests that the channels opened by Ckm have a small conductance (about 15 pS in a physiological K-gradient), which seems to rule out a role for large conductance channels in rabbit and rat portal vein (Beech & Bolton,

1989a; Noack *et al.*, 1992a) and pulmonary artery (Langton *et al.*, 1992) smooth muscles.

The reason for the Mg-dependence of the action of (−)-Ckm is unknown but the possibility that the response might depend on Mg-NDP is worthy of discussion. We have observed previously that 10 μM Ckm induced an average outward current of 44 pA at − 40 mV in portal vein smooth muscle cells (Beech & Bolton, 1989a), considerably less than was observed in the present experiments when GDP was in the pipette solution. In addition, averaging our responses to 10 μM (−)-Ckm at − 37 mV in this study gives 55 ± 5 pA ($n = 11$) without GDP in the pipette and 135 ± 16 pA ($n = 22$) with 1 mM GDP in the pipette. From these observations it is tempting to speculate that the response to (−)-Ckm might be Mg-dependent because Mg-GDP in some way modulates the action of (−)-Ckm. NDP-induced enhancement of KCO effects on K_{ATP} has been observed in other cell types. Allard & Lazdunski (1992) found that pinacidil activated skeletal muscle K_{ATP} only if NDPs were present. Shen *et al.* (1991) found that nicorandil, but not pinacidil or cromakalim, required the presence of Mg-NDPs in order to activate cardiac K_{ATP} channels. Potentiation of the action of (−)-Ckm by a NDP might be an explanation for the observation that vasodilatation of the rabbit ear artery to (−)-Ckm is augmented by hypoxia (Randall & Griffith, 1993). This observation may seem to contradict results on the response to Ckm in metabolically compromised conventional whole-cells (Noack *et al.*, 1992b; Beech *et al.*, 1993) but as discussed in the preceding paper (Beech *et al.*, 1993) $[ATP]_i$ might have been low (< 100 μM) in these recordings and so metabolic poisoning would not raise $[NDP]_i$ sufficiently to affect the action of Ckm or $[NDP]_i$ may have been so low that Ckm did not act. Further experiments will be required to test thoroughly the hypothesis that NDPs modulate the action of KCOs and other explanations for the Mg-dependence of (−)-Ckm response will also need to be considered.

We are grateful for support from the Wellcome Trust, the World Health Organization and the MRC. We thank Ms S.A. Prestwich for measuring ATP by h.p.l.c. for us and Dr T.C. Hamilton (SKB) for the cromakalim and levcromakalim.

References

ALLARD, B. & LAZDUNSKI, M. (1992). Nucleotide diphosphates activate the ATP-sensitive potassium channel in mouse skeletal muscle. *Pflügers Arch.*, **422**, 185–192.

AMMÄLÄ, C., BOKVIST, K., GALT, S. & RORSMAN, P. (1991). Inhibition of ATP-regulated K^+-channels by a photoactivatable ATP-analogue in mouse pancreatic β-cells. *Biochim. Biophys. Acta*, **1092**, 347–349.

ASHCROFT, S.J.H. & ASHCROFT, F.M. (1992). The sulphonylurea receptor. *Biochim. Biophys. Acta*, **1175**, 45–59.

BEECH, D.J. & BOLTON, T.B. (1989a). Properties of the cromakalim-induced potassium conductance in smooth muscle cells isolated from the rabbit portal vein. *Br. J. Pharmacol.*, **98**, 851–864.

BEECH, D.J. & BOLTON, T.B. (1989b). Two components of potassium current activated by depolarization of single smooth muscle cells from the rabbit portal vein. *J. Physiol.*, **418**, 293–309.

BEECH, D.J., ZHANG, H.-L., NAKAO, K. & BOLTON, T.B. (1993). K channel activation by nucleotide diphosphates and its inhibition by glibenclamide in vascular smooth muscle cells. *Br. J. Pharmacol.* **110**, 573–582.

BOLTON, T.B. & BEECH, D.J. (1992). Smooth muscle potassium channels: their electrophysiology and function. In *Potassium Channel Modulators: Pharmacological, Molecular and Clinical Aspects*. ed. Weston, A.H. & Hamilton, T.C. Chapter 7, pp. 144–180. Oxford: Blackwell Scientific Publications.

CARL, A., BOWEN, C.H., GELBAND, C.H., SANDERS, K.M. & HUME, J.R. (1992). Cromakalim and lemakalim activate Ca^{2+}-dependent K^+ channels in canine colon. *Pflügers Arch.*, **421**, 67–76.

CLAPP, L.H. & GURNEY, A.M. (1992). ATP-sensitive K^+ channels regulate resting potential of pulmonary arterial smooth muscle cells. *Am. J. Physiol.*, **262**, H916–H920.

CRÉPEL, V., KRNJEVIC, K. & BEN-ARI, Y. (1992). Glibenclamide depresses the slowly inactivating outward current (I_D) in hippocampal neurons. *Can. J. Physiol. Pharmacol.*, **70**, 306–307.

EDWARDS, G., DUTY, S., TREZISE, D.J. & WESTON, A.H. (1992). In *Potassium Channel Modulators: Pharmacological, Molecular and Clinical Aspects*. ed. Weston, A.H. & Hamilton, T.C. Chapter 14, pp. 369–421. Oxford: Blackwell Scientific Publications.

FAN, Z., NAKAYAMA, K. & HIRAOKA, M. (1990). Multiple actions of pinacidil on adenosine triphosphate-sensitive potassium channels in guinea-pig ventricular myocytes. *J. Physiol.*, **430**, 273–295.

HORN, R. & MARTY, A. (1988). Muscarinic activation of ionic currents measured by a new whole-cell recording method. *J. Gen. Physiol.*, **92**, 145–159.

INOUE, I. (1986). Modification of K conductance of the squid axon membrane by SITS. *J. Gen. Physiol.*, **88**, 507–520.

INOUE, I., NAKAYA, Y., NAKAYA, S. & MORI, H. (1989). Extracellular Ca^{2+}-activated K channel in coronary artery smooth muscle cells and its role in vasodilation. *FEBS Lett.*, **255**, 281–284.

KAJIOKA, S., OIKE, M. & KITAMURA, K. (1990). Nicorandil opens a calcium-dependent potassium channel in smooth muscle cells of the rat portal vein. *J. Pharmacol. Exp. Ther.*, **254**, 905–913.

KAJIOKA, S., KITAMURA, K. & KURIYAMA, H. (1991). Guanosine diphosphate activates an adenosine 5'-triphosphate-sensitive K^+ channel in the rabbit portal vein. *J. Physiol.*, **444**, 397–418.

KLÖCKNER, U. & ISENBERG, G. (1992). ATP suppresses activity of Ca^{2+}-activated K^+ channels by Ca^{2+} chelation. *Pflügers Arch.*, **420**, 101–105.

KLÖCKNER, U., TRIESCHMANN, U. & ISENBERG, G. (1989). Pharmacological modulation of calcium and potassium channels in isolated vascular smooth muscle cells. *Arzneimittel-Forschung*, **39**, 120–126.

KOMORI, S. & BOLTON, T.B. (1991). Calcium release induced by inositol 1,4,5-trisphosphate in single rabbit intestinal smooth muscle cells. *J. Physiol.*, **433**, 495–517.

KOVACS, R.J. & NELSON, M.T. (1991). ATP-sensitive K^+ channels from aortic smooth muscle incorporated into planar bilayers. *Am. J. Physiol.*, **261**, H604–H609.

LANGTON, P.D., CLAPP, L.H., DART, C., GURNEY, A.M. & STANDEN, N.B. (1992). Whole cell K^+ current activated by lemakalim in isolated myocytes from rabbit pulmonary artery: estimate of unitary conductance and density by noise analysis. *J. Physiol.*, **459**, 254P.

LEIBOWITZ, M.D., SUTRO, J.B. & HILLE, B. (1986). Voltage-dependent gating of veratridine-modified Na channels. *J. Gen. Physiol.*, **87**, 25–46.

LORENZ, J.N., SCHNERMANN, J., BROSIUS, F.C., BRIGGS, J.P. & FURSPAN, P.B. (1992). Intracellular ATP can regulate afferent arteriolar tone via ATP-sensitive K^+ channels in the rabbit. *J. Clin. Invest.*, **90**, 733–740.

NAKAO, K. & BOLTON, T.B. (1991). Cromakalim-induced potassium currents in single dispersed smooth muscle cells of rabbit artery and vein. *Br. J. Pharmacol.*, **102**, 155P.

NICHOLS, C.G., NIGGLI, E. & LEDERER, W.J. (1990). Modulation of ATP-sensitive potassium channel activity by flash-photolysis of 'caged-ATP' in rat heart cells. *Pflügers Arch.*, **415**, 510–512.

NOACK, Th., EDWARDS, G., DEITMER, P. & WESTON, A.H. (1992a). Characterization of potassium currents modulated by BRL 38227 in rat portal vein. *Br. J. Pharmacol.*, **106**, 717–726.

NOACK, Th., EDWARDS, G., DEITMER, P. & WESTON, A.H. (1992b). Potassium channel modulation in rat portal vein by ATP depletion: a comparison with the effects of levcromakalim (BRL 38227). *Br. J. Pharmacol.*, **107**, 945–955.

OKABE, K., KAJIOKA, S., NAKAO, K., KITAMURA, K., KURIYAMA, H. & WESTON, A.H. (1990). Actions of cromakalim on ionic currents recorded from single smooth muscle cells of the rat portal vein. *J. Pharmacol. Exp. Ther.*, **252**, 832–839.

QUAST, U. & COOK, N.S. (1989). *In vitro* and *in vivo* comparison of two K^+ channel openers, diazoxide and cromakalim, and their inhibition by glibenclamide. *J. Pharmacol. Exp. Ther.*, **250**, 261–271.

RANDALL, M.D. & GRIFFITH, T.M. (1993). Modulation of vasodilatation to levcromakalim by hypoxia and EDRF in the rabbit isolated ear: a comparison with pinacidil, sodium nitroprusside and verapamil. *Br. J. Pharmacol.*, **109**, 386–393.

REEVE, H.L., VAUGHAN, P.F.T. & PEERS, C. (1992). Glibenclamide inhibits a voltage-gated K^+ current in the human neuroblastoma cell line SH-SY5Y. *Neurosci. Lett.*, **135**, 37–40.

ROBERTSON, D.W. & STEINBERG, M.I. (1990). Potassium channel modulators: scientific applications and therapeutic promise. *J. Med. Chem.*, **33**, 1529–1541.

RUDY, B. (1988). Diversity and ubiquity of K channels. *Neuroscience*, **25**, 729–749.

RUSSELL, S.N., SMIRNOV, S.V. & AARONSON, P.I. (1992). Effects of BRL 38227 on potassium currents in smooth muscle cells isolated from rabbit portal vein and human mesenteric artery. *Br. J. Pharmacol.*, **105**, 549–556.

SCHWANSTECHER, C., DICKEL, C. & PANTEN, U. (1992). Cytosolic nucleotides enhance the tolbutamide sensitivity of the ATP-dependent K^+ channel in mouse pancreatic B cells by their combined actions at inhibitory and stimulatory receptors. *Mol. Pharmacol.*, **41**, 480–486.

SHEN, W.K., TUNG, R.T., MACHULDA, M.M. & KURACHI, Y. (1991). Essential role of nucleotide diphosphates in nicorandil-mediated activation of cardiac ATP-sensitive K^+ channel. *Circ. Res.*, **69**, 1152–1158.

SILBERBERG, S.D. & VAN BREEMEN, C. (1992). A potassium current activated by lemakalim and metabolic inhibition in rabbit mesenteric artery. *Pflügers Arch.*, **420**, 118–120.

STANDEN, N.B., QUAYLE, J.M., DAVIES, N.W., BRAYDEN, J.E., HUANG, Y. & NELSON, M.T. (1989). Hyperpolarizing vasodilators activate ATP-sensitive K^+ channels in arterial smooth muscle. *Science*, **245**, 177–180.

STRONG, P.N., WEIR, S.W., BEECH, D.J., HIESTAND, P. & KOCHER, H. (1989). Effects of potassium channel toxins from *Leiurus quinquestriatus hebraeus* venom on responses to cromakalim in rabbit blood vessels. *Br. J. Pharmacol.*, **98**, 817–826.

WAKATSUKI, T., NAKAYA, Y. & INOUE, I. (1992). Vasopressin modulates K^+-channel activities of cultured smooth muscle cells from porcine coronary artery. *Am. J. Physiol.*, **263**, H491–H496.

(Received March 18, 1993
Revised June 21, 1993
Accepted June 23, 1993)

Br. J. Pharmacol. (1993), **110**, 591–596

Effects of phospholipase A_2 inhibitors on coupling of α_2-adrenoceptors to inwardly rectifying potassium currents in guinea-pig submucosal neurones

[1]R.J. Evans & A. Surprenant

Vollum Institute, L-474, 3181 SW Sam Jackson, Oregon Health Sciences University, Portland, Oregon 97201, U.S.A.

1 Noradrenaline hyperpolarizes guinea-pig submucosal neurones by opening inwardly rectifying potassium channels. Intracellular recordings were made from submucosal neurones and the possible involvement of the phospholipase A_2 pathway in this response was examined.

2 The non-specific phospholipase A_2 inhibitors, quinacrine (10 μM) and 4-bromophenacyl bromide (4-BPB, 10 μM) inhibited nerve-evoked inhibitory synaptic potentials (i.p.s.ps) and hyperpolarizations to somatostatin and UK 14304. Quinacrine and 4-BPB also blocked the inward rectification present in current-voltage curves in the absence of somatostatin or UK 14304.

3 The more selective phospholipase A_2 inhibitor, cyclosporin A (10 μM) and the lipoxygenase and cyclo-oxygenase inhibitor, eicosatetraynoic acid (ETYA, 20 μM) and nordihydroguairetic acid (NDGA, 20 μM) did not alter i.p.s.ps or hyperpolarizations to UK 14304.

4 Exogenously applied arachidonic acid (1–300 μM) did not mimic the i.p.s.p. or the hyperpolarization to UK 14304.

5 We conclude that arachidonic acid or its eicosanoid metabolites produced by phospholipase A_2 stimulation are unlikely to be involved in the receptor G-protein coupled activation of potassium currents in submucosal neurones. The inhibition of the noradrenaline-induced hyperpolarization by quinacrine and 4-BPB is most likely due primarily to blockade of the basal inwardly rectifying potassium conductance present in these neurones.

Keywords: Enteric neurones; arachidonic acid; phospholipase A_2; electrophysiology; G-protein coupled receptors

Introduction

Arachidonic acid can be released following the activation of phospholipase A_2 by receptor-coupled G proteins (Axelrod *et al.*, 1988; Piomelli & Greengard, 1990). Arachidonic acid or its eicosanoid metabolites have been shown to act as second messengers in neuronal inhibition by G-protein-coupled receptors which act by increasing potassium conductances (Piomelli *et al.*, 1987; Kurachi *et al.*, 1989; Volterra & Siegelbaum, 1989; Miller *et al.*, 1992). This mechanism of action has been particularly well characterized for the FMRF-amide induced activation of the S-channel in *Aplysia* neurones (see review by Volterra & Siegelbaum, 1989). There is much less information regarding the involvement of this pathway in activation of G-protein coupled potassium conductances in mammalian neurones. In rat hippocampal pyramidal neurones the increase in neuronal M-current by somatosatin can be mimicked by the application of arachidonic acid or its eicosanoid metabolite, leukotriene C_4 (Schweitzer *et al.*, 1990) and arachidonic acid has been shown to open potassium channels in excised membrane patches obtained from these neurones (Premkumar *et al.*, 1990).

The opening of potassium channels following the activation of inhibitory receptors has been studied extensively in guinea-pig submucosal neurones (North, 1989). These neurones receive inhibitory synaptic inputs through the activation of α_2-adrenoceptors by noradrenaline released from sympathetic nerves and by somatostatin released from intrinsic enteric nerves (Mihara *et al.*, 1987a,b; Surprenant & North, 1988; Bornstein *et al.*, 1988). These hyperpolarizations are mediated through the activation of an inwardly rectifying potassium conductance. The transduction is blocked by pertussis toxin (Surprenant & North, 1988), and is guanosine 5'-triphosphate-sensitive (Shen *et al.*, 1992) demonstrating the activation is G-protein coupled. The involvement of protein kinases A and C as second messengers in this transduction pathway has been discounted (Surprenant & North, 1988). We have shown previously that the opening of potassium channels by noradrenaline can be recorded in excised patches of submucosal neurones (Shen *et al.*, 1992). These results suggest that either the potassium channel is modulated directly by the G-protein coupled receptor or the second messenger system is closely associated with the cell membrane. A possible candidate for such a second messenger system is the production of arachidonic acid and its metabolites from membrane phospholipid by the membrane-bound phospholipase, phospholipase A_2 (Kennedy, 1992). Recently, it has been suggested that α_2 adrenoceptor activation may be coupled to the stimulation of phospholipase A_2 and the production of arachidonic acid (Jones *et al.*, 1991; Gonzales *et al.*, 1991). The aim of the present study was to examine whether arachidonic acid or its metabolites may be involved in the hyperpolarizations to somatostatin and α_2-adrenoceptor activation in guinea-pig submucosal neurones.

Methods

Submucosal plexus preparations were obtained from the small intestine of guinea-pigs (150–250 g); methods of tissue preparation were as described previously (Surprenant, 1984). Tissues were superfused at 3–4 ml min^{-1} with a physiological solution of the following composition (mM): NaCl 126, NaH_2PO_4 1.2, $MgCl_2$ 1.2, $CaCl_2$ 2.5, KCl 5, $NaHCO_3$ 25 and glucose 11; gassed with 95% O_2 and 5% CO_2. The temperature was maintained at 34–36°C. Test agents were added to the superfusion medium to give the required final concentration.

Changes in membrane potential of submucosal neurones

[1] Author for correspondence at present address: Department of Physiology & Pharmacology, University of Strathclyde, Glasgow G1 1XW, Scotland.

were recorded with glass microelectrodes, filled with 1 M KCl and 1% neurobiotin (Vector laboratories) with tip resistances of 70–180 MΩ. Signals were recorded with an Axoclamp 2A amplifier and displayed on a Gould 2400S chart recorder. When successful impalements were obtained with microelectrodes of approximately 70–90 MΩ, membrane currents were measured with a single-electrode voltage clamp amplifier (Axoclamp 2A) with a switching frequency of 1–3 kHz. Steady-state voltage/current relationships were obtained by measuring membrane current during slow (5 mV s^{-1}) ramps of membrane potential. Signals were also digitised at 5–10 kHz and data were acquired using pClamp 5.5 software.

A blunt glass microelectrode (tip diameter 20–50 μm) filled with physiological saline was used to evoke synaptic potentials from submucosal neurones following the stimulation of adjacent ganglia (for nicotinic excitatory postsynaptic potentials (e.p.s.ps) 0.1 Hz, pulse width 0.1 ms, 5–15 V, and noradrenergic inhibitory postsynaptic potentials (i.p.s.ps) 5 pulses 20 Hz, pulse width 0.2 ms, 50 V). I.p.s.ps and agonist-induced hyperpolarizations were recorded at − 60 mV; nicotinic e.p.s.ps were recorded at a holding potential of − 90 mV in order to suppress action potential initiation.

Acetylcholine (ACh) (1 mM) was applied by ionophoresis from fire polished patch clamp electrodes (resistance 3–5 MΩ). Duration of the ionophoretic pulses ranged from 10 to 50 ms (30–50 V). Ionophoretic pulses were delivered at a frequency of 0.1 Hz throughout the course of the experiment.

Drug effects are expressed as a percentage of the response before drug application; all values are mean ± s.e.mean. Tests of significance were by Student's t test; $P<0.05$ was considered statistically significant.

Drugs

The following drugs were used, acetylcholine, arachidonic acid (sodium salt), 4-bromophenacyl bromide (4-BPB), 5,8, 11,14-eicosatetraynoic acid (ETYA), nordihydroguaiaretic acid (NDGA), quinacrine, tetrodotoxin and somatostatin (Sigma); cyclosporin A (Sandoz), UK 14304 (5-bromo-6-(2-imidazolin-2-ylamino)-quinoxaline, gift from Pfizer). Drugs were made up as concentrated stock solutions. 4-BPB was dissolved in dimethylsulphoxide (DMSO), arachidonic acid, ETYA and NDGA were made up in ethanol; these solvents had no effects on responses when applied in vehicle control experiments.

Results

Electrophysiological properties of submucosal neurones

Recordings were made from submucosal neurones that exhibited noradrenergic inhibitory postsynaptic potentials (i.p.s.ps) and/or were hyperpolarized by the α_2-adrenoceptor agonist, UK 14304 or somatostatin. Resting membrane potentials ranged from − 48 mV to − 63 mV (mean ± s.e.mean = − 54 ± 1.6 mV, $n = 31$). These neurones, which also show nicotinic excitatory postsynaptic potentials (e.p.s.ps), are classified as S or type 1 neurones (Nishi & North, 1973; Hirst *et al.*, 1974). Electrical stimulation (5 pulses at 20 Hz) evoked i.p.s.ps; the peak amplitude of these was 26.8 ± 1 mV ($n = 20$) (Figure 2). Superfusion with UK 14304 (100 nM) or somatostatin (10 nM) hyperpolarized these submucosal neurones by 24.8 ± 1.3 mV ($n = 20$) and 24.6 ± 3 mV ($n = 4$) respectively. Agonist-induced hyperpolarizations were reversed on washout (Figure 1).

Effects of phospholipase A_2 inhibitors on i.p.s.ps and hyperpolarizations to UK 14034 and somatostatin

The non-specific phospholipase A_2 inhibitors, quinacrine (mepacrine) and 4-BPB, and the relatively more specific

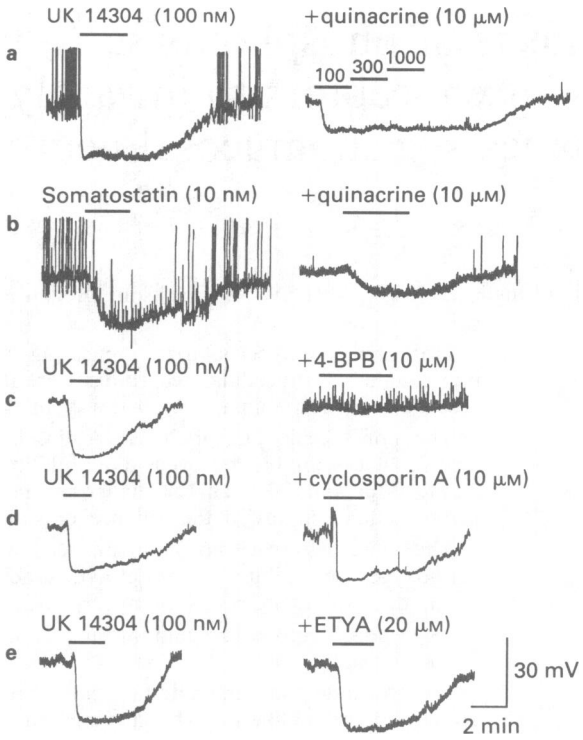

Figure 1 Effects of phospholipase A_2 inhibitors, quinacrine, 4-BPB, and cyclosporin A, and the cyclo-oxygenase and lipoxygenase inhibitor ETYA on somatostatin and α_2-adrenoceptor-mediated hyperpolarizations. Traces in (a)-(e) are recordings obtained before (lefthand records) and during the application of phospholipase A_2 inhibitors (righthand records); each set of recordings were obtained in separate experiments. (a,b) Quinacrine (10 μM) reduced the hyperpolarization produced by the α_2-adrenoceptor agonist, UK 14304 (UK, a) or somatostatin (b). (c) 4-BPB (10 μM) abolished the UK 14304-induced hyperpolarization; note the high frequency of spontaneous nicotinic e.p.s.ps in the presence of 4-BPB. (d,e) The hyperpolarization in response to UK 14304 was unaltered in the presence of cyclosporin A (10 μM) (d) or ETYA (20 μM) (e). For abbreviations, see text.

inhibitor cyclosporin A (Wallach & Brown, 1981; Blackwell & Flower, 1983; Fan & Lewis, 1985; Niwa *et al.*, 1986; Schweitzer *et al.*, 1990; El-Etr *et al.*, 1992) were used to examine whether phospholipase A_2 may be coupled to the-G-protein activation of inwardly rectifying potassium currents in submucosal neurones. Quinacrine (10 μM) reduced significantly the nerve evoked i.p.s.p. (Figure 2a), and the hyperpolarizations to UK 14304 (100 nM) and somatostatin (10 nM) by 92 ± 4% ($n = 8$), 58 ± 8% ($n = 11$) and 70 ± 5% ($n = 4$) respectively (Figure 1). Increasing the concentration of UK 14304 ten fold produced no further hyperpolarization (Figure 1a) indicating that quinacrine was not acting competitively. 4-BPB (10 μM) reduced the nerve-evoked i.p.s.p. by >95% ($n = 5$; Figure 2b) and reduced the hyperpolarization to UK 14304 by 94 ± 8% ($n = 4$; Figure 1c). An increase in the frequency of spontaneous e.p.s.ps was often recorded during the application of 4-BPB (e.g. Figure 1c). The inhibition of the UK 14304-induced hyperpolarization by quinacrine and 4-BPB was similar when experiments were carried out in the presence of tetrodotoxin (1 μM) to block indirect effects that might occur due to possible release of neurotransmitters by quinacrine or 4-BPB ($n = 2$). The effects of quinacrine and 4-BPB were not reversed after 20 min washout. Cyclosporin A (10 μM) had no effect on the i.p.s.p. amplitude (Figure 2c) or the hyperpolarization to UK 14304 (Figure 1d; 105.5 ± 2.5% ($n = 8$) and 108.7 ± 3.3% ($n = 6$) of control respectively).

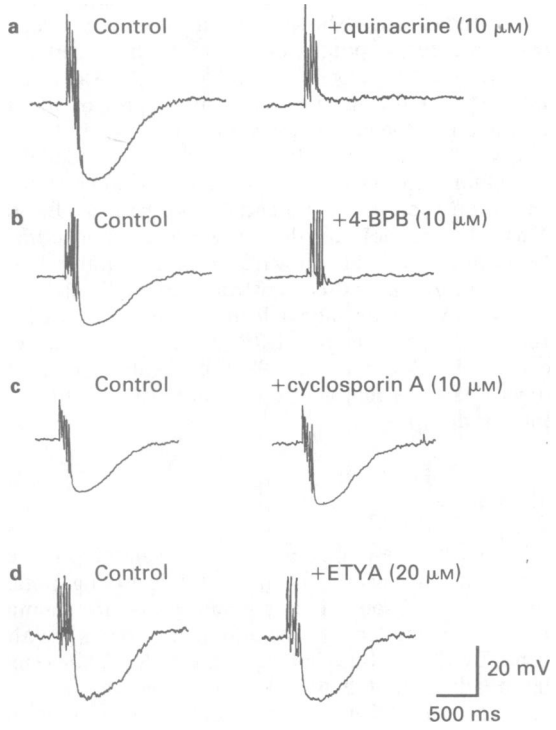

Figure 2 Effects of phospholipase A_2 inhibitors, quinacrine, 4-BPB, and cyclosporin A, and the cyclo-oxygenase and lipoxygenase inhibitor ETYA on nerve evoked i.p.s.ps. I.p.s.ps were evoked by electrical stimulation of adjacent ganglia with 5 pulses at 20 Hz. Traces in (a)-(d) are recordings obtained before (lefthand records) and during the application of drugs (righthand records); each set of recordings were obtained in separate experiments. (a,b) Quinacrine (10 μM) (a) and 4-BPB (10 μM) (b) reduced nerve evoked i.p.s.ps by >95%. (c,d) The amplitude of nerve evoked i.p.s.ps was unaffected by cyclosporin A (10 μM) (c) or ETYA (20 μM) (d). For abbreviations, see text.

Effects of cyclo-oxygenase and lipoxygenase inhibitors on hyperpolarizations to UK 14304

Arachidonic acid can be metabolised by two main routes: by cyclo-oxygenase to produce prostaglandins, and/or by lipoxygenase to produce hydroperoxyeicosatetraenoic acid derivatives. In this study neither the lipoxygenase and cyclo-oxygenase inhibitor ETYA (20 μM; Figure 1e) nor the lipoxygenase inhibitor NDGA (20 μM) inhibited the hyperpolarizations to UK 14304; UK 14304-induced hyperpolarizations were 89 ± 5% ($n = 5$) and 115 ± 15% ($n = 2$) of control respectively. Similarly, ETYA (20 μM) did not alter the i.p.s.p. amplitude (96 ± 4% of control i.p.s.p., $n = 3$; Figure 2d).

Effects of exogenously applied arachidonic acid

The exogenous application of arachidonic acid or its metabolites have been demonstrated to mimic G-protein activation in those cases where phospholipase A_2 stimulation has been well documented in signal transduction (Buttner *et al.*, 1989; Schweitzer *et al.*, 1990). In the present study superfusion with arachidonic acid (1–20 μM) produced no significant change in membrane potential ($n = 4$). Higher concentrations (100–300 μM) also did not alter the membrane potential ($n = 2$) or produced a 10–15 mV depolarization ($n = 3$). Arachidonic acid (100 μM) was without effect when it was applied in the presence of ETYA to prevent the enzymatic degradation of arachidonic acid ($n = 2$). Therefore, it appears that the depolarization to the higher concentrations of arachidonic acid may have been due to an action by one or more of its eicosanoid metabolites. Alternatively, these high concentrations of arachidonic acid may well have caused direct membrane damage which would be expected to result in a depolarization.

Effects of quinacrine on nicotinic responses and action potentials

In addition to its action as a phospholipase inhibitor, quinacrine has been shown to block ion channels and nicotinic ACh receptors (Adams & Feltz, 1980; Kehl, 1991; Mironov & Lux, 1992). We further examined the effects of quinacrine on nicotinic synaptic and ionophoretic potentials and on directly evoked action potentials. Quinacrine (10 μM) reduced nicotinic e.p.s.p.s by >95% ($n = 4$; Figure 3a). Ionophoretic application of ACh evoked nicotinic depolarizing potentials or inward currents; these were inhibited by 63 ± 9% by quinacrine (10 μM, $n = 8$; Figure 3b). Directly evoked action potentials were recorded in response to depolarizing current

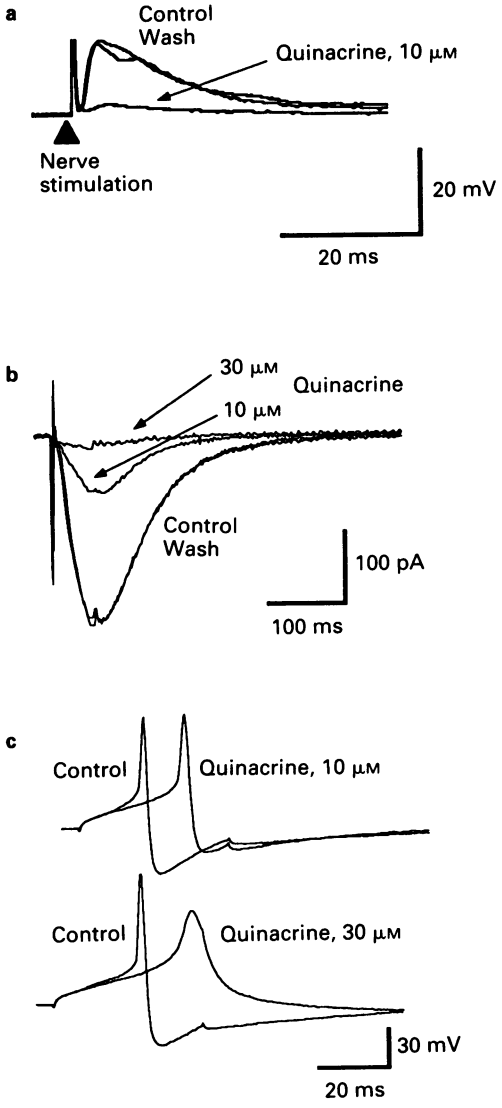

Figure 3 Effects of quinacrine on nicotinic responses and action potentials. (a) Records show averages of 10 nicotinic e.p.s.ps evoked at 0.1 Hz. Quinacrine (10 μM) reversibly reduced nicotinic e.p.s.ps by >95%. (b) Records show averages of 10 inward currents evoked by the ionophoretic application of acetylcholine (ACh, 1 mM) (50 ms pulse width, 30 V). Nicotinic inward currents were reduced reversibly by quinacrine (10–30 μM). (c) Injection of depolarizing current pulses (40 ms) evoked action potentials. The action potential threshold and duration was increased, and the peak amplitude and undershoot decreased by the application of quinacrine (10–30 μM).

pulses; quinacrine depressed the amplitude and increased the duration of these action potentials (Figure 3c).

Effects of quinacrine and 4-BPB on the voltage-current relationship

To determine if the inhibitory effects of quinacrine and 4-BPB may be independent of their action as phospholipase inhibitors, steady state voltage/current relations were examined between − 40 mV and − 140 mV. The control voltage/current curve shows marked inward rectification at potentials negative to E_K (Figure 4a; see Surprenant & North, 1988). Application of UK 14304 produced a hyperpolarization associated with an increase in membrane conductance (Figure 4). Previous studies have shown that it is the opening of an inwardly rectifying potassium current that mediates the hyperpolarization (Surprenant & North, 1988). Quinacrine (10 μM) reduced the inward rectification present in the absence of agonist; the conductance ratio measured at − 60 and − 115 mV was reduced from 1:3 ± 0.3 to 1:0.93 ± 0.1 ($n = 3$). Quinacrine produced no significant alteration in the current/voltage curve at potentials positive to E_K (about − 90 mV; Figure 4c). In the presence of quinacrine, UK 14304 produced a small outward current at potentials positive to E_K but no inward current was recorded negative to E_K (Figure 4c). A similar blockade of inward rectification was recorded in the presence of 4-BPB (30 μM, $n = 3$). Lower, and more selective (Okada *et al.*, 1989), concentrations of 4-BPB (3–10 μM) partially inhibited the basal inward rectification of the membrane ($n = 3$).

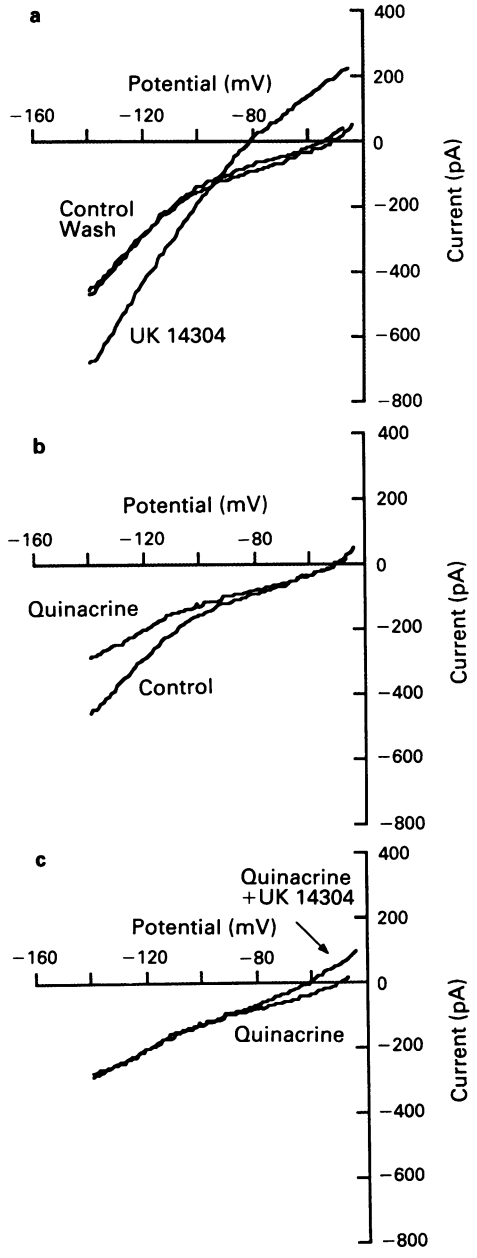

Figure 4 Effects of quinacrine on the voltage-current relationship. (a) The voltage-current curve shows marked inward rectification at potentials negative to E_K. UK 14304 (100 nM) produced a hyperpolarization associated with an increase in the membrane conductance. (b) In control physiological solution, quinacrine (10 μM) reduced the inward rectification at potentials negative of E_K with no effect on the voltage/current relationship at potentials positive of E_K. (c) In the presence of quinacrine the UK 14304-induced outward current recorded at potentials positive to E_K was greatly reduced and no inward current was recorded at potentials negative to E_K. All recordings obtained from the same neurone.

Discussion

The aim of the present study was to examine whether the receptor coupled opening of inwardly rectifying potassium current by activation of α_2-adrenoceptors in submucosal neurones was mediated by arachidonic acid or its metabolites generated by the action of phospholipase A_2. Quinacrine and 4-BPB greatly inhibited both the noradrenergic i.p.s.p. and the agonist-induced hyperpolarizations; these results initially suggested a possible involvement of the phospholipase A_2 pathway in signal transduction following α_2-adrenoceptor stimulation. However, we also found that quinacrine blocked a number of other ionic currents in these neurones, including the nicotinic current and currents underlying the directly evoked action potential. These actions of quinacrine probably account for the inhibition of spontaneous action potential firing that was observed in a number of cells when quinacrine was applied (e.g. Figure 1a,b). These results are in keeping with previous studies which have demonstrated that quinacrine blocks nicotinic currents (Adams & Feltz, 1980), fast transient outward potassium currents (Kehl, 1991), calcium currents (Mironov & Lux, 1992; Sargent *et al.*, 1992) and calcium and creep currents in isolated atrial myocytes (Bielfeld *et al.*, 1986; Yang & Vassalle, 1989). In the present study, quinacrine and 4-BPB also blocked the inward rectification present in the voltage/current curves recorded in control solution (Figure 4), in a manner analogous to the blockade of the inwardly rectifying potassium channels by rubidium or barium (Surprenant & North, 1988). Barium and rubidium inhibit somatostatin and α_2-adrenoceptor-activated potassium conductance increases in these neurones by this blockade of the inward rectification of the resting membrane (Surprenant & North, 1988). As has been described previously for barium (North & Surprenant, 1985), quinacrine and 4-BPB inhibited the outward current to UK 14304 recorded at potentials positive to E_K. It has not yet been established whether α_2-adrenoceptor activation shifts the current-voltage relation for the resting inward rectifier to more positive potentials or whether an additional conductance the pharmacology of which is identical to the inward rectifier present in these cells is activated (see Surprenant & North, 1988; Shen *et al.*, 1992). In any event, the most likely explanation for the actions of quinacrine and 4-BPB in inhibiting the somatostatin and UK 14304-induced hyperpolarization is a direct blockade of the inwardly rectifying potassium channels the activity of which is increased by these agonists. The inhibition by quinacrine and 4-BPB of the postsynaptic α_2-adrenoceptor response (the agonist-induced hyperpolarization as well as the adrenergic i.p.s.p.) were irreversible or only slowly reversible while the inhibition of the nicotinic e.p.s.p. was rapidly reversible. The inhibition of the e.p.s.p. is probably due to direct blockade of the nicotinic receptor-channel as has been described for the quinacrine-induced blockade of the endplate potential at frog neuromuscular junction

(Adams & Feltz, 1980). We have not examined possible mechanisms of action of quinacrine or 4-BPB in inhibiting the α_2-adrenoceptor response but because of its slow time course its action may involve more than direct blockade of the inward rectifying potassium channels. The present results, in addition to the previously mentioned studies, make it clear that neither quinacrine nor 4-BPB-mediated inhibition can be considered adequate criteria for involvement of the phospholipase A_2 pathway in a given cellular effect.

In the present study the more specific phospholipase A_2 inhibitor, cyclosporin A, or the inhibitors of arachidonic acid metabolism, ETYA and NDGA, had no effect on the response of submucosal neurones to α_2-adrenoceptor activation. In addition arachidonic acid itself did not mimic the UK 14304-induced membrane hyperpolarization of submucosal neurones. These results strongly indicate that in guinea-pig submucosal neurones the increase in the inwardly rectifying potassium current following the activation of α_2-adrenoceptors is not likely to be mediated by arachidonic acid or its eicosanoid metabolites produced through the stimulation of phospholipase A_2. Previous studies on submucosal neurones have failed to provide evidence for a role of protein kinase A, protein kinase C or nitric oxide in mediating the hyperpolarization to α_2-adrenoceptor or somatostatin receptor activation (Mihara *et al.*, 1987a; Surprenant & North, 1988; R.J.E. & A.S., unpublished observations). The present finding that the phospholipase A_2 pathway also is unlikely to play a role in transducing this response strengthens the conclusion that receptor-activated G-proteins modulate the activity of inwardly rectifying potassium channels directly.

This work was supported by U.S. Department of Health & Human service grant NS 25996.

References

ADAMS, P.R. & FELTZ, A. (1980). Quinacrine (mepacrine) action at frog end-plate. *J. Physiol.*, **306**, 261–281.

AXELROD, J., BURCH, R.M. & JELSEMA, C.L. (1988). Receptor-mediated activation of phospholipase A_2 via GTP-binding proteins: arachidonic acid and its metabolites as second messengers. *Trends Neurosci.*, **11**, 117–123.

BLACKWELL, G.J. & FLOWER, R.J. (1983). Inhibition of phospholipase. *Br. Med. Bull.*, **39**, 260–264.

BIELFELD, D.R., HADLEY, R.W., VASSILEV, P.M. & HUME, J.R. (1986). Membrane electrical properties of vesicular Na-Ca exchange inhibitors in single-atrial myocytes. *Circ. Res.*, **59**, 381–389.

BORNSTEIN, J.C., COSTA, M. & FURNESS, J.B. (1988). Intrinsic and extrinsic inhibitory synaptic inputs to submucous neurones of the guinea-pig small intestine. *J. Physiol.*, **398**, 371–390.

BUTTNER, N., SIEGELBAUM, S.A. & VOLTERRA, A. (1989). Direct modulation of *Aplysia* S-K+ channels by a 12-lipoxygenase metabolite of arachidonic acid. *Nature*, **342**, 553–555.

EL-ETR, M., MARIN, P., TENCE, M., DELUMEAU, J.-C., CORDIER, J., GLOWINSKI, J. & PREMONT, J. (1992). 2-Chloradenosine potentiates the al-adrenergic activation of phospholipase C through a mechanism involving arachidonic acid and glutamate in striatal astrocytes. *J. Neurosci.*, **12**, 1363–1369.

FAN, T.-P.D. & LEWIS, G.P. (1985). Mechanism of cyclosporin A-induced inhibition of prostacyclin synthesis by macrophages. *Prostaglandins*, **30**, 735–747.

GONZALES, R., SHERBOURNE, C.D., GOLDYNE, M.E. & LEVINE, J.D. (1991). Noradrenaline-induced prostaglandin production by sympathetic postganglionic neurons is mediated by α_2-adrenergic receptors. *J. Neurochem.*, **57**, 1145–1150.

HIRST, G.D.S., HOLMAN, M.E. & SPENCE, I. (1974). Two types of neurones in myenteric plexus of duodenum in the guinea-pig. *J. Physiol.*, **236**, 303–326.

JONES, S.B., HALENDA, S.P. & BYLUND, D. (1991). α_2-Adrenergic receptor stimulation of phospholipase A_2 and of adenylate cyclase in transfected chinese hamster ovary cells is mediated by different mechanisms. *Mol. Pharmacol.*, **39**, 239–245.

KEHL, S.J. (1991). Quinidine-induced inhibition of the fast transient outward K^+ current in rat melanotrophs. *Br. J. Pharmacol.*, **103**, 1807–1813.

KENNEDY, M.B. (1992). Second messengers and neuronal function. In *An Introduction to Molecular Neurobiology*. ed. Hall, Z.W. pp. 207–246. Sunderland, Massachusetts: Sinauer.

KURACHI, Y., ITO, H., SUGIMOTO, T., SHIMIZU, T., MIKI, I. & UI, M. (1989). Arachidonic acid metabolites as intracellular mediators of the G protein-gated cardiac K^+ channel. *Nature*, **337**, 555–557.

MIHARA, S., NORTH, R.A. & SUPRENANT, A. (1987a). Somatostatin increases an inwardly rectifying potassium conductance in guinea-pig submucous neurones. *J. Physiol.*, **390**, 335–356.

MIHARA, S., NISHI, S., NORTH, R.A. & SURPRENANT, A. (1987b). A non-adrenergic non-cholinergic slow inhibitory post-synaptic potential in neurones of the guinea-pig submucous plexus. *J. Physiol.*, **390**, 357–365.

MILLER, B., SARANTIS, M., TRAYNELIS, S.F. & ATTWELL, D. (1992). Potentiation of NMDA receptor currents by arachidonic acid. *Nature*, **355**, 722–725.

MIRONOV, S.L. & LUX, H.D. (1992). The selective action of quinacrine on high-threshold calcium channels in rat hippocampal cells. *Br. J. Pharmacol.*, **106**, 751–755.

NISHI, S. & NORTH, R.A. (1973). Intracellular recording from myenteric plexus of guinea-pig ileum. *J. Physiol.*, **231**, 471–491.

NIWA, Y., KANO, T., TANIGUCHI, S., MIYACHI, Y. & SAKANE, T. (1986). Effect of cyclosporin A on the membrane-associated events in human leukocytes with special reference to the similarity with dexamethasone. *Biochem. Pharmacol.*, **35**, 947–951.

NORTH, R.A. (1989). Drug receptors and the inhibition of nerve cells. *Br. J. Pharmacol.*, **18**, 13–28.

NORTH, R.A. & SURPRENANT, A. (1985). Inhibitory synaptic potentials resulting from α_2-adrenoceptor activation in guinea-pig submucous plexus neurones. *J. Physiol.*, **358**, 17–32.

OKADA, D., YAMAGISHI, S. & SUGIYAMA, H. (1989). Differential effects of phospholipase inhibitors in long-term potentiation in the rat hippocampal mossy fiber synapses and Schaffer/commissural synapses. *Neurosci. Lett.*, **100**, 141–146.

PIOMELLI, D. & GREENGARD, P. (1990). Lipoxygenase metabolites of arachidonic acid in neuronal transmembrane signalling. *Trends Pharmacol. Sci.*, **11**, 367–373.

PIOMELLI, D., VOLTERRA, A., DALE, N., SIEGELBAUM, S.A., KANDEL, E.R., SCHWARTZ, J.H. & BELLARDETTI, F. (1987). Lipoxygenase metabolites of arachidonic acid as second messengers for presynaptic inhibition of *Aplysia* sensory cells. *Nature*, **328**, 38–43.

PREMKUMAR, L.S., GAGE, P.W. & CHUNG, S.-H. (1990). Coupled potassium channels induced by arachidonic acid in cultured neurons. *Proc. R. Soc. B.*, **242**, 17–22.

SARGENT, C.A., VESTERQVIST, O., MCCULLOUGH, J.R., OGLETREE, M.L. & GROVER, G.J. (1992). Effect of phospholipase A_2 inhibitors quinacrine and 7,7-dimethyleicosadienoic acid in isolated globally ischemic rat hearts. *J. Pharmacol. Exp. Ther.*, **262**, 1161–1167.

SCHWEITZER, P., MADAMBA, S. & SIGGINS, G.R. (1990). Arachidonic acid metabolites as mediators of somatostatin induced increase of neuronal M-current. *Nature*, **346**, 464–467.

SHEN, K.-Z., NORTH, R.A. & SURPRENANT, A. (1992). Potassium channels opened by noradrenaline and other transmitters in excised membrane patches of guinea-pig submucosal neurones. *J. Physiol.*, **445**, 581–599.

SURPRENANT, A. (1984). Slow excitatory synaptic potentials recorded from neurones of guinea-pig submucosal plexus. *J. Physiol.*, **351**, 343–362.

SURPRENANT, A. & NORTH, R.A. (1988). Mechanism of synaptic inhibition by noradrenaline acting at α_2-adrenoceptors. *Proc. R. Soc. B.*, **234**, 85–114.

VOLTERRA, A. & SIEGELBAUM, S.A. (1989). Antagonistic modulation of S-K+ channel activity by cyclic AMP and arachidonic acid metabolites. Role for two G proteins. *Ann. N.Y. Acad. Sci.*, **559,** 219–239.

WALLACH, D.P. & BROWN, V.J.R. (1981). Studies on the arachidonic acid cascade-1. *Biochem. Pharmacol.*, **30,** 1315–1324.

YANG, L. & VASSALLE, M. (1989). Quinacrine decreases the slow inward current and force in guinea pig ventricular tissue. *Eur. J. Pharmacol.*, **170,** 261–263.

(Received January 26, 1993
Revised April 28, 1993
Accepted May 24, 1993)

Br. J. Pharmacol. (1993), **110**, 597–602

Monocrotaline pyrrole-induced changes in angiotensin-converting enzyme activity of cultured pulmonary artery endothelial cells

Cindy M. Hoorn & [1]Robert A. Roth

Department of Pharmacology and Toxicology, Michigan State University, East Lansing, Michigan 48824, U.S.A.

1 Changes in the structural and functional integrity of endothelium have been recognized as relatively early features of delayed and progressive pulmonary vascular injury caused by the pyrrolizidine alkaloid, monocrotaline (MCT). Although a number of investigators have evaluated angiotensin-converting enzyme (ACE) activity in the lungs of rats treated with MCT, the exact nature of changes in activity of this enzyme and the role they may play in MCT pneumotoxicity remain controversial.

2 We examined the direct effects of monocrotaline pyrrole (MCTP), a toxic metabolite of MCT, on cultured endothelial cell ACE activity. Post-confluent monolayers of porcine or bovine pulmonary artery endothelial cells (PECs or BECs, respectively) were treated with a single administration of MCTP at time 0; then they were examined for their ability to degrade the synthetic peptide, [^{3}H]-benzoyl-Phe-Ala-Pro.

3 In PECs, which are relatively insensitive to the direct cytolytic effects of MCTP, monolayer ACE activity was unchanged initially but gradually decreased within 4 days after treatment with a high concentration of MCTP (150 μM). This decrease was transient, and PEC monolayer ACE activity returned to the control value by 10 days post treatment.

4 BEC monolayer ACE activity was also unchanged initially but rapidly declined within 4 days after MCTP treatment and remained depressed throughout the post treatment period. BECs were quite sensitive to the cytolytic effects of MCTP and the decline in ACE activity occurred coincident with the decrease in monolayer cellularity and appearance of marked cytotoxicity.

5 We conclude that high concentrations of MCTP decrease endothelial ACE activity. The decline in ACE activity is delayed and the magnitude and duration of the decrease corresponds to the degree of MCTP-induced cytotoxicity. This suggests that altered endothelial ACE activity is unlikely to be a direct effect of MCTP on the enzyme but may reflect the delayed cell injury which results from exposure to this compound.

Keywords: Monocrotaline; monocrotaline pyrrole; angiotensin-converting enzyme; cultured endothelium; pulmonary hypertension; response to injury

Introduction

The pyrrolizidine alkaloid, monocrotaline (MCT), causes delayed and progressive pulmonary vascular injury in rats and other sensitive species (Schoental & Head, 1955; Valdivia *et al.*, 1967; Hayashi & Lalich, 1967; Peckham *et al.*, 1974), resulting in the development of pulmonary hypertension and right ventricular hypertrophy (Chesney *et al.*, 1974; Meyrick & Reid, 1979; Sugita *et al.*, 1983). The pulmonary vascular endothelium has been suggested as a likely cellular target for initial injury, and changes in endothelial structural and functional integrity have been noted relatively early in the course of MCT pneumotoxicity *in vivo* (Hilliker *et al.*, 1982; Bruner *et al.*, 1983; Reindel *et al.*, 1990). It has been suggested that persisent changes in endothelial cell function may play a role in the development and/or maintenance of MCT-induced pulmonary hypertension (Reindel *et al.*, 1990; Roth & Reindel, 1990; Reindel & Roth, 1991b).

The pulmonary vascular endothelium carries out a number of complex functions which are important in the maintenance of vascular homeostasis and in regulating the vascular response to circulating mediators (for a review of this subject, see Fajardo, 1989). One of these functions is the cleavage of circulating, inactive angiotensin I (AI) to the potent vasoconstrictor, angiotensin II (AII), by the action of the exopeptidase known as angiotensin-converting enzyme (ACE) (Yang *et al.*, 1970; Erdos, 1975). It has been suggested that pulmonary vascular disease might be associated with changes in pulmonary activity of this enzyme (Gillis & Catravas, 1982; Dobuler *et al.*, 1982; Catravas *et al.*, 1988).

A number of investigators have evaluated ACE in lungs of rats treated with MCT in an effort to correlate changes in enzyme activity with the development or progression of MCT-induced cardiopulmonary changes. The results of these studies have been disparate. Some investigators report that there is a decrease in lung ACE activity (Kay *et al.*, 1982; Keane *et al.*, 1982), whereas others contend that apparent changes in lung ACE activity are due to a dilution of this activity by the increased lung mass seen in this model (Huxtable *et al.*, 1978; LaFranconi & Hustable, 1983); transient increases in ACE activity have also been reported (Molteni *et al.*, 1984). From these results of work done *in vivo*, it is difficult to draw definitive conclusions about ACE activity in lung vasculature injured by MCT.

Monocrotaline pyrrole (MCTP) is a putative, toxic metabolite of MCT. Injection of a relatively low dose of chemically synthesized MCTP into rats results in a spectrum of pulmonary changes which are comparable to those produced by MCT, including changes in endothelial cells (Bruner *et al.*, 1983). MCTP has also been shown to be toxic to cultured bovine and porcine pulmonary artery endothelial cells (BECs and PECs, respectively) (Reindel & Roth, 1991; Reindel *et al.*, 1991). This cultured endothelial cell model makes it possible to investigate the direct effects of MCTP treatment on endothelial cell function. The purpose of this study was to determine whether MCTP affects ACE activity in cultured

[1] Author for correspondence.

endothelium and to characterize the development of any changes that occur.

Methods

Preparation of endothelial cells

Lines of PECs and BECs were derived from segments of pulmonary artery by modifications of the methods of Jaffe *et al.* (1987) and Booyse *et al.* (1975), as described by Reindel & Roth (1991). PECs and BECs exhibited characteristic cobblestone morphology in culture and were further characterized as described in Reindel *et al.* (1991).

BECs or PECs were maintained in Medium 199 (M199; GIBCO, Grand Island, NY, U.S.A.) containing 10% fetal bovine serum (FBS; Intergen, Purchase, NY, U.S.A.) and 1% penicillin (100 units ml^{-1})-streptomycin (100 $\mu g\ ml^{-1}$)-fungizone (0.25 $\mu g\ ml^{-1}$) (antibiotic-antimycotic; GIBCO) or Opti-MEM (GIBCO) containing 3% FBS and 1% antibiotic-antimycotic, respectively. Cells were passed by enzymatic dissociation with 0.025% trypsin-0.27 mM EDTA (GIBCO) at a ratio of 1:3 or 1:4. Cells used in these studies were between passages 4 and 10.

Preparation of MCTP

MCTP was prepared from MCT (Transworld Chemical, Washington, DC, U.S.A.) via an N-oxide intermediate by the method of Mattocks (1968). MCTP isolated from this synthesis procedure has Ehrlich activity (Mattocks & White, 1971) and a structure compatible with MCTP as determined by mass spectrometry and nuclear magnetic resonance (Bruner *et al.*, 1986). MCTP was dissolved in N,N-dimethylformamide (DMF; Sigma Chemical Co., St. Louis, MO, U.S.A.) at a concentration of 20 mg kg^{-1}, and all dilutions of MCTP were made with DMF. A 2.5 μl volume of MCTP solutions or DMF vehicle (0 μM MCTP) per millilitre of medium was used to achieve the nominal concentrations of MCTP (0, 1.5, 15 or 150 μM) used in the study.

Assay of angiotensin-converting enzyme activity

PECs and BECs were plated into 12-well tissue culture clusters (25 mm diameter) and allowed to form confluent monolayers. Monolayers were not used to assay ACE activity until at least 10 days after plating because ACE activity of cultured endothelial cells is not restored after dissociation and replating until cells have been maintained in a confluent state for this length of time (DelVecchio & Smith, 1981). Mature monolayers were treated with a single administration of MCTP (0, 1.5, 15 or 150 μM) on day 0. ACE activity of monolayers were analysed at 8 h and 2, 4 and 7 days (also at 10 days, for PEC monolayers) post treatment using the standard radioassay protocol provided by Ventrex Laboratories, Inc. (Portland, ME, U.S.A.). The assay involves cleavage of the synthetic peptide [^{3}H]-benzoyl-Phe-Ala-Pro by endothelial ACE to form [^{3}H]-benzoyl-phenylalanine and the dipeptide, alanyl-proline. The tritiated product, soluble in organic scintillant, was extracted, separated and counted in a liquid scintillation counter. At the times indicated post treatment, monolayers were washed thoroughly with ACE assay buffer (0.05 M HEPES, 0.1 M NaCl; pH 7.5, 37°C). At a time 0, 2 ml of buffered substrate ([^{3}H]-benzoyl-Phe-Ala-Pro: specific activity 20 Ci $mmol^{-1}$, diluted to 10^5 c.p.m. 100 μl^{-1} in assay buffer) were added to each well in a shaking water bath at 37°C. At 10 min intervals, 50 μl aliquots of the reaction mixture were removed to each of 2 test tubes containing 1 ml of 0.1 N HCl to stop the reaction; 1 ml of Ventrex scintillation cocktail No. 2 was added to each tube. The tubes were mixed for 30 s, then spun in a centrifuge for 3 min at 500 *g*. An aliquot (500 μl) of the upper counting phase was transferred to a 2 ml microvial (Ventrex) for measurement of radioactivity; 50 μl aliquots of the reaction buffer were also counted in aqueous scintillant to determine total c.p.m. per well. Monolayer ACE activity was determined in the presence or absence of the specific ACE inhibitor, captopril (10^{-6} M) to ensure that conversion of substrate was due to the action of ACE. In addition, wells without cells were used as a negative control. ACE activity was calculated by a simplified form of the integrated first-order rate equation as derived by Ryan (1988). A unit of ACE activity is defined as that quantity of enzyme required to hydrolyse substrate at an initial rate of 1% min^{-1} at 37°C.

Effects of MCTP on monolayer cellularity

After determination of ACE activity as described above, monolayers were washed three times with calcium- and magnesium-free Hank's balanced salt solution to remove non-adherent cells. Adherent cells were enzymatically removed from the plate surface with 0.025% trypsin-0.27 mM EDTA solution (GIBCO) and counted in a Coulter counter (Model ZM).

Statistical analysis

ACE activity data are presented as means of 5 (PECs) or 3 (BECs) separate experiments, each consisting of duplicate wells at each concentration of MCTP. The standard error of difference (Steel & Torrie, 1980) for each data set is presented. Data were analysed with a blocked analysis of variance (Crunch Statistical Package, Version 3.12; Crunch Software Corporation, Oakland, CA, U.S.A.). Individual comparisons between treatment groups (MCTP and DMF vehicle) were

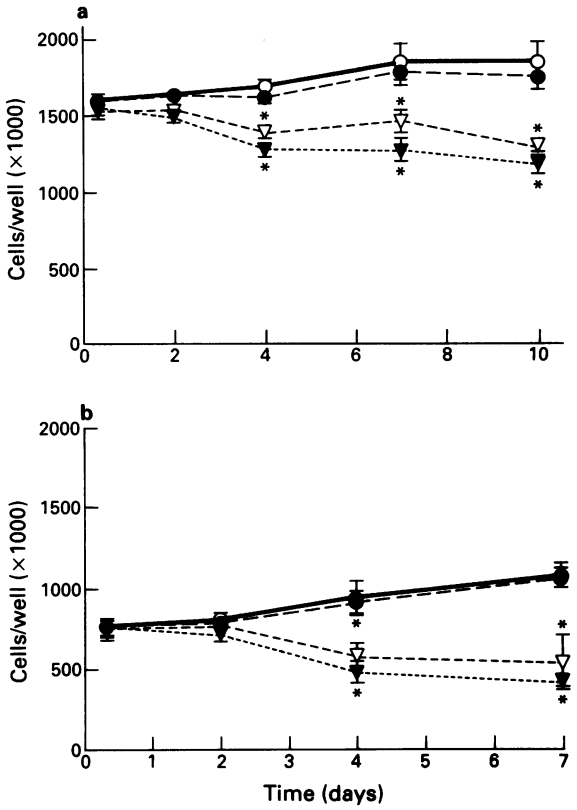

Figure 1 Cellularity of PEC (a) and BEC (b) monolayers exposed to a single administration of 1.5 (●), 15 (▽) or 150 (▼) μM monocrotaline pyrrole (MCTP) or N,-N-dimethylformamide (DMF) vehicle (○) on day 0. Values represent the means of replicate studies ($n = 5$ for PECs; $n = 3$ for BECs). *Significantly different from vehicle control ($P < 0.05$).

made by Tukey's omega test ($P<0.05$) (Steel & Torrie, 1980).

Cell numbers are presented as means ± s.e.mean. These data were analysed by a completely random analysis of variance, and individual comparisons were made by Tukey's omega test ($P<0.05$).

Results

Effects of MCTP on cellularity

The effects of MCTP on cellularity of PEC and BEC monolayers are shown in Figures 1a and b respectively. Cell monolayers were treated once with MCTP at zero time. Whereas PEC and BEC cell numbers continued to increase slightly with time in wells treated with vehicle or the lowest concentration of MCTP, they declined in monolayers treated with the higher doses of MCTP, beginning at day 4 post treatment. When examined by phase contrast microscopy, all monolayers appeared to remain intact and free of obvious gaps throughout the post treatment period. PECs and BECs treated with higher concentrations of MCTP (15 or 150 μM) demonstrated distinct morphological changes as monolayer cellularity decreased. These changes have been described previously (Reindel & Roth, 1991; Reindel *et al.*, 1991) and include cell enlargement, vacuole formation and nuclear changes in BECs. A milder enlargement with a shift toward a more spindle-like shape occurred in PECs.

Changes in ACE activity

Changes in ACE activity of mature monolayers of PECs and BECs after a single exposure to MCTP are shown in Figure 2. ACE activity of PEC monolayers (Figure 2a) treated with 150 μM MCTP decreased gradually, reaching a nadir at 4 days post treatment then returning to control levels by 10 days post treatment. BEC monolayers also showed a concentration-dependent decline in ACE activity with MCTP treatment, but the decrease was much more marked and persistent (Figure 2b). In monolayers treated with the highest concentration of MCTP, ACE activity was significantly decreased by 2 days post treatment, and after 4 days these monolayers demonstrated virtually no ACE activity. In BECs, the intermediate MCTP concentration also led to reduced ACE activity after day 2. In both PECs and BECs, cells treated with 1.5 μM MCTP exhibited levels of ACE activity similar to those seen in controls.

Cellular ACE activity

Cellular ACE activity after MCTP treatment is expressed in Figure 3 as a function of PEC and BEC number (i.e., units of activity per million cells). Although the total activities of vehicle-treated PEC and BEC monolayers were similar (see Figure 2), activities normalised to cell number were quite different. BECs (Figure 3b) had about twice the ACE activity per million cells than PECs (Figure 3a). The delayed, transient decrease in ACE activity of PECs treated with 150 μM MCTP was still evident, but cellular ACE activity returned to the control value by 7 days and was increased by 10 days

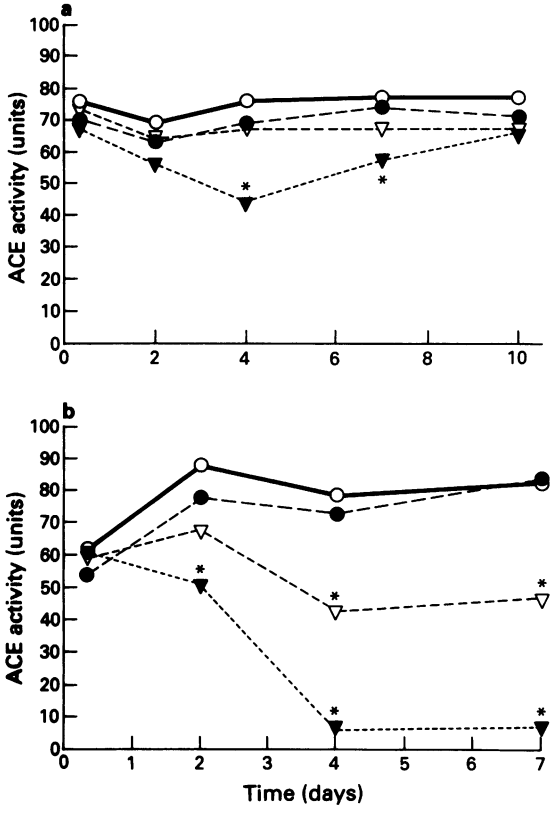

Figure 2 Angiotensin-converting enzyme (ACE) activity of monolayers of PECs (a) and BECs (b) exposed to a single administration of 1.5 (●), 15 (▽) or 150 (▼) μM monocrotaline pyrrole (MCTP) or N,N-dimethylformamide (DMF) vehicle (○) at time 0. One unit of ACE activity is defined as that quantity of enzyme required to hydrolyze substrate at an initial rate of 1% min^{-1} at 37°C. Values represent the means of replicate studies ($n = 5$ for PECs; $n = 3$ for BECs). Standard error of difference = 3.89 PECs; 7.55 BECs. *Significantly different from vehicle control ($P<0.05$).

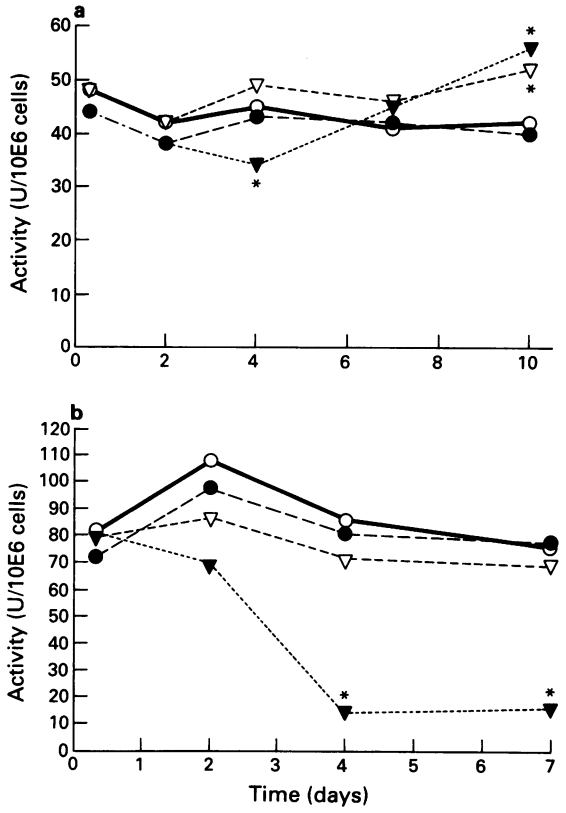

Figure 3 Angiotensin-converting enzyme (ACE) activity of mature monolayers of PECs (a) and BECs (b) expressed as a function of cell number. Cell monolayers were exposed to a single administration of 1.5 (●), 15 (▽) or 150 (▼) μM monocrotaline pyrrole (MCTP) or N,N-dimethylformamide (DMF) vehicle (○) at time 0. Values represent the means of replicate studies ($n = 5$ for PECs; $n = 3$ for BECs). Standard error of difference = 2.44 PECs; 9.58 BECs. *Significantly different from vehicle control ($P<0.05$).

post treatment. Cells treated with 15 μM MCTP showed no change in activity until day 10, at which time cellular ACE activity was elevated. In BECs, cellular ACE activity was significantly depressed by 4 days post treatment in cells treated with the highest concentration of MCTP. However, decreases in cellular ACE activity were not evident in BECs treated with 15 μM MCTP. PECs and BECs treated with 1.5 μM MCTP exhibited similar ACE activity to vehicle-treated controls.

Discussion

A number of conditions which result in pulmonary injury or alterations in pulmonary blood flow have been associated with changes in angiotensin-converting enzyme activity in lung or serum. A rapid, transient decrease in lung ACE and a corresponding increase in serum ACE as is seen following administration of α-naphthylthiourea (ANTU) or paraquat (Hollinger *et al.*, 1980a,b) may reflect direct damage to the vascular endothelium. In other cases, changes in ACE activity appear to be compensatory and occur coincident with or subsequent to the development of pulmonary hypertension (Keane *et al.*, 1982; Jederlinic *et al.*, 1988; Oparil *et al.*, 1988).

The latter scenario has been described for MCT pneumotoxicity in the rat. Kay and coworkers reported that MCT treatment results in vascular remodelling and consequent pulmonary hypertension by 10–14 days post treatment with an accompanying decrease in lung ACE activity per mg protein and decreased conversion of AI to AII beginning by day 10 (Kay *et al.*, 1982; Keane & Kay, 1984). Molteni *et al.* (1984) reported a transient increase in pulmonary ACE activity after 1 week of MCT treatment followed by a persistent decline in activity during weeks 2 to 6 of treatment. Kay and Keane maintained that the alterations in ACE activity seen with MCT treatment occur in response to the pulmonary hypertensive conditions and may be a protective mechanism to limit this physiological change (Kay *et al.*, 1982; Keane *et al.*, 1982). This view is held by Molteni and coworkers as well, but they further suggest that the transient increase in ACE activity which they find in their model precedes vascular remodelling and reflects endothelial injury and dysfunction (Molteni *et al.*, 1984).

In a separate study, Shale *et al.* (1986) found that lung ACE (reported as nmol min^{-1}/lung and nmol min^{-1} mg^{-1} protein) decreased when MCT was given in an oral dosing regimen which did not produce pulmonary hypertension or right ventricular hypertrophy. Although this supports the idea that ACE does not play a causative role in the development of these sequelae, it also suggests that the decrease in ACE activity seen with MCT treatment is not solely a response to increased pulmonary vascular pressure. Rather, it suggests an early, direct effect of MCT on the lung. The increased pulmonary tissue mass due to inflammation and hyperplasia after MCT treatment may in fact dilute what is really an unchanged endothelial ACE content at this stage in the injury. This conclusion is in agreement with the findings of Huxtable and co-workers, who maintain that decreases in lung ACE activity in MCT-treated animals can be attributed to dilution by an increased total lung mass (Huxtable *et al.*, 1978; LaFranconi & Huxtable, 1983).

Our objective in performing this study was to determine whether MCTP would directly alter ACE activity in an endothelial cell system *in vitro*. Although we found that MCTP does decrease endothelial ACE activity *in vitro*, our results raise a number of interesting points with respect to changes in ACE activity after cell injury. In both PECs and BECs, decreases in ACE activity did not occur immediately after administration of MCTP; rather, changes were delayed for several days. This suggests that the decrease in ACE activity was not due to a direct interaction of MCTP with the enzyme or to other changes which may occur at the cell surface at the time of treatment. MCTP is quite reactive and much of it probably binds to cells rapidly after administration *in vitro*. However, the inactivation of ACE does not appear to be an early or immediate change effected by MCTP, even at relatively high concentrations. Ryan & Catravas (1990) suggest that, in addition to enzyme dysfunction, changes in ACE activity may occur as a result of changes in the microenvironment of the enzyme. Some of the delayed, cytotoxic changes which occur as a consequence of exposure to hypoxia or MCTP treatment could result in subtle alterations of the endothelial cell surface which are incompatible with ACE function.

There are clear species differences in the response of pulmonary artery endothelial cells to treatment with MCTP (Reindel *et al.*, 1991). While BECs are quite sensitive to the cytolytic effects of MCTP, PECs appear to be relatively resistant. However, both cell types show distinct changes in morphology after MCTP treatment. The differences noted with respect to ACE activity of BEC and PEC monolayers after MCTP treatment are also pronounced, and these seem to parallel the morphological and cytotoxic changes. For example, the transient nature of the decrease in PECs corresponds with the decline in cell numbers, and the more dramatic and persistent fall in ACE activity in BECs reflects the more marked cytotoxic response of this cell type.

Recent work with ACE inhibitors and AII receptor antagonists suggests that AII may be important in the pathophysiology of the vascular response to injury (Zakheim *et al.*, 1975; Grotendorst *et al.*, 1982; Molteni *et al.*, 1985; Schweigerer *et al.*, 1987; Powell *et al.*, 1990; Clozel *et al.*, 1991). Bell & Madri (1990) propose that blockade of ACE activity may decrease local generation of AII and reduce vascular wall injury by enhancing wound closure, increasing the antithrombotic tendency of the area and decreasing the rate of smooth muscle cell infiltration. ACE activity declined substantially in our cells after treatment with MCTP only after there was evidence of cytotoxicity; changes in enzyme activity may have occurred in response to these alterations and might function to limit the local damage. In PECs, in which the cellular damage was less pronounced, the changes in ACE activity were also quite subtle and transient. These cells eventually had increased ACE activity on a cellular basis by 10 days post treatment, which may reflect more persistent alterations in the cells' response to injury.

It is important to point out that the most dramatic changes in ACE activity in both PECs and BECs occurred only at the highest concentrations of MCTP. Whether the pulmonary vascular endothelium experiences such an exposure *in vivo* after a pulmonary hypertension-producing dose of MCT or MCTP is open to question (Reindel *et al.*, 1990). Our results indicate clearly that direct inhibition of endothelial cell ACE does not happen at MCTP exposures that probably occur *in vivo*. It appears likely that changes in ACE activity seen *in vivo* occur indirectly from altered lung mass or through a response of the endothelium to injury (e.g., modified gene expression), altered vascular surface area and/or changes in blood flow or pressure.

In summary, ACE activity in pulmonary artery endothelium is altered after exposure to relatively high concentrations of MCTP *in vitro*, and this alteration is clearly not secondary to hypoxia, increased pressure, or other complicating haemodynamic factors that may be present *in vivo*. The decline in ACE activity is delayed, and the magnitude and duration of the decrease corresponds to the degree of MCTP-induced cytotoxicity. These changes apparently are not due to a direct action of MCTP on the enzyme but may occur as a response to the delayed cell injury which results from exposure to this compound.

The authors would like to thank Dr Gregory Fink of the Department of Pharmacology and Toxicology at Michigan State University

for his valuable assistance with the statistical analyses used in this study. We are also grateful to Dr Stephen Malcolm of the Department of Biological Sciences at Western Michigan University for his help in editing the manuscript. This work was supported by NIH Grant No. ES02581. C.M.H. was supported by NRSA No. ES05477; R.A.R. was supported in part by the Burroughs-Wellcome Toxicology Scholar Award.

References

BELL, L. & MADRI, J.A. (1990). Influence of the angiotensin system on endothelial and smooth muscle cell migration. *Am. J. Pathol.*, **137**, 7–12.

BOOYSE, F.M., SEDLAK, B.J. & RAFELSON, M.E. (1975). Culture of arterial endothelial cells: characterization and growth of bovine aortic cells. *Thromb. Diath. Haemorrh.*, **35**, 825–839.

BRUNER, L.H., CARPENTER, L.J., HAMLOW, P. & ROTH, R.A. (1986). Effect of a mixed function oxidase inducer and inhibitor on monocrotaline pyrrole pneumotoxicity. *Toxicol. Appl. Pharmacol.*, **85**, 416–427.

BRUNER, L.H., HILLIKER, K.S. & ROTH, R.A. (1983). Pulmonary hypertension and ECG changes from monocrotaline pyrrole in the rat. *Am. J. Physiol.*, **245**, H300–H306.

CATRAVAS, J.D., BURCH, S.E., SPURLOCK, B. & MILLS, L.R. (1988). Early effects of ionizing radiation on pulmonary endothelial angiotensin converting enzyme and 5'-nucleotidase, *in vivo*. *Toxicol. Appl. Pharmacol.*, **94**, 342–355.

CHESNEY, C.F., ALLEN, J.R. & HSU, I.C. (1974). Right ventricular hypertrophy in monocrotaline treated rats. *Exp. Mol. Pathol.*, **20**, 257–268.

CLOZEL, J.P., HESS, P., MICHAEL, C, SCHIETINGER, K. & BAUMGARTNER, H.R. (1991). Inhibition of converting enzyme and neointima formation after vascular injury in rabbits and guinea pigs. *Hypertension*, **18** (Suppl II), II-55–II-59.

DELVECCHIO, P.J. & SMITH, J.R. (1981). Expression of angiotensin-converting enzyme activity in cultured pulmonary artery endothelial cells. *J. Cell. Physiol.*, **108**, 337–345.

DOBULER, K.J., CATRAVAS, J.D. & GILLIS, C.N. (1982). Early detection of oxygen-induced lung injury in conscious rabbits: reduced activity of angiotensin converting enzyme and removal of 5-hydroxytryptamine. *Am. Rev. Respir. Dis.*, **126**, 534–539.

ERDOS, E.G. (1975). Angiotensin converting enzyme. *Circ. Res.*, **36**, 247–255.

FAJARDO, L.F. (1989). The complexity of endothelial cells: a review. *Am. J. Clin. Pathol,*. **92**, 241–250.

GILLIS, C.N. & CATRAVAS, J.D. (1982). Altered removal of vasoactive substances in the injured lung: detection of lung microvascular injury. *Ann. NY Acad. Sci.*, **384**, 458–474.

GROTENDORST, G.R., CHANG, T., SEPPA, H.E.J., KLEINMAN, H.K. & MARTIN, G.R. (1982). Platelet-derived growth factor is a chemoattractant for vascular smooth muscle cells. *J. Cell. Physiol.*, **113**, 261–266.

HAYASHI, Y. & LALICH, J.J. (1967). Renal and pulmonary alterations induced in rats by a single injection of monocrotaline. *Proc. Soc. Exp. Biol. Med.*, **124**, 392–396.

HILLIKER, K.S., BELL, T.G. & ROTH, R.A. (1982). Pneumotoxicity and thrombocytopenia after a single injection of monocrotaline. *Am. J. Physiol.*, **242**, H573–H579.

HOLLINGER, M.A., GIRI, S.N., PATWELL, S., ZUCKERMAN, J.E., GORIN, A. & PARSONS, G. (1980a). Effect of acute lung injury on angiotensin converting enzyme in serum, lung lavage, and effusate. *Am. Rev. Respir. Dis.*, **121**, 373–376.

HOLLINGER, M.A., PATWELL, S., ZUCKERMAN, J.E., GORIN, A.B., PARSONS, G. & GIRI, S.N. (1980b). Effect of paraquat on serum angiotensin converting enzyme. *Am. Rev. Respir. Dis.*, **121**, 795–798.

HUXTABLE, R., CIARAMITARO, D. & EISENSTEIN, D. (1978). The effect of a pyrrolizidine alkaloid, monocrotaline, and a pyrrole, dehydroretronecine, on the biochemical functions of the pulmonary endothelium. *Mol. Pharmacol.*, **14**, 1189–1203.

JAFFE, E.A. (1987). Cell biology of endothelial cells. *Hum. Pathol.*, **18**, 234–239.

JEDERLINIC, P., HILL, N.S., OU, L.C. & FANBURG, B.L. (1988). Lung angiotensin converting enzyme activity in rats with differing susceptibilities to chronic hypoxia. *Thorax*, **43**, 703–707.

KAY, J.M., KEANE, P.M., SUYAMA, K.L. & GAUTHIER, D. (1982). Angiotensin converting enzyme activity and evolution of pulmonary vascular disease in rats with monocrotaline pulmonary hypertension. *Thorax*, **37**, 88–96.

KEANE, P.M. & KAY, J.M. (1984). Lung angiotensin converting enzyme activity in monocrotaline pulmonary hypertension (letter). *Thorax*, **39**, 159–160.

KEANE, P.M., KAY, J.M., SUYAMA, K.L., GAUTHIER, D. & ANDREW, K. (1982). Lung angiotensin converting enzyme activity in rats with pulmonary hypertension. *Thorax*, **37**, 198–204.

LAFRANCONI, W.M. & HUXTABLE, R.J. (1983). Changes in angiotensin-converting enzyme activity in lungs damaged by the pyrrolizidine alkaloid monocrotaline. *Thorax*, **38**, 307–309.

MATTOCKS, A.R. (1968). Toxicity of pyrrolizidine alkaloids. *Nature, (Lond.)*, **217**, 723–728.

MATTOCKS, A.R. & WHITE, I.N.H. (1971). The conversion of pyrrolizidine alkaloids to N-oxides and to dihydropyrrolizidine derivatives by rat liver microsomes *in vitro*. *Chem. Biol. Interact.*, **3**, 383–396.

MEYRICK, B. & REID, L. (1979). Development of pulmonary arterial changes in rats fed Crotalaria spectabilis. *Am. J. Pathol.*, **94**, 37–50.

MOLTENI, A., WARD, W.F., TS'AO, C.H., PORT, C.D. & SOLLIDAY, N.H. (1984). Monocrotaline-induced pulmonary endothelial dysfunction in rats. *Proc. Soc. Exp. Biol. Med.*, **176**, 88–94.

MOLTENI, A., WARD, W.F., TS'AO, C.H., SOLLIDAY, N.H. & DUNNE, M. (1985). Monocrotaline-induced pulmonary fibrosis in rats: amelioration by captopril and penicillamine (42151). *Proc. Soc. Exp. Biol. Med.*, **180**, 112–120.

OPARIL, S., NARKATES, A.J., JACKSON, R. & ANN, H.S. (1988). Altered angiotensin-converting enzyme in lung and extrapulmonary tissues of hypoxia-adapted rats. *J. Appl. Physiol.*, **65**, 218–227.

PECKHAM, J.C., SANGSTER, L.T. & JONES, O.H. JR (1974). *Crotalaria spectabilis* poisoning in swine. *J. Am. Vet. Med. Assoc.*, **165**, 633–638.

POWELL, J.S., MULLER, R.K.M., ROUGE, M., KUHN, H., HEFTI, F. & BAUMGARTNER, H.R. (1990). The proliferative response to vascular injury is suppressed by angiotensin-converting enzyme inhibition. *J. Cardiovasc. Pharmacol.*, **16** (Suppl. 4), S42–S49.

REINDEL, J.F., GANEY, P.E., WAGNER, J.G., SLOCOMBE, R.F. & ROTH, R.A. (1990). Development of morphologic, hemodynamic, and biochemical changes in lungs of rats given monocrotaline pyrrole. *Toxicol. Appl. Pharmacol.*, **106**, 179–200.

REINDEL, J.F., HOORN, C.M., WAGNER, J.G. & ROTH, R.A. (1991). Comparison of the responses of bovine and porcine pulmonary artery endothelial cells to monocrotaline pyrrole. *Am. J. Physiol. (Lung Cell. Mol. Physiol. 5)*, **261**, L406–L414.

REINDEL, J.F. & ROTH, R.A. (1991). The effects of monocrotaline pyrrole on cultured pulmonary artery endothelial and smooth muscle cells. *Am. J. Pathol.*, **138**, 707–719.

ROTH, R.A. & REINDEL, J.F. (1990). Lung vascular injury from monocrotaline pyrrole, a putative hepatic metabolite. In *Biological Reactive Intermediates*, IV. ed. Witmer, C.M., Snyder, R.R. & Jollow, D. pp. 477–487. New York, NY: Plenum Press.

RYAN, J.W. (1988). Angiotensin-converting enzyme, dipeptidyl carboxypeptidase I, and its inhibitors. In *Methods in Enzymology*, Vol. 163. ed. diSabato, G. pp. 194–210. New York, NY: Academic Press.

RYAN, J.W. & CATRAVAS, J.D. (1990). Angiotensin converting enzyme as an indicator of pulmonary microvascular function. In *Focus on Pulmonary Pharmacology and Toxicology*. ed. Hollinger, M.A. pp. 183–210. Boca Raton, FL: CRC Press, Inc.

SCHOENTAL, R. & HEAD, M.A. (1955). Pathological changes in rats as a result of treatment with monocrotaline. *Br. J. Cancer*, **9**, 229–237.

SCHWEIGERER, L., NEUFELD, G,. FRIEDMAN, J., ABRAHAM, J.A., FIDDES, J.C. & GOSPODAROWICZ, D. (1987). Capillary endothelial cells express basic fibroblast growth factor, a mitogen that promotes their own growth. *Nature (Lond.)*, **325**, 257–259.

SHALE, D.J., WISEMAN, M.S. & COOKSON, W.O.C.M. (1986). Effect of monocrotaline ingestion on the distribution of protein and angiotensin converting enzyme activity in the rat lung. *Thorax*, **41**, 914–918.

STEEL, R.G.D. & TORRIE, J.H. (1980). *Principles and Procedures of Statistics: A Biometrical Approach*. p. 381. New York: McGraw-Hill, Inc.

SUGITA, T., HYERS, T.M., DAUBER, I.M., WAGNER, W.W., McMURTRY, I.F. & REEVES, J.T. (1983). Lung vessel leak precedes right ventricular hypertrophy in monocrotaline-treated rats. *J. Appl. Physiol.*, **54**, 371.

VALDIVIA, E., LALICH, J.J., HAYASHI, H. & SONNAD, J. (1967). Alterations in pulmonary alveoli after a single injection of monocrotaline. *Arch. Pathol.*, **84**, 64–76.

YANG, H.Y.T., ERDOS, E.G. & LEVIN, Y. (1970). A dipeptidyl carboxypeptidase that converts angiotensin I and inactivates bradykinin. *Biochem. Biophys. Acta*, **214**, 374–376.

ZAKHEIM, R.M., MATTIOLI, L., MOLTENI, A., MULLIS, K.B. & BARTLEY, J. (1975). Prevention of pulmonary vascular changes of chronic alveolar hypoxia by inhibition of angiotensin-1-converting enzyme in the rat. *Lab. Invest.*, **33**, 57–61.

(Received September 21, 1992
Revised April 19, 1993
Accepted May 24, 1993)

Br. J. Pharmacol. (1993), **110**, 603–608

Competitive inhibition by procaine of carbachol-induced stimulus-secretion coupling in rat pancreatic acini

Nobuhiro Ikei, *Julia Busik, *Yoshiaki Habara & [1,*†]Tomio Kanno

Otsuka Assay Laboratories, Diagnostic Division; Otsuka Pharmaceutical Co., Tokushima 771-01, Japan; *Laboratory of Cellular Metabolism, Department of Molecular Physiology, National Institute for Physiological Sciences, Okazaki 444, Japan and †Department of Physiology, Faculty of Veterinary Medicine, Hokkaido University, Sapporo 060, Japan

1 Procaine (0.03–10 mM) inhibited carbacbol (CCh)-induced amylase release from rat isolated pancreatic acini in a competitive manner. Kinetic analysis of the relation between CCh concentrations and the amount of amylase released in the presence of various procaine concentrations indicated that procaine caused competitive inhibition with the affinity constant (pA_2) value of 5.00 ± 0.08.

2 Receptor binding assay confirmed that procaine (0.01–10 mM) competitively inhibited [N-methyl-^{3}H]-scopolamine chloride ([^{3}H]-NMS) binding to its receptor with binding affinity (pK_i) of 4.63 ± 0.10.

3 Procaine transformed CCh-evoked $[Ca^{2+}]_i$ dynamics: the initial rise in $[Ca^{2+}]_i$ followed by a gradual decay during continuous stimulation with 3 μM CCh was transformed by 0.3 mM procaine to the oscillatory $[Ca^{2+}]_i$ dynamics, which resembled the response to 0.3 μM CCh in the absence of procaine. The initial phase of $[Ca^{2+}]_i$ oscillation corresponded to the initial phase of CCh-induced amylase release in isolated perfused acini.

4 Procaine (0.3–3 mM) did not inhibit the secretory response to cholecystokinin octapeptide (CCK-8) in isolated incubated acini. A higher concentration of procaine (10 mM) caused weak but significant inhibition of the response to only limited concentrations of CCK-8, 30 and 100 pM. Procaine lower than 10 mM was ineffective on [^{125}I]-BH-CCK-8 binding, although procaine (10 mM) caused weak but significant inhibition of the binding.

Keywords: Exocrine secretion; pancreas; procaine; amylase release; $[Ca^{2+}]_i$; carbachol; cholecystokinin (CCK)

Introduction

The term 'stimulus-secretion coupling' originally expressed the sequence of events set in motion by acetylcholine (ACh) which results in the release of catecholamines from the adrenal medulla. This term has since been applied to a variety of secretory systems including the exocrine pancreas (Kanno, 1972). A cardinal intracellular signal in the coupling is the increase in cytoplasmic concentration of calcium ion, $[Ca^{2+}]_i$. Information on $[Ca^{2+}]_i$ dynamics in various types of cells has become available following the development of the bioluminescent probe, aequorin (Cobbold, 1989 for reference) and of Ca^{2+}-sensitive fluorescent probes (Grynkiewicz *et al.*, 1985; Tsien *et al.*, 1985). Spatial and temporal $[Ca^{2+}]_i$ dynamics in stimulus-secretion coupling of rat pancreatic acinar cells have been monitored by a digital image analysing technique using Fura-2 (Kanno *et al.*, 1989; Habara & Kanno, 1991).

An approach to elucidate the cardinal role of $[Ca^{2+}]_i$ dynamics in the coupling may be pharmacological analysis with local anaesthetics, since it was reported that the local anaesthetic, tetracaine, reduced both acetylcholine-induced $^{45}Ca^{2+}$ uptake and catecholamine secretion in the chromaffin cells of the adrenal gland (Douglas & Kanno, 1967; Rubin *et al.*, 1967; Rubin, 1970). In the present study, recordings were made of $[Ca^{2+}]_i$ dynamics and of amylase release evoked by stimulation with carbachol (CCh) or the C-terminal octapeptide of cholecystokinin (CCK-8). In addition, binding assays for muscarinic or cholecystokinin (CCK) receptors were used to elucidate the mechanism of the inhibitory action of procaine on stimulus-secretion coupling, which is activated by binding of CCh or CCK-8 to respective receptors in the rat pancreatic acinar cell.

[1] Author for correspondence at Okazaki address.

Methods

Male rats (Sprague-Dawley) of 200–250 g b.w. were fasted overnight and used for the experiments.

Isolation and incubation of pancreatic acini

HEPES-buffered Ringer Solution (HR; pH 7.4) was used for preparing, incubating, and perfusing isolated acini. The composition of the standard solution was as follows (mM): NaCl 118, KCl 4.7, NaH_2PO_4 1.0, $MgCl_2$ 1.13, $CaCl_2$ 2.5, D-glucose 5.5, HEPES 10.0. The solution was supplemented with soybean trypsin inhibitor (0.1 mg ml^{-1}), bovine serum albumin (2 mg ml^{-1}), Eagle's minimal essential amino acids medium, and 2.0 mM L-glutamine. The solution was gassed with 100% O_2. Pancreatic acini were prepared by the method of Hootman *et al.* (1986) with slight modifications as reported previously (Habara *et al.*, 1986). The isolated acini were preincubated for 30 min prior to the experiments. The dose-response curves were obtained by stimulating acini with increasing concentrations of CCh or CCK-8 in the absence or the presence of various concentrations of procaine for 30 min at 37°C. After 30 min stimulation with secretagogue, 1 ml aliquot was taken from the flask and centrifuged at 12,000 × *g* for 20 s. The supernatant was kept on ice for amylase determination.

Perfusion

An aliquot of acinar suspension was loaded onto a Millipore filter held in a plastic holder (Imamura *et al.*, 1983) and was perfused at a rate of 1 ml HR min^{-1} with a Perista Minipump. Initial collections of perfusate were made at 20 min intervals for 60 min and subsequent collections at every 2 min thereafter. Acini were continuously stimulated with CCh in the absence or the presence of 0.3 mM procaine.

Receptor binding assay

The possible antagonism of procaine with muscarinic receptors was examined by use of a specific muscarinic antagonist, [^{3}H]-NMS (2.94 TBq mmol^{-1}), as described in previous reports (Hootman *et al.*, 1986; Habara *et al.*, 1986). Acini were incubated with 0.5 nM [^{3}H]-NMS in a total volume of 5 ml of HR in the presence of varying concentrations of atropine or procaine or carbachol for 60 min at 37°C. The binding reaction was then stopped by pouring the medium onto Whatman GF/A glass fibre filters in a vacuum filtering manifold and rinsed three times with 5 ml of chilled 0.9% NaCl. Filters were then placed in scintillation vials, extracted for several hours in a cocktail consisting of 10% Solvable in Atomlight, and counted for radioactivity with an Aloka liquid scintillation spectrometer. The ability of procaine to interact with pancreatic acinar CCK receptors was characterized by use of [^{125}I]-BH-CCK-8 (81.4 TBq mmol^{-1}) as described in a previous paper (Miller *et al.*, 1981). Acini were incubated with 13 pM [^{125}I]-BH-CCK-8 in a total volume of 1 ml of HR in the presence of various concentrations of CCK-8 and procaine for 30 min at 37°C. The binding reaction was then terminated as described in [^{3}H]-NMS experiments. Saline containing 0.2% BSA was used for rinsing solution. Radioactivity of the filters was measured with an Aloka gamma counter.

Fura-2-AM loading and digital image analysis

Fura-2-AM loading and measurement of fluorescence ratio with double excitation wavelengths were carried out as reported previously (Kanno *et al.*, 1989). In brief, acini were loaded with a final concentration of 10 μM Fura-2-AM for 40 min at 37°C with mild shaking. After pelleting and rinsing, acini resuspended in fresh HR were transferred onto a Cell-Tak coated non-fluorescent glass cover slide mounted in a Sykus-Moore chamber and allowed to attach to the cover slide for several minutes. The chamber was then installed on a stage of a modified inverted microscope (TMD-2, Nikon, Tokyo, Japan) equipped with an inlet of perfusing solution and an outlet by suction. At 5 s intervals, a pair of fluorescence images of the emissions (510 nm) formed by excitation at 340 and 380 nm were obtained with a silicon intensified target (SIT) camera and data processing was carried out with an Argus 50 (Hamamatsu Photonics, Hamamatsu, Japan) as described previously (Kanno *et al.*, 1989; Habara & Kanno, 1991). Regulation of excitation wavelengths was controlled with a personal computer which is on-line with a filter exchange unit and SIT camera.

Measurement of amylase release

Amylase activity present in incubation or perfusion media was determined by the modified method of Bernfeld using soluble Zulkowsy starch as substrate (Kanno, 1975). Amylase activity was expressed as a percentage of the total enzyme activity initially present in acinar cells.

Affinity constant analysis

Schild plots and standard analysis for linear regression were adopted for the analysis of antagonism in the functional studies (Arunlakshana & Schild, 1959). In the binding studies, the pK_i values are negative logarithms of K_i values which were derived from the IC_{50} value, according to the following equation (Cheng & Prusoff, 1973), $K_i = IC_{50}/(1 + [L]/K_d)$, where [L] and K_d are the concentration of [^{3}H]-NMS (= 0.5 nM) and dissociation constant (= 180 pM), respectively. The K_d value of [^{3}H]-NMS was employed from the results of Hootman *et al.* (1991), because the pancreatic acini were prepared according to their method.

Statistics

The results are presented as mean ± s.e.mean. Statistical analyses were carried out by Student's *t* test.

Materials

Procaine hydrochloride and HEPES (N-2-hydroxyethylpiperazine-*N'*-2-ethanesulphonic acid) were purchased from Nacalai Tesque (Kyoto, Japan); collagenase (purified; CLSPA) was from Worthington Biochemical (Freehold, NJ, U.S.A.); soybean trypsin inhibitor (type 1-S), bovine serum albumin (Fraction V) and carbamylcholine chloride (carbachol, CCh) were from Sigma Chemical (St. Louis, MO, U.S.A.); cholecystokinin octapeptide (CCK-8) was from Peptide Institute (Minoh, Japan); Eagle's minimal essential amino acids medium (50 × concentrate) was from Flow Laboratories (Irvine, Scotland); Cell-Tak from Collaborative Research (Bedford, MA, U.S.A.); soluble Zulkowsky starch was from Merck (Darmstadt, Germany); Fura-2-AM from Dojindo Laboratories (Kumamoto, Japan). [N-methyl-^{3}H]-scopolamine chloride ([^{3}H]-NMS), [^{125}I]-Bolton & Hunter-labelled cholecystokinin octapeptide (BH-CCK-8), Solvable, and Atomlight were from Du Pont/New England Nuclear (Boston, MA, U.S.A.). Millipore filter (type SM, pore size 5 μm) was from Nihon Millipore Kogyo (Yonezawa, Japan).

Results

Effect of procaine on amylase release induced by CCh or CCK-8 stimulation in isolated incubated acini

The effect of procaine on secretagogue-induced amylase release was examined in isolated incubated acini. Figure 1 illustrates the relation between the concentrations of CCh or CCK-8 and the level of amylase release in the absence or the presence of various concentrations of procaine. When the procaine concentration was increased stepwise from zero to 10 mM, the dose-response relation for CCh was shifted to the right in a concentration-dependent manner. The maximal responses to CCh in the presence of various procaine concentrations were not significantly different from the maximal response to CCh alone. In contrast to CCh, the CCK-8-

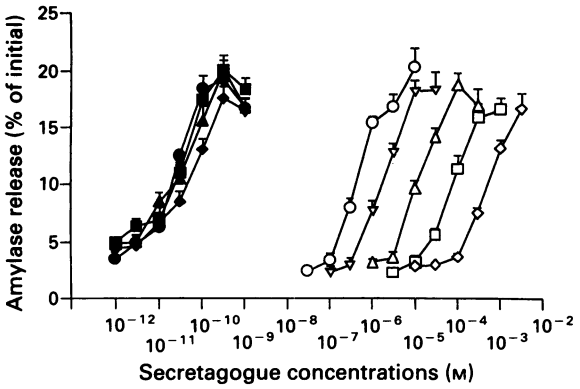

Figure 1 Dose-response relation of amylase release induced by carbachol (CCh) or cholecystokinin octapeptide (CCK-8) in the absence or the presence of procaine. CCh or CCK-8 at different concentrations as indicated was added to the incubation media and amylase released over 30 min was determined. Each value represents the mean ± s.e.mean obtained from 6 (CCh) or 5 (CCK-8) experiments. Each symbol represents the value obtained in following conditions: CCh without procaine (○); CCh with 0.03 mM procaine (▽); CCh with 0.3 mM procaine (△); CCh with 3 mM procaine (□); CCh with 10 mM procaine (◇); CCK-8 without procaine (●); CCK-8 with 0.3 mM procaine (▲); CCK-8 with 3 mM procaine (■); CCK-8 with 10 mM procaine (◆).

induced secretory response was not affected by procaine (0.3–3 mM), but amylase release induced by CCK-8 (30 pM or 100 pM) stimulation was significantly decreased by 10 mM procaine. The dose-response curve was slightly shifted downward in the presence of 10 mM procaine (Figure 1).

The inhibitory effect of procaine on CCh-stimulated amylase release was further analysed by a method of Arunlakshana & Schild (1959) in Figure 2. The pA_2 for procaine was 5.00 ± 0.08 ($n = 6$). The slope of the line in Figure 2 was 0.98 ± 0.04 ($n = 6$), which was not significantly different from unity. On the contrary, kinetic analysis of the inhibitory action of procaine on CCK-8 induced amylase release was also carried out, but it did not give us a definite conclusion as to the mode of inhibition.

Effect of procaine on [^{3}H]-NMS or [^{125}I]-BH-CCK-8 binding

A view that procaine may compete with CCh at the receptor site was further confirmed by examining the inhibitory effect of procaine on [^{3}H]-NMS binding to isolated incubated acini. The results presented in Figure 3 show that procaine competitively inhibited [^{3}H]-NMS binding. The pK_i value for procaine calculated from binding studies was 4.63 ± 0.10 ($n = 3$). This value was not significantly different from the pA_2 value ($P > 0.05$). The data depicted in the Figure 3 were calculated according to Hill equation and yielded a Hill coefficient of 1.07 ± 0.06 ($n = 3$) which was not significantly different from unity.

Procaine concentrations of less than 10 mM were ineffective on [^{125}I]-BH-CCK-8 binding, although 10 mM procaine caused weak but significant inhibition of the binding.

Effect of procaine on secretagogue-induced amylase release and temporal dynamics of [Ca^{2+}]$_i$ in acini

The effect of procaine on $[Ca^{2+}]_i$ dynamics induced by secretagogues at various concentrations was examined in isolated perfused acini and the corresponding effect on the time course of the secretory response was compared in the other preparations. In the absence of procaine, 0.3 μM CCh induced $[Ca^{2+}]_i$ oscillation (Figure 4b) and sustained amylase release (Figure 4a). Procaine (0.3 mM) inhibited $[Ca^{2+}]_i$ dynamics and secretory response induced by continuous stimulation with 0.3 μM CCh (Figure 4c and d).

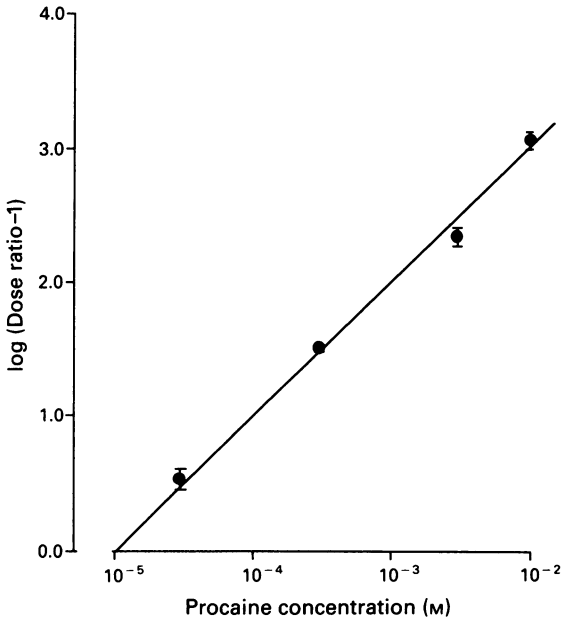

Figure 2 Schild plot of procaine inhibition of amylase release. Dose-ratios for procaine were calculated from Figure 1. Values are the mean ± s.e.mean of 6 experiments.

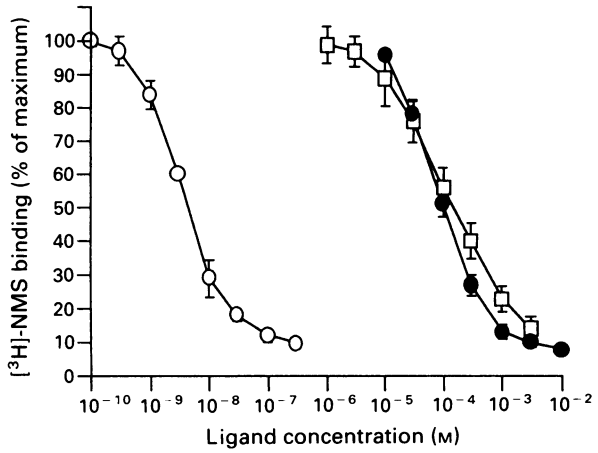

Figure 3 Effect of procaine on [N-methyl-^{3}H]-scopolamine ([^{3}H]-NMS) binding to acini. Acini were incubated in HR containing 0.5 nM [^{3}H]-NMS for 60 min at 37°C in the presence of varying concentrations of atropine (○), procaine (●), or carbachol (CCh) (□). The results were represented as a percentage of maximum. Values are the mean ± s.e.mean of 3 experiments in which duplicate measurements were carried out.

When isolated pancreatic acini were stimulated with 3 μM CCh, $[Ca^{2+}]_i$ reached peak levels, on which small oscillatory spikes were superimposed, within 2 min after the initiation of the stimulation, and gradually returned to the stable level (Figure 5b). This pattern of $[Ca^{2+}]_i$ was transformed by 0.3 mM procaine to $[Ca^{2+}]_i$ oscillation, which resembled the response to 0.3 μM CCh in the absence of procaine (Figure 5d). Amylase release was rapidly increased and reached the peak level within 4 min after the initiation of stimulation and was maintained at a stable level during stimulation (Figure 5a). The initial phase of $[Ca^{2+}]_i$ oscillation corresponded to the initial phase of amylase release (Figure 5c).

When the preparation was stimulated with 100 μM CCh, $[Ca^{2+}]_i$ rose rapidly to the peak level followed by sharp decay, and amylase release increased to an initial phase followed by second plateau phase. Addition of 0.3 mM procaine prolonged the CCh-evoked $[Ca^{2+}]_i$ increase and initial phase of amylase release.

Procaine (0.3 mM) was ineffective by itself on $[Ca^{2+}]_i$ dynamics and secretory response, and did not inhibit the responses to CCK-8 (10–1000 pM). However, procaine at a higher concentration, 10 mM, caused weak inhibition of the responses to CCK-8. When isolated pancreatic acini were stimulated with CCK-8 at a lower concentration, 10 or 30 pM, $[Ca^{2+}]_i$ increased with oscillatory spikes and amylase release was gradually increased followed by a plateau phase. Addition of 10 mM procaine attenuated the $[Ca^{2+}]_i$ oscillation, and decreased both the rate of rise in amylase release and the level of plateau phase. When the preparation was stimulated with CCK-8 at a higher concentration, 100 or 1000 pM, $[Ca^{2+}]_i$ rapidly reached the peak level followed by a rapid decay, and amylase release was increased rapidly to reach the initial transient phase followed by gradual decay. Addition of 10 mM procaine induced slight inhibition of the $[Ca^{2+}]_i$ increase and delayed the declining phase of the secretory response to CCK-8. Procaine alone (10 mM) was ineffective on both responses.

Discussion

Cholinoceptor

The present study carried out in the isolated incubated preparations of rat pancreatic acini gave us the following

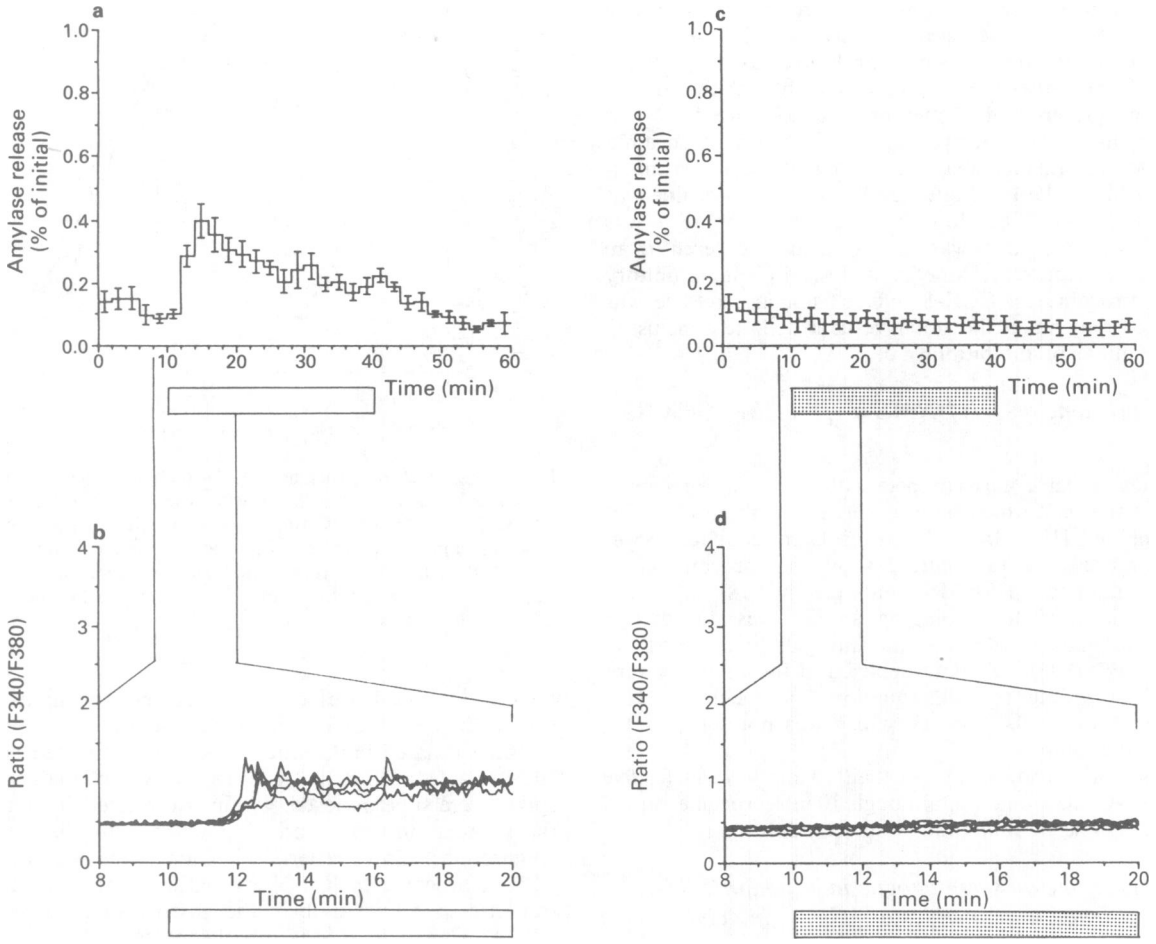

Figure 4 Effect of 0.3 mM procaine on 0.3 μM carbachol (CCh)-induced amylase release and $[Ca^{2+}]_i$ dynamics in isolated perfused rat pancreatic acini. (a) Time course of amylase release induced by continuous stimulation with 0.3 μM CCh. The values are the mean ± s.e.mean obtained from 5 experiments. Open horizontal bar indicates the period of CCh perfusion. (b) Shows the changes in $[Ca^{2+}]_i$ measured in four different regions of the same acinus, and is part of a continuous recording of $[Ca^{2+}]_i$ dynamics (indicated by the thin lines) at a high magnification of time scale in order to distinguish the $[Ca^{2+}]_i$ dynamics during the perfusion with CCh. $[Ca^{2+}]_i$ is expressed as fluorescence ratio (F340/F380). Similar records were obtained in three other experiments. (c) Time course of amylase released induced by 0.3 μM CCh in the presence of 0.3 mM procaine. The values are the mean ± s.e.mean obtained from 5 experiments. (d) Time course of $[Ca^{2+}]_i$ dynamics induced by perfusion with 0.3 μM CCh in the presence of 0.3 mM procaine. Stippled horizontal bar indicates the perfusion period with CCh and procaine. Similar records were obtained in three other experiments. Other explanations as in (b).

results; (1) the maximal responses to CCh in the presence of various procaine concentrations were not significantly different from the maximal response to CCh alone (Figure 1); (2) the dose-response relation for the CCh-induced amylase release showed a parallel shift to the right by increasing doses of procaine (Figure 1); and (3) the slope of the Schild plots thus obtained was not significantly different from unity (Figure 2). These results are compatible with a view that procaine is a competitive antagonist for the muscarinic receptor in pancreatic acinar cells. This view was further strengthened by the receptor binding experiments, indicating that the pK_i value was not significantly different from the pA_2. The coincidence of two values, pK_i and pA_2, indicates that the main mechanism of procaine inhibition on CCh-induced pancreatic secretion may certainly be at the muscarinic receptor level, and that the drug may cause little, if any, inhibitory effects on the Ca^{2+} entry step and on the steps between $[Ca^{2+}]_i$ increase and exocytosis. Furthermore, the Hill coefficient calculated from the results of the receptor binding experiments was 1.07 ± 0.06, which was not significantly different from unity, indicating that the mode of procaine binding with the receptor is single order. This conclusion coincides with that obtained by characterizing muscarinic cholinoceptors on rat pancreatic acini (Dehaye *et al.*, 1984).

The conclusion that procaine is a competitive muscarinic antagonist in the pancreatic acinar cells is compatible with previous findings obtained in other types of cells. Richelson *et al.* (1978) concluded by measuring CCh-induced guanosine 3':5'-cyclic monophosphate (cyclic GMP) formation in cultured neuroblastoma clone of mouse that local anaesthetics, including procaine, were apparently competitive inhibitors of CCh. Sharkey *et al.* (1988) concluded from a binding assay using [^{3}H]-quinuclidinyl benzilate that local anaesthetics including procaine could act as antimuscarinic agents in heart and brain of rat. Hisayama *et al.* (1989) suggested that local anaesthetics including procaine may interact directly with the muscarinic M_2 receptor sites in a competitive manner in smooth muscle of guinea-pig. In addition, the pK_i value of 4.63 is similar to the value obtained in heart ($pK_i = 5.5$) or medulla ($pK_i = 4.4$) or taenia caecum ($pK_i = 5.03$), all of which have M_2 type muscarinic receptors (Sharkey *et al.*, 1988; Hisayama *et al.*, 1989).

CCK receptor

The present experiments demonstrated that procaine at a much higher concentration (10 mM) caused weak but significant inhibition of [^{125}I]-BH-CCK-8 binding, whereas the

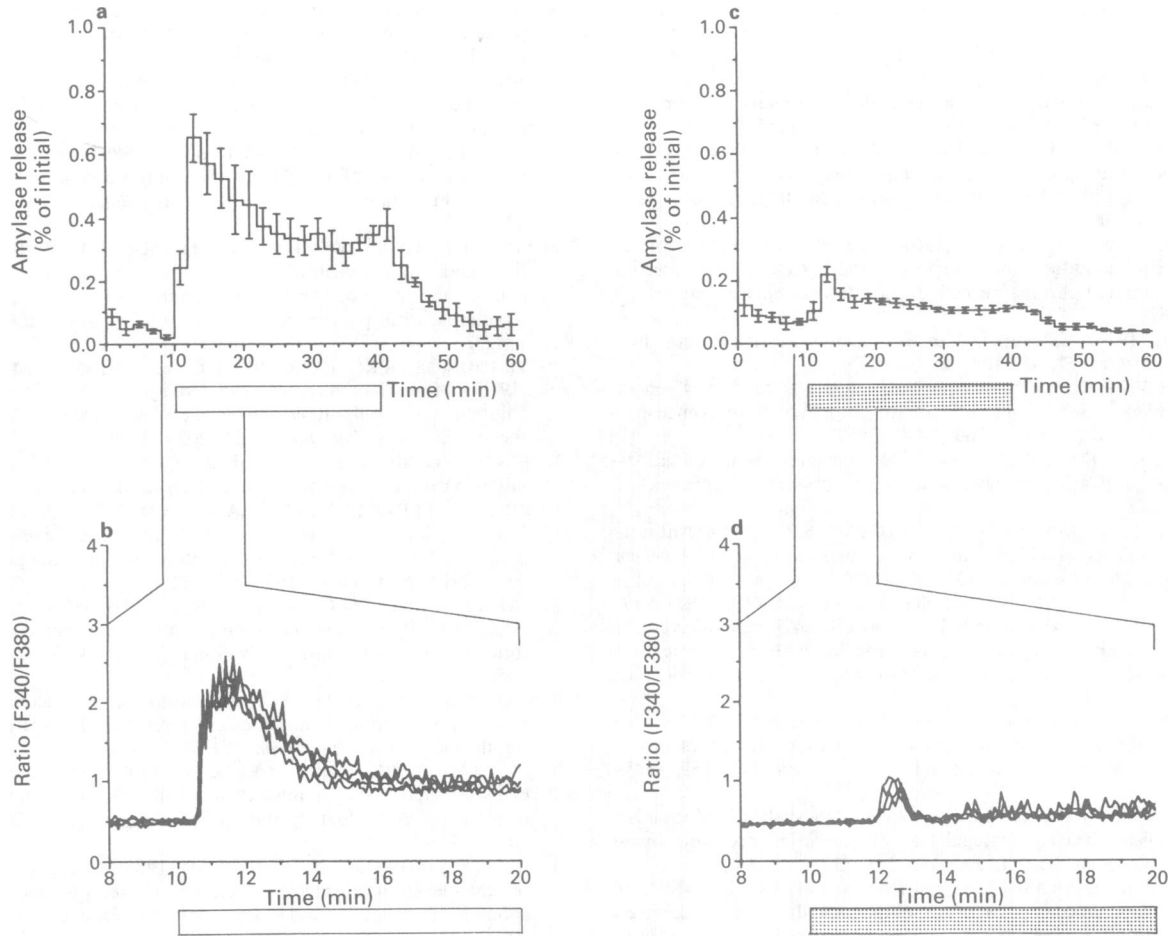

Figure 5 Effect of 0.3 mM procaine on 3 μM carbachol (CCh)-induced amylase release and $[Ca^{2+}]_i$ dynamics in perfused acini. Symbols and explanations except CCh concentration as in Figure 4.

drug at concentrations lower than 10 mM was without effect on binding. The weak inhibitory effect of procaine on CCK-8-induced secretory response was further confirmed in isolated incubated acini: procaine (0.3–3 mM) failed to inhibit the secretory response evoked by CCK-8 stimulation at various concentrations. A higher concentration of procaine (10 mM) caused a weak but significant inhibition of the response to only limited concentrations (30 and 100 pM) of CCK-8.

The weak inhibitory effect of procaine at a much higher concentration may not be entirely due to the disturbance by procaine at the binding sites of CCK-8 but may also be due to action on the steps between receptor binding and exocytosis. Precise mechanisms of the inhibitory action of procaine on CCK-8-induced responses remained to be elucidated, although the following views have been proposed in various preparations; (1) local anaesthetics including procaine may inhibit the Ca^{2+}-induced Ca^{2+} release in various preparations (Thorens & Endo, 1975; Endo, 1977; Yagi *et al.*, 1985) and (2) local anaesthetics including procaine may interfere with Na^+ channel, Ca^{2+} channel, various membrane-associated proteins including adenylate cyclase, guanylate cyclase, calmodulin-sensitive proteins, ion-pumping enzymes (Na^+/K^+-ATPase and Ca^{2+}/Mg^{2+}-ATPase), phospholipase A_2, and phospholipase C (for reference see Butterworth & Strichartz, 1990; Charlesworth *et al.*, 1992).

Correlation between $[Ca^{2+}]_i$ dynamics and time course of amylase release

A cardinal intracellular signal in stimulus-secretion coupling is the increase in $[Ca^{2+}]_i$, the dynamics of which may correlate with the time course of secretory responses to secretagogues. To analyse the correlation, however, it should be noted that the $[Ca^{2+}]_i$ dynamics were recorded from a single acinar cell, whereas the secretory response was the mean of a population of many cells. The mean of asynchronous oscillatory $[Ca^{2+}]_i$ dynamics induced by continuous stimulation with CCh at a low concentration (0.3 μM) in different acini may correspond to a gradual increase in secretory response followed by a plateau phase (Figure 4). The dual phase of $[Ca^{2+}]_i$ dynamics, an initial rapid rise followed by gradual decay, caused by continuous stimulation with CCh at a higher concentration (3 μM) apparently resembled the dual phase of the time course of the secretory response (Figure 5). The pattern of $[Ca^{2+}]_i$ dynamics caused by stimulation with 3 μM CCh in the absence of procaine was transformed to the pattern caused by stimulation with 0.3 μM CCh in the solution containing 0.3 mM procaine. These results again support the view that the $[Ca^{2+}]_i$ dynamics correlated with the secretory response, and that procaine inhibits the muscarinic receptor and, in turn, decreases the CCh-induced Ca^{2+} entry.

References

ARUNLAKSHANA, O. & SCHILD, H.O. (1959). Some quantitative uses of drug antagonists. *Br. J. Pharmacol. Chemother.*, **14**, 48–58.

BUTTERWORTH, J.F. & STRICHARTZ, G.R. (1990). Molecular mechanisms of local anesthesia: a review. *Anesthesiology*, **72**, 711–734.

CHARLESWORTH, P., JACOBSON, I., POCOCK, G. & RICHARDS, C.D. (1992). The mechanism by which procaine inhibits catecholamine secretion from bovine chromaffin cells. *Br. J. Pharmacol.*, **106**, 802–812.

CHENG, Y.C. & PRUSOFF, W.H. (1973). Relationship between the inhibition constant (K_i) and the concentration of inhibitor which causes 50 per cent inhibition (I_{50}) of an enzymatic reaction. *Biochem. Pharmacol.*, **22,** 3099–3108.

COBBOLD, P.H. (1989). Oscillatory calcium signals in hormone-stimulated cells. *News Physiol. Sci.*, **4,** 211–215.

DEHAYE, J., WINAND, J., POLOCZEK, P. & CHRISTOPHE, J. (1984). Characterization of muscarinic cholinergic receptors on rat pancreatic acini by N-[^{3}H]methylscopolamine binding. *J. Biol. Chem.*, **259,** 294–300.

DOUGLAS, W.W. & KANNO, T. (1967). The effect of amethocaine on acetylcholine-induced depolarization and catecholamine secretion in the adrenal chromaffin cell. *Br. J. Pharmacol. Chemother.*, **30,** 612–619.

ENDO, M. (1977). Calcium release from the sarcoplasmic reticulum. *Physiol. Rev.*, **57,** 71–108.

GRYNKIEWICZ, G., POENIE, M. & TSIEN, R.Y. (1985). A new generation of Ca^{2+} indicators with greatly improved fluorescence properties. *J. Biol. Chem.*, **260,** 3440–3450.

HABARA, Y. & KANNO, T. (1991). Dose-dependency in spatial dynamics of $[Ca^{2+}]_c$ in pancreatic acinar cells. *Cell Calcium*, **12,** 533–542.

HABARA, Y., WILLIAMS, J.A. & HOOTMAN, S.R. (1986). Antimuscarinic effects of chloroquine in rat pancreatic acini. *Biochem. Biophys. Res. Commun.*, **137,** 664–669.

HISAYAMA, T., TAKAYANAGI, I., KUMAGAI, N. & KUBO, H. (1989). Interaction of 8-(N,N-diethylamino)octyl 3,4,5-trimethoxybenzoate hydrochloride, ryanodine and procaine with muscarinic cholinergic M_2 receptor sites in smooth muscle. *J. Pharmacol. Exp. Ther.*, **249,** 646–651.

HOOTMAN, S.R., BROWN, M.E., WILLIAMS, J.A. & LOGSDON, C.D. (1986). Regulation of muscarinic acetylcholine receptors in cultured guinea pig pancreatic acini. *Am. J. Physiol.*, **251,** G75–G83.

HOOTMAN, S.R., VALLES, S.M. & KOVALCIK, S.A. (1991). Mechanism of agonist-induced downregulation of muscarinic receptors in rat pancreatic acini. *Am. J. Physiol.*, **261,** G128–G135.

IMAMURA, K., WAKASUGI, H., SHINOZAKI, H. & IBAYASHI, H. (1983). Dynamic analysis of secretagogue-induced amylase secretion from rat pancreatic acini studied by perifusion system. *Jpn. J. Physiol.*, **33,** 687–698.

KANNO, T. (1972). Calcium-dependent amylase release and electrophysiological measurements in cells of the pancreas. *J. Physiol.*, **226,** 353–371.

KANNO, T. (1975). The electrogenic sodium pump in the hyperpolarization and secretory effects of pancreozymin in the pancreatic acinar cell. *J. Physiol.*, **245,** 599–616.

KANNO, T., SAITO, T. & YAMASHITA, T. (1989). Spatial and temporal oscillation of $[Ca^{2+}]_i$ during continuous stimulation with CCK-8 in isolated rat pancreatic acini. *Biomed. Res.*, **10,** 475–478.

MILLER, L.J., ROSENZWEIG, S.A. & JAMIESON, J.D. (1981). Preparation and characterization of a probe for the cholecystokinin octapeptide receptor, N$^{\alpha}$(^{125}I-desaminotyrosyl)CCK-8, and its interactions with pancreatic acini. *J. Biol. Chem.*, **256,** 12417–12423.

RICHELSON, E., PRENDERGAST, F.G. & DIVINETZ-ROMERO, S. (1978). Muscarinic receptor-mediated cyclic GMP formation by cultured nerve cells–ionic dependence and effects of local anesthetics. *Biochem. Pharmacol.*, **27,** 2039–2048.

RUBIN, R.P. (1970). The role of calcium in the release of neurotransmitter substances and hormones. *Pharmacol. Rev.*, **22,** 389–428.

RUBIN, R.P., FEINSTEIN, M.B., JAANUS, S.D. & PAIMRE, M. (1967). Inhibition of catecholamine secretion and calcium exchange in perfused cat adrenal glands by tetracaine and magnesium. *J. Pharmacol. Exp. Ther.*, **155,** 463–471.

SHARKEY, J., RITZ, M.C., SCHENDEN, J.A., HANSON, R.C. & KUHAR, M.J. (1988). Cocaine inhibits muscarinic cholinergic receptors in heart and brain. *J. Pharmacol. Exp. Ther.*, **246,** 1048–1052.

THORENS, S. & ENDO, M. (1975). Calcium-induced calcium release and 'depolarization'-induced calcium release: their physiological significance. *Proc. Jpn. Acad.*, **51,** 473–478.

TSIEN, R.Y., RINK, T.J. & POENIE, M. (1985). Measurement of cytosolic free Ca^{2+} in individual small cells using fluorescence microscopy with dual excitation wavelengths. *Cell Calcium*, **6,** 145–157.

YAGI, S., MATSUMURA, N. & ENDO, M. (1985). Effects of inhibitors of calcium-induced calcium release on receptor-mediated responses of smooth muscles and platelets. *Proc. Jpn. Acad.*, **61,** 399–402.

(Received October 16, 1992
Revised May 13, 1993
Accepted May 25, 1993)

Br. J. Pharmacol. (1993), **110**, 609–612

Effect of capsazepine on the release of calcitonin gene-related peptide-like immunoreactivity (CGRP-LI) induced by low pH, capsaicin and potassium in rat soleus muscle

Paolo Santicioli, *Elena Del Bianco, *Michela Figini, †Stuart Bevan & [1]Carlo Alberto Maggi

Pharmacology Department, A Menarini Pharmaceuticals, Via Sette Santi 3, 50131, Florence, Italy; *Dept. of Internal Medicine, University of Florence, Florence, Italy and †Sandoz Institute for Medical Research, 5 Gower Place, London

1 We have determined the effect of the competitive antagonist capsazepine at the capsaicin receptor on the release of calcitonin gene-related peptide-like immunoreactivity (CGRP-LI) from rat isolated soleus muscle induced by capsaicin (1 μM), by superfusion with low pH medium (pH 5) or by KCl (80 mM).

2 Each one of the three stimuli tested produced a marked CGRP-LI release. Total evoked release (fmol g^{-1}) was 482 ± 69, 169 ± 20 and 253 ± 43 for capsaicin, low pH medium and KCl, respectively.

3 Prior application of capsaicin (10 μM for 30 min followed by 30 min of washout) to produce capsaicin desensitization *in vitro* abolished CGRP-LI release induced by the three stimuli.

4 Capsazepine (1–100 μM, 45 min preincubation) inhibited the evoked CGRP-LI release. Capsaicin-induced release was significantly inhibited by 77, 92 and 96% with 10, 30 and 100 μM capsazepine, respectively. Low pH-induced release was inhibited by 78, 84, 88 and 93% with 3, 10, 30 and 100 μM capsazepine, respectively. KCl-induced release was significantly inhibited by 55 and 93% with 30 and 100 μM (but not with 10 μM) capsazepine, respectively.

5 These findings demonstrate that capsazepine prevents low pH- and capsaicin-induced CGRP-LI release from rat soleus muscle at concentrations which do not affect the release evoked by KCl. These findings imply a relationship between the action of low pH and activation of the capsaicin receptor. At high concentrations, capsazepine produces a nonspecific inhibitory effect on CGRP-LI release from peripheral endings of the capsaicin-sensitive primary afferent neurone.

Keywords: Calcitonin gene-related peptide (CGRP); protons; rat soleus muscle; capsaicin-sensitive primary afferents; capsazepine

Introduction

Capsaicin-sensitive primary afferent neurones are known to exert an 'efferent' function by releasing sensory neuropeptides, tachykinins and calcitonin gene-related peptide (CGRP), from their peripheral endings. Pronounced chemosensitivity is a distinguishing feature of the capsaicin-sensitive primary afferents: peripheral release of sensory neuropeptides is evoked by a number of chemical stimuli, including mediators or inflammation (bradykinin, 5-hydroxytryptamine etc.) and conditions (elevated extracellular K^+ and H^+ concentrations) which are commonly encountered during inflammation/tissue damage (Maggi, 1991a for review).

In recent years, much information has been gained on the mechanisms through which capsaicin and related molecules act on primary afferent neurones (Maggi *et al.*, 1991b; Bevan & Szolcsanyi, 1991 for reviews). The selective action of capsaicin is mediated through the stimulation of a specific 'vanilloid' receptor, identified by the use of resiniferatoxin, an ultrapotent capsaicin analogue (Szallasi & Blumberg, 1990). Stimulation of the capsaicin or 'vanilloid' receptor opens a novel type of cation channel leading to calcium and sodium entry into the sensory neurones (Bevan & Szolcsanyi, 1991). In peripheral terminals of capsaicin-sensitive afferents, the increased cation conductance is believed to underlie the capsaicin-induced depolarization and generation of afferent impulses, whilst calcium entry is the trigger for the concomitant local secretion of sensory neuropeptides (Maggi, 1991b).

Determination of the mechanism of action of capsaicin on primary afferent neurones has been facilitated by the development of pharmacological tools which selectively block capsaicin action on primary afferent neurones. Bevan *et al.* (1991, 1992a) developed the benzazepine derivative, capsazepine, as the first example of a competitive receptor antagonist for the vanilloid receptor. Capsazepine has been shown to antagonize selectively capsaicin action at both central and peripheral endings of primary afferent neurones (Urban & Dray, 1991; Bevan *et al.*, 1992a; Belvisi *et al.*, 1992; Maggi *et al.*, 1993) and the nature of the antagonism is compatible with competitive interaction at the capsaicin receptor. The selectivity of capsazepine for the vanilloid receptor makes it an extremely useful tool to investigate the possibility that an endogenous ligand exists for this receptor. Another tool which, at certain concentrations, acts as a selective capsaicin antagonist is the dye, ruthenium red (Amann & Maggi, 1991, for review). In contrast to capsazepine, ruthenium red does not bind to the vanilloid receptor and its action is characterized by noncompetitive antagonism of capsaicin-induced primary afferent stimulation (Bevan *et al.*, 1992a; Maggi *et al.*, 1993). Although the precise mechanism of action of ruthenium red is unclear, there is evidence that it prevents the opening of the cation channel coupled to the vanilloid receptor (Dray *et al.*, 1990; Amann & Maggi, 1991 for review). According to this model, ruthenium red not only prevents the action of capsaicin on sensory neurones, but also blocks the action of other stimuli which share with the vanilloid receptor the same cation channel for sensory neurone stimulation. A notable case for this is the action of protons (low pH media) which activate the efferent function of capsaicin-sensitive afferent neurones in a ruthenium red-sensitive manner (Geppetti *et al.*, 1991; Del Bianco *et al.*, 1991; Santicioli *et al.*, 1992a). Patch clamp studies on membranes of primary afferents have demonstrated that capsaicin and protons open the same cation channel (Bevan *et al.*, 1993).

[1] Author for correspondence.

In a recent study we demonstrated that application of low pH medium produced release of CGRP-LI of sensory origin from the rat soleus muscle and that release evoked by low pH medium or capsaicin is selectively reduced by ruthenium red, the release evoked by KCl being unaffected (Santicioli *et al.*, 1992a). In the present study we aimed to investigate the effect of capsazepine on CGRP-LI release induced by these three stimuli from rat soleus muscle. Preliminary results of this study were presented at a Meeting of the British Pharmacological Society (Santicioli *et al.*, 1992b).

Methods

Male albino Wistar rats (Charles River, Italy) weighing 250–300 g were anaesthetized with urethane (1.2 g kg^{-1}, i.p.). The soleus muscle was excised from both legs and the animals killed with an excess dose of the anaesthetic. The muscles were placed in oxygenated (96% O_2, 4% CO_2, pH 7.4) Krebs solution of the following composition (mM): NaCl 119, $NaHCO_3$ 25, KH_2PO_4 1.2, $MgSO_4$ 1.5, KCl 4.7, $CaCl_2$ 2.5 and glucose 11. In each experiment, the soleus muscles were excised from the legs of 2 rats: tissues were sliced (thickness 0.4 mm) with a MacIlwain tissue chopper, the chopped muscles pooled and divided (150–250 mg each) into 4 thermostated (37°C) 1 ml perspex chambers and superfused at rate of 0.4 ml min^{-1} with oxygenated Krebs solution containing 0.1% (w/v) bovine serum albumin (BSA) and 10 μM thiorphan. All values in the text and figures are mean ± s.e.mean of replicates of different experiments.

Thiorphan was added to inhibit endopeptidase 24.11, minimize CGRP-degradation and enhance CGRP-LI recovery in superfusates (Katayama *et al.*, 1991; Davies *et al.*, 1992). For experiments aiming to assess the effect of low pH solutions, phosphate buffer solutions at pH 7.4 and 5 were prepared and used as described in previous studies (Geppetti *et al.*, 1991; Del Bianco *et al.*, 1991; Santicioli *et al.*, 1992a). The soleus muscle was placed in phosphate buffered physiological salt solution at pH 7.4 after excision and during equilibration. In these experiments, the phosphate buffer solutions were gassed with 100% O_2.

After a 45 min stabilization period, 5 min fractions were collected into polypropylene tubes containing acetic acid (final concentration 2 N). In some experiments, in order to induce a long lasting blockade of primary afferents, capsaicin (10 μM) was left in contact with the tissue for 30 min and then washed out for 30 min before sample collection and application of low pH medium. Controls were run in the presence of capsaicin vehicle (0.001% ethanol).

To study the effect of capsazepine on CGRP-LI release evoked by the various stimuli, the samples were incubated with the drug for 45 min before application of the stimuli. At the end of the experiment the samples from each chamber were collected and weighed.

The fractions were freeze-dried, reconstituted with the assay buffer (0.1 M phosphate buffer at pH 7.4 containing 0.9% NaCl, 0.01% NaN_3 and 0.1% bovine serum albumin (BSA)) and their CGRP-LI content was determined by radioimmunoassay (RIA), as described previously (Geppetti *et al.*, 1991; Del Bianco *et al.*, 1991; Santicioli *et al.*, 1992a).

Drugs used were: capsaicin and thiorphan (Sigma). Capsazepine was synthesized at the Sandoz Institute for Medical Research.

In each experiment the total evoked release (TER) of CGRP-LI produced by the various stimuli above the basal values was calculated. Statistical analysis was performed by means of two-tailed Student's *t* test for paired and unpaired data, or by analysis of variance, when applicable.

Results

Application of capsaicin (1 μM), high potassium medium (80 mM) or superfusion with low pH medium (pH 5) produced a clearcut increase in CGRP-LI outflow (Figure 1). TER (fmol g^{-1} wet wt) produced by these three stimuli was 482 ± 69, 169 ± 20 and 253 ± 43 for capsaicin, low pH medium and KCl, respectively.

Prior application of capsaicin totally prevented CGRP-LI outflow induced by a subsequent application of capsaicin, pH 5 buffer solution or KCl ($n = 4–6$ for each agonist, Figure 1, open columns).

Capsazepine (1–100 μM) did not produce CGRP-LI release on its own. In the presence of capsazepine, the CGRP-LI release evoked by the three stimuli was depressed in a concentration-dependent manner, but the concentrations of the drug which inhibited the evoked release were different for the three agonsits (Figure 2). In particular, the capsaicin-evoked CGRP-LI release was inhibited by 10 μM capsazepine and abolished at higher concentrations. The CGRP-LI release evoked by low pH medium was significantly inhibited by 3 μM capsazepine and further depressed and abolished by

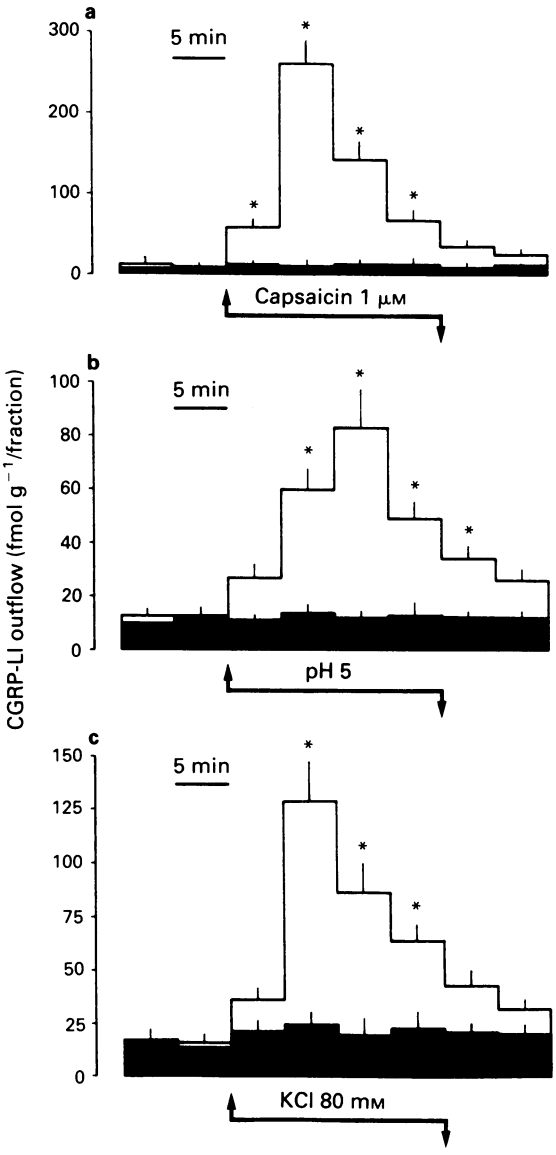

Figure 1 Calcitonin gene-related peptide-like immunoreactivity (CGRP-LI) release evoked by capsaicin (1 μM, a), superfusion with low pH medium (pH 5, b) or KCl (80 mM, c) from the rat isolated soleus muscle, in control (open columns) or capsaicin-pretreated (10 μM for 30, 30 min, before, solid columns) preparation. In each panel, the horizontal bars indicate the period of application of the various stimuli. Each value is mean ± s.e.mean of 4–16 replicates. Significantly different from basal values: $*P < 0.05$.

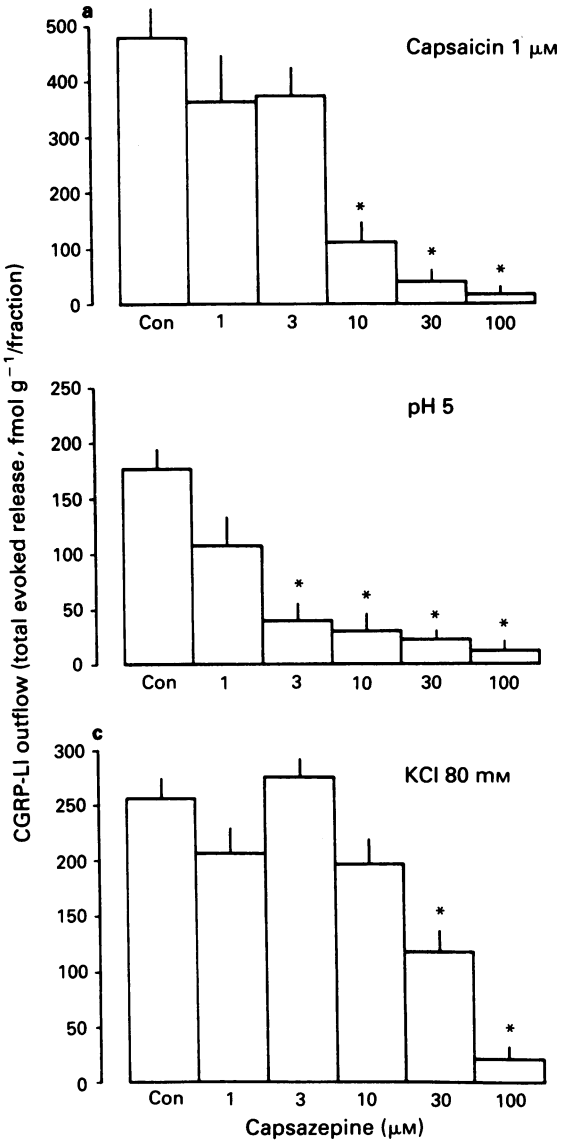

Figure 2 Effect of capsazepine (1–100 μM) on calcitonin gene-related peptide-like immunoreactivity (CGRP-LI) release induced by capsaicin (1 μM) (a), low pH medium (pH 5), (b) or KCl (80 mM) (c) from rat soleus muscle. Con = control. Each value is mean ± s.e. mean of 4–8 replicates. Significantly different from controls: $*P<0.05$.

higher concentrations. The KCl-induced release was only reduced at 30 μM and was abolished at 100 μM capsazepine.

Discussion

The rat soleus muscle receives a CGRP-containing, capsaicin-sensitive afferent innervation. In skeletal muscle, another source of CGRP exists, the peripheral terminals of somatic motorneurones (Yamamoto & Tohyama, 1989, for review). Capsaicin pretreatment, at a dose regimen which completely depletes CGRP-LI in e.g. the rat urinary bladder, only partially reduces (50–60%) CGRP-LI levels of the soleus muscle (Santicioli *et al.*, 1992a), which is consistent with dual CGRP innervation. On the other hand the available evidence indicates that only the 'sensory' source of neuronal CGRP is released from skeletal muscle by depolarizing media (Sakaguchi *et al.*, 1991). In agreement with this notion, CGRP-LI release evoked by KCl was totally prevented by *in vitro* application of high capsaicin concentrations (capsaicin desensitization). Therefore, peripheral endings of primary afferent neurones are the only source of releasable CGRP-LI in our preparation.

The main finding of this study is that the competitive vanilloid receptor antagonist, capsazepine, not only prevents the capsaicin-evoked CGRP-LI outflow, but also significantly inhibits that induced by low pH. Up to 10 μM, the action of capsazepine is, in some way, selective, because no inhibition of KCl-induced CGRP-LI release was observed. At higher concentrations (30–100 μM) capsazepine possesses a non-specific inhibitory action on the neurosecretory process, as indicated by inhibition of the response to KCl. Capsazepine is a competitive antagonist of the vanilloid receptor (Bevan *et al.*, 1992a) and its failure to antagonize the capsaicin- (1 μM) induced CGRP-LI release at concentrations below 10 μM is likely to be due to the competitive nature of interaction. The magnitude of response to low pH is smaller than that to capsaicin and this may explain the greater efficacy of capsazepine. In preliminary experiments (data not shown) we attempted to use lower capsaicin concentrations but the evoked CGRP-LI release was too variable for pharmacological analysis of the inhibitory effect of capsazepine.

A major finding of this study is that capsazepine antagonized CGRP-LI release evoked by low pH medium at a concentration of 3 μM while the response to KCl, which is quantitatively comparable to that evoked by low pH, was only inhibited at 30 μM capsazepine. While this work was in progress, Franco-Cereceda & Lundberg (1992) showed that CGRP-LI release induced by low pH (pH 5) or lactic acid (5 mM) from guinea-pig isolated, perfused heart was inhibited by 10 μM capsazepine. In a subsequent study, Lou & Lundberg (1992) showed that acid-induced nasal irritation and bronchoconstriction in guinea-pigs and CGRP-LI release from guinea-pig perfused lung was inhibited by capsazepine. Our findings in rat soleus agree with the reports of Franco-Cereceda & Lundberg (1992) and Lou & Lundberg (1992) in that capsazepine inhibits release of sensory neuropeptides induced by low pH at concentrations which do not affect afferent stimulation by other stimuli.

These findings are difficult to reconcile with the data presented by Bevan *et al.* (1992b) showing that neither the amplitude of the proton-activated current, nor the acid-induced $^{86}Rb^+$ efflux from dorsal root ganglion (DRG) neurones in culture or acid-induced depolarization of rat vagal nerve fibres are affected by capsazepine at concentrations, that are fully effective in blocking the corresponding responses activated by capsaicin. Likewise, peripheral nociceptor activation by low pH medium in a rat tail-spinal cord preparation is unaffected by capsazepine at concentrations which block the response to capsaicin (Dray *et al.*, 1992). On this basis, the hypothesis that occupancy of the vanilloid receptor by capsazepine might interfere with stimulation of the coupled cation channel by protons seems untenable.

Our findings and those of Franco-Cereceda & Lundberg (1992) and Lou & Lundberg (1992) have a common point in that the interaction of capsazepine with the effect of low pH has been investigated at the level of peptide release from peripheral endings of capsaicin-sensitive primary afferent neurones.

On this basis it would be premature to draw a parallel between the proton-activated cation current on DRG neurone membranes (Bevan *et al.*, 1992b; 1993) and the low pH-induced neuropeptide release from peripheral endings of primary afferent neurones. In particular, the possibility cannot be excluded that, when applying low pH media to peripheral tissues, a mediator is generated from one or more of the multiple cell types which are present which, in turn, may act on primary afferents. In other words, the action of low pH on sensory neuropeptide release in the periphery could have been stimulated by the generation of some intermediate factor(s) rather than by a direct action of protons on sensory nerve terminals. This implies that if such a factor(s) exists, it could be an endogenous ligand for the vanilloid receptor, and thus account for blockade of the response to low pH media

by both capsazepine (Franco-Cereceda & Lundberg, 1992; Lou & Lundberg, 1992 and present findings) and ruthenium red (Geppetti *et al.*, 1991; Del Bianco *et al.*, 1991; Santicioli *et al.*, 1992a). On the other hand, although KCl-induced CGRP-LI release was not affected by capsazepine at concentrations that inhibit the effect of low pH, the possibility cannot be entirely ruled out that the neurosecretory process is not-specifically inhibited by capsazepine. In particular, there is evidence that KCl-evoked CGRP-LI release from peripheral endings of primary afferent neurones in rats involves the activation of ω-conotoxin-sensitive calcium channels (Maggi & Giuliani, 1991) which may be a target for the nonspecific effect of capsazepine on evoked CGRP-LI release. The present findings indicate that at concentrations of 30 μM or higher, capsazepine exerts a generalized depressant action on evoked peptide release and therefore caution against an uncontrolled use of this compound as a selective capsaicin receptor antagonist.

References

AMANN, R. & MAGGI, C.A. (1991). Ruthenium red as a capsaicin antagonist. *Life Sci.*, **49**, 849–856.

BELVISI, M., MIURA, M., STRETTON, D. & BARNES, P.J. (1992). Capsazepine as a selective antagonist of capsaicin-induced activation of C-fibres in guinea-pig bronchi. *Eur. J. Pharmacol.*, **215**, 341–344.

BEVAN, S., FORBES, C.A. & WINTER, J. (1993). Protons and capsaicin activate the same ion channel in rat isolated dorsal root ganglion neurons. *J. Physiol.*, **459**, 401P.

BEVAN, S.J., HOTHI, S., HUGHES, G., JAMES, I.F., RANG, H.P., SHAH, K., WALPOLE, C.S.J. & YEATS, J.C. (1992a). Capsazepine: a competitive antagonist of the sensory neuron excitant capsaicin. *Br. J. Pharmacol.*, **107**, 544–552.

BEVAN, S.J., RANG, H.P. & SHAH, K. (1992b). Capsazepine does not block the proton-induced activation of rat sensory neurones. *Br. J. Pharmacol.*, **107**, 235P.

BEVAN, S.J., JAMES, I.F., RANG, H.P., SHAH, K. & YEATS, J.C. (1991). The development of a capsaicin antagonist for the sensory neurone excitant, capsaicin. *Br. J. Pharmacol.*, **102**, 77P.

BEVAN, S. & SZOLCSANYI, J. (1991). Sensory neuron-specific actions of capsaicin: mechanisms and applications. *Trends Pharmacol. Sci.*, **11**, 330–333.

DAVIES, D., MEDEIROS, M.S., KEEN, J., TURNER, A.J. & HAYNES, L.W. (1992). Endopeptidase 24.11 cleaves a chemotactic factor from α-CGRP. *Biochem. Pharmacol.*, **43**, 1753–1756.

DEL BIANCO, E., SANTICIOLI, P., TRAMONTANA, M., MAGGI, C.A., CECCONI, R. & GEPPETTI, P. (1991). Different pathways by which extracellular Ca^{2+} promotes CGRP release from central terminals of capsaicin-sensitive afferent of guinea-pigs: effect of capsaicin, high K+ and low pH media. *Brain Res.*, **566**, 46–53.

DRAY, A., FORBES, C.A. & BURGESS, G.M. (1990). Ruthenium red blocks the capsaicin-induced increase in intracellular calcium and activation of membrane currents in sensory neurones, as well as the activation of peripheral nociceptors in vitro. *Neurosci. Lett.*, **110**, 52–59.

DRAY, A., PATEL, I., NAEEM, S., RUEFF, A. & URBAN, L. (1992). Studies with capsazepine on peripheral nociceptor activation by capsaicin and low pH: evidence for a dual effect of capsaicin. *Br. J. Pharmacol.*, **107**, 236P.

FRANCO-CERECEDA, A. & LUNDBERG, J.M. (1992). Capsazepine inhibits low pH- and lactic acid-evoked release of CGRP from sensory nerves in guinea-pig heart. *Eur. J. Pharmacol.*, **221**, 183–184.

GEPPETTI, P., DEL BIANCO, E., PATACCHINI, R., SANTICIOLI, P., MAGGI, C.A. & TRAMONTANA, M. (1991). Low pH-induced release of CGRP from capsaicin-sensitive sensory nerves: mechanism of action and biological response. *Neuroscience*, **41**, 295–301.

KATAYAMA, M., NADEL, J.A., BUNNETT, N.W., DI MARIA, G.U., HAXHIU, M. & BORSON, D.B. (1991). Catabolism of CGRP and substance P by neutral endopeptidase. *Peptides*, **12**, 563–567.

LOU, Y.P. & LUNDBERG, J.M. (1992). Inhibition of low pH evoked activation of airway sensory nerves by capsazepine, a novel capsaicin receptor antagonist. *Biochem. Biophys. Res. Commun.*, **189**, 537–544.

MAGGI, C.A. (1991a). The pharmacology of the efferent function of sensory nerves. *J. Autonom. Pharmacol.*, **11**, 173–208.

MAGGI, C.A. (1991b). Capsaicin and primary afferent neurons: from basic science to human therapy? *J. Autonom. Nerv. System*, **33**, 1–14.

MAGGI, C.A., BEVAN, S., WALPOLE, C.S.J., RANG, H.P. & GIULIANI, S. (1993). A comparison of capsazepine and ruthenium red as capsaicin antagonists in the rat isolated urinary bladder and vas deferens. *Br. J. Pharmacol.*, **108**, 801–805.

MAGGI, C.A. & GIULIANI, S. (1991). The neurotransmitter role of CGRP in the rat and guinea-pig ureter: effect of a CGRP antagonist and species-related differences in the action of ω-conotoxin on CGRP release from primary afferents. *Neuroscience*, **43**, 261–268.

SAKAGUCHI, M., INAISHI, Y., KASHIHARA, Y. & KUNO, M. (1991). Release of CGRP from nerve terminals in rat skeletal muscle. *J. Physiol.*, **434**, 257–270.

SANTICIOLI, P., DEL BIANCO, E., GEPPETTI, P. & MAGGI, C.A. (1992a). Release of CGRP-like immunoreactivity from rat isolated soleus muscle by low pH, capsaicin and potassium. *Neurosci. Lett.*, **143**, 19–22.

SANTICIOLI, P., DEL BIANCO, E., GIACHETTI, A. & MAGGI, C.A. (1992b). Capsazepine inhibits low-pH and capsaicin-induced release of CGRP from rat soleus muscle. *Br. J. Pharmacol.*, **107**, 464P.

SZALLASI, A. & BLUMBERG, P.M. (1990). Specific binding of resiniferatoxin: an ultrapotent capsaicin analog by dorsal root ganglion membranes. *Brain Res.*, **524**, 106–111.

URBAN, L. & DRAY, A. (1991). Capsazepine, a novel capsaicin antagonist, selectivity antagonises the effects of capsaicin in the mouse spinal cord in vitro. *Neurosci. Lett.*, **134**, 9–11.

YAMAMOTO, A.I. & TOHYAMA, M. (1989). CGRP in the nervous tissue. *Prog. Neurobiol.*, **33**, 335–386.

(Received March 19, 1993
Revised May 13, 1993
Accepted May 27, 1993)

Br. J. Pharmacol. (1993), **110**, 613-618

Comparison of the anti-inflammatory properties of formoterol, salbutamol and salmeterol in guinea-pig skin and lung

[1]C.J. Whelan, M. Johnson & C.J. Vardey

Department of Cardiovascular and Respiratory Pharmacology, Glaxo Group Research Ltd., Park Road, Ware, Herts. SG12 0DP

1 We have compared some anti-inflammatory properties of formoterol, salbutamol and salmeterol in guinea-pig skin and lung.

2 Intradermal formoterol (1×10^{-10} to 1×10^{-8} mol/site), salbutamol (1×10^{-8} and 1×10^{-7} mol/site) and salmeterol (1×10^{-8} and 1×10^{-7} mol/site) inhibited bradykinin-induced plasma protein extravasation (PPE) in guinea-pig skin. A maximally effective dose of formoterol (1×10^{-9} mol/site) and salbutamol (1×10^{-8} mol/site) inhibited PPE in guinea-pig skin for 2-4 h and 1-2 h respectively, whereas salmeterol (1×10^{-8} mol/site) was effective for >6 h.

3 Inhaled formoterol (nebuliser concentration 0.1 to 100 $\mu g\ ml^{-1}$) inhibited histamine-induced plasma protein extravasation (PPE) in guinea-pig lung, with significant inhibition being observed at 10 and 100 $\mu g\ ml^{-1}$. Formoterol (100 $\mu g\ ml^{-1}$) inhibited PPE in guinea-pig lung for 2-4 h, a duration of action intermediate between that previously obtained for salbutamol (1 h) and salmeterol (>6 h).

4 Formoterol, like salbutamol, had no effect on neutrophil accumulation or granulocyte-dependent PPE (zymosan-induced) in guinea-pig skin. Formoterol inhibited neutrophil accumulation (lipopolysaccharide-induced) in guinea-pig lung but at doses greater than those required to inhibit granulocyte-independent PPE (histamine-induced). In contrast, salmeterol inhibited neutrophil accumulation and granulocyte-dependent PPE in guinea-pig skin and inhibited neutrophil accumulation in guinea-pig lung at doses which inhibit granulocyte-independent PPE.

5 Inhaled formoterol (nebuliser concentration 100 $\mu g\ ml^{-1}$) and salmeterol (100 $\mu g\ ml^{-1}$) both inhibited PAF-induced eosinophil accumulation in guinea-pig lung. However, unlike salmeterol, this effect of formoterol was observed only at suprabronchodilator doses.

6 We conclude that to inhibit neutrophil accumulation, at doses which inhibit granulocyte-independent PPE, agonists acting at β-adrenoceptors on vascular endothelium require a duration of action greater than that of salbutamol and formoterol. However, we speculate that the mechanism of inhibition of eosinophil accumulation in guinea-pig lung by β_2-adrenoceptor agonists may involve an action on β_2-adrenoceptors on a cell type other than the endothelial cell.

Keywords: Formoterol; salbutamol; salmeterol; β_2-adrenoceptor agonists; vascular permeability; neutrophil; eosinophil; skin; lung

Introduction

We have previously shown that the long-acting β_2-adrenoceptor agonist, salmeterol, inhibited zymosan- and lipopolysaccharide- induced neutrophil accumulation in guinea-pig skin and lung respectively, at doses which produce a sustained inhibition of histamine-induced increased vascular permeability (Whelan & Johnson, 1992). The same dose-range of salmeterol also inhibited platelet activating factor (PAF)-induced eosinophil accumulation in guinea-pig lung (Whelan & Johnson, 1992). In contrast, the short-acting β_2-adrenoceptor agonist, salbutamol, inhibited histamine-induced plasma protein extravasation (PPE), but had little or no effect on neutrophil or eosinophil accumulation (Whelan & Johnson, 1992).

Formoterol is another β_2-adrenoceptor agonist which produces prolonged bronchodilatation in man (Faulds *et al.*, 1991). It has recently been reported to produce long-lasting inhibition of PPE (Erjefalt & Persson, 1991) and inhibition of antigen-induced eosinophil accumulation in guinea-pigs (Sugiyama *et al.*, 1992). Furthermore, like salmeterol (Twentyman *et al.*, 1990; Dahl, 1991), formoterol has been shown to inhibit allergen-induced late-phase responses in man (Gronneberg & Zetterstrom, 1992; Palmqvist *et al.*, 1992), data which are consistent with the concept that long-acting β_2-adrenoceptor agonists may have acute anti-inflammatory activity *in vivo* (Johnson *et al.*, 1992). However, *in vitro* and *in vivo* studies have shown that the duration of action of formoterol is intermediate between that of salmeterol and salbutamol (Nials *et al.*, 1990).

The objective of the present study was to extend our earlier observations (Whelan & Johnson, 1992) by comparing the effects of formoterol, salbutamol and salmeterol as inhibitors of PPE and granulocyte accumulation in guinea-pig lung and skin, and to use the data to explore further the relationship between duration of action of β_2-adrenoceptor agonists and acute anti-inflammatory effects *in vivo*.

Methods

Plasma protein extravasation

Guinea-pig skin Male guinea-pigs (300-400 g) were anaesthetized with ketamine (40 mg kg^{-1}, i.m.) and xylazine (8 mg kg^{-1}, i.m.). Each animal received an intracardiac injection of iodinated (^{125}I) human serum albumin (^{125}I-HSA; 20 kBq) in heparinised (10 u ml^{-1}) saline. The abdomen of each animal was shaved, and into this shaved area, six intradermal injections (50 µl) of a β_2-adrenoceptor agonist or vehicle (1% dimethylsulphoxide (DMSO) in saline) were administered. After 30 min, one site of the six received an injection of sterile saline (50 µl) while the other five sites were injected with bradykinin (1×10^{-10}-1×10^{-6} mol/site) in

[1] Author for correspondence.

50 µl sterile saline. Thirty min after bradykinin, animals were killed with pentobarbitone sodium (Expiral) and a plasma sample prepared. Each injection site was removed with a hollow punch and the radioactivity contained within the skin samples, and an aliquot of plasma, determined in a scintillation counter (LKB compugamma). From these data, the plasma content of each skin sample was determined as described previously (Whelan & Johnson, 1992). All data described are corrected for the plasma content of the vehicle-injected site.

In experiments where the duration of action of β_2-adrenoceptor agonists was determined in guinea-pig skin, [^{125}I]-HSA and β_2-adrenoceptor agonists were administered under isoflurane anaesthesia as described above. At intervals after the intradermal injection of β_2-adrenoceptor agonists, animals were anaesthetized with ketamine and xylazine and the same sites were injected with bradykinin. Thirty minutes after injection of bradykinin, animals were killed and PPE determined as described above.

Guinea-pig lung Histamine-induced PPE in guinea-pig lung was determined as described previously (Whelan & Johnson, 1992). Briefly, following intracardiac injection of [^{125}I]-HSA (20 kBq), male guinea-pigs (300–400 g) were exposed to an aerosol of histamine (500 µg ml^{-1}) for 1 min. Thirty minutes after histamine challenge, guinea-pigs were killed with an overdose of pentobarbitone sodium injected intraperitoneally. A blood sample was taken and the lungs were lavaged twice with 10 ml heparinized phosphate-buffered saline. The radioactivity in an aliquot of plasma and 5 ml of the pooled bronchoalveolar lavage fluid (BALF) was measured in a scintillation counter. From these data, PPE (expressed as µl plasma ml^{-1} BALF) was calculated.

In experiments where potency was determined, guinea-pigs were exposed to aerosols of formoterol (nebulizer concentration 0.1–100 µg ml^{-1}) as described by Ball *et al.* (1991), 30 min before challenge with histamine (500 µg ml^{-1}). The duration of action was determined by increasing the interval between treatment of guinea-pigs with formoterol and challenge with histamine.

Granulocyte accumulation

Guinea-pig skin Guinea-pig peritoneal granulocytes were elicited, isolated and labelled with ^{111}In as described previously (Whelan & Johnson, 1992). Labelled granulocytes were resuspended in saline, mixed with [^{125}I]-HSA and reinjected into male guinea-pigs (300–400 g) under ketamine (40 mg kg^{-1}, i.m.) and xylazine (8 mg kg^{-1}, i.m.) anaesthesia. At the same time, the abdomen of each animal was shaved, and six intradermal injections (50 µl) of a β_2-adrenoceptor agonist or vehicle (1% DMSO) were administered. Thirty minutes after injection of β_2-adrenoceptor agonist, each animal received an injection of saline (50 µl) into one site, while the other sites were injected with zymosan (0.2 mg). Granulocyte accumulation and PPE were measured 4 h after injection of zymosan as described previously (Whelan & Johnson, 1992). All data described are corrected for the granulocyte and plasma content of a vehicle-injected site.

Guinea-pig lung Male guinea-pigs (250–350 g) were exposed to aerosols of lipopolysaccharide (LPS, 100 µg ml^{-1}) or platelet activating factor (PAF, 100 µg ml^{-1}) for 10 min. Four hours after LPS, or 24 h after PAF, guinea-pigs were killed with pentobarbitone sodium, the lungs lavaged and neutrophil (LPS) and eosinophil (PAF) accumulation measured as described previously (Whelan & Johnson, 1992). Animals were exposed to aerosols of β_2-adrenoceptor agonists or vehicle as described above, 30 min before challenge with either LPS or PAF.

Statistical analysis

Data obtained for plasma protein extravasation in skin and for granulocyte accumulation in skin and lung were normally distributed and are expressed as arithmetic means ± s.e.mean. Where appropriate, levels of statistical significance were calculated by Student's *t* test.

In lung, histamine-induced increases in plasma protein extravasation were log normally distributed. These data are expressed as geometric means and 95% confidence limits. Where appropriate, levels of statistical significance were calculated, on the log transformed data, by Student's *t* test. A difference was considered to be significant when $P<0.05$. Experimental design was such that in any given experiment, each β_2-adrenoceptor agonist group was compared with a time-matched vehicle-treated group, thus, avoiding multiple comparisons.

Drugs and reagents

For intradermal administration, formoterol, salbutamol and salmeterol (Glaxo Group Research) were dissolved in DMSO to produce a stock solution of 2×10^{-1} mol l^{-1}. This was diluted in sterile saline to produce a final solution for intradermal injection containing 1% DMSO or less. For aerosol administration, formoterol, salbutamol and salmeterol were dissolved in saline with the addition of a few drops of acetic acid where necessary. Bradykinin, histamine dihydrochloride, lipopolysaccharide (E. coli 026:B6), platelet activating factor and heparin were purchased from Sigma Ltd., Poole, U.K. ^{125}I-iodinated human serum albumin (specific activity 92.5 kBq mg^{-1} albumin) and [^{111}In]-oxine were purchased from Amersham International plc., Amersham, Bucks.

Results

Plasma protein extravasation

Guinea-pig skin Intradermal injection of bradykinin (1×10^{-10} to 1×10^{-6} mol/site) induced a dose-related PPE such that the highest dose of bradykinin used (1×10^{-6} mol/site) caused the extravasation of 21.3 ± 2.68 µl plasma ($n = 23$, Figure 1).

Formoterol, salmeterol and salbutamol inhibited PPE induced by bradykinin (1×10^{-10} to 1×10^{-6} mol/site). When injected 30 min prior to bradykinin (1×10^{-6} mol/site), intradermal formoterol (1×10^{-10} to 1×10^{-8} mol/site) significantly ($P<0.05$) inhibited PPE in guinea-pig skin (Figure 1), with a peak effect being obtained at 1×10^{-9} mol/site. A

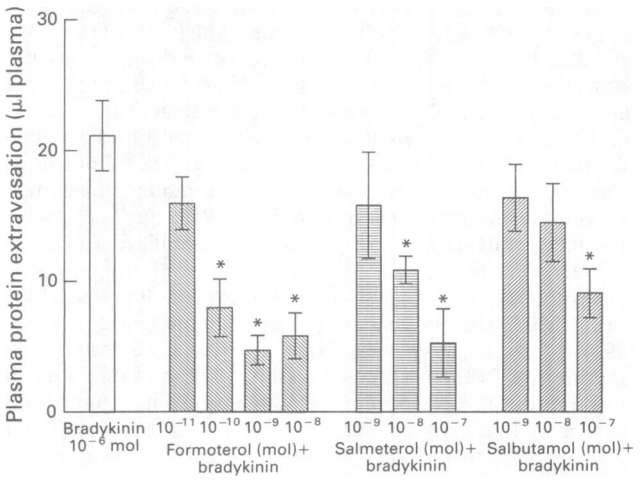

Figure 1 Inhibition of bradykinin (1×10^{-6} mol/site)-induced plasma protein extravasation (PPE) in guinea-pig skin by intradermal formoterol (1×10^{-11}–1×10^{-8} mol/site), salmeterol (1×10^{-9}–1×10^{-7} mol/site) and salbutamol (1×10^{-9}–1×10^{-7} mol/site). Each column represents the mean and s.e.mean of at least 6 determinations. *Significant reduction relative to vehicle + bradykinin group ($P<0.05$).

lower dose of formoterol (1×10^{-11} mol/site) was also effective, but this inhibition was not statistically significant ($P > 0.05$). Similarly, salmeterol (1×10^{-8} and 1×10^{-7} mol/site), and salbutamol (1×10^{-8} and 1×10^{-7} mol/site), significantly ($P < 0.05$) inhibited bradykinin-induced PPE (Figure 1). Lower doses (1×10^{-9} mol/site) of salbutamol and salmeterol had no significant inhibitory effect ($P > 0.05$; Figure 1). In these experiments, 1×10^{-9} mol/site formoterol was equivalent to 1×10^{-7} mol/site salmeterol and both were more effective than 1×10^{-7} mol/site salbutamol (Figure 1).

In experiments where the duration of action of β_2-adrenoceptor agonists in guinea-pig skin was determined, formoterol (1×10^{-9} mol/site) caused a marked inhibition (82.3%, $P < 0.05$) of PPE when injected 30 min before bradykinin (Figure 2). However, the inhibitory activity of formoterol was progressively lost, such that no significant inhibition ($P > 0.05$) was seen after 4 h (Figure 2). In contrast to formoterol, a less effective dose of salmeterol (1×10^{-8} mol/site, 64.4% inhibition at 30 min) significantly inhibited PPE ($P < 0.05$) even when administered up to 6 h before bradykinin, while, in these experiments, the inhibitory effects of salbutamol (1×10^{-8} mol/site, 52.3% inhibition at 30 min, $P < 0.05$) were lost after 2 h (Figure 2). The duration of action of formoterol, salmeterol and salbutamol obtained with lower doses of bradykinin (1×10^{-8} and 1×10^{-7} mol/site) were similar to those obtained with the higher dose of bradykinin (1×10^{-6} mol/site, data not shown).

Guinea-pig lung When guinea-pigs were challenged with aerosols of histamine (500 μg ml^{-1}), the plasma protein content of BALF increased from 1.19 (95% c.l. 0.82–1.73, $n = 7$) μl plasma ml^{-1} to 4.71 (3.43–6.48, $n = 12$) μl plasma ml^{-1} (Figure 3).

Formoterol (nebuliser concentration 0.1–100 μg ml^{-1}), administered to guinea-pigs by inhalation 30 min prior to challenge with histamine, caused a concentration-related inhibition of PPE (Figure 3). Unlike data previously obtained for salmeterol and salbutamol (Whelan & Johnson, 1992), the concentration-effect curve for formoterol appeared shallow, in that while a small degree of inhibition of PPE was apparent at concentrations of 0.1 and 1.0 μg ml^{-1}, greater concentrations of formoterol (10 and 100 μg ml^{-1}) were required to reduce significantly ($P < 0.05$) histamine-induced PPE (Figure 3).

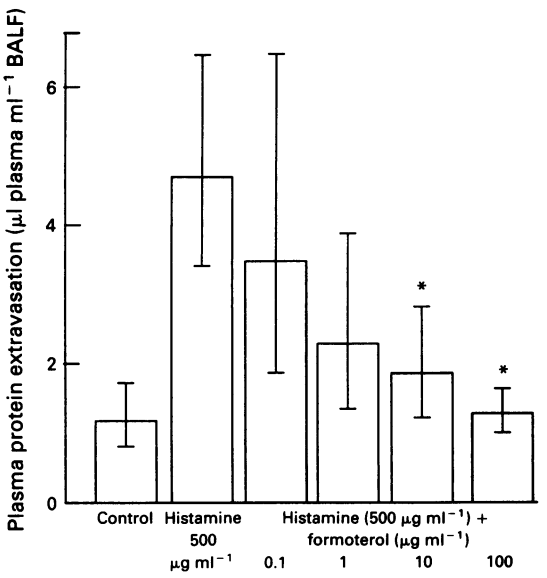

Figure 3 Histamine-induced plasma protein extravasation (PPE) in guinea-pig lung. Inhibition of PPE by inhaled formoterol (0.1–100 μg ml^{-1}). All doses are nebuliser concentrations given 30 min prior to challenge with histamine (500 μg ml^{-1}). Data are the geometric means and 95% confidence limits of at least 6 determinations. *Significant inhibition relative to histamine alone ($P < 0.05$).

Inhibition of histamine-induced PPE by formoterol (100 μg ml^{-1}) was evident 30 min and 1 h after administration. However, no significant ($P > 0.05$) inhibition of PPE was observed when formoterol was administered 2 h or 4 h before histamine (Figure 4).

Granulocyte accumulation

Guinea-pig skin: zymosan-induced granulocyte accumulation and PPE Four hours after injection of zymosan (0.2 mg/site), an increased granulocyte content and PPE were observed in guinea-pig skin (Table 1). Intradermal formoterol (1×10^{-9} and 1×10^{-8} mol/site) had no significant ($P > 0.05$)

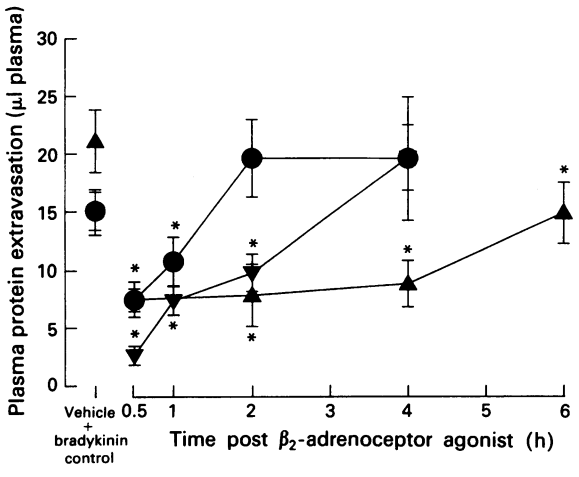

Figure 2 Bradykinin-induced plasma protein extravasation (PPE) in guinea-pig skin. Data are time courses for inhibition of PPE by formoterol (1×10^{-9} mol/site; ▼), salbutamol (1×10^{-8} mol/site; ●) and salmeterol (1×10^{-8} mol/site; ▲) injected intradermally at the times indicated prior to injection with bradykinin (1×10^{-6} mol/site). Each point represents the mean ± s.e.mean of at least 6 determinations. *Significant inhibition relative to vehicle + bradykinin group ($P < 0.05$).

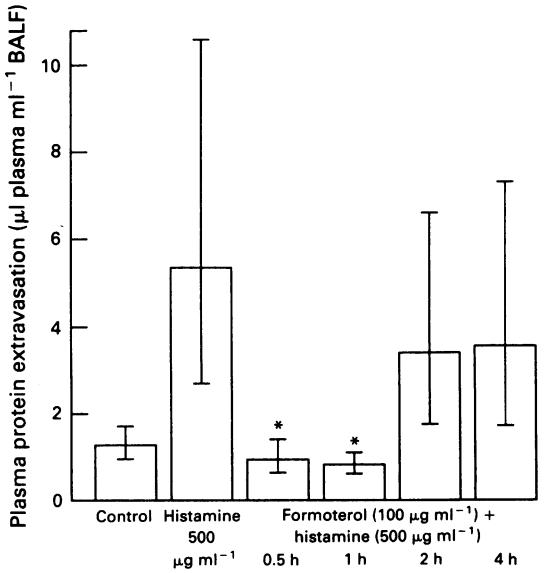

Figure 4 Histamine-induced plasma protein extravasation (PPE) in guinea-pig lung. The time course of inhibition of PPE by inhaled formoterol (100 μg ml^{-1}) administered at the time indicated prior to challenge with histamine (500 μg ml^{-1}). Each column represents the geometric mean and 95% confidence limits of at least 6 determinations. *Significant inhibition relative to histamine alone ($P < 0.05$).

Table 1 Inhibition of granulocyte accumulation and plasma protein extravasation (PPE) in guinea-pig skin by β_2-adrenoceptor agonists administered 30 min before zymosan (0.2 mg/site, i.d.): measurements were made 4 h later

Agonist	Dose (mol/site)	Granulocytes ($\times 10^3$)/site Control	Granulocytes ($\times 10^3$)/site Test	PPE (μl plasma site) Control	PPE (μl plasma site) Test	n
Formoterol	10^{-9}	983.2 ± 118.8	760.0 ± 79.3	39.40 ± 4.91	29.77 ± 4.05	6
	10^{-8}	342.7 ± 53.8	247.4 ± 47.3	13.86 ± 1.37	11.43 ± 1.78	6
Salmeterol	10^{-8}	332.0 ± 21.8	222.7 ± 22.1*	8.81 ± 0.70	4.99 ± 1.64*	8
	10^{-7}	332.0 ± 21.8	185.3 ± 59.2*	8.81 ± 0.70	4.50 ± 1.26*	6
Salbutamol	10^{-7}	973.1 ± 202.9	769.2 ± 150.8	22.10 ± 5.40	11.48 ± 2.40	6

Each value is the mean ± s.e.mean of n observations.
*Significantly different from control ($P<0.05$).

inhibitory effect (Table 1). However, in parallel experiments, intradermal injection of salmeterol (1×10^{-8} and 1×10^{-7} mol/site) significantly ($P<0.05$) inhibited both zymosan-induced granulocyte accumulation and PPE (Table 1), whereas the short-acting compound, salbutamol, (1×10^{-7} mol/site) again had no effect, findings that are consistent with those described previously (Whelan & Johnson, 1992).

Guinea-pig lung: LPS-induced neutrophil accumulation Exposure of guinea-pigs to aerosols of LPS (100 μg ml^{-1}), as described previously (Whelan & Johnson, 1992), caused a significant ($P<0.05$) increase in BALF neutrophil count to 771.3 ± 87.2 cells μl^{-1} (mean ± s.e.mean, $n = 9$), 4 h after challenge. Pretreatment of guinea-pigs with aerosols of formoterol (nebuliser concentrations up to 100 μg ml^{-1}), 30 min before challenge with LPS, had no significant ($P>0.05$) inhibitory effect on LPS-induced neutrophilia. A higher concentration of formoterol (1000 μg ml^{-1}) was required to inhibit significantly ($P<0.05$) LPS-induced neutrophilia by 46.2%, the BALF neutrophil count being reduced to 414.3 ± 66.0 cells μl^{-1} ($n = 9$). These findings for formoterol are similar to those previously reported for salbutamol (Whelan & Johnson, 1992). In contrast in parallel experiments, salmeterol (10 and 100 μg ml^{-1}) significantly ($P<0.05$) reduced LPS-induced neutrophil accumulation from 793.0 ± 108.5 cells μl^{-1} ($n = 6$) to 319.7 ± 59.1 and 297.2 ± 50.6 cells μl^{-1} ($n = 6$) respectively, confirming data published previously (Whelan & Johnson, 1992).

PAF-induced eosinophil accumulation Exposure of guinea-pigs to aerosols of PAF (nebuliser concentration 100 μg ml^{-1}) caused a 2–5 fold increase in BALF eosinophil count 24 h after challenge. Pretreatment of guinea-pigs with aerosols of formoterol (100 μg ml^{-1}) or salmeterol (100 μg ml^{-1}) resulted in a significant ($P<0.05$) decrease in PAF-induced eosinophilia (Table 2). Lower concentrations of formoterol (1 and 10 μg ml^{-1}) or salmeterol (10 μg ml^{-1}) had a smaller inhibitory effect on PAF-induced eosinophil accumulation which was not statistically significant ($P>0.05$). Thus, in terms of the threshold nebuliser concentration (100 μg ml^{-1}) required to produce statistically significant inhibition ($P<0.05$), formoterol and salmeterol appear equipotent.

Discussion

In an earlier study, we postulated that a long duration of action was necessary for β_2-adrenoceptor agonists to inhibit aspects of acute inflammation, such as granulocyte accumulation (Whelan & Johnson, 1992). This hypothesis was based on the observation that the long-acting β_2-adrenoceptor agonist, salmeterol, but not the short-acting compound, salbutamol, inhibited granulocyte accumulation in guinea-pig lung and skin, by an action on β_2-adrenoceptors.

The experiments described in the present report confirm and extend these findings by comparing the anti-inflammatory profile of formoterol, another β_2-adrenoceptor agonist (Anderson, 1991) with that of salmeterol and salbutamol. Formoterol inhibits PPE in guinea-pig skin and lung, findings that are consistent with those described for other β_2-adrenoceptor agonists (Persson *et al.*, 1982; Whelan & Johnson, 1992). As a bronchodilator, formoterol is approximately 10 times more potent than salmeterol in guinea-pigs and dose-effect curves for the two compounds appear to be parallel (Nials *et al.*, 1990). However, concentration-effect curves for inhibition of PPE by formoterol in guinea-pig lung appeared shallow, in that while formoterol appeared to be more potent than salmeterol at threshold concentrations, the concentrations required to achieve significant inhibition of PPE were similar to those obtained previously for salmeterol (Whelan & Johnson, 1992). Thus, in contrast, to salmeterol, which inhibits PPE at bronchodilator doses, formoterol appears to inhibit PPE significantly in guinea-pig lung only at doses that are greater than those reported to produce bronchodilatation in this species (Nials *et al.*, 1990).

Table 2 Inhibition of platelet activating factor (PAF)-induced eosinophil accumulation in guinea-pig lung by inhaled formoterol and salmeterol

	β_2-Agonist nebuliser concentration (μg ml^{-1})	Eosinophils (cells μl^{-1} BALF) Formoterol	Eosinophils (cells μl^{-1} BALF) Salmeterol
Control	–	34.0 ± 7.5 (6)	59.1 ± 9.1 (9)
PAF	–	123.8 ± 16.7† (6)	104.3 ± 16.5† (9)
PAF + β_2-Agonist	1.0	68.0 ± 15.7 (6)	NT
PAF + β_2-Agonist	10	75.2 ± 18.9 (6)	65.8 ± 17.4 (9)
PAF + β_2-Agonist	100	46.2 ± 13.0* (6)	43.2 ± 9.1* (9)

Animals were exposed for 3 min to aerosols of β_2-adrenoceptor agonists. Thirty min later, the animals were exposed for 10 min to aerosols of PAF (100 μg ml^{-1}) and lungs were lavaged 24 h later. Each value is the mean ± s.e.mean of (n) observations.
†Significantly greater than control ($P<0.05$).
*Significantly different from PAF alone ($P<0.05$).
NT = Not tested.

As an inhibitor of PPE in both guinea-pig skin and lung, formoterol has a duration of action of 2–4 h. In contrast, in skin, an equipotent dose of salmeterol has a duration of effect in excess of 6 h, while this is only 2 h for salbutamol, similar profiles to those reported previously in guinea-pig lung (Whelan & Johnson, 1992). Thus, in both guinea-pig skin and lung, formoterol appears to have a duration of action intermediate between that of salbutamol and salmeterol. Furthermore, this duration is similar to that obtained for formoterol-induced bronchodilatation in guinea-pigs by Nials *et al.* (1990).

Inhibition of PPE by β_2-adrenoceptor agonists is believed to be due to an action of these agents on the venular endothelium (Persson *et al.*, 1982; Gudgeon & Martin, 1989), leading to a reduction in the number, or size, of inter-endothelial cell gap junctions. We have previously postulated that inhibition of granulocyte accumulation by salmeterol is also due to a long-lasting action on β_2-adrenoceptors on venular endothelium (Whelan & Johnson, 1992), since high concentrations of β_2-adrenoceptor agonists are generally required to have a direct inhibitory effect on leukocytes *in vitro* (Busse & Sosman, 1984; Baker & Fuller, 1990; Nijkamp *et al.*, 1992). Furthermore, unlike inhibition of granulocyte accumulation by salmeterol *in vivo* (Whelan & Johnson, 1992), these effects are not reversed by β-adrenoceptor antagonists such as propranolol (Baker & Fuller, 1990).

The availability of formoterol has allowed us to investigate further the relationship between the duration of action of β_2-adrenoceptor agonists and inhibition of granulocyte accumulation in guinea-pig lung and skin. The finding that formoterol, unlike salmeterol, did not inhibit neutrophil accumulation or granulocyte-dependent PPE (zymosan), at doses which inhibit granulocyte-independent PPE (histamine or bradykinin), suggests that compounds with a duration of action greater than that of formoterol are necessary for inhibition of this inflammatory process. This observation supports our hypothesis that inhibition of granulocyte accumulation is a feature of β_2-adrenoceptor agonists with a long duration of action (Whelan & Johnson, 1992).

In contrast to the lack of inhibition of neutrophil accumulation, both formoterol and salmeterol inhibited PAF-induced eosinophil accumulation in guinea-pig lung. This finding is consistent with reports in the literature that inhaled formoterol inhibits antigen-induced eosinophil accumulation in dog and guinea-pig lung (Anderson, 1991; Sugiyama *et al.*, 1992). In the present study, formoterol and salmeterol were approximately equipotent as inhibitors of PAF-induced eosinophil accumulation in guinea-pig lung, whereas formoterol is approximately 10 times more potent than salmeterol as a bronchodilator in guinea-pigs (Nials *et al.*, 1990). Thus, like inhibition of PPE, salmeterol inhibits eosinophil accumulation in guinea-pigs at bronchodilator doses, but formoterol is only effective at doses greater than those required to produce bronchodilatation.

The finding that formoterol is more potent as an inhibitor of PAF-induced eosinophilia than LPS-induced neutrophilia, may indicate that β_2-adrenoceptor agonists inhibit eosinophil accumulation through a different mechanism from neutrophil accumulation. The differential effect of the β_2-agonists on neutrophil recruitment and the associated granulocyte-dependent PPE, suggests that only compounds with a duration of action similar to salmeterol will inhibit this response at doses which inhibit granulocyte-independent PPE (Whelan & Johnson, 1992), whereas higher doses of shorter-acting compounds, such as formoterol, are required to produce an equivalent effect. Thus, in the experiments where higher doses of formoterol were used, it is possible that the duration of action was sufficient to produce an equivalent inhibition of neutrophil accumulation.

It is unlikely that even salmeterol is exerting an effect on the endothelium when eosinophil accumulation is taking place during the 24 h following challenge with PAF. Thus, it is possible that bronchodilator doses of salmeterol, and suprabronchodilator doses of formoterol, inhibit an early event in the process of eosinophil recruitment. However, salbutamol, at bronchodilator doses, has no effect on PAF-induced eosinophil accumulation in guinea-pigs (Whelan & Johnson, 1992), suggesting that this event must be occurring after the inhibitory effects of salbutamol have waned. In contrast, fenoterol, another short-acting β_2-adrenoceptor agonist, has been reported to inhibit antigen-induced eosinophil accumulation in guinea-pig lung (Fugner, 1989), but at doses which may have resulted in a prolonged duration of action. Alternatively, because of its higher intrinsic activity (O'Donnell & Wanstall, 1978), it is also possible that fenoterol exerts an effect on eosinophil accumulation which salbutamol does not. However, salmeterol also has low intrinsic activity (Dougall *et al.*, 1991), thus efficacy *per se* is unlikely to account for these differences, unless β_2-adrenoceptor agonists act at more than one site to inhibit eosinophil recruitment.

Although the process by which eosinophils are recruited into tissues is poorly defined, it appears to involve the generation of interleukin-5 (Lopez *et al.*, 1988; Sanjar *et al.*, 1992) and the expression of adhesion molecules such as VLA-4 on eosinophils (Dobrina *et al.*, 1991) and VCAM-1 on endothelium (Moser *et al.*, 1992). β_2-adrenoceptor agonists could exert an inhibitory effect at many levels in this complex process, and, further studies will be necessary before the mechanism by which these compounds inhibit eosinophilia in guinea-pig lung can be elucidated.

The duration of action of formoterol is dependent on the concentration or dose used, whereas salmeterol appears to be intrinsically long-acting (Johnson *et al.*, 1993), properties which may influence the anti-inflammatory profiles of the compounds. The finding that formoterol has a duration of action between that of salbutamol and salmeterol contrasts with data in the literature, which show formoterol to exhibit long-acting anti-inflammatory effects in animals (O'Donnell & Anderson, 1991; Erjefalt & Persson, 1991; Advenier *et al.*, 1992) and man (Gronneberg & Zetterstrom, 1990a,b; 1992; Palmqvist *et al.*, 1992). However, in these studies, few comparative results relating to potency were presented and, it is possible that high doses of formoterol were used that resulted in an extended duration of action. For example, Erjefalt & Persson (1991) found formoterol to have a duration of action of over 10 h as an inhibitor of PPE in guinea-pig lung. However, the dose of formoterol used was at least 10 times greater than that required to produce a maximal inhibition of PPE in guinea-pig trachea. In the experiments in the present paper, where formoterol was up to 100 times more potent than salbutamol in inhibiting PPE, the duration of action was determined with doses which produced just maximal inhibition of PPE, a difference which could account for the shorter duration of action of formoterol in our hands.

Furthermore, in human skin, a 25 fold greater dose of formoterol was required to inhibit anti-IgE-induced late-phase cutaneous reactions than the immediate wheal and flare responses (Gronneberg & Zetterstrom, 1990b). Similarly, in atopic subjects, inhalation of a high dose of formoterol (30 μg) was shown to inhibit the late-phase bronchoconstriction seen following allergen challenge (Palmqvist *et al.*, 1992). Moreover, in the same study, an equibronchodilator dose of salbutamol (500 μg), 2.5 times the therapeutic dose, also inhibited late-phase bronchoconstriction, a finding which contrasts with earlier reports showing that, at therapeutic doses, salbutamol has no effect (Cockcroft & Murdock, 1987). In the present study, salmeterol inhibited both PPE and granulocyte accumulation in guinea-pigs at doses which have been reported to produce bronchodilatation (Nials *et al.*, 1990), whereas suprabroncholidator doses of formoterol were required to produce similar effects, a finding which is consistent with those described above in man.

In man, therefore, one might expect the same dose of an inherently long-acting compound, such as salmeterol, unlike

formoterol and salbutamol, to inhibit both early and late phase reactions in lung and skin. Indeed, Twentyman *et al.* (1990) and Dahl, (1991) have reported that at therapeutic doses, salmeterol (50 μg) inhibits the acute and late-phase response to allergen in atopic subjects.

In conclusion, the data presented show that, at equipotent doses, the duration of action of formoterol as an inhibitor of PPE in guinea-pig skin and lung is intermediate between that of salbutamol and salmeterol. Whereas salmeterol inhibits neutrophil accumulation at doses which inhibit PPE, this does not apply to formoterol, indicating that a duration of action in excess of that of formoterol is required to inhibit this aspect of acute inflammation. In contrast, formoterol, like salmeterol, inhibits eosinophil accumulation in guinea-pig lung, but the doses of formoterol are greater than those required to produce bronchodilatation in this species. We speculate that the mechanism of inhibition of eosinophil accumulation by β_2-adrenoceptor agonists may therefore be different from that of inhibition of neutrophil accumulation.

References

ADVENIER, C., QIAN, Y., LAW KOUNE, J.-D., MOLIMARD, M., CANDENAS, M.-L. & NALINE, E. (1992). Formoterol and salbutamol inhibit bradykinin and histamine induced airway microvascular leakage in guinea-pig. *Br. J. Pharmacol.*, **105**, 792–798.

ANDERSON, G.P. (1991). Pharmacology of formoterol: an innovative bronchodilator. In. *Agents and Actions Supplements*, vol 34: *New Drugs for Asthma Therapy.*, ed Anderson, G.P., Chapman, I.D., Morley, J. pp. 97–115. Basel, Boston, Berlin: Birkhauser.

BAKER, A.J. & FULLER, R.W. (1990). Anti-inflammatory effect of salmeterol on human alveolar macrophages. *Am. Rev. Respir. Dis.*, **141**, A394.

BALL, D.I., BRITTAIN, R.T., COLEMAN, R.A., DENYER, L.H., JACK, D., JOHNSON, M., LUNTS, L.H.C., NIALS, A.T., SHELDRICK, K.E. & SKIDMORE, I.F. (1991). Salmeterol, a novel long-acting β_2-adrenoceptor agonist: characterization of pharmacological activity *in vitro* and *in vivo*. *Br. J. Pharmacol.*, **104**, 665–671.

BUSSE, W.W. & SOSMAN, J.M. (1984). Isoproterenol inhibition of isolated human neutrophil function. *J. Allergy Clin. Immunol.*, **73**, 404–410.

COCKCROFT, D.W. & MURDOCK, K.Y. (1987). Comparative effects of inhaled salbutamol, sodium cromoglycate, and beclomethasone dipropionate on allergen-induced early asthmatic responses, late asthmatic responses and increased bronchial responsiveness to histamine. *J. Allergy Clin. Immunol.*, **79**, 734–740.

DAHL, R. (1991). Are β_2-adrenoceptor agonists 'anti-inflammatory'? *Eur. Respir. Dis.*, **4**, Suppl. 14, 183s.

DOBRINA, A., MENEGAZZI, R., CARLOS, T.M., NARDON, E., CRAMER, R., ZACCHI, T., HARLAN, J.M. & PATRIARCA, P. (1991). Mechanisms of eosinophil adherence to cultured vascular endothelial cells. Eosinophils bind to the cytokine-induced endothelial ligand vascular cell adhesion molecule-1 via the very late activation antigen-4 receptor. *J. Clin. Invest.*, **88**, 20–26.

DOUGALL, I.G., HARPER, D., JACKSON, D.M. & LEFF, P. (1991). Estimation of the efficacy and affinity of the β_2-adrenoceptor agonist salmeterol in guinea-pig trachea. *Br. J. Pharmacol.*, **104**, 1057–1061.

ERJEFALT, I. & PERSSON, C.G.A. (1991). Long duration and high potency of antiexudative effects of formoterol in guinea-pig tracheobronchial airways. *Am. Rev. Respir. Dis.*, **144**, 788–791.

FAULDS, D., HOLLINGSHEAD, L.M. & GOA, K.L. (1991). Formoterol. A review of its pharmacological properties and therapeutic potential in reversible obstructive airways disease. *Drugs*, **42**, 115–137.

FUGNER, A. (1989). Formation of oedema and accumulation of eosinophils in the guinea-pig lung. Inhibition by beta-stimulants. *Int. Arch. Allergy Appl. Immunol.*, **88**, 225–227.

GRONNEBERG, R. & ZETTERSTROM, O. (1990a). Inhibition of anti-IgE induced skin response in normals by formoterol, a new β_2-adrenoceptor agonist, and terbutaline, 1. Dose response relation and duration of effect of early wheal and flare response. *Allergy*, **45**, 334–339.

GRONNEBERG, R. & ZETTERSTROM, O. (1990b). Inhibition of anti-IgE induced skin response in normals by formoterol, a new β_2-adrenoceptor agonist, and terbutaline. 2. Effect on the late phase reaction. *Allergy*, **45**, 340–346.

GRONNEBERG, R. & ZETTERSTROM, O. (1992). Inhibitory effects of formoterol and terbutaline on the development of late phase skin reactions. *Clin. Exp. Allergy*, **21**, 257–263.

GUDGEON, J.R. & MARTIN, W. (1989). Modulation of arterial endothelial permeability: studies on an *in vitro* model. *Br. J. Pharmacol.*, **98**, 1267–1274.

JOHNSON, M., BUTCHERS, P.R., COLEMAN, R.A., NIALS, A.T., STRONG, P., SUMNER, M.J., VARDEY, C.J. & WHELAN, C.J. (1993). The pharmacology of salmeterol. *Life Sci.*, **52**, 2131–2143.

JOHNSON, M., VARDEY, C.J. & WHELAN, C.J. (1992). The therapeutic potential of long-acting β_2-adrenoceptor agonists in allergic inflammation. *Clin. Exp. Allergy.*, **22**, 177–181.

LOPEZ, A.F., SANDERSON, C.J., GAMBLE, J.R., CAMPBELL, H.D., YOUNG, I.G. & VADAS, M.A. (1988). Recombinant human interleukin 5 is a selective activator of human eosinophil function. *J. Exp. Med.*, **167**, 219–224.

MOSER, R., FEHR, J. & BRUIJNZEEL, P.L.B. (1992). IL-4 controls the selective endothelium-driven transmigration of eosinophils from allergic individuals. *J. Immunol.*, **149**, 1432–1438.

NIALS, A.T., BUTCHERS, P.R., COLEMAN, R.A., JOHNSON, M. & VARDEY, C.J. (1990). Salmeterol and formoterol: are they both long-acting β_2-adrenoceptor agonists? *Br. J. Pharmacol.*, **99**, 120P.

NIJKAMP, F.P., ENGELS, F., HENRICKS, P.A.J. & VAN OOSTERHOUT, A.J.M. (1992). Mechanisms of β-adrenergic receptor regulation in lungs and its implications for physiological responses. *Physiol. Rev.*, **72**, 323–367.

O'DONNELL, S.R. & ANDERSSON, G.P. (1991). Attenuation by formoterol of tracheal plasma exudation by topical bradykinin in rat trachea *in vivo*. *Br. J. Pharmacol.*, **104**, 293P.

O'DONNELL, S.R. & WANSTALL, J.C. (1978). Evidence that the efficacy (intrinsic activity) of fenoterol is higher than that of salbutamol on β-adrenoceptors in guinea-pig trachea. *Eur. J. Pharmacol.*, **47**, 333–340.

PALMQVIST, M., BALDER, B., LOWHAGEN, O., MELANDER, B., SVEDMYR, N. & WAHLANDER, L. (1992). Late asthmatic reaction decreased after pretreatment with salbutamol and formoterol, a new long-acting β_2-agonist. *J. Allergy Clin. Immunol.*, **89**, 844–849.

PERSSON, C.G.A., ERJEFALT, I., GREGA, G.J. & SVENSJÖ, E. (1982). The role of β-receptor agonists in the inhibition of pulmonary edema. *Ann. N.Y. Acad. Sci.*, **384**, 544–557.

SANJAR, S., MCCABE, P.J., FATTAH, D., HUMBLES, A.A. & POLE, S.M. (1992). TRFK5, an antibody to interleukin 5, selectively inhibits antigen-induced eosinophil accumulation in the guinea-pig lung. *Am. Rev. Respir. Dis.*, **145**, A40.

SUGIYAMA, H., OKADA, C., BEWTRA, A.K., HOPP, R.J. & TOWNLEY, R.G. (1992). The effect of formoterol on the late asthmatic phenomenon in guinea pigs. *J. Allergy. Clin. Immunol.*, **89**, 858–866.

TWENTYMAN, O.P., FINNERTY, J.P., HARRIS, A., PALMER, J. & HOLGATE, S.T. (1990). Protection against allergen-induced asthma by salmeterol. *Lancet*, **336**, 1338–1342.

WHELAN, C.J. & JOHNSON, M. (1992). Inhibition by salmeterol of increased vascular permeability and granulocyte accumulation in guinea-pig lung and skin. *Br. J. Pharmacol.*, **105**, 831–838.

(Received February 5, 1993
Revised May 17, 1993
Accepted May 28, 1993)

Br. J. Pharmacol. (1993), **110**, 619–626

Salmeterol, a long-acting β_2-adrenoceptor agonist mediating cyclic AMP accumulation in a neuronal cell line

Karen E. McCrea & [1]Stephen J. Hill

Department of Physiology & Pharmacology, Medical School, Queen's Medical Centre, Nottingham NG7 2UH

1 The accumulation of cyclic AMP stimulated by salmeterol, a long-acting β_2-adrenoceptor agonist and by isoprenaline, a non-selective β-adrenoceptor agonist have been compared in the B50 neuroblastoma cell line.

2 Salmeterol produced a concentration-dependent increase in the accumulation of total [^{3}H]-cyclic AMP in B50 cells yielding an EC_{50} value of 37 nM which was lower than that obtained with isoprenaline (294 nM). The maximum response to salmeterol was only 46% of that obtained with isoprenaline.

3 The β_2-adrenoceptor antagonist, ICI 118551, inhibited the responses to both salmeterol (apparent K_D 2.2 nM) and isoprenaline (apparent K_D 1.6 nM). However, the β_1-adrenoceptor antagonist, atenolol, produced no significant effect at concentrations up to 100 μM.

4 Salmeterol (1 μM) changed the concentration-response curve of isoprenaline in the manner of a partial agonist interacting with a full agonist. The K_D of salmeterol obtained from the interaction was 55.6 nM.

5 Whereas salmeterol has a slow onset of action in airway smooth muscle compared to other β_2-adrenoceptor agonists, in B50 monolayers both salmeterol and isoprenaline produced a rapid increase in cyclic AMP accumulation ($t_{1/2}$ 1.1 min and 0.4 min respectively).

6 Despite the existence of cyclic AMP efflux mechanisms that exist in this cell line it was possible to investigate the duration of agonist action by measuring intracellular levels of the second messenger. Replacement of drug-containing medium with fresh buffer led to a rapid reduction in intracellular levels of cyclic AMP in isoprenaline-stimulated cells whereas cyclic AMP accumulation was sustained for much longer periods in salmeterol-stimulated cells. However, the persistent action of salmeterol could be reversed by the addition of a β_2-selective antagonist.

7 These results confirm that salmeterol has a high affinity, but low efficacy (relative to isoprenaline) for β_2-adrenoceptors coupled to cyclic AMP accumulation and that the drug persists at its site of action for long periods in the B50 neuronal cell line.

Keywords: Salmeterol; isoprenaline; β_2-adrenoceptor; cyclic AMP accumulation; B50 neuroblastoma cell line

Introduction

β_2-Adrenoceptor agonists are currently the most widely used group of bronchodilator drugs employed to relieve airway obstruction in asthma (Barnes *et al.*, 1984). These β_2-agonists induce the elevation of adenosine 3:5-cyclic monophosphate (cyclic AMP) content in tissues in response to adenylate cyclase activation via a stimulatory G protein (G_s) (Gilman, 1987; Birnbaumer, 1990). In airway smooth muscle, increased cellular cyclic AMP accumulation leads to the stimulation of cyclic AMP-dependent protein kinase A (PKA) which in turn phosphorylates a range of other proteins, including myosin light chain kinase, associated with the contractile apparatus of the cell (Barnes, 1986) and ion channels (Kume *et al.*, 1989), leading ultimately to smooth muscle relaxation.

Recently, a new bronchodilator drug, salmeterol, has been developed (Bradshaw *et al.*, 1987) which has been shown to be a potent and highly selective β_2-adrenoceptor agonist and which displays a long duration of action in airway smooth muscle (Brittain, 1990; Ball *et al.*, 1991). The mechanism underlying the long duration of action of salmeterol at β_2-adrenoceptors remains to be established but it has been postulated that it involves two processes: (a) an interaction between the saligenin head of the molecule and the active site and (b) the binding of the long non-polar N-substituent sidechain within a distinct hydrophobic core region of the receptor protein, which has been termed the 'exo-site' (Jack, 1991). Such an arrangement enables the head group to associate freely with and dissociate from the active site of the β_2-adrenoceptor whilst the sidechain remains firmly attached to the receptor protein (Ball *et al.*, 1991). A notable feature of studies performed in strips of airway smooth muscle, however, is the slow onset of action of salmeterol (Ball *et al.*, 1991). This suggests that the duration of action of salmeterol might be partly determined by slow diffusion of this lipophilic molecule to its active site within the smooth muscle segment.

The B50 neuroblastoma cell line (Schubert *et al.*, 1974), derived from the rat central nervous system, has recently been shown to express β_2-, but not β_1-adrenoceptors, coupled to cyclic AMP accumulation (Ruck *et al.*, 1990). The aim of this study was to evaluate the pharmacological characteristics of the cyclic AMP response elicited by salmeterol in monolayer cultures of a neuronal cell line, where the onset and offset of agonist action should be less sensitive to diffusional influences than in smooth muscle segments. A preliminary account of some of this work has been communicated to the British Pharmacological Society (McCrea *et al.*, 1992).

Methods

Cell culture

B50 cells (European Collection of Animal Cell Cultures, Porton Down, Salisbury, Wilts.), passages 3–17, were cultured at 37°C under an atmosphere of 10% CO_2 in humidified air in 75 cm^3 flasks (Costar). The growth medium was Dulbecco's modified Eagles medium (DMEM) supplemented

[1] Author for correspondence.

with 2 mM L-glutamine and 10% (v/v) foetal calf serum (FCS). Cells were passaged every 4 days using a split ratio of 1:6. Experiments were performed in 24 well cluster dishes, normally 3 days after seeding, on confluent monolayers.

Measurement of [^{3}H]-cyclic AMP accumulation

Cyclic AMP production was assayed by a modification of the method described previously for brain slices (Donaldson *et al.*, 1988). Monolayer cultures were incubated with [^{3}H]-adenine (2 μCi/well) for 2 h at 37°C in 1 ml/well Hanks/HEPES (20 mM) buffer, pH 7.4. Prelabelled cell monolayers were then washed 3 times with Hanks/HEPES buffer (1 ml/well) containing the type IV phosphodiesterase (PDE) inhibitor, rolipram (0.1 mM) (Ruck *et al.*, 1990). Where appropriate, antagonist drugs were equilibrated with the cells for 30 min prior to the addition of agonist. Agonists, or the appropriate vehicle controls were finally added in 10 μl of buffer and the incubation terminated after the appropriate length of time by the addition of 50 μl of 10 M HCl to each well which led to cell lysis.

In some experiments it was necessary to analyse intra- and extracellular cyclic AMP content independently. These assays were performed as above. However, before the termination of each agonist-stimulated incubation, supernatant buffer was carefully removed from each well for the analysis of extracellular [^{3}H]-cyclic AMP content (as described below). An identical volume of fresh Hanks/HEPES buffer (1 ml) was then rapidly applied to each well followed immediately by cell lysis in the normal way, thereby enabling intracellular [^{3}H]-cyclic AMP content to be determined.

[^{3}H]-cyclic AMP was isolated by sequential Dowex-alumina chromatography (Donaldson *et al.*, 1988). [^{3}H]-cyclic AMP, in 0.95 ml aliquots of the supernatant layers, and [^{14}C]-cyclic AMP (100 μl), which was used as a tracer, were applied to Dowex 50 ion exchange resin (0.6 ml) in plastic Econo columns (Bio-Rad), previously treated with 5 ml 1 M HCl and 20 ml distilled water. Columns were washed with 3 ml distilled water and were than placed above similar plastic columns containing 0.6 g neutral alumina (previously washed with 20 ml of 0.1 M imidazole before use). [^{3}H]-cyclic AMP was eluted from Dowex onto the alumina columns with distilled water (4–5 ml). The alumina columns were then placed directly above scintillation vials and [^{3}H]-cyclic AMP was eluted in 5 ml of 0.1 M imidazole. Radioactivity was determined by liquid scintillation counting. Recovery of cyclic AMP from the columns was routinely 70–80%. Furthermore, additional 50 μl aliquots were removed from the supernatant and used to determine the total radioactivity present in each sample; these 'totals' were then used to correct for variations in the number of cells present in each well.

In order to confirm the separation of cyclic AMP from other adenine nucleotides by this procedure, 1 ml aliquots of 150 μM solutions of ATP, ADP, cyclic AMP, AMP, adenosine and adenine were subjected to Dowex 50 chromatography. Sequential 1 ml aliquots of water were applied to each column and the eluate optical density was measured at 260 nm. Triplicate determinations were made for each compound. ATP and ADP were completely eluated within the first three 1 ml fractions. Cyclic AMP was eluted during fractions 4 to 6 and AMP (17%) began to elute, after the normal cyclic AMP collection period, during fractions 8 to 10. Adenine and adenosine were completely retained on the columns for the full 10 fraction collection period.

Data analysis

Accumulation of [^{3}H]-cyclic AMP was expressed as either radioactivity in d.p.m. (individual experiments) or as a percentage of the maximal stimulation by an agonist (maximal response minus basal). Agonist concentration-response curves were fitted to a logistic equation using the non-linear regression programme GraphPAD. The equation fitted was:

$$\%\ \text{of maximal response} = \frac{E_{max} \times X^n}{(EC_{50})^n + X^n}$$

where E_{max} is the maximal response (100%), X is the agonist concentration, EC_{50} is the concentration of agonist producing half maximal response and n is the slope parameter.

Antagonist inhibition curves were analysed using the same programme according to the expression.:

$$\%\ \text{of maximal response} = 100 - \frac{100 \times A^n}{(IC_{50})^n + A^n}$$

where IC_{50} is the concentration producing half maximal inhibition of the response to 1 μM agonist and A is the antagonist concentration.

Apparent antagonist dissociation constants (K_D) were calculated assuming competitive antagonism using a modification of the null method first described by Lazareno & Roberts (1987). Briefly, a concentration-response curve to agonist was generated and a concentration (X^1; normally 1 μM) of agonist was chosen which gave a response greater than 50% of the maximum agonist response. The concentration of antagonist (IC_{50}) required to reduce the response to this concentration of agonist by 50% was then determined. From the agonist concentration-response curve obtained in the absence of antagonist, the concentration of agonist (X^o) that yielded a response equivalent to 50% of that produced by X^1 (in the absence of antagonist) was also identified. The apparent K_D was then calculated from the expression:

$$\frac{X^1}{X^o} = \frac{IC_{50}}{K_D} + 1$$

where X^1/X^o is equivalent to the agonist dose-ratio that would be used in the analysis of parallel dose-response curves obtained in the presence and absence of an IC_{50} concentration of antagonist.

The dissociation constant for the partial agonist (K_p) salmeterol was determined by a method described by Stephenson (1956). The concentration of isoprenaline (D_1) that produced the same cyclic AMP response as that to 1 μM salmeterol was first determined. Concentration-response curves for isoprenaline were then constructed in the presence and absence of a fixed concentration of salmeterol (1 μM) termed P. The concentrations of isoprenaline that produced equivalent cyclic AMP responses in the absence (D_2; $D_2 > D_1$) and presence (D_3) of salmeterol were calculated. The dissociation constant of the partial agonist was determined from the expression:

$$\frac{D_3}{(D_2 - D_1)} = 1 + \frac{P}{K_p}$$

Values were expressed as means ± s.e.mean and *n* in the text refers to the number of separate experiments. In individual experiments, data points were calculated from the mean (± s.e.mean) of 4 determinations. Statistical analysis was performed by use of unpaired Student's *t* tests.

Chemicals

2,8-[^{3}H]-adenine (specific activity 31 Ci mmol^{-1}) and 8-[^{14}C]-cyclic AMP (specific activity 306 mCi mmol^{-1}) were purchased from New England Nuclear (Herts.) and Amersham International (Bucks.), respectively. Dowex 50W, H^+-form (200–400 mesh), neutral alumina (type WN-3), imadazole, (±)-isoprenaline hydrochloride and atenolol were obtained from Sigma (Dorset). DMEM, FCS and horse serum were purchased from Northumbria Biologicals (Northumberland) and glutamine from Flow Laboratories (Herts.). The gifts of salmeterol free base (Glaxo, Herts.). ICI 118551 hydrochloride (erythro-DL-1-(7-methylindan-4-yloxy)-3-isopropyl-aminobutane-2-ol; ICI Pharmaceuticals, Cheshire) and rolipram (Schering, Berlin, Germany) are gratefully acknowledged.

Stock solutions of drugs were prepared in Hanks/HEPES buffer except for ICI 118551 (Bilski *et al.*, 1983) which was dissolved in ethanol and salmeterol which was prepared as stock solution of 10 mM in Hanks/HEPES buffer with the addition of one drop of glacial acetic acid per ml.

Results

Comparison of salmeterol- and isoprenaline-stimulated cyclic AMP accumulation

Previous investigations have shown that the onset of the action of salmeterol is delayed compared with other β-adrenoceptor agonists in isolated airway smooth muscle (Ball *et al.*, 1991; Dougall *et al.*, 1991). This is probably due to the lipophilic nature of this molecule. However, 1 μM salmeterol stimulated a rapid increase in [^{3}H]-cyclic AMP accumulation in B50 cell monolayers reaching a steady-state level within 5 min; this response appeared to be maintained for at least 20 min (Figure 1). The mean $t_{1/2}$ obtained in three separate experiments was 1.13 ± 0.09 min. A rapid onset of cyclic AMP production was also produced by 1 μM isoprenaline ($t_{1/2}$ 0.44 ± 0.03 min, $n = 4$).

B50 cells treated with 10 μM salmeterol only produced a 1.7 ± 0.1 fold increase in [^{3}H]-cyclic AMP over basal levels ($n = 4$). However, in the presence of rolipram (0.1 mM) the response to salmeterol was enhanced (2.9 ± 0.2 fold over basal levels, $n = 4$). Rolipram was therefore included in all subsequent experiments. Salmeterol stimulated the formation of [^{3}H]-cyclic AMP in B50 cells in a concentration-dependent manner (Figure 2a). Concentration-response analysis yielded an EC_{50} value of 36.7 ± 18.4 nM ($n = 4$) and a slope parameter of 0.64 ± 0.07 ($n = 4$). Accumulation of cyclic AMP induced by isoprenaline (10 min incubation period) was much greater than that stimulated by salmeterol (Figure 3). Treatment with 10 μM isoprenaline led to a 7.9 ± 0.9 fold rise in second messenger formation ($n = 22$) compared to basal levels whereas the same concentration of salmeterol gave only 46.0 ± 4.2% ($n = 6$) of this response. The EC_{50} value and slope parameter for isoprenaline were 294 ± 84 nM and 0.89 ± 0.04 respectively ($n = 22$).

Effect of β-adrenoceptor antagonists on salmeterol-stimulated cyclic AMP accumulation

Preincubation of B50 cell monolayers with various concentrations of the β_2-selective antagonist, ICI 118551, for 30 min attenuated cyclic AMP accumulation when cells were stimulated by 1 μM salmeterol for a further 10 min period (Figure 2b). Increasing doses of ICI 118551 also inhibited cyclic AMP formation in B50 cells treated with isoprenaline (1 μM). The mean apparent dissociation constants (K_D) obtained for ICI 118551 were 2.2 ± 0.7 nM ($n = 3$) and 1.6 ± 0.5 nM ($n = 3$) in salmeterol- and isoprenaline-stimulated cells respectively.

Inclusion of the β_1-selective antagonist, atenolol, in the assay system did not alter salmeterol- and isoprenaline-stimulated (1 μM) [^{3}H]-cyclic AMP production at concentrations up to 100 μM atenolol (results not shown; $n = 3$).

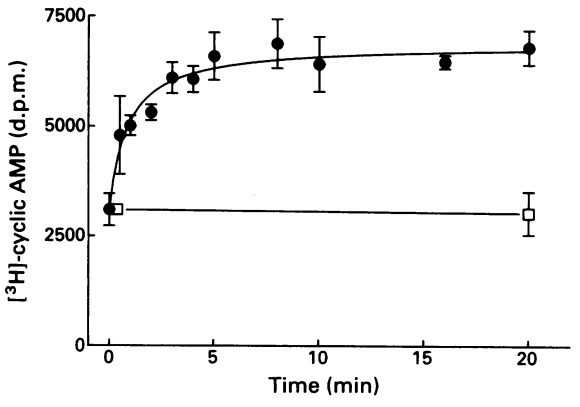

Figure 1 Time course showing the accumulation of total [^{3}H]-cyclic AMP in response to 1 μM salmeterol in B50 cell monolayers. Data were obtained in the presence (●) or absence (□) of agonist. Each data point represents the mean ± s.e.mean of quadruplicate determinations in a single experiment. This experiment was repeated twice yielding similar results.

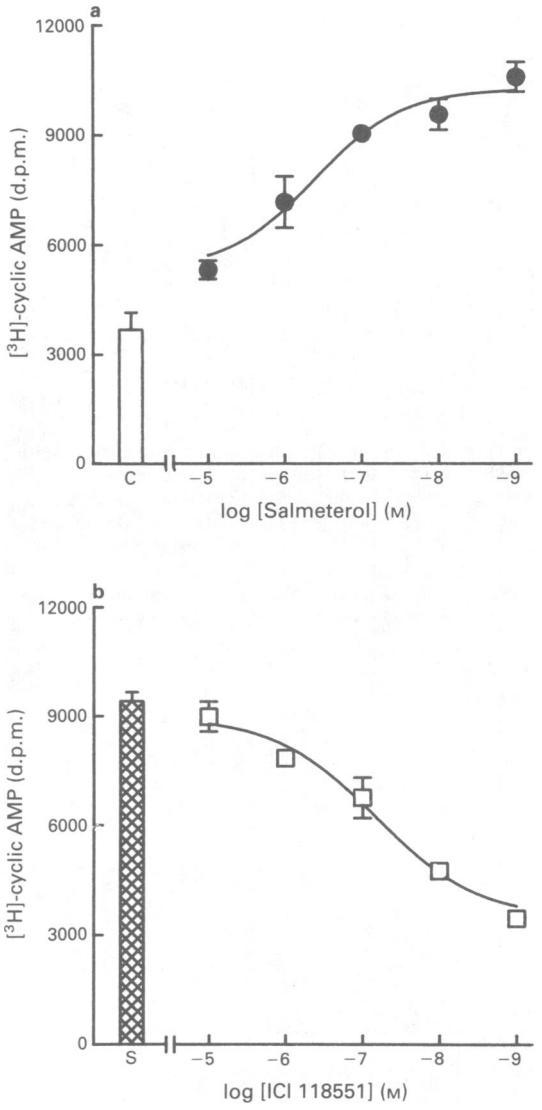

Figure 2 (a) Salmeterol-stimulated accumulation of [^{3}H]-cyclic AMP in the presence of 0.1 mM rolipram. The basal accumulation of total cyclic AMP is represented by the column labelled C. (b) Concentration-response curve for the inhibition of salmeterol-induced [^{3}H]-cyclic AMP accumulation by the β_2-selective antagonist, ICI 118551. The response to 1 μM salmeterol is shown by the cross-hatched column marked S. Cell monolayers were preincubated with ICI 118551 for 30 min before stimulation with 1 μM salmeterol for a further 10 min. The results of (a) and (b) were obtained in the same experiment. Data represent the means ± s.e.mean of results from 4 incubations in a single experiment. Where not shown, s.e.means were within the size of the symbol. Similar results were obtained in 2 other experiments.

Investigation of full/partial agonist interactions

In this series of experiments the ability of salmeterol to antagonize the effects of a more efficacious agonist (isoprenaline) was investigated. B50 cell monolayers were

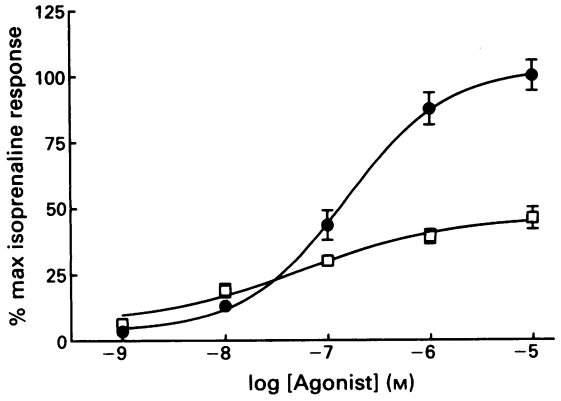

Figure 3 Comparison of concentration-response curves for [^{3}H]-cyclic AMP accumulation stimulated by isoprenaline (●) and salmeterol (□) for a 10 min period. Responses are expressed as a percentage (after subtraction of basal values) of the maximum response to isoprenaline (10 μM) which was measured in each experiment. Data represent the combined mean ± s.e.mean of quadruplicate determinations obtained in each of 6 experiments. Where not shown, s.e.means were within the size of the symbol.

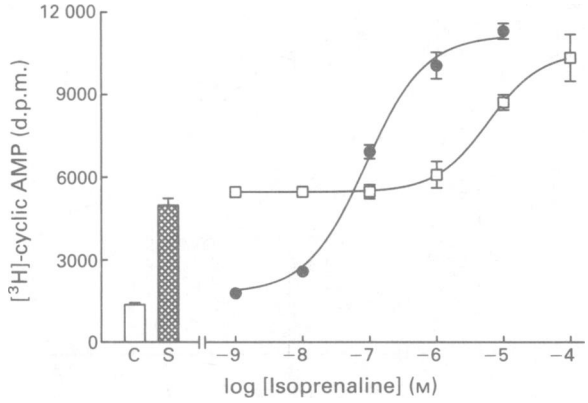

Figure 4 The effect of salmeterol on the [^{3}H]-cyclic AMP response to various concentrations of isoprenaline. Both drugs were added simultaneously to the assay system and the incubation continued for 10 min. The concentration-response curve for isoprenaline is shown in the absence (●) and presence (□) of 1 μM salmeterol. The basal accumulation of cyclic AMP and the response to 1 μM salmeterol are shown by the columns labelled C and S respectively. Each data point represents the mean ± s.e.mean of quadruplicate determinations. Where not shown, s.e.means were within the size of the symbol. This experiment was repeated 3 times with similar results.

simultaneously stimulated with various concentrations of isoprenaline in the presence or absence of 1 μM salmeterol (Figure 4). In the presence of salmeterol (1 μM), the response to high concentrations of isoprenaline (>0.1 μM) was attenuated by salmeterol. Analysis of these data yielded a value of 55.6 ± 28.2 nM ($n = 4$) for the dissociation constant (K_p) of the partial agonist, salmeterol.

Efflux of cyclic AMP from B50 cells

Whilst investigating the long term effects of salmeterol on cyclic AMP accumulation it became apparent that the second messenger accumulated in the extracellular medium. To investigate this phenomenon more closely, time courses for isoprenaline- and salmeterol-stimulated cyclic AMP accumulation were re-examined by analysing both extra- and intracellular [^{3}H]-cyclic AMP content obtained from supernatant layers and lysed cells respectively.

Figure 5 shows the time courses for the intracellular accumulation, excretion and total levels (intra- and extracellular) of cyclic AMP from B50 cells in the presence of isoprenaline (1 μM) or salmeterol (1 μM). In each case cyclic AMP accumulated rapidly within the cells, but after a variable lag period [^{3}H]-cyclic AMP levels in the extracellular fluid began to increase significantly. The basal accumulation of [^{3}H]-cyclic AMP was also monitored in all experiments at $t = 0$ and $t = 120$ min. During each 2 h assay period, the basal accumulation of both intra- and extracellular cyclic AMP was found to increase (1.3 ± 0.1 fold ($n = 3$) and 1.6 ± 0.2 fold ($n = 3$) respectively) due to the presence of rolipram in the incubation medium.

In B50 cells, after 5 min incubation with 1 μM isoprenaline, the total accumulation of cyclic AMP appeared to rise to a high steady-state level (Figure 5a). However, intracellular levels of cyclic AMP rose initially (7.0 ± 1.0 fold over basal levels, $n = 3$) but thereafter declined. After a 60 min incubation period for example, intracellular levels of the second messenger were only 14.7% of maximal levels (Figure 5a) and within 2 h levels of the second messenger had decreased to 6.2% of those measured at the peak of the response (Figure 5a). Profiles of time courses from several other experiments also showed this decrease in intracellular levels of cyclic AMP after the initial peak response. After 60 min and 120 min, intracellular levels of the second messenger were only 37.4% ± 11.4% and 17.4 ± 6.0% ($n = 3$) of those

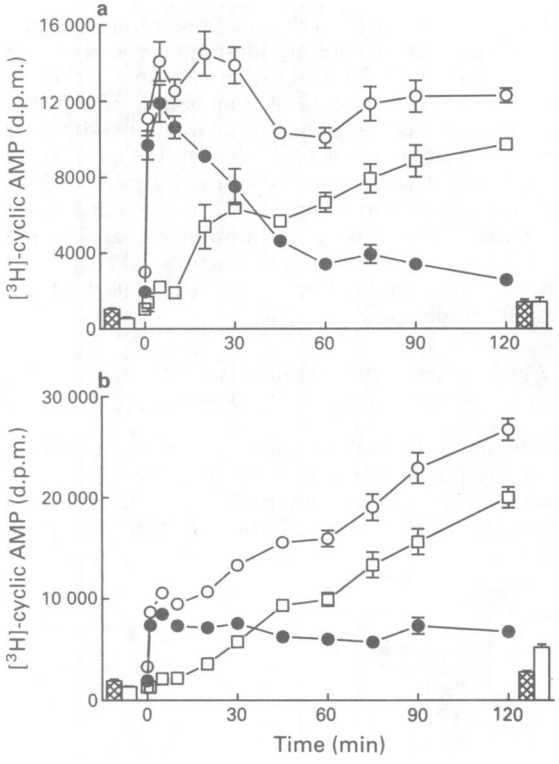

Figure 5 Time courses for the appearance of intracellular (●), extracellular (□) and total (intra- and extracellular) (○) [^{3}H]-cyclic AMP accumulation after stimulation of B50 cells with 1 μM isoprenaline (a) or 1 μM salmeterol (b) (drugs were added at $t = 0$). Extracellular cyclic AMP represents the [^{3}H]-cyclic AMP present in 1 ml of the incubation medium. The intracellular level of [^{3}H]-cyclic AMP was monitored by lysing the cells in an equal volume of freshly applied Hanks/HEPES medium (after removal of the incubation medium). The basal accumulation of intra- and extracellular [^{3}H]-cyclic AMP at $t = 0$ and $t = 120$ min are represented by the cross-hatched and open columns respectively. Data in each graph represent means ± s.e.mean of quadruplicate determinations in a single experiment. Where not shown, s.e.means were within the size of the symbol. All assays were repeated on at least 2 further occasions and similar results were obtained within each experiment.

measured at the peak of the response. Furthermore, the accumulation of intracellular cyclic AMP had fallen to 1.7 ± 0.4 fold over time-matched basal levels ($n = 3$) by the end of this incubation period. In contrast, after this 2 h incubation period extracellular levels of cyclic AMP were 5.0 ± 0.3 fold higher than time-matched basal values ($n = 3$) (Figure 5a).

A simple assay was then performed in order to determine whether the decrease in intracellular levels of [^{3}H]-cyclic AMP during these time course experiments was a consequence of uptake of isoprenaline into cells, metabolism of the drug or receptor desensitization. Cells were preincubated with 1 μM isoprenaline for 30 min. Cell monolayers were then washed twice with fresh prewarmed buffer before the cells were rechallenged with isoprenaline (1 μM) at $t = 40$ min. The accumulation of intra- and extracellular [^{3}H]-cyclic AMP was then assessed as before. Figure 6 shows that the removal of isoprenaline from the incubation medium led to a rapid decrease in both intra- and extracellular levels of cyclic AMP. After isoprenaline (1 μM) was re-introduced, the accumulation of cyclic AMP began to increase again both intra- and extracellularly. However, intracellular accumulation of cyclic AMP did not attain the initial peak value observed after the original application of isoprenaline. Instead, the profile of cyclic AMP accumulation mirrored that in which isoprenaline had not been washed out of the incubation medium (Figures 6 and 5a). These data support the idea that isoprenaline induces β_2-adrenoceptor desensitization in B50 cells.

In cell monolayers treated with salmeterol (1 μM), the total accumulation of cyclic AMP appeared to rise rapidly and increase in a linear manner during the 2 h assay period (Figure 5b). Intracellular levels of cyclic AMP also rapidly increased over a 5 min incubation period (3.3 ± 0.6 fold over basal levels, $n = 3$) (Figure 5b). However, the decline of intracellular cyclic AMP was less pronounced than that observed in isoprenaline-stimulated cells over longer periods of incubation (Figure 5b). After 60 min and 120 min, intracellular levels of cyclic AMP had decreased to $62.2 \pm 4.5\%$ and $72.6 \pm 20.3\%$ ($n = 3$) of those measured at the peak of the response. In addition, after this 2 h incubation period, levels of the second messenger remained 2.1 ± 0.3 fold higher than time-matched basal values ($n = 3$) (Figure 5b). Furthermore, the extracellular levels of cyclic AMP increased in a linear fashion and were 3.6 ± 0.3 fold higher ($n = 3$) than the equivalent control values 2 h after the application of salmeterol to these cells.

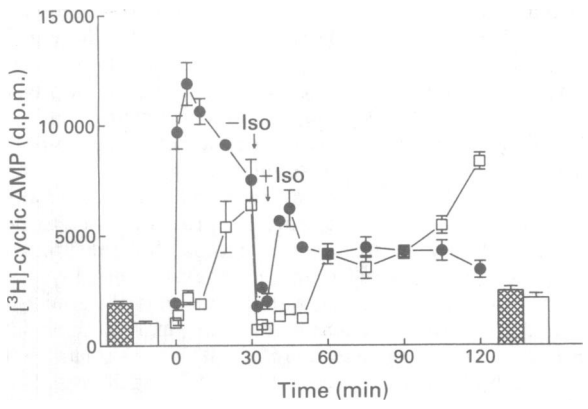

Figure 6 Influence of isoprenaline rechallenge on the time course of [^{3}H]-cyclic AMP accumulation. B50 cell monolayers were incubated with 1 μM isoprenaline for 30 min, washed twice with Hanks/HEPES buffer and re-stimulated with 1 μM isoprenaline at $t = 40$ min (as shown by the arrows). Intracellular (●) and extracellular (□) levels of cyclic AMP were measured throughout the 2 h incubation period. Basal levels of intra- and extracellular [^{3}H]-cyclic AMP at $t = 0$ and $t = 120$ min are represented by the cross-hatched and open columns respectively. Each point represents the mean ± s.e.mean of 4 determinations in a single experiment.

The long duration of action of salmeterol

B50 cell monolayers were incubated with either 1 μM isoprenaline or salmeterol for 5 min before the drug-containing buffer was removed, the cells washed twice and drug-free buffer was replaced in each well. As before, levels of intracellular, extracellular and basal cyclic AMP were determined during the assay period. Isoprenaline-stimulated cells showed a rapid decrease in total [^{3}H]-cyclic AMP accumulation after the removal of drug-containing media with levels of the second messenger returning to basal values within 5 min. Furthermore, intracellular levels of cyclic AMP also rapidly decreased over the same period and cyclic AMP extrusion was not observed during the 60 min assay period (Figure 7a).

However, in salmeterol-stimulated cells, removal of drug-containing media did not appear to alter the total accumulation of cyclic AMP (Figure 7b) which remained at a high level during the 2 h incubation period (Figure 7b). Profiles of the time courses showing intra- and extracellular [^{3}H]-cyclic AMP production were similar to those obtained when the cell monolayers had not been washed with drug-free buffer (Figures 7b and 5b). Levels of intracellular cyclic AMP measured after 60 min and 120 min were $48.8 \pm 3.7\%$ and $48.1 \pm 1.1\%$ respectively of those observed after the initial peak response ($n = 3$). At the end of the incubation period, intracellular levels of the second messenger were still 1.6 ± 0.2 fold higher than time-matched basal levels ($n = 3$)

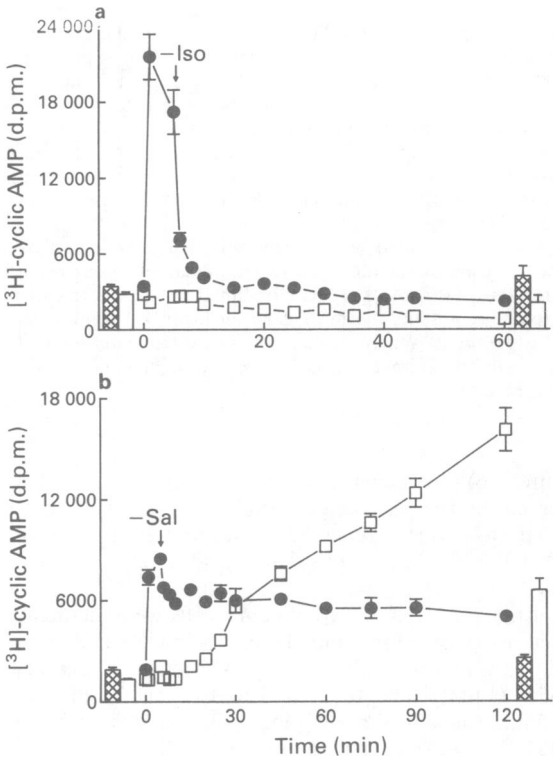

Figure 7 The effect of removing isoprenaline- and salmeterol-containing medium from the assay system on [^{3}H]-cyclic AMP accumulation. Isoprenaline (Iso, 1 μM) (a) or salmeterol (Sal, 1 μM) (b) was removed from the assay medium after a 5 min incubation (as shown by the arrow) by replacing the existing buffer with fresh prewarmed medium that contained rolipram (0.1 mM) but not salmeterol. Intracellular (●) and extracellular (□) levels of [^{3}H]-cyclic AMP were measured throughout the appropriate assay period as described in the Methods section. Basal levels of [^{3}H]-cyclic AMP measured at $t = 0$ and at the end of the appropriate assay period are represented by cross-hatched (intracellular) and open (extracellular) columns respectively. Data represent the means ± s.e.mean of quadruplicate determinations in a single experiment. Where not shown, s.e.means were within the size of the symbol. Similar results were obtained in 2 additional experiments.

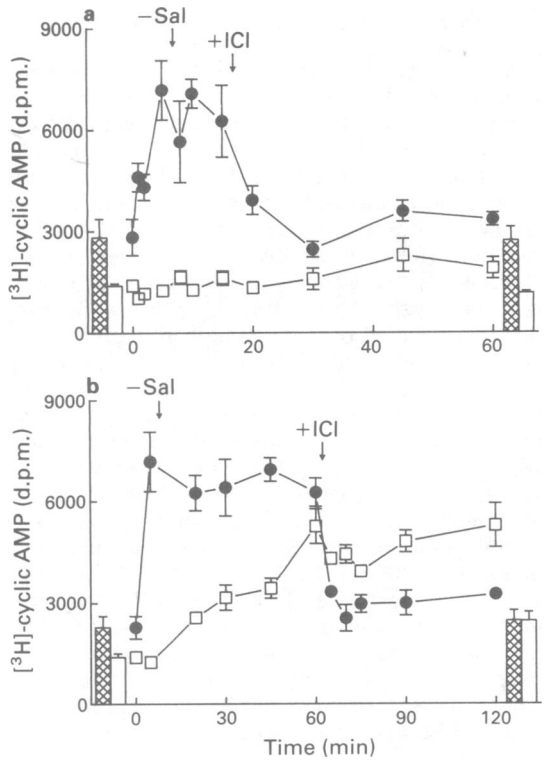

Figure 8 Influence of ICI 118551 challenge on the time course of [^{3}H]-cyclic AMP accumulation. Salmeterol (Sal, 1 μM)-containing buffer was removed from the assay medium after a 5 min incubation (as shown by the arrow) by washing twice with prewarmed Hanks/HEPES buffer (which contained 0.1 mM rolipram). ICI 118551 (1 μM) was then applied to each well at (a) $t = 15$ min or (b) $t = 60$ min (see arrows). Both intra- (●) and extracellular (□) levels of [^{3}H]-cyclic AMP were measured throughout the appropriate assay period. The basal accumulation of [^{3}H]-cyclic AMP measured at $t = 0$ and at the end of each assay period is represented by cross-hatched (intracellular) and open (extracellular) columns respectively. The results of (a) and (b) were obtained in the same experiment. Each point represents the mean ± s.e.mean of 4 determinations in a single experiment. Where not shown, s.e.means were within the size of the symbol. Similar results were obtained in 2 additional experiments.

(Figure 7b). A substantial portion of cyclic AMP was observed in the extracellular fluid. At the end of the 2 h incubation period cyclic AMP accumulation had risen to 2.9 ± 0.3 fold above equivalent basal levels ($n = 3$) (Figure 7b).

In a further series of experiments, cells were incubated with salmeterol (1 μM) for 5 min before being washed twice with fresh prewarmed buffer. The β_2-selective antagonist ICI 118551 (1 μM) was then added to each well at either $t = 15$ min or $t = 60$ min (Figure 8). In cells treated with 1 μM ICI 118551 at $t = 15$ min, intracellular levels of [^{3}H]-cyclic AMP rapidly returned to basal values and extracellular levels of [^{3}H]-cyclic AMP remained low (Figure 8a). Figure 8b shows that the response to salmeterol was well maintained following washout of drug-containing buffer until the administration of ICI 118551 at $t = 60$ min. At this point, intracellular levels of [^{3}H]-cyclic AMP rapidly fell towards basal values whereas the extracellular accumulation of cyclic AMP appeared to plateau, indicating that extracellular cyclic AMP was not rapidly metabolized by phosphodiesterases.

Discussion

Previous pharmacological studies have shown that salmeterol is a potent and highly selective β_2-adrenoceptor agonist with a long duration of action in guinea-pig (Ball *et al.*, 1991; Dougall *et al.*, 1991) and human (Ullman & Svedmyr, 1988a,b) airway smooth muscle. In this investigation we have examined some general features of salmeterol-stimulated cyclic AMP accumulation in the rat neuroblastoma B50 cell line (Schubert *et al.*, 1974). Monolayer cultures of this cell line provide a simple model system in which to investigate the effect of this long-acting agonist on β_2-adrenoceptor-stimulated cyclic AMP accumulation (Ruck *et al.*, 1990).

In the presence of rolipram (0.1 mM), an inhibitor of the cyclic AMP selective (type IV) phosphodiesterase isoenyzme (Reeves *et al.*, 1987; Donaldson *et al.*, 1988; Nicholson *et al.*, 1991), salmeterol potently stimulated cyclic AMP accumulation in B50 cell monolayers. The slope of the concentration-response curve to salmeterol was similar to that obtained with isoprenaline. However, salmeterol (EC_{50} 37 nM) was found to be 8 fold more potent than isoprenaline (EC_{50} 294 nM). The [^{3}H]-cyclic AMP response to salmeterol was potently antagonized by the β_2-selective antagonist, ICI 118551 (O'Donnell & Wanstall, 1980; Bilski *et al.*, 1983; Molenaar & Summers, 1987). The apparent K_D value for ICI 118551 (2.2 ± 0.7 nM), calculated assuming competitive antagonism, was similar to the value obtained for antagonism of the cyclic AMP response elicited by isoprenaline (K_D 1.6 ± 0.5 nM) which suggests that both drugs activate identical receptor populations. This K_D value agrees well with other β_2-adrenoceptor K_D values (0.5 nM in guinea-pig uterus: Bilski *et al.*, 1983; 0.6 nM in bovine trachea: Hall & Hill, 1988). In the presence of the β_1-selective antagonist, atenolol, the cyclic AMP response to both drugs was not altered. Taken together these results provide strong evidence that the cyclic AMP response to salmeterol is mediated via β_2-adrenoceptors.

It has previously been shown that salmeterol has a slower onset of action on airway smooth muscle than other β-adrenoceptor agonists including isoprenaline, salbutamol, clenbuterol and formoterol (Ball *et al.*, 1991; Dougall *et al.*, 1991) which is thought to be due to the lipophilicity of this large molecule. In B50 cells, however, maximal accumulation of [^{3}H]-cyclic AMP was rapid in response to both salmeterol ($t_{1/2}$ 1.13 min) and isoprenaline ($t_{1/2}$ 0.44 min). This rapid onset of action by salmeterol in B50 cells is likely to be a consequence of the use of cell monolayers which significantly reduces the diffusion barriers that exist when a drug is introduced into a tissue environment.

A direct comparison of concentration-response curves to both drugs indicated that salmeterol was capable of generating only 46% of the cyclic AMP response elicited by a maximal concentration of isoprenaline. This suggests that salmeterol behaves as a partial agonist in this system. This finding agrees well with a previous investigation that also showed that salmeterol has a lower efficacy than isoprenaline for β_2-adrenoceptors in guinea-pig tracheal strips (Ball *et al.*, 1991; Dougall *et al.*, 1991). Since salmeterol is also more potent than isoprenaline in stimulating cyclic AMP accumulation in B50 cells, salmeterol appears to have a higher affinity than isoprenaline for the β_2-adrenoceptor. In order to determine the affinity of this partial agonist for the β_2-adrenoceptor, full/partial agonist interactions were employed. The pattern obtained was as expected for a partial agonist. Our estimate from this interaction of the apparent dissociation constant (K_p) for salmeterol (55.6 nM) was similar to that estimated by Coleman *et al.* (1990) and Dougall *et al.* (1991).

Whilst investigating the duration of action of salmeterol in B50 cells it was noted that a substantial portion of the cyclic AMP produced by these monolayers in response to both salmeterol and isoprenaline accumulated in the extracellular medium. Cyclic AMP efflux systems have been observed in some bacteria and a variety of cultured animal cells (Makman & Sutherland, 1965; King & Mayer, 1974; Mawe *et al.*, 1974; Rindler *et al.*, 1978; Marley *et al.*, 1991). In B50 cells stimulated by either agonist there was a rapid elevation of intracellular cyclic AMP but extracellular levels of this

second messenger appeared only after a short lag period (5–10 min). After the initial increase in intracellular cyclic AMP in isoprenaline-stimulated cells (10 min incubation period), levels of the second messenger began to decrease in a linear fashion over a 2 h interval whereas extracellular levels of cyclic AMP continued to rise over the same period. In intact cellular systems, intracellular cyclic AMP would normally be expected to achieve a plateau level (even in the presence of a competitive phosphodiesterase inhibitor such as rolipram) at which a steady state is reached between cyclic AMP synthesis and cyclic AMP breakdown via phosphodiesterase (Donaldson *et al.*, 1988). Consequently, this decrease in intracellular cyclic AMP levels following β_2-adrenoceptor stimulation may be due to reduced cyclic AMP synthesis as a consequence of ongoing receptor desensitization (Leftkowitz *et al.*, 1990), uptake of isoprenaline into B50 cells and metabolism of the drug during the 2 h assay period or it may be secondary to the activation of cyclic AMP extrusion mechanisms. In this latter case, a new steady state level of cyclic AMP would be established within B50 cells following the development of an additional cyclic AMP removal mechanism.

The idea that receptor desensitization is being observed is supported by data from an experiment in which isoprenaline was removed from the incubation medium but cells were then rechallenged with the same dose of β-agonist (1 μM). After cell monolayers were exposed to a second stimulation by isoprenaline, intracellular [^{3}H]-cyclic AMP accumulation did increase but not to the levels observed after the initial challenge of isoprenaline. Instead, levels of cyclic AMP were similar to the accumulation of cyclic AMP measured in cells that had not undergone a washing process and renewed stimulation with isoprenaline, suggesting that receptor desensitization mechanisms are operating in B50 cells following isoprenaline stimulation.

β_2-Adrenoceptors in B50 monolayers stimulated by salmeterol did not appear to undergo such rapid desensitization since intracellular levels of cyclic AMP were maintained above basal values throughout the assay period although some reduction in cyclic AMP accumulation was observed during the 2 h incubation period. Furthermore, the level of extracellular cyclic AMP (which does not appear to be broken down rapidly by phosphodiesterases; cf. Figure 8) continues to increase almost linearly (indicative of substantial on-going cyclic AMP synthesis) between 30 and 120 min following salmeterol administration. This reduced degree of desensitization (compared to isoprenaline) may be a consequence of the lower efficacy of salmeterol. Alternatively, it is possible that the lipophilic nature of this β_2-agonist might alter the conformation of the agonist-receptor complex and thus sterically hinder phosphorylation of particular amino acid residues on the β_2-adrenoceptor by protein kinase A and β-adrenoceptor kinase or inhibit the putative functioning of β-arrestin in uncoupling the receptor from G_S (Lefkowitz *et al.*, 1990).

It is possible that the extrusion phenomenon serves, along with phosphodiesterase activity, to maintain low intracellular concentrations of cyclic AMP. Furthermore, extracellular cyclic AMP may have an important physiological role. Receptors for cyclic AMP are thought to be located on the external surfaces of plasma membranes in *Euglena* (Carré & Edmonds, 1992) and four cyclic AMP receptor subtypes (cAR1-4) have been cloned and sequenced in *Dictyostelium* (Klein *et al.*, 1988; Saxe *et al.*, 1991a,b). The efflux process appears to involve an active transport mechanism which depends on a chemical source of energy such as ATP (Doore *et al.*, 1975). Rindler *et al.* (1978) have shown that inhibitors of mitochondrial function and glycolysis (e.g. oligomycin, valinomycin and FCCP) reduced ATP concentrations in C6 rat glioma cells and avian erythrocytes and cyclic AMP efflux was inhibited by a corresponding degree.

Although cyclic AMP efflux exists in B50 cells, it is still possible to study the long term effects of salmeterol in these monolayers by measuring intracellular cyclic AMP accumulation. In isoprenaline-treated cells that had been washed with drug-free medium after a 5 min stimulatory period, intracellular cyclic AMP levels rapidly decreased towards basal values. Furthermore, cyclic AMP efflux from these cells was negligible indicating that isoprenaline is easily removed from its site of action by this simple washing process. When the same procedure was performed on salmeterol-stimulated cells, intracellular levels of cyclic AMP were sustained above basal values and extrusion of cyclic AMP from B50 cells was observed. Overall the profile of cyclic AMP production and excretion was similar to that in which salmeterol stimulation of cells had been maintained. These data are consistent with the hypothesis (Jack, 1991; Ball *et al.*, 1991) that the lipophilic nature of this molecule allows it to anchor at the putative 'exo-site' within the β_2-adrenoceptor protein and from which it cannot be displaced by washing with drug-free medium, thereby allowing salmeterol to persist at its site of action. However, as has been observed in guinea-pig trachea (Ball *et al.*, 1991), the action of salmeterol can nevertheless be reversed by the administration of a β_2-selective antagonist (ICI 118551).

In conclusion, salmeterol appears to be a potent and selective β_2-adrenoceptor agonist with a long duration of action in B50 cells *in vitro*. It behaves as a partial agonist in this system and since it is more potent than isoprenaline in stimulating cyclic AMP accumulation in these cells, this suggests that salmeterol has a higher affinity than isoprenaline for the β_2-adrenoceptor. However, it is intriguing that there is no obvious sign of receptor desensitization over a 120 min period of stimulation despite the continued presence of salmeterol at its site of action.

We thank Malcolm Johnson for helpful discussions and Glaxo Group Research Ltd. for financial support.

References

BALL, D.I., BRITTAIN, R.T., COLEMAN, R.A., DENYER, L.H., JACK, D., JOHNSON, M., LUNTS, L.H.C., NIALS, A.T., SHELDRICK, K.E. & SKIDMORE, I.F. (1991). Salmeterol, a novel, long-acting β_2-adrenoceptor agonist: characterization of pharmacological activity *in vitro* and *in vivo*. *Br. J. Pharmacol.*, **104**, 665–671.

BARNES, P.J. (1986). Bronchodilator mechanisms. In *Asthma: Clinical Pharmacology and Therapeutic Progress*. ed. Kay, A.B. pp. 146–160. Oxford: Blackwell.

BARNES, P.J., IND, P.W. & DOLLERY, C.T. (1984). Beta-adrenoceptors in asthma and their responses to agonists. In *Asthma: Physiology, Immunopharmacology and Treatment*. ed. Kay, A.B., Austen, K.F. & Lichtenstein, L.M. pp. 339–358. London: Academic Press.

BILSKI, A.J., HALLIDAY, S.E., FITZGERALD, J.D. & WALE, J.C. (1983). The pharmacology of a β_2-selective adrenoceptor antagonist ICI 118,551. *J. Cardiovasc. Res.*, **5**, 430–437.

BIRNBAUMER, L. (1990). G proteins in signal transduction. *Annu. Rev. Pharmacol. Toxicol.*, **30**, 675–705.

BRADSHAW, J., BRITTAIN, R.T., COLEMAN, R.A., JACK, D., KENNEDY, I., LUNTS, L.H.C. & SKIDMORE, I.F. (1987). The design of salmeterol, a long-acting selective β_2-adrenoceptor agonist. *Br. J. Pharmacol.*, **92**, 590P.

BRITTAIN, R.T. (1990). Approaches to a long-acting, selective β_2-adrenoceptor stimulant. *Lung*, **168**, 111–114.

CARRÉ, I.A. & EDMUNDS, L.N. Jr. (1992). cAMP-dependent kinases in the algal flagellate *Euglena gracilis*. *J. Biol. Chem.*, **267**, 2135–2137.

COLEMAN, R.A., JOHNSON, M., NIALS, A.T. & SUMNER, M.J. (1990). Salmeterol, but not formoterol, persists at β_2-adrenoceptors *in vitro*. *Br. J. Pharmacol.*, **99**, 121P.

DONALDSON, J. BROWN, A.M. & HILL, S.J. (1988). Influence of rolipram on the cyclic 3',5'-adenosine monophosphate response to histamine and adenosine in slices of guinea-pig cerebral cortex. *Biochem. Pharmacol.*, **37**, 715–723.

DOORE, B.J., BASHER, M.M., SPITZER, N., MAWE, R.C. & SAIER, M.H. Jr. (1975). Regulation of adenosine 3':5'-monophosphate efflux from rat glioma cells in culture. *J. Biol. Chem.*, **250**, 4371–4372.

DOUGALL, I.G., HARPER, D., JACKSON, D.M. & LEFF, P. (1991). Estimation of the efficacy and affinity of the β_2-adrenoceptor agonist salmeterol in guinea-pig trachea. *Br. J. Pharmacol.*, **104**, 1057–1061.

GILMAN, A.G. (1987). G proteins: transducers of receptor-generated signals. *Annu. Rev. Biochem.*, **56**, 615–649.

HALL, I.P. & HILL, S.J. (1988). β-adrenoceptor stimulation inhibits histamine-stimulated inositol phospholipid hydrolysis in bovine tracheal smooth muscle. *Br. J. Pharmacol.*, **95**, 1204–1212.

JACK, D. (1991). A way of looking at agonism and antagonism: lessons from salbutamol, salmeterol and other β-adrenoceptor agonists. *Br. J. Clin. Pharmacol.*, **31**, 501–514.

KING, C.D. & MAYER, S.E. (1974). Inhibition of egress of adenosine 3',5'-monophosphate from pigeon erythrocytes. *Mol. Pharmacol.*, **10**, 941–953.

KLEIN, P., SUN, J.J., SAXE, C.L., KIMMEL, A.R., JOHNSON, R.L. & DEVREOTES, P.N. (1988). A chemoattractant receptor controls development in *Dictyostelium discoideum*. *Science*, **241**, 1467–1472.

KUME, H., TAKAI, A., TOKUNO, H. & TOMITA, T. (1989). Regulation of Ca^{2+} dependent K^+ channel activity in tracheal myocytes by phosphorylation. *Nature*, **341**, 152–154.

LAZERENO, S. & ROBERTS, F.F. (1987). Measuring muscarinic antagonist potency using stimulated phosphoinositide breakdown in rat cortex slices. *Br. J. Pharmacol.*, **92**, 677P.

LEFKOWITZ, R.J., HAUSDORFF, W.P. & CARON, M.G. (1990). Role of phosphorylation in desensitization of the β-adrenoceptor. *Trends Pharmacol. Sci.*, **11**, 190–194.

MAKMAN, R.S. & SUTHERLAND, E.W. (1965). Adenosine 3',5'-cyclic monophosphate in E. coli. *J. Biol. Chem.*, **240**, 1309–1314.

MARLEY, P.D., THOMSON, K.A., JACHNO, K. & JOHNSTON, M.J. (1991). Histamine-induced increases in cyclic AMP levels in bovine adrenal medullary cells. *Br. J. Pharmacol.*, **104**, 839–846.

MAWE, R., DOORE, B., McCAMAN, M., FEUCHT, B. & SAIER, M. (1974). Regulation of cyclic AMP excretion in bacteria and cultured animal cells. *J. Cell Biol.*, **63**, 211a.

McCREA, K.E., JOHNSON, M. & HILL, S.J. (1992). The effect of salmeterol on cyclic AMP accumulation in a neuronal cell line. *Br. J. Pharmacol.*, **104**, 249P.

MOLENAAR, P. & SUMMERS, R.J. (1987). Characterization of $beta_1$ and $beta_2$ adrenoceptors in guinea-pig atrium: functional and receptor binding studies. *J. Pharmacol. Exp. Ther.*, **241**, 1041–1047.

NICHOLSON, C.D., CHALLISS, R.A.J. & SHAHID, M. (1991). Differential modulation of tissue function and therapeutic potential of selective inhibitors of cyclic nucleotide phosphodiesterase isoenzymes. *Trends Pharmacol. Sci.*, **12**, 19–27.

O'DONNELL, S.R. & WANSTALL, J.C. (1980). Evidence that ICI 118,551 is a potent highly β_2-selective adrenoceptor antagonist and can be used to characterize beta-adrenoceptor populations in tissues. *Life Sci.*, **27**, 671–677.

REEVES, M.L., LEIGH, B.K. & ENGLAND, P.J. (1987). The identification of a new cyclic nucleotide phosphodiesterase in human and guinea-pig cardiac ventricle. *Biochem. J.*, **241**, 537–543.

RINDLER, M.J., BASHOR, M.M., SPITZER, N. & SAIER, M.H. Jr. (1978). Regulation of adenosine 3',5'-monophosphate efflux from animal cells. *J. Biol. Chem.*, **253**, 5431–5436.

RUCK, A., MILLNS, P., KENDALL, D.A. & HILL, S.J. (1990). Expression of β_2-adrenoceptors mediating cyclic AMP accumulation in astroglial and neuronal cell lines derived from the rat CNS. *Biochem. Pharmacol.*, **40**, 2371–2375.

SAXE, C.L., JOHNSON, R.L., DEVREOTES, P.N. & KIMMEL, A.R. (1991a). Multiple genes for cell surface cAMP receptors in *Dictyostelium discoideum*. *Dev. Genet.*, **12**, 6–13.

SAXE, C.L., JOHNSON, R.L., DEVREOTES, P.N. & KIMMEL, A.R. (1991b). Expression of a cAMP receptor gene of *Dictyostelium* and evidence for a multi gene family. *Genes Dev.*, **5**, 1–8.

SCHUBERT, D., HEINEMANN, S., CARLISLE, W., TARIKAS, H., KIMES, B., PATRICK, J., STEINBACH, J.H., CULP, W. & BRANDT, B.L. (1974). Clonal cell lines from the rat central nervous system. *Nature*, **249**, 224–227.

STEPHENSON, R.P. (1956). A modification of receptor theory. *Br. J. Pharmacol. Chemother.*, **11**, 379–393.

ULLMAN, A. & SVEDMYR, N. (1988a). Salmeterol, a new long acting inhaled β_2-adrenoceptor agonist: comparison with salbutamol in adult asthmatic patients. *Thorax*, **43**, 674–678.

ULLMAN, A. & SVEDMYR, N. (1988b). Inhaled salmeterol a new β_2-adrenoceptor agonist produces sustained bronchodilation in asthmatic patients without causing tachyphylaxis. *Am. Rev. Resp. Disease*, **137**, 32.

(Received March 15, 1993
Revised May 17, 1993
Accepted June 2, 1993)

Br. J. Pharmacol. (1993), **110**, 627–632

The effect of nitric oxide on the efficacy of synaptic transmission through the chick ciliary ganglion

T.R.D. Scott & [1]M.R. Bennett

The Neurobiology Laboratory, Department of Physiology, University of Sydney, N.S.W. 2006, Australia

1 The effect of nitric oxide on the efficacy of synaptic transmission in the chick ciliary ganglion of post-hatched birds has been determined by use of the size of the postganglionic compound action potential resulting from chemical transmission through the ganglion as a measure of synaptic efficacy.

2 Sodium nitroprusside (100 μM) increased the synaptic efficacy by an average 26%. This is likely to be due to its ability to release nitric oxide, as potassium ferricyanide (100 μM) did not cause a potentiation. Sodium azide (100 μM), shown in sympathetic ganglia to stimulate production of cyclic GMP, did not modulate synaptic efficacy significantly.

3 8-Br-cyclic-GMP (100 μM) increased synaptic efficacy by an average 61%. The addition of 8-Br-cyclic-AMP (100 μM) had less effect, increasing transmission by on average 46%.

4 The nitric oxide synthase blocker, N^G-nitro-L-arginine methyl ester (L-NAME, 100 μM) was added prior to the tetanic stimulation of the preganglionic nerves at 30 Hz for 20 s, a procedure known to produce both post-tetanic potentiation and long-term potentiation of synaptic transmission through the ganglion. L-NAME reduced the long-term potentiation by an average of 47% but did not significantly change the post-tetanic potentiation.

5 Following the brief application of 8-Br-cyclic AMP, 8-Br-cyclic GMP and sodium nitroprusside there was an enhancement of the efficacy of synaptic transmission that persisted after the withdrawal of the drugs. The maximum increase in synaptic efficacy following the brief addition of 8-Br-cyclic GMP was 116%, sodium nitroprusside was 110% and 8-Br-cyclic AMP was 126%.

6 These results suggest that nitric oxide modulates synaptic transmission through the ganglion by acting on an endogenous guanylate cyclase that produces cyclic GMP.

Keywords: Nitric oxide; ciliary ganglia; cyclic GMP

Introduction

Nitric oxide has been implicated in the maintenance of long-term potentiation (LTP) in the hippocampus (see for example, Haley *et al.*, 1992). As a form of LTP occurs in the avian ciliary ganglion (Scott & Bennett, 1993), it is possible that a component of the maintenance of this LTP is also due to nitric oxide. In avian ciliary neurones, nitric oxide synthase is exclusively found in the giant nerve terminal calyx in the avian ciliary ganglion (Chan, 1992), so that it is unlikely that nitric oxide acts as a retrograde messenger in the way that has been suggested in CA1 pyramidal neurones in the hippocampus (for a review see, Bredt & Snyder, 1992). Nevertheless, nitric oxide is known to decrease calcium-activated potassium currents in the ganglion by a mechanism that is independent of any effect on the calcium influx through calcium channels (Cetiner & Bennett, 1992). This result supports the hypothesis that nitric oxide might act to increase transmitter secretion by increasing the duration of the terminal action potential following blockade of the fast calcium-dependent potassium current, I_c. Such a mechanism has been suggested to underly the potentiation of transmitter secretion from nerve terminals in *Aplysia* neurones (Kandel & Hawkins, 1992). One problem with this idea is that nitric oxide also decreases the transient and sustained whole-cell calcium currents in the ganglion (Khurana & Bennett, 1993). Thus on the one hand calcium influx across the nerve terminal membrane may be increased by nitric oxide to increase the duration of the action potential and therefore the open time of voltage-sensitive calcium channels. On the other hand however, these channels themselves may be depressed, thus decreasing the calcium influx. In the present work it is shown that an endogenous nitric oxide synthase in the nerve terminal of the ganglion does play a role in the maintenance of LTP and the method by which this might occur is investigated.

[1]Author for correspondence.

Methods

One to five day post-hatched white leghorn chicks (*Gallus gallus*) were used in all experiments. Animals were decapitated and a craniectomy performed to expose the right ciliary ganglion. The ciliary ganglion with the attached right eye and oculomotor nerves were removed. The right eye was dissected to free the ciliary nerve from within the eye (see Pilar & Tuttle, 1982 for a further description of the dissection). The ciliary ganglion with its attached oculomotor and ciliary nerves were then placed in a tissue bathing chamber. The bath was perfused at a rate of approximately 2 ml min^{-1} with Tyrode solution of the following composition (in mM): Na^+ 140, K^+ 5, Mg^{2+} 1, Ca^{2+} 3, Cl^- 153, glucose 10, HEPES 10, equilibrated by bubbling with 95% O_2, 5% CO_2 and pH adjusted to 7.2–7.4 with NaOH. Stimulation was applied to the oculomotor nerve through a glass suction electrode. The application of the stimulating pulse (a square wave of 14 V and duration 0.09 ms) was through a radio-frequency isolation unit. Experiments were conducted at room temperature (17 to 20°C).

Recordings of compound action potentials from the postganglionic ciliary nerve were made by using a fine suction electrode. Signals obtained from this nerve were amplified by an Axoclamp 2A amplifier (Axon Instruments). These signals were digitized using a Labmaster A-D board and recorded and analysed on an IBM-compatible computer using the pCLAMP (Fetchex, Fetchan) software package (Axon Instruments).

Drugs used here were hexamethonium chloride, 8-

bromoadenosine 3':5'-cyclic monophosphate (8-Br-cyclic AMP), 8-bromoguanosine 3':5'-cyclic monophosphate (8-Br-cyclic GMP), sodium azide (NaN_3), potassium ferricyanide (FCN), sodium nitroprusside (SNP) and N^G-nitro-L-arginine methyl ester (L-NAME). These were purchased from Sigma Chemical Company.

Hexamethonium (300 μM), a nicotinic cholinoceptor antagonist, was routinely added to the bathing solution in order to reduce the size of the chemical component of the biphasic compound action potential. Supramaximal stimulation was applied to the preganglionic oculomotor nerve. The reduction in the compound action potential by hexamethonium permitted measurement of an increase in synaptic efficacy. An increase in the synaptic efficacy, such as that which might follow tetanic stimulation during post-tetanic potentiation (PTP) and LTP, or following the addition of a potentiating drug, was reflected by a significant increase in the number of the postsynaptic population reaching action potential firing threshold. This was indicated by an increase in the amplitude of the chemical component of the compound action potential.

Protocols for the measurement of LTP and PTP were followed routinely. Upon the attachment of the suction electrodes to the pre- and postganglionic nerves, the preganglionic oculomotor nerve was stimulated at a frequency of 0.033 Hz. Only preparations with evoked compound action potentials larger than 1 mV were used. Hexamethonium (300 μM) was then added to the bathing solution. This was allowed to perfuse the ganglion for at least 60 min so that the chemical phase of the compound action potential could be reduced (by at least 60% of its original value) and a control measurement for its amplitude established. The preparation was stimulated at 0.033 Hz during this period.

Activity-dependent potentiation was produced by tetanic stimulation of 30 Hz for 20 s and applied following the establishment of a control level of synaptic efficacy. It has been shown that the frequency of this tetanic stimulation occurs within the normal operating range of ciliary ganglia (Fujii, 1992). Following tetanic stimulation of the ciliary ganglion, recordings of the PTP and LTP time courses were made by measuring the amplitude of the chemical phase of the evoked compound action potential. Addition of drugs to the bathing solution was carried out at least 60 min after the previous tetanic stimulation. Any drug was allowed to perfuse the ganglion for at least 60 min before tetanic stimulation was reapplied.

For the brief exposure of the ganglia to NO, 8-Br-cyclic AMP and 8-Br-cyclic GMP (as defined by the horizontal bars in Figure 3), the drug was applied directly to the bath and then quickly washed from the bath. A test was made to ensure that any change in synaptic efficacy in these experiments was due to the drug action, and not to another factor to do with the exchange and washing. This involved the addition of normal bath solution directly to the bath for 3 min followed by the same washing procedure as used with drug application. No change in the synaptic efficacy was observed over the time course of an hour indicating that the effects of the brief drug addition were the result of the drugs action.

The ordinates of the figures are expressed in terms of percentage of control. A control value (V_{ctl}) was obtained by averaging the amplitude of the chemical component of the compound action potential for the 15 min prior to drug addition or tetanic stimulation (measured by evoking compound action potentials at a frequency of 0.033 Hz). Following this, compound action potentials were again evoked at a frequency of 0.033 Hz. The amplitudes of these post-tetanic compound action potentials (V) were measured. The percentage increase was calculated as:

$$\% \text{ of control} = 100 \times \frac{V}{V_{ctl}}$$

Data are expressd as mean ± standard error of the mean (s.e.mean) and n gives the number of experiments. The significance of the difference between n pairs of observations made before and after application of a drug was calculated by Student's paired t test. P values of 0.05 or less were considered to represent significant differences.

Results

The efficacy of transmission through the ciliary ganglion was determined as described previously (Scott & Bennett, 1993). The size of the compound action potential recorded in the postganglionic ciliary nerve due to chemical transmission

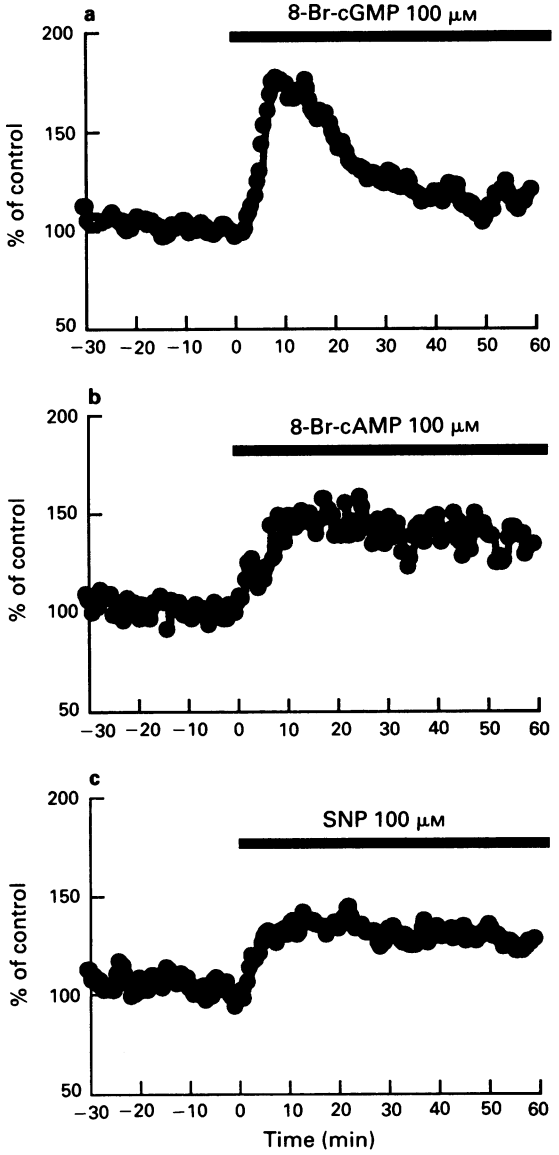

Figure 1 The effects of 8-Bromo-cyclic GMP (8-Br-cGMP), 8-bromo-cyclic AMP (8-Br-cAMP) and sodium nitroprusside (SNP) on transmission through the ciliary ganglion. The ordinate scale gives the percentage of the amplitude of the chemical component of the compound action potential with respect to its amplitude during the control period recorded from the postganglionic ciliary nerve. Measurement is made by stimulating at 30 s intervals and the control amplitude is established by averaging these recordings for 15 min before application of the drug or tetanic stimulation. (a) Shows the effect of addition of 100 μM 8-Br-cyclic GMP at time zero; (b) shows the effect of the addition of 100 μM 8-Br-cyclic AMP at time zero; (c) shows the effect of the addition of 100 μM SNP at time zero. The horizontal bar indicates the time of application of the respective drugs.

through the ganglion in the presence of 300 μM of hexamethonium was used as a measure of synaptic efficacy. The oculomotor nerve was stimulated every 30 s and the size of the chemical component of the action potential noted. Application of 100 μM 8-Br-cyclic GMP increased the synaptic efficacy in all 5 ganglia studied, with an average increase of 61 ± 31% (Figure 1a). Application of 100 μM of 8-Br-cyclic AMP also enhanced transmission through the ganglion, by an average of 46 ± 20% in 5 experiments (Figure 1b).

In order to determine if an endogenous nitric oxide-sensitive, soluble guanylate cyclase was likely to be present in the ganglion for the production of cyclic GMP, sodium nitroprusside (100 μM) was applied to the preparation. This increased the size of the compound action potential by an average of 26 ± 12% in 12 ganglia (Figure 1c). Sodium azide (100 μM), an agent shown to stimulate the formation of cyclic GMP in sympathetic ganglia (Quenzer *et al.*, 1980a,b; Ariano *et al.*, 1982; Ando *et al.*, 1983; Volle & Quenzer, 1983), was applied to the ganglion in five experiments. Surprisingly, this showed no significant effect on the efficacy of synaptic transmission. The action of sodium azide in stimulating cyclic GMP formation is known to be much less effective in autonomic ganglia than is the action of sodium nitroprusside (Quenzer *et al.*, 1980a). In order to check that the effects of sodium nitroprusside ($Na_2Fe(CN)_5NO$) were due to its production of nitric oxide, five ganglia were bathed in 100 μM potassium ferricyanide ($K_3Fe(CN)_6$). There was no change in the compound action potential.

The existence of a nitric oxide-sensitive system in the ganglion, presumably operating through cyclic GMP, raises the question of whether an endogenous nitric oxide modulates transmission. In order to test this, the nitric oxide synthase blocker L-NAME (100 μM) was added to the preparation,

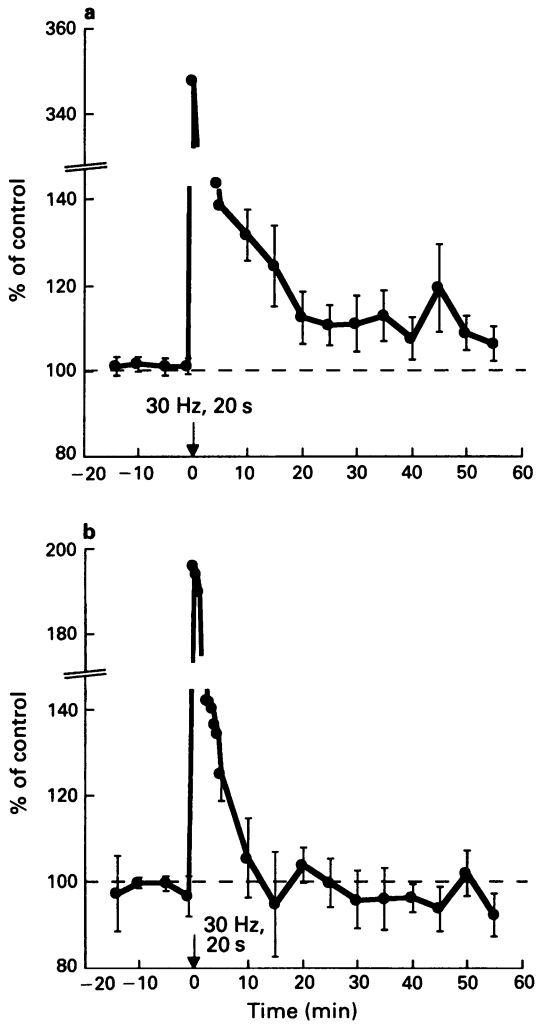

Figure 2 The effect of blocking nitric oxide synthase with N^G-nitro-L-arginine methyl ester (L-NAME) on post-tetanic potentiation and long-term potentiation of chemical transmission in the ganglion. The ordinate scale gives the percentage of control of the chemical component of the compound action potential as in Figure 1. Each point represents the mean ± s.e.mean for five experiments. (a) Tetanic stimulation of the ganglion at 30 Hz for 20 s produces the usual post-tetanic and long-term potentiation time courses; (b) the same ganglia were perfused for at least 60 min with 100 μM L-NAME and tetanic stimulation was reapplied to the presynaptic oculomotor nerve.

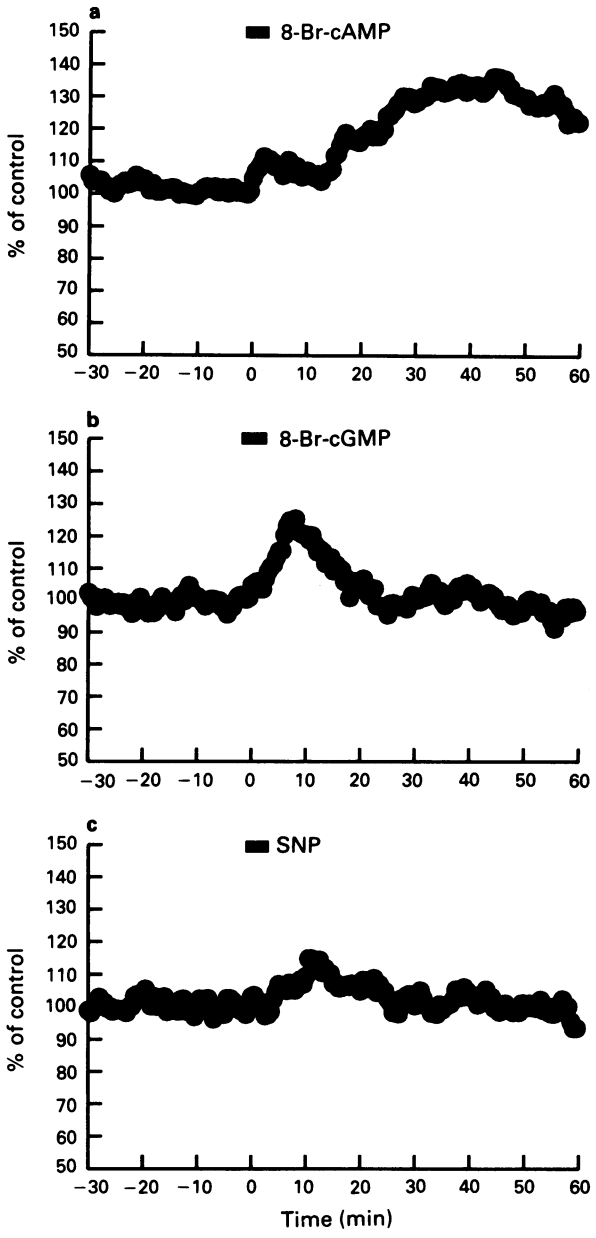

Figure 3 The result of a brief application of 8-bromo-cyclic AMP (8-Br-cAMP), 8-bromo-cyclic GMP (8-Br-cGMP), and sodium nitroprusside: (a) exposure of the ganglion to 1 mM 8-Br-cyclic AMP for 3 min at time zero increased the efficacy of synaptic transmission which was maximal at time 40 min and measured as 134% of the control in this case. (b) Exposure of the ganglion to 1 mM 8-Br-cyclic GMP for 3 min at time zero increased the efficacy of synaptic transmission which was maximal at time 10 min and measured as 125% of the control in this case. (c) Exposure of the ganglion to 1 mM sodium nitroprusside (SNP) for 3 min at time zero increased the efficacy of synaptic transmission which was maximal at time 10 min and measured as 114% of the control in this case.

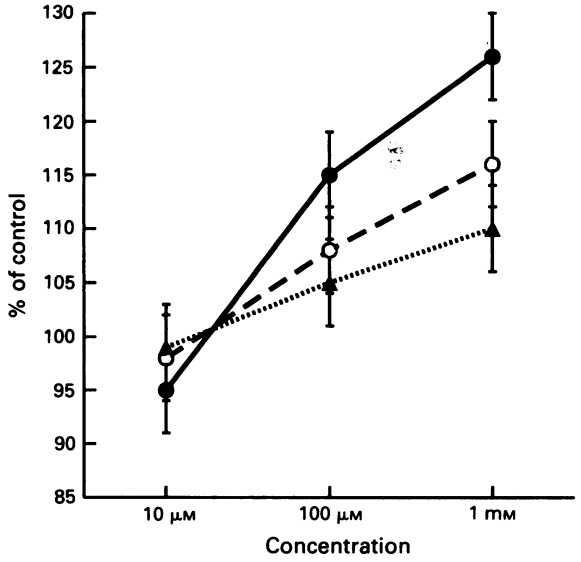

Figure 4 The dose-response curve of the maximal increase in the efficacy of synaptic transmission following drug exposure at the indicated concentration for 3 min. The maximal responses for cyclic AMP (●), cyclic GMP (○) and sodium nitroprusside (▲) exposure were taken at time 40 min, 10 min and 10 min respectively after initial drug exposure.

and the effect of this on transmission and potentiation monitored. L-NAME did not affect transmission through the ganglia but it did significantly decrease LTP by an average of 48% ± 13% in 5 preparations ($P < 0.05$; Figure 2). There was no significant effect on PTP ($P > 0.25$). In one preparation the LTP doubled in the presence of L-NAME; we have no explanation for this.

Given that NO, cyclic GMP and cyclic AMP are likely to be involved in the enhancement of synaptic efficacy, ganglia were exposed for 3 min to each of these drugs at a concentration of 1 mM to see whether the resultant potentiation would be maintained following the drug removal (Figure 3). Application of 1 mM 8-Br-cyclic AMP produced a slowly increasing potentiation that reached a maximum of 126 ± 4% of control ($n = 3$) at time 40 min (Figure 3a). The exposure of the ganglion to 8-Br-cyclic GMP produced a potentiation that was maximal at 10 min after the drug application to a value of 116 ± 7% of control ($n = 3$; Figure 3b). The potentiation produced by SNP reached a maximal level 10 min after stimulation (110 ± 2%; $n = 3$; Figure 3c). Both the 8-Br-cyclic AMP and SNP evoked effects returned to control levels approximately 25 min after drug application. Each of the potentiations resulting from the actions of these drugs was proportional to the drug concentration over the range 10 μM to 1 mM (Figure 4).

Discussion

Nicotinamide adenine dinucleotide phosphate (NADPH) diaphorase (Dawson *et al.*, 1991; Hope *et al.*, 1991) can be used as a marker for neurones that contain NO synthase. In the autonomic nervous system such neurones are found in the intermedio-lateral cell column of the spinal cord giving rise to the preganglionic sympathetic nerves (Valtschanoff *et al.*, 1992; Blottner & Baumgarten, 1992) and in pelvic ganglia, as well as in the intramural plexuses of the gastrointestinal tract and lower urinary tract (Grozdanovic *et al.*, 1992). Antibodies to nitric oxide synthase have confirmed these findings with NADPH-diaphorase histochemistry (Bredt *et al.*, 1990) as well as allowing for its ultrastructural localization. This has shown that the synthase is not associated with any subcellular organelle or with the plasma membane (Llewellyn-Smith *et al.*, 1992), but is patchily distributed in both the neurone cell bodies as well as in nerve terminals. NADPH-positive stained neurones are found throughout the ciliary ganglion of avian embryos but are restricted to the superficial layers of the ganglion after hatching (Scott *et al.*, 1992). Ultrastructural localisation of antibodies to the synthase show that it is exclusively found in the giant calyciform preganglionic terminal on the ciliary neurones, with no antibody in the neurone somas (Chan, 1992). Therefore, it appears very likely that nitric oxide may act as a cotransmitter or modulator of transmission in the ciliary ganglion rather than a retrograde messenger as has been proposed for neurones in the hippocampus (see for example, Böhme *et al.*, 1991).

There is now considerable evidence suggesting that nitric oxide acts as a transmitter in the peripheral nervous system. The inhibitory neurones of the gastrointestinal tract that use neither noradrenaline nor acetylcholine as transmitters (Bennett *et al.*, 1963), the so called NANC neurones, appear in most cases to use nitric oxide as their transmitter (Gillespie *et al.*, 1989; Li & Rand, 1989; Hobbs & Gibson, 1990; Bult *et al.*, 1990; Desai *et al.*, 1991; Boeckxstaens *et al.*, 1991; Christinck *et al.*, 1991). There is also evidence that nitric oxide can act as an autoexcitatory agent to potentiate the release of transmitters. For example, the secretion of noradrenaline in the regulation of haemodynamics is facilitated by the action of endogenous nitric oxide (Halbrugge *et al.*, 1991).

Endogenous nitric oxide is generated and released from the ciliary ganglion during LTP, as this was reduced by about 40% in the presence of L-NAME without any affect on PTP. Cyclic GMP may be involved in the action of nitric oxide, as addition of 8-Br-cyclic GMP increased the efficacy of transmission through the ganglion by about 40%, that is to about the same extent as did sodium nitroprusside, a result similar to that observed for sympathetic ganglia (Briggs, 1992). The classical pathway for the action of nitric oxide, namely through the haeme group of guanylate cyclase capturing nitric oxide, with a subsequent conformational change in the enzyme leading to the production of cyclic GMP and phosphorylation of a substrate through cyclic GMP-dependent kinase (Bredt & Snyder, 1992), is one mode of action observed in sympathetic ganglia (Dun *et al.*, 1978). In these ganglia the increase in cyclic GMP accompanying nerve stimulation (Weight *et al.*, 1974) is probably confined to the nerve terminals as depolarization of the ganglion with high potassium concentrations does not lead to an increase in cyclic GMP if the ganglion has been denervated (Quenzer *et al.*, 1980a,b; Ando *et al.*, 1983). This increase in the terminal cyclic GMP may be due to the action of secreted acetylcholine acting on terminal muscarinic receptors to inhibit secretion (Morita *et al.*, 1982), as acetylcholine increases the cyclic GMP content of the ganglion through an atropine-sensitive mechanism (Kebabian *et al.*, 1975). Whether acetylcholine secreted at the ciliary nerve terminals also acts to stimulate the production of cyclic GMP in these terminals in order to increase transmitter secretion has not been determined.

In the present case it has been shown that 8-Br-cyclic AMP can increase the efficacy of synaptic transmission through the ganglion by about 40% as is the case for sympathetic ganglia (Briggs, 1992). As this is about the same increase in efficacy as that produced by sodium nitroprusside, it is possible that nitric oxide also acts through the cyclic AMP pathway. In sympathetic ganglia, analogues of cyclic AMP give a long-lasting increase in the evoked secretion of acetylcholine through a mechanism that does not involve extracellular calcium (Briggs *et al.*, 1985; 1988). The question immediately arises as to how nitric oxide could increase cyclic AMP and also elevate transmitter secretion. One way involves the ability of cyclic GMP to inhibit cyclic AMP phosphodiesterase (Maurice & Haslam, 1990a,b): this mechanism ensures that if cyclic GMP levels in the nerve terminal are elevated by nitric oxide then so will those of cyclic AMP. It

is interesting in this regard that recent biochemical studies have shown that there is a large increase in the phosphorylation of a protein kinase A substrate in the ciliary ganglion after its exposure to sodium nitroprusside (Lengyel *et al.*, 1993). In the hippocampus cyclic AMP is elevated in an NMDA-receptor dependent way during LTP indicating an involvement of cyclic AMP-dependent protein kinase (Chetkovitch *et al.*, 1991). The effect of blocking cyclic AMP production on LTP in the ciliary ganglion has not yet been investigated.

The effects of cyclic AMP in elevating transmission through the ciliary ganglion were more sustained than those due to cyclic GMP (see Figures 1 and 3). One possible explanation is that cyclic GMP has two actions in the ganglion: one already mentioned involves the elevation of cyclic AMP through the ability of cyclic GMP to inhibit cyclic AMP phosphodiesterase; the other could involve the elevation of a protein phosphatase through protein kinase G. It has recently been shown that calcium-activated potassium channels in rat pituitary tumour cells are stimulated by cyclic GMP acting through a protein phosphatase (White *et al.*, 1993). If cyclic AMP stimulation through cyclic GMP inhibits these channels in the ciliary ganglion but cyclic GMP-dependent protein phosphatase stimulates them, then the action of exogenous cyclic GMP may be transient compared with that of exogenous cyclic AMP. It remains to be seen whether this hypothesis survives experimental testing.

The present results suggest the following model for the action of nitric oxide in the maintenance phase of LTP in the ciliary ganglion. High-frequency stimulation of the calyciform nerve terminal leads to the influx of sufficient calcium into the terminal to activate nitric oxide synthase (Chan, 1992; Garthwaite, 1991); the nitric oxide so produced acts on guanylate cyclase located in the terminal resulting in the increase in transmitter secretion in autonomic ganglia but no change in the sensitivity of postsynaptic receptors (Kuba & Kumamoto, 1990; Scott & Bennett, 1993). The principal effect of the cyclic GMP produced is to phosphorylate cyclic AMP phosphodiesterase, so that this can no longer metabolize cyclic AMP (Maurice & Haslam, 1990a). The subsequent increase in cyclic AMP in the terminal leads to the phosphorylation of a protein kinase A substrate (Lengyel *et al.*, 1993), which may be identified as the calcium-activated potassium channels in the terminal. This results in a decrease in the opening of these channels (Cetiner & Bennett, 1992), with a consequent increase in the duration of the terminal action potential and a very large increase in the transient calcium concentration required during vesicle exocytosis at the active zones of the terminal. Whether there is an autophosphorylation form of protein kinase A in the terminal which will allow for a sustained effect of this pathway on transmitter secretion is not known. Nor is it known whether the decrease in calcium channel opening produced by nitric oxide is such as to compensate for the enhancement expected from the increase in duration of the action potential. The present work suggests however that the processes described in the above model may occur: blocking nitric oxide synthase with L-NAME decreases LTP whereas adding nitric oxide exogenously increases the efficacy of transmission through the ganglion as does the addition of either cyclic GMP or cyclic AMP. Whether there is a pathway from cyclic GMP to calcium-calmodulin kinase II remains to be investigated, as blocking this kinase prevents LTP (Scott & Bennett, 1993), indicating that it is important in the expression of LTP.

References

ANDO, M., NAMBA., T., OKUYA, M. & NAGATA, Y. (1983). Effect of axotomy on the cyclic GMP increase induced by preganglionic stimulation and high extracellular K^+ concentration in superior cervical sympathetic ganglion of the rat. *Brain Res.*, **267**, 313–321.

ARIANO, M.A., BRIGGS, C.A. & MCAFEE, D.A. (1982a). Cellular localization of cyclic nucleotide change in rat superior cervical ganglion. *Cell. Mol. Neurobiol.*, **2**, 143–156.

BENNETT, M.R., BURNSTOCK, G. & HOLMAN, M.E. (1963). The effect of K and Cl ions on the inhibitory potential recorded in the guinea pig taenia coli. *J. Physiol.*, **169**, P1.

BLOTTNER, D. & BAUMGARTEN, H. (1992). Nitric oxide synthetase (NOS)-containing sympathoadrenal cholinergic neurons of the rat IML-cell column: evidence from histochemistry, immunohistochemistry, and retrograde labeling. *J. Comp. Neurol.*, **316**, 45–55.

BOECKXSTAENS, G.E., PELCKMANS, P.A., BULT, H., DEMAN, J.G., HERMAN, A.G. & VANMAERCKE, Y.M. (1991). Evidence for nitric oxide as a mediator of non-adrenergic, non-cholinergic relaxations induced by ATP and GABA in the canine gut. *Br. J. Pharmacol.*, **102**, 434–438.

BÖHME, G.A., BON, C., STUTZMANN, J., DOBLE, A. & BLANCHARD, J. (1991). Possible involvement of nitric oxide in long-term potentiation. *Eur. J. Pharmacol.*, **199**, 379–381.

BREDT, D.S., HWANG, P.M. & SNYDER, S.H. (1990). Localization of nitric oxide synthase indicating a neural role for nitric oxide. *Nature*, **347**, 768–770.

BREDT, D.S. & SNYDER, S.H. (1992). Nitric oxide, a novel neuronal messenger. *Neuron*, **8**, 3–11.

BRIGGS, C.A., (1992). Potentiation of nicotinic transmission in the rat superior cervical sympathetic ganglion: effects of cGMP and nitric oxide generators. *Brain Res.*, **573**, 139–146.

BRIGGS, C.A., MCAFEE, D.A. & MCCAMAN, R.E. (1985). Long-term potentiation of synaptic acetylcholine release in the superior cervical ganglion of the rat. *J. Physiol.*, **363**, 181–190.

BRIGGS, C.A., MCAFEE. D.A. & MCCAMAN, R.E. (1988). Long-term regulation of synaptic acetylcholine release and nicotine transmisson: the role of cyclic AMP. *Br. J. Pharmacol.*, **93**, 399–411.

BULT, H., BOECKXSTAENS, G.E., PELKMANS, P.A., JORDAENS, F.H., VAN MAERCKE, Y.M. & HERMAN, A.G. (1990). Nitric oxide as an inhibitory non-adrenergic non-cholinergic neurotransmitter. *Nature*, **345**, 346–347.

CETINER, M. & BENNETT, M.R. (1992). Nitric oxide modulation of calcium activated potassium channels in parasympathetic neurones of cultured avian ciliary ganglia. *Proc. Aust. Physiol. Pharmacol. Soc.*, **23**, 192.

CHAN, N. (1992). Localization of nitric oxide synthase in the chick ciliary ganglion. *B.Sc(hons) Thesis*, Department of Physiology, *The University of Sydney*.

CHETKOVICH, D.M., GRAY, R., JOHNSTON, D. & SWEATT, J.D. (1991). N-Methyl-D-aspartate receptor activation increases cAMP levels and voltage-gated Ca^{2+} channel activity in area CA1 of hippocampus. *Proc. Natl. Acad. Sci. U.S.A.*, **88**, 6467–6471.

CHRISTINCK, F., JURY, J., CAYABYAB, F. & DANIEL, E.E. (1991). Nitric oxide may be the final mediator of nonadrenergic, noncholinergic inhibitory junction potentials in the gut. *J. Can. Physiol. Pharmacol.*, **69**, 1448.

DAWSON, T., BREDT, D.S., FOTUHI, M., HWANG, P.M. & SNYDER, S.H. (1991). Nitric oxide synthase and neuronal NADPH diaphorase are identical in brain and peripheral tissues. *Proc. Natl. Acad. Sci. U.S.A.*, **88**, 7797–7801.

DESAI, K.M., SESSA, W.C. & VANE, J.R. (1991). Involvement of nitric oxide in the reflex relaxation of the stomach to accommodate food or fluid. *Nature*, **351**, 477–478.

DUN, N.J., KAIBARA, K. & KARCZMAR, A.G. (1978). Muscarinic and cGMP induced membrane potential changes: differences in lectrogenic mechanisms. *Brain Res.*, **150**, 658–661.

FUJII, J.T. (1992). Repetitive firing properties in subpopulations of the chick edinger westphal nucleus. *J. Comp. Neurol.*, **316**, 279–286.

GARTHWAITE, G. (1991). Glutamate, nitric oxide and cell-cell signalling in the nervous system. *Trends Neurosci.*, **14**, 60–67.

GILLESPIE, J.S., LIU, X. & MARTIN, W. (1989). The effects of L-arginine and N^G-monomethyl L-arginine on the response of the rat anococcygeneus muscle to NANC nerve stimulation. *Br. J. Pharmacol.*, **98**, 1080–1082.

GROZDANOVIC, Z., BAUMGARTEN, H.G. & BRÜNING, G. (1992). Histochemistry of nadph-diaphorase, a marker for neuronal nitric oxide synthase, in the peripheral autonomic nervous system of the mouse. *Neurosci.*, **48**, 225–235.

HALBRUGGE, T., LUTSCH, K., THYEN, A. & GRAEFE, K.-H. (1991). Role of nitric oxide formation in the regulation of haemodynamics and the release of noradrenaline and adrenaline. *Naunyn-Schmied. Arch. Pharmacol.*, **344**, 720–727.

HALEY, J.E., WILCOX, G.L. & CHAPMAN, P.F. (1992). The role of nitric oxide in hippocampal long-term potentiation. *Neuron*, **8**, 211–216.

HOBBS, A.J. & GIBSON, A. (1990). L-N^G-nitro-arginine and its methyl ester are potent inhibitors of non-adrenergic, non-cholinergic transmission in the rat anococcygeus. *Br. J. Pharmacol.*, **100**, 749–792.

HOPE, B.T., MICHAEL, G.J., KNIGGE, K.M. & VINCENT, S.R. (1991). Neuronal NADPH diaphorase is a nitric oxide synthase. *Proc. Natl. Acad. Sci. U.S.A.*, **88**, 2811–2814.

KANDEL, E.R. & HAWKINS, R.D. (1992). The biological basis of learning and individuality. *Sci. Am.*, **267**, 53–60.

KEBABIAN, J.W., STEINER, A.L. & GREENGARD, P. (1975). Muscarinic cholinergic regulation of cyclic guanosine 3',5'-monophosphate in autonomic ganglia: possible role in synaptic transmission. *J. Pharmacol. Exp. Ther.*, **193**, 474–488.

KHURANA, G. & BENNETT, M.R. (1993). Nitric oxide and arachidonic acid modulation of calcium currents in postganglionic neurones of cultured avian ciliary ganglia. *Br. J. Pharmacol.*, **109**, 480–485.

KUBA, K. & KUMAMOTO, E. (1990). Long-term potentiation in vertebrate synapses: a variety of cascades with common subprocesses. *Prog. Neurobiol.*, **34**, 197–269.

LENGEYL, I., NICHOL, K., BENNETT, M.R., ROSTAS, J. & DUNKLEY, P. (1993). Protein phosphorylation in chick ciliary ganglion. *Proc. Int. Soc. Neurosci.*, (in press).

LI, C.G. & RAND, M.J. (1989). Evidence for a role of nitric oxide in the neurotransmitter system mediating relaxation of the rat anococcygeus muscle. *Clin. Exp. Pharmacol. Physiol.*, **16**, 933–938.

LLEWELYN-SMITH, I.J., PHEND, K.D., MINSON, J.B., PILOWSKY, P.M. & CHALMERS, J.P. (1992). Glutamate-immunoreactive synapses on retrogradely labelled sympathetic preganglionic neurons in rat thoracic spinal cord. *Brain Res.*, **581**, 67–80.

MAURICE, D.H. & HASLAM, R.J. (1990a). Molecular basis of the sysnegistic inhibition of platelet function by nitrovasodilators and activators of adenylate cyclase: inhibition of cyclic AMP breakdown by cyclic GMP. *Mol. Pharmacol.*, **37**, 671–681.

MAURICE, D.H. & HASLAM, R.J. (1990b). Nitroprusside enhances isoprenaline-induced increase in cAMP in rat aortic smooth muscle. *Eur. J. Pharmacol.*, **191**, 471–475.

MORITA, K., NORTH, R.A. & TOKIMASA, T. (1982). Muscarinic presynaptic inhibition of synaptic transmission in myenteric plexus of guinea-pig ileum. *J. Physiol.*, **333**, 141–149.

PILAR, G. & TUTTLE, J.B. (1983). A simple neuronal system with a range of uses: the avian ciliary ganglion. In *Progress in Cholinergic Biology: Model Cholinergic Synapses* ed. Hanin, I. & Goldberg, A.M. pp. 213–247. New York: Raven Press.

QUENZER, L.F., PATTERSON, B.A. & VOLLE, R.L. (1980a). The cyclic nucleotide content of the rat superior cervical ganglion. *J. Pharmacol. Exp. Ther.*, **215**, 297–303.

QUENZER, L.F., PATTERSON, B.A. & VOLLE, R.L. (1980b). K +-induced accumulation of guanosine 3', 5'-monophosphate in sympathetic ganglia. *J. Neurochem.*, **34**, 1782–1784.

SCOTT, T.R.D. & BENNETT, M.R. (1992). Long-term potentiation of chemical transmission in the avian ciliary ganglion. *Proc. Aust. Physiol. Soc.*, **23**, 182P.

SCOTT, T.R.D. & BENNETT, M.R. (1993). The effect of ions and second messengers on long-term potentiation of chemical transmission in avian ciliary ganglion. *Br. J. Pharmacol.*, (in press).

SCOTT, T.R.D., NICOL, K.A., CHAN, N. & BENNETT, M.R. (1992). Nitric oxide synthase localization in autonomic ganglia and its participation in long-term potentiation. *Proc. Aust. Physiol. Pharmacol. Soc.*, **23**, 191P.

VALTSCHANOFF, J.G., WEINBERG, R.J. & RUSTIONI, A. (1992). NADPH diaphorase in the spinal cord of rats. *J. Comp. Neurol.*, **321**, 209–222.

VOLLE, R.L. & QUENZER, L.F. (1983). Regulation of cyclic GMP levels in nerve tissue. *Fed. Proc.*, **42**, 3099–3102.

WEIGHT, F.F., PETZOLD, G. & GREENGARD, P. (1974). Cyclic guanosine 3', 5' monophosphate in sympathetic ganglia: increase associated with sympathetic ganglia. *Science*, **186**, 942–944.

WHITE, R.E., LEE, A.B., SHCHERBATKO, A.D., LINCOLN, T.M., SCHOHBRUNN, A. & ARMSTRONG, D.L. (1993). Potassium channel stimulations by natriuretic peptides through cGMP-dependent dephosphorylation. *Nature*, **361**, 263–266.

(Received March 4, 1993
Revised May 14, 1993
Accepted June 2, 1993)

Br. J. Pharmacol. (1993), **110**, 633–638

Adenylate cyclase-mediated vascular responses of rabbit aorta, mesenteric artery and skin microcirculation

A.J. Wilson & [1]J.B. Warren

Department of Applied Pharmacology, National Heart & Lung Institute, London SW3 6LY

1 The importance of adenylate cyclase-mediated vascular relaxation in the macro and microcirculation was assessed in rabbit aortic and coeliac artery bioassay rings *in vitro* and skin microvessels *in vivo*.

2 The neuropeptide pituitary adenylate cyclase-activating polypeptide (PACAP38), the β-agonist, isoprenaline, and the prostaglandins, PGE_1 and PGE_2, were compared with the activity of nitroprusside, which acts by stimulating guanylate cyclase.

3 In aortic tissue the relative relaxant potencies were ($-\log$ M EC_{50}, 100% = response to nitroprusside 10^{-6} M): nitroprusside 7.0, PACAP38 6.8, isoprenaline 6.3; PGE_1 and PGE_2 were weak constrictors. In coeliac artery rings relative potencies were ($-\log$ M EC_{50}, 100% = response to nitroprusside 10^{-5} M): PACAP38 6.6, PGE_1 6.6, nitroprusside 6.5, PGE_2 4.9, and isoprenaline 4.3.

4 Comparative potencies when injected into anaesthetized rabbit skin *in vivo* were ($-\log$ mol/site required to increase blood red cell flux by 75%): PACAP38 13.0, PGE_2 10.7, isoprenaline 9.7, PGE_1 9.1, nitroprusside <7.

5 Nitroprusside, the most effective relaxant tested in the aorta, was 10^7 fold less potent than PACAP in its effect on skin blood flow. PGE_1 and PGE_2 were constrictors of the aorta, of intermediate effect in the coeliac artery, but potent vasodilators of the microcirculation.

6 In this model, the importance of adenylate cyclase-mediated vascular relaxation increases with decreasing vessel size.

Keywords: Prostaglandins; pituitary adenylate cyclase activating polypeptide; cyclic AMP; cyclic GMP; β-adrenoceptors; nitric oxide

Introduction

The cyclic nucleotides adenosine and guanosine 3′:5′-cyclic monophosphates (cyclic AMP and cyclic GMP, respectively) have both been implicated as intracellular second messengers which mediate vascular smooth muscle relaxation. Adenylate cyclase can be stimulated to generate cyclic AMP by several first messengers, including prostaglandins, β-adrenoceptor agonists and some of the neuropeptides (Andersson, 1973; Scheid *et al.*, 1979; Schoeffter *et al.*, 1987; Sata *et al.*, 1988; Warren *et al.*, 1991; Wood & Owen, 1992). The elevation in concentration of cyclic AMP activates cyclic AMP-dependent protein kinases, leading to actin myosin relaxation. The stimulation of soluble guanylate cyclase to generate cyclic GMP is by nitric oxide, the endogenous nitrovasodilator released by several cell types, which is a key component of endothelium-derived relaxing factor (EDRF) (Moncada & Higgs, 1991).

Many of the studies of EDRF and nitric oxide have involved bioassay systems using rabbit aorta or large vessel endothelial cells in culture. In these systems the inhibition of nitric oxide synthase abolishes the relaxant activity derived from endothelial cells (Gryglewski *et al.*, 1986; Moncada & Higgs, 1991). Agonists such as bradykinin which cause the release of EDRF also stimulate endothelial cells in culture to increase substantially their release of prostaglandins (Gryglewski *et al.*, 1986). However, preventing the synthesis of prostaglandins with cyclo-oxygenase inhibitors does not affect relaxant activity (Gryglewski *et al.*, 1986). Furthermore, pre-contracted rabbit aortic rings do not relax in response to vasodilator prostaglandins (Bunting *et al.*, 1976) suggesting that the prostaglandin-adenylate cyclase vasodilator pathway is not important in these systems when compared to the nitric oxide-guanylate cyclase pathway.

The nitric oxide-guanylate cyclase vasodilator pathway does not predominate to the same extent in smaller blood vessels. For example, the peptide bradykinin is a potent stimulus to nitric oxide release from endothelial cells from large vessels, yet in rabbit coeliac artery bradykinin relaxes this vessel by a cyclo-oxygenase dependent mechanism (Aiken, 1974; Cherry *et al.*, 1982; Ritter *et al.*, 1989). Another stimulus to endothelium-derived nitric oxide in large arteries, acetylcholine, acts by a nitric oxide independent mechanism in the rat small mesenteric artery (Garland & McPherson, 1992) and is only a weak vasodilator in skin (Williams, 1982).

In the microcirculation, prostaglandins E_1, E_2, and I_2, as well as vasoactive intestinal polypeptide (VIP) and calcitonin gene-related peptide are potent vasodilators in man and experimental animals and all stimulate adenylate cyclase (Williams & Peck, 1977; Joyner *et al.*, 1979; Messina *et al.*, 1975; 1980; Messina & Kaley, 1980; Williams, 1982). Pituitary adenylate cyclase activating polypeptide (PACAP) is approximately 100 fold more potent than VIP at stimulating adenylate cyclase in several cell lines and has similar potency as a vasodilator of large vessels and the microcirculation (Warren *et al.*, 1991; 1992c).

The aim of the present study was to define the relative sensitivity of rabbit aorta, coeliac artery and the skin microcirculation to four agonists which stimulate adenylate cyclase. This has been compared with the sensitivity of these tissues to nitroprusside, given as a nitric oxide donor. Nitroprusside was chosen as it readily releases nitric oxide in tissue (Newman *et al.*, 1990). Both aortic and coeliac artery rings were studied without endothelium and in the presence of indomethacin to remove any complicating effects of endogenous nitric oxide or prostaglandin release.

Methods

Aortic and coeliac arteries

Aortic and coeliac arteries were dissected from male New Zealand White rabbits which had been killed with an over-

[1] Author for correspondence.

dose of sodium pentobarbitone. They were placed in Krebs-Henseleit solution of the following composition (mM): NaCl 118, KCl 4.7, $MgSO_4.7H_2O$ 1.2, NaH_2PO_4 1.2, $NaHCO_3$ 25, $CaCl_2$ 1.5, which was bubbled with 5% CO_2 in air (pH 7.4). The blood vessels were cleaned of connective tissue and cut into 3 mm rings. The endothelium was removed by rotating gently around the closed tips of a pair of fine forceps.

Superfusion bioassay system

Rings of aorta or coeliac artery were mounted on hooks attached to a force transducer (Dynameter UF1, Pioden Controls Ltd, Canterbury, Kent) and amplifier (Transbridge TBM4, World Precision Instruments, Sarasota, Florida, U.S.A.) and the output recorded on a Maclab analogue to digital conversion system and Macintosh Apple computer (Apple Computer Inc, Cupertino, Ca, U.S.A.). They were maintained at 37°C and perfused continuously at 2 ml min^{-1} with Krebs-Henseleit buffer bubbled with 5% CO_2 in air. The bioassay rings were adjusted over a minimum period of 100 min to maintain a resting tension of 2–3 g for the aorta and 1–1.5 g for the coeliac artery rings. Rings were then perfused with buffer containing potassium 100 mM for 2 min and allowed a further 45 min to return to baseline. The rings were contracted by perfusing with buffer containing 1 μM phenylephrine and the absence of endothelium confirmed by the lack of response to 1 μM acetylcholine given for 1 min. Albumin (0.3% w/v) was added to the buffer for peptide dilutions and also to the bioassay perfusate to prevent peptide sticking to plastic tubing.

All doses of the agonists were perfused over the bioassay tissue for 1 min, the concentration of phenylephrine being maintained at 1 μM and indomethacin 10 μM added to all solutions. The relaxation response of each bioassay ring was determined by giving 1 μM nitroprusside for 1 min and results are expressed as a percentage of this response. Drugs were given in the concentration range 10^{-10}–10^{-4} M and 6–10 rings were used at each drug concentration.

Measurement of skin blood flow

The microcirculation vasodilator response to intradermal injections was assessed by measuring skin blood flow *in vivo* with a laser Doppler flow probe (Perimed II, Stockholm, Sweden; Warren *et al.*, 1992a,b,c; 1993). Male New Zealand White rabbits, 2.5–3.5 kg, were anaesthetized with sodium pentobarbitone 30 mg kg^{-1}, i.v. The dorsal skin was shaved with electric clippers and depilated with a commercial depilating cream (Immac). The dorsal skin was then rinsed thoroughly with warm water and the animal left for 1 h before measurements were made. The animal remained anaesthetized throughout the procedure in an air-conditioned room at 24 ± 1°C and was not allowed to recover consciousness.

Up to 10 sites were marked out in each quadrant of dorsal skin and baseline blood flow was measured in each site with the laser-Doppler flow probe. The probe was held at right angles to the skin by a plastic guide. Each reading took 15 s with a 10 s interval between readings and the mean of three readings per site were taken. Results were recorded as red blood cell flux (the number of moving red cells detected by the laser beam × mean cell velocity) and expressed as a percentage of a standardized signal. The laser Doppler was set at 4 Hz, gain 10 and a time constant of 3 s. The output was recorded on a Maclab and Macintosh Apple Computer (Apple Computer Inc, Cupertino, Ca, U.S.A.) set at an input of 10 V and chart speed of 2 mm s^{-1}.

Skin blood flow protocols

Test agents dissolved in phosphate buffered saline or control buffer were injected intradermally with a 27 wire gauge needle in 100 μl volumes and the change in red cell flux measured at 30 min. Experiments were repeated four times in each rabbit so that each datum point per rabbit is the mean of four sites. Test compounds were injected in a randomized site pattern. Results are expressed as the percentage change from basal.

Cell culture

Vascular smooth muscle cells were prepared by non-enzymatic methods from rabbit aorta (Warren *et al.*, 1990). The endothelium and adventitia were removed from a length of lower thoracic aorta resected from a New Zealand White rabbit that had been killed with an overdose of sodium pentobarbitone. The medial layer was cut into 1 mm squares and seeded into a culture flask. Smooth muscle cells grew out from these explants and, when confluent, were passaged using a rubber policeman. Contaminating cells were identified by microscopy and removed by selective scraping when passaging. Flasks were passaged 1:3 approximately every 6 weeks and cells used between passages 3 and 7. The identity of the smooth muscle cells was confirmed by their spindle shaped aligned appearance, by electron microscopy and by positive immuno-staining for alpha smooth muscle actin. Smooth muscle cells were cultured in Dulbecco's Modified Eagles Medium (DMEM) supplemented with 20% foetal calf serum, glutamine 480 mg l^{-1}, penicillin 60,000 u l^{-1}, streptomycin 60 mg l^{-1}, thymidine 2 mg l^{-1}, insulin 5 mg l^{-1}, transferrin 5 mg l^{-1} and selenium 5 μg l^{-1}; this medium was changed every 3–4 days.

For the incubation experiments cells were passaged into 24 well plates (Falcon, Becton Dickinson, London UK) and used when confluent at 4–5 days.

Measurement of cyclic AMP

Aortic smooth muscle cells in multi-well plates were washed three times with Krebs-Henseleit buffer and left in 270 μl of buffer, containing phenylephrine 1 μM and indomethacin 10 μM for 45 min. The plates were kept throughout the experiment in an incubator at 37°C in an atmosphere of 5% CO_2 in air. Test compounds were added in 30 μl volumes to the wells, to give a final volume of 300 μl, and incubated for a further 15 min. The reaction was then stopped by adding 300 μl tri-chloroacetic acid 1 M at 4°C and the plates left overnight at 4°C. The test agents used (final concentration ranges) were: PACAP38 10^{-13}–10^{-7} M, prostaglandin E_1 (PGE_1) 10^{-10}–10^{-6} M, PGE_2 10^{-10}–10^{-5} M, isoprenaline 10^{-10}–10^{-6} M and nitroprusside 10^{-6} M. All incubations were in the presence of the phosphodiesterase inhibitor rolipram 100 μM, other than the control wells.

To extract the cyclic nucleotides, 500 μl was removed from each well, centrifuged, and the supernatant added to 50 μl of 25 mM EDTA and vortexed. Freon:tri-n-octylamine, 1: v/v, 100 μl was added and vortex mixed. The mixture was centrifuged and 450 μl of the upper aqueous phase removed and neutralized with 50 μl $NaHCO_3$ (120 mM).

For the radio-immunoassay of cyclic AMP, 100 μl samples were taken in duplicate. Goat cyclic AMP antibody, 100 μl, was added together with 50 μl of adenosine 3′:5′-cyclic phosphoric acid 2′-O-succinyl-3 [^{125}I]-iodotyrosine methyl ester, 2,000 Ci $mmol^{-1}$, to give total c.p.m. in the range 10,000–15,000. The mixture was left overnight at 4°C. Charcoal suspension in potassium phosphate buffer was added at 4°C, vortex mixed, left for 15 min, centrifuged, and 800 μl of supernatant removed and radioactivity measured in a gamma counter.

For the protein assay, cells were removed from the plate wells with 0.1 M NaOH and protein measured with a spectrophotometric dye method using Bradford reagent.

Drugs and chemicals

PACAP38 was obtained from Penninsula Laboratories, St Helen's, UK. PGE_1 and PGE_2 were from Cascade Biochem

Ltd, Reading, UK and adenosine 3':5'-cyclic phosphoric acid 2'-O-succinyl-3 [^{125}I]-iodotyrosine methyl ester from Amersham International Ltd, Amersham, UK. Rolipram was the generous gift of Schering AG, Berlin, Germany. Freon:tri-n-octylamine was from the Aldrich Chemical Co, Gillingham, UK. [1R-[1α(Z),2β,3β,5α]]-(+)-7-[5-([1,1'-biphenyl]-4-ylmethoxy)-3-3-hydroxy-2-(1-piperidinyl)cyclopentyl]-4-heptenoic acid, hydrochloride (GR32191B) was the generous gift of Glaxo Group Research, Greenford, UK.

Foetal calf serum, DMEM, penicillin and streptomycin were obtained from Gibco (Paisley, UK). Gas mixtures were obtained from BOC Medical Gases (Middlesex, UK). Other drugs and chemicals were obtained from Sigma (Poole, UK).

Statistical analysis

Results are expressed as mean ± s.e.mean. In the bioassay experiments of vascular rings, 6–10 rings were used for each drug concentration tested. For the measurement of skin blood flow, all data points are the mean of 4 animals, each experiment performed 4 times in each rabbit. In experiments measuring cyclic AMP generation, all data points are the mean of 6 experiments and each assay was performed in duplicate. Statistical comparisons were made by analysis of variance and taken as significantly different if $P<0.05$.

Results

Vasodilator effects in aorta

The mean resting tension of the aortic rings was 2.44 ± 0.08 g and this increased to 10.55 ± 0.66 g with phenylephrine 1 μM. There was no vasodilatation in response to acetylcholine, confirming that the endothelium had been removed. Nitroprusside 1 μM caused a mean maximal reduction in contraction of − 64%. The maximal response to 10 μM nitroprusside was not significantly different from the response to 1 μM. The response to nitroprusside 1 μM was taken as − 100% and results expressed as a percentage of this response.

Nitroprusside, PACAP38 and isoprenaline caused dose-dependent relaxation of pre-contracted aortic rings (Figure 1). The following potencies (− log M EC_{50}, 100% = response to nitroprusside 1 μM) were observed: nitroprusside, 7.0; PACAP38, 6.8 and isoprenaline, 6.3. Both of the prostaglandins tested had no effect up to 10^{-7} M but caused some contraction of aortic rings at higher concentrations. The isoprenaline dose-response was significantly different from the PACAP38, nitroprusside and prostaglandin responses: $P<0.05$, ANOVA.

To determine if high doses of PGE_2 could stimulate constrictor thromboxane receptors, the thromboxane receptor antagonist, GR32191B, was tested on aortic rings without endothelium. At a concentration of 100 μM it reversed the constrictor effects of thromboxane-mimetic, U46619 at 10 nM, but did not affect the contraction produced by phenylephrine 1 μM. Rings contracted with phenylephrine 1 μM contracted a further 44 ± 3% with PGE_2 10 μM in the absence, and 42 ± 2% in the presence, of 100 μM GR32191B (results are mean ± s.e., $n=4$; − 100% = fall in tension in response to nitroprusside 1 μM).

Vasodilator effects in coeliac artery

Phenylephrine was a less effective constrictor of coeliac artery than of aorta and therefore used at a higher concentration of 10 μM which elevated resting tension from a mean of 1.37 ± 0.05 g to 5.53 ± 0.73 g (with 1 μM phenylephrine the corresponding figure was 2.45 ± 0.80 g). A higher dose of nitroprusside was used (10 μM) and results expressed as a percentage of this response. Nitroprusside 10 μM caused a − 72% relaxation of the phenylephrine-induced contraction and only a − 20% relaxation at 1 μM.

Figure 2 shows that PACAP38 was of similar potency to nitroprusside as a relaxant of pre-contracted coeliac artery. In contrast to their vasoconstrictor effects in aortic tissue, both prostaglandins were vasodilators in the coeliac artery with PGE_1 being of equivalent potency to PACAP38. The vasodilator potency (− log M EC_{50}, − 100% = response to nitroprusside 10 μM) was PACAP38, 6.6, PGE_1, 6.6; nitroprusside, 6.5; PGE_2, 4.9; isoprenaline, 4.3. PGE_2 and isoprenaline were each significantly different from the other three, $P<0.05$ in each case.

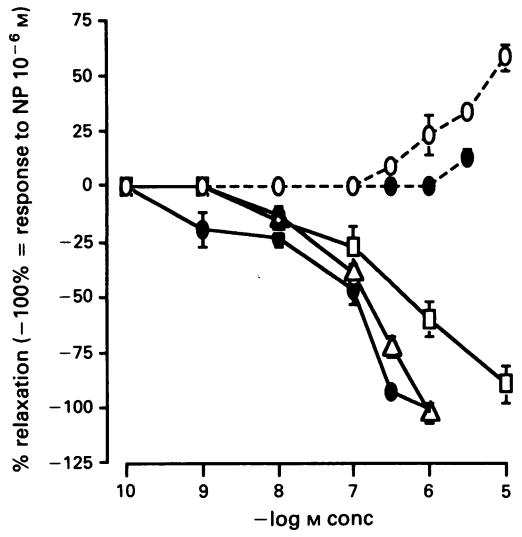

Figure 1 Graph showing the concentration-dependent effect of five agonists on rabbit aorta. Aortic rings were precontracted with phenylephrine 1 μM in the presence of indomethacin 10 μM. Agonists were given for 1 min in the superfusate of the bioassay: prostaglandin E_1 (●– – –●); E_2 (○– – –○); isoprenaline (□——□) and PACAP38 (Δ——Δ). Results are expressed as a percentage of the relaxation to nitroprusside 1 μM (●——●). Results are the mean ± s.e.mean of 6–10 rings.

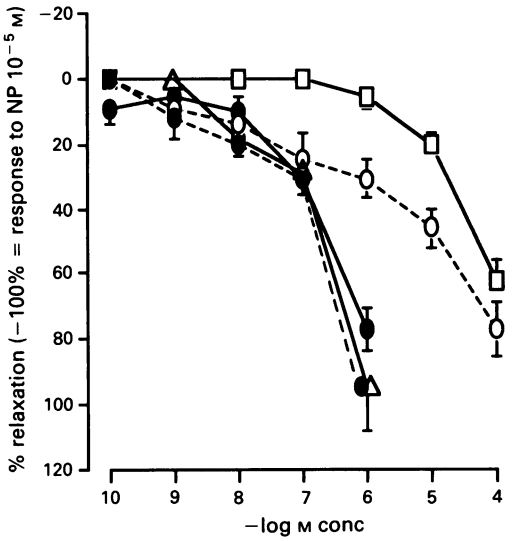

Figure 2 Graph showing the concentration-dependent effect of five agonists on rabbit coeliac artery rings. Rings were precontracted with phenylephrine 10 μM in the presence of indomethacin 10 μM. Agonists were given for 1 min in the superfusate of the bioassay: prostaglandin E_1 (●– – –●); E_2 (○– – –○); isoprenaline (□——□) and PACAP38 (Δ——Δ). Results are expressed as a percentage of the relaxation to nitroprusside 10 μM (●——●). Results are the mean ± s.e.mean of 6–10 rings.

Effects on skin blood flow

Of the agonists tested on skin blood flow *in vivo*, PACAP38 was the most potent and nitroprusside the least potent, there being a 10^7 fold shift in the dose response between them (Figure 3). Both PACAP38 and nitroprusside were significantly different from the other three agonists and from each other ($P<0.05$ in each case, ANOVA). Comparative potencies (− log mol/site of the dose required to increase basal flow by 75%) were: PACAP38 13.0, PGE_2 10.7, isoprenaline 9.7, PGE_1 9.1, nitroprusside <7. Sodium nitroprusside was not given in doses higher than 10^{-7} mol per site, as a preliminary experiment measuring blood pressure in rabbits with an intra-arterial cannula suggested that at 10^{-6} mol per site, or above, nitroprusside injected intradermally can affect systemic blood pressure.

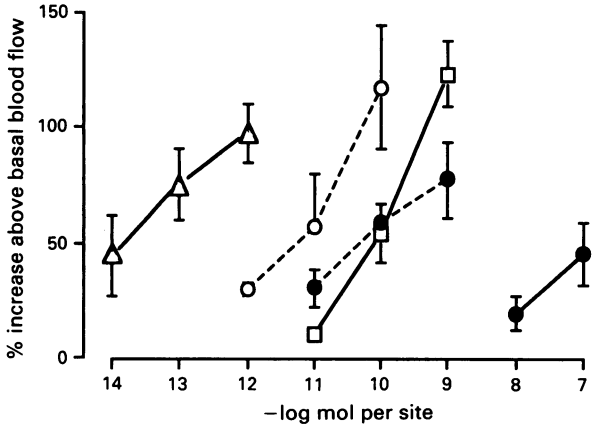

Figure 3 A comparison of the vasodilator effects of five agonists on skin blood flow in the shaved dorsal skin of the anaesthetized rabbit. Each agonist was injected in 100 µl aliquots and blood flow measured at 30 min with a laser Doppler flow probe: prostaglandin E_1 (●- - -●); E_2 (O- - -O); isoprenaline (□——□); PACAP38 (Δ——Δ) and nitroprusside (●——●). Each point represents the mean ± s.e.mean of 4 rabbits and each experiment was repeated four times in each rabbit. Results are expressed as the percentage increase in basal blood flow.

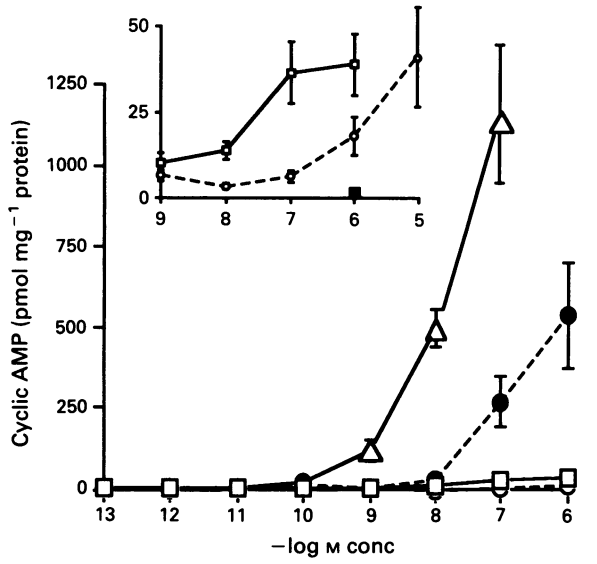

Figure 4 Graph showing the concentration-dependent effect of five agonists on cyclic AMP production by cultured rabbit aortic smooth muscle cells. Intracellular cyclic AMP was measured by radioimmunoassay after a 15 min incubation with each dose of agonist in the presence of a phosphodiesterase inhibitor. Nitroprusside (■) had no effect whereas the other four agonists tested increased cyclic AMP concentrations significantly and were significantly different from each other: prostaglandin E_1 (●- - -●); E_2 (O- - -O); isoprenaline (□——□) and PACAP38 (Δ——Δ). Results are expressed as the concentration of cyclic AMP per mg of protein. Each point is the mean ± s.e.mean of six experiments.

Stimulation of adenylate cyclase

Nitroprusside had no effect on cyclic AMP generation in cultured aortic vascular smooth muscle cells whereas all four of the remaining agonists caused dose-dependent increases (Figure 4). The order of potency was PACAP38 > PGE_1 > isoprenaline > PGE_2 and the agonists were significantly different from each other ($P<0.05$ in each case).

Discussion

The present study shows that within a single species, the adenylate cyclase-mediated responses to the four agonists tested were more prominent in the microcirculation than the macrocirculation. PGE_1 and PGE_2 were constrictors of the aorta, of intermediate effect in the coeliac artery, but potent vasodilators in skin, consistent with the concept that prostaglandins are important vasodilators of the microcirculation (Messina *et al.*, 1975; 1980; Messina & Kaley, 1980).

The results confirm PACAP38 as a vasorelaxant (Warren *et al.*, 1991; 1992c) and in addition show it to be particularly effective at increasing blood flow in the skin microcirculation. PACAP is a powerful stimulus to adenylate cyclase in many tissues and it is likely that PACAP causes vasorelaxation via the generation of cyclic AMP in vascular smooth muscle (Warren *et al.*, 1991). It stimulated adenylate cyclase in aortic smooth muscle cells in culture in the present experiments at much lower concentrations than the other three agonists tested.

The prostaglandins did not relax precontracted aortic rings and this is well described (Bunting *et al.*, 1976). The sensitivity of the aortic rings to PACAP suggests intracellular adenylate cyclase is coupled to the vasodilator mechanism in this tissue and that the insensitivity to prostaglandins may be at the receptor level. The contraction observed with higher concentrations of prostaglandins could be caused by cross reactivity with vasoconstrictor receptors. These are unlikely to be thromboxane receptors as the constrictor effects of higher concentrations of PGE_2 were not inhibited by GR32191, a compound known to be a specific thromboxane receptor antagonist (Humphrey *et al.*, 1990).

The radio-immunoassay data show both prostaglandins stimulated cyclic AMP generation in aortic smooth muscle cells in culture indicating that the receptors are linked to adenylate cyclase but that any vasodilator effect may have been negated by the stimulation of constrictor receptors.

Isoprenaline, PACAP, PGE_1 and PGE_2 all caused a dose-dependent elevation in intracellular cyclic AMP in rabbit cultured vascular smooth muscle cells. This supports the hypothesis, although does not prove it, that they act via this mechanism. It is possible to measure cyclic AMP in snap-frozen vascular bioassay rings which allows the elevation in cyclic AMP to be correlated with biological effect, but the maximal elevation in cyclic AMP observed with this method is too small to generate dose-response curves (Vuorinen *et al.*, 1992). For this reason, we chose to measure cyclic AMP generation in cultured cells in the presence of a phosphodiesterase inhibitor as the magnitude of the response allows agonist dose-response curves to be compared. Rabbit aorta was chosen as the source of vascular smooth muscle cells as they grow readily from explants and their identity can be confirmed by their morphology and staining characteristics. Repeating these studies with cultured microvascular smooth muscle cells would be of interest but it is not technically possible to grow these cells in sufficient numbers for such an experiment.

It is important not to over interpret the cyclic AMP radioimmunoassay data. The correlation between an elevation of intracellular cyclic AMP concentration and biological activity for different agonists can vary because of the phenomenon of compartmentalization (Buxton & Bruton, 1979). For example, some agonists cause a highly localized but effective elevation in cyclic AMP concentration with little change in total intracellular cyclic AMP content. Others, such as forskolin, affect many compartments causing an increase in total intracellular cyclic AMP which appears disproportionate to the biological effect. One group has used cell fixation by microwave irradiation to study cyclic nucleotide accumulation and shown that intracellular accumulation patterns are agonist-specific and dose-dependent (Barsony & Marx, 1990). For example, the effect of forskolin was maximal in the nucleus whereas isoprenaline and PGE_2 caused accumulation of cyclic AMP along the plasma membrane (Barsony & Marx, 1990).

Nitroprusside was the most potent relaxant tested in rabbit aorta but was the weakest when tested in the microcirculation. Similarly, the nitric oxide donor, isosorbide dinitrate, in a dose which causes a fall in systemic blood pressure through its action on large arteries, has little effect on flow in most microvascular beds (Wanless *et al.*, 1987). However, the microcirculation of rabbit skeletal muscle does dilate in response to endogenous nitric oxide released in response to acetylcholine (Persson *et al.*, 1990). The microvessels of rat and rabbit skin are capable of synthesizing and responding to nitric oxide, for instance after challenge with endotoxin or ultraviolet light (Pons *et al.*, 1992; Warren *et al.*, 1992b; 1993). The response to these inflammatory stimuli is mediated by the inducible form of nitric oxide synthase. This enzyme generates greater quantities of nitric oxide than the constitutive nitric oxide synthase, which may explain the effectiveness of inflammatory stimuli in causing vasodilatation. All of the present experiments were carried out in rabbit tissue but it seems likely that similar findings occur in man. PACAP38 is a powerful vasodilator of the human microcirculation as well as forearm resistance vessels (Warren *et al.*, 1992a). Prostaglandins and β_2-adrenoceptor agonists have similar vasodilator potency in man and rabbit. Nitroprusside causes arterial relaxation at low concentrations in man but is a weak vasodilator in the skin microcirculation (Warren *et al.*, unpublished observations).

In conclusion, aorta, coeliac artery and skin microvessels of the rabbit were all responsive to stimulators of adenylate cyclase. Tissue receptor differences appear to account for the variations seen with the agonists used, but in general the importance of adenylate cyclase-mediated vasodilatation increased with decreasing vessel size. The role of adenylate cyclase within the microcirculation has implications for our understanding of the mechanism of action of anti-inflammatory drugs, such as cyclo-oxygenase inhibitors, which suppress increased blood flow in inflamed tissue yet have little effect on systemic blood pressure.

Supported by the British Heart Foundation.

References

AIKEN, J.W. (1974). Inhibitors of prostaglandin synthesis specifically antagonize bradykinin and angiotensin-induced relaxations of the isolated coeliac artery from rabbit. *Pharmacologist*, **16**, 295–300.

ANDERSSON, R. (1973). Role of cyclic AMP and Ca++ in mechanical and metabolic events in isometrically contracting vascular smooth muscle. *Acta Physiol. Scand.*, **87**, 84–95.

BARSONY, J. & MARX, S.J. (1990). Immunocytology on microwave-fixed cells reveals rapid and agonist-specific changes in subcellular accumulation patterns for cAMP or cGMP [published erratum appears in *Proc. Natl. Acad. Sci. U.S.A.*, 1990, May; 87(9): 3633]. *Proc. Natl. Acad. Sci. U.S.A.*, **87**, 1188–1192.

BUNTING, S., GRYGLEWSKI, R., MONCADA, S. & VANE, J.R. (1976). Arterial walls generate from prostaglandin endoperoxides a substance (prostaglandin X) which relaxes strips of mesenteric and coeliac arteries and inhibits platelet aggregation. *Prostaglandins*, **12**, 897–913.

BUXTON, I.L.O. & BRUTON, L.L. (1979). Compartments of cyclic AMP and protein kinase in mammalian cardiomyocytes. *J. Biol. Chem.*, **76**, 1570–1574.

CHERRY, P.D., FURCHGOTT, R.F., ZAWADZKI, J.V. & JOTHIANANDAN, D. (1982). Role of endothelial cells in relaxation of isolated arteries by bradykinin. *Proc. Natl. Acad. Sci. U.S.A.*, **72**, 2106–2110.

GARLAND, C.J. & MCPHERSON, G.A. (1992). Evidence that nitric oxide does not mediate the hyperpolarization and relaxation to acetylcholine in the rat small mesenteric artery. *Br. J. Pharmacol.*, **105**, 429–435.

GRYGLEWSKI, R.J., MONCADA, S. & PALMER, R.M.J. (1986). Bioassay of prostacyclin and endothelium-derived relaxing factor (EDRF) from porcine aortic endothelial cells. *Br. J. Pharmacol.*, **87**, 685–694.

HEESEN, B.J. & DE MEY, J.G. (1990). Effects of cyclic AMP-affecting agents on contractile reactivity of isolated mesenteric and renal resistance arteries of the rat. *Br. J. Pharmacol.*, **101**, 859–864.

HUMPHREY, P.P.A., HALLET, P., HORNBY, E.J., WALLIS, C.J., COLLINGTON, E.W. & LUMLEY, P. (1990). Pathophysiological actions of thromboxane A2 and their pharmacological antagonism by thromboxane receptor blockade with GR32191. *Circulation*, **81**, I42–I52.

JOYNER, W.L., SVENSJ:O, E. & ARFORS, K.E. (1979). Simultaneous measurements of macromolecular leakage and arteriolar blood flow as altered by PGE1 and beta 2-receptor stimulant in the hamster cheek pouch. *Microvasc. Res.*, **18**, 301–310.

MESSINA, E. & KALEY, G. (1980). Microcirculatory responses to prostacyclin and PGE2 in the rat cremaster muscle. *Adv. Prostaglandins Thromboxane Res.*, **7**, 719–722.

MESSINA, E.J., RODENBURG, J., SLOMIANY, B.L., ROBERTS, A.M., HINTZE, T.H. & KALEY, G. (1980). Microcirculatory effects of arachidonic acid and a prostaglandin endoperoxide (PGH2). *Microvasc. Res.*, **19**, 288–296.

MESSINA, E.J., WEINER, R. & KALEY, G. (1975). Inhibition of bradykinin vasodilation and potentiation of norepinephrine and angiotensin vasoconstriction by inhibition of prostaglandin synthesis in skeletal muscle of the rat. *Circ. Res.*, **37**, 430–437.

MONCADA, S. & HIGGS, E.A. (1991). Nitric oxide: physiology, pathophysiology and pharmacology. *Pharmacol. Rev.*, **43**, 109–141.

NEWMAN, C.M., WARREN, J.B., TAYLOR, G.W., BOOBIS, A.R. & DAVIES, D.S. (1990). Rapid tolerance to the hypotensive effects of glyceryl trinitrate in the rat: prevention by N-acetyl-L- but not N-acetyl-D-cysteine. *Br. J. Pharmacol.*, **99**, 825–829.

PERSSON, M.G., GUSTAFSSON, L.E., WIKLUND, N.P., HEDQVIST, P. & MONCADA, S. (1990). Endogenous nitric oxide as a modulator of rabbit skeletal muscle microcirculation *in vivo*. *Br. J. Pharmacol.*, **100**, 463–466.

PONS, F., WILLIAMS, T.J. & WARREN, J.B. (1992). Mechanisms underlying vasodilation induced by E.Coli lipopolysaccharide (lps) in the rabbit cutaneous microvasculature. *Br. J. Pharmacol.*, **107**, 289P.

RITTER, J.M., DOKTOR, H.S. & CRAGOE, E.J.Jr. (1989). Actions of bradykinin and related peptides on rabbit coeliac artery rings. *Br. J. Pharmacol.*, **96**, 23–28.

SATA, T., LINDEN, J., LIU, L.W., KUBOTA, E. & SAID, S.I. (1988). Vasoactive intestinal peptide evokes endothelium-dependent relaxation and cyclic AMP accumulation in rat aorta. *Peptides*, **9**, 853–858.

SCHEID, C.R., HONEYMAN, T.W. & FAY, F.S. (1979). Mechanism of beta-adrenergic relaxation of smooth muscle. *Nature*, **277**, 32–36.

SCHOEFFTER, P., LUGNIER, C., DEMESY-WAELDELE, F. & STOCLET, J.C. (1987). Role of cyclic AMP- and cyclic GMP-phosphodiesterases in the control of cyclic nucleotide levels and smooth muscle tone in rat isolated aorta. A study with selective inhibitors. *Biochem. Pharmacol.*, **36**, 3965–3972.

VUORINEN, P., PORSTI, I., METSA-KETELA, T., MANNINEN, V., VAPAATALO, H. & LAUSTIOLA, K.E. (1992). Endothelium-dependent and -independent effects of exogenous ATP, adenosine, GTP and guanosine in vascular tone and cyclic nucleotide accumulation of rat mesenteric artery. *Br. J. Pharmacol.*, **105**, 279–284.

WANLESS, R.B., ANAND, I.S., GURDEN, J., HARRIS, P. & POOLE-WILSON, P.A. (1987). Regional blood flow and hemodynamics in the rabbit with adriamycin cardiomyopathy: effects of isosorbide dinitrate, dobutamine and captopril. *J. Pharmacol. Exp. Ther.*, **243**, 1101–1105.

WARREN, J.B., BRADY, A.J. & TAYLOR, G.W. (1990). Vascular smooth muscle influences the release of endothelium-derived relaxing factor. *Proc. R. Soc. B*, **241**, 127–131.

WARREN, J.B., COCKCROFT, J., LARKIN, S.W., KAJEKAR, R., MACRAE, A., GHATEI, M.A. & BLOOM, S.R. (1992a). Pituitary adenylate cyclase activating polypeptide (PACAP) is a potent vasodilator in humans. *J. Cardiovasc. Pharmacol.*, **20**, 83–87.

WARREN, J.B., COUGHLAN, M.L. & WILLIAMS, T.J. (1992b). Endotoxin-induced vasodilation in anesthetized rat skin involves nitric oxide and prostaglandin synthesis. *Br. J. Pharmacol.*, **106**, 953–957.

WARREN, J.B., DONNELLY, L.E., CULLEN, S., ROBERTSON, B.E., GHATEI, MA., BLOOM, S.R. & MACDERMOT, J. (1991). Pituitary adenylate cyclase-activating polypeptide: a novel, long-lasting, endothelium-independent vasorelaxant. *Eur. J. Pharmacol.*, **197**, 131–134.

WARREN, J.B., LARKIN, S.W., KAJEKAR, R., COUGHLAN, M. & WILLIAMS, T.J. (1992c). Pituitary adenylate cyclase activating polypeptide is a potent vasodilator and oedema potentiator in rabbit skin *in vivo*. *Br. J. Pharmacol.*, **106**, 331–334.

WARREN, J.B., LOI, R.K. & COUGHLAN, M.L. (1993). Involvement of nitric oxide synthase in the delayed vasodilator response to ultraviolet light irradiation in rat skin *in vivo*. *Br. J. Pharmacol.*, **109**, 802–806.

WILLIAMS, T.J. (1982). Vasoactive intestinal polypeptide is more potent than prostaglandin E2 as a vasodilator and oedema potentiator in rabbit skin. *Br. J. Pharmacol.*, **77**, 505–509.

WILLIAMS, T.J. & PECK, M.J. (1977). Role of prostaglandin-mediated vasodilatation in inflammation. *Nature*, **270**, 530–532.

WOOD, L.M. & OWEN, D.A.A. (1992). A comparison of vasodilator activity of agents activating cyclic nucleotides with those inhibiting their metabolism in rabbit isolated ear artery. *Br. J. Pharmacol.*, **96**, 718–724.

(Received April 6, 1993
Revised May 27, 1993
Accepted June 2, 1993)

Br. J. Pharmacol. (1993), **110**, 639–644

Enhancement by calcitonin gene-related peptide of nicotinic receptor-operated noncontractile Ca^{2+} mobilization at the mouse neuromuscular junction

[1]Ikuko Kimura, Hiroshi Tsuneki, Katsuya Dezaki & Masayasu Kimura

Department of Chemical Pharmacology, Faculty of Pharmaceutical Sciences, Toyama Medical and Pharmaceutical University, 2630 Sugitani, Toyama 930-01, Japan

1 The involvement of calcitonin gene-related peptide (CGRP) in the mechanism of nicotinic acetylcholine receptor-operated noncontractile Ca^{2+} mobilization (not accompanied by twitch tension) was investigated by measuring Ca^{2+}-aequorin luminescence at the neuromuscular junction of mouse diaphragm muscle treated with neostigmine.

2 Noncontractile Ca^{2+} transients were enhanced by 4-aminopyridine (100 μM), a K^+ channel blocker, and inhibited by botulinum toxin (1–100 μg, i.p.) and hexamethonium (10–100 μM), a neuronal nicotinic receptor antagonist.

3 Noncontractile Ca^{2+} transients were diminished by $CGRP_{8-37}$ (10–20 μM), a CGRP antagonist. CGRP (0.3–10 nM) prolonged the duration of noncontractile Ca^{2+} transients. The effect of CGRP was suppressed by $CGRP_{8-37}$ (0.1 μM).

4 Noncontractile Ca^{2+} transients were inhibited by H-89 (0.1–1 μM), a protein kinase-A inhibitor. The catalytic subunit of protein kinase-A and AA373 (300 μM), a protein kinase-A activator, prolonged the duration of noncontractile transients. The prolongations either by CGRP or by AA373 were not observed in the presence of H-89 (0.1 μM).

5 Contractile (accompanied by twitch tension) but not noncontractile Ca^{2+} transients were decreased by 12-O-tetradecanoyl phorbol 13-acetate (TPA, 0.3–1 μM), a protein kinase-C activator. Phospholipase A_2 increased only contractile Ca^{2+} transients. Calmodulin-related agents affected neither type of Ca^{2+} transients.

6 These results provide the first evidence that nicotinic acetylcholine receptor-operated noncontractile Ca^{2+} mobilization is promoted by nerve-released CGRP activating protein kinase-A, and is dependent on the accumulated amounts of acetylcholine at the neuromuscular junction where desensitization might readily develop.

Keywords: Calcitonin gene-related peptide; protein kinase-A; nicotinic acetylcholine receptor; intracellular calcium; protein kinase-C; phospholipase A_2

Introduction

Noncontractile and contractile Ca^{2+} transients are simultaneously generated at the endplate region by nerve stimulation in the presence of a cholinesterase inhibitor in mouse diaphragm muscles (Kimura *et al.*, 1991a). The noncontractile transients are triggered by the prolonged action of acetylcholine (ACh) on the postsynaptic nicotinic ACh receptor (AChR). Competitive nicotinic AChR antagonists are 10 fold more potent on noncontractile Ca^{2+} transients than on contractile Ca^{2+} transients (Kimura *et al.*, 1989).

Noncontractile Ca^{2+} mobilization occurs neither by Ca^{2+} release from sarcoplasmic reticulum, nor by simple Ca^{2+} influx through the nicotinic AChR-channel as a component of endplate current (Kimura *et al.*, 1991a,b). Contractile Ca^{2+} transients are related partly to Ca^{2+} release from the sarcoplasmic reticulum (Kimura *et al.*, 1990). The duration of noncontractile Ca^{2+} transients was much longer than that of contractile transients. We considered the possibility that the long-lasting, noncontractile Ca^{2+} may be mobilized via some pathway of signal transduction.

The neuropeptide calcitonin gene-related peptide (CGRP) coexists with ACh in the nerve terminals of the rodent neuromuscular junction (Takami *et al.*, 1985). CGRP enhances the nicotinic AChR desensitization through the phosphorylation of the nicotinic AChR by protein kinase-A (Mulle *et al.*, 1988). Hence, the properties of noncontractile Ca^{2+} mobilization which is triggered by the accumulated ACh in the synaptic cleft were studied to test whether they are also affected by CGRP and protein kinase A-related agents.

The present study was designed to elucidate which pathway of signal transduction is involved in postsynaptic nicotinic AChR-operated noncontractile Ca^{2+} mobilization at the neuromuscular junction. Two characteristic properties are described here concerning noncontractile Ca^{2+} transients: These are: (1) their dependence on the amount of ACh released from nerve terminal, and (2) whether they are promoted by released CGRP.

Methods

Muscle preparations

Male ddY mice (7–9 weeks old, 28–42 g) were killed by decapitation. A segment of the phrenic nerve-diaphragm muscle was isolated and fixed in a chamber. Modified Krebs solution (mM: NaCl 122, KCl 5.9, $CaCl_2$ 2.5, $MgCl_2$ 1.2, $NaHCO_3$ 15.5 and glucose 11.5) was equilibrated with 95% O_2 and 5% CO_2, maintained at 36°C and perfused through the chamber.

Measurement of Ca^{2+} transients

We adopted the procedures used in a previous study for measuring Ca^{2+}-aequorin luminescence (Ca^{2+} transients) and twitch tension (Kimura *et al.*, 1990). In brief, the aequorin

[1] Author for correspondence.

solution (1 mg ml^{-1}) was pressure-injected into 40–50 fibres near the ends of the fine branches where miniature endplate potentials were obtained. The phrenic nerve was then stimulated at 0.1 Hz with supramaximal square pulses (0.4–0.8 V) of 0.1 ms duration. Aequorin luminescence was led to a photomultiplier tube (Hamamatsu Photonics, Shizuoka, Japan) and measured by a photon counter (Hamamatsu Photonics). The signals were averaged 6 or 30 times by a signal processor (San-ei, Tokyo, Japan).

Drugs and solutions

Type A botulinum toxin (Wako Pure Chemical, Osaka, Japan) was injected into mice by a bolus i.p. injection 40 min prior to dissection.

Adenosine 3':5'-cyclic monophosphate (cyclic AMP; Sigma Chemical, MO, U.S.A.), calmodulin (Calbiochem, Tokyo), catalytic subunit of protein kinase-A (Sigma) and phospholipase A_2 (Sigma) were dissolved in 5 μM EDTA, and then passed through a column of Chelex 100 (50–100 mesh; Bio-Rad Laboratories, CA, U.S.A.). A similar amount of the above solutions was injected by nitrogen gas at 5 to 6 atm for 2 s through a micropipette into the muscle fibres with aequorin (Wako). Injection pipettes were filled with the above drugs at 100 fold higher concentrations than those reported as effective concentrations in other tissues, because the volume of muscle fibre within which aequorin is thought to diffuse was estimated as about 100 fold larger than that of aequorin droplets expelled by pressure at 5 atm for 2 s in the air.

AA373 (3-(2'-hydroxy-4',5'-diethoxybenzoyl)propionic acid) (Takeda Chemical, Osaka), 4α-phorbol 12, 13-didecanoate (0.1% *N*,*N*-dimethylformamide solution; Funakoshi, Tokyo), 4-aminopyridine (Nacalai Tesque, Kyoto, Japan), 8-bromo cyclic AMP (Sigma), α-CGRP (human; Asahi-Kasei Industrial, Shizuoka), $CGRP_{8-37}$ (human; Peninsula Laboratories, CA), H-7 (1-(5-isoquinolinesulphonyl)-2-methylpiperazine dihydrocholoride; MBL, Tokyo), H-85 (*N*-[2-(*N*-formyl-*p*-chlorocinnamylamino)ethyl]-5-isoquinolinesulphonamide), H-89 (*N*-[2-(*p*-bromocinnamylamino)ethyl]-5-isoquinolinesulphonamide) and KN-62 (1-[*N*,*O*-bis(5-isoquinolinesulphonyl)-*N*-methyl-L-tyrosyl]-4-phenylpiperazine) (0.001–0.05% dimethyl sulphoxide solution; provided by Prof. H. Hidaka, Department of Pharmacology, Nagoya University School of Medicine), indomethacin (0.1% *N*, *N*-dimethylformamide solution; Sigma), isoprenaline (Kaken Pharmaceutical, Tokyo), neostigmine methylsulphate (Sigma), 12-O-tetradecanoyl phorbol 13-acetate (TPA, 0.03–0.1% *N*, *N*-dimethylformamide solution; Sigma), staurosporine (0.01% *N*, *N*-dimethylformamide solution; Kyowa Medix, Tokyo), theophylline (Nacalai), W-5 (*N*-(6-aminohexyl)-1-naphthalenesulphonamide hydrochloride; MBL) and W-7 (*N*-(6-aminohexyl)-5-chloro-1-naphthalenesulphonamide hydrochloride; Nacalai) were bath-applied.

Experimental protocol

After intracellular injection by pressure or preincubation with the above drugs, neostigmine was added for 15 min. The records for 30 signals of Ca^{2+} transients obtained during the last 5 min were analyzed. The duration of noncontractile Ca^{2+} transients consists of time to peak (T_1) and decay time (T_2). Decay time was expressed as the period from peak to e^{-1} amplitude of the signal.

Statistical analysis

Data are expressed as mean ± s.e. One-way analysis of variance (ANOVA), multiple-range test and Student's *t* test were used to evaluate statistical differences between the means. The levels of significance were taken as $P = 0.05$ or 0.01. The 50% inhibitory concentrations (IC_{50}) on peak amplitude of noncontractile Ca^{2+} transients were calculated by direct assay on log concentration-response curves, where each response was presented as a percentage of the noncontractile response in the presence of neostigmine alone.

Results

Involvement of ACh in noncontractile Ca^{2+} mobilization

4-Aminopyridine (100 μM), a K^+ channel blocker that enhances the release of ACh (Somogyi *et al.*, 1987), increased the peak amplitude of both noncontractile and contractile Ca^{2+} transients, but did not affect the duration of noncontractile transients (data not shown). Botulinum toxin produces a highly effective blockade of quantal ACh release (Stanley & Drachman, 1983). Type A botulinum toxin (1 to 100 μg, bolus i.p.) completely suppressed the generation of both types of Ca^{2+} transient but did not affect mechanical or luminescence responses following direct stimulation of muscle segments (data not shown). Hexamethonium (10 to 100 μM), an antagonist of presynaptic nicotinic AChRs mediating a positive feed-back mechanism (Wessler *et al.*, 1986), inhibited the peak amplitude of noncontractile Ca^{2+} transients but not their duration (Figure 1). The IC_{50} for hexamethonium was

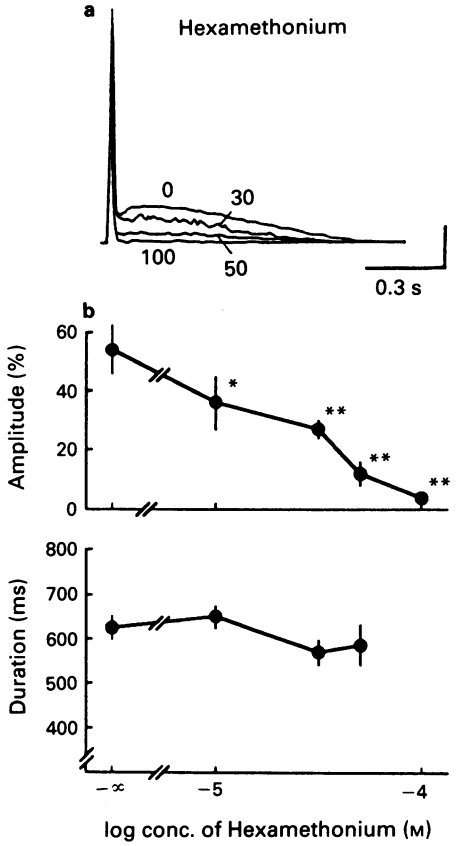

Figure 1 Involvement of a presynaptic nicotinic AChR in the mobilization of noncontractile Ca^{2+} in diaphragm muscles treated with 0.3 μM neostigmine. (a) Typical traces of Ca^{2+} transients in the presence of hexamethonium at the concentrations indicated (μM). The large, rapid increase in Ca^{2+} represents the contractile transients, and the slower prolonged increase represents the noncontractile transients. Ordinate calibration bar represents 50% amplitude. (b) Log concentration-response curves of hexamethonium on the peak amplitude and the duration, of noncontractile Ca^{2+} transients, respectively. Increasing concentrations of hexamethonium were added to the neostigmine solution every 5 min after a 15 min application of neostigmine, and the records for 6 signals during the last 1 min were analysed. Peak amplitude of either type of Ca^{2+} transients was expressed as a percentage of contractile Ca^{2+} transients obtained before the application of neostigmine. $n = 4$ to 8. $^*P < 0.05$ and $^{**}P < 0.01$; significantly different from the control response to neostigmine alone, by multiple-range test.

30 μM (23.3–38.7, 95% confidence limits). Contractile Ca^{2+} transients were not affected by hexamethonium (data not shown).

Enhancing effect of CGRP on noncontractile Ca^{2+} transients

$CGRP_{8-37}$ (10 to 20 μM), a competitive CGRP antagonist (Poyner *et al.*, 1992), shortened the duration of noncontractile Ca^{2+} transients, whereas it did not affect the peak amplitude (Figure 2a). CGRP (0.3 to 10 nM) prolonged the duration of noncontractile Ca^{2+} transients without affecting their peak amplitude (Figure 2b). When the duration was divided into two time phases, T_1 and T_2 (see methods), the lengthening of the duration by CGRP could be attributed to an increase in T_2 (Table 1), suggesting a delay of the inactivation process. A low concentration (0.1 μM) of $CGRP_{8-37}$, which had no effect on noncontractile Ca^{2+} transients, suppressed the enhancing effect of 10 nM CGRP on the duration of noncontractile transients (Figure 2b). H-89 (0.1 μM), a selective inhibitor of protein kinase-A (Chijiwa *et al.*, 1990), also suppressed the lengthening effect of 10 nM CGRP. Contractile Ca^{2+} transients were affected neither by $CGRP_{8-37}$ nor by CGRP (data not shown).

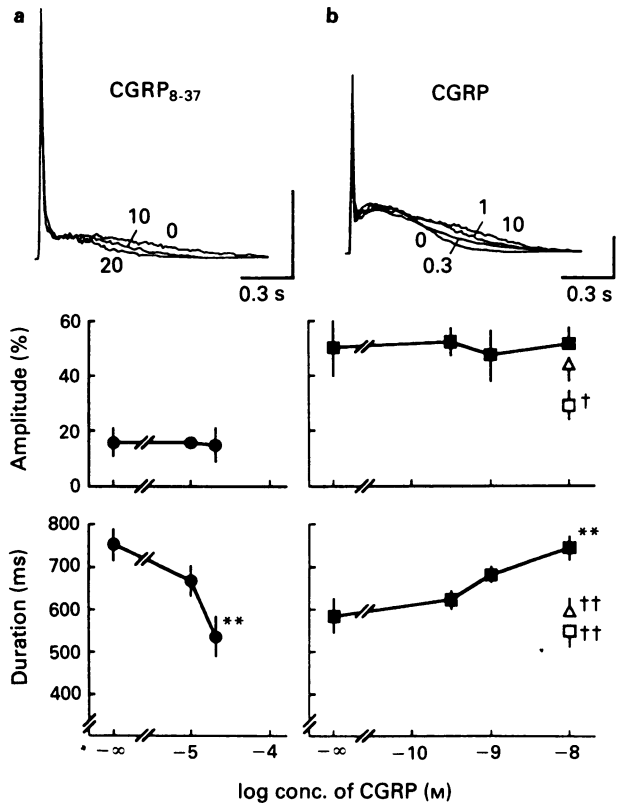

Figure 2 Involvement of calcitonin gene-related peptide (CGRP) in the mobilization of noncontractile Ca^{2+} in diaphragm muscles treated with 0.3 μM neostigmine. $CGRP_{8-37}$ was preincubated for 90 min before neostigmine was added. Responses to $CGRP_{8-37}$ and their control responses to neostigmine alone were examined in nonperfused solution to minimize losses. CGRP was preincubated for 15 min before neostigmine was added. $CGRP_{8-37}$ (0.1 μM) or H-89 were added 10 min before addition of CGRP. (a) Upper: typical traces of Ca^{2+} transients in the presence of $CGRP_{8-37}$ at the concentrations indicated (μM). Ordinate calibration bars represent 50% amplitude. Middle and lower: log concentration-response curves of $CGRP_{8-37}$ (●) on the peak amplitude and the duration of noncontractile Ca^{2+} transients, respectively. (b) Upper: typical traces in the presence of CGRP (0.3–10 nM). Middle and lower: log concentration-response curves of CGRP without any blockers (■), with 0.1 μM $CGRP_{8-37}$ (△) and with 0.1 μM H-89 (□) on the peak amplitude and the duration, of noncontractile transients, respectively. Peak amplitude of either type of Ca^{2+} transients was expressed as a percentage of contractile Ca^{2+} transients obtained before the application of neostigmine. $n = 5$ to 10. $^{**}P < 0.01$; significantly different from the control response to neostigmine alone, by one-way ANOVA. $^{\dagger}P < 0.05$ and $^{\dagger\dagger}P < 0.01$; significantly different from the effects of CGRP without $CGRP_{8-37}$ and H-89, by Student's *t* test.

Table 1 Influence of protein kinase-A system on duration of noncontractile Ca^{2+} transients

Drug		T_1 (ms)	T_2 (ms)	*Total duration*[a] (ms)	n
Control[b]		154 ± 8	429 ± 40	583 ± 40	9
CGRP	(10 nM)	193 ± 23	550 ± 29*	743 ± 27**	8
PKA	(10 μM)[c]	162 ± 13	519 ± 28	681 ± 27†	7
AA373	(300 μM)	161 ± 8	559 ± 20*	719 ± 18*	7
H-89	(0.3 μM)	171 ± 12	343 ± 17‡	514 ± 23‡‡	7
H-85	(0.3 μM)	199 ± 17	434 ± 32	634 ± 29	7

[a]Total duration consists of time to peak (T_1) and decay time (T_2). [b]Duration of noncontractile Ca^{2+} transients in the presence of 0.3 μM neostigmine alone. [c]Catalytic subunit of protein kinase-A (PKA) was intracellularly injected with aequorin.
Statistical differences were evaluated by Student's *t* test.
$^{*}P < 0.05$ and $^{**}P < 0.01$; significantly different from control responses to neostigmine alone, determined by two-tail test.
$^{\dagger}P < 0.05$ represents one-tail significance.
$^{\ddagger}P < 0.05$ and $^{\ddagger\ddagger}P < 0.01$; significantly different from the effect of H-85, determined by two-tail test.

Promoting effect of protein kinase-A activator and suppressing effect of a kinase inhibitor on noncontractile Ca^{2+} transients

H-89 (0.1 to 1 μM) decreased both the peak amplitude and the duration of noncontractile Ca^{2+} transients, whereas H-85 (0.1 to 1 μM), a noneffective analogue of H-89, had no effect (Figure 3a). The IC_{50} for H-89 on the peak amplitude was 0.14 μM (0.07–0.50). The shortening of the duration by H-89 (0.3 μM) was due to a decrease in T_2 (Table 1). These results demonstrate that H-89 decreased noncontractile transients both by suppressing the activation process and by promoting the inactivation process for Ca^{2+} mobilization. AA373 (300 μM), a protein kinase-A activator (Kimura *et al.*, 1977), prolonged the duration of noncontractile transients 1.2 fold, especially T_2, without affecting the peak amplitude of both noncontractile and contractile Ca^{2+} transients (Figure 3b, Table 1). AA373 failed to prolong the duration in the presence of H-89 (0.1 μM). The catalytic subunit of protein kinase-A (10 μM in an injection pipette) also prolonged the duration 1.2 fold (Table 1). These results indicate that the influence of protein kinase-A activation is similar to that of the CGRP application.

Enhancing effect of cyclic AMP on contractile Ca^{2+} transients

The increase in contractile Ca^{2+} transients after cholinesterase inhibition was enhanced by 10 μM isoprenaline (30 min treatment) (Table 2). Cyclic AMP (0.3 mM in the pipette) and 100 μM 8-bromo cyclic AMP (30 min), a cyclic AMP analogue able to enter the cell membrane, also enhanced the contractile responses 2.3 and 1.4 fold, respectively. The duration of noncontractile transients, however, was not prolonged under such conditions. The prolonging effects of cyclic AMP and isoprenaline were observed only at 3–30 fold higher concentrations. Theophylline (100 μM for 30 min) significantly increased only the duration of noncontractile transients.

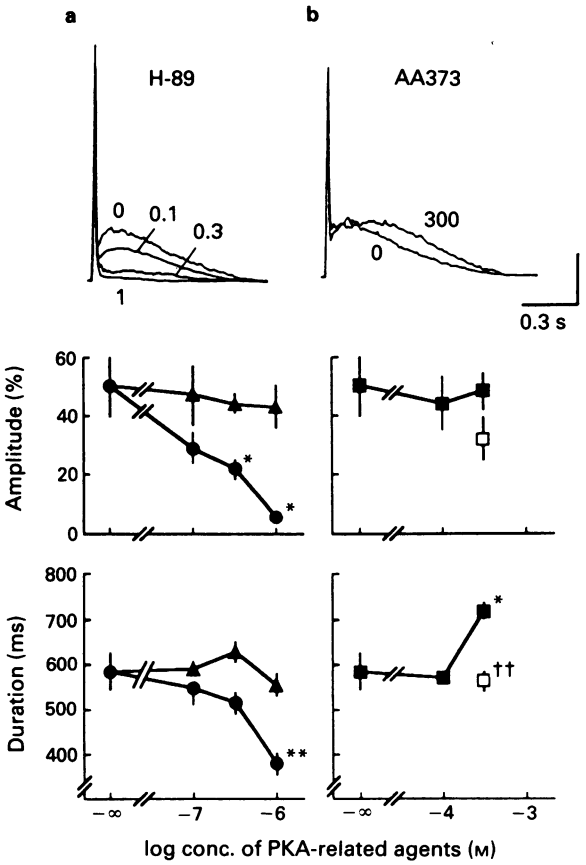

Figure 3 Involvement of protein kinase A (PKA)-activation in the mobilization of noncontractile Ca^{2+} in diaphragm muscles treated with 0.3 μM neostigmine. H-89, H-85 and AA373 were present for 30 min before neostigmine was added. H-89 (0.1 μM) was added 10 min before addition of AA373. (a) Upper: typical traces of Ca^{2+} transients in the presence of H-89 at the concentrations indicated (μM). Ordinate calibration bar represents 50%. Middle and lower: log concentration-response curves of H-89 (●) and H-85 (▲) on the peak amplitude and the duration, of noncontractile Ca^{2+} transients, respectively. (b) Upper: typical traces in the presence of 300 μM AA373. Middle and lower: log concentration-response curves of AA373 without (■) and with 0.1 μM H-89 (□) on the peak amplitude and the duration, of noncontractile transients, respectively. Peak amplitude of either type of Ca^{2+} transients was expressed as a percentage of contractile Ca^{2+} transients obtained before the application of neostigmine. $n = 4$ to 9. $*P<0.05$ and $**P<0.01$; significantly different from the control response to neostigmine alone, by one-way ANOVA. $††P<0.01$, significantly different from the effects of AA373 without H-89, by Student's t test.

Table 2 Influence of cyclic AMP on contractile and noncontractile Ca^{2+} transients

Drug		Contractile amplitude (%)	Noncontractile amplitude (%)	Noncontractile duration (ms)	n
Control[a]		228 ± 25	42 ± 8	560 ± 43	9
8-Br cyclic AMP	(100 μM)	317 ± 36†	44 ± 8	609 ± 16	8
Isoprenaline	(10 μM)	417 ± 35**	48 ± 8	583 ± 36	8
	(30 μM)	308 ± 33†	46 ± 8	720 ± 19**	8
Theophylline	(100 μM)	279 ± 42	41 ± 5	691 ± 22**	16
		(kcps)[b]	(kcps)	(ms)	
Cyclic AMP	(0 mM)[c]	12.0 ± 2.4	2.2 ± 0.3	574 ± 25	9
	(0.3 mM)[c]	27.0 ± 6.0*	3.7 ± 0.7	588 ± 25	10
	(10 mM)[c]	32.5 ± 4.8**	3.8 ± 0.7	719 ± 29**	8

[a]Contractile Ca^{2+} transients before pretreatment with cyclic AMP-related agents were regarded as 100% amplitude only in this table, since contractile transients were increased by these agents alone. [b]Kilocounts per second. Ca^{2+} signals before injection of cyclic AMP could not be obtained. Then data are expressed as absolute luminescence values. [c]Drug concentrations in an injection pipette.
Statistical differences were evaluated by Student's t test. $*P<0.05$ and $**P<0.01$; determined by two-tail test. $†P<0.05$ represents one-tail significance.

Table 3 Involvement of signal transduction systems in contractile and noncontractile Ca^{2+} mobilization

Drug		Contractile amplitude (%)	Noncontractile amplitude (%)	Noncontractile duration (ms)	n
Control[a]		250 ± 13	50 ± 10	583 ± 40	9
Protein kinase-C					
TPA	(0.3 μM)	148 ± 16**	50 ± 28	550 ± 27	4
	(1 μM)	126 ± 15**	49 ± 9	541 ± 18	9
4α-PDD[b]	(1 μM)	227 ± 14	46 ± 3	626 ± 36	7
Staurosporine	(10 nM)	238 ± 21	45 ± 8	573 ± 27	7
H-7	(10 μM)	244 ± 17	47 ± 6	597 ± 39	8
Calmodulin					
Calmodulin	(10000 u ml^{-1})[d]	233 ± 16	50 ± 11	629 ± 29	9
W-7	(10 μM)	179 ± 18**	16 ± 3*	154 ± 25**	7
W-5	(10 μM)	187 ± 20*	15 ± 2*	387 ± 61*	7
KN-62	(5 μM)	231 ± 43	50 ± 9	546 ± 29	8
Phospholipase A_2					
PLA_2[c]	(1000 u ml^{-1})[d]	330 ± 31	51 ± 6	605 ± 16	9
	(10000 u ml^{-1})[d]	457 ± 76*	52 ± 10	580 ± 21	9
Indomethacin	(10 μM)	240 ± 22	51 ± 8	642 ± 37	9

[a]Responses of each type of Ca^{2+} transients to 0.3 μM neostigmine alone. [b]4α-Phorbol 12, 13-didecanoate. [c]Phospholipase A_2 (1000 unit ml^{-1}). [d]Drug concentrations in an injection pipette.
$*P<0.05$ and $**P<0.01$; determined by one-way ANOVA.

Suppressing effect of a protein kinase-C activator on contractile Ca^{2+} transients

TPA (0.3 to 1 μM, 30 min treatment), a specific activator of protein kinase-C (Nishizuka, 1984), reduced the increase in contractile Ca^{2+} transients to 0.5 fold but not the noncontractile component, whereas the noneffective analogue 4α-phorbol 12, 13-didecanoate (1 μM, 30 min) affected neither type of Ca^{2+} transient (Table 3). Staurosporine (10 nM, 30 min) and H-7 (10 μM, 30 min), nonselective protein kinase-C inhibitors (Rüegg & Burgess, 1989), did not alter either component of the Ca^{2+} signal.

No involvement of calmodulin in Ca^{2+} mobilization

Intracellular injection of calmodulin (10000 unit ml^{-1} in the pipette) changed neither contractile nor noncontractile Ca^{2+} transients (Table 3). Both W-7 (10 μM, 30 min treatment), a calmodulin inhibitor (Hidaka *et al.*, 1980), and W-5 (10 μM, 30 min), a noneffective analogue of W-7, suppressed contractile and noncontractile Ca^{2+} transients by the same extent, demonstrating that the calmodulin inhibitor affected Ca^{2+} transients by a mechanism unrelated to the inhibition of calmodulin; the effect may be due to nicotinic AChR-channel blockade. KN-62 (5 μM, 30 min), a calmodulin kinase II inhibitor (Tokumitsu *et al.*, 1990), affected neither type of Ca^{2+} transient.

Enhancing effect of phospholipase A_2 on contractile Ca^{2+} transients

Phospholipase A_2 (1000 to 10000 unit ml^{-1} in the injection pipette) promoted only the increase in contractile transients, but not noncontractile transients (Table 3). Indomethacin (10 μM, 30 min treatment), a cyclo-oxygenase inhibitor, had no effect on either type of Ca^{2+} mobilization.

Discussion

Noncontractile Ca^{2+} mobilization is induced by the accumulation of ACh after cholinesterase inhibition, at the neuromuscular junction. However, the mechanism of noncontractile Ca^{2+} mobilization has not been clarified. The duration of endplate potentials is prolonged by the continued action of ACh in anticholinesterase-treated muscle (Katz & Miledi, 1975; Burd & Ferry, 1987), then desensitization of the nicotinic AChR can readily occur to nerve stimulation (Magleby & Pallotta, 1981). Noncontractile Ca^{2+} which is mobilized under such a desensitizable condition may prevent the nicotinic AChR from responding to excessive stimuli.

The peak amplitude of noncontractile Ca^{2+} transients was enhanced by 4-aminopyridine and inhibited either by botulinum toxin or by hexamethonium. These results demonstrate that the peak amplitude of noncontractile transients depends on evoked ACh release from presynapse. In particular, the inhibitory effect of hexamethonium suggests that the autofacilitation of ACh release is an essential process in noncontractile Ca^{2+} mobilization, since hexamethonium reduces the ACh release by blocking a presynaptic nicotinic AChR which mediates the positive feed-back mechanism (Wessler *et al.*, 1986). Hexamethonium has little effect on the postsynaptic nicotinic AChR at the low concentrations used in this study (Milne & Byrne, 1981). We cannot, however, rule out the possibility that another type of nicotinic AChR, such as a neuronal nicotinic AChR, might exist on the postsynaptic side to mobilize noncontractile Ca^{2+}. The direct activation of the postsynaptic nicotinic AChR by neostigmine can be excluded from the mechanism of Ca^{2+} mobilization, because it did not generate noncontractile Ca^{2+} transients after the blockade of quantal ACh release by botulinum toxin.

Noncontractile Ca^{2+} transients were shortened by the CGRP antagonist $CGRP_{8-37}$, and prolonged by CGRP. It has been reported that the CGRP is released in part from the motor nerve by prolonged terminal depolarization, although the major source of CGRP release is from sensory terminals of skeletal muscle (Sakaguchi *et al.*, 1991). The CGRP binds to CGRP receptors located at the neuromuscular junction (Poyner *et al.*, 1992; Popper & Micevych, 1989). Our results suggest that the mobilization of noncontractile Ca^{2+} may be promoted by endogenous CGRP of the neuromuscular synapse. The release of CGRP may be initiated through the positive feed-back mechanism of ACh release during the accumulation of ACh.

CGRP induces a localized increase in the cyclic AMP level in endplate-rich region, indirectly leading to the activation of protein kinase-A (Matsumoto *et al.*, 1992). The protein kinase-A inhibitor H-89 suppressed noncontractile Ca^{2+} transients. The duration of noncontractile transients was prolonged either by the protein kinase-A activator, AA373 or by the catalytic subunit of the kinase. The prolongations by CGRP were completely suppressed by H-89. These results indicate that CGRP may activate protein kinase-A to mobilize noncontractile Ca^{2+}. The prolonging effects of isoprenaline and cyclic AMP were observed only at higher concentrations than those increasing contractile transients, whereas CGRP prolonged the noncontractile transients without affecting the contractile responses. Although the low sensitivity to added cyclic AMP appears to reflect problems of access of cyclic AMP to the relevant compartment of muscle fibre, cyclic AMP-independent activation of protein kinase-A by CGRP may be one of pathways in noncontractile Ca^{2+} mobilization. A presynaptic role of protein kinase-A (Van der Kloot & Brănisteanu, 1992) contributes less to the prolongation of noncontractile Ca^{2+} transients, because the prolongation was observed by intracellular injection of the catalytic subunit of protein kinase-A or a high concentration of cyclic AMP into muscle fibres. Nicotinic AChR phosphorylation by protein kinase-A causes agonist-independent activation of the nicotinic AChR in the single-channel recording (Ferrer-Montiel *et al.*, 1991). Hence, CGRP-induced prolongation of noncontractile Ca^{2+} transicents, especially T_2 (decay time in the Ca^{2+} signal reflecting an inactivation process), may be related to the receptor-channel opening via phosphorylation by protein kinase-A.

It has been shown that a protein kinase-C activator TPA alters the conductance and the gating behaviour of the nicotinic AChR-channel (Eusebi *et al.*, 1987). The decrease in contractile Ca^{2+} transients by TPA is probably correlated with phosphorylation of the nicotinic AChR by protein kinase-C. The presynaptic effect of TPA may not relate to this decrease, since phorbol ester enhances the ACh release in mouse phrenic nerve-diaphragm preparations (Murphy & Smith, 1987). In contrast to contractile transients, the noncontractile transients were not inhibited by TPA. The protein kinase-C inhibitors, staurosporine and H-7, did not affect noncontractile transients, demonstrating that the mechanism of noncontractile Ca^{2+} mobilization is not related to the enzyme activity of protein kinase-C. On the other hand, phospholipase A_2 increased only contractile transients. This increase may be in part due to arachidonic acid-induced Ca^{2+} release from the sarcoplasmic reticulum (Cheah, 1981). Calmodulin-related agents affected neither type of Ca^{2+} transients. Thus, the postsynaptic signalling pathways examined in this study, other than the protein kinase-A system, were not involved in the processes of noncontractile Ca^{2+} mobilization.

CGRP promotes nicotinic AChR desensitization through phosphorylation by protein kinase-A (Miles *et al.*, 1989). In addition, intracellular Ca^{2+} influx through the nicotinic AChR enhances the desensitization via phosphorylation of the receptor by protein kinase-C (Huganir & Greengard, 1990). However, the interaction between the cyclic AMP (protein kinase-A) system and Ca^{2+} system with respect to desensitization remains unclear. We suggest the possibility that CGRP may mobilize noncontractile Ca^{2+} during desensitization. Noncontractile Ca^{2+} may translocate protein kinase-C to the plasma membrane and promote the kinase activation by co-factors such as diacylglycerol, because protein kinase-C binds to the membrane in a Ca^{2+}-dependent manner (Bazzi & Nelsestuen, 1988). Protein kinase-C phosphorylates the nicotinic AChR, inducing desensitization of the receptor (Eusebi *et al.*, 1987). Thus, the protein kinase-A system may cooperate with the Ca^{2+} system to promote nicotinic AChR desensitization.

In conclusion, noncontractile Ca^{2+} mobilization was promoted by nerve-released CGRP activating protein kinase-A, and was dependent on the accumulated amounts of ACh at the neuromuscular junction, whereas contractile Ca^{2+} mobilization was inhibited by protein kinase-C and enhanced by phospholipase A_2.

We are grateful to Dr Ricardo Miledi (University of California, Irvine, U.S.A.) for his comments on this manuscript. We thank Dr Hiroyoshi Hidaka (Nagoya University School of Medicine) and Asahi-Kasei Industrial for providing samples, and Dr Takashi Kondoh (ERATO) for his skilful technical assistance. This work was supported in part by special Coordination Funds for Promoting Science and Technology (1991) from the Science and Technology Agency, Japan, and in part by a Sasakawa Scientific Research Grant (1991) from the Japanese Science Society.

References

BAZZI, M.D. & NELSESTUEN, G.L. (1988). Constitutive activity of membrane-inserted protein kinase-C. *Biochem. Biophys. Res. Commun.*, **152**, 336–343.

BURD, P.F. & FERRY, C.B. (1987). A prolonged contraction at the end-plate region of the diaphragm of rats and mice after anticholinesterases *in vitro*. *J. Physiol.*, **391**, 429–440.

CHEAH, A.M. (1981). Effect of long chain unsaturated fatty acids on the calcium transport of sarcoplasmic reticulum. *Biochim. Biophys. Acta*, **648**, 113–119.

CHIJIWA, T., MISHIMA, A., HAGIWARA, M., SANO, M., HAYASHI, K., INOUE, T., NAITO, K., TOSHIOKA, T. & HIDAKA, H. (1990). Inhibition of forskolin-induced neurite outgrowth and protein phosphorylation by a newly synthesized selective inhibitor of cyclic AMP-dependent protein kinase, *N*-[2-(*p*-bromocinnamylamino) ethyl]-5-isoquinolinesulfonamide (H-89), of PC12D pheochromocytoma cells. *J. Biol. Chem.*, **265**, 5267–5272.

EUSEBI, F., GRASSI, F., NERVI, C., CAPORALE, C., ADAMO, S., ZANI, B.M. & MOLINARO, M. (1987). Acetylcholine may regulate its own nicotinic receptor-channel through the C-kinase system. *Proc. R. Soc.* B, **230**, 355–365.

FERRER-MONTIEL, A.V., MONTAL, M.S., DÍAZ-MUÑOZ, M. & MONTAL, M. (1991). Agonist-independent activation of acetylcholine receptor channels by protein kinase A phosphorylation. *Proc. Natl. Acad. Sci. U.S.A.*, **88**, 10213–10217.

HIDAKA, H., YAKAMI, T., NAKA, M., TANAKA, T., HAYASHI, H. & KOBAYASHI, R. (1980). Calcium-regulated modulator protein interacting agents inhibit smooth muscle calcium-stimulated protein kinase and ATPase. *Mol. Pharmacol.*, **17**, 66–72.

HUGANIR, R.L. & GREENGARD, P. (1990). Regulation of neurotransmitter receptor desensitization by protein phosphorylation. *Neuron*, 5, 555–567.

KATZ, B. & MILEDI, R. (1975). The nature of the prolonged endplate depolarization in anti-esterase treated muscle. *Proc. R. Soc.* B, **192**, 27–38.

KIMURA, M., KIMURA, I. & KOBAYASHI, S. (1977). The activation of cyclic 3',5'-adenosine monophosphate-dependent protein kinase on sarcoplasmic reticulum fractions of various smooth muscles and its related novel relaxants. *Biochem. Pharmacol.*, **26**, 994–996.

KIMURA, M., KIMURA, I., KONDOH, T. & TSUNEKI, H. (1991a). Noncontractile acetylcholine receptor-operated Ca^{++} mobilization: suppression of activation by open channel blockers and acceleration of desensitization by closed channel blockers in mouse diaphragm muscle. *J. Pharmacol. Exp. Ther.*, **256**, 18–23.

KIMURA, I., KONDOH, T. & KIMURA, M. (1989). Postsynaptic nicotinic ACh receptor-operated Ca^{2+} transients with neostigmine in phrenic nerve-diaphragm muscles of mice. *Brain Res.*, **507**, 309–311.

KIMURA, I., KONDOH, T. & KIMURA, M. (1990). Changes in intracellular Ca^{2+} produced in the mouse diaphragm by neuromuscular blocking drugs. *J. Pharm. Pharmacol.*, **42**, 626–631.

KIMURA, I., KONDOH, T., TSUNEKI, H. & KIMURA, M. (1991b). Reversed effect of caffeine on non-contractile and contractile Ca^{2+} mobilization operated by acetylcholine receptor in mouse diaphragm muscle. *Neurosci. Lett.*, **127**, 28–30.

MAGLEBY, K.L. & PALLOTTA, B.S. (1981). A study of desensitization of acetylcholine receptors using nerve-released transmitter in the frog. *J. Physiol.*, **316**, 225–250.

MATSUMOTO, N., WANG, X.-B. & UCHIDA, S. (1992). Different natures of supersensitivity of adenylate cyclase stimulated by calcitonin gene-related peptide and isoproterenol in rat diaphragm after denervation and reserpine treatment. *J. Neurochem.*, **58**, 357–361.

MILES, K., GREENGARD, P. & HUGANIR, R.L. (1989). Calcitonin gene-related peptide regulates phosphorylation of the nicotinic acetylcholine receptor in rat myotubes. *Neuron*, **2**, 1517–1524.

MILNE, R.J. & BYRNE, J.H. (1981). Effects of hexamethonium and decamethonium on end-plate current parameters. *Mol. Pharmacol.*, **19**, 276–281.

MULLE, C., BENOIT, P., PINSET, C., ROA, M. & CHANGEUX, J.-P. (1988). Calcitonin gene-related peptide enhances the rate of desensitization of the nicotinic acetylcholine receptor in cultured mouse muscle cells. *Proc. Natl. Acad. Sci. U.S.A.*, **85**, 5728–5732.

MURPHY, R.L.W. & SMITH, M.E. (1987). Effects of diacylglycerol and phorbol ester on acetylcholine release and action at the neuromuscular junction in mice. *Br. J. Pharmacol.*, **90**, 327–334.

NISHIZUKA, Y. (1984). The role of protein kinase C in cell surface signal transduction and tumour promotion. *Nature*, **308**, 693–698.

POPPER, P. & MICEVYCH, P.E. (1989). Localization of calcitonin gene-related peptide and its receptors in a striated muscle. *Brain Res.*, **496**, 180–186.

POYNER, D.R., ANDREW, D.P., BROWN, D., BOSE, C. & HANLEY, M.R. (1992). Pharmacological characterization of a receptor for calcitonin gene-related peptide on rat, L6 myocytes. *Br. J. Pharmacol.*, **105**, 441–447.

RÜEGG, U.T. & BURGESS, G.M. (1989). Staurosporine, K-252 and UCN-01: potent but nonspecific inhibitors of protein kinases. *Trends Pharmacol. Sci.*, **10**, 218–220.

SAKAGUCHI, M., INAISHI, Y., KASHIHARA, Y. & KUNO, M. (1991). Release of calcitonin gene-related peptide from nerve terminals in rat skeletal muscle. *J. Physiol.*, **434**, 257–270.

SOMOGYI, G.T., VIZI, E.S., CHAUDHRY, I.A., NAGASHIMA, H., DUNCALF, D., FOLDES, F.F. & GOLDINER, P.L. (1987). Modulation of stimulation-evoked release of newly formed acetylcholine from mouse hemidiaphragm preparation. *Naunyn-Schmied Arch. Pharmacol.*, **336**, 11–15.

STANLEY, E.F. & DRACHMAN, D.B. (1983). Botulinum toxin blocks quantal but not non-quantal release of ACh at the neuromuscular junction. *Brain Res.*, **261**, 172–175.

TAKAMI, K., KAWAI, Y., SHIOKAWA, S., LEE, Y., GIRGIS, S., HILLYARD, C.J., MACINTYRE, I., EMSON, P.C. & TOHYAMA, M. (1985). Immunohistochemical evidence for the coexistence of calcitonin gene-related peptide- and choline acetyltransferase-like immunoreactivity in neurons of the rat hypoglossal, facial and ambiguus nuclei. *Brain Res.*, **328**, 386–389.

TOKUMITSU, H., CHIJAWA, T., HAGIWARA, M., MIZUTANI, A., TERASAWA, M. & HIDAKA, H. (1990). KN-62, 1-[*N*,*O*-bis(5-isoquinolinesulfonyl)-*N*-methyl-L-tyrosyl]-4-phenylpiperazine, a specific inhibitor of Ca^{2+}/calmodulin-dependent protein kinase II. *J. Biol. Chem.*, **265**, 4315–4320.

VAN DER KLOOT, W. & BRĂNISTEANU, D.D. (1992). Effects of activators and inhibitors of protein kinase A on increases in quantal size at the frog neuromuscular junction. *Pflügers Arch.*, **420**, 336–341.

WESSLER, I., HALANK, M., RASBACK, J. & KILBINGER, H. (1986). Presynaptic nicotine receptors mediating a positive feed-back on transmitter release from the rat phrenic nerve. *Naunyn-Schmied Arch. Pharmacol.*, **334**, 365–372.

(Received March 2, 1993
Revised June 1, 1993
Accepted June 3, 1993)

Br. J. Pharmacol. (1993), **110**, 645–650

Partial agonist effect of the platelet-activating factor receptor antagonists, WEB 2086 and WEB 2170, in the rat perfused heart

Weimin Hu, Ila K. McNicholl, Patrick C. Choy & [1]Ricky Y.K. Man

Department of Pharmacology and Therapeutics, and Department of Biochemistry and Molecular Biology, Faculty of Medicine, University of Manitoba, Winnipeg, Manitoba, Canada R3E OW3

1 WEB 2086 and WEB 2170 are potent platelet-activating factor (PAF) receptor antagonists and have been used widely as pharmacological tools to investigate the actions of PAF in a variety of biological systems.

2 Low concentrations of WEB 2086 and WEB 2170 blocked the vasoconstrictor action of PAF in the rat perfused heart. In this study, we observed that moderate concentrations of WEB 2086 and WEB 2170 increased the perfusion pressure in rat isolated hearts under constant flow perfusion. The vasoconstrictor actions of WEB 2086 and WEB 2170 were not observed with a structurally different PAF receptor antagonist, FR-900452.

3 To determine whether this vasoconstrictor action of WEB 2086 involved non-specific effects or was via the activation of PAF receptors, hearts were pretreated with 1000 pmol PAF or 50 μM FR-900452. These pretreatments attenuated the vasoconstrictor action of 1 μM WEB 2086, suggesting that the action of WEB 2086 may be mediated via PAF receptors. Pretreatment with the leukotriene receptor antagonist (L-649,923, 5 μM) and the leukotriene synthesis inhibitor (MK-886, 10 μM) that are known to block the vasoconstrictor action of PAF receptor activation also attenuated the vasoconstrictor action of WEB 2086. Pretreatment with PAF or MK-886 attenuated the vasoconstrictor action of 0.5 μM WEB 2170.

4 When PAF receptors were activated by PAF in the perfused heart, significant amounts of leukotriene C_4 and leukotriene $C_4/D_4/E_4$ were detected in the coronary effluent. However, no significant amount of these leukotrienes was detected in the coronary effluent when hearts were perfused with 1 μM WEB 2086 or 0.5 μM WEB 2170.

5 In summary, our results indicate that WEB 2086 and WEB 2170 possess partial agonist effects in the rat perfused heart where they produced vasoconstriction via the activation of PAF receptor. This action could be attenuated by PAF pretreatment or a PAF receptor antagonist. The vasoconstrictor action of WEB 2086 and WEB 2170 involved the production of leukotrienes. But unlike the vasoconstrictor action of PAF, no significant amount of leukotrienes was detected in the effluent suggesting that the vasoconstrictor action of WEB 2086 and WEB 2170 may be explained on the basis of intracellularly or locally produced leukotrienes.

Keywords: Platelet-activating factor receptor antagonists; WEB 2086; WEB 2170; FR-900452; partial agonist; rat perfused heart

Introduction

Platelet-activating factor (PAF) is a lipid mediator that has a variety of biological actions (Braquet *et al.*, 1987) it has been demonstrated to bind to the cell membrane with high affinity suggesting that its action is mediated by the activation of specific receptors located on the cell membrane (Valone *et al.*, 1982; Hwang *et al.*, 1983). The PAF receptor has now been cloned and sequenced (Honda *et al.*, 1991) thus confirming the existence of a specific receptor for PAF. To examine the biological effects of PAF, a number of PAF receptor antagonists have been developed. These antagonists have been useful in demonstrating many pathophysiological roles of PAF including platelet activation and thrombosis, shock, allergy and immune responses (Braquet *et al.*, 1987). Using receptor binding assays, several studies show that PAF receptor antagonists compete with PAF for the same high affinity site and prevent the activation of the receptor by PAF (Braquet *et al.*, 1987; Saunders & Handley, 1987). In the rat perfused heart, PAF produces a vasodilatation followed by a vasoconstriction (Man *et al.*, 1990). Leukotriene B_4 (LTB_4) may be involved in the vasodilator effect while LTC_4 and/or LTD_4 may be involved in the vasoconstrictor effect in the perfused heart (Hu *et al.*, 1991b). We have recently examined the selectivity of a number of PAF receptor antagonists for their ability to block the vasodilator and vasoconstrictor actions of PAF in the rat perfused heart (Hu & Man, 1991a). During the course of this study, we observed that WEB 2086 showed a small vasoconstrictor action during the 10 min pretreatment period. This effect may be due to a non-specific effect of WEB 2086 on the coronary blood vessels. Alternatively, WEB 2086 may produce vasoconstriction if it possesses a partial agonist action on the PAF receptor. Although there is no report on commonly used PAF receptor antagonists with a partial agonist effect, there is a recent paper indicating that a PAF structural analogue (hexanolamine PAF, a putative PAF receptor antagonist) showed partial agonist activity (Grigoriadis & Stewart, 1991). The present study was designed to investigate if WEB 2086 and its structural analogue WEB 2170 possess partial agonist action.

Methods

Rat heart perfusion

Following cervical dislocation, hearts from Sprague-Dawley rats (250–350 g) were rapidly excised and placed in cool

[1] Author for correspondence at: Ricky Y.K. Man, Department of Pharmacology, University of Manitoba, 770 Bannatyne Avenue, Winnipeg, Manitoba, Canada R3E OW3.

Krebs-Henseleit solution (4°C) oxygenated with 95% O_2: 5% CO_2. The solution had the following composition (in mM): NaCl 120, NaH_2PO_4 1.18, $MgSO_4$ 1.18, KCl 4.76, $CaCl_2$ 1.25, $NaHCO_3$ 25.0, and glucose 5.5. The aorta was cannulated for coronary perfusion. The heart was allowed to beat spontaneously. The temperature of the perfusate was maintained at 37 ± 0.5°C and the coronary flow was controlled by a roller pump. The perfusion pressure was measured by a pressure transducer attached to a side arm of the aortic cannula. The perfusion pressure was recorded on a Gould chart recorder and monitored with a digital display of the perfusion pressure. The detailed methodology of the isolated heart perfusion system has been described previously (Man *et al.*, 1990). All stock solutions to be used in subsequent sections were made fresh daily and kept at 4°C between experiments. In these experiments, only one concentration of the drug was used in each heart.

Vasoactive effect of PAF receptor antagonists

Hearts were equilibrated with Krebs-Henseleit solution for 20 min. During the equilibration period, the flow rate was adjusted to obtain a control perfusion pressure of 65–75 mmHg. The vasoactive actions of PAF receptor antagonists were determined by the perfusion of the heart with Krebs-Henseleit solution containing the appropriate amount of the PAF receptor antagonist for 10 min under constant flow perfusion. The vasoactive effect was measured as changes in the perfusion pressure (Man *et al.*, 1990). WEB 2086 (3-[4-(2-chlorophenyl)-9-methyl-6H-thieno[3,2-f][1,2,4]-triazolo-[4,3-a][1,4]-diazepine-2-yl]-1-(4-morpholinyl)-1-propanone, Boehringer Ingelheim, KG) and WEB 2170 (5-(2-chlorophenyl)-3,4-dihydro-10-methyl-3-((4-morpholinyl)carbonyl)-2H, 7H-cyclopenta(4,5)thieno[3,2-f][1,2,4]triazolo-[4,3-a] [1,4] diazepine, Boehringer Ingelbeim, KG) were dissolved in Krebs-Henseleit solution. FR-900452 (1-methyl-3-(1-(5-methylthiomethyl-6-oxo-3-(2-oxo-3-cyclopenten-1-ylidene)-2-piperazinyl)ethyl)-2-indolinone, Fujisawa Pharmacological Co., Japan) was dissolved in ethanol then diluted in Krebs-Henseleit solution to a final concentration of 50 μM in 0.1% ethanol. This amount of ethanol has been shown not to affect the coronary vascular effects of PAF (Hu *et al.*, 1991b).

Effect of WEB 2170 on the vasodilator and vasoconstrictor effects of PAF

Following a 20 min equilibration period, hearts were pretreated with a solution containing the appropriate amount of WEB 2170 for 10 min. PAF (1-*O*-alkyl-2-acetyl-*sn*-glycero-3-phosphocholine, prepared from bovine heart, Sigma Chemical Co.) was prepared in saline (0.9% NaCl) containing 0.25% bovine serum albumin (Sigma Chemical Co.). A bolus injection of PAF (100 pmol) was given in a volume of 0.1 ml and over a 1 s period, into the perfusion line 5–6 cm proximal to the aortic cannula. Changes in perfusion pressure were recorded. To serve as controls, the effect of PAF was determined in hearts with no WEB 2170 pretreatment.

Mechanism of vasoconstrictor action of WEB 2086 and WEB 2170

To determine the involvement of PAF receptors in the action of WEB 2086 and WEB 2170, PAF receptors were blocked by PAF pretreatment or FR-900452. For pretreatment with PAF, a bolus injection of 1000 pmol of PAF was given in a volume of 0.1 ml. The perfusion pressure returned to baseline level with 5 min and pretreatment with PAF has been shown to abolish any subsequent response to PAF in the perfused heart (Piper & Stewart, 1986; Hu *et al.*, 1991a). Changes in perfusion pressure induced by 1 μM WEB 2086 were determined after the PAF pretreatment. In separate experiments, the effect of 0.5 μM WEB 2170 on the perfusion pressure was examined after the same PAF pretreatment. The effect of WEB 2086 was also determined after a 10 min pretreatment with 50 μM FR-900452.

The leukotriene receptor antagonist, L-649,923 (sodium (βS*, R*)-4-(3-4(-acetyl-4-hydroxy-2-propylphenoxy)-propylthio)-γ-hydroxy-β-methylbenzenebutanoate, Merck Frosst Canada Inc., Jones *et al.*, 1986) was dissolved in distilled water and the leukotriene synthesis inhibitor, MK-886 (3-[1-(4-chlorobenzyl)-3-*t*-butyl-thio-5-isopropylindol-2-yl]-2,2-dimethylpropanoic acid, Merck Frost Canada Inc., Gillard *et al.*, 1989) was dissolved in ethanol, and then diluted in Krebs-Henseleit solution to a concentration of 5 μM and 10 μM respectively. The effects of WEB 2086 and WEB 2170 were examined in separate experiments after the heart had been pretreated for 10 min with either L-649,923 or MK-886. The cyclo-oxygenase inhibitor, indomethacin, was added to the perfusion solution at the start of the stabilization period and the vasoactive action of the PAF receptor antagonist was tested after 45 min of perfusion in the presence of indomethacin.

Radioimmunoassay for leukotrienes

Leukotrienes were determined by a competitive binding radioummunoassay using a commercially available kit from Amersham International (U.K.). Samples of effluent from rat perfused isolated heart were collected into test tubes for periods of 0–2, 2–5 and 5–10 min after various protocols. Samples were capped and stored at − 20°C. The concentration of leukotrienes in the effluent from rat perfused heart was determined without prior extraction or purification.

LTC_4: effluent (100 μl) from perfused rat heart was mixed with 100 μl of [5, 6, 8, 9, 11, 12, 14, 15 (n)-^{3}H]-LTC_4, followed by 100 μl of specific antiserum to LTC_4 and 100 μl of assay buffer. The mixture was incubated overnight at 4°C. Then 500 μl of dextran-coated charcoal was added to the mixture in an ice-bath for 10 min to remove unbound leukotrienes. After centrifugation at 2,000 *g* for 10 min at 4°C, the supernatant was decanted into 10 ml of aqueous scintillation fluid and the radioactivity measured in a β-scintillation counter (Beckmann). The concentration of LTC_4 in each sample was determined from the standard curve. The sensitivity of the LTC_4 assay was 8 pg/tube.

$LTC_4/D_4/E_4$: effluent (100 μl) from perfused rat heart was mixed with 100 μl of [14, 15 (n)-^{3}H]-LTC_4, followed by 100 μl of antiserum to the leukotrienes and 100 μl of assay buffer. The mixture was incubated overnight at 4°C. Then 250 μl of dextran-coated charcoal was added to the mixture in an ice-bath for 15 min to remove unbound leukotrienes. After centrifugation at 2,000 *g* for 15 min at 4°C, the supernatant was decanted into 10 ml of aqueous scintillation fluid and the radioactivity measured in a β-scintillation counter. The concentration of leukotrienes in each sample was determined from a standard curve. The sensitivity for LTC_4 in this assay was 12.5 pg/tube. Compared to LTC_4 (100%), the cross-reactivity for LTD_4 was 181.8% and the cross-reactivity for LTE_4 was 92.7%.

Statistical analyses

Data were analysed by the Student's *t* test and analysis of variance (ANOVA) followed by Duncan's test where appropriate. Values are expressed as means ± standard deviations (s.d.) and $P < 0.05$ was considered statistically significant.

Results

Effects of WEB 2086 and WEB 2170 on the perfusion pressure of rat perfused hearts

In our previous study, we demonstrated that pretreatment with a low concentration of WEB 2086 (0.5 μM) blocked the vasoconstrictor action of 100 pmol PAF in the rat perfused

heart while a higher concentration of WEB 2086 (100 μM) blocked both the vasodilator and vasoconstrictor actions of PAF (Hu & Man, 1991a). However a gradual increase in the perfusion pressure with some concentrations of WEB 2086 was observed during the pretreatment period with this PAF receptor antagonist. This time course of perfusion pressure change was much slower than that observed with PAF (Figure 1). Since a 10 min pretreatment period was used in our previous study, the same time period was used to determine changes in perfusion pressure after 10 min of perfusion in the presence of WEB 2086. Statistically significant increases in perfusion pressure were observed with 1 μM of WEB 2086, a moderate concentration of WEB 2086 (65.5 ± 0.7 and 80.9 ± 5.7 mmHg before and after 10 min of perfusion, $n = 10$, $P < 0.001$). This concentration of WEB 2086 was chosen for subsequent experiments. For comparison, WEB 2170, a structurally similar PAF receptor antagonist was also studied. A gradual increase in perfusion pressure in the presence of WEB 2170 was also observed (Figure 1). This is in contrast to the much faster time course for the coronary vascular effect of PAF (Figure 1). The increase in perfusion pressure by various concentrations of WEB 2170 is shown in Figure 2. Concentrations of 0.02–1.0 μM WEB 2170 produces consistent vasoconstriction in the rat perfused heart. In order to determine the ability of WEB 2170 to block the vasodilator and vasoconstrictor effects of PAF, experiments were conducted with a 10 min perfusion period with various concentrations of WEB 2170 prior to testing the coronary vascular effect of 100 pmol PAF. A low concentration of WEB 2170 (0.02 μM) did not affect the vasodilator nor vasoconstrictor effects of 100 pmol PAF while 0.05, 0.1 and 0.5 μM WEB 2170 blocked the vasoconstrictor effect of PAF but had no effect on the vasodilator effect of PAF (Table 1). WEB 2170 (1 μM) appeared to block both the vasodilator and vasoconstrictor effects of PAF. Since an equivalent concentration of WEB 2170 to WEB 2086 (1 μM) would be more potent than WEB 2086 in blocking the vasodilator effect of PAF in the perfused heart, 0.5 μM of WEB 2170 was used for further studies.

Unlike WEB 2086 and WEB 2170, FR-900452, a PAF receptor antagonist with a different chemical structure (Okamoto *et al.*, 1986), did not affect the perfusion pressure at a concentration that blocked both the vasodilatation and vasoconstriction produced by 100 pmol PAF (66.0 ± 0.9 and 68.3 ± 4.6 mmHg before and after 10 min of perfusion with a solution containing 50 μM FR-900452, $n = 8$, $P > 0.05$).

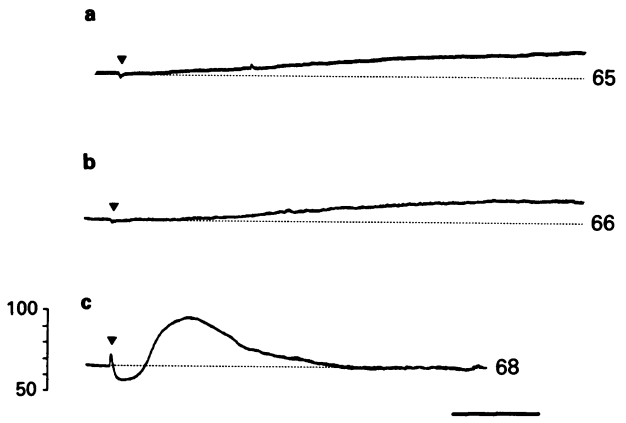

Figure 1 Time course of typical perfusion pressure changes by 1 μM WEB 2086 (a), 0.5 μM WEB 2170 (b) and 100 pmol PAF (c). The time scale is 2 min for (a) and (b) and 1 min for (c). Vertical scale represents the perfusion pressure in mmHg. Arrows indicate the time of application of the various treatments. Values in each panel represent the baseline perfusion pressure and are highlighted by the dotted lines.

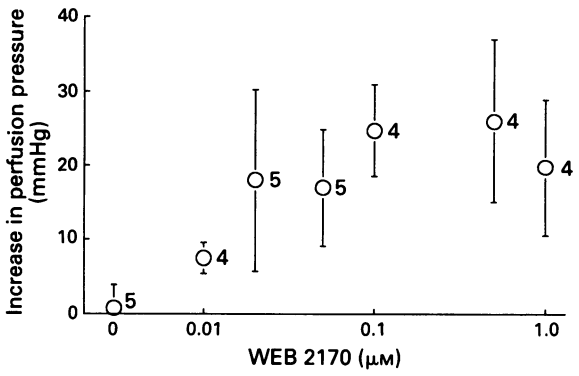

Figure 2 Effect of various concentrations of WEB 2170 on the perfusion pressure of rat perfused hearts. Changes in perfusion pressure were recorded at the end of a 10 min perfusion period in the absence or presence of various concentrations of WEB 2170. Values represent mean ± s.d., n = number of hearts used in each group.

The mechanism for the vasoconstrictor action of WEB 2086 and WEB 2170

Pretreatment with PAF or FR-900452 had been shown to be effective in blocking the coronary vascular effect of PAF in the rat heart (Piper & Stewart, 1986; Hu *et al.*, 1991a). These pretreatments attenuated the vasonconstrictor action of 1 μM WEB 2086 (Figure 3). These results suggested that the action of WEB 2086 may be mediated via PAF receptors. Pretreatment with the leukotriene receptor antagonist L-649,923 (5 μM) or the leukotriene synthesis inhibitor MK-886 (10 μM) has been shown to block the vasoactive actions of PAF (Hu *et al.*, 1991b). These pretreatments also significantly attenuated the vasoconstrictor action of WEB 2086 (Figure 4). Pretreatment with 2.8 μM indomethacin had no significant effect on the vasoconstrictor action of WEB 2086 (14.8 ± 7.3 mmHg, $n = 4$). Pretreatment with 1000 pmol PAF or MK-886 significantly attenuated the vasoconstrictor action of 0.5 μM WEB 2170 (Figure 5).

Determination of leukotrienes in the coronary effluent

The vasoconstrictor action of PAF in the rat perfused heart has been shown to be due to the release of leukotrienes (Piper & Stewart, 1986; Hu *et al.*, 1991b; Hu & Man, 1991b).

Table 1 Effect of WEB 2170 on the vasodilator and vasoconstrictor effects of 100 pmol PAF in the rat perfused heart[a]

Concentration of WEB 2170 (μM)	*Peak vasodilator effect* (mmHg)[b]	*Peak vasoconstrictor effect* (mmHg)[b]	n
0	− 8.6 ± 5.5	27.8 ± 4.8	8
0.02	− 14.6 ± 5.0	21.3 ± 9.7	5
0.05	− 14.2 ± 3.7	NC	5
0.1	− 10.6 ± 1.1	NC	5
0.5	− 9.5 ± 4.6	NC	5
1.0	− 3.4 ± 2.3*	NC	5

Values represent mean ± s.d., n = number of experiments. NC denotes no detectable change (increase) in perfusion pressure. Statistical analysis were performed by ANOVA followed by Duncan's test.

*$P < 0.05$ when compared to the appropriate data in the absence of WEB 2170.

[a]Hearts were perfused for 10 min with various concentrations of WEB 2170; 100 pmol PAF was administered as a single bolus injection. Each heart received only one concentration of WEB 2170 and one injection of PAF.

[b]With constant flow perfusion, decrease in perfusion pressure represents vasodilatation (negative value) and increase in perfusion pressure represents vasoconstriction.

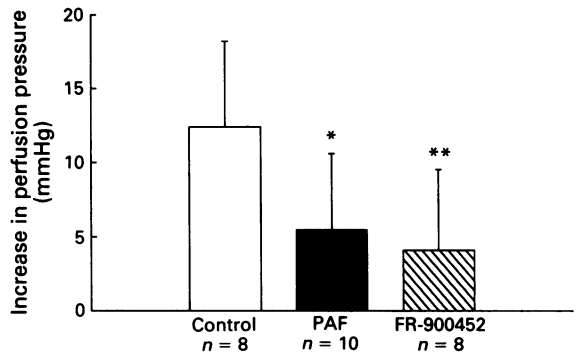

Figure 3 Effect of pretreatment with 1000 pmol PAF bolus injection and 50 μM FR-900452 on perfusion pressure changes by 1 μM WEB 2086 in rat perfused hearts. Values represent mean ± s.d., n = number of hearts used in each group. Control indicates no pretreatment. $^*P<0.05$ and $^{**}P<0.01$ when compared to the corresponding control value.

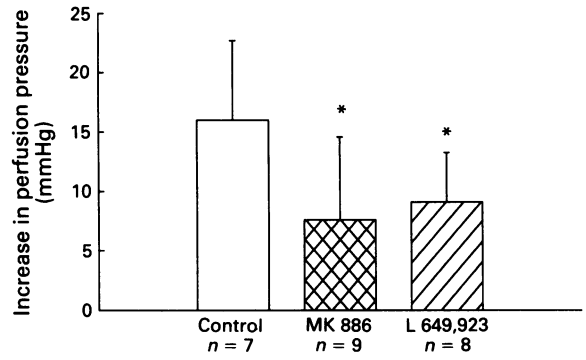

Figure 4 Effect of pretreatment with 10 μM MK-886 and 5 μM L-649,923 on perfusion pressure changes by 1 μM WEB 2086 in rat perfused hearts. Values represent mean ± s.d., n = number of hearts used in each group. Control indicates no pretreatment. $^*P<0.05$ when compared to the corresponding control value.

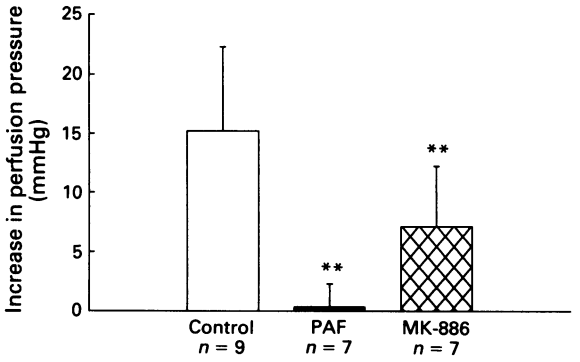

Figure 5 Effect of pretreatment with 1000 pmol PAF bolus injection and 10 μM MK-886 on perfusion pressure changes by 0.5 μM WEB 2170 in rat perfused hearts. Values represent mean ± s.d., n = number of hearts used in each group. Control indicates no pretreatment. $^{**}P<0.01$ when compared to the corresponding control value.

The amount of LTC_4 and the combined amount of $LTC_4/D_4/E_4$ in the effluent were measured by radioimmunoassay. Significant amounts of leukotrienes were detected in the coronary effluent during the initial 2 min after 1000 pmol PAF was administered (Table 2). This time interval corresponded to the maximal effect of PAF after a bolus injection. Since the effects of WEB 2086 and WEB 2170 on perfusion pressure were gradual, effluents were collected at 0–2, 2–5 and 5–10 min intervals. No detectable or very small amounts of leukotrienes were found in the effluent from hearts perfused with 1 μM WEB 2086 or 0.5 μM WEB 2170 at all intervals examined (Table 2).

Table 2 The concentration of leukotrienes in the coronary effluent after a bolus injection of PAF, and perfusion with 1 μM WEB 2086 and 0.5 μM WEB 2170 in the rat perfused heart[a]

	PAF (1000 pmol)	*WEB 2086* (1 μM)	*WEB 2170* (0.5 μM)
LTC_4 (pg ml^{-1} effluent)			
0–2 min	1183 ± 293 (3)	10 ± 20 (4)	30 ± 52 (3)
2–5 min		– (4)	17 ± 21 (3)
5–10 min		– (4)	30 ± 52 (3)
$LTC_4/D_4/E_4$ (pg ml^{-1} effluent)			
0–2 min	1700 ± 360 (3)	66 ± 31 (4)	43 ± 49 (4)
2–5 min		70 ± 50 (4)	– (4)
5–10 min		53 ± 41 (4)	23 ± 45 (4)

Values represent mean ± s.d. Number in parentheses indicated the number of experiments.
– denotes no detectable amount.
[a]Leukotrienes were measured by radioimmunoassay and each sample was determined in duplicate. Background amounts of LTC_4 and $LTC_4/D_4/E_4$ (perfusion with normal buffer only) were 45 ± 17 and 78 ± 73 pg ml^{-1} effluent respectively (n = 4).

Discussion

The major finding of this study was the moderate coronary vasoconstrictor actions of the PAF receptor antagonist, WEB 2086 and its structural analogue, WEB 2170. We propose that this action is mediated by the partial agonist effect of WEB 2086 and WEB 2170. The evidence in support of a partial agonist action of WEB 2086 and WEB 2170 is as follows: pretreatment with a bolus injection of PAF that would abolish subsequent response to PAF in the perfused heart, significantly attenuated the vasoconstriction produced by WEB 2086 and WEB 2170; FR-900452, a PAF receptor antagonist (Okamoto *et al.*, 1986) that we showed to be devoid of any significant coronary vascular effect in the heart, also attenuated the vasoconstriction produced by WEB 2086; the activation of PAF receptors by PAF in the heart led to the production of vasoactive leukotrienes and the vasoconstriction could be blocked by leukotriene receptor antagonists and a leukotriene synthesis inhibitor (Piper & Stewart, 1986; Hu *et al.*, 1991b). Our results also demonstrated that MK-886 and L-649,923 decreased the vasoconstrictor action of WEB 2086 and WEB 2170.

It should be noted that the vasoconstrictor action of WEB 2086 was not completely abolished by pretreatment with PAF, FR-900452, MK-886 or L-649,923 at concentrations that had been shown to block completely the coronary vascular effects of PAF in our previous studies (Hu *et al.*, 1991b; Hu & Man, 1991a). Previous studies showed that PAF may block subsequent responses to PAF in the heart by receptor desensitization or depletion of vasoactive leukotrienes release (Piper & Stewart, 1986; Man *et al.*, 1990; Hu *et al.*, 1991a). Since the coronary vascular effects of PAF involve the release of leukotrienes (Hu *et al.*, 1991b), the leukotriene synthesis inhibitor MK-886 and the leukotriene receptor antagonist L-649,923 should be effective in blocking the effect of PAF. It has been suggested that cyclo-oxygenase products are involved in mediating the vasoconstrictor action of PAF in the heart (Piper & Stewart, 1986; 1987). However, our results indicated that the partial angonist action of WEB 2086 did not involve vasoactive cyclo-oxygenase products since indomethacin had no effect on the vasoconstrictor action of WEB 2086 under our experimental conditions. This is compatible with our previous data showing that the coronary

vascular effects of PAF via the activation of PAF receptors in the heart did not involve vasoactive cyclo-oxygenase products directly although cyclo-oxygenase products were present in the coronary effluent (Hu & Man, 1991b). Our results therefore suggest that a component of the vasoconstrictor action of WEB 2086 may be due to non specific action on the coronary blood vessels.

It is intriguing that activation of PAF receptors by PAF was accompanied by the release of leukotrienes into the coronary effluent while the partial agonist action of WEB 2086 and WEB 2170, though involving leukotrienes and attenuated by a leukotriene synthesis inhibitor or a leukotriene receptor antagonist, does not result in significant amounts of leukotrienes in the coronary effluent. This suggests that the vasoconstrictor action of WEB 2086 and WEB 2170 may be mediated by intracellularly or locally produced leukotrienes. Hence no significant amount of leukotrienes can be found in the coronary effluent in the presence of WEB 2086 and WEB 2170.

An alternate hypothesis to explain the present results may be that WEB 2086 and WEB 2170 release PAF. Pretreatment with PAF and FR-900452 would therefore be effective in attenuating the vasoconstrictor effect. Since the coronary vascular effect of PAF is mediated by leukotrienes, pretreatment with L-649,923 and MK-886 would also be expected to have an effect. One difficulty with this hypothesis is that if PAF is released by WEB 2086 and WEB 2170, then detectable amounts of leukotrienes in the coronary effluent should be observed as a result of PAF released. Moreover, PAF produces an initial vasodilatation. However, vasodilatation was not observed with WEB 2086 and WEB 2170 in the present study.

In our previous study (Hu & Man, 1991a) and this study, low concentrations of WEB 2086 and WEB 2170 blocked the vasoconstrictor effect of PAF and at higher concentrations blocked the vasodilator effect of PAF in the rat perfused heart. Thus WEB 2086 and WEB 2170 should be considered to possess antagonist action under these experimental conditions. Since a partial agonist can occupy the PAF receptors and prevent further activation of PAF receptors by a full agonist, WEB 2086 and WEB 2170 with partial agonists actions would be capable of blocking the actions of PAF. However, we were not able to define the partial agonist action of WEB 2086 and WEB 2170 as a percentage of a full agonist such as PAF since the time course of pressure changes initiated by WEB 2086 and WEB 2170 were very different from that of the agonist PAF. In contrast to the slow time course of WEB 2086 and WEB 2170 on perfusion pressure changes (peak effect not observed even after 5 min, Figure 1), the effect of PAF was much faster. Peak effect was observed within 1 to 2 min with PAF and the perfusion pressure gradually returned to baseline level by 5 min even with a continuous infusion of PAF (Man *et al.*, 1990).

Currently, there has been no report of a partial agonist action of most commonly used PAF receptor antagonists. WEB 2086 is considered to be a PAF receptor antagonist devoid of agonist action in most systems tested (Meade & Heuer, 1990). However, the results from the present study suggest a partial agonist effect of WEB 2086 in the rat heart. If there are PAF receptor subtypes as suggested by recent reports (Lambrecht & Parnham, 1986; Hwang, 1988; Stewart & Dusting, 1988; Kroegel *et al.*, 1989; Hu & Man, 1991a), then it is possible that WEB 2086 only has partial agonist action on one receptor subtype and is a full antagonist on the other receptor subtype. If the PAF receptor subtype where WEB 2086 is a full antagonist is predominant in most systems, then it will be difficult to notice the partial agonist action of WEB 2086 on the other PAF receptor subtype that is not dominant. Since our previous data suggested that the rat heart contained both PAF receptor subtypes, we would expect to observe both the full antagonist and the partial agonist actions of WEB 2086. However, the presence of PAF receptor subtypes remains to be fully elucidated.

Recently hexanolamine PAF, a structural analogue of PAF with putative PAF receptor antagonist action, had been shown to exhibit partial agonist action (Grigoriadis & Stewart, 1991). Although the 1-*O*-hexadecyl form of hexanolamine PAF showed partial agonist activity, the 1-*O*-octadecyl form (U66985) was devoid of agonist activity (Tokumura *et al.*, 1985). It is also of interest that U66983, with 3 methylene residues between the phosphate and choline nitrogen, showed agonist activity while U66982, with 10 methylene residues, had weak antagonist activity (Tokumura *et al.*, 1985). The possible sites for the partial agonist and antagonist actions of WEB 2086 and WEB 2170 are currently not known.

WEB 2170, a structural analogue of WEB 2086, has been shown to be slightly more potent that WEB 2086 and has similar properties (Meade & Heuer, 1990). Our results also suggested that WEB 2170, like WEB 2086, has partial agonist action and produced coronary vasoconstriction. In contrast, FR-900452, a structurally different PAF receptor antagonist, does not share this property with WEB 2086 and WEB 2170. It remains to be determined if other commonly used PAF receptor antagonists behave as full receptor antagonists or under certain circumstances act as partial agonists as in the case of WEB 2086 and WEB 2170.

We wish to thank Boehringer Ingelheim KG and Boehringer Ingelheim (Canada) Ltd. for the supply of WEB 2086 and WEB 2170. We also wish to thank Dr Okamoto of Fujisawa Pharmaceutical Co. Ltd. for the supply of FR-900452 and Dr Ford-Hutchinson of Merck Frosst Canada Inc. for the supply of L-649,923 and MK-886. This study was supported by the MRC of Canada.

References

BRAQUET, P., TOUQUI, L., SHEN, T.Y. & VARGAFTIG, B.B. (1987). Perspectives in platelet-activating factor research. *Pharmacol. Rev.*, **39**, 97–145.

GILLARD, J., FORD-HUTCHINSON, A.W., CHAN, C., CHARLESON, S., DENIS, D., FOSTER, A., FORTIN, R., LEGER, S., MCFARLANE, C.S., MORTON, H., PIECHUTA, H., RIENDEAU, D., ROUZER, C.A., ROKACH, J., YOUNG, R., MACINTYRE, D.E., PETERSON, L., BACH, T., EIERMANN, G., HOPPLE, S., HUMES, J., HUPE, L., LUELL, S., METZGER, J., MEURER, R., MILLER, D.K., OPAS, E. & PACHOLOK, S. (1989). L-663,536 (MK-886) (3-[1-(4-chlorobenzyl) -3-*t*-butyl-thio-5-isopropylindol-2-yl]-2,2-dimethylpropanoic acid), a novel, orally active leukotriene biosynthesis inhibitor. *Can. J. Physiol. Pharmacol.*, **67**, 456–464.

GRIGORIADIS, G. & STEWART, A.G. (1991). 1-*O*-hexadecyl-2-acetyl-*sn*-glycer-3-phospho(N,N,N trimethyl)hexanolamine: an analogue of platelet-activating factor with partial agonist activity. *Br. J. Pharmacol.*, **104**, 171–177.

HONDA, Z., NAKAMURA, M., MIKI, I., MINAMI, M., WATANABE, T., SEYAMA, Y., OKADO, H., TOH, H. ITO, K., MIYAMOTO, T. & SHIMIZU, T. (1991). Cloning by functional expression of platelet-activating factor receptor from guinea-pig lung. *Nature*, **349**, 342–346.

HU, W., CHOY, P.C. & MAN, R.Y.K. (1991a). Characterization of the coronary vascular responses to platelet-activating factor in the isolated perfused heart. *Lipids*, **26**, 700–704.

HU, W., KINNAIRD, A.A.A. & MAN, R.Y.K. (1991b). Mechanisms of the coronary vascular effects of platelet-activating factor in the rat perfused heart. *Br. J. Pharmacol.*, **103**, 1097–1102.

HU, W. & MAN, R.Y.K. (1991a). Differential actions of platelet-activating factor (PAF) receptor antagonists on the vasodilator and vasoconstrictor effects of PAF in the rat perfused heart. *Br. J. Pharmacol.*, **104**, 773–775.

HU, W. & MAN, R.Y.K. (1991b). Interaction of vasoactive substances released by platelet-activating factor in the rat perfused heart. *Br. J. Pharmacol.*, **104**, 933–937.

HWANG, S.-B. (1988). Identification of a second putative receptor of platelet-activating factor from human polymorphonuclear leukocytes. *J. Biol. Chem.*, **263**, 3225–3233.

HWANG, S.-B., LEE, C.-S.C., CHEAH, M.J. & SHEN, T.Y. (1983). Specific receptor sites for 1-*O*-alkyl-1-*O*-acetyl-*sn*-glycero-3-phosphocholine (platelet activating factor) on rabbit platelet and guinea pig smooth muscle membranes. *Biochemistry*, **224**, 4756–4763.

JONES, T.R., YOUNG, R., CHAMPION, E., CHARETTE, L., DENIS, D., FORD-HUTCHINSON, A.W., FRENETTE, R., GAUTHIER, J.-Y., GUINDON, Y., KAKUSHIMA, M., MASSON, P., McFARLANE, C., PIECHUTA, H., ROKACH, J., ZAMBONI, R., DEHAVEN, R.N., MAYCOCK, A. & PONG, S.S. (1986). L-649,923, sodium ($\beta S^*, R^*$)-4-(3-4(-acetyl-4-hydroxy-2-propylphenoxy)-propylthio)-γ-hydroxy -β-methylbenzenebutanoate, a selective, orally active leukotriene receptor antagonist. *Can. J. Physiol. Pharmacol.*, **64**, 1068–1075.

KROEGEL, C., YUKAWA, T., WESTWICK, J. & BARNES, P.J. (1989). Evidence for two platelet-activating factor receptors on eosinophils: dissociation between PAF-induced intracellular calcium mobilization degranulation and superoxides anion generation in eosinophils. *Biochem. Biophys. Res. Commun.*, **162**, 511–521.

LEMBRECHT, G. & PARNHAM, J. (1986). Kadsurenone distinguishes between different platelet-activating factor receptor subtypes on macrophages and polymorphonuclear leucocytes. *Br. J. Pharmacol.*, **87**, 287–289.

MAN, R.Y.K., HU, W. & KINNAIRD, A.A.A. (1990). Coronary vascular response to platelet-activating factor in the perfused rat heart. *J. Lipid Mediators*, **2**, 75–83.

MEADE, C.J. & HEUER, H.O. (1990). Hetrazepines as PAF antagonists. In *Platelet-Activating Factor Antagonists. New Developments for Clinical Application.* ed. O'Flaherty, J.T. & Ramwell, P.W. pp. 47–80. Texas: Portofolio Publishing.

OKAMOTO, M., YOSHIDA, K., NISHIKAWA, M., ANDO, T., IWAMI, M. KOHSAKA, M. & AOKI, H. (1986). FR-900452, a specific antagonist of platelet activating factor (PAF) produced by *Streptomyces phaeofaciens. J. Antibiotics*, **39**, 198–204.

PIPER, P.J. & STEWART, A.G. (1986). Coronary vasoconstriction in the rat, isolated perfused heart induced by platelet-activating factor is mediated by leukotriene C4. *Br. J. Pharmacol.*, **88**, 595–605.

PIPER, P.J. & STEWART, A.G. (1987). Antagonism of vasoconstriction induced by platelet-activating factor in guinea-pig perfused hearts by selective platelet-activating factor receptor antagonists. *Br. J. Pharmacol.*, **90**, 771–783.

SAUNDERS, R.N. & HANDLEY, D.A. (1987). Platelet-activating factor antagonists. *Annu. Rev. Pharmacol. Toxicol.*, **27**, 237–255.

STEWART, A.G. & DUSTING, G.J. (1988). Characterization of receptors of platelet-activating factor on platelets, polymorphonuclear leukocytes and macrophages. *Br. J. Pharmacol.*, **94**, 1225–1233.

TOKUMURA, A., HOMMA, H. & HANAHAN, D.K. (1985). Structural analogs of alkylacetylglycerophosphocholine inhibitory behaviour on platelet activation. *J. Biol. Chem.*, **260**, 12710–12714.

VALONE, F.H., COLES, H.E., REINHOLD, V.R. & GOETZL, E.J. (1982). Specific binding of phospholipid platelet-activating factor by human platelets. *J. Immunol.*, **129**, 1637–1641.

(Received November 24, 1992
Revised June 2, 1993
Accepted June 4, 1993)

Br. J. Pharmacol. (1993), **110**, 651–656

Differential effects of acetylcholine, nitric oxide and levcromakalim on smooth muscle membrane potential and tone in the rabbit basilar artery

[1]Frances Plane & Christopher J. Garland

Department of Physiology and Pharmacology, University of Southampton, Bassett Crescent East, Southampton, SO9 3TU

1 Endothelium-dependent hyperpolarization of smooth muscle cells in isolated, pre-contracted segments of rabbit basilar artery in response to acetycholine (100 μM) was abolished in the presence of glibenclamide (10 μM).

2 Acetylcholine-evoked relaxation was unaffected by either glibenclamide or 65 mM potassium chloride, indicating that the change in membrane potential did not form an essential component of relaxation and that high concentrations of potassium did not inhibit the release or action of endothelium-derived relaxing factor in this vessel.

3 Saturated solutions of nitric oxide (NO) gas in solution (150 μM), which evoked maximal relaxation of arterial segments pre-contracted and depolarized by noradrenaline (10–100 μM), did not alter the membrane potential of either unstimulated or depolarized smooth muscle cells.

4 The potassium channel opener levcromakalim, evoked concentration-dependent relaxation and hyperpolarization in pre-constricted smooth muscle cells. The threshold concentrations for hyperpolarization and relaxation, the EC_{50} values and the maximally effective concentration of levcromakalim (around 30 nM, 150 nM and 10 μM, respectively) were not significantly different, and both components of the response were inhibited by glibenclamide (10 μM), indicating a close coupling between the two responses.

5 In the presence of 65 mM potassium chloride, the hyperpolarization to levcromakalim was abolished, while a small relaxation (25 ± 4%) persisted, indicating an additional mechanism for relaxation to this agent.

6 These results show that different mechanisms underlie the relaxant action of potassium channel openers, NO and endothelium-derived factors in cerebral arteries and provide further evidence that in the basilar artery, in contrast to some other vessels, endothelium-dependent hyperpolarization to acetylcholine is not important for smooth muscle relaxation.

Keywords: Glibenclamide; hyperpolarization; levcromakalim; membrane potential; nitric oxide; potassium channels; vascular smooth muscle

Introduction

The relaxation of blood vessels evoked by muscarinic agonists is usually accompanied by hyperpolarization of the smooth muscle cell membrane, both events being mediated by the release of a diffusible factor from the endothelium (Chen *et al.*, 1988; 1991; Feletou & Vanhoutte, 1988). Endothelium-derived relaxing factor (EDRF) has now been identified as nitric oxide (NO; Palmer *et al.*, 1987), or a closely related compound, but the possibility that NO may contribute to endothelium-dependent hyperpolarization and the mechanism underlying this response is the subject of some controversy.

Inhibitors of NO synthase did not reduce acetylcholine-evoked hyperpolarization in the guinea-pig coronary and rat small mesenteric artery, indicating the involvement of an endothelium-derived hyperpolarizing factor (EDHF) distinct from NO (Chen *et al.*, 1991; Garland & McPherson, 1992). However, in the guinea-pig uterine artery both the relaxation and hyperpolarization evoked by acetylcholine were depressed by the NO synthase inhibitor L-N^G-monomethyl arginine (L-NMMA), indicating that NO may contribute to both smooth muscle hyperpolarization and relaxation in this particular vessel (Tare *et al.*, 1990). Additionally, in both the guinea-pig uterine artery and the rat small mesenteric artery, exogenous NO can stimulate both smooth muscle relaxation and membrane hyperpolarization under certain conditions (Tare *et al.*, 1990; Garland & McPherson, 1992).

The role of glibenclamide-sensitive potassium channels in the endothelium-dependent hyperpolarization evoked by acetylcholine is also controversial and may vary between different vessels. For example, in the rabbit middle cerebral artery, acetylcholine-evoked hyperpolarization was reduced by the sulphonylurea compound glibenclamide, whereas in the guinea-pig isolated coronary artery and rat small mesenteric arteries this agent did not block responses to acetylcholine (Standen *et al.*, 1989; Brayden, 1990; Eckman *et al.*, 1992; Garland & McPherson, 1992). Furthermore, in the rat small mesenteric artery, although acetylcholine-induced hyperpolarization was not abolished by glibenclamide, hyperpolarization to NO was inhibited (Garland & McPherson, 1992), providing further indirect evidence that NO may contribute to endothelium-dependent hyperpolarization in some vessels.

Glibenclamide also inhibits the smooth muscle relaxation which is evoked by potassium channel opening drugs (KCOs) such as levcromakalim, suggesting that membrane hyperpolarization, mediated by the opening of glibenclamide-sensitive potassium channels, is the major mechanism underlying the decrease in vascular tone (Buckingham *et al.*, 1989; Winquist *et al.*, 1989; McHarg *et al.*, 1990). This hypothesis is based largely on separate experiments showing that KCOs can increase the resting membrane potential of unstimulated vascular smooth muscle cells, and can also relax isolated, pre-contracted vessels. There is relatively little information on the membrane effects of KCOs under conditions of smooth muscle depolarization. Minoxidil sulphate and cromakalim have both been shown to reduce the subsequent depolarizing action of noradrenaline in the rabbit portal vein and

[1] Author for correspondence at: Department of Pharmacology, University Walk, Bristol BS8 1TD.

mesenteric artery, respectively (Leblanc *et al.*, 1989; McHarg *et al.*, 1990). However, although smooth muscle relaxation elicited by KCO's is reduced in isolated arteries precontracted with high concentration of extracellular potassium, consistent with a role for potassium channels in relaxation (Parsons *et al.*, 1991a), in only one study have the membrane events underlying this response been reported (Nakashima *et al.*, 1990).

The fact glibenclamide can inhibit the membrane hyperpolarization evoked by NO, and in some vessels that to endothelium derived factor(s), suggests an important role for the potassium channels which are activated by agents like levcromakalim, which are also glibenclamide-sensitive. The reported variation in the ability of NO to elicit smooth muscle hyperpolarization, and in the sensitivity of endothelium-dependent hyperpolarization to glibenclamide, could then be explained in a number of ways, including a variation in either the endothelium-derived mediator of hyperpolarization or in the distribution of potassium channels. Regional differences in the distribution of potassium channels have been suggested within the cerebral circulation of the rat, as not all of the arteries arising from the circle of Willis are hyperpolarized by KCOs (McCarron *et al.*, 1991; McPherson & Stork, 1992).

In the rabbit isolated basilar artery, acetylcholine-evoked hyperpolarization is both small in amplitude and transient. In addition, it is diminished on repeated application of the agonist. In contrast, the relaxation to acetylcholine is both sustained and reproducible with repeated exposures (Rand & Garland, 1992). However, both responses are attenuated by inhibitors of NO synthase indicating that, as in the guinea-pig uterine artery, NO may contribute to both components of the response to acetylcholine (Rand & Garland, 1992). Surprisingly, exogenous NO failed to evoke any significant hyperpolarization in smooth muscle cells of the rabbit basilar artery, even at concentrations which caused a maximal reversal of induced tone (15 μM; Rand & Garland, 1992). However, this concentration was close to the threshold for membrane hyperpolarization to NO in the rat mesenteric artery, so that higher concentrations might be required to demonstrate hyperpolarization if the potassium channels which mediate this response are sparse in this particular vessel (Garland & McPherson, 1992).

The aims of the present study were to investigate the glibenclamide-sensitivity of acetylcholine-evoked hyperpolarization and relaxation in the rabbit basilar artery, and to examine the possibility that very high concentrations of NO may be required for smooth muscle hyperpolarization. Furthermore, the effects of the KCO, levcromakalim, on both smooth muscle tone and membrane potential, under both resting and depolarized conditions, were also examined. The aim was to determine if the small size of the membrane responses evoked by acetylcholine, and the apparent lack of hyperpolarization to NO, could reflect an absence of KCO and glibenclamide-sensitive potassium channels in this artery.

Methods

White rabbits of either sex (2–3 kg) were anaesthetized with sodium pentobarbitone (60 mg kg^{-1}, i.v.) and killed by rapid exsanguination. The brain was removed and placed in Krebs buffer at room temperature. The basilar artery was carefully removed, cleaned and cut into cylindrical segments 2 mm in length. Segments were then mounted in a tissue chamber for simultaneous recording of changes in smooth muscle membrane potential and tension, as previously described (Garland, 1987). Briefly, two tungsten wires (40 μm diameter) were passed through the lumen of the segment and each wire attached to a metal foot in a myograph (model 400 A, J.P. Trading, Denmark). The tissue segment was stretched between the wires under a previously determined optimal preload of 500 mg and superfused at 5–6 ml min^{-1} with Krebs buffer which had been bubbled with 95% O_2/5% CO_2. All experiments were carried out on tissues with a functionally intact endothelium unless otherwise stated.

Drugs were equilibrated with the perfusate before it entered the tissue chamber. Nitric oxide solutions were injected close to the artery segment, from a gas-tight syringe in volumes not greater than 200 μl.

Electrophysiology

Measurement of smooth muscle membrane potential was made with a glass microelectrode advanced through the adventitial surface of the artery segment. The electodes were filled with 2 M KCl and had resistances of 60–120 MΩ. Membrane electrical events were recorded through a high-input impedance d.c. preamplifier (Neurolog 102G) and, together with data from the isometric force transducer, stored on disc (CVMS, McPherson Scientific).

Solutions and drugs

Tissues were maintained in Krebs buffer of the following composition (mM): NaCl 122, $NaHCO_3$ 25.5, KCl 5.2, $MgSO_4$ 1.2, $CaCl_2$ 1.6, disodium EDTA 0.027, ascorbate 0.114 and glucose 9.4. All K^+-rich Krebs solutions were prepared by direct replacement of NaCl with KCl. At the end of each experiment, tissues were maximally contracted with 100 mM K^+-Krebs solution.

Drugs used were acetylcholine chloride (BDH), noradrenaline bitartrate (arterenol, Sigma), levcromakalim (gift from Smith Kline Beecham) and glibenclamide (gift from Hoechst).

Preparation of nitric oxide solutions

Nitric oxide gas (research grade, BDH) was injected into Krebs solution which had been bubbled with helium (BOC) for 45–60 min. Nitric oxide solution was injected into the tissue chamber in volumes of 200 μl with a gas tight syringe. Control injections of helium-gassed Krebs solution were made to assess the extent of any potential injection artifacts.

Analysis of data

Relaxations are expressed as a percentage decrease in the tone induced by either noradrenaline or potassium chloride. Data are expressed as mean ± s.e.mean. The significance between mean values was calculated by Student's t test, with rejection of the null hypothesis at the 5% level ($P<0.05$).

Results

Membrane and tension responses to acetylcholine

Smooth muscle cells in the basilar artery were electrically quiescent, and the mean resting membrane potential was -63.7 ± 7.1 mV (80 cells from 28 preparations). When first applied to noradenaline precontracted tissues (mean background contraction and depolarization of 4.5 ± 0.9 mN and 10.5 ± 2.2 mV, $n=4$), acetylcholine (100 μM) evoked 95 ± 3.5% relaxation of the induced tone and hyperpolarized the smooth muscle cell membrane by 8.1 ± 1.0 mV ($n=4$ paired observations). Subsequent exposures to acetylcholine were followed by a relaxation of similar magnitude (93.9 ± 4.6% on fifth exposure). However, as previously described (Rand & Garland, 1992), the amplitude of the accompanying hyperpolarization decreased with each application of acetylcholine, although in contrast to the previous study, a small but significant change in membrane potential was still observed even on a fifth exposure (4.1 ± 1.5 mV; $n=4$). The threshold concentrations for acetylcholine-evoked hyperpolarization and relaxation were 1 μM and 0.1 μM, respectively (Figure 1a).

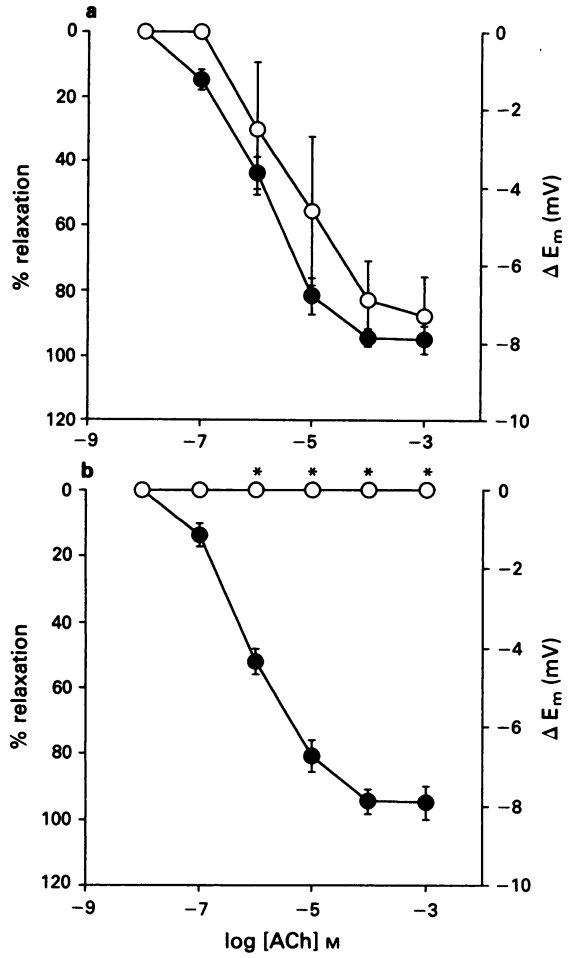

Figure 1 Mean concentration-response curves for acetylcholine in the rabbit basilar artery precontracted with noradrenaline (10–100 μM). Points show relaxation (●) and hyperpolarization (○) and are the mean ± s.e.mean from 4 separate experiments. (a) Control concentration-response curves for the second application of acetylcholine. (b) Concentration-response curves in the presence of glibenclamide. $*P<0.05$ compared to control responses.

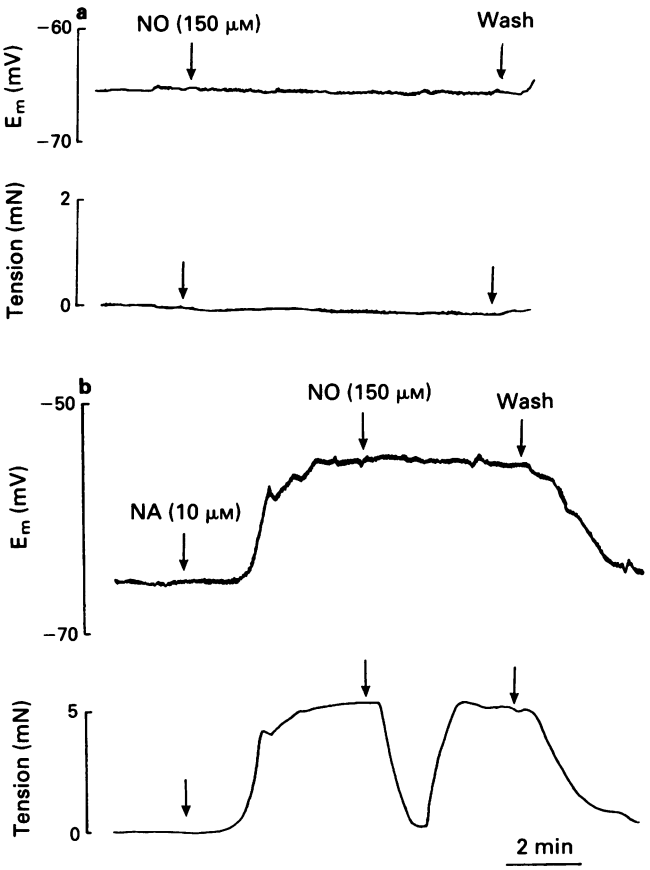

Figure 2 Representative traces showing simultaneous records of membrane potential and changes in tension elicited by NO in the absence and presence of noradrenaline to induce contraction and depolarization. (a) NO (150 μM) had no effect on resting membrane potential or tension in the unstimulated rabbit basilar artery. The resting membrane potential of the cell shown in this trace was − 67 mV. (b) Noradrenaline (10 μM) elicited contraction of approximately 5 mN and depolarized the smooth muscle by approximately 10 mV (resting membrane potential − 65 mV). NO (150 μM) initiated a transient relaxation of the induced tone but had no effect on the membrane potential of the smooth muscle cell.

When glibenclamide (10 μM) was added after the first exposure to acetylcholine, the subsequent membrane hyperpolarization was abolished, although at this time relaxations were not significantly altered (Figures 1b). Furthermore, the acetylcholine-evoked relaxations were also unaltered when potassium chloride (65 mM) was used to induce tone instead of noradrenaline. The EC_{50} values for acetylcholine-evoked relaxation in the presence of either noradrenaline or potassium were 1.5 ± 0.2 μM and 1.65 ± 0.4 μM, respectively ($n = 4$; $P>0.05$), and the maximal relaxations obtained were 94.8 ± 3.8% and 94.5 ± 4.5%, respectively $n = 4$; $P>0.05$).

Membrane and tension responses to nitric oxide

In tissues contracted and depolarized with noradrenaline (10–100 μM), NO (0.5–15 μM) initiated transient relaxations which reversed within 20–25 s. Maximal relaxation of induced tone (85.4 ± 6.7%; $n = 4$) was achieved at a concentration of 15 μM NO and the EC_{50} value was 2.0 ± 0.9 μM ($n = 4$).

Over the concentration-range which produced relaxation of induced tone, NO (0.5–15 μM) had no significant effect on the membrane potential of unstimulated smooth muscle cells, in contrast to the small hyperpolarization (around 2 mV) reported by Rand & Garland (1992). Furthermore, at a concentration 10 times higher than that required to evoke maximal relaxation, 150 μM, NO did not elicit any smooth muscle hyperpolarization, either in the absence (Figure 2a) or presence (Figure 2b) of prior membrane depolarization to noradrenaline.

Membrane and tension responses to levcromakalim

Levcromakalim (1–100 μM) evoked concentration-dependent hyperpolarization in unstimulated smooth muscle cells (mean resting membrane potential − 63.3 ± 6.8 mV; 39 cells from 14 preparations), which was maintained for over 20 min in the continued presence of the drug. In these experiments, levcromakalim had no significant effect on the resting level of tone. The maximal hyperpolarization to levcromakalim (100 μM) was 14 ± 3.2 mV ($n = 6$). Glibenclamide (10 μM), had no significant effect on either the tone or membrane potential of unstimulated smooth muscle cells during exposures of up to 20 min, but abolished levcromakalim-evoked hyperpolarization.

In tissues depolarized and contracted with noradrenaline (mean background contraction and depolarization 4.98 ± 0.7 mN and 12.7 ± 2.5 mV, respectively; $n = 4$), levcromakalim (0.01–10 μM) evoked concentration-dependent relaxation of the induced tone, which was accompanied by smooth muscle hyperpolarization. The threshold concentration (30 nM), EC_{50} values (140 ± 25 nM and 175 ± 15 nM; $n = 4$) and the concentration of levcromakalim required for a maximal response (10 μM; $n = 4$) with both hyperpolarization and relaxation were not significantly different (Figure 3a). Following prior exposure to glibenclamide (10 μM) for

Table 1 Comparison of relaxation and smooth muscle hyperpolarization evoked by levcromakalim in the rabbit basilar artery pre-contracted with noradrenaline or potassium chloride

	Noradrenaline (10–100 μM)	25 mM *KCl*	35 mM *KCl*	65 mM *KCl*
Mean level of contraction (mN)	4.98 ± 0.7	3.1 ± 0.6	14.5 ± 2.1	23.0 ± 3.9
Mean level of depolarization (mV)	12.7 ± 2.5	22.1 ± 2.9	29.4 ± 2.0	44.1 ± 4.0
% maximal relaxation to levcromakalim (100 μM)	95.0 ± 5.1	97.0 ± 4.1	74.0 ± 6.9	25.0 ± 4.0
Maximal membrane potential change to levcromakalim (100 μM; mV)	25.0 ± 2.3	26.0 ± 2.1	15.0 ± 4.9	0

Each value is the mean of 4 observations ± s.e.mean.

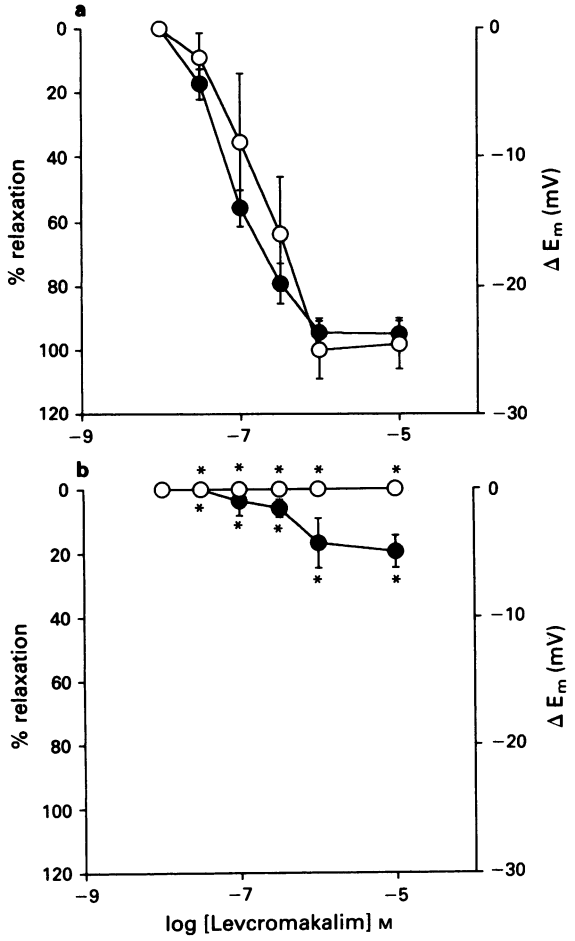

Figure 3 Mean concentration-response curves for levcromakalim in the rabbit basilar artery contracted with noradrenaline (10–100 μM). Points show relaxation (●) and hyperpolarization (○) and are the mean ± s.e.mean from 4 separate experiments. (a) Control concentration-response curves to levcromakalim. (b) Concentration-response curves in the presence of glibenclamide (10 μM). *$P<0.05$ compared to controls.

20 min, the maximal levcromakalim-evoked relaxation was reduced to 19.4 ± 5.0% ($n = 4$) and the accompanying smooth muscle hyperpolarization was abolished (Figure 3b). Levcromakalim-evoked responses were also reduced in the presence of elevated external potassium concentrations. In arterial segments preconstricted with 25 mM potassium chloride, levcromakalim evoked concentration-dependent relaxation and hyperpolarization which was not significantly different from the responses observed in noradrenaline precontracted tissues. The maximal changes in tension and smooth muscle membrane potential evoked by levcromakalim in the presence of 25 mM potassium chloride were 97 ± 4.1% and 26 ± 2.1 mV respectively ($n = 4$; $P>0.05$). In contrast, when 35 mM and 65 mM potassium chloride were used, both the smooth muscle relaxation and hyperpolarization evoked by levcromakalim were depressed. Table 1 shows the maximal relaxation and change in membrane potential evoked by levcromakalim (100 μM) in tissues precontracted with either noradrenaline or potassium chloride. In the presence of 35 mM potassium chloride, the maximal relaxation and change in membrane potential evoked by levcromakalim were reduced by approximately 24% and 42%, respectively. In arterial segments contracted with 65 mM potassium, levcromakalim-evoked hyperpolarization was abolished although a small relaxation (25 ± 4%) still persisted.

Discussion

These data confirm and extend our previous study, which indicated that membrane hyperpolarization did not make an important contribution to the smooth muscle relaxation evoked by either acetylcholine or exogenous NO in the rabbit basilar artery (Rand & Garland, 1992). The present study demonstrated that the small hyperpolarization evoked by acetylcholine was inhibited by glibenclamide, whereas smooth muscle relaxation was unaffected. The ability of glibenclamide to block acetylcholine-induced hyperpolarization is similar to its action in the rabbit middle cerebral artery (Standen *et al.*, 1989; Brayden, 1990). The maximal hyperpolarization in response to acetylcholine, at 8 mV, was not marked, but by comparison to the action of levcromakalim might be predicted to stimulate a relaxation of around 30–40% (see Figure 3). This relaxation would, however, be masked by the relaxation induced by other mechanisms initiated by lower concentrations of acetycholine. As the activation of glibenclamide-sensitive potassium channels also mediates smooth muscle hyperpolarization to the KCO levcromakalim and, in some vessels, NO and endothelium-derived factors, these agents may all share an ability to activate the same type of potassium channel under certain conditions.

Smooth muscle relaxation in the basilar artery was also unaffected by precontraction with a high concentration of potassium (65 mM), a concentration which is known to inhibit smooth muscle hyperpolarization to acetylcholine (Chen *et al.*, 1989; Waldron *et al.*, 1993), demonstrating that this concentration of potassium does not inhibit either the action or the release of EDRF in this vessel.

Glibenclamide did not modify either the resting membrane potential or tension in the basilar artery, indicating a low open probability for glibenclamide-sensitive channels at this potential. This observation was not complicated by an action exerted via the endothelium, as glibenclamide was without effect in both endothelium-intact and denuded tissues. Glibenclamide also had no effect on resting tension and membrane potential in the rabbit middle cerebral artery (Brayden, 1990), whereas in the rat small mesenteric and guinea-pig coronary artery, glibenclamide caused membrane depolarization and smooth muscle contraction in unstimulated tissues (McPherson & Angus, 1990; 1991; Eckman *et al.*, 1992). These contrasting results suggest a variation in the characteristics of the glibenclamide-sensitive potassium channels present in these different vessels and in their contribution

to smooth muscle tone. Variation has also been observed in the sensitivity of acetycholine-evoked hyperpolarization to glibenclamide. The mesenteric artery smooth muscle cells, although depolarized by glibenclamide, developed a hyperpolarization which was not reduced in overall size by glibenclamide (Garland & McPherson, 1992), while in the basilar artery the relatively small hyperpolarization was abolished. These differences could be explained by different populations of potassium channels in the two arteries.

The majority of evidence, from a range of isolated blood vessels, suggests that the endothelium-dependent hyperpolarization which is evoked by cholinomimetics is not mediated by NO. For example, in the guinea-pig coronary artery, endothelium-dependent relaxation can be reduced independently of hyperpolarization by the NO synthase inhibitor nitroarginine. In contrast, a number of studies including the present one, have failed to demonstrate significant membrane hyperpolarization in response to concentrations of exogenous NO which are capable of stimulating maximal smooth muscle relaxation (Komori *et al.*, 1988; Brayden, 1990; Chen *et al.*, 1991; Rand & Garland, 1992). However, NO-evoked hyperpolarization has been demonstrated in smooth muscle cells in rat small mesenteric arteries and in the guinea-pig uterine artery, indicating that in some vessels NO may at least contribute to acetylcholine-induced hyperpolarization (Tare *et al.*, 1990; Garland & McPherson, 1992). In the rabbit isolated basilar artery, although NO did not alter the membrane potential, both the hyperpolarization and relaxation stimulated by acetylcholine were reduced by the NO synthase inhibitors L-NMMA and N^G-nitro-L-arginine methyl ester (L-NAME), indicating that NO contributes in some way to the hyperpolarization in this artery (Rand & Garland, 1992). Why NO failed to alter the membrane potential in the basilar artery when glibenclamide-sensitive potassium channels are present, and NO can activate such channels in other arteries, is not clear. One possibility is that glibenclamide can block more than one type of potassium channel, fitting in with its variable action on the resting membrane potential in different arteries. In this case, the NO-sensitive channels present in the mesenteric artery may not be present in the basilar artery. In the basilar artery, even saturated solutions of NO failed to change the smooth muscle membrane potential although they caused a total reversal of contraction. These concentrations of NO were 10 fold greater than in our previous study, when we did observe a slight hyperpolarization of 2 mV, which was not large enough to contribute significantly to relaxation. The reason for our failure to record similar effects in the present study is not clear, particularly as the sensitivity of the tissues to NO and the maximal relaxation attained were similar in both studies, and the degree of preconstriction and depolarization to noradrenaline were comparable.

In contrast to NO, levcromakalim evoked both concentration-dependent smooth muscle relaxation and hyperpolarization in the rabbit basilar artery, indicating that the lack of hyperpolarization to NO did not reflect an absence of levcromakalim-sensitive potassium channels. The different responses to levcromakalim and NO in the basilar artery are in contrast to studies in the rat mesenteric artery (McPherson & Angus, 1991; Garland & McPherson, 1992), where both cromakalim and NO hyperpolarized the resting membrane potential, both via a glibenclamide-sensitive pathway. Taken together, these observations again suggest a variation in the type of potassium channels which are present in each of these arteries.

Although membrane hyperpolarization to NO has yet to be investigated at the single channel level, the picture is much clearer in the case of KCOs, based on extensive patch-clamp studies with levcromakalim (Noack *et al.*, 1992a,b). These data have provided evidence that levcromakalim can activate small conductance potassium channels, which are ATP-sensitive and appear to be identical to the channels which are opened by depletion of the cellular substrates required for oxidative metabolism. These experiments also showed that levcromakalim could influence the open probability of other potassium channels, such as those which carry the delayed rectifier current. Levcromakalim and cromakalim have very similar actions on the mesenteric and basilar arteries, so may very well act by similar mechanisms in these vessels. In contrast, the hyperpolarization to NO, but not cromakalim was blocked by prior depolarization in the mesenteric artery, consistent with the idea of separate potassium channels mediating the responses to KCOs and NO, with both sensitive to glibenclamide.

Unlike NO, levcromakalim does not stimulate guanylyl cyclase in vascular smooth muscle cells, rather the relaxation appears to follow the opening of membrane potassium channels, subsequent hyperpolarization and a reduction in the open probability of voltage-dependent calcium channels (Hamilton *et al.*, 1986; Weir & Weston, 1986; Coldwell & Howlett, 1987; Taylor *et al.*, 1988; Noack *et al.*, 1992a,b). Most data on KCO's have been derived from separate measurements of smooth muscle tension and membrane potential, giving a circumstantial link between relaxation and hyperpolarization (Cavero *et al.*, 1989; Winquist *et al.*, 1989). Additionally, in vessels such as the guinea-pig coronary artery, relaxation of noradrenaline-contracted arterial segments by levcromakalim, was depressed by the presence of glibenclamide, indicating that the two events are causally linked (Eckman *et al.*, 1992). To date, there have been only a limited number of studies on the membrane events which accompany smooth muscle relaxation in response to KCOs in depolarized tissues. In the present study, simultaneous recordings showed that levcromakalim stimulated concentration-dependent hyperpolarization in unstimulated segments of the rabbit basilar artery and reversed the depolarization and contraction in the presence of noradrenaline. Both components of the response were inhibited by pre-incubation with glibenclamide (10 μM). Also, in the presence of 65 mM potassium, levcromakalim-evoked relaxations were reduced to a similar level to those obtained in noradrenaline-contracted tissues in the presence of glibenclamide, whereas membrane hyperpolarization was abolished at this time. This finding directly demonstrates that the attenuation of KCO-evoked relaxation observed in the presence of high concentrations of potassium is due to a reduced hyperpolarization (Masuzawa *et al.*, 1990; Parsons *et al.*, 1991a,b), and also supports the contention that a change in smooth muscle membrane potential represents the driving force for relaxation to this agent. This is an important observation, because the reduced relaxation in tissues preconstricted with high concentrations of potassium had been suggested to reflect functional antagonism, i.e. the high level of tone induced by potassium directly reducing the efficacy of the relaxing agent (Cook & Small, 1991). This is clearly not the case in the basilar artery. However, the finding that higher concentrations of levcromakalim can evoke changes in tone which are independent of an increase in membrane potential also indicates another, as yet undefined mechanism may also be involved, possibly an alteration in intracellular smooth muscle calcium handling (Bray *et al.*, 1988; 1991).

In summary, smooth muscle hyperpolarization to both acetylcholine and levcromakalim is abolished by glibenclamide. However, although the relaxation to levcromakalim is also almost totally blocked, relaxation to acetylcholine is not altered. This supports other evidence that endothelium-dependent hyperpolarization to cholinomimetics is not an important mechanism for relaxation in the basilar artery. In addition, NO *per se* provides no stimulus for hyperpolarization, as even saturated solutions of this agent failed to modify the membrane potential in this vessel.

This work was made possible by financial support from the Wellcome Trust, Levcromakalim and glibenclamide were generously supplied by SmithKline Beecham and Hoechst, respectively.

References

BRAY, K.M., WESTON, A.H., DUTY, S., NEWGREEN, D.T., LONGMORE, J., EDWARDS, G. & BROWN, T.J. (1991). Differences between the effects of cromakalim and nifedipine on agonist-induced responses in the rabbit aorta. *Br. J. Pharmacol.*, **102**, 337–344.

BRAY, K.M., WESTON, A.H., McHARG, A.D., NEWGREEN, D.T., SOUTHERTON, J.S. & DUTY, S. (1988). Further studies on the actions of the K-channel openers cromakalim (BRL 34915) and pincadil, in rabbit aorta. *Pflügers Arch.*, **411**, R202.

BRAYDEN, J.E. (1990). Membrane hyperpolarization is a mechanism of endothelium-dependent cerebral vasodilatation. *Am. J. Physiol.*, **259**, H668–H673.

BUCKINGHAM, R.E., HAMILTON, T.C., HOWLETT, D.R., MOOTOO, S. & WILSON, C. (1989). Inhibition by glibenclamide of the vasorelaxant action of cromakalim in the rat. *Br. J. Pharmacol.*, **97**, 57–64.

CAVERO, I., MODOT, S. & MESTRE, M. (1989). Vasorelaxant effects of cromakalim in rats are mediated by glibenclamide-sensitive potassium channels. *J. Pharmacol. Exp. Ther.*, **248**, 1261–1268.

CHEN, G., HASHITANI, H. & SUZUKI, H. (1989). Endothelium-dependent relaxation and hyperpolarization of canine artery smooth muscle in relation to the electrogenic Na^+-K^+ pump. *Br. J. Pharmacol.*, **98**, 950–956.

CHEN, G., SUZUKI, H. & WESTON, A.H. (1988). Acetylcholine releases endothelium-derived hyperpolarizing factor and EDRF from rat blood vessels. *Br. J. Pharmacol.*, **95**, 1165–1174.

CHEN, G., YAMAMOTO, Y., MIWA, K. & SUZUKI, H. (1991). Hyperpolarization of arterial smooth muscle induced by endothelial humoral substances. *Am. J. Physiol.*, **260**, H1888–H1892.

COLDWELL, M.C. & HOWLETT, D.R. (1987). Specificity of action of the novel anti-hypertensive agent, BRL 34915 as a potassium channel activator; comparison with nicorandil. *Biochem. Pharmacol.*, **36**, 3663–3669.

COOK, S.J. & SMALL, R.C. (1991). K^+-rich media and the relaxant actions of bronchodilator drugs in guinea-pig trachealis. *Br. J. Pharmacol.*, **104**, 401P.

ECKMAN, D.M., FRANKOVICH, J.D. & KEEF, K.D. (1992). Comparison of the actions of acetylcholine and levcromakalim in the guinea-pig coronary artery. *Br. J. Pharmacol.*, **106**, 9–16.

FELETOU, M. & VANHOUTTE, P.M. (1988). Endothelium-dependent hyperpolarization of canine coronary artery smooth muscle. *Br. J. Pharmacol.*, **93**, 515–524.

GARLAND, C.J. (1987). The role of membrane depolarization in the contractile response of the rabbit basilar artery to 5-hydroxytryptamine. *J. Physiol.*, **392**, 333–348.

GARLAND, C.J. & McPHERSON, G.A. (1992). Evidence that nitric oxide does not mediate the hyperpolarization and relaxation to acetylcholine in the rat small mesenteric artery. *Br. J. Pharmacol.*, **105**, 429–435.

HAMILTON, T.C., WEIR, S.W. & WESTON, A.H. (1986). Comparison of the effects of BRL 34915 and verapamil on electrical and mechanical activity in rat portal vein. *Br. J. Pharmacol.*, **88**, 103–111.

KOMORI, K., LORENZ, R.R. & VANHOUTTE, P.M. (1988). Nitric oxide, ACh and electrical and mechanical properties of canine arterial smooth muscle. *Am. H. Physiol.*, **24**, H207–H212.

LEBLANC, N., WILDE, D.W., KEEF, K.D. & HUME, J.R. (1989). Electrophysiological mechanisms of minoxidil sulfate-induced vasodilation of rabbit portal vein. *Circ. Res.*, **65**, 1102–1111.

MASUZAWA, K., ASANO, M., MATSUDA, T., IMAIZUMI, Y. & WATANABE, M. (1990b). Possible involvement of ATP-sensitive K^+ channels in the relaxant response of dog middle cerebral artery to cromakalim. *J. Pharmacol. Exp. Ther.*, **255**, 818–825.

McCARRON, J.G., QUAYLE, J.M., HALPERN, W. & NELSON, M.T. (1991). Cromakalim and pinacidil dilate small mesenteric arteries but not small cerebral arteries. *Am. J. Physiol.*, **261**, H287–H291.

MCHARG, A.D., SOUTHERTON, J.S. & WESTON, A.H. (1990). A comparison of the actions of cromakalim and nifedipine on rabbit isolated mesenteric artery. *Eur. J. Pharmacol.*, **185**, 137–146.

McPHERSON, G.A. & ANGUS, J.A. (1990). Characterization of responses to cromakalim and pinacidil in smooth and cardiac muscle by use of selective antagonists. *Br. J. Pharmacol.*, **100**, 201–206.

McPHERSON, G.A. & ANGUS, J.A. (1991). Evidence that acetylcholine mediated hyperpolarization of the rat small mesenteric artery does not involve the K^+ channel opened by cromakalim. *Br. J. Pharmacol.*, **103**, 1184–1190.

McPHERSON, G.A. & STORK, A.P. (1992). The resistance of some rat cerebral arteries to the vasorelaxant effect of cromakalim and other K^+-channel openers. *Br. J. Pharmacol.*, **105**, 51–58.

NAKASHIMA, M., LI, Y.I., SEKI, N. & KURIYAMA, H. (1990). Pinacidil inhibits neuromuscular transmission indirectly in the guinea-pig and rabbit mesenteric arteries. *Br. J. Pharmacol.*, **101**, 581–586.

NOACK, T., EDWARDS, G., DEITMER, P. & WESTON, A.H. (1992a). Characterization of potassium currents modulated by BRL 38227 in rat portal vein. *Br. J. Pharmacol.*, **106**, 717–726.

NOACK, T., EDWARDS, G., DEITMER, P. & WESTON, A.H. (1992b). Potassium channel modulation in rat portal vein by ATP depletion: a comparison with the effects of levcromakalim (BRL 38227). *Br. J. Pharmacol.*, **107**, 945–955.

PALMER, R.M.J., FERRIGE, A.G. & MONCADA, S. (1987). Nitric oxide release accounts for the biological activity of endothelium-derived relaxing factor. *Nature*, **327**, 524–526.

PARSONS, A.A., KSOLL, E., MACKERT, J.R.L., SCHILLING, L. & WAHL, M. (1991a). Comparison of cromakalim-induced relaxation of potassium precontracted rabbit, cat and rat isolated cerebral arteries. *Naunyn-Schmied Arch. Pharmacol.*, **343**, 384–392.

PARSONS, A.A., SCHILLING, L. & WAHL, M. (1991b). Analysis of acetylcholine-induced relaxation of rabbit isolated middle cerebral artery: effects of inhibitors of NO-synthesis, Na,K-ATPase, and ATP-sensitive K channels. *J. Cereb. Blood Flow Metab.*, **11**, 700–704.

RAND, V.E. & GARLAND, C.J. (1992). Endothelium-dependent relaxation to acetylcholine in the rabbit basilar artery: importance of membrane hyperpolarization. *Br. J. Pharmacol.*, **106**, 143–150.

STANDEN, N.B., QUAYLE, J.M., DAVIES, N.W., BRAYDEN, J.E., HUANG, Y. & NELSON, M.T. (1989). Hyperpolarizing vasodilators activate ATP-sensitive K^+ channels in arterial smooth muscle. *Science*, **245**, 177–180.

TARE, M., PARKINGTON, H.C., COLEMAN, H.A., NEILD, T.O. & DUSTING, G.J. (1990). Hyperpolarization and relaxation of arterial smooth muscle caused by nitric oxide derived from the endothelium. *Nature*, **346**, 69–71.

TAYLOR, S.G., SOUTHERTON, J.S., WESTON, A.H. & BAKER, J.R.L. (1988). Endothelium-dependent effects of acetylcholine in rat aorta: a comparison with sodium nitroprusside and cromakalim. *Br. J. Pharmacol.*, **64**, 853–863.

WALDRON, G.J., McPHERSON, G.A. & GARLAND, C.J. (1993). Acetycholine-induced relaxation in the rat isolated mesenteric artery: relative importance of smooth muscle hyperpolarization. *Br. J. Pharmacol.*, **108**, 3P.

WEIR, S.W. & WESTON, A.H. (1986). The effects of BRL 34915 and nicorandil on electrical and mechanical activity and on ^{86}Rb efflux in rat blood vessels. *Br. J. Pharmacol.*, **88**, 121–128.

WINQUIST, R.J., HEANEY, L.A., WALLACE, A.A., BASKIN, E.P., STEIN, R.B., GARCIA, M.L. & KACZOROWSKI, G.J. (1989). Glyburide blocks the relaxation response to BRL 34915 (cromakalim), minoxidil sulfate and diazoxide in vascular smooth muscle. *J. Pharmacol. Exp. Ther.*, **248**, 149–156.

(Received January 22, 1993
Revised May 11, 1993
Accepted June 4, 1993)

Br. J. Pharmacol. (1993), **110**, 657–664

Bradykinin-induced airflow obstruction and airway plasma exudation: effects of drugs that inhibit acetylcholine, thromboxane A_2 or leukotrienes

Ivana Kawikova, Hirokazu Arakawa, Claes-Göran Löfdahl, Bengt-Eric Skoogh & [1]Jan Lötvall

Lung Pharmacology Group, Department of Clinical Pharmacology and Division of Respiratory Medicine, (Department of Medicine), University of Göteborg, Göteborg, Sweden

1 The mechanisms behind bradykinin-induced effects in the airways are considered to be largely indirect. The role of cholinergic nerves and eicosanoids, and their relationship in these mechanisms were investigated in guinea-pigs.

2 The role of cholinergic nerves was studied in animals given atropine (1 mg kg^{-1}, i.v.), hexamethonium (2 mg kg^{-1}, i.v.), or vagotomized. To study the role of eicosanoids, animals were pretreated with a thromboxane A_2 (TxA_2) receptor antagonist (ICI 192,605; 10^{-6} mol kg^{-1}, i.v.) or with a leukotriene (LT) receptor $C_4/D_4/E_4$ antagonist (ICI 198,615; 10^{-6} mol kg^{-1}, i.v.).

3 After pretreatment with a drug, bradykinin (150 nmol) was instilled into the tracheal lumen. We measured both airway insufflation pressure (Pi), to assess airway narrowing, and the content of Evans blue dye in airway tissue, to assess plasma exudation.

4 Bradykinin instillation into the trachea caused an increase in Pi and extravasation of Evans blue dye. The increase in Pi was significantly attenuated by atropine or the TxA_2 receptor antagonist, but not by hexamethonium, vagotomy or the LT receptor antagonist.

5 The bradykinin-induced exudation of Evans blue dye was significantly attenuated in the intrapulmonary airways by the TxA_2 receptor antagonist, but not by atropine, hexamethonium, cervical vagotomy or the LT receptor antagonist.

6 A thromboxane-mimetic, U-46619 (20 nmol kg^{-1}, i.v. or 10 nmol intratracheally), caused both an increase in Pi and extravasation of Evans blue dye at all airway levels. Atropine pretreatment slightly attenuated the peak Pi after the intratracheal administration of U-46619, but not after i.v. administration.

7 We conclude that peripheral cholinergic nerves are involved in bradykinin-induced airflow obstruction but not plasma exudation, and that TxA_2 is involved in both airflow obstruction and airway plasma exudation induced by bradykinin given via the airway route. TxA_2-induced airflow obstruction is mediated only to a minor degree, via the release of acetylcholine in the airways.

Keywords: Asthma; bronchoconstriction; airway oedema; inflammation; plasma exudation; cholinergic nerves; bradykinin; thromboxane; leukotrienes

Introduction

Bradykinin, a plasma-derived inflammatory peptide, has been implicated in asthma (Regoli & Barabe, 1980; Barnes *et al.*, 1988). Bradykinin produces bronchoconstriction in asthmatics, but to a lesser extent in normal subjects (Simonsson *et al.*, 1973; Fuller *et al.*, 1987). It has also been shown that asthmatics have elevated concentrations of bradykinin in plasma during active disease and of the bradykinin precursor kininogen in broncho-alveolar lavage fluid after allergen challenge (Abe *et al.*, 1967; Christiansen *et al.*, 1987).

In experimental animals, bradykinin causes airway narrowing *in vivo* (Collier *et al.*, 1960; Ichinose *et al.*, 1990; Lötvall *et al.*, 1991), exudation of plasma from the airway microcirculation (Saria *et al.*, 1983; Erjefält & Persson, 1989; Lötvall *et al.*, 1991) and airway smooth muscle contraction *in vitro* (Bhoola *et al.*, 1962; Dusser *et al.*, 1988).

The mechanisms of bradykinin-induced effects in the airways have been the subject of many studies. It has been suggested that cholinergic nerves (Ichinose *et al*, 1990), sensory neuropeptides (Kaufman *et al.*, 1980; Saria *et al.*, 1988; Ichinose *et al.*, 1990), metabolites of arachidonic acid (Collier *et al.*, 1960; Ichinose *et al.*, 1990) and platelet activating factor (Rogers *et al.*, 1990) are involved in these responses. Moreover, peptide-degrading enzymes, such as neutral endopeptidase 24.11 and angiotensin-converting enzyme, modulate the responses to bradykinin (Dusser *et al.*, 1988; Lötvall *et al.*, 1991). The relationships between the different mediators which are involved in bradykinin responses and the exact metabolites of arachidonic acid that are involved, have not yet been elucidated. Furthermore, the results of different studies are sometimes contradictory. For example, Collier *et al.* (1960) found that neither anticholinoceptor drugs nor section of the cervical vagi had any effect on the bronchoconstrictor response to bradykinin, whereas Ichinose *et al.* (1990) found that atropine had a significant inhibitory effect.

In this study we wanted to investigate the role of cholinergic nerves and of metabolites of arachidonic acid, as well as their relationship in the mechanism of bradykinin-induced effects in the airways of guinea-pigs given bradykinin directly into the tracheal lumen. To evaluate the role of cholinergic nerves, we used atropine or hexamethonium pretreatment, or cervical vagotomy before bradykinin instillation. To elucidate the importance of arachidonic acid metabolites in bradykinin-nduced airway responses, a thromboxane A_2 receptor antagonist (ICI 192,605) or a leukotriene $C_4/D_4/E_4$ receptor antagonist (ICI 198,615) was given before bradykinin instillation. Finally, we studied the relationship between cholinergic nerves and thromboxane A_2 by administering U-46619, a stable thromboxane A_2-mimetic, to animals pretreated with

[1]Author for correspondence at: Department of Clinical Pharmacology, Fack 2, Sahlgrenska Sjukhuset, S-413 45 Göteborg, Sweden.

atropine. In all these experiments, we monitored airway insufflation pressure as a measurement of airway narrowing and quantified the amount of Evans blue dye in the airways as a measurement of plasma exudation.

Methods

Preparation

This study was approved by the Animal Ethics Committee in Göteborg. We used male Dunkin-Hartley guinea-pigs weighing 350–550 g for the study involving bradykinin and 450–700 g for the study involving U-46619 (total $n = 118$). The animals were anaesthetized with ketamine (100 mg kg^{-1}, i.p.) and xylazine (10–12 mg kg^{-1}, i.m.). Additional doses were given as required to maintain adequate anaesthesia. The animals were placed on a heated blanket (Harvard model 507061, Harvard Apparatus Ltd., Edenbridge, Kent), which maintained body temperature at approximately 37°C. The left carotid artery was cannulated and the catheter was connected to a pressure transducer (Spectramed, Viggo, Helsingborg, Sweden). Another polyethylene catheter was inserted into the right external jugular vein for the i.v. administration of drugs and fluids. A tracheal cannula (10 mm length and 2.7 mm internal diameter) was inserted into the upper cervical trachea through a tracheostomy, secured with a suture and connected to a constant volume mechanical ventilator (Harvard model 50-1718, Harvard Apparatus Ltd., Edenbridge, Kent). Animals were placed in a supine position at an angle of 20°, with the head at a higher level to allow the instilled material to reach the lower airway levels. A tidal volume of 10 ml kg^{-1} and a frequency of 60 breaths per min was used. The ventilatory circuit had a total volume of 18 ml. Insufflation pressure (Pi) was measured with a differential pressure transducer (Model FCO40; ±1,000 mmH_2O, Furness Controls Ltd., Bexhill, Sussex) which was attached to a catheter connected to a side port of the intratracheal cannula. The signals from the blood pressure transducer were amplified with an analogue preamplifier (Kungsbacka mät & registerteknik AB, Sweden). All the signals were digitised using a 12-bit analog-digital board (National Instruments, Austin, TX, U.S.A.) connected to a Macintosh II computer (Apple Computer Inc., Cupertino, CA, U.S.A.) and monitored with software (LabView, National Instruments, Austin, TX, U.S.A.).

Protocol

After preparation, all the animals were treated with suxamethonium (5 mg, i.v.) to avoid artefacts of spontaneous breathing and with propranolol (1 mg kg^{-1}, i.v.) to inhibit the sympathomimetic effects of bradykinin administration (Piper *et al.*, 1967). The animals were divided into twelve groups, to study the effect of atropine, hexamethonium, cervical vagotomy, ICI 192,605 or ICI 198,615 on bradykinin-induced effects in the airways. Each group had a separate control group, which was given the vehicle for each drug or which was not vagotomized before the airway instillation of bradykinin (150 nmol). The eleventh group was a control which was not treated and which was given a tracheal instillation of the vehicle for bradykinin (0.9% saline). The twelfth group was a control pretreated with the vehicle for ICI 198,615 before the instillation of the vehicle for bradykinin (0.9% saline) into the tracheal lumen. Ten minutes after the administration of suxamethonium and propranolol, the animals were pretreated with the relevant drugs or vehicles: atropine (1 mg kg^{-1}, i.v.); hexamethonium (2 mg kg^{-1}, i.v.); ICI 192,605 (10^{-6} mol kg^{-1}, i.v.); ICI 198,615 (10^{-6} mol kg^{-1}, i.v.), or the vehicle for each drug; 0.9% saline, $NaHCO_3$ in 0.9% saline, 0.9% saline and [1 M NaOH, PEG 400 and 10 nM NaH_2PO_4] in 0.9% saline respectively. In a separate group, both cervical vagi were sectioned by surgical procedures. The control group for vagotomy was dissected around the vagi, but the nerves were not cut. Eight minutes later, Evans blue dye (20 mg kg^{-1}) was administered i.v. for 1 min. Two minutes later, the lungs were hyperinflated with twice the tidal volume, by manually blocking the outflow of the ventilator, and bradykinin or saline was instilled into the airways. Instillation into the tracheal lumen was performed by flushing 50 µl of 3 mM bradykinin with 1 ml of air through a needle, directly into the tracheal lumen via the tracheal cannula, with the point of the needle inside the lower part of the tracheal cannula. The distribution of instilled liquid into the airway tree has been studied by use of pen ink and Evans blue dye. We found that most of the ink/dye was macroscopically located at the level of the trachea and main bronchi immediately after intratracheal instillation, but we also found staining around the intrapulmonary airways, suggesting that the dye had also reached this airway level (unpublished observation).

Airway insufflation pressure (Pi) and mean systemic blood pressure were monitored every 15 s over 1 min and subsequently every 30 s for another 5 min after bradykinin instillation. The animals were disconnected from the ventilator and the thoracic cavity was opened. A catheter was inserted into the aorta through the left ventricle and the systemic circulation was perfused with 50 ml of 0.9% NaCl to remove the Evans blue dye from the bronchial circulation. Another catheter was inserted via the right ventricle into the pulmonary artery and the pulmonary circulation was perfused with 20 ml of 0.9% NaCl.

Another four groups of animals were used to evaluate the role of cholinergic nerves in airway responses induced by U-46619, a thromboxane mimetic. These groups were anaesthetized, tracheostomized and given propranolol, suxamethonium and Evans blue dye in the same way as all the other animals. U-46619 was administered intravenously (20 nmol kg^{-1}) or intratracheally (10 nmol in 50 µl of 0.9% NaCl) after the animals were pretreated with atropine (1 mg kg^{-1}, i.v.) or saline (0.9%). Airway insufflation pressure (Pi) and mean systemic blood pressure were monitored and the amount of Evans blue dye in the airway tissue was quantified.

Measurement of plasma exudation

After perfusion, the trachea and lungs were dissected out *en bloc*, the parenchyma was carefully scraped off and the extraneous tissue was removed. The trachea, main bronchi and intrapulmonary airways were then separated from one another and the intrapulmonary airways were divided into two portions of approximately equal length, arbitrarily called proximal and distal. We did not attempt to remove any plasma from the intraluminal portion of the airways. All the tissues were dried in a freeze-drier for 24 h (MicroModulyo, Edwards High Vacuum International, West Sussex), weighed when dry and Evans blue dye was extracted by keeping the tissues in 2 ml of formamide in a 40°C water bath for another 16 h. Absorption at 620 nm was measured in a spectrophotometer (Beckman DB, Ingeniörsfirman Hugo Tillquist, Stockholm, Sweden). Extravasated Evans blue dye was quantified by interpolation on a standard curve of dye concentrations in the range of 0–15 µg ml^{-1} and expressed as ng dye mg^{-1} dry tissue. The Evans blue dye measurement has previously been shown to correlate with the extravasation of radiolabelled albumin into guinea-pig airways (Rogers *et al.*, 1989).

Drugs

The following drugs were used: ketamine (Parke-Davis, S.A. Barcelona, Spain), xylazine (Bayer Leverkusen, Bayer Sverige AB, Mölndal, Sweden), Evans blue dye (Aldrich Chemical Co., Inc., Milwaukee, U.S.A.), propranolol (ICI Pharmaceuticals, Macclesfield, Cheshire), suxamethonium (Kabi-

Vitrum AB, Stockholm, Sweden), atropine, hexamethonium and bradykinin (Sigma Chemical Co. Ltd., Poole, Dorset).

U-46619 (9α, 11α-dideoxymethanoepoxy-prostaglandin $F_{2\alpha}$) (Cayman Chemical Co Inc., Ann Arbor, MI, U.S.A.), ICI 192,605 (4(z)-6-(2-o-chlorophenyl-4-o-hydroxyphenyl-1,3-dioxan-*cis*-5-yl)hexenoic acid), a thromboxane A_2 receptor antagonist (Jessup *et al.*, 1988), and ICI 198,615 ([1-[[2-methoxy-4[[(phenylsulphonyl)amin]carbonyl]phenyl]methyl]-1H-indazol-6-yl]carbamic acid cyclopentylester) a leukotriene $C_4/D_4/E_4$ receptor antagonist (Shirley & Cheng, 1991), were kindly donated by ICI Pharmaceuticals.

Data analysis

Data are reported as the mean ± s.e.mean. The peak Pi, immediate area under the curve (i-AUC = from 0 min to 1.5 min), more sustained AUC (s-AUC = from 1.5 min to 6 min), total AUC (t-AUC = from 0 min to 6 min) were calculated to evaluate the differences in airway narrowing. The amounts of Evans blue dye at the four airway levels were compared to determine any differences in plasma exudation. The mean baseline blood pressure and the lowest mean blood pressure after bradykinin instillation were calculated to estimate the effect of bradykinin on the systemic circulation. Non-parametric analysis (Mann-Whitney U-test) was used to determine significance of differences between groups. A value of $P<0.05$ was considered significant. Data were analysed with a Macintosh computer using StatView II.

Results

Role of cholinergic nerves in bradykinin-induced airway effects

Airway insufflation pressure There was no significant difference in baseline pulmonary insufflation pressure (Pi) between atropinized or untreated animals (Figure 1a). The instillation of 50 μl of 0.9% saline into the tracheal lumen induced a small increase in Pi (from 8.9 ± 0.6 cmH_2O to 16.5 ± 1.2 cmH_2O). Bradykinin instilled into the trachea (50 μl of 3 mM; 150 nmol) produced a biphasic response in Pi. The immediate sharp peak reached a maximum between 30–45 s after instillation (Figure 1a; peak Pi 35 ± 4 cmH_2O). A more slowly progressing sustained response was observed between 3.5 and 4 min (Figure 1a; Pi 28 ± 3 cmH_2O). Atropine pretreatment significantly inhibited both the immediate and the more sustained response to bradykinin ($P<0.05$; Figure 1a and Table 1). Peak Pi and the area under the curves were not significantly different in the group pretreated with atropine before bradykinin instillation compared with sham stimulation (50 μl of 0.9% saline; Table 1).

In animals pretreated with hexamethonium, the baseline Pi was not significantly affected (10.4 ± 0.2 mmHg) compared with untreated animals (11.2 ± 0.3 mmHg). The bradykinin-induced increase in Pi (peak Pi: 37 ± 2.7 mmHg) was not significantly affected by hexamethonium (peak Pi: 47 ± 5.8 mmHg, $P=0.2$; Figure 2a and Table 1).

There was no significant difference in baseline Pi between vagotomized animals compared with control animals (8 ± 0.3 and 8 ± 0.4 cmH_2O respectively). Cervical vagotomy did not significantly affect the changes in Pi induced by bradykinin instillation (Figure 3a and Table 1; Peak Pi 41 ± 5 and 35 ± 4 cmH_2O in vagotomized and control animals respectively).

Evans blue dye Bradykinin (150 nmol) instilled into the lumen of the trachea produced a significant extravasation of Evans blue dye into the trachea, main bronchi and intrapulmonary airways, as compared with instilled 0.9% saline ($P<0.005$). Atropine (Figure 1b) or hexamethonium (Figure 2b) did not influence this effect. In vagotomized animals, however, we found a slight but significant enhancement of the extravasation of Evans blue dye in the proximal intrapulmonary airways (Figure 3b; $P<0.05$), but no significant effect was found at any other airway level.

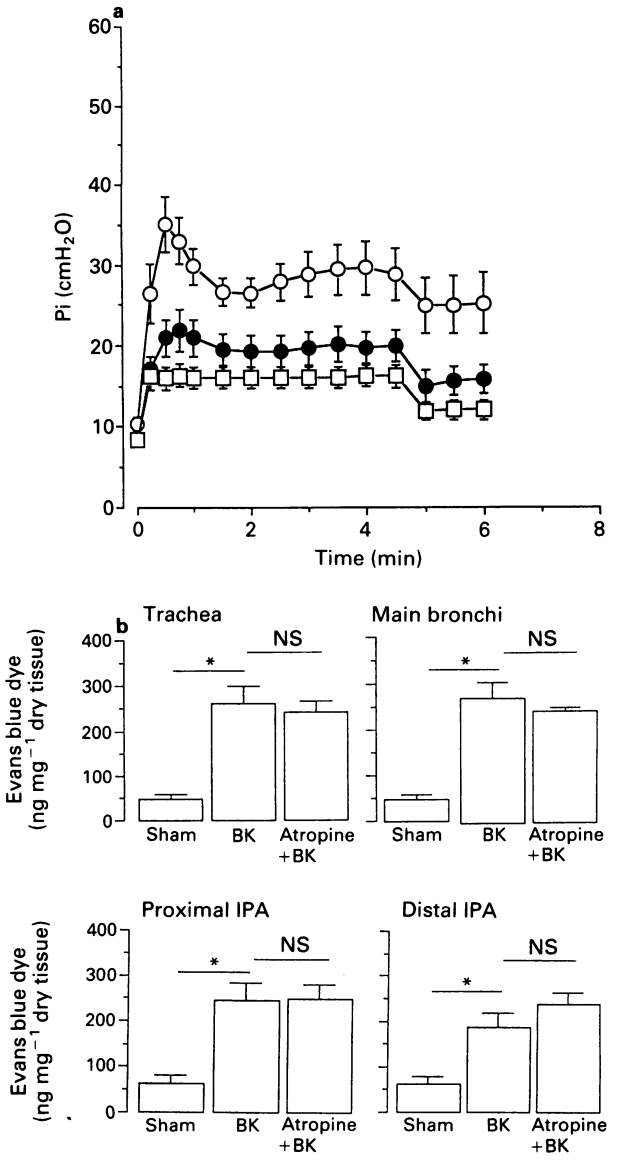

Figure 1 (a) Time course of the increase in airway insufflation pressure (Pi) induced by a tracheal instillation of 0.9% saline (sham, □, $n=8$), bradykinin in untreated animals (○, $n=13$) and bradykinin after pretreatment with atropine (●, $n=11$). There was a significant difference in the response to bradykinin between the untreated and atropinized group ($P<0.05$). (b) The amount of Evans blue dye at different airway levels after an intratracheal instillation of 0.9% saline (sham, $n=8$), bradykinin (BK) in untreated animals ($n=13$), and bradykinin after pretreatment with atropine ($n=11$). IPA = intrapulmonary airways. Data are shown as mean ± s.e.mean, * $P<0.05$; NS $P>0.05$.

Mean blood pressure There was no significant difference in baseline mean systemic blood pressure between the group pretreated with atropine and its control group (37 ± 3 and 37 ± 2 mmHg respectively) or with hexamethonium (36 ± 2 mmHg in the group pretreated with hexamethonium and 38 ± 2 mmHg in controls), whereas the vagotomized group had a higher mean blood pressure compared with its control group (52 ± 3 mmHg in the vagotomized group and 39 ± 2 mmHg in controls, $P<0.05$). Instilled bradykinin produced a significant fall in systemic blood pressure, reaching the lowest values approximately 2 min after bradykinin (lowest mean blood pressure 20 ± 2 mmHg after bradykinin instillation compared with 29 ± 3 mmHg after the instillation of

Table 1 The role of cholinergic nerves in bradykinin (BK)-induced airway effects

	Sham	*BK*	*Atropine + BK*	*BK*	*Hexamethonium + BK*	*BK*	*Vagotomy + BK*
i-AUC	21 ± 2	37 ± 3*	26 ± 3†	46 ± 2*	53 ± 5*	35 ± 4*	53 ± 5*
s-AUC	60 ± 5	112 ± 12*	75 ± 8†	128 ± 12*	175 ± 27*	111 ± 17*	119 ± 10*
t-AUC	82 ± 6	148 ± 15*	100 ± 10†	174 ± 14*	228 ± 31*	147 ± 21*	160 ± 13*

The effect of atropine, vagotomy and hexomethonium on i-AUC (immediate area under the curve = 0–1.5 min), s-AUC (sustained area under the curve = 1.5–6 min) and t-AUC (total area under the curve = 0–6 min) in guinea-pigs given bradykinin into the tracheal lumen.
*$P<0.05$ compared with sham exposed animals.
†$P<0.05$ compared with untreated animals exposed to bradykinin.
Values are shown as mean ± s.e.mean.

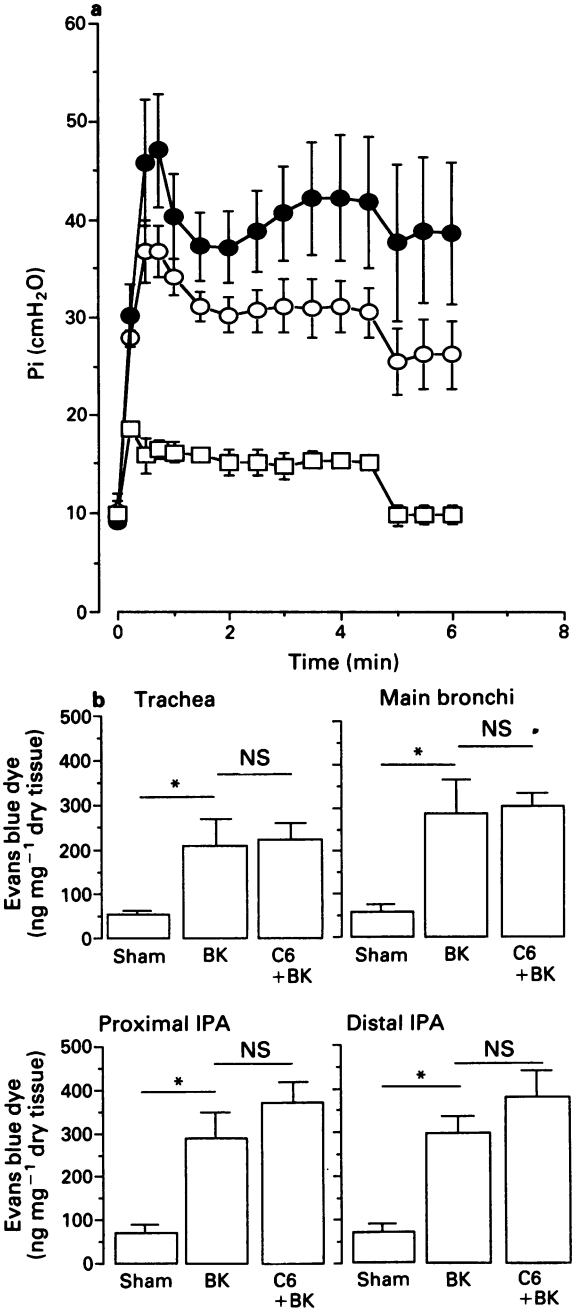

Figure 2 (a) Time course of increase in airway insufflation pressure (Pi) induced by a tracheal instillation of 0.9% saline (sham, □, $n = 8$), bradykinin in untreated animals (○, $n = 6$) and bradykinin after pretreatment with hexamethonium (●, $n = 6$). (b) The amount of Evans blue dye at different airway levels after an intratracheal instillation of 0.9% saline (sham, $n = 8$), or after an intratracheal instillation of bradykinin (BK) in untreated animals ($n = 6$) and in animals pretreated with hexamethonium (C6, $n = 6$). IPA = intrapulmonary airways. Data are shown as mean ± s.e.mean, *$P<0.05$; NS $P>0.05$.

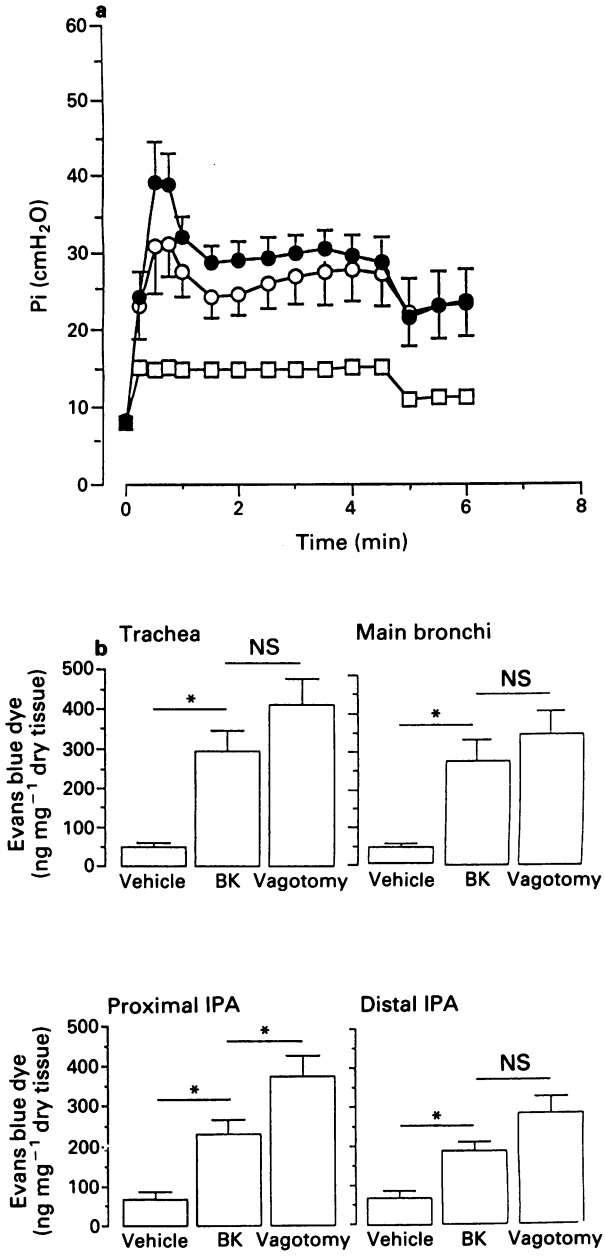

Figure 3 (a) Time course of the increase in airway insufflation pressure (Pi) induced by a tracheal instillation of 0.9% saline (sham; □; $n = 8$), bradykinin in untreated animals (○, $n = 11$) and bradykinin after cervical vagotomy (●, $n = 9$). (b) The amount of Evans blue dye at different airway levels after an intratracheal instillation of 0.9% saline (sham, $n = 8$), bradykinin (BK) in untreated animals ($n = 11$) and bradykinin after cervical vagotomy ($n = 9$). IPA = intrapulmonary airways. Data are shown as mean ± s.e.mean, *$P<0.05$; NS $P>0.05$.

0.9% saline; $P<0.05$). Atropine or hexamethonium pretreatment, or vagotomy, had no significant effect on the lowest mean blood pressure measured after bradykinin instillation (20 ± 2 mmHg in the group pretreated with atropine compared with 20 ± 2 mmHg in its control group, 22 ± 2 mmHg in the group pretreated with hexamethonium compared with 19 ± 2 mmHg in its control group and 21 ± 1 mmHg in the vagotomized group compared with 20 ± 2 mmHg in its control group).

Role of arachidonic acid metabolites in bradykinin-induced airway effects

Thromboxane A_2 The thromboxane A_2 receptor antagonist, ICI 192,605 (10^{-6} mol kg^{-1}, i.v.), did not influence baseline Pi compared with the vehicle (Figure 4a). Pretreatment with ICI 192,605 significantly suppressed both the immediate and the more sustained response in Pi to bradykinin (Figure 4a; $P<0.005$). Peak Pi, i-AUC, s-AUC and t-AUC were significantly higher in the group pretreated with ICI 192,605 before bradykinin instillation compared with sham stimulation ($P<0,05$; Table 2).

The bradykinin-induced extravasation of Evans blue dye was significantly attenuated in both the proximal and distal intrapulmonary airways after pretreatment with ICI 192,605, but it was not significantly affected in the trachea and main bronchi (Figure 4b; $P<0.05$).

Animals pretreated with ICI 192,605 had a significantly lower mean baseline blood pressure (27 ± 2 mmHg) than the group pretreated with the vehicle and given bradykinin (46 ± 4 mmHg, $P<0.05$). However, the lowest mean blood pressure measured after bradykinin instillation was not significantly different in animals pretreated with ICI 192,605 compared with their controls (21 ± 2 and 21 ± 1 mmHg respectively).

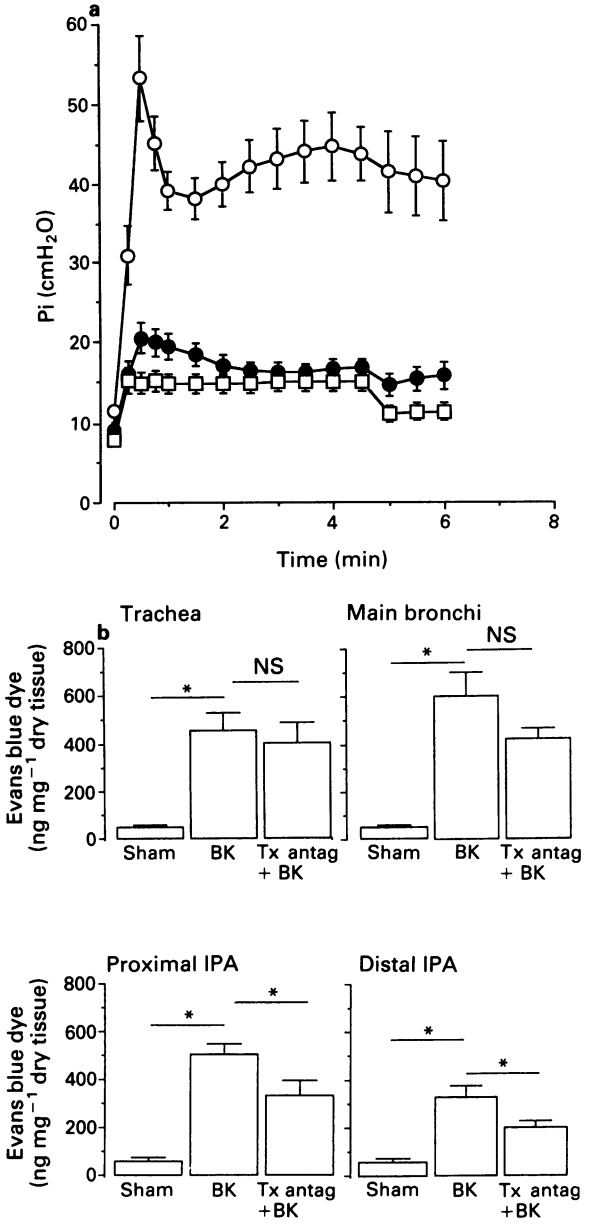

Figure 4 (a) Time course of the increase in airway insufflation pressure (Pi) induced by a tracheal instillation of 0.9% saline (sham, □, $n=8$), bradykinin in untreated animals (150 nmol, ○, $n=6$) and bradykinin after pretreatment with ICI 192,605 (10^{-6} mol kg^{-1}, i.v., ●, $n=7$), ($P<0.005$). (b) The amount of Evans blue dye at different airway levels after an intratracheal instillation of 0.9% saline (sham, $n=8$), bradykinin (BK) and bradykinin after pretreatment with ICI 192,605. IPA = intrapulmonary airways. Data are shown as mean ± s.e.mean, *$P<0.05$; NS $P>0.05$.

Leukotrienes The leukotriene $C_4/D_4/E_4$ receptor antagonist, ICI 198,615 (10^{-6} mol kg^{-1}, i.v.), did not affect baseline Pi compared with the vehicle (Figure 5a). Neither the bradykinin-induced increase in Pi (Table 2) nor the effect on Evans blue dye extravasation were significantly affected by ICI 198,615 (Figure 5b). ICI 198,615 had no significant effect on baseline mean blood pressure (32 ± 3 and 39 ± 5 mmHg in animals pretreated with ICI 198,615 and vehicle respectively) or lowest mean blood pressure after bradykinin instillation (15 ± 1 and 19 ± 2 mmHg respectively).

Thromboxane-mimetic, U-46619

Intravenous U-46619 There was no difference in baseline Pi between atropinized and untreated animals (10 ± 1 and 10 ± 1 cmH_2O respectively). The administration of U-46619 (20 nmol kg^{-1}, i.v.) caused an increase in airway insufflation pressure, which was not significantly influenced by atropine pretreatment (Table 3). Furthermore, the time course of the Pi response to U-46619, measured as the areas under the curves, was not significantly different in the group pretreated with atropine before U-46619 administration compared with the animals pretreated with the vehicle (Table 3). The intravenous administration of U-46619 produced an extravasation of Evans blue dye in the trachea, main bronchi and both the proximal and distal intrapulmonary airways. Atropine appeared to have a small potentiating effect on the U-46619-induced plasma exudation in the intrapulmonary airways (Table 4).

There was no difference in baseline mean systemic blood pressure between animals pretreated with atropine and the control group (42 ± 4 and 44 ± 5 mmHg, respectively). Intravenous U-46619 caused an increase in mean blood pressure, which reached its maximum level after approximately 60 s, but atropine did not influence this effect.

U-46619 administered into the trachea U-46619 (10 nmol in 50 µl of 0.9% NaCl) administered directly into the tracheal lumen produced an immediate increase in Pi, which reached a peak within 1 min (Table 3). When the thromboxane-mimetic was administered via this route, there was a slight but significant attenuation of the peak Pi, but the immediate, sustained or total areas under the curve were not significantly affected (Table 3). The tracheal administration of U-46619 produced an extravasation of Evans blue dye in the trachea, main bronchi and both the proximal and distal intrapulmonary airways (Table 4). Atropine appeared to have a slight attenuating effect on the U-46619-induced plasma exudation in the distal intrapulmonary airways.

The administration of U-46619 into the trachea caused an increase in mean systemic blood pressure, which reached its maximum level at approximately 60 s. Atropine did not influence this effect of U-46619 (data not shown).

Table 2 The role of eicosanoids in bradykinin (BK)-induced airway effects

	Sham	*BK*	*TxA_2 antagonist + BK*	*Vehicle + sham*	*BK*	*LT antagonist + BK*
i-AUC	21 ± 2	53 ± 4*	28 ± 1*†	20 ± 2	42 ± 2*	44 ± 5*
s-AUC	60 ± 5	187 ± 19*	74 ± 4*†	46 ± 4	143 ± 7*	145 ± 20*
t-AUC	82 ± 6	241 ± 22*	103 ± 4*†	66 ± 7	185 ± 8*	189 ± 24*

The effects of ICI 192,605, a TxA_2 receptor antagonist and ICI 198,615, a LT receptor antagonist on i-AUC (immediate are under the curve = 0–1.5 min), s-AUC (sustained area under the curve = 1.5–6 min) and t-AUC (total area under the curve = 0–6 min) in guinea-pigs given bradykinin into the tracheal lumen.
*$P<0.05$ compared with sham exposed animals.
†$P<0.05$ compared with untreated animals exposed to bradykinin.
Values are shown as mean ± s.e.mean.

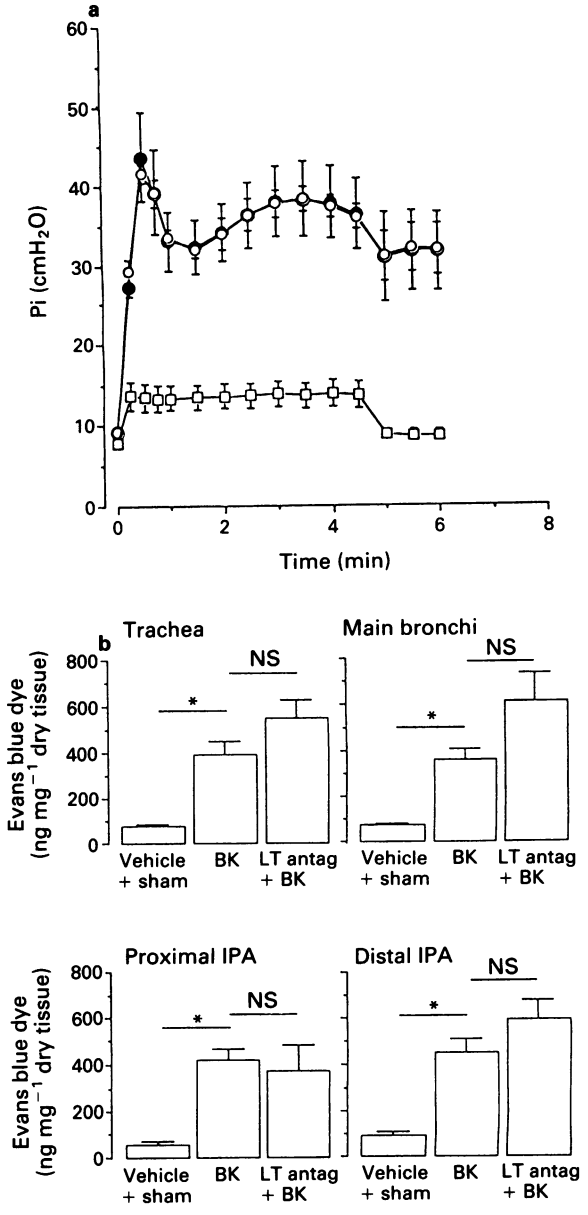

Figure 5 (a) Time course of the increase in airway insufflation pressure (Pi) induced by a tracheal instillation of 0.9% saline in animals pretreated with the vehicle for ICI 198,615 (sham, □; $n = 5$), bradykinin instillation in untreated animals (○, $n = 6$) and bradykinin instillation after pretreatment with ICI 198,615 (●, $n = 6$). (b) The amount of Evans blue dye at different airway levels after an intratracheal instillation of 0.9% saline in animals pretreated with the vehicle for ICI 198,615 (sham, $n = 5$), bradykinin (BK) in untreated animals and bradykinin after pretreatment with ICI 198,615. IPA = intrapulmonary airways. Data are shown as mean ± s.e.mean, $P<0.05$; NS $P>0.05$.

Discussion

In the present study, we have investigated the role of cholinergic nerves and arachidonic acid metabolites in bradykinin-induced airflow obstruction and airway plasma exudation in the guinea-pig. We found that atropine, but not hexamethonium or cervical vagotomy, attenuated the airflow obstruction induced by bradykinin, but not the induced plasma exudation. By contrast, in animals pretreated with the thromboxane A_2 receptor antagonist, both bradykinin-induced airflow obstruction and plasma exudation in the intrapulmonary airways were attenuated, suggesting that thromboxane A_2 plays an important role in bradykinin-induced airway responses. The release of leukotrienes did not appear to be involved, because a leukotriene $C_4/D_4/E_4$ receptor antagonist produced no effect.

Cholinergic nerves

Our finding that atropine, but not cervical vagotomy, attenuated bradykinin-induced airflow obstruction suggests that bradykinin activates peripheral cholinergic fibres, which cause the release of acetylcholine, without any activation of central reflexes. It is likely that anaesthetized guinea-pigs have an intact central nervous cholinergic innervation to the airways, because Hay *et al.* (1990) showed that cholinergic airflow obstruction can be induced in this species by electrical stimulation of specific areas in the dorsal medulla. Ichinose *et al.* (1990) used different anaesthetics from the present study (urethane versus ketamine and xylazine) and still demonstrated that atropine had an inhibitory effect on bradykinin-induced airflow obstruction. Furthermore, hexamethonium did not influence the responses, implying that activation of cholinergic nerves via cholinergic ganglia was unimportant in the responses to bradykinin. Our data thus suggest that, in this model, the bradykinin-induced activation of cholinergic nerves is located at the level of postganglionic fibres within the airway wall, and excludes central cholinergic reflexes.

The amount of Evans blue dye exudation in airway tissue after bradykinin was not inhibited by atropine, hexamethonium or cervical vagotomy, thus implying that plasma exudation is independent of the release of acetylcholine. This is not surprising, since the cholinergic agent, methacholine, does not produce airway microvascular leakage in guinea-pigs (Lötvall *et al.*, 1990). By contrast, there was a trend towards a potentiation of bradykinin-induced Evans blue dye extravasation in the peripheral airways after atropine, cervical vagotomy and hexamethonium. These findings are not completely explained by the present study. Possibly a relative increase in the tone of sympathetic nerves after inhibition of cholinergic nerves may influence the bronchial blood flow, and subsequently the plasma exudation induced by bradykinin.

Arachidonic acid metabolites

To evaluate the role of metabolites of arachidonic acid, we pretreated animals with either a TxA_2 receptor antagonist

Table 3 The effect of atropine on U46619-induced airflow obstruction

	Intravenous		*Intratracheal*	
	U-46619 (n = 6)	*Atropine + U-46619 (n = 6)*	*U-46619 (n = 6)*	*Atropine + U-46619 (n = 6)*
Peak Pi	58 ± 2	60 ± 1	66 ± 3	55 ± 2*
i-AUC	68 ± 3	70 ± 2	66 ± 5	59 ± 2
s-AUC	179 ± 35	193 ± 9	241 ± 21	217 ± 9
t-AUC	280 ± 30	263 ± 10	307 ± 26	276 ± 11

The effect of atropine on peak Pi, i-AUC (immediate area under the curve = 0–1.5 min), s-AUC (sustained area under the curve = 1.5–6 min) and t-AUC (total area under the curve = 0–6 min) in guinea-pigs given U-46619, intravenously or into the tracheal lumen.
Values are shown as mean ± s.e.mean, $*P < 0.05$.

Table 4 The effect of atropine on U46619-induced airway plasma exudation

	Intravenous		*Intratracheal*	
	U-46619 (n = 6)	*Atropine + U-46619 (n = 6)*	*U-46619 (n = 6)*	*Atropine + U-46619 (n = 6)*
Trachea	244 ± 41	255 ± 37	158 ± 34	129 ± 15
Main bronchi	350 ± 38	352 ± 47	279 ± 60	223 ± 60
Proximal IPA	391 ± 40	501 ± 66*	452 ± 50	389 ± 53
Distal IPA	390 ± 21	529 ± 61*	452 ± 50	309 ± 30*

The effect of atropine on exudation of Evans blue dye into airway tissue (ng mg^{-1} dry tissue) in guinea-pigs given U-46619 intravenously or into the tracheal lumen.
IPA = intrapulmonary airways.
Values are shown as mean ± s.e.mean, $*P < 0.05$.

(ICI 192,605) or a LT $C_4/D_4/E_4$ receptor antagonist (ICI 198,615) at doses that are known strongly to inhibit responses to the thromboxane-mimetic (Jessup *et al.*, 1988; Lötvall *et al.*, 1992) or leukotrienes (Shirley & Cheng, 1991). We found that the TxA_2 receptor antagonist incompletely suppressed the increase in airway insufflation pressure caused by bradykinin instilled into the tracheal lumen. The TxA_2 receptor antagonist significantly decreased, but did not abolish, the extravasation of Evans blue dye in the intrapulmonary airways, thereby suggesting that TxA_2 plays a partial role in bradykinin-induced airway microvascular leakage at this airway level. These two findings imply that TxA_2 is one of the important mediators of bradykinin-induced airway responses in the guinea-pig, but that other mechanisms are also involved. The involvement of prostanoids in bradykinin-induced plasma exudation has recently been implied by Rogers *et al.* (1990), who found that indomethacin had an inhibitory effect in intrapulmonary airways after i.v. bradykinin. This finding is further supported by another study in our laboratory, where we found that the thromboxane synthase inhibitor, OKY-046, significantly suppressed airway narrowing and plasma exudation in the intrapulmonary airways after bradykinin (Arakawa *et al.*, 1992). In addition, a TxA_2-mimetic (U-46619) alone produces airway microvascular leakage in guinea-pigs when administered by the i.v. route (Lötvall *et al.*, 1992) or via the airway route as shown in the present study.

Ichinose and co-workers (1990) found no effect of indomethacin on airflow obstruction induced by bradykinin administered via tracheal instillation. This discrepancy could be explained by small differences in the experimental protocol. Both we and Rogers *et al.* (1990) gave each animal a single dose of bradykinin, whereas Ichinose *et al.* (1990) gave increasing doses of bradykinin.

The specific leukotriene receptor antagonist, ICI 198,615, did not significantly affect the observed bradykinin-induced airflow obstruction or airway microvascular leakage, in contrast to the obvious effects of the thromboxane A_2 receptor antagonist. This finding is in agreement with Rogers *et al.* (1990) who also found that the same leukotriene receptor antagonist failed to influence the extravasation of Evans blue dye in airway tissue caused by i.v. bradykinin. In our laboratory, we have previously found that ICI 198,615, used at the same dose as in the present study, attenuates the allergen-induced exudation of plasma in the airways of guinea-pigs, further urguing that the drug is active (Lötvall *et al.*, 1993). In another study, we have observed a lack of effect by BW B70C, a 5-lipoxygenase inhibitor, (3 mg kg^{-1}, i.v.) on bradykinin-induced airflow obstruction and airway plasma exudation (Kawikova & Lötvall, unpublished observations), which further argues against any involvement of leukotrienes in bradykinin-induced airway responses.

Thromboxane versus cholinergic nerves

We have found that both cholinergic nerves and thromboxane A_2 are involved in the mechanism of bradykinin-induced airway responses. Chung *et al.* (1985) showed that a low dose of U-46619, a TxA_2-mimetic, enhanced the airway response to electrical field stimulation, but not to methacholine, thereby suggesting an increase in the prejunctional release of acetylcholine. We administered U-46619 to animals both i.v. and via the tracheal route and expected to observe an attenuation of airflow obstruction in animals pretreated with atropine. However, atropine did not have any significant effect on this response when U-46619 was given i.v., but we observed a small attenuating effect when it was administered via the trachea. The bradykinin-induced activation of peripheral cholinergic nerves may therefore, in part, be mediated via thromboxane A_2, although additional mechanisms are also likely to work in parallel. It is likely that the bradykinin-induced activation of cholinergic fibres and the release of thromboxane is due primarily to the activation of different receptors for bradykinin (Farmer *et al.*, 1989; 1991). How-

ever, further studies are required to support this hypothesis.

In animals given i.v. U-46619, atropine appeared to have a small augmenting effect on Evans blue dye extravasation in the intrapulmonary airways, but not when the thromboxane-mimetic was given via the trachea. It is possible that some variation in parasympathetic activity may influence the bronchial vasculature and thus the bronchial blood flow in response to the thromboxane-mimetic. This response may also be different when U-46619 is administered by the different routes. To our knowledge, no studies have been conducted to evaluate the effect of local or systemic thromboxane on bronchial blood flow in guinea-pigs. It is unlikely that the local release of acetylcholine affects airway plasma exudation, because the inhalation of methacholine does not produce plasma exudation in the guinea-pig (Lötvall *et al*, 1990).

We conclude that, in the guinea-pig, both cholinergic nerves and thromboxane A_2 are involved in bradykinin-induced airflow obstruction and that thromboxane A_2 is involved in bradykinin-induced plasma exudation in the intrapulmonary bronchi. In man, the mechanisms of bradykinin-induced airflow obstruction are also controlled in part via the activation of cholinergic mechanisms (Simonsson *et al.*, 1973; Fuller *et al.*, 1987). In one small study, the inhibition of cyclo-oxygenase in asthmatics had no significant effect on bradykinin-induced airway responses, but a small but significant inhibitory effect was found in a larger study (Fuller *et al.*, 1987; Polosa *et al.*, 1990). However, the exact role of thromboxane A_2 in bradykinin-induced airway plasma exudation in man remains to be investigated.

Supported by the Swedish Heart and Lung Foundation and the Swedish Medical Research Council. I.K. is supported by a special Visiting Researcher's Grant from the Swedish Heart and Lung Foundation. The authors would like to thank Dr Vaclav Spicka for valuable discussions and Anna Bergendal and Lena Bernsten for administrative assistance.

References

ABE, K., WATANABE, N., KUMAGAI, N., MOURI, T., SEKI, T. & YOSHINAGA, K. (1967). Circulating plasma kinin in patients with bronchial asthma. *Experimentia*, **23**, 626 – 627.

ARAKAWA, H., KAWIKOVA, I., LÖFDAHL, C.G., SKOOGH, B.E. & LÖTVALL, J. (1992). Bradykinin-induced airway responses in guinea pig: effects of inhibition of cyclooxygenase and thromboxane synthetase. *Eur. J. Pharmacol.*, **229**, 131 – 136.

BARNES, P.J., CHUNG, K.F. & PAGE, C.P. (1988). Inflammatory mediators and asthma. *Pharmacol.Rev.*, **40**, 49 – 84

BHOOLA, K.D., COLLIER, H.O.J., SCHACHTER, M. & SHORLEY, P.G. (1962). Actions of some peptides on bronchial muscle. *Br. J. Pharmacol. Chemother.*, **19**, 190 – 197.

CHRISTIANSEN, S.C., PROUD, D. & COCHRANE, C.G. (1987). Detection of tissue kallikrein in the bronchoalveolar lavage fluid of asthmatic subjects. *J. Clin. Invest.*, **79**, 188 – 197.

CHUNG, K.F., EVANS, T.W., GRAF, P.D. & NADEL, J.A. (1985). Modulation of cholinergic neurotransmission in canine airways by thromboxane mimetic U46619. *Eur. J. Pharmacol.*, **117**, 373 – 375.

COLLIER, H.O., HOLGATE, J.A., SCHACHTER, M. & SHORLEY, P.G. (1960). The bronchoconstrictor action of bradykinin in the guinea pig. *Br. J. Pharmacol. Chemother*, **15**, 290 – 297.

DUSSER, D.J., NADEL, J.A., SEKIZAWA, K., GRAF, P.D. & BORSON, D.B. (1988). Neutral endopeptidase and angiotensin converting enzyme inhibitors potentiate kinin-induced contraction of ferret trachea. *J. Pharmacol. Exp. Ther.*, **244**, 531 – 536.

ERJEFÄLT, I. & PERSSON, C.G.A. (1989). Inflammatory passage of plasma macromolecules into airway wall and lumen. *Pulm. Pharmacol.*, **2**, 93 – 102.

FARMER, S.G., BURCH, R.M., MEEKER, S.N. & WILKINS, D.E. (1989). Evidence for pulmonary bradykinin B3 receptor. *Mol. Pharmacol.*, **36**, 1 – 8.

FARMER, S.G., ENSOR, J.E. & BURCH, R.M. (1991). Evidence that cultured airway smooth muscle contain bradykinin B_2 and B_3 receptors. *Am. J. Respir. Cell. Mol. Biol.*, **4**, 273 – 277.

FULLER, R.W., DIXON, C.M.S., CUSS, F.M. & BARNES, P.J. (1987). Bradykinin-induced bronchoconstriction in humans: mode of action. *Am. Rev. Respir. Dis.*, **135**, 176 – 180.

HAY, J.A., DEL PRADO, M. & CHAPMAN, R.W. (1990). Activation of a novel medullary pathway elicits a vagal, cholinergic bronchoconstriction in guinea pigs. *Pulm. Pharmacol.*, **3**, 53 – 54

ICHINOSE, M., BELVISI, M. & BARNES, P.J. (1990). Bradykinin-induced bronchoconstriction in guinea pig in vivo: role of neural mechanisms. *J. Pharmacol. Exp. Ther.*, **253**, 594 – 599.

JESSUP, C.L., JESSUP, R. & WAYNE, M. (1988). ICI 192,605, a potent, selective thromboxane A_2 receptor antagonist on smooth muscle. *Br. J. Pharmacol.*, **95**, 675P.

KAUFMAN, M.P., COLERIDGE, H.M., COLERIDGE, J.C.G. & BAKER, G. (1980). Bradykinin stimulates afferent vagal C-fibers in intrapulmonary airways of dogs. *J. Appl. Physiol.*, **48**, 511 – 517.

LÖTVALL, J. ARAKAWA, H., KAWIKOVA, I., HAYES, J., LÖFDAHL, C.G. & SKOOGH, B.E. (1993). Role of eicosanoids in acute airway responses to allergen-conjugate in guinea pigs sensitised to free TMA. *Am. Rev. Respir. Dis.*, **147**, (suppl).

LÖTVALL, J., ELWOOD, W., TOKUYAMA, K., SAKAMOTO, T., BARNES, P.J. & CHUNG, K.F. (1992). A thromboxane mimetic, U-46619, produces plasma exudation in airways of the guinea pig. *J. Appl. Physiol.*, **72**, 2415 – 2419.

LÖTVALL, J.O., LEMEN, R.J., HUI, K.P., BARNES, P.J. & CHUNG, K.F. (1990). Airflow obstruction after substance P aerosol: contribution of airway pulmonary edema. *J. Appl. Physiol.*, **69**, 1473 – 1478.

LÖTVALL, J.O., TOKUYAMA, K., BARNES, P.J. & CHUNG, K.F. (1991). Bradykinin-induced airway microvascular leakage is potentiated by captopril and phosphoramidon. *Eur. J. Pharmacol.*, **200**, 221 – 217.

PIPER, J.P., COLLIER, H.O.J. & VANE, J.R. (1967). Release of catecholamines in the guinea pig by substances involved in anaphylaxis. *Nature*, **213**, 838 – 890.

POLOSA, R., PHILLIPS, G.D., LAI, C.K.W. & HOLGATE, S.T. (1990). Contribution of histamine and prostanoids to bronchoconstriction provoked by inhaled bradykinin in atopic asthma. *Allergy*, **45**, 174 – 182.

REGOLI, D. & BARABE, J. (1980). Pharmacology of bradykinin and related kinins. *Pharmacol. Rev.*, **32**, 1 – 46.

ROGERS, D.F., BOSCHETTO, P. & BARNES, P.J. (1989). Plasma exudation: correlation between Evans blue dye and radiolabeled albumin in guinea pig airways in vivo. *J. Pharmacol. Meth.*, **21**, 309 – 315.

ROGERS, D.F., DIJK, S. & BARNES, P.J. (1990). Bradykinin-induced plasma exudation in guinea-pig airways: involvement of platelet activating factor. *Br. J. Pharmacol.*, **101**, 739 – 745.

SARIA, A., LUNDBERG, J.M., SKOTFISH, G. & LEMBECK, F. (1983). Vascular protein leakage in various tissues induced by substance P, capsaicin, bradykinin, serotonin, histamine and by antigen challenge. *Naunyn-Schmied. Arch. Pharmacol.*, **324**, 212 – 218.

SARIA, A., MARTLING, C.-R., YAN, Z., THEODORSSON-NORHEIM, E., GAMSE, R. & LUNDBERG, J. M. (1988). Release of multiple tachykinins from capsaicin-sensitive sensory nerves in the lung by bradykinin, histamine, dimethylphenyl piperazinium, and vagal nerve stimulation. *Am. Rev. Respir. Dis.*, **137**, 1330 – 1335.

SHIRLEY, J.T. & CHENG, J.B. (1991). Competition of leukotrienes and ICI 198,615 for [^{3}H]LTD_4 binding sites in guinea pig lung membranes suggests the involvement of two LTD_4 receptor subtypes. *J. Pharmacol. Exp. Ther.*, **258**, 531 – 536.

SIMONSSON, B.G., SKOOGH, B.E., BERGH, N.P., ANDERSSON, R. & SVEDMYR, N. (1973). In vivo and in vitro effect of bradykinin on bronchial muscle tone in normal subjects and patients with airways obstruction. *Respiration*, **30**, 378 – 388.

(Received January 26, 1993
Revised May 17, 1993
Accepted June 4, 1993)

Br. J. Pharmacol. (1993), **110**, 665–676

An electrophysiological investigation of the properties of 5-HT_3 receptors of rabbit nodose ganglion neurones in culture

John A. Peters, [1]Hilary M. Malone & [2]Jeremy J. Lambert

Neuroscience Research Group, Department of Pharmacology and Clinical Pharmacology, Ninewells Hospital and Medical School, Dundee University, Dundee, DD1 9SY

1 The biophysical and pharmacological properties of 5-hydroxytryptamine (5-HT)-evoked currents in rabbit nodose ganglion neurones in culture have been determined by use of the whole-cell and outside-out membrane patch recording modes of the patch-clamp technique.

2 In 49% of cells investigated the bath application of 10^{-5} M 5-HT at negative holding potentials elicited an inward current. The whole-cell response to 5-HT reversed in sign ($E_{5\text{-}HT}$) at approximately -2 mV and exhibited inward rectification.

3 The influence of various ion substitutions upon $E_{5\text{-}HT}$ established that the 5-HT-evoked current is mainly mediated by a mixed Na^+, K^+ cation conductance with little or no contribution from Cl^- ions. The omission of Ca^{2+} and Mg^{2+} from the extracellular solution enhanced the amplitude of the 5-HT-induced current.

4 On isolated outside-out membrane patches, the bath application of 10^{-6} M 5-HT induced single channel currents with a chord conductance of approximately 17 pS at -70 mV and an average slope conductance of 19 pS over the range -100 to -40 mV. The 5-HT-induced single channels exhibited modest inward rectification and were reduced in frequency, but not amplitude, by the 5-HT_3 receptor antagonist metoclopromide (10^{-6} M).

5 The bath application of 5-HT (3×10^{-7}–3×10^{-5} M) to whole cells voltage clamped at -60 mV produced dose-dependent inward currents which were mimicked by 2-methyl-5-HT and 1-phenylbiguanide with equipotent molar ratios, relative to 5-HT, of 2.5 and 32 respectively.

6 Whole-cell inward currents produced by the local pressure application of 5-HT (10^{-5} M) were unaffected by 10^{-6} M methysergide, 10^{-6} M ketanserin or 10^{-6} M citalopram, but were concentration-dependently antagonized by the selective 5-HT_3 receptor antagonists tropisetron ($IC_{50} = 4.6 \times 10^{-11}$ M) ondansetron ($IC_{50} = 5.7 \times 10^{-11}$ M), and bemesetron ($IC_{50} = 3.3 \times 10^{-10}$ M). The response to 5-HT was also blocked by the non-selective antagonists metoclopramide ($IC_{50} = 1.2 \times 10^{-8}$ M), cocaine ($IC_{50} = 8.3 \times 10^{-8}$ M) and (+)-tubocurarine ($IC_{50} = 1.6 \times 10^{-7}$ M).

Keywords: 5-HT_3 receptor; nodose ganglion neurone; 5-HT_3 receptor agonists; 5-HT_3 receptor antagonists; 5-HT_3 receptor-evoked currents; 5-HT_3 receptor electrophysiology

Introduction

5-HT_3 receptor antagonists are used in the treatment of emesis induced by radiation and cytotoxic drugs in anti-cancer therapies (Sanger, 1992). Additionally, postoperative nausea and vomiting, and the emesis associated with migraine, may be reduced by these agents (Sanger, 1992). The emesis induced by some cytotoxic agents is dependent on the integrity of the vagus nerve, suggesting a role for vagal afferent fibres in this behaviour. Hence, the 5-HT_3 receptors located on vagal afferent terminals in the area postrema and the nucleus tractus solitarius (NTS), and those on peripheral terminals in the upper gut, are proposed sites of action for the antiemetic effect of these receptor antagonists. Little is known of the functional properties of these 5-HT_3 receptors, as their anatomical location makes them inaccessible to electrophysiological techniques such as whole-cell and patch-clamp recording. However, the recent use of whole-cell recording techniques on rat NTS neurones, to determine the influence of 5-HT_3 receptor agonists and antagonists upon spontaneous synaptic potentials, has allowed the pharmacological properties of the presynaptically located receptors to be investigated indirectly (Glaum *et al.*, 1992).

An alternative approach is to study the properties of 5-HT_3 receptors located on the neuronal cell body. It is well known that activation of 5-HT_3 receptors results in a depolarization of both nodose ganglion neurones and the isolated vagus nerve (Higashi & Nishi, 1982; Azami *et al.*, 1985; Round & Wallis, 1986). Furthermore, radioligand binding and autoradiographic techniques have clearly demonstrated the presence of specific 5-HT_3 receptor antagonist binding sites on both the nodose ganglion and vagus nerve (Hoyer *et al.*, 1989; Kilpatrick *et al.*, 1989; Laporte *et al.*, 1992). Hence, 5-HT_3 receptors could be synthesized in the cell body and axonally transported along the vagus nerve to their central and peripheral locations (Hoyer *et al.*, 1989). Consistent with this suggestion, in the rat, nodose ganglionectomy results in a large reduction of the number of 5-HT_3 antagonist recognition sites in the NTS (Pratt & Bowery, 1989; Pratt *et al.*, 1990; Laporte *et al.*, 1992). Additionally, a recent study employing *in situ* hybridization did not detect 5-HT_3 receptor mRNA in the medullary dorsal vagal complex (Tecott *et al.*, 1993). Hence, in the present study we have used whole-cell and patch-clamp techniques to determine some of the biophysical and pharmacological properties of the 5-HT_3 receptors of rabbit isolated nodose ganglion neurones. Some preliminary reports of this work have appeared (Peters *et al.*, 1990a; 1991b; Malone *et al.*, 1991a,b).

Methods

Cell isolation and culture

Adult male New Zealand white rabbits were anaesthetized with halothane and killed by exsanguination. The nodose ganglia were rapidly excised and enzymatically dissociated

[1] Present address: Department of Pharmacology, University of California, San Francisco, California.
[2] Author for correspondence.

into a single cell suspension essentially according to the method of Ikeda et al. (1986). In brief, each excised ganglion was immersed in Hank's balanced salt solution (Gibco), and following the removal of the connective tissue capsule, divided into 3–4 segments. The latter were transferred into 10 ml of Earl's balanced salt solution comprising (in mM): NaCl 116.0, KCl 5.0, $CaCl_2$ 1.0, $MgSO_4$ 0.5, NaH_2PO_4 1.0, $NaHCO_3$ 25.0, glucose 25.0 and HEPES 10, supplemented with trypsin (550 u), collagenase type I (7600 u) and DNase type 1 (1540 u). The solution and tissue fragments were gassed with 95% O_2/5% CO_2 and maintained at 34°C in a shaking water bath for up to 30 min. At 10 min intervals, the fragments were triturated, by use of a fire polished pasteur pipette, to aid dissociation of the tissue. Upon complete dispersal of the tissue, enzymatic digestion was inhibited by the addition of 10 ml of Hank's balanced salt solution supplemented with foetal calf serum (FCS: 10% vol/vol), 10 mM $CaCl_2$ and 5 mM HEPES. The cell suspension was centrifuged at 100 g for 5 min and the resulting pellet resuspended in growth medium comprising: Dulbecco's modified Eagle's medium (DMEM) supplemented with FCS (10% vol/vol), streptomycin (50 mg l^{-1}), penicillin (5×10^4 iu l^{-1}) and nerve growth factor (50 μg l^{-1}). Aliquots of the cell suspension (0.5 ml) were transferred into 35 mm diameter petri dishes (Nunclon), pre-coated with poly-l-lysine (5 μg cm^{-2}) and pre-filled with 2 ml of the above growth medium. Cells were incubated at 37°C in an atmosphere of 90% air/10% CO_2 at 100% relative humidity and used in electrophysiological recordings after periods of 1 to 5 days *in vitro*.

Electrophysiological recordings

Agonist-activated macroscopic- and single channel-currents were recorded from whole cells and outside-out membrane patches respectively by use of standard patch-clamp techniques (Hamill et al., 1981). In some whole-cell, and all outside-out patch recording configurations, a List L/M EPC 7 converter headstage and amplifier were employed to record agonist-evoked electrical signals. In whole-cell recordings, series resistance compensation (30 to 70%) was applied to reduce errors in the voltage-clamp. Whole-cell recordings were also conducted with an Axoclamp 2A amplifier (Axon Instruments) in discontinuous single electrode voltage-clamp mode. The switching frequency used (8–14 KHz) allowed for complete settling of the headstage voltage monitor waveform during each cycle. Calculated or recorded voltage errors of <3 mV at the peak of an agonist-induced current were regarded as acceptable. The List L/M EPC7 and Axoclamp 2A recording systems yielded qualitatively similar results. Patch electrodes were fabricated from borosilicate glass capillary tubing (Corning type 7052; Garner Glass Company, Claremont, CA), and when filled with the solutions detailed below had measured resistances of 2–5 MΩ and 10–15 MΩ when intended for whole-cell and single channel recordings respectively. In the majority of experiments, cells were continually superfused (3–5 ml min^{-1}) with an extracellular recording medium (E_1) comprising (in mM): NaCl 140, KCl 2.8, $CaCl_2$ 1.0, $MgCl_2$ 2.0, HEPES 10.0, pH 7.2. In experiments designed to evaluate the ionic basis of agonist-induced responses, the extracellular concentration of Cl^- was reduced to 8.8 mM by the total replacement of NaCl with Na isethionate. A reduction in the extracellular concentration of Na was accomplished by the partial replacement of NaCl with an osmotically equivalent amount of sucrose. Patch electrodes were generally filled with a solution (I_1) containing (in mM): CsCl 140, $MgCl_2$ 2.0, HEPES 10, $CaCl_2$ 0.1, EGTA 1.1 (free $[Ca^{2+}] = 10^{-8}$ M at pH 7.2). Caesium was chosen as the predominant internal cation in order to suppress membrane potassium conductances. Occasionally, KCl alone (solution I_2), or a mixture of KCl and tetraethylammonium chloride replaced CsCl in the patch pipette solution. The uses of these modified internal salines are specified in the Results. All external and internal salines were titrated to pH 7.2 with NaOH; Na ions so introduced were included in the calculation of sodium ion concentrations.

Changes in reference electrode potential that could occur during the superfusion of cells with modified recording media were minimized by the use of a salt bridge, containing 3 M KCl in 4% (w/v) agar, which connected the recording chamber to a reservoir containing an Ag/AgCl electrode immersed in standard extracellular medium. Liquid junction potentials arising at the tip of the patch pipette prior to 'giga-seal' formation (Barry & Lynch, 1991) were estimated as previously described (Peters et al., 1989) and taken into account when setting the holding potential in voltage-clamp experiments. At least 20 min were allowed between the establishment of a whole-cell recording and the commencement of an experimental series. During this time, diffusional exchange of small ions between the pipette and cell interior would be complete (Pusch & Neher, 1988) and the Donnan potential arising from poorly mobile cytoplasmic anions would have fallen towards zero millivolts (Barry & Lynch, 1991). All recordings were performed at ambient temperature (18–24°C) and, unless stated otherwise, at a holding potential of −60 mV.

In most experiments, 5-HT was locally applied to cells either by pressure ejection (1.4×10^5 Pa, 5–100 ms, 0.1 Hz) from modified patch pipettes filled with 5-HT (10^{-5} M) in recording medium, but in the case of ion substitution experiments, 5-HT was applied by ionophoresis. Ionophoretic pipettes contained 20 mM 5-HT dissolved in twice distilled deionized water (pH 3.5–4.0) and had resistances in the range 40–80 MΩ. A World Precision Instruments Intra 767 electrometer was employed to provide ejection and retaining currents to the pipette. In experiments where the potencies of agonists was compared, compounds were applied under gravity feed from a reservoir coupled by polyethylene tubing to a pipe of approximately 1 mm diameter placed within 2 mm of the neurone under study. The same system was employed to apply 5-HT to excised outside-out membrane patches. All antagonist compounds were applied by the superfusion system.

Data analysis

Whole-cell and single channel currents recorded from outside-out membrane-patches were low-pass filtered at cut-off frequencies of 0.5 and 1.0 KHz (Bessel characteristic) respectively and recorded onto tape using a Racal store 4DS FM tape recorder. The former were analysed and displayed by computer programme as previously described (Peters et al., 1989), or were replayed onto a chart recorder and inspected by eye. Single channel current amplitudes were measured on a Tektronix 5110 oscilloscope equipped with a 5D10 waveform digitizer, or were analysed by the procedure described by Hales and Lambert (1991). In the latter case, the mean single channel current amplitude was determined from the peak of a single Gaussian function fitted to an all points current amplitude histogram. The manual and automated procedures gave identical estimates of channel current amplitude. The IC_{50} values of antagonists acting against whole-cell currents evoked by pressure applied 5-HT were determined from full log concentration-effect relationships. Each of these was fitted iteratively with a sigmoidal function, by use of Fig P version 6 software (Biosoft, Cambridge), to obtain the IC_{50} and slope factor. All quantitative data are expressed as the arithmetic mean ± the standard error of the mean.

Drugs used

All cell culture reagents and antibiotics were obtained from GIBCO. The drugs used in electrophysiological recordings were: acetylcholine bromide (ACh), cocaine hydrochloride, γ-aminobutyric acid (GABA), 5-hydroxytryptamine creatinine sulphate complex (5-HT), metoclopramide hydrochloride

and (+)-tubocurarine chloride (all Sigma), 2-methyl-5-HT hydrochloride and ondansetron hydrochloride (Glaxo), methysergide hydrogen maleate and tropisetron (ICS 205-930) (Sandoz), 1-phenylbiguanide and bemesetron (MDL-72222) (Research Biochemicals Incorporated), ketanserine tartrate (Janssen) and citalopram hydrogen bromide (Lundbeck). With the exception of tropisetron and bemesetron, which were initially dissolved in a minimal volume of 1 N HCl, all drugs were prepared as concentrates in twice distilled deionised water.

Results

Rabbit nodose ganglion neurones – general properties

Current-clamp recordings from rabbit nodose ganglion neurones were made by utilizing a KCl-based pipette saline (I_2) and a NaCl-based bath saline (E_1; see Methods). Under these recording conditions the mean resting membrane potential was -55.7 ± 1.5 mV ($n = 12$). To estimate the cell input resistance the amplitude of the anelectrotonic potential elicited by injecting current (-0.05 to -0.1 nA, 200 ms, 1.0 Hz) was measured. The cell input resistance determined in this manner was 338.3 ± 55.6 MΩ ($n = 12$). Depolarizing current pulses elicited action potentials which overshot 0 mV by $+53 \pm 2.5$ mV ($n = 4$). Previous studies have demonstrated that rabbit nodose ganglion cells express $GABA_A$, nicotinic and 5-HT$_3$ receptors (Wallis *et al.*, 1982). Under voltage-clamp, at holding potential (V_h) of -60 mV, the bath application of GABA (10^{-5} M) produced an inward current on all cells tested ($n = 50$). On the same population of cells 64% responded to ACh (10^{-5} M) and 49% responded to 5-HT (10^{-5} M) with an inward current. On responsive cells, the inward current induced by these agonists varied in amplitude across cells from < -50 pA to > 10 nA.

Properties and ionic basis of the 5-HT-evoked response

Under constant current recording conditions, the brief application of 5-HT (10^{-5} M, 1.4×10^5 Pa, 10–30 ms) to sensitive cells, induced a rapid membrane depolarization and an associated fall of the cell input resistance. The depolarization was sufficient to evoke an action potential discharge. When these cells were voltage-clamped at their resting potential, identical applications of 5-HT induced a transient inward current.

For the KCl based pipette saline (I_2) and the NaCl based bath saline (E_1) detailed in the Methods, the amplitude of the 5-HT-induced inward current decreased with membrane depolarization and reversed in sign ($E_{5\text{-HT}}$) at -1.6 ± 1.3 mV ($n = 5$). The complete substitution of KCl by CsCl in the pipette saline had little influence on $E_{5\text{-HT}}$ (-2.4 ± 0.3 mV, $n = 32$) suggesting K^+ and Cs^+ to be equipermeant. With either K^+ or Cs^+ as the predominant internal cation, inward rectification of the macroscopic current response was apparent when response amplitude was plotted as a function of holding potential (Figure 1). The degree of inward rectification was quantified by calculating the chord conductance at holding potentials of -80 and $+40$ mV. At the latter potential, chord conductance was reduced to $61.8 \pm 4.1\%$ ($n = 6$) and $55.8 \pm 5.9\%$ ($n = 5$) of the value observed at -80 mV with Cs^+ or K^+ respectively as the predominant internal cation. Reducing the internal concentration of K^+ from 140 mM to 20 mM, by partial substitution of KCl with tetraethylammonium chloride, produced a positive shift in $E_{5\text{-HT}}$ to 32.5 ± 3.3 mV ($n = 3$). A reduction

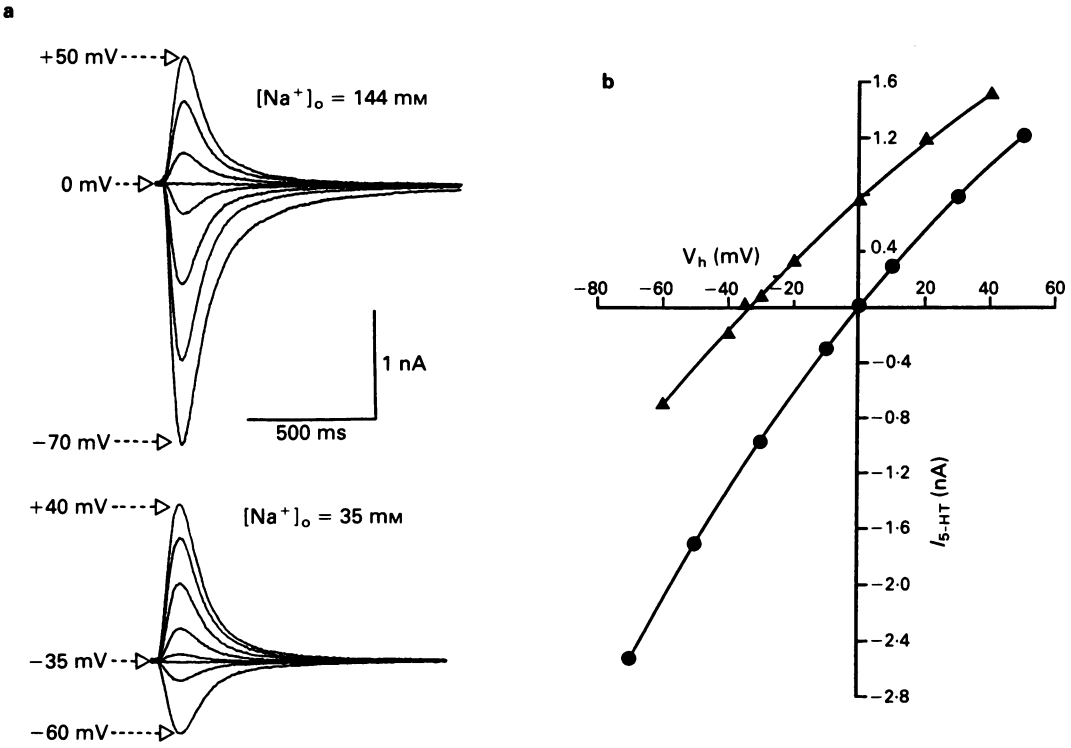

Figure 1 5-Hydroxytryptamine (5-HT)-induced currents are associated with an increase in membrane conductance to Na ions. (a) The traces illustrate transmembrane currents in response to ionophoretically applied 5-HT (0.8 nC, 0.1 Hz) recorded at holding potentials (V_h) ranging between -70 and $+50$ mV. The traces illustrated were obtained in extracellular solution containing 144 mM Na^+ (upper panel) and in a solution in which extracellular Na^+ $[Na^+]_o$ was reduced to 35 mM by the partial replacement of NaCl with sucrose (lower panel). Each trace is the computer-generated average of 4 responses to ionophoretically applied 5-HT. Leakage currents have been substracted. The neurone was dialysed with a Cs^+-based pipette solution (I_1, see Methods). (b) Graphical depiction of the data shown in (a) illustrating the relationship between holding potential and 5-HT-evoked current amplitude with $[Na^+]_o$ equal to 144 mM (●) and 35 mM (▲). Note that the reduction in $[Na^+]_o$ produces a large (35 mV) hyperpolarizing shift in the reversal potential ($E_{5\text{-HT}}$) of the 5-HT-evoked current. Curves were fitted to the data points by eye.

of the external concentration of NaCl by iso-osmotic replacement with sucrose, to effect a reduction of the Na^+ concentration to 35 mM, resulted in a negative shift of $E_{5\text{-HT}}$ to -33.7 ± 1.6 mV ($n = 3$; Figure 1). By contrast, the replacement of extracellular Cl^- alone by isethionate, produced a hyperpolarizing shift in $E_{5\text{-HT}}$ of only 1 mV, to -3.2 ± 1.1 mV ($n = 3$). Collectively these observations suggest that the current evoked by 5-HT is mainly mediated by a mixed Na^+, K^+ cation conductance with little or no contribution from Cl^- ions. Assuming the response to be mediated solely by Na^+ and K^+, and employing the value of $E_{5\text{-HT}}$ obtained with salines E_1 and I_2 (i.e. -2.4 mV), the ratio of Na and K permeabilities (P_{Na}/P_K) was calculated from the Golman-Hodgkin-Katz voltage equation (e.g. Lambert *et al.*, 1989) to be 0.9 (cf. Higashi & Nishi, 1982).

In N1E-115 and N18 neuroblastoma cells the divalent cations Mg^{2+} and Ca^{2+} inhibit 5-HT_3-mediated currents in a voltage-independent manner (Peters *et al.*, 1988; Yang, 1990). Consistent with these observations, in the present experiments the omission of Ca^{2+} and Mg^{2+} from the extracellular solution enhanced the amplitude of the 5-HT-induced current recorded at -60 mV to $249.0 \pm 18.7\%$ ($n = 3$) of control (Figure 2). Potentiation of the 5-HT-evoked current was observed at all holding potentials examined (-80 to $+40$ mV) and occurred in the absence of any detectable shift in $E_{5\text{-HT}}$.

The properties of 5-HT-activated single channels

On 7 of the 16 outside-out membrane patches challenged, all of which were excised from 5-HT sensitive whole-cells, the application of 10^{-6} M 5-HT induced the appearance of single channel events (Figure 3). The single channel currents had a mean amplitude of -1.12 ± 0.03 pA ($n = 7$) at a holding potential of -70 mV. 5-HT-induced whole-cell currents (recorded using pipette and bath salines identical to those employed in experiments upon excised patches) had a reversal potential of approximately -2 mV. Utilizing this value, the chord conductance of the 5-HT-activated channel was calculated to be 16.5 ± 0.47 pS ($n = 7$). A slightly higher value of 19.3 ± 0.6 pS ($n = 3$) was derived from the slope of the relationship between single channel amplitude and holding potential over the range -40 to -100 mV (Figure 3). The small difference between the values of slope and chord conductance is most probably a consequence of inward rectification of the single channel current which was noted to occur at holding potentials positive to -40 mV (see Figure 3).

Metoclopramide is a reversible antagonist of the rabbit nodose ganglion 5-HT_3 receptor (see below). The bath application of 10^{-6} M metoclopramide greatly reduced the frequency of 5-HT-activated single channels, but had no influence on their amplitude (Figure 4). The effect on frequency was reversed upon washout of the antagonist. This observation suggests that the single channel events are a consequence of 5-HT_3 receptor activation.

The agonist actions of 5-HT, 2-methyl 5-HT and 1-phenylbiguanide

5-HT (3×10^{-7}–3×10^{-5} M) applied for approximately 30 s by superfusion elicited transient, concentration-dependent,

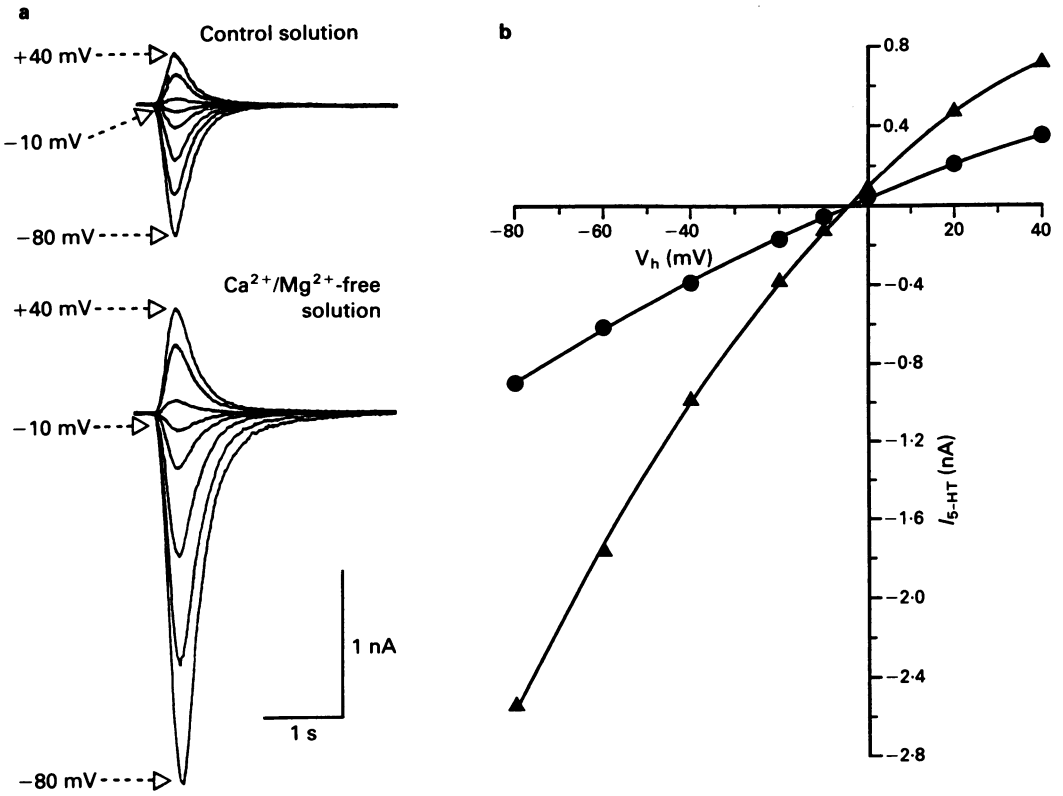

Figure 2 Extracellular Ca^{2+} and Mg^{2+} depress the current response to 5-hydroxytryptamine (5-HT). (a) Superimposed traces illustrating membrane currents recorded at holding potentials (V_h) ranging between -80 and $+40$ mV in response to ionophoretically applied 5-HT. Both sets of currents were obtained from the same nodose ganglion neurone in the presence of 1 mM Ca^{2+} and 2 mM Mg^{2+} (upper traces) and subsequently in the nominal absence of divalent cations (lower traces). Note that the 5-HT-evoked current recorded at all holding potentials is potentiated in the divalent cation deficient solution. Each trace is the computer-generated average of 4 responses to ionophoretically applied 5-HT (0.6 nC, 0.1 Hz). Leakage currents have been subtracted. The neurone was dialysed with a Cs^+-based pipette solution I_1 (see Methods). (b) Graph illustrating the relationship between holding potential and 5-HT-induced amplitude in the presence (●) and absence (▲) of divalent cations. Note that the reversal potential ($E_{5\text{-HT}}$) of the current response to 5-HT (Ca – 4 mV) is unchanged in the divalent cation-free solution. Curves were fitted to the data points by eye.

inward current responses on whole-cells (Figure 5a). During the construction of concentration-effect relationships, sensitivity to 5-HT remained constant as demonstrated by the reproducibility of inward current responses to a fixed, submaximal, concentration (3 μM) of 5-HT (Figure 5b). The lowest concentration of 5-HT necessary to evoke a detectable current was estimated to be 3×10^{-7} M. A maximally effective concentration of 5-HT could not be reliably determined because of unsatisfactory control of the membrane potential during large agonist-induced responses. Responses elicited by concentrations of 5-HT greater than 3×10^{-7} M displayed densensitization, the rate of onset of which increased in a dose-dependent manner (see Figure 5a). The interval (approximately 150 s) between successive applications of the agonist was sufficient to allow full recovery from desensitization to occur. The 5-HT$_3$ receptor agonists 2-methyl-5-HT and 1-phenylbiguanide mimicked the response to 5-HT with potencies lower than that of 5-HT itself. In the experiment depicted in Figure 5a,b, agonists were applied in the sequence; 5-HT, 1-phenylbiguanide, 2-methyl-5-HT, with only one concentration of each agonist being applied in each of five successive sequences. This protocol was adopted to minimize the impact of any undetected shift in agonist sensitivity upon relative potency estimates. As the inability to determine the maximal inward current response to agonists precluded the calculation of EC_{50} values, the potencies of

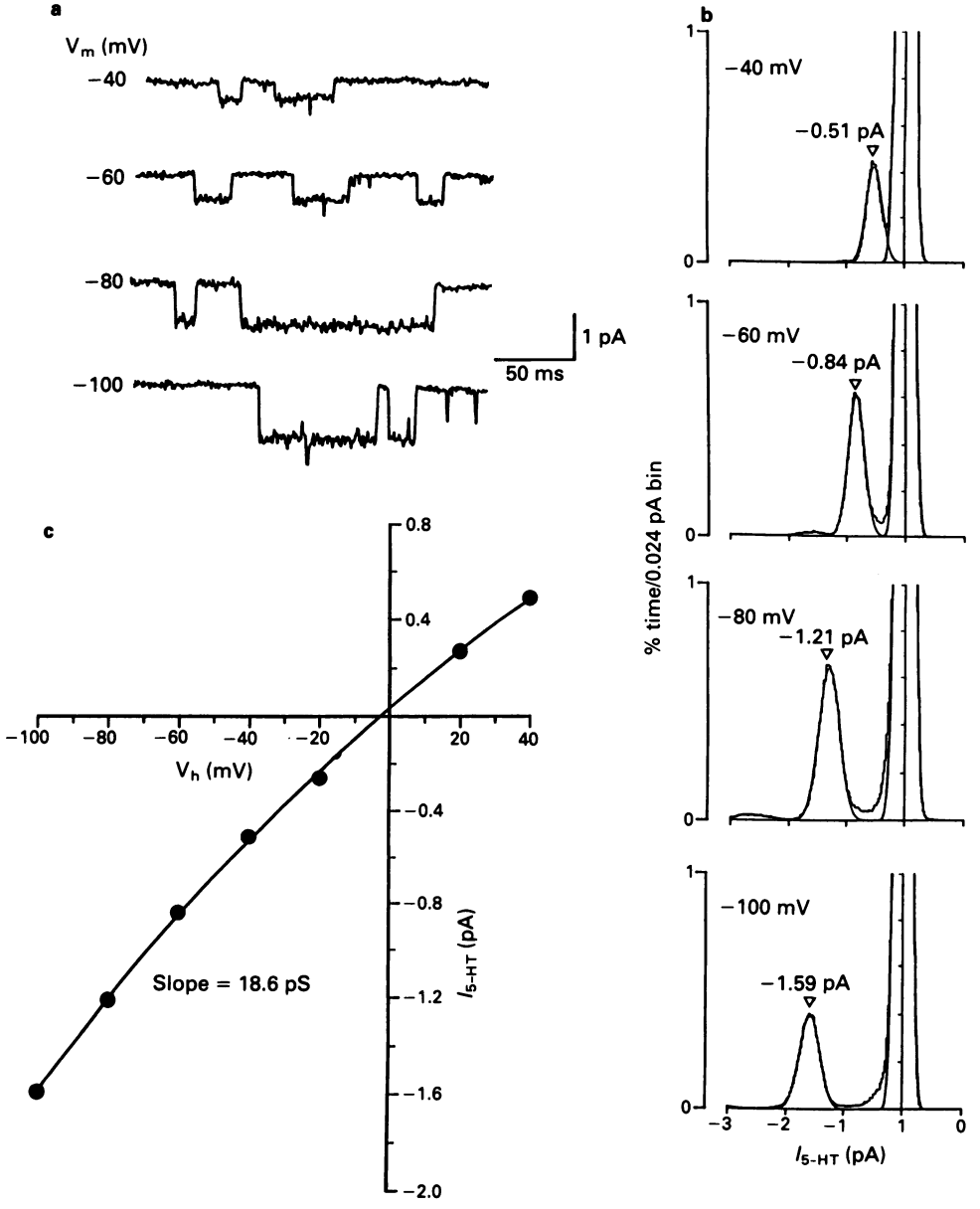

Figure 3 The conductance of 5-hydroxytryptamine (5-HT)-induced single channel currents. (a) The bath application of 5-HT (10^{-6} M) to an isolated outside-out membrane patch excised from a rabbit nodose ganglion neurone induces the appearance of single channel currents. The amplitude of the 5-HT-induced single channels increases with hyperpolarization ($V_h = -40$ to -100 mV) of the membrane patch. (b) 'All points' amplitude histograms constructed at the holding potential indicated ($V_h = -40$ to -100 mV) for a 30–60 s continuous recording, brief extracts of which are shown in (a). At each holding potential, the truncated distribution which occurs around 0 pA represents the baseline 'noise'. The single channel amplitude was determined by simultaneously fitting 2 Gaussian distributions (one to the single channel distribution and one to the baseline noise). The channel amplitude thus obtained is indicated at each holding potential by the inverted triangle (see Hales & Lambert, 1991). (c) The amplitude of the 5-HT-induced single channel current (determined as in (b)) as a function of the holding potential (V_h). The illustrated line is fitted by eye. The slope of this relationship (between -100 and -40 mV) gives a single channel conductance of 18.6 pS for this membrane patch. The currents illustrated in (a) are low pass filtered (Bessel characteristic) at 1.0 KHz. The 'all points' histograms illustrated in (b) were derived from records similarly low pass filtered and digitised at 50 μS per point.

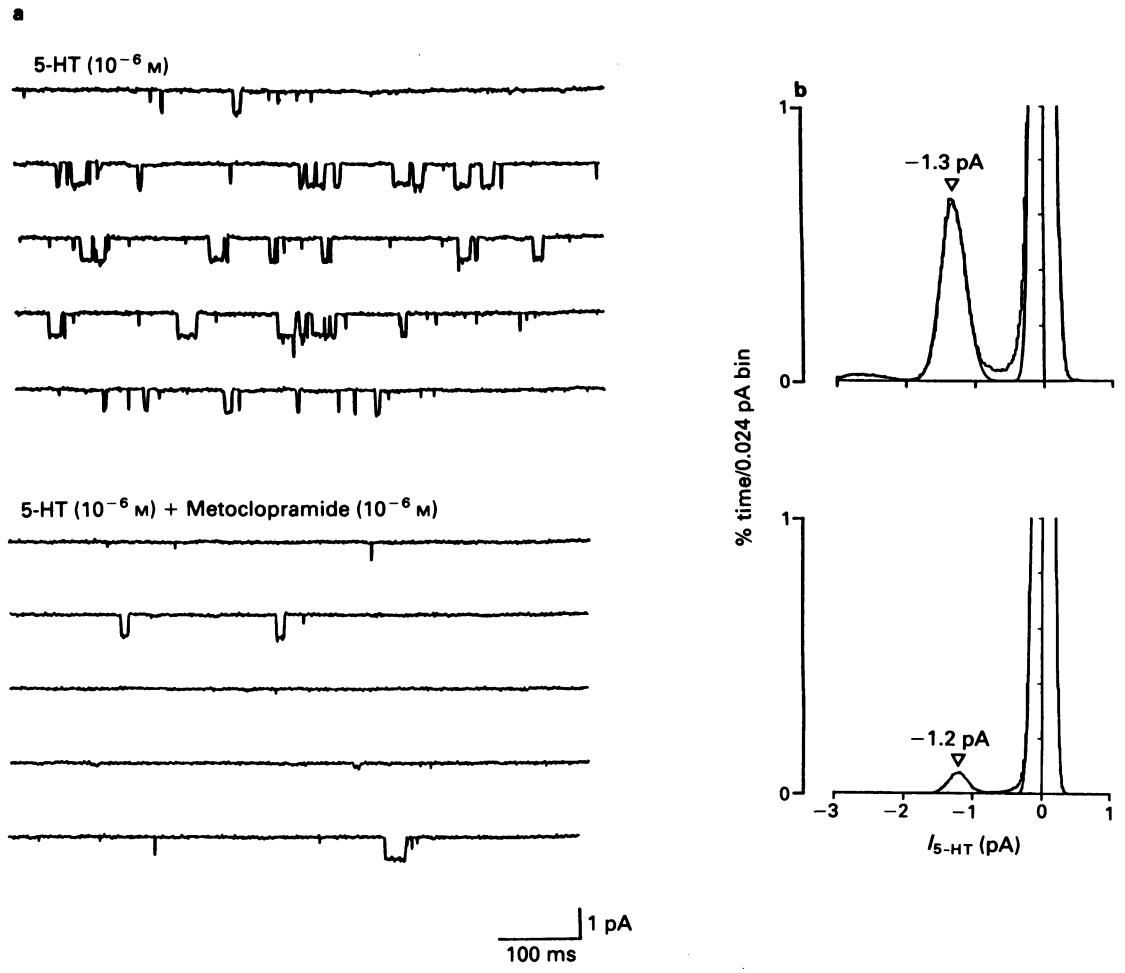

Figure 4 Antagonism of 5-hydroxytryptamine (5-HT)-induced single channel currents by metoclopramide. (a) The upper set of traces illustrate single channel currents activated by the bath application of 10^{-6} M 5-HT to an outside-out membrane patch voltage-clamped at a holding potential of − 80 mV. The lower set of traces is taken from the same membrane patch subsequently bathed in 10^{-6} M 5-HT and 10^{-6} M metoclopramide. Note, from the visual inspection of these records that metoclopramide appears to have reduced the frequency of single channel events, but had little or no effect on the single channel amplitude. (b) 'All points' amplitude histograms constructed for 30–60 s records taken from this membrane patch for 5-HT (10^{-6} M) and 5-HT (10^{-6} M) in the presence of metoclopramide (10^{-6} M). The histograms are fitted by two Gaussian distributions (baseline noise and the single channel current) which reveal that the amplitude of the 5-HT-induced current (− 1.3 pA) is little influenced by the metoclopramide (− 1.2 pA). By contrast, the frequency of open events is clearly reduced by the metoclopramide. The effect of metoclopramide was reversible upon washout (not shown). The currents illustrated in (a) are low pass filtered (Bessel characteristic) at 1.0 KHz. The 'all points' histograms illustrated in (b) were derived from records similarly low pass filtered and digitized at 50 μS per point. Details of the Gaussian fitting are given in Hales & Lambert, 1991.

2-methyl-5-HT and 1-phenylbiguanide, relative to that of 5-HT, were assessed by interpolating from their concentration-effect relationships doses that produced an inward current response equivalent to that elicited by 3×10^{-6} M 5-HT (Figure 5b). The equipotent molar ratios thus determined were 2.5 ± 0.4 ($n = 3$) and 31.8 ± 1.2 ($n = 3$) for 2-methyl-5-HT and 1-phenylbiguanide respectively.

Methysergide, ketanserin and citalopram

The bath application of methysergide; a mixed '5-HT_1-like' and 5-HT_2 receptor antagonist, had little effect on the 5-HT-evoked responses. Inward currents elicited by the local pressure application of 5-HT were reduced by $4 \pm 1\%$ of control ($n = 6$) in the presence of 10^{-6} M methysergide. Similarly, the 5-HT_2 receptor antagonist ketanserin (10^{-6} M) produced only a $5 \pm 1\%$ reduction of the control response to 5-HT ($n = 7$). The bath application of citalopram (10^{-8}–10^{-6} M), a selective 5-HT uptake inhibitor (Pawlowski *et al.*, 1981), had no effect upon the inward current produced by the local pressure application of 5-HT. For example, the 5-HT current in the presence of 10^{-6} M citalopram was $100 \pm 2\%$ of control ($n = 3$).

Ondansetron

Ondansetron is a selective 5-HT_3 receptor antagonist (Butler *et al.*, 1988). Preliminary experiments demonstrated that 10^{-9} M ondansetron completely inhibited the 5-HT-induced current. The antagonist action of ondansetron was slowly reversed upon washout (Figure 6a). The time to 50% recovery from block was approximately 16 and 11 min on the 2 cells in which full recovery could be demonstrated. Hence, the concentration-effect relationship (10^{-11}–10^{-9} M) for this antagonist was performed cumulatively, allowing at least 5 min equilibration with each antagonist concentration tested (Figure 6a). From such studies, the IC_{50} value determined for ondansetron was $57 \pm 5 \times 10^{-12}$ M with a slope factor of 1.06 ± 0.16 (Figure 7b). Concentration-response curves to 5-HT (3×10^{-7}–10^{-3} M) were constructed in the presence and absence of 10^{-10} M ondansetron (Figure 6b,c). Unfortunately, in these experiments the maximum response to 5-HT could not be determined as the large agonist-evoked current (> 10 nA) compromised the fidelity of the voltage-clamp. However, the non-parallel displacement of this limited dose-response curve suggests, at least superficially, a non-competitive action of ondansetron.

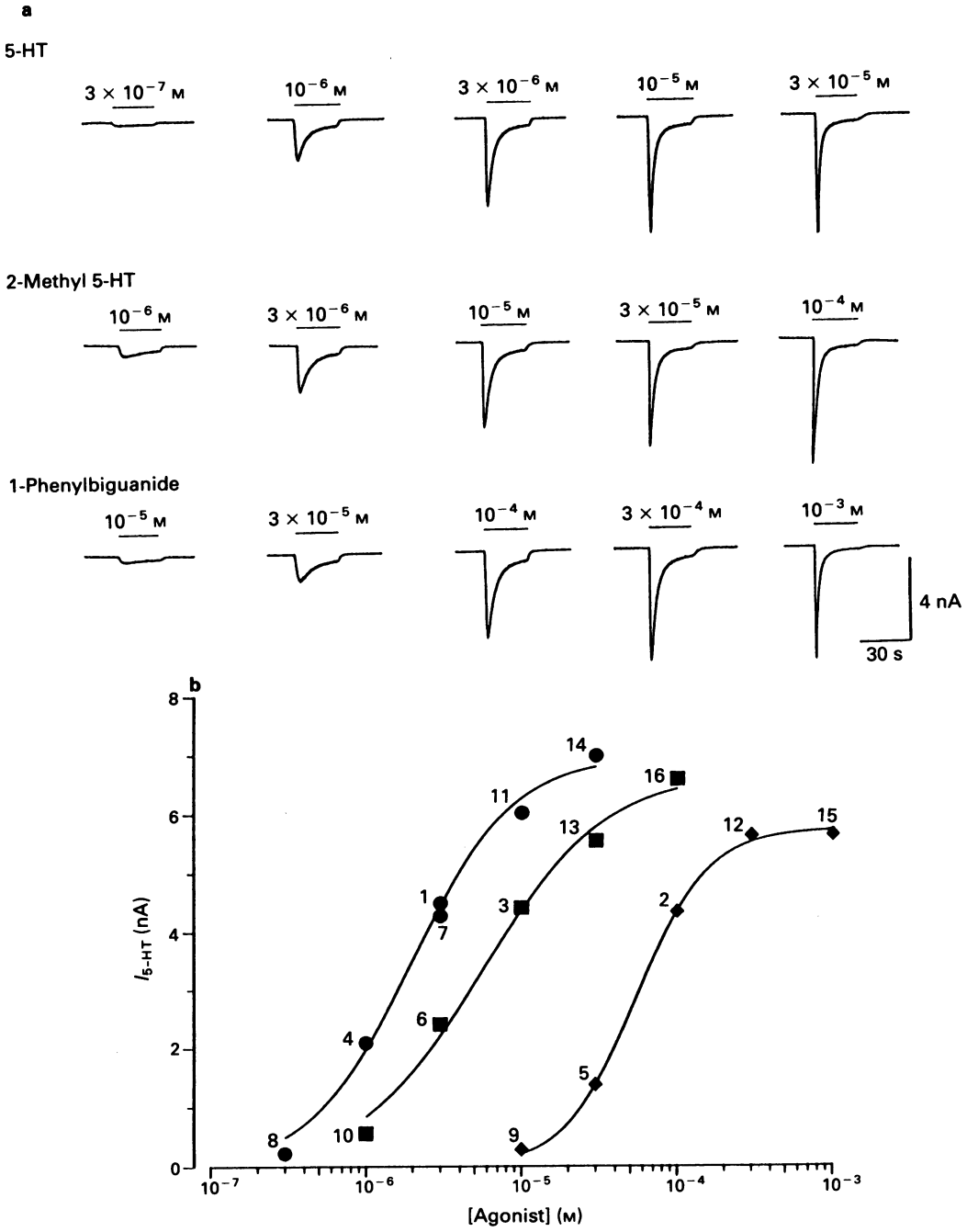

Figure 5 A comparison of the whole cell currents activated by 5-hydroxytryptamine (5-HT), 2-methyl-5-HT and 1-phenylbiguanide. (a) Inward currents activated by the bath application of 5-HT (3×10^{-7} M–3×10^{-5} M), 2-methyl-5-HT (10^{-6} M–10^{-4} M) and 1-phenylbiguanide (10^{-5} M–10^{-3} M) recorded from the same rabbit nodose ganglion neurone voltage-clamped at − 60 mV are illustrated. For all agonists, the inward current was concentration-dependent and exhibited desensitization. The current induced by 1-phenylbiguanide appeared to reach a true maximum, which was less than the current produced by the maximal concentration of 5-HT (3×10^{-5} M) or 2-methyl-5-HT (10^{-4} M) tested. The maximum current produced by the latter two agonists could not be determined because of the unsatisfactory control of the membrane potential during large agonist-induced responses. (b) The relationship between the concentration of bath applied 5-HT (●), 2-methyl 5-HT (■) and 1-phenylbiguanide (◆) plotted on the x-axis (log scale) and the inward current produced (y-axis). Numbers adjacent to symbols indicate the order in which the various concentrations of agonists were applied to the cell. The lines to the data points were fitted by eye. All recordings were low pass filtered at 500 Hz.

Tropisetron and bemesetron

The 5-HT-induced current was completely inhibited by 10^{-9} M tropisetron and 10^{-8} M bemesetron. As with ondansetron, the inhibitory actions of these antagonists were slowly reversed upon washout (Figure 7a). Hence, the concentration-effect relationships for tropisetron (10^{-11} M–10^{-9} M) and bemesetron (10^{-10}–10^{-8} M) were determined using cumulative applications of the antagonists (Figure 7a). From these studies the IC_{50} values and slope factors for tropisetron and bemesetron were $46 \pm 4.4 \times 10^{-12}$ M; 1.05 ± 0.1 and $328 \pm 24.7 \times 10^{-12}$ M; 1.12 ± 0.12 respectively (Figure 7b).

Metoclopramide, cocaine and (+)-tubocurarine

Metoclopramide, cocaine and (+)-tubocurarine are non-selective 5-HT$_3$ receptor antagonists (Fozard & Mobarok Ali, 1978; Higashi & Nishi, 1982; Yakel & Jackson, 1988; Fozard,

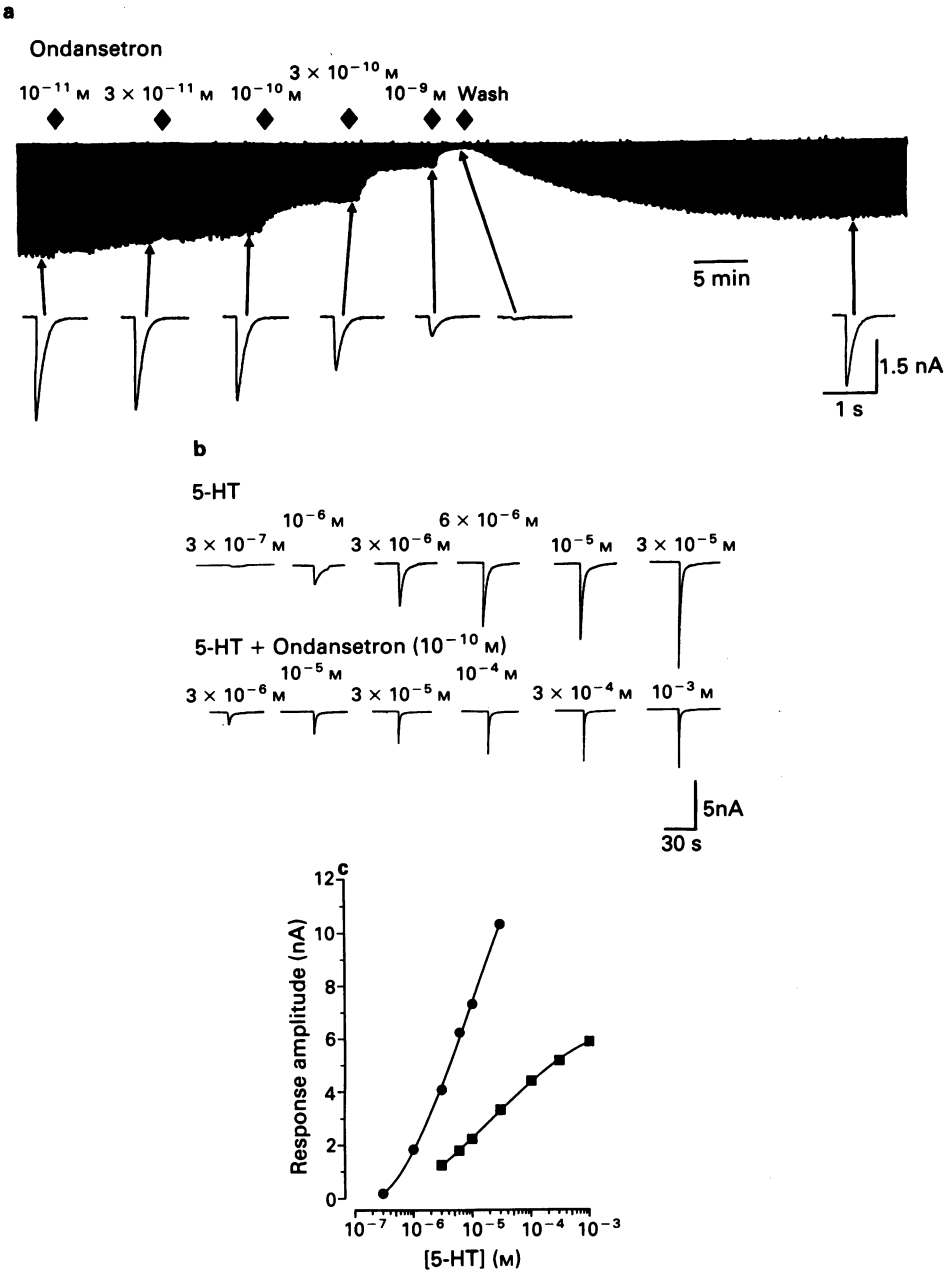

Figure 6 Inhibition of the 5-hydroxytryptamine (5-HT)-induced currents by ondansetron. (a) Ondansetron (10^{-11} M–10^{-9} M) produced a dose-dependent inhibition of the inward current evoked by the local pressure application of 5-HT (10^{-5} M; 1.4×10^5 Pa; 20 ms; 0.1 Hz). The upper trace is shown on a compressed time scale to illustrate the onset of antagonism and the relatively slow recovery from blockade by ondansetron of the 5-HT-induced inward current. Hence, individual 5-HT-induced currents cannot be discerned. In the lower trace individual 5-HT-induced currents are shown on an expanded time scale at the time during the experiment indicated by the arrows. (b) Whole-cell currents produced by the bath application of 5-HT (3×10^{-7} M–10^{-3} M) in the absence and presence of 10^{-10} M ondansetron. (c) The relationship between the concentration of bath applied 5-HT and whole-cell current amplitude in the absence (●) and the presence (■) of ondansetron (10^{-10} M). Although, the maximum current to 5-HT could not be determined due to large (> 10 nA) agonist-induced currents which compromised the fidelity of the voltage-clamp, inspection of this figure clearly illustrates that ondansetron produced a non-parallel dextral shift of the 5-HT dose-response curve. All currents illustrated were recorded from rabbit nodose ganglion neurones voltage clamped at – 60 mV. All recordings were low pass filtered at 500 Hz.

1989; Peters *et al.*, 1990b). Preliminary experiments established that the 5-HT-induced inward current was antagonized to < 10% of control by 3×10^{-7} M metoclopramide, 10^{-6} M cocaine or 3×10^{-6} M (+)-tubocurarine. Unlike blockade by ondansetron, tropisetron and bemesetron, the inhibitory effects of these antagonists readily reversed upon washout (Figure 7a). Therefore, the concentration-effect relationships for these compounds were constructed against 5-HT responses which had fully recovered from inhibition (by washout of the previous dose) before subsequent drug application. From these studies the IC_{50} values and slope factors were: metoclopramide $11.6 \pm 0.96 \times 10^{-9}$ M; 1.18 ± 0.1; cocaine $83.4 \pm 7.1 \times 10^{-9}$ M; 1.12 ± 0.1 and for (+)-tubocurarine $156 \pm 13.6 \times 10^{-9}$ M; 1.07 ± 0.1 respectively (Figure 7b).

Discussion

Dissociated rabbit nodose ganglion neurones maintained in cell culture had a mean resting potential of – 56 mV, a value which agrees well with that determined in intact ganglia *in*

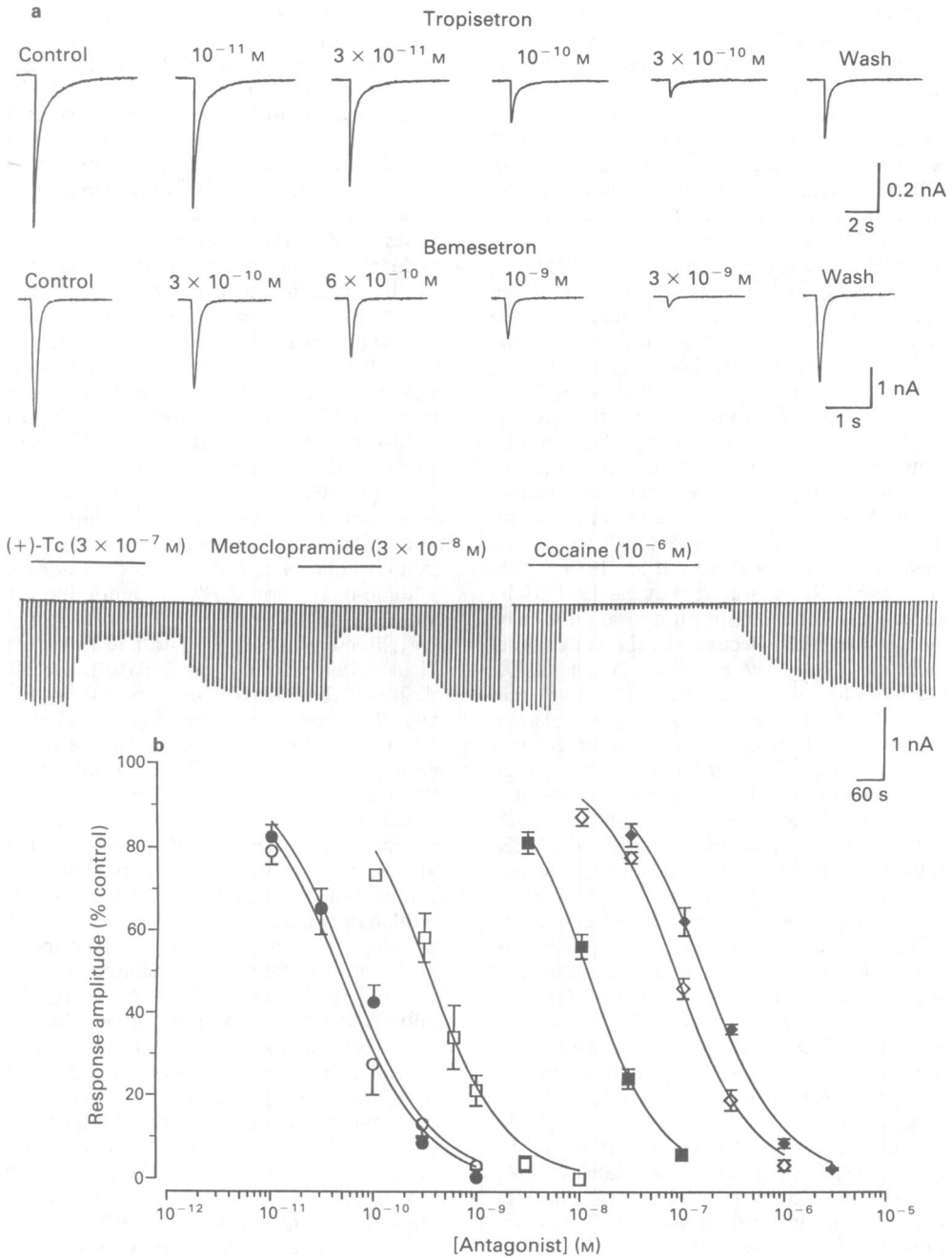

Figure 7 A comparison of the 5-hydroxytryptamine (5-HT) antagonist actions of ondansetron, tropisetron, bemestron, (+)-tubocurarine, metoclopramide and cocaine. (a) The inward current produced by locally applied 5-HT (10^{-5} M; 1.4×10^5 Pa; 20–40 mS; 0.1 Hz) is dose-dependently inhibited by the bath application of tropisetron (upper traces) and bemesetron (lower traces). The antagonism is only partially reversed by washout for 30 min. By contrast, the antagonist actions of (+)-tubocurarine ((+)-Tc, 3×10^{-7} M), metoclopramide (3×10^{-8} M) and cocaine (10^{-6} M) are well reversed by washout. Records illustrated for (+)-tubocurarine, metoclopramide and cocaine are taken from the same neurone. (b) The concentration-dependent inhibition of 5-HT-induced currents by tropisetron (○), ondansetron (●), bemesetron (□), metoclopramide (■), (+)-tubocurarine (◆) and cocaine (◇). The relationship between the concentration of bath applied antagonist (log scale; x axis) is plotted against the inhibition of the 5-HT-induced inward current (expressed as a percentage of control; y axis). Each point is the mean ± s.e.mean (vertical lines) of 3 to 11 observations. The lines fitting the data points were determined as described in the Methods. All currents illustrated were low pass filtered at 500 Hz and were recorded from cells voltage-clamped at − 60 mV.

vitro (Stansfeld & Wallis, 1985). However, the input resistance of 340 MΩ shown here is substantially greater than that of 22–34 MΩ previously found in intracellular recordings performed on the whole ganglion (Stansfeld & Wallis, 1985). It is probable that intracellular electrodes introduce a 'shunt' conductance at the site of impalement. This, together with morphological differences between dissociated neurones and those within intact ganglia, seem likely to account for the higher input resistance obtained here.

In the present study, all cells tested responded to GABA, 49% to 5-HT and 64% to ACh. Previous studies utilizing rabbit nodose ganglia *in vitro* have shown that most type A neurones respond to GABA, but are unaffected by either 5-HT or nicotinic cholinoceptor agonists (Higashi *et al.*, 1982; Stansfeld & Wallis, 1984; 1985). By contrast, of the type C cell population, 70–80% respond to GABA, 80–90% to 5-HT and 33–70% to nicotinic agonists (Higashi *et al.*, 1982; Stansfeld & Wallis, 1984). In this study, no attempt was made to categorize the neuronal cell type, either by electrophysiological or anatomical criteria. However, the dissociation and cell culture procedure employed here for the rabbit, results in the survival and maintenance of mainly

C-type neuronal cell bodies of the rat nodose ganglion (Ikeda *et al.*, 1986). The responsiveness of many neurones to 5-HT and ACh is consistent with the cultures containing a substantial population of type C cells.

In a previous voltage-clamp study of the response to 5-HT in rabbit nodose ganglion neurones, Higashi and Nishi (1982) demonstrated the current to be carried predominantly by Na and K ions. Qualitatively similar results were obtained in the present investigation, and the ratio of Na and K permeabilities (P_{Na}/P_K) was calculated to be 0.9. Most voltage-clamp studies of 5-HT_3 receptor populations indicate a P_{Na}/P_K ratio close to unity, and inward rectification of the macroscopic current response, as described here, is often observed (Lambert *et al.*, 1989; Yakel *et al.*, 1990; Yang, 1990; see Peters *et al.*, 1992 for further references). The nominal absence of Ca^{2+} and Mg^{2+} from the extracellular medium greatly potentiated the amplitude of the current response to ionophoretically applied 5-HT. These results confirm a previous finding of enhanced responsiveness to 5-HT in the rabbit nodose ganglion in the absence of divalent cations (Stansfeld & Wallis, 1984) and agree with several other studies which have shown Ca^{2+} and Mg^{2+} to depress 5-HT_3 receptor-mediated responses (Peters *et al.*, 1988; Yang, 1990; Yakel *et al.*, 1990; Robertson & Bevan, 1991). The mechanism of this effect is uncertain, but it appears not to be due to an alteration in the ionic selectivity of the ion channel integral to the receptor (Peters *et al.*, 1988; Yang, 1990). Voltage-dependent blockade of the ion channel by Ca^{2+} and Mg^{2+} has been suggested from recent studies performed on a cloned homo-oligomeric 5-HT_3 receptor expressed in *Xenopus laevis* oocytes (Maricq *et al.*, 1991). Additionally, in NCB 20 hybridoma cells the antagonism of 5-HT_3 receptor-mediated responses by Zn^{2+} and Cd^{2+} increases with membrane hyperpolarization (Lovinger, 1991). By contrast, studies performed on N18 and N1E-115 neuroblastoma cells did not detect voltage-dependency in the blocking actions of Ca^{2+} or Mg^{2+} (Peters *et al.*, 1988; Yang, 1990). Several studies employing radiolabelled 5-HT_3 receptor antagonists suggest divalent cations to have little influence upon the affinity of agonist or antagonist binding (Hoyer & Neijt, 1988; Bolanos *et al.*, 1990, but see Stanton *et al.*, 1990). However, divalent cations have been shown to reduce the specific binding of a radiolabelled 5-HT_3 receptor agonist, [^{3}H]-m-chlorophenylbiguanide, to N1E-115 neuroblastoma cell membrane homogenates (Lummis *et al.*, 1993).

On outside-out membrane patches excised from rabbit nodose ganglion neurones, 5-HT gates an ion channel with a conductance of 17–19 pS. However, it is evident that the conductance of the channel integral to the 5-HT_3 receptor can differ substantially across preparations (Peters *et al.*, 1991a; 1992). For guinea-pig submucous plexus neurones, a single channel conductance (15 pS) comparable to that of the rabbit nodose ganglion has been demonstrated (Derkach *et al.*, 1989). However, a second conductance of 9 pS was also present (Derkach *et al.*, 1989). In coeliac ganglion neurones from the same species, the smaller conductance (10 pS) was predominant (Surprenant *et al.*, 1991). The chord conductance of the 5-HT_3 receptor of rat superior cervical ganglion neurones rectifies inwardly, but at very negative holding potentials (− 104 mV), has a value similar to the larger conductance of the guinea-pig submucous plexus neurones and that shown here for the rabbit nodose ganglion neurones (Yang *et al.*, 1992). However, fluctuation analysis performed on macroscopic currents recorded from rat superior cervical ganglion neurones suggests the presence of a second conductance, too low to be discerned from the background noise in isolated patch recordings (Yang *et al.*, 1992). Certainly, extremely low conductances (< 1 pS) have been obtained for the 5-HT_3 receptors of some murine neuroblastoma cell lines (Lambert *et al.*, 1989; Peters & Lambert, 1989; Yang, 1990; Peters *et al.*, 1992), although in a related cell line (NG 108-15) measurable conductances of 7 and 12 pS have been demonstrated (Shao *et al.*, 1991). The diverse single channel conductances may suggest different forms of the 5-HT_3 receptor. For the nicotinic receptor, amino acids have been identified in the proposed M2 region (thought to form the ion channel) which play a crucial role in determining ion conductance (Galzi *et al.*, 1991). Interestingly, identical or equivalent amino acids occupy these positions in recently cloned 5-HT_3 receptor subunits from NCB-20 cells (Maricq *et al.*, 1991) and N1E-115 cells (Hope *et al.*, 1993). A comparison of the amino acid sequences derived from 5-HT_3 clones which exhibit divergent single channel conductances might clarify the molecular determinants of ion permeation for this receptor channel complex.

2-Methyl-5-HT and 1-phenylbiguanide mimicked the actions of 5-HT, albeit with reduced potency. Equipotent molar ratios for the agonists were estimated to be 2.5 and 31.8 respectively. Broadly similar estimates of the potency of 2-methyl-5-HT, relative to 5-HT, have been made in a variety of 5-HT_3 receptor-containing cell lines and peripheral neuronal preparations from several species (see Peters *et al.*, 1993 for references). In most instances, 2-methyl-5-HT has been found to act as a partial agonist, this being particularly clear in voltage-clamp recordings performed on the NG108-15, PC12 and N1E-115 cell lines, *Xenopus* oocytes expressing a homo-oligomeric 5-HT_3 receptor cloned from the latter, and frog dorsal root ganglion neurones (Sepulveda *et al.*, 1991; Boess *et al.*, 1992; Furukawa *et al.*, 1992; Yakushiji & Akaike, 1992; Hope *et al.*, 1993). In such studies, the efficacy of 2-methyl-5-HT has been estimated to lie in the range 0.09–0.26, considering the efficacy of 5-HT to be unity. Here, the maximal inward current response to 5-HT, and thus the efficacy of 2-methyl-5-HT, could not be reliably determined. Nevertheless, inspection of Figure 5 suggests the efficacy of 2-methyl-5-HT in rabbit nodose ganglion neurones to be considerably higher than that found in the comparable voltage clamp studies cited above. Few data exist concerning the actions of 1-phenylbiguanide at the single cell level. In extracellular recordings performed on the rat isolated vagus nerve and superior cervical ganglion, the potency of 1-phenylbiguanide was found to be similar to, or slightly less than, that of 5-HT (e.g. Ireland & Tyers, 1987; Newberry & Gilbert, 1989). By contrast, 1-phenylbiguanide is devoid of agonist or antagonist activity in guinea-pig tissues (Butler *et al.*, 1990). From the present data, 1-phenylbiguanide appears to be much less potent as an agonist at rabbit nodose ganglion neurones than in rat peripheral neurones.

Ondansetron, tropisetron and bemesetron were potent antagonists of 5-HT-evoked currents in rabbit nodose ganglion neurones. Antagonist potencies similar to those determined here have been obtained for ondansetron in rabbit isolated heart and vagus nerve (Butler *et al.*, 1988) and for tropisetron in the rabbit heart, vagus nerve, superior cervical and nodose ganglia (Richardson *et al.*, 1985; Round & Wallis, 1986). Bemesetron was far more potent than in previous experiments made in rabbit superior cervical and nodose ganglion neurones (Round & Wallis, 1987). However, in some ganglionic preparations both the nature (competitive/non-competitive) and the potency of bemesetron as an antagonist changes over the course of several hours suggesting the equilibration of some antagonists with the 5-HT_3 receptors in these tissues to be a slow process (Azami *et al.*, 1985; Round & Wallis, 1987). Hence, comparisons of such data with those obtained in single cell studies may be of limited value.

The antagonist actions of ondansetron, tropisetron and bemesetron reversed relatively slowly. In comparable single cell voltage-clamp studies, similar slow recoveries have been observed for bemesetron in N18 and N1E-115 cells, rat superior cervical and nodose ganglion neurones, and for tropisetron in N1E-115 cells (Lambert *et al.*, 1989; Yang, 1990; Lovinger & White, 1991; Yang *et al.*, 1992). Such data suggest these high affinity antagonists dissociate slowly from the 5-HT_3 receptor. By comparison, the response to bath applied 5-HT peaks and subsequently desensitizes

within several seconds. Such different time courses clearly prevent equilibrium being achieved between agonist and antagonist binding within the brief time that the electrophysiological response may be observed. Hence, it is not surprising that in the present experiments ondansetron produced a non-parallel shift of the 5-HT dose-response curve. Presumably a similar explanation underlies the apparently non-competitive kinetics observed with tropisetron in N1E-115 cells and PC12 cells (Neijt *et al.*,1988; Furikawa *et al.*, 1992).

(+)-Tubocurarine, metoclopramide and cocaine, unlike the antagonists discussed above, exerted a rapidly developing and reversible antagonism of the 5-HT-evoked current response. In the intact rabbit nodose ganglion *in vitro*, concentrations of (+)-tubocurarine similar to those employed here were shown to competitively antagonize the 5-HT$_3$ receptor-mediated response. However, an additional non-competitive component of blockade was observed with higher concentrations of (+)-tubocurarine (Higashi & Nishi, 1982). In murine tissues, concentrations of (+)-tubocurarine as low as 1 nM are sufficient to produce substantial blockade of inward current responses elicited by 5-HT$_3$ receptor activation (Yakel & Jackson, 1988; Peters *et al.*, 1990b; Yang, 1990). Several observations, including a lack of voltage- and use-dependency in the blocking action of (+)-tubocurarine in N1E-115 neuroblastoma cells (Peters *et al.*, 1990b) and the parallel dextral displacement of the concentration-effect relationship to 2-methyl-5-HT in intact mouse superior cervical ganglia *in vitro* in the presence of (+)-tubocurarine are consistent with a competitive mode of action (Newberry *et al.*, 1991). At the opposite extreme, 5-HT$_3$ receptor mediating depolarizing or inward current responses in peripheral neurones of the guinea-pig are resistant to antagonism by (+)-tubocurarine at all but heroic doses (approximately 10^{-5} M; Vanner & Surprenant, 1990; Malone *et al.*, 1991a).

In the present study, metoclopramide and cocaine exhibited moderate potency as 5-HT$_3$ receptor antagonists. Although extensively studied in multicellular or organ systems (see Fozard, 1989 and Peters *et al.*, 1991a for reviews), little comparative data are available for these compounds from single cell studies. However, it would appear that cocaine is relatively weak in blocking 5-HT$_3$ receptor-evoked currents in isolated nodose ganglion neurones of the mouse, rat and guinea-pig when compared with the rabbit (Malone *et al.*, 1991a; Weight *et al.*, 1992).

In conclusion, the present study has attempted to characterize both physiologically and pharmacologically the 5-HT$_3$ receptors present upon the soma of vagal primary afferent neurones. Whether the observed properties are in all respects shared by the 5-HT$_3$ receptor populations located at the central and peripheral terminals of such neurones cannot presently be answered. However, in the absence of contradictory information, it seems parsimonious to employ the present results as a working model.

The work was supported by a grant from the Wellcome Trust. We thank Lynn Connolly and Gillian Thomson for typing the manuscript.

References

AZAMI, J., FOZARD, J.R., ROUND, A.A. & WALLIS, D.I. (1985). The depolarizing action of 5-hydroxytryptamine on rabbit vagal primary afferent and sympathetic neurones and its selective blockade by MDL 72222. *Naunyn Schmied. Arch. Pharmacol.*, **328**, 423–429.

BARRY, P.H. & LYNCH, J.W. (1991). Liquid junction potentials and small cell effects in patch-clamp analysis. *J. Membr. Biol.*, **121**, 101–117.

BOESS, F.G., SEPULVEDA, M.-I., LUMMIS, S.C.R. & MARTIN, I.L. (1992). 5-HT$_3$ receptors in NG108-15 neuroblastoma × glioma cells: effect of the novel agonist 1-(m-chlorophenyl)-biguanide. *Neuropharmacology*, **31**, 561–564.

BOLANOS, F.J., SCHECHTER, L.E., MIQUEL, M.C., EMERIT, M.B., RUMIGNY, J.F., HAMON, M. & GOZLAN, H. (1990). Common pharmacological and physicochemical properties of 5-HT$_3$ binding sites in rat cerebral cortex and NG108-15 clonal cells. *Biochem. Pharmacol.*, **40**, 1541–1550.

BUTLER, A., ELSWOOD, C.J., BURRIDGE, J., IRELAND, S.J., BUNCE, K.T., KILPATRICK, G.J. & TYERS, M.B. (1990). The pharmacological characterization of 5-HT$_3$ receptors in three isolated preparations derived from guinea-pig tissues. *Br. J. Pharmacol.*, **101**, 591–598.

BUTLER, A., HILL, J.M., IRELAND, S.J., JORDAN, C.C. & TYERS, M.B. (1988). Pharmacological properties of GR38032F, a novel antagonist at 5-HT$_3$ receptors. *Br. J. Pharmacol.*, **94**, 397–412.

DERKACH, V., SURPRENANT, A. & NORTH, R.A. (1989). 5-HT$_3$ receptors are membrane ion channels. *Nature*, **339**, 706–709.

FOZARD, J.R. (1989). The development and early clincial evaluation of selective 5-HT$_3$ receptor antagonists. In *The Peripheral Actions of 5-Hydroxytryptamine*. ed. Fozard, J.R. pp. 354–376. Oxford: Oxford University Press.

FOZARD, J.R. & MOBAROK ALI, A.T.M. (1978). Blockade of neuronal tryptamine receptors by metoclopramide. *Eur. J. Pharmacol.*, **49**, 109–112.

FURUKAWA, K., AKAIKE, N., ONODERA, H. & KOGURE, K. (1992). Expression of 5-HT$_3$ receptors in PC12 cells treated with NGF and 8-Br-c-AMP. *J. Neurophysiol.*, **67**, 812–819.

GALZI, J.-L., REVAH, F., BESSIS, A. & CHANGEUX, J.-P. (1991). Functional architecture of the nicotinic acetylcholine receptor: from electric organ to brain. *Ann. Rev. Pharmacol.*, **31**, 37–72.

GLAUM, S.R., BROOKS, P.A., SPYER, M.K. & MILLER, R.J. (1992). 5-Hydroxytryptamine-3 receptors modulate synaptic activity in the rat nucleus tractus solitarius *in vitro*. *Brain Res.*, **589**, 62–68.

HALES, T.G. & LAMBERT, J.J. (1991). The actions of propofol on inhibitory amino acid receptors of bovine adrenomedullary chromaffin cells and rodent central neurones. *Br. J. Pharmacol.*, **104**, 619–628.

HAMILL, O.P., MARTY, A., NEHER, E., SAKMANN, B. & SIGWORTH, F.J. (1981). Improved patch-clamp techniques for high resolution current recordings from cells and cell-free membrane patches. *Pflügers Archiv.*, **391**, 85–100.

HIGASHI, H. & NISHI, S. (1982). 5-Hydroxytryptamine receptors on visceral primary afferent neurones of rabbit nodose ganglia. *J. Physiol.*, **323**, 543–567.

HIGASHI, H., UEDA, N., NISHI, S., GALLAGHER, J.P. & SHINNICK-GALLAGHER, P. (1982). Chemoreceptors for serotonin (5-HT), acetylcholine (ACh), bradykinin (BK), histamine (H) and γ-aminobutyric acid (GABA) on rabbit visceral afferent neurones. *Brain Res. Bull.*, **8**, 23–32.

HOPE, A.G., DOWNIE, D.L., SUTHERLAND, L., LAMBERT, J.J., PETERS, J.A. & BURCHELL, B. (1993). Cloning and functional expression of an apparent splice variant of the murine 5-HT$_3$ R-A subunit. *Eur. J. Pharmacol. (Mol. Pharmacol. Section)*, **245**, 187–192.

HOYER, D. & NEIJT, H.C. (1988). Identification of serotonin 5-HT$_3$ recognition sites in membranes of N1E-115 neuroblastoma cells by radioligand binding. *Mol. Pharmacol.*, **33**, 303–309.

HOYER, D., WAEBER, C., KARPF, A., NEIJT, H. & PALACIOS, J.M. (1989). [^{3}H] ICS 205-930 labels 5-HT$_3$ recognition sites in membranes of cat and rabbit vagus nerve and superior cervical ganglion. *Naunyn-Schmied. Arch. Pharmacol.*, **340**, 396–402.

IKEDA, S.R., SCHOFIELD, G.G. & WEIGHT, F.F. (1986). Na^+ and Ca^{2+} currents of acutely isolated adult rat nodose ganglion cells. *J. Neurophysiol.*, **55**, 527–539.

IRELAND, S.J. & TYERS, M.B. (1987). Pharmacological characterization of 5-hydroxytryptamine-induced depolarizations of the rat isolated vagus nerve. *Br. J. Pharmacol.*, **90**, 229–238.

KILPATRICK, G.J., JONES, B.J. & TYERS, M.B. (1989). Binding of the 5-HT$_3$ ligand, [^{3}H] GR65630 to rat area postrema, vagus nerve and the brain of several species. *Eur. J. Pharmacol.*, **159**, 157–164.

LAMBERT, J.J., PETERS, J.A., HALES, T.G. & DEMPSTER, J. (1989). The properties of 5-HT$_3$ receptors in clonal cell lines studied by patch-clamp techniques. *Br. J. Pharmacol.*, **97**, 27–40.

LAPORTE, A.M., KIDD, E.J., VERGE, D., GOZLAN, H. & HAMON, M. (1992). Autoradiographic mapping of central 5-HT_3 receptors. In *Central and Peripheral 5-HT_3 Receptors*. ed. M. Hamon. pp. 157–187. London: Academic Press.

LOVINGER, D.M. (1991). Inhibition of 5-HT_3 receptor-mediated ion current by divalent metal cations in NCB-20 neuroblastoma cells. *J. Neurophysiol.*, **66**, 1329–1337.

LOVINGER, D.M. & WHITE, G. (1991). Ethanol potentiation of 5-hydroxytryptamine$_3$ receptor-mediated ion current in neuroblastoma cells and isolated adult mammalian neurones. *Mol. Pharmacol.*, **40**, 263–270.

LUMMIS, S.C.R., BAKER, J. & SEPULVEDA, M.-I. (1993). Characterisation of a radiolabelled 5-HT_3 receptor agonist, [^{3}H] m-chlorophenylbiguanide. *Br. J. Pharmacol.*, **108**, 104P.

MALONE, H.M., PETERS, J.A. & LAMBERT, J.J. (1991a). (+)-Tubocurarine and cocaine reveal species differences in the 5-HT_3 receptors of rabbit, mouse and guinea-pig nodose ganglion neurones. *Br. J. Pharmacol.*, **104**, 68P.

MALONE, H.M., PETERS, J.A. & LAMBERT, J.J. (1991b). Physiological and pharmacological properties of 5-HT_3 receptors of rabbit, mouse and guinea-pig nodose ganglion neurones. *Soc. Neurosci., abs.*, **17**, 601.

MARICQ, A.V., PETERSON, A.S., BRAKE, A.J., MYERS, R.M. & JULIUS, D. (1991). Primary structure and functional expression of the 5-HT_3 receptor, a serotonin-gated ion channel. *Science*, **254**, 432–437.

NEIJT, H.C., TE DUITS, I.J. & VIJVERBERG, H.P.M. (1988). Pharmacological characterization of serotonin 5-HT_3 receptor-mediated electrical response in cultured mouse neuroblastoma cells. *Neuropharmacology*, **27**, 301–307.

NEWBERRY, N.R., CHESHIRE, S.H. & GILBERT, M.J. (1991). Evidence that the 5-HT_3 receptors of rat, mouse and guinea-pig superior cervical ganglion may be different. *Br. J. Pharmacol.*, **102**, 615–620.

NEWBERRY, N.R. & GILBERT, M.J. (1989). 5-Hydroxytryptamine evokes three distinct responses in the rat superior cervical ganglion *in vitro*. *Eur. J. Pharmacol.*, **162**, 197–205.

PAWLOWSKI, L., RUCZYNSKA, J. & GORKA, Z. (1981). Citalopram: a new potent inhibitor of serotonin (5-HT) uptake with central 5-HT-mimetic properties. *Psychopharmacology*, **74**, 161–165.

PETERS, J.A., HALES, T.G. & LAMBERT, J.J. (1988). Divalent cations modulate 5-HT_3 receptor-induced currents in N1E-115 neuroblastoma cells. *Eur. J. Pharmacol.*, **151**, 491–495.

PETERS, J.A. & LAMBERT, J.J. (1989). Electrophysiology of 5-HT_3 receptors in neuronal cell lines. *Trends Pharmacol. Sci.*, **10**, 172–175.

PETERS, J.A., LAMBERT, J.J. & COTTRELL, G.A. (1989). An electrophysiological investigation of the characteristics and function of $GABA_A$ receptors on bovine adrenomedullary chromaffin cells. *Pflügers Arch.*, **415**, 95–103.

PETERS, J.A., LAMBERT, J.J. & MALONE, H.M. (1991a). Physiological and pharmacological aspects of 5-HT_3 receptor function. In *Aspects of Synaptic Transmission: LTP, Galanin, Opioids, Autonomic and 5-HT*. ed. Stone, T.W. pp. 283–313. London: Taylor and Francis.

PETERS, J.A., LAMBERT, J.J. & MALONE, H.M. (1993). Electrophysiological studies of 5-HT_3 receptors. In *5-HT_3 Receptor Antagonists*. ed. Jones, B., King, F.D. & Sanger, G.J. Florida: CRC Inc. (in press).

PETERS, J.A., MALONE, H.M. & LAMBERT, J.J. (1990a). 5-Hydroxytryptamine$_3$ receptor mediated responses on adult rabbit nodose ganglion neurones in cell culture. *Eur. J. Pharmacol.*, **183**, 1112.

PETERS, J.A., MALONE, H.M. & LAMBERT, J.J. (1990b). Antagonism of 5-HT_3 receptor mediated currents in murine N1E-115 neuroblastoma cells by (+)-tubocurarine. *Neurosci. Lett.*, **110**, 107–112.

PETERS, J.A., MALONE, H.M. & LAMBERT, J.J. (1991b). Characterization of 5-HT_3 receptor mediated electrical responses in nodose ganglion neurones and clonal neuroblastoma cells maintained in culture. In *Serotonin: Molecular Biology, Receptors and Functional Effects*. ed. Fozard, J.R. & Saxena, P.R. pp. 84–94. Basel: Birkhauser.

PETERS, J.A., MALONE, H.M. & LAMBERT, J.J. (1992). Recent advances in the electrophysiological characterization of 5-HT_3 receptors. *Trends Pharmacol. Sci.*, **13**, 391–397.

PRATT, G.D. & BOWERY, N.G. (1989). The 5-HT_3 receptor ligand, [^{3}H] BRL 43694, binds to presynaptic sites in the nucleus tractus solitarius of the rat. *Neuropharmacology*, **28**, 1367–1376.

PRATT, G.D., BOWERY, N.G., KILPATRICK, G.J., LESLIE, R.A., BARNES, N.M., NAYLOR, R.J., JONES, B.J., NELSON, D.R., PALACIOS, J.M., SLATER, P. & REYNOLDS, D.J.M. (1990). Consensus meeting agrees distribution of 5-HT_3 receptors in mammalian hind brain. *Trends Pharmacol. Sci.*, **11**, 135–137.

PUSCH, M. & NEHER, E. (1988). Rates of diffusional exchange between small cells and a measuring patch pipette. *Pflügers Arch.*, **411**, 204–211.

RICHARDSON, B.P., ENGEL, G., DONATSCH, P. & STADLER, P.A. (1985). Identification of serotonin M-receptor subtypes and their specific blockade by a new class of drugs. *Nature*, **316**, 126–131.

ROBERTSON, B. & BEVAN, S. (1991). Properties of 5-hydroxytryptamine$_3$ receptor-gated currents in adult rat dorsal root ganglion neurones. *Br. J. Pharmacol.*, **102**, 272–276.

ROUND, A.A. & WALLIS, D.I. (1986). The depolarizing action of 5-hydroxytryptamine on rabbit vagal afferent and sympathetic neurones and its selective blockade by ICS 205-930. *Br. J. Pharmacol.*, **88**, 485–494.

ROUND, A. & WALLIS, D.I. (1987). Further studies on the blockade of 5-HT depolarizations of rabbit vagal afferent and sympathetic ganglion cells by MDL 72222 and other antagonists. *Neuropharmacology*, **26**, 39–48.

SANGER, G.J. (1992). The involvement of 5-HT_3 receptors in visceral function. In *Central and Peripheral 5-HT_3 Receptors*. ed. Hamon, M. pp. 207–255. London: Academic Press.

SEPULVEDA, M.-I., LUMMIS, S.C.R. & MARTIN, I.L. (1991). The agonist properties of m-chlorophenylbiguanide and 2-methyl-5-hydroxytryptamine on 5-HT_3 receptors in N1E-115 neuroblastoma cells. *Br. J. Pharmacol.*, **104**, 536–540.

SHAO, X.M., YAKEL, J.L. & JACKSON, M.B. (1991). Differentiation of NG108-15 cells alters channel conductance and desensitization kinetics of the 5-HT_3 receptor. *J. Neurophysiol.*, **65**, 630–638.

STANSFELD, C.E. & WALLIS, D.I. (1984). Generation of an unusual depolarizing response in rabbit primary afferent neurones in the absence of divalent cations. *J. Physiol.*, **352**, 49–72.

STANSFELD, C.E. & WALLIS, D.I. (1985). Properties of visceral primary afferent neurons in the nodose ganglion of the rabbit. *J. Neurophysiol.*, **54**, 245–260.

STANTON, J.A., WATLING, K.J. & BEER, M.S. (1990). Effect of Ca^{2+} and Mg^{2+} ions on the binding of QICS 205-930 to the 5-HT_3 recognition site in rat brain whole cortex. *Br. J. Pharmacol.*, **100**, 395P.

SURPRENANT, A., MATSUMOTO, S. & GERZANICH, V. (1991). 5-HT_3 receptors in guinea-pig coeliac neurons. *Soc. Neurosci., Abs.*, **17**, 239.12.

TECOTT, L.H., MARICQ, A.V. & JULIUS, D. (1993). Nervous system distribution of the serotonin 5-HT_3 receptor mRNA. *Proc. Natl. Acad. Sci. U.S.A.*, **90**, 1430–1434.

VANNER, S. & SURPRENANT, A. (1990). Effect of 5-HT_3 receptor antagonists on 5-HT and nicotinic depolarizations in guinea-pig submucosal neurones. *Br. J. Pharmacol.*, **99**, 840–844.

WALLIS, D.I., STANSFELD, C.E. & NASH, H.L. (1982). Depolarizing responses recorded from nodose ganglion cells of the rabbit evoked by 5-hydroxytryptamine and other substances. *Neuropharmacology*, **21**, 31–40.

WEIGHT, F.F., FAN, P. & VISENTIN, P. (1992). Cocaine antagonises 5-HT activation of 5-HT_3 channels in neurones from rat nodose ganglion. *Br. J. Pharmacol.*, **107**, 12P.

YAKEL, J.L. & JACKSON, M.B. (1988). 5-HT_3 receptors mediate rapid responses in cultured hippocampus and a clonal cell line. *Neuron*, **1**, 615–621.

YAKEL, J.L., SHAO, X.M. & JACKSON, M.B. (1990). The selectivity of the channel coupled to the 5-HT_3 receptor. *Brain Res.*, **533**, 46–52.

YAKUSHIJI, T. & AKAIKE, N. (1992). Blockade of 5-HT_3 receptor-mediated currents in dissociated frog sensory neurones by benzoxazine derivative, Y-25130. *Br. J. Pharmacol.*, **107**, 853–857.

YANG, J. (1990). Ion permeation through 5-HT-gated channels in neuroblastoma N18 cells. *J. Gen. Physiol.*, **96**, 1177–1198.

YANG, J., MATHIE, A. & HILLE, B. (1992). 5-HT_3 receptor channels in dissociated rat superior cervical ganglion neurones. *J. Physiol.*, **488**, 237–256.

(Received March 26, 1993
Revised June 1, 1993
Accepted June 8, 1993)

Br. J. Pharmacol. (1993), **110**, 677–680

Differential affinity of dihydroimidazoquinoxalines and diimidazoquinazolines to the α1β2γ2 and α6β2γ2 subtypes of cloned $GABA_A$ receptors

[1]Wha Bin Im, Haesook K. Im, Jeffrey F. Pregenzer, Beverly J. Hamilton, Donald B. Carter, E. Jon Jacobsen, Ruth E. TenBrink & Philip F. VonVoigtlander

The Upjohn Company, CNS Diseases Research, Kalamazoo, Michigan 49001, U.S.A.

1 In this study, we compared two series of newly discovered ligands for their selectivity to benzodiazepine sites in the α1β2γ2 and the α6β2γ2 subtypes of cloned γ-aminbutyric $acid_A$ ($GABA_A$) receptors, the latter being unique in not interacting with classical benzodiazepines.

2 The prototype compounds, U-85575 (12-chloro-5-(5-cyclopropyl-1',2',4'- oxadiazol-3'-yl)-2,3-dihydro-diimidazo[1,5-a;1,2-c]quinazoline), and U-92330 (5-acetyl-3-(5'-cyclopropyl-1',2',4'-oxadiazole-3'-yl)-7-chloro-4,5-dihydro[1,5-a]quinoxaline), appear to share an overlapping recognition site with classical benzodiazepines on the $GABA_A$ receptor, because their potentiation of GABA-mediated Cl^- currents in both subtypes were sensitive to Ro 15-1788, a classical benzodiazepine antagonist.

3 Minor changes in the ring substituents of the drugs reduced their affinity to the α6β2γ2 subtype more pronouncedly than to the α1β2γ2 subtype. The diimidazoquinazoline containing a 2-methyl group which projected below the plane of the rigid ring showed a markedly lower affinity to the α6β2γ2 subtype as compared to its stereoisomer having the methyl group above the plane of the ring. Also, the dihydroimidazoquinoxalines containing the 5-benzoyl group showed a lower affinity to the α6β2γ2 subtype than the 5-acetyl counterpart. In particular, the 5-benzoyl analogue containing a 6-fluoro group showed no interaction with the α6β2γ2 subtype even at the concentration of 10 μM, probably due to stabilization of the benzoyl group in the out-of-plane region by the steric and electrostatic effects of the 6-fluoro group.

4 We propose that the benzodiazepine site of the α6β2γ2 subtype shares overlapping regions with that of the α1β2γ2 subtype, but has a sterically restricted out-of-plane region, which may be also incompatible with the 5-phenyl group of classical benzodiazepines.

Keywords: $GABA_A$ receptor; α1β2γ2; α6β2γ2; diimidazoquinazoline; dihydroimidazoquinoxaline; benzodiazepine site

Introduction

Benzodiazepines and related non-benzodiazepine hypnotic or anxiolytic agents interact with γ-aminobutyric acid ($GABA_A$) receptors, the supermolecular receptor-Cl^- channel complexes made of heteromultimeric subunits (Costa, 1979; Yokohama *et al.*, 1982; Haefely *et al.*, 1985; Barnard *et al.*, 1987; Schofield, 1989; Sieghart, 1992). In mammalian brains, several subunits with families of isotypes exist for $GABA_A$ receptors (Schofield, 1989; Sigel *et al.*, 1990; Verdoorn *et al.*, 1990; Sieghart, 1992). The most widespread subunits in the brain, α1, β2, and γ2, have been expressed in human kidney cells, and the cloned receptors (α1β2γ2) have been shown to interact with ligands for benzodiazepine sites (Pritchett *et al.*, 1989a,b; Puia *et al.*, 1991). Interestingly, different isotypes of the α subunit, when expressed with the β2 and γ2 subunits, influenced the selectivity of the cloned receptors to benzodiazepine ligands: The α1β2γ2 subtype showed higher affinity to zolpidem (imidazopyridines), Ro 15-1788 and the β-carbolines than the α2β2γ2 and α3β2γ2 subtypes (Pritchett *et al.*, 1989a,b; Puia *et al.*, 1992). The three subtypes (α1β2γ2, α2β2γ2 and α3β2γ2) interact with the classical benzodiazepines with nearly equal affinity (Pritchett & Seeburg, 1990; Puia *et al.*, 1992). The α6β2γ2 subtype in cerebellar granule cells differs from the above ones in that it does not accommodate the classical benzodiazepines, although it shares several other ligands for benzodiazepine sites with the other subtypes (i.e., Ro 15-4513; Luddens *et al.*, 1990). In the course of studying subtype selectivity, we discovered two new series of ligands which displayed markedly differential affinity to the α1β2γ2 and α6β2γ2 subtypes, depending on their particular substituents.

Here we report that U-92330, 5-acetyl-3-(5'-cyclopropyl-1',2',4' -oxadiazole-3'-yl)-7-chloro-4,5-dihydroimidazo[1,5-a]-quinoxaline, and U-85575, 12-chloro-5-(5-cyclopropyl-1',2',4'-oxadiazol-3'-yl)-2,3-dihydro-diimidazo[1,5-a;1,2-c]quinazoline (Figure 1), interact with both α1β2γ2 and α6β2γ2 subtypes, but the 5-benzoyl analogues of U-92330 and the 2-methyl analogues of U-85575 display markedly reduced affinities to α6β2γ2 as compared with their affinity to the α1β2γ2 subtype. It appears that the presence of an alkyl or aromatic group in the out-of-plane region with respect to the ring system reduces their affinity to the α6β2γ2 subtype due to the presence of at least one sterically restricted region as compared to that of the α1β2γ2 subtype.

Methods

$GABA_A$ receptor expression

DNA manipulations and general baculovirus methods (Sf9 cell cultivation, infection and isolation, and purification of recombinant viruses) were performed as described elsewhere (Carter *et al.*, 1992). The Sf-9 cells were infected at a multiplicity of infection of three plaque-forming units of viruses; AcNPV-α1 or-α6, AcNPV-β2 and AcNPV-γ2. Infected cells were used for electrophysiological measurements at 48 h post infection, or for membrane preparations at 60 h post infection.

The stable cell-lines expressing α1 or α6 (Khrestchatisky *et al.*, 1989; Luddens *et al.*, 1990), β2 (Ymer *et al.*, 1989), and γ2 (Shivers *et al.*, 1989) subunits of $GABA_A$ receptors were derived by transfection of plasmids containing cDNA and a plasmid encoding G418 resistance into the human kidney

[1] Author for correspondence.

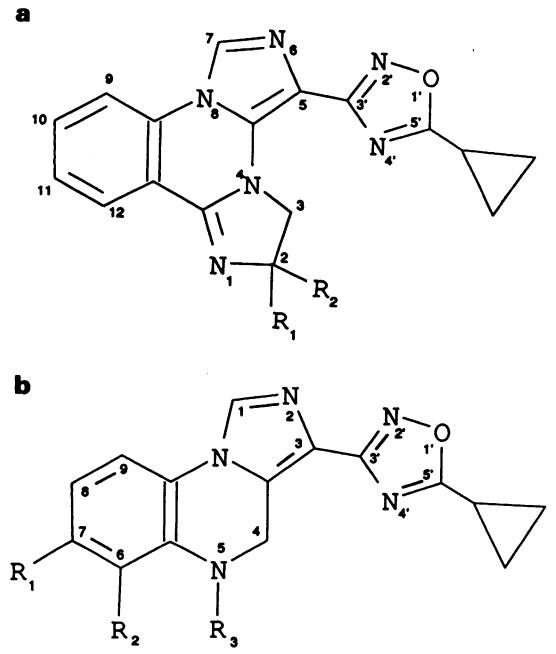

Figure 1 Chemical structures of the diimidazoquinazolines (a) and dihydroimidazoquinoxalines (b).

cells (A293 cells) as described elsewhere (Hamilton *et al.*, 1993). After two weeks of selection in 1 mg ml^{-1} G418, cells positive for all three $GABA_A$ receptor mRNAs by Northern blotting were used for electrophysiology to measure GABA-induced Cl^- currents.

Equilibrium binding

For the binding study, Sf-9 cells infected with baculovirus carrying cDNAs for α1 or α6, β2 and γ2 subunits were harvested in 2 l batches 60 h post infection. The membranes were prepared following the procedures described elsewhere (Carter *et al.*, 1992), and were stored at −80°C in a solution containing 300 mM sucrose, 5 mM Tris/HCl, pH 7.5, and glycerol to a final concentration of 20%. Equilibrium binding of [^{3}H]-flunitrazepam or [^{3}H]-Ro 15-4513 (ethyl 8-azido-5,6-dihydro-5-methyl-6-oxo-4H-imidazo[1,5-a][1,4]benzodiazepine-3-carboxylate) to the $GABA_A$ receptors was measured in a 500 µl volume of normal saline containing 6 nM [^{3}H]-flunitrazepam or [^{3}H]-Ro 15-4513, varying concentrations of test ligands, and 50 µg of membrane protein. The mixture was incubated for 60 min at 4°C, filtered over Whatman glass fibre filters, and washed four times with cold normal saline. The filter was then counted for radioactivity in the presence of a scintillation cocktail (Insta gel).

Electrophysiology

The whole cell configuration of the patch clamp techniques (Hamill *et al.*, 1981) was used to record to GABA-mediated Cl^- currents as described previously (Verdoorn *et al.*, 1990). The pipette solution contained (mM) CsCl 140, EGTA11, $MgCl_2$2, ATP 0.5 and HEPES 10, pH 7.3, and the external solution contained (mM): NaCl 130, KCl 5, $MgCl_2$ 1, $CaCl_2$ 1.8 and HEPES 5, pH 7.2, (normal saline). GABA and drugs were dissolved at the indicated concentrations in the external solution, and were applied through a Y-tube (Murase *et al.*, 1989) placed within 100 µm of the cells. The current through the pipette was recorded with an Axopatch 1D amplifier and a CV-4 headstage (Axon Instrument Co.). The currents were recorded with Gould Recorder 220. Experiments were carried out at a holding potential of −60 mV at room temperature (21–24°C).

Results and discussion

Functional characteristics

U-92330 was examined for its functional characteristics in the α1β2γ2 and α6β2γ2 subtypes expressed in Sf-9 cells (Figure 2a). The drug at 1 µM (saturating concentration) enhanced GABA-mediated Cl^- currents by 112 ± 25% ($n = 4$) in α1β2γ2 and by 148 ± 43% ($n = 3$) in α6β2γ2, as normalized to GABA (5 µM) response. Its potentiation of Cl^- current in the two subtypes was overcome by Ro 15-1788 (ethyl-8-fluoro-5,6-dihydro-5-methyl-6-oxo-4H-imidazo[1,5-a][1,4]benzodiazepine-3-carboxylate; 10 µM), suggesting that the drug shares an overlapping recognition site with the classical benzodiazepine antagonist. Interestingly, Ro 15-1788 enhanced GABA mediated Cl^- currents by 76 ± 40% ($n = 3$) in the α6β2γ2, but not in the α1β2γ2 subtype. We obtained similar results with the cloned receptors expressed in human embryonic kidney cells (A293 cells) (Figure 2b). In A293 cells, U-92330 at 1 µM enhanced Cl^- currents by 140 ± 27% ($n = 5$) in the α1β2γ2 and by 257 ± 35% ($n = 4$) in the α6β2γ2 subtype in a Ro 15-1788-sensitive way. Also, Ro 15-1788 increased Cl^- currents by 96 ± 38% ($n = 6$) only in the α6β2γ2 subtype. U-92038, the 5-benzoyl counterpart of U-92330, was also an agonist in the two subtypes expressed in A293 cells; the drug at a concentration of 5 µM increased GABA-mediated Cl^- currents by 155 ± 15% ($n = 3$) in the α1β2γ2 and by 203 ± 10% ($n = 3$) in the α6β2γ2 subtype.

U-85575, representing the diimidazoquinazolines, was also an agonist in the subtypes expressed in A293 cells; the drug at 5 µM enhanced Cl^- current by 45 ± 10% in the α1β2γ2 subtype in a Ro 15-1788-sensitive manner (data not shown), as found earlier (Im *et al.*, 1992) and by 126 ± 20% in the α6β2γ2 subtype.

It has been proposed in an earlier study (Kleingoor *et al.*, 1991) that inverse agonists, but not full agonists, modulate the α6β2γ2 subtype in A293 cells. Our current finding that the dihydroimidazoquinoxalines, the diimidazoquinazolines and Ro 15-1788 were agonists in the α6β2γ2 indicates that the chemical moiety responsible for agonistic activity for the α6β2γ2 is different from those for the α1β2γ2 subtype. Furthermore, the benzodiazepine site in α6β2γ2 is involved in a positive as well as negative modulation of the receptor function.

Binding characteristics

In agreement with earlier studies, the classical benzodiazepines like flunitrazepam and diazepam had no effect on binding of [^{3}H]-Ro 15-4513 in the cell membranes expressing the α6β2γ2 subtype of $GABA_A$ receptors (expressed in Sf-9 cells using baculovirus) even at concentrations of 5 µM (data not shown). In Table 1, we compare the K_i values of U-85575 and its 2-methyl stereoisomers in cell membranes expressing the α1β2γ2 and α6β2γ2 subtypes. U-85575 blocked binding of [^{3}H]-flunitrazepam with a K_i value of 0.3 nM in the α1β2γ2 subtype as found earlier, and that of [^{3}H]-Ro 15-4513 with a K_i value of 68 nM in the α6β2γ2 subtype. The similar ratio of the K_i value in α1β2γ2 to that in α6β2γ2 (about 200) was also observed with U-90168, the analogue of U-85575 with the 2-methyl substituent projected above the plane-of-the-ring, its K_i being 1 nM in α1β2γ2 and 181 nM in α6β2γ2. The ratio, however, became greater (860) with U-90167, a stereoisomer of U-90168, with its methyl substituent projected below the plane-of-the-ring; its K_i value was 3.8 nM in α1β2γ2 and 3270 nM in α6β2γ2. This difference between the stereoisomers indicates that the benzodiazepine site on the α6β2γ2 subtype (as compared to α1β2γ2) has a sterically restricted region where the 2'-methyl group of U-90167 (projected below the plane-of-the-ring) comes in contact.

The prototype compound of the dihydroimidazoquinoxalines, U-92330, blocked binding of [^{3}H]-flunitrazepam in the α1β2γ2 subtype with a K_i value of 2.4 ± 0.1 nM and blocked

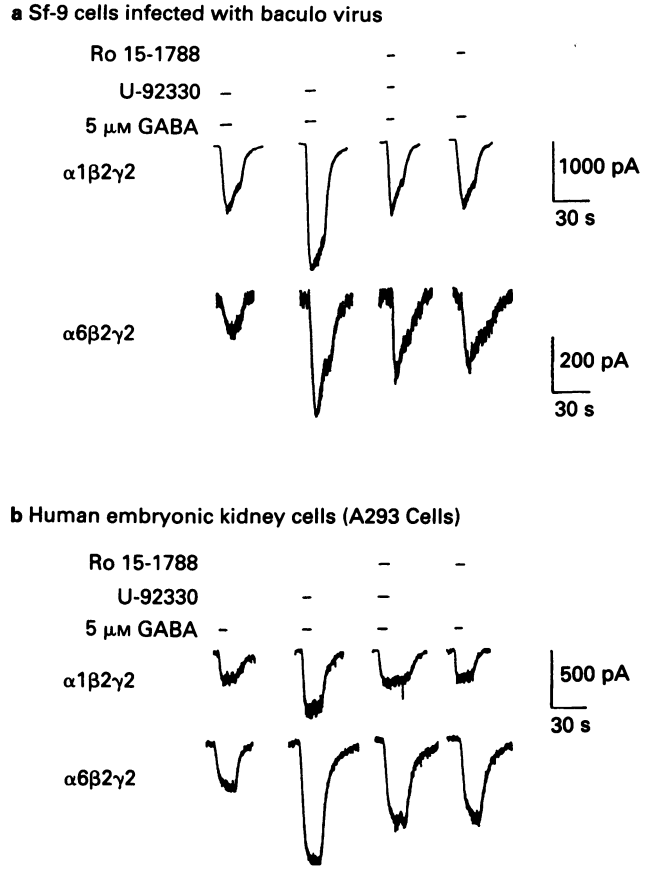

Figure 2 Traces showing the ability of U-92330 to potentiate γ-aminobutyric acid (GABA)-induced Cl^- currents and its sensitivity to Ro 15-1788 in the α1β2γ2 and the α6β2γ2 subtypes of $GABA_A$ receptors expressed in (a) Sf-9 insect cells or (b) human embryonic kidney cells. Whole cell currents induced by GABA at 5 μM were measured in the absence or presence of U-92330 (5 μM), Ro 15-1788 (10 μM), or a combination of the two. The currents were induced under a holding potential of −60 mV and a symmetrical Cl gradient.

binding of [^{3}H]-Ro 15-4513 in the α6β2γ2 subtype with a K_i value of 35 ± 8.3 nM (Table 1). We compared the affinity of three pairs of U-92330 analogues containing either the 5-acetyl or 5-benzoyl moiety in the two subtypes. In α1β2γ2, the K_i values were very similar among the three pairs, ranging from 0.4 to 1.7 nM, although the K_i values of the 5-acetyl analogues tended to be slightly higher than the 5-benzoyl analogues (Table 1). In α6β2γ2, however, the 5-acetyl analogues displayed considerably lower K_i values (higher affinity) as compared to the 5-benzoyl analogues. U-92330, U-92593 and U-92842 (the 5-acetyl analogues) blocked the binding of [^{3}H]-Ro 15-4513 in cell membranes expressing the α6β2γ2 subtype with the K_i value of 35 ± 8.3, 107 ± 21 and 81 ± 1.1 nM, respectively, while the corresponding 5-benzoyl analogues, U-92038, U-92594 and U-92130 displayed a K_i value of 1024 ± 49, > 10,000 and 681 ± 4.2 nM, respectively. In particular, U-92594, the 5-benzoyl analogue containing a fluoro substituent at C6 (R2), had no interaction with the α6β2γ2 subtype, even at a concentration of 10,000 nM.

The overlay of the two common rings, the benzene and imidazole moieties, of the diimidazoquinazolines and the dihydroimidazoquinoxalines shows that the 5-benzoyl group of U-92594 may occupy the same general region as the 2-methyl group of U-90167 (see Figure 1). Furthermore, molecular mechanics studies using the AMBER force field show that the 5-benzoyl group of U-92594 is out-of-the-plane with respect to the ring system, as is the 2-methyl group of U-90167 (Figure 3). The exact location of the benzoyl group of U-92594, however, is not as clear as the 2-methyl group of

Table 1 Comparison of binding affinity of the diimidazoquinazoline and the dihydroimidazoquinoxaline analogues in cloned γ-aminobutyic $acid_A$ ($GABA_A$) receptor subtypes

Diimidazoquinazolines	R_1	R_2	*Binding*, K_i (nM) $\alpha_1\beta_2\gamma_2$	$\alpha_6\beta_2\gamma_2$
U-85575	H	H	0.3 ± 0.1	68 ± 5
U-90167	CH_3	H	3.8 ± 0.5	3270 ± 250
U-90168	H	CH_3	1.0 ± 0.2	181 ± 42

Dihydroimidazoquinoxaline	R_1	R_2	R_3	$\alpha_1\beta_2\gamma_2$	$\alpha_1\beta_2\gamma_2$
U-92330	Cl	H	Acetyl	1.7 ± 0.4	35 ± 8
U-92038	Cl	H	Benzoyl	1.3 ± 0.1	1024 ± 49
U-92593	H	F	Acetyl	0.8 ± 0.2	107 ± 21
U-92594	H	F	Benzoyl	0.4 ± 0.1	> 10,000
U-91842	F	H	Acetyl	0.6 ± 0.1	81 ± 1
U-92130	F	H	Benzoyl	0.4 ± 0.1	681 ± 4

Binding of [^{3}H]-flunitrazepam was measured in the membranes from Sf-9 insect cells expressing the α1β2γ2 subtype and that of [^{3}H]-Ro 15-4513 in the insect cell membranes expressing the α6β2γ2 subtype as described in the Methods. The IC_{50} value was obtained from dose-response curves consisting of six different concentrations, and was converted to K_is by use of the equation, $K_i = IC_{50}/(1 + [\text{Test ligand}]/K_d$ of flunitrazepam or Ro 15-4513). The data represent the mean ± standard errors from at least three separate experiments. It should be noted that the K_i values of several drugs were obtained with [^{3}H]-Ro 15-4513 in the α1β2γ2 subtype and were not noticeably different from those obtained with [^{3}H]-flunitrazepam.

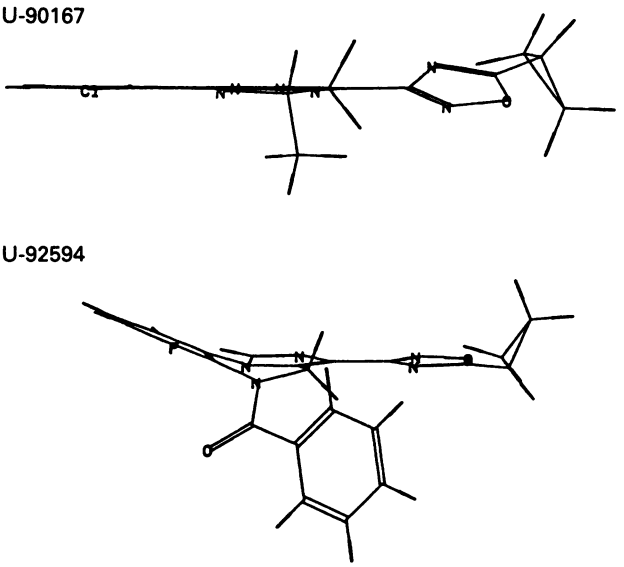

Figure 3 Side-view of minimum energy structures of U-90167 and U-92594.

U-90167, due to amide rotamers. Perhaps the steric and electrostatic effects of the adjacent fluorine may restrict the mobility of the benzoyl group and bring it in contact with a sterically restricted region on the α6β2γ2 subtype as with the 2-methyl group of U-90167. The close interaction of the C6 fluoro substituent and the 5-benzoyl group was further underscored by the observation that the 5-benzoyl analogues with the C7-fluoro substituent (U-92130) have a much higher affinity for the α6β2γ2 subtype (K_i = 681 nM) than the 6-fluoro-5-benzoyl analogue, U-92594 (K_i > 10,000).

Earlier studies (Tebib *et al.*, 1987) have assigned the 5-phenyl group of diazepam to be out-of-plane with respect to the parent ring system. This could account, at least in part,

for the lack of interaction of diazepam with the $\alpha6\beta2\gamma2$ subtype of $GABA_A$ receptors. It appears that the benzodiazepine site of the $\alpha6\beta2\gamma2$ subtype shares many common recognition regions with that of the $\alpha1\beta2\gamma2$ subtype, but has at least a sterically restricted area which poorly accommodates bulky hydrophobic groups in the out-of-plane region.

Wieland *et al.* (1992) have shown in the $\alpha6\beta2\gamma2$ subtype that mutation of arginine-100 to histidine in the $\alpha6$ subunit confers the ability to interact with classical benzodiazepines, thus confirming the equivalence of arginine-100 in $\alpha6$ to histidine-101 in the other α subunits ($\alpha1$, $\alpha2$, $\alpha3$ or $\alpha5$), which play a key role for interaction with classical benzodiazepines. It is tempting to speculate that the Arg-100 in the $\alpha6$ subunit may be responsible for creating the sterically restricted area in the benzodiazepine recognition site of the $\alpha6\beta2\gamma2$ subtype.

References

BARNARD, E.A., DARLISON, M.G. & SEEBURG, P. (1987). Molecular biology of the $GABA_A$ receptor: the receptor/channel superfamily. *Trends Neurosci.*, **10**, 502–509.

CARTER, D.B., THOMSEN, D.R., IM, W.B., LENNON, D.J., NGO, D.M., GALE, W., IM, H.K., SEEBURG, P.H. & SMITH, M.W. (1992). Functional expression of $GABA_A$ Cl^- channels and benzodiazepine binding sites in Baculovirus infected insect cells. *Bio/Technology*, **6**, 679–681.

COSTA, E. (1979). The role of gamma-aminobutyric acid in the action of 1,4-benzodiazepines. *Trends Pharmacol. Sci.*, **1**, 41–44.

HAEFELY, W., KYBURZ, E., GERECKE, M. & MOHLER, H. (1985). Recent advances in the molecular pharmacology of benzodiazepine receptors and in the structure-activity relationship of their agonists and antagonists. *Adv. Drug Res.*, **14**, 165–322.

HAMILL, O.P., MARTY, A., NEHER, E., SAKMANN, B. & SIGWORTH, F.J. (1981). Improved patch-clamp techniques for high resolution current recording from cells and cell-free membrance patches. *Pflugers. Arch.*, **391**, 85–100.

HAMILTON, B.J., LENNON, D.J., IM, H.K., IM, W.B., SEEBURG, P.H. & CARTER D.B. (1993). Stable expression of cloned rat $GABA_A$ receptor subunits in a human kidney cell line. *Neurosci. Lett.*, (in press).

IM, H.K., IM, W.B., PREGENZER, J.F., PETKE, J.D., HAMILTON, B.J., CARTER, D.B., VONVOIGTLANDER, P.F., HANSEN, H.C. & KRISTIANSEN, M. (1992). Differential potentiation of $GABA_A$ receptor function by two steroisomers of diimidazoquinazoline analogues. *Br. J. Pharmacol.*, **107**, 622–627.

KHRESTCHATISKY, M., MACLENNON, A.J., CHIANG, M.-Y., XU, W. JACKSON, M.B., BRECHA, N., STERNINI, C., OLSEN, R.W. & TOBIN, A.J. (1989). A novel α subunit in rat brain $GABA_A$ receptors. *Neuron.*, **3**, 745–753.

KLEINGOOR, M., BLANKENFELD, P.H., SEEBURG, P.H. & KETTENMANN, H. (1991). Inverse but not full benzodiazepine agonists modulate recombinant $\alpha6\beta2\gamma2$ $GABA_A$ receptors transfected human embryonic kidney cells. *Neurosci. Lett.*, **130**, 169–172.

LUDDENS, H., PRICHETT, D.B., KOHLER, M., KILLISH, I., KEINANEN, K., MONYER, H., SPRENGEL, R. & SEEBURG, P.H. (1990). Cerebellar $GABA_A$ receptor selective for a behavioral alcohol antagonist. *Nature*, **346**, 648–651.

MURASE, K., RYU, P.D. & RANDIC, M. (1989). Excitatory and inhibitory amino acids and peptide induced responses in acutely isolated rat spinal dorsal horn neurons. *Neurosci. Lett.*, **103**, 56–63.

PRITCHETT, D.B., SONTHEOMER, H., SHIVERS, B.D., YMER, S., KETTENMANN, H, SCHOFIELD, P.R. & SEEBURG, P.H. (1989a). Importance of a novel $GABA_A$ receptor subunit for benzodiazepine pharmacology. *Nature*, **338**, 582–585.

PRITCHETT, D.B., LUDDENS, H. & SEEBURG, P.H. (1989b). Type I and Type II $GABA_A$-benzodiazepine receptors produced in transfected cells. *Science*, **245**, 1389–1392.

PRITCHETT, D.B. & SEEBURG, P.H. (1990). γ-Aminobutyric $acid_A$ receptor α_5 subunit creates novel Type II benzodiazepine receptor pharmacology. *J. Neurochem.*, **54**, 1802–1804.

PUIA, G., VICINI, S., SEEBURG, P.H. & COSTA, E. (1991). Influence of recombinant $GABA_A$ receptor subunit composition on the action of allosteric modulators of GABA-gated Cl^- currents. *Mol. Pharmacol.*, **39**, 691–696.

PUIA, G., DUCIC, I., VICINI, S., & COSTA, E. (1992). Molecular mechanisms of the partial allosteric modulatory effects of bretazenil at γ-aminobutyric acid type A receptor. *Proc. Natl. Acad. Sci.*, **89**, 3620–3624.

SCHOFIELD, P.R. (1989). The $GABA_A$ receptor: Molecular biology reveals a complex picture. *Trends Pharmacol. Sci.*, **10**, 476–478.

SHIVERS, B.D., KILLISCH, I., SPRENGEL, R., SONHEIMER, H., KOHLER, M., SCHOFIELD, P.R. & SEEBURG, P.H. (1989). Two novel $GABA_A$ receptor subunits exist in distinct neuronal subpopulations. *Neuron.*, **3**, 327–337.

SIEGHART, W. (1992). $GABA_A$ receptors: ligand-gated Cl^- ion channels modulated by multiple drug-binding sites. *Trends Pharmacol. Sci.*, **13**, 446–450.

SIGEL, E., BAUR, R., TRUBE, G., MOHLER, H. & MALHERBE, P. (1990). The effect of the subunit composition of rat brain $GABA_A$ receptors on channel function. *Neuron*, **5**, 703–711.

TEBIB, S., BOURGUIGNON, J.-J. & WERMUTH, G.-G (1987). The active analog approach applied to the pharmacophore identification of benzodiazepine receptor ligands. *J. Computer-Aided Mol. Des.*, **1**, 153–928.

VERDOORN, T.A., DRAGUHN, A., YMER, S., SEEBURG, P.H. & SAKMANN, B. (1990). Functional properties of recombinant rat $GABA_A$ receptors depend upon subunit composition. *Neuron.*, **4**, 919–928.

WIELAND, H.A., LUDDENS, H. & SEEBURG, P.H. (1992). A single histidine in $GABA_A$ receptors is essential for benzodiazepine agonist binding. *J. Biol. Chem.*, **267**, 1426–1429.

YMER, S., SCHOFIELD, P.R., DRAGUHN, A., WERNER, P., KOHLER, M. & SEEBURG, P.H. (1989). $GABA_A$ receptor β subunit heterogeneity: Functional expression of cloned cDNAs. *EMBO J.*, **6**, 1665–1670.

YOKOHAMA, J.W., RITTER, B. & NEUBERT, A.D. (1982). 2-Arylpyrazolo-[4,3-c]quinoline-3-ones: Novel agonist, partial agonist, and antagonist of benzodiazepines. *J. Med. Chem.*, **25**, 337–339.

(Received April 5, 1993
Revised June 9, 1993
Accepted June 10, 1993)

Br. J. Pharmacol. (1993), **110**, 681–686

Pharmacological characterization of the dopamine receptor coupled to cyclic AMP formation expressed by rat mesenteric artery vascular smooth muscle cells in culture

[1]Alistair S. Hall, Susan E. Bryson, Peter F.T. Vaughan, Stephen G. Ball & Anthony J. Balmforth

Department of Cardiovascular Studies, University of Leeds LS2 9JT

1 Mesenteric artery vascular smooth muscle cells derived from male Wistar rats and grown in culture were prelabelled with [^{3}H]-adenine and exposed to a range of dopamine receptor agonists and antagonists. Resultant [^{3}H]-cyclic AMP formation was determined and concentration-effect curves constructed, in the presence of propranolol (10^{-6} M) and the phosphodiesterase inhibitor IBMX (5×10^{-4} M).

2 K_a apparent values for D_1/DA_1 dopamine receptor agonists SKF 38393, fenoldopam, 6,7-ADTN, and dopamine were 0.06, 0.59, 4.06 and 5.77×10^{-6} M respectively. Although fenoldopam and SKF 38393 were more potent than dopamine, they were partial agonists with efficacies, relative to dopamine of approximately 48% and 24% respectively. 6,7-ADTN, in contrast, behaved as a full agonist.

3 Dopamine-stimulated cyclic AMP formation was inhibited in a concentration-dependent manner by the D_1/DA_1 dopamine receptor selective antagonists, SCH 23390 and *cis*-flupenthixol (K_i values 0.53 and 36.1×10^{-1} M respectively). In contrast, the D_2/DA_2 dopamine receptor selective antagonists, domperidone and (−)-sulpiride, were less potent (K_i values 2.06 and 5.82×10^{-6} M respectively). Furthermore, the stereoisomers of SCH 23390 and *cis*-flupenthixol, SCH 23388 and trans-flupenthixol, were at least two orders of magnitude less potent (K_i values 0.14 and 13.2×10^{-6} M respectively) indicating the stereoselective nature of this receptor.

4 Our results indicate that rat mesenteric artery vascular smooth muscle cells in culture express a dopamine receptor coupled to cyclic AMP formation, which has the pharmacological profile, characteristic of the D_1 dopamine receptor subfamily.

Keywords: Rat mesenteric artery; cyclic AMP; dopamine receptor; vascular smooth muscle

Introduction

Specific dopamine receptors located on cells within the renal vasculature and cortex are now known to be responsible for inducing vasodilatation, diuresis and natriuresis by linkage to the enzymes adenylate cyclase and phospholipase C (Anderson *et al.*, 1990). These receptors have been further localized to the vascular media and renal tubules, whilst a second pharmacologically distinct receptor subtype, has been identified on the endothelial and neuronal cells of the vascular intima and adventitia (Amenta, 1990).

Cardiovascular dopamine receptors have traditionally been referred to using the DA_1/DA_2 dopamine receptor nomenclature proposed by Goldberg & Kohli in 1979. This scheme contrasts with one suggested by Kebabian & Calne earlier that same year (Kebabian & Calne, 1979). These authors proposed a D_1/D_2 nomenclature for dopamine receptors whether located within the periphery or within the central nervous system. The use of separate nomenclatures, whilst based primarily on anatomical location, has persisted due to some reported differences in pharmacological profiles, particularly with regard to the relative potency of partial agonists SKF 38393 and fenoldopam (SKF 82526). However, it remains unclear the extent to which these anomalies result from the differing experimental techniques used in the study of dopamine receptors at each location rather than true differences in receptor pharmacology at these sites (Hieble, 1987).

We have developed an intact cell culture model of the peripherally derived, adenosine 3':5'-cyclic monophosphate (cyclic AMP) stimulating, vascular DA_1 dopamine receptor. This approach is identical to the one previously used by members of our group to study the centrally derived D_1 dopamine receptor (Balmforth *et al.*, 1988b) and also the peripherally derived DA_1 dopamine receptor (Bryson *et al.*, 1992) expressed by human glial, and rat glomerular mesangial cells respectively. Vascular smooth muscle cell cultures derived from the rat superior mesenteric arterial-tree represent the small calibre resistance vessels that are of importance in the regulation of blood pressure and also regional blood flow (Campbell & Campbell, 1987). We have reported preliminary evidence that these cells in culture express a dopamine receptor coupled to the stimulation of cyclic AMP (Balmforth *et al.*, 1988a) and now describe a detailed pharmacological profile of the dopamine receptor expressed in this system.

Methods

Cell culture

Rat mesenteric artery vascular smooth muscle cells were cultured by a modification of the technique of enzymatic dissociation (Gunther *et al.*, 1982). Briefly, four male Wistar rats weighing 150–250 g were killed by stunning, cervical dislocation and decapitation. Following excision of the mesenteric vascular tree under sterile conditions, the vessels were cleaned of excess adipose and adventitial tissue and the mesenteric veins discarded. Arteries were then cut into 1 mm segments and placed in 5 ml of enzyme dissociation mixture (serum-free medium containing; collagenase 2.5 mg ml^{-1}, elastase 0.05 mg ml^{-1} and soyabean trypsin inhibitor 0.5 mg ml^{-1}). Following 10 min incubation at 37°C, any residual adipose, adventitial, or endothelial tissues were

[1] Author for correspondence.

removed by a process of trituration and centrifugation (1 min, 600 g). Muscular tubes derived in this way were placed in 10 ml of fresh enzyme dissociation mixture and incubated at 37°C for a further 30 min, being triturated periodically to facilitate the process of tissue dissociation. Cells were harvested by centrifugation at 600 g for 6 min, and suspended in 5 ml of Dulbecco's modified Eagle's medium (DMEM) containing 20% foetal calf serum, 2×10^{-6} M L-glutamine, 1,000 u ml^{-1} penicillin G sodium, 100 μg ml^{-1} streptomycin sulphate, 0.25 μg ml^{-1} amphotericin B and 100 μg ml^{-1} gentamycin. Confirmation of the purity and identity of cells cultured was obtained by phase microscopy and by staining cells with a fluorescent antibody to rat vascular smooth muscle α-actin. Cells were seeded into a 25 cm^2 tissue culture flask and maintained in a humidified atmosphere of 2% CO_2, 98% air at 37°C with medium being changed at intervals of 2–3 days. Cells for assays were subcultured in 6-well multidishes each containing 4 ml of medium and plated at a seeding density of 2×10^4 cells ml^{-1}. Assays were performed 7 days after subculture, using cells between the second and fifth passage in all experiments.

Assay for cyclic AMP formation in intact cells

The method for measurement of intracellular cyclic AMP formation is a modification of the prelabelling technique as described previously by (Balmforth *et al.*, 1988b). Briefly, cell adenine nucleotide pools were labelled by replacing used with fresh medium (2 ml), containing 4 μCi of [^{3}H]-adenine, and incubating at 37°C for 2 h, after which cells were washed three times with serum-free medium (2 ml). Cyclic AMP formation was stimulated by addition of agonists (when appropriate in the presence of antagonists) in serum-free medium containing the phosphodiesterase inhibitor 3-isobutyl-1-methylxanthine (IBMX, 0.5 mM). Propranolol (10^{-6} M) was present for all experiments except for those in which dopamine agonist activity at α-, β-adrenoceptor, and DA_2 dopamine receptor sites was investigated. This concentration of propranolol was chosen as it was observed to inhibit isoprenaline (10^{-5} M) without attenuating cyclic AMP formation stimulated by D_1/DA_1 dopamine receptor agonists SKF 38393 (10^{-5} M) and fenoldopam (10^{-5} M). All antagonist concentration-effect studies assessed inhibition of dopamine-induced (10^{-4} M) cyclicAMP formation. After 12 min at 37°C (time of maximal cyclic AMP formation) incubations were terminated by aspiration of the medium and subsequent addition of 1.5 ml of ice-cold 5% trichloroacetic acid (TCA) containing [^{14}C]-cyclic AMP (1.25 nCi ml^{-1}) as an internal standard. Cyclic AMP was isolated from the TCA extracts by sequential chromatography on Dowex AG50W-X4 anion exchange and neutral alumina columns (Salomon *et al.*, 1974). The [^{3}H]-cyclic AMP content of each sample was corrected for quench and [^{14}C]-cyclic AMP recovery (60–80%) and expressed in units of d.p.m. well (disintegrations per minute per well) using a Hewlett Packard 2000CA scintillation counter.

Data analysis

Concentration-effect curves were drawn for agonists and antagonists using the 'Graphpad' iterative curve-fitting computer programme (ISI Software). Sigmoid curves generated from the experimental data points (± s.e. mean) were not constrained by fixing any numeric parameters such as the slope, or the maximum, minimum and EC_{50}/IC_{50} values. In this way the K_a apparent affinity constant was determined objectively for each agonist studied. A K_i value was determined using the Cheng-Prussof equation, $K_i = IC_{50}/1 + (L/K_a)$ where IC_{50} = concentration of antagonist required to inhibit 50% of dopamine-stimulated responses, L = concentration of dopamine used in the assay and K_a = concentration of dopamine producing 50% of the maximal dopamine-stimulated cyclic AMP response (Cheng & Prusoff, 1973). All results are expressed as the geometric mean with the upper and lower 95% confidence limits in parentheses.

Materials

Dopamine hydrochloride, (±)-propranolol hydrochloride, 3-isobutyl-1-methylxanthine (IBMX), collagenase (type 1), elastase (type 1), and soyabean trypsin inhibitor were purchased from Sigma Chemicals (Poole, Dorset.) SCH 23388 (S-[-7-chloro-8-hydroxy-3-methyl-1-phenyl-2, 3, 4, 5-tetrahydro-1H-3-benzazipine hydrochloride), (+)-SKF 38393 (R-[+]-1-phenyl-2,3,4,5-tetrahydro-1H-3-benzazepine-7,8-diol hydrochloride), 6,7-ADTN (2-amino-6,7-dihyroxy-1,2,3,4-tetrahydronapthalene hydrochloride) and (−)-sulpiride from Semat (U.K.) Ltd. (St. Albans, Hertfordshire); [8-^{3}H]-adenine and adenine [U-^{14}C]-cyclic AMP from Amersham International P.L.C. (Amersham, Bucks). Dowex AG50W-X4 (200–400 mesh) and neutral alumina AG7 (100–200 mesh) from Biorad (Watford, Hertfordshire). All tissue culture reagents and plastics were purchased from Gibco (Paisley, Scotland). The following reagents were generously donated: SCH 23390 (R-[+]-7-chloro-8-hydroxy-3-methyl-1-phenyl-2,3,4,5-tetrahydro-1H-3-benzazipine-maleate) from Schering (Bloomfield, NJ, U.S.A.); *cis*-flupenthixol and *trans*-flupenthixol from H. Lundbeck A/S (Copenhagen, Denmark); domperidone maleate from Janssen Pharmaceuticals (Wantage, Oxon); fenoldopam methane sulphonate from Smith, Kline and French Research (Welwyn, Hertfordshire).

Results

Effect of catecholamine receptor antagonists

Addition of dopamine (10^{-4} M) to vascular smooth muscle cells produced an approximate six-fold increase in cyclic AMP formation as compared to the control values obtained for cells exposed to IBMX (5×10^{-4} M) alone. This stimulation was equivalent to that observed for isoprenaline (10^{-5} M) though only a fifth of that observed for forskolin (10^{-5} M) (data not shown). Dopamine (10^{-4} M)-stimulated cyclic AMP formation was not potentiated by the addition of the α-adrenoceptor antagonist phentolomine (10^{-6} M) nor the D_2/DA_2 dopamine receptor antagonist (−)-sulpiride (10^{-6} M) (Figure 1). The β-adrenoceptor antagonist, propranolol (10^{-6} M) produced either partial or no inhibition of dopamine-induced cyclic AMP formation. Furthermore the increase in cyclic AMP levels produced by dopamine was almost completely inhibited by the D_1/DA_1-dopamine receptor antagonist, SCH 23390 (10^{-6} M). These initial data suggested the presence of both DA_1-dopamine and β-adrenoceptors linked to cyclic AMP formation. As a small effect of dopamine mediated via β-adrenoceptors could not be excluded, and to prevent any confounding effects of the other dopamine receptor agonists via the β-adrenoceptors expressed in this system (Hall *et al.*, 1992) further characterization of the dopamine receptor was undertaken in the presence of propranolol (10^{-6} M).

Effect of dopamine receptor agonists

Each agonist studied produced a concentration-related stimulation of cyclic AMP formation, though the benzazepines, SKF 38393 and fenoldopam (SKF 82526), were observed to be partial agonists with efficacies (maximal levels of stimulated cyclic AMP formation) relative to dopamine (10^{-4} M) of approximately 24% and 48% respectively (Figure 2). When the relative potencies of the different dopamine receptor agonists investigated were compared on the basis of their K_a apparent values (agonist concentration giving half-maximal stimulation) the following potency series was observed; SKF 38393 > fenoldopam > 6, 7–ADTN = dopamine, with K_a apparent values of 0.06 (0.02–0.07), 0.59

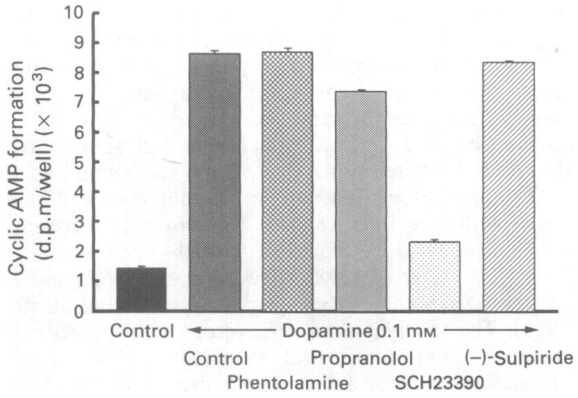

Figure 1 The effects of 10^{-6} M phentolomine, propranolol, SCH 23390, and (−)-sulpiride (acting at α, β adrenoceptors, D_1/DA_1 and D_2/DA_2 dopamine receptors, respectively) on dopamine-induced (10^{-4} M) cyclic AMP formation. Each column is the mean (± s.e.mean) of triplicate determinations of a single representative experiment.

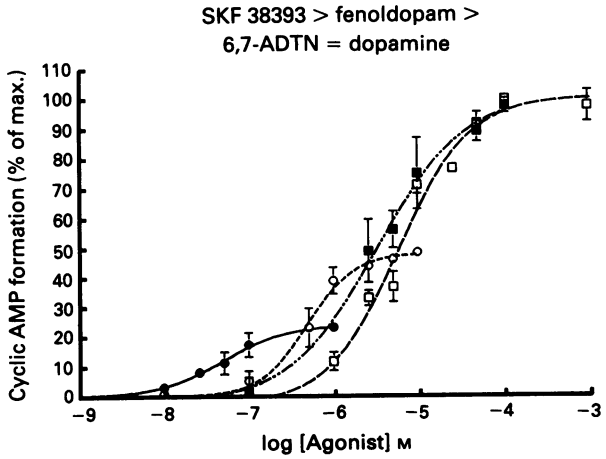

Figure 2 The stimulation of cyclic AMP formation induced by D_1/DA_1 dopamine receptor agonists (+)-SKF 38393 (●), fenoldopam (○), 6,7-ADTN (■) and dopamine (□). K_a apparent values were 0.06, 0.59, 4.06, and 5.77×10^{-6} M respectively. Dopamine (10^{-4} M) was included as a standard with each concentration-effect curve, in order to determine the efficacy of each drug. Each point is the mean (s.e.mean) of at least three separate experiments expressed as a percentage of maximal cyclic AMP formation induced by dopamine (13.40, 5.54, 4.78 and 12.94 thousands d.p.m./well respectively) after basal values have been subtracted (1.51, 1.15, 1.34 and 2.00 thousands d.p.m./well respectively).

(0.59–0.60), 4.06 (1.50–5.68), and 5.77 (4.04–7.26) × 10^{-6} M, respectively.

Effect of dopamine receptor antagonists

The D_1/DA_1 dopamine receptor antagonists, SCH 23390 (10^{-6} M) and *cis*-flupenthixol (10^{-4} M), completely inhibited maximal dopamine-induced (10^{-4} M) cyclic AMP production, achieving 50% inhibition in the sub-micromolar range (Figure 3). In contrast, the dopamine D_2/DA_2 receptor antagonists domperidone and (−)-sulpiride were observed to be significantly less potent inhibitors of dopamine-induced (10^{-4} M) cyclic AMP formation. K_i values were 0.53 (0.27–1.15), 36.1 (27.55–90–84), 2,060 (1573–3,493) and 5,820 (4,015–7,332) × 10^{-9} M respectively. The potency series observed for these antagonists was therefore SCH 23390 > *cis*-flupenthixol >> domperidone = (−)-sulpiride. The potencies of dopamine D_1/DA_1 receptor antagonists SCH 23390 and *cis*-flupenthixol were also compared with the potencies of their stereo-isomers SCH 23388 and *trans*-flupenthixol, in order to investigate the stereo selective properties of the receptor (Figure 4). Both SCH 23388 and *trans*-flupenthixol were at least two orders of magnitude less potent than their stereo-isomers, with K_i values of 143(53–149) and 13,240 (3,200–22,580) nM respectively.

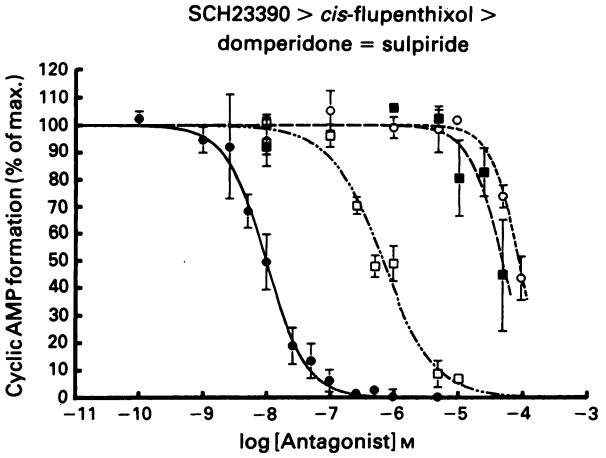

Figure 3 Concentration-effect curves for the D_1/DA_1 dopamine selective antagonists, SCH 23390 (●) and *cis*-flupenthixol (□) as compared to D_2/DA_2 dopamine selective antagonists domperidone (■) and (−)-sulpiride (○). K_i values were 0.53, 36.1, 2,060, and $5,820 \times 10^{-9}$ M respectively. Each point is the mean (± s.e.mean) of at least three seperate experiments expressed as a percentage of dopamine-induced (10^{-4} M) cyclic AMP formation in the absence of any antagonist (8.76, 4.53, 6.43 and 5.01 thousands d.p.m./well respectively) and with basal values subtracted (2.49, 1.47, 1.44 and 2.08 thousands d.p.m./well respectively).

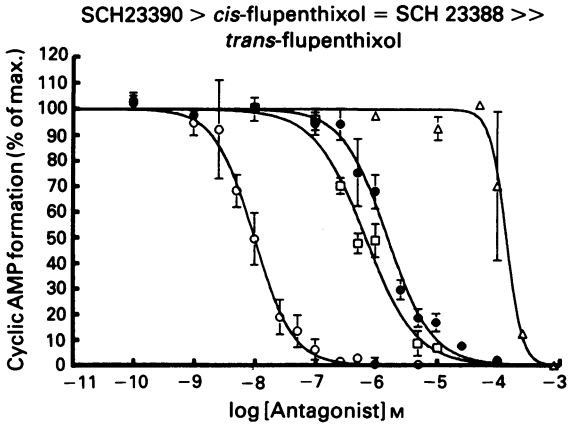

Figure 4 The relative potency of D_1/DA_1 dopamine receptor antagonists SCH 23390 (○) and *cis*-flupenthixol (□) as compared with their stereoisomers SCH 23388 (●) and *trans*-flupenthixol (△). K_i values were 0.53, 36.1, 143, and $13,240 \times 10^{-9}$ M respectively. Each point is the mean (± s.e.mean) of at least three separate experiments expressed as a percentage of dopamine-induced (10^{-4} M) cyclic AMP formation in the absence of any antagonist (8.76, 4.53, 5.42 and 1.14 thousands d.p.m./well respectively) and with basal values subtracted (2.49, 1.47, 1.51 and 1.14 thousands d.p.m./well respectively).

Discussion

We have confirmed our previous finding (Balmforth *et al.*, 1988a) that rat mesenteric artery vascular smooth muscle cells in culture express dopamine receptors linked to the stimulation of adenylate cyclase. Moreover, by using intact cells, instead of homogenates as previous workers (Murthy *et al.*, 1976; Nakajima *et al.*, 1977; Kotake *et al.*, 1981) an

increased contrast, between basal and maximal stimulation of cyclic AMP by dopamine, has been achieved. This enhanced resolution is comparable to that observed for intact-cell models of the dopamine receptors located on bovine parathyroid (Brown *et al.*, 1980), human glial (Balmforth *et al.*, 1988b) and also rat mesangial cells (Bryson *et al.*, 1992). Increased sensitivity, combined with the use of selective dopamine receptor agonists and antagonists, allowed us to characterize more fully the vascular dopamine receptor. Furthermore, the use of identical experimental techniques to those previously used by our group to characterize dopamine receptors expressed by mesangial and glial cell types (Balmforth *et al.*, 1988b; Bryson *et al.*, 1992) permits direct comparison of observed pharmacological profiles.

Several other properties make this experimental model particularly suitable for studying the pharmacological and biochemical properties of the vascular dopamine receptor (Furchgott, 1972). These features include (a) the virtual absence of contamination with other vascular and non-vascular cell types (b) the ability to manipulate the extracellular environment and maintain controlled experimental conditions for relatively long periods and (c) the ability to study receptor-coupled events without the artifact of tissue diffusion barriers and without the disruption of cell membranes and of subcellular structures.

The benzazepine compound SCH 23390 is a potent and selective D_1/DA_1 dopamine receptor antagonist (Hyttel, 1983) with a K_i in the nanomolar range. We observed concentration-dependent inhibition of dopamine-induced stimulation of cyclic AMP formation with this compound (K_i 0.53×10^{-9} M). By comparison, the weakly active stereoisomer of SCH 23390, SCH 23388, was a poor antagonist of dopamine-induced increases in cyclic AMP. Thus as observed initially for the D_1 dopamine receptor expressed by rat striatal homogenates (Stoof & Kebabian, 1984; Barnett *et al.*, 1986) and subsequently for the D_1 dopamine and DA_1 dopamine receptors expressed by human glial and rat mesangial cells in culture (Balmforth *et al.*, 1988b; Bryson *et al.*, 1992) the orientation of the phenyl substituent of SCH 23390 is critical for potent antagonism. In addition, stereoselectivity was also apparent from the difference (greater than two orders of magnitude) in the concentration-effect curves of the stereoisomers *cis*- and *trans*-flupenthixol.

In contrast to both SCH 23390 and *cis*-flupenthixol the D_2/DA_2 dopamine receptor selective antagonists domperidone and (−)-sulpiride were observed to be of very low potency. Furthermore, no enhancement of dopamine-induced stimulation of cyclic AMP formation was observed in the presence of either domperidone or (−)-sulpiride, indicating the absence of DA_2 dopamine receptors, coupled to the inhibition of adenylate cyclase, in this preparation. Some previous investigators have suggested that vascular tissues may express DA_2 dopamine receptors (Missale *et al.*, 1988; Munch *et al.*, 1991). However, it should be noted that both groups performed radio ligand binding studies on membrane preparations derived from homogenized arteries. It is highly probable, therefore, that neuronal and endothelial cell types, possibly expressing the DA_2 dopamine receptor subtypes, were also present. Detailed autoradiographic imaging indicates that dopamine DA_2 receptors are likely to be located within the adventitia and endothelium, having no direct association with vascular smooth muscle cells (Amenta, 1990). Our own data would strongly support these findings, indicating localization of a DA_1 dopamine but not a DA_2 dopamine receptor on vascular smooth muscle cells.

Vascular smooth muscle cells derived from the rat mesenteric arterial-tree also express β-adrenoceptors both *in vivo* (Nichols & Hiley, 1985) and *in vitro* (Hall *et al.*, 1992). For this reason all dopamine receptor characterization studies were performed in the presence of the β-adrenoceptor antagonist propranolol (10^{-6} M). In contrast with *in vivo* observations, isolated vascular smooth muscle cells in culture do not express functional α-adrenoceptors (Bobik, 1987). No adequate explanation for this interesting observation has yet been proposed. However, irrespective of the mechanism, the absence of α-adrenoceptors in our system conveniently avoids the need for an α-adrenoceptor antagonist to prevent dopamine interactions at these sites.

We have observed that 6,7-ADTN is a full agonist at the vascular dopamine receptor, equipotent to dopamine, and with a K_a apparent value in the micromolar range. This is consistent with previous reports for dopamine receptors, coupled to adenylate cyclase, derived both from the periphery (Kotake *et al.*, 1981; Bryson *et al.*, 1992) and also those derived from the central nervous system (Balmforth *et al.*, 1988b). The vascular dopamine receptor expressed in our experimental system demonstrated a greater affinity for D_1/DA_1 dopamine receptor selective agonists, SKF 38393 and fenoldopam, than for either 6,7-ADTN or dopamine, giving the following relative potency series, SKF 38393 > fenoldopam > 6,7-ADTN = dopamine. However, both SKF 38393 and fenoldopam stimulated much lower maximal levels of cyclic AMP formation than either dopamine or 6,7-ADTN giving the relative efficacy series 6,7-ADTN = dopamine > fenoldopam > SKF 38393. Our potency series is consistent with those reported for radioligand binding and second messenger studies of the centrally derived D_1 dopamine (Balmforth *et al.*, 1988b; Anderson *et al.*, 1990; Sibley & Monsma, 1992), and also the peripherally derived DA_1 dopamine receptors (Hughes & Sever, 1989; Bryson *et al.*, 1992). However, these contrast with the potency series reported for the DA_1 dopamine receptor when studied using the physiological endpoint of vasorelaxation (Cavero *et al.*, 1982; Hilditch & Drew, 1985; Anderson *et al.*, 1990). Though at first this would appear to represent a discrepancy, further consideration suggests that it is not. Both SKF 38393 and fenoldopam act as partial agonists at the vascular DA_1 dopamine receptor in this, as in most other *in vitro* experimental systems. For example Hilditch & Drew (1985) report that SKF 38393 produced no detectable relaxation of isolated rabbit splenic arteries. However, by using SKF 38393 as an antagonist instead, they were able to confirm the DA_1 dopamine receptor of the high affinity for this compound.

A further explanation of the discrepancy between our own, and previous reported agonist potency series for the DA_1 dopamine receptor, concerns the contrasting use of the α-adrenoceptor antagonist phenoxybenzamine. Many *in vitro* and *in vivo* experiments have been performed following exposure to large concentrations of phenoxybenzamine (3×10^{-5} M for up to 60 min; Goldberg & Kohli, 1979; Brodde, 1982). This compound has often been used in preference to alternative more selective α-adrenoceptor antagonists as it also inhibits reuptake of noradrenaline into sypathetic nerve terminals and thereby prevents the confounding effects of endogenous catecholamine release (Cuceddu *et al.*, 1974). However, we have observed that phenoxybenzamine produces potent and specific inhibition of the vascular dopamine receptor (Hall *et al.*, 1993). Possible alkylation of DA_1 dopamine receptor sites by phenoxybenzamine, would be expected to result in a reduction of receptor number. Because the maximum response produced by a partial agonist requires occupation of all expressed receptors, the effects of fenoldopam and SKF 38393 may be markedly attenuated as a result. In contrast the effect produced by the full agonists dopamine and 6,7-ADTN might be expected to remain relatively intact, if spare receptors were present.

The potency series for both antagonists and agonists which we have observed in this series of investigations, are consistent with those described for the centrally derived human glial cell D_1 dopamine receptor, and the peripherally derived rat glomerular mesangial DA_1 dopamine receptor (Balmforth *et al.*, 1988b; Bryson *et al.*, 1992) previously characterized by members of our group using identical experimental techniques. Furthermore, our results are consistent with radioligand binding studies performed on membrane preparations derived from homogenates of the rat striatum (Stoof &

Kebabian, 1984) and also from the human renal cortex (Hughes & Sever, 1989). This leads us to the conclusion that rat mesenteric artery vascular smooth muscle cells in culture express a dopamine receptor coupled to cyclic AMP formation, which has the pharmacological profile, characteristic of the D_1 dopamine receptor subfamily (Sibley & Monsma, 1992).

Attempts to identify mRNA of the recently sequenced, centrally derived, dopamine D_1 and D_5 receptor subtypes, in homogenized tissues derived from the rat liver, heart, kidney, lung, and spleen, have so far been unsuccessful (Dearry *et al.*, 1990; Monsma *et al.*, 1990; Sunahara *et al.*, 1990; 1991). It remains unclear however, whether this failure has been due to a lack of resolution in the techniques which have been employed in these studies, or whether it has been due to the absence of the D_1 and D_5 dopamine receptor subtypes within the periphery. Such data suggest, that despite identical pharmacological profiles, the peripherally derived vascular dopamine receptor may be structurally distinct from cyclic AMP, stimulating dopamine receptors expressed within the central nervous system. The continued though perhaps temporary, use of the DA_1 dopamine receptor nomenclature therefore provides a helpful distinction when describing the vascular dopamine receptor. However, were future work to confirm that the DA_1 dopamine receptor is structurally distinct from both the D_1 (D_{1A}) and the D_5 (D_{1B}) subtypes, then adoption of the D_{1C} receptor nomenclature proposed by Sibley & Monsma (1992) would become much more appropriate.

References

AMENTA, F. (1990). Density and distribution of dopamine receptors in the cardiovascular system and the kidney. *J. Auton. Pharmacol.*, **10** (Suppl.1) s11–s18.

ANDERSON, P.H., GINGRICH, J.A., BATES, M.D., DEARRY, A., FARLARDEAU, P., SENOGLES, S.E. & CARON, M.G. (1990). Dopamine receptor subtypes: beyond the D_1/D_2 classification. *Trends Pharmacol. Sci.*, **11**, 231–237.

BALMFORTH, A.J., LYALL, F., MORTON, J.I. & BALL, S.G. (1988a). Cultured mesenteric vascular smooth muscle cells express dopamine DA_1-receptors. *Eur. J. Pharmacol.*, **155**, 305–308.

BALMFORTH, A.J., YASUNARI, K., VAUGHAN, P.F.T. & BALL, S.G. (1988b). Characterization of dopamine and β-adrenergic receptors linked to cyclic AMP formation in intact cells of the clone D384 derived from a human astrocytoma. *J. Neurochem.*, **51**, 1510–1515.

BARNETT, A., AHN, H., BILLARD, W., GOULD, E.H., KOHLI, J.D., GLOCK, P. & GOLDBERG, L.I. (1976). Relative activities of SCH 23390 and its analogs in three tests for D_1/DA_1 dopamine receptor antagonism. *Eur. J. Pharmacol.*, **128**, 249–253.

BOBIK, A. (1987). Biochemical pharmacology of noradrenergic, serotonin, and histamine receptor systems in vascular smooth muscle. In *Vascular Smooth Muscle in Culture* (2). ed. Campbell J.H. & Campbell, G.R.: Florida, CRC Press Inc. pp. 105–119.

BRODDE, O.E. (1982). Vascular dopamine receptors: demonstration and characterization by *in vitro* studies. *Life Sci.*, **34**, 289–306.

BROWN, E.M., ATTIE, M.F., REEN, S., GARDNER, D.G., KEBABIAN, J. & AURBACH, G.D. (1980). Characterization of dopaminergic receptors in dispersed bovine parathyroid cells. *Mol. Pharmacol.*, **18**, 335–340.

BRYSON, S.E., DREW, G.M., HALL, A.S., BALL, S.G. & BALMFORTH A.J. (1992). Characterization of the dopamine receptor expressed by rat glomerular mesangial cells in culture. *Eur. J. Pharmacol. Mol. Pharmacol. Sect.*, **225**, 1–7.

CAMPBELL, J.H. & CAMPBELL, G.R. (1987). Methods of growing vascular smooth muscle in culture. In *Vascular Smooth Muscle in Culture* (1). ed. Campbell, J.H. & Campbell, G.R.: Florida: CRC Press Inc. pp. 15–23.

CAVERO, I., MASSINGHAM, R. & LEFEVRE-BORG, F. (1982). Peripheral dopamine receptors, potential targets for a new class of antihypertensive agents. *Life Sci.*, **31**, 939–948.

CHENG, Y.C. & PRUSOFF, W.H. (1973). Relationship between the inhibition constant (Ki) and the concentration of inhibitor which causes 50 percent inhibition (I_{50}) of an enzymic reaction. *Biochem. Pharmacol.*, **22**, 3099–3108.

CUCEDDU, L.X., BARNES, E., LANGER, S.Z. & WEINER, N. (1974). Release of norepinephrine and dopamine-β-hydroxylase by nerve stimulation. I. Role of neuronal and extraneuronal uptake and of alpha presynaptic receptors. *J. Pharmacol. Exp. Ther.*, **190**, 431–450.

DEARRY, A., GINGRICH, J.A., FALARDEAU, P., FREMEAU, R.T. & CARON, M.G. (1990). Molecular cloning and expression of the gene for a human D_1 dopamine receptor. *Nature*, **347**, 72–76.

FURCHGOTT, R.F. (1972). The classification of adrenoceptors (adrenergic receptors). An evaluation from the standpoint of receptor theory. In *Handbook of Experimental Pharmacology*. ed. Baschko, H.J. & Muscholl E. New York Springer pp. 283–335.

GOLDBERG, L.I. & KOHLI, J.D. (1979). Peripheral pre- and postsynaptic dopamine receptors: are they different from dopamine receptors in the CNS? *Comm. Psycopharmacol.*, **3**, 447–456.

GUNTHER, S., ALEXANDER, R.W., ATKINSON, W.J. & GIMBRONE, M.A. (1982). Functional angiotensin II receptors in cultured vascular smooth muscle cells. *J. Cell. Biol.*, **92**, 289–295.

HALL, A.S., BRYSON, S.E., BALL, S.G.B. & BALMFORTH, A.J. (1992). Pharmacological characterization of the beta adrenoceptor coupled to cyclic-AMP formation expressed by rat mesenteric artery vascular smooth muscle cells in culture. *J. Hyperten.*, **9**, S96-S97.

HALL, A.S., BRYSON, S.E., BALL, S.G.B. & BALMFORTH, A.J. (1993). Phenoxybenzamine mediated inhibition of the vascular dopamine receptor. *Eur. J. Pharmacol.*, (in press).

HIEBLE, J.P. (1987). Peripheral actions of dopamine receptor agonists. In *Annual Reports in Medicinal Chemistry*. pp. 107–116. Bristol; Academic Press Inc.

HILDITCH, A. & DREW, G.M. (1985). Peripheral dopamine receptor subtypes–a closer look. *Trends Pharmacol. Sci.*, **6**, 396–400.

HUGHES, A. & SEVER, P. (1989). Specific binding of ^{125}I SCH 23982, a selective dopamine (D_1) receptor ligand to plasma membranes derived from human kidney cortex. *Biochem. Pharmacol.*, **35**, 781–785.

HYTTEL, J. (1983). SCH 23390–the first selective dopamine D_1 antagonist. *Eur. J. Pharmacol.*, **91**, 153–158.

KEBABIAN, J.W. & CALNE, D.B. (1979). Multiple receptors for dopamine. *Nature*, **277**, 93–96.

KOTAKE, C., HOFFMAN, P.C., GOLDBERG, L.I. & CANNON, J.G. (1981). A comparison of the effects of dopamine and beta-adrenergic antagonists on adenylate cyclase of renal glomeruli and striatum. *Mol. Pharmacol.*, **20**, 429–434.

MISSALE, C., CASTELLETTI, L., MEMO, M., CARRUBA, M.O. & SPANO, P.T. (1988). Identification and characterization of postsynaptic D_1- and D_2- dopamine receptors in the cardiovascular system. *J. Cardiovasc. Pharmacol.*, **11**, 643–650.

MONSMA, F.T., MAHAN, L.G., MCVITTE, L.D., GERFEN, C.R. & SIBLEY, D.R. (1990). Molecular cloning and expression of a D_1 dopamine receptor linked to adenylate cyclase activation. *Proc. Natl. Acad. Sci. U.S.A.*, **87**, 6723–6727.

MUNCH, G., RAETHER, A., SCHOFFEL, E. & ILLES, P. (1991). Postsynaptic DA_1- and DA_2- receptors in jejunal arteries of rabbits. *J. Cardivasc. Pharmacol.*, **18**, 469–471.

MURTHY, V.V., GILBERT, J.C., GOLDBERG, L.I. & KUO, J.F. (1976). Dopamine sensitive adenylate cyclase in canine renal artery. *J. Pharm. Pharmacol.*, **28**, 567–571.

NAKAJIMA, T., NAITCH, F. & KURMA, I. (1977). Dopamine sensitive adenylate cyclase in rat kidney particulate preparation. *Eur. J. Pharmacol.*, **41**, 163–169.

NICHOLS, A.J. & HILEY, C.R. (1985). Identification of adrenoceptors and dopamine receptors mediating vascular responses in the superior mesenteric arterial bed of the rat. *J. Pharm. Pharmacol.*, **37**, 110–115.

SALOMON, Y., LONDOS, C. & RODBELL, M. (1974). A highly sensitive adenylate cyclase assay. *Annl. Biochem.*, **58**, 541–548.

SIBLEY, D.R. & MONSMA, F.J. (1992). Molecular biology of the dopamine receptors. *Trends. Pharmacol. Sci.*, **13**, 61–69.

STOOF, J.C. & KEBABIAN, J.W. (1984). Two dopamine receptors: biochemistry, physiology and pharmacology. *Life Sci.*, **35**, 2281–2296.

SUNAHARA, R.K., GUAN, H.C., O'DOWD, B.F., SEEMAN, P., LAURIER, L.G., NG, G., GEORGE, S.R., TORCHIA, J., VAN TOL, H.H.M. & NIZNIK, H.B. (1991). Cloning of the gene for a human dopamine D_5 receptor with higher affinity for dopamine than D_1. *Nature*, **350**, 614–619.

SUNAHARA, R.K., NIZNIK, H.B. & WEIBER, D.M. (1990). Human dopamine D_1 receptor encoded by an intronless gene on chromosome 5. *Nature*, **347**, 80–83.

(Received April 7, 1993
Revised June 7, 1993
Accepted June 14, 1993)

Br. J. Pharmacol. (1993), **110**, 687–692

Characterization of receptors for endothelins in the perfused arterial and venous mesenteric vasculatures of the rat

[1]Pedro D'Orléans-Juste, Audrey Claing, *Timothy D. Warner, †Mitsuo Yano & Sabine Télémaque

Department of Pharmacology, Medical School, Université de Sherbrooke, Sherbrooke (Québec) J1H 5N4, Canada; *The William Harvey Research Institute, St. Bartholomew's Hospital Medical College, Charterhouse Square, London EC1M 6BQ and †Banyu Pharmaceutical Co., Ltd., Tsukuba Research Institute, Tsukuba Techno-Park Ohu, Okubo 3, Tsukuba 300-33, Japan

1 Endothelin-1 and -3 induced marked arterial and venous constrictions in the perfused mesenteric vasculature of the rat with endothelin-3 being at least 20 times less active than endothelin-1, on both arterial and venous sides of the vasculature.

2 Two ET_B selective agonists, BQ-3020 and IRL 1620 (500 pmol), induced weak constrictions of the venous mesenteric vasculature and were inactive in the arterial side at doses up to 1000 pmol.

3 In mesenteric vasculatures precontracted with either methoxamine (arterial side) or the thromboxane A_2-mimetic, U46619 (venous side), acetylcholine or bradykinin produced vasodilatations of both arterial and venous vessels, whereas endothelin-3 induced vasodilatations only on the arterial side.

4 A selective ET_A receptor antagonist, BQ-123, blocked, in a concentration-dependent and reversible fashion, the vasoconstrictions induced by endothelin-1 on both sides of the mesenteric circulation (IC_{50}; arterial side: 0.013 μM; venous side: 0.032 μM).

5 In contrast, the vasodilator responses induced by endothelin-3 on the arterial side of the precontracted mesenteric vasculature were not affected by BQ-123.

6 The present study illustrates the presence of ET_A receptors which are responsible for vasoconstriction by endothelins in the arterial and venous mesenteric vasculatures. Furthermore, we suggest that the vasodilatations induced by endothelin-3 in the arterial vasculature uniquely, are ET_B receptor-mediated.

Keywords: Endothelin-1; endothelin-3; vascular effects; antagonist; BQ-123; endothelin receptors; mesenteric vasculature; IRL 1620; BQ-3020

Introduction

The responses of the venous and arterial portions of the mesenteric vasculature of the rat to the potent vasoactive peptides, endothelin-1 and endothelin-3, were recently described (Warner *et al.*, 1989; Warner, 1990). In these two studies, endothelin-1 was shown to be a potent vasoconstrictor of both sides of the rat mesenteric perfused vasculature. In addition, various groups have shown that endothelins have transient depressor properties *in vivo* in conscious and anaesthetized rats as well as in the mesenteric vasculature of the rat *in vitro* (de Nucci *et al.*, 1988; Yanagisawa *et al.*, 1988; Warner *et al.*, 1989; Gardiner *et al.*, 1990; Le Monnier de Gouville *et al.*, 1990; Douglas & Hiley, 1991). The release of vasodilator factors by endothelin-1 in this vascular bed is in accordance with the finding that the vasopressor effects of endothelins are modulated by the release of vasodilator factors, such as endothelium-derived nitric oxide (EDNO) and prostacyclin (de Nucci *et al.*, 1988).

The recent cloning of at least two distinct receptor types, namely ET_A (Arai *et al.*, 1990) and ET_B (Sakurai *et al.*, 1990), has prompted studies to characterize which receptors are involved in the various effects of endothelins. For instance, ET_A receptor activation has been initially associated with the vasoconstrictor effect of endothelins, whereas it was suggested that ET_B receptors were responsible for the release of EDNO (Webb, 1991). However, these concepts have been recently challenged as the vasoconstriction of some venous blood vessels as well as the rabbit pulmonary artery have been shown to be mediated via the activation of ET_B receptors (Ihara *et al.*, 1992b; Moreland *et al.*, 1992). ET_B-mediated vasoconstrictions in the rabbit pulmonary artery were further characterized by the use of the selective ET_B receptor agonists, IRL 1620 (Suc-[Glu^9,$Ala^{11,15}$]-endothelin-1(8-21); Takai *et al.*, 1992) and BQ-3020 ([$Ala^{11,15}$]-endothelin-1(6-21); Ihara *et al.*, 1992b).

Ihara *et al.* (1992a) have shown that the potent, selective ET_A receptor antagonists, BQ-153 and BQ-123, markedly suppress the pressor effects of endothelin-1 in conscious rats without affecting its initial hypotensive effect. Furthermore, this group suggested that the pressor response to endothelin-1 is due to the activation of ET_A receptors whereas its initial hypotensive effect, which is perhaps due to the release of EDNO (Whittle *et al.*, 1989) and which remained unaffected by the ET_A-receptor antagonists, is mediated by ET_B receptors (Ihara *et al.*, 1992a). These observations were confirmed by Bigaud & Pelton (1992) and Douglas *et al.* (1992). Interestingly, both groups demonstrated that BQ-123 not only reduced the pressor effect but also potentiated the initial depressor response to endothelin-1 in conscious (Bigaud & Pelton, 1992) as well as in anaesthetized rats (Douglas *et al.*, 1992). In addition, the ET_B receptor-mediated vasodilator properties of endothelins have very recently been characterized in rat aortic rings by Karaki *et al.* (1993) using a selective ET_B receptor antagonist, IRL 1038.

In contrast to the ET_B-mediated vasodilator properties of endothelin-1, we have recently shown that the endothelin-induced release of prostacyclin from rat perfused lung is mediated via the activation of ET_A receptors (D'Orléans-Juste *et al.*, 1992). This suggests that even though both ET_A and ET_B receptors are present in pulmonary tissues (D'Orléans-Juste *et al.*, 1992; Nakamichi *et al.*, 1992), the production of endogenous modulators of the vascular effects of endothelin-1 may be triggered by receptors other than ET_B.

As the haemodynamic effects of endothelins are clearly due to a series of interconnected events including the production

[1] Author for correspondence.

of additional vasorelaxant factors, such as EDNO and prostacyclin, the use of an isolated segmental vasculature, such as the perfused mesenteric bed, is useful in allowing the pharmacological delineation of the constrictor and EDNO-releasing properties of various peptides including the endothelins (Warner, 1990; D'Orléans-Juste et al., 1991; Claing et al., 1992). Hence, this model was chosen to quantify the receptors involved in the responses of the rat mesenteric vasculature to endothelin-1 and endothelin-3.

Methods

The rat mesenteric vascular bed perfused simultaneously through the arterial and venous vasculatures

The rat mesentery was prepared as described previously (Warner, 1990). Male albino Wistar rats (250–350 g) were killed by stunning and exsanguination. The abdomen was opened and the ileocolic and colic branches of the superior mesenteric artery were tied. The portal mesenteric vein was freed of connective and adipose tissues and was then cannulated (Portex tube size 3FG) 1.0–1.3 cm distal to the portal mesenteric junction. The superior mesenteric artery was cannulated as described previously (McGregor, 1965). Warm (37°C), oxygenated (95% O_2: 5% CO_2) Krebs solution (concentration in mM: NaCl 117.5, KCl 4.7, KH_2PO_4 1.2, $CaCl_2$ 2.5, $MgSO_4$ 1.2, $NaHCO_3$ 25, glucose 5.5) containing heparin (100 u ml^{-1}) was then perfused through the mesenteric artery at a flow of 2 ml min^{-1} for 5 min. Following this initial perfusion period, the mesentery was separated from the intestine by cutting close to the intestinal border. The venous and arterial vasculatures were subsequently perfused independently at flow rates of 2 ml min^{-1} with Krebs solution containing indomethacin (5 μM). The pressor responses to the endothelins, angiotensin II and noradrenaline, as well as the vasodilatations induced by endothelins, acetylcholine and bradykinin were measured with pressure transducers (Statham, model P-23A) and recorded on a Grass physiograph (model 7D).

Venous and arterial contractions of the mesenteric vasculature in response to endothelin-1, endothelin-3, angiotensin II and noradrenaline

Following an equilibration period of 45 min, the vasoconstrictor effects of endothelin-1, endothelin-3, BQ-3020, IRL 1620, angiotensin II and noradrenaline were measured on both sides of the mesenteric vasculature. Agonists were administered by bolus injections in volumes of 1 μl. Individual drugs (maximum of four different drugs on each preparation) were administered consecutively at time intervals varying from 10 min (angiotensin II, noradrenaline) to 45 min (endothelin-1, endothelin-3) to avoid tachyphylaxis. After the first administration of the different agonists, BQ-123 (cyclo[D-Asp-L-Pro-D-Val-L-Leu-D-Trp]) (0.01–1 μM) was infused starting from 15 min before the second administration of the agonists. The IC_{50} of the antagonist was estimated by monitoring the pressor responses of endothelin-1 at the highest dose (arterial: 100 pmol, venous: 25 pmol) in the presence of increasing concentrations of BQ-123 (0.001–1 μM).

Endothelium-dependent vasodilatation

In order to quantify endothelium-dependent relaxations, the perfusion pressures on both sides of the mesenteric circulation were increased by infusing a sympathomimetic, methoxamine (100 μM), on the arterial side and a thromboxane A_2-mimetic, U46619 (0.5 μM), on the venous side (Warner, 1990). The perfusion flow rate was increased to 5 ml min^{-1} on the arterial side to reduce spontaneous activity (Warner, 1990). When a steady elevation in perfusion pressure was reached on both sides, endothelium-dependent vasodilators of the arterial and venous mesenteric vasculature of the rat (bradykinin, acetylcholine or endothelin-3: Warner et al., 1989; Warner, 1990; D'Orléans-Juste et al., 1991; Claing et al., 1992) were administered as bolus injections. In some experiments, BQ-123 (0.1 μM) was infused starting from 15 min before the administration of bradykinin, acetylcholine or endothelin-3.

Drugs

Endothelin-1 and endothelin-3 were purchased from Peninsula Laboratories (Belmont, CA, U.S.A.). Bradykinin and angiotensin II were synthesized in the laboratory of Dr D. Regoli (Department of Pharmacology, Université de Sherbrooke, Sherbrooke, Québec, Canada). Acetylcholine, indomethacin, noradrenaline and methoxamine were purchased from Sigma (St. Louis, MO, U.S.A.). U46619 (9,11-dideoxy-9α,11α-methanoepoxy prostaglandin $F_{2\alpha}$) was purchased from Cayman Chemical Company (Ann Arbor, U.S.A.). The ET_A receptor antagonist, BQ-123 and the ET_B receptor agonist, BQ-3020, were synthesized at Banyu Pharmaceutical Company (Tsukuba, Japan). The ET_B receptor agonist, IRL 1620, was synthesized at Ciba-Geigy (Takarazuka, Japan).

Endothelin-1, endothelin-3, BQ-3020, IRL 1620 and BQ-123 were dissolved in phosphate-buffered saline (pH: 7.4, Sigma, St. Louis, MO, U.S.A.). All other agents were dissolved in saline (NaCl: 0.9%) or distilled water, except for indomethacin which was dissolved in Trizma base (pH: 7.4, 0.2 M, Sigma).

Statistics

Results are shown as mean values ± s.e. mean for n experiments. Statistical differences between and within groups were compared by analysis of variance (ANOVA; Wallenstein et al., 1980). Statistical significance was assumed when $P<0.05$.

Results

Effects of BQ-123 on endothelin-1-induced arterial and venous pressor responses

The basal perfusion pressures of the arterial and venous sides of the mesenteric vasculature were 5.7 ± 0.9 mmHg ($n = 11$) and 1.8 ± 0.3 mmHg ($n = 7$), respectively, when perfused at 2 ml min^{-1}. Increasing the perfusion flow to 5 ml min^{-1} increased the perfusion pressure of the arterial vasculature to 14.3 ± 1.1 mmHg ($n = 14$).

Infusion of BQ-123 had no effect on the basal perfusion pressure of either side of the vasculature while it markedly reduced the increases in perfusion pressures induced by endothelin-1 (25 pmol) (control, arterial side: 3.4 ± 0.3 mmHg, venous side: 10.9 ± 0.8 mmHg; + BQ-123 (0.1 μM), arterial side: 0.7 ± 0.1 mmHg, venous side: 1.9 ± 0.3 mmHg, $n = 6–8$, $P<0.001$; Figure 1). The response to endothelin-1 was almost restored to control values, 30 min after stopping the infusion of the antagonist (arterial side: 2.6 ± 0.8 mmHg, venous side: 8.0 ± 1.0 mmHg, $n = 6–8$, not significantly different from control).

Characteristically, endothelin-1 was 5–10 times less active in the arterial (Figure 2a) mesenteric vasculature than in the venous vessels (Figure 2b) (e.g. arterial side, 25 pmol: 2.7 ± 0.2 mmHg, 50 pmol: 4.6 ± 0.6 mmHg, $n = 11$: venous side, 5 pmol: 3.0 ± 0.3 mmHg, 10 pmol: 8.0 ± 0.6 mmHg, $n = 7$). BQ-123 (0.01–1 μM) induced a concentration-dependent antagonism (50 ± 5% to 100 ± 1%, $n = 5–8$, $P<0.001$) of the contractions evoked by endothelin-1 (25–100 pmol) on the arterial side of the mesenteric vasculature (Figure 2a). The IC_{50} value of BQ-123, estimated against the highest dose of endothelin-1 used in the present study (100 pmol), was 0.013 μM. In addition, 30 min after the cessation of the

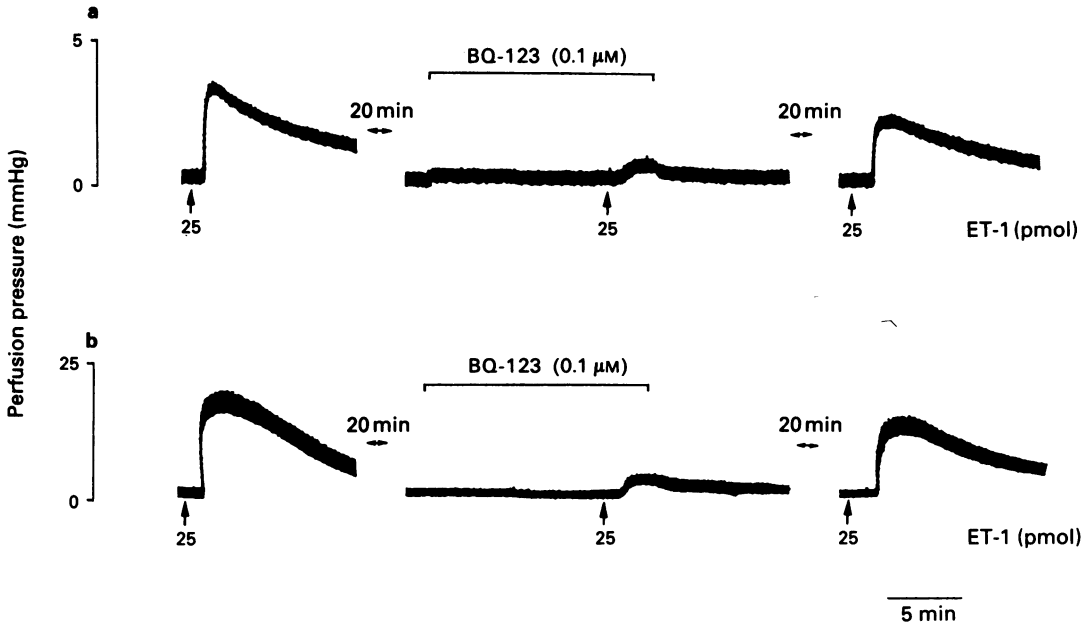

Figure 1 Typical trace illustrating the pressor effect of endothelin-1 (ET-1: 25 pmol) in the absence and presence of BQ-123 (0.1 μM, 15 min) in the arterial (a) and venous (b) mesenteric vasculatures of the rat. This trace is representative of 7 other experiments.

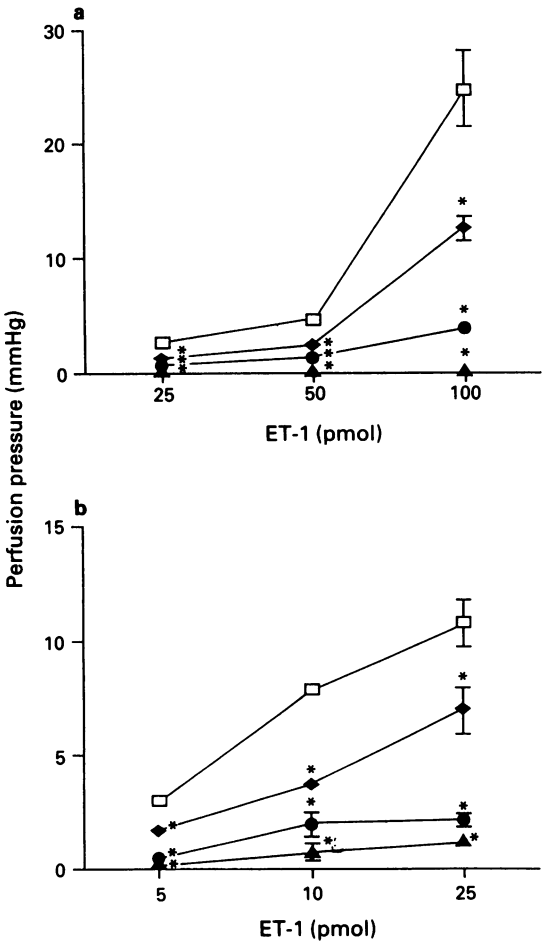

Figure 2 The dose-dependent effect of endothelin-1 in absence (□) and presence of BQ-123 (◆: 0.01 μM, ●: 0.1 μM, ▲: 1 μM) on the arterial (a) and venous (b) mesenteric vasculatures of the rat. Each point is the mean ± s.e. mean of 5–8 determinations. *$P<0.001$.

infusion of BQ-123 (0.01–0.1 μM), the responses of arterial mesenteric vasculature were completely recovered for the smaller doses of endothelin-1 (25 pmol: 2.6 ± 0.7 mmHg, 50 pmol: 4.0 ± 1.0 mmHg), but only partially for the highest dose (100 pmol: 15.2 ± 4.1 mmHg). However, at the highest concentration of BQ-123 (1 μM), the response was only partially restored, 30 min after the cessation of the infusion (50 ± 8%, $n = 5$ of control values for each dose of endothelin-1 tested, results not shown).

BQ-123 (0.01–1 μM) induced a concentration-dependent antagonism (35 ± 9 to 90 ± 2%, $n = 5–7$, $P<0.001$) of the vasoconstrictions induced by endothelin-1 (5–25 pmol) in the venous vasculature (Figure 2b). The IC_{50} value for BQ-123, estimated against the dose of 25 pmol of endothelin-1 was 0.032 μM. The response to endothelin-1 (5–25 pmol) was totally restored 30 min after the cessation of the infusion of the lower concentrations of the antagonist (0.01–0.1 μM: 8.0 ± 1.0 mmHg for the dose of 25 pmol of ET-1), but for BQ-123 given at 1 μM, the response was restored to only 50 ± 10% of the control value for the three doses of ET-1.

Endothelin-3 increased the perfusion pressures of both sides of the rat mesenteric vasculature (arterial side, 1000 pmol: 3.8 ± 0.6 mmHg, venous side, 200 pmol: 8.0 ± 1.1 mmHg, $n = 5$). However, doses of endothelin-3, 20 times higher than endothelin-1, were required to obtain similar vasoconstrictions (endothelin-1; arterial side, 50 pmol: 4.3 ± 1.1 mmHg, venous side, 10 pmol: 7.9 ± 0.6 mmHg, $n = 5–8$).

BQ-3020 or IRL 1620, caused only small increases in the perfusion pressure on the venous side (BQ-3020, 500 pmol: 1.1 ± 0.1 mmHg; IRL 1620, 500 pmol: 1.8 ± 0.4 mmHg, $n = 4–5$), and were inactive as vasoconstrictors, even at doses of 1000 pmol on the arterial mesenteric vasculature.

Lack of effect of BQ-123 on the pressor responses induced by angiotensin II or noradrenaline

BQ-123 (1 μM) did not affect the vasoconstrictions induced by angiotensin II (100 pmol: venous, control: 8.4 ± 0.2 mmHg; + BQ-123: 9.4 ± 0.5 mmHg, $n = 4$; Figure 3b) or noradrenaline (1000 pmol: control, arterial side:

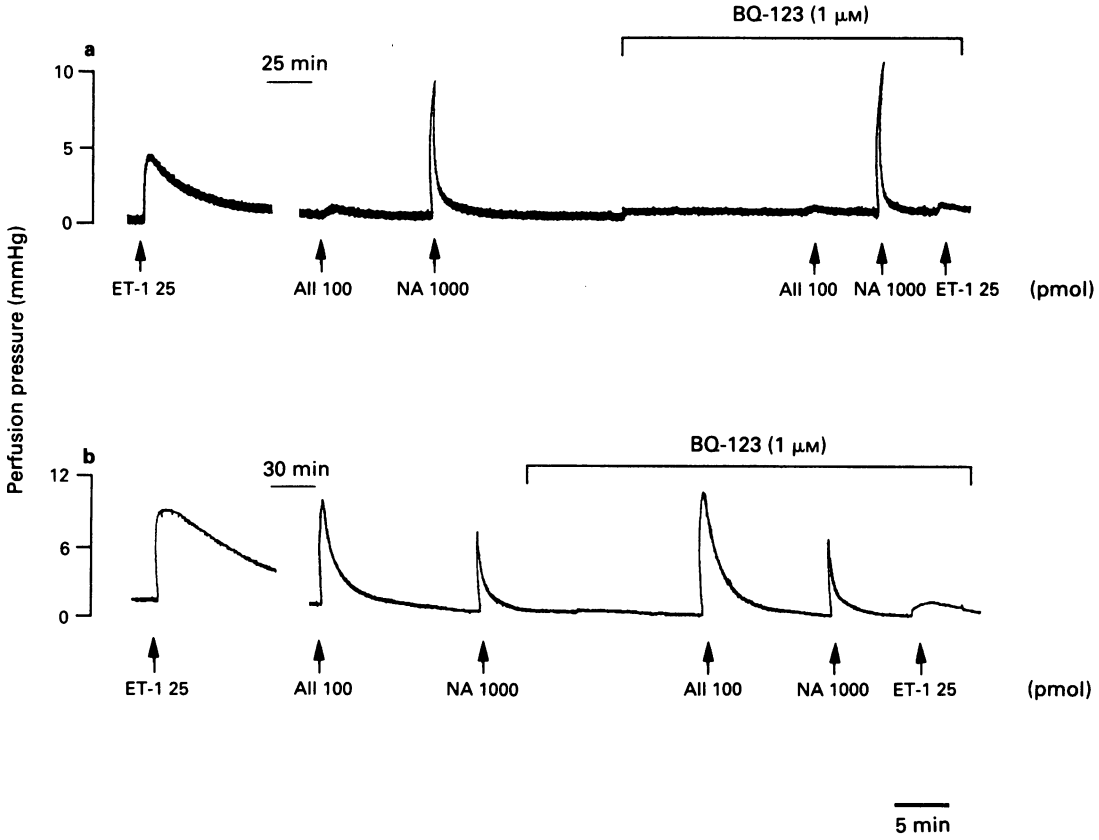

Figure 3 Typical trace illustrating the effect of endothelin-1 (ET-1: 25 pmol), angiotensin II (AII: 100 pmol) and noradrenaline (NA: 1000 pmol) in the absence and presence of BQ-123 (1 μM) in the arterial (a) and venous (b) mesenteric vasculatures of the rat. This trace is representative of 3 other experiments.

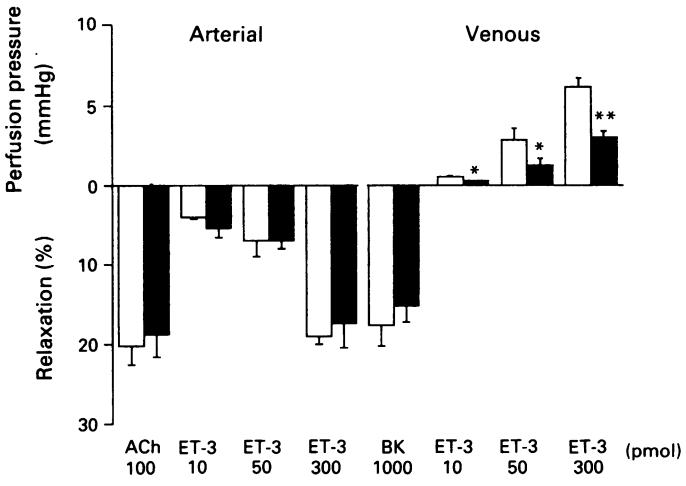

Figure 4 The dose-dependent effect of endothelin-3 (ET-3: 10–300 pmol) and the vasodilator effects of acetycholine (ACh: 100 pmol) and bradykinin (BK: 1000 pmol) on the precontracted arterial (methoxamine, 100 μM) and venous (U46619, 0.5 μM) vasculature in the absence (open columns) or presence (solid columns) of BQ-123 (0.1 μM). Columns indicate the mean with s.e. mean of 4–8 determinations. $*P<0.01$; $**P<0.001$.

8.1 ± 1.3 mmHg, venous side: 4.6 ± 1.0 mmHg; + BQ-123, arterial side: 9.5 ± 3.1 mmHg, venous side: 5.1 ± 0.8 mmHg, $n = 4$: Figure 3a and b), while it markedly decreased those induced by endothelin-1 (25 pmol) on both sides of the mesenteric vasculature (Figures 3a and b).

Comparison of the vasoconstrictor and vasodilator effects of endothelin-3 in the perfused mesenteric vascular bed

Infusions of methoxamine (100 μM, arterial side) or U46619 (0.5 μM, venous side) increased the perfusion pressures by 35.1 ± 3.2 mmHg ($n = 14$) and 12.3 ± 0.9 mmHg ($n = 12$), respectively (Figure 4). Endothelin-3 (10–300 pmol) induced dose-dependent vasodilatations of the arterial vessels, and vasoconstrictions of the venous side of the mesenteric vasculature. In addition, acetylcholine (100 pmol) and bradykinin (1000 pmol) induced marked vasodilatations of the arterial and venous portion of the mesenteric bed, respectively (20 ± 3% and 18 ± 3%, $n = 5–6$). BQ-123 (0.1 μM) had no significant effect on the vasodilator response of the arterial vessels to endothelin-3, but significantly reduced its venoconstrictor effects. The antagonist had no effect on the vasodilatation induced by acetylcholine (100 pmol: 19 ± 3%) in the arterial vasculature nor by bradykinin (1000 pmol: 16 ± 2%) in the venous vasculature (Figure 4).

Discussion

Bolus *i.v.* administration of endothelin-1 induces a prolonged pressor response preceded by an initial transient depressor response in conscious and anaesthetized rats (de Nucci *et al.*, 1988; Yanagisawa *et al.*, 1988; Gardiner *et al.*, 1990). The selective ET_A receptor antagonists, BQ-153 and BQ-123, significantly reduce the pressor response to endothelin-1 in conscious rats, yet do not alter its initial hypotensive effect (Ihara *et al.*, 1992a). The latter observation strongly suggests that while the pressor response to endothelin-1 is predominantly mediated by the activation of ET_A receptors, the initial hypotensive response may be due to the activation

of ET_B receptors (Ihara *et al.*, 1992a) and the possible release of EDNO (Whittle *et al.*, 1989).

In order to examine this possibility, we have tested the endothelins in the double perfused mesenteric bed of the rat, in which it is possible to assess separately the EDNO-releasing and vasoconstrictor properties of various peptides and autacoids (Warner, 1990).

The present study shows that the selective ET_A receptor antagonist, BQ-123, markedly reduced in a specific and concentration-dependent fashion, the constrictor effects of endothelin-1 in both the arterial and venous sides of the mesenteric circulation of the rat. This confirms that endothelin-1 vasoconstricts the mesenteric bed via the activation of ET_A receptors. In addition, our results show that BQ-123, even at high concentrations, did not affect the vasodilatations induced by endothelin-3. This peptide was used as a vasodilator agent, instead of endothelin-1, since it is a less potent vasoconstrictor agent within this preparation and so more readily permits the characterization of the vasodilator properties of endothelins, which have been reported *in vivo* and in various vascular beds (Warner *et al.*, 1989; Lidbury *et al.*, 1990).

Spinella *et al.* (1991) have reported the antagonist properties of an endothelin analogue ([D-Asp^1]-endothelin-1), which markedly reduced the vasoconstrictive properties of endothelin-1 in the rat perfused lung. In addition, this group has shown that the antagonist was selective for endothelin-1 and did not affect the increase in perfusion pressure induced by endothelin-3 in the same experimental model. In contrast, in the present study, we have shown that BQ-123 also markedly reduced the vasoconstrictions induced by endothelin-3 in the rat perfused mesenteric bed. The recent cloning of two endothelin receptor subtypes, namely ET_A (Arai *et al.*, 1990) and ET_B (Sakurai *et al.*, 1990), has included the observation that the endothelins (endothelin-1, 2 and 3) show different orders of potency on these two receptor subtypes. On the ET_A receptor, endothelin-1 is much more potent than endothelin-3, whereas on the ET_B receptor, both peptides are equipotent (Arai *et al.*, 1990; Sakurai *et al.*, 1990). As shown in the present study, endothelin-1 was found to be 20 to 40 times more active than endothelin-3 at constricting both sides of the rat mesenteric vasculature, thus suggesting that the vasoconstrictor effects of endothelin-1 in this vasculature are mediated by the activation of ET_A receptors. This hypothesis is confirmed by experiments using BQ-123, which markedly reduced the vasoconstrictor responses to endothelin-1 and -3. The increase in perfusion pressure caused by BQ-3020 or IRL 1620, two highly selective ET_B receptor agonists (Ihara *et al.*, 1992b; Takai *et al.*, 1992) in the venous mesenteric vasculature, illustrates the presence of a relatively small proportion of non-ET_A receptors in the mesenteric vasculature, as initially reported by Randall *et al.* (1989) in the blood perfused mesenteric bed of the rat.

Our data also indicate that endothelins release EDNO via the activation of ET_B receptors in the arterial mesenteric vasculature. This conclusion is reinforced by the observations of Karaki *et al.* (1993) who have reported ET_B-mediated vasodilator properties of endothelin-3 in rat aortic rings. It is also noteworthy that endothelin-3 induced marked vasodilatation in the arterial, but not in the venous portion of the mesenteric vasculature, even though the veins responded to bradykinin with endothelium-dependent vasodilatations (Warner, 1990).

In conclusion, we have shown that endothelin-1 and endothelin-3 induced arterial and venous constrictions via the activation of ET_A receptors and arterial vasodilatation via the activation of BQ-123-insensitive receptors, probably of the ET_B type, in the mesenteric vasculature of the rat.

The authors would like to thank Ms H. Morin for her secretarial work and Mr M. Takai (Ciba-Geigy, Japan) for the generous supply of IRL 1620. The work was performed with the financial support of the Medical Research Council of Canada and the Heart and Stroke Foundation of Québec. S.T. has a studentship of the Fonds de la recherche en santé du Québec. P.D.J. is a scholar of the Heart and Stroke Foundation of Canada.

References

ARAI, H., HORI, S., ARAMORI, I., OHKUBO, H. & NAKANISHI, S. (1990). Cloning and expression of a cDNA encoding an endothelin receptor. *Nature*, **348**, 730–732.

BIGAUD, M. & PELTON, J.T. (1992). Discrimination between ET_A- and ET_B-receptor-mediated effects of endothelin-1 and [Ala^{1,3,11,15}] endothelin-1 by BQ-123 in the anaesthetized rat. *Br. J. Pharmacol.*, **107**, 912–918.

CLAING, A., TÉLÉMAQUE, S., CADIEUX, A., FOURNIER, A., REGOLI, D. & D'ORLÉANS-JUSTE, P. (1992). Nonadrenergic and noncholinergic arterial dilatation and venoconstriction are mediated by calcitonin gene-related peptide$_1$ and neurokinin-1 receptors, respectively, in the mesenteric vasculature of the rat after perivascular nerve stimulation. *J. Pharmacol. Exp. Ther.*, **263**, 1226–1232.

D'ORLÉANS-JUSTE, P., CLAING, A., TÉLÉMAQUE, S., WARNER, T.D. & REGOLI, D. (1991). Neurokinins produce selective venoconstriction via NK-3 receptors in the rat mesenteric vascular bed. *Eur. J. Pharmacol.*, **204**, 329–334.

D'ORLÉANS-JUSTE, P., TÉLÉMAQUE, S., CLAING, A., IHARA, M. & YANO, M. (1992). Human big-endothelin-1 and endothelin-1 release prostacyclin via the activation of ET_1 receptors in the rat perfused lung. *Br. J. Pharmacol.*, **105**, 773–775.

DE NUCCI, G., THOMAS, R., D'ORLÉANS-JUSTE, P., ANTUNES, E., WALDER, C., WARNER, T.D. & VANE, J.R. (1988). Pressor effects of circulating endothelin are limited by its removal in the pulmonary circulation and by the release of prostacyclin and endothelium-derived relaxing factor. *Proc. Natl. Acad. Sci. USA*, **85**, 9797–9800.

DOUGLAS, S.A., ELLIOTT, J.D. & OHLSTEIN, E.H. (1992). Regional vasodilatation to endothelin-1 is mediated by a non-ET_A receptor subtype in the anaesthetized rat: effect of BQ-123 on systemic haemodynamic responses. *Eur. J. Pharmacol.*, **221**, 315–324.

DOUGLAS, S.A. & HILEY, C.R. (1991). Responses to endothelin-1, human proendothelin (1–38) and porcine proendothelin (1–39) in the rat on intravenous administration and in the blood perfused mesentery. *Neurochem. Int.*, **18**, 445–454.

GARDINER, S.M., COMPTON, A.M. & BENNETT, T. (1990), Regional haemodynamic effects of endothelin-1 and endothelin-3 in conscious Long Evans and Brattleboro rats. *Br. J. Pharmacol.*, **99**, 107–112.

IHARA, M., NOGUCHI, K., SAEKI, T., FUKURODA, T., TSUCHIDA, S., KIMURA, S., FUKAMI, T., ISHIKAWA, K., NISHIKIBE, M. & YANO, M. (1992a). Biological profiles of highly potent novel endothelin antagonists selective for the ET_A receptor. *Life Sci.*, **50**, 247–255.

IHARA, M., SAEKI, T., FUKURODA, T., KIMURA, S., OZAKI, S., PATEL, A.C. & YANO, M. (1992b). A novel radioligand [^{125}I]BQ-3020 selective for endothelin (ET_B) receptors. *Life Sci.*, **51**, PL47–52.

KARAKI, H., SUDJARWO, S.A., HORI, M., SAKATA, K., URADE, Y., TAKAI, M. & OKADA, T. (1993). ET_B receptor antagonist, IRL 1038, selectively inhibits the endothelin-induced endothelium-dependent vascular relaxation. *Eur. J. Pharmacol.*, **231**, 371–374.

LE MONNIER DE GOUVILLE, A.C., MONDOT, S., LIPPTON, H., HYMAN, A. & CAVERO, I. (1990). Hemodynamic and pharmacological evaluation of the vasodilator and vasoconstrictor effects of endothelin-1 in rats. *J. Pharmacol. Exp. Ther.*, **252**, 300–311.

LIDBURY, P.S., THIEMERMANN, C., KORBUT, R. & VANE, J.R. (1990). Endothelins release tissue plasminogen activator and prostanoids. *Eur. J. Pharmacol.*, **186**, 205–212.

MCGREGOR, D.D. (1965). The effect of sympathetic nerve stimulation on vasoconstrictor responses in perfused mesenteric blood vessels of the rat. *J. Physiol.*, **177**, 21–30.

MORELAND, S., MCMULLEN, D.M., DELANEY, C.L., LEE, V.G. & HUNT, J.T. (1992). Venous smooth muscle contains vasoconstrictor ET_B-like receptors. *Biochem. Biophys. Res. Commun.*, **184**, 100–106.

NAKAMICHI, K., IHARA, M., KOBAYASHI, M., SAEKI, T., ISHIKAWA, K. & YANO, M. (1992). Different distribution of endothelin receptor subtypes in pulmonary tissues revealed by the novel selective ligands BQ-123 and [$Ala^{1,3,11,15}$]-endothelin-1. *Biochem. Biophys. Res. Commun.*, **182**, 144–150.

RANDALL, M.D., DOUGLAS, S.A. & HILEY, C.R. (1989). Vascular activities of endothelin-1 and some alanyl substituted analogues in resistance beds of the rat. *Br. J. Pharmacol.*, **98**, 685–699.

SAKURAI, T., YANAGISAWA, M., TAKUWA, Y., MIYAZAKI, H., KIMURA, S., GOTO, K. & MASAKI, T. (1990). Cloning of a cDNA encoding a non-isopeptide-selective subtype of the endothelin receptor. *Nature*, **348**, 732–735.

SPINELLA, M.J., MALIK, A.B., EVERITT, J. & ANDERSEN, T.T. (1991). Design and synthesis of a specific endothelin-1 antagonist: effects on pulmonary vasoconstriction. *Proc. Natl. Acad. Sci. U.S.A.*, **88**, 7443–7446.

TAKAI, M., UMEMURA, I., YAMASAKI, K., WATAKABE, T., FUJITANI, Y., ODA, K., URADE, Y., INUI, T., YAMAMURA, T. & OKADA, T. (1992). A potent and specific agonist, Suc-[Glu^9, $Ala^{11,15}$]-endothelin-1(8–21), IRL 1620, for the ET_B receptor. *Biochem. Biophys. Res. Commun.*, **184**, 953–959.

WALLENSTEIN, S., ZUCKER, C.L. & FLEISS, J.L. (1980). Some statistical methods useful in circulation research. *Circ. Res.*, **47**, 1–9.

WARNER, T.D. (1990). Simultaneous perfusion of rat isolated superior mesenteric arterial and venous beds: comparison of their vasoconstrictor and vasodilator responses to agonists. *Br. J. Pharmacol.*, **99**, 427–433.

WARNER, T.D., DE NUCCI, G. & VANE, J.R. (1989). Rat endothelin is a vasodilator in the isolated perfused mesentery of the rat. *Eur. J. Pharmacol.*, **159**, 325–326.

WEBB, D.J., (1991). Endothelin receptors cloned, endothelin converting enzyme characterized and pathophysiological roles for endothelin proposed. *Trends Pharmacol. Sci.*, **12**, 43–46.

WHITTLE, B.J., LOPEZ-BELMONTE, J. & REES, D.D. (1989). Modulation of the vasodepressor actions of acetylcholine, bradykinin, substance P and endothelin in the rat by a specific inhibitor of nitric oxide formation. *Br. J. Pharmacol.*, **98**, 646–652.

YANAGISAWA, M., KURIHARA, H., KIMURA, S., TOMOBE, Y., KOBAYASHI, M., MITSUI, Y., YAZAKI, Y., GOTO, K. & MASAKI, T. (1988). A novel potent vasoconstrictor peptide produced by vascular endothelial cells. *Nature*, **332**, 411–415.

(Received October 19, 1992
Revised June 7, 1993
Accepted June 11, 1993)

Br. J. Pharmacol. (1993), **110**, 693–700

Identification of both NK_1 and NK_2 receptors in guinea-pig airways

Katherine T. McKee, Lorna Millar, Ian W. Rodger & [1]Kathleen M. Metters

Department of Pharmacology, Merck Frosst Centre for Therapeutic Research, P.O. Box 1005, Pointe-Claire, Dorval, Québec H9R 4P8, Canada

1 NK_1 and NK_2 receptors have been characterized in guinea-pig lung membrane preparations by use of [^{125}I-Tyr^8]-substance P and [^{125}I]-neurokinin A binding assays in conjunction with tachykinin-receptor selective agonists ([Sar^{9}Met(O$_2$)^{11}]substance P for NK_1 and [βAla^8]neurokinin A (4–10) for NK_2) and antagonists (CP-99,994 for NK_1 and SR48968 for NK_2).

2 The presence of high affinity, G-protein-coupled NK_1 receptors in guinea-pig lung parenchymal membranes has been confirmed. The rank order of affinity for competing tachykinins was as predicted for an NK_1 receptor: substance P = [Sar^{9}Met(O$_2$)^{11}]substance P > substance P-methyl ester = physalaemin > neurokinin A = neurokinin B >> [βAla^8]neurokinin A (4–10). The novel NK_1 antagonist CP-99,994 has a K_i of 0.4 nM at this NK_1 site.

3 In order to characterize [^{125}I]-neurokinin A binding to guinea-pig lung, the number of [^{125}I]-neurokinin A specific binding sites was increased 3–4 fold by purification of the parenchymal membranes over discontinuous sucrose gradients. The rank order of affinity determined for NK_1- and NK_2-receptor agonists and antagonists in competition for these sites showed that the majority (80%) of [^{125}I]-neurokinin A specific binding was also to the NK_1 receptor.

4 Under conditions where the guinea-pig lung parenchymal NK_1 receptor was fully occupied by a saturating concentration of either [Sar^{9}Met(O$_2$)^{11}]substance P (1 μM) or CP-99,994 (2.7 μM), residual [^{125}I]-neurokinin A specific binding was inhibited in a concentration-dependent manner by both [βAla^8]neurokinin A and SR48968. This result shows that the NK_2 receptor is also present in these preparations.

5 Similar studies using guinea-pig tracheal membranes demonstrated that [^{125}I]-neurokinin A specific binding was composed of a NK_1-receptor component (60%), inhibited by both [Sar^{9}Met(O$_2$)^{11}]substance P and CP-99,994, and a significant NK_2-receptor component, inhibited by both [βAla^8]neurokinin A and SR48968.

6 In summary, these data demonstrate that guinea-pig lung parenchyma and guinea-pig trachea express both NK_1 and NK_2 receptors.

Keywords: Tachykinin; substance P; CP-99,994; SR48968; guinea-pig airways; neurogenic inflammation; radioligand binding

Introduction

Substance P (SP), neurokinin A (NKA) and neurokinin B (NKB) form part of the mammalian tachykinin family of biologically active peptides (Maggio, 1988). The wide spectrum of neuronal and non-neuronal physiological events involving tachykinins are receptor-mediated. These peptides all share the conserved carboxyl-terminal sequence (Phe-X-Gly-Leu-Met-NH_2) which is essential for receptor activation, while their diverse amino terminal domains are thought to govern receptor selectivity (Krause *et al.*, 1992). Substance P, NKA and NKB have been shown to interact preferentially with NK_1, NK_2 and NK_3 receptors, respectively, three distinct G-protein-coupled receptor types which have now been cloned and sequenced (Masu *et al.*, 1987; Yokoto *et al.*, 1989; Shigemoto *et al.*, 1990).

The results of *in vitro* and *in vivo* studies show that tachykinins are mediators of bronchoconstriction, plasma extravasation, mucous production and vasodilatation, all characteristic of neurogenic inflammation in the respiratory tract (Barnes *et al.*, 1990). These peptides are released from sensory nerve fibres originating in the airway epithelium in response to a variety of noxious stimuli (Solway & Leff, 1991), producing pronounced spasmogenic effects on respiratory smooth muscle. In addition, SP and NKA are known to modulate immune cell function through their effects on T-lymphocytes, B-lymphocytes, macrophages, mast cells and monocytes (Casale, 1991). It has been proposed, therefore, that the tachykinins may contribute to the pathogenesis of certain respiratory disease states such as bronchial asthma, both by decreasing airway calibre and modulating the cells involved in the inflammatory response.

The precise role played by the individual tachykinins and their receptor types in pulmonary pathophysiology is currently being elucidated. It has been demonstrated that plasma extravasation in guinea-pig upper airways (trachea and main bronchi) is mediated via NK_1 receptors (Murai *et al.*, 1992), whereas in lower airways (secondary bronchi and intraparenchymal airways) plasma extravasation is mediated via both NK_1 and NK_2 receptors (Tousignant *et al.*, 1993a,b). Similarly, bronchoconstriction in guinea- pig airways appears to be mediated via both NK_1 and NK_2 receptor types (Regoli *et al.*, 1987). In support of these functional studies suggesting that guinea-pig respiratory tissues contain multiple tachykinin-receptor types, several groups have characterized NK_1 receptors in guinea-pig lung membranes by radioligand binding techniques (Coats & Gerard, 1989; Aharony *et al.*, 1991; Geraghty *et al.*, 1992). However, as yet, NK_2 receptors have not been identified unambiguously to be present in these preparations.

Delineating the receptor types present in guinea-pig lung is complicated by the non-selectivity of the endogenous tachykinins normally used as probes and, in addition, the extreme susceptibility of these peptides to metabolism by a variety of proteases. These problems have been partially alleviated by the development of metabolically stable and highly selective peptide agonists {[Sar^9,Met(O$_2$)^{11}]-SP (Regoli

[1] Author for correspondence.

et al., 1988) at the NK_1 site and [β-Ala^8]NKA (4–10) (Rovero et al., 1989) at the NK_2 site} and non-peptide antagonists {CP-99,994 (McLean et al., 1992) at the NK_1 site and SR48968 (Emonds-Alt et al., 1992) at the NK_2 site}. In this paper we have used these selective agonists and antagonists, in conjunction with radioligand binding techniques, to identify both NK_1 and NK_2 receptors in guinea-pig lung parenchyma and trachea.

Methods

Guinea-pig lung parenchymal and tracheal membrane preparation

Guinea pigs (male; 350 g) were killed by cervical dislocation and the lung tissues removed. All subsequent procedures were performed either on ice or at 4°C. The tracheae were removed and processed as described below. The remaining connective tissue, major airways and large blood vessels were then dissected away and the lung tissue (principally parenchyma) was finely minced prior to homogenization in 10 volumes of 10 mM HEPES/KOH, pH 7.4, containing 0.25 M sucrose, 2 mM EDTA, 2 mM phenylmethylsulphonyl fluoride, 10 μg ml^{-1} pepstatin, 10 μg ml^{-1} leupeptin, and 10 μM E-64, using 5 s bursts of a Polytron homogenizer (Brinkman Instruments). The homogenate was then subjected to differential centrifugation at 1,000 *g* for 10 min, at 10,000 *g* for 15 min, and finally at 100,000 *g* for 40 min. The resulting pellets were washed by resuspension in 20 vol of 10 mM HEPES/ KOH, pH 7.4, followed by centrifugation at 150,000 *g* for 40 min. The final membrane pellets were resuspended in 50 mM Tris/HCl, pH 7.4, at a final concentration of 7–10 mg ml^{-1} of membrane protein and stored at − 80°C.

For the [^{125}I]-NKA binding assays, the guinea-pig lung membranes were further purified over discontinuous sucrose gradients. The 100,000 *g* membrane fraction was resuspended in 10 mM HEPES/KOH, pH 7.4, containing 10% (w/v) sucrose, at a final protein concentration of 1–2 mg ml^{-1}. The tissue suspension was then carefully layered over 10 mM HEPES/KOH, pH 7.4, containing 40% (w/v) sucrose in a 3:2 (v/v) ratio. The discontinuous sucrose gradient was centrifuged in a swinging bucket rotor at 83,000 *g* for 60 min. The membrane fraction located at the interface of the sucrose gradient layers was recovered using an automated pump (Buchler Instruments) and then washed by a 10 fold dilution in 10 mM HEPES/KOH, pH 7.4, followed by centrifugation at 150,000 *g* for 40 min. The final membrane pellets were again resuspended in 50 mM Tris/HCl, pH 7.4, at a final concentration of 3–5 mg ml^{-1} of membrane protein and stored at − 80°C.

Guinea-pig tracheal membranes were prepared by homogenization, as described for the parenchymal preparations. The homogenate was initially centrifuged at 1,000 *g* for 15 min, and then at 100,000 *g* for 40 min. The membrane pellets were resuspended at 50 mM Tris/HCl, pH 7.4, at a final concentration of 3–8 mg ml^{-1} of tracheal membrane protein and stored at − 80°C.

[^{125}I]-neurokinin radioreceptor binding assays

[^{125}I]-neurokinin ([^{125}I]-NK) binding assays were routinely performed in 50 mM Tris/HCl, pH 7.4, containing 0.01% (w/v) bovine serum albumin, 200 μM chymostatin, 100 μM leupeptin, 100 μM phosphoramidon, 100 μM captopril, 250 μM bestatin, and 0.005% (v/v) 2-mercaptoethanol. For the guinea-pig lung parenchymal [^{125}I-Tyr^8]-SP binding assay, the 250 μl incubations also included 1 mM $MnCl_2$, 20–25 pM [^{125}I-Tyr^8]-SP and 75 μg of membrane protein. Non-specific binding was determined in the presence of 1 μM SP. For the guinea-pig lung parenchymal [^{125}I]-NKA binding assay, the 500 μl incubations also included 3 mM $MnCl_2$, 20–25 pM [^{125}I]-NKA and 250 μg of sucrose-purified membrane protein. For the guinea-pig tracheal [^{125}I]-NKA binding assay the 500 μl incubation also included 10 mM $MnCl_2$, 50 pM [^{125}I]-NKA and 300–500 μg of membrane protein. Non-specific binding was determined in the presence of 1 μM NKA. Aliquots of frozen membrane preparations were initially resuspended in the presence of EDTA, to give a final concentration of 1 mM in the incubation medium.

Incubations were conducted for 1 h for [^{125}I-Tyr^8]-SP binding assays and 2 h for [^{125}I]-NKA binding assays, both at room temperature. Bound and free radioligand was then separated by rapid filtration, under vacuum, through Whatman GF/B filters presoaked for 4 h, at 4°C, in 20 mM Tris/HCl, pH 7.4, containing 0.1% polyethylenimine and 0.01% (w/v) bovine serum albumin (BSA). The filters were washed with approximately 16 ml of 20 mM Tris/HCl, pH 7.4, containing 0.01% (w/v) BSA and the residual radioactivity bound to the filters determined by gamma counting, with an efficiency of approximately 80%.

In all experiments specific binding was defined as the difference between total binding and non-specific binding, determined in the presence of an excess (> 10000 fold) of the appropriate unlabelled competing ligand. Specific binding was linear with respect to both membrane protein concentration and radioligand concentration, and routinely represented 70–90% of the total radioligand bound to the membrane protein.

Data calculation

The first-order dissociation rate constant (k_{-1}) was determined as the slope obtained by linear regression analysis of plots of ln B/B_0 on the y-axis, versus incubation time in min on the x-axis, where B is the amount of radioligand bound at a given incubation time and B_0 is the amount of radioligand bound at time zero. This analysis was also employed to determine the observed association rate constant (k_{obs}) which was then expressed as k_{obs}/[radioligand].

Scatchard plot analysis was performed by linear transformation of saturation binding curves using Accufit Saturation-One Site data analysis software (Beckman Instruments Inc.) based on the linear transformation of Scatchard (1949) and Rosenthal (1967). Hill coefficients were determined as the slope obtained by linear regression analysis of plots of log $B/(B_{max}-B)$ (y-axis) versus log [radioligand] (x-axis), where B is the amount of specific binding at a given radioligand concentration and B_{max} is the maximum specific binding observed (Hill, 1910).

Sigmoidal equilibrium competition curves were analysed by custom designed software employing a non-linear least-squares curve fitting routine based on a four parameter logistic equation to determine IC_{50} values and slope factors (apparent Hill coefficients). The corresponding K_i values were calculated from the equation $K_i = IC_{50}/1 + ([\text{radioligand}]/K_D)$.

Reverse phase high performance liquid chromatography

Reverse phase high performance liquid chromatography (r.p.-h.p.l.c) was employed to assess the stability of the [^{125}I]-NKs under radioreceptor binding assay conditions. [^{125}I]-neurokinin binding assays were performed in a final incubation volume of 500 μl of 50 mM Tris/HCl, pH 7.4, essentially as described above, but omitting $MnCl_2$, which was found to interfere with r.p.-h.p.l.c. analysis. The incubation medium also contained different combinations of the following inhibitors: leupeptin (0–100 μM), phosphoramidon (0–100 μM), captopril (0–100 μM), chymostatin (0–200 μM) and bestatin (0–250 μM). Control incubations were performed both in the absence of inhibitors and the absence of membranes.

Following a 1 h or 2 h incubation at room temperature for [^{125}I-Tyr^8]-SP and [^{125}I]-NKA binding assays, respectively, the membranes were recovered by centrifugation at 150,000 *g* for 15 min, at 4°C. The supernatant containing the unbound

radioligand was removed, the resulting membrane pellet resuspended by sonication in 250 µl of 0.1% (v/v) trifluoroacetic acid (TFA) and the supernatant containing the bound radioligand recovered by a second centrifugation, conducted under the same conditions. Unbound and bound radioligand fractions were analysed by r.p.-h.p.l.c., using a Nova Pak C_{18} column (0.39 × 15 cm; Waters Associates) equilibrated in 0.1% (v/v) TFA. Following the initial 5 min wash with 0.1% (v/v) TFA, the [^{125}I]-peptide(s) was eluted with a linear gradient from 0 to 60% (v/v) acetonitrile in 0.1% TFA, developed over 60 min, at a flow rate of 1 ml min^{-1}. The radioactivity profile was monitored by on-line solid scintillation counting using a flow-through h.p.l.c. radioactivity monitor. The recovery following r.p.-h.p.l.c. was 100%.

Protein determination

Protein concentration was determined by monitoring the absorbance at 562 nm produced by the formation of protein-Cu^{1+}-bicinchoninic acid complexes in alkaline solution (Smith *et al.*, 1985), with BSA used as the standard.

Materials

Guinea-pigs were obtained from Charles River (LaSalle Québec, Canada); [^{125}I-Tyr^8]-SP (2200 Ci mmol^{-1}) and [^{125}I]-NKA (2200 Ci mmol^{-1}) were from New England Nuclear (Mississauga, Ontario, Canada); SP, NKA, neurokinin B, SP methyl ester, physalaemin, [Sar^9,Met(O$_2$)^{11}]SP, and [β-Ala^8]-NKA (4–10) were from Peninsula Laboratories, Inc. (Belmont, CA, U.S.A.); MEN 10,376 (H-Asp-Tyr-(D)Trp-Val-(D)Trp-(D)Trp-Lys-NH_2) was from IAF BioChem (Montréal, Québec, Canada); CP-99,994 ((+),(2S,3S)-3-(2-methoxybenzylamino)-2-phenylpiperidine), L-736,322 ((−),(2R,3R)-3-(2-methoxybenzylamino)-2-phenylpiperidine), RP67580 (7,7-diphenyl-2[1-imino-2(2-methoxyphenyl)-ethyl]perhydroisoindol-4-one (3aR,7aR)), RP68651 (7,7-diphenyl-2[1-imino-2(2-methoxyphenyl)-ethyl]perhydroisoindol-4-one (3aS,7aS)) and SR49868 ((S)-N-methyl-N[4-(4-acetylamino-4-phenyl piperidino)-2-(3,4-dichlorophenyl)butyl]benzamide) were synthesized by Merck Research Laboratories; E-64 and GTPγS were from Boehringer Mannheim (Laval, Québec, Canada); eledoisin, senktide, bestatin, captopril, chymostatin, leupeptin, pepstatin, phosphoramidon, phenylmethylsulphonyl fluoride, EDTA and polyethylenimine were from the Sigma Chemical Company (St. Louis, Missouri, U.S.A.); the protein determination kit was from Pierce (Rockford, U.S.A.). All other reagents were of analytical grade.

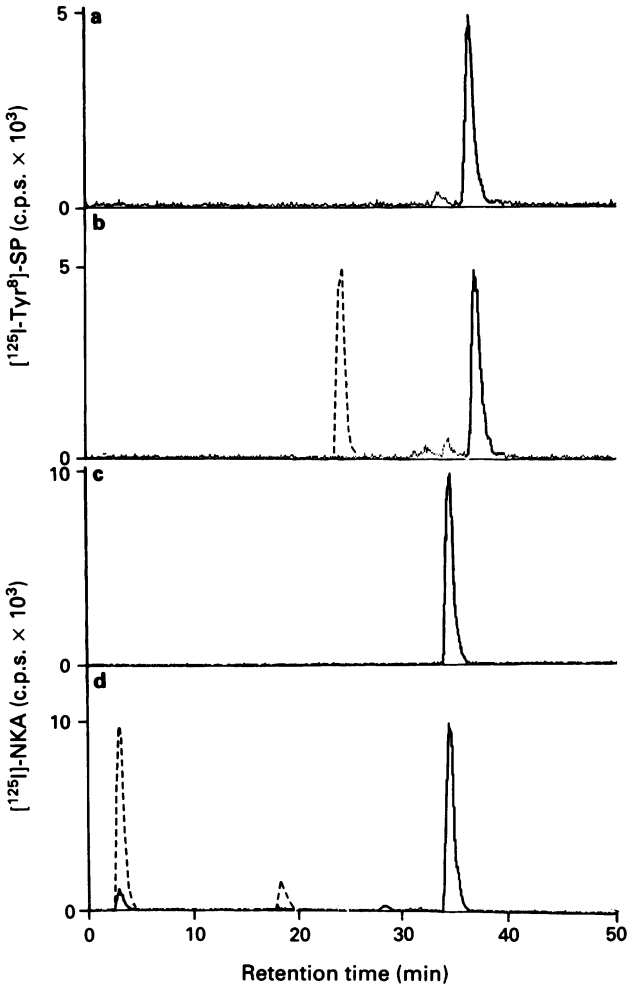

Figure 1 R.p.-h.p.l.c. analysis of [^{125}I-Tyr^8]-substance P ([^{125}I-Tyr^8]-SP) and [^{125}I]-neurokinin A ([^{125}I]-NKA) metabolism. The stability of [^{125}I-Tyr^8]-SP and [^{125}I]-NKA during radioreceptor binding assays was assessed by r.p.-h.p.l.c., as described in the Methods. (a) and (c) show the elution positions of the [^{125}I-Tyr^8]-SP and [^{125}I]-NKA standards; (b) and (d) show the profile of unbound radiolabelled material following incubation of [^{125}]-Tyr^8]-SP and [^{125}I]-NKA in the absence (- - - -) and presence (———) of an inhibitor mixture of leupeptin (100 µM), phosphoramidon (100 µM), captopril (100 µM), chymostatin (200 µM) and bestatin (250 µM). The profile obtained for bound radiolabelled material was essentially the same (data not shown).

Results

[^{125}I]-neurokinin metabolism

Both [^{125}I-Tyr^8]-SP and [^{125}I]-NKA were completely degraded when incubated with guinea-pig lung parenchymal membranes, in the absence of protease inhibitors, under the conditions used for [^{125}I]-NK binding assays (Figure 1). Both radioligands were stable when incubated in the absence of membranes. Extensive r.p.-h.p.l.c. analysis of binding assay incubations was conducted in order to establish the precise inhibitor mixture necessary to prevent [^{125}I]-NK metabolism. Protease inhibitors effective against different classes of enzymes were evaluated over a concentration range up to 500 µM, both singly and in various combinations. The following inhibitors were all found to be essential in blocking a component of [^{125}I]-NK degradation at the concentration indicated, and were routinely included in [^{125}I]-NK binding assay incubations: phosphoramidon (100 µM) for neutral endopeptidase (EC 3.4.24.11), bestatin (250 µM) for aminopeptidase, captopril (100 µM) for angiotensin coverting enzyme (EC 3.14.5.1), chymostatin (200 µM) for chymotrypsin-like serine proteases, and leupeptin (100 µM) for trypsin-like serine proteases. Thiorphan, a specific neutral endopeptidase inhibitor, was found to be equipotent with phosphoramidon in inhibiting [^{125}I]-NK breakdown, while the cysteine protease inhibitor E-64 and the aspartic protease inhibitor pepstatin had no effect. Analysis by r.p.-h.p.l.c. showed that the chosen mixture inhibited over 90% of the [^{125}I]-NK degradation previously observed, in both the unbound and bound radioligand fractions, over the binding assay incubation period (Figure 1). The inhibitor mixture also blocked over 95% of the metabolism of [^{125}I]-NKA by guinea-pig tracheal membranes.

Characterization of the NK_1 receptor in guinea-pig lung parenchymal membranes

Enhancement by divalent cations [^{125}I-Tyr^8]-SP specific binding to guinea-pig lung parenchymal membranes was enhanced in the presence of divalent cations with $Mn^{2+} > Mg^{2+} >> Ca^{2+}$ (Figure 2). The optimum divalent cation concentration was 1 mM for Mn^{2+}, which resulted in a 5–6 fold increase in [^{125}I-Tyr^8]-SP specific binding, from a baseline level of 595 ± 71 c.p.m. to 3450 ± 170 c.p.m. ($n = 3$). Divalent cation concentrations greater than 10 mM proved

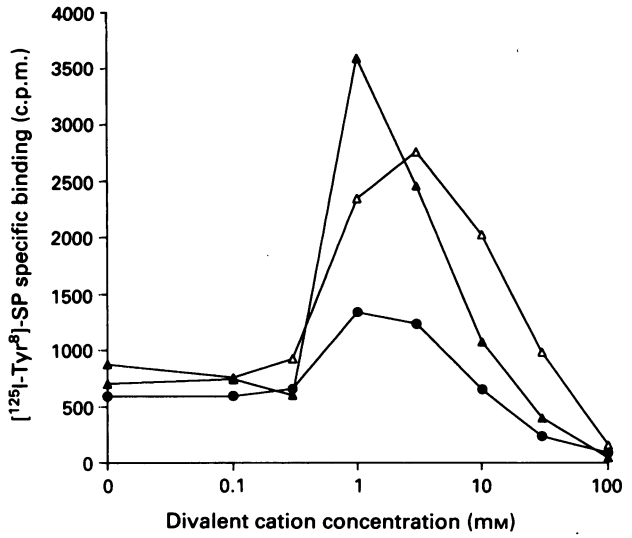

Figure 2 Effect of divalent cations on [^{125}I-Tyr^8]-substance P ([^{125}I-Tyr^8]-SP) specific binding to guinea-pig lung membranes. [^{125}I-Tyr^8]-SP binding assays were performed, as described in the Methods, in the presence of 0–100 mM $MnCl_2$ (▲), $MgCl_2$ (△) and $CaCl_2$ (●). Results are expressed as specific binding in c.p.m. as a function of divalent cation concentration. These are representative data from three experiments giving similar values.

inhibitory, with complete abolition of [^{125}I-Tyr^8]-SP specific binding observed at 100 mM, in all cases.

Rates of association and dissociation The rate of association of [^{125}I-Tyr^8]-SP to guinea-pig lung parenchymal membranes was slow, with an observed association rate constant (k_{obs}/[radioligand]) of approximately 2×10^9 min^{-1} M^{-1} ($n = 2$). Equilibrium was reached over a 1 h incubation period. Addition of a large excess of unlabelled competing SP (1 μM) resulted in a time-dependent dissociation of [^{125}I-Tyr^8]-SP, with a first-order dissociation rate constant (k_{-1}) of 0.018 min^{-1} ($n = 2$). The addition of 100 μM GTPγS with the competing SP, however, provoked complete dissociation of [^{125}I-Tyr^8]-SP binding to non-specific levels within 1 min (Figure 3).

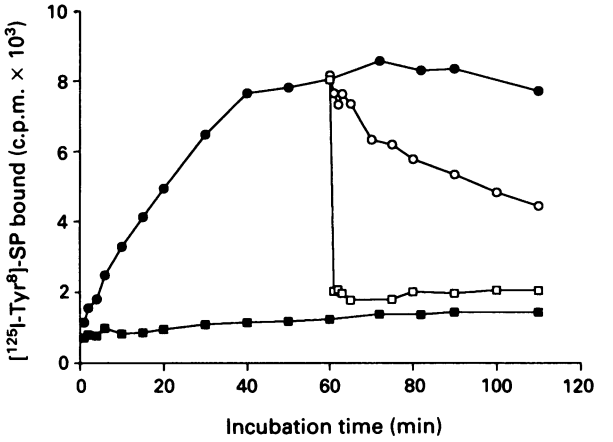

Figure 3 Association and dissociation of [^{125}I-Tyr^8]-substance P ([^{125}I-Tyr^8]-SP) binding to guinea-pig lung membranes. The rates of association of total (●) and non-specific (■) binding of [^{125}I-Tyr^8]-SP to guinea-pig lung parenchymal membranes were followed, at the required time intervals, by removing and filtering 250 μl aliquots from homogeneous binding assay mixtures incubated in the absence (●) or presence (■) of 1 μM SP. At 60 min the rate of dissociation of total binding was monitored, in the same manner, following addition of either 1 μM SP (○), or 1 μM SP with 100 μM GTPγS (□).

Analyses by Scatchard and Hill plot [^{125}I-Tyr^8]-SP specific binding to guinea-pig lung parenchymal membranes was saturable, as demonstrated by incubation with an increasing concentration (2–200 pM) of [^{125}I-Tyr^8]-SP, in the presence and absence of 1 μM unlabelled SP. Scatchard analysis of the deduced specific binding saturation curve demonstrated that [^{125}I]-Tyr^8]-SP specific binding conformed to a single binding site model, with a K_D of 46 ± 4 pM ($n = 3$) and a maximum number of binding sites (B_{max}) of 67 ± 6 fmol mg^{-1} of membrane protein ($n = 3$). Analysis of the specific binding data by Hill plot gave a straight line, with a Hill coefficient of 0.96 ± 0.01 ($n = 3$), close to unity. This confirms that [^{125}I-Tyr^8]-SP was binding in an independent manner to a site, or sites, with one apparent affinity in these preparations, with no evidence for cooperativity.

Equilibrium competition curves Tachykinin-receptor agonists and antagonists were used to compete for [^{125}I-Tyr^8]-SP specific binding to guinea-pig lung parenchymal membranes (Table 1). The most potent competing ligands were the NK_1 preferring SP and the selective NK_1 agonist [Sar^{9}Met(O$_2$)^{11}]-SP, which were equipotent, with IC_{50} values of approximately 0.1 nM. Substance P-methyl ester and the amphibian peptide physalaemin, which also interact preferentially with NK_1 receptors, were only 10–20 fold less potent than SP. In comparison, NKA, NKB and eledoisin, which bind preferentially to NK_2 and NK_3 receptors, respectively, were less effective in competing for [^{125}I-Tyr^8]-SP specific binding to guinea-pig lung parenchymal membranes, being 300–600 fold less potent than SP. Most strikingly, the highly selective NK_2 agonist [βAla^8]NKA (4–10) was considerably less potent when competing for these [^{125}I-Tyr^8]-SP specific binding sites, with an IC_{50} value of 4.4 μM, while the NK_3-selective agonist senktide (Wormser *et al.*, 1986) was inactive.

In agreement with the profile obtained for tachykinin-receptor agonists the selective NK_1-receptor antagonist CP-99,994 was a potent competing ligand for [^{125}I-Tyr^8]-SP specific binding to guinea-pig lung parenchymal membranes, with an IC_{50} value of 0.6 ± 0.1 nM (Table 1). The related **2R,3R** enantiomer L-736,322 was 1,000 fold less potent with an IC_{50} value of 633 ± 118 nM. In contrast, the NK_1 antagonist (−)-RP67580 (Garret *et al.*, 1991) was 300 fold less potent than CP-99,994 in competition assays, with an IC_{50} of 181 ± 31 nM. In this case, the related (+)-enantiomer RP68651 was totally inactive at concentrations up to 20 μM. In comparison, the NK_2-selective antagonists SR48968 and MEN 10,376 (Maggi *et al.*, 1991) were poor competitors for [^{125}I-Tyr^8]-SP specific binding to these preparations, with IC_{50} values of 1.1 μM and > 10 μM, respectively.

Characterization of [^{125}I]-neurokinin A specific binding to guinea-pig lung parenchymal membranes

Enhancement by divalent cations Initial binding assays investigating the effect of divalent cations on [^{125}I]-NKA specific binding to guinea-pig lung parenchymal membranes were conducted using the 100,000 *g* membrane fraction. Under the experimental conditions there was no detectable [^{125}I]-NKA specific binding to these preparations in the absence of divalent cations, but [^{125}I]-NKA specific binding was substantially increased in the presence of both Mg^{2+} and Ca^{2+}. Further experiments demonstrated, however, that Mg^{2+}- and Ca^{2+}-enhanced [^{125}I]-NKA specific binding was not inhibited by GTPγS, neurokinins, other than NKA, nor by receptor antagonists, and did not, therefore, represent specific binding to a tachykinin receptor (data not shown).

In contrast to the results with Mg^{2+} and Ca^{2+}, only a slight enhancement of [^{125}I]-NKA specific binding to guinea-pig lung parenchymal membranes was observed in the presence of Mn^{2+}. Further purification of the guinea-pig parenchymal lung membranes over discontinuous sucrose gradients, however, resulted in a 3–4 fold increase in the number of Mn^{2+}-dependent, [^{125}I]-NKA specific binding sites,

Table 1 Competition curves: tachykinin-receptor agonists and antagonists were used to compete for [^{125}I-Tyr^8]-substance P ([^{125}I-Tyr^8]-SP) specific binding to guinea-pig lung parenchymal membranes and [^{125}I]-neurokinin A ([^{125}I]-NKA) specific binding to sucrose-purified guinea-pig lung parenchymal membranes

	[^{125}I-Tyr^8]-SP		*[^{125}I]-NKA*	
Competing ligand	*IC_{50} (nM)*	*Slope factor*	*IC_{50} (nM)*	*Slope factor*
Agonist				
NK_1				
SP	0.083 ± 0.004 (10)	0.98 ± 0.02 (9)	0.17 ± 0.09 (3)	1.25 ± 0.05 (3)
[Sar^{9}Met(O$_2$)^{11}]SP	0.11 ± 0.01 (3)	0.92 ± 0.03 (3)	0.12 ± 0.01 (6)*	0.96 ± 0.12 (5)
SP-methyl ester	1.35 ± 0.09 (3)	0.85 ± 0.03 (3)	0.84 ± 0.42 (3)	0.58 ± 0.04 (3)
Physalaemin	1.5 ± 0.4 (3)	1.1 ± 0.2 (3)	0.3 (1)	0.73 (1)
NK_2				
NKA	31 ± 5 (3)	0.74 ± 0.04 (3)	2.3 ± 0.3 (4)	0.96 ± 0.07 (4)
[β-Ala^8]NKA (4–10)	4393 ± 472 (3)	0.73 ± 0.1 (3)	87 ± 11 (3)	0.69 ± 0.09 (3)
NK_3				
NKB	28.4 ± 0.3 (3)	0.83 ± 0.04 (3)	9 (2)	0.79 (2)
senktide	> 10000 (3)		> 10000 (3)	
Antagonist				
NK_1				
CP-99,994	0.6 ± 0.1 (3)	1.03 ± 0.02 (3)	0.47 ± 0.05 (4)*	0.64 ± 0.11 (4)
L-736,322	633 ± 118 (3)	1.05 ± 0.06 (3)	447 (2)*	0.53 (2)
RP67580	181 ± 31 (3)	0.93 ± 0.03 (3)	ND	
RP68651	> 20000 (2)		ND	
NK_2				
SR48968	1170 ± 202 (3)	0.92 ± 0.07 (3)	617 ± 71 (3)	0.66 ± 0.11 (3)
MEN 10376	> 10000 (3)		7763 ± 872 (3)	0.57 ± 0.06 (3)

IC_{50} values and slope factors (apparent Hill coefficients) were determined as described in the Methods and are shown ± s.e.mean with the number of observations given in parentheses. ND = not determined. Maximum specific binding was defined as the difference between total binding and non-specific binding determined in the presence of 1 μM of SP or NKA, respectively. The maximum inhibition of specific binding (I_{max}) was 100% in all cases except for the inhibition of [^{125}I]-NKA specific binding by [Sar^{9}Met(O$_2$)^{11}]SP, CP-99,994 and L-736,322 where I_{max} was 80% (*). The IC_{50} values and slope factors for these three competing ligands were calculated with non-specific binding determined in the presence of 1 μM of [Sar^{9}Met(O$_2$)^{11}]SP or CP-99,994 or 30 μM L-736,322, respectively.

from 0.59 ± 0.03 to 1.87 ± 0.06 fmol of [^{125}I]-NKA bound mg^{-1} membrane protein ($n = 3$). The optimal Mn^{2+} concentration for both purified and non-purified membrane preparations was 3 mM. In addition, Mn^{2+}-enhanced [^{125}I]-NKA specific binding fulfilled the criteria for binding specifically to a tachykinin receptor(s), as described in the following sections.

Rates of association and dissociation The profile obtained for the association and dissociation of [^{125}I]-NKA specific binding to sucrose-purified parenchymal membranes was directly comparable to the profile previously observed for [^{125}I-Tyr^8]-SP specific binding to guinea-pig lung parenchymal membranes. The rate of association of Mn^{2+}-dependent [^{125}I]-NKA specific binding to sucrose-purified parenchymal membranes was very slow (k_{obs}/[radioligand] = 0.8 × 10^9 min^{-1} M^{-1}, $n = 2$). In this case equilibrium was attained over a 2 h incubation at room temperature. The rate of dissociation provoked by addition of excess competing NKA (1 μM) was also slow ($k_{-1} = 0.01$ min^{-1}, $n = 2$), while the addition of GTPγS (100 μM) with the NKA, again resulted in the rapid and complete dissociation of [^{125}I]-NKA binding to non-specific levels.

Equilibrium competition curves Selected tachykinin-receptor agonists and antagonists were used to compete for [^{125}I]-NKA specific binding to sucrose-purified guinea-pig lung parenchymal membranes. The rank order of potency observed for the peptide agonists was SP = [Sar^{9}Met(O$_2$)^{11}]SP > SP-methyl ester > NKA > NKB >> [βAla^8]NKA (4–10), with senktide inactive at concentrations up to 10 μM. This was directly comparable with the rank order of potency determined for these ligands in competition for [^{125}I]-Tyr^8]-SP specific binding to guinea-pig lung parenchymal membranes (Table 1).

The results for inhibition of [^{125}I]-NKA specific binding to sucrose-purified guinea-pig lung parenchymal membranes by NK_1- and NK_2-receptor antagonists were also comparable with the data obtained for inhibition of [^{125}I-Tyr^8]-SP specific binding to guinea-pig lung parenchymal membranes by these compounds. Thus, the NK_1-selective CP-99,994 was the most potent competing ligand, displaying an IC_{50} value of 0.47 ± 0.05 nM, with the related stereoisomer L-736,322 again 1000 fold less potent. The NK_2-selective SR48968 and MEN 10,376, however, were still relatively poor in competition for [^{125}I]-NKA specific binding to these preparations, displaying IC_{50} values of 0.62 ± 0.07 μM and 7.8 ± 0.9 μM, respectively (Table 1).

The highly NK_1-selective [Sar^{9}Met(O$_2$)^{11}]SP and CP-99,994, however, only inhibited approximately 80% of the [^{125}I]-NKA specific binding to sucrose-purified guinea-pig lung parenchymal membranes (Figure 4). [^{125}I]-NKA binding assays were therefore conducted in the presence of saturating concentrations of [Sar^{9}Met(O$_2$)^{11}]SP (1 μM) or CP-99,994 (2.7 μM) to abolish the NK_1-receptor binding component. Under these conditions, the remaining [^{125}I]-NKA specific binding could be completely inhibited in a concentration-dependent manner by both [βAla^8]NKA (4–10) and SR48968, with IC_{50} values of 27 ± 7 nM ($n = 3$) and 0.23 ± 0.04 nM ($n = 4$), respectively (Figure 4), while the NK_3-selective agonist senktide was inactive at concentrations up to 10 μM.

Characterization of [^{125}I]-neurokinin A specific binding to guinea-pig tracheal membranes

[^{125}I]-NKA binding assay Due to the relatively low amount of membrane protein obtained from guinea-pig tracheal preparations, a limited series of experiments was conducted to identify the tachykinin-receptor types present in this tissue. The characteristics of [^{125}I]-NKA specific binding to guinea-pig tracheal membranes were essentially the same as those observed for sucrose-purified guinea-pig lung parenchymal membranes. [^{125}I]-NKA specific binding was enhanced by Mn^{2+} ions, although in this case the optimum cation concentration was 10 mM. In addition, the equilibrium for [^{125}I]-NKA specific binding to guinea-pig tracheal membranes was reached over a 2 h incubation period, and the dissociation of the radioligand provoked by addition of excess competing

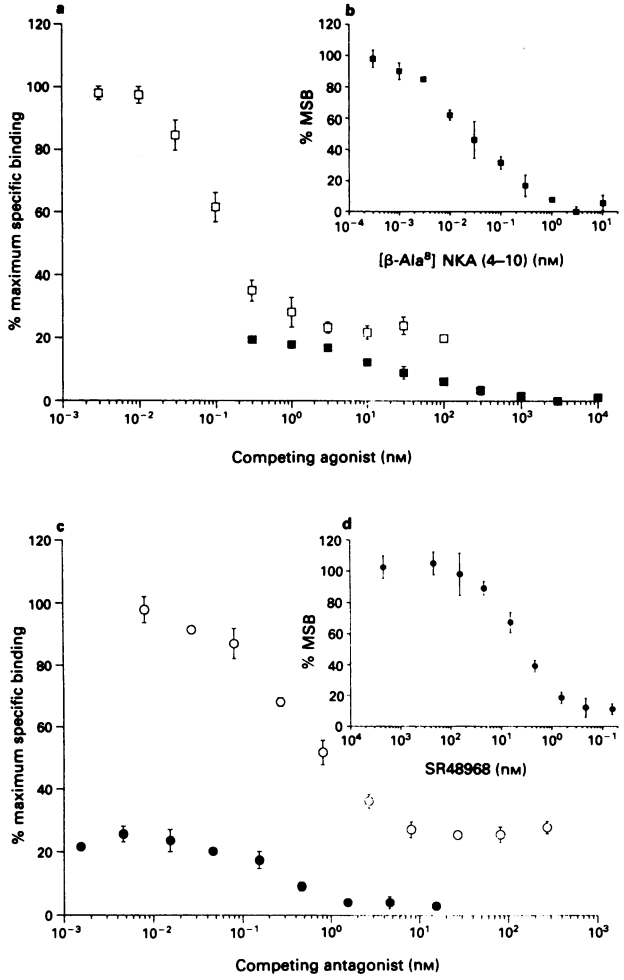

Figure 4 Competition for [^{125}I]-neurokinin A ([^{125}I]-NKA) specific binding to sucrose-purified guinea-pig lung parenchymal membranes by selective tachykinin-receptor agonists and antagonists. [^{125}I]-NKA binding assays were performed, as described in the Methods, in the presence of 3 pM–300 nM of either [Sar^9,Met(O$_2$)^{11}]SP (□), (a), or CP-99,994 (○). Residual [^{125}I]-NKA specific binding was then competed for with 0.3 nM–10 μM [β-Ala^8]NKA (4–10) (■, in the presence of 1 μM [Sar^9,Met(O$_2$)^{11}]SP, (a), or 30 pM–30 nM SR48968 (●), in the presence of 2.7 μM CP-99,994 (c). The inhibition curves for [β-Ala^8]NKA (4–10) and SR48968 expressed as a function of the percentage maximum specific binding determined in the presence of 1 μM [Sar^9,Met(O$_2$)^{11}]SP and 2.7 μM CP-99,994, respectively, are shown in (b) and (d). The IC_{50} values for competing NK_1- and NK_2-receptor agonists and antagonists were calculated on the basis of the maximum specific binding to the individual NK_1- and NK_2-receptor components.

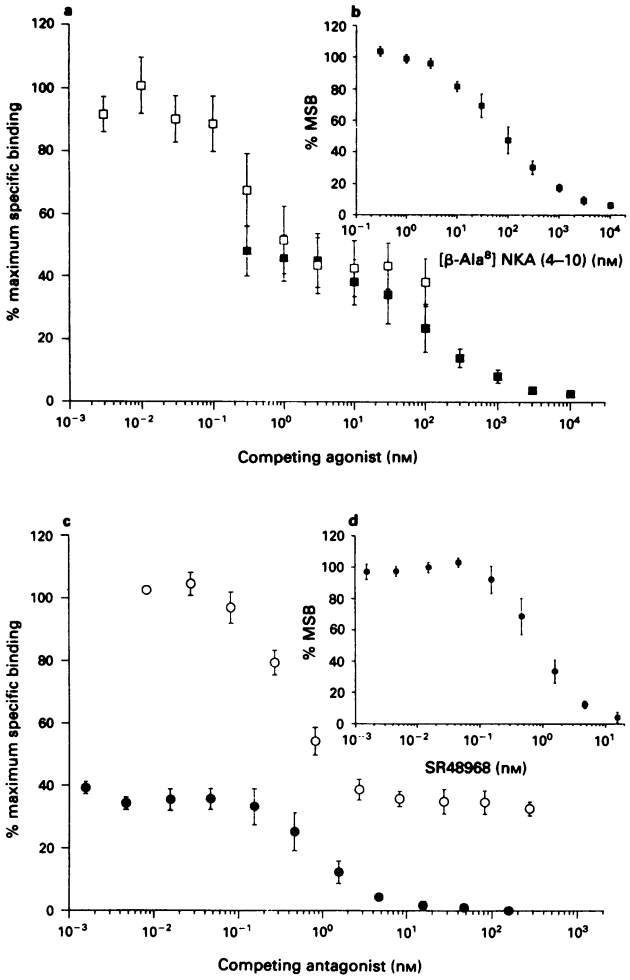

Figure 5 Competition for [^{125}I]-neurokinin A ([^{125}I]-NKA) specific binding to guinea-pig tracheal membranes by tachykinin-receptor selective agonists and antagonists. [^{125}I]-NKA binding assays were conducted as described in Figure 4. (a) Shows the concentration-dependent inhibition of [^{125}I]-NKA specific binding by [Sar^9,Met(O$_2$)^{11}]SP (□), and also [β-Ala^8]NKA (4–10) (■) when competed for in the presence of 1 μM [Sar^9,Met(O$_2$)^{11}]SP. (c) Shows the concentration-dependent inhibition of [^{125}I]-NKA specific binding by CP-99,994 (○) and also by SR48968 (●) when titrated in the presence of 2.7 μM CP-99,994. The inhibition curves for [β-Ala^8]NKA (4–10) and SR48968 expressed as a function of the percentage maximum specific binding in the presence of 1 μM [Sar^9,Met(O$_2$)^{11}]SP and 2.7 μM CP-99,994, respectively, are shown in (b) and (d). The IC_{50} values for competing NK_1- and NK_2-receptor agonists and antagonists were calculated on the basis of the maximum specific binding to the individual NK_1- and NK_2-receptor components.

NKA was significantly increased by simultaneous addition of 100 μM GTPγS.

Equilibrium competition curves Approximately 60% of [^{125}I]-NKA specific binding to guinea-pig tracheal membranes could be inhibited in a concentration-dependent manner by the NK_1-selective [Sar^{9}Met(O$_2$)^{11}]SP and CP-99,994, with IC_{50} values of 0.2 nM ($n = 2$) and 0.5 nM ($n = 2$), respectively (Figure 5). The remaining [^{125}I]-NKA specific binding component could then be completely inhibited in a concentration-dependent manner by either the NK_2-selective agonist [βAla^8]NKA (4–10) or antagonist SR-48968, with IC_{50} values of 88 nM and 0.9 nM ($n = 2$) (Figure 5).

Discussion

[^{125}I-Tyr^8]-substance P and [^{125}I]-NKA binding assays were employed to characterize NK_1 and NK_2 receptors in guinea-pig lung parenchymal and tracheal membrane preparations. Both radioligands were completely degraded by peptidases present in the tissue preparations. It is well established that neutral endopeptidase inactivates neurokinins in a variety of tissues, including guinea-pig airways (Dusser *et al.*, 1988; Devillier *et al.*, 1988; Webber, 1989). Inhibition of this enzyme alone, however, was insufficient to prevent metabolism of radiolabelled neurokinins under our experimental conditions. Thus, it was essential to include inhibitors of

angiotensin converting enzyme, aminopeptidase and several serine-protease activities. These results are in contrast to previous studies where neutral endopeptidase inhibitors either alone (Aharony *et al.*, 1991), or in combination with low concentrations of serine-protease inhibitors (Coats & Gerard, 1989; Geraghty *et al.*, 1992), appeared sufficient to maintain integrity of the radioligands used. In several studies this difference may be explained by the use of the radiolabel [^{125}I-Bolton-Hunter]SP, which is more resistant to proteolysis, particularly by aminopeptidase. In this case, however, it is highly likely that the unlabelled competing peptides will be degraded and, consequently, their potency underestimated.

The specific binding of [^{125}I-Tyr^8]-SP to guinea-pig lung parenchymal membranes was found to be of high affinity, saturable, enhanced by Mn^{2+}, dissociated by the GTP analogue GTPγS, and inhibited by tachykinin-receptor agonists with the following rank order of potency: SP = [Sar^{9}Met(O$_2$)^{11}]SP > SP-methyl ester = physalaemin > NKA >> [βAla^8]NKA (4–10) >> senktide. These results are consistent with previous studies describing the NK_1 receptor in a variety of systems, including the NK_1 monoreceptor dog carotid artery preparation (Regoli *et al.*, 1988) and in expression systems for the cloned rat and human NK_1 receptors (Hershey *et al.*, 1990; Takeda *et al.*, 1991). Our data convincingly demonstrate, therefore, that [^{125}I-Tyr^8]-SP binds to the NK_1 receptor in guinea-pig lung parenchyma.

Of particular interest is the observation that two structurally different NK_1-receptor antagonists, CP-99,994 (McLean *et al.*, 1992) and RP67580 (Garret *et al.*, 1991), display a 300 fold difference in potency at the guinea-pig lung NK_1 receptor, with K_i values of 0.4 nM and 127 nM, respectively. CP-99,994 is structurally related to CP-96345, the first selective non-peptide NK_1 antagonist to be described (Snider *et al.*, 1991). CP-96345 is approximately 100 fold more potent in competition for binding to the guinea-pig NK_1 receptor than with the rat NK_1 receptor. In contrast, RP67580 is a potent antagonist at the rat NK_1 receptor, with a K_i of 4.16 nM (Watling, 1992), but, as shown in this study, is 30 fold less active at the guinea-pig NK_1 receptor. These results, therefore, support the proposal that there is a distinct species-dependent structure-activity relationship for NK_1 antagonists (Garret *et al.*, 1991; Snider *et al.*, 1991; Appell *et al.*, 1992).

In order to characterize the NK_2 receptor in guinea-pig lung the number of detectable [^{125}I]-NKA specific binding sites in parenchymal membranes was increased 3–4 fold by purification over discontinuous sucrose gradients. The ability of tachykinin-receptor agonists and antagonists to compete for [^{125}I]-NKA specific binding was directly comparable to their potency in competition for [^{125}I-Tyr^8]-SP specific binding to parenchymal membranes. Thus, both the rank order of potency and the determined IC_{50} values were almost identical, demonstrating that the majority of [^{125}I]-NKA specific binding to sucrose-purified guinea-pig lung parenchymal membranes was also to the NK_1 receptor.

Notwithstanding this conclusion, the NK_1-receptor selective ligands [Sar^{9}Met(O$_2$)^{11}]SP and CP-99,994 were observed to inhibit only 80% of the [^{125}I]-NKA specific binding to sucrose-purified guinea-pig lung parenchymal membranes. In addition, the NK_2-preferring agonists NKA and [βAla^8]NKA (4–10) were more potent in competing for [^{125}I]-NKA specific binding than for [^{125}I-Tyr^8]-SP specific binding. Therefore, the possibility that [^{125}I]-NKA was also binding to the NK_2 receptor in sucrose-purified guinea-pig lung parenchymal membranes was investigated. When [^{125}I]-NKA binding assays were conducted in the presence of saturating concentrations of NK_1-selective ligands in order to fully occupy the NK_1 receptor, the remaining [^{125}I]-NKA specific binding sites could be inhibited in a concentration-dependent manner by the NK_2-selective ligands [βAla^8]NKA (4–10) and SR48968, but not by the NK_3-selective agonist senktide. The IC_{50} values determined for [βAla^8]NKA (4–10) and SR48968 in the presence of NK_1 ligands were in agreement with the potencies of these ligands at the NK_2 receptor (Emonds-Alt *et al.*, 1992). These data, therefore, strongly suggest the presence of a small population of NK_2 receptors in guinea-pig parenchyma and are consistent with the recent description of NK_2-mediated plasma extravasation in guinea-pig intraparenchymal airways (Tousignant *et al.*, 1993a).

Similar results were obtained investigating [^{125}I]-NKA specific binding to guinea-pig tracheal membranes. The profile of partial inhibition by selective ligands shows that this tissue contains a dual population of NK_1 and NK_2 receptors. The identification of both these tachykinin-receptor types supports similar conclusions from pharmacological studies which concluded that tachykinin-mediated contraction of guinea-pig trachea occurs as a result of activation of both NK_1 and NK_2 receptors (Ireland *et al.*, 1991).

In addition to the reports demonstrating that the NK_1 receptor type displays profound species differences, there are many studies supporting the hypothesis that species homologues of the NK_2 receptor also exist (for review see Maggi *et al.*, 1993). The rank order of potency of NK_2-receptor antagonists has led to the broad classification of the guinea-pig, rabbit and human receptors as NK_{2A} where MEN 10,207 > L-659877 > R396, and the hamster and rat receptors as NK_{2B}, where this order of potency is reversed. This classification of NK_{2A} and NK_{2B} receptors is, however, somewhat misleading as it is, as yet, essentially a reflection of species differences rather than the existence of true NK_2 receptor subtypes. Whereas there are several studies suggesting that subtypes of both NK_1 and NK_2 receptors exist within the same species, including the guinea-pig, the evidence is principally pharmacological and awaits clarification at the molecular level (Carruette *et al.*, 1992; Maggi *et al.*, 1993). In this report the small population of NK_2 receptors present in guinea-pig airways, combined with the low amounts of membrane available from tracheal tissue, has limited the study to the identification of the tachykinin receptor types present in these tissues and has precluded a detailed pharmacological characterization of these binding sites.

In summary, this paper confirms the presence of the NK_1 receptor in guinea-pig lung parenchymal membranes and, in addition, demonstrates that these tissues also express detectable levels of NK_2 receptors. We also provide evidence for the presence of both NK_1 and NK_2 receptors in guinea-pig trachea. These results are entirely consistent with functional studies describing NK_1- and NK_2-mediated events in guinea-pig airways at the level of both the parenchyma and the trachea. While the presence of mRNA coding for both NK_1 and NK_2 receptors in human lung has already been shown (Hopkins *et al.*, 1991; Graham *et al.*, 1991), this is the first unambiguous identification of NK_2 receptors in airway tissues by use of radioligand binding techniques.

The authors would like to thank Jeffrey Hale for the synthesis of SR49868, Simon Owen for the synthesis of CP-99,994, L-736,322, RP67580 and RP68651 and Barbara Sholzberg for secretarial assistance.

References

AHARONY, D., CATANESE, C.A. & WOODHOUSE, D.P. (1991). Binding of the novel ligand [4,5-^{3}H-Leu^{10}]substance P to high-affinity NK-1 receptors on guinea pig lung membranes: modulation by GTP analogs and sulfhydryl modifying agents. *J. Pharmacol. Exp. Ther.*, **259**, 146–155.

APPELL, K.C., FRAGALE, B.J., LOSCIG, S., SINGH, S. & TOMCZUK, B.E. (1992). Antagonists that demonstrate species differences in neurokinin-1 receptors. *Mol. Pharmacol.*, **41**, 772–778.

BARNES, P.J., BELVISI, M.G. & ROGERS, D.F. (1990). Modulation of neurogenic inflammation: novel approaches to inflammatory disease. *Trends Pharmacol. Sci.*, **11**, 185–189.

CARRUETTE, A., MOUSSAOUI, S.M., CHAMPION, A., COTTEZ, D., GONIOT, P. & GARRET, C. (1992). Comparison in different tissue preparations of the in vitro pharmacological profile of RP67580, a new non-peptide substance P antagonist. *Neuropeptides*, **23**, 245–250.

CASALE, T.B. (1991). Neuropeptides and the lung. *J. Allergy Clin. Immunol.*, **88**, 1–14.

COATS, S.R. & GERARD, N.P. (1989). Characterization of the substance P receptor in guinea pig lung tissues. *Am. J. Respir. Cell Mol. Biol.*, **1**, 269–275.

DEVILLIER, P., ADVENIER, C., DRAPEAU, G., MARSAC, J. & REGOLI, D. (1988). Comparison of the effects of epithelium removal and of an enkephalinase inhibitor on the neurokinin-induced contractions of guinea-pig isolated trachea. *Br. J. Pharmacol.*, **94**, 675–684.

DUSSER, D.J., UMENO, E., GRAF, P.D., DJOKIC, T., BORSON, D.B. & NADEL, J.A. (1988). Airway neutral endopeptidase-like enzyme modulates tachykinin-induced bronchoconstriction *in vivo*. *J. Appl. Physiol.*, **65**, 2585–2591.

EMONDS-ALT, X., VILAIN, P., GOULAOUIC, P., PROIETTO, V., VAN BROECK, D., ADVENIER, C., NALINE, E., NELIAT, G., LE FUR, G. & BRELIERE, J.C. (1992). A potent and selective non-peptide antagonist of the neurokinin A (NK_2) receptor. *Life Sci.*, **50**, PL101–PL106.

GARRET, C., CARRUETTE, A., FARDIN, V., MOUSSAOUI, S., PEYRONEL, J.-F., BLANCHARD, J.-C. & LADURON, P.M. (1991). Pharmacological properties of a potent and selective nonpeptide substance P antagonist. *Proc. Natl. Acad. Sci. U.S.A.*, **88**, 10208–10212.

GERAGHTY, D.P., MUSSAP, C.J. & BURCHER, E. (1992). Radioiodinated substance P, neurokinin A, and eledoisin bind predominantly to NK1 receptors in guinea pig lung. *Mol. Pharmacol.*, **41**, 147–153.

GRAHAM, A., HOPKINS, B., POWELL, S.J., DANKS, P. & BRIGGS, I. (1991). Isolation and characterisation of the human lung NK-2 receptor gene using rapid amplification of cDNA ends. *Biochem. Biophys. Res. Commun.*, **177**, 8–16.

HERSHEY, A.D. & KRAUSE, J.E. (1990). Molecular characterization of a functional cDNA encoding the rat substance P receptor. *Science*, **247**, 958–962.

HILL, A.V. (1910). The possible effects of the aggregation of the molecules of haemoglobin on its dissociation curves. *J. Physiol.*, **40**, IV–VII.

HOPKINS, B., POWELL, S.J., DANKS, P., BRIGGS, I. & GRAHAM, A. (1991). Isolation and characterisation of the human lung NK-1 receptor cDNA. *Biochem. Biophys. Res. Commun.*, **180**, 1110–1117.

IRELAND, S.J., BAILEY, F., COOK, A., HAGAN, R.M., JORDAN, C.C. & STEPHENS-SMITH, M.L. (1991). Receptors mediating tachykinin-induced contractile responses guinea-pig trachea. *Br. J. Pharmacol.*, **103**, 1463–1469.

KRAUSE, J.E., TAKEDA, Y. & HERSHEY, A.D. (1992). Structure, functions and mechanisms of substance P receptor action. *J. Invest. Dermatol.*, **98**, 2S–7S.

MAGGI, C.A., GIULIANI, S., BALLATI, L., LECCI, A., MANZINI, S., PATACCHINI, R., RENZETTI, A.R., ROVERO, P., QUARTARA, L. & GIACHETTI, A. (1991). In vivo evidence for tachykininergic transmission using a new NK-2 receptor selective antagonist, MEN 10,376. *J. Pharmacol. Exp. Ther.*, **257**, 1172–1178.

MAGGI, C.A., PATACCHINI, R., ROVERO, P. & GIACHETTI, A. (1993). Tachykinin receptors and tachykinin receptor antagonists. *J. Auton. Pharmacol.*, **13**, 23–93.

MAGGIO, J.E. (1988). Tachykinins. *Annu. Rev. Neurosci.*, **11**, 13–28.

MASU, Y., NAKAYAMA, K., TAMAKI, H., HARADA, Y., KUNO, M. & NAKANISHI, S. (1987). cDNA cloning of bovine substance-K receptor through oocyte expression system. *Nature*, **329**, 836–838.

MCLEAN, S., GANONG, A., SEYMOUR, P.A., SNIDER, R.M., DESAI, M.C., ROSEN, T., BRYCE, D.K., LONGO, K.P., REYNOLDS, L.S., ROBINSON, G., SCHMIDT, A.W., SIOK, C. & HEYM, J. (1992). Pharmacology of CP-99,994: a nonpeptide antagonist of the tachykinin NK_1 receptor. *Regul. Pept.*, (Supplement 1) S120.

MURAI, M., MORIMOTO, H., MAEDA, Y. & FUJII, T. (1992). Effects of the tripeptide substance P antagonist, FR113680, on airway constriction and airway edema induced by neurokinins in guinea-pigs. *eur. J. Pharmacol.*, **217**, 23–29.

REGOLI, D., DRAPEAU, G., DION, S. & D'ORLEANS-JUSTE, P. (1987). Pharmacological receptors for substance P and neurokinins. *Life Sci.*, **40**, 109–117.

REGOLI, D., DRAPEAU, G., DION, S. & COUTURE, R. (1988). New selective agonists for neurokinin receptors: pharmacological tools for receptor characterization. *Trends Pharmacol. Sci.*, **9**, 290–295.

ROSENTHAL, H.D. (1967). A graphic method for the determination and presentation of binding parameters in a complex system. *Anal. Biochem.*, **20**, 525–532.

ROVERO, P., PESTELLINI, V., PATACCHINI, R., GIULIANI, S., SANTICIOLI, P., MAGGI, C.A., MELI, A. & GIACHETTI, A. (1989). A potent and selective agonist for NK-2 tachykinin receptor. *Peptides*, **10**, 593–595.

SCATCHARD, G. (1949). The attraction of proteins for small molecules and ions. *Ann. NY Acad. Sci.*, **51m** 660–672.

SHIGEMOTO, R., YOKOTA, Y., TSUCHIDA, K. & NAKANISHI, S. (1990). Cloning and expression of a rat neuromedin K receptor cDNA. *J. Biol. Chem.*, **265**, 623–628.

SMITH, P.K., KROHN, R.I., HERMANSON, G.T., MALLIA, A.K., GARTNER, F.H., PROVENZANO, M.D., FUJIMOTO, E.K., GOEKE, N.M., OLSON, B.J. & KLENK, D.C. (1985). Measurement of protein using bicinchoninic acid. *Anal. Biochem.*, **150**, 76–85.

SNIDER, R.M., CONSTANTINE, J.W., LOWE III, J.A., LONGO, K.P., LEBEL, W.S., WOODY, H.A., DROZDA, S.E., DESAI, M.C., VINICK, F.J., SPENCER, R.W. & HESS, H.-J. (1991). A potent nonpeptide antagonist of the substance P (NK_1). *Science*, **251**, 435–437.

SOLWAY, J. & LEFF, A.R. (1991). Sensory neuropeptide and airway function. *J. Appl. Physiol.*, **71**, 2077–2087.

TAKEDA, Y., CHOU, K.B., TAKEDA, J., SACHAIS, B.S. & KRAUSE, J.E. (1991). Molecular cloning, structural characterization and functional expression of the human substance P receptor. *Biochem. Biophys. Res. Commun.*, **179**, 1232–1240.

TOUSIGNANT, C., CHAN, C.-C., GUEVREMONT, D., BRIDEAU, C., MACCOSS, M. & ROGER, I.W. (1993a). NK_2 receptors mediate plasma extravasation in guinea pig lower airways. *Br. J. Pharmacol.*, **108**, 383–386.

TOUSIGNANT, C., CHAN, C.-C., YOUNG, D., GUEVREMONT, D. & RODGER, I.W. (1993b). NK_1-receptor mediated plasma extravasation in guinea-pig and rat airways: comparison of [^{125}I] human fibrinogen and [^{99m}Tc] human serum albumin as markers of leakage. *Can. J. Physiol. Pharmacol.*, (in press).

WATLING, K.J. (1992). Nonpeptide antagonists herald new era in tachykinin research. *Trends Pharmacol. Sci.*, **13**, 266–269.

WEBBER, S.E. (1989). Receptors mediating the effects of substance P and neurokinin A on mucus secretion and smooth muscle tone of the ferret trachea: potentiation by an enkephalinase inhibitor. *Br. J. Pharmacol.*, **98**, 1197–1206.

WORMSER, U., LAUFER, R., HART, Y., CHOREV, M., GILON, C. & SELINGER, Z. (1986). Highly selective agonists for substance P receptor types. *EMBO J.*, **5**, 2805–2808.

YOKOTA, Y., SASAI, Y., TANAKA, K., FUJIWARI, T., TSUCHIDA, K., OHKUBO, H. & NAKANISHI, S. (1989). Molecular characterization of a functional cDNA for rat substance P receptor. *J. Biol. Chem.*, **264**, 17649–17652.

(Received October 30, 1992
Revised May 17, 1993
Accepted June 11, 1993)

Br. J. Pharmacol. (1993), **110**, 701–706

Modulation of adjuvant arthritis by endogenous nitric oxide

Armando Ialenti, [1]*Salvador Moncada & Massimo Di Rosa

Department of Experimental Pharmacology, University of Naples 'Federico II', via Domenico Montesano, 49, 80131 – Napoli, Italy and *Wellcome Research Laboratories, Langley Court, Beckenham, Kent, BR3 3BS

1 The role of endogenous nitric oxide (NO) in adjuvant arthritis in Lewis rats has been studied by use of L-arginine, the amino acid from which NO is synthesized, and N^G-nitro-L-arginine methyl ester (L-NAME), an inhibitor of NO synthase. Prolonged modulation (35 days) of the L-arginine: NO pathway in rats was achieved by dissolving test compounds in the drinking water (L-arginine: 3, 10 and 30 mg ml^{-1}; L-NAME: 0.1, 1 and 10 mg ml^{-1}).

2 Arthritis was exacerbated by L-arginine and suppressed by L-NAME in a dose-related fashion. Combined treatment with L-NAME (1 mg ml^{-1}) and L-arginine (30 mg ml^{-1}) did not modify the arthritis.

3 Reduced weight gain, which is a feature of adjuvant arthritis, was modified by these compounds so that L-arginine reduced weight gain whereas L-NAME increased weight gain compared with that in control animals.

4 D-Arginine (30 mg ml^{-1}), N^G-nitro-D-arginine methyl ester (D-NAME: 1 mg ml^{-1}) and L-lysine (30 mg ml^{-1}), an amino acid not involved in the generation of NO, were without effect on either arthritis or body weight gain.

5. Antigen-stimulated proliferation of T-lymphocytes as well as generation of nitrite (NO_2^-) and release of acid phosphatase from macrophages were all enhanced in L-arginine-treated arthritic rats and reduced in L-NAME-treated animals.

6 These results suggest that endogenous NO modulates adjuvant arthritis, possibly by interfering with the activation of T-lymphocytes and/or macrophages.

Keywords: Adjuvant arthritis; L-arginine; lymphocyte proliferation; macrophage activation; N^G-nitro-L-arginine methyl ester

Introduction

Adjuvant-induced arthritis in the rat is an experimental immunopathy that is thought to share many features with human rheumatoid arthritis and, as such, is one of the most widely used models for studying the anti-inflammatory/antirheumatic properties of compounds (for review see Billingham & Davies, 1979). Chronic polyarthritis is induced in the rat by intradermal injection of an oil emulsion of dead mycobacteria, usually *M. tuberculosis*.

Although the aetiology and pathogenesis of adjuvant arthritis are not yet fully understood, there is substantial evidence that immunological mechanisms are involved and that T-lymphocytes play a major role (for review see Cohen, 1991). L-Arginine exerts a trophic effect on the thymus and improves host immunity. Thus it has been shown that L-arginine enhances the lymphocyte cell count of the thymic gland, blastogenesis of these lymphocytes in response to mitogens, skin allograft rejection and tumour regression (for review see Barbul, 1986).

The biosynthesis of nitric oxide (NO) from L-arginine is a pathway for the regulation of cell function and communication (for review see Moncada *et al.*, 1991). In all cell types so far studied, NO is generated following oxidation and cleavage of the terminal nitrogen atom(s) of L-arginine by an enzyme, the NO synthase. At least two types of NO synthase have been identified so far. The enzyme found in endothelial cells and brain is constitutive, Ca^{2+}-dependent and releases picomolar amounts of NO for a short period following receptor stimulation. In contrast, the enzyme found in the macrophage is induced following stimulation with cytokines or endotoxin, is Ca^{2+}-independent, and releases nanomolar amounts of NO for a long period.

Nitric oxide produced by the constitutive enzyme modulates various functions, such as vascular tone and neurotransmission in the central nervous system, via activation of the soluble guanylate cyclase. The production of NO by the inducible enzyme has been identified as a major mechanism of the cytostatic/cytotoxic action of activated macrophages on target cells. This occurs as a result of combination of NO with iron-sulphur centres in key enzymes of the respiratory cycle and of the pathway for DNA synthesis in the target cells (Hibbs *et al.*, 1990).

The NO synthase is inhibited *in vitro* and *in vivo* by some analogues of L-arginine (Rees *et al.*, 1990; McCall *et al.*, 1991). The identification of these inhibitors has provided an important pharmacological tool for investigating the relevance of NO in biological processes.

In this study we have investigated the effect of L-arginine and of N^G-nitro-L-arginine methyl ester (L-NAME), an inhibitor of NO synthase, on adjuvant arthritis in the rat. We have also studied the effects of D-arginine, N^G-nitro-D-arginine methyl ester (D-NAME) and L-lysine, an amino acid not involved in the biosynthesis of NO. The possible involvement of the L-arginine: NO pathway in T-lymphocyte proliferation and macrophage activation in arthritic rats was also studied, since it has been shown that murine T-lymphocyte clones express the inducible NO synthase and generate NO following stimulation with cytokines (Kirk *et al.*, 1990).

Some of these results were presented at the meeting of The British Pharmacological Society held in Cambridge on 5–7th January, 1993.

Methods

Animals

Male Lewis rats (Nossan, Italy) weighing 160–180 g were used for this study. Animals were housed in propylene cages with food and water *ad libitum*. The light cycle was automatically controlled (on 07 h 00 min; off 19 h 00 min) and the room temperature thermostatically regulated to 22 ± 1°C. Prior to the experiments animals were housed in these conditions for 6–8 days to become acclimatized.

[1] Author for correspondence.

Treatments

Prolonged modulation of NO production in Lewis rats was achieved by spontaneous ingestion of test compounds dissolved in drinking water. The water intake of a Lewis rat was found in pilot experiments to be 26–28 ml day^{-1}. When the tap water was replaced with the solution of test compounds a transient (3–4 days) reduction (23–24 ml day^{-1}) in water intake was observed, after which it returned to normal values.

Animals were divided into several groups. Two groups were given tap water: one of these did not receive any treatment and was used for recording weight gain and other parameters in normal animals during the time of the experiments (naive rats), the other served as control of the adjuvant arthritis (control rats). Other groups were given solutions of test compounds in various concentrations or combinations (see Results). In preliminary experiments it was established that Lewis rats given solutions of test compounds at the concentrations described, gained weight at the same rate as rats given tap water to drink.

Arthritis

Four days after the start of treatment, adjuvant arthritis was induced in all rats (except the naive group) by a single intradermal injection (0.1 ml) into the right foot pad of 0.3 mg heat-killed *M. tuberculosis* in Freund's incomplete adjuvant.

The magnitude of the inflammatory response was evaluated by measuring the volume of the contralateral (non-injected) hind paw (secondary lesion). The paw volume was determined by plethysmometry (Basile, Italy) immediately after immunization and every 7 days for a period of 35 days. Weight gain, a further parameter of severity of arthritis (Newbold, 1963), was also recorded on these days. Eight animals were used per group for measurement of arthritis and weight gain.

Splenocyte and macrophage collection

Three groups of 15 animals were used for these studies; one served as a control group, the others were treated with either L-arginine (30 mg ml^{-1}) or L-NAME (1 mg ml^{-1}). Three rats from each group were killed at weekly intervals, i.e. on day 7, 14, 21, 28, 35. On the same days three naive rats were also killed in order to evaluate the splenocyte and macrophage activities (see below) in non-arthritic rats. The spleens were removed and single cell suspensions were prepared in Dulbecco's modified Eagle's medium supplemented with 2 mM glutamine, 25 mM HEPES, penicillin (100 units ml^{-1}), streptomycin (100 $\mu g\ ml^{-1}$) and 10% foetal calf serum (complete medium).

Lymphocytes of each spleen were separately isolated from cell suspension by density-gradient centrifugation using Ficoll-Paque and then resuspended (10^6 cells ml^{-1}) in complete medium. Cell viability, assessed by the trypan blue dye exclusion method, was 93–95%.

At the same time as removal of the spleen, peritoneal cells were also collected by washing the cavity with 8 ml sterile phosphate-buffered saline (PBS, pH 7.2) containing heparin (50 u ml^{-1}). Cells were washed twice and plated onto 35 mm Petri dishes ($4–5 \times 10^6$ cells per dish) containing complete medium (see above). After 3 h at 37°C in 5% CO_2 humidified air, nonadherent cells were removed by washing with sterile PBS containing 1 mM EDTA.

Macrophages (80–85% of total cells) were removed from the culture dishes by vigorous pipetting, centrifuged (300 *g* for 10 min) and resuspended in complete medium at a concentration of 10^6 cells ml^{-1}. Macrophage viability (95–98%) was determined by exclusion of trypan blue.

T-lymphocyte proliferation

T-lymphocyte proliferation assays were carried out in triplicate and performed in 96-microwell plates. Cells (10^5 cells per well) were stimulated with *M. tuberculosis* (final concentration 5 $\mu g\ ml^{-1}$) and incubated for 7 days at 37° in 5% CO_2 humidified air. One μCi of [^{3}H]-thymidine (47 Ci $mmol^{-1}$) was then added to each well. After a 6 h incubation at 37°C, cultures were harvested on glass fibre strips and [^{3}H]-thymidine incorporation was measured in a beta counter. The data are expressed as mean total c.p.m. ± s.e.mean.

Macrophage activation

Macrophages were plated in 24 well culture plates at a concentration of 2.5×10^5 cells ml^{-1} and incubated for 24 h. Aliquots of the medium were then collected for assay of nitrite (NO_2^-), acid phosphatase (AP) and lactic dehydrogenase (LDH). Each assay was carried out in triplicate.

Nitrite levels were measured with Griess reagent as previously described (Di Rosa *et al.*, 1990) and results were expressed as nmol of NO_2^- generated by 10^6 cells in 24 h.

AP activity was evaluated with β-glycerophosphate as a substrate and measuring the amount of inorganic P released in 30 min by 100 μl of medium, according to the method of Gianetto & De Duve (1955). Results are expressed as μmol of inorganic P liberated in 30 min by the enzyme released in 24 h by 10^6 cells.

LDH activity was assayed by measuring the amount of pyruvic acid reduced to lactic acid by 100 μl of medium in 30 min, according to the method of Cabaud & Wroblewski (1958). Results are expressed as μmol of pyruvic acid transformed in 30 min by the enzyme released in 24 h by 10^6 cells.

Statistics

Data are expressed as the mean ± s.e.mean; statistical analysis of the data was performed using a Pharm/PCS computer programme. Means were compared by Student's test for unpaired data.

Drugs

M. tuberculosis and PBS were obtained from Difco. All reagents for cell culture except foetal calf serum (Flow Labs) were from Gibco. [^{3}H]-thymidine was obtained from Amersham and Ficoll-Paque from Pharmacia. D-NAME was synthesized by Bachem (Switzerland) and all other chemicals were purchased from Sigma.

Results

Arthritis

In each group of rats ($n = 8$) a single intradermal injection of adjuvant to the right hind paw resulted in a gradual increase in volume of the left paw (secondary lesion), which reached a peak value 21 days after immunization (Figure 1). In the rats given L-arginine (30 mg ml^{-1}) arthritis was exacerbated throughout the time course of the development of the arthropathy while in aminals receiving L-NAME (1 mg ml^{-1}) the process was greatly suppressed (Figure 1).

Rats given L-arginine had a dose-related increase in paw swelling throughout the time course of the arthritis (Figure 2). The greatest response (+ 44%, $P < 0.01$) was observed in rats drinking 30 mg ml^{-1} L-arginine. Rats given L-NAME showed a dose-related reduction in paw swelling throughout the time course of the arthritic reaction (Figure 2). The greatest reduction (− 50%, $P < 0.01$) was observed in rats drinking 10 mg ml^{-1} L-NAME. Rats given a combination of L-arginine (30 mg ml^{-1}) and L-NAME (1 mg ml^{-1}) had a foot volume increase that was slightly, but not significantly,

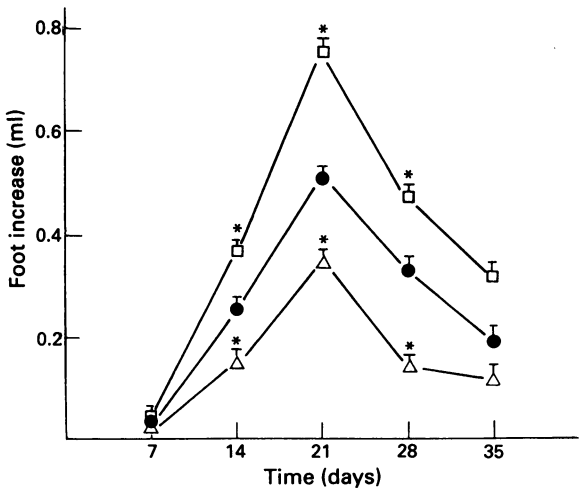

Figure 1 Effect of L-arginine and N^G-nitro-L-arginine methyl ester (L-NAME) on adjuvant arthritis (secondary lesion). The control group (●) was given tap water. Other groups were given L-arginine 30 mg ml^{-1} (□) or L-NAME 1 mg ml^{-1} (△) dissolved in drinking water. Data are expressed as mean ± s.e.mean from 8 animals. *$P<0.01$ vs control group.

above the control value (Figure 2). The arthritis occurring at day 21 in rats given D-arginine (30 mg ml^{-1}), D-NAME (1 mg ml^{-1}) and L-lysine (30 mg ml^{-1}) was similar to that observed in control rats.

Weight gain

In all groups of rats ($n = 8$) the average weight gain was related to the severity of arthritis. At the time of the peak foot volume increase (day 21) the average weight gain of naive rats was 73 ± 4 g whereas control arthritic rats gained only 51 ± 3 g ($P<0.01$ vs naive). The effects of the various test compounds on weight gain mirrored their effect on the severity of the arthritis so that on day 21 weight gain was significantly reduced compared with the control group in those rats drinking L-arginine while it was significantly greater in those drinking L-NAME. The effects of L-arginine and L-NAME on weight gain were dose-related (Figure 3).

In contrast, in rats given D-arginine, D-NAME and L-lysine the weight gain was not significantly different from that of the control group, neither was the weight increase of rats given a combination of L-NAME (1 mg ml^{-1}) and L-arginine (30 mg ml^{-1} Figure 3).

Proliferation of T-lymphocytes

The proliferation of T-lymphocytes stimulated with *M. tuberculosis* (5 μg ml^{-1}) was evaluated at weekly intervals in three rats from the control, the L-arginine (30 mg ml^{-1})- and L-NAME (1 mg ml^{-1})-treated groups. In each group the proliferative response observed at day 7 increased up until day 21 (peak response) and then decreased to approximately the initial value (day 7) at day 35 (Figure 4). Thus, in each group the time course of the proliferative response paralleled the development of arthritis. The proliferation of T-lymphocytes taken from L-arginine-treated animals was always greater than that observed in those from control rats. The difference between the two groups was significant ($P<0.01$) at days 14, 21, 28 and 35. The proliferation of T-lymphocytes collected from L-NAME-treated rats was always less than that in cells from control rats and was significantly reduced ($P<0.01$) on days 14, 21 and 28 (Figure 4). The incorporation of [^{3}H]-thymidine in stimulated T-lymphocytes from naive rats ranged from 13,296 to 15,019 c.p.m. ($n = 15$) (Figure 4).

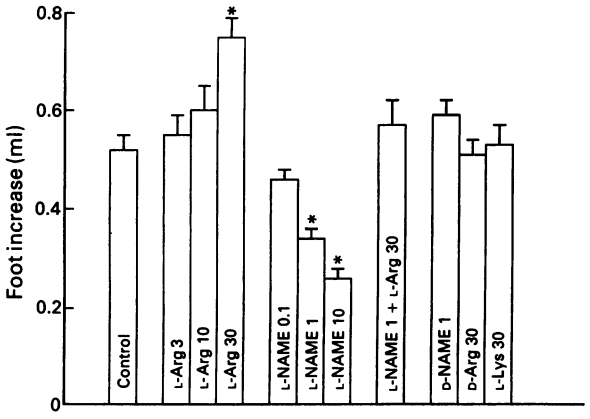

Figure 2 Adjuvant arthritis (secondary lesion) on day 21 post adjuvant challenge. The control group was given tap water and the other groups were given solutions of test compounds at the concentrations (mg ml^{-1}) shown inside the columns. L-Arg and D-Arg: L- and D-arginine; L-NAME and D-NAME: N^G-nitro-L-arginine methyl ester and N^G-nitro-D-arginine methyl ester; L-Lys = L-lysine. Data are expressed as mean ± s.e.mean from 8 animals. *$P<0.01$ vs control group.

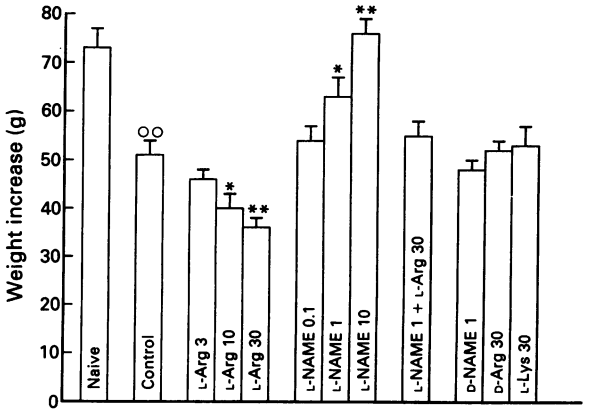

Figure 3 Increase in body weight on day 21 post adjuvant challenge. The naive and control groups were given tap water and the other groups were given solutions of test compounds at the concentrations (mg ml^{-1}) shown inside the columns: compounds as in Figure 2. Data are expressed as mean ± s.e.mean from 8 animals. $^{OO}P<0.01$ vs naive group; **$P<0.01$; *$P<0.05$ vs control group.

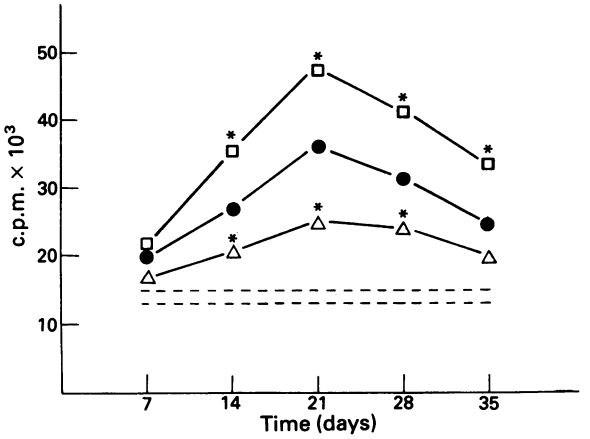

Figure 4 Effect of L-arginine and N^G-nitro-L-arginine methyl ester (L-NAME) on antigen-stimulated [^{3}H]-thymidine incorporation in spleen lymphocytes collected at different times from arthritic rats. The control group (●) was given tap water and the other groups were given L-arginine 30 mg ml^{-1} (□) or L-NAME 1 mg ml^{-1} (△) dissolved in drinking water. Each point represents the mean c.p.m. product by 10^5 cells separately collected from 3 rats. Standard errors were always less than 5% of the respective means and are not shown because they are covered by the symbols. The [^{3}H]-thymidine incorporation in cells obtained from naive rats ($n = 15$) lay within the dotted lines. *$P<0.01$ vs control group.

Macrophage activation

During the development of the arthritis, peritoneal macrophages were collected at weekly intervals from those rats used for evaluation of T-lymphocyte proliferation (see above). Macrophages were incubated in complete medium for 24 h in order to evalue NO_2^- production, as well as the release of both AP and LDH. These biochemical parameters were also evaluated in macrophages from naive rats.

Nitrite production These results are shown in Figure 5. In the control group the NO_2^- production increased from day 7 to day 14 and day 21. Thereafter the NO_2^- production declined on day 28 and was further reduced on day 35. Macrophages from the L-arginine-treated group produced larger amounts of NO_2^-, although the time course of NO_2^- generation followed a pattern similar to that exhibited by the cells from the control group. In contrast, NO_2^- production by macrophages from the L-NAME-treated group was greatly decreased when compared to that of the control group. Furthermore, in this group the time course of NO_2^- production did not have the clear bell shape observed in the other two groups. The difference between the control group and those treated with L-arginine or L-NAME was significant ($P<0.01$) at each time. The amount of NO_2^- produced by macrophages from naive rats ranged from 8.8 to 10.5 ($n = 15$) (Figure 5).

Acid phosphatase These results are shown in Figure 6. In the macrophages from the control group the release of AP gradually increased from day 7 to day 14 and day 21. Thereafter the release of AP declined on day 28 and was further reduced on day 35.

The AP release from the macrophages collected from the L-arginine-treated group was greater than that occurring in the cells from the control rats at each time interval. The difference between the two groups was significant ($P<0.05$) on day 21. Macrophages from L-NAME-treated rats always released smaller amounts of AP than the respective control cells. The difference between the two groups was significant on days 21 ($P<0.01$) and 28 ($P<0.05$). The AP release from naive rat macrophages ranged from 45 to 52 ($n = 15$) (Figure 6).

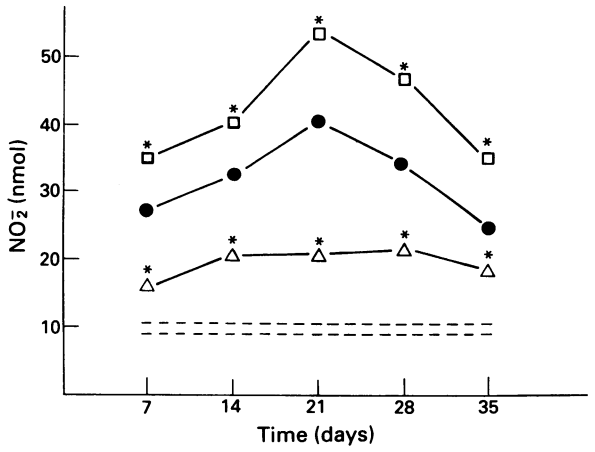

Figure 5 Effect of L-arginine and N^G-nitro-L-arginine methyl ester (L-NAME) on nitrite (NO_2^-) generation by peritoneal macrophages collected at different times from arthritic rats. The control group (●) was given tap water and the other groups were given L-arginine 30 mg ml^{-1} (□) or L-NAME 1 mg ml^{-1} (△) dissolved in drinking water. Each point represents the mean value of NO_2^- (nmol produced in 24 h by 10^6 cells separately collected from 3 rats). Standard errors were always less than 5% of the respective means and are not shown because they are covered by the symbols. The production of NO_2^- by cells from naive rats ($n = 15$) lay within the dotted lines. *$P<0.01$ vs control group.

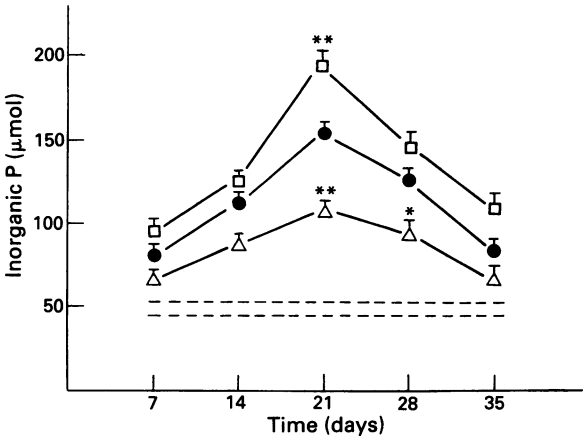

Figure 6 Effect of L-arginine and N^G-nitro-L-arginine methyl ester (L-NAME) on the release of acid phosphatase from peritoneal macrophages collected at different times from arthritic rats. The control group (●) was given tap water and the other groups were given L-arginine 30 mg ml^{-1} (□) or L-NAME 1 mg ml^{-1} (△) dissolved in drinking water. Each point represents the mean value ± s.e.mean of inorganic P (μmol) liberated in 30 min by the enzyme released in 24 h by 10^6 cells separately collected from 3 rats. The acid phosphatase released by cells from naive rats ($n = 15$) lay within the dotted lines. **$P<0.01$; *$P<0.05$ vs control group.

Lactic dehydrogenase The release of LDH (expressed as μmol of pyruvic acid transformed in 30 min by the enzyme released by 10^6 cells in 24 h) from macrophages of the three groups was virtually the same at any time. Thus it ranged from 67.2 to 69.2 ($n = 15$) in macrophages from control rats, from 66.4 to 69.6 ($n = 15$) in cells from the L-arginine-treated group and from 67.6 to 70.4 ($n = 15$) in the L-NAME-treated group. These values were virtually identical to the LDH release by macrophages from naive rats, which ranged from 65.2 to 67.8 ($n = 15$).

Discussion

Our results show that the L-arginine:NO pathway plays a role in adjuvant arthritis induced in the rat. Thus, ingestion of L-arginine, but not D-arginine or L-lysine, dose-dependently exacerbated the arthritis, which was reduced by L-NAME and unaffected by D-NAME. A combination of L-arginine and L-NAME led to an arthritic process similar to that in control animals.

Adjuvant arthritis is an experimental immunopathy which involves a T-lymphocyte-mediated delayed hypersensitivity reaction (Cohen, 1991). The disease is transferable to naive recipient rats by inoculation of specific T cells from treated animals and the proliferative response of these cells correlates with the incidence and severity of the arthritis (Holoshitz *et al.*, 1982; 1984).

Throughout the time course of the syndrome, T-lymphocytes from L-arginine-treated rats exhibited an enhanced proliferative response, whereas this was markedly depressed in L-NAME-treated animals. Furthermore, macrophages from L-arginine-treated rats generated greater amounts of NO_2^- and released higher levels of AP than those from the control group, whereas both NO_2^- generation and AP release were significantly reduced in cells from L-NAME-treated rats. The cytoplasmic enzyme LDH remained unaltered in macrophages during the development of arthritis, showing that lysosomal enzyme release was selective and not due to non-specific cell damage. Thus, manipulation of the L-arginine:NO pathway in the whole animal results in cellular changes which parallel the severity of the arthritis.

It has been shown that L-arginine improves host immunity, since it augments the number of thymic lymphocytes and the

response of T cells to mitogens, as well as enhancing tumour regression (Barbul *et al.*, 1980; 1985; Reynolds *et al.*, 1987). Furthermore, dietary supplements of L-arginine increase the activity of both natural-killer and lymphokine-activated-killer cells in healthy volunteers (Park *et al.*, 1991) and enhance development and interleukin (IL)-2 receptor expression in cytotoxic T-lymphocytes of mice (Reynolds *et al.*, 1988). It is therefore possible that increased lymphocyte proliferation leads to enhanced macrophage activation and thus an amplification of the general immunological response. The role of the L-arginine:NO pathway in lymphocytes is at present unclear. However, it has recently been observed that stimulated murine T-lymphocytes generate NO following induction of NO synthase (Kirk *et al.*, 1990).

The interaction of T cells with macrophages results in the production by both types of cells of several cytokines including IL-1, interferon-γ (IFN-γ) and tumour necrosis factor-α (TNF-α) which have been implicated in immune arthritis and are known to play a role in macrophage activation (Cooper *et al.*, 1988; Hom *et al.*, 1988; Thorbecke *et al.*, 1992). It has been shown that the leishmanicidal activity of macrophages correlates with their ability to express NO synthase following activation with IFN-γ or TNF-α (Liew *et al.*, 1991). Macrophage-derived NO is not only cytotoxic for invading micro-organisms and tumours, but may also produce host tissue damage (Kolb *et al.*, 1991; Kroncke *et al.*, 1991). Furthermore, cytokines might lead to induction of NO synthase in tissues other than the macrophages, including endothelial cells and chondrocytes, all of which may contribute to the general inflammatory response.

Although we did not measure cytokine levels in our experiments, it is interesting that the weight gain of arthritic rats given L-arginine was significantly lower than in control animals while L-NAME caused a significant and dose-dependent increase in weight gain. It is well known that TNF-α or cachectin is closely linked to the loss in weight occurring in animals suffering from chronic inflammation and/or infection (Beutler & Cerami, 1989). The effects of L-arginine and L-NAME on weight gain, which appear to be correlated to their respective pro- and anti-inflammatory actions, may possibly involve a modulatory role of these agents on the formation and/or the effects of TNF-α in arthritic rats.

In vitro inhibition of the L-arginine:NO pathway by L-NMMA has been reported to cause an increase in T cell proliferation induced by mitogens or alloantigens, suggesting an inhibitory role for NO in these models of T cell activation (Hoffman *et al.*, 1990; Albina *et al.*, 1991). The reasons for the apparent discrepancy between these *in vitro* and our *in vivo* findings and those described above, which indicate an enhancing role for NO in the immune system, need to be reconciled.

Although our results point towards an effect of the different treatments in the cellular immunological mechanism, it is important to recognize that L-NAME induces increases in blood pressure and reduction in blood flow in different organs (Gardiner *et al.*, 1990). Furthermore, L-arginine may increase vasodilatation and vascular permeability at the inflammatory site, as we have recently shown in some models of acute inflammation (Ialenti *et al.*, 1992). These vascular effects may also influence the development of the arthritic process in a way which remains to be determined.

Glucocorticoids inhibit the induction of NO synthase in macrophages, thus part of the anti-inflammatory and immunosuppressive actions of these steroids is due to this inhibition (Di Rosa *et al.*, 1990). It may be that the well-known suppressive effect of glucocorticoids in adjuvant arthritis may depend, at least in part, on a similar mechanism, i.e. the inhibition of the induction of NO synthase in T-lymphocytes and/or macrophages. It is also possible that selective inhibitors of the inducible NO synthase(s) that is expressed in stimulated macrophages and T-lymphocytes may represent a new class of antirheumatic-immunosuppressive agent.

The authors wish to thank Annie Higgs for her assistance in the preparation of the manuscript.

References

ALBINA, J.E., ABATE, J.A. & HENRY, W.L. Jr. (1991). Role of IFNγ in the induction of the nitric oxide-synthesizing pathway. *J. Immunol.*, **147**, 144–148.

BARBUL, A. (1986). Arginine: biochemistry, physiology, and therapeutic implications. *J. Parente. Enteral Nutr.*, **10**, 227–238.

BARBUL, A., FISCHEL, R.S., SHIMAZU, S., WASSERKRUG, H.L., YOSHIMURA, N.N., TAO, R.C. & EFRON, G. (1985). Intravenous hyperalimentation with high arginine levels improves wound healing and immune function. *J. Surg. Res.*, **38**, 328–334.

BARBUL, A., WASSERKRUG, H.L., SEIFTER, E., RETTURA, G., LEVENSON, S.M. & EFRON, G. (1980). Immunostimulatory effects of arginine in normal and injured rats. *J. Surg. Res.*, **29**, 228–235.

BEUTLER, B. & CERAMI, A. (1989). The biology of cachectin/TNFα – a primary mediator of the host response. *Annu. Rev. Immunol.*, **7**, 625–655.

BILLINGHAM, M.E.J. & DAVIES, E.G. (1979). Experimental models of arthritis in animals as screening tests for drugs to treat arthritis in man. In *Anti-inflammatory drugs*. ed Vane, J.R. & Ferreira, S.H. *Handbook of Exp. Pharmacol.*, vol. 50/2, pp. 108–144. Berlin:Springer.

CABAUD, P.G. & WROBLEWSKI, F. (1958). Colorimetric measurement of lactic dehydrogenase activity of body fluids. *Am. J.Clin Pathol.*, **30**, 234–236.

COHEN, I.R. (1991). Autoimmunity to chaperonins in the pathogenesis of arthritis and diabetes. *Annu. Rev. Pharmacol.*, **9**, 567–589.

COOPER, S.M., SRIRAM, S. & RANGES, G.E. (1988). Suppression of murine collagen-induced arthritis with monoclonal anti-Ia antibodies and augmentation with IFNγ. *J. Immunol.*, **141**, 1958–1962.

DI ROSA, M., RADOMSKI, M., CARNUCCIO, R. & MONCADA, S. (1990). Glucocorticoids inhibit the induction of nitric oxide synthase in macrophages. *Biochem. Biophys. Res. Commun.*, **172**, 1246–1252.

GARDINER, S.M., COMPTON, A.M., BENNETT, T., PALMER, R.M.J. & MONCADA, S. (1990). Regional haemodynamic changes during oral ingestion of N^G-nitro-L-arginine methyl ester in conscious Brattleboro rats. *Br. J. Pharmacol.*, **101**, 10–12.

GIANETTO, R. & DE DUVE, C. (1955). Comparative study of the binding of acid phosphatase, β-glucuronidase and cathepsin by rat-liver particles. *Biochem. J.*, **59**, 433–438.

HIBBS, J.B. Jr., TAINTOR, R.R., VAVRIN, Z., GRANGER, D.L., DRAPIER, J.-C., AMBER, I.J. & LANCASTER, J.R. Jr. (1990). Synthesis of nitric oxide from a terminal guanidino nitrogen atom of L-arginine: a molecular mechanism regulating cellular proliferation that targets intracellular iron. In *Nitric Oxide from L-Arginine: a Bioregulatory System*. ed. Moncada, S. & Higgs, E.A. pp. 189–223, Amsterdam: Elsevier.

HOFFMAN, R.A., LANGREHR, J.M., BILLAR, T.R., CURRAN, R.D. & SIMMONS, R.L. (1990). Alloantigen-induced activation of rat splenocytes is regulated by the oxidative metabolism of L-arginine. *J. Immunol.*, **145**, 2220–2226.

HOM, J.T., BENDELE, A.M. & CARLSON, D.G. (1988). In vivo administration with IL-1 accelerates the development of collagen-induced arthritis in mice. *J. Immunol.*, **141**, 834–841.

HOLOSHITZ, J., MATITIAU, A. & COHEN, I.R. (1984). Arthritis induced in rats by cloned T lymphocytes responsive to mycobacteria but not to collagen Type II. *J. Clin. Invest.*, **73**, 211–215.

HOLOSHITZ, J., NAPARSTEK, Y., BEN-NUN, A. & COHEN, I.R. (1982). Lines of T lymphocytes induce or vaccinate against autoimmune arthritis. *Science*, **219**, 56–58.

IALENTI, A., IANARO, A., MONCADA, S. & DI ROSA, M. (1992). Modulation of acute inflammation by endogenous nitric oxide. *Eur. J. Pharmacol.*, **211**, 177–182.

KIRK, S.J., REGAN, M.C. & BARBUL, A. (1990). Cloned murine T lymphocytes synthetize a molecule with the biological characteristics of nitric oxide. *Biochem. Biophys. Res. Commun.*, **173**, 660–665.

KOLB, H., KIESEL, U., KRONCKE, K.D. & KOLB-BACHOFEN, V. (1991). Suppression of low dose streptozotocin induced diabetes in mice by administration of a nitric oxide synthase inhibitor. *Life Sci.*, **49**, 213–217.

KRONCKE, K.D., KOLB-BACHOFEN, V., BERSCHICK, B., BURKART, V. & KOLB, H. (1991). Activated macrophages kill pancreatic syngeneic islet cells via arginine-dependent nitric oxide generation. *Biochem. Biophys. Res. Commun.*, **175**, 752–758.

LIEW, F.Y., LI, Y., MOSS, D., PARKINSON, C., ROGERS, M.V. & MONCADA, S. (1991). Resistance to *Leishmania major* infection correlates with the induction of nitric oxide synthase in murine macrophages. *Eur. J. Immunol.*, **21**, 3009–3014.

MCCALL, T.B., FEELISCH, M., PALMER, R.M.J. & MONCADA, S. (1991). Identification of N-iminoethyl-L-ornithine as an irreversible inhibitor of nitric oxide synthase in phagocytic cells. *Br. J. Pharmacol.*, **102**, 234–238.

MONCADA, S., PALMER, R.M.J. & HIGGS, E.A. (1991). Nitric oxide: physiology, pathophysiology and pharmacology. *Pharmacol. Rev.*, **43**, 109–142.

NEWBOLD, B.B. (1963). Chemotherapy of arthritis induced in rats by injection of mycobacterial adjuvant. *Br. J. Pharmacol.*, **21**, 127–136.

PARK, K.G.M., HAYES, P.D., GARLICK, P.J., SEWELL, H. & EREMIN, O. (1991). Stimulation of lymphocyte natural cytotoxicity by L-arginine. *Lancet*, **337**, 645–646.

REES, D.D., PALMER, R.M.J., SCHULZ, R., HODSON, H.F. & MONCADA, S. (1990). Characterization of three inhibitors of endothelial nitric oxide synthase *in vitro* and *in vivo*. *Br. J. Pharmacol.*, **101**, 746–752.

REYNOLDS, J.V., ZHANG, S., THOM, A.K., ZIEGLER, M.M. NAJI, A. & DALY, J.M. (1987). Arginine as immunomodulator. *Surgical Forum*, **38**, 415–418.

REYNOLDS, J.V., DALY, J.M., ZHANG, S., EVANTASH, E., SHOU, J., SIGAL, R. & ZIEGLER, M.M. (1988). Immunomodulatory mechanisms of arginine. *Surgery*, **104**, 142–151.

THORBECKE, G.J., SHAH, R., LEU, C.H., KURUVILLA, A.P., HARDISON, A.M. & PALLADINO, M.A. (1992). Involvement of endogenous tumor necrosis factor α and transforming growth factor β during induction of collagen type II arthritis in mice. *Immunology*, **89**, 7375–7379.

(Received January 4, 1993
Revised May 21, 1993
Accepted June 15, 1993)

Br. J. Pharmacol. (1993), **110**, 707–712

Activation of protein kinase C potentiates postsynaptic acetylcholine response at developing neuromuscular synapses

[1]Wen-Mei Fu & Jiann-Liang Lin

Pharmacological Insititute, College of Medicine, National Taiwan University, Taipei, Taiwan

1 Phorbol 12-myristate 13-acetate (TPA, 1 μM) and phorbol 12,13-dibutyrate (PDBu, 2 μM), activators of protein kinase C (PKC), increased the mean amplitude and decay time of the spontaneous synaptic currents of *Xenopus* nerve-muscle coculture, whereas, 4α-phorbol (2 μM) which is an inactive phorbol analogue had no effect.

2 Staurosporine (0.5 μM) and H-7 (10 μM), inhibitors of PKC, inhibited the potentiation effects of TPA on the spontaneous synaptic currents.

3 Effects of TPA on the postsynaptic acetylcholine (ACh) sensitivity were examined by iontophoresis of ACh to the surface of embryonic muscle cells of 1-day-old *Xenopus* cultures. TPA increased both the amplitude and decay time of ACh-induced whole-cell currents in isolated myocytes.

4 TPA concentration-dependently increased the mean open time of low-conductance ACh channels but did not affect those of high-conductance ACh channels. PDBu but not 4α-phorbol exhibited similar effects to TPA. Staurosporine and H-7 inhibited the increasing effects of TPA.

5 These results suggest that activation of PKC might be involved in synaptogenesis at developing neuromuscular synapses by the postsynaptic potentiation of ACh sensitivity.

Keywords: Phorbol 12-myristate 13-acetate (TPA); protein kinase C; ACh response; embryonic myocyte

Introduction

The characteristics of postsynaptic nicotinic acetylcholine (ACh) receptor channels determine the property of synaptic transmission at the neuromuscular junction. It has also been suggested that protein phosphorylation (one of the principal mechanisms of regulation of cellular metabolism) plays a major role in the regulation of synaptic function (Greengard, 1978), a fundamental event in signal transduction is receptor phosphorylation (Nestler & Greengard, 1984). Protein phosphorylation has been correlated with modulation of receptor activity by either enhancing or terminating the action of ligand (Hemmings *et al.*, 1989). The principal effect of adenosine 3':5'-cyclic monophosphate (cyclic AMP)-dependent processes on muscle and electric organ AChRs has been reported to be an enhancement of the receptor phosphorylation as well as the rate of agonist-induced receptor desensitization (Huganir *et al.*, 1986; Middleton *et al.*, 1986; 1988; Mulle *et al.*, 1988). On the other hand, phorbol 12-myristate 13-acetate (TPA), an activator of protein kinase C, has also been reported to reduce ACh sensitivity in cultured myotubes (Eusebi *et al.*, 1985). The physiological role of desensitization or reduction of sensitivity of AChR remains unclear.

Recently, we have provided the first evidence that membrane permeable analogues of cyclic AMP and forskolin increased the ACh responses in the embryonic myocytes of *Xenopus* cell cultures (Fu & Poo, 1991). Furthermore, calcitonin gene-related peptide (CGRP) which is released from the nerve terminals and elevates postysynpatic cyclic AMP has also been shown to potentiate spontaneous synaptic currents and increase mean open time of ACh channels in *Xenopus* embryonic myocytes (Lu *et al.*, 1993). The involvement of cyclic AMP-dependent protein kinase (PKA) in the action of CGRP was implicated, since intracellular loading of a PKA inhibitor into the myocyte prevented the CGRP effects. In the present study, we examined further the effect of activation of protein kinase C (PKC) on the properties of ACh channels and the synaptic currents during the early phase of neuromuscular synaptogenesis. We found that agents activating PKC increased the synaptic currents and iontophoretic ACh-induced currents in these embryonic myocytes. The present findings suggest that PKC and released trophic factors which activate PKC may be important in the physiological modulation of synaptic function during the early phase of synaptic development.

[1] Author for correspondence.

Methods

Culture preparations

Xenopus nerve-muscle cultures were prepared as previously described (Spitzer & Lamborghini, 1976; Anderson *et al.*, 1977; Sanes & Poo, 1989). Briefly, the neural tube and the associated myotomal tissue of 1-day-old *Xenopus* embryos at stage 20–22 (Nieuwkoop & Faber, 1967) were dissociated in the Ca^{2+}- and Mg^{2+}-free Ringer solution supplemented with EDTA. The cells were plated on clean glass coverslips and were used for experiments after 24 h incubation at room temperature (20–22°C). The culture medium consisted of 50% (vol/vol) Ringer solution (composition mM: NaCl 115, $CaCl_2$ 2, KCl 2.5, HEPES 10, pH 7.6), 49% L-15 Leibovitz medium (Sigma), and 1% foetal bovine serum (GIBCO). Most of the experiments utilized the spherical myocytes in these cultures. Previous studies have shown that synapses formed between spinal neurones and these spherical myocytes have structural and functional properties similar to those observed *in vivo* (Evers *et al.*, 1989).

Electrophysiology

Whole-cell and cell-attached patch-clamp recording methods were similar to those described previously (Hamill *et al.*, 1981; Evers *et al.*, 1989). Whole-cell recording method was used in voltage-clamp configuration to monitor membrane currents induced by iontophoresis of ACh at isolated myocytes and synaptic currents at innervated myocytes. The solution inside the whole-cell recording pipettes contained mM: KCl 150, NaCl 1, $MgCl_2$ 1 and HEPES 10 (pH 7.2). Iontophoresis of ACh was applied to the surface of the myocyte by conventional glass microelectrodes filled with 3 M ACh

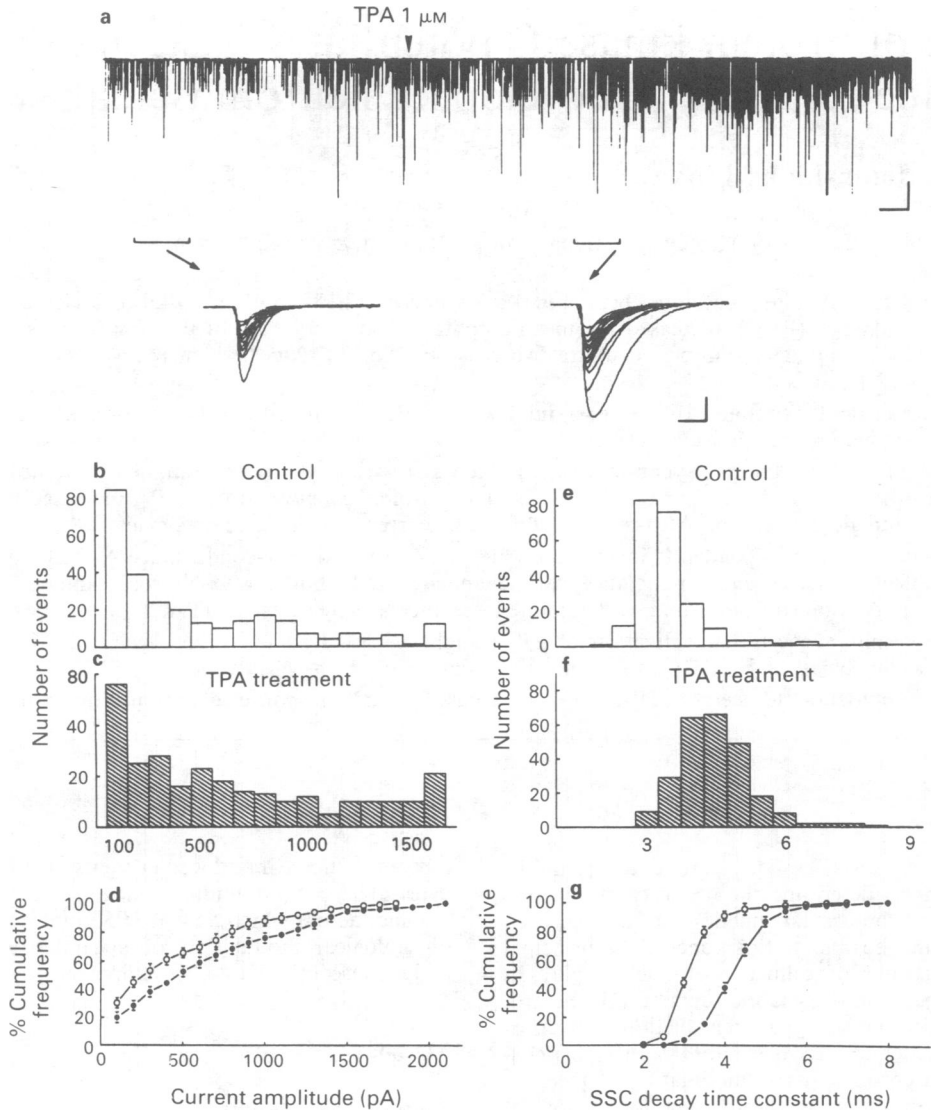

Figure 1 Potentiation of synaptic activity by phorbol 12-myristate 13-acetate (TPA). (a) Continuous trace depicts membrane current measured by gigaohm-seal, whole-cell recording method from an innervated myocyte in 1-day-old *Xenopus* culture. The myocyte was voltage-clamped at − 60 mV. Spontaneous synaptic currents (SSCs) appear as random downward deflection (filtered at 150 Hz). TPA was applied to the culture at time marked by the arrow. Samples of synaptic currents before and after drug application were superimposed and shown below the trace at higher time resolution (filtered at 10 kHz). Note the increase in the average amplitude and decay time of the synaptic currents after TPA treatment. Bars: 30 s, 170 pA and 3 ms, 150 pA for slow and fast traces, respectively. (b,c) Histograms of amplitude distribution for all SSC events before (b) and after (c) TPA application at the same synapse as in (a). (e,f) Histograms of decay time distribution for all SSC events before (e) and after (f) TPA application. (d,g) % cumulative frequency of amplitude (d) and decay time (g) distribution of all SSC events obtained from 4 cells. The difference between two sets of data obtained from control (○) and TPA-treated (●) is significant ($P < 0.05$, two-tail t test).

chloride (resistance 100–200 MΩ). The iontophoretic current of 2 ms duration was supplied by a Grass stimulator (SD9) through a microelectrode amplifier (Getting M5), which provided a braking current between 2 to 10 nA. For single channel recording, the patch pipettes were coated with Sylgard (Dow Corning) before polishing to reduce the capacitance of the electrode and the noise of the current recordings. The pipette was filled with Ringer solution containing low concentrations of ACh (1–5 nM). Single channel activities were recorded with a patch clamp amplifier (Dagan 8900) and the current signal was filtered at 3 kHz. The data were digitized by a digitizing unit (Neuro-Corder DR390) and stored on a videotape recorder for later playback on a storage oscilloscope (Tektronix 5113) and on oscillographic recorder (Gould RS3200) or for anlysis by a microcomputer. For single channel analysis, the current signals were digitized at either 50 or 100 μs intervals and analysed with PClamp programme (Axon Inst.). The amplitude and duration of individual events were measured and stored in the computer. Events corresponding to opening of more than one channel were excluded from the open time analysis. Events with open time shorter than 500 μs were not analysed because of possible attenuation and distortion. Open duration histograms were fitted with a single exponential and the amplitude histograms were fitted with Gaussian distribution curves, using least-squares method in both cases. All recordings were made at room temperature in culture medium. The results are expressed as the mean ± s.e.mean. The statistical significance was evaluated by Student's t test.

The following chemicals were used: acetylcholine (ACh), TPA (phorbol 12-myristate 13-acetate), PDBu (phorbol 12, 13-dibutyrate) and 4α-phorbol (Sigma), staurosporine (Boehringer) and H-7 (1-(5-isoquinolinesulphonyl)-2-methylpiperazine dihydrochloride) (Seikagaku Kogyo Co., Japan).

Results

Effects of protein kinase C (PKC) activators on spontaneous synaptic currents

In nerve-muscle cultures prepared from 1-day-old *Xenopus* embryos, synaptic contacts are established between dissociated spinal neurones and myotomal myocytes within the first day of culture. Spontaneous synaptic currents (SSCs) are readily detectable from the innervated myocytes by whole-cell voltage-clamp recording. These currents have been shown to be caused by spontaneous pulsatile ACh secretion from the neurone, since they were abolished by bath application of (+)-tubocurarine and unaffected by tetrodotoxin (Xie & Poo, 1986). Figure 1a depicts the recording of SSCs from an innervated myocyte before and after application of TPA (1 μM). Bath application of TPA increased the frequency and the amplitude and decay time of the SSCs. The change in amplitude and decay time distribution was apparent on comparing the amplitude and decay time histograms of SSCs before and after exposure to TPA in the same cell (Figure 1b,c,e and f). Figure 1d and g show the cumulative frequency (%) obtained from 4 cells. TPA treatment shifted the curves to the right. PDBu, another PKC activator, also increased both amplitude and decay time of the SSC currents, but 4α-phorbol, an inactive phorbol analogue, had no effect (Figure 2). Figure 3 summarizes the results obtained with these phorbol ester analogues on the amplitude and decay time of the SSCs and also showed that staurosporine and H-7 (both PKC inhibitors), inhibited the potentiating effects of TPA. The increase in SSC frequency induced by TPA resulted from presynaptic potentiation of spontaneous ACh secretion. The increase in amplitude, on the other hand, could be caused by a higher amount of transmitter molecules in the ACh quanta or by an elevated sensitivity of the muscle cell membrane toward ACh. In the following experiment, we tested directly the effect of TPA on ACh sensitivity of embryonic myocytes.

Potentiation of muscle acetylcholine sensitivity by TPA

Gigaohm-seal, whole-cell recording of single non-innervated myocyte in 1-day-old *Xenopus* cultures was performed in voltage-clamp mode. Identical ACh pulses were applied repetitively by focal iontophoresis at the muscle surface, and the ACh-induced membrane currents were recorded. Figure 4

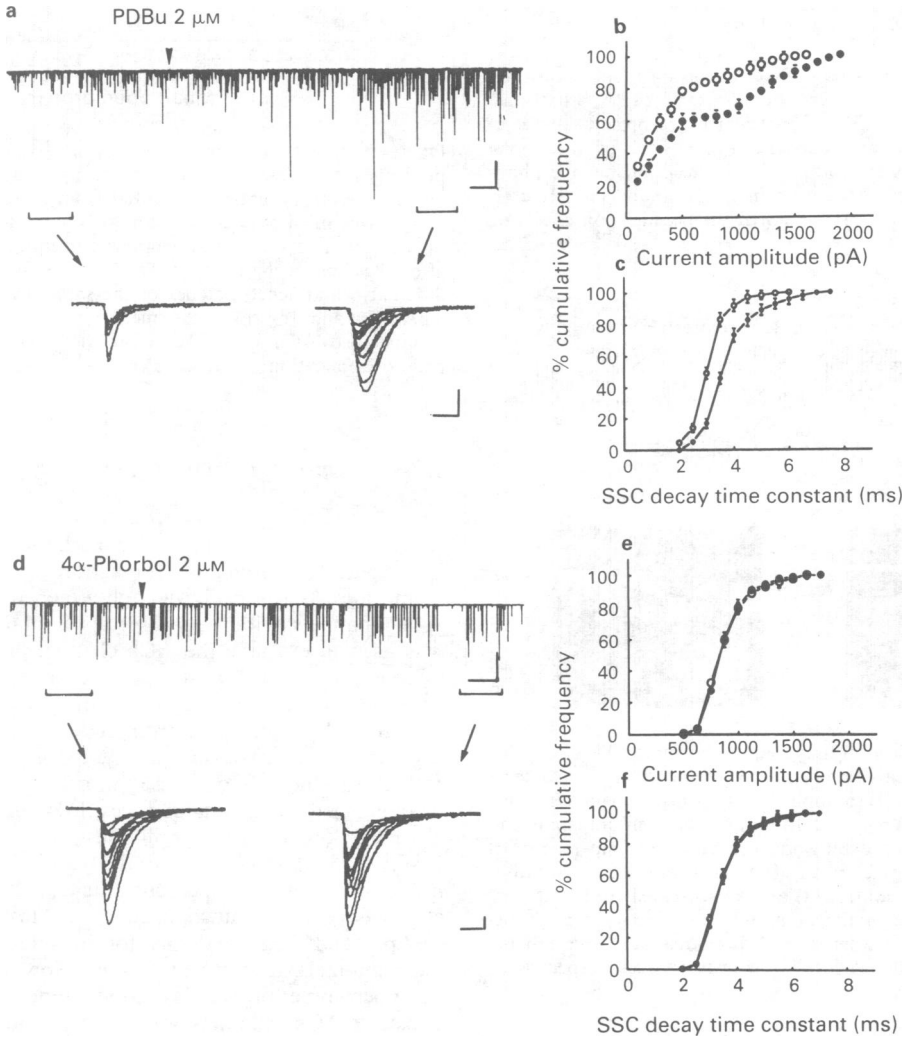

Figure 2 Effects of phorbol analogues on the spontaneous synaptic currents. Continuous traces in (a) and (d) depict membrane current measured by whole-cell recording from an innervated myocyte which was voltage-clamped at −60 mV. Spontaneous synaptic currents (SSCs) appear as random downward deflections. Samples of synaptic currents were shown below at higher time resolution. Note that phorbol 12,13-dibutyrate (PDBu) (a) but not 4α-phorbol (d) increased the amplitude and decay time of the synaptic currents. Bars: 30 s, 160 pA and 3 ms, 150 pA for slow and fast traces, respectively. (b,c,e and f) % cumulative frequency of amplitude (b,e) and decay time (c,f) distribution of all SSC events obtained from 4 cells. The difference between two sets of data points obtained from control (○) and PDBu-treated (●) is significant ($P<0.05$, two-tail t test). There is no significant difference between control (○) and 4α-phorbol-treated (●) groups ($P>0.05$).

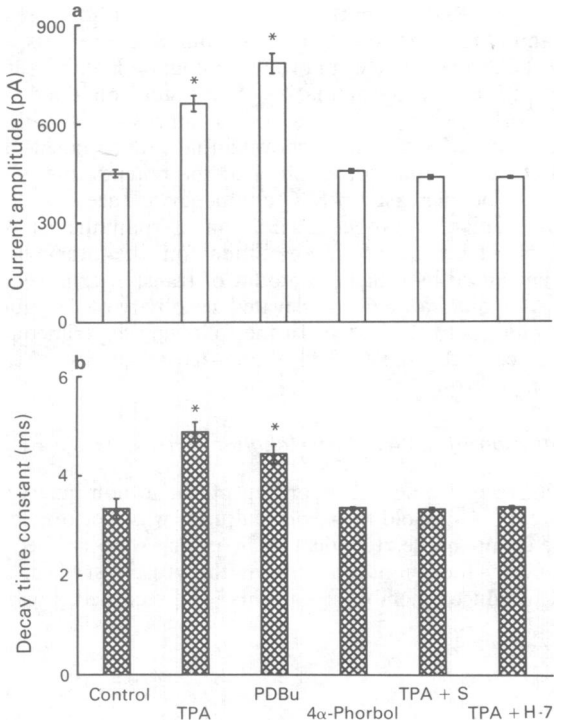

Figure 3 Effects of protein kinase C activation on the spontaneous synaptic currents. Phorbol 12-myristate 13-acetate (TPA, 1 μM) and phorbol 12,13-dibutyrate (PDBu, 2 μM) which are protein kinase C activators increased the amplitude and decay time of the spontaneous synaptic currents, but 4α-phorbol (2 μM), an inactive phorbol analogue, had no effect. Staurosporine (0.5 μM) and H-7 (10 μM), both protein kinase C inhibitors, inhibited the potentiation effects of TPA. ($n = 5-8$).

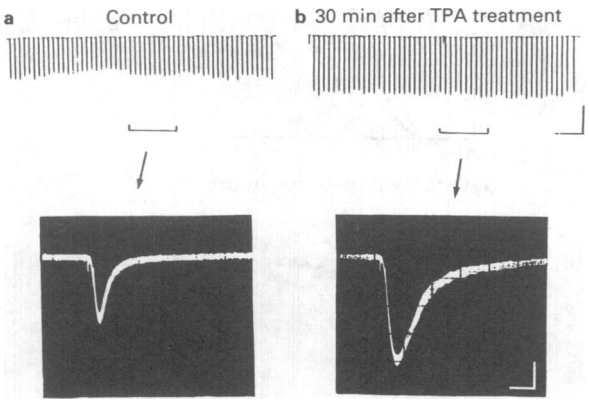

Figure 4 Effects of phorbol 12-myristate 13-acetate (TPA) on the acetylcholine (ACh) sensitivity of isolated myocyte. Identical iontophoretic pulses of ACh were applied to the surface of an isolated myocyte in a 1-day-old *Xenopus* culture, and the membrane current of the myocyte was recorded by whole-cell voltage-clamp recording (Vc: − 60 mV). Oscilloscopic traces of 10 superimposed consecutive ACh-induced currents of control (a) and TPA-treated (b) are shown below. Note the increase in the amplitude and decay time of the membrane currents 30 min after TPA (1 μM) treatment. Scale bars: 8 s, 320 pA and 10 ms, 200 pA for slow and fast traces, respectively.

depicts the recording of ACh-induced membrane currents before and 30 min after TPA application. Similar to the effects of TPA on synaptic currents, both the peak amplitude and the decay time of ACh-induced currents were significantly increased. The mean amplitude and decay time of ACh-induced current after TPA treatment was 198.1 ± 20.8% and 149.0 ± 19.6% ($n = 9$) that of the control (prior to the TPA treatment), respectively.

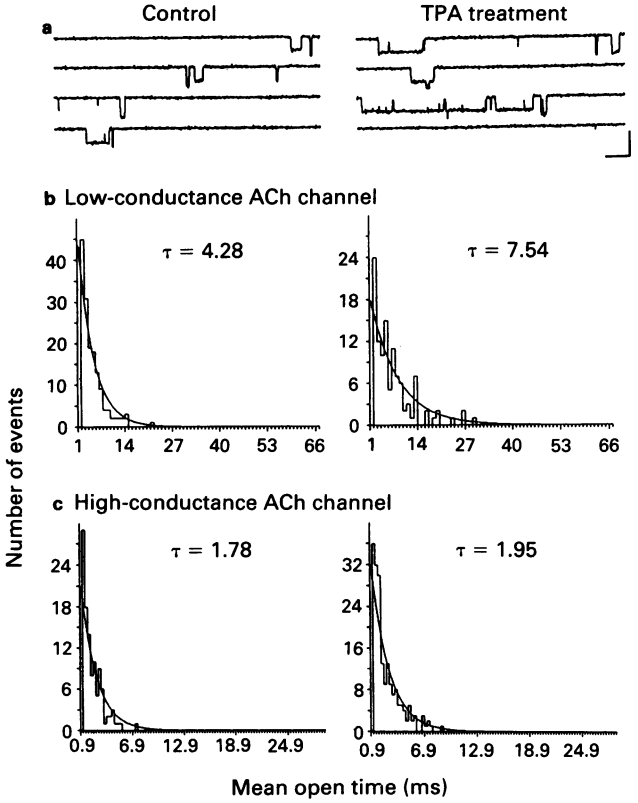

Figure 5 Effects of phorbol 12-myristate 13-acetate (TPA) on the properties of single acetylcholine (ACh) channel. Recordings were made at + 60 mV applied potential from cell-attached patches. The pipette was filled with Ringer containing 1 nM of ACh. (a) Samples of recordings of single ACh channel currents before (left panel) and after (right panel) bath application of 1 μM TPA were obtained from different cell-attached patches of the same myocyte. Bars: 7 ms and 8 pA. (b) and (c) show the mean open time of low- and high-conductance ACh channels before (left panels) and after (right panels) application of 1 μM TPA.

Effects of protein kinase C activators on single ACh channel

Single channel recordings were made on isolated myocyte to investigate the mechanism of action of TPA on the muscle membrane ACh sensitivity. Cell-attached patch recording of ACh channels with micropipettes containing 1–5 nM ACh was used to examine the ACh channel properties before and after extracellular exposure of the myocyte to TPA. Figure 5a shows samples of single channel events observed before and after TPA exposure from different patches of the same myocyte when myocyte was hyperpolarized + 60 mV from rest. ACh channels on these embryonic muscle cells can be distinguished as two major types, low- and high-conductance channels; the current amplitudes were 5.07 ± 0.04 pA and 7.51 ± 0.05 pA ($n = 6$), respectively. We found that the amplitude of single channel currents for both types of ACh channels remained unchanged after TPA treatment (5.09 ± 0.02 pA and 7.52 ± 0.04 pA for low- and high-conductance ACh channels, respectively, $n = 6$). However, the mean channel open time of the low-conductance but not high-conductance ACh channels was increased after TPA treatment (Figure 5b and c). TPA concentration-dependently increased the mean open time of low-conductance ACh channels (Figure 6). The involvement of protein kinase C activation as the mechanism of action of TPA was further supported by the inhibitory effect of staurosporine and H-7 (both PKC inhibitors) on the action of TPA (Figure 7). Furthermore, PDBu but not 4α-phorbol increased the mean open time of low-conductance ACh channels (Figure 7).

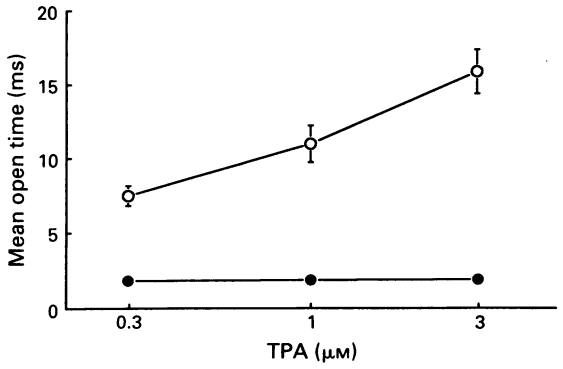

Figure 6 Concentration-dependent increase of mean open time of single acetylcholine (ACh) channel by phorbol 12-myristate 13-acetate (TPA). Each data point is obtained from at least 7 patches at each concentration. Note that TPA concentration-dependently increased the mean open time of low-conductance (○) but not high-conductance (●) ACh channels.

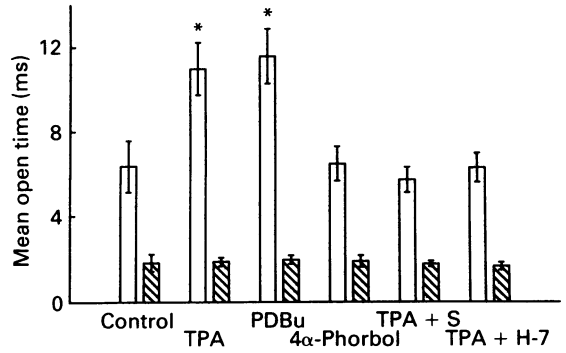

Figure 7 Effects of protein kinase C activation on the mean open time of single acetylcholine (ACh) channel. Phorbol 12-myristate 13-acetate (TPA, 1 μM) and phorbol 12, 13-dibutyrate (PDBu, 2 μM) which are protein kinase C activators increased the mean open time of low-conductance (open columns) but not high-conductance (hatched columns) ACh channels, but 4α-phorbol (2 μM), an inactive phorbol analogue, had no effect. Staurosporine (0.5 μM) and H-7 (10 μM), both protein kinase C inhibitors, inhibited the increasing effect of TPA.

Discussion

The characteristics of postsynaptic nicotinic acetylcholine (ACh) channels determine the property of synaptic transmission at the neuromuscular junction. Phosphorylation reactions are known to be able to modulate synaptic transmission both pre- and post-synaptically (Kennedy, 1983; Nestler *et al.*, 1984). Phosphorylation of the muscle ACh receptor (AChR) has been implicated in playing a role in the regulation of the receptor ion channelling. Cyclic AMP-elevating agents, which act presumably by activating cyclic AMP-dependent protein kinase (PKA) were shown to enhance receptor desensitization (Albuquerque *et al.*, 1986; Middleton *et al.*, 1986). On the other hand, many important phosphorylation reactions are mediated by protein kinase C (PKC) (Nishizuka, 1986; Huganir & Greengard, 1987; Nishizuka, 1988), which can be specifically activated by the phorbol ester, TPA. TPA was shown to enhance spontaneous ACh secretion in this experiment, in accordance with previous reports showing that TPA enhanced neurotransmitter release presynaptically at motor nerve terminals (Eusebi *et al.*, 1986; Haimann *et al.*, 1987; Murphy & Smith, 1987; Shapira *et al.*, 1987; Caratsch *et al.*, 1988). Although there is growing evidence that PKC can modulate the activity of voltage-dependent Ca^{2+}, Cl^- and K^+ conductance (Kaczmarek, 1987; Shearman *et al.*, 1989), reports of effects of PCK on ligand-gated channels are rare. Recently, it was reported that the effects of PKC on the postsynaptic sensitivity of AChR showed species differences. TPA causes a transient decrease in ACh sensitivity at the junctional AChRs of adult frog muscle fibres (Caratsch *et al.*, 1986) and a sustained decrease in ACh sensitivity accompanied by a decrease in both channel conductance and opening probability at the extrajunctional AChRs of embryonic chick myotubes (Eusebi *et al.*, 1985; 1987). On the other hand, TPA causes an early decrease followed by a delayed increase and again a decrease to below pretreatment level in rat skeletal muscle (Caratsch *et al.*, 1989). In the present study, we obtained evidence that activation of PKC increases postsynaptic ACh responses in embryonic myocytes.

In this work, we have demonstrated that TPA and PDBu potentiate ACh responses in the embryonic myocyte of 1-day-old *Xenopus* culture. The involvement of PKC in this effect is further supported by the inhibitory effect on the action of TPA of staurosporine and H-7 (both PKC inhibitors) together with the lack of potentiating effect of 4α-phorbol, which does not activate PKC (Castagna *et al.*, 1982). Developmental changes of ACh receptor channels have been studied extensively in *Xenopus* muscle cells *in vitro* (Brehm *et al.*, 1984a; Rohrbough & Kidokoro, 1990) as well as *in vivo* (Kullberg *et al.*, 1981; Brehm *et al.*, 1984b; Owens & Kullberg, 1989). Shortly after the initial insertion of ACh receptor channels, the majority of channels are an embryonic type (low-conductance channels) which have a prolonged mean open time and lower conductance. The adult-type channels (high-conductance channels) are rare at the early stages but they are detectable from the beginning. They have about 50% greater unitary conductance than embryonic-type channels and shorter mean open time. During development, the relative population of the adult-type channels increases (Kidokoro & Gruener, 1982; Brehm *et al.*, 1984a). The results of this study demonstrate that application of TPA increased the amplitude and decay time of iontophoretic ACh-induced whole-cell current. Measurement of single ACh channel activity was consistent with this result. The open duration and opening probability of low-conductance ACh channels but not those of high-conductance channels were increased by the application of TPA. These potentiating effects of PKC on ACh channels of *Xenopus* embryonic myocytes appear very similar to those observed in PKA modulation (Fu & Poo, 1991). It is possible that the muscle cells used in previous studies may have reached a more mature stage of development and their ACh channels lost their susceptibility to potentiation, as we found for older *Xenopus* myocytes (unpublished data). *In vitro* studies indicate that all four subunits of the AChR from *Torpedo* electric organ and rat muscle can be phosphorylated by several kinases (Huganir & Greengard, 1983; Huganir *et al.*, 1984; Steinbach & Zempel, 1987). PKA phosphorylates the r and δ subunits, PKC phosphorylates the α and δ subunits. Their results show that the rate of desensitization was enhanced for the phosphorylated AChRs. It remains to be determined whether the potentiation of AChR response by PKC in *Xenopus* embryonic myocytes is mediated by the phosphorylation of the receptor subunits and which phosphorylated subunits are responsible for this potentiating action.

Spontaneous synaptic activity begins soon after nerve-muscle contact. This early activity is known to be responsible for inducing spontaneous muscle contractions during the early phase of synaptogenesis. Kidokoro & Saito (1988) have found that spontaneous synaptic activity is responsible for the accelerated development of striation in the innervated myocyte. Maturation of synaptic specialization could also be influenced by the presence of the activity and the increase of intracellular Ca^{2+} concentration through the influx from AChR channels. Thus this work provides an indication that extracellular agents such as primary neurotransmitters, co-transmitters or hormones which are capable of activating

PKC, may regulate synaptic ion channels and synaptic maturation at embryonic developing neuromuscular synapses.

This work was supported by a grant from National Science Council of Taiwan (NSC82-0412-B002-95).

References

ALBUQUERQUE, E.X., DESHPANDE, S.S., ARACAVA, Y., ALKONDON, M. & DALY, J.W. (1986). A possible involvement of cyclic AMP in the expression of desensitization of the nicotinic acetylcholine receptor. *FEBS Lett.*, **199**, 113–120.

ANDERSON, M.J., COHEN, M.W. & ZORYCHIA, E. (1977). Effects of innervation on the distribution of acetylcholine receptors on cultured muscle cells. *J. Physiol.*, **268**, 731–756.

BREHM, P., KIDOKORO, Y. & MOODY-CORBETT, F. (1984a). Acetylcholine receptor channel properties during development of *Xenopus* muscle cells in culture. *J. Physiol.*, **357**, 203–217.

BREHM, P., KULIBERG, R. & MOODY-CORBETT, F. (1984b). Properties of non-junctional acetylcholine receptor channels in innervated muscle of *Xenopus laevis*. *J. Physiol.*, **350**, 631–648.

CARATSCH, C.G., GRASSI, F., MOLINARO, M. & EUSEBI, F. (1986). Postsynaptic effects of the phorbol ester TPA on frog end-plates. *Pflügers Arch.*, **407**, 409–413.

CARATSCH, C.G., KNOFLACH, F., GRASSI, F. & EUSEBI, F. (1989). Regulation of acetylcholine receptor function by the phorbol ester TPA in rat skeletal muscle. *Naunyn-Schmied. Arch. Pharmacol.*, **340**, 82–86.

CARATSCH, C.G., SCHUMACHER, S., GRASSI, F. & EUSEBI, F. (1988). Influence of protein kinase C-stimulation by a phorbol ester on neurotransmitter release at frog end-plates. *Naunyn-Schmied. Arch. Pharmacol.*, **337**, 9–12.

CASTAGNA, M., TAKAI, Y., KAIBUCHI, K., SANO, K., KIKKAWA, Y. & NISHIZUKA, Y. (1982). Direct activation of calcium-activated, phospholipid-dependent protein kinase by tumor-promoting phorbol esters. *J. Biol. Chem.*, **257**, 7847–7851.

EUSEBI, F., GRASSI, F., MOLINARO, M. & ZANI, B.M. (1987). Acetylcholine regulation of nicotinic receptor channels through a putative G protein in chick myotubes. *J. Physiol.*, **393**, 635–645.

EUSEBI, F., MOLINARO, M. & CARATSCH, C.G. (1986). Effects of phorbol ester on spontaneous transmitter release at frog neuromuscular junction. *Pflügers Arch.*, **406**, 181–183.

EUSEBI, F., MOLINARO, M. & ZANI, B.M. (1985). Agents that activate protein kinase C reduce acetylcholine sensitivity in cultured myotubes. *J. Cell Biol.*, **100**, 1339–1342.

EVERS, J., LASER, M., SUN, Y., XIE, Z. & POO, M.M. (1989). Studies of nerve-muscle interactions in *Xenopus* cell culture: analysis of early synaptic currents. *J. Neurosci.*, **9**, 1523–1539.

FU, W.M. & POO, M.M. (1991). Modulation of acetylcholine channel by DBcAMP in *Xenopus* cell culture. *Soc. Neurosci.*, **17**, 1096 (Abstr).

GREENGARD, P. (1978). Phosphorylated proteins as physiological effectors. *Science*, **199**, 146–152.

HAIMANN, C., MELDOLESI, J. & CECCARELLI, B. (1987). The phorbol ester, 12-0-tetradecanoylphorbol-13-acetate, enhances the evoked quanta release of acetylcholine at the frog neuromuscular junction. *Pflügers Arch.*, **408**, 27–31.

HAMILL, O.P., MARTY, A., NEHER, E., SAKMANN, B. & SIGWORTH, F.J. (1981). Improved patch-clamp techniques for high-resolution current recording from cell and cell-free membrane patches. *Pflügers Arch.*, **391**, 85–100.

HEMMINGS, H.C., NARIN, A.C., MCGUINESS, T.L., HUGANIR, R.L. & GREENGARD, P. (1989). Role of protein phosphorylation in neuronal signal transduction. *FASEB J.*, **3**, 1583–1592.

HUGANIR, R.L., DELCOUR, A.H., GREENGARD, P. & HESS, G.P. (1986). Phosphorylation of the nicotinic acetylcholine receptor regulates its rate of desensitization. *Nature*, **321**, 774–776.

HUGANIR, R.L. & GREENGARD, P. (1983). cAMP-dependent protein kinase phosphorylates the nicotinic acetylcholine receptor. *Proc. Natl. Acad. Sci. U.S.A.*, **80**, 1130–1134.

HUGANIR, R.L. & GREENGARD, P. (1987). Regulation of receptor function by protein phosphorylation. *Trends Pharmacol. Sci.*, **8**, 472–477.

HUGANIR, R.L., MILES, K. & GREENGARD, P. (1984). Phosphorylation of the nicotinic acetylcholine receptor by an endogenous tyrosine-specific protein kinase. *Proc. Natl. Acad. Sci. U.S.A.*, **81**, 6968–6972.

KACZMAREK, L.K. (1987). The role of protein kinase C in the regulation of ion channels and neurotransmitter release. *Trends Neurosci.*, **10**, 30–34.

KENNEDY, M.B. (1983). Experimental approaches to understanding the role of protein phosphorylation in the regulation of neuronal function. *Annu. Rev. Neurosci.*, **6**, 493–525.

KIDOKORO, Y. & GRUENER, R. (1982). Distribution and density of α-bungarotoxin binding sites on innervated and noninnervated *Xenopus* muscle cells in culture. *Develop. Biol.*, **91**, 78–85.

KIDOKORO, Y. & SAITO, M. (1988). Early cross-striation formation in twitching *Xenopus* myocytes in culture. *Proc. Natl. Acad. Sci. U.S.A.*, **85**, 1978–1982.

KULLBERG, R., BREHM, P. & STEINBACH, J.H. (1981). Nonjunctional acetylcholine receptor channel open time decreases during development of *Xenopus* muscle. *Nature*, **289**, 411–413.

LU, B., FU, W.M., GREENGARD, P. & POO, M.M. (1993). CGRP enhances nicotinic ACh channel activity at developing neuromuscular synapses through cAMP-dependent protein kinase. *Nature*, **363**, 76–79.

MIDDLETON, P., JARAMILLO, F. & SCHUETZE, S.M. (1986). Forskolin increases the rate of acetylcholine receptor desensitization at rat soleus endplate. *Proc. Natl. Acad. Sci. U.S.A.*, **83**, 4967–4971.

MIDDLETON, P., RUBIN, L.L. & SCHUETZE, S.M. (1988). Desensitization of acetylcholine receptors in rat myotubes is enhanced by agents that elevate intracellular cAMP. *J. Neurosci.*, **8**, 3405–3412.

MULLE, C., BENOIT, P., PINSET, C., ROA, M. & CHANGEUX, J.-P. (1988). Calcitonin gene-related peptide enhances the rate of desensitization of the nicotinic acetylcholine receptor in cultured mouse muscle cells. *Proc. Natl. Acad. Sci. U.S.A.*, **85**, 5728–5732.

MURPHY, R.L.W. & SMITH, M.E. (1987). Effects of diacylglycerol and phorbol ester on acetylcholine release and action at the neuromuscular junction in mice. *Br. J. Pharmacol.*, **90**, 327–334.

NESTLER, E.J. & GREENGARD, P. (1984). *Protein Phosphorylation in the Nervous System* (New York: Wiley).

NESTLER, E.G., WALAAS, S.I. & GREENGARD, P. (1984). Neuronal phosphoprotein: physiological and clinical implications. *Science*, **225**, 1365–1370.

NIEUWKOOP, P.D. & FABER, J. (1967). *Normal Table of* Xenopus laevis. Second Edition. Amsterdam: North Holland.

NISHIZUKA, Y. (1986). Studies and perspectives of protein kinase C. *Science*, **233**, 305–312.

NISHIZUKA, Y. (1988). The molecular heterogeneity of protein kinase C and its implications for cellular regulation. *Nature*, **334**, 661–665.

OWENS, J.L. & KULLBERG, R. (1989). In vivo development of nicotinic acetylcholine receptor channel in *Xenopus* myotomal muscle. *J. Neurosci.*, **9**, 1018–1028.

ROHRBOUGH, J. & KIDOKORO, Y. (1990). Changes in kinetic of acetylcholine receptor channels after initial expression in *Xenopus* myocyte culture. *J. Physiol.*, **425**, 245–269.

SANES, D.H. & POO, M.M. (1989). In vitro analysis of position- and lineage dependent selectivity in the formation of neuromuscular synapse. *Neuron*, **2**, 1237–1244.

SHAPIRA, R., SILBERBERG, S.D., GINSBURG, S. & RAHAMIMOFF, R. (1987). Activation of protein kinase C augments evoked transmitter release. *Nature*, **325**, 58–60.

SHEARMAN, M.S., SEKIGUCHI, K. & NISHIZUKA, Y. (1989). Modulation of ion channel activity: a key function of the protein kinase C enzyme family. *Pharmacol. Rev.*, **41**, 211–237.

SPITZER, N.C. & LAMBORGHINI, J.C. (1976). The development of the action potential mechanism of amphibian neurons isolated in culture. *Proc. Natl. Acad. Sci. U.S.A.*, **73**, 1641–1645.

STEINBACH, J.H. & ZEMPEL, J. (1987). What does phosphorylation do for the nicotinic acetylcholine receptor? *Trends Neurosci.*, **10**, 61–64.

XIE, A. & POO, M.M. (1986). Initial events in the formation of neuromuscular synapse. *Proc. Natl. Acad. Sci. U.S.A.*, **83**, 7069–7073.

(Received April 22, 1993
Revised June 4, 1993
Accepted June 30, 1993)

Br. J. Pharmacol. (1993), **110**, 713–718

Enhancement of D_2 receptor agonist-induced inhibition by D_1 receptor agonist in the ventral tegmental area

Toshihiko Momiyama, *[1]Masashi Sasa & Shuji Takaori

Department of Pharmacology, Faculty of Medicine, Kyoto University, Kyoto 606-01, and *Department of Pharmacology, Hiroshima University School of Medicine, Hiroshima 734, Japan

1 A microiontophoretic study was performed on chloral hydrate-anaesthetized rats to examine the role of D_1 receptors in the ventral tegmental area (VTA) neurones, which are inhibited by autoreceptor and D_2 receptor agonists.

2 Inhibition by microiontophoretic application of quinpirole (a D_2 agonist) of antidromic spikes elicited by stimulation of the nucleus accumbens in dopaminergic neurones of the VTA, was significantly enhanced by simultaneous application of SKF 38393 (D_1 agonist), although SKF 38393 alone had little effect on the neurones.

3 In addition, quinpirole-induced inhibition was antagonized by iontophoretic application of domperidone (D_2 antagonist), but was not affected by SCH 23390 (D_1 antagonist).

4 Furthermore, SKF 38393-induced enhancement of inhibition by quinpirole was antagonized by simultaneous application of SCH 23390.

5 These results suggest that activation of D_1 receptors located on the VTA dopaminergic neurones or on non-dopaminergic nerve terminals is not essential for inducing inhibition of the dopaminergic neurones, but enhances D_2 receptor-mediated inhibition directly or indirectly via inhibitory neurones.

Keywords: Ventral tegmental area; D_1 receptor; D_2 receptor; SKF 38393; quinpirole; domperidone; SCH 23390

Introduction

The ventral tegmental area (VTA) is composed of dopamine-containing neurones and non-dopaminergic neurones. Both neurone types project to limbic areas such as the nucleus accumbens (Acc) and frontal cortex (Anden *et al.*, 1966; Beckstead *et al.*, 1979; Simon *et al.*, 1979). The spontaneous and/or glutamate-induced firing of VTA dopaminergic neurones are reported to be inhibited by dopamine as well as dopamine agonists such as apomorphine, LY 141865, (+)-amphetamine and quinpirole (LY 171555), through dopamine autoreceptors (Aghajanian & Bunney, 1977; Wang, 1981b; White & Wang, 1984a,b). Recently, we have also found that dopamine, a D_2 agonist, talipexole (B-HT 920) and a dopamine autoreceptor agonist, OPC-4392, produced D_2 receptor antagonist-reversible inhibition of the antidromic spike induced by stimulation of the Acc in dopaminergic neurones of the VTA (Momiyama *et al.*, 1990; 1991). Similar results in the VTA neurones were also obtained by Seutin *et al.* (1990) with systemic injection of talipexole. However, an autoradiographic study shows that in addition to D_2 receptors, D_1 receptors also exist in the VTA of man and rats (Boyson *et al.*, 1986; Dawson *et al.*, 1986; 1988; Cortes *et al.*, 1989). Furthermore, a recent biochemical study has demonstrated that neurones, probably in the ventral tegmental area, superio-medial to the lateral mammillary nuclei, express mRNAs of a subtype of the D_1 receptor (D_{1B}) (Tiberi *et al.*, 1991). Therefore, a microiontophoretic study was performed to elucidate the role of D_1 receptors in the VTA.

Methods

Twenty-eight male Wistar rats weighing 270–350 g were anaesthetized with chloral hydrate (400 mg kg^{-1}, i.p.). After tracheal cannulation, the animals were fixed in a stereotaxic apparatus and immobilized with gallamine triethiodide (80 mg/animal, i.p.) under artificial respiration. ECG (II lead) was continuously recorded to monitor the anaesthetic condition of the animal. When the experiments exceeded 5 h, a supplemental dose of 200 mg kg^{-1} chloral hydrate was administered. Gallamine triethiodide (40 mg/animal) was also given when required. Lignocaine was sprayed on all pressure points and incision sites repeatedly throughout the experiments. Body temperature was maintained between 36.5–37.5°C with a heating pad.

A bipolar stimulating electrode with a tip 0.1 mm in diameter was inserted into the Acc (1.7–2.2 mm anterior to bregma, 1.5–2.0 mm lateral to midline, 7.5–8.0 mm from the cortical surface) (Paxinos & Watson, 1986) ipsilateral to the recording site to activate the VTA neurones antidromically. A stimulus composed of a rectangular pulse (0.1 ms duration and 0.1–0.3 mA) was applied to the Acc every 1.6 s. The stimulus intensity was 1.5 times higher than the threshold which was the minimum current to produce an antidromic action potential in the VTA neurone. Single neuronal activities were extracellularly recorded in the VTA (4.7–5.0 mm posterior to bregma, 0.5–1.0 mm lateral to midline, 7.5–8.8 mm from the cortical surface) (Paxinos & Watson, 1986) using a glass-insulated silver wire microelectrode (electrical resistance; 1–2 MΩ) attached along a seven-barreled micropipette with an outer diameter of 3–5 μm. The distance between the tips of the recording electrode and micropipette was 20–30 μm.

Each seven-barreled micropipette was filled with 0.2 M dopamine hydrochloride (Sigma, pH 5.5), 30 mM SKF 38393 (2, 3, 4, 5-tetrahydro-1-phenyl-1 H-3-benzazepine-7,8-diol hydrochloride; Smith Kline and French Lab., pH 6.0), 10 mM quinpirole (LY 171555; Eli Lilly Co., pH 5.5), 5 mM SCH 23390 ((**R**)-(+)-8-chloro-2, 3, 4, 5-tetrahydro-3-methyl-5-[phenyl-1H-3-benzazepine-7-ol hemimaleate; Schering Corp., dissolved in 0.3% tartrate, pH 4.0), 30 mM domperidone (Kyowa Hakko, dissolved in 1% lactate, pH 4.5), 1 M monosodium L-glutamate (Sigma, pH 7.4) and 3 M NaCl. These chemicals were applied iontophoretically to the immediate vicinity of the target neurone being recorded, with a microiontophoresis programmer (WP-I, model 160). NaCl solution (3 M) was used for automatic current-balancing and for checking the current effects. Retaining currents of ap-

[1] Author for correspondence.

proximately − 20 nA were used between application periods for all these drugs except L-glutamate, which was retained with a + 20 nA current and applied as an anion.

The successive responses to Acc stimulation displayed on an oscilloscope (Nihon-Kohden VC-11) were photographed. The mean number and latency of spikes produced by Acc stimulation in each neurone were obtained by 10 successive responses before and during iontophoretic application of each drug; then, the mean spike number and latency of each group of neurones were calculated from the mean value of each neurone. The statistical significance of the data was determined by the paired t test. The positions of the stimulating and recording electrode tips were marked by passing a direct current of 0.3 mA for 10 s and 20 μA for 2 min, respectively, and histologically checked by staining with cresyl violet. Typical examples of the locations of recording and stimulating electrodes are shown in Figure 1a and b, respectively. Other details of the experiment have been previously reported (Akaike *et al.*, 1984; Momiyama *et al.*, 1990; 1991).

Results

Forty-five neurones were antidromically activated by Acc stimulation. Of these 45 neurones, 39 were histologically confirmed to be located in the VTA. As previously reported (Momiyama *et al.*, 1990; 1991), VTA neurones activated by antidromic Acc stimulation were classified into type I and II neurones according to their responses to Acc stimulation; presumably corresponding to dopaminergic and non-dopaminergic neurones, respectively, since they had long and short latencies of the antidromic spike, respectively (Figure 2a and b).

Effects of agonists

The effects of microiontophoretic application of dopamine, quinpirole and SKF 38393 were examined in 16 type I neurones and 13 type II neurones. In 15 of 16 type I neurones, antidromic spike generation was inhibited by dopamine at a current of 40 nA, although that of the remaining one neurone was not affected (Figure 3b). When dopamine (40 nA) was applied for 60 s, the mean spike number of 16 type I neurones significantly ($P<0.01$) decreased to 0.41 ± 0.05 from the control (1.06 ± 0.02), while the spike latency was not affected (Table 1a). Quinpirole also inhibited antidromic spike generation current-dependently in type I neurones without affecting the spike latency; the inhibition of the antidromic spike generation during application of 20, 40 and 70 nA of quinpirole was seen in 7, 11 and 14 of 16 type I neurones, respectively (Figure 3c,d and e). The mean spike number of 16 type I neurones upon Acc stimulation current-dependently and significantly ($P<0.01$) decreased from 1.06 ± 0.02 to 0.83 ± 0.04, 0.68 ± 0.05 and 0.43 ± 0.06 during application of quinpirole at currents of 20, 40 and 70 nA, respectively (Table 1a). However, SKF 38393 at a current of 40 nA did not significantly affect antidromic spikes in 15 of 16 type I neurones, although an inhibition of the spike generation was seen in the remaining neurone and at a current of 70 nA, the drug did not affect any of the 16 type I neurones tested (Figure 2f and g). The mean spike number of 16 type I neurones was unaffected by SKF at a current of 40 or 70 nA, (Table 1a). In contrast, simultaneous application of SKF 38393 with quinpirole enhanced the quinpirole-induced inhibition of antidromic spikes of type I neurones upon Acc stimulation without affecting the spike latency. When SKF 38393 at a current of 70 nA was simultaneously applied, significant ($P<0.05$) enhancement of quinpirole (20 nA)-induced inhibition was observed in 6 of 16 type I neurones, compared with the spike number during application of quinpirole alone at a current of 20 nA (Figure

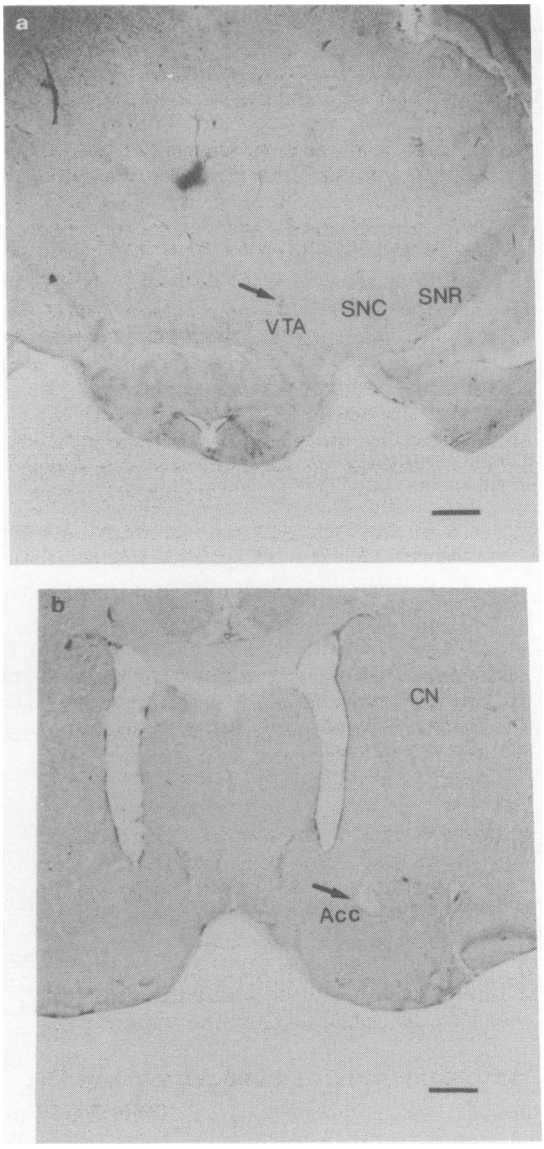

Figure 1 (a) The location of the recording electrode (arrow) within the ventral tegmental area (VTA). (b) The location of stimulating electrode (arrow) within the nucleus accumbens (Acc). Abbreviations: CN, caudate nucleus; SNC, substantia nigra pars compacta; SNR, substantia nigra pars reticulata. Calibration bar: 1.0 mm.

Figure 2 Spikes of type I (a) and type II (b) neurones in the ventral tegmental area elicited by stimulation of the nucleus accumbens antidromically: (▲) indicate stimulus artifacts. Calibration: 5 ms, 1 mV.

Table 1 Effects of dopamine, quinpirole (LY 171555) and SKF 38393 on antidromic spikes elicited by stimulation of the nucleus accumbens in type I (a) and type II (b) neurones of the ventral tegmental area

	Number of spikes		*Latency* (ms)
a *Type I neurone* ($n = 16$)			
Control	1.06 ± 0.02		9.36 ± 0.40
DA (40 nA)[a]	0.41 ± 0.05*	(15)[b]	9.34 ± 0.40
LY (20 nA)	0.83 ± 0.04*	(7)	9.36 ± 0.40
LY (40 nA)	0.68 ± 0.05*	(11)	9.35 ± 0.43
LY (70 nA)	0.43 ± 0.06*	(14)	9.35 ± 0.43
SKF (40 nA)	1.03 ± 0.06	(1)	9.37 ± 0.40
SKF (70 nA)	1.05 ± 0.05	(0)	9.36 ± 0.40
SKF (70 nA) + LY (20 nA)	0.46 ± 0.06†	(13)[b] (6)[c]	9.36 ± 0.40
SKF (40 nA) + LY (40 nA)	0.44 ± 0.06†	(14)[b] (3)[c]	9.35 ± 0.43
b *Type II neurone* ($n = 13$)			
Control	1.08 ± 0.08		2.85 ± 0.43
DA (40 nA)[a]	1.05 ± 0.09	(1)[b]	2.85 ± 0.43
LY (20 nA)	1.06 ± 0.10	(0)	2.85 ± 0.42
LY (40 nA)	0.98 ± 0.10	(2)	2.79 ± 0.50
LY (70 nA)	0.98 ± 0.10	(2)	2.79 ± 0.50
SKF (40 nA)	1.03 ± 0.09	(1)	2.85 ± 0.43
SKF (70 nA)	1.04 ± 0.09	(1)	2.85 ± 0.43
SKF (70 nA) + LY (20 nA)	0.98 ± 0.10	(2)[b] (1)[c]	2.88 ± 0.43
SKF (40 nA) + LY (40 nA)	0.95 ± 0.12	(2)[b] (1)[c]	2.83 ± 0.55

Each value represents the mean ± s.e.
Each drug was applied iontophoretically for 60 s.
[a]Current applied; [b]number of neurones, in which spike generation by stimulation of the nucleus accumbens was significantly ($P < 0.05$) inhibited, when tested in 16 type I and 13 type II neurones; [c]number of neurones in which quinpirole-induced inhibition was enhanced by SKF, when tested in 16 type I and 13 type II neurones.
*$P < 0.01$, significantly different from control;
†$P < 0.01$, significantly different from LY (20 nA) or LY (40 nA) alone.
DA: dopamine, LY: quinpirole, SKF: SKF 38393.
SKF + LY: simultaneous application of SKF 38393 and quinpirole.

3h, Table 2). The inhibition of the antidromic spike generation was seen in 13 of 16 type I neurones when SKF 38393 at a current of 70 nA and quinpirole at a current of 20 nA were simultaneously applied (Tables 1a and 2). Similar effects were observed during simultaneous application of SKF 38393 at a current of 40 nA with quinpirole at a current of 40 nA (Figure 3i, Table 2). The mean spike number of 16 type I neurones significantly ($P < 0.01$) decreased from 0.83 ± 0.04 to 0.46 ± 0.06 during simultaneous application of SKF 38393 (70 nA) and quinpirole (20 nA), and from 0.68 ± 0.05 to 0.44 ± 0.06 with SKF 38393 (40 nA) plus quinpirole (40 nA), compared with the controls by quinpirole alone (Tables 1a and 2). However, when dopamine (40 nA), quinpirole (20, 40 and 70 nA) or SKF 39393 (40 and 70 nA) alone was given to 13 type II neurones, there were no effects on the antidromic

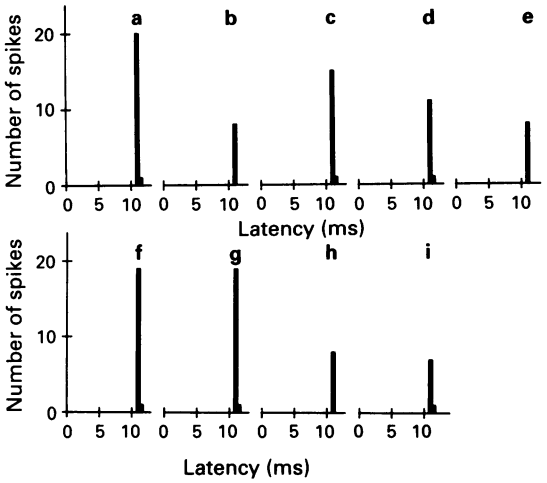

Figure 3 Effects of microiontophoretic application of dopamine, quinpirole and SKF 38393 on antidromic spikes elicited by stimulation of the nucleus accumbens in a type I neurone in the ventral tegmental area. The poststimulus latency histogram was obtained from 20 successive responses of the neurones. (a) Control; (b) during iontophoretic application of dopamine at a dose of 40 nA; (c), (d) and (e): during application of quinpirole at doses of 20, 40 and 70 nA, respectively; (f) and (g) during application of SKF 38393 at doses of 40 and 70 nA; (h) and (i) simultaneous application of SKF 38393 (70 nA) with quinpirole (20 nA) and SKF 38393 (40 nA) with quinpirole (40 nA), respectively.

Table 2 Effects of quinpirole (LY) in the presence of SKF 38393 (SKF) on number of antidromic spikes elicited by stimulation of the nucleus accumbens in type I neurones in the ventral tegmental area

Neurone no.	*Control*	*LY* (20 nA)	*LY* (40 nA)	*SKF* (70 nA) + *LY* (20 nA)	*SKF* (40 nA) + *LY* (40 nA)
1	1.0[n]	1.0	0.8	0.5**	0.5**
2	1.0	0.7*	0.7*	0.4**	0.4**
3	1.2	0.7*	0.6**	0.4**	0.2**
4	1.0	0.9	0.7*	0.2**	0.6*
5	1.0	0.4**	0.5**	0.5**	0.2**
6	1.0	0.8	0.6*	0.4**	0.4**
7	1.1	0.6*	0.5**	0.3**	0.3**
8	1.2	1.1	0.9	0.4**	0.4**
9	1.0	0.9	0.5**	0.2**	0.3**
10	1.0	0.9	0.6*	0.3**	0.3**
11	1.0	1.0	1.0	0.9	0.7*
12	1.2	0.8*	0.7**	0.4**	0.4**
13	1.0	0.8	0.9	0.8	0.8
14	1.0	0.7*	0.3**	0.3**	0.1**
15	1.0	1.0	1.0	0.9	0.9
16	1.2	0.9*	0.6*	0.5**	0.6**
Mean	1.06	0.83**	0.68**	0.46††	0.44††
s.e.	0.02	0.04	0.05	0.06	0.06

n: mean spike number of 10 successive responses.
*$P < 0.05$, significantly different from the control. **$P < 0.01$, significantly different from the control.
††$P < 0.01$, significantly different from LY (20 nA) or LY (40 nA) alone.

spike elicited by Acc stimulation in most of the neurones examined, although the inhibition was seen in 1–2 neurones (Figures 4b–g, Table 1b). In addition, SKF 38393 given simultaneously with quinpirole had no effect on the antidromic spikes in 12 of 13 type II neurones tested, although enhancement of the inhibition was seen in the remaining one neurone (Figure 4h and i, Table 1b).

Effects of antagonists

When domperidone (40 nA) was applied 30 s prior to the application of quinpirole (40 nA), the quinpirole-induced inhibition was antagonized during application of domperidone in 5 of 10 type I neurones (Figure 5a–d). The mean spike number of 10 type I neurones significantly ($P<0.01$) decreased to 0.69 ± 0.03 from 1.09 ± 0.05 during microiontophoretic application of quinpirole, and then increased to 1.07 ± 0.05 in the presence of domperidone (Table 3).

To examine whether or not activation of D_1 receptors by intrinsic dopamine enhances the inhibition resulting from D_2 receptor stimulation in the VTA type I neurones, the effects of SCH 23390 (D_1 antagonist) on the quinpirole-induced inhibition were investigated. When SCH 23390 at currents up to 70 nA was applied 30 s prior to, and then simultaneously with quinpirole (40 and 70 nA), quinpirole-induced inhibition was not antagonized in any of 10 type I neurones (Figure 5e and f). There was no significant difference in the mean spike number between application of SCH 23390 plus quinpirole and quinpirole alone (Table 3).

Effect of SCH 23390 on SKF 38393-induced enhancement

SCH 23390 at a current of 40 nA was applied iontophoretically for 30 s and then SKF 38393 and quinpirole at a current of 40 nA were given simultaneously in the presence of SCH 23390. Under these conditions, an enhancement by SKF 38393 of quinpirole-induced inhibition of antidromic spike generation in VTA type I neurones was antagonized by SCH 23390. As shown in Table 4, the mean number of antidromic spikes of 10 type I neurones tested was significantly ($P<0.01$) decreased by iontophoretic application of quinpirole (40 nA) from 1.13 ± 0.08 to 0.68 ± 0.06 (Table 4). The inhibitory effect induced by quinpirole was significantly ($P<0.01$) enhanced from 0.68 ± 0.06 to

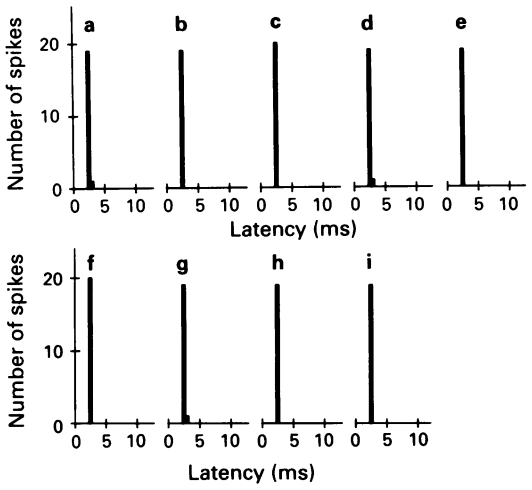

Figure 4 Effect of microiontophoretic application of dopamine, quinpirole and SKF 38393 on antidromic spikes elicited by nucleus accumberns stimulation in a type II neurone in the ventral tegmental area. The poststimulus latency histogram was obtained from 20 successive responses of the neurone. (a) Control; (b) during iontophoretic application of dopamine at a dose of 40 nA; (c), (d) and (e) during application of quinpirole at doses of 20, 40 and 70 nA, respectively; (f) and (g) during application of SKF 38393 at doses of 40 and 70 nA; (h) and (i) simultaneous application of SKF 38393 (70 nA) with quinpirole (20 nA) and SKF 38393 (40 nA) with quinpirole (40 nA), respectively.

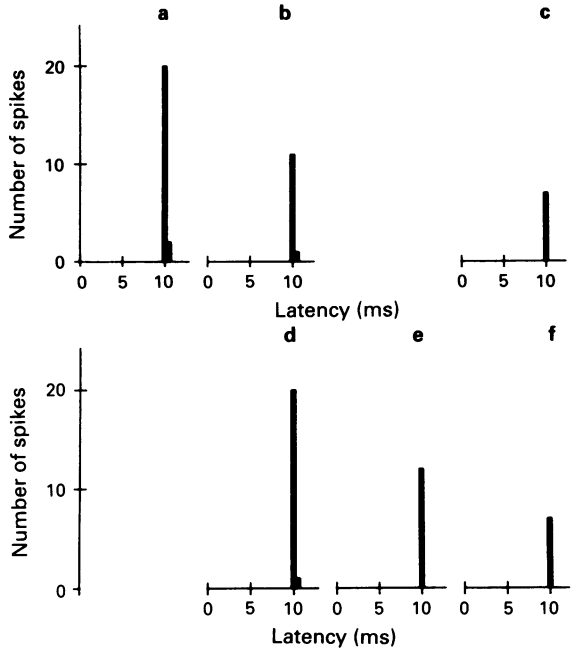

Figure 5 Antagonistic effects of domperidone and SCH 23390 on quinpirole-induced inhibition of antidromic spikes elicited by stimulation of nucleus accumbens in a type I neurone in the ventral tegmental area. The poststimulus latency histogram was obtained from 20 successive responses of the neurone. (a) Control; (b) and (c) during iontophoretic application of quinpirole at doses of 40 and 70 nA, respectively; (d) simultaneous application of domperidone at a dose of 40 nA with quinpirole (40 nA); (e) during simultaneous application of SCH 23390 at a dose of 40 nA with quinpirole (40 nA); (f) during simultaneous application of SCH 23390 (70 nA) and quinpirole (70 nA).

Table 3 Effect of quinpirole (LY) on antidromic spikes of type I neurones in the VTA upon Acc stimulation, and antagonistic effects of domperidone (Dom) and SCH 23390 (SCH) on quinpirole-induced inhibition of the spike

	Number of spikes	*Latency* (ms)
Control	1.09 ± 0.05	10.01 ± 0.43
LY (40 nA)[a]	0.69 ± 0.03* (9)[b]	10.05 ± 0.40
LY (70 nA)	0.41 ± 0.04* (10)	10.07 ± 0.40
Dom (40 nA) + LY (40 nA)	1.07 ± 0.05† (0)	10.12 ± 0.39
SCH (40 nA) + LY (40 nA)	0.68 ± 0.05* (9)	10.06 ± 0.40
SCH (70 nA) + LY (70 nA)	0.36 ± 0.04* (10)	10.06 ± 0.41

$n = 10$
Each value represents the mean ± s.e.
Each drug was applied iontophoretically for 60 s.
*$P<0.01$, significantly different from control.
†$P<0.01$, significantly different from LY alone.
[a]Current applied; [b]number of neurones, in which spike generation by stimulation of the nucleus accumbens was significantly ($P<0.05$) inhibited.
Dom + LY and SCH + LY: simultaneous application of domperidone with quinpirole, and SCH 23390 with quinpirole, respectively.

Table 4 Effect of SCH 23390 (SCH) on SKF 38393 (SKF) -induced enhancement of inhibition by quinpirole (LY) in type I neurones

	Number of spikes	*Latency* (ms)
Control	1.13 ± 0.08	11.39 ± 0.59
DA (40 nA)[a]	0.46 ± 0.05*	11.44 ± 0.59
LY (40 nA)	0.68 ± 0.06*	11.51 ± 0.56
SKF (40 nA)	1.08 ± 0.06	11.46 ± 0.54
SKF (40 nA) + LY (40 nA)	0.46 ± 0.04††	11.56 ± 0.55
SCH (40 nA) + SKF (40 nA) + LY (40 nA)	0.73 ± 0.08†	11.43 ± 0.56

$n = 10$.
Each value represents the mean ± s.e.
Each drug was applied iontophoretically for 60 s.
*$P < 0.01$, significantly different from control.
††$P < 0.01$, significantly different from LY alone.
†$P < 0.01$, significantly different from the value without SCH.
[a]Current applied.
SKF + LY: simultaneous application of LY with SKF.
SCH + SKF + LY: simultaneous application of SCH with SKF and LY.

0.46 ± 0.04 by simultaneous application of SKF 38393 (40 nA) with quinpirole (Table 4). Furthermore, when quinpirole (40 nA), SKF 38393 (40 nA) and SCH 23390 (40 nA) were simultaneously applied to these 10 type I neurones, the mean number of antidromic spikes was significantly ($P < 0.01$) increased from 0.46 ± 0.04 to 0.73 ± 0.08, compared with the value without SCH 23390 (Table 4).

Discussion

The present study confirmed the previous findings that the VTA neurones projecting to the Acc are composed of two types (Wang, 1981a; Momiyama *et al.*, 1990; 1991): type I and type II neurones, probably corresponding to dopaminergic and non-dopaminergic neurones, respectively, since in the former neurones, an antidromic spike elicited by Acc stimulation had a long duration and latency while the latter neurones, in contrast, had a short duration and latency (Grace & Bunney, 1980; Wang, 1981a; Momiyama *et al.*, 1990; 1991).

Microiontophoretically applied dopamine and quinpirole inhibited antidromic spikes elicited by Acc stimulation in type I neurones. The quinpirole-induced inhibition was antagonized by simultaneous application of domperidone, suggesting that this inhibition is mediated by D_2 receptors located in dopaminergic neurones of the VTA, as shown in our previous studies (Momiyama *et al.*, 1990; 1991). These results are also in accordance with those obtained by White & Wang with D_2 agonists, LY 141865 and bromocriptine, as well as a D_2 antagonist, sulpiride, on spontaneous firing of the VTA neurones (White & Wang, 1984a,b).

On the other hand, microiontophoretic application of SKF 38393 alone had little effect on antidromic spikes of type I neurones. The quinpirole-induced inhibition of the antidromic spikes was not affected by blocking D_1 receptors with SCH 23390. This suggests that D_1 receptors alone in the VTA are not essential for dopamine-mediated inhibition of dopaminergic neurones. However, the inhibitory effects of quinpirole were significantly enhanced in the presence of SKF 38393, suggesting that activation of D_1 receptors induces synergistic effects on D_2 receptor-mediated inhibition in the VTA. Similar synergistic effects by activation of both D_1 and D_2 receptors have also been found in globus pallidus neurones (Walters *et al.*, 1987), the caudate nucleus and the Acc neurones (Wachtel *et al.*, 1989), although the effects of D_1 and D_2 receptor activation were opposite in some caudate nucleus neurones in our studies (Akaike *et al.*, 1987; Ohno *et al.*, 1987). However, Wachtel *et al.* (1989) have reported that the ability of dopamine agonists to stimulate D_2 receptors in the VTA neurones was not altered by manipulation of D_1 receptor occupation. These differences are probably due to the low currents of the D_1 agonist applied in the presence of the D_2 agonist. Furthermore, in the present study, enhancement of quinpirole-induced inhibition by SKF 38393 was antagonized by simultaneous application of SCH 23390, a selective D_1 antagonist, indicating that this enhancement by SKF 38393 is mediated by D_1 type receptors. Our electrophysiological study suggests that D_1 type receptors are distributed in the VTA which have some modulatory function, although it is not as essential as that of D_2 receptors. One possibility suggested by our results is that under normal conditions, dopamine acts on the D_2 receptors located on the dendrites of dopaminergic neurones in the VTA, and that excess dopamine released from dendrites may also activate D_1 receptors, thereby enhancing the D_2 receptor-mediated inhibitory effects, although activation of the D_1 receptors is not always necessary to inhibit these neurones.

However, contradictory results have been reported regarding the existence of D_1 receptors in the VTA. One autoradiographic study found no D_1 receptors in the pars compacta of the substantia nigra or the VTA (Alter & Hauser, 1987); however, other autoradiographic studies indicated the existence of both D_1 and D_2 receptors in the VTA (Boyson *et al.*, 1988; Dawson *et al.*, 1986; 1988; Cortes *et al.*, 1989). *In situ* hybridization histochemistry studies have demonstrated that the D_1 receptor mRNA was not expressed in the VTA dopaminergic neurones (Dearry *et al.*, 1990; Sunahara *et al.*, 1990; Weiner *et al.*, 1991; Meador-Woodruff *et al.*, 1992). Recently, however, Mansour *et al.* (1992) have reported that there are marked discrepancies between D_1 receptor binding and mRNA in some brain regions; D_1 receptor binding can be observed in the VTA, but no D_1 receptor mRNA can be detected there. They have discussed whether these discrepancies may be due to technical problems such as ligand and probe sensitivity, and to specific transport of dopamine receptors synthesized. Therefore, conflicting results – that D_1 receptors in the VTA dopaminergic neurones are observed by autoradiographic studies, but their mRNA cannot be detected by *in situ* hybridization – appear not always to mean the lack of D_1 rceptors.

However, iontophoretically applied SKF 38393 does not influence only the neurone recorded, but also affects other neuronal elements in the vicinity of the iontophoretic pipette. Therefore, it is possible that the SKF 38393-induced response is mediated by non-dopaminergic elements within the VTA e.g. it may activate D_1 type receptors located on the terminals of GABAergic neurones originating in the Acc and enhance release of GABA, eventually potentiating D_2 receptor-mediated inhibition.

The authors are grateful to Smith Kline & Franch Laboratories (Philadelphia, PA, U.S.A.), Eli Lilly and Company (Indianapolis, U.S.A.), Schering-Plough Corporation (Bloomfield, NJ, U.S.A.) and Kyowa Hakko Company (Tokyo, Japan) for the gifts of SKF 38393, quinpirole, SCH 23390 and domperidone, respectively. This work was supported in part by a Grant-in Aid for Scientific Research from the Ministry of Education, Science and Culture, Japan.

References

AGHAJANIAN, G.K. & BUNNEY, B.S. (1977). Dopamine 'autoreceptors': pharmacological characterization by microiontophoretic single cell recording studies. *Naunyn-Schmied. Arch. Pharmacol.*, **297**, 1–7.

AKAIKE, A., SASA, M. & TAKAORI, S. (1984). Microiontophoretic studies of the dopaminergic inhibition from the ventral tegmental area to the nucleus accumbens. *J. Pharmacol. Exp. Ther.*, **229**, 859–864.

AKAIKE, A., OHNO, Y., SASA, M. & TAKAORI, S. (1987). Excitatory and inhibitory effects of dopamine on neuronal activity of the caudate nucleus neurons *in vitro*. *Brain Res.*, **418**, 262–272.

ALTER, C.A. & HAUSER, K. (1987). Topography of substantia nigra innervation by D_1 receptor-containing striatal neurons. *Brain Res.*, **410**, 1–11.

ANDEN, N.E., DHALSTROM, A., FUXE, K., LARSON, K., OLSON, L. & UNGERSTEDT, U. (1966). Ascending monoamine neurons to telecephalon and diencephalon. *Acta Physiol. Scand.*, **67**, 313–326.

BECKSTEAD, R.M., DOMESICK, V.B. & NAUTA, W.J.H. (1979). Efferent connections of substantia nigra and ventral tegmental area in the rat. *Brain Res.*, **175**, 191–207.

BOYSON, S.J., MCGONIGLE, P. & MOLINOFF, P.B. (1986). Quantitative autoradiographic localization of D_1 and D_2 subtypes of dopamine receptors in rat brain. *J. Neurosci.*, **6**, 3177–3188.

CORTES, R., GUEYE, B., PAZOS, A., PROBST, A. & PALACIOS, J.M. (1989). Dopamine receptors in human brain: autoradiographic distribution of D_1 sites. *Neuroscience*, **28**, 263–273.

DAWSON, T.M., GEHLERT, D.R., MCCABE, R.T., BARNETT, A. & WAMSLEY, J.K. (1986). D-1 dopamine receptors in the rat brain: a quantitative autoradiographic analysis. *J. Neurosci.*, **6**, 2352–2365.

DAWSON, T.M., BARONE, P. & SIDHU, A. (1988). The D_1 dopamine receptor in the rat brain: quantitative autoradiographic localization using an iodinated ligand. *Neuroscience*, **26**, 83–100.

DEARRY, A., GINGRICH, J.A., FALARDEAU, P., FREMEAU R.T. Jr., BATES, M.D. & CARON, M.G. (1990). Molecular cloning and expression of the gene for a human D_1 dopamine receptor. *Nature*, **347**, 72–76.

GRACE, A.A. & BUNNEY, B.S. (1980). Nigral dopamine neurons: intracellular recording and identification with L-Dopa injection and histofluorescence. *Science*, **210**, 654–656.

MANSOUR, A., MEADOR-WOODRUFF, J.H., ZHOU, Q., CIVELLI, O., AKIL, H. & WATSON, S.J. (1992). A comparison of D_1 receptor binding and mRNA in rat brain using receptor autoradiographic and in situ hydridization techiques. *Neuroscience*, **48**, 959–971.

MEADOR-WOODRUFF, J.H., MANSOUR, A., GRANDY, D.K., DAMASK, S.P., CIVELLI, O. & WATSON, Jr. S.J. (1992). Distribution of D_5 dopamine receptor mRNA in rat brain. *Neurosci. Lett.*, **145**, 209–212.

MOMIYAMA, T., SASA, M. & TAKAORI, S. (1990). D-2 receptor-mediated inhibition by a substituted quinolinone derivative, 7-{3-[4-(2,3-dimethylphenyl) piperazinyl]propoxy}-2(1H)-quinolinone (OPC-4392), of dopaminergic neurons in the ventral tegmental area. *Life Sci.*, **47**, 761–769.

MOMIYAMA, T., SASA, M. & TAKAORI, S. (1991). Inhibition by talipexole, a thiazolo-azepine derivative, of dopaminergic neurons in the ventral tegmental area. *Life Sci.*, **49**, 535–543.

OHNO, Y., SASA, M. & TAKAORI, S. (1987). Coexistence of inhibitory dopamine D-1 and excitatory D-2 receptors on the same caudate nucleus neurons. *Life Sci.*, **40**, 1937–1945.

PAXINOS, G. & WATSON, C. (1986). *The Rat Brain in Stereotaxic Coordinates*. 2nd Edition, Sydney: Academic Press.

SEUTIN, V., MOREAU, J.S., GIESBERS, I., MASSOTTE, L. & DRESSE, A. (1990). Effects of B-HT 920 on monoaminergic neurons of the rat brain: an electrophysiological in vivo and in vitro study. *Naunyn-Schmied. Arch. Pharmacol.*, **242**, 502–507.

SIMON, H., LE MOAL, M. & CALAS, A. (1979). Efferents and afferents of the ventral tegmental A10 region studied after local injection of [^{3}H]leucine and horseradish peroxidase. *Brain Res.*, **178**, 17–40.

SUNAHARA, R.K., NIZNIK, H.B., WEINER, D.M., STORMANN, T.M., BRANN, M.R., KENNEDY, J.M., GELERNTER, J.E., ROZMAHEL, R., YANG, Y., ISRAEL, Y., SEEMAN, P. & O'DOWD, B.F. (1990). Human dopamine D_1 receptor encoded by an intronless gene on chromosome 5. *Nature*, **347**, 80–83.

TIBERI, J., JARVIE, K.R., SILVIA, C., FALARDEAU, P., GINGRICH, J.A., GODINOT, N., BERTRAND, L., YANG-FENG, T.L., FREMEAU, Jr. R.T. & CARON, M.G. (1991). Cloning, molecular characterization, and chromosomal assignment of a gene encoding a second D_1 dopamine receptor subtype: differential expression pattern in rat brain compared with the D_{1A} receptor. *Proc. Natl. Acad. Sci. U.S.A.*, **88**, 7491–7495.

WACHTEL, S.R., HU, X.T., GALLOWAY, M.P. & WHITE, F.J. (1989). D_1 dopamine receptor stimulation enables the postsynaptic, but not autoreceptor, effects of D_2 dopamine agonists in nigrostriatal and mesoaccumbens dopamine systems. *Synapse*, **4**, 327–346.

WALTERS, J.R., BERGSTROM, D.A., CARLSON, J.H., CHASE, T.N. & BRAUN, A.R. (1987). D_1 dopamine receptor activation required for postsynaptic expression of D_2 agonist effects. *Science*, **236**, 719–722.

WANG, R.Y. (1981a). Dopaminergic neurons in the ventral tegmental area. I. Identification and characterization. *Brain Res. Rev.*, **3**, 123–140.

WANG, R.Y. (1981b). Dopaminergic neurons in the ventral tegmental area. II. Evidence for autoregulation. *Brain Res. Rev.*, **3**, 141–151.

WEINER, D.M., LEVEY, A.I., SUNAHARA, R.K., NIZNIK, H.B., O'DOWD, B.F., SEEMAN, P. & BRANN, M.R. (1991). D_1 and D_2 dopamine receptor mRNA in rat brain. *Proc. Natl. Acad. Sci. U.S.A.*, **88**, 1859–1863.

WHITE, F.J. & WANG, R.Y. (1984a). A 10 dopamine neurons: role of autoreceptors in determining firing rate and sensitivity to dopamine agonists. *Life Sci.*, **34**, 1161–1170.

WHITE, F.J. & WANG, R.Y. (1984b). Pharmacological characterization of dopamine autoreceptors in the rat ventral tegmental area: microiontophoretic studies.[1] *J. Pharmacol. Exp. Ther.*, **231**, 275–280.

(Received November 23, 1992
Revised April 24, 1993
Accepted June 16, 1993)

Br. J. Pharmacol. (1993), **110**, 719–723

Protection by oestradiol against the development of cardiovascular changes associated with monocrotaline pulmonary hypertension in rats

Michel Y. Farhat, Ming-Fong Chen, Tahira Bhatti, Azhar Iqbal, Seedabarum Cathapermal & [1]Peter W. Ramwell

Department of Physiology and Biophysics, Georgetown University Medical Center, Washington D.C. 20007, U.S.A.

1 We studied the effects of oestradiol 17β on the development of pulmonary vascular changes and right ventricular (RV) hypertrophy in response to monocrotaline in male Sprague-Dawley rats.

2 Rats were treated with either placebo or oestradiol 17β (10 mg) in the form of slow release pellets implanted subcutaneously 48 h before monocrotaline administration. Rats were injected with either saline or a single dose of monocrotaline (60 mg kg^{-1}, i.m.). Pulmonary vascular changes and RV hypertrophy were studied at 4 weeks following monocrotaline administration.

3 Monocrotaline induced a significant increase in the ratio of right ventricle (RV) to left ventricle-plus-septum (LV + S) weights. Monocrotaline-treated rats also showed significant myointimal proliferation in small pulmonary arteries, decrease of arterial numbers and increase in the number of abnormal alveolar macrophages.

4 Oestradiol 17β attenuated myointimal hyperplasia in pulmonary vessels, decreased the RV/(LV + S) ratio in monocrotaline-treated rats. Oestradiol 17β had no significant effect on control animals.

5 Oestradiol treatment prevented the increase in lung wet to dry weight ratio, observed 7 days post monocrotaline administration.

6 These results suggest that oestradiol 17β protects against the pulmonary vascular remodelling and RV hypertrophy associated with monocrotaline-induced pulmonary hypertension in the rat. Oestradiol also protects against microvascular leak observed in the early days of lesion.

Keywords: Oestrogen; monocrotaline; myointimal hyperplasia; right ventricular hypertrophy; pulmonary hypertension; microvascular leak

Introduction

Monocrotaline-induced pulmonary hypertension is an important model for the study of the pathogenesis of chronic inflammatory pulmonary conditions that involve the interstitium and vessels of the lung. Endothelial cell damage produced early by the metabolites of monocrotaline is thought to lead to the development of structural and functional changes (Butler, 1970; Roth & Reindel, 1991; Schultze *et al.*, 1991). A single monocrotaline injection causes pulmonary oedema, inflammatory lung parenchyma changes, pulmonary hypertension and right ventricular hypertrophy (Meyrick *et al.*, 1980; Ghodsi & Will, 1981; Roth & Reindel, 1991). The pulmonary vascular lesions are characterized by medial hyperplasia and hypertrophy of muscular pulmonary arteries and capillary endothelial cell changes (Meyrick *et al.*, 1980; Ghodsi & Will, 1981; Meyrick & Reid, 1982).

The development of monocrotaline-induced pulmonary hypertension appears to be sexually differentiated (Kiyatake *et al.*, 1992). Female rats treated with monocrotaline develop a lower degree of pulmonary hypertension than their male counterparts, suggesting a possible protective role of oestrogen in this animal model. Oestradiol has been shown to inhibit myointimal proliferation in the aorta of renal hypertensive rats (Wolinsky, 1972), prevent the development of atherosclerosis in the rabbit aorta (Fischer & Swain, 1985), and decrease the size of atherosclerotic plaque in monkeys and rabbits via changing the cholesterol metabolism (Kushwaha & Hazzard, 1981; Williams *et al.*, 1990). Oestradiol treatment also blunts pulmonary vascular responses to pressor agonists and inhibits hypoxic pulmonary vasoconstriction (Gordon *et al.*, 1986). However, the effect of oestrogen on the pathogenesis and development of different forms of pulmonary vascular injury, including monocrotaline-induced pulmonary hypertension remains unclear.

The purpose of this study was to evaluate the effect of oestrogen treatment on the structural changes in the right heart and pulmonary vasculature observed in monocrotaline-induced pulmonary hypertension in the rat.

Methods

Animals and treatment protocol

Ten week old male Sprague-Dawley rats (weighing between 250 to 300 g; Charles River Laboratories, Willmington, MA, U.S.A.) were treated with a single intramuscular injection of saline or monocrotaline (60 mg kg^{-1}). An aqueous solution of monocrotaline was prepared as described by Hayashi *et al.* (1967) wherein, 200 mg was dissolved in 1.2 ml of 1 N HCl, diluted with distilled water to about 5 ml and neutralized with 0.5 N NaOH; the volume was then adjusted to 10 ml with distilled water.

All animals were treated with either placebo or oestradiol-17β (10 mg) in the form of slow release pellets, implanted subcutaneously 2 days before monocrotaline injection. Pellets were purchased from Innovative Research of America (Toledo, OH, U.S.A.) and were fused and compressed individually with filter material including cholesterol, microcrystalline cellulose, α-lactose, di- and tricalcium phosphate, calcium and magnesium stearate, and stearic acid (Osborne *et al.*, 1985). The pellet doses were chosen so as to sustain rat blood oestradiol levels of about 10 ng ml^{-1}. The development of pulmonary vascular changes and right ventricular (RV)

[1] Author for correspondence.

hypertrophy both in the presence and absence of oestradiol treatment was studied at 4 weeks following monocrotaline administration. All of the animals were housed at constant temperature and kept in a 12 h light-dark cycle in the Research Resources Facility of Georgetown University Medical Center, where they had free access to food and water.

Preparation of tissues

At the end of the study period, rats were anaesthetized with pentobarbitone (60 mg kg^{-1}, i.p.). The trachea was cannulated and rats were ventilated with room air at a tidal volume of 2.5 ml and a frequency of 60 breaths min^{-1}, using a small animal respirator (Model 680, Harvard Apparatus Co., Dover, MA, U.S.A.). A blood sample was collected from the abdominal aorta for the determination of plasma oestradiol levels by radioimmunoassay (Jurjen *et al.*, 1975). Lungs were perfused *in situ* from the right ventricle with heparinized (heparin sodium, 5 units ml^{-1}) lactated Ringer solution for 10 min at a pressure of 20 mmHg, followed by Karnovsky's fixative (Karnovsky, 1956) for 20 min. The trachea was then perfused with the same fixative at a pressure of 25 cmH_2O for 10 min. The lungs and heart were removed en bloc. Tissues from both lungs were immersed in the fixative overnight, then transferred to the 0.1 M sodium-cacodylate buffer (pH 7.3) and stored at 4°C for 1 week before structural study.

The development of pulmonary hypertension was confirmed by right ventricular hypertrophy which was expressed as an increase in right ventricular free wall (RV)/left ventricle-plus-septum (LV + S) in the absence of a change in (LV + S) weight (Fulton *et al.*, 1952). Both atria, valves and fatty tissue of the heart were trimmed from the ventricles. The RV was separated from the LV + S, which were blotted and weighed separately.

Morphology

Histological sections were prepared from lung tissues and stained with haematoxylin-eosin as well as with a multiple stain (ethylene alcohol, methyl alcohol, basic fuchsin, and toluidine blue) to demonstrate internal and external elastic laminae for morphometric studies. The number of abnormal alveolar macrophages was also determined.

Measurement of medial thickness was made on muscular arteries with an external diameter of 30–100 and 100–200 μm respectively, with a computerized morphometer (The Morphometer, Woods Hole Educational Associates, Woods Hole, MA, U.S.A.). For each artery, medial thickness was expressed as:

(external diameter – luminal diameter)/external diameter × 100

The external diameter is the distance between and including the two external elastic laminae intersected by the diameter. Because vessels were often not perfectly circular in cross-section, each vessel was measured twice at right angles to the first measurements. In each section, ten vessels were measured, and the average was calculated. To determine the number of abnormal alveolar macrophages and small arteries (external diameter < 100 μm), macrophages, arteries and alveoli were counted in 10 consecutive fields at × 500 magnification in each lung section and expressed per 100 alveoli (Meyrick *et al.*, 1980; Ono & Voelkel, 1991).

Histological evaluation was carried out using a double blind study, in which the treatment status was unknown to the investigators.

Determination of lung perivascular oedema

In one group of animals, 7 days following monocrotaline or vehicle administration, lungs were excised as previously described, and weighed immediately to the nearest mg to determine wet weights. Lung samples were then allowed to stand at room temperature until a stable dry weight was obtained. The extent of lung oedema was quantified by the ratio of wet to dry weight (Sugita *et al.*, 1983). These values were compared to those obtained from oestradiol-treated animals.

Statistical analysis

All data were expressed as means ± standard deviations (s.d.). Data were analysed by unpaired Student's *t* test and Fisher's Multiple Comparison Test, to determine significant differences between various experimental groups.

Significance was achieved at $P < 0.05$.

Materials

Crotaline was purchased from Sigma Chemical Co., St. Louis, MO, U.S.A.; and heparin sodium Organon Inc., West Orange, NJ, U.S.A.

Results

Animal behaviour and body weight changes

Monocrotaline-treated (M) rats showed loss of appetite and failed to gain weight 4 weeks after injection. Two monocrotaline-treated rats became lethargic after 3 weeks and were killed with a high dose of pentobarbitone sodium (100 mg kg^{-1}). Subsequent autopsy showed severe pulmonary oedema. Body weight loss was less in oestrogen-treated animals, and these animals did not show any significant change in behaviour. Oestradiol-treated control (E) animals however, exhibited a significant decrease in body weight as compared to placebo controls (C) (Figure 1). Plasma oestradiol levels in oestradiol-treated animals ranged between 8.1 and 14.6 ng ml^{-1}.

Structural studies

Right ventricular hypertrophy and heart weight index As shown in Table 1, monocrotaline induced a significant increase in the RV/(LV + S) ratio at 4 weeks (0.48 ± 0.07 vs 0.29 ± 0.04 in C, $P < 0.05$). Oestradiol treatment protected against monocrotaline-induced increase in ventricular ratio, but had no effect in placebo-treated animals. There was no significant difference in the (LV + S)/body weight ratio among all groups.

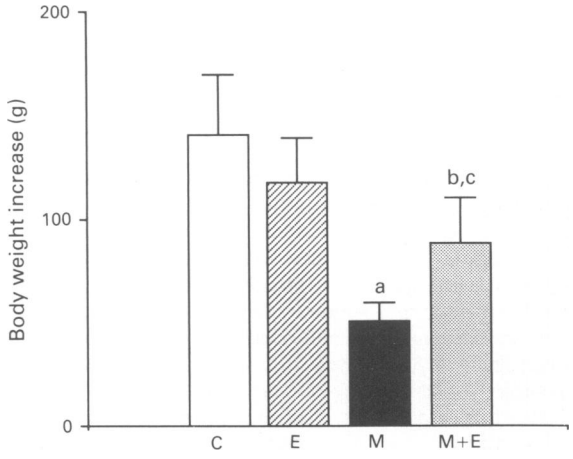

Figure 1 Effect of oestradiol 17β treatment on body weight gain in monocrotaline-treated male rats. Measurements were made 4 weeks following monocrotaline administration. C: control. M: monocrotaline. E: oestradiol. M + E: monocrotaline + oestradiol-treated rats. Each value represents the mean ± s.d. from 4 to 6 animals. $^{a}P < 0.001$ vs C; $^{b}P < 0.02$ vs M and $^{c}P < 0.02$ vs C.

Table 1 Effect of oestradiol 17β on right ventricular hypertrophy in monocrotaline-treated male rats

	RV/(LV + S)	*(LV + S)/BW* ($\times 10^{-3}$)
C ($n = 6$)	0.29 ± 0.01	2.15 ± 0.36
E ($n = 6$)	0.28 ± 0.05	2.13 ± 0.30
M ($n = 4$)	0.48 ± 0.07[ab]	2.08 ± 0.15
M + E ($n = 6$)	0.35 ± 0.05	2.19 ± 0.14

C: control. M: monocrotaline. E: oestradiol. M + E: monocrotaline + oestradiol-treated rats. BW: body weight. LV: left ventricle. RV: right ventricle. S: septum.
[a]$P < 0.005$ vs C; [b]$P < 0.01$ vs M + E.

Myointimal proliferation Monocrotaline induced a 2 fold medial thickening in small muscular arteries with external diameter of less than 200 μm. The percentage myointimal thickening was more significant in those arteries with an external diameter of 30 to 100 μm (13.9 ± 2.1 in M vs 7.1 ± 1.5 in C; $P < 0.05$). Oestradiol significantly prevented monocrotaline-induced medial hypertrophy (Figure 2) 4 weeks after treatment (9.2 ± 1.9 in M + E; $P < 0.01$ vs M), but had no significant effect on placebo-treated animals (Table 2).

Abnormal alveolar macrophages and arterial numbers Sections of lung tissue from monocrotaline-treated rats showed an increase in number of inflammatory cells in lung parenchyma with perivascular infiltration. Lung histology showed increased numbers of foamy alveolar macrophages (50.9 ± 14.1/100 alveoli) in intra-alveolar spaces (Table 2). Oestradiol significantly reduced the numbers of abnormal alveolar macrophages induced by monocrotaline (30.9 ± 10.7/100 alveoli; $P < 0.05$). Monocrotaline treatment also slightly reduced the alveolar numbers in each × 500 magnification field. However, Figure 3 shows that monocrotaline-treated rats had the least arterial (external diameter < 100 μm) density among the four groups studied. Oestradiol 17β significantly protected against the monocrotaline-induced decrease in arterial density (3.6 ± 0.07 in M vs 5.1 ± 1.1/100 alveoli in M + E; $P < 0.05$).

Microvascular leak Monocrotaline induced a significant increase in water content of the lung. The wet to dry weight changed from 5.31 ± 0.06 in C to 5.73 ± 0.07 in M ($P < 0.001$) after 7 days. Oestradiol 17β treatment had no effect on basal lung weight ratio but significantly ($P < 0.01$) inhibited the increase in water content induced by monocrotaline (Figure 4). There was no significant change in lung dry weight to body weight ratio in all groups of study.

Discussion

This study shows that oestradiol significantly improves survival and prevents right ventricular hypertrophy as well as medial hypertrophy in small pulmonary arteries of monocrotaline-treated rats. These data suggest that oestradiol may protect against the development of monocrotaline-induced pulmonary hypertension.

Monocrotaline induces a dose-dependent injury to pulmonary vascular endothelium, leading to a time-related progression of medial proliferation in pulmonary vessels, as well as right ventricular hypertrophy and pulmonary hypertension (Ghodsi & Will, 1981; Meyrick & Reid, 1982; Roth & Reindel, 1991). The delayed and progressive nature of the injury to endothelial cells seems enigmatic, since reactive metabolites of monocrotaline bind rapidly to tissue macromolecules or are rapidly inactivated in aqueous environments

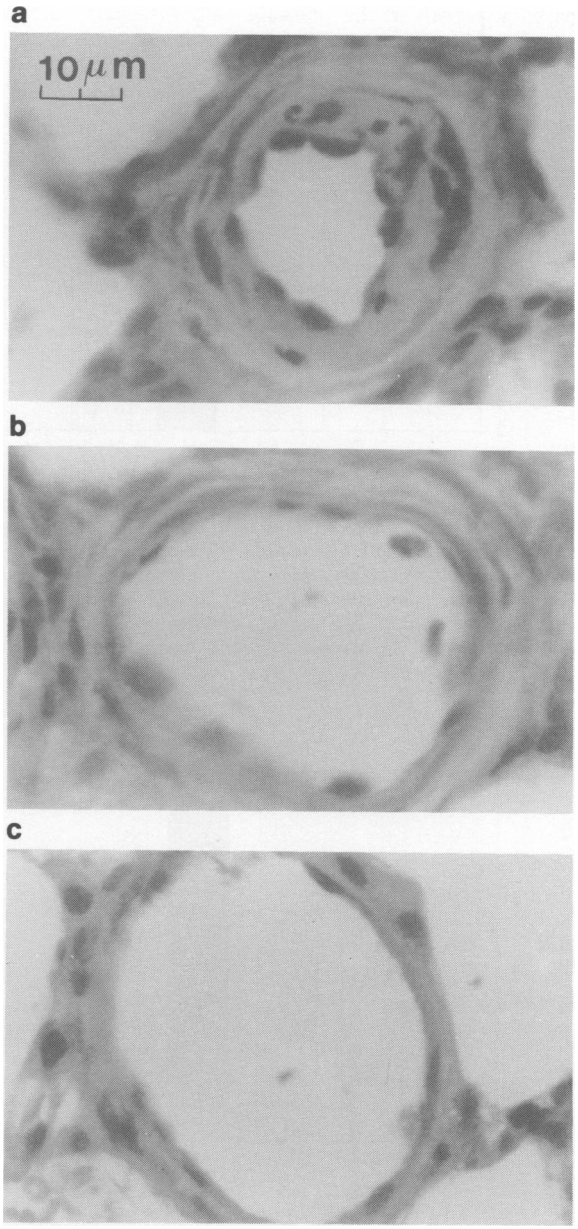

Figure 2 Cross-section (× 500) of small pulmonary artery from lungs of monocrotaline (a), monocrotaline + oestradiol-treated (b), and control (c) rats at 4-weeks following monocrotaline injection, showing the protective effect of oestrogen on pulmonary vascular hypertrophy induced by monocrotaline.

Table 2 Effect of oestradiol 17β on monocrotaline pneumotoxicity in male rats

	MT (%) 30 to 100 μm	*MT* (%) 100 to 200 μm	*Alveoli /field*	*Macro /100 alveoli*
C ($n = 6$)	7.1 ± 1.5	5.9 ± 1.2[a]	23.8 ± 4.8	0
E ($n = 6$)	6.6 ± 1.0	5.7 ± 1.4	22.7 ± 5.1	0
M ($n = 4$)	13.9 ± 2.1[bc]	11.0 ± 2.6	18.4 ± 4.0	50.9 ± 14.1
M + E ($n = 6$)	9.2 ± 1.9	6.6 ± 1.8[a]	22.0 ± 5.0	30.9 ± 10.7

The parameters measured are: % medial thickness (MT%) of small pulmonary arteries (external diameters of 30–100 μm and 100–200 μm), number of alveoli per magnification field (× 500) and number of abnormal alveolar macrophages per 100 alveoli. C: control. M: monocrotaline. E: oestradiol. M + E: monocrotaline + oestradiol-treated rats.
[a]$P < 0.02$ vs M; [b]$P < 0.005$ vs C; [c]$P < 0.01$ vs M + E.

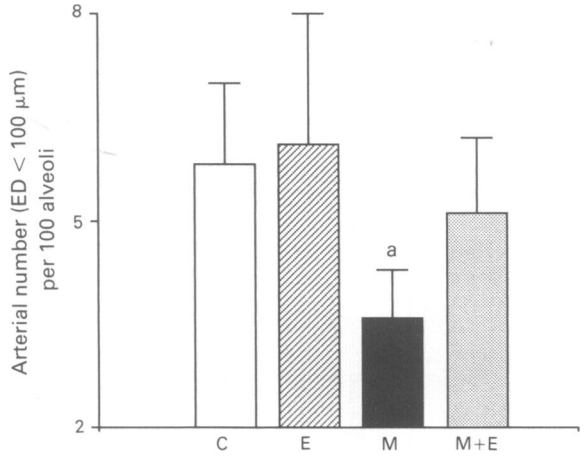

Figure 3 Effect of oestradiol 17β on arterial number in monocrotaline-treated male rats. The number of small pulmonary arteries with external diameter (ED) $<100\,\mu m$ is measured. C: control. M: monocrotaline. E: oestradiol. M + E: monocrotaline + oestradiol-treated rats. Oestradiol treatment (M + E) significantly protected against the decrease in number of arteries observed in monocrotaline-treated rats. Each value represents mean ± s.d. from 4 to 6 animals. $^aP<0.02$ vs C.

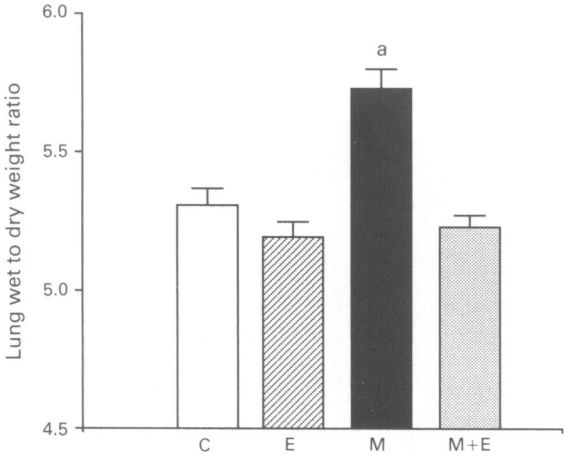

Figure 4 Effect of oestradiol 17β on pulmonary oedema in monocrotaline-treated male rats. Oedema is measured as the lung wet to dry weight ratio, 7 days post monocrotaline administration. C: control. M: monocrotaline. E: oestradiol. M + E: monocrotaline + oestradiol-treated rats. Oestradiol treatment protected against monocrotaline-induced increase in lung water content. Each value represents the mean ± s.d. from 4 to 6 animals. $^aP<0.01$ vs M + E.

(Roth & Reindel, 1991). In fact, it has been suggested that monocrotaline metabolites may not be directly toxic to endothelial cells but may trigger some indirect mechanisms, such as production and release of endogenous mediators of injury (e.g. leukotrienes, cytokines) (Rosenberg & Rabinovitch, 1988; Ito *et al.*, 1988; Ono & Voelkel, 1991; 1992), or inhibit production of endothelium-dependent relaxing factor and cytoprotective compounds like prostacyclin.

We find that smaller arteries displayed greater medial proliferation than the larger ones (Table 2), which is in accordance with previous reports (Meyrick & Reid, 1982; Ono & Voelkel, 1991). We also find that oestradiol significantly reduced right ventricular hypertrophy (Table 1) and decreased pulmonary vascular medial thickening in oestradiol-treated monocrotaline rats. Since there is, in general, a positive correlation between progressive pulmonary hypertension, thickening of the medial wall of the small pulmonary vessels, and right ventricular hypertrophy (Meyrick *et al.*, 1980; Ghodsi & Will, 1981) it is possible that a reduction of pulmonary hypertension and RV hypertrophy by oestradiol treatment might also be a consequence of the reduction in lung vessel thickening.

In addition, the histology of monocrotaline-induced pulmonary hypertension showed profuse inflammatory cell infiltration in the lung parenchyma and abnormal macrophages in alveolar spaces. Oestrogen treatment however, reduced the number of abnormal alveolar macrophages per field (Table 2). Natural and synthetic oestrogens are known to stimulate phagocytosis and clearance of intravenously administered particles by tissue elements of the mononuclear phagocyte system in mice (Loose & Diluzio, 1976; Boorman *et al.*, 1980). It is not clear whether oestrogen decreases inflammation in our model by a direct anti-inflammatory effect or indirectly via attenuating monocrotaline toxicity.

There are several possible mechanisms by which oestradiol may act to attenuate the monocrotaline-induced pulmonary vascular remodelling. Firstly, oestradiol may stimulate angiogenesis (Wolinsky, 1972; Khosla *et al.*, 1981) and hence increase the overall cross-sectional area of pulmonary vascular bed, changing the flow-resistive characteristics of the pulmonary vasculature in monocrotaline-treated animals.

Secondly, oestradiol could decrease the smooth muscle mass in pulmonary vessels, as demonstrated in systemic arteries of hypertensive rats (Wolinsky, 1972), thus leading to a blunted response of monocrotaline-induced myointimal proliferation. We have observed that oestradiol causes a significant attenuation of cardiac transplant myointimal proliferation (Foegh *et al.*, 1987), and inhibition of [^{3}H]-thymidine uptake in arterial segments from the left anterior descending coronary artery of the pig, *in vitro* (unpublished observation). On the other hand, we have also shown that in pulmonary vessels oestradiol potentiates [^{3}H]-thymidine uptake by vascular smooth muscle cells. This mitogenic effect of oestrogen however, is abolished in presence of an intact endothelium, suggesting that endothelial injury or dysfunction may be important (Farhat *et al.*, 1992).

Thirdly, oestradiol has been shown to cause arterial dilatation in several systemic vascular beds (Rosenfeld *et al.*, 1976), and to alter the response of isolated systemic vessels to various vasoconstrictor agents (Colucci *et al.*, 1982). *In vivo* studies also show a blunted pulmonary vascular reactivity to hypoxia, angiotensin II and prostaglandin $F_{2\alpha}$ during pregnancy (Moore & Reeves, 1980; Fuchs *et al.*, 1982; Sylvester *et al.*, 1985), and following oestradiol treatment (Wetzel *et al.*, 1984). Increased production of prostacyclin or other endothelial derived vasodilators may be implicated in this effect (Resnick, 1981). On the other hand, oestradiol 17β has been shown to increase contractions and increase vascular sensitivity to catecholamines in bovine isolated radial arteries (Chan & Kalsner, 1982), rabbit saphenous veins (Rorie & Muldoon, 1979) and rat small mesenteric arteries (Colucci *et al.*, 1982). We have also observed that oestradiol treatment enhances pulmonary vascular response of the rat isolated perfused lung to the thromboxane-mimetic, U46619 (Farhat & Ramwell, 1992). These data suggest that oestrogen plays a role in the regulation of the pulmonary vascular reactivity, and that the effect of oestrogen may depend on the identity of the vessel in the experimental model, as well as on the nature of the agonist used.

On the other hand, endothelial injury by monocrotaline results in increased permeability, perivascular oedema (Plestina & Stoner, 1972; Roth & Reindel, 1991) and increased lung weight which occurs within a few hours after monocrotaline administration (Reindel *et al.*, 1990). Evidence indicates that the structural and functional changes observed at a later stage in the pulmonary arteries and right ventricle may be secondary to those earlier cellular or subcellular events (Ghodsi & Will, 1981; Roth & Reindel, 1991). Our data show that oestradiol treatment prevents monocrotaline-induced microvascular leakage, suggesting that oestradiol may protect against endothelial injury by monocrotaline. Endothelial damage is not caused directly by monocrotaline

but by its metabolic products. Monocrotaline is converted to reactive pyrroles by the mixed function oxidase system of the liver (Hilliker *et al.*, 1983). Oestradiol may have a direct inhibitory effect on the conversion of monocrotaline to its toxic metabolite, monocrotaline pyrrole. Kiyatake *et al.* (1992) have shown that liver homogenates from female rats produced significantly lower concentrations of monocrotaline pyrrole than those from males. This was associated with a lower right ventricular pressure observed in female rats suggesting a gender difference in the severity of monocrotaline-induced pulmonary hypertension.

In conclusion, chronic treatment with oestradiol significantly attenuates pulmonary vascular remodelling and right ventricular hypertrophy in monocrotaline pulmonary hypertension in the rat. Our data suggest that oestradiol may exert its protective effect by preventing monocrotaline-induced endothelial injury. This is the first indication of a protective effect of oestrogen in this animal model and may open new avenues to understanding the role of oestrogen in other forms of pulmonary vascular injury.

This work is supported by NHLBI grant HL 36802.

References

BOORMAN, G.A., LUSTER, M.I., DEAN, J.H. & WILSON, R.E. (1980). The effect of adult exposure to diethylstilbestrol in the mouse on macrophage function and numbers. *J. Reticuloendothel. Soc.*, **28,** 547–560.

BUTLER, W.H. (1970). An ultrastructural study of the pulmonary lesion induced by pyrrole derivatives of the pyrrolizidine alkaloids. *J. Pathol.*, **102,** 15–21.

CHAN, C. & KALSNER, S. (1982). Termination of responses to sympathetic nerve stimulation and to noradrenaline in a perfused arterial preparation: the role of neuronal and extraneuronal uptake. *J. Pharmacol. Exp. Ther.*, **222,** 731–740.

COLUCCI, W.S., GIMBRONE, M.A.Jr., MCLAUGHLIN, M.K., HALPERN, W. & ALEXANDER, R.W. (1982). Increased vascular catecholamine sensitivity and -adrenergic receptor affinity in female and estrogen treated male rats. *Circ. Res.*, **50,** 805–811.

FARHAT, M.Y. & RAMWELL, P.W. (1992). Estradiol potentiates the vasopressor response of the isolated perfused rat lung to the thromboxane mimic U46619. *J. Pharmacol. Exp. Ther.*, **261,** 686–691.

FARHAT, M.Y., VARGAS, R., DINGAAN, B. & RAMWELL, P.W. (1992). *In vitro* effect of oestradiol on thymidine uptake in pulmonary vascular smooth muscle cell: role of the endothelium. *Br. J. Pharmacol.*, **107,** 679–683.

FISCHER, G.M. & SWAIN, M.L. (1985). Effects of estradiol and progesterone on the increased synthesis of aortic collagen in atherosclerotic rabbit aortas. *Atherosclerosis*, **54,** 177–185.

FOEGH, M.L., KHIRABADI, B.S., NAKANISHI, R., VARGAS, R. & RAMWELL, P.W. (1987). Estradiol protects against experimental cardiac transplant atherosclerosis. *Transpl. Proc.*, **19,** 90–95.

FUCHS, K.Y., MOORE, G. & ROUNDS, S. (1982). Pulmonary vascular reactivity is blunted in pregnant rats. *J. Appl. Physiol.*, **53,** 703–707.

FULTON, R.M., HUTCHINSON, E. & JONES, A.M. (1952). Ventricular weight in cardiac hypertrophy. *Br. Heart J.*, **14,** 413–420.

GHODSI, F. & WILL, J.A. (1981). Changes in pulmonary structure and function induced by monocrotaline intoxication. *Am. J. Physiol.*, **240,** H149–H155.

GORDON, J.B., WETZEL, R.C., MCGEADY, M.L., ADKINSON, N.F. & SYLVESTER, J.T. (1986). Effects of indomethacin on estradiol-induced attenuation of hypoxic vasoconstriction in lamb lungs. *J. Appl. Physiol.*, **61,** 2116–2121.

HAYASHI, Y., HUSSA, J.F. & LALICH, J.J. (1967). Cor pulmonale in rats. *Lab. Invest.*, **16,** 875–880.

HILLIKER, K.S., BELL, T.G. & ROTH, R.A. (1983). Monocrotaline pyrrole-induced pulmonary hypertension in Fawn-hooded rats with platelet storage pool deficiency: 5-hydroxytryptamine uptake by isolated perfused lungs. *Thromb. Haemostas.*, **50,** 844–847.

ITO, K., NAKASHIMA, T., MURAKAMI, K. & MURAKAMI, T. (1988). Altered function of pulmonary endothelium following monocrotaline-induced lung vascular injury in rats. *Br. J. Pharmacol.*, **94,** 1175–1183.

JURJEN, H., PRATT, J.J. & WOLDRING, M.G. (1975). Radioimmunoassay of plasma estradiol without extraction and chromatography. *J. Clin. Endocrinol. Metab.*, **40,** 19–25.

KARNOVSKY, M.J. (1956). A formaldehyde-glutaraldehyde fixation of high osmolarity for use in electron microscopy. *J. Cell. Biol.*, **27,** 137–138.

KHOSLA, S.S., SMITH, G.J.W., PARKS, P.A. & ROONEY, S.A. (1981). Effects of estrogen on fetal rabbit lung maturation: morphological and biochemical studies. *Pediatr. Res.*, **15,** 1274–1281.

KIYATAKE, K., KANEKO, N., OKADA, O., KAKUSAKA, I., NAGAO, K. & KURIYAMA, T. (1992). Role of liver microsome for sexual difference in monocrotaline-treated rats. *Am. Rev. Respir. Dis.*, **145,** A620.

KUSHWAHA, R.S. & HAZZARD, W.R. (1981). Exogenous estrogens attenuate dietary hypercholesterolemia and athereosclerosis in the rabbit. *Metabolism*, **30,** 359–366.

LOOSE, L.D. & DILUZIO, N.R. (1976). Dose-related reticuloendothelial system stimulation by diethylstilbestrol. *J. Reticuloendothel. Soc.*, **29,** 457–460.

MEYRICK, B., GAMBLE, W. & REID, L. (1980). Development of Crotalia pulmonary hypertension: hemodynamic and structural study. *Am. J. Physiol.*, **239,** H692–H702.

MEYRICK, B.O. & REID, L.M. (1982). Crotalia-induced pulmonary hypertension; uptake of H^3-thymidine by the cells of the pulmonary circulation and alveolar walls. *Am. J. Pathol.*, **106,** 84–94.

MOORE, L.G. & REEVES, J.T. (1980). Pregnancy blunts pulmonary vascular reactivity in dogs. *Am. J. Physiol.*, **239,** H297–H301.

ONO, S. & VOELKEL, N.F. (1991). PAF antagonists inhibit monocrotaline-induced lung injury and pulmonary hypertension. *J. Appl. Physiol.*, **71,** 2483–2492.

ONO, S. & VOELKEL, N.F. (1992). PAF receptor blockade inhibits lung vascular changes in the rat monocrotaline model. *Lung*, **170,** 31–40.

OSBORNE, C.K., HOBBS, K. & CLARK, G.M. (1985). Effect of estrogens and antiestrogens on growth of human breast cancer cells in athymic nude mice. *Cancer Res.*, **45,** 584–590.

PLESTINA, R. & STONER, H.B. (1972). Pulmonary edema in rats given monocrotaline pyrrole. *J. Pathol.*, **106,** 235–249.

REINDEL, J.F., GANEY, P.E., WAGNER, J.G., SLOCOMBE, R.F. & ROTH, R.A. (1990). Development of morphologic, hemodynamic, and biochemical changes in lungs of rats given monocrotaline pyrrole. *Toxicol. Appl. Pharmacol.*, **106,** 179–200.

RESNICK, R. (1981). The endocrine regulation of uterine blood flow in the nonpregnant uterus: a review. *Am. J. Obstet. Gynecol.*, **140,** 151–156.

RORIE, D.K. & MULDOON, S.M. (1979). Increased reactivity of isolated rabbit saphenous vein after treatment with estrogen and progesterone. *Blood Vessels*, **16,** 252–258.

ROSENBERG, H.C. & RABINOVITCH, M. (1988). Endothelial injury and vascular reactivity in monocrotaline pulmonary hypertension. *Am. J. Physiol.*, **255,** H1484–H1491.

ROTH, R.A. & REINDEL, J.F. (1991). Lung vascular injury from monocrotaline pyrrole, a putative hepatic metabolite. *Adv. Exp. Med. Biol.*, **283,** 477–487.

SCHULTZE, A.E., WAGNER, J.G. WHITE, S.M. & ROTH, R.A. (1991). Early indications of monocrotaline pyrrole-induced lung injury in rats. *Toxicol. Appl. Pharmacol.*, **109,** 41–50.

SUGITA, T., HYERS, T.M., DAUBER, I.M., WAGNER, W.W., MCMURTRY, I.F. & REEVES, J.T. (1983). Lung vessel leak precedes right ventricular hypertrophy in monocrotaline-treated rats. *J. Appl. Physiol.: Respir. Environ. Exercise Physiol.*, **54,** 371–374.

SYLVESTER, J.T., GORDON, J.B., MALAMET, R.L. & WETZEL, R.C. (1985). Prostaglandins and estradiol-induced attenuation of hypoxic pulmonary vasoconstriction. *Chest*, **88,** 252S–254S.

WETZEL, R.C., ZACUR, H.A. & SYLVESTER, J.T. (1984). Effect of puberty and estradiol on hypoxic vasomotor response in isolated sheep lungs. *J. Appl. Physiol. Resp. Environ. Exercise Physiol.*, **56,** 1199–1203.

WILLIAMS, J.K., ADAMS, M.R. & KLOPFENSTEIN, H.S. (1990). Estrogen modulates responses of atherosclerotic coronary arteries. *Circulation*, **81,** 1680–1687.

WOLINSKY, J.H. (1972). Effect of estrogen and progesterone treatment on the response of aorta of male rats to hypertension: morphological and chemical studies. *Circ. Res.*, **30,** 341–349.

(Received February 8, 1993
Revised May 7, 1993
Accepted May 19, 1993)

Br. J. Pharmacol. (1993), **110**, 724–735

Repeated administration of desipramine and a $GABA_B$ receptor antagonist, CGP 36742, discretely up-regulates $GABA_B$ receptor binding sites in rat frontal cortex

[1]Gerard D. Pratt* & [2]Norman G. Bowery

Department of Pharmacology, The School of Pharmacy, 29– 39 Brunswick Square, London WC1N 1AX.

1 $GABA_B$ receptor binding site densities within laminar regions of the rat frontal cortex were examined autoradiographically following repeated administration (21 days) of the antidepressants desipramine, paroxetine and amitriptyline in addition to the $GABA_B$ receptor antagonists, CGP 35348 and CGP 36742. β_1-Adrenoceptor autoradiography was studied in parallel with that for $GABA_B$ receptor sites.

2 The effects of these compounds were examined concomitantly on the $GABA_B$ receptor-mediated inhibition of forskolin- and enhancement of noradrenaline-stimulated cyclic AMP production.

3 $GABA_B$ receptor binding was increased by both desipramine (20 mg kg^{-1}, p.o. and 10 mg kg^{-1}, i.p.) and CGP 36742 (100 mg kg^{-1}, i.p.) in the outer laminar region of the frontal cortex by around 50% above control levels. Conversely, no significant changes were mediated by paroxetine, amitriptyline, CGP 35348 or the $GABA_B$ receptor agonist, baclofen.

4 With the exception of paroxetine, all compounds down-regulated the total β-adrenoceptor population throughout frontal cortical laminae which was attributable to the β_1-adrenoceptor subtype. In contrast, the reduction in β-adrenoceptors mediated by CGP 35348 and CGP 36742 did not occur as a consequence of reduced β_1-adrenoceptor numbers.

5 Protracted treatment with CGP 35348, failed to influence forskolin-stimulated cyclic AMP production; however, a significant increase in the accumulation of cyclic AMP produced in response to forskolin was seen after treatment with CGP 36742.

6 Such discretely localized changes in $GABA_B$ receptor densities induced by desipramine and CGP 36742 may provide an explanation for the discrepancies reported in membrane binding studies and possibly implicate a role for $GABA_B$ receptor antagonists in antidepressant therapy.

Keywords: $GABA_B$ receptors; antidepressants; autoradiography; β-adrenoceptors; adenylyl cyclase; $GABA_B$ receptor antagonists

Introduction

Since the introduction of the tricyclic antidepressant, imipramine in 1957, much research has focussed upon attempting to find a common biochemical denominator from which a neurochemical inbalance would trigger depression. The clinical observation that reserpine can produce depression suggested that the disease may be a consequence of a monoamine deficit. In support of this, synaptic levels of the monoamines, noradrenaline (NA) and 5-hydroxytryptamine (5-HT) are increased by both tricyclic antidepressants and monoamine oxidase inhibitors by the prevention of either their uptake or breakdown, respectively. Adaptations to the populations of central cortical monoamine receptors following chronic antidepressant administration are now well-documented. Down-regulation of the numbers of both β-adrenoceptors (Banerjee *et al.*, 1977) and 5-HT_2 receptors (Peroutka & Snyder, 1980) has been consistently found with a variety of antidepressant classes and is believed to be a prerequisite for their therapeutic actions.

Focus turned to the GABAergic system following the observations that the levels of γ-aminobutyric acid (GABA) are reduced in the cerebrospinal fluid (Gold *et al.*, 1980) and the plasma (Berrettini *et al.*, 1982) of depressed patients. In addition, since the GABA agonists, progabide and fengabine have antidepressant actions both in animal models as well as clinically (Lloyd *et al.*, 1983; Musch & Garreau, 1986), attention was directed to GABA receptors and in particular to the possible alterations in the $GABA_B$ receptor subtype following chronic antidepressant administration. This stemmed from observations of increased $GABA_B$ receptor binding to rat cerebral cortical membranes following subcutaneous infusions of a variety of antidepressants (Pilc & Lloyd, 1984; Lloyd *et al.*, 1985). These effects were substantiated using intraperitoneal administration (Szekely *et al.*, 1987) and also in mouse cortical membranes (Suzdak & Gianutsos, 1986). Moreover, $GABA_B$ receptors are reduced in the frontal cortex following olfactory bulbectomy (Lloyd & Pichat, 1986). Furthermore, increased $GABA_B$ receptor functionality with respect to baclofen-induced nociception is reduced by chronic desipramine (Borsini *et al.*, 1986) whereas baclofen-induced hypothermia and $GABA_B$ receptor-mediated inhibition of 5-HT release (Gray & Green, 1987) are enhanced by repeatedly administered antidepressants or electroconvulsive therapy (ECT) (Gray *et al.*, 1987). Additionally, chronic imipramine treatment enhances the $GABA_B$ receptor-mediated potentiation of NA-stimulated adenylyl cyclase activity (Suzdak & Gianutsos, 1986).

Not all researchers, however, have been able to demonstrate $GABA_B$ receptor up-regulation after such dosing regimes. Cross & Horton (1988) failed to observe any significant changes in $GABA_B$ binding sites following repeated administration of desipramine or zimeldine, despite the fact that 5-HT_2 binding site densities were significantly reduced in the same membrane preparations. Moreover, $GABA_B$ receptors are not altered in drug-free suicide victims (Cross *et al.*, 1988). Interestingly, although the binding of [^{3}H]-GABA to $GABA_B$ sites in rat frontal cortical membranes was increased after prolonged treatment with desipramine and imipramine, [^{3}H]-baclofen binding was unaffected by these drugs (Szekely *et al.*, 1987). Furthermore, although

[1] Present address: Institute of Pharmacology, University of Zurich, Gloriastrasse 32, CH-8006, Zurich, Switzerland.
[2] Author for correspondence.

[^{3}H]-dihydroalprenolol binding sites were down-regulated by infusions of imipramine, desipramine, tranylcypromine and phenelzine, $GABA_B$ receptor densities were not influenced by these antidepressants (McManus & Greenshaw, 1991).

It was hypothesized that if indeed $GABA_B$ receptor densities are increased following repeated antidepressant administration, it could be that certain undetected changes may arise from a discrete localization within certain cerebral cortical laminae which would be considerably diluted in a membrane preparation. The aim of the present study, therefore, was firstly to employ receptor autoradiography in an attempt to resolve these discrepancies. Since this technique offers the advantage of retaining the morphology of the brain intact, such an approach should enable the detection of possible changes within individual laminal regions of the frontal cortex. Autoradiographical examination of $GABA_B$ receptor sites within laminar regions of the frontal cortex was investigated in parallel with β_1-adrenoceptors after treatment with a variety of antidepressants, an established $GABA_B$ receptor antagonist, CGP 35348 (Olpe *et al.*, 1990) and also a novel $GABA_B$ receptor antagonist, CGP 36742 (Bittiger *et al.*, 1992).

Secondly, since activation of $GABA_B$ receptors inhibits forskolin-induced stimulation of adenylyl cyclase (Wojcik & Neff, 1984; Karbon & Enna, 1985; Hill, 1985) and potentiates the accumulation of adenosine 3′:5′-cyclic monophosphate (cyclic AMP) produced in response to noradrenaline (Karbon & Enna, 1985; Hill, 1985), such receptor up-regulation might be detected through these $GABA_B$ receptor-linked transduction mechanisms. An increase in the number of $GABA_B$ binding sites might be expected to confer a greater inhibition of forskolin- and enhancement of noradrenaline-stimulated cyclic AMP production by (−)-baclofen. The effects of the compounds were therefore examined concomitantly on these $GABA_B$ receptor-linked second messenger responses.

Methods

Drug-treatment protocols

In one study, male Wistar rats (160–200 g; Interfauna) were anaesthetized with halothane, and subcutaneously implanted with Alzet 2002 minipumps (Alza Corporation, USA). The minipumps were filled with 200 µl of a concentration of imipramine sufficient to deliver a proposed daily infused dose of 10 mg kg^{-1} for 14 days. Following the removal of the minipumps under halothane anaesthesia, animals were separated into two groups to compare drug-free periods of 24 and 48 h. A second group of rats was injected intraperitoneally for 14 days with imipramine (5 mg kg^{-1}) in order to compare this route of administration with that of subcutaneous infusion. These animals were prepared for perfusion-fixation after a further 24 h and were subjected to halothane anaesthesia to control for its possible influence on the action of imipramine. For this study, the binding kinetic parameters B_{max} and K_D were assessed by non-linear regression analysis as described by DeBlasi *et al.* (1989), using a range of GABA concentrations at a fixed concentration of [^{3}H]-GABA (50 nM).

In a second study, male CFY rats (140–180 g; Interfauna) caged in groups of 5 animals were dosed orally for 21 days with amitriptyline (30 mg kg^{-1}), desipramine (20 mg kg^{-1}), paroxetine (10 mg kg^{-1}) or (±)-baclofen (10 mg kg^{-1}). Additionally, desipramine (10 mg kg^{-1}) and the $GABA_B$ receptor antagonists, CGP 35348 and CGP 36742 (both at a concentration of 100 mg kg^{-1}) were injected intraperitoneally. In this study, the effects of antidepressant treatment on $GABA_B$ receptor binding parameters were determined using saturation analysis by varying the concentration of [^{3}H]-GABA (37.5–300 nM; 4 concentrations). Binding to β-adrenoceptors, using (−)-[^{125}I]-iodopindolol (18.75–300 pM; 5 concentrations) and resolved β_1-adrenoceptors (in the presence of the β_2-adrenoceptor antagonist, ICI 118,551) was performed on adjacent sections. In addition, the effects of these compounds were examined on the $GABA_B$ receptor-mediated modulation of forskolin and noradrenaline-stimulated adenylyl cyclase activity by baclofen. Drug concentrations are expressed in terms of their salt:base ratios.

Autoradiographical procedures

Tissue preparation Male Wistar rats (180–250 g) were anaesthetized with sodium pentobarbitone (Nembutal, 40 mg kg^{-1}, i.p.) and perfused-fixed with 250 ml of 0.1% paraformaldehyde in 0.01 M phosphate-buffered saline (0.9%) (pH 7.4) via intra-cardiac administration through the left ventricle. Brains were mounted onto a cork slice with 'Tissue Tek' (Miles Scientific), frozen in iso-pentane cooled to approximately − 40°C in liquid nitrogen and stored at − 80°C until required. Parasagitally-orientated sections (10 µm) were cut at − 20°C with a cryostat and thaw-mounted onto glass microscope slides to be stored at − 20°C until use.

Localization of $GABA_B$ receptor binding sites Frozen brain sections were thawed for 45 min and pre-incubated at room temperature for 60 min in 200 ml Tris-HCl buffer (50 mM; pH 7.4) containing 2.5 mM $CaCl_2$. After thorough drying under ambient conditions, sections were incubated individually for 20 min with 150 µl buffer containing [^{3}H]-GABA. Selectivity for $GABA_B$ sites was achieved in the presence of 40 µM isoguvacine (to prevent binding to $GABA_A$ sites). Non-specific binding was defined by (−)-baclofen (100 µM). Following incubation, excess radiolabel was aspirated from the section which then received 2 × 3 s washes in room temperature buffer. Sections were allowed to dry under a stream of cold air prior to their apposition to tritium-sensitive 'Hyperfilm' (Amersham) for between 3 and 4 weeks to generate autoradiograms.

Localization of β-adrenoceptor binding sites Frozen brain sections were thawed for 45 min and then incubated for 60 min at room temperature in a Tris-HCl/saline buffer (20 mM Trizma base; 135 mM NaCl; pH 7.4) containing (−)-[^{125}I]-iodopindolol. β-Adrenoceptor binding was resolved into the β_1-adrenoceptor subtype in the presence of the β_2-adrenoceptor antagonist, ICI 118,551 (50 nM). Non-specific binding was defined by use of (−)-isoprenaline (200 µM). Following incubation, sections were washed for 2 × 5 min periods in buffer at 4°C, rinsed for 3 s in ice-cold distilled water to remove buffer salts and then quickly dried in a stream of cold air. Sections were apposed to 'Hyperfilm' for between 24 and 48 h to generate autoradiograms with calibrated brain paste standards made according to the following method of Clarke & Hall (1986).

Autoradiographical analysis After the required duration of exposure, 'Hyperfilm' was developed and fixed in D-19 developer and 'Unifix' (Kodak), respectively. Autoradiographical density measurements were restricted to the frontal cortex of rat brain which was taken to represent approximately the anterior one-third region of the cerebral cortex (as described by plate 82; Paxinos & Watson, 1986). Optical densities of radioligand binding were measured with a 'Quantimet 970' image analysis system (Cambridge Instruments) againt calibrated ^{3}H micro-scales (Amersham). Scatchard plots were constructed from optical density values, converted to fmol mg^{-1} tissue using the simple relationship:

$$1\text{nCi} = 1/\text{specific activity (Ci mmol}^{-1}) \times 1000 \text{ fmol}$$

Adenylyl cyclase studies

This protocol was based essentially on the methods of Hill (1985) and Watling & Bristow (1986). Freshly removed

brains from stunned and decapitated male Wistar rats (180–250 g) were dissected on ice and cross-chopped slices of cerebral cortex (250 μm × 250 μm) prepared with a McIlwain tissue chopper. Slices were dispersed in 10 ml Krebs-Ringer bicarbonate (KRB) buffer of the following composition (mM); NaCl 118, KCl 4.7, $CaCl_2$ 2.5, $MgSO_4$ 1.2, KH_2PO_4 1.2, $NaHCO_3$ 25, glucose 11 and ascorbic acid 0.005%. They were then transferred to a larger volume of KRB (100 ml/brain), continually gassed with O_2:CO_2 (95%:5%) and washed for 90 min (with one buffer change after 30 min). Following this, excess KRB buffer was aspirated and 50 μl aliquots of the resulting tissue suspension added to fresh KRB. Following pre-incubation for 10 min at 37°C, adenylyl cyclase activity was initiated by the addition of either forskolin (10 μM) or noradrenaline (100 μM) in 50 μl aliquots to give a final assay volume of 500μl. After 10 min the reaction was terminated in a boiling water-bath (3 min). Aliquots (50 μl) of the supernatant were then assayed for cyclic AMP content by a radioimmunoassay based on the method of Brown *et al.* (1972). Estimates of the protein concentrations of brain tissue were made by the method of Bradford (1976). Statistical evaluation of the effects of chronic drug treatment on both receptor binding parameters and adenylyl cyclase activity were made by oneway analysis of variance followed by Dunnett's multiple comparison test.

Radioligands and drugs

The following were used: [2,8-^{3}H]-adenosine 3',5'–cyclic phosphate ammonium salt (specific activity = 34.2 Ci mmol^{-1}); (−)-[^{125}I]-iodopindolol (specific activity = 2200 Ci-mmol^{-1}) (New England Nuclear); 4-amino-*n*-[2,3-^{3}H]-butyric acid (GABA) (specific activity = 92.5 Ci mmol^{-1}) (Amersham); isoguvacine (Cambridge Research Biochemicals); baclofen isomers, CGP 35348 (*p*-(3-aminopropyl)-diethoxymethyl-phosphinic acid) and CGP 36742 (*p*-(3-aminopropyl)-*p*-n-butylphosphinic acid) were kindly supplied by Dr H. Bittiger, Ciba-Geigy Ltd. Basel, Switzerland; ICI 118,551 (erythro-DL-1-(7-methylindan-4-y(oxy)-3-isopropyl-aminobutan-2-ol) was kindly supplied by ICI Pharmaceuticals, Macclesfield.

Drugs were dissolved in saline or distilled water.

Results

Chronic antidepressant administration on $GABA_B$ receptor binding

Administration for 14 days The effects of imipramine administered for 14 days either intraperitoneally (5 mg kg^{-1})

Table 1 The effect of imipramine, administered intraperitoneally and via subcutaneously implanted minipumps for 14 days, on [^{3}H]-γ-aminobutyric acid ([^{3}H]-GABA) binding to $GABA_B$ sites in rat frontal cortex

Treatment	n	*Lamina I*	*Laminae II–III*	*Lamina V*	*Lamina VI*
			B_{max} (fmol mg^{-1} tissue)		
Control	5	211.9 ± 23.0	264.2 ± 26.8	197.4 ± 19.2	139.9 ± 18.6
Imipramine (1)	5	270.8 ± 29.8	305.4 ± 22.4	217.3 ± 23.5	134.4 ± 17.3
Imipramine (2)	5	231.4 ± 48.7	292.2 ± 55.0	215.9 ± 49.0	NC
Imipramine (3)	4	286.9 ± 42.0	319.2 ± 69.3	209.8 ± 69.3	151.3 ± 12.2
			K_D (nM)		
Control	5	77.5 ± 10.3	86.5 ± 15.9	90.6 ± 20.2	117.3 ± 24.1
Imipramine (1)	5	90.0 ± 19.1	95.2 ± 14.0	91.8 ± 15.6	110.2 ± 20.6
Imipramine (2)	5	81.8 ± 26.5	82.0 ± 36.6	118.0 ± 42.2	NC
Imipramine (3)	4	86.5 ± 15.9	95.8 ± 25.2	90.7 ± 46.6	114.8 ± 14.2

(1) 10 mg kg^{-1}, s.c., 24 h drug-free period
(2) 10 mg kg^{-1}, s.c., 48 h drug-free period
(3) 5 mg kg^{-1}, i.p., 24 h drug-free period
NC: not calculated

Table 2 The effects of repeatedly administered (21 days) antidepressants on the binding of [^{3}H]-γ-aminobutyric acid ([^{3}H]-GABA) to $GABA_B$ sites in rat frontal cortex

Treatment	*Dose* (mg kg^{-1})	*Lamina I*	*Laminae II–III*	*Lamina V*	*Lamina VI*
			B_{max} (fmol mg^{-1} tissue)		
Control		236.6 ± 25.0	254.6 ± 42.3	228.8 ± 38.5	209.4 ± 22.2
Desipramine	20 p.o.	316.0 ± 26.0*	299.2 ± 26.2	252.0 ± 23.9	237.7 ± 27.3
Amitriptyline	30 p.o.	290.5 ± 40.9	283.5 ± 34.4	239.8 ± 22.2	232.6 ± 27.8
Paroxetine	10 p.o.	268.5 ± 38.7	299.1 ± 44.3	NC	177.5 ± 29.2
Baclofen	10 p.o.	297.4 ± 24.9	266.4 ± 11.8	194.1 ± 10.1	250.4 ± 18.7
Desipramine	10 i.p.	352.0 ± 50.7*	275.1 ± 11.9	224.2 ± 4.8	190.8 ± 23.4
CGP 35348	100 i.p	241.4 ± 7.4	255.2 ± 16.9	190.4 ± 6.9	161.1 ± 7.3
CGP 36742	100 i.p.	367.1 ± 36.1*	307.4 ± 17.3	259.4 ± 11.6	221.1 ± 9.8
			K_D (nM)		
Control		70.1 ± 16.1	59.2 ± 19.3	74.6 ± 22.3	85.8 ± 17.4
Desipramine	20 p.o.	106.5 ± 26.8	72.2 ± 14.9	76.7 ± 13.5	85.6 ± 17.5
Amitriptyline	30 p.o.	76.9 ± 13.6	55.6 ± 10.2	68.9 ± 7.6	103.8 ± 18.1
Paroxetine	10 p.o.	84.1 ± 24.0	76.4 ± 21.2	NC	70.3 ± 31.2
Baclofen	10 p.o.	71.6 ± 1.5	48.5 ± 4.0	40.5 ± 6.6	111.3 ± 20.7
Desipramine	10 i.p.	81.0 ± 12.3	44.9 ± 11.2	55.9 ± 7.2	61.0 ± 24.4
CGP 35348	100 i.p.	59.5 ± 6.5	56.0 ± 8.2	41.7 ± 3.3	46.8 ± 6.4*
CGP 36742	100 i.p.	132.5 ± 20.3*	82.9 ± 10.1	90.8 ± 10.1	103.5 ± 10.9

*$P < 0.05$ Dunnett's multiple comparison test (n = between 3 and 5 rats/group)
NC: not calculated

or by continuous infusion (10 mg kg^{-1}) from subcutaneously implanted osmotic minipumps on [^{3}H]-GABA binding to GABA$_B$ receptors in rat frontal cortex are summarised in Table 1. Following a 24 h (but not 48 h) drug-free period, subcutaneous infusion of imipramine produced an apparent increase in GABA$_B$ binding sites in lamina I amounting to 28% above control; however, statistical significance was not achieved ($P = 0.074$). Nevertheless, this trend of increased GABA$_B$ binding in lamina I was also evidence following intraperitoneal injections of imipramine (5 mg kg^{-1}). Such changes were also reflected, but to a lesser extent, in laminae II and III. Since the osmotic pumps offered no apparent advantages over intraperitoneal injections, the latter route was used in the subsequent study for comparison with oral administration.

Administration for 21 days Since this second study involved drug administration by both oral and intraperitoneal routes, control values for [^{3}H]-GABA binding to GABA$_B$ sites were derived from the mean of six animals, three dosed orally and three dosed intraperitoneally, there being no significant difference in the results from these two groups.

Chronic treatment with desipramine for 21 days significantly increased the B_{max} of GABA$_B$ binding sites in lamina I by 34% and 49% (p.o. and i.p., respectively). By contrast, although amitriptyline and paroxetine (as well as the GABA$_B$ receptor agonist, (±)-baclofen), also appeared to increase the B_{max} of GABA$_B$ binding, the values did not differ significantly from control (Table 2).

The GABA$_B$ receptor antagonist, CGP 35348 (100 mg kg^{-1}, i.p.), failed to increase GABA$_B$ receptor numbers, however, CGP 36742, at the same dose produced a significant enhancement (+55%) of GABA$_B$ binding in lamina I, comparable to that mediated by desipramine. With the exception of CGP 36742, none of these treatments significantly altered the affinity of [^{3}H]-GABA for GABA$_B$ sites in any of the frontal cortical laminae studied. A significant reduction in receptor affinity was produced by CGP 36742, denoted by an increased K_D of 89% above control. Thus, it would appear that the ability of this compound to up-regulate markedly GABA$_B$ receptors possibly occurs at the expense of a reduction in the affinity of the endogenous ligand for its receptor. The effects of these chronic treatments are shown autoradiographically (Figure 1) and by Scatchard analysis (Figure 2).

Drug-induced modulation of β-adrenoceptor binding

Figure 3 shows the effects of the repeated administration of CGP 35348, CGP 36742 and the antidepressants, on binding to β-adrenoceptors in the frontal cortex, assessed autoradiographically using (−)-[^{125}I]-iodopindolol. Quantitative measurements of the radioligand binding were examined over the concentration range (18.75–300 pM) to produce Scatchard plots of total and β_1-adrenoceptor binding (Figure 4) from which B_{max} and $K_D$values were derived (Table 3).

Whilst no apparent reduction in binding was produced by paroxetine in the frontal cortex, chronic treatment with amitriptyline and desipramine produced a clear down-regulation of both total and β_1-adrenoceptor binding in all laminae of this region. Similarly, oral administration of the GABA$_B$ receptor agonist, baclofen, produced a β-adrenoceptor down-regulation of a similar magnitude to that mediated by amitriptyline. Resolution into the β_1-adrenoceptor subtype, revealed that the observed drug-induced modifications were attributable to this subsite in all frontal cortical laminae. Moreover, with the exception of desipramine (i.p.) in laminae II and III, no significant changes in receptor affinity were observed.

Both the GABA$_B$ receptor antagonists, CGP 35348, and CGP 36742, down-regulated the total β-adrenoceptor population to a similar degree as observed with amitriptyline. However, the resolved β_1-adrenoceptor subtype was not significantly affected by either treatment which may implicate the preferential involvement of β_2-adrenoceptors in this response. Furthermore, both GABA$_B$ receptor antagonists and desipramine significantly increased the affinity of the total β-adrenoceptor population (with the exception of CGP 35348 in laminae II and III) for (−)-[^{125}I]-iodopindolol, as exemplified by reduced K_D values of between 14% and 40%. In contrast, the affinities of resolved β_1-adrenoceptors were unaffected by such treatments (with the exception of desipramine in laminae II and III). By ranking the individual B_{max} values for GABA$_B$ receptors in desipramine- and CGP 36742-treated rats with the corresponding B_{max} values for β-adrenoceptors, no positive correlation was apparent (Spearman's rank correlation coefficient, $r_s = 0.13$; $P >> 0.05$).

Table 3 The effects of repeatedly administered (21 days) antidepressants on (−)-[^{125}I]-iodopindolol binding to β-adrenoceptors in rat frontal cortex

Treatment	*Dose* (mg kg^{-1})	*Total* *Lamina I*	*Total* *Laminae II–III*	*Total* *Laminae V–VI*	β_1 *Lamina I*	β_1 *Laminae II–III*	β_1 *Laminae V–VI*
		B_{max} (fmol mg^{-1} tissue)					
Control		1.88 ± 0.06	1.92 ± 0.05	1.51 ± 0.02	1.46 ± 0.06	1.55 ± 0.05	1.15 ± 0.04
Desipramine	20 p.o.	1.29 ± 0.08*	1.44 ± 0.04*	1.09 ± 0.04*	0.73 ± 0.06*	0.92 ± 0.06*	0.62 ± 0.05*
Amitriptyline	30 p.o.	1.37 ± 0.06*	1.57 ± 0.07*	1.22 ± 0.07*	0.97 ± 0.10*	1.27 ± 0.11*	0.92 ± 0.07*
Paroxetine	10 p.o.	1.78 ± 0.01	1.80 ± 0.01	1.36 ± 0.04	1.33 ± 0.03	1.38 ± 0.05	0.94 ± 0.04
Baclofen	10 p.o.	1.41 ± 0.08*	1.51 ± 0.01*	1.16 ± 0.02*	1.02 ± 0.09	1.14 ± 0.08*	0.79 ± 0.09
Desipramine	10 i.p.	0.98 ± 0.09*	1.21 ± 0.05*	0.92 ± 0.03*	0.69 ± 0.03*	0.85 ± 0.03*	0.57 ± 0.04*
CGP 35348	100 i.p.	1.40 ± 0.04*	1.56 ± 0.05*	1.20 ± 0.04*	1.26 ± 0.12	1.37 ± 0.14	1.03 ± 0.09
CGP 36742	100 i.p.	1.46 ± 0.05*	1.59 ± 0.07*	1.18 ± 0.06*	1.30 ± 0.08	1.40 ± 0.08	0.98 ± 0.07
		K_D (pM)					
Control		52.5 ± 5.3	46.5 ± 4.0	41.4 ± 2.4	83.7 ± 9.6	73.4 ± 8.7	81.6 ± 6.8
Desipramine	20 p.o.	48.2 ± 5.9	46.9 ± 1.3	40.3 ± 1.3	68.4 ± 9.5	62.7 ± 3.9	70.2 ± 7.1
Amitriptyline	30 p.o.	49.7 ± 1.7	49.6 ± 2.8	47.0 ± 4.3	64.7 ± 3.1	79.3 ± 4.5	84.5 ± 7.6
Paroxetine	10 p.o.	58.5 ± 2.5	53.4 ± 2.8	42.1 ± 2.1	90.2 ± 8.1	76.9 ± 5.6	68.9 ± 4.8
Baclofen	10 p.o.	48.0 ± 10.7	39.1 ± 2.4	36.0 ± 2.9	86.2 ± 11.7	73.4 ± 8.1	64.0 ± 3.7
Desipramine	10 i.p.	31.2 ± 5.2*	31.0 ± 2.8*	30.0 ± 3.2*	58.9 ± 11.1	48.2 ± 5.0*	55.8 ± 14.5
CGP 35348	100 i.p.	37.8 ± 2.2*	38.8 ± 2.7	35.4 ± 1.2*	79.3 ± 12.8	67.4 ± 10.8	68.4 ± 6.1
CGP 36742	100 i.p.	34.6 ± 1.5*	32.6 ± 3.4*	27.7 ± 3.2**	86.7 ± 7.1	73.9 ± 12.0	64.4 ± 8.0

*$P < 0.05$ Dunnett's multiple comparison test (n = between 3 and 5 rats/group)

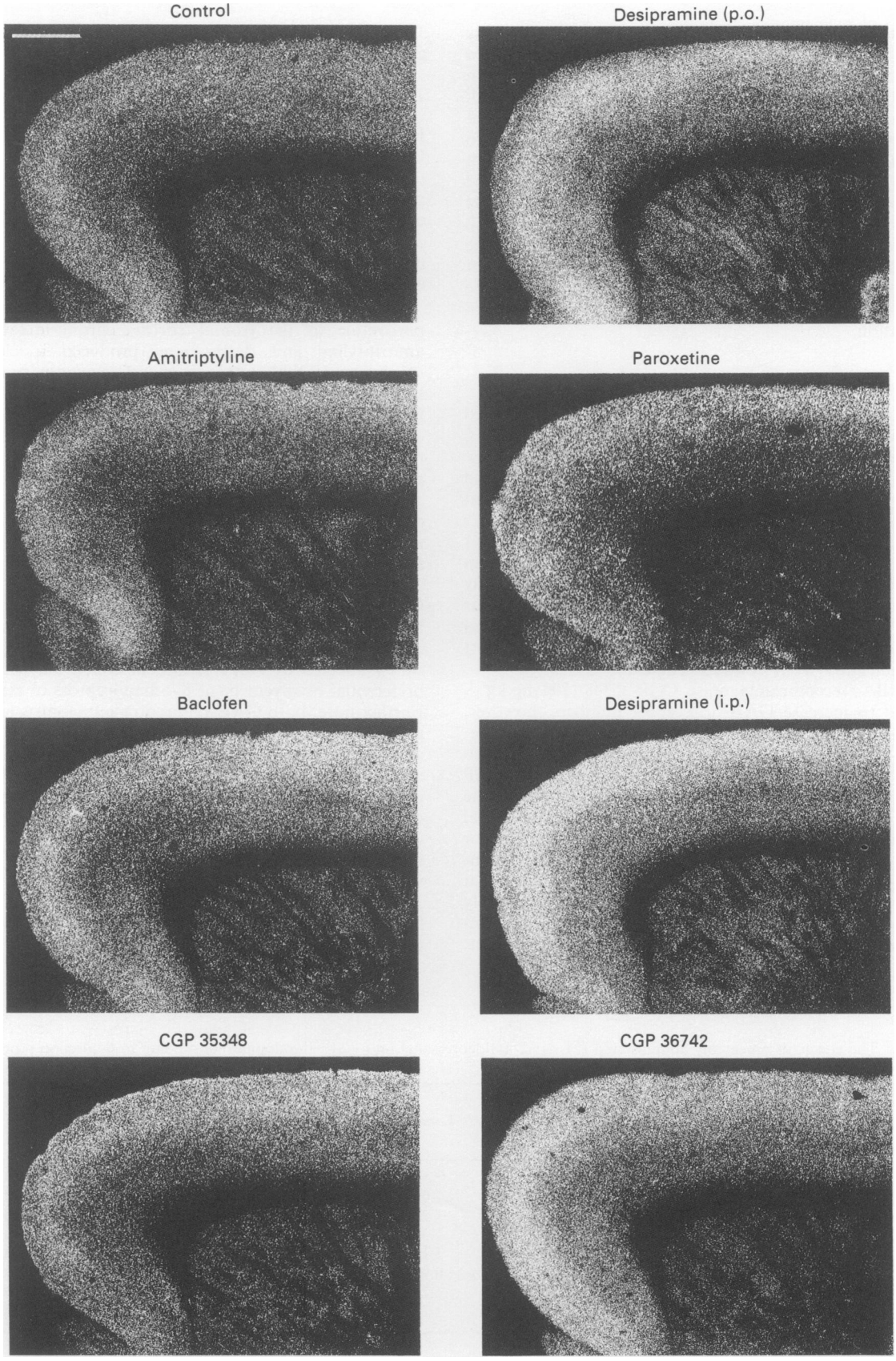

Figure 1 Autoradiograms showing the binding of [^{3}H]-γ-aminobutyric acid ([^{3}H]-GABA) (37.5 nM) to $GABA_B$ receptor sites in the frontal cortex of rats treated with antidepressants, CGP35348 and CGP 36742. Rats were treated orally with amitriptyline (30 mg kg^{-1}), desipramine (20 mg kg^{-1}), paroxetine (10 mg kg^{-1}) or baclofen (10 mg kg^{-1}) whilst intraperitoneal injections of desipramine (10 mg kg^{-1}), CGP 35348 (100 mg kg^{-1}) or CGP 36742 (100 mg kg^{-1}) were also administered for a period of 21 days. Following a 24 h drug-free period, animals were prepared for perfusion-fixation prior to $GABA_B$ receptor autoradiography. Sections were incubated for 20 min with [^{3}H]-GABA and the selective labelling of $GABA_B$ receptors was achieved in the presence of 40 μM isoguvacine. Non-specific binding was defined by 100 μM (−)-baclofen. Of particular interest is the increase in $GABA_B$ binding density in the outer laminae of the frontal cortex following protracted treatment with desipramine (p.o. and i.p.) and with CGP 36742. (Bar = 1 mm).

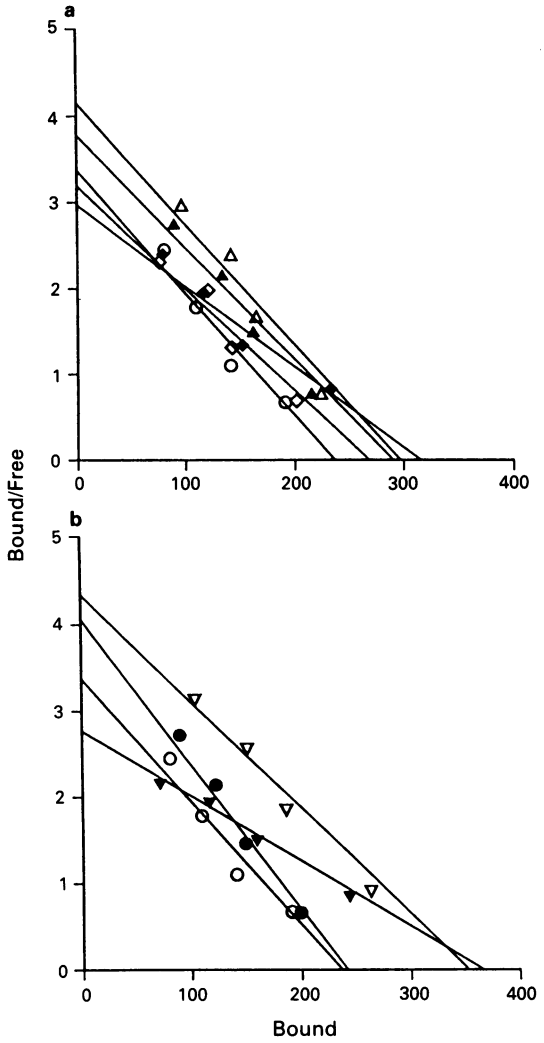

Figure 2 Scatchard plots of GABA$_B$ receptor binding in the frontal cortex (Lamina I) of control (○; $r = 0.97$) and (a) amitriptyline- (30 mg kg^{-1} ▲; $r = 0.91$), desipramine- (20 mg kg^{-1} ◆; $r = 0.84$), paroxetine- (10 mg kg^{-1} ◇; $r = 0.84$) or baclofen- (10 mg kg^{-1} △; $r = 0.94$) orally-treated rats. (b) Desipramine- (10 mg kg^{-1} ▽, $r = 0.96$), CGP 35348- (100 mg kg^{-1} ●; $r = 0.89$) or CGP 36742- (100 mg kg^{-1} ▼; $r = 0.97$) intraperitoneally-treated rats. K_D and B_{max} of the binding of [^{3}H]-GABA (at concentrations of 37.5, 75, 150 and 300 nM) were derived by linear regression analysis and data points represent the mean of 5 animals for which triplicate determinations were made. (Bound = fmol mg^{-1} tissue; Bound/Free = fmol mg^{-1} tissue/nM).

Effects of repeated antidepressant treatment on GABA$_B$ receptor transduction

A summary of the effects of desipramine, amitriptyline, baclofen, CGP 35348 and CGP 36742 on GABA$_B$ receptor-modulation of forskolin and noradrenaline-stimulated adenylyl cyclase is shown in Table 4. With the exception of tissue from rats treated intra-peritoneally with desipramine, forskolin-induced increases in cyclic AMP formation were significantly inhibited by (−)-baclofen (100 μM) in all cases. Similarly, the augmentation of noradrenaline-stimulated cyclic AMP production induced by (−)-baclofen amounted in most instances to around 100%, except in the case of desipramine (i.p.) where cyclic AMP levels were enhanced by only 66%. Moreover, the responsiveness of adenylyl cyclase to noradrenaline stimulation alone, was significantly reduced following repeated administration of amitriptyline (p.o.) and desipramine (i.p.). Although protracted treatment with the GABA$_B$ receptor antagonist, CGP 35348, failed to influence the forskolin-stimulated system, a significant increase in the accumulation of cyclic AMP produced in response to forskolin was seen after treatment with CGP 36742. Since the response to (−)-baclofen did not differ significantly from control tissue, this might suggest an increase in the GABA$_B$ receptor-mediated effect.

Discussion

The inconsistencies surrounding reports of the modulation of GABA$_B$ receptor populations by chronic treatment with antidepressants have remained largely unresolved. From a summary of the main findings, predominantly from five laboratories (Table 5), it is immediately apparent that many methodological differences abound which may account for the existing discrepancies. In an attempt to arbitrate these conflicting reports, the present study has examined the effects of a number of chronically administered antidepressants on the GABA$_B$ receptor population in the rat frontal cortex using receptor autoradiography. This approach has enabled a more detailed analysis of GABA$_B$ sites located within distinct laminal areas of this brain region and has therefore advanced the findings of existing studies in which only synaptic membranes of the frontal cortex had been employed.

The use of osmotic minipumps in drug administration confers the advantage of effecting a slow infusion over a required period which serves to maintain more consistent plasma drug levels than would perhaps be expected following daily oral or intraperitoneal injections. Although infusion and intraperitoneal injections of imipramine appeared to increase the B_{max} of GABA$_B$ receptor binding, most notably in

Table 4 The effects of chronic treatment with antidepressants and GABA$_B$ receptor antagonists GABA$_B$ receptor-modulated forskolin- and noradrenaline-stimulated adenylyl cyclase activity

Treatment	*Dose* (mg kg^{-1})	n	*Forskolin* *Basal*	*Alone*	+ (−)-*Baclofen*	*Noradrenaline* *Basal*	*Alone*	+ (−)-*Baclofen*
Control (p.o.)		5	0.31 ± 0.06	4.08 ± 0.56	2.49 ± 0.37^b	0.27 ± 0.04	1.36 ± 0.19	2.31 ± 0.42^b
Desipramine	20 p.o.	4	0.63 ± 0.06^c	5.28 ± 0.15	4.45 ± 0.29^{b,d}	0.87 ± 0.06^c	1.81 ± 0.18	2.77 ± 0.34^c
Amitriptyline	30 p.o.	4	0.26 ± 0.05	2.93 ± 0.39	1.96 ± 0.39^c	0.24 ± 0.07	0.69 ± 0.10^a	1.12 ± 0.07^c
Baclofen	10 p.o.	5	0.39 ± 0.05	5.06 ± 1.13	3.01 ± 0.46^b	0.24 ± 0.05	1.08 ± 0.14	1.74 ± 0.18^c
Control (i.p.)		5	0.36 ± 0.05	4.28 ± 0.50	2.99 ± 0.31^b	0.41 ± 0.06	1.59 ± 0.20^a	2.46 ± 0.35^c
Desipramine	10 i.p.	3	0.37 ± 0.08	1.87 ± 0.50^a	2.16 ± 0.64	0.33 ± 0.08	0.65 ± 0.06	0.93 ± 0.10^{b,d}
CGP 35348	100 i.p.	5	0.34 ± 0.08	4.03 ± 0.40	3.13 ± 0.17^b	0.32 ± 0.06	1.38 ± 0.06	2.08 ± 0.20^c
CGP 36742	100 i.p.	5	0.47 ± 0.06	6.19 ± 0.32^a	3.85 ± 0.40^c	0.53 ± 0.06	1.76 ± 0.12	2.91 ± 0.21^c

Values represent the mean (± s.e.mean) amount of cyclic AMP accumulated (pmol min^{-1} mg^{-1} protein).
$^aP < 0.05$ forskolin/noradrenaline stimulation alone vs control (Dunnett's multiple comparison test).
$^bP < 0.05$ forskolin/noradrenaline stimulation vs (−)-baclofen (100 μM) (Student's t test).
$^cP < 0.01$ forskolin/noradrenaline stimulation vs (−)-baclofen (100 μM) (Student's t test).
$^dP < 0.01$ (−)-baclofen response (100 μM), drug-treatment vs control (Dunnett's multiple comparison test).
$^eP < 0.05$ basal cyclic AMP levels vs control (Dunnett's multiple comparison test).

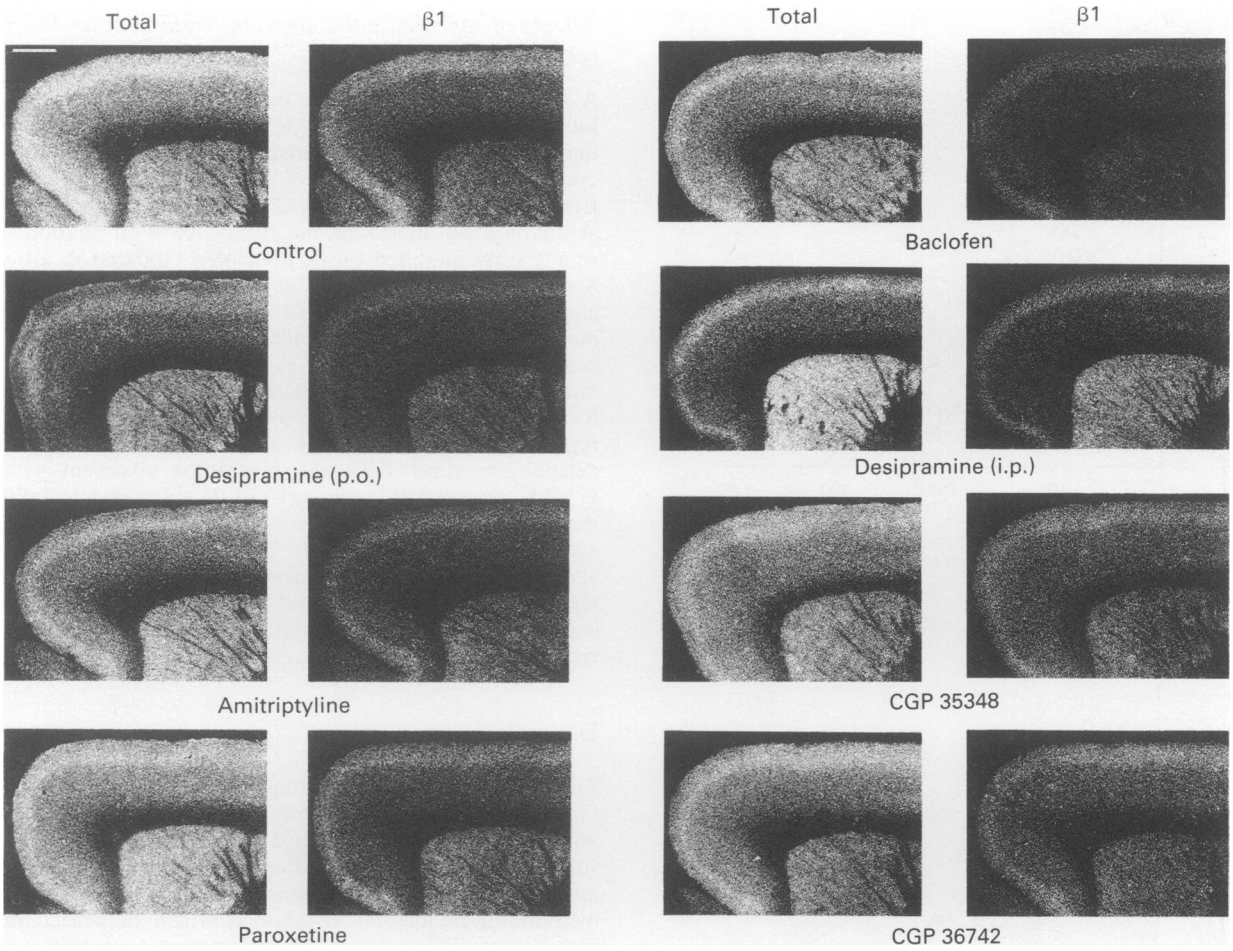

Figure 3 Autoradiograms of total (β_1 and β_2) and resolved β_1-adrenoceptor binding in parasagittal sections of the brains of rats treated with antidepressants, CGP35348 and CGP 36742. Rats were treated orally with amitriptyline (30 mg kg^{-1}), desipramine (20 mg kg^{-1}), paroxetine (10 mg kg^{-1}) or baclofen (10 mg kg^{-1}) whilst intraperitoneal injections of desipramine (10 mg kg^{-1}), CGP 35348 (100 mg kg^{-1}) or CGP 36742 (100 mg kg^{-1}) were also administered for a period of 21 days. Following a 24 h drug-free period, animals were prepared for perfused-fixation prior to β-adrenoceptor autoradiography. Sections were incubated for 60 min with (−)-[^{125}I]-iodopindolol (18.75–300 pM). Non-specific binding was defined by use of 200 μM (−)-isoprenaline whilst the selective labelling of β_1-adrenoceptors was achieved in the presence of the β_2-adrenoceptor antagonist, ICI 118,551 (50 nM). (Bar = 1 mm).

the outer lamina (I) of the frontal cortex, significance was not achieved. These findings agree with those of McManus & Greenshaw (1991) but are in contrast to the up-regulation of $GABA_B$ receptors mediated by both imipramine (Suzdak & Gianutsos, 1986; Szekely *et al.*, 1987) and its demethylated metabolite, desipramine (Pilc & Lloyd, 1984; Lloyd *et al.*, 1985; Szekely *et al.*, 1987).

The antidepressants employed in the second study (desipramine, paroxetine and amitriptyline) were selected on the basis of their ability to inhibit selectively the uptake of NA, 5-HT or both monoamines. From the localized increase in $GABA_B$ receptor binding induced by desipramine in lamina I of the frontal cortex, it could be interpreted that this modulation of $GABA_B$ receptors may have occurred as a consequence of the selective inhibition of noradrenaline uptake, since both amitriptyline and paroxetine were ineffective under the conditions employed in this study. However, this would contradict the findings of Lloyd *et al.* (1985) since $GABA_B$ receptor binding site densities in rat cortical membranes were up-regulated by chronic subcutaneous infusions of both amitriptyline and fluoxetine as well as desipramine.

In addition to the possible modulation of $GABA_B$ receptors, the effects of the antidepressants on β-adrenoceptor binding were also examined with the aim of correlating potentially up-regulated $GABA_B$ receptors with down-regulated β-adrenoceptors. In light of this, desipramine significantly reduced the β-adrenoceptor population in all laminae of the frontal cortex, attributable to a reduction in the β_1-adrenoceptor sub-type. These findings agree with the autoradiographical study of Ordway *et al.* (1988) who observed a reduction in β_1- but not β_2-adrenoceptors throughout the somatosensory cortex following administration of desipramine. Selective β_1-adrenoceptor modulation by desipramine has also been demonstrated in cortical membrane preparations (Minneman *et al.*, 1979; Beer *et al.*, 1987; Heal *et al.*, 1989) and the reduction in β_1-adrenoceptors mediated by amitriptyline, substantiates the findings of Heal *et al.* (1989) and Nelson *et al.* (1990).

The failure of paroxetine (10 mg kg^{-1}), to down-regulate β-adrenoceptors, at a concentration known to inhibit 5-HT uptake, confirms its lack of effect in membrane binding studies (Nelson *et al.*, 1990). Although receptor autoradiography has shown that the 5-HT uptake inhibitors fluoxetine and sertraline decrease β-adrenoceptors in rat frontoparietal cortex (Byerley *et al.*, 1987; 1988), the changes induced by fluoxetine (10 mg kg^{-1}) were marginal, with a larger, more widespread down-regulation induced by repeated doses of 30 mg kg^{-1}. The effects of sertraline were limited to deeper laminae of the cortex.

Repeated administration of the $GABA_B$ receptor agonist, baclofen, reduces the B_{max} of high affinity $GABA_B$ receptors in mouse cortical membranes as well as suppressing the

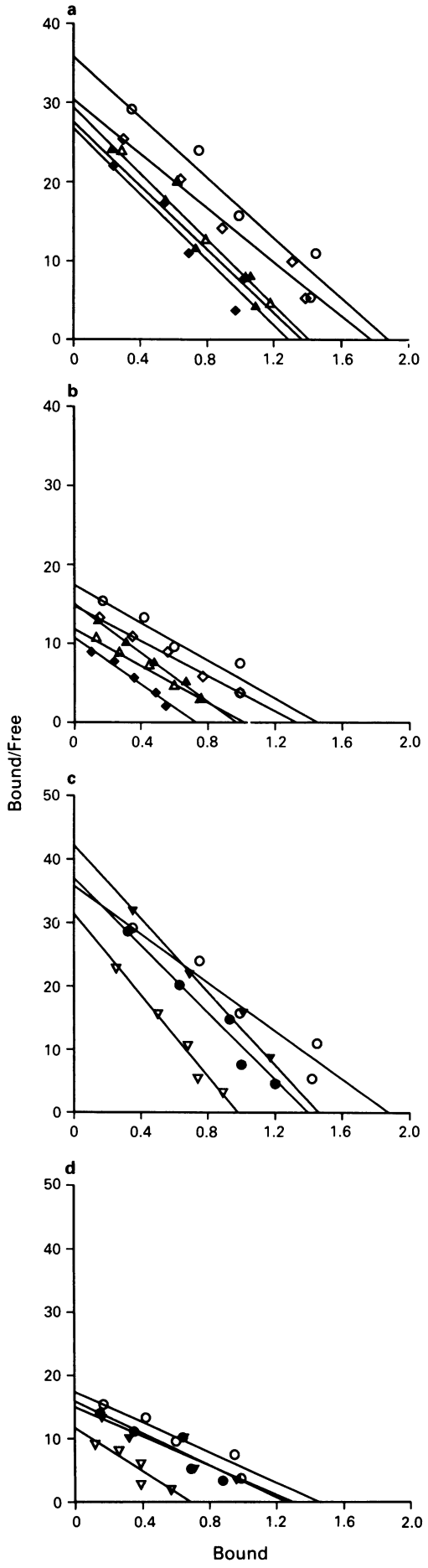

ability of baclofen to potentiate NA-stimulated cyclic AMP accumulation (Suzdak & Gianutsos, 1985a; 1986). In the present study, such a reduction of GABA$_B$ receptors was not apparent after chronic baclofen treatment which may reflect the differing routes of administration used, or, that after a period of 21 days had elapsed, tolerance to the effects of the agonist may have ensued. This treatment protocol did not, however, preclude a significant reduction in β-adrenoceptor populations.

The emergence of the centrally-active GABA$_B$ receptor antagonists, CGP 35348 (Olpe *et al.*, 1990) and CGP 36742 (Bittiger *et al.*, 1992), should facilitate our understanding of the possible physiological roles for central GABA$_B$ receptors. Although CGP 35348 enters the CNS, it does so rather rapidly and since its effects are short lasting (Olpe *et al.*, 1990), this could explain why after its repeated administrations, no alteration in GABA$_B$ receptor populations in the frontal cortex was observed. Conversely, CGP 36742 increased the B_{max} of GABA$_B$ receptors in lamina I, to a similar extent to that induced by desipramine. In view of the comparable affinities of the two antagonists (Olpe *et al.*, 1990; Bittiger *et al.*, 1992), this suggests that a possible longer half-life of CGP 36742 may be responsible for mediating the receptor regulation. It was therefore intriguing that whereas both antagonists reduced the total β-adrenoceptor population, the modulation was not attributable to the β_1-adrenoceptor sub-type (in contrast to the antidepressant effects already described). This indicates a possible involvement of β_2-adrenoceptors, although in cortical regions this sub-type constitutes only 20–25% of the total β-adrenoceptor population (Rainbow *et al.*, 1984; Beer *et al.*, 1987; Ordway *et al.*, 1988; De Paermentier *et al.*, 1989) and may be associated with non-nerve cell components such as glia and blood vessels (Minneman *et al.*, 1979). The discrepancy may point to different sensitivities between neuronal GABA$_B$ receptors and those functionally-linked to non-neuronal elements. Clearly, clarification of such a link between GABA$_B$ receptor antagonists and β_2-adrenoceptors requires further experimental investigation.

To provide a functional index of GABA$_B$ receptor modulation, the sensitivities of both forskolin- and noradrenaline-stimulated adenylyl cyclase systems were examined in brain slices following repeated administration of the aforementioned compounds. The sensitivity of adrenoceptors to noradrenaline stimulation was significantly reduced after chronic treatment with both desipramine (i.p.) and amitriptyline, which was likely to be a consequence of down-regulated β-adrenoceptors (Minneman *et al.*, 1979; Beer *et al.*, 1987; Heal *et al.*, 1989). Since the ability of (−)-baclofen to enhance the effect of noradrenaline was unaltered from control levels by these treatments, a drug-induced modulation of these particular GABA$_B$ receptors was not evident. The failure of desipramine (p.o.) to reduce the cyclic AMP response, despite down-regulated numbers of β-adrenoceptors

Figure 4 Scatchard plots of (a) total (β_1 and β_2) and (b) resolved β_1-adrenoceptor binding (in the presence of 50 nM ICI 118,551) in the frontal cortex (lamina I) of control (○; $r = 0.86$ and 0.89) and amitriptyline- (30 mg kg^{-1} ▲; $r = 0.93$ and 0.97), desipramine- (20 mg kg^{-1} ◆; $r = 0.87$ and 0.89), paroxetine- (10 mg kg^{-1} ◇; $r = 0.95$ and 0.99) or baclofen- (10 mg kg^{-1} △; $r = 0.95$ and 0.96) orally-treated rats. (c) Total (β_1 and β_2) and (d) resolved β_1-adrenoceptor binding (in the presence of 50 nM ICI 118,551) to the frontal cortex (lamina I) of control (○; $r = 0.86$ and 0.89) and desipramine- (10 mg kg^{-1} ▽ $r = 0.95$ and 0.81), CGP 35348- (100 mg kg^{-1} ●; $r = 0.93$ and 0.84) or CGP 36742- (100 mg kg^{-1} ▼; $r = 0.90$ and 0.83) intraperitoneally-treated rats. The kinetic parameters, K_D and B_{max} of the binding of (−)-[^{125}I]-iodopindolol (at concentrations of 18.75, 37.5, 75, 150 and 300 pM) were derived by linear regression analysis and data points represent the mean of 5 animals for which triplicate determinations were made. (Bound = fmol mg^{-1} tissue; Bound/Free = fmol mg^{-1} tissue/nM).

Table 5 Summary of published studies examining the effects of chronic antidepressant treatments on $GABA_B$ receptor binding in brain membranes

Reference	*Drugs*	*Dose* (mg kg^{-1})	*Duration*	*Drug-free period*	*Region/ species*	*Radioligand conditions*	*Results* re: $GABA_B$ B_{max}	*Additional findings*
Pilc & Lloyd (1984)	Amitriptyline Desipramine Citalopram Viloxazine Pargyline	10 s.c. 5 s.c. 10 s.c. 10 s.c. 20 s.c.	18 day mini-pumps	24 h	Frontal cortex Wistar Rat	[^{3}H]-GABA (8–160 nM) saturation	+ 63%** + 39%* + 52%** + 66%** + 57%*	only viloxazine increased $GABA_B$ binding acutely (10 nM). No chronic effects on $GABA_B$ binding, GABA levels or GAD activity.
Lloyd *et al.* (1985)	Nomifensine Desipramine Desipramine Zimeldine	5 s.c. 1.25 s.c. 5 s.c. 10 s.c.	18 days mini-pumps	72 h	Frontal cortex Wistar rat	[^{3}H]-GABA (10 nM) 1–750 μM GABA displacement	+ 16% + 41% − 3%[a] + 34%[a]	*In frontal cortex* DMI, Map, Vilox, Cital, Zimel, Nomi, Ami, Parg, Traz, Mian (s.c.), ECS; Fluox, Prog, Feng, Val (i.p.) produced increases in $GABA_B$ binding of between 27% and 88% at 10 nM [^{3}H]-GABA. *In Hippocampus* DMI, Vilox and Cital significantly increased $GABA_B$ binding.
Suzdak & Gianutsos (1986)	Baclofen Imipramine	10 i.p. 32 i.p.	14 days	24 hrs	Whole cortex Mouse (CD1)	[^{3}H]-GABA (1–1000 nM) saturation	− 16%*[b] + 17%*[c] + 24%*[b] + 15%*[c]	Chronic baclofen reduced the baclofen-induced potentiation of NA-stimulated adenylyl cyclase whereas imipramine augmented the potentiation.
Szekely *et al.* (1987)	Desipramine Imipramine Maprotiline	10 i.p. 7.5 i.p. 10 i.p.	21 days twice daily	48 h	Frontal cortex Sprague-Dawley rat	[^{3}H]-GABA (5–400 nM) [^{3}H]−(-)-Bac (5–150 nM) saturation	[^{3}H]-GABA [^{3}H]-(−)-Bac + 28%** No + 24%** change − 6%	Antidepressants failed to affect the potency of (−)-baclofen to inhibit forskolin-stimulated adenylyl cyclase in membrane studies.
Cross & Horton (1988)	Desipramine Zimeldine Desipramine Zimeldine	1.25 & 5 p.o. 1.25 & 5 p.o. 5 & 10 p.o. 5 & 10 p.o.	21 days twice daily	24 h	Whole cortex Frontal cortex Wistar rat	[^{3}H]-GABA (1 nM) 5–150 nM GABA displacement	No change	DMI (5 and 10 mg kg^{-1}, p.o.) and Zimel (10 mg kg^{-1}, p.o.) significantly reduced 5-HT_2 binding sites in frontal cortex but not hippocampus.
Cross *et al.* (1988)	Post-mortem depressed suicide victims	–	–	–	Frontal/Temporal cortex Human	[^{3}H]-GABA (1 nM) 5–300 nM GABA displacement	No change in K_D or B_{max} of drug-free or AD-treated suicide victims	Kinetic parameters were also unaffected in hippocampal membranes.

Table 5 Summary of published studies examining the effects of chronic antidepressant treatments on $GABA_B$ receptor binding in brain membranes

Reference	*Drugs*	*Dose* (mg kg^{-1})	*Duration*	*Drug-free period*	*Region/ species*	*Radioligand conditions*	*Results* re: $GABA_B$ B_{max}	*Additional findings*
Motohashi *et al.* (1989)	Lithium chloride	1.5 mEq kg^{-1}	14 days	24 h	Hippocampus	[^{3}H]-(−)-Bac(10–80 nM) saturation	+ 52%*	No changes in $GABA_B$ binding in frontal cortex or [^{3}H]-muscimol binding in either region.
	Carbamazepine	50 i.p.					+ 38%*	
					Wistar rat			
McManus & Greenshaw (1991)	Imipramine	30 s.c.	28 days	None	Frontal cortex	[^{3}H]-GABA (1 mM) 5–160 nM GABA displacement	No change	B_{max} of [^{3}H]-dihydroalprenolol binding reduced with all treatments.
	Desipramine	10 s.c.	mini-pumps					
	Tranylcypromine	1 s.c.			Sprague-Dawley rat			
	Phenelzine	10 s.c.						

[a]Changes refer to the high affinity components of a curvilinear Scatchard plot.
[b]High affinity binding site.
[c]Low affinity binding site.
*$P<0.05$; **$P<0.01$ Student's t test.

Abbreviations DMI (desipramine); Map (maprotiline); Vilox (viloxazine); Cital (citalopram); Zimel (zimeldine); Nomi (nomifensine); Ami (amitriptyline); Parg (pargyline); Traz (trazodone); Mian (mianserin); ECS (electroconvulsive shock); Fluox (fluoxetine); Prog (progabide); Feng (fengabine); Val (sodium valproate); NA (noradrenaline); GAD (glutamic acid decarboxylase); [^{3}H]-(−)-Bac ([^{3}H]-(−)-baclofen); AD (antidepressant).

is difficult to interpret but may be associated with the higher basal cyclic AMP content found in these animals which could have masked any drug-induced modulation of adenylyl cyclase activity. Protracted treatment with baclofen decreases the sensitivity of β-adrenoceptors to noradrenaline activation in addition to suppressing the ability of baclofen to augment this response (Suzdak & Gianutsos, 1986). Although there was some indication that such an effect may have occurred in the present study, significant differences from control values were not obtained. Furthermore, no additional drug-induced modulations of the $GABA_B$ receptor-mediated noradrenergic potentiation of β-adrenoceptor activation were detected.

Focussing on the forskolin-activated adenylyl cyclase system, with the exception of desipramine (i.p.), the (−)-baclofen-induced inhibition of activated cyclic AMP production was evident following all of the chronic treatments. Since protracted treatment with desipramine (p.o. and i.p.) as well as CGP 36742, significantly up-regulates $GABA_B$ receptor sites in the outer lamina (I) of the frontal cortex, it was anticipated that such an increase in the $GABA_B$ receptor population would be reflected by an enhancement of the ability of (−)-baclofen to inhibit the stimulatory action of forskolin. In the case of desipramine (p.o.), the levels of cyclic AMP produced in response to forskolin alone were not significantly increased after this treatment. However, although in the presence of (−)-baclofen, the amount of significantly increased after this treatment. However, in the presence of (−)-baclofen, the amount of accumulated cyclic AMP was significantly greater than the control value which may reflect $GABA_B$ receptor up-regulation.

Protracted treatment with CGP 36742 significantly increased the levels of cyclic AMP formed by forskolin alone. Moreover, although the percentage inhibition of this effect by baclofen was enhanced, unlike desipramine, the increased cyclic AMP levels observed in the presence of (−)-baclofen after treatment with CGP 36742 were not significantly different from the control response. This indicates an enhancement of the $GABA_B$ receptor-mediated effect and provides a functional correlate of the $GABA_B$ receptor up-regulation induced by CGP 36742. Moreover, since treatment with CGP 36742 failed to modulate those $GABA_B$ receptors associated functionally with the noradrenaline-stimulated adenylyl cyclase system, this further supports the contention that the $GABA_B$ receptors linked with these two transduction mechanisms may be heterogeneous.

In conclusion, of the compounds tested, only desipramine and CGP 36742 were able to mediate consistently an up-regulatory signal for $GABA_B$ receptors. Secondly, where drug-induced increases in the $GABA_B$ receptor population were evident in the frontal cortex, such changes were restricted to the outer lamina (I) of this region. Since desipramine specifically inhibits the uptake of noradrenaline, some speculation regarding the influence of this antidepressant (as well as CGP 36742) on $GABA_B$ receptors in this discrete anatomical location would seem most appropriately interpreted in relation to both the noradrenergic system and known markers of GABAergic activity.

Although desipramine enhances the release of GABA from the rat thalamus (Korf & Venema, 1983), the mechanism(s) through which $GABA_B$ receptors in the frontal cortex are up-regulated by chronic treatment with antidepressants still remain to be elucidated. Activation of $GABA_B$ receptors inhibits noradrenaline release in cerebral cortex (Bowery *et al.*, 1980; Suzdak & Gianutsos, 1985b), suggesting a presynaptic inhibitory action on noradrenergic terminals. Low (but not high) affinity $GABA_B$ sites are associated with noradrenergic cortical terminals since only the former are reduced following a unilateral lesion of the dorsal noradrenergic bundle (Karbon *et al.*, 1983). However, since the changes in $GABA_B$ receptor sites reported in the present study pertain to a high affinity component, this implies that such $GABA_B$ receptors may not necessarily be linked with the noradrenergic system in depression. Such a hypothesis,

however, contradicts the findings of Lloyd *et al.* (1985) and Suzdak & Gianutsos (1986) where both high and low affinity sites were increased by antidepressants.

One of the predicted effects of a $GABA_B$ receptor antagonist would be to inhibit the suppression of noradrenaline release induced by GABA acting at presynaptic $GABA_B$ receptors on noradrenergic terminals. Although there is no experimental evidence to support this at present, CGP 35348 inhibits the release of [^{3}H]-GABA from cortical slices (Waldmeier & Baumann, 1990). The $GABA_B$ receptors increased following chronic treatment with CGP 36742, again, are likely to represent presynaptic $GABA_B$ autoreceptors. Blockade of terminal $GABA_B$ receptors on noradrenergic neurones would lead to an increase in synaptic concentrations of noradrenaline, thus facilitating postsynaptic β-adrenoceptor down-regulation. Persistent occupation of a receptor by an antagonist would eventually lead to a compensatory 'supersensitization', thus those $GABA_B$ receptors up-regulated by chronic treatment with CGP 36742, could be attributed to these terminal receptors.

Such hypotheses are purely speculative at this stage and do not account for possible modulations of post-synaptic $GABA_B$ receptors or changes in other brain regions. Nonetheless, it is hoped that these findings will provide a significant step forward in our understanding of the role of $GABA_B$ receptors in depression.

References

BANERJEE, S.P., KUNG, L.S., RIGGI, S.J. & CHANDA, S.K. (1977). Development of β-adrenergic receptor subsensitivity by antidepressants. *Nature*, **268**, 455–456.

BEER, M., HACKER, S., POAT, J. & STAHL, S.M. (1987). Independent regulation of β_1 and β_2-adrenoceptors. *Br. J. Pharmacol.*, **92**, 827–834.

BERRETTINI, W.H., NURNBERGER, J.I., HARE, T.A., GERSHON, E.S. & POST, R.M. (1982). Plasma and CSF GABA in affective illness. *Br. J. Psychiatry*, **141**, 483–487.

BITTIGER, H., BERNASCONI, R., FROESTL, W., HALL, R., JAEKEL, J., KLEBS, K., KRUEFER, L., MICKEL, S.J., MONDADORI, C., OLPE, H.R., PFANNKUCH, F., POZZA, M., PROBST, A., VAN RIEZEN, H., SCHMUTZ, M., SCHUETZ, H., STEINMANN, M.W., VASSOUT, A. & WALDMEIER, P. (1992). $GABA_B$ antagonists: potential new drugs. *Pharmacol. Commun.*, **2**, 70–74.

BORSINI, F., GIULIANI, S. & MELI, A. (1986). Functional evidence for altered activity of GABAergic receptors following chronic despramine treatment in rats. *J. Pharm. Pharmacol.*, **38**, 934–935.

BOWERY, N.G., HILL, D.R., HUDSON, A.L., DOBLE, A. MIDDLEMISS, D.N., SHAW, J. & TURNBULL, M. (1980). (−)Baclofen decreases neurotransmitter release in the mammalian CNS by an action at a novel GABA receptor. *Nature*, **283**, 92–94.

BRADFORD, M.M. (1976). A rapid and sensitive method for the quantification of microgram quantities of protein utilising the principle of protein-dye binding. *Anal. Biochem.*, **72**, 248–254.

BROWN, B.L., ELKINS, R.P. & ALBANO, J.D.M. (1972). Saturation assay for cyclic AMP using endogenous binding protein. In *Adv. Cyclic Nucl. Res.*, Vol. 2, pp. 25–40. New York: Raven Press.

BYERLEY, W.F., MCCONNELL, E.J., MCCABE, R.T., DAWSON, T.M., GROSSER, B.I. & WAMSLEY, J.K. (1987). Chronic administration of sertraline, a selective serotonin uptake inhibitor, decreased the density of β-adrenergic receptors in rat frontoparietal cortex. *Brian Res.*, **421**, 377–381.

BYERLEY, W.F., MCCONNELL, E.J., MCCABE, R.T., DAWSON, T.M., GROSSOR, B.I. & WAMSLEY, J.K. (1988). Decreased beta-adrenergic receptors in rat brain after chronic administration of the selective uptake inhibitor fluoxetine. *Psychopharmacol.*, **94**, 141–143.

CLARKE, C.R. & HALL, M.D. (1986). Hormone receptor autoradiography: recent developments. *Trends Biochem. Sci.*, **11**, 195–199.

CROSS, J.A. & HORTON, R.W. (1988). Effects of chronic oral administration of the antidepressants, desmethylimipramine and zimelidine on rat cortical $GABA_B$ binding sites: a comparison with 5-HT_2 binding site changes. *Br. J. Pharmacol.*, **93**, 331–336.

CROSS, J.A., CHEETHAM, S.C., CROMPTON, M.R., KATONA, C.L.E. & HORTON, R.W. (1988). Brain $GABA_B$ binding sites in depressed suicide victims. *Psychiatr. Res.*, **26**, 119–129.

DE BLASI, A., O'REILLY, K. & MOTULSKY, H.J. (1989). Calculating receptor number from binding experiments using same compound as radioligland and competitor. *Trends Pharmacol. Sci.*, **10**, 227–229.

DE PAERMENTIER, F., CHEETHAM, S.C., CROMPTON, M.R. & HORTON, R.W. (1989). β-adrenoceptors in human brain labelled with [^{3}H]dihydroalprenolol and [^{3}H]CGP 12177. *Eur. J. Pharmacol.*, **167**, 397–405.

GOLD, B.I., BOWERS, M.B., ROTH, R.H. & SWEENEY, D.W. (1980). GABA levels in CSF of patients with psychiatric disorders. *Am. J. Psychiatry*, **137**, 362–364.

GRAY, J.A. & GREEN, A.R. (1987). Increased $GABA_B$ receptor function in mouse frontal cortex after repeated administration of antidepressant drugs or electroconvulsive shocks. *Br. J. Pharmacol.*, **92**, 357–362.

GRAY, J.A., GOODWIN, G.M., HEAL, D.J. & GREEN, A.R. (1987). Hypothermia induced by baclofen, a possible index of $GABA_B$ receptor function in mice, is enhanced by antidepressant drugs and ECS. *Br. J. Pharmacol.*, **92**, 863–870.

HEAL, D.J., BUTLER, S.A., HURST, E.M. & BUCKETT, W.R. (1989). Antidepressant treatments, including sibutramine hydrochloride and electroconvulsive shock, decrease β_1- but not β_2-adrenoceptors in rat cortex. *J. Neurochem.*, **53**, 1019–1025.

HILL, D.R. (1985). $GABA_B$ receptor modulation of adenylate cyclase activity in rat brain slices. *Br. J. Pharmacol.*, **84**, 249–257.

KARBON, E.W., DUMAN, R. & ENNA, S.J. (1983). Biochemical identification of multiple $GABA_B$ binding sites: association with noradrenergic terminals in rat forebrain. *Brain Res.*, **274**, 393–396.

KARBON, E.W. & ENNA, S.J. (1985). Characterisation of the relationship between gamma-aminobutyric acid B agonists and transmitter-coupled nucleotide-generating systems in rat brain. *Molec. Pharmacol.*, **27**, 53–59.

KORF, J. & VENEMA, K. (1983). Desmethylimipramine enhances the release of endogenous GABA and other neurotransmitters from the thalamus. *J. Neurochem.*, **40**, 946–950.

LLOYD, K.G., MORSELLI, P.L., DEPOORTERE, H., FOURNIER, V., ZIVKOVIC, R., SCATTON, B., BROEKKAMP, C.L., WORMS, P. & BARTHOLINI, G. (1983). The potential use of GABA agonists in psychiatric disorders: evidence from studies with progabide in animal models and clinical trials. *Pharmacol. Biochem. Behav.*, **18**, 957–966.

LLOYD, K.G., THURET, F. & PILAC, A. (1985). Upregulation of γ-aminobutyric acid $(GABA)_B$ binding sites in rat frontal cortex: a common action of repeated administration of different classes of antidepressants and electroshock. *J. Pharmacol. Exp. Ther.*, **235**, 191–199.

LLOYD, K.G. & PICHAT, P. (1986). Decrease in $GABA_B$ binding to the frontal cortex of olfactory bulbectomised rats. *Br. J. Pharmacol.*, **87**, 36P.

MCMANUS, D.J. & GREENSHAW, A.J. (1991). Differential effects of antidepressants on $GABA_B$ and β-adrenergic receptors in rat cerebral cortex. *Biochem. Pharmacol.*, **42**, 1525–1528.

MINNEMAN, K.P., DIBNER, M.D., WOLFE, B.B. & MOLINOFF, P.B. (1979). β_1- and β_2-adrenergic receptors in rat cerebral cortex are independently regulated. *Science*, **204**, 866–868.

MOTOHASHI, N., IKAWA, K. & KARIYA, T. (1989). $GABA_B$ receptors are up-regulated by chronic treatment with lithium or carbamazepine. GABA hypotheis of affective disorders? *Eur. J. Pharmacol.*, **166**, 95–99.

MUSCH, B. & GARREAU, M. (1986). An overview of the antidepressant activity of fengabine in open clinical trials. In *Biological Psychiatry*. ed. Shagass C. pp. 920–922. New York: Elsevier.

NELSON, D.R., PALMER, K.J. & JOHNSON, A.M. (1990). Effect of prolonged 5-hydroxytryptamine uptake inhibition by paroxetine on cortical β_1 and β_2-adrenoceptors in rat brain. *Life. Sci.*, **47**, 1683–1691.

OLPE, H.-R., KARLSSON, G., POZZA, M.F., BRUGGER, F., STEINMANN, M., VAN RIEZEN, H., FAGG, G., HALL, R.G., FROESTL, W. & BITTIGER, H. (1990). CGP 35348: a centrally active blocker of $GABA_B$ receptors. *Eur. J. Pharmacol.*, **187**, 27–38.

ORDWAY, G.A., GAMBARANA, C. & FRAZER, A. (1988). Quantitative autoradiography of central beta adrenoceptor subtypes: comparison of the effects of chronic treatment with desipramine or centrally administered l-isoproterenol. *J. Pharmacol. Exp. Ther.*, **247**, 379–389.

PAXINOS, G. & WATSON, C. (1986). *The Rat Brain in Stereotaxic Coordinates*. Sydney: Academic Press.

PEROUTKA, S.J. & SNYDER, S.H. (1980). Long term antidepressant treatment decreases spiroperidol-labelled serotonin receptor binding. *Science*, **210**, 88–90.

PILC, A. & LLOYD, K.G. (1984). Chronic antidepressants and GABA 'B' receptors: a GABA hypothesis of antidepressant drug action. *Life Sci.*, **35**, 2149–2154.

RAINBOW, T.C., PARSONS, B. & WOLFE, B.B. (1984). Quantitative autoradiography of β_1- and β_2-adrenergic receptors in rat brain. *Proc. Natl. Acad. Sci. U.S.A.*, **81**, 1585–1589.

SUZDAK, P.D. & GIANUTSOS, G. (1985a). Parallel changes in the sensitivity of gamma-aminobutyric acid and noradrenergic receptors following chronic administration of antidepressant and GABAergic drugs. A possible role in affective disorders. *Neuropharmacol.*, **24**, 217–222.

SUZDAK, P.D. & GIANUTSOS, G. (1985b). Differential coupling of GABA-A and GABA-B receptors to the noradrenergic system. *J. Neural Transm.*, **62**, 77–89.

SUZDAK, P.D. & GIANUTSOS, G. (1986). Effect of chronic imipramine or baclofen on $GABA_B$ binding and cyclicAMP production in cerebral cortex. *Eur. J. Pharmacol.*, **131**, 129–133.

SZEKELY, A.M., BARBACCIA, M.L. & COSTA, E. (1987). Effect of a protracted antidepressant treatment on signal transduction and [^{3}H](−)-baclofen binding at $GABA_B$ receptors. *J. Pharmacol. Exp. Ther.*, **243**, 155–159.

WALDMEIER, P.C. & BAUMANN, P.A. (1989). $GABA_B$ receptors and transmitter release. In *$GABA_B$ Receptors in Mammalian Function*. ed Bowery, N.G., Bittiger, H. & Olpe, H.-R., pp. 63–80. Chichester, Wiley.

WATLING, K.J. & BRISTOW, D.R. (1986). $GABA_B$ receptor-mediated enhancement of vasoactive intestinal peptide-stimulated cyclicAMP production in slices of rat cerebral cortex. *J. Neurochem.*, **46**, 1755–1762.

WOJCIK, W.J. & NEFF, N.H. (1984). Gamma-aminobutyric acid B receptors are negatively coupled to adenylate cyclase in brain and in the cerebellum these receptors may be associated with granule cells. *Molec. Pharmacol.*, **25**, 24–28.

(Received September 2, 1992
Revised May 17, 1993
Accepted May 19, 1993)

Br. J. Pharmacol. (1993), **110**, 736–738

Differential inhibition by N^G-monomethyl-L-arginine of vasodilator effects of acetylcholine and methacholine in human forearm vasculature

[1]P.J. Chowienczyk, J.R. Cockcroft & J.M. Ritter

Department of Clinical Pharmacology, UMDS, Guy's and St Thomas' Hospitals, London, SE1

1 We compared the effects of N^G-monomethyl-L-arginine (L-NMMA), an NO synthase inhibitor, on vasodilatation produced by acetylcholine and methacholine in human forearm vasculature.

2 Acetylcholine (83 nmol min^{-1}) infused into the brachial artery of 8 healthy volunteers caused a submaximal increase in forearm blood flow, measured by venous occlusion plethysmography, from 3.3 ± 0.5 (mean ± s.e.mean) to 13.3 ± 1.7 ml min^{-1} 100 ml^{-1}.

3 Co-infusion of L-NMMA (4 μmol min^{-1}) with acetylcholine (83 nmol min^{-1}) over 6 min resulted in a 58% ± 12% fall in the response to acetylcholine whereas during co-infusion of saline over the same time period in the same subjects ($n = 8$) on a different day the response to acetylcholine fell by only 9% ± 17% ($P < 0.01$).

4 Methacholine (1.5 and 15 nmol min^{-1}) increased forearm blood flow from 2.5 ± 0.4 to 5.9 ± 0.9 and from 3.2 ± 0.4 to 17.0 ± 1.9 ml min^{-1} 100 ml^{-1} respectively.

5 Co-infusion of L-NMMA (4 μmol min^{-1}) had no significant effect on the response to methacholine (1.5 or 15 nmol min^{-1}) when compared with saline control ($n=8$). Co-infusion of a higher dose of L-NMMA (8 μmol min^{-1}) with methacholine (1.5 nmol min^{-1}) did not significantly inhibit the vasodilator response ($n=7$).

6 These results suggest that, in human forearm vasculature, methacholine acts predominantly through mechanisms other than the L-arginine/nitric oxide pathway.

Keywords: Endothelium; muscarinic receptors; nitric oxide; N^G-monomethyl-L-arginine; acetylcholine; methacholine; human forearm vasculature

Introduction

N^G-monomethyl-L-arginine (L-NMMA), an inhibitor of nitric oxide (NO) synthase, inhibits vasodilator responses to acetylcholine in human forarm resistance vessels (Vallance *et al.*, 1989). This suggests that acetylcholine causes vasodilatation in this vascular bed at least in part through the L-arginine/NO pathway. It has been assumed that other muscarinic agonists such as methacholine also act on this vascular bed through the L-arginine/NO pathway (Creager *et al.*, 1990; 1992; Liao *et al.*, 1991) However, increasing recognition of the heterogeneity of muscarinic receptor subtypes in vasculature (Dauphin & Hamel, 1991) and their actions in producing both endothelium-dependent and endothelium-independent vasodilatation (Brayden & Bevan, 1985; Rubanyi *et al.*, 1986; Nield *et al.*, 1990; Jaiswal *et al.*, 1991) makes this assumption questionable. We demonstrated recently that in patients with hypercholesterolaemia (a condition in which endothelial dysfunction is well documented in animals and in human coronary vessels) forearm resistance vessel responses to acetylcholine are reduced whereas responses to methacholine are not (Chowienczyk *et al.*, 1992). In the present study we therefore compared effects of L-NMMA on vasodilator responses to acetylcholine and methacholine to determine whether or not this inhibitor of NO synthase influences responses to these muscarinic agonists similarly.

Methods

Studies were performed on healthy normotensive, normocholesterolaemic subjects aged 22–47 years, following informed consent and with the approval of the local ethical committee. Eight subjects were studied on 4 separate occasions in variable order, one week or more apart. They received acetylcholine with saline, acetylcholine with L-NMMA, methacholine with saline and methacholine with L-NMMA. Drugs were obtained from Sigma, UK (methacholine), CooperVision, UK (acetylcholine) and Calbiochem, UK (L-NMMA). L-NMMA was passed through a 0.2 μm filter immediately before use. Experiments were done in a temperature controlled clinical laboratory (20–22°C). Forearm blood flow (ml min^{-1} per 100 ml forearm volume) was measured in both arms simultaneously by venous occlusion plethysmography (Whitney, 1953) with electronically calibrated temperature compensated mercury in silastic strain gauges (Hokanson *et al.*, 1975). During measurements the hands were excluded from the circulation by inflation of wrist cuffs to 180 mmHg. Upper arm cuffs were inflated intermittently to 40 mmHg. A 27 gauge needle was inserted under sterile conditions into the left brachial artery under local anaesthesia (1% lignocaine) and sterile saline (140 mM sodium chloride), or drugs dissolved in saline, infused at 1 ml min^{-1}. Following insertion of the needle subjects rested for 15 min. Saline was then infused for a further 14 min during which baseline measurements were recorded and a constant rate infusion of acetylcholine (83 nmol min^{-1}) or methacholine (15 nmol min^{-1}) commenced; 4 min after the start of the agonist infusion, either saline or L-NMMA (4 μmol min^{-1}) was co-infused for 6 min. Forearm blood flow was measured during infusion of saline alone, during infusion of agonist alone (from 2 to 4 min) and during co-infusion of agonist with L-NMMA or saline (during the last 2 min of co-infusion). Flows were recorded for 10 s in every 15 s and the mean of 3 to 5 measurements used for analysis. A further group of 8 subjects was studied on two occasions, methacholine (1.5 nmol min^{-1}) with saline being infused on one occasion and methacholine with L-NMMA (4

[1] Author for correspondence at: Department of Clinical Pharmacology, St Thomas's Hospital, Lambeth Palace Road, London SE1 7EH.

μmol min^{-1}) on the other. Seven subjects were studied on two further occasions when methacholine (1.5 nmol min^{-1}) with saline was infused on one occasion and with L-NMMA (8 μmol min^{-1}) on the other.

Statistics

Results are presented as means (± s.e.mean). Changes in vasodilator response due to L-NMMA or saline (control) were expressed as a percentage of blood flow response (increase above baseline) during agonist administration immediately before co-infusion. Data were analysed by analysis of variance for repeated measures. Differences were considered significant when $P<0.05$.

Results

Blood flow in the non-infused (control) arm did not change significantly throughout the experiment on any study day, confirming that at the doses used acetylcholine, methacholine and L-NMMA did not cause systemic effects when infused into the brachial artery. Blood flow in the infused arm is shown in Table 1. Acetylcholine (83 nmol min^{-1}) produced approximately a four fold rise in blood flow. Blood flow during methacholine (1.5 and 15 nmol min^{-1}) was approximately 50% lower and 25% higher respectively than during acetylcholine infusion.

During co-infusion of saline there was some tachyphylaxis to both vasodilators ($P<0.01$) which did not differ significantly for acetylcholine or either dose of methacholine. Percentage change in response to acetylcholine and methacholine during L-NMMA co-infusion relative to saline control is shown in Figure 1. L-NMMA (4 μmol min^{-1}) inhibited the response to acetylcholine (83 nmol min^{-1}) by 49% ± 15% of saline control ($P<0.01$). In contrast L-NMMA (4 μmol min^{-1}) had no effect on responses to methacholine (15 nmol min^{-1}, $P=0.82$ or 1.5 nmol min^{-1}, $P=0.88$). There was also no significant effect of L-NMMA (8 μmol min^{-1}) on the response to methacholine (1.5 nmol min^{-1}, $P=0.51$).

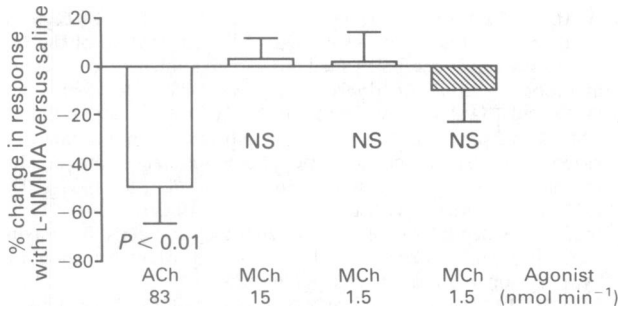

Figure 1 Percentage change in response to acetylcholine (ACh) and methacholine (MCh) relative to saline control after 6 min co-infusion of N^G-monomethyl-L-arginine (L-NMMA) 4 μmol min^{-1} (open columns) or 8 μmol min^{-1} (hatched column).

Discussion

L-NMMA inhibits vasodilatation caused by brachial artery infusion of acetylcholine (Vallance *et al.*, 1989). These workers infused L-NMMA followed by acetylcholine. A possible confounding factor in this approach is that L-NMMA lowers basal blood flow, and there is a strong positive correlation between basal blood flow and response to acetylcholine in this preparation (Chowienczyk *et al.*, 1993). In the present study we infused vasodilator agonists before starting co-infusion of L-NMMA. The blood flow during L-NMMA infusion was therefore higher than in the study by Vallance *et al.* (1989) reducing the concentration of L-NMMA in the forearm vasculature. Despite this we observed very similar inhibition to that reported by Vallance *et al.* (1989) confirming their conclusion that part, at least, of the vasodilatation caused by acetylcholine in forearm vasculature is mediated by the L-arginine/NO pathway. The order of addition of L-NMMA and acetylcholine markedly influences the development of inhibition of acetylcholine induced relaxation of rings of rabbit aorta (Furchgott *et al.*, 1990) The explanation for this pattern of inhibition is not clear; possible explanations include substrate depletion or agonist dependent access of L-NMMA to its site of action (Furchgott *et al.*, 1990). It is possible that the potency of L-NMMA in the forearm is similarly determined by the order of infusion of acetylcholine and L-NMMA. Alternatively, there might be reduced extraction of L-NMMA in proximal vessels at higher flows. This has been proposed as the explanation of the findings that in general, over a narrow range of flow rates, the response to a drug is more closely related to the dose of drug infused than the calculated concentration (Robinson, 1990).

The principle finding of the present study is that whereas L-NMMA inhibits the vasodilator action of acetylcholine in forearm vasculature substantially it has no effect on responses to methacholine. The doses of acetylcholine and methacholine used cause submaximal vasodilatation, and are similar to those used in previous studies of endothelial function in hypertension and hyperlipidaemia (Linder *et al.*, 1990; Creager *et al.*, 1990). In our first study, blood flow during infusion of methacholine was approximately 25% greater than during acetylcholine infusion, suggesting the possibility that the lack of inhibition of methacholine by L-NMMA was due to greater dilution of the inhibitor. However the second study excluded this possibility by showing that a lower dose of methacholine that caused approximately 50% of the blood

Table 1 Effect of N^G-monomethyl-L-arginine (L-NMMA) or saline on vasodilatator responses to acetylcholine (ACh) and methacholine (MCh)

	Forearm bloodflow (ml min^{-1} 100 ml^{-1})				
Study day†	*Baseline*	*Agonist*	*Agonist with saline/L-NMMA*	*%change with saline/L-NMMA*	
ACh(83)/saline	3.8 ± 0.5	12.9 ± 1.7	10.7 ± 1.2	−9 ± 17	**
ACh(83)/L-NMMA(4)	3.3 ± 0.5	13.3 ± 1.7	7.3 ± 1.6	−58 ± 12	**
MCh(15)/saline	4.0 ± 1.2	14.8 ± 3.0	13.1 ± 2.7	−16 ± 9	NS
MCh(15)/ L-NMMA(4)	3.2 ± 0.4	17.0 ± 1.9	15.0 ± 1.7	−13 ± 6	NS
MCh(1.5)/saline	2.1 ± 0.4	6.4 ± 0.9	5.2 ± 0.7	−25 ± 6	NS
MCh(1.5)/ LNMMA(4)	2.5 ± 0.4	5.9 ± 0.9	5.0 ± 0.8	−23 ± 12	NS
MCh(1.5)/saline	2.2 ± 0.3	6.4 ± 0.7	5.1 ± 0.7	−20 ± 7	NS
MCh(1.5)/ L-NMMA(8)	2.1 ± 0.4	5.5 ± 0.7	4.4 ± 0.6	−29 ± 13	NS

** $P<0.0.1$, NS = not significant.
† Agonist dose in nmol min^{-1}; L-NMMA dose in μmol min^{-1}.

flow response to acetylcholine was also uninhibited by L-NMMA (4 μmol min^{-1}). It was possible that a higher dose of L-NMMA would have inhibited the response to methacholine, but in the third series of experiments doubling the dose of L-NMMA did not significantly inhibit the vasodilator response to methacholine (1.5 nmol min^{-1}).

There are several possible explanations for the differential effect of L-NMMA on acetylcholine and methacholine. Muscarinic receptor subtypes initiating vascular relaxation to acetylcholine *in vitro* are complex (Rubanyi *et al.*, 1986; Nield *et al.*, 1990; Jaiswal *et al.*, 1991), and differential inhibition of different agonists by L-NMMA could result from actions on receptor subtypes linked with more than one effector mechanism, not all of which involve the L-arginine/NO pathway. Endothelium-dependent relaxations resistant to NO synthase inhibitors are well recognised (Nagao *et al.*, 1992; Nagao & Vanhoutte 1992) and are thought to result from endothelium-derived hyperpolarizing factor (Chen *et al.*, 1988; Feletou & Vanhoutte, 1988). Endothelium-independent relaxation may be due to activation of muscarinic receptors on vascular smooth muscle (Brayden & Bevan, 1985; Nield *et al.*, 1990; Jaiswal *et al.*, 1991). Vasoconstriction is also mediated by muscarinic receptors on smooth muscle (Furchgott & Zawadski, 1980; Jaiswal *et al.*, 1991) and therefore muscarinic receptor subtypes are linked to opposing vasodilator and constrictor pathways. Inhibition of noradrenaline release from nerves and release of prostacyclin from the endothelium have been excluded as important mechanisms of vasodilatation in this preparation for both acetylcholine (Linder *et al.*, 1990) and methacholine (Creager *et al.*, 1990).

Different mechanisms of vasodilatation by acetylcholine and methacholine may result from the metabolic instability of acetylcholine (Duff *et al.*, 1952) influencing the site of action of the agonist. Destruction of acetylcholine by cholinesterase at the interface between circulating blood and vessel wall or within the vessel wall might favour actions of arterially administered acetylcholine initiated by receptors on the luminal surface of the endothelium and linked with the L-arginine/NO pathway, while preventing access to receptors on the abluminal endothelial cell surface or on nerve endings or vascular smooth muscle. Methacholine is less susceptible to enzymic inactivation than is acetylcholine, so more of its effect might be mediated by actions deep to the luminal surface of the endothelium. There is evidence that sensitivity to inhibitors of the L-arginine/NO pathway varies with size of resistance vessel (Nagao *et al.*, 1992). The instability of acetylcholine in blood might result in a greater fraction of the vasodilator response to acetylcholine being mediated through relatively proximal resistance arteries more sensitive to inhibition by L-NMMA.

Irrespective of the explanation placed on the selective inhibition of acetylcholine by L-NMMA demonstrated in this study, the lack of effect of L-NMMA on responses to methacholine has important implications for the interpretation of studies that have used this agonist as a putative probe of endothelial function in this preparation (Creager *et al.*, 1990; 1992; Liao *et al.*, 1991). The present findings suggest that the vasodilator effect of methacholine in human forearm vasculature is mediated mainly through mechanisms other than the L-arginine/NO pathway.

This work was supported by the British Heart Foundation.

References

BRAYDEN, J.E. & BEVAN, J.A. (1985). Neurogenic muscarinic vasodilatation in the cat. An example of endothelial cell-independent cholinergic relaxation. *Circ. Res.*, **56**, 205–211.

CHEN, G., SUZUKI, H. & WESTON, A.H. (1988). Acetylcholine releases endothelium-dependent hyperpolarizing factor and EDRF from rat blood vessels. *Br. J. Pharmacol.*, **95**, 1165–1174.

CHOWIENCZYCK, P.J., COCKCROFT, J.R. & RITTER, J.M. (1993). Responses to brachial artery administration of acetylcholine depend on forearm length in man. *Br. J. Clin. Pharmacol.*, **35**, 542P.

CHOWIENCZYCK, P.J., WATTS, G.F., COCKCROFT, J.R. & RITTER, J.M. (1992). Impaired endothelium-dependent vasodilatation of forearm resistance vessels in hypercholesterolaemia. *Lancet*, **340**, 1430–1432.

CREAGER, M.A., COOKE, J.P., MENDELSOHN, M.E., GALLAGHER. S.J., COLEMAN, S.M., LOSCALZO, J. & DZAU, V.J. (1990). Impaired vasodilatation of forearm resistance vessels in hypercholesterolaemic humans. *J. Clin. Invest.*, **86**, 228–234.

CREAGER, M.A., GALLAGHER, S.J., GIRED, X.J., COLEMAN, S.M., DZAU, V.J. & COOKE, J.P. (1992). L-Arginine improves endothelium-dependent vasodilatation in hypercholesterolaemic humans. *J. Clin Invest.*, **90**, 1248–1254.

DAUPHIN, F. & HAMEL, E. (1991). Identification of multiple muscarinic binding site subtypes in cat and human cerebral vasculature. *J. Pharmacol. Exp. Ther.*, **260**, 660–667.

DUFF, F., GREENFIELD, A.D.M., SHEPERD, J.T. & THOMPSON, I.D. (1952). A quantitative study of the response to acetylcholine and histamine of the blood vessels of the human hand and forearm. *J. Physiol.*, **120**, 160–170.

FELETOU, M. & VANHOUTTE, P.M. (1988). Endothelium-dependent hyperpolarization of canine coronary smooth muscle. *Br. J. Pharmacol.*, **93**, 515–524.

FURCHGOTT, R.F., JOTHIANANDAN, D. & FREAY, A.D. (1990). Endothelium-derived relaxing factor: some old and new findings. In *Nitric Oxide from L-Arginine: a Bioregulatory System.* ed. Moncada, S. & Higgs, E.A. pp. 12–14. New York: Elsevier.

FURCHGOTT, R.F. & ZAWADZKI, J.V. (1980). The obligatory role of endothelial cells in the relaxation of arterial smooth muscle by acetylcholine. *Nature*, **288**, 373–376.

HOKANSON, D.E., SUMNER, D.S. & STRANDNESS D.E. Jr (1975) An electrically calibrated plethysmograph for direct measurement of limb blood flow. *IEEE Trans. Biomed. Eng.*, **22**, 25–29.

JAISWAL, N., LAMBRECHT, G., MUTSCHLER, E., TACKE, R. & MALIK, K.U. (1991). Pharmacological characterization of the vascular muscarinic receptors mediating relaxation and contraction in rabbit aorta. *J. Pharmacol. Exp Ther.*, **258**, 842–850.

LIAO, J.K., BETTMAN, M.A., SANDOR, T., TUCKER, J.I., COLEMAN, S.M. & CREAGER, M.A. (1991). Differential impairment of vasodilator responsiveness of peripheral resistance and conduit vessels in humans with atherosclerosis. *Circ. Res.*, **68**, 1027–1034.

LINDER, L., KIOWSKI, W., BÜHLER, F.R. & LÜSCHER, T.F. (1990). Indirect evidence for release of endothelium derived relaxing factor in human forearm circulation in vivo. Blunted response in hypertension. *Circulation*, **81**, 1726–1767.

NAGAO, T., ILLIANO, S. & VANHOUTTE, P.M. (1992). Heterogeneous distribution of endothelium-dependent relaxations resistant to N^G-nitro-L-arginine in rats. *Am. J. Physiol.*, **263**, H1090–H1094.

NAGAO, T. & VANHOUTTE, P.M. (1992). Hyperpolarization as a mechanism for endothelium-dependent relaxations in the porcine coronary artery. *J. Physiol.*, **445**, 355–367.

NIELD, T.O., SHEN, K.Z. & SURPRENANT, A. (1990). Vasodilatation of arterioles by acetylcholine released from single neurones in the guinea pig submucosal plexus. *J. Physiol.*, **420**, 247–265.

ROBINSON, B.F. (1990). Assessment of responses to drugs in forearm resistance vessels and hand veins of man: Techniques and problems. In *Dose-Response Relationship of Drugs.* ed. Kuhlmann, J. & Wingender, W. pp. 40–43. München: W. Zuckschwerdt.

RUBANYI, G.M., MCKINNEY, M. & VANHOUTTE, P.M. (1986). Biphasic release of endothelium-derived relaxing factor(s) by acetylcholine from perfused canine femoral arteries. Characterisation of muscarinic receptors. *J. Pharmacol. Exp. Ther.*, **240**, 802–808.

VALLANCE, P., COLLIER, J. & MONCADA, S. (1989). Effects of endothelium-derived nitric oxide on peripheral arteriolar tone in man. *Lancet*, **ii**, 997–1000.

WHITNEY, R.J. (1953). The measurement of volume changes in human limbs. *J. Physiol.*, **121**, 1–27.

(Received June 1, 1993
Accepted June 10, 1993)

Br. J. Pharmacol. (1993), **110**, 739–746

Pulmonary effects of endogenous and exogenous nitric oxide in the pig: relation to cigarette smoke inhalation

[1]K. Alving, C. Fornhem & J.M. Lundberg

Department of Pharmacology, Karolinska Institute, S-17177, Stockholm, Sweden

1 Pentobarbitone-anaesthetized pigs were challenged with cigarette smoke (unfiltered or filtered through a Cambridge glass fibre filter to remove the particulate phase including nicotine), as well as nicotine aerosol and the gas phase components nitric oxide (NO) and carbon monoxide (CO); the effects on the bronchial and pulmonary circulations, and pulmonary airway mechanics, were examined. The relative importance of endogenous NO mechanisms in the pig lung was also studied by giving the NO synthesis inhibitor N^G-nitro-L-arginine (L-NOARG; 50 mg kg^{-1}) intravenously. Mean arterial pressure and blood flow in the bronchial, pulmonary and femoral circulations were measured, the latter with ultrasonic flow probes around the supplying arteries, and vascular resistance (VR) was calculated. Changes in pulmonary airways resistance (R_{pulm}) and lung dynamic compliance (C_{dyn}) were also determined. Finally, the concentration of NO in inhaled air during cigarette smoke and NO gas challenges was continuously monitored by a chemiluminescence method and the relative contribution of NO in cigarette smoke-induced vascular effects in the pig lung was calculated.

2 Cigarette smoke challenge, with or without a Cambridge filter, caused a rapid vasodilator response in the bronchial circulation and the major part (75%) of this response was probably caused by NO present in smoke. NO challenge caused profound bronchial vasodilatation with dose-response characteristics between 10 and 100 p.p.m. The small part of the cigarette smoke-induced response not explained by the NO content may be caused by CO, showing weak vasodilator effect in the bronchial circulation. The L-NOARG-induced relative increase in bronchial VR was 2–3 times higher than the changes in pulmonary, femoral and systemic VR, suggesting a strong influence of endothelial NO mechanisms on basal tone in the bronchial circulation.

3 Challenge with unfiltered cigarette smoke induced variable responses in the pulmonary circulation, whereas inhalation of filtered smoke caused consistent pulmonary vasodilatation. The major part of this vasodilator response was probably caused by NO, which was a potent dilator of the pulmonary circulation with maximal effect achieved with as little as 10 p.p.m. The effect of NO may be opposed in unfiltered smoke by the particulate phase (but not nicotine), presumably by inducing sympathetic reflexes. L-NOARG caused similar relative increases in pulmonary, femoral and systemic VR.

4 Cigarette smoke inhalation induced bronchodilatation in the pentobarbitone-anaesthetized pig as revealed by changes in R_{pulm} and C_{dyn}. Both NO and nicotine may contribute to this response. NO inhalation reduced R_{pulm} in the basal state with maximal effect at 30 p.p.m. The mechanism for NO-induced bronchodilatation may be indirect in the pig, since pretreatment with L-NOARG blocked the response. L-NOARG did not affect basal R_{pulm}.

5 In conclusion, bronchial vasodilatation caused by continuous cigarette smoke inhalation in the pig, seems to be largely mediated (approximately 75%) by NO. The remaining part could be mediated by CO. Cigarette smoke particles, but not nicotine, may counteract NO-induced relaxation in the pulmonary circulation, thus resulting in variable effects in the pulmonary circulation during challenge with unfiltered cigarette smoke. NO also acts as a bronchodilator in the pig, but the mechanism may be indirect. Finally, endogenous NO mechanisms appear to be strongly involved in the control of basal tone in the bronchial circulation, less so in the pulmonary circulation and not at all in bronchial smooth muscle.

Keywords: Cigarette smoke; nitric oxide; bronchial circulation; pulmonary circulation; vasodilatation; nicotine; carbon monoxide; nitrogen dioxide; bronchodilatation

Introduction

Since the finding that nitric oxide (NO) is identical with endothelium-derived relaxing factor (Ignarro *et al.*, 1987; Palmer *et al.*, 1987), the interest in NO as an endogenous modulator of vascular tone has evolved, mostly thanks to the development of inhibitors of the L-arginine pathway (see Moncada *et al.*, 1991). It has also been postulated that NO is a non-adrenergic, non-cholinergic relaxatory transmitter in the tracheal smooth muscle (Tucker *et al.*, 1990). Furthermore, NO synthase has been shown to be present together with vasoactive intestinal polypeptide (VIP) in parasympathetic perivascular nerves (Kummer *et al.*, 1992; Ceccatelli *et al.*, 1993). However, the precise role of NO in the control of airway smooth muscle tone remains unclear (see Jansen *et al.*, 1992). Besides the endogenous production of NO, this compound can also be found in high amounts in cigarette smoke (Norman & Keith, 1965). We have previously shown that cigarette smoke challenge in the lower airways of the pig caused a marked vasodilator response in the bronchial circulation, a response that did not seem to involve neuronal activation, mast cell degranulation or prostaglandin release (Matran *et al.*, 1990). Interestingly, both cigarette smoke and NO have been shown to increase the levels of guanosine 3′:5′-cyclic monophosphate (cyclic GMP), the second messenger for NO, in lung tissue (Arnold *et al.*, 1977), and cigarette smoke has been shown to relax the pulmonary circulation of the pig isolated lung (Gilman *et al.*, 1981). Although inhalation of NO can cause relaxation of the hypertensive pul-

[1] Author for correspondence.

monary circulation in the rat isolated lung (Archer *et al.*, 1990) as well as in the intact sheep (Frostell *et al.*, 1991), pig (Weitzberg *et al.*, 1991) and man (Frostell *et al.*, 1993), cigarette smoke inhalation does not seem to reduce pulmonary artery pressure in patients with pulmonary hypertension (Richards *et al.*, 1990). We have recently shown that bronchial blood flow changes induced by intermittent cigarette smoke challenge correlated with NO levels in the smoke and that only cigarette smoke free from particles and nicotine (vapour phase) relaxed the pulmonary circulation in the pig *in vivo* (Alving *et al.*, 1992). In this study we have examined the vasodilator effects of cigarette smoke administered continuously in concentrations more relevant to normal smoking and the relative contribution to these responses of NO and carbon monoxide (CO). We have also studied the effects of nicotine to evaluate the importance of nicotine versus particles in counteracting the gas phase-induced pulmonary vasodilatation. Furthermore, the effect of cigarette smoke and the above mentioned smoke constituents on lower airway calibre was examined. Finally, the importance of endogenous NO production in the control of smooth muscle tone in the bronchial and pulmonary circulations, as well as in the lower airways, was evaluated by using a potent and stereospecific inhibitor of endothelial NO synthesis (N^G-nitro-L-arginine; L-NOARG) (Mülsch & Busse, 1990).

Methods

The experiments were approved by the Local Ethical Committee for animal research.

Surgical preparation

Twenty-eight domestic pigs of either sex (12 weeks old, 20–25 kg body weight) were fasted overnight and premedicated with ketamine hydrochloride (20 mg kg^{-1}, i.m.). Anaesthesia was induced with sodium pentobarbitone (16 mg kg^{-1}) introduced into an ear vein; the adequacy of anaesthesia was tested by pinching the interdigital skin, and skeletal muscle relaxation was achieved with pancuronium bromide (0.2 mg kg^{-1}). Anaesthesia was thereafter checked by continuous measurement of heart rate and arterial blood pressure and by intermittent pinching of the interdigital skin during intermission of pancuronium bromide delivery. After a low tracheostomy the pigs were intubated and ventilated with a mixture of air and oxygen using an Engström respirator. A catheter was put into the caval vein via a femoral vein and used for continuous infusion of pentobarbitone (10 mg kg^{-1} h^{-1}), pancuronium (0.6 mg kg^{-1} h^{-1}), Ringer solution with glucose (250 ml h^{-1}) and for intravenous (i.v.) challenges. A Swan-Ganz thermodilution catheter was put into the pulmonary artery through the other femoral vein for measurements of pulmonary artery pressure (PAP), pulmonary capillary wedge pressure and central venous pressure; heparin (7500 iu) was given as a bolus by this catheter. A femoral artery was cannulated for continuous recordings of mean arterial pressure (MAP) and heart rate (HR). Arterial blood gas partial pressures and pH were regularly monitored with an automatic blood gas analyser (IL 1302, Metric AB, Solna, Sweden) to ensure a Po_2 of 11–14 kPa, a Pco_2 of 4.5–5.5 kPa and a pH of 7.4–7.5. Arterial glucose levels and haematocrit were determined at the beginning and the end of the experiments and were found to be maintained within normal values. Body temperature was maintained at 38–39°C with a heating pad connected to a thermostat. In some groups of animals a left side thoracotomy was done and the pericardium was opened, an ultrasonic flow probe was placed around the pulmonary artery and connected to an ultrasonic blood flow meter (T202S, Transonic System Inc., Ithaca, NY, U.S.A.) for continuous recording of absolute blood flow (cardiac output). After a right side thoracotomy the bronchial artery, which supplies the tracheobronchial tree from the lower trachea down to the peripheral bronchioles, was dissected free and a flow probe was placed around the vessel. A femoral artery was also exposed and a flow probe was placed around the vessel. The tracheal pressure was measured by connecting an outlet of the tracheal tube to a Statham PM 131 TC pressure transducer and was used as a measure of transpulmonary pressure since the intrapleural pressure was equal to atmospheric pressure due to the thoracotomy. Airflow was measured with a heated Fleisch pneumotachograph no. 1 connected to a Statham PM 15 E pressure transducer and airflow and transpulmonary pressure signals were sent to an E80 T pulmonary computer (Processdata AB, Uppsala, Sweden) for on-line calculations of pulmonary resistance (R_{pulm}) and dynamic lung compliance (C_{dyn}). All the cardiovascular and pulmonary parameters were continuously recorded on Grass polygraphs and simultaneously collected on an Apple Macintosh data acquisition system for analyses and graphical presentation.

Experimental procedure

An aerosol of nicotine bitartrate (2.5 mg) dissolved in 2 ml saline was generated using an ultrasonic nebulizer (NB 108, Engström Medical, Stockholm, Sweden) and delivered over 2.5 min to the lungs. Nicotine (100 μg kg^{-1}) was given as a bolus i.v. injection. The lower airways were also challenged with cigarette smoke from a Kentucky 2R1 research cigarette containing 2.5 mg nicotine (Diana & Vaught, 1990) delivered over 2.5 min, using a Walton Horizontal Smoking Machine (Guerin *et al.*, 1979) connected to the respirator. Smoke challenges were done with or without a Cambridge CM-113 glass fibre filter that removes particulate matter and nicotine from the cigarette smoke (Wartman *et al.*, 1959). Furthermore, pigs were challenged with NO (300 p.p.m. in nitrogen), CO (300 p.p.m. in nitrogen) and nitrogen dioxide (NO_2; 200 p.p.m. in nitrogen) over 2.5 min administered via the respirator to give final calculated concentrations of 10, 30 and 100 p.p.m. The ganglionic blocking agent chlorisondamine (3 mg kg^{-1}, i.v.) was given 20 min before challenges. The inhibitor of NO synthesis N^G-nitro-L-arginine (L-NOARG) was dissolved in warm saline and infused over 2 min (50 mg kg^{-1}, i.v.) followed by a constant infusion of 50 mg kg^{-1} h^{-1} that continued until challenges were ended (2 h). Haemoglobin was dissolved in saline and infused i.v. over 10 min ($\leqslant$ 10 mg kg^{-1}) or given as an aerosol (100 mg) to the lower airways. Methylene blue was dissolved in saline and infused i.v. over 10 min ($\leqslant$ 40 mg kg^{-1}). The concentration of inhaled NO and NO_2 was continuously monitored, by a chemiluminescence method (CLD 700 AL NO/NOx analyser, Eco Physics, Basel, Switzerland; see Fontijn *et al.*, 1970), during challenge with filtered cigarette smoke and NO by sampling at a site close to the endotracheal tube.

The animals were divided into groups according to Table 1. Challenges were repeated before and after treatment with chlorisondamine or L-NOARG.

Calculations

Blood flow was recorded in ml min^{-1} (cardiac output in l min^{-1}) and vascular resistance (VR) in the bronchial and femoral circulations was defined as MAP minus central venous pressure divided by local blood flow. Pulmonary VR was defined as PAP minus pulmonary capillary wedge pressure divided by cardiac output and systemic VR as MAP minus central venous pressure divided by cardiac output. Results for VR and pulmonary mechanics are expressed as peak relative changes (percentage) compared to baseline. For MAP, HR, cardiac output and PAP absolute changes are given. Data are presented as mean ± s.e.mean. The Wilcoxon signed rank test for non-parametric comparisons was used for statistical analyses.

Table 1 A summary of the different groups of pigs used in the study

n	*Treatment*	*Challenge*	*Cardiac output*
6	Chlorisondamine	Smoke ± filter	No
5	-	Nicotine	No
8	L-NOARG	Smoke + filter, NO, CO	Yes
4	Hb ($n = 2$), MB ($n = 2$)	NO, NO_2	Yes
5	(NO measurements)	Smoke + filter, NO	No

Cardiac output was measured in some of the protocols as indicated.
Hb = haemoglobin, MB = methylene blue.

Drugs

Ketamine hydrochloride (Parke Davis, Barcelona, Spain), sodium pentobarbitone (NordVacc, Stockholm, Sweden), pancuronium bromide (Organon, Oss, The Netherlands), nicotine bitartrate (Swedish Tobacco Company, Stockholm, Sweden), NO, CO and NO_2 in nitrogen (AGA, Stockholm, Sweden), chlorisondamine (Ciba-Geigy, Basel, Switzerland), methylene blue (Sigma, St. Louis, Mo., U.S.A.), bovine haemoglobin (Sigma) and L-NOARG (Sigma) were obtained as indicated.

Results

Effects of cigarette smoke and nicotine

Continuous exposure of the lungs to unfiltered smoke from one cigarette over 2.5 min resulted in a marked increase in bronchial blood flow with a calculated decrease in bronchial vascular resistance (VR), suggesting a vasodilator response in the bronchial circulation (Figure 1). Pretreatment with the ganglionic blocker, chlorisondamine (3 mg kg^{-1}, i.v.) resulted *per se* in reduced MAP and HR by 23% and 27%, respectively, and a slight reduction (< 15%) of pulmonary VR and R_{pulm} was also noted. Bronchial VR and C_{dyn} were not significantly changed by chlorisondamine. This dose of chlorisondamine abolished the responses to nicotine given i.v. ($\leqslant 250\ \mu g\ kg^{-1}$). Pretreatment with chlorisondamine or the insertion of a Cambridge filter did not change the response to cigarette smoke in the bronchial circulation (Figure 1). Unfiltered smoke did not consistently relax the pulmonary circulation as revealed by changes in PAP (Figure 2a). However, filtered smoke induced a consistent decrease in PAP. Nicotine aerosol (2.5 mg) delivered over 2.5 min also caused a slight relaxation of the pulmonary circulation (Figure 3), but the responses to smoke were not significantly changed by pretreatment with the ganglionic nicotine receptor antagonist, chlorisondamine (Figure 2a). Exposure of the lungs to unfiltered smoke caused an increase in MAP and this response was reduced by chlorisondamine pretreatment and almost totally blocked by a Cambridge filter (Figure 2b). Nicotine aerosol slightly lowered MAP (Figure 3). Cigarette smoke or nicotine aerosol did not induce any consistent changes in HR. Unfiltered smoke administered to the lower airways produced a clear-cut bronchodilator response as revealed by a decrease in R_{pulm} and increase in C_{dyn} (Figure 4). The bronchial response was reduced, but not abolished, by insertion of a Cambridge filter, but was not affected by chlorisondamine. Nicotine aerosol also induced a small reduction of R_{pulm}, but inconsistent changes in C_{dyn} (Figure 3). If nicotine was given as a bolus i.v. injection (100 $\mu g\ kg^{-1}$), an increase in PAP, MAP and R_{pulm}, and a decrease in C_{dyn} was noted instead (Figure 3). Nicotine did not produce any clear-cut effects on the bronchial VR by either route of administration.

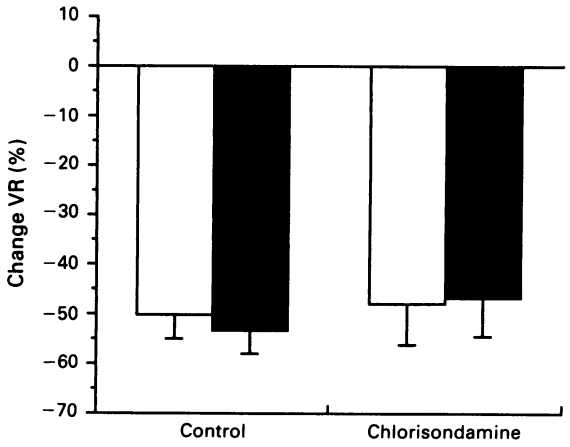

Figure 1 Maximal relative changes in bronchial VR after inhalation challenge over 2.5 min with smoke from one Kentucky 2R1 standard cigarette, without (open columns) and with (solid columns) a Cambridge filter, and before and after treatment with the ganglionic blocker chlorisondamine (3 mg kg^{-1}, i.v.). Data are presented as means with s.e.mean ($n = 6$). No significant difference was noted (Wilcoxon's signed rank test).

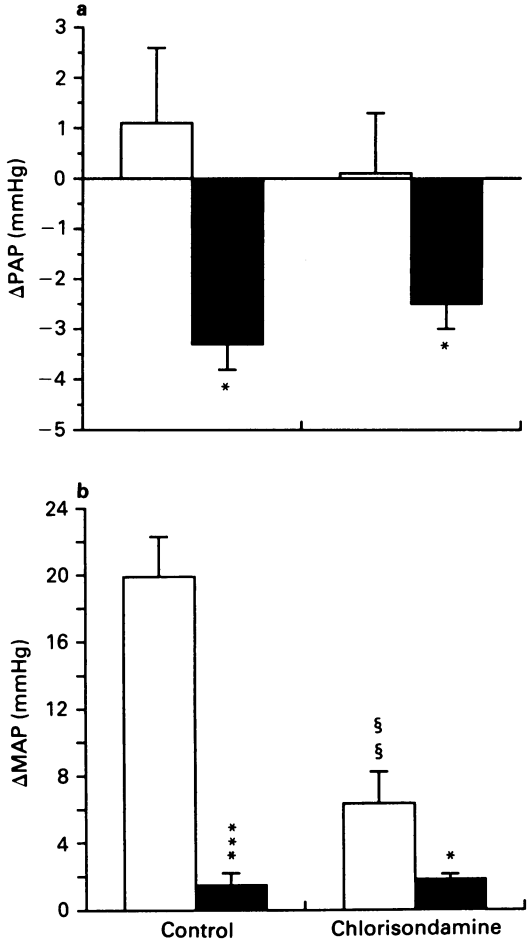

Figure 2 Maximal absolute changes in pulmonary artery pressure (PAP) (a) and mean arterial pressure (MAP) (b) after inhalation challenge over 2.5 min with smoke from one Kentucky 2R1 standard cigarette, without (open columns) and with (solid columns) a Cambridge filter, and before and after treatment with the ganglionic blocker, chlorisondamine (3 mg kg^{-1}, i.v.). Data are presented as means with s.e.mean ($n = 6$). $^{*}P < 0.05$, $^{***}P < 0.001$ compared to 'without filter' and §§$P < 0.01$ compared to control (Wilcoxon's signed rank test).

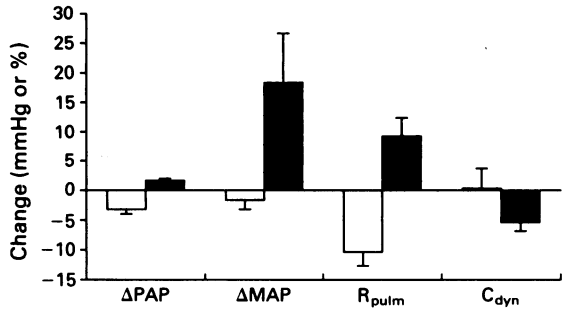

Figure 3 Maximal absolute (pulmonary artery pressure (PAP) and mean arterial pressure (MAP)) or relative (R_{pulm} and C_{dyn}) changes after inhalation challenge over 2.5 min with nicotine aerosol (2.5 mg; open columns) and after a bolus i.v. injection with nicotine (100 $\mu g\,kg^{-1}$, solid columns). Data are presented as means with s.e.mean ($n = 5$). Note the qualitative difference between administration routes.

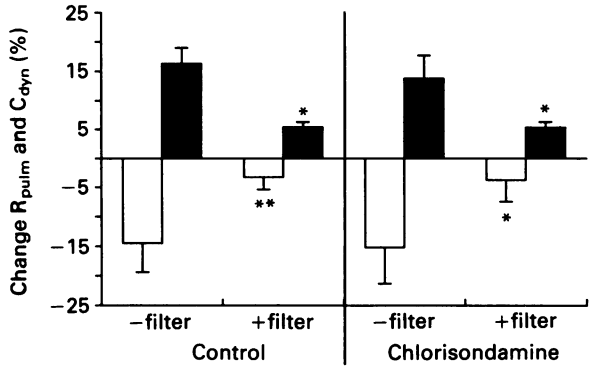

Figure 4 Maximal relative changes in R_{pulm} (open columns) and C_{dyn} (solid columns) after inhalation challenge over 2.5 min with smoke from one Kentucky 2R1 standard cigarette, without and with a Cambridge filter, and before and after treatment with the ganglionic blocker, chlorisondamine (3 $mg\,kg^{-1}$, i.v.). Data are presented as means with s.e.mean ($n = 6$). $^*P<0.05$, $^{**}P<0.01$ compared to 'without filter'(Wilcoxon's signed rank test).

Effects of NO, CO and NO_2

Administration of NO over 2.5 min at calculated final concentrations of 10, 30 and 100 p.p.m. caused vasodilator responses in the bronchial circulation in a dose-related fashion (Figure 5). A small vasodilator response to NO was also seen in the pulmonary circulation, with maximum relaxation achieved at 10 p.p.m. (Figure 5). Inhalation of NO (up to 100 p.p.m.) did not induce any systemic cardiovascular effects in the pig. A bronchodilator response, with a decrease in R_{pulm} and an increase in C_{dyn}, was also noted after challenge with NO with maximal responses at 30 p.p.m. ($-17.2 \pm 5.8\%$ for R_{pulm} and $+5.6 \pm 0.9\%$ for C_{dyn}), showing no further increase in the response at 100 p.p.m. (Figure 6). The vasodilator response in the bronchial circulation could not be altered by pretreatment with haemoglobin ($\leqslant 10\ mg\,kg^{-1}$, i.v. and 100 mg aerosol, $n = 2$) or methylene blue ($\leqslant 40\ mg\,kg^{-1}$, i.v., $n = 2$). At the higher i.v. doses of haemoglobin or methylene blue, profound systemic cardiovascular effects with fall in MAP was noted, thus making further increases in the doses impossible.

Administration of CO to the lungs induced a small vasodilator response in the bronchial circulation at 100 p.p.m. (Figure 7), but not at lower concentrations (10–30 p.p.m.). In contrast, in the pulmonary circulation a vasoconstrictor response was noted at 100 p.p.m. (Figure 7). CO did not induce any major systemic cardiovascular effects acutely and did not affect R_{pulm} or C_{dyn}.

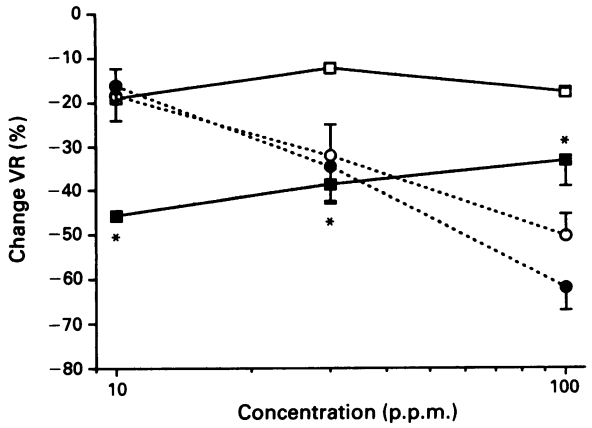

Figure 5 Maximal relative changes in bronchial VR (●,○) and pulmonary VR (■,□) after inhalation challenge over 2.5 min with NO (10, 30 and 100 p.p.m.) before (○,□) and after (●,■) treatment with the NO synthase inhibitor N^G-nitro-L-arginine (50 mg kg^{-1}, i.v.). Data are presented as means with s.e.mean ($n = 8$). $^*P<0.05$ compared to control (Wilcoxon's signed rank test).

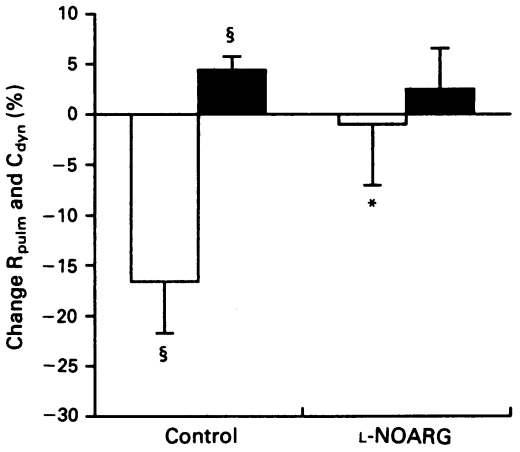

Figure 6 Maximal relative changes in R_{pulm} (open columns) and C_{dyn} (solid columns) after inhalation challenge over 2.5 min with NO (100 p.p.m.) before and after treatment with the NO synthase inhibitor N^G-nitro-L-arginine (50 mg kg^{-1}, i.v.). Data are presented as means with s.e.mean ($n = 8$). $^*P<0.05$ compared to control and $\S P<0.05$ compared to baseline (Wilcoxon's signed rank test).

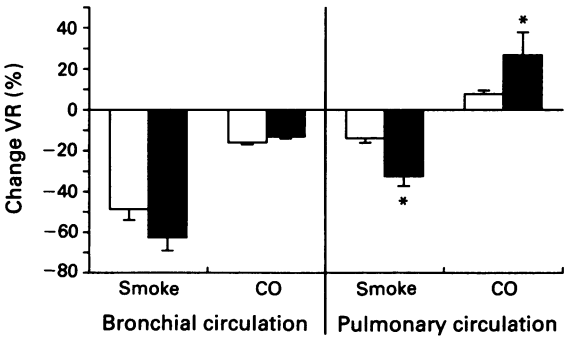

Figure 7 Maximal relative changes in bronchial and pulmonary vascular resistance (VR) after inhalation challenge over 2.5 min with smoke from one Kentucky 2R1 standard cigarette with a Cambridge filter, and CO (100 p.p.m.) before (open columns) and after (solid columns) treatment with the NO synthase inhibitor N^G-nitro-L-arginine (50 mg kg^{-1}, i.v.). Data are presented as means with s.e.mean ($n = 8$). $^*P<0.05$ compared to control (Wilcoxon's signed rank test).

Challenge with NO_2 caused vasodilator responses at 100 p.p.m. in the bronchial and pulmonary circulations, but at lower magnitudes compared to equal amounts of NO (<18% decrease in VR, $n = 4$). At lower doses NO_2 produced only minor vasodilator effects in the lung. At 100 p.p.m. NO_2 also caused systemic cardiovascular effects with increases in MAP (+34 ± 14 mmHg) and HR (+18 ± 6 beat min^{-1}), and variable effects on pulmonary airway mechanics.

Basal effects of the NO synthase inhibitor, L-NOARG

Intravenous infusion of 50 mg kg^{-1} L-NOARG over 5 min induced profound systemic cardiovascular effects peaking at about 5 min after completion of the loading dose (Table 2). MAP and PAP returned to somewhat lower levels at 10–15 min but were then maintained at elevated levels throughout the infusion period (50 mg kg^{-1} h^{-1} for 2 h). MAP and PAP were increased by more than 50%, concomitant with a slight bradycardia and a decrease in cardiac output (Table 2). There were no changes in central venous pressure or pulmonary capillary wedge pressure. The relative increase in pulmonary and femoral VR was close to the increase in systemic VR (Table 2). However, in the bronchial circulation, vasoconstrictor responses greatly exceeding the increase in systemic VR were noted. The vasoconstrictor effect in the bronchial circulation did not start to return to baseline within the observation period (2 h).

There was no significant change in R_{pulm} after infusion of L-NOARG but a reduction in C_{dyn} was noted (Table 2).

Influence of L-NOARG on the responses to NO, cigarette smoke and CO

The dose-response curve for the NO-induced vasodilator responses in the bronchial circulation was not significantly affected by pretreatment with L-NOARG (Figure 5). However, the relaxation response in the pulmonary circulation was markedly increased and maximal effect was achieved at 10 p.p.m. Similarly, the vasodilator response to filtered cigarette smoke in the bronchial circulation was not significantly changed by L-NOARG, but the response in the pulmonary circulation was increased (Figure 7). Interestingly, the constrictor response seen in the pulmonary circulation after challenge with 100 p.p.m. CO was increased after pretreatment with L-NOARG (Figure 7).

The bronchodilator response to NO in control animals, at least the fall in R_{pulm} was abolished after pretreatment with L-NOARG (Figure 6).

Measurements of NO in cigarette smoke

The concentration of NO in filtered cigarette smoke was continuously measured near the opening of the endotracheal tube during challenge, and simultaneous measurements of bronchial blood flow were done. Tracings of typical experiments are shown in Figure 8. The actual peak levels of NO as measured with the chemiluminescence method were 8.6 ± 0.5, 25.2 ± 0.4 and 82.7 ± 1.6 p.p.m. for NO 10, 30 and 100 p.p.m., respectively, i.e. about 85% of expected. The NO level during cigarette smoke challenge peaked at the time of finishing the cigarette at a concentration of 74.5 ± 13.3 p.p.m. The insertion of a Cambridge filter did not affect the NO levels in inhaled air. No NO_2 could be detected in cigarette smoke or in the NO gas. The blood flow in the bronchial circulation changed rapidly and showed a pattern very similar to the NO levels (Figure 8). Also, the fall in PAP coincided with the presence of high levels of NO. When the integrated areas under the curves for blood flow changes and NO levels during cigarette smoke and NO gas challenge were calculated, it was found that the ratio of total blood flow change divided by NO levels was somewhat higher for cigarette smoke (1.78 ± 0.70, $n = 5$) compared to NO gas (1.34 ± 0.20, $n = 5$; $P<0.05$ by Wilcoxon's signed rank). The ratio of blood flow changes divided by NO levels for NO gas challenge was thus about 75% of that for cigarette smoke challenge. A similar discrepancy was, however, not seen for dilator responses in the pulmonary circulation, when comparing challenges with NO gas and filtered cigarette smoke.

Table 2 Baseline values for cardiovascular parameters and airway mechanics, and maximal absolute (Δ) or relative (%) changes induced by N^G-nitro-L-arginine (L-NOARG) (50 mg kg^{-1}, i.v.)

Parameter	*Baseline*	*Change*
MAP (mmHg)	107 ± 5	+56 ± 4 (Δ)
PAP (mmHg)	20.6 ± 1.3	+ 13.6 ± 2.4 (Δ)
HR (beat min^{-1})	112 ± 5	− 11 ± 3 (Δ)
Cardiac output (l min^{-1})	1.47 ± 0.15	−0.37 ± 0.05 (Δ)
Systemic VR (mmHg l^{-1} min^{-1})	68.5 ± 7.6	+ 141 ± 7.2 (%)
Pulmonary VR (mmHg l^{-1} min^{-1})	13.0 ± 1.3	+ 122 ± 14.1 (%)
Femoral VR (mmHg ml^{-1} min^{-1})	2.0 ± 0.3	+ 110 ± 16.0 (%)
Bronchial VR (mmHg ml^{-1} min^{-1})	11.9 ± 1.5	+ 391 ± 62.2 (%)
R_{pulm} (cmH_2O l^{-1} min^{-1})	7.6 ± 0.7	− 2.6 ± 3.3 (%)
C_{dyn} (ml cmH_2O^{-1})	23.1 ± 1.7	− 7.2 ± 0.9 (%)

Data are presented as mean ± s.e.mean ($n = 8$). All changes, except for R_{pulm}, are statistically significant ($P<0.05$) by Wilcoxon's signed rank test.

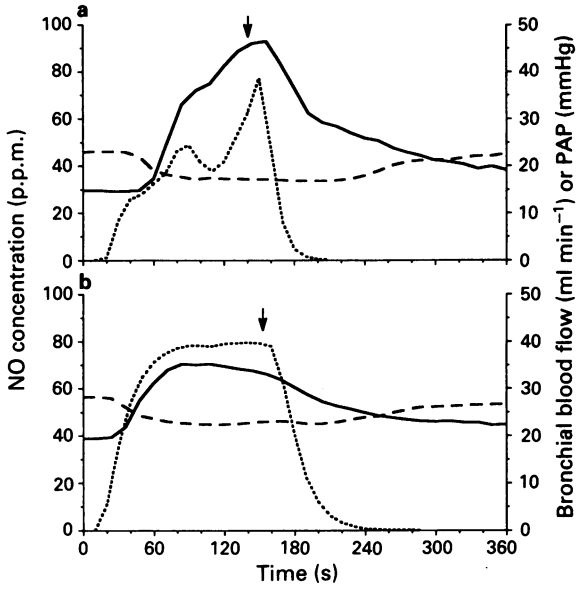

Figure 8 Typical changes in bronchial blood flow (solid line), pulmonary artery pressure (PAP) (broken line) and NO concentration in inhaled air (dotted line), during inhalation challenge with smoke from one Kentucky 2R1 standard cigarette (a) or pure NO (b). Measurements of bronchial blood flow and NO concentrations were made simultaneously in untreated pigs (calculations of area under the curve were made from these experiments, see text), whereas changes in PAP were measured from an elevated baseline in pigs treated with the NO synthase inhibitor N^Gnitro-L-arginine during identical challenge procedures. The arrows indicate the end of cigarette smoke generation and NO delivery, respectively.

Discussion

In this study we have examined the pulmonary effects of exogenous NO and the role of endogenously produced NO in the control of smooth muscle tone in the lung in relation to cigarette smoke-induced effects. Challenge with cigarette smoke in the lower airways, in concentrations relevant for

normal smoking in man (Norman & Keith, 1965), induced profound vasodilator changes in the pig bronchial circulation. This effect did not seem to be mediated by nicotine or the particulate phase and was apparently not dependent on a central reflex mechanism under our conditions of anaesthesia. Also, we have previously shown that the cigarette smoke-induced relaxation in the bronchial circulation is not dependent on activation of capsaicin-sensitive C-fibre afferents and subsequent local axon reflexes causing peptide release (Matran *et al.*, 1990). It therefore seemed likely that one or several gas phase components could be responsible for the observed effects, presumably by direct effects on the vessels. We have recently shown that the fluctuating blood flow response seen in the bronchial circulation during intermittent cigarette smoke challenge correlated significantly with the NO concentration (<20 p.p.m.) in the inhaled smoke (Alving *et al.*, 1992). This is consistent with the finding that cigarette smoke caused acute fluctuations in the cyclic GMP content of the dog isolated lung (Maron *et al.*, 1984). In this study we could show that administration of NO in concentrations ranging from 10 to 100 p.p.m. caused dose-related bronchial vasodilatation. Continuous burning of one cigarette over 2.5 min resulted in peak NO levels close to 100 p.p.m. in our system. Similar changes in bronchial blood flow were induced by equivalent doses of pure NO. Up to 10 fold higher concentrations of NO can be found in fresh puffs of cigarette smoke (Norman & Keith, 1965), indicating profound vasodilator effects on the bronchial vasculature during normal smoking. When comparing the total increase in bronchial blood flow (area under the curve) caused by cigarette smoke and NO, respectively, and the total increase in NO levels, it could be concluded that a major part of the cigarette smoke-induced vasodilator effect on the bronchial circulation is likely to be mediated by NO present in the smoke. Approximately 25% of the response may not be caused by NO, however, indicating that other vapour phase components also are involved. Administration of NO_2 induced vasodilatation in the bronchial circulation, at least at the highest dose (100 p.p.m.), but at this concentration profound systemic cardiovascular effects and bronchoconstrictor responses were noted. Since such effects were not seen during challenge with filtered smoke, and since no NO_2 was detected by chemiluminescence in smoke, NO_2 may not contribute to the bronchial vasodilator effects seen during cigarette smoke challenge. The absence of NO_2 in fresh cigarette smoke has been demonstrated also by others (Norman & Keith, 1965). CO, on the other hand, induced some bronchial vasodilatation without causing systemic changes or bronchoconstriction. Although the CO-induced effects were relatively small compared to NO at the same concentration, CO may still contribute to cigarette smoke-induced vasodilator effects in the bronchial circulation, since the content of CO is high in cigarette smoke (First, 1984). The mechanism for the CO-induced effects in the bronchial circulation remains unclear, especially since inhalation of CO caused a vasoconstrictor response in the pulmonary circulation of the pig. It has been suggested, that CO may cause direct activation of soluble guanylate cyclase (Marks *et al.*, 1991). It seems clear, at least, that CO is not a general vasodilator. We tried to block the vasodilator effects of exogenous NO by pretreatment with haemoglobin or methylene blue, which would capture NO or inhibit guanylate cyclase, respectively, but doses high enough to block the effects of the high concentration of NO found in cigarette smoke could not be given to the animals. Furthermore, these pretreatment procedures would not distinguish between NO and CO.

Besides the very potent effects of exogenous NO on the bronchial circulation, the endogenous control of bronchial blood flow involving L-arginine pathways, and thus NO production, seemed to be relatively strong in this vascular bed compared to other organs. The effect of an NO-synthesis inhibitor in human vessels of the hand *in vivo* has been reported to consist of mainly arteriolar constriction, without any marked effects on the venous side (Vallance *et al.*, 1989). In the pig *in vivo* a similar picture was noted since central venous pressure was largely unchanged by the NO-synthesis inhibitor L-NOARG. In addition to the discrimination between the arterial and venous side of both the systemic and pulmonary circulations, we also found marked variations in the effect of L-NOARG on resistance vessels in different vascular beds, with the bronchial circulation being the most sensitive of the vascular beds examined. Interestingly, vagal control of the pig bronchial circulation has been shown to be primarily of sensory origin, without any parasympathetic influence (Matran *et al.*, 1989b), in contrast to the pulmonary circulation (Matran *et al.*, 1991) and many other vascular beds. Furthermore, the sensory neuropeptide, substance P, which induces vasodilatation mainly by endothelium-dependent mechanisms (Furchgott, 1984), was found to be a very potent dilator of the bronchial circulation in the pig (Matran *et al.*, 1989a). The importance of NO mechanisms in vagally-induced vasodilatation in the bronchial circulation remains to be studied. It is possible that the bronchial circulation is mainly under local control involving the endothelium and sensory nerves, since total pharmacological blockade of autonomic innervation did not change basal VR in the bronchial circulation of the pig (Matran *et al.*, 1993).

Challenge with unfiltered cigarette smoke caused variable responses in the pig pulmonary circulation *in vivo*, in spite of a slightly elevated PAP (from 16 to 20 mmHg) in this open-chest preparation. This is consistent with findings in awake human subjects, where cigarette smoking did not reduce PAP, either in normal individuals (Goldbarg *et al.*, 1971) or in patients with pulmonary hypertension (Richards *et al.*, 1990), although pure NO relaxes the preconstricted pulmonary circulation at as little as 10 p.p.m. in human volunteers (Frostell *et al.*, 1993) as well as in the pig (present results). Alternatively, an increase in cardiac output could result in unaltered PAP in spite of a vasodilator response in the pulmonary circulation. However, PAP tended to increase during inhalation of unfiltered cigarette smoke both in awake human subjects (Goldbarg *et al.*, 1971; Richards *et al.*, 1990) and in the anaesthetized pig. Recently, we showed that filtration of cigarette smoke through a Cambridge filter resulted in consistent relaxant responses in the pig pulmonary circulation, which indicated that the particulate phase or nicotine mediates counteracting vasoconstrictor responses, masking NO-induced relaxation (Alving *et al.*, 1992). In the present study, the combined findings that chlorisondamine did not unveil cigarette smoke-induced relaxation, and that challenge with nicotine aerosol reduced the PAP, speaks against nicotine as the counteracting constrictor agent. Most studies on the cardiovascular actions of nicotine have dealt with intravascular administration of nicotine, where cardiac activation and vasoconstriction in the pulmonary circulation have been noted (Larson *et al.*, 1965; Samanék & Aviado, 1966). If nicotine was given i.v. to the pig, in a dose close to the total amount found in the smoke from one cigarette, increases in MAP, PAP (present results), and HR (Alving & Franco-Cereceda, 1993) were noted, in contrast to responses seen after aerosol administration. This indicates that different mechanisms were activated by nicotine, causing opposite cardiovascular effects, depending on the route of administration. The bronchial circulation, however, was not significantly affected by either route of administration (Alving & Franco-Cereceda, 1993; present data). It should be stressed that the absorption into the systemic circulation of nicotine in cigarette smoke (free base) and aqueous solution (salt) may be different in that the particle-bound free base may be more easily absorbed than the water solution. This would result in more restricted local effects of nicotine when given as an aerosol challenge compared with cigarette smoke, since the latter may induce both local and systemic effects (Aviado & Samanék, 1965). Another explanation could be that the counteracting pressor effect in the pulmonary circulation was mediated by the particulate phase causing central sym-

pathetic reflexes, which would constrict the pig pulmonary circulation (Matran, 1991). The latter was also supported by the fact that unfiltered cigarette smoke caused consistent pulmonary vasodilatation in the pig isolated lung, where such reflexes would be absent (Gilman *et al.*, 1981).

Cigarette smoke challenge also induced clear-cut bronchodilatation in the anaesthetized pig. This is in contrast to effects in awake human subjects where a bronchoconstrictor response independent of nicotine has been reported (Nadel & Comroe, 1961). It has been suggested that this bronchoconstriction is caused by inert particles in the smoke (Widdicombe *et al.*, 1962), inducing vagal cholinergic reflexes (Sterling, 1967). Similarly, inhalation of an irritant compound, capsaicin, evoked a bronchoconstrictor response in man that was found to be due to a cholinergic reflex mechanism (Fuller *et al.*, 1985). In the pentobarbitone-anaesthetized pig, however, bronchoconstrictor responses to capsaicin aerosol could not be elicited (Alving *et al.*, 1991), in spite of a clear-cut vagal cholinergic control of bronchial tone in the pig (Matran *et al.*, 1991). It may be suggested that central parasympathetic reflexes are supressed by the pentobarbitone anaesthesia (see Adams *et al.*, 1987), or alternatively, that the bronchoconstrictor response is dependent on laryngeal stimulation (Nadel & Widdicombe, 1962), which could not occur in the tracheostomized pig. In the pig, airway sympathetic nerve stimulation does not seem to produce bronchodilatation (Leff *et al.*, 1985; Matran, 1991), resembling the situation in man (Richardson & Beland, 1976), and this suggests that some other mechanism for the cigarette smoke-induced bronchodilatation in the pig should be searched for. It has been shown *in vitro* that nicotine induces a slight contraction followed by a prolonged relaxation in pig isolated bronchi (Macht & Ting, 1921), and that the nicotinic agonist dimethylphenylpiperazinium chloride produces tetrodotoxin-resistant relaxation in pig isolated trachea (Kannan & Johnson, 1992). Challenge with nicotine aerosol in the pig *in vivo* produced a slight decrease in R_{pulm}, indicating relaxation of central airways, as well as relaxation of the pulmonary circulation and a fall in MAP. The mechanism for the nicotine-induced relaxation is at present unknown. Besides the effect of nicotine on R_{pulm}, NO may also contribute to the relaxation response induced by cigarette smoke in the pig lower airways. The bronchodilatation induced by NO inhalation seemed to be indirect, however, since pretreatment with L-NOARG blocked this response. L-NOARG *per se* did not affect R_{pulm}, suggesting that NO mechanisms are not involved in the basal control of bronchial smooth muscle tone, although it has been suggested that the non-adrenergic, non-cholinergic relaxation response to electrical field stimulation in the trachea is NO-mediated (Tucker *et al.*, 1990). The fall in C_{dyn} induced by L-NOARG may be secondary to pressor effects in the pulmonary circulation. Nevertheless, a clear-cut bronchodilator response to exogenous NO was noted in the basal state, and this effect was even more pronounced when bronchial tone was elevated by histamine (Alving, unpublished results). The residual bronchodilator response to cigarette smoke seen after insertion of a Cambridge filter was less than the response induced by NO in equal amounts, indicating the presence of bronchoconstrictor mediators as well in the gas phase of cigarette smoke.

In conclusion, we suggest that the major part of the vasodilatation in the pig bronchial and pulmonary circulations caused by the vapour phase of cigarette smoke is mediated by NO. The apparent counteracting effect in the pulmonary circulation of the particulate phase probably does not involve nicotine, but may be due to particles causing sympathetic reflexes. NO inhalation also relaxes the central airways of the pig, which together with nicotine could be responsible for the cigarette smoke-induced relaxation in the airways. Finally, the basal tone of the bronchial circulation seems to be under marked control of endogenous NO-mechanisms, whereas inhibition of the L-arginine pathway induces changes in pulmonary VR close to changes in systemic VR. NO mechanisms do not seem to be involved in the basal control of bronchial smooth muscle tone.

This study was supported by grants from the Swedish Medical Research Council (14P-10162, 14X-6554, 04X-10354), the Swedish Society of Medicine, the AGA AB Medical Research Fund, the Åke Wiberg Foundation, the American Council for Tobacco Research, the Swedish Tobacco Company, and the Swedish Environmental Protection Board. We thank Miss Margareta Stensdotter for expert technical assistance.

References

ADAMS, L., SCHNEIDER, D.A., SCHERTEL, E.R., STRONG, E.B. & GREEN, J.F. (1987). Respiratory reflexes in the anaesthetized miniature swine. *Respir. Physiol.*, **70**, 343–357.

ALVING, K., FORNHEM, C., WEITZBERG, E. & LUNDBERG, J.M. (1992). Nitric oxide mediates cigarette smoke-induced vasodilatory responses in the lung. *Acta Physiol. Scand.*, **146**, 407–408.

ALVING, K. & FRANCO-CERECEDA, A. (1993). The ability of ruthenium red to reduce the autonomic reflexes and peptide release evoked by capsaicin administration in the pig *in vivo*. *Acta Physiol. Scand.*, **147**, 315–321.

ALVING, K., MATRAN, R. & LUNDBERG, J.M. (1991). Capsaicin-induced local effector responses, autonomic reflexes and sensory neuropeptide depletion in the pig. *Naunyn-Schmied. Arch. Pharmacol.*, **343**, 37–45.

ARCHER, S.L., RIST, K., NELSON, D.P., DEMASTER, E.G., COWAN, N. & WEIR, E.K. (1990). Comparison of the hemodynamic effects of nitric oxide and endothelium-dependent vasodilators in intact lungs. *J. Appl. Physiol.*, **68**, 735–747.

ARNOLD, W.P., ALDRED, R. & MURAD, F. (1977). Cigarette smoke activates guanylate cyclase and increases guanosine 3', 5'-monophosphate in tissues. *Science*, **198**, 934–936.

AVIADO, D.M., & SAMANÉK, M. (1965). Bronchopulmonary effects of tobacco and related substances. I. Bronchoconstriction and bronchodilatation: influence of lung denervation. *Arch. Environ. Health*, **11**, 141–151.

CECCATELLI, S., LUNDBERG, J.M., FAHRENKRUG, J., BREDT, D.S., SNYDER, S.H. & HÖKFELT, T. (1992). Evidence for involvement of nitric oxide in the regulation of hypothalamic portal blood flow. *Neuroscience*, **57**, 769–772.

DIANA, J.N. & VAUGHT, A. (1990). *Research Cigarettes*. Lexington, KY, U.S.A.: University of Kentucky Printing Services.

FIRST, M.W. (1984). Environmental tobacco smoke measurements: retrospect and prospect. *Eur. J. Resp. Dis.*, **65** (suppl. 133), 9–16.

FONTIJN, A., SABADELL, A.J. & RONCO, R.J. (1970). Homogeneous chemiluminescent measurement of nitric oxide with ozone. Implications for continuous selective monitoring of gaseous air pollutants. *Anal. Chem.*, **42**, 575–579.

FROSTELL, C., FRATACCI, M.-D., WAIN, J.C., JONES, R. & ZAPOL, W.M. (1991). Inhaled nitric oxide. A selective pulmonary vasodilator reversing hypoxic pulmonary vasoconstriction. *Circulation*, **83**, 2038–2047.

FROSTELL, C.G., BLOMQVIST, H., HEDENSTIERNA, G., LUNDBERG, J.M. & ZAPOL, W. (1993). Inhaled nitric oxide selectively reverses human hypoxic pulmonary vasoconstriction without causing systemic vasodilatation. *Anesthesiology*, **78**, 427–435.

FULLER, R.W., DIXON, C.M.S. & BARNES, P.J. (1985). Bronchoconstrictor response to inhaled capsaicin in humans. *J. Appl. Physiol.*, **58**, 1080–1084.

FURCHGOTT, R.F. (1984). The roles of the endothelium in the responses of vascular smooth muscle to drugs. *Annu. Rev. Pharmacol. Toxicol.*, **24**, 175–197.

GILMAN, M.J., SYLVESTER, J.T., KENNEDY, T.P., MENKES, H.A. & TRAYSTMAN, R.J. (1981). Vascular effects of cigarette smoke in isolated pig lungs. *Am. Rev. Resp. Dis.*, **124**, 549–553.

GOLDBARG, A.N., KRONE, R.J. & RESNEKOV, L. (1971). Effects of cigarette smoking on hemodynamics at rest and during exercise. I Normal subjects. *Chest*, **60**, 531–536.

GUERIN, M.R., STAKELY, J.R., HIGGINS, C.E., MONEYHUN, J.H. & HOLMBERG, R.W. (1979). Inhalation bioassay chemistry. Walton horizontal smoking machine for inhalation exposure of rodents to cigarette smoke. *J. Natl. Cancer Inst.*, **63**, 441–448.

IGNARRO, L.J., BUGA, G.M., WOOD, K.S., BYRNS, R.E. & CHAUDHURI, G. (1987). Endothelium-derived relaxing factor produced and released from artery and vein is nitric oxide. *Proc. Natl. Acad. Sci. U.S.A.*, **84**, 9265–9269.

JANSEN, A., DRAZEN, J., OSBORNE, J.A., BROWN, R., LOSCALZO, J. & STAMLER, J.S. (1992). The relaxant properties in guinea pig airways of S-nitrosothiols. *J. Pharmacol. Exp. Ther.*, **261**, 154–160.

KANNAN, M.S. & JOHNSON, D.E. (1992). Functional innervation of pig tracheal smooth muscle: neural and non-neural mechanisms of relaxation. *J. Pharmacol. Exp. Ther.*, **260**, 1180–1184.

KUMMER, W., FISCHER, A., MUNDEL, P., MAYER, B., HOBA, B., PHILIPPIN, B. & PREISSLER, U. (1992). Nitric oxide synthase in VIP-containing vasodilator nerve fibres in the guinea-pig. *Neuroreport*, **3**, 653–655.

LARSON, R.K., FUKUDA, P. & MURRAY, J.F. (1965). Systemic and pulmonary vascular effects of nicotine in anaesthetized dogs. *Am. Rev. Respir. Dis.*, **91**, 556–564.

LEFF, A.R., MUNOZ, N.M., TALLET, J. & DAVID, A.C. (1985). Autonomic response characteristics of porcine smooth muscle *in vivo*. *J. Appl. Physiol.*, **58**, 1176–1188.

MACHT, D.I. & TING, G.-C. (1921). A study of antispasmodic drugs on the bronchus. *J. Pharmacol. Exp. Ther.*, **18**, 373–398.

MARKS, G.S., BRIEN, J.F., NAKATSU, K. & McLAUGHLIN, B.E. (1991). Does carbon monoxide have a physiological function? *Trends Pharmacol. Sci.*, **12**, 185–188.

MARON, M.B., CROWE, T.D. & BRAUGHLER, J.M. (1984). Cigarette smoke causes acute fluctuations in the cyclic GMP content of the isolated intact lung. *Respiration*, **45**, 39–44.

MATRAN, R. (1991). Neural control of lower airway vasculature. Involvement of classical transmitters and neuropeptides. *Acta Physiol. Scand.*, **142** (suppl. 601), 1–54.

MATRAN, R., ALVING, K. & LUNDBERG, J.M. (1990). Cigarette smoke, nicotine and capsaicin aerosol-induced vasodilatation in the pig respiratory mucosa. *Br. J. Pharmacol.*, **100**, 535–541.

MATRAN, R., ALVING, K. & LUNDBERG, J.M. (1991). Differential bronchial and pulmonary vascular responses to vagal stimulation in the pig. *Acta Physiol. Scand.*, **143**, 387–394.

MATRAN, R., ALVING, K. & LUNDBERG, J.M. (1993). Differential development of tachyphylaxis to sensory and autonomic nerve activation by capsaicin in the pig, *in vivo*. *Br. J. Pharmacol.*, (in press).

MATRAN, R., ALVING, K., MARTLING, C.-R., LACROIX, J.S. & LUNDBERG, J.M. (1989a). Effects of neuropeptides and capsaicin on tracheobronchial blood flow of the pig. *Acta Physiol. Scand.*, **135**, 335–342.

MATRAN, R., ALVING, K., MARTLING, C.-R., LACROIX, J.S. & LUNDBERG, J.M. (1989b). Vagally mediated vasodilatation by motor and sensory nerves in the tracheal and bronchial circulation of the pig. *Acta Physiol. Scand.*, **135**, 29–37.

MONCADA, S., HIGGS, E.A., HODSON, H.F., KNOWLES, R.G., LOPEZ-JARAMILLO, P., McCALL, T., PALMER, R.M.J., RADOMSKI, M.W., REES, D.D. & SCHULZ, R. (1991). The L-arginine:nitric oxide pathway. *J. Cardiovasc. Pharmacol.*, **17** (suppl. 3), S1–S9.

MÜLSCH, A. & BUSSE, R. (1990). N^G-nitro-L-arginine (N^5-[imino(nitroamino)methyl]-L-ornithine) impairs endothelium-dependent dilations by inhibiting cytosolic nitric oxide synthesis from L-arginine. *Naunyn-Schmied. Arch. Pharmacol.*, **341**, 143–147.

NADEL, J.A. & COMROE, J.H. JR (1961). Acute effects of inhalation of cigarette smoke on airway conductance. *J. Appl. Physiol.*, **16**, 713–716.

NADEL, J.A. & WIDDICOMBE, J.G. (1962). Reflex effects of upper airway stimulation on total lung resistance and blood pressure. *J. Appl. Physiol.*, **17**, 861–865.

NORMAN, V. & KEITH, C.H. (1965). Nitrogen oxides in tobacco smoke. *Nature*, **205**, 915–916.

PALMER, R.M.J., FERRIGE, A.G. & MONCADA, S.A. (1987). Nitric oxide release accounts for the biological activity of endothelium-derived relaxing factor. *Nature*, **327**, 524–526.

RICHARDS, A.M., IKRAM, H., CROZIER, I.G., NICHOLLS, M.G. & JANS, S. (1990). Ambulatory pulmonary arterial pressure in pulmonary hypertension: variability, relation to systemic arterial pressure, and plasma catecholamines. *Br. Heart J.*, **63**, 103–108.

RICHARDSON, J.B. & BELAND, J. (1976). Nonadrenergic inhibitory nervous system in human airways. *J. Appl. Physiol.*, **41**, 764–771.

SAMANÉK, M. & AVIADO, D.M. (1966). Cardiopulmonary effects of tobacco and related substances. III. Pulmonary vascular effects of cigarette smoke and nicotine. *Arch. Environ. Health*, **12**, 717–724.

STERLING, G.M. (1967). Mechanism of bronchoconstriction caused by cigarette smoking. *Br. Med. J.*, **3**, 275–277.

TUCKER, J.F., BRANE, S.R., CHARALAMBONS, L., HOBBS, A.J. & GIBSON, A., (1990). L-N^G-nitroarginine inhibits non-adrenergic, non-cholinergic relaxations of guinea-pig isolated tracheal smooth muscle. *Br. J. Pharmacol.*, **100**, 663–668.

VALLANCE, P., COLLIER, J. & MONCADA, S. (1989). Nitric oxide synthesised from L-arginine mediates endothelium dependent dilatation in human veins *in vivo*. *Cardiovasc. Res.*, **23**, 1053–1057.

WARTMAN, W.B. JR, COGBILL, E.C. & HARLOW, E.S. (1959). Determination of particulate matter in concentrated aerosols. Application to analysis of cigarette smoke. *Anal. Chem.*, **31**, 1705–1709.

WEITZBERG, E., RUDEHILL, A., ALVING, K. & LUNDBERG, J.M. (1991). Nitric oxide inhalation selectively attenuates pulmonary hypertension and arterial hypoxia in porcine endotoxin shock. *Acta Physiol. Scand.*, **143**, 451–452.

WIDDICOMBE, J.G., KENT, D.C. & NADEL, J.A. (1962). Mechanism of bronchoconstriction during inhalation of dust. *J. Appl. Physiol.*, **17**, 613–616.

(Received February 15, 1993
Revised June 3, 1993
Accepted June 18, 1993)

Br. J. Pharmacol. (1993), **110**, 747–752

Activation of the phospholipase C pathway by ATP is mediated exclusively through nucleotide type P_2-purinoceptors in C2C12 myotubes

[1]Robert H. Henning, Marry Duin, Adriaan den Hertog & Adriaan Nelemans

Department of Pharmacology/Clinical Pharmacology, University of Groningen, Bloemsingel 1, 9713 BZ Groningen, The Netherlands

1 The presence of a nucleotide receptor and a discrete ATP-sensitive receptor on C2C12 myotubes has been shown by electrophysiological experiments. In this study, the ATP-sensitive receptors of C2C12 myotubes were further characterized by measuring the formation of inositol(1,4,5)trisphosphate ($Ins(1,4,5)P_3$) and internal Ca^{2+}.

2 The nucleotides ATP and UTP caused a concentration-dependent increase in $Ins(1,4,5)P_3$ content with comparable time courses (EC_{50}: ATP $33 \pm 2\,\mu M$, UTP $80 \pm 4\,\mu M$). ADP was less effective in increasing $Ins(1,4,5)P_3$ content of the cells, while selective agonists for P_1-, P_{2X}- and P_{2Y}-purinoceptors, adenosine, α,β-methylene ATP and 2-methylthio ATP, appeared to be ineffective.

3 Under Ca^{2+}-free conditions, the basal level of $Ins(1,4,5)P_3$ was lower than in the presence of Ca^{2+}, and the ATP- and UTP-induced formation of $Ins(1,4,5)P_3$ was diminished.

4 The $Ins(1,4,5)P_3$ formation induced by optimal ATP and UTP concentrations was not additive. ATP- and UTP-induced $Ins(1,4,5)P_3$ formation showed cross-desensitization, whereas cross-desensitization was absent in responses elicited by one of the nucleotides and bradykinin.

5 The change in $Ins(1,4,5)P_3$ content induced by effective nucleotides was inhibited by suramin. Schild plots for suramin inhibition of $Ins(1,4,5)P_3$ formation in ATP- and UTP-stimulated myotubes showed slopes greater than unity (1.63 ± 0.09 and 1.37 ± 0.11, respectively). Apparent pA_2 values were 4.50 ± 0.48 and 4.41 ± 0.63 for ATP and UTP, respectively.

6 Stimulation of the cells with ATP or UTP induced a rapid increase in intracellular Ca^{2+}, followed by a slow decline to basal levels. Ca^{2+} responses reached lower maximal values and did not show the slow phase in the absence of extracellular Ca^{2+}. The ATP and UTP-evoked increase in intracellular Ca^{2+} was not additive and showed cross-desensitization. Cross-desensitization was absent in myotubes stimulated with one of the nucleotides and bradykinin.

7 These results show that ATP- and UTP-induced formation of $Ins(1,4,5)P_3$, Ca^{2+} release from internal stores and Ca^{2+}-influx from the extracellular space are mediated exclusively via the nucleotide type P_2-purinoceptor in mouse C2C12 myotubes.

Keywords: Nucleotide receptor; ATP; UTP; inositol (1,4,5)trisphosphate ($Ins(1,4,5)P_3$); P_2-purinoceptor; intracellular Ca^{2+}; C2C12 myotubes

Introduction

Receptors sensitive to ATP have been classified according to their sensitivity to selective ATP analogues (Burnstock, 1990). In addition to the established P_2-purinoceptor subclasses (O'Connor *et al.*, 1990; Thomas *et al.*, 1991) the existence of nucleotide receptors was proposed (Davidson *et al.*, 1990), which are sensitive to the purine, adenosine triphosphate (ATP) and also the pyrimidine, uridine triphosphate (UTP). Nucleotide receptors have been shown in pituitary cells (Davidson *et al.*, 1990), mesangial cells (Pfeilschifter, 1990), myotubes (Henning *et al.*, 1992a), DDT_1 MF-2 smooth muscle cells (Van der Zee *et al.*, 1992) and PC12 cells (Murrin & Boarder, 1992).

Recently, a nucleotide receptor and a not yet classified discrete ATP-sensitive receptor were defined in mouse C2C12 myotubes. Stimulation of the nucleotide receptor resulted in a Ca^{2+}-influx and activation of Ca^{2+}-regulated K^+-channels, while the Na^+-channels were opened via the distinct ATP-receptor (Henning *et al.*, 1992a). It is also suggested that in chick myotubes, the ATP-induced membrane current is mediated via two distinct ATP-sensitive receptors (Thomas *et al.*, 1991).

The membrane current evoked by ATP-receptor subtypes may be caused by activation of different second messenger systems or by activation of receptor-coupled ion-channels (Burnstock, 1990). To characterize the ATP-sensitive receptors on C2C12 myotubes we investigated their coupling to the phospholipase C pathway by measuring the formation of $Ins(1,4,5)P_3$ and intracellular Ca^{2+} mobilization.

Methods

Cell culture

C2C12 cells, a murine myoblast cell line (Yaffee & Saxel, 1977) were obtained from the American Tissue Type Collection, Rockville, U.S.A. and cultured in 9.6 cm^2 plastic wells at 37°C in Dulbecco's modified essential medium, 7 mM $NaHCO_3$ and 10 mM HEPES (DMEM) supplemented with 10% foetal calf serum. When cells reached 80% confluence, medium was changed to DMEM supplemented with 5% horse serum. Myotubes were used 7 days after initiating myoblast fusion.

Inositol phosphates

$Ins(1,4,5)P_3$ contents of the myotubes was assessed by mass measurement using a radioligand binding assay. Before the

[1] Author for correspondence.

experiment, the cells were washed three times with a buffer of the following composition (mM): NaCl 125, KCl 6, $CaCl_2$ 1.2, $MgCl_2$ 2.5, NaH_2PO_4 1.2, glucose 11, HEPES 10 (pH 7.4). In the Ca^{2+}-free buffer $CaCl_2$ was omitted and EGTA (0.4 mM) and $MgCl_2$ (3.5 mM) were added. The reaction was started by the addition of ATP or analogues and stopped by addition of trichloroacetic acid (TCA: 5%, 300 µl) after removing the buffer. Experiments were conducted at 22°C. The TCA was extracted (three times) with water-saturated diethylether, the samples were neutralized with KOH and stored at −40°C. The samples were assayed for Ins(1,4,5)P_3 content as described before (Den Hertog *et al.*, 1992), using a standard curve of Ins(1,4,5)P_3 in ether-extracted TCA solution.

Intracellular Ca^{2+}

Cytoplasmic free Ca^{2+} levels were determined by fura-2 fluorescence. Cells plated on glass coverslips were loaded with fura-2-AM (1 µM) for 30 min at 37°C in the buffer containing 0.2% BSA. Recordings were made at excitation wavelengths of 340 and 380 nm and an emission wavelength of 510 nm at 22°C using a fluorescence spectrophotometer (Hitachi). Data are expressed as the ratio between the two wavelengths representing Ca^{2+}-free (380 nm) and Ca^{2+}-bound (340 nm) fluorescent probe.

Data analysis

Data are presented as mean ± s.e.mean unless stated otherwise and are considered statistically different at $P<0.05$ (unpaired Student's *t* test). Concentration-response curves were fitted to the averaged data by a least-squares non-linear regression programme (SigmaPlot 4.0, Jandel Scientific).

Drugs

Adenosine, α,β-methylene adenosine 5'-triphosphate (α,β-meATP) and fura-2-AM were obtained from Boehringer, Mannheim (Germany). Adenosine 5'-triphosphate (ATP), adenosine 5'-diphosphate (ADP) and uridine 5'-triphosphate (UTP) were obtained from Serva, Heidelberg (Germany). 2-(methylthio) adenosine 5'-triphosphate (2-MeSATP) was obtained from Research Biochemicals Inc., Natick, Mass. (U.S.A.), suramin from Bayer, Leverkusen (Germany) and bradykinin from Sigma, St. Louis (U.S.A.). D-[2-^{3}H]-inositol 1,4,5-trisphosphate was obtained from Du Pont-New England Nuclear (U.S.A.).

Results

Ins(1,4,5)P_3 formation

The basal Ins(1,4,5)P_3 content of the C2C12 myotubes, as measured by radioligand binding assay, was 1.07 ± 0.12 pmol mg^{-1} protein ($n = 60$). The myotubes responded to application of ATP (300 µM) with a rapid transient increase in Ins(1,4,5)P_3 content of about four times the basal level, followed by a slow decline towards basal values after about 5 min (Figure 1a). During prolonged stimulation with ATP (1 h) a further decline in Ins(1,4,5)P_3 content was observed (Figure 1b). Similar experiments were conducted in C2C12 myotubes using UTP as an agonist. The characteristics of the increase in Ins(1,4,5)P_3 content of myotubes stimulated with UTP (300 µM) were similar to those observed with ATP (Figure 1c), including the effect of prolonged exposure to the agonist (Figure 1d). The specific P_{2X}- and P_{2Y}-purinoceptor agonists, α,β-MeATP and 2-MeS ATP and the P_1-purinoceptor agonist adenosine, did not change the basal Ins(1,4,5)P_3 content of the myotubes (α,β-MeATP (100 µM): 1.36 ± 0.29 pmol mg^{-1} protein, 2-MeS ATP (100 µM): 1.36 ± 0.17 pmol mg^{-1} protein and adenosine (1 mM) 1.08 ± 0.30 pmol mg^{-1} protein ($n = 4$)).

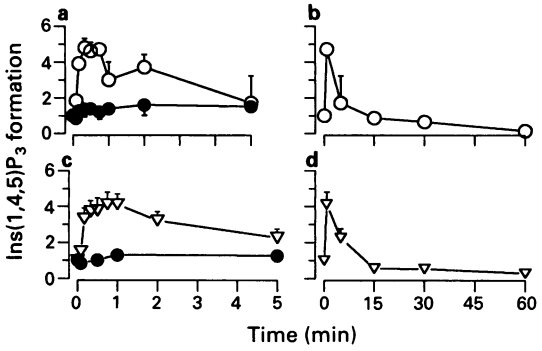

Figure 1 Changes in inositol (1,4,5)trisphosphate (Ins(1,4,5)P_3) content of the myotubes evoked by stimulation with different agonists. (a) Increase in Ins(1,4,5)P_3 content after stimulation with ATP (○, 300 µM); this effect is abolished in the presence of suramin (●, 500 µM). (b) Prolonged stimulation with ATP (300 µM); (c) stimulation with UTP (▽, 300 µM) induces similar changes in Ins(1,4,5)P_3 content as with ATP, also inhibited by suramin (●, 500 µM). (d) Prolonged stimulation with UTP (300 µM). Ins(1,4,5)P_3 formation is expressed as pmol mg^{-1} protein. Data are obtained from 4 or more experiments.

The maximum Ins(1,4,5)P_3 levels measured on stimulation of the cells with ATP, ADP and UTP (10 µM−1 mM) was reached after 45 s. These maximum values were used to plot concentration-response curves. It was found that ATP was slightly more potent than UTP regarding the formation of Ins(1,4,5)P_3 (EC_{50}: ATP 33 ± 2 µM; UTP 80 ± 4 µM), whereas ADP was less effective (Figure 2). The optimal increase in Ins(1,4,5)P_3 content was found in the presence of ATP (1 mM) and UTP (1 mM). Simultaneous addition of these nucleotides (1 mM) did not produce an additive effect on Ins(1,4,5)P_3 levels (Figure 2).

To study whether nucleotide-induced Ins(1,4,5)P_3 formation in C2C12 cells was mediated via a single receptor, the effect of subsequent addition of three agonists, ATP, UTP and bradykinin, was investigated. Bradykinin (30 µM) also induced Ins(1,4,5)P_3 formation with a similar time course as observed for the nucleotides, producing a peak at 45 s (not shown). Myotubes were pretreated for 15 min with the first agonist. Subsequently, a second agonist was administered still in the presence of the first agonist and Ins(1,4,5)P_3 content of

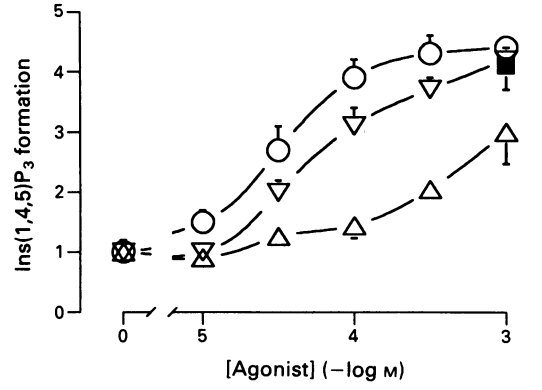

Figure 2 Concentration-dependent changes in inositol (1,4,5)trisphosphate (Ins(1,4,5)P_3) content of the myotubes evoked by ATP (○), ADP (△) and UTP (▽). The increase in Ins(1,4,5)P_3 content evoked by optimal concentrations of ATP (1 mM) and UTP (1 mM) at 45 s stimulation are non-additive (■). Ins(1,4,5)P_3 formation is expressed as pmol mg^{-1} protein. Data are obtained from 4 or more experiments.

the cells was measured after 45 s. Typically, Ins(1,4,5)P_3 formation induced after preincubation of the cells by an agonist by application of a second dose of the same agonist was reduced to about 30%. Preincubation of the cells with ATP (1 mM) also significantly decreased Ins(1,4,5)P_3 formation evoked by UTP (1 mM) but did not affect the bradykinin (30 μM)-induced increase in Ins(1,4,5)P_3 (Figure 3). Likewise, preincubation with UTP decreased ATP-induced Ins(1,4,5)P_3 formation, not affecting bradykinin-induced Ins(1,4,5)P_3 formation (Figure 3). Further, preincubation with bradykinin did not affect ATP- or UTP-induced Ins(1,4,5)P_3 formation (Figure 3).

The P_2-purinoceptor antagonist, suramin, is known to block the ATP- and UTP-induced changes in membrane potential of C2C12 myotubes (Henning *et al.*, 1992a). Application of ATP in the presence of suramin (500 μM) did not cause a significant change in Ins(1,4,5)P_3 content of the myotubes (Figure 1a). Similarly, suramin (500 μM) also abolished the UTP-induced changes (Figure 1c) and ADP-mediated (1 mM) increase in Ins(1,4,5)P_3 formation (not shown). To examine further the supposition that nucleotides act via the same purinceptor, the antagonistic properties of suramin on ATP- and UTP-induced Ins(1,4,5)P_3 formation were investigated after pretreatment of the cells (20 min) with various suramin concentrations (50 μM, 150 μM and 300 μM). Suramin appeared to displace the concentration-response curves for ATP and UTP in parallel (Figure 4a,b). However, the slopes of the Schild plots deviated markedly from unity, being 1.63 ± 0.09 and 1.37 ± 0.11 for ATP and UTP, respectively (Figure 4c). The apparent pA_2 values for suramin in myotubes stimulated with ATP and UTP were 4.50 ± 0.48 and 4.41 ± 0.63, respectively.

The profile of the ATP-evoked biphasic change in membrane potential was different under Ca^{2+}-free conditions, represented by the abolition of the transient hyperpolarization and a slower decline of the depolarizing phase (Henning *et al.*, 1992a). To examine whether these changes in membrane potential were related to the formation of Ins(1,4,5)P_3, its formation was measured in cells stimulated with ATP (300 μM) in the absence of external Ca^{2+}. The basal level of Ins(1,4,5)P_3 was decreased by preincubation of the cells (10 min) under Ca^{2+}-free conditions (Figure 5). A pronounced increase in Ins(1,4,5)P_3 reaching a lower maximum value than in the presence of external Ca^{2+} and a relative faster decline was observed on receptor stimulation with ATP (300 μM) in the absence of extracellular Ca^{2+} (Figures 1a,5).

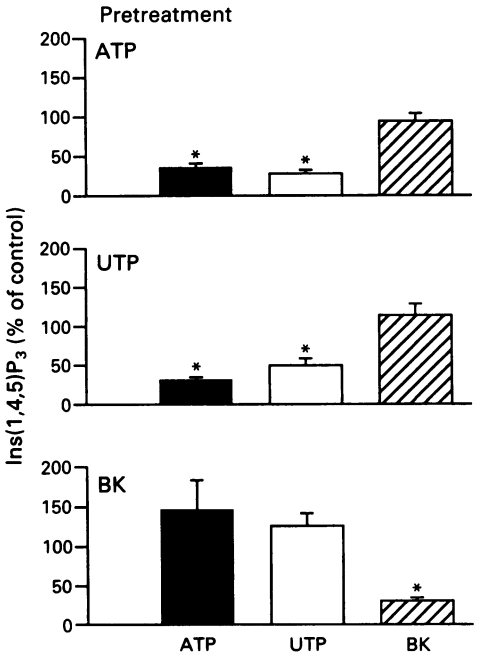

Figure 3 Cross-desensitization of inositol (1,4,5)trisphosphate (Ins(1,4,5)P_3) formation elicited by ATP, UTP and bradykinin in C2C12 myotubes. Myotubes were stimulated for 45 s after pretreatment for 15 min. Data are expressed as percentage of the Ins(1,4,5)P_3 content elicited by the agonist in non-pretreated cells, which amounted to 4.6 ± 1.2 pmol mg^{-1} protein, 4.2 ± 0.6 pmol mg^{-1} protein and 3.5 ± 0.5 pmol mg^{-1} protein, for ATP (1 mM), UTP (1 mM) and bradykinin (BK; 30 μM), respectively ($n = 4$). The basal Ins(1,4,5)P_3 level was 1.06 ± 0.12 pmol mg^{-1} protein; $n = 4$. *Significant decrease in Ins(1,4,5)P_3 formation compared to cells that were not pretreated, $P < 0.01$.

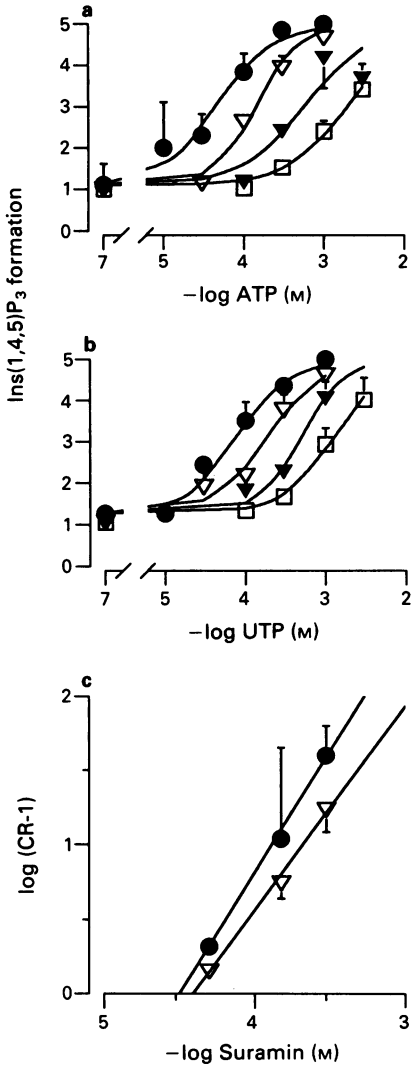

Figure 4 The antagonistic effect of suramin on nucleotide-induced inositol (1,4,5)trisphosphate (Ins(1,4,5)P_3) formation in C2C12 myotubes. (a) Concentration-response curve for ATP (●) and in the presence of suramin (50 μM, ▽; 150 μM, ▼; 300 μM, □). Values are expressed as mean ± s.e.mean ($n \geq 4$). (b) Concentration-response curve for UTP (●) and in the presence of suramin (50 μM, ▽; 150 μM, ▼; 300 μM, □), values are expressed as mean ± s.e.mean ($n = 4$). (c) Schild plot for data derived from data in (a) and (b) showing suramin action on ATP- (●) and UTP- (▽) induced Ins(1,4,5)P_3 formation. The concentration-response ratios (CR) were calculated at the EC_{50} of Ins(1,4,5)P_3 formation. Regression lines were calculated by the method of least squares ($r > 0.98$; $P < 0.05$). Intercepts with the X-axis were 4.50 ± 0.48 and 4.41 ± 0.63, while the slopes measured are 1.63 ± 0.09 and 1.37 ± 0.11 for ATP and UTP, respectively.

Internal Ca^{2+}

The nucleotide receptor regulation of internal Ca^{2+} was studied using fura-2 as a fluorescent probe in myotubes

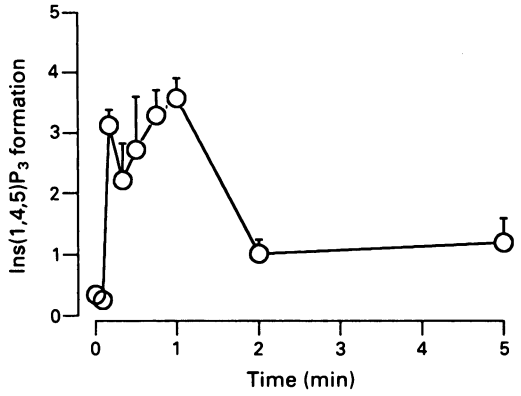

Figure 5 The increase in inositol (1,4,5)trisphosphate ($Ins(1,4,5)P_3$) content after stimulation with ATP (300 μM) under extracellular Ca^{2+}-free conditions. $Ins(1,4,5)P_3$ formation is expressed as pmol mg^{-1} protein. Data are obtained from 4 experiments.

stimulated by ATP and UTP. Under normal conditions, ATP and UTP evoked a rapid increase in intracellular Ca^{2+}, followed by a slow decline to basal levels (Figure 6a,b). Maximum concentrations of ATP (1 mM) and UTP (1 mM) evoked a comparable increase in intracellular Ca^{2+} (Figure 6a). Under Ca^{2+}-free conditions, the basal internal Ca^{2+} concentration and the transient rise in intracellular Ca^{2+} of myotubes stimulated with ATP and UTP (Figure 6b) were less pronounced than in the presence of external Ca^{2+} (Figure 6a). Further, the slow phase of the Ca^{2+} response evoked by both nucleotides under normal conditions was absent in Ca^{2+}-free medium (Figure 6b). Stimulation of the cells with the specific P_{2X}-, P_{2Y}- and P_1-purinoceptor agonists, α,β-MeATP (100 μM), 2-MeS ATP (100 μM) and adenosine (1 mM), did not change intracellular Ca^{2+} (not shown).

To examine whether ATP and UTP-induced Ca^{2+} responses were mediated through the same receptor, the response to subsequent stimulation with the nucleotides was determined. Stimulation of the cells with UTP (1 mM) did not produce a rise in intracellular Ca^{2+} if cells were pretreated for 10 min with ATP (1 mM; Figure 7a) and *vice versa* (not shown). However, bradykinin (20 μM) induced a rapid increase in intracellular Ca^{2+} of myotubes pretreated

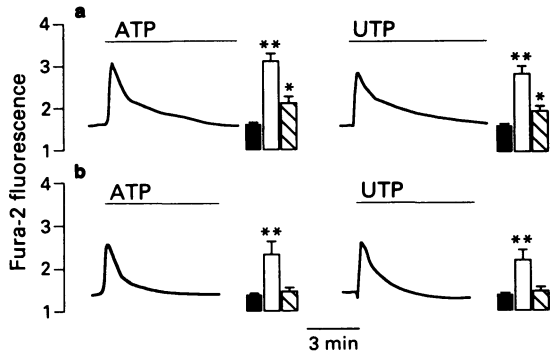

Figure 6 The effect of ATP and UTP on intracellular Ca^{2+}, using fura-2 fluorescence. The presence of the nucleotides is represented by a horizontal bar. Data are expressed as the fluorescence ratio (R = F340/F380). (a) Typical responses caused by ATP (1 mM, left panel) and UTP (1 mM, right panel) in the presence of extracellular Ca^{2+}. (b) Typical responses to ATP (1 mM, left panel) and UTP (1 mM, right panel) evoked under Ca^{2+}-free conditions not showing the slow phase. The corresponding columns represent the basal levels (solid columns), peak levels (open columns) and levels at 3 min (hatched columns) of the fluorescence ratio obtained after stimulation in 7 or more experiments (mean ± s.e.mean). $*P<0.01$, $**P<0.001$ compared with basal values.

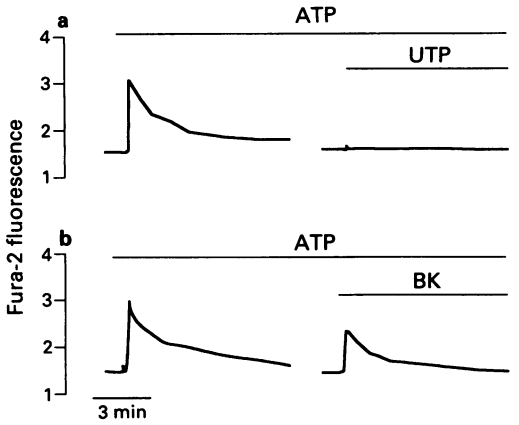

Figure 7 The response in intracellular Ca^{2+} after pretreatment of the cells for 10 min with ATP. The presence of ATP and the subsequent addition of the second agonist is indicated by horizontal bars. (a) The absence of the effect of UTP (1 mM) in myotubes pretreated with ATP (1 mM). (b) Myotubes pretreated with ATP (1 mM), showing a rapid increase in internal Ca^{2+} upon administration of bradykinin (BK; 20 μM). Data are expressed as the fluorescence ratio (R = F340/F380) obtained in at least 3 experiments.

for 10 min with ATP (1 mM; Figure 7b) and UTP (1 mM; not shown).

Discussion

The results presented here show that nucleotide receptors are activated by ATP and UTP in C2C12 myotubes. This is shown by the formation of $Ins(1,4,5)P_3$ and increase in intracellular Ca^{2+} demonstrated upon stimulation with these nucleotides, while stimulation of the myotubes with ATP analogues, assumed to interact specifically with P_1-, P_{2X}- and P_{2Y}-purinoceptors (Burnstock, 1990; Cusack & Hourani, 1990), was ineffective. Further, the involvement of P_{2T}-purinoceptors is ruled out, as ATP is supposed to act as an antagonist for these receptors. P_{2Z}-purinoceptors are also excluded in view of the agonist effect of UTP (Cusack & Hourani, 1990).

The formation of $Ins(1,4,5)P_3$ in myotubes stimulated with ATP and UTP showed a similar time course and corresponding $Ins(1,4,5)P_3$ levels were reached at optimal agonist concentrations, while ADP was less effective. The $Ins(1,4,5)P_3$ content of ATP- and UTP-stimulated cells decreased below initial levels during prolonged stimulation of the myotubes, which might be attributed to a negative feedback on receptor-activated processes by protein kinase C as established in various cell types (Leeb-Lundberg, *et al.*, 1985; Bauhal *et al.*, 1985; Berridge, 1987). Besides the similarity in time course of formation of $Ins(1,4,5)P_3$ and increase in internal Ca^{2+}, the $Ins(1,4,5)P_3$ formation induced by optimal concentrations of ATP and UTP was not additive. Further, ATP- and UTP-induced formation of $Ins(1,4,5)P_3$ and mobilization of internal Ca^{2+} showed cross-desensitization, whereas cross-desensitization was absent in myotubes stimulated with one of these nucleotides and bradykinin. Consequently, these observations strongly suggest that the $Ins(1,4,5)P_3$ formation and changes in internal Ca^{2+} in C2C12 myotubes elicited by ATP and UTP are mediated by a single receptor, identified as a nucleotide type P_2-purinoceptor.

The observations on $Ins(1,4,5)P_3$ formation in C2C12 myotubes are comparable with nucleotide receptor-activated $Ins(1,4,5)P_3$ formation in other cells (Davidson *et al.*, 1990; Pfeilschifter, 1990; Murrin & Boarder, 1992). The nucleotide

receptor-induced formation of Ins(1,4,5)P_3 in C2C12 myotubes was inhibited by suramin, as reported for ATP/UTP mediated inositol phosphate formation in DDT_1 MF-2 cells (Hoiting *et al.*, 1990; Van der Zee *et al.*, 1992). The antagonistic property of suramin on Ins(1,4,5)P_3 formation in ATP and UTP-stimulated C2C12 myotubes was characterized by comparable pA_2 values. Besides the observations made in the cross-desensitization experiments, this also suggests that ATP and UTP mediate their signal via the same receptor. However, similar slopes and pA_2 values are common for suramin antagonism of different types of P_2-purinoceptors, such as P_{2X}- and P_{2T}-purinoceptors (Leff *et al.*, 1990; Hourani *et al.*, 1992) and were also observed in the suramin-induced reversal of skeletal muscle paralysis (Henning *et al.*, 1992b).

Stimulation of the nucleotide receptors of C2C12 myotubes under Ca^{2+}-free conditions was accompanied by a transient formation of Ins(1,4,5)P_3 and a concomitant rise in internal Ca^{2+}. The increase in intracellular Ca^{2+} can be readily explained by the Ca^{2+} release from intracellular stores activated by Ins(1,4,5)P_3, a process recognized in many cell types (Berridge, 1987; Berridge & Irvine, 1989). Moreover, stimulation of the nucleotide receptor also activated a Ca^{2+}-influx from the extracellular space, as demonstrated by the larger amplitude and slower decay of the Ca^{2+} response in the presence of extracellular Ca^{2+}. In turn, this receptor-mediated influx of Ca^{2+} apparently enhanced the formation of Ins(1,4,5)P_3. In accord, phospholipase C activity has been shown to be dependent on the internal Ca^{2+} concentration (Uhing *et al.*, 1986; Martin *et al.*, 1986; Taylor *et al.*, 1991). It should be noted that the nucleotide receptor-evoked formation of Ins(1,4,5)P_3 and increase in intracellular Ca^{2+} in myotubes of the mouse C2C12 cell line show similar characteristics to the responses obtained in primary embryonic chick myotubes by stimulation of a yet unclassified P_2-purinoceptor with ATP (Häggblad & Heilbronn, 1988; Erikson & Heilbronn, 1989).

Stimulation of nucleotide receptors on C2C12 myotubes caused a transient hyperpolarization followed by a slowly declining depolarization (Henning *et al.*, 1992a). The depolarization evoked via the nucleotide receptor is probably due to enhancement of the Ca^{2+}-influx. Supplementary to this Ca^{2+}-influx evoked via nucleotide receptors, the additional depolarization caused by ATP is supposed to be due to a Na^+-influx produced by stimulation of discrete ATP-sensitive receptors (Henning *et al.*, 1992a). In view of the similar effects of ATP and UTP on Ins(1,4,5)P_3 and internal Ca^{2+} obtained in myotubes preincubated with the other compound, it is unlikely that the discrete ATP-sensitive receptor of C2C12 myotubes is coupled to these pathways. The transient hyperpolarization elicited by the nucleotide receptor is supposed to be due to the opening of Ca^{2+}-regulated K^+-channels (Henning *et al.*, 1992a). Under Ca^{2+}-free conditions, however, a transient Ca^{2+} release from internal stores was observed, not accompanied by a hyperpolarization (Henning *et al.*, 1992a). Thus, a second component dependent on external Ca^{2+} is apparently necessary to open the Ca^{2+}-regulated K^+-channels upon stimulation of the nucleotide receptor. The formation of Ins(1,3,4,5)P_4 from Ins(1,4,5)P_3 via the 3-kinase is Ca^{2+}-dependent (Biden & Wollheim, 1986; Imboden & Pattison, 1987) and might be involved as the second component to activate these K^+-channels, as shown in DDT_1 MF-2 cells (Molleman *et al.*, 1991). A further study to elucidate the mechanism responsible for the hyperpolarization is in progress.

In conclusion, the results presented here show that ATP- and UTP-mediated formation of Ins(1,4,5)P_3, causing a rise in internal Ca^{2+} by release from internal stores and activation of Ca^{2+}-entry from the extracellular space, are exclusively mediated by nucleotide receptors in mouse C2C12 myotubes.

This study was partly sponsored by grant 900-549-133 from The Netherlands Organisation for Scientific Research (NWO).

References

BAUHAL, A.J., BALLA, T., HUNYADY, L., HAUSDORF, W., GUILLEMETTE, G. & CATT, K.J. (1985). Angiotensin II and guanidine nucleotides stimulate formation of inositol 1,4,5-trisphosphate and its metabolites in permeabilized adrenal glomerulosa cells. *J. Biol. Chem.*, **263**, 6087–6092.

BERRIDGE, M.J. (1987). Inositol triphosphate and diacylglycerol: two interacting second messengers. *Annu. Rev. Biochem.*, **56**, 159–193.

BERRIDGE, M.J. & IRVINE, R.F. (1989). Inositol phosphates and cell signalling. *Nature*, **341**, 197–205.

BIDEN, T.J. & WOLLHEIM, C.B. (1986). Ca^{++} regulates the inositol tris/tetrakisphosphate pathway in intact and broken preparations of insulin secreting RINm5F cells. *J. Biol. Chem.*, **261**, 11931–11934.

BURNSTOCK, G. (1990). Purinergic mechanisms. *Ann. N.Y. Acad. Sci.*, **603**, 1–17.

CUSACK, N.J. & HOURANI, S.M.O. (1990). Subtypes of P_2-purinoceptors. *Ann. N.Y. Acad. Sci.*, **603**, 172–181.

DAVIDSON, J., WAKEFIELD, I.K., SOHNINS, U., VAN DER MERWE, P.A. & MILLER, R.P. (1990). A novel extracellular nucleotide receptor coupled to phoshoinositidase-C in pituitary cells. *Endocrinology*, **126**, 80–87.

DEN HERTOG, A., HOITING, B., MOLLEMAN, A., VAN DEN AKKER, J., DUIN, M. & NELEMANS, S.A. (1992). Calcium release from separate receptor-specific intracellular stores induced by histamine and ATP in a hamster cell line. *J. Physiol.*, **454**, 591–607.

ERIKSON, H. & HEILBRONN, E. (1989). Extracellularly applied ATP alters the calcium flux through dihydropyridine-sensitive channels in cultured chick myotubes. *Biochem. Biophys. Res. Commun.*, **3**, 878–885.

HÄGGBLAD, J. & HEILBRONN, E. (1988). P_2-purinoceptor-stimulated phosphoinositide turnover in chick myotubes. *FEBS Lett.*, **235**, 133–136.

HENNING, R.H., NELEMANS, S.A., VAN DEN AKKER, J. & DEN HERTOG, A. (1992a). The nucleotide receptors on mouse C2C12 myotubes. *Br. J. Pharmacol.*, **106**, 853–858.

HENNING, R.H., NELEMANS, S.A., SCAF, A.H.J., VAN EEKEREN, J., AGOSTON, S. & DEN HERTOG, A. (1992b). Suramin reverses non-depolarizing neuromuscular blockade in rat diaphragm. *Eur. J. Pharmacol.*, **216**, 73–79.

HOITING, B., MOLLEMAN, A., NELEMANS, A. & DEN HERTOG, A. (1990). P_2-purinoceptor-activated membrane currents and inositol tetrakisphosphate formation are blocked by suramin. *Eur. J. Pharmacol.*, **181**, 127.

HOURANI, S.M.O., HALL, D.A. & NIEMAN, C.J. (1992). Effects of the P_2-purinoceptor antagonist, suramin, on human platelet aggregation induced by adenosine 5'-diphosphate. *Br. J. Pharmacol.*, **105**, 453–457.

IMBODEN, J.B. & PATTISON, G. (1987). Regulation of inositol 1,4,5-trisphosphate kinase activity after stimulation of human T cell antigen receptor. *J. Clin. Invest.*, **79**, 1538–1541.

LEEB-LUNDBERG, L.M.F., COTECCHIA, S., LOMASNEY, J.W., DE BERNARDIS, J.F., LEFKOWITZ, R.J. & CARON, M.G. (1985). Phorbol esters promote α_1-adrenergic receptor phosphorylation and receptor uncoupling from inositol phosphate metabolism. *Proc. Natl. Acad. Sci. U.S.A.*, **82**, 5651–5655.

LEFF, P., WOOD, B.E. & O'CONNOR, S.E. (1990). Suramin is a slowly-equilibrating but competitive antagonist at P_2 receptors in rabbit isolated ear artery. *Br. J. Pharmacol.*, **101**, 645–649.

MARTIN, T.F.J., BAJJALIEH, S.M., LUCAS, D.O. & KOWALCHYK, J.A. (1986). Thyrotropin-releasing hormone stimulation of polyphosphoinositide hydroloysis in GH3 cell membranes is GTP dependent but insensitive to cholera or pertussis toxin. *J. Biol. Chem.*, **261**, 2918–2927.

MOLLEMAN, A., HOITING, B., DUIN, M., VAN DEN AKKER, J., NELEMANS, S.A. & DEN HERTOG, A. (1991). Potassium channels regulated by inositol 1,3,4,5-tetrakisphosphate and internal calcium in DDT_1 MF2 smooth muscle cells. *J. Biol. Chem.*, **266**, 5658–5663.

MURRIN, R.J. & BOARDER, M.R. (1992). Neuronal 'nucleotide' receptor linked to phospholipase C and phospholipase D? Stimulation of PC12 cells by ATP analogues and UTP. *Mol. Pharmacol.*, **41**, 561–568.

O'CONNOR, S.E., DAINTY, I.A. & LEFF, P. (1991). Further subclassification of ATP receptors based on agonist studies. *Trends Pharmacol. Sci.*, **12**, 137–141.

PFEILSCHIFTER, J. (1990). Comparison of extracellular ATP and UTP signalling in rat renal mesangial cells. *Biochem. J.*, **272**, 469–472.

TAYLOR, S.J., CHAE, H.Z., RHEE, S.G. & EXTON, J.H. (1991). Activation of the β_1 isozyme of phospholipase C by α subunits of the G_q class of G proteins. *Nature*, **350**, 516–518.

THOMAS, S.A., ZAWISA, M.J., LIN, X. & HUME, R.I. (1991). A receptor that is highly specific for extracellular ATP in developing chick skeletal muscle *in vitro*. *Br. J. Pharmacol.*, **103**, 1963–1969.

UHING, R.J., PRPIC, V., JIANG, H. & EXTON, J.H. (1986). Hormone-stimulated polyphosphoinositide breakdown in rat liver plasma membrane. Role of guanine nucleotides and calcium. *J. Biol. Chem.*, **261**, 2140–2146.

VAN DER ZEE, L., NELEMANS, S.A. & DEN HERTOG, A. (1992). Nucleotide receptors on DDT_1 MF-2 vas deferens cells. *Eur. J. Pharmacol.*, **215**, 317–320.

YAFFEE, D. & SAXEL, O. (1977). Serial passage and differentiation of myogenic cells isolated from dystrophic mouse muscle. *Nature*, **270**, 725–727.

(Received January 4, 1993
Revised June 11, 1993
Accepted June 29, 1993)

Br. J. Pharmacol. (1993), **110**, 753–760

Similar effects of ethanol and flumazenil on acquisition of a shuttle-box avoidance response during withdrawal from chronic ethanol treatment

[1]Hugh E. Criswell & George R. Breese

Brain and Development Research Center and Center for Alcohol Studies, University of North Carolina School of Medicine, Chapel Hill, North Carolina 27599-7250, U.S.A.

1 Acquisition of a two-way shuttle-box avoidance response is facilitated by ethanol. This facilitated acquisition of an avoidance response to ethanol was attenuated during withdrawal from chronic-ethanol diet intake (i.e. tolerance developed by ethanol). The deficit in the avoidance task after chronic ethanol treatment could be overcome by increasing the dose of ethanol.

2 Flumazenil, a benzodiazepine antagonist, also facilitated acquisition of the avoidance response in control rats. This response to flumazenil was significantly reduced during withdrawal from chronic-ethanol treatment. This reduced avoidance responding during withdrawal also could be overcome by increasing the dose of flumazenil.

3 The benzodiazepine-inverse agonist, RO 15-4513, produced a deficit in avoidance responding that was antagonized by both ethanol and flumazenil in a dose-related manner.

4 To determine whether flumazenil has the properties of a benzodiazepine agonist, it was established that, unlike the benzodiazepine chlordiazepoxide, flumazenil did not enhance the ethanol-induced deficit in the aerial righting reflex. Additionally, flumazenil blocked the action of chlordiazepoxide in this procedure, consistent with the benzodiazepine antagonist action of flumazenil.

5 Data collected are consistent with the hypothesis that an endogenous substance with the properties of a benzodiazepine-inverse agonist antagonizes the anticonflict actions of acutely administered ethanol during withdrawal from chronic-ethanol exposure.

Keywords: Flumazenil; ethanol; chronic ethanol treatment; shuttle-box avoidance; avoidance conflict responding; aerial righting reflex; anxiogenic; anxiolytic; RO 15-4513; ethanol tolerance

Introduction

In 1980, our laboratory compared the effects of ethanol and benzodiazepines on performance in various behavioural tasks and concluded they may share a common mechanism of action (Frye *et al.*, 1980; Vogel *et al.*, 1980). However, ethanol does not compete with a benzodiazepine for receptor binding (Frye *et al.*, 1980; Breese *et al.*, 1983). Several early studies have indicated that ethanol, like benzodiazepines, has an anticonflict action (Conger, 1956; Barry *et al.*, 1963; Mansfield *et al.*, 1977; Vogel *et al.*, 1980). More recently, our laboratory (Frye *et al.*, 1981; Criswell & Breese, 1989) demonstrated that chlordiazepoxide and ethanol facilitated acquisition of a shuttle-box avoidance response, a finding consistent with other studies demonstrating that the two-way avoidance task may have a conflict component (Gray, 1977; Fernandez-Teruel *et al.*, 1991a,b). During withdrawal from chronic-ethanol treatment, acquisition of the avoidence response was not facilitated by either ethanol or chlordiazepoxide, suggestive that there was cross-tolerance between these drugs (Criswell & Breese, 1989). This latter observation provided additional support for the position that ethanol has actions similar to those of the benzodiazepines but the basis of the tolerance to the action of chlordiazepoxide and ethanol in the avoidance task following withdrawal from chronic-ethanol treatment was unknown.

File *et al.* (1989) reported that flumazenil, a benzodiazepine antagonist, reversed the deficit to ethanol seen in a conflict procedure in rats withdrawn from chronic ethanol treatment. Furthermore, in a social interaction test, flumazenil alone reversed the behavioural response associated with withdrawal from chronic-ethanol or from chronic-benzodiazepine administration (Baldwin & File, 1987; File *et al.*, 1989; File & Hitchcott, 1990). The effect of flumazenil in these conflict tasks during withdrawal from ethanol or a benzodiazepine (File & Hitchcott, 1990) could be explained if flumazenil had a benzodiazepine agonist action or if it was antagonizing the effect of an endogenous compound with benzodiazepine-inverse agonist activity (File *et al.*, 1989; File & Hitchcott, 1990).

It is not known whether the reduced responding to ethanol in the avoidance task observed during withdrawal from chronic-ethanol treatment would be attenuated by flumazenil, as has been demonstrated in another conflict task (File *et al.*, 1989). For this reason, the present investigation examined (1) the effect of the benzodiazepine antagonist, flumazenil, alone and on the action of an acute dose of ethanol in rats performing the avoidance procedure, (2) the effect of varying doses of flumazenil and ethanol on shuttle-box avoidance responses following withdrawal from chronic ethanol treatment; (3) whether a benzodiazepine-inverse agonist would produce a deficit in the acquisition of the avoidance response; (4) the action of ethanol and flumazenil on the deficit produced by a benzodiazepine-inverse agonist in the avoidance task, and (5) the possibility that the anticonflict action of flumazenil was due to a benzodiazepine agonist-like action of this drug. From these data, it could be assessed whether findings were consistent with the hypothesis of File *et al.* (1989) that an endogenous compound with benzodiazepine-inverse agonist properties is responsible for the deficit in the anticonflict action of ethanol during withdrawal from chronic-ethanol treatment (Criswell & Breese, 1989; 1990).

Some of these data were presented in abstract form at the annual Research Society on Alcoholism meeting (Criswell & Breese, 1990).

[1] Author for correspondence.

Methods

Animals

Male Sprague-Dawley rats weighing 250 to 275 g were obtained from Charles River Laboratories (Raleigh, NC, U.S.A.). The animals were maintained in our animal facilities until they reached 350 to 550 g. Rats were in the animal facility for at least two weeks before being used. The rats were housed individually with a 12 h light-dark cycle and allowed free access to food and water or a liquid diet as described below.

Shuttle-box avoidance task

The functional response measured in this investigation was the rate of acquisition of a two-way shuttle-box avoidance procedure, with a tone as the warning stimulus (Criswell & Breese, 1989). For the experimental procedure, each rat was allowed a 5 min adaptation period prior to avoidance training after being placed in a shuttle-box (Lehigh Valley Electronics). Following this adaptation period, the onset of a tone signalled the beginning of a 10 s avoidance period during which the animals could shuttle to the opposite side of the cage to avoid a 0.7 m footshock. Failure to respond within the 10 s period resulted in shock onset. Footshock was terminated when the animals moved to the far side of the cage (escaped) or at the end of a 5 s period. Avoidance of the shock or shock termination initiated a 30 s intertrial interval. Data were collected for 100 trials with the number of avoidance responses, escapes from shock, crosses during the intertrial interval, and response omissions (failure to escape within 5 s) recorded at the end of each 25 trial block for analysis. During the first few training trials, some rats made responses during the avoidance period before having received their first shock; therefore, data were analysed only for the last 75 trials out of the 100 trial session. Since the avoidance task does not require food and water deprivation, the behavioural consequences of chronic exposure to ethanol in a liquid diet can be assessed (Criswell & Breese, 1989).

In the latter portions of this investigation, we encountered a shift in the number of untreated rats exhibiting low rates of avoidance responding during acquisition. Rech (1966) and Fernandez-Teruel *et al.* (1991a,b) have described such differences within populations of rats. This has been described as a 'batch' effect by File & Hitchcott (1990). Therefore, we initiated a screening programme as new batches of rats ($n = 36$) were acquired from the supplier, whereby 4 to 6 animals were tested without drug prior to being assigned to an experiment. Only batches of rats from which this screen produced a mean of 30 or fewer avoidance responses during the last 75 trials were used to evalute the actions of ethanol and flumazenil. A possible 'floor' effect was avoided with treatments which were expected to produce a negative action on avoidance responding by choosing batches of rats with a mean of 45 avoidance responses or greater during acquisition. Rats with such high response scores were used to examine the action of a benzodiazepine inverse agonist, RO-15-4513, in the avoidance task and to evaluate performance in the avoidance task of a group withdrawn from chronic ethanol administration. The rats given saline or liquid diet with each experiment provided a cross-validation of our original measure of acquisition of the task (i.e. screen) for appointment to the appropriate experimental protocol.

Aerial righting

The impairment of aerial righting induced by ethanol in the presence or absence of chlordiazepoxide or flumazenil was measured by the modified procedure of Leitch *et al.* (1977) described by Frye & Breese (1982). The animals were held upside down by grasping the back of the neck and tail and dropped onto a soft surface (i.e. a foam rubber pad). Landing on all four feet on two consecutive releases was considered a successful trial. The distance from the back of the rat to the foam rubber pad was the measured height. A control rat is able to demonstrate aerial righting at a height of approximately 5 cm. Rats treated with ethanol or chlordiazepoxide were not released from heights above 50 cm.

Drugs and treatments

Ethanol (Aaper Alcohol and Chemical Co., Shelbyville, KY, U.S.A.) was administered i.p. as a 10% (weight-volume) solution in saline. This concentration minimizes the irritating effects of the ethanol. Chlordiazepoxide (Hoffman LaRoche, Nutley, NJ, U.S.A.) was dissolved in saline and administered i.p. (1 ml kg^{-1} volume). Ethanol was administered chronically by making a nutritionally complete liquid diet containing ethanol available to the rats as previously described (Frye *et al.*, 1981). Control rats received liquid diet with the ethanol replaced by an equicaloric amount of dextrose. For the experiments involving 12-day exposure to chronic ethanol, all animals were habituated to the control liquid diet for 2 days. On day 3, a diet containing 5% ethanol was substituted for the control liquid diet in the experimental group. After 2 days, the concentration of ethanol was increased to 7.5% and 2 days later to 10% where it remained for 8 days. Control animals were limited to 70 ml day^{-1} of liquid diet. Animals drinking the ethanol-liquid diet ingested 11.6 ± 0.7 g kg^{-1} day^{-1}. This diet regimen results in similar weight gains for the two groups (Frye *et al.*, 1981). Whereas the chronic-ethanol treated rats exhibit tremors and irritability to handling, they did not have spontaneous seizures or seizures to the sound exposure in the avoidance task.

Following chronic exposure of the rats to control liquid diet or ethanol-containing liquid diet, the diet was removed and replaced by lab-chow. After 7–9 h of withdrawal from the ethanol-containing or control-liquid diets, treated and control rats were given saline or various doses of ethanol, i.p. This protocol demonstrated tolerance to acute action of ethanol in the avoidance task in the rats withdrawn from chronic treatment (Criswell & Breese, 1989). Additional rats received saline or various doses of flumazenil (RO 15-1788; Hoffmann-La Roche Pharmaceutical Co., Nutley, NJ. U.S.A.), either alone or 5 min prior to ethanol. In other experiments to evaluate the agonist properties of flumazenil, either flumazenil or chlordiazepoxide (Hoffmann-La Roche Pharmaceutical Co.) were given alone or in combination with ethanol and the effect of these drug treatments on aerial righting was evaluated. The benzodiazepine-inverse agonist RO-15-4513 (ethyl 8-azido-5,6-dihydro-5 methyl-6-oxo-4H-imidazo[1,5-a][1,4]benzodiazepine-3-carboxylate; Hoffmann-La Roche Pharmaceutical Co.) was suspended in 0.25% carboxylmethylcellulose and injected i.p.

Statistics

Total number of avoidance responses, response omissions, intertrial interval crosses during the last 75 trials of a 100 trial session (see avoidance task) and aerial righting distance were analysed by ANOVA (Winer, 1962). Individual means were compared to controls using the Dunnett test (Winer, 1962).

Results

Effects of flumazenil on the response to acutely administered ethanol in the avoidance task

In agreement with previous work (Frye & Breese, 1981; Criswell & Breese, 1989), an acute dose of ethanol caused an increase in avoidance responding in rats treated with control-liquid diet (Figure 1). Flumazenil pretreatment did not block

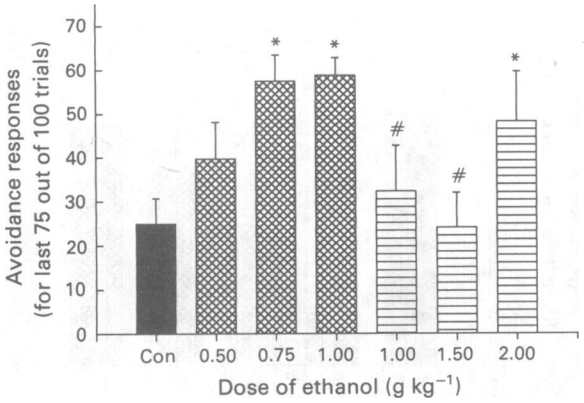

Figure 1 Dose-response effects of ethanol on acquisition of a two-way shuttle-box avoidance response following withdrawal from control or ethanol-liquid diet. The solid column (■) refers to a control (Con) group which was formed from rats that received ethanol-liquid diet or control-liquid diet, after it was established that there was no difference in the responses for these groups ($P>0.05$); (▩) refer to groups of rats that received various doses of acutely administered ethanol (0.5, 0.75, 1.0 g kg^{-1}) during withdrawal from control-liquid diet; (▤) refer to groups of rats that were tested with various doses of ethanol (1.0, 1.5, 2.0 g kg^{-1}) during withdrawal from ethanol-containing liquid diet administered for 12 days. Ethanol was administered 10 min prior to behavioural testing. There were no differences in the number of response omissions or intertrial crosses between groups ($P>0.1$). The mean ± s.e.mean of 5 to 10 rats are shown for each dose of ethanol. *$P<0.05$ when compared to saline control. †$P<0.05$ when compared to the response to 1 g kg^{-1} of ethanol in the CLD group.

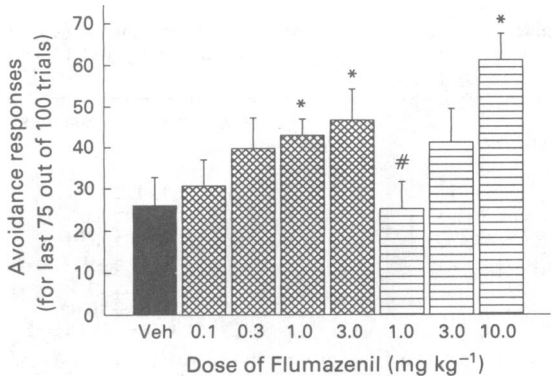

Figure 2 Effect of increasing doses of flumazenil on acquisition of an avoidance task in control rats and in rats following withdrawal from 12 days on an ethanol-liquid diet. Responses to vehicle in rats that received either control diet or ethanol-liquid diet were not significantly different ($P>0.05$) and were combined (Veh). This group is designated (■). Other rats that received 12 days of a control-liquid diet were given various doses of flumazenil (Flu) and are referred to by (▩). Rats treated for 12 days on an ethanol-liquid diet and then withdrawn are designated by (▤). Each dose of flumazenil or vehicle was administered i.p. 5 min prior to testing. n for all groups was from 8 to 13, except for the 1 mg kg^{-1} CLD group ($n=28$) and the 10 mg kg^{-1} ELD group ($n=6$). There were no differences in response omissions between groups ($P>0.05$) and only the 3 mg kg^{-1} group in the untreated group showed a greater number of intertrial crosses than did controls ($P<0.05$). Each value and bar represent the mean ± s.e.mean. *$P<0.05$ when compared to the Veh group. †$P<0.05$ when compared to the CLD-Flu 1.0 mg kg^{-1} group.

Table 1 Effect of flumazenil on the ethanol-induced facilitation of the acquisition of an avoidance task in control rats*

Treatment	*Drug doses* (mg kg^{-1})	*Avoidance responses* (n/75 trials)	n
Vehicle	–	31 ± 6	12
Flumazenil	3	47 ± 7*	11
Ethanol	1	56 ± 5*	11
Ethanol + flumazenil	1 + 3	59 ± 5*	11

*Flumazenil (Flu; 3 mg kg^{-1}) was administered i.p 5 min prior to testing. Ethanol (EtOH; 1 g kg^{-1}) was administered 10 min prior to testing. No antagonism of the response to ethanol was observed when the two drugs were co-administered (Et + Flu; $P>0.1$). There were no differences in response omissions between the groups ($P>0.05$) and only the Et + Flu group showed a greater number of intertrial crosses than the control group ($P<0.05$). n = number. *$P<0.05$ when compared to vehicle control.

the facilitated avoidance responding produced by ethanol (Table 1), indicating that blockade of benzodiazepine receptors does not affect the ethanol-induced increase in avoidance responding. However, flumazenil itself produced a significant increase in avoidance responding (Table 1; Figure 2), demonstrating that flumazenil induces the same behavioural action in this task as ethanol and chlordiazepoxide (Criswell & Breese, 1989). The dose-response effect of flumazenil in the avoidance task was shallow (Figure 2).

Effect of flumazenil and ethanol in rats withdrawn from chronic ethanol treatment

Chronic-ethanol treatment for 12 days antagonized the acute action of ethanol in the avoidance task for doses of ethanol up to 1.5 g kg^{-1} (Figure 1). A higher dose of ethanol (2 g kg^{-1}) was able to overcome the reduced responses observed for lower doses of ethanol in the avoidance task during withdrawal from chronic-ethanol treatment (Figure 1). Additionally, Figure 2 shows that 12 days on the chronic ethanol-liquid diet also reduced the usual facilitation of avoidance responding by 1 mg kg^{-1} of flumazenil. As observed when the dose of ethanol was increased, this reduced effectiveness of flumazenil during withdrawal was overcome if the dose of flumazenil was increased to 10 mg kg^{-1} (Figure 2).

Effect of the benzodiazepine-inverse agonist R0-15-4513 on avoidance responding and reversal by flumazenil and ethanol

Various doses of R0-15-4513, a benzodiazepine-inverse agonist (Mereu *et al.*, 1987; Bonetti *et al.*, 1989; Mehta & Ticku, 1989) were administered to groups of rats chosen for their rapid acquisition of this avoidance response (see Methods). In these rats, R0 15-4513 decreased acquisition of the avoidance response in a dose-related fashion (Figure 3). Conversely, the deficit in avoidance responding produced by RO 15-4513 could be overcome in a dose-related fashion by flumazenil (Table 2). As expected, ethanol also antagonized the reduced avoidance responding produced by RO-15-4513 (Figure 4). Due to a probable 'ceiling effect', ethanol and flumazenil alone had no significant action on avoidance responding in these rats ($P>0.1$; data not shown).

However, we did establish that RO 15-4513 induced a significant deficit in rats with intermediate levels of responding (data not shown), indicating that this action of RO 15-4513 is not dependent upon the performance level of the animals.

The effect of ethanol withdrawal on acquisition of avoidance responding also was examined in a group of rats selected for rapid acquisition of the avoidance response. A significant reduction in responding was observed in these rats during withdrawal from 12 days of chronic-ethanol exposure (chronic ethanol-liquid diet = 41.0 ± 8.5 avoidance response/last 75 trials vs control-liquid diet = 63.6 ± 2.8 avoidance responses/last 75 trials; $P<0.05$). Thus, a behavioural response like that for RO-15-4513 was observed during acute withdrawal from the chronic-ethanol treatment in these rats that had high avoidance response scores during acquisition.

Table 2 Effect of flumazenil (Flu) on the deficit in acquisition of an avoidance task produced by RO-15-4513 (RO) in control rats*

Treatments	*Drug doses*	*Avoidance responses* (*n*/75 trials)	n
Veh	0	41.1 ± 4.1	17
Flumazenil (Flu)	1	48.1 ± 5.6	8
RO-15-4513 (RO)	1	16.3 ± 5.9†	7
Flu + RO	0.3 + 1	11.2 ± 4.1	4
Flu + RO	0.6 + 1	32.0 ± 13.7	5
Flu + RO	1.0 + 1	43.3 ± 10.0*	6

*Rats were taken from groups shown to aquire a two-way shuttle box avoidance response (see Methods). Various doses of flumazenil (Flu, 0.3, 0.6 and 1 mg kg^{-1}) were administered i.p. just prior to rats receiving 1 mg kg^{-1} of RO-15-4513 (RO) which was 5 min before testing. The dose of ethanol is 1 g kg^{-1}. There were no differences in response omissions or intertrial crosses between the group ($P<0.1$). '0' under drug doses indicates that no drug was administered. See Figure 3 for deficit in responding during acquisition of the avoidance response for RO-15-4513. n = number.
†$P<0.05$ when compared to vehicle.
*$P<0.05$ when compared to RO-15-4513.

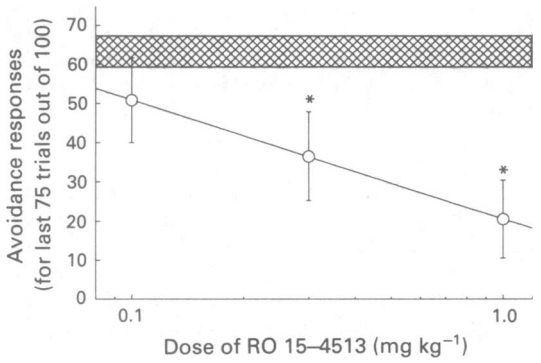

Figure 3 Dose response curve for the effect of RO 15-4513 on acquisition of an avoidance task. Naive rats were selected from a group which had been shown to make a high number of avoidance responses (see Methods). (○) Is the dose-response curve for RO 15-4513; points show mean ± s.e.mean for 6 rats. The vehicle response in the avoidance task is illustrated by the cross-hatched bar above the curve (vehicle response ± s.e.mean). Vehicle or RO 15-4513 were injected i.p. 5 min prior to testing. There were no differences in the number of response omissions or intertrial crosses between groups ($P>0.05$). *$P<0.05$ when compared to vehicle treatment.

Interactions of flumazenil with ethanol and chlordiazepoxide on aerial righting

The possibility that flumazenil possessed benzodiazepine agonist properties was tested by comparing the action of the benzodiazepine, chlordiazepoxide, to increase ethanol sedation to any change in sedation produced by flumazenil when combined with ethanol. In accordance with previous studies (Barthalmus *et al.*, 1978; Okamoto *et al.*, 1985), chlordiazepoxide enhanced the ethanol-induced deficit in aerial righting (Figure 5). Subsequently, it was reasoned that if flumazenil had a benzodiazepine agonist action, flumazenil, like chlordiazepoxide, would enhance the deficit in aerial righting produced by ethanol. The effects of flumazenil on the deficit in aerial righting produced by ethanol and chlordiazepoxide are shown in Figure 6. Flumazenil had no action in this task either to block or augment the action of ethanol (Figure 6). On the other hand, flumazenil (3 mg kg^{-1}) blocked the aerial righting deficit produced by 10 mg kg^{-1} of chlordiazepoxide (Figure 7). Furthermore, flumazenil (3 mg kg^{-1}) blocked the

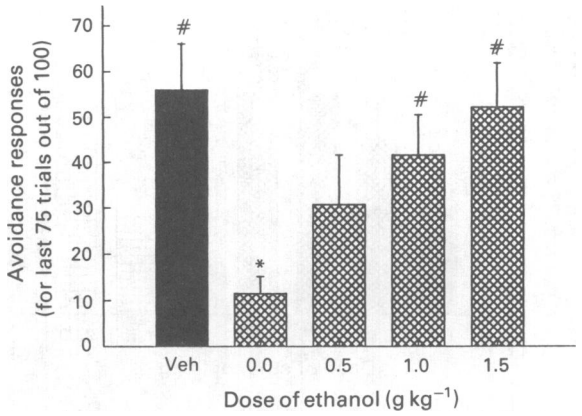

Figure 4 Reversal by ethanol of the effect of RO 15-4513 on performance in the shuttle-box avoidance task. The control group (no drug) which received only vehicle (Veh) 5 min prior to testing is designated by (■). Various doses of ethanol, (▩) were administered 5 min before 1 mg kg^{-1} of RO 15-4513 to a group of rats that readily acquired the avoidance response (see Methods). Testing began 5 min after administration of RO 15-4513 (1.0 mg kg^{-1}). The group designated as the 0.0 dose of ethanol in the column with cross-hatches received vehicle plus RO-15-4513. There were no differences in the number of response omissions or intertrial crosses between the drug-treated and control groups ($P>0.05$). The mean ± s.e.mean of 4–6 rats are shown for each dose. Ethanol (1 g kg^{-1}) alone did not produce a significant change from vehicle (see text). *$P<0.05$ when compared to vehicle alone (Veh). †$P<0.05$ when compared to RO-15-4513 alone designated to the 0.0 dose.

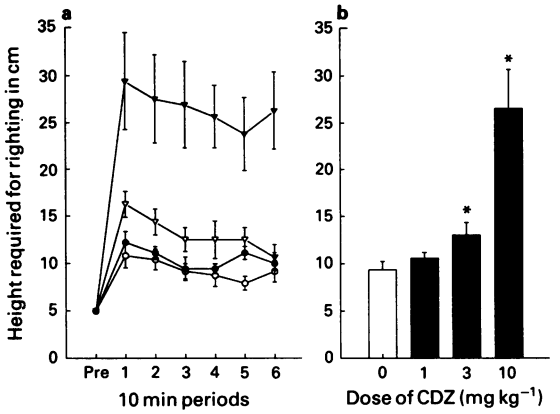

Figure 5 Dose-response relationship for enhancement by chlordiazepoxide (CDZ) of the ethanol-induced aerial-righting deficit. (a) Shows the mean ± s.e.mean of height required for righting for each 10 min period: (○) group that received ethanol alone; (●) group that received ethanol and 1 mg kg^{-1} of CDZ; (▽) group that received ethanol plus 3 mg kg^{-1} of CDZ; (▼) group that received ethanol plus 10 mg kg^{-1} of CDZ. Chlordiazepoxide (1, 3 or 10 mg kg^{-1}) was administered 5 min prior to ethanol (1.5 g kg^{-1}) administration. Aerial righting was assessed every 10 min for 1 h. Rats given only saline have scores of approximately 5 cm (Frye & Breese, 1982), as designated by Pre in (a). The columns in (b) depict the mean ± s.e.mean score for aerial righting scores for the rats in (a) for the total time period (1 h): (□) group that received only ethanol; (■) are the three doses of CDZ (1, 3 and 10 mg kg^{-1}). The score for aerial righting observed after 10 mg kg^{-1} of chlordiazepoxide (CDZ) alone is presented in Figure 6. Each group consisted of 8 to 12 rats. *$P<0.05$ when compared to ethanol alone.

increased deficit in aerial righting produced by chlordiazepoxide when administered to rats given ethanol (Figure 7). Thus, flumazenil continued to act as a benzodiazepine antagonist when given with only chlordiazepoxide as well as when chlordiazepoxide and ethanol were combined. Consequently, these results provide evidence that flumazenil is not acting as a benzodiazepine agonist at the doses used in the avoidance task but acts only as a benzodiazepine antagonist.

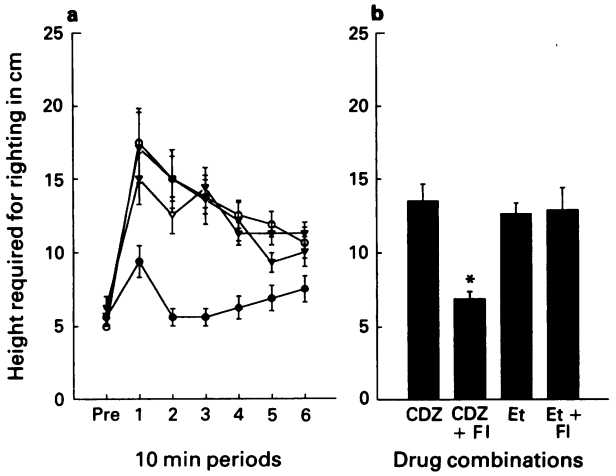

Figure 6 Effect of flumazenil on the aerial-righting deficit induced by chlordiazepoxide or ethanol. (a) Shows the mean ± s.e.mean aerial-righting score for 4 groups of 8 rats tested every 10 min for 1 h. Flumazenil (Fl, 3 mg kg^{-1}) was administered 5 min prior to either chlordiazepoxide (CDZ; 10 mg kg^{-1}) or ethanol (Et, 1.5 g kg^{-1}). Control data (Pre) were obtained immediately prior to drug administration; and (○) group that received CDZ; (▽) refers to the group that received only ethanol; (●) group that received CDZ plus flumazenil, and (▼) group that received ethanol and flumazenil. (b) The columns in this panel shown the mean ± s.e.mean aerial righting score for the accumulated 1 h period for each of the drug combinations in (a). These groups include CDZ, Et, CDZ + Fl, and Et + Fl as noted under the columns. Flumazenil alone did not affect aerial righting in untreated rats ($P > 0.1$). *$P < 0.05$ when compared to the chlordiazepoxide-treated group.

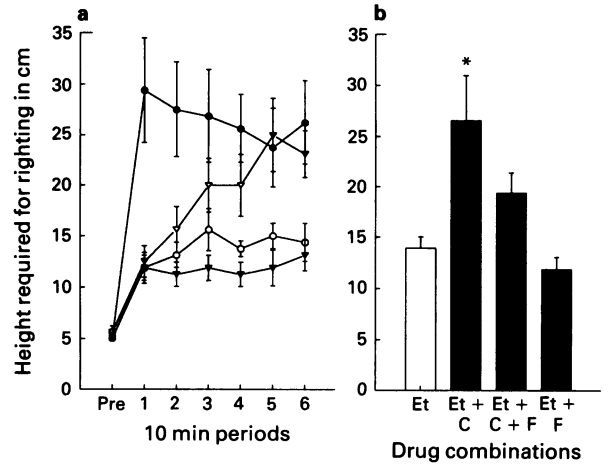

Figure 7 Effect of flumazenil on the chlordiazepoxide enhancement of ethanol-induced aerial-righting deficit. (a) Shows the mean ± s.e.mean aerial righting scores every 10 min for rats given ethanol (Et, 1.5 g kg^{-1}) 5 min after the following treatments were administered: saline (○, ethanol alone); ethanol plus 10 mg kg^{-1} chlordiazepoxide (●), ethanol plus 3 mg kg^{-1} of flumazenil (▼) or ethanol with both flumazenil and chlordiazepoxide (▽). Flumazenil blocked the enhancement of the ethanol-induced aerial-righting deficit by CDZ for the first 20 min ($P < 0.05$), but did not block the action of ethanol alone. (b) The columns show mean ± s.e.mean aerial righting score for the accumulated 1 h test period for each group in (a); (□) is for ethanol (Et) alone. The ■ are for the following groups: ethanol plus CDZ (Et + C); ethanol plus flumazenil (Et + F), and ethanol plus CDZ plus flumazenil (Et + C + F). Flumazenil alone did not affect aerial righting in untreated rats ($P > 0.1$). Eight rats were tested in each group. *$P < 0.05$ when compared to ethanol alone.

Discussion

Ethanol can facilitate acquisition of a two-way shuttle-box avoidance response (Frye & Breese, 1981; Criswell & Breese, 1989). This facilitatory effect of ethanol on avoidance responding has previously been cited as an indication that ethanol and chlordiazepoxide exhibit a type of anticonflict action in this task (Gray, 1977; Criswell & Breese, 1989; Fernandez-Teruel *et al.*, 1991a,b), similar to that seen in the acute lick suppression paradigm where shock suppressed licking is enhanced by these drugs (Vogel *et al.*, 1971; 1980). While motor stimulants such as (+)-amphetamine can facilitate avoidance responding (Rech *et al.*, 1966), the effect of ethanol in the avoidance task cannot be attributed to enhanced locomotion, because no dose of ethanol causes an increased locomotion in our Sprague-Dawley rats (unpublished data; Frye & Breese, 1981; Criswell & Breese, 1989). In the present work, tolerance to the action of ethanol in facilitating avoidance responding was observed during withdrawal from 12 days of chronic-ethanol treatment (i.e. liquid diet containing ethanol), replicating our previous findings (Criswell & Breese, 1989). In an earlier study, tolerance to ethanol during withdrawal from chronic ethanol treatment was accompanied by cross-tolerance to the action of a benzodiazepine in this task (Criswell & Breese, 1989). Tolerance to the anticonflict action of ethanol during withdrawal from chronic ethanol treatment also has been reported by File *et al.* (1989). Furthermore, an anxiogenic response has been observed in these behavioural tasks during withdrawal from chronic administration of both ethanol and benzodiazepines (Baldwin & File, 1987; File *et al.*, 1989; File & Hitchcott, 1990; Baldwin *et al.*, 1991). This series of studies suggested that there was a link between the tolerance to the anticonflict action of ethanol during withdrawal from chronic-ethanol treatment and benzodiazepine receptor mechanisms.

Flumazenil, a benzodiazepine antagonist, has been reported to reduce the anxiogenic response associated with withdrawal from chronic benzodiazepine or ethanol administration (Baldwin & File, 1987; File *et al.*, 1989; File & Hitchcott, 1990), as does ethanol (Figure 2). Nevertheless, unlike a benzodiazepine or ethanol (Frye *et al.*, 1980; 1983), flumazenil does not prevent the majority of symptoms associated with the ethanol-withdrawal syndrome (Little *et al.*, 1985; Adinoff *et al.*, 1986; Chan *et al.*, 1991). Furthermore, flumazenil did not reduce the acute action of ethanol in the avoidance task in control rats, indicating that this action of ethanol was not due to a direct action on benzodiazepine receptors. However, this investigation demonstrated that flumazenil facilitated acquisition of the avoidance response in control rats. This behavioural response exhibited by flumazenil resembled that seen after administration of ethanol or a benzodiazepine (Criswell & Breese, 1989).

Based on results obtained with flumazenil, File *et al.* (1989) proposed the hypothesis that tolerance to the anticonflict action of ethanol during withdrawal from chronic-ethanol treatment was related to an increase in an endogenous substance acting as a benzodiazepine-inverse agonist. Therefore, one purpose of the present investigation was to determine if flumazenil would affect tolerance to the anticonflict action of ethanol in the avoidance task during withdrawal, as had been noted in another conflict task (File *et al.*, 1989). During withdrawal from 12 days of chronic-ethanol treatment, the facilitated responding in the avoidance task following 1 mg kg^{-1} of flumazenil was reduced to levels observed in rats given vehicle (i.e. tolerance like that observed to ethanol and chlordiazepoxide after chronic ethanol exposure). Administration of a higher dose of flumazenil during withdrawal from chronic ethanol treatment reinstated responding to a level similar to that observed when a lower dose of flumazenil was administered to rats receiving control liquid diet. As noted for flumazenil, increasing the dose of ethanol also overcame the tolerance observed following withdrawal from chronic ethanol treatment, providing additional evidence for similarities between ethanol and flumazenil in the avoidance task. While metabolic factors could contribute to the decreased response to ethanol after chronic-ethanol treatment (e.g. increased ethanol metabolism), a similar ex-

planation for the results with flumazenil seems unlikely. Two additional explanations for these data would be that flumazenil was antagonizing the action of an endogenous substance acting as a benzodiazepine-inverse agonist (i.e. as suggested by File *et al.*, 1989) or that flumazenil was acting as a benzodiazepine agonist to produce an anticonflict action in the avoidance task.

With the logic that an endogenous benzodiazepine inverse agonist might be present during withdrawal, it was reasoned that, if withdrawal from chronic ethanol was increasing the presence of an endogenous benzodiazepine-inverse agonist, then administration of a benzodiazepine-inverse agonist like RO-15-4513 (Mereu *et al.*, 1987), should produce a deficit in responding in the avoidance task and this deficit should be antagonized by flumazenil. In rats chosen for their rapid acquisition of avoidance responding (see Methods), a dose-related deficit in acquisition of the avoidance response was noted after RO-15-4513 administration. This finding is consistent with other reports that benzodiazepine-inverse agonists produce deficits in behavioural tasks with a conflict component (Corda *et al.*, 1983; File & Pellow, 1984; Fernandez-Teruel *et al.*, 1991,a,b; Takada *et al.*, 1992). In earlier work, File & Lister (1983) reported that the anxiogenic response to a β-carboline in the social interaction test is blocked by flumazenil, just as it antagonizes the anticonflict action of a benzodiazepine (Barrett *et al.*, 1985). Ethanol as well as flumazenil effectively reversed the deficit in the avoidance task produced by RO 15-4513. This demonstration that doses of ethanol or flumazenil could antagonize RO-15-4513 in the avoidance task would predict that doses of both ethanol and flumazenil could be found that would produce an effect in tolerant animals like that seen in control rats. This in fact was the case. Since RO-15-4513 acts directly on $GABA_A$ receptors, ethanol could be enhancing γ-aminobutyric acid (GABA) responsiveness or acting through a parallel neural system to overcome the action of RO-15-4513 to reduce responding in the avoidance task. However, flumazenil reversal of both the effect of RO-15-4513 and the tolerance to the anticonflict action of ethanol observed in the avoidance task, seemed most likely to be due to a direct action on benzodiazepine receptors, an interpretation consistent with the hypothesis proposed by File *et al.* (1989). Nonetheless, we next examined the alternative possibility that flumazenil possessed benzodiazepine agonist activity to produce behavioural changes in the avoidance task (i.e. was having an agonist action on benzodiazepine receptors).

The possible agonist activity of flumazenil at the benzodiazepine receptor was supported by *in vitro* data in which high concentrations of flumazenil had been reported to possess a benzodiazepine-like agonist action (Skerritt & MacDonald, 1983; Mehta & Ticku, 1989). However, under most *in vivo* conditions, flumazenil has not been reported to exhibit the pharmacological properties of a benzodiazepine agonist (Crawley *et al.*, 1984; Barrett *et al.*, 1985; Koob *et al.*, 1986; Thomas *et al.*, 1990), including a discrimination task for a benzodiazepine (Pugh, *et al.*, 1992). Such a lack of behavioural action of flumazenil was observed in the present investigation when, unlike chlordiazepoxide, it did not affect the sedation induced by ethanol (i.e. did not affect the deficit in aerial righting induced by ethanol; Figure 6). Further, flumazenil not only blocked the deficit produced by chlordiazepoxide on aerial righting, but also antagonized the facilitation of the ethanol-induced aerial righting deficit produced by chlordiazepoxide. Thus, the present evaluation of flumazenil in combination with ethanol and chlordiazepoxide provided convincing evidence that, at doses used in the avoidance task, flumazenil possesses no discernible benzodiazepine agonist action, but rather is an effective benzodiazepine antagonist. Of course, this absence of an effect of flumazenil on aerial righting contrasts with the action of flumazenil to facilitate responding in the avoidance task. File & Hitchott (1990) as well as Fernandez-Teurel *et al.* (1991a,b) have implied that the circumstance under which behavioural measures are taken determine whether flumazenil will affect behaviour. Our present data are consistent with this view. Thus, the data collected in the avoidance task and the lack of evidence that flumazenil acts as a benzodiazepine agonist are in support of the view that an endogenous benzodiazepine-inverse agonist could be involved both in the general poor learning by rats in this behavioural paradigm (Fernandez-Teurel *et al.*, 1991a,b), as well as in the reduced anti-conflict action (i.e. tolerance) to ethanol and flumazenil in the avoidance task during withdrawal from chronic ethanol treatment (File *et al.*, 1989; File & Hitchcott, 1990).

Schatzkik *et al.* (1989) has provided evidence for an increased sensitivity of receptors for inverse agonists and decreased sensitivity of benzodiazepines following withdrawal from chronic lorazepam treatment. Similarly, Buck & Harris (1990) provided evidence that chronic ethanol administration densensitizes benzodiazepine receptors to agonist action while simultaneously increasing their sensitivity to inverse agonists. This change in benzodiazepine receptor function would be expected to produce behavioural changes similar to those observed in the present study, if a benzodiazepine-inverse agonist were to be present in brain to influence these sensitized receptors. However, in the latter study, the increase in sensitivity to a benzodiazepine-inverse agonist was observed after acute as well as chronic ethanol administration, suggesting that this change in receptor sensitivity is associated with acute ethanol tachyphylaxis. Tolerance to the effect of ethanol on shuttle-box avoidance acquisition is not observed until rats have been treated with ethanol for at least seven days (Criswell & Breese, 1989).

There have been nunerous attempts to isolate substances from brain that act on the benzodiazepine receptor (Braestrup *et al.*, 1980; Guidotti *et al.*, 1983; Peña *et al.*, 1986). It seem relatively clear that endogenous benzodiazepines exist in brain (Sangameswaran *et al.*, 1986; Wolfman *et al.*, 1991). Likewise, there are endogenous compounds which are purported to have properties of a benzodiazepine-inverse agonist (Guidotti *et al.*, 1983; Peña *et al.*, 1986; Novas *et al.*, 1988). Assuming that these endogenous compounds have an action in the brain, the absence of an effect of flumazenil in the aerial righting reflex would relate to a physiological state where little endogenous benzodiazepine agonist or inverse agonist were present in brain. Conversely, when rats are performing the avoidance task during withdrawal from chronic ethanol (i.e. aversive situation), the content of the endogenous benzodiazepine-inverse agonist in brain would be expected to increase to a greater degree than would be observed under normal conditions. As noted earlier, others have suggested that the behaviour conditions dictate whether flumazenil has an effect in a behavioural task (File & Hitchcott, 1990; Fernandez-Teurel *et al.*, 1991a,b). In any case, the similar actions of ethanol and flumazenil, in the absence of any evidence for a benzodiazepine agonist like action of flumazenil, provide support for the hypothesis that an endogenous benzodiazepine-inverse agonist is responsible for the reduced effectiveness of flumazenil and ethanol in the avoidance task following withdrawal from chronic-ethanol treatment (File *et al.*, 1989). The endogenous peptide, diazepam binding inhibitor (DBI), which was isolated from mammalian brain (Guidotti *et al.*, 1983), acts as a benzodiazepine inverse agonist (Ferrero *et al.*, 1984; 1986). This endogenous peptide is reportedly low during normal conditions, but is increased by stressful and anxiety producing situations (Ferrero *et al.*, 1988; Ferrarese *et al.*, 1991a,b). Consequently, defining the potential role of this endogenous peptide in the behavioural change in conflict behaviour in the avoidance task during withdrawal from chronic ethanol treatment would be a logical extension of our present investigation.

This work was supported by U.S. Public Health Services Grants AA-08024, HD-0331 and MH-33127. The authors acknowledge the excellent manuscript preparation by Ms Doris Lee.

References

ADINOFF, B., MAJCHROWICZ, E., MARTIN, P.R. & LINNOILA, M. (1986). The benzodiazepine antagonist RO 15-1788 does not antagonize the ethanol withdrawal syndrome. *Biol. Psychiatry*, **21**, 643–649.

BALDWIN, H.A. & FILE, S.E. (1987). Reversal of increased anxiety during benzodiazepine withdrawal: evidence for an anxiogenic endogenous ligand for the benzodiazepine receptor. *Brain Res. Bull.*, **20**, 603–606.

BALDWIN, H.A., RASSNICK, S., RIVIER, J., KOOB, G.F. & BRITTON, K.T. (1991). CRF antagonist reverses the 'amnogenic' response to ethanol withdrawal in the rat. *Psychopharmacol.*, **103**, 227–232.

BARRETT, J.E., BRADY, L.S. & WITKIN, J.M. (1985). Behavioral studies with anxiolytic drugs. I. Interactions of the benzodiazepine antagonist Ro 15-1788 with chlordiazepoxide, pentobarbital and ethanol. *J. Pharmacol. Exp. Ther.*, **233**, 554–559.

BARRY, H. III, WAGNER, S.A. & MILLER, N.E. (1963). Effects of several drugs on performance in an approach-avoidance conflict. *Psychol. Rep.*, **12**, 215–221.

BARTHALMUS, G.T., LEANDER, J.D. & MCMILLAN, D.E. (1978). Combined effects of ethanol and diazepam on performance and acquisition of serial position sequences by pigeons. *Psychopharmacology*, **59**, 101–102.

BONETTI, E.P., BURKARD, W.P., GABL, M., HUNKELER, W., LOREZ, H.-P., MARTIN, J.R., MOEHLER, H., OSTERRIEDER, W., PIERI, L., POLC, P., RICHARDS, J.G., SCHAFFNER, R., SCHERSCHLICHT, R., SCHOCH, P. & HAEFELY, W.E. (1989). Ro 15-4513, partial inverse agonism at the BZR and interaction with ethanol. *Pharmacol. Biochem. & Behav.*, **31**, 733–749.

BRAESTRUP, C., NIELSEN, M. & OLSEN, C.E. (1980). Urinary and brain β-carboline-3-carboxylates as potent inhibitors of brain benzodiazepine receptors. *Proc. Natl. Acad. Sci. U.S.A.*, **77**, 2288–2292.

BREESE, G.R., FRYE, G.D., VOGEL, R.A., MANN-KOEPKE, K. & MUELLER, R.A. (1983). Comparisons of behavioral and biochemical effects of ethanol and chlordiazepoxide. In *Stress and Alcohol Use* ed. Pohorecky, L.A. & Brick, J. pp. 261–276. Amsterdam: Elsevier Sci. Publ. Co. Inc.

BUCK, K.J. & HARRIS, R.A. (1990). Benzodiazepine agonist and inverse agonist actions of $GABA_A$ receptor-operated chloride channels. II. Chronic effects of ethanol. *J. Pharmacol. Exp. Ther.*, **253**, 713–719.

CHAN, A.W.K., LEONG, F.W., SCHANLEY, D.L., LANGAN, M.C. & PENETRANTE, F. (1991). Flumazenil (Ro 15-1788) does not affect ethanol tolerance and dependence. *Pharmacol. Biochem. Behav.*, **39**, 659–663.

CONGER, J.J. (1956). Alcoholism: theory, problem and challenge. Reinforcement theory and the dynamics of alcoholism. *J. Stud. Alc.*, **17**, 296–305.

CORDA, M.G., BLAKER, W.D., MENDELSON, W.B., GUIDOTTI, A. & COSTA, E. (1983). β-Carbolines enhance shock-induced suppression of drinking rats. *Proc. Natl. Acad. Sci. U.S.A.*, **80**, 2072–2076.

CRAWLEY, J.N., SKOLNICK, P. & PAUL, S.M. (1984). Absence of intrinsic antagonist actions of benzodiazepine antagonists on an exploratory model of anxiety in the mouse. *Neuropharmacology*, **23**, 531–537.

CRISWELL, H.E. & BREESE, G.R. (1989). A conflict procedure not requiring deprivation: evidence that chronic ethanol treatment induces tolerance to the anti-conflict action of ethanol and chlordiazepoxide. *Alcohol. Clin. Exp. Res.*, **13**, 680–685.

CRISWELL, H.E. & BREESE, G.R. (1990). Evidence for the involvement of an endogenous benzodiazepine-inverse agonist in the tolerance to the anticonflict action of ethanol. *Alcohol. Clin. Exp. Res.*, **14**, 279.

FERNANDEZ-TERUEL, A., ESCORIHUELA, R.M., NÚÑEZ, J.F., ZAPATA, A., BOIX, F., SALAZAR, W. & TOBEÑA, A. (1991a). The early acquisition of two-way (shuttle box) avoidance as an anxiety-mediated behavior: psychopharmacological validation. *Brain Res. Bull.*, **26**, 173–176.

FERNANDEZ-TERUEL, A., ESCORIHUELA, R.M., TOBENA, A. & DRISCOLL, P. (1991b). Stress and putative endogenous ligands for benzodiazepine receptors: the importance of characteristics of the aversive situation and of differential emotionality in experimental animals. *Experientia*, **47**, 1051–1056.

FERRARESE, C., MENNINI, T., PECORA, N., GOBBI, M., APPOLLONIO, I., BERNASCONI, P., FRIGO, M., REGONDI, C., PIERPAOLI, C., FRATTOLA, L. & GARATTINI, S. (1991a). Acute noise stress in rats increases the levels of diazepam binding inhibitor (DBI) in hippocampus and adrenal gland. *Psychopharmacology*, **103**, 339–342.

FERRARESE, C., MENNINI, T., PECORA, N., PIERPAOLI, C., FRIGO, M., MARZORATI, C., GOBBI, M., BIZZI, A., CODEGONI, A., GARATTINI, S. & FRATTOLA, L. (1991b). Diazepam binding inhibitor (DBI) increases after acute stress in rat. *Neuropharmacology*, **30**, 1445–1452.

FERRERO, A., BENNA, P., COSTA, P., TARENZI, L., BAGGIO, G., BERGAMASCO, B. & BERGAMINI, L. (1988). Diazepam binding inhibitor-like immunoreactivity (DBI-LIK) in human CSF: correlations with neurological disorders. *J. Neurol. Sci.*, **87**, 327–349.

FERRORA, A., GUIDOTTI, A., CONTI-TRONCONI, B. & COSTA, E. (1984). A brain octadecaneuropeptide generated by tryptic digestion of DBI (diazepam binding inhibitor) functions as a pro-conflict ligand of benzodiazepine recognition sites. *Neuropharmacology*, **23**, 1359–1362.

FERRERO, P., SANTI, M.R., CONTI-TRONCONI, B., COSTA, E. & GUIDOTTI, A. (1986). Study of an octadecaneuropeptide derived from diazepam binding inhibitor (DBI) biological activity and presence in rat brain. *Proc. Natl. Acad. Sci. U.S.A.*, **83**, 827–831.

FILE, S.E., BALDWIN, H.A. & HITCHCOTT, P.K. (1989). Flumazenil but not nitrendipine reverses the increased anxiety during ethanol withdrawal in the rat. *Psychopharmacology*, **98**, 262–264.

FILE, S.E. & HITCHCOTT, P.K. (1990). A theory of benzodiazepine dependence that can explain whether flumazenil will enhance or reverse the phenomena. *Psychopharmacology*, **101**, 525–532.

FILE, S.E. & LISTER, R.G. (1983). Interactions of ethyl-β-carboline-3-carboxylate and Ro 15-1788 with CGS 8216 in an animal model of anxiety. *Neurosci. Lett.*, **39**, 91–94.

FILE, S.E. & PELLOW, S. (1984). FG 7142, a β-carboline, has an anxiogenic action in the social interaction test. *Br. J. Pharmacol.*, **82**, 240.

FRYE, G.D. & BREESE, G.R. (1981). An evaluation of the locomotor stimulating action of ethanol in rats and mice. *Psychopharmacology*, **73**, 17–22.

FRYE, G.D. & BREESE, G.R. (1982). GABAergic modulation of ethanol-induced motor impairment. *J. Pharmacol. Exp. Ther.*, **223**, 750–756.

FRYE, G.D., MCCOWN, T.J. & BREESE, G.R. (1983). Differential sensitivity of ethanol withdrawal signs in the rat to GABA-mimetics: blockade of audiogenic seizures but not forelimb tremors. *J. Pharmacol. Exp. Ther.*, **226**, 720–725.

FRYE, G.D., CHAPIN, R.E., VOGEL, R.A., MAILMAN, R.B., KILTS, C.D., MUELLER, R.A. & BREESE, G.R. (1981). Effects of acute and chronic 1,3-butanediol treatment on central nervous system function: a comparison with ethanol. *J. Pharmacol. Exp. Ther.*, **216**, 306–314.

FRYE, G.D., VOGEL, R.A., MAILMAN, R.B., ONDRUSEK, M.G., WILSON, J.H., MUELLER, R.A. & BREESE, G.R. (1980). A comparison of behavioural and neurochemical effects of ethanol and chlordiazepoxide. In *Alcohol and Aldehyde Metabolizing Systems*. Vol. IV. ed. Thurman, R.D. pp. 727–737. New York: Plenum Publishing Corp.

GRAY, J.A. (1977). Drug effects on fear and frustration: possible limbic site of action of minor tranquillizers. In *Handbook of Psychopharmacology* Vol. 8, ed. Iversen, L.L., Inversen, S.D. & Snyder, S.H. pp. 433–529. New York: Plenum Publishing Corp.

GUIDOTTI, A., FORCHETTI, C., CORDA, M.G., KONKEL, D., BENNETT, C.D. & COSTA, E. (1983). Isolation, characterization, and purification to homogeneity of an endogenous polypeptide with agonistic action on benzodiazepine receptors. *Proc. Natl. Acad. Sci. U.S.A.*, **80**, 3531–3535.

KOOB, G.F., BRAESTRUP, C. & THATCHER-BRITTON, K. (1986). The effects of FG 7142 and Ro 15-1788 on the release of punished responding produced by chlordiazepoxide and ethanol in rat. *Psychopharmacology*, **90**, 173–178.

LEITCH, G.J., BARKES, D.J., SIEGMANN, F.S. & GUTHRIE, G.D. (1977). Possible role of GABA in the development of tolerance to alcohol. *Experientia*, **33**, 496–497.

LITTLE, H.J., TAYLOR, S.C., NUTT, D.J. & COWEN, P.J. (1985). The benzodiazepine antagonist, R0 15-1788 does not decrease ethanol withdrawal convulsions in rats. *Eur. J. Pharmacol.*, **107**, 375–377.

MANSFIELD, J.G., EATON, N.K., CUNNINGHAM, C.L. & BROWN, J.S. (1977). Ethanol and approach-avoidance conflict in the rat. *Physiol. Psychol.*, **5**, 175–203.

MEHTA, A.K. & TICKU, M.K. (1989). Benzodiazepine and beta-carboline interactions with $GABA_A$ receptor-gated chloride channels in mammalian cultured spinal cord neurons. *J. Pharmacol. Exp. Ther.*, **249**, 418–423.

MEREU, G., PASSINO, N., CARCANGIU, P., BOI, V. & GESSA, G.L. (1987). Electrophysiological evidence that R0 15-4513 is a benzodiazepine receptor inverse agonist. *Eur. J. Pharmacol.*, **135**, 453–454.

NOVAS, M.L., WOLFMAN, C., MEDINA, J.H. & DEROBERTIS, E. (1988). Proconvulsant and 'anxiogenic' effects of n-butyl-β-carboline-3-carboxylate, an endogenous benzodiazepine binding inhibitor from brain. *Pharmacol. Biochem. Behav.*, **30**, 331–336.

OKAMOTO, M., RAO, S.N., AARONSON, L.M. & WALEWSKI, J.L. (1985). Ethanol drug interaction with chlordiazepoxide and pentobarbitol. *Alcohol. Clin. Exp. Res.*, **9**, 516–521.

PEÑA, D., MEDINA, J.H., NOVAS, M.L., PALADINI, A.C. & DE ROBERTIS, E. (1986). Isolation and identification in bovine cerebral cortex of n-butyl-β-carboline-3-carboxylate, a potent benzodiazepine binding inhibitor. *Proc. Natl. Acad. Sci. U.S.A.*, **83**, 4952–4956.

RECH, R.H. (1966). Amphetamine effects on poor performance of rats in a shuttle-box. *Psychopharmacologia*, **9**, 110–117.

PUGH, S.L., BOONE, M.S. & EMMETT-OGLESBY, M.W. (1992). Tolerance, cross-tolerance and withdrawal in rats made dependent on diazepam. *J. Pharmacol. Exp. Ther.*, **262**, 751–758.

SANGAMESWARAN, L., FALES, H.M., FRIEDRICH, P. & DEBLAS, A.L. (1986). Purification of a benzodiazepine from bovine brain and detection of benzodiazepine-like immunoreactivity in human brain. *Proc. Natl. Acad. Sci. U.S.A.*, **83**, 9236–9240.

SCHATZKIK, A., LOPEZ, F., GREENBLATT, D.J., SHADER, R.I. & MILLER, L.G. (1989). Lorazepam discontinuation promotes 'inverse agonist' effects of benzodiazepines. *Br. J. Pharmacol.*, **98**, 451–454.

SKERRITT, J.H. & MACDONALD, R.L. (1983). Benzodiazepine Ro 15-1788: electrophysiological evidence for partial agonist activity. *Neurosci. Lett.*, **43**, 321–326.

THOMAS, D.A., WEISS, S.J. & SCHINDLER, C.W. (1990). Effects of chlordiazepoxide and flumazenil on preference for punished and unpunished response alternatives in rats. *Psychopharmacology*, **102**, 333–338.

TAKADA, K., BARRETT, J.E., ALLEN, M.S., COOK, J.M. & KATZ, J.L. (1992). Punishment of schedule-controlled behavior with β-carboline injections: antagonism and comparisons with other compounds. *J. Pharmacol. Exp. Ther.*, **261**, 138–145.

VOGEL, J.R., BEER, B. & CLODY, D.E. (1971). A simple and reliable conflict procedure for testing anti-anxiety agents. *Psychopharmacologia*, **21**, 1–7.

VOGEL, R.A., FRYE, G.D., WILSON, J.H., KUHN, C.M., KOEPKE, K.M., MAILMAN, R.B., MUELLER, R.A. & BREESE, G.R. (1980). Attenuation of the effects of punishment by ethanol: comparisons with chlordiazepoxide. *Psychopharmacology*, **7**, 123–129.

WINER, R.J. (1962). *Statistical Principles in Experimental Design*. New York: McGraw-Hill.

WOLFMAN, C., CUNHA, C. DA., JERUSALINSKY, D., LEVI DE STEIN, M., VIOLA, H., IZQUIERDO, I. & MEDIAN, J.H. (1991). Habituation and inhibitory avoidance training alter brain regional levels of benzodiazepine-like molecules and are affected by intracerebral flumazenil microinjection. *Brain Res.*, **548**, 74–80.

(Received March 29, 1993
Revised June 4, 1993
Accepted June 17, 1993)

Br. J. Pharmacol. (1993), **110**, 761–771

Pharmacological profile of valsartan: a potent, orally active, nonpeptide antagonist of the angiotensin II AT_1-receptor subtype

[1]Leoluca Criscione, Marc de Gasparo, Peter Bühlmayer, Steven Whitebread, Hans-peter R. Ramjoué & Jeanette Wood

Cardiovascular Research Department, Pharmaceuticals Division, CIBA-GEIGY Limited, CH-4002 Basel, Switzerland.

1 The pharmacological profile of valsartan, (S)-N-valeryl-*N*-{[2'-(1H-tetrazol-5-yl)biphenyl-4-yl]-methyl}-valine, a potent, highly selective, and orally active antagonist at the angiotensin II (AII) AT_1-receptor, was studied *in vitro* and *in vivo*.

2 Valsartan competed with [^{125}I]-AII at its specific binding sites in rat aortic smooth muscle cell membranes (AT_1-receptor subtype) with a K_i of 2.38 nM, but was about 30,000 times less active in human myometrial membranes (AT_2-receptor subtype).

3 In rabbit aortic rings incubated for 5 min with valsartan, at concentrations of 2, 20 and 200 nM, the concentration-response curve of AII was displaced to the right and the maximum response was reduced by 33%, 36% and 40%, respectively. Prolongation of the incubation time with valsartan to 1 h or 3 h, further reduced the maximum response by 48% or 59% (after 20 nM) and by 59% or 60% (after 200 nM) respectively. After 3 h incubation an apparent pK_B value of 9.26 was calculated. Contractions induced by noradrenaline, 5-hydroxytryptamine, or potassium chloride were not affected by valsartan. No agonistic effects were observed in the rabbit aorta at concentrations of valsartan up to 2 μM.

4 In bovine adrenal glomerulosa, valsartan inhibited AII-stimulated aldosterone release without affecting the maximum response (pA_2 8.4).

5 In the pithed rat, oral administration of valsartan (10 mg kg^{-1}) shifted the AII-induced pressor response curves to the right, without affecting responses induced by the electrical stimulation of the sympathetic outflow or by noradrenaline. Animals treated with valsartan 24 h before pithing also showed significant inhibition of the response to AII.

6 In conscious, two-kidney, one-clip renal hypertensive rats (2K1C), valsartan decreased blood pressure in a dose-dependent manner after single i.v. or oral administration. The respective ED_{30} values were 0.06 mg kg^{-1} (i.v.) and 1.4 mg kg^{-1} (p.o.). The antihypertensive effect lasted for at least 24 h after either route of administration. After repeated oral administration for 4 days (3 and 10 mg kg^{-1} daily), in 2K1C renal hypertensive rats, systolic blood pressure was consistently decreased, but heart rate was not significantly affected.

7 In conscious, normotensive, sodium-depleted marmosets, valsartan decreased mean arterial pressure, measured by telemetry, after oral doses of 1–30 mg kg^{-1}. The hypotensive effect persisted up to 12 h after 3 and 10 mg kg^{-1} and up to 24 h after 30 mg kg^{-1}.

8 In sodium-depleted marmosets, the hypotensive effect of valsartan lasted longer than that of losartan (DuP 753). In renal hypertensive rats, both agents had a similar duration (24 h), but a different onset of action (valsartan at 1 h, losartan between 2 h and 24 h).

9 These results demonstrate that valsartan is a potent, specific, highly selective antagonist of AII at the AT_1-receptor subtype and does not possess agonistic activity. Furthermore, it is an efficacious, orally active, blood pressure-lowering agent in conscious renal hypertensive rats and in conscious normotensive, sodium-depleted primates.

Keywords: Aldosterone; AT_1-receptor; human myometrium; hypertension; losartan; marmoset; pithed rat; rabbit aorta; renal hypertensive rats; telemetry; valsartan

Introduction

The octapeptide, angiotensin II (AII) which is formed from its precursor, the decapeptide angiotensin I, by the proteolytic action of the angiotensin-converting enzyme (ACE), has been shown to play a key role in the regulation of blood pressure and fluid and electrolyte homeostasis (for review see Hofbauer & Wood, 1986). Prevention of the formation of AII, via inhibition of ACE, has provided a powerful strategy for the treatment of hypertension and congestive heart failure (Ondetti *et al.*, 1977; Kramer *et al.*, 1983; CONSENSUS trial, 1987; Ondetti, 1991). Attempts to develop therapeutic agents capable of blocking AII at its receptor failed in the past, due to the antagonists being peptides that lacked oral activity (Pals *et al.*, 1979). In addition, saralasin, the most extensively investigated compound in this class, displayed unwanted agonistic properties (Pals *et al.*, 1971; Hofbauer *et al.*, 1976). More recently, starting from imidazole derivatives first described by Furukawa *et al.* (1982), it has been possible to identify and characterize specific, nonpeptide, AII-receptor antagonists (Duncia *et al.*, 1990; Carini *et al.*, 1990; Weinstock *et al.*, 1991; Bühlmayer *et al.*, 1991; Mantlo *et al.*, 1991).

Whitebread *et al.* (1989) first reported the existence of one subtype of AII receptor in vascular smooth-muscle cells, and a second in human uterus, while both subtypes were found in the rat and human adrenal glomerulosa, in rat uterus and

[1] Author for correspondence at: Ciba-Geigy Ltd, K 125.9.01, CH-4002 Basel, Switzerland.

human renal artery. Similar results, also relating to other tissues and species, have subsequently been reported (Chiu *et al.*, 1989; see also Smith *et al.*, 1992 for review). An international committee (Bumpus *et al.*, 1991) has proposed the designations AT_1 for the receptor subtype sensitive to DuP 753 (losartan), and AT_2 for the subtype sensitive to PD 123177 (Blankley *et al.*, 1991) and CGP 42 112 A (Whitebread *et al.*, 1989; 1991). The AT_1-receptor subtype is the one responsible for the well-known effects of AII, such as vasoconstriction, aldosterone and adrenaline release, water intake, and cellular proliferation (Criscione *et al.*, 1990; Herblin *et al.*, 1991; Timmermans *et al.*, 1991a; Chiu *et al.*, 1991c; Smith *et al.*, 1992), whereas the pathophysiological role of the AT_2-receptor subtype is not yet well understood (Criscione *et al.*, 1990; Herblin *et al.*, 1991; Dudley *et al.*, 1991; Timmermans *et al.*, 1991c). Recent reports, however, indicate that the AT_2 receptor does not interact with guanine-nucleotide-binding protein (Bottari *et al.*, 1991), but may stimulate tyrosine phosphatase activity (Bottari *et al.*, 1992).

Losartan (initially described as DuP 753), was the first orally active antagonist of the AT_1-receptor subtype (Timmermans *et al.*, 1990; Wong *et al.*, 1990d; Smith *et al.*, 1992). This compound is an efficacious antihypertensive agent in animals (Wong *et al.*, 1990a,d) and is also active in man (Christen *et al.*, 1991). The blood pressure-lowering effect of losartan in rats, however, depends partly on its conversion to the active, hepatically generated carboxylic acid metabolite, EXP3174, which is about 20 times more potent than the parent compound as an AT_1-receptor antagonist (Wong *et al.*, 1990c; Timmermans *et al.*, 1991b). The formation of an active metabolite in the liver is seen as a potential problem in predicting dosages of losartan for patients with impaired liver function (Wong *et al.*, 1991a). Moreover, the metabolism of losartan seems to differ in rats, monkeys, and man (Stearns *et al.*, 1992), and there are species-specific differences in its pharmacokinetics (Smith *et al.*, 1992).

The present paper describes the *in vitro* and *in vivo* pharmacological profile of valsartan, (known as CGP 48933), (S)-N-valeryl-*N*-{[2'-(1H-tetrazol-5-yl)biphenyl-4-yl]-methyl}-valine, (Figure 1). The novelty of this structure resides in the replacement of the heterocycle imidazole of losartan with a nonplanar, acylated amino acid. In some experiments *in vivo*, the effects of valsartan have been compared with those of losartan. A preliminary account of this work has been published as an abstract (Criscione *et al.*, 1992).

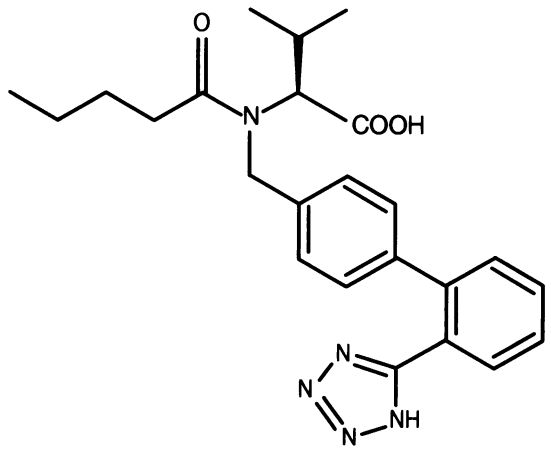

Figure 1 Chemical structure of valsartan, (S)-N-valeryl-*N*-{[2'-(1H-tetrazol-5-yl)biphenyl-4-yl]-methyl}-valine.

Methods

Binding of valsartan to the AII receptor of smooth muscle cells from rat aorta and human myometrium

A primary culture of rat aortic smooth muscle cells (SMC) was grown on Dulbecco's Minimum Essential Medium (DMEM) containing 4.5 g l^{-1} glucose and supplemented with 4 mM L-glutamine, 15% foetal calf serum and penicillin-streptomycin, 200 iu–200 μg ml^{-1}. At confluence, the cells were washed twice with phosphate-buffered saline (PBS) and harvested with a rubber policeman. They were homogenized (Polytron setting 8, 1 × 8 s) in 20 mM sodium bicarbonate and centrifuged for 30 min at 60,000 *g* in a Beckman centrifuge (L7-35). The pellet was resuspended in 50 mM Tris-HCl buffer, pH 7.4, containing 125 mM NaCl, 6.5 mM $MgCl_2$, 1 mM EDTA, and a cocktail of peptidase inhibitors (antipain, phosphoramidon, leupeptin, pepstatin, bestatin, amastatin, each at 1.25 μg ml^{-1}) with a tight-fitting teflon-pestle homogenizer. The membrane preparations were kept in aliquots at – 80°C until used; no apparent loss of AII-binding activity was seen under these conditions. Protein concentration was measured according to the method of Bradford (1976) using bovine serum albumin (BSA) as standard.

Human uteri were obtained from informed and consenting patients undergoing hysterectomy. The tissue was cut in small pieces, immediately frozen on dry ice and kept at – 80°C until required. It was homogenized in 20 mM sodium bicarbonate (Polytron setting 8, 3 × 8 s) and centrifuged at 600 *g* for 20 min at 4°C. The pellet was resuspended and treated similarly once more. The pooled supernatants were then centrifuged at 60,000 *g*, and the pellet was resuspended in buffer, as described above.

The experiments were performed using an automatic pipetting and filtration device (Filter-Prep 101, Ismatec, Zurich, Switzerland). Briefly, 20–30 μg protein was incubated at 25°C for 60 min with [^{125}I]-AII (175 pM) and varying concentrations of unlabelled competitors, dissolved in dimethylsulphoxide (DMSO); the final concentration of the latter in the incubation was 1%. The binding experiments were performed in the presence or absence of BSA (Chiu *et al.*, 1991a). The reaction was terminated by the addition of 2 ml ice-cold buffer. Bound and free radioactivities were separated by immediate filtration through Whatman GF/F filters, pretreated with 0.2% BSA in PBS, which were washed 3 times with 2 ml cold PBS. The radioactivity trapped on the filter was measured in a gamma counter (Pharmacia-LKB, Uppsala, Sweden) at 70% efficiency. Nonspecific binding was determined in the presence of 1 μM unlabelled AII. Degradation of the radioligands during the incubation was always less than 10%, as determined by thin layer chromatography, using the method described by Whitebread *et al.* (1991).

Functional antagonism, specificity, and potency of valsartan in rabbit isolated aortic rings

Rabbits (2–2.5 kg, Chinchilla, male, Dr K. Thomae, Germany) were killed by a blow to the neck and the descending thoracic aorta quickly removed. From each aorta, rings of 2–3 mm width were prepared and mounted between two parallel hooks under an initial resting tension of 2.5 g. Thereafter, rings were immersed in a 20 ml tissue bath containing a modified Krebs-Henseleit solution of the following composition (mM): NaCl 119, KCl 4.8, $CaCl_2$ 2.53, $NaHCO_3$ 24.8, Mg_2SO_4 1.2, KH_2PO_4 1.2 and glucose 10; at 37°C, gassed with 95% O_2 and 5% CO_2. Each preparation was allowed to equilibrate for at least 1 h. Isometric responses were measured with a force transducer (K30, Hugo Sachs Electronics, Freiburg, Germany) coupled to a tissue-bath data-acquisition system (Buxco Electronics, Inc., Sharon, CT, U.S.A.). Data were analyzed with the Buxco digital computer

and a software package (Branch Technology, Dexter, MI, U.S.A.).

In a first series of experiments, contractions of rabbit aortic rings were induced with graded, cumulative concentrations of AII (Hypertensin CIBA), noradrenaline, 5-hydroxytryptamine (5-HT) or potassium chloride. Control rings were incubated with appropriate concentrations of the vehicle (DMSO). Valsartan or solvent was added to the organ-bath 5 min before the dose-response curves of the various vasoconstrictor agents were determined.

In a second series of experiments, contractions induced by graded, cumulative concentrations of AII were tested after the rings had been incubated with valsartan or solvent for 1 h or 3 h respectively.

Effects of valsartan on AII-induced aldosterone release in bovine adrenal glomerulosa cells

Bovine adrenal glands were obtained from a local slaughterhouse and processed within 45–60 min. Adrenals from 5–7 animals were collected and placed in ice-cold, potassium-free Medium 199 (Amimed, Muttenz, Switzerland). After removal of adherent fat, 0.5 mm-thick slices of capsular tissue with adherent glomerulosa tissue were cut with a Staddie-Riggs microtome. Glomerulosa tissue slices (about 8 g of tissue) were washed in three volumes of ice-cold, potassium-free Medium 199 with 0.4% BSA. The tissue was minced with scissors and incubated for 45 min at 37°C in 25 ml of potassium-free Medium 199, pH 7.3, containing 0.4% BSA, 10 mg ml^{-1} dispase and 25 $\mu g\ ml^{-1}$ DNase from bovine pancreas (Boehringer Grade II, Mannheim), under constant agitation at 150 r.p.m. in an atmosphere of 95% O_2/5% CO_2. Cells were dispersed by aspirating and expelling tissue 10–20 times with a narrow-bore 10 ml pipette every 15 min during the incubation period. The cell suspension was centrifuged (350 *g*, 8 min, 4°C), the pellet resuspended in 25 ml enzyme solution, and the enzymatic procedure repeated for 30 min. Following dissociation, the cell suspension was filtered through a 70 μm nylon filter, and the cells washed 3 times in potassium-free Medium 199 containing 0.4% BSA. The cell pellet was resuspended in Medium 199 containing 5.5 mM potassium and 0.1% BSA. The final cell suspension was filtered through a 100 μm nylon filter. Cells were counted in a haemocytometer and cell viability (usually >90%) was assessed by trypan blue exclusion. The yield from 10–14 adrenals was $6–8 \times 10^7$ cells. For use in a subsequent incubation, one half of the cell preparation was stored at 4°C in DMEM supplemented with 10% foetal calf serum. These cells were found to be responsive to AII for at least 12–16 h.

For aldosterone release, adrenal cells were suspended in Medium 199 containing 5.5 mM potassium and 0.1% BSA, at a concentration of 5.21×10^5 cells ml^{-1}. Aliquots of 960 μl (5×10^5 cells) were distributed into 35-mm, six-well, tissue-culture plates. AII, with or without test compound, was added in 40 μl of Medium 199 at the indicated concentrations. The cells were incubated for 2 h at 37°C under 95% O_2/5% CO_2 with constant shaking at 70 cycles min^{-1} and then centrifuged at 1200 *g* at 4°C for 10 min. Aldosterone in the supernatant was measured directly with a radioimmunoassay kit (Coat-a-Count) from Diagnostic Products Corporation (Buehlmann Laboratories).

Functional antagonism, specificity, and potency of valsartan in vivo *in pithed rats*

Male rats of the Sprague-Dawley-derived strain of *Rattus norvegicus* (Tif: RAIf) (280–350 g) were obtained from Tierfarm AG, Sisseln, Switzerland. They were pithed under Pentothal anaesthesia, according to the technique of Gillespie & Muir (1967). Immediately after pithing, the rats were ventilated with room air, enriched with 33% O_2, using a respiratory pump (Harvard Model 683, South Natick, Mass, USA, at 50 cycles min^{-1}, 10 ml kg^{-1}). The body temperature of the rats was maintained at 37°C by a thermostatically controlled heating lamp and monitored with a rectal thermometer (Systag TCU-82, Rüschlikon, Switzerland). The left common carotid artery was cannulated for mean arterial pressure (MAP) measurement (Isotec transducer, Miamisbourg, OH, U.S.A.; Hellige recorder, Freiburg im Breisgau, Germany). Drugs were administered through a cannula placed in the right jugular vein. Atropine (0.3 mg kg^{-1}) and tubocurarine (2 mg kg^{-1}) were given i.v., 10 min apart, after pithing. Thereafter, rats were challenged with AII (0.03 to 100 $\mu g\ kg^{-1}$), the electrical stimulation of the sympathetic outflow (0.1 to 10 Hz, 40mA, 1 ms, for 10 s), or noradrenaline (0.03 to 30 $\mu g\ kg^{-1}$).

Rats were given orally 10 mg kg^{-1} of valsartan 2 h ($n = 7$), 4 h ($n = 8$) or 24 h ($n = 5$) prior to the challenge with the pressor agents. Control rats ($n = 7$), received 2 ml kg^{-1} of the solvent.

Antihypertensive effect of valsartan in renal hypertensive rats (2K1C)

Male normotensive (WKY) rats, aged 5–6 weeks (IFFA, CREDO, L'Arberesle, France), were made hypertensive by constriction (0.2 mm silver clip) of one renal artery under light ether anaesthesia (Goldblatt 2K1C). Rats were used 5–7 weeks after clipping. Systolic blood pressure (SBP) and heart rate (HR) were measured indirectly in the tail arteries of conscious restrained rats with an inflatable cuff and a piezoelectric detector attached to a pen recorder (W + W Electronics blood-pressure recorder, Model 8005, Comerio, Italy). The rats were placed in individual restraining tubes, transferred to an oven preheated to 30°C, and left there for 1 h for the arteries in the tail to dilate. SBP and HR were measured weekly after the renal clip was implanted. Only rats with a SBP higher than 220 mmHg were used.

Intravenous administration An on-line computerized system was used for continuous intra-arterial measurements of MAP and HR in unrestrained rats, as described previously (Bunkenburg *et al.*, 1991). Catheters were implanted in a femoral vein and an artery under halothane anaesthesia at least 48 h before an experiment. Throughout the experimental procedure, the rats were kept in individual cages where they could move freely with access to food and water.

Valsartan was given by single bolus i.v. injection in doses ranging from 0.01 to 10 mg kg^{-1}. Each animal received only one dose. One group received the ACE inhibitor, enalaprilat (3 mg kg^{-1} i.v.). MAP and HR were measured continuously throughout the experiment.

In another group of rats, the nonselective β-adrenoceptor antagonist, propranolol (1 mg kg^{-1}, i.v.) was administered 30 min before an i.v. bolus injection of valsartan (3 mg kg^{-1}). MAP and HR were measured continuously as described above.

Single oral administration Rats were treated with single doses (1, 3 and 10 mg kg^{-1}) of valsartan, given by gavage. SBP and HR were measured in conscious restrained rats (by the tail-cuff method described above) before and 2, 4 or 24 h after administration of valsartan. The rats were returned to their cages between measurements. In a separate study, losartan was given orally at a dose of 10 mg kg^{-1} p.o.

Repeated oral administration Rats were treated once daily for 4 days with 3 or 10 mg kg^{-1} of valsartan. SBP and HR were measured by the tail-cuff method before and 2, 4 or 24 h after each administration. The rats were restrained for the measurement, but were returned to their cages between measurements.

In all experiments *in vivo*, the compounds were dissolved by addition of NaOH (0.1 M) and the pH adjusted to about 8 with HCl (0.1 M). Control rats received equivalent volumes of the solvent mixture.

Hypotensive effect of valsartan in conscious, normotensive sodium-depleted marmosets

Experiments were performed in conscious freely moving marmosets (250–350 g in weight, aged 1–3 years) with an implanted transmitter unit (AM Unit, model TA11PA-C40, Data Sciences, Inc., St. Paul, Minnesota, U.S.A.), for the measurement of blood pressure by telemetry (Schnell & Wood, 1993). The pressure transmitters were implanted into the peritoneal cavity under aseptic conditions and light anaesthesia (combination of alfaxalonum (10 mg kg^{-1}), atropine (0.15 mg kg^{-1}), and diazepam (0.75 mg kg^{-1}) i.m.). With the aid of a microscope, the ascending aorta was exposed through a midline incision in the abdomen and the sensor catheter was placed in the aorta below the renal artery pointing upstream. The transmitter was sutured to the inner abdominal wall with a continuous suture. Immediately after surgery the marmosets were given penicillin and piroxicam (5000 iu and 2 mg per animal, respectively). The marmosets were allowed to recover for at least 4 weeks before any experiment was started. One week before beginning an experiment, the marmosets were maintained on a low sodium diet consisting of laboratory chow (NAFAG 9627, Gossau, Switzerland) supplemented with fruit. They received furosemide (approximately 5 mg day^{-1}) in their drinking water (0.2 mg ml^{-1}) for 48 h before drug administration.

MAP and HR were measured continuously while the marmosets were freely moving in their normal cages commencing 48 h before drug administration. The compounds were given by gavage. MAP was monitored for a further 24 h. The marmosets received either vehicle (0.9% saline, 1 ml kg^{-1}), valsartan or losartan in doses of 1, 3, 10 and 30 mg kg^{-1}. Values for MAP and HR were averaged over a 1 h period and changes calculated using each marmoset as its own control; each post-administration value was subtracted from the value for the corresponding period of time in the pretreatment period.

Drugs

The drugs used were obtained from commercial suppliers: ^{125}I-labelled AII and Sar^{1}Ile^8 AII (2200 Ci $mmol^{-1}$) (Anawa; Wangen, Switzerland); unlabelled AII, Sar^{1}Ile^8 AII, Sar^{1}Ala^8 AII (Bachem; Bubendorf, Switzerland); peptidase inhibitors (Novabiochem; Läufelfingen, Switzerland); culture media (Amimed; AG, Muttenz, Switzerland); 5-HT and noradrenaline (Fluka, Switzerland); Hypertensin CIBA (CIBA-GEIGY, Basel, Switzerland); heparin and diazepam (Roche, Basel, Switzerland); halothane (Hoechst, Zurich, Switzerland); atropine (Siegfried A.G., Zofingen, Switzerland); tubocurarine (Wellcome AG, Reinach, Switzerland); Pentothal (Abbott AG, Cham, Switzerland); saffan (Glaxovet Ltd., Uxbridge, U.K.); penicillin (Duplocilline LA, (Veterinaria AG), Zurich, Switzerland); piroxicam (Piroxicam-mepha, Mepha Pharma AG, Aesch, Switzerland). Enalapril was kindly supplied by MSD. Valsartan, losartan and propranol were synthesized in the Chemistry Department of Ciba-Geigy.

Statistical analysis

Dose-response curves were analyzed using the four-parameter logistic method of De Lean *et al.* (1978) to estimate IC_{50} or EC_{50}. Inhibition constants (K_i) were calculated from competitive binding experiments according to the formula $K_i = IC_{50}/(1 + L/K_d)$, where L is the concentration of radioactive ligand and K_d its dissociation constant. K_i was calculated from the reciprocal analysis of [^{125}I]-Sar^{1}Ile^8-AII binding in the presence and absence of valsartan, using the formula $K_i = [\text{valsartan}]/((K_{d'}/K_d)-1)$, where $K_{d'}$ is the apparent K_d in the presence of [valsartan]. K_d was calculated using the LIGAND programme (Munson & Rodbard, 1980). In the isolated aortic rings, the conventional Schild analysis for estimation of potency could not be used because valsartan reduced the maximum response to AII. Instead, apparent pK_B values were derived by using a double-reciprocal regression plot as described by Kenakin (1984) and Robertson *et al.* (1992). In adrenal glomerulosa cells (inhibition of aldosterone biosynthesis), the maximum response to AII was not affected by valsartan, thus a pA_2 value was calculated according to Wiest *et al.* (1991).

MAP, SBP and HR are presented as means of absolute or changes over the time period of interest and expressed as mean ± s.e.mean. The ED_{30} of valsartan, i.e. dose which decreased either MAP or SBP by 30 mmHg, was derived by linear regression. Data were analyzed by analysis of variance followed by Bonferroni's method or Student's unpaired *t* test at time points of interest. Significance level was taken as $P<0.05$.

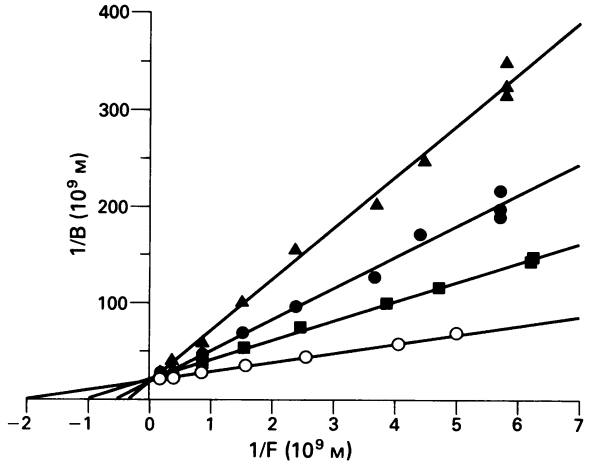

Figure 2 Reciprocal analysis of [^{125}I]-Sar^{1}Ile^8-AII binding to rat aortic smooth muscle cell membranes in the presence and absence (control ○) of three concentrations of valsartan (■ 1, ● 2, ▲ 4 nM). Radioligand (0.175 nM) was incubated for 60 min at 25°C with unlabelled Sar^{1}Ile^8-AII (0.05–5 nM). The K_d values for the control was 0.50 nM. The K_i values at the three concentrations of valsartan were 0.87, 0.85 and 0.88 nM. B = bound Sar^{1}Ile^8-AII; F = unbound Sar^{1}Ile^8-AII.

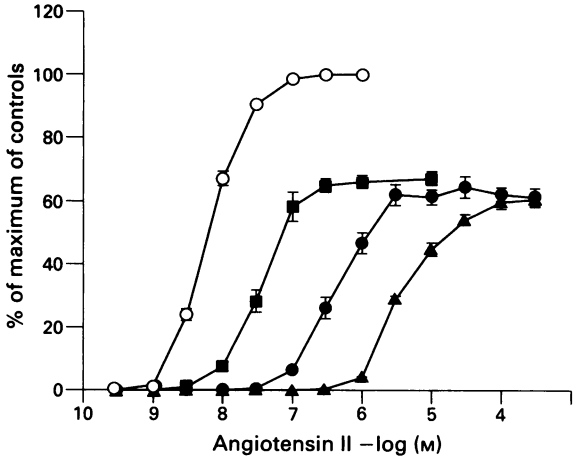

Figure 3 Inhibitory effects of valsartan (■ 2, ● 20, ▲ 200 nM, incubated for 5 min) on the contractions induced by angiotensin II (AII) in rabbit aortic rings. Results are expressed as percentage of the maximum response obtained with AII in rings treated with appropriate concentrations of the solvent (○). Values represent the mean ± s.e.mean of 12–14 experiments.

Results

Binding of valsartan to the AII receptor of smooth muscle cells (SMC) from rat aorta (AT_1) and human myometrium (AT_2)

Valsartan competed for [^{125}I]-AII binding to membranes from SMC and human myometrium with K_i values of 2.38 ± 0.31 nM (mean ± s.e.mean; $n = 5$) and 57.7 ± 9.4 μM ($n = 5$), respectively, giving a selectivity factor of more than 30,000. By contrast, the peptide antagonist, Sar^{1}Ile^8-AII, bound with high affinity to both receptor subtypes (K_i 0.85 ± 0.07 nM and 0.23 ± 0.04 nM, $n = 4$, respectively). The corresponding K_d values for AII were 1.28 ± 0.16 nM ($n = 11$) and 0.44 ± 0.035 nM ($n = 10$). A reciprocal analysis of [^{125}I]Sar^{1}Ile^8-AII binding to SMC in the absence or presence of 1, 2 or 4 nM valsartan demonstrated that this compound is a competitive inhibitor at the receptor level, as in the presence of inhibitor, the B_{max} (y-intersect) remained unchanged (Figure 2).

The results quoted above were all obtained in the absence of BSA in the incubation medium. In vascular SMC, valsartan had a 3 fold lower affinity in the presence of BSA (K_i 7.06 ± 0.63 nM, $n = 9$; K_d for AII: 0.67 ± 0.09 nM, $n = 7$). In human myometrium, valsartan inhibited binding by 39 ± 1.8%, $n = 5$, at 100 μM.

Functional antagonism, specificity, and potency of valsartan in rabbit isolated aortic rings

Valsartan, when incubated for 5 min at concentrations of 2, 20 or 200 nM, displaced the concentration-response curve of AII to the right and reduced the maximum contractile response to AII by 33%, 36% and 40%, respectively (Figure 3). When the rings were incubated for 1 h or 3 h with 20 nM valsartan, the AII concentration-response curve was further displaced to the right and the maximum response was decreased by 48% and 59% respectively. After 200 nM, the maximum response to AII was similarly reduced after 1 h (by 59%) or after 3 h (by 60%), and the EC_{50} values for AII were not significantly affected (6.5 and 8.9 μM respectively). After 3 h incubation, an apparent pK_B value of 9.26 was calculated. In Figure 4, the effects of the three different incubation times (5 min, 1 h or 3 h) with 20 nM valsartan are given. In this experiment, the calculated EC_{50} for AII was 15 nM (control) and 410 nM after incubation for 5 min with 20 nM valsartan. The EC_{50} for AII increased 2 fold after

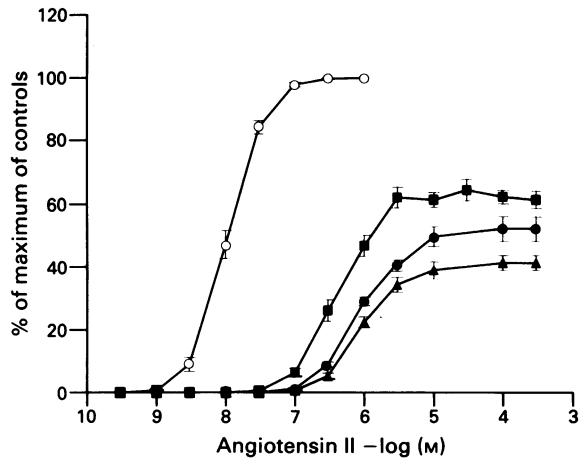

Figure 4 Inhibitory effects of 20 nM valsartan incubated for 5 min (■), 1 h (●), or 3 h (▲), on the contractions induced by angiotensin II (AII) in rabbit aortic rings. Results are expressed as percentage of the maximum response obtained with AII in rings treated with appropriate concentrations of the solvent (○). Values represent the means ± s.e.mean of 4–14 experiments.

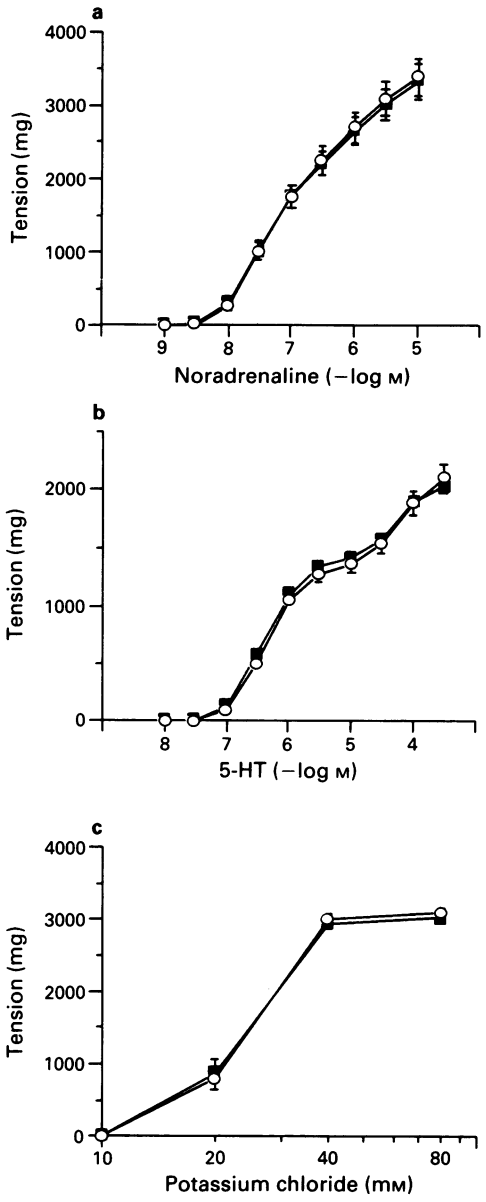

Figure 5 Effects of vehicle (○) or valsartan (■ 2 μM) on the concentration-response curves of rabbit aortic rings for contractions induced by noradrenaline (a), 5-hydroxytryptamine (5-HT) (b) and potassium chloride (c). Values represent the means ± s.e.mean of 8 experiments in each group.

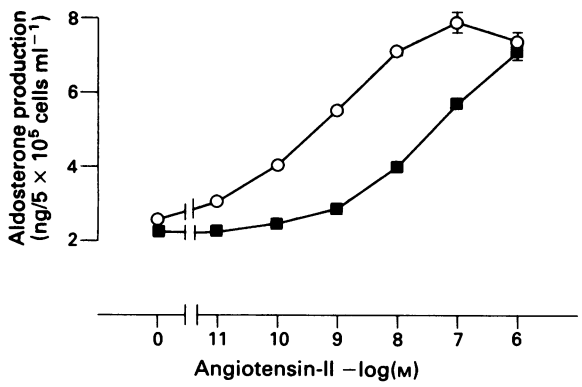

Figure 6 Effects of vehicle (○) or valsartan (■ 300 nM) on angiotensin II-stimulated aldosterone production in dispersed bovine adrenal glomerulosa cells. Values represent means ± s.e.mean of six determinations. Error bars smaller than the symbols were omitted.

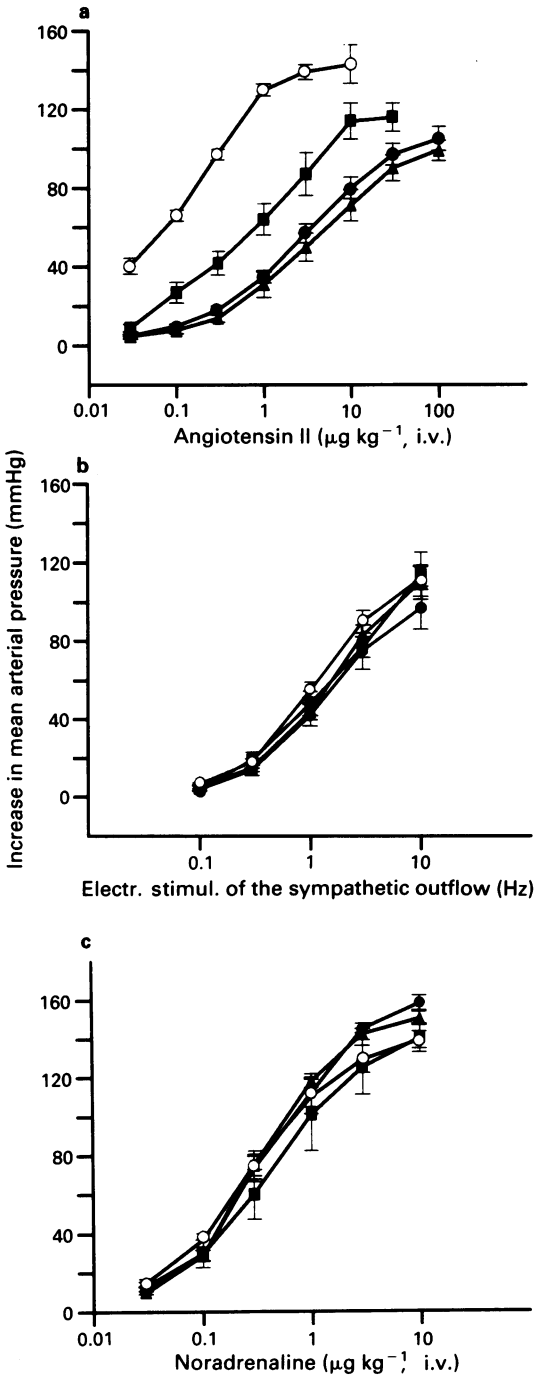

Figure 7 Effects of oral application of vehicle (○) or valsartan 10 mg kg^{-1} on the pressor-response curves to angiotensin II (a), electrical stimulation of the sympathetic outflow (b) and noradrenaline (c) in pithed rats. Animals were treated with valsartan 2 h (▲), 4 h (●) and 24 h (■) prior to challenge with the three pressor agents. Values represent the means ± s.e.mean of 5–8 experiments in each group. In (a), all three treatment regimes were significantly different fron controls, and the 24 h regime was significantly different from the 2 and 4 h regimes respectively.

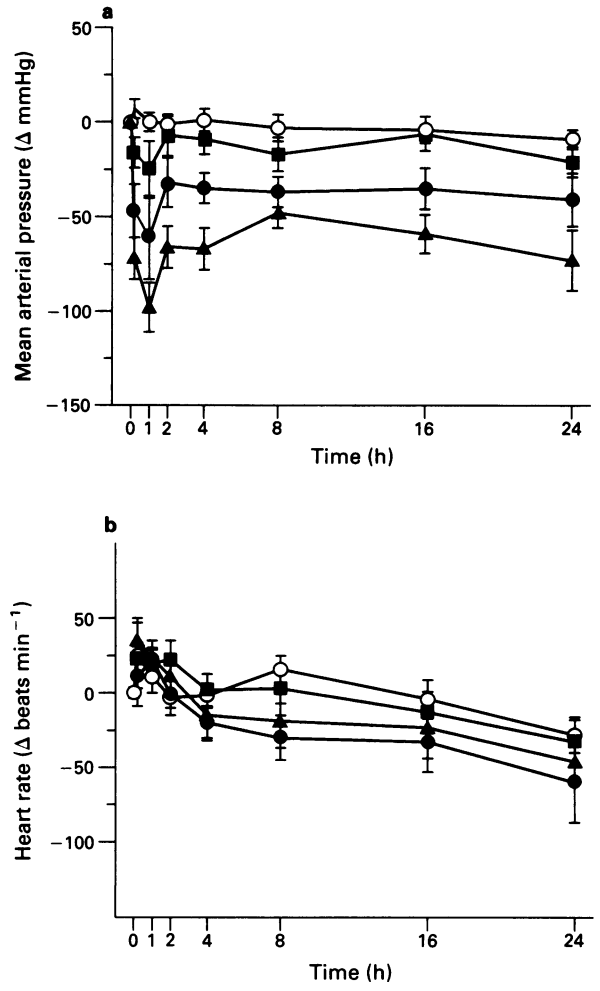

Figure 8 Effects of intravenous administration of vehicle (○) or valsartan (■ 0.03, ● 0.1, ▲ 1 mg kg^{-1}) on mean arterial pressure (a) and heart rate (b) in conscious, renal hypertensive rats (2K1C). Values represent the means ± s.e.mean of 5–7 animals per group.

incubation for 1 h (920 nM) or 3 h (930 nM). At a concentration of 2 μM, the compound had no effect on contractions induced by noradrenaline, 5-HT, or potassium chloride (Figure 5). No agonistic effects were observed up to a concentration of 2 μM.

Effects of valsartan on AII-induced aldosterone release in bovine adrenal glomerulosa cells

The addition of increasing concentrations of AII (10 pM to 10 μM) to dispersed adrenal glomerulosa cells results in a concentration-dependent stimulation of aldosterone production. As shown in Figure 6, the maximum AII-induced aldosterone response was more than 3 times the basal aldosterone values. The addition of valsartan (300 nM) to this system inhibited aldosterone production, as indicated by the parallel shift to the right of the AII concentration-response curve (Figure 6). The calculated ED_{50} values for AII in the presence and absence of the antagonist were 49 nM and 0.64 nM, respectively. The pA_2 value was calculated to be 8.41 (K_B = 3.9 nM). Valsartan did not affect the aldosterone release induced by the addition of 5.5 mM potassium (results not shown).

Functional antagonism, specificity and duration of action of valsartan in vivo *in pithed rats*

Valsartan at a dose of 10 mg kg^{-1} p.o. did not significantly affect basal MAP values in any of the three time regimes. Vehicle-treated rats had an initial MAP of 57 ± 3.6 mmHg, (n = 7); the 2 h group, 51 ± 5.2 mmHg, (n = 6); the 4 h group, 51 ± 3.1 mmHg; (n = 8); and the 24 h group, 47 ± 3.4 mmHg, (n = 5). The pressor-response curves to AII were significantly shifted to the right after all three time regimes. The effects at 24 h, however, were significantly less pronounced than after 2 h and 4 h respectively (Figure 7a). The pressor-response curves to electrical stimulation of the sympathetic outflow or to noradrenaline were not affected by the compound at any time regime (Figure 7,b,c).

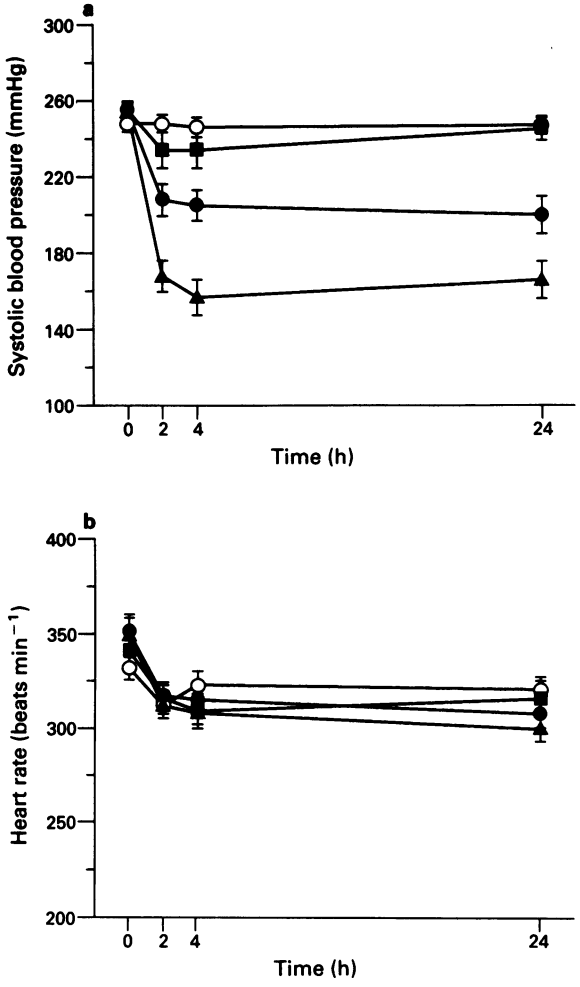

Figure 9 Effects of oral administration of vehicle (○) and valsartan (■ 1, ■ 3, ▲ 10 mg kg^{-1}) on systolic blood pressure (a) and heart rate (b) in conscious renal hypertensive rats (2K1C). Values represent means ± s.e.mean of 16–29 animals per group.

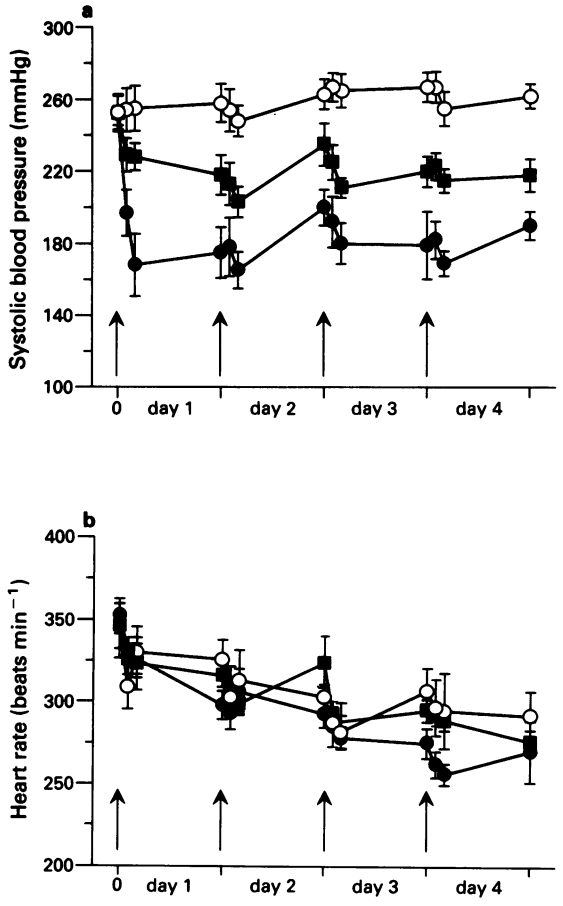

Figure 11 Effects of repeated oral administration of vehicle (○) or valsartan (■ 3 mg kg^{-1}) and (● 10 mg kg^{-1}) on systolic blood pressure (a) and heart rate (b) in conscious renal hypertensive rats (2K1C). Rats were treated once daily for 4 days at time points indicated by the arrows. Measurements were performed 2, 4 and 24 h after each administration. Values represent the means ± s.e.mean of 6 rats in each group.

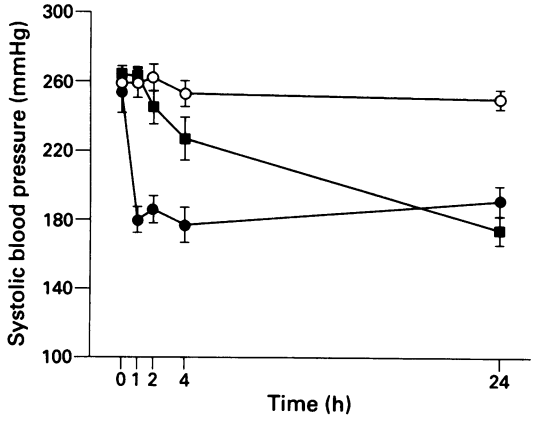

Figure 10 Effects of oral administration of vehicle (○), losartan (■ 10 mg kg^{-1}), and valsartan (● 10 mg kg^{-1}) on systolic blood pressure in conscious, renal hypertensive rats (2K1C). Measurements were performed 1, 2, 4 and 24 h after a single administration. Values represent means ± s.e.mean of 5–12 animals per group.

Antihypertensive effect of valsartan in conscious renal hypertensive rats (2K1C)

Intravenous administration Valsartan (0.03–1 mg kg^{-1}, n = 5–7) decreased MAP in a dose-dependent manner (Figure 8a). The 3 mg kg^{-1} and 10 mg kg^{-1} doses did not have any additional antihypertensive effect (data not shown). The dose which produced a decrease of 30 mmHg (ED_{30}) was calculated to be 0.06 mg kg^{-1}. The initial immediate decrease in MAP was accompanied by a transient increase in HR in the first 30–60 min after injection. The antihypertensive effects of doses of 0.1 mg kg^{-1} and above persisted for up to 24 h (Figure 8a). The maximum response induced by 3 mg kg^{-1} of valsartan (− 105 ± 7 mmHg) at 60 min was similar to that induced by the same dose of the ACE inhibitor enalaprilat (− 106 ± 8 mmHg) at 60 min. The transient increase in HR observed after i.v. administration of valsartan was prevented by pretreatment with propranolol 1 mg kg^{-1} (30 min before) (data not shown).

Single oral administration Valsartan in oral doses of 1, 3 or 10 mg kg^{-1}, decreased SBP in a dose-dependent manner. The maximal decreases were of − 20.9 ± 8.6 (n = 16), − 49.7 ± 8.1, (n = 29) and − 97.4 ± 11.4 (n = 17) mmHg respectively. The dose which produced a decrease of 30 mmHg (ED_{30}) was calculated to be 1.4 mg kg^{-1}. With the threshold dose of 1 mg kg^{-1}, the antihypertensive response persisted for less

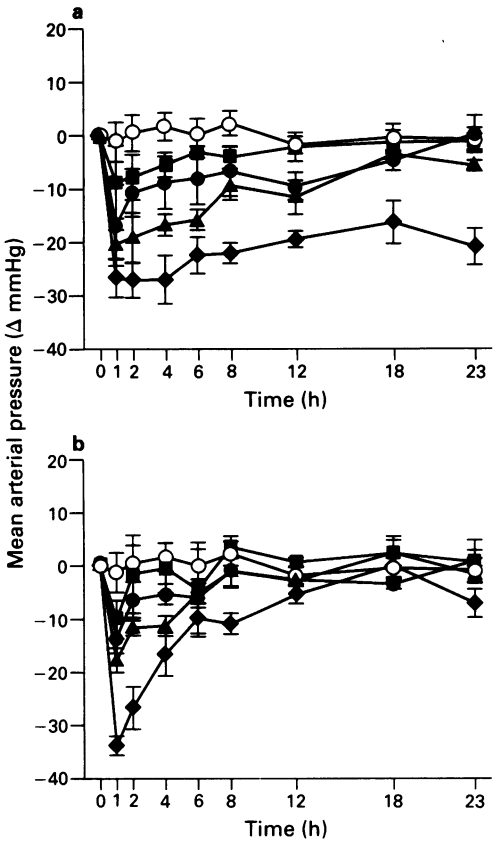

Figure 12 Effect of oral administration of vehicle (○) or valsartan (a) or vehicle and losartan (b) on mean arterial pressure in conscious, freely moving and sodium-depleted marmosets. The doses for both agents were 1 (■), 3 (●), 10 (▲) and 30 (◆) mg kg^{-1}. Values represent means ± s.e.mean of 4–6 animals per group.

than 24 h, whereas with the doses of 3 and 10 mg kg^{-1} the effect lasted for at least 24 h (Figure 9a). HR tended to decrease during the experiment in all groups and there was no significant effect of valsartan (Figure 9b). Compared with losartan, valsartan had a more rapid onset of action, whereas the effect of both compounds 24 h after administration was similar (Figure 10).

Repeated oral administration On the first day of administration of doses of 3 or 10 mg kg^{-1} (Figure 11a), the blood pressure-lowering effect was similar to that seen in the single-dose experiment (Figure 9a). The antihypertensive effects persisted for 24 h after the first dose. After the administration of the second, third and fourth dose, a small, non significant additional fall in SBP was observed. SBP remained consistently decreased during the treatment period. HR, was not significantly affected by valsartan when compared to the vehicle control group (Figure 11b).

Hypotensive effect of valsartan in conscious, normotensive, sodium-depleted marmosets

Valsartan induced dose-dependent reductions in MAP in conscious freely-moving sodium-depleted marmosets (Figure 12a). The threshold dose was about 1 mg kg^{-1}. With doses of 3 mg kg^{-1} and above, the maximum response developed within 1 h of administration. The response persisted for up to 12 h after valsartan at 3 and 10 mg kg^{-1} and for more than 24 h after the 30 mg kg^{-1} dose. Losartan also induced dose-dependent reductions in MAP in this model, but the duration of the hypotensive response was much shorter than with valsartan. MAP had recovered 10–12 h after the 30 mg kg^{-1} p.o. dose of losartan (Figure 12b). Neither of the AII antagonists had a significant effect on HR in the dose-range tested when compared with the vehicle-treated marmosets.

Discussion

In this paper, we present evidence that valsartan is a potent, highly specific, and orally active nonpeptide receptor antagonist of the AT_1 receptor subtype. Moreover, these data clearly demonstrate that valsartan is an efficacious and long-acting antihypertensive agent in renal hypertensive rats, and also lowers blood pressure in normotensive sodium-depleted marmosets.

Valsartan inhibited binding of AII to AT_1-receptors in aortic SMC, with a 30,000 fold higher affinity than for AII receptors in human myometrium, which are exclusively of the AT_2-receptor subtype. Valsartan is a competitive inhibitor at the receptor level. The high specificity for the AT_1-receptor subtype is substantiated by the fact that at a concentration of 10 μM valsartan lacks affinity for a series of other receptors, including: α_1-, α_2-, β_1-adrenoceptors, histamine$_1$, substance P, $GABA_A$, $GABA_B$, muscarinic, 5-HT_1 and 5-HT_2, and calcium channels (S. Bischoff, H. Bittiger, K. Hauser, H. Rogg, Research Dept. Ciba-Geigy, unpublished data). The specificity of the compound was confirmed in functional studies in rabbit aortic rings. In this preparation, valsartan inhibited AII-induced contractions whereas it did not affect contractions induced by 5-HT, potassium chloride, or noradrenaline, even at a concentration of 2 μM. At this very high concentration no contractions were observed in the aortic rings, indicating that the compound lacks agonistic properties and acts as a pure antagonist. As observed with other nonpeptide AT_1-receptor antagonists (Wong *et al.*, 1990c; 1991a; Chiu *et al.*, 1991a; Robertson *et al.*, 1992), the rightward displacement of the AII concentration-response curve induced by valsartan was accompanied by a reduction in the maximal response. In contrast, no reduction in the maximum contractions to AII has been observed in rabbit aorta treated with losartan (Chiu *et al.*, 1991b). This difference may be due to the alcoholic moiety in the structure of losartan, instead of the carboxylic acid moiety contained in compounds displaying the insurmountable type of antagonism. As demonstrated also for another AT_1-receptor antagonist, GR117289 (Robertson *et al.*, 1992), both effects were dependent on the incubation time. For valsartan, an incubation time of about 1 h was needed to reach equilibrium. The reduction in the maximum response to AII by these agents, described as insurmountable antagonism, has been ascribed to a slowly reversible antagonism at the receptor site (Timmermans *et al.*, 1991c; Robertson *et al.*, 1992). It is worth noting, however, that in bovine isolated glomerulosa cells, valsartan inhibited AII-induced aldosterone release, without affecting the maximum response to AII. This observation is compatible with a competitive antagonistic profile of valsartan. In addition, as depicted in Figure 2, valsartan displayed a competitive type of antagonism at the receptor level in SMC. This apparent discrepancy might be explained by the different protocols used, since in the binding and in the aldosterone release studies, valsartan and AII were given simultaneously, whereas in the aortic ring studies valsartan was given prior to the addition of AII. Thus, in the presence of an antagonist slowly dissociating in the aortic rings, the time for an agonist to reach an equilibrium with the receptor becomes longer. A similar profile to that of valsartan, was observed with the AT_1-receptor antagonist, L-158,809, which was a competitive inhibitor in binding and aldosterone release studies and non-competitive in rabbit aorta (Chang *et al.*, 1992).

The inhibition by valsartan of the AII-induced release of aldosterone *in vitro* is consistent with similar findings made with losartan (Smith *et al.*, 1992). Losartan and an analogue, DuP 532 are also reported to inhibit AII-induced aldosterone release *in vivo* in normotensive rats (Wong *et al.*, 1990b; 1991a). Similar results have been observed with val-

sartan at a dose of 10 mg kg^{-1} (de Gasparo *et al.*, 1992).

The specificity of the antagonistic effects of valsartan was also observed after oral administration *in vivo*. In pithed rats, valsartan displaced to the right the dose-pressor-curve of AII, without affecting responses to noradrenaline or electrical stimulation of the sympathetic outflow. These effects were observed 2, 4 h and to a lesser extent, 24 h after a single oral administration of valsartan. Thus, the long duration of the antihypertensive effect of valsartan, observed in renal hypertensive rats, appears to be due to a blockade of the AT_1-receptor. Long lasting inhibition of AII-induced pressor responses have also been reported with losartan in normal male volunteers (Christen *et al.*, 1991).

In conscious, renal hypertensive rats, valsartan induced dose-related decreases in blood pressure after both i.v. and oral administration. Transient tachycardia was observed after i.v. injection, but not after oral administration. As with systemic vasodilators, the initial increase in HR appeared to be due to a transient activation of the sympathetic nervous system, since it was prevented by pretreatment with propranolol. A similar increase in HR, has also been observed after i.v. administration of losartan in spontaneously hypertensive rats (Wong *et al.*, 1990d) and in conscious water-deprived and water-replete Brattleboro rats (Batin *et al.*, 1991). Particularly in water-deprived Brattleboro rats, which are characterized by a marked activation of the renin-angiotensin system, the hypotension induced by losartan was due to a marked increase in total peripheral conductance, indicating that this class of compounds possesses vasodilator properties (Batin *et al.*, 1991).

After i.v. or oral administration of valsartan, the antihypertensive effect of the compound in renal hypertensive rats persisted for up to 24 h, and the maximum effect was similar to that induced in the same model by an angiotensin converting-enzyme inhibitor. Compared to losartan, valsartan had a more rapid onset of action after oral administration, and its maximum effect was reached after about 1 h, whereas the maximum antihypertensive effect of losartan developed between 4 and 24 h after administration. This latency in the biological response to losartan in rats, which has also been observed by other authors (Wong *et al.*, 1991b), appears to be due to the formation of an active, hepatically-generated carboxylic acid metabolite, EXP3174. This active metabolite is approximately 20 times more potent than the parent compound (Wong *et al.*, 1990c; Timmermans *et al.*, 1991b) and after oral administration in hypertensive rats has an onset of action similar (Wong *et al.*, 1990c) to that reported here for valsartan.

The long duration of action of valsartan observed after single administration was confirmed in the repeated administration study, where valsartan was given once daily for 4 days. Despite its long action, no signs of accumulation of effect were observed. Although plasma concentrations of AII have been shown to increase after administration of AT_1-receptor antagonists (Bunkenburg *et al.*, 1991), no signs of tolerance to the antihypertensive effects were observed. Indeed, the data from this study indicate that in renal hypertensive rats the blood pressure can be persistently maintained at almost normotensive levels throughout the period of treatment.

The sodium-depleted marmoset is a primate model of a normal, but renin-angiotensin-dependent, blood pressure. It has been used to evaluate the hypotensive efficacy of renin inhibitors, since these agents are primate-specific and cannot be tested in rats (Wood *et al.*, 1989). In conscious, freely moving marmosets, with MAP measured by telemetry, valsartan decreased blood pressure after oral administration to an extent comparable to that observed after renin or converting-enzyme inhibitors (Wood *et al.*, 1989). Although the oral efficacy and duration of action of these two compounds was similar in the renal hypertensive rats, valsartan had a longer duration of action than losartan in the marmosets. As in the results described here, losartan also has a shorter duration of action in rhesus monkeys than in rats (Stearns *et al.*, 1992). This may be because nonhuman primates do not metabolize losartan to its more active metabolite. Liver slices from rhesus monkeys, in contrast to liver slices from rats and man, do not convert losartan to its more active carboxylic acid metabolite, but to less potent glucuronidation metabolites of the tetrazole moiety (Stearns *et al.*, 1992). As previously suggested the formation of an active metabolite in the liver may make it difficult to predict the dosage of losartan for patients with impaired liver function. Therefore, an orally effective AT_1-receptor antagonist that is not dependent for its action on an active metabolite could have advantages over losartan (Wong *et al.*, 1991a).

In conclusion, valsartan is a highly specific, orally active antagonist of the AT_1-receptor subtype. Its blood-pressure-lowering effect after oral administration is not accompanied by reflex tachycardia, and persists at least 24 h in renal hypertensive rats and 12–24 h in sodium-depleted marmosets.

We thank, R. Burdet, N. Flubacher, P. Forgiarini, E. Halmo, E. Hermes, M. Mele, D. Monna, H.P. Mueller, O. Peter, C. Rodriguez, C. Schnell, H. Thomann and S. Walther for their excellent technical support and Walter Fuchs for preparing the figures.

References

BATIN, P., GARDINER, S.M., COMPTON, A.M., KEMP, P.A. & BENNETT, T. (1991). Cardiac haemodynamic effects of the non-peptide, angiotensin II-receptor antagonist, DuP 753, in conscious Long Evans and Brattleboro rats. *Br. J. Pharmacol.*, **103**, 1585–1591.

BLANKLEY, C.J., HODGES, J.C., KLUTCHKO, S.R., HIMMELSBACH, R.J., CHUCHOLOWSKI, A., CONNOLLY, C.J., NEERGAARD, S.J., VAN NIEUWENHZE, M.S., SEBASTIAN, A., QUIN, J., III, ESSENBURG, A.D. & COHEN, D.M. (1991). Synthesis and structure-activity relationships of a novel series of non-peptide angiotensin II receptor binding inhibitors specific for the AT_2 subtype. *J. Med. Chem.*, **34**, 3248–3260.

BOTTARI, S.P., TAYLOR, V., KING, I.N., BOGDAL, Y., WHITEBREAD, S. & DE GASPARO, M. (1991). Angiotensin II AT_2 receptors do not interact with guanine nucleotide binding properties. *Eur. J. Pharmacol., Mol. Pharmacol.*, **207**, 157–163.

BOTTARI, S.P., KING, I.N., REICHLIN, S., DAHLSTROEM, I., LYDON, N. & DE GASPARO, M. (1992). The angiotensin AT_2 receptor stimulates protein tyrosine phosphatase activity and mediates inhibition of particulate guanylate cyclase. *Biochem. Biophys. Res. Commun.*, **183**, 206–211.

BRADFORD, M.M. (1976). A rapid and sensitive method for the quantification of microgram quantities of protein utilizing the principle of protein-dye binding. *Anal. Biochem.*, **72**, 248–254.

BÜHLMAYER, P., CRISCIONE, L., FUHRER, W., FURET, P., DE GASPARO, M., STUTZ, S. & WHITEBREAD, S. (1991). Nonpeptidic angiotensin II antagonists: synthesis and *in vitro* activity of a series of novel naphthalene and tetrahydronaphthalene derivatives. *J. Med. Chem.*, **34**, 3105–3114.

BUMPUS, F.M., CATT, K.J., CHIU, A.T., DE GASPARO, M., GOODFRIEND, T., HUSAIN, A., PEACH, M.J., TAYLOR, D.G. JR & TIMMERMANS, P.B.M.W.M. (1991). Nomenclature for angiotensin receptors: a report of the nomenclature committee of the Council for High Blood Pressure Research. *Hypertension*, **17**, 720–721.

BUNKENBURG, B., SCHNELL, C., BAUM, H.-P., CUMIN, F. & WOOD, J.M. (1991). Prolonged angiotensin II antagonism in spontaneously hypertensive rats. Hemodynamic and biochemical consequences. *Hypertension*, **18**, 278–288.

CARINI, D.J., DUNCIA, J.V., JOHNSON, A.L., CHIU, A.T., PRICE, W.A., WONG, P.C. & TIMMERMANS, P.B. (1990). Nonpeptide angiotensin II receptor antagonists: n-((benzyloxy)benzyl) imidazoles and related compounds as potent antihypertensives. *J. Med. Chem.*, **33**, 1330–1336.

CHANG, R.S.L., SIEGEL, P.K.S., CLINESCHMIDT, B.V., MANTLO, N.B., CHAKRAVARTY, P.K., GREENLEE, W.J., PATCHETT, A.A. & LOTTI, V.J. (1992). In vitro pharmacology of L-158,809, a new highly potent and selective angiotensin II receptor antagonist. *J. Pharmacol. Exp. Ther.*, **262**, 133–138.

CHIU, A.T., HERBLIN, W.F., ARDECKY, R.J., MCCALL, D.E., CARINI, D.J., DUNCIA, J.V., PEASE, L.J., WONG, P.C., WEXLER, R.R., JOHNSON, A.L. & TIMMERMANS, P.B.M.W.M. (1989). Identification of angiotensin II receptor subtypes. *Biochem. Biophys. Res. Commun.*, **165**, 196–203.

CHIU, A.T., CARINI, D.J., DUNCIA, J.V., LEUNG, K.H., MCCALL, D.E., PRICE, W.A. JR, WONG, P.C., SMITH, R.D., WEXLER, R.R. & TIMMERMANS, P.B.M.W.M. (1991a). DuP 532. A second generation of nonpeptide angiotensin II receptor antagonists. *Biochem. Biophys. Res. Commun.*, **177**, 209–217.

CHIU, A.T., MCCALL, D.E., PRICE, W.A. Jr., WONG, P.C., CARINI, D.J., DUNCIA, J.V., WEXLER, R.R., YOO, S.E., JOHNSON, A.L. & TIMMERMANS, P.B.M.W.M. (1991b). *In vitro* pharmacology of DuP 753. *Am. J. Hypertens.*, **4** Suppl, 282S–287S.

CHIU, A.T., ROSCOE, W.A., MCCALL, D.E. & TIMMERMANS, P.B.M. W.M. (1991c). Angiotensin II-1 receptors mediate both vasoconstriction and hypertrophic responses in rat aortic smooth-muscle cells. *Receptor*, **1**, 133–140.

CHRISTEN, Y., WAEBER, B., NUSSBERGER, J., PORCHET, M., BORLAND, R.M., LEE, R.J., MAGGON, K., SHUM, L., TIMMERMANS, P.B.M.W.M. & BRUNNER, H.R. (1991). Oral administration of DuP 753, a specific angiotensin II receptor antagonist, to normal male volunteers: inhibition of pressor response to exogenous angiotensin I and II. *Circulation*, **83**, 1333–1342.

CONSENSUS TRIAL: THE CONSENSUS TRIAL STUDY GROUP (1987). Effects of enalapril on mortality in severe congestive heart failure. *N. Engl. J. Med.*, **316**, 1429–1435.

CRISCIONE, L., DE GASPARO, M., BUEHLMAYER, P., WHITEBREAD, S., RAMJOUE, H.P. & WOOD, J.M. (1992). Pharmacological profile of CGP 48933: a specific, orally active nonpeptide antagonist of AT_1 angiotensin II receptor subtype. *Hochdruck*, **12**, 43.

CRISCIONE, L., THOMANN, H., WHITEBREAD, S., DE GASPARO, M., BUEHLMAYER, P., HEROLD, P., OSTERMAYER, F.A. & KAMBER, B. (1990). Binding characteristics and vascular effects of various angiotensin II antagonists. *J. Cardiovasc. Pharmacol.*, **16**, S56–S59.

DE GASPARO, M., WHITEBREAD, S., LEVENS, N., RAMJOUE, H.P., CRISCIONE, L., ROGG, H., BAUM, H.P., BRECHLER, V., BUEHLMAYER, P., WOOD, J.M. & BOTTARI, S.P. (1992). Pharmacology of angiotensin II-receptor subtypes. In *Cellular and Molecular Biology of the Adrenal Cortex*. ed. Saez, J.M., Vol. 22, pp. 3–17. Colloque INSERM: John Libbey Eurotext Ltd.

DE LEAN, A., MUNSON, P.J. & RODBARD, D. (1978). Simultaneous analysis of families of sigmoidal curves: application to bioassay, radioligand assay, and physiological dose-response curve. *Am. J. Physiol.*, **235**, E97–E111.

DUDLEY, D.T., HUBBELL, S.E. & SUMMERFELT, R.M. (1991). Characterization of angiotensin II (AT_2) binding sites in R3T3 cells. *Mol. Pharmacol.*, **40**, 360–367.

DUNCIA, J.V., CHIU, A.T., CARINI, D.J., GREGORY, G.B., JOHNSON, A.L., PRICE, W.A., WELLS, G.J., WONG, P.C., CALABRESE, J.C. & TIMMERMANS, P.B. (1990). The discovery of potent nonpeptide angiotensin II receptor antagonists: a new class of potent antihypertensives. *J. Med. Chem.*, **33**, 1312–1329.

FURUKAWA, Y., KISHIMOTO, S. & NISHIKAWA. (1982). *Hypotensive imidazole deriviates*. US Patent 4,340,598 issued to Takeda Chemical Industries, Ltd., Osaka, Japan. US patent.

GILLESPIE, J.S. & MUIR, T.C. (1967). A method of stimulating the complete sympathetic outflow from the spinal cord to the blood vessels in the pithed rat. *Br. J. Pharmacol.*, **30**, 78–87.

HERBLIN, W.F., CHIU, A.T., MCCALL, D.E., ARDECKY, R.J., CARINI, D.J., DUNCIA, J.V., PEASE, L.J., WONG, P.C., WEXLER, R.R., JOHNSON, A.L. & TIMMERMANS, P.B.M.W.M. (1991). Angiotensin II receptor heterogeneity. *Am. J. Hypertens.*, **4** Suppl, 299S–302S.

HOFBAUER, K.G. & WOOD, J.M. (1986). The renin-angiotensin system: inhibitors and antagonists. In *Handbook of Hypertension*, Vol 6: *Pathology of Hypertension, Regulatory Mechanisms* ed. Zanchetti, A. & Tarazi, R.C. pp. 466–488. Amsterdam: Elsevier Science Publisher.

HOFBAUER, K.G., ZSCHIEDRICH, H. & GROSS, F. (1976). Regulation of renin release and intrarenal formation of angiotensin: studies in the isolated rat kidney. *Clin. Exp. Pharmacol. Physiol.*, **3**, 73–93.

KENAKIN, T.P. (1984). Drugs and drug responses in isolated tissues. *Pharmacol. Rev.*, **36**, 165–222.

KRAMER, B.L., MASSIE, B.M. & TOPIC, N. (1983). Controlled trial of captopril in chronic heart failure: a rest and exercise hemodynamic study. *Circulation*, **67**, 807–816.

MANTLO, N.B., CHAKRAVARTY, P.K., ONDEYKA, D.L., SIEGL, P.K.S., CHANG, R.S., LOTTI, V.J., FAUST, K.A., CHEN, T.-B., SCHORN, T.W., SWEET, C.S., EMMERT, S.E., PATCHETT, A.A. & GREENLEE, W.J. (1991). Potent, orally active imidazo[4,5-*b*]pyridine-based angiotensin II receptor antagonists. *J. Med. Chem.*, **34**, 2919–2922.

MUNSON, P.J. & RODBARD, D. (1980). LIGAND: a versatile computerized approach for the characterisation of ligand binding systems. *Anal. Biochem.*, **107**, 220–239.

ONDETTI, M.A. (1991). Angiotensin converting enzyme inhibitors: an overview. *Hypertension*, **18** Suppl. 3, III134–III135.

ONDETTI, M.A., RUBIN, A. & CUSHMAN, D.W. (1977). Design of specific inhibitors of angiotensin converting enzyme: a new class of orally active antihypertensive agents. *Science*, **196**, 441–444.

PALS, D.T., MASUCCI, I., DENNING, G.S. JR, SIPES, F. & FESSLER, D.C. (1971). Role of the pressor action of angiotensin II in experimental hypertension. *Circ. Res.*, **29**, 673–681.

PALS, D.T., DENNING, Jr., G.S. & KEENAN, R.E. (1979). Historical development of saralasin. *Kidney Int.*, **15**, S7–S10.

ROBERTSON, M.J., BARNES, J.C., DREW, G.M., CLARK, K.L., MARSHALL, F.H., MICHEL, A., MIDDLEMISS, D., ROSS, B.C., SCOPES, D. & DOWLE, M.D. (1992). Pharmacological profile of GR117289 *in vitro*: a novel, potent and specific non-peptide angiotensin AT_1 receptor antagonists. *Br. J. Pharmacol.*, **107**, 1173–1180.

SCHNELL, R.C. & WOOD, J.M. (1993). Measurement of blood pressure and heart rate by telemetry in conscious unrestrained marmosets. *Am. J. Physiol.*, **264**, H1509–H1516.

SMITH, R.D., CHIU, A.T., WONG, P.C., HERBLIN, W.F. & TIMMERMANS, P.B.M.W.M. (1992). Pharmacology of nonpeptide angiotensin II receptor antagonists. *Annu. Rev. Pharmacol. Toxicol.*, **32**, 135–165.

STEARNS, R.A., MILLER, R.R., DOSS, G.A., CHAKRAVARTY, P.K., ROSEGAY, A., GATTO, G.J. & CHIU, S.-H.L. (1992). The metabolism of DuP 753, a nonpeptide angiotensin II receptor antagonist, by rat, monkey, and human liver slices. *Drug Metab. Dispos.*, **20**, 281–287.

TIMMERMANS, P.B.M.W.M., CARINI, D.J., CHIU, A.T., DUNCIA, J.V., PRICE, W.A. JR, WELLS, G.J., WONG, P.C., WEXLER, R.R. & JOHNSON, A.L. (1990). Nonpeptide angiotensin II receptor antagonists: a novel class of antihypertensive agents. *Blood Vessels*, **27**, 295– 300.

TIMMERMANS, P.B.M.W.M., CARINI, D.J., CHIU, A.T., DUNCIA, J.V., PRICE, W.A. JR, WELLS, G.J., WONG, P.C., JOHNSON, A.L. & WEXLER, R.R. (1991a). The discovery of a new class of highly specific nonpeptide angiotensin II receptor antagonists. *Am. J. Hypertens.*, **4** Suppl, 275S–281S.

TIMMERMANS, P.B.M.W.M., CARINI, D.J., CHIU, A.T., DUNCIA, J.V., PRICE, W.A. JR, WELLS, G.J., WONG, P.C., WEXLER, R.R. & JOHNSON, A.L. (1991b). Angiotensin II receptor antagonists: from discovery to antihypertensive drugs. *Hypertension*, **18** Suppl. 3, III136–III142.

TIMMERMANS, P.B.M.W.M., WONG, P.C., CHIU, A.T. & HERBLIN, W.F. (1991c). Nonpeptide angiotensin II receptor antagonists. *Trends Pharmacol. Sci.*, **12**, 55–62.

WEINSTOCK, J., KEENAN, R.M., SAMANEN, J., HEMPEL, J., FINKELSTEIN, J.A., FRANZ, R.G., GAITANOPOULOS, D.E., GIRARD, G.R., GLEASON, J.G., HILL, D.T., MORGAN, T.M., PEISHOFF, C.E., AIYAR, N., BROOKS, D.P., FREDRICKSON, T.A., OHLSTEIN, E.H., RUFFOLO, R.R. JR, STACK, E.J., SULPIZIO, A.C., WEIDLEY, E.F. & EDWARDS, R.M. (1991). 1-(Carboxybenzyl)-imidazole-5-acrylic acids: potent and selective angiotensin II receptor antagonists. *J. Med. Chem.*, **34**, 1514–1517.

WHITEBREAD, S., MELE, M., KAMBER, B. & DE GASPARO, M. (1989). Preliminary biochemical characterization of two angiotensin II receptor subtypes. *Biochem. Biophys. Res. Commun.*, **163**, 284–291.

WHITEBREAD, S.E., TAYLOR, V., BOTTARI, S.P., KAMBER, B. & DE GASPARO, M. (1991). Radioiodinated CGP 42112A: a novel high affinity and highly selective ligand for the characterization of angiotensin AT_2 receptors. *Biochem. Biophys. Res. Commun.*, **181,** 1365–1371.

WIEST, S.A., RAMPERSAUD, A., ZIMMERMAN, K. & STEINBERG, M.I. (1991). Characterization of distinct angiotensin II binding sites in rat adrenal gland and bovine cerebellum using selective nonpeptide antagonists. *J. Cardiovasc. Pharmacol.*, **17,** 177–184.

WONG, P.C., PRICE, W.A., CHIU, A.T., DUNCIA, J.V., CARINI, D.J., WEXLER, R.R., JOHNSON, A.L. & TIMMERMANS, P.B. (1990a). Nonpeptide angiotensin II receptor antagonists IX. Antihypertensive activity in rats of DuP 753, an orally active antihypertensive agent. *J. Pharmacol. Exp. Ther.*, **252,** 726–732.

WONG, P.C., PRICE, W.A. JR, CHIU, A.T., CARINI, D.J., DUNCIA, J.V., JOHNSON, A.L., WEXLER, R.R. & TIMMERMANS, P.B. (1990b). Nonpeptide angiotensin II receptor antagonists studies with EXP 9270 and DuP 753. *Hypertension*, **15,** 823–834.

WONG, P.C., PRICE, W.A. JR, CHIU, A.T., DUNCIA, J.V., CARINI, D.J., WEXLER, R.R., JOHNSON, A.L. & TIMMERMANS, P.B. (1990c). Nonpeptide angiotensin II receptor antagonists. XI. Pharmacology of EXP 3174: an active metabolite of DuP 753, an orally active antihypertensive agent. *J. Pharmacol. Exp. Ther.*, **255,** 211–217.

WONG, P.C., PRICE, W.A. JR, CHIU, A.T., DUNCIA, J.V., CARINI, D.J., WEXLER, R.R., JOHNSON, A.L. & TIMMERMANS, P.B. (1990d). Hypotensive action of DuP 753, an angiotensin II antagonist, in spontaneously hypertensive rats. Nonpeptide angiotensin II receptor antagonists. X. *Hypertension*, **15,** 459–468.

WONG, P.C., HART, S.D., CHIU, A.T., HERBLIN, W.F., CARINI, D.J., SMITH, R.D., WEXLER, R.R. & TIMMERMANS, P.B.M.W.M. (1991a). Pharmacology of DuP 532, a selective and noncompetitive AT_1 receptor antagonist. *J. Pharmacol. Exp. Ther.*, **259,** 861–870.

WONG, P.C., PRICE, W.A., Jr., CHIU, A.T., DUNCIA, J.V., CARINI, D.J., WEXLER, R.R., JOHNSON, A.L. & TIMMERMANS, P.B.M. W.M. (1991b). *In vivo* pharmacology of DuP 753. *Am. J. Hypertens.*, **4,** Suppl., 288S–298S.

WOOD, J.M., CRISCIONE, L., DE GASPARO, M., BUEHLMAYER, P., RUEEGER, H., STANTON, J.L., JUPP, R.A. & KAY, J. (1989). CGP 38 560 an orally active, low-molecular-weight renin inhibitor with high potency and specificity. *J. Cardiovasc. Pharmacol.*, **14,** 221–226.

(Received December 17, 1992
Revised May 12, 1993
Accepted May 18, 1993)

Br. J. Pharmacol. (1993), **110**, 772–776

Effect of a calcitonin gene-related peptide antagonist ($CGRP_{8-37}$) on skin vasodilatation and oedema induced by stimulation of the rat saphenous nerve

K. Jane Escott & [1]Susan D. Brain

Pharmacology Group, Division of Biomedical Sciences, King's College, Manresa Road, London SW3 6LX

1 The effect of the calcitonin gene-related peptide antagonist ($CGRP_{8-37}$, 400 nmol kg^{-1}, i.v.) on the increased blood flow induced by calcitonin gene related peptide (CGRP), vasodilator prostaglandins, and topical capsaicin was measured with a laser Doppler blood flow meter in rat abdominal skin.

2 The saphenous nerve was electrically stimulated and the effect of $CGRP_{8-37}$ (400 nmol kg^{-1}, i.v.) on the increased blood flow (measured by laser Doppler flowmetry) and oedema formation (measured by the extravascular accumulation of [^{125}I]-albumin) was investigated in the rat hind paw.

3 $CGRP_{8-37}$ (400 nmol kg^{-1}, i.v.) had no effect on basal cutaneous blood flow at uninjected sites and sites injected with Tyrode buffer, but acted selectively to inhibit the increased blood flow induced by intradermal CGRP (10 pmol/site, $P<0.05$), but not that induced by prostaglandin E_2 (PGE_2, 300 pmol/site) or carba-prostacyclin ($cPGI_2$, 100 pmol/site).

4 Capsaicin (0.1–33 mM), applied topically, acted in a dose-related manner to increase blood flow. $CGRP_{8-37}$ (400 nmol kg^{-1}, i.v.) almost totally inhibited blood flow induced by capsaicin (10 mM; $P<0.05$) but did not significantly inhibit blood flow induced by a higher dose of capsaicin (33 mM).

5 The increased blood flow induced by short stimulation of the saphenous nerve (10 V, 1 ms, 2 Hz for 30 s) was inhibited by 76%, 5 min after i.v. $CGRP_{8-37}$ (400 nmol kg^{-1}, i.v., $P<0.05$).

6 A longer (5 min) electrical stimulation of the saphenous nerve caused oedema formation, in addition to increased blood flow. The oedema formation was significantly inhibited by $CGRP_{8-37}$ (400 nmol kg^{-1}, i.v., $P<0.05$).

7 The results suggest that the potent microvascular vasodilator neuropeptide, CGRP, is responsible for the increased blood flow observed after short stimulation of the saphenous nerve and that endogenous CGRP contributes in a pro-inflammatory manner to neurogenic oedema formation in the rat hind paw.

Keywords: Calcitonin gene-related peptide (CGRP); substance P; neurokinin-1 receptors; saphenous nerve; skin blood flow; laser Doppler flowmetry; neurogenic inflammation

Introduction

Our group has previously studied the release and activity of the 37 amino acid vasodilator sensory neuropeptide calcitonin gene-related peptide (CGRP) in the rabbit cutaneous microvasculature. The studies show that the increased blood flow induced in rabbit skin by intradermal injection of capsaicin and analogues (e.g. olvanil), can be inhibited by the co-injection of the 8–37 amino acid C-terminal peptide of CGRP ($CGRP_{8-37}$), a selective competitive antagonist of CGRP (Chiba *et al.*, 1989; Gardiner *et al.*, 1990; Han *et al.*, 1990). Early experiments suggested that $CGRP_{8-37}$ could partially inhibit capsaicin-induced vasodilatation (Hughes & Brain, 1991), whilst more recent experiments using $CGRP_{8-37}$ synthesized by improved techniques have shown that a 60% increase in blood flow in response to capsaicin (100 nmol/site) is totally inhibited by $CGRP_{8-37}$ (Hughes *et al.*, 1992). We have concluded from these results that CGRP is an important vasodilator neuropeptide released from capsaicin sensitive nerves in rabbit skin. It is generally assumed that substance P, which is often co-localised with CGRP also has an important vasoactive effect. However, substance P is an extremely weak vasodilator in rabbit skin (Brain *et al.*, 1985) and a neurokinin-1 (NK_1) receptor selective antagonist had little effect on capsaicin-induced blood flow in this species (Hughes *et al.*, 1992).

In this study we have investigated the release and activity of CGRP in rat skin, where neurokinins (especially substance P) have been established as potent vasoactive mediators (Lembeck & Holzer 1979; Gamse & Saria 1985; Brain & Williams 1989). We know, from a previous study that $CGRP_{8-37}$ cannot be administered intradermally in the rat due to a pro-inflammatory activity, possibly related to basic residues in the N-terminus region (Brain *et al.*, 1992). Thus we have administered $CGRP_{8-37}$ intravenously (i.v.) which has been shown to be effective in inhibiting the hypotensive effects of i.v. CGRP in several studies (Donoso *et al.*, 1990; Gardiner *et al.*, 1990). We have examined the ability of $CGRP_{8-37}$ to influence the sensory nerve-dependent pro-inflammatory responses in the rat in response to capsaicin administration and electrical stimulation of the saphenous nerve.

Methods

Blood flow and oedema formation were measured in the skin of male Wistar rats (200–300 g), anaesthetized with sodium pentobarbitone (Sagatal, May and Baker, initial i.p. injection 50–80 mg kg^{-1}, maintained by additional 20 mg kg^{-1} h^{-1}, given i.v.). Body temperature was maintained at 36–38°C by automatic control of a heating pad. Rats were pretreated with guanethidine (20 mg kg^{-1}, s.c.) 24 h before saphenous nerve stimulation, to prevent vasoconstriction induced by concomitant stimulation of the sympathetic fibres of the saphenous nerve (Gamse & Saria, 1987).

Measurement of blood flow in abdominal skin

The animal was anaesthetized, and the abdominal skin

[1] Author for correspondence.

shaved and depilated. Thirty minutes later $CGRP_{8-37}$ or vehicle were given i.v. and blood flow was measured at several sites with a laser Doppler flowmeter. Prostaglandins, CGRP or Tyrode were injected intradermally (50 μl) and capsaicin or vehicle (20% alcohol: 10% Tween 80: 70% saline) were applied topically (5 μl). Blood flow was measured again between 5–10 min after application of test agents. Blood flow changes were measured with a Moor dual probe laser Doppler (MBF3D) and measured as flux, as previously discussed in detail (Lawrence & Brain, 1992). The results are expressed as percentage change in blood flow compared with pre-injected sites in Figures 1 and 2. In some experiments the protocols were designed to measure responses to vasoactive agents and to saphenous nerve stimulation in the same animals.

Measurement of blood flow after saphenous nerve stimulation

After induction of anaesthesia the hind limbs of the rat were shaved and depilated with a commercial cream. The jugular vein was cannulated for i.v. administration of anaesthetic and test agents. The saphenous nerves were carefully dissected in both legs (stimulated or sham legs) tied centrally, placed on bipolar platinum electrodes and immersed in mineral oil. In order to study antidromic vasodilatation one laser Doppler probe was positioned and secured over the hind paw skin in a region innervated by the saphenous nerve, i.e. medio-dorsal side of the skin of the hind paw, as confirmed by the observation of Evans Blue dye extravasation after saphenous nerve stimulation. The other probe was positioned in a corresponding site on the sham treated hind paw to monitor basal blood flow throughout the experiment. Not earlier than 30 min after the preparation was finished, antidromic stimulation was performed using the following parameters: 10 V, 1 ms, 2 Hz for 30 s. Three stimulations were given at 20–30 min intervals. To investigate the effect of $CGRP_{8-37}$ on blood flow changes induced by saphenous nerve stimulation, $CGRP_{8-37}$ (400 nmol kg^{-1}), or vehicle (0.1% BSA in saline) were administered i.v. 5 min prior to the second stimulation. Results in Figure 3 show the flux in 3a and 3b; whilst Figure 3c shows percentage change in the vasodilator response to saphenous nerve stimulation, after i.v. treatments.

Measurement of oedema in the hind paw after saphenous nerve stimulation

The saphenous nerves were prepared as described above and left for 5 min. Then Evans Blue (25 mg kg^{-1}) and ^{125}I-labelled human serum albumin (50 kBq) were injected into the rat via the tail vein. $CGRP_{8-37}$ (400 nmol kg^{-1}) or vehicle (0.1% BSA) were administered via the jugular vein, at least 5 min prior to stimulation. Then the nerve was stimulated: 10 V, 1 ms, 2 Hz for 5 min. After stimulation, a blood sample was obtained by cardiac puncture and then the animal killed by anaesthetic overdose. The oedematous area of skin of the hind paw (as observed by Evans blue dye extravasation) was removed and weighed. An approximately equal amount of skin was also removed from the sham hind paw and weighed. Radioactivity was counted in 100 μl of plasma and hind paw skin samples. Plasma extravasation was expressed as μl of plasma in 100 mg of skin and a ratio calculated: sham versus stimulated hind paw oedema for each rat.

Statistical analysis

Results are expressed as mean ± s.e.mean. Abdominal, dorsal skin and paw blood flow data were analysed by Bonferroni's modified *t* test, the standard error estimate for the analysis of variance was used to allow comparison of multiple sites. The significance of the hind paw skin oedema after saphenous nerve stimulation was tested by Student's unpaired *t* test.

Materials

The following drugs were used: prostglandin E_1 (PGE_1) from Sigma Chemical Company, U.K., human α-calcitonin gene-related peptide (CGRP) a gift from Dr U. Ney, Celltech, U.K., human $CGRP_{8-37}$ from Bachem, U.K., synthetic capsaicin-pelargonic acid vanillylamide from Fluka Chemicals Ltd., U.K., carba-prostacyclin ($cPGI_2$) from Cascade Biochem. Ltd., U.K., and guanethidine from Ciba-Geigy, U.K. CGRP, PGE_1 and PGI_2 were stored in stock solutions at − 20°C and then diluted with Tyrode solution immediately prior to use. $CGRP_{8-37}$ was prepared in 0.1% bovine serum albumin (BSA) in saline. Capsaicin was dissolved in ethanol at 100 mg ml^{-1} and diluted in a solution of alcohol:Tween 80:saline, at a ratio of 20:10:70. ^{125}I-labelled human serum albumin was obtained from Amersham International, U.K. Immac (Reckitt & Colman, U.K.) was used to remove remaining hair stubble. The composition of the Tyrode solution was a follows (mM): NaCl 136.89, KCl 2.68, NaH_2PO_4 0.42, $NaHCO_3$ 11.9, $MgCl_2$ 1.05 and glucose 5.55.

Results

The intradermal injection of CGRP, PGE_1 and carba-prostacyclin ($cPGI_2$) led to an increased blood flow as measured by laser Doppler flowmetry, in keeping with previous observations (Brain & Williams, 1989). $CGRP_{8-37}$ (400 nmol kg^{-1}, i.v.) had no significant effect on basal blood flow as shown in Figure 1. However, this figure shows that $CGRP_{8-37}$ significantly inhibited the increased blood flow induced by CGRP but not that induced by the prostaglandins. These results indicate that the administration of intravenous $CGRP_{8-37}$ can be used to investigate the release of vasoactive amounts of endogenous CGRP.

The effect of the application of topical capsaicin on rat cutaneous blood flow is shown in Figure 2. Capsaicin increased blood flow in a dose-related manner, whilst the vehicle had no effect on blood flow when tested at the highest concentration used. The graph is similar to that obtained by Lynn and co-workers (1992). $CGRP_{8-37}$ caused an almost

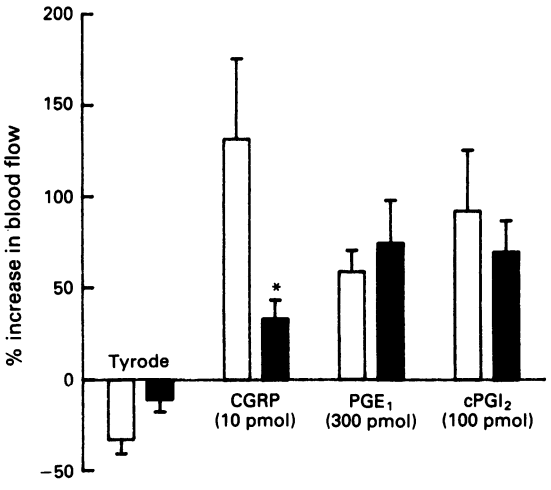

Figure 1 The effect of calcitonin gene-related peptide (CGRP) and vasodilator prostaglandins on blood flow in rat abdominal skin. Results are expressed as percentage change in local skin blood flow at each injected site compared with blood flow at the site before injection. The results from control rats (0.1% BSA, i.v.) are shown by the open columns and from rats treated with $CGRP_{8-37}$ (400 nmol kg^{-1}, i.v.) are shown by the solid columns. The results are expressed as the mean ± s.e.mean of 9 rats in each group. A significant effect of $CGRP_{8-37}$ on the vasodilator activity of CGRP is shown by $*P<0.05$.

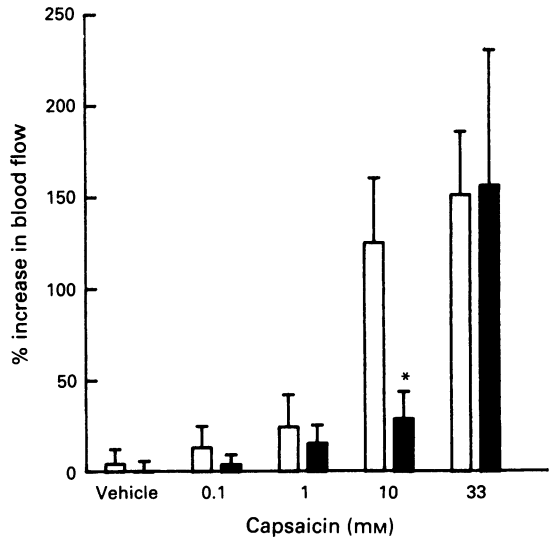

Figure 2 The effect of topical capsaicin on blood flow in rat abdominal skin. Results are expressed as percentage increase in local blood flow at each injected site compared with blood flow at the site before injection. The open columns represent control rats (0.1% BSA, i.v.) and the solid columns are animals treated with $CGRP_{8-37}$ (400 nmol kg^{-1}, i.v.). Each column is the mean ± s.e.mean of 9 rats. $CGRP_{8-37}$ significantly inhibited the vasodilator activity of capsaicin at a dose of 10 nM, as shown by $*P<0.05$.

total inhibition of blood flow induced by capsaicin (10 mM). However, little inhibitory effect of a higher dose of capsaicin, 33 mM was observed.

A short (30 s) electrical stimulation of the saphenous nerve caused an increased blood flow which returned to baseline levels within 5–10 min after stimulation. This response was repeatable at least three times, as shown in Figure 3a. $CGRP_{8-37}$ caused an inhibition of the peak response as shown in Figure 3b. The group data, with an inhibition of stimulated blood flow at both time points after saphenous nerve stimulation are shown in Figure 3c. No evidence of oedema formation was observed within this short stimulation period. By comparison increasing the stimulation period to 5 min led to the well established neurogenic oedema formation (shown in Figure 4) as first described by Jancso *et al.* (1967). The oedema was significantly attenuated by $CGRP_{8-37}$. The results suggest that $CGRP_{8-37}$ acted to inhibit approximately 50% of the oedema formation induced by electrical stimulation of the saphenous nerve.

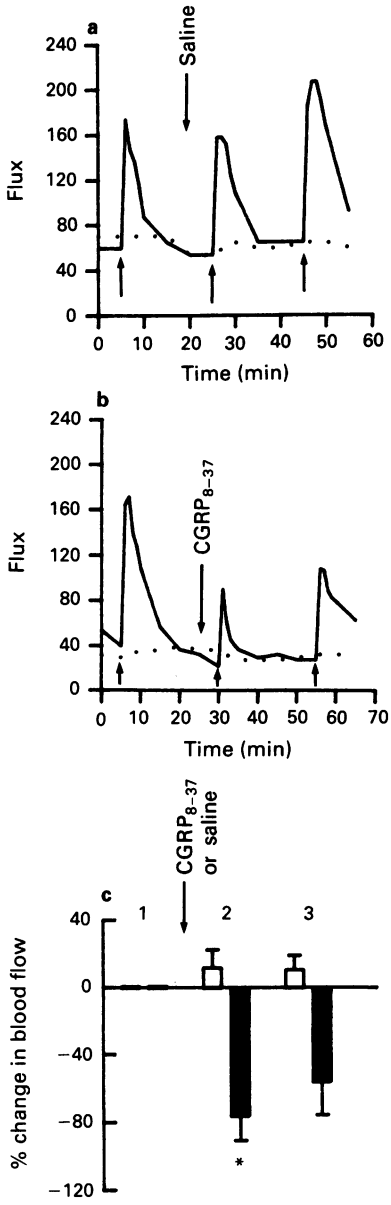

Figure 3 Effect of $CGRP_{8-37}$ on blood flow in the skin of rat hind paw after saphenous nerve stimulation (10 V, 1 ms, 2 Hz, for 30 s). (a) Effect of repeated stimulations of the saphenous nerve on blood flow in the skin of a rat hind paw. The rat received vehicle (0.1% BSA in saline, i.v.) 5 min prior to the second stimulation. (b) Effect of $CGRP_{8-37}$ (400 nmol kg^{-1}, i.v., 5 min before the second stimulation) on saphenous-induced blood flow in the rat hind paw skin. The results for (a) and (b) are expressed as Flux (arbitrary unit) and the dotted line indicates flux recorded on the contralateral paw. Stimulation of the saphenous nerve is represented by the upward arrows. (c) Collected results to show the effect of $CGRP_{8-37}$ on blood flow induced by saphenous nerve stimulation. Results are expressed as percentage change in blood flow compared to the first stimulation and are the mean ± s.e.mean of 4 rats in each group. In each group $CGRP_{8-37}$ or vehicle were administered i.v. at least 5 min prior to the second stimulation. $CGRP_{8-37}$ inhibited blood flow after the second stimulation ($*P<0.05$) and the third stimulation.

Discussion

The results show that $CGRP_{8-37}$ acts in a selective manner to antagonize the actions of exogenous CGRP in increasing blood flow. $CGRP_{8-37}$ also significantly inhibited the increased blood flow induced by topical capsaicin (10 mM) and saphenous nerve stimulation, as well as oedema formation induced by saphenous nerve stimulation. $CGRP_{8-37}$ failed to inhibit the increased blood flow induced by the highest dose of capsaicin (33 mM). The reason for this is unclear; possibly a maximal response combined with the release of increased levels of CGRP resulted in an inability of $CGRP_{8-37}$ to inhibit the increased blood flow. Alternatively other vasodilator mediators might be involved in mediating the increased blood flow induced by this dose of capsaicin.

The stimulation of the saphenous nerve in rats previously treated with guanethidine, to deplete a sympathetic component, has become an established small animal model of neurogenic inflammation, since Lembeck & Holzer (1979) provided evidence that substance P acts as a neurogenic mediator of antidromic vasodilatation and neurogenic plasma extravasation. In those experiments, blood flow was measured by femoral vein outflow. In the present experiments blood flow is measured by laser Doppler flowmetry. The use of the laser Doppler blood flow meter to measure saphenous nerve-stimulated increased blood flow was first used by Gamse & Saria (1987). It became immediately apparent that an increase in blood flow could be induced by a mild and short electrical stimulation when compared with the electrical stimulation necessary for the

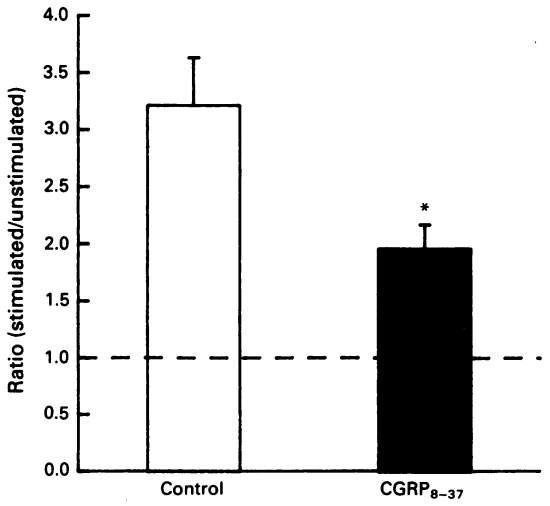

Figure 4 Effect of $CGRP_{8-37}$ (400 nmol kg^{-1}, i.v.) on oedema formation after electrical stimulation of the saphenous nerve (10 V, 1 ms, 2 Hz for 5 min). Results are expressed as the ratio of plasma extravasation in the stimulated compared to the sham-treated hind paw skin. The dashed line at 1 indicates the basal level of plasma extravasation in unstimulated paws. Results are expressed as mean ± s.e. mean of 10 rats in each group. $CGRP_{8-37}$ (solid column) significantly reduced plasma extravasation as indicated by $*P<0.05$, in comparison to the control rats (0.1% BSA, i.v., open column).

observation of oedema formation. The reason for this is not clear. It is probably related to the potency of endogenous CGRP as a vasodilator in skin. It is also possible that CGRP is released from A-delta fibres in addition to C-fibre nerves in initial saphenous nerve stimulation (Janig & Lisney, 1989). The present results are compatible with the suggestion that CGRP is the principle vasodilator released after mild and short stimulation of sensory nerves and this is in keeping with the findings of Delay-Goyet and co-workers (1992) who published a brief communication with similar findings whilst this study was in progress. They also investigated the effect of a neurokinin-1 antagonist (RP67580) and showed that this had no effect on saphenous nerve stimulation-mediated changes in blood flow.

Thus our findings indicate that CGRP mediates the increase in cutaneous blood flow observed with saphenous nerve stimulation. Results of previous studies in our group show that CGRP, does not act by itself to increase microvascular permeability, but as a consequence of its vasodilator activity potentiates oedema formation induced by mediators of increased microvascular permeability such as substance P and neurokinin A, in species that include the rat (Brain & Williams, 1985; 1989). We therefore investigated whether $CGRP_{8-37}$ could affect oedema formation induced by saphenous nerve stimulation. The results show an approximately 50% inhibition. Similar experimental protocols have been used to investigate the effect of recently developed non-peptide NK_1 receptor antagonists on oedema formation induced by saphenous nerve stimulation. CP96345 (Lembeck *et al.*, 1992; Xu *et al.*, 1992) and RP67580 (Garret *et al.*, 1991) almost completely abolished oedema formation, whilst a NK_2 receptor antagonist, Men10207, had no inhibitory effect (Xu *et al.*, 1992). These results are in keeping with the previous suggestion that the NK_1 receptor mediates increased microvascular permeability (Andrews *et al.*, 1989). The partial inhibitory activity of $CGRP_{8-37}$, on oedema formation induced by saphenous nerve stimulation, indicates that endogenously-released CGRP is involved in neurogenic oedema formation. An increase in blood flow is observed and this is concomitant with oedema formation (Shepheard *et al.*, 1992). It is unlikely that substance P acts directly via NK_1 receptors to increase blood flow as the selective NK_1 receptor agonist, GR73632, does not increase blood flow in rat skin, although it has potent oedema inducing effects which are potentiated by CGRP (Birch *et al.*, 1992; Richards *et al.*, 1993). Further it is known that the selective NK_1 receptor antagonist RP67580 does not affect the increased blood flow induced by stimulation of the saphenous nerve at levels sufficient to induce oedema formation (Shepheard *et al.*, 1992). Thus a vasodilator component is likely to be involved in the resulting oedema formation. There are several possibilities as to the identity of this vasodilator. Firstly the increased blood flow could be totally induced by CGRP at concentrations that were not possible to antagonize in the present experiments when oedema formation occurs in response to a 5 min electrical stimulation period. It should be remembered that $CGRP_{8-37}$ is a peptide antagonist which is poorly characterized whilst CP96345 and RP67580 are non-peptide structures, developed on the basis of their affinity and selectivity as NK_1 receptor antagonists. Alternatively it is possible that substance P is released from the saphenous nerve in sufficient quantities to stimulate mast cell degranulation and thus the release of the vasoactive amines histamine and 5-hydroxytryptamine (5-HT). This has been suggested by previous studies where evidence for the involvement of histamine and 5-HT has been obtained (Lembeck & Holzer, 1979; Morton & Chahl, 1980). However this would appear unlikely as the amines do not participate in the oedema response which, as discussed above, is completely inhibited by NK_1 receptor antagonists. It is also possible that another distinct, perhaps novel vasodilator, in addition to CGRP, is released from sensory nerves upon saphenous nerve stimulation. This is the most exciting possibility but we have no evidence to date that this is so.

We consider that the involvement of CGRP in neurogenic oedema formation is of interest. It has recently been demonstrated that the NK_1 receptor antagonist, RP67580, inhibits oedema formation in the rat dura induced by trigeminal nerve stimulation (Shepheard *et al.*, 1993); a neurogenic model that is considered to be relevant to migraine in man. Also increased CGRP levels have been measured in venous blood samples taken from patients with migraine (Goadsby *et al.*, 1990). As CGRP is colocalized with substance P it could be released in the rat dura in vasodilator amounts. It is not known whether the endogenous release of CGRP is pro-inflammatory in terms of vasodilatation or oedema formation in the rat dura; but our results obtained in this study would suggest that such a possibility may exist. However, it should also be pointed out that CGRP, at vasodilator doses, is anti-inflammatory in the hamster cheek pouch causing a clear inhibition of mediator induced oedema formation (Raud *et al.*, 1991). Our studies suggest that this anti-inflammatory mechanism does not operate in rat skin or paw (Newbold & Brain, 1993); but the collected findings highlight the possibility that CGRP could well have multiple effects on the inflammatory response.

In conclusion we have shown that $CGRP_{8-37}$ inhibits vasodilatation induced by topical capsaicin and saphenous nerve stimulation in the rat and thus provide evidence that endogenous CGRP is the major vasodilator mediator in these models of neurogenic inflammation. $CGRP_{8-37}$ also significantly inhibited neurogenic oedema formation induced by stimulation of the saphenous nerve. We consider this is good evidence to suggest that CGRP potentiates oedema formation when co-released from sensory nerves with substance P.

K.J.E. is the recipient of an MRC/Glaxo collaborative studentship. We thank Dr H. Connors and Dr D. Beattie from Glaxo Group research, U.K. for their helpful discussion and Dr U. Ney from Celltech, U.K. for the gift of the human α-CGRP.

References

ANDREWS, P.V., HELME, R.D. & THOMAS, K.L. (1989). NK_1 receptor mediation of neurogenic plasma extravasation in rat skin. *Br. J. Pharmacol.*, **97**, 1232–1238.

BIRCH, P.J., HARRISON, S.M., HAYES, A.G., ROGERS, H. & TYERS, M.B. (1992). The non-peptide NK_1 receptor antagonist (±)-CP-96,345, produces antinociceptive and anti-oedema effects in the rat. *Br. J. Pharmacol.*, **105**, 508–510.

BRAIN, S.D., CAMBRIDGE, H., HUGHES, S.R. & WILSONCROFT, P. (1992). Evidence that calcitonin gene-related peptide contributes to inflammation in the skin and joint. *Proc. Natl. Acad. Sci. U.S.A.*, **657**, 412–419.

BRAIN, S.D. & WILLIAMS, T.J. (1985). Inflammatory oedema induced by synergism between calcitonin gene-related peptide (CGRP) and mediators of increased vascular permeability. *Br. J. Pharmacol.*, **86**, 855–860.

BRAIN, S.D. & WILLIAMS, T.J. (1989). Interactions between the tachykinins and calcitonin gene-related peptide lead to the modulation of oedema formation and blood flow in rat skin. *Br. J. Pharmacol.*, **97**, 77–82.

BRAIN, S.D., WILLIAMS, T.J., TIPPINS, J.R., MORRIS, H.R. & MACINTYRE, I. (1985). Calcitonin gene-related peptide is a potent vasodilator. *Nature*, **313**, 54–56.

CHIBA, T., YAMAGUCHI, A., YAMATANI, T., NAKAMURA, A., MORISHITA, T., INUI, T., FUKASE, M., NODA, T. & FUJITA, T. (1989). Calcitonin gene-related peptide receptor antagonist human CGRP(8–37). *Am. J. Physiol.*, **256**, E331–E335.

DELAY-GOYET, P., SATOH, H. & LUNDBERG, J.M. (1992). Relative involvement of substance P and CGRP mechanisms in antidromic vasodilation in the rat skin. *Acta. Physiol. Scand.*, **146**, 537–538.

DONOSO, M.V., FOURNIER, A., ST-PIERRE, S. & HUIDOBRO-TORO, J.P. (1990). Pharmacological characterization of CGRP1 receptor subtype in the vascular system of the rat: studies with hCGRP fragments and analogs. *Peptides*, **11**, 885–889.

GAMSE, R. & SARIA, A. (1985). Potentiation of tachykinin-induced plasma protein extravasation by calcitonin gene-related peptide. *Eur. J. Pharmacol.*, **114**, 61–66.

GAMSE, R. & SARIA, A. (1987). Antidromic vasodilatation in the rat hindpaw measured by laser Doppler flowmetry: pharmacological modulation. *J. Auton. Nerv. Syst.*, **19**, 105–111.

GARDINER, S.M., COMPTOM, A.M., KEMP, P.A., BENNETT, T., BOSE, C., FOULKES, R. & HUGHES, B. (1990). Antagonistic effect of human α-CGRP[8-37] on the in vivo regional haemodynamic actions of human αCGRP. *Biochem. Biophys. Res. Commun.*, **171**, 938–943.

GARRET, C., CARUETTE, A., FARDIN, V., MOUSSAOUI, S., PEYRONEL, J.-F., BLANCHARD, J.-C. & LADURON, P.M. (1991). Pharmacological properties of a potent and selective nonpeptide substance P antagonist. *Proc. Natl. Acad. Sci. U.S.A.*, **88**, 10208–10212.

GOADSBY, P.J., EDVINSSON, L. & EKMAN, R. (1990). Vasoactive peptide release in the extracerebral circulation of humans during migraine headache. *Ann. Neurol.*, **28**, 183–187.

HAN, S.P., NAES, L. & WESTFALL, T.C. (1990). Inhibition of periarterial nerves stimulation-induced vasodilatation of the mesenteric arterial bed by CGRP(8-37) and CGRP receptor desensitization. *Biochem. Biophys. Res. Commun.*, **168**, 786–791.

HUGHES, S.R. & BRAIN, S.D. (1991). A calcitonin gene-related peptide (CGRP) antagonist ($CGRP_{8-37}$) inhibits microvascular responses induced by CGRP and capsaicin in skin. *Br. J. Pharmacol.*, **104**, 738–742.

HUGHES, S.R., BUCKLEY, T.L. & BRAIN, S.D. (1992). Olvanil: more potent than capsaicin at stimulating the efferent function of sensory nerves. *Eur. J. Pharmacol.*, **219**, 481–484.

JANIG, W. & LISNEY, S.J.W. (1989). Small diameter myelinated afferents produce vasodilatation but not plasma extravasation in rat skin. *J. Physiol.*, **415**, 477–486.

JANSCO, N., JANSCO-GABOR, A. & SZOLCSANYII, J. (1967). Direct evidence for neurogenic inflammation and its prevention by denervation and by pretreatment with capsaicin. *Br. J. Pharmacol.*, **31**, 138–151.

LAWRENCE, E. & BRAIN, S.D. (1992). Responses to endothelins in the rat cutaneous microvaculature: a modulatory role of locally-produced nitric oxide. *Br. J. Pharmacol.*, **106**, 733–738.

LEMBECK, F., DONNERER, J., TSUCHIYA, M. & NAGAHISA, A. (1992). The non-peptide tachykinin antagonist, CP-96,345, is a potent inhibitor of neurogenic inflammation. *Br. J. Pharmacol.*, **105**, 527–530.

LEMBECK, F. & HOLZER, P. (1979). Substance P as neurogenic mediator of antidromic vasodilation and neurogenic plasma extravasation. *Naunyn-Schmied Arch. Pharmacol.*, **310**, 175–183.

LYNN, B., YE, W. & COTSELL, B. (1992). The actions of capsaicin applied topically to the skin of the rat on C-fibre afferents, antidromic vasodilatation and substance P levels. *Br. J. Pharmacol.*, **107**, 400–406.

MORTON, C.R. & CHAHL, L.A. (1980). Pharmacology of the neurogenic oedema response to electrical stimulation of the saphenous nerve in the rat. *Naunyn-Schmied. Arch. Pharmacol.*, **314**, 271–276.

NEWBOLD, P. & BRAIN, S.D. (1993). The modulation of inflammatory oedema by calcitonin gene-related peptide. *Br. J. Pharmacol.*, **108**, 705–710.

RAUD, J., LUNDERBERG, T., BRODDA-JANSEN, G. THEODORSSON, E. & HEDQVIST, P. (1991). Potent anti-inflammatory action of calcitonin gene-related peptide. *Biochem. Biophys. Res. Commun.*, **180**, 1429–1435.

RICHARDS, K.J., CAMBRIDGE, H. & BRAIN, S.D. (1993). Comparative effects of a neurokinin-1 (NK_1) receptor agonist, GR73632, and CGRP on microvascular tone and permeability in rat skin. *Neuropeptides*, **24**, 206.

SHEPHEARD, S.L., COOK, D.A., WILLIAMSON, D.J., HURLEY, C.J., HILL, R.G. & HARGREAVES, R.J. (1992). Inhibition of neurogenic plasma extravasation but not vasodilation in the hind limb of the rat by the non-peptide NK-1 receptor antagonist (±) RP 67580. *Br. J. Pharmacol.*, **107**, 150P.

SHEPHEARD, S.L., WILLIAMSON, D.J., HILL, R.G. & HARGREAVES, R.J. (1993). The non-peptide neurokinin$_1$ receptor antagonist, RP 67580, blocks neurogenic plasma extravasation in the dura mater of rats. *Br. J. Pharmacol.*, **108**, 11–12.

XU, J.-X., DALSGAARD, J.-C., MAGGI, C.A. & WIESENFELD-HALLIN, Z. (1992). NK-1, but not NK-2, tachykinin receptors mediate plasma extravasation induced by antidromic C-fiber stimulation in rat hindpaw: demonstrated with the NK-1 antagonist CP-96,345 and the NK-2 antagonist Men 10207. *Neurosci. Lett.*, **139**, 249–252.

(Received March 30, 1993
Revised May 10, 1993
Accepted May 18, 1993)

Br. J. Pharmacol. (1993), **110**, 777–782

Use of the endothelin antagonists BQ-123 and PD 142893 to reveal three endothelin receptors mediating smooth muscle contraction and the release of EDRF

[1]Timothy D. Warner, Graham H. Allcock, Roger Corder & John R. Vane

The William Harvey Research Institute, St. Bartholomew's Hospital Medical College, Charterhouse Square, London EC1M 6BQ

1 We have compared the receptors mediating the contractions of rings of rat thoracic aorta or rabbit pulmonary artery and rat stomach strips in response to the endothelin/sarafotoxin (ET/SX) family of peptides and to those mediating endothelium-dependent vasodilatations within the isolated perfused mesentery of the rat. To discriminate ET_A receptors from ET_B receptors we have used the criteria that ET-1 is more active than SX6c on ET_A receptors, and that the ET/SX peptides are equiactive on ET_B receptors. We have also assessed the effects of the ET_A receptor-selective antagonist BQ-123, and the non-selective ET receptor antagonist PD 142893 on the responses of each preparation to the ET/SX peptides.

2 ET-1-induced constrictions of the rat thoracic aorta (EC_{50} 3×10^{-10} M), a prototypic ET_A receptor-mediated response, or isolated perfused mesentery of the rat were antagonized by BQ-123 (10^{-5} M) or PD 142893 (10^{-5} M). SX6c did not constrict either the rat isolated perfused mesentery or the rat thoracic aorta. Thus, ET_A receptors mediate these constrictions.

3 ET-1 and SX6c were approximately equipotent in constricting rabbit pulmonary artery rings (EC_{50}s $3-6 \times 10^{-10}$ M). Neither BQ-123 (10^{-5} M) nor PD 142893 antagonized the contractions induced by ET-1. These effects suggest mediation by ET_B receptors but PD 142893 (10^{-5} M) did give a 3 fold antagonism of constrictions induced by SX6c.

4 SX6c was more potent than ET-1 in contracting the rat stomach strip (threshold concentrations 10^{-10} and 3×10^{-10} M). Contractions to ET-1 or SX6c were unaffected by BQ-123 (10^{-5} M), again indicative of ET_B receptor-mediated events. PD 142893 (10^{-5} M) was ineffective against ET-1 but produced a 3 fold antagonism of SX6c.

5 In the rat isolated perfused mesentery ET-1 or SX6c (0.3–300 pmol) were equipotent in producing dose-related vasodilatations that were unaffected by BQ-123 (10^{-6} M), indicative of an ET_B receptor-mediated response. In contrast to the other ET_B-mediated responses, PD 142893 (10^{-6} M) strongly antagonized these vasodilatations.

6 Thus, ET_A receptors mediate constrictions of the rat thoracic aorta and rat isolated perfused mesentery whereas ET_B receptors mediate constrictions of the rabbit pulmonary artery and rat stomach strip and endothelium-dependent dilatations within the mesentery. However, within the group of ET_B receptor-mediated responses, endothelium-dependent vasodilatations are sensitive to PD 142893, whereas contractions of the isolated smooth muscle preparations are not. Thus, the receptor present on the endothelium responsible for the release of nitric oxide in response to the ET/SX peptides is most probably different from that present on smooth muscle that mediates BQ-123-insensitive contractions.

Keywords: Endothelin-1; endothelin receptors; endothelium-dependent relaxations

Introduction

The endothelins constitute a family of three structurally very closely related peptides (Inoue *et al.*, 1989) that may well be expressed in all mammalian species for the genes for endothelin-1 (ET-1), endothelin-2 (ET-2) and endothelin-3 (ET-3) are present for instance in human, porcine, rat and murine tissues (Inoue *et al.*, 1989; Saida *et al.*, 1989). Among non-mammalian species the endothelins are closely related to the sarafotoxins, which are present in the venom of *Atractaspis engaddensis* (Kloog *et al.*, 1988; Bdolah *et al.*, 1989). The effects of these peptides are considered to be mediated by two receptors. The ET_A receptor has several hundred fold more affinity for binding ET-1, ET-2 or SX6b than ET-3 or SX6c whereas the ET_B receptor binds the ET/SX peptides with equal affinity (Ambar *et al.*, 1989; Arai *et al.*, 1990; Sakurai *et al.*, 1990; Saeki *et al.*, 1991; Williams *et al.*, 1991; Clozel *et al.*, 1992). Contractions of different isolated smooth muscle preparations may be mediated by either ET_A or ET_B receptors (Harrison *et al.*, 1992; Hay, 1992; Moreland *et al.*, 1992). In addition, the ET_B receptor is present on endothelial and other cells and mediates the release of endothelium-derived relaxing factor/nitric oxide (EDRF/NO) (Warner *et al.*, 1989; Ishii *et al.*, 1991). However, there have also been reports of an endothelial receptor that selectively responds to ET-3 (Emori *et al.*, 1990) and mediates a prolonged release of EDRF/NO (Warner *et al.*, 1992b). Thus, the classification of receptors as ET_A and ET_B may not describe all the existing receptor subtypes. BQ-123 (cyclo(-D-Trp-D-Asp-Pro-D-Val-Leu-)) is a selective ET_A receptor antagonist (Ihara *et al.*, 1992) and PD 142893 (Ac-(3,3-D-diphenylalanyl)-L-Leu-L-Asp-L-Ile-L-Ile-L-Trp trifluoroacetate) is a non-selective ET_A/ET_B receptor antagonist (Hingorani *et al.*, 1992; LaDouceur *et al.*, 1992; Cody *et al.*, 1992). Using these antagonists and ET-1 and SX6c as agonists we have compared the receptors mediating the constrictor responses of the rat aorta (a prototypic ET_A receptor mediated response, Maggi *et al.*, 1989) that is antagonized by BQ-123 (pA_2 6.93, Sumner *et al.*, 1992), the rabbit pulmonary artery (a prototypic ET_b receptor mediated response; Maggi *et al.*, 1990; Panek *et al.*, 1992) and the rat stomach strip, and the vasodilatations of the rat mesentery (a

[1] Author for correspondence.

prototypic endothelium-endothelin receptor mediated response; Warner *et al.*, 1989).

Some of these data have been presented to the British Pharmacological Society (Warner *et al.*, 1992a; 1993).

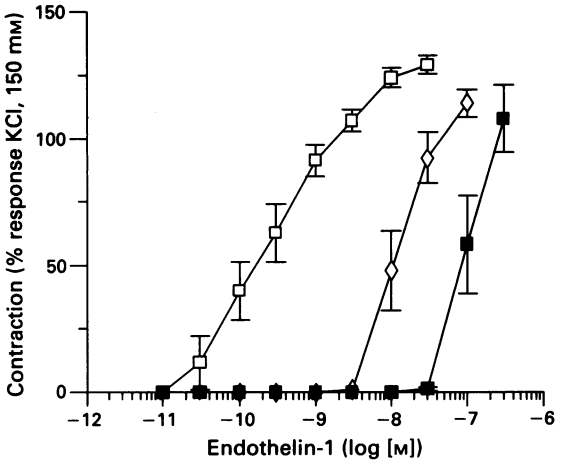

Figure 1 Effects of BQ-123 and PD 142893 on the contractile responses of the rat thoracic aorta to endothelin-1 (ET-1). Data are presented as the contractions of rings of rat thoracic aorta to ET-1 expressed as % of the contraction to KCl (150 mM). Control (□); BQ-123 (10^{-5} M), (■); PD 142893 (10^{-5} M), (◇). Results are calculated as the mean (± s.e.mean) ($n \geq 6$).

Methods

Organ bath experiments

Male Wistar rats (250–400 g) or New Zealand white rabbits were killed with thiopentone sodium (Sagatal, 120 mg kg^{-1}, i.p. or i.v.). Strips prepared from the fundus of the rat stomach (resting tension 2 g) and rings of rat aorta with the endothelium removed (2–3 mm, resting tension 1 g) and the first branches of the rabbit pulmonary artery (3 mm, resting tension 1 g) were set up in isolated organ baths containing 10 ml of Krebs buffer. Responses of the tissues were detected by isometric transducers (Hugo Sachs Electronik, Germany) and displayed on a chart recorder (Graphtec WR3101). The bathing Krebs solution, which was gassed with 95% O_2:5% CO_2 at a temperature of 37°C, contained bacitracin (3 mg l^{-1}), bovine serum albumin (50 mg l^{-1}), indomethacin (5×10^{-6} M), thiorphan (10^{-6} M), captopril (10^{-6} M) and bestatin (10^{-6} M) to exclude indirect effects induced by the production of prostanoids and to minimize the possible local metabolism by tissue enzymes (Maggi *et al.*, 1989). In a range of different isolated tissues we have found that this can produce up to a 1 log unit decrease in the threshold concentration of ET-1 (data not shown, Maggi *et al.*, 1990). After an equilibration period of 1 h the tissues were contracted by 0.15 M KCl. After wash out the tissues were incubated with either BQ-123 (10^{-5} M), PD 142893 (10^{-5} M) or vehicle for 20 min before being exposed to cumulative concentrations of ET-1 (10^{-11} to 3×10^{-7} M). Each tissue was used for only one curve. Contractile responses to the ET/SX peptides were standardized

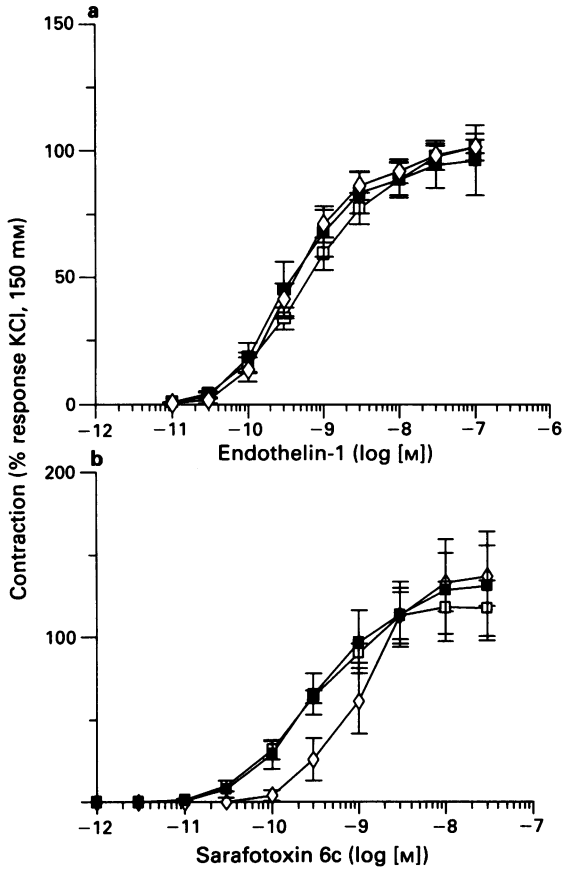

Figure 2 (a) Effects of BQ-123 and PD 142893 on the contractile responses of the rabbit pulmonary artery to endothelin-1 (ET-1). Data are presented as the contractions of rings of rabbit pulmonary artery to ET-1 expressed as % of the contraction to KCl (150 mM). (b) Effects of BQ-123 and PD 124893 on the contractile responses of the rabbit pulmonary artery to sarafotoxin 6c (SX6c). Control (□); BQ-123 (10^{-5} M), (■); PD 142893 (10^{-5} M), (◇). Results are calculated as the mean (± s.e.mean) ($n \geq 6$).

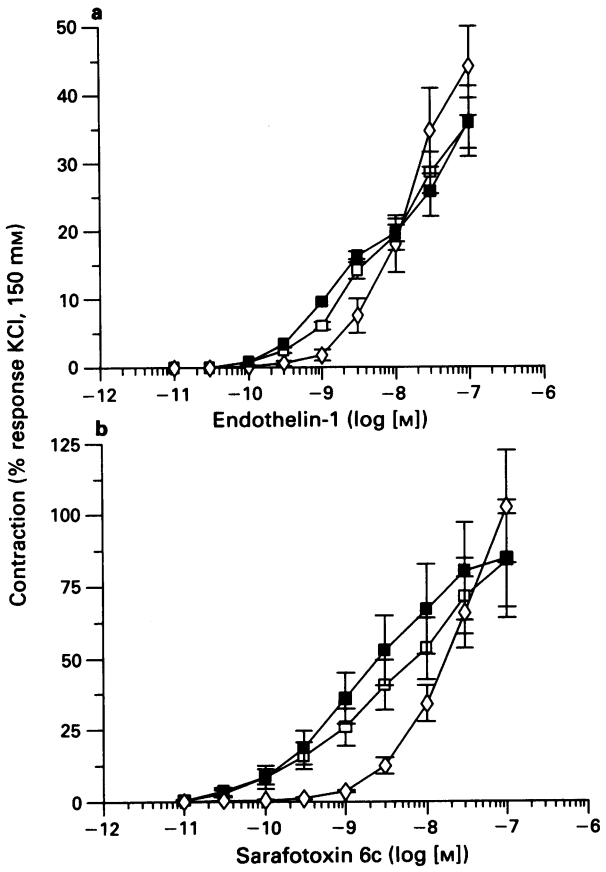

Figure 3 (a) Effects of BQ-123 and PD 142893 on the contractile responses of the rat stomach strip to endothelin-1 (ET-1). (b) Effects of BQ-123 and PD 142893 on the contractile responses of the rat stomach strip to sarafotoxin 6c (SX6c). Data are presented as the contractions of the tissues to ET-1 expressed as % of the contraction to KCl (150 mM). Control (□); BQ-123 (10^{-5} M), (■); PD 142893 (10^{-5} M), (◇). Results are calculated as the mean (± s.e.mean) ($n \geq 6$).

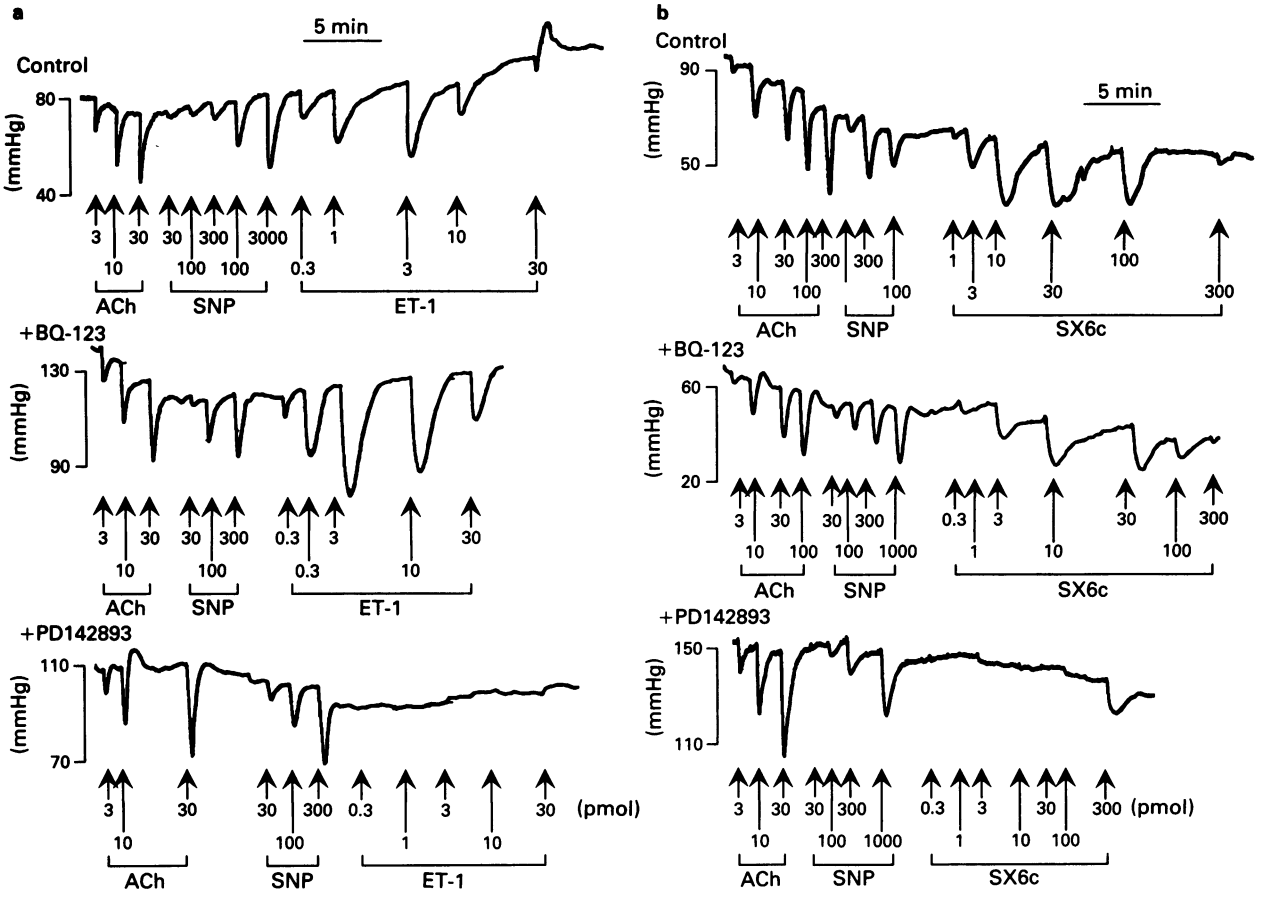

Figure 4 Representative traces of the effects of BQ-123 and PD 142893 on the vasodilatations of the rat mesentery in response to bolus injections of endothelin-1 (ET-1, 0.3–30 pmol) or sarafotoxin 6c (SX6c, 0.3–300 pmol). (a) Vasodilatations of the rat mesentery to ET-1. Upper panel, control; middle panel, in the presence of BQ-123 (10^{-6} M); lower panel, in the presence of PD 142893 (10^{-6} M). (b) Vasodilatations of the rat mesentery to SX6c. Upper panel, control; middle panel, in the presence of BQ-123 (10^{-6} M); lower panel, in the presence of PD 142893 (10^{-6} M). Tone was introduced into the preparations by the infusion of methoxamine (5×10^{-5}–1×10^{-4} M). ACh – acetylcholine (3–300 pmol); SNP – sodium nitroprusside (30–3000 pmol). Each trace is representative of at least 4 experiments.

by comparison to the KCl contraction. In some experiments we confirmed the removal of the endothelial cells from preparations by the lack of relaxation in response to acetylcholine (10^{-6} M).

Isolated perfused mesentery of the rat

The isolated perfused mesentery of the rat was prepared by the method of McGregor (1965). Male albino Wistar rats were anaesthetized with pentobarbitone sodium (120 mg kg^{-1}, i.p.), the abdomen opened and the ileocolic and colic branches of the superior mesenteric artery ligated. The superior mesenteric artery was cannulated and the superior mesenteric vascular bed perfused via the artery for 5 min (2 ml min^{-1}) with Krebs buffer containing heparin (100 u ml^{-1}). The animal was then killed by cutting the diaphragm. The intestine was separated from the mesentery and the preparation supported on a petri-dish and the arteries perfused at a constant flow of 5 ml min^{-1} with warmed (37°C) and gassed (95% O_2:5% CO_2) Krebs buffer containing indomethacin (5×10^{-6} M) to block cyclo-oxygenase activity. Changes in perfusion pressure were measured with a transducer approximately 15 cm from the tip of the arterial cannula (Warner *et al.*, 1989). After an equilibration period of 30 min the mesenteric vessels were constricted by methoxamine (5×10^{-5} M). Vehicle, BQ-123 (10^{-6} M) or PD 142893 (10^{-6} M) was then infused for 10 min before and continued during, injection of drugs in volumes of 1–3 μl to minimize any injection artefacts.

Materials

The Krebs buffer had the following composition (mM): NaCl 118, KCl 4.7, KH_2PO_4 1.2, $MgSO_4.7H_2O$ 1.17, $CaCl_2$. $6H_2O$ 2.5, $NaHCO_3$ 25 and glucose 5.6. BQ-123 and PD 142893 were synthesized by Parke-Davis, MI, U.S.A. ET-1 and SX6c were purchased from Peptide Institute (Osaka, Japan). BQ-123 and the ET/SX peptides were reconstituted in 0.9% w/v saline containing 1% w/v bovine serum albumin and 10 mM sodium bicarbonate. PD 142893 was reconstituted in dimethylsulphoxide (DMSO, 10^{-3} M) and added directly to the organ baths or further diluted into buffer (as for BQ-123 and the ET/SX peptides) for infusion into the rat mesentery. Bovine serum albumin, bacitracin, thiorphan, captopril, bestatin, methoxamine, phenylephrine, sodium nitroprusside and acetylcholine were obtained from Sigma Chemical Co. (Poole, Dorset) and dissolved in either distilled water or saline. Indomethacin (from Sigma) was made as a stock solution in sodium bicarbonate (5%). The salts for the Krebs solution were obtained from BDH (Lutterworth, Leics.).

Statistics

Statistical differences between points were determined by an unpaired two tail Student's t test and between concentration-response curves by two-way analysis of variance. $P<0.05$ was taken as significant.

Results

Rat thoracic aorta (RTA)

Control constrictions of the RTA induced by KCl were 1.2 ± 0.1 g ($n = 50$). ET-1 caused contractions of the RTA with a threshold concentration of 3×10^{-11} M and an EC_{50} of 3×10^{-10} M (Figure 1a). In the presence of BQ-123 (10^{-5} M) or PD 142893 (10^{-5} M) the concentration of ET-1 to produce 75% of the response to KCl (150 mM) was increased from 5×10^{-10} to 1.5×10^{-7} M or 2×10^{-8} M, respectively (Figure 1a, $P < 0.05$ for each). SX6c (up to 10^{-7} M, $n = 4$) did not constrict the RTA.

Rabbit pulmonary artery (RbPA)

Control constrictions of the RbPA induced by KCl were 2.1 ± 0.1 g ($n = 50$). ET-1 caused concentration-dependent contractions of the RbPA (EC_{50}, 6×10^{-10} M) which were unaffected by BQ-123 or PD 142893 (Figure 2a, $P > 0.05$ for each). Contractions induced by SX6c (EC_{50}, 3×10^{-10} M) were antagonized by PD 142893 (EC_{50}, 10^{-9} M, $P < 0.05$) but not by BQ-123 (Figure 2b).

Rat stomach strip (RSS)

Control constrictions of the RSS induced by KCl were 2.4 ± 0.1 g ($n = 50$). SX6c was more potent than ET-1 in contracting the RSS (threshold concentrations, 10^{-10} M and 3×10^{-9} M; concentrations to produce 30% of the response to KCl (150 mM) 7×10^{-10} and 5×10^{-8} M, Figures 3a and 3b). Contractions induced by ET-1 were unaffected by either BQ-123 or PD 142893 (Figure 3a, $P > 0.05$ for each), whereas contractions induced by SX6c (Figure 3b) were antagonized by PD 142893 (concentration to produce 30% of the response to KCl (150 mM) 8×10^{-9} M, $P < 0.05$), although not by BQ-123 (Figure 3b).

Rat isolated perfused mesentery (RMes)

Methoxamine (5×10^{-5} M) increased the perfusion pressure of the RMes by 91 ± 6 mmHg ($n = 36$). In preconstricted preparations ET-1 (Figure 4a) or SX6c (0.3–300 pmol, Figure 4b) produced dose-related vasodilatations. For ET-1 the higher doses caused short-lived vasodilatations followed by prolonged vasoconstrictions. SX6c produced only vasodilatations without secondary vasoconstrictions, although doses of greater than 30 pmol produced progressively smaller vasodilatations (Figure 4b) possibly due to receptor desensitization. BQ-123 (10^{-6} M) had no effect on either the magnitude or the duration of the vasodilatations caused by ET-1 (Figures 4a, 5a and 5b) or SX6c (Figures 4b, 6a and 6b). Infusion of PD 142893 (10^{-6} M) significantly decreased both the magnitude and the duration of the responses to ET-1

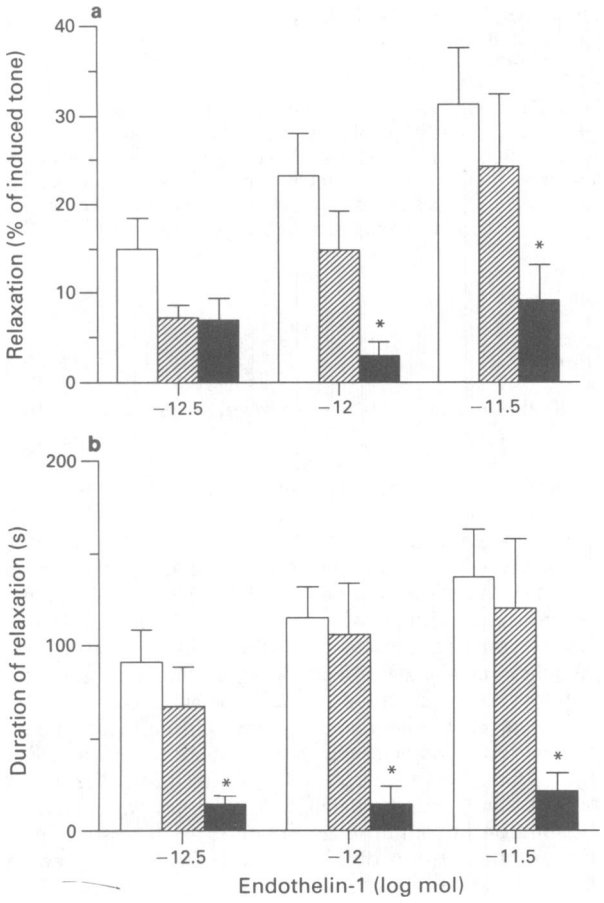

Figure 5 Effect of BQ-123 or PD 142893 on vasodilatations in response to endothelin-1 (ET-1) in the rat mesentery. (a) Vasodilatations in response to bolus injections of ET-1 expressed as % relaxation of tone induced by infusion of methoxamine (5×10^{-5}–1×10^{-4} M). (b) Duration of vasodilatations in response to bolus injections of ET-1. Control, open columns; BQ-123 (10^{-6} M), hatched columns; PD 142893 (10^{-6} M), solid columns. Each column represents the mean ± s.e.mean of at least 4 determinations.

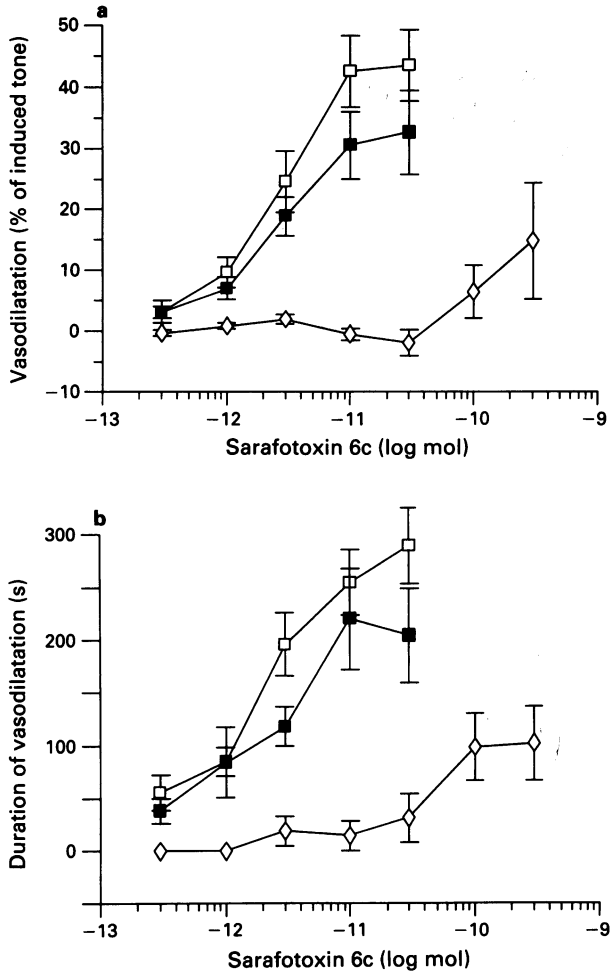

Figure 6 Effect of BQ-123 or PD 142893 on vasodilatations in response to sarafotoxin 6c (SX6c) in the rat mesentery. (a) Vasodilatations in response to bolus injections of SX6c expressed as % relaxation of tone induced by infusion of methoxamine (5×10^{-5}–1×10^{-4} M). (b) Duration of vasodilatations in response to bolus injections of SX6c. Control (□); BQ-123 (10^{-6} M), (■); PD 142893 (10^{-6} M) (◇). Results are calculated as the mean (± s.e.mean) ($n \geq 6$).

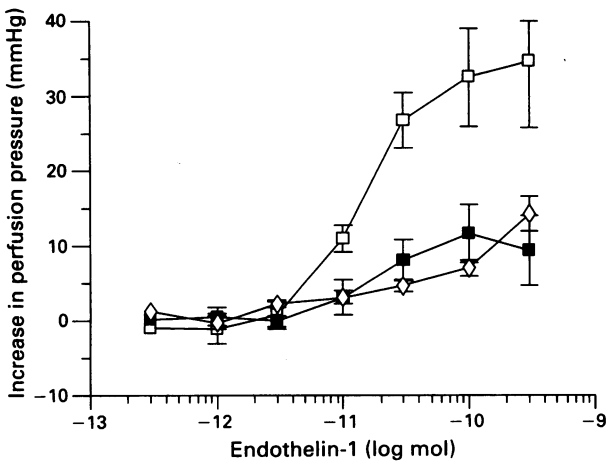

Figure 7 Effect of BQ-123 or PD 142893 on vasoconstriction in response to endothelin-1 (ET-1) in the rat mesentery. Data are expressed as the maximum increase in perfusion pressure following bolus injection of ET-1. Control (□); BQ-123 (10^{-6} M) (■); PD 142893 (10^{-6} M) (◇). Results are calculated as the mean (± s.e.mean) ($n \geqslant 6$).

(Figures 4a, 5a and 5b) or SX6c (Figures 4b, 6a and 6b), causing, for instance, a rightwards shift of 2 orders of magnitude in the dose-response curve to SX6c. BQ-123 and PD 142893 both strongly antagonized the secondary vasoconstriction induced by ET-1 (Figures 4a, 4b and 7). BQ-123 and PD 142893 did not affect endothelium-dependent vasodilatations in response to acetylcholine, or endothelium-independent vasodilatations in response to sodium nitroprusside (Figures 4a and 4b, $n \geqslant 8$ for each).

Discussion

Here we have compared the activities of the two endothelin receptor antagonists, BQ-123 and PD 142893, on the responses to ET-1 and SX6c of isolated vascular and non-vascular preparations. Our data indicate that the division ET_A and ET_B may not be sufficient to describe all endothelin-receptor subtypes, for the ET_B receptors present on smooth muscle are functionally distinct from those present on the endothelium.

The effects of ET-1 that are mediated via ET_A receptors are sensitive to blockade by BQ-123, whereas those that are mediated via ET_B receptors are BQ-123-insensitive (Ihara *et al.*, 1992; Hay, 1992; Moreland *et al.*, 1992; Sumner *et al.*, 1992). For instance, BQ-123 antagonizes the constrictions of the guinea-pig aorta induced by ET-1 but not the guinea-pig bronchus, and so these responses have been described as ET_A and ET_B receptor-mediated, respectively (Hay, 1992). We found that BQ-123 effectively antagonized constrictions of the RTA (Sumner *et al.*, 1992) and RMes induced by ET-1, but not those of the RbPA or RSS. Thus, constrictions of the RTA and RMes induced by ET-1 represent ET_A receptor-mediated events, whereas the contractions of the RbPA and RSS as well as the vasodilatations of the RMes are ET_B receptor-mediated events. This would correlate with the relative potencies of the other ET/SX peptides because we also observed that SX6c was very much less potent than ET-1 as a constrictor of the RTA (Panek *et al.*, 1992) or RMes, typical of an ET_A receptor-mediated response, whereas in the RbPA (Maggi *et al.*, 1989; Panek *et al.*, 1992) or RSS (Spokes *et al.*, 1989) SX6c was equipotent with, or even more potent than ET-1, typical of ET_B receptor-mediated responses.

Thus, the relative activities of the ET/SX peptides and the effects of BQ-123 are consistent with a division of ET-receptors into two groups ET_A and ET_B. However, our experiments using PD 142893 are not consistent with this idea. PD 142893 antagonized ET_A-mediated responses, i.e. constrictions of the RTA or RMes, in agreement with previous reports (Cody *et al.*, 1992). However, PD 142893 revealed differences in those effects of ET-1 that were insensitive to BQ-123, in that it antagonized effectively the vasodilatations of the RMes induced by ET-1, but it had no effect on ET-1-induced constrictions of the RbPA or RSS. PD 142893 slightly inhibited constrictions of the RbPA or RSS induced by SX6c, causing approximately three fold shifts in the SX6c concentration-response curves. In comparison PD 142893, at a ten times lower concentration, caused a 100 fold shift in the vasodilator response curve to SX6c in the RMes. This suggests that the ET_B receptors consist of two populations. Although all appear to be equally sensitive to the ET/SX peptides and insensitive to the effects of BQ-123, some such as those mediating the release of EDRF/NO are blocked more readily by PD 142893. These apparent differences between ET_B receptors may correspond with recent reports that different populations of high- and low-affinity ET_B receptors are present in brain (Sokolovsky *et al.*, 1992). As low stringency Southern blot analysis of human genomic DNA revealed only two genes, most probably corresponding to the ET_A and ET_B receptors (Sakamoto *et al.*, 1991), this third receptor type may represent a post-translational modification of the ET_B receptor, or a novel, unidentified receptor with low sequence similarities to the other two receptors.

Our finding that neither BQ-123 nor PD 142893 antagonized the effects of ET-1 on the RbPA is consistent with data derived from receptor binding assays (Panek *et al.*, 1992) and confirms earlier reports that ET_A receptors are not uniformly expressed on vascular smooth muscle (Harrison *et al.*, 1992; Moreland *et al.*, 1992). It is also in agreement with our observations that BQ-123 does not fully antagonize the pressor effects of the ET/SX peptides in the ganglion-blocked rat (McMurdo *et al.*, 1993) nor the vasoconstrictions in response to the ET/SX peptides in all vascular beds in the anaesthetized rat (Cristol *et al.*, 1993).

In conclusion, our results suggest that there are at least three ET receptor types. Constrictions of the RTA and RMes appear to be mediated by ET_A receptors, as defined both by the selective effects of the ET/SX peptides and by antagonism with BQ-123. Endothelium-dependent vasodilatations of the RMes and contractions of the RbPA and RSS fit the profile of effects mediated by ET_B receptors, as defined by the non-selectivity of the ET/SX peptides and the lack of antagonism by BQ-123. However, the difference in sensitivity of these ET_B receptor-mediated responses to PD 142893 distinguish the release of EDRF/NO and the constrictions of the isolated smooth muscle preparations as being mediated by different receptor types.

This work was supported by the Parke-Davis Pharmaceutical Research Division of Warner-Lambert Co. We thank Drs A. Doherty and W. Cody of the Chemistry Department for providing the ET antagonists BQ-123 and PD 142893 (Ac-(3,3-D-diphenylalanyl)-L-Leu-L-Asp-L-Ile-L-Ile-L-Trp trifluoroacetate) for these studies.

References

AMBAR, I., KLOOG, Y., SCHVARTZ, I., HAZUM, E. & SOKOLOVSKY, M. (1989). Competitive interaction between endothelin and sarafotoxin: binding and phosphoinositides hydrolysis in rat atria and brain. *Biochem. Biophys. Res. Commun.*, **158**, 195–201.

ARAI, H., HORI, S., ARAMORI, I., OHKUBO, H. & NAKANISHI, S. (1990). Cloning and expression of cDNA encoding an endothelin receptor. *Nature*, **348**, 730–732.

BDOLAH, A., WOLLBERG, G., FLEMINGER, G. & KOCHVA, E. (1989). SRTX-d, a new native peptide of the endothelin/sarafotoxin family. *FEBS Lett.*, **256**, 1–3.

CLOZEL, M., GRAY, G.A., BREU, W., LÖFFLER, B.-M. & OSTERWALDER, R. (1992). The endothelin ET_B receptor mediates both vasodilatation and vasoconstriction *in vivo*. *Biochem. Biophys. Res. Commun.*, **186**, 867–873.

CODY, W.L., DOHERTY, A.M., HE, J.X., DEPUE, P.L., RAPUNDALO, S.T., HINGORANI, G.A., MAJOR, T.C., PANEK, R.L., DUDLEY, D.T., HALEEN, S.J., LADOUCEUR, D., HILL, K.E., FLYNN, M.A. & REYNOLDS, E.E. (1992). Design of a functional hexapeptide antagonist of endothelin. *J. Med. Chem.*, **35**, 3301–3303.

CRISTOL, J.-P., WARNER, T.D., THIEMERMANN, C. & VANE, J.R. (1993). Vasoconstrictor effects of endothelins and sarafotoxins in the systemic circulation and renal vasculature of the anaesthetised rat are mediated by different receptors. *Br. J. Pharmacol.*, **108**, 776–779.

EMORI, T., HIRATA, Y. & MARUMO, F. (1990). Specific receptors for endothelin-3 in cultured bovine endothelial cells and its cellular mechanism of action. *FEBS Lett.*, **263**, 261–264.

HARRISON, V.J., RANDRIANTSOA, A. & SCHOEFFER, P. (1992). Heterogeneity of endothelin-sarafotoxin receptors mediating contraction of pig coronary artery. *Br. J. Pharmacol.*, **105**, 511–513.

HAY, D.W.P. (1992). Pharmacological evidence for distinct endothelin receptors in guinea-pig bronchus and aorta. *Br. J. Pharmacol.*, **106**, 759–761.

HINGORANI, G., MAJOR, T., PANEK, R., FLYNN, M., REYNOLDS, E., HE, X., CODY, W., DOHERTY, A. & RAPUNDALO, S. (1992). In vitro pharmacology of a non-selective (ET_A/ET_B) endothelin receptor antagonist, PD 142893 (Ac-(β-phenyl)D-Phe-L-Leu-L-Asp-L-Ile-L-Ile-L-Trp trifluoroacetate). *FASEB J.*, **6**, A1003.

IHARA, M., NOGUCHI, K., SAEKI, T., FUKURODA, T., TSUCHIDA, S., KIMURA, S., FUKAMI, T., ISHIKAWA, K., NISHIKIBE, M. & YANO, M. (1992). Biological profiles of highly potent endothelin antagonists selective for the ET_A receptor. *Life Sci.*, **50**, 247–255.

INOUE, A., YANAGISAWA, M., KIMURA, S., KASUYA, Y., MIYAUCHI, T., GOTO, K. & MASAKI, T. (1989). The human endothelin family: three structurally and pharmacologically distinct isopeptides predicted by three separate genes. *Proc. Natl. Acad. Sci. U.S.A.*, **86**, 2863–2867.

ISHII, K., WARNER, T.D., SHENG, H. & MURAD, F. (1991). Endothelin increases cyclic GMP levels in LLC-PK_1 porcine kidney epithelial cells via formation of an endothelium-derived relaxing factor-like substance. *J. Pharmacol. Exp. Ther.*, **259**, 1102–1108.

KLOOG, Y., AMBAR, I., SOKOLOVSKY, M., KOCHVA, E., WOLLBERG, Z. & BDOLAH, A. (1988). Sarafotoxin, a novel vasoconstrictor peptide: phosphoinositide hydrolysis in rat heart and brain. *Science*, **242**, 268–270.

LADOUCEUR, D.M., DAVIS, L.J., KEISER, J.A., DOHERTY, A.M., CODY, W.L., HE, F.X. & HALEEN, S.J. (1992). Effects of the endothelin receptor antagonist, PD 142893 (Ac-(β-phenyl)D-Phe-L-Leu-L-Asp-L-Ile-L-Ile-L-Trp. TFA) on endothelin-1 (ET-1) induced vasodilation and vasoconstriction in regional arterial beds of the anaesthetized rat. *FASEB J.*, **6**, A1004.

MAGGI, C.A., GIULIANI, S., PATACCHINI, R., ROVERO, P., GIACHETTI, A. & MELI, A. (1989). The activity of peptides of the endothelin family in various mammalian smooth muscle preparations. *Eur. J. Pharmacol.*, **174**, 23–31.

MAGGI, C.A., GIULIANI, S., PATACCHINI, R., SANTICIOLI, P., GIACHETTI, A. & MELI, A. (1990). Further studies on the response of the guinea-pig isolated bronchus to endothelins and sarafotoxin S6b. *Eur. J. Pharmacol.*, **176**, 1–9.

MCGREGOR, D.D. (1965). The effect of sympathetic nerve stimulation on vasoconstrictor responses in perfused mesenteric blood vessels of the rat. *J. Physiol.*, **177**, 21–30.

MCMURDO, L., CORDER, R., THIEMERMANN, C. & VANE, J.R. (1993). Incomplete inhibition of the pressor effects of endothelin-1 and related peptides in the anaesthetised rat with BQ-123 provides evidence for more than one vasoconstrictor receptor. *Br. J. Pharmacol.*, **108**, 557–561.

MORELAND, S., MCMULLEN, D.M., DELANEY, C.L., LEE, V.G. & HUNT, J.T. (1992). Venous smooth muscle contains vasoconstrictor ET_B-like receptors. *Biochem. Biophys. Res. Commun.*, **184**, 100–106.

PANEK, R.L., MAJOR, T.C., HINGORANI, G.P., DOHERTY, A.M., TAYLOR, D.G. & RAPUNDALO, S.T. (1992). Endothelin and structurally related analogs distinguish between endothelin receptor subtypes. *Biochem. Biophys. Res. Commun.*, **183**, 566–571.

SAEKI, T., IHARA, M., FUKURODA, T., YAMAGIWA, M. & YANO, M. (1991). [$Ala^{1,3,11,15}$]Endothelin-1 analogs with ET_B agonistic activity. *Biochem. Biophys. Res. Commun.*, **179**, 286–292.

SAIDA, K., MITSUI, Y. & ISHIDA, N. (1989). A novel peptide, vasoactive intestinal constrictor, of a new (endothelin) peptide family. *J. Biol. Chem.*, **264**, 14613–14616.

SAKAMOTO, A., YANAGISAWA, M., SAKURAI, T., TAKUWA, Y., YANAGISAWA, H. & MASAKI, T. (1991). Cloning and functional expression of human cDNA for the ET_B endothelin receptor. *Biochem. Biophys. Res. Commun.*, **178**, 656–663.

SAKURAI, T., YANAGISAWA, M., TAKUWA, Y., MIYAZAKI, H., KIMURA, S., GOTO, K. & MASAKI, T. (1990). Cloning of a cDNA encoding a non-isopeptide-selective subtype of the endothelin receptor. *Nature*, **348**, 732–735.

SOKOLOVSKY, M., AMBAR, I. & GALRON, R. (1992). A novel subtype of endothelin receptors. *J. Biol. Chem.*, **267**, 20551–20554.

SPOKES, R.A., GHATEI, M.A. & BLOOM, S.R. (1989). Studies with endothelin-3 and endothelin-1 on rat blood pressure and isolated tissues: evidence for multiple endothelin receptor subtypes. *J. Cardiovasc. Pharmacol.*, **13**(Suppl. 5), S191–S192.

SUMNER, M.J., CANNON, T.R., MUNDIN, J.W., WHITE, D.G. & WATTS, I.S. (1992) Endothelin ET_A and ET_B receptors mediate vascular smooth muscle contraction. *Br. J. Pharmacol.*, **107**, 858–860.

WARNER, T.D., ALLCOCK, G.H., CORDER, R. & VANE, J.R. (1992a). BQ123 and different isolated preparations reveal heterogeneity in the receptors mediating contractions to endothelin-1. *Br. J. Pharmacol.*, **107**, 103P.

WARNER, T.D., ALLCOCK, G.H. & VANE, J.R. (1993). The endothelin receptor antagonist PD 142893 inhibits endothelium-dependent vasodilatations induced by endothelin/sarafotoxin peptides. *Br. J. Pharmacol.*, **109**, 56P.

WARNER, T.D., MITCHELL, J.A., DE NUCCI, G. & VANE, J.R. (1989). Endothelin-1 and endothelin-3 release EDRF from isolated perfused arterial vessels of rat and rabbit. *J. Cardiovasc. Pharmacol.*, **13**(Suppl. 5), S85–S88.

WARNER, T.D., SCHMIDT, H.H.H.W. & MURAD, F. (1992b). Interactions of endothelins and EDRF in bovine native endothelial cells: selective effects of endothelin-3. *Am. J. Physiol.*, **262**, H1600–H1605.

WILLIAMS, D.L., Jr., JONES, K.L., PETTIBONE, D.J., LIS, E.V. & CLINESCHMIDT, B.V. (1991). Sarafotoxin S6c: an agonist which distinguishes between endothelin receptor subtypes. *Biochem. Biophys. Res. Commun.*, **175**, 556–561.

(Received February 12, 1993
Revised June 14, 1993
Accepted June 23, 1993)

Br. J. Pharmacol. (1993), **110**, 783–789

Characterization of endothelin receptors mediating the effects of the endothelin/sarafotoxin peptides on autonomic neurotransmission in the rat vas deferens and guinea-pig ileum

[1] Timothy D. Warner, Graham H. Allcock, Emma J. Mickley & John R. Vane

The William Harvey Research Institute, St. Bartholomew's Hospital Medical College, Charterhouse Square, London EC1M 6BQ

1 To characterize the receptors mediating the effects of the endothelin/sarafotoxin family of peptides on the responses to electrical stimulation of the rat vas deferens (RVD) and guinea-pig ileum (GPI) we have used endothelin-1 (ET-1), ET-3, sarafotoxin 6b (SX6b) and SX6c as agonists and the endothelin-receptor antagonists BQ-123 (ET_A receptor selective) and PD 142893 (non-selective).

2 In the RVD, ET-1 and SX6b increased the twitches induced by field stimulation starting at a threshold concentration of 10^{-10} M while the threshold concentration for ET-3 was 3×10^{-9} M. SX6c (up to 3×10^{-8} M) did not potentiate the twitches. SX6b produced significantly ($P<0.05$) greater potentiations than ET-1 at concentrations of 3×10^{-9} M and higher, and 10^{-7} M ET-3 also produced a significantly greater effect than ET-1 at the same concentration. Thus, at threshold the rank order of peptides was ET-1 = SX6b > ET-3 >>> SX6c, and at concentrations of 3×10^{-8} M and higher, SX6b > ET-3 > ET-1 >>> SX6c.

3 In the presence of BQ-123 or PD 142893 (10^{-5} M) the threshold concentrations for ET-1 to augment the twitches were increased 30 fold. In the same conditions neither SX6b nor ET-3 potentiated the responses. The relative activities of the endothelin/sarafotoxin peptides and the effectiveness of the endothelin receptor antagonists are consistent with postjunctional ET_A receptors mediating these effects.

4 In the transmurally stimulated GPI the endothelin/sarafotoxin peptides produced two effects; an increase in the basal tension of the tissues and an inhibition of the twitch responses. To increase the basal tension the peptides had the order of potency ET-1 > SX6b >> ET-3 = SX6c. These direct effects of ET-1 or SX6b were strongly antagonized (100 fold) by either BQ-123 (10^{-5} M) or PD 142893 (10^{-5} M). Thus, ET_A receptors mediate contractions of the GPI induced by these peptides.

5 The endothelin/sarafotoxin peptides were approximately equipotent at depressing twitches of the GPI in response to transmural stimulation (EC_{50}s, 4×10^{-11} to 1.5×10^{-10} M). The depressions induced by ET-1 were unaffected by either BQ-123 (10^{-5} M) or PD 142893 (10^{-5} M). BQ-123 produced a small (three fold) antagonism of the inhibitory effects of ET-3 or SX6c. These results indicate that a receptor of the ET_B type mediates the inhibitory effects of the endothelin/sarafotoxin peptides on neurotransmission in the GPI.

6 Thus, both ET_A receptors and ET_B receptors mediate the effects of the endothelin/sarafotoxin peptides on neurotransmission.

Keywords: endothelin-1; endothelin receptors; endothelium-dependent relaxations

Introduction

The endothelin/sarafotoxin peptides potently affect responses to autonomic nerve stimulation. For instance, endothelin-1 (ET-1) inhibits the release of noradrenaline (Wiklund *et al.*, 1988; Tabuchi *et al.*, 1989) or acetylcholine (Wiklund *et al.*, 1989; Hiley *et al.*, 1989) from sympathetic or parasympathetic nerve endings. ET-1 also potentiates contractions through a postjuctional effect, as in the vas deferens of the rat (Hiley *et al.*, 1989; Maggi *et al.*, 1989; Wiklund *et al.*, 1990) or mouse (Rae & Calixto, 1990). The endothelin receptors mediating these effects have not been characterized although two receptors for the endothelin/sarafotoxin peptides have been identified. The ET_A receptor, is more selective for ET-1 or SX6b whereas the other, the ET_B receptor, is isopeptide non-selective (Ambar *et al.*, 1989; Arai *et al.*, 1990; Sakurai *et al.*, 1990; Saeki *et al.*, 1991; Williams *et al.*, 1991; Clozel *et al.*, 1992). BQ-123 (cyclo(-D-Trp-D-Asp-Pro-D-Val-Leu-) is a selective ET_A receptor antagonist (Ihara *et al.*, 1992) and PD 142893 (Ac-(3,3-D-diphenylalanine)-L-Leu-L-Asp-L-Ile-L-Ile-L-Trp) has been shown to be a non-selective ET_A/ET_B receptor antagonist (Cody *et al.*, 1992), although we have found it to have little activity against ET_B receptors except for those present on endothelial cells (Warner *et al.*, 1993). Using these antagonists and ET-1, ET-3, sarafotoxin 6b (SX6b) and SX6c as agonists we have characterized the receptors that mediate the effects of the endothelin/sarafotoxin peptides on autonomic neurotransmission in the guinea-pig ileum and rat vas deferens.

Some of these data were presented to the British Pharmacological Society (Allcock *et al.*, 1993).

Methods

Organ bath experiments

Male Wistar rats (250–400 g) or Dunkin-Hartley guinea-pigs (350–450 g) were killed with thiopentone sodium (Sagatal, 120 mg^{-1} kg^{-1} i.p. or i.v.). Rat vas deferens (RVD), *pars prostatica*, or sections of guinea-pig ileum (GPI) were mounted in isolated organ baths containing 10 ml of Krebs buffer under resting tensions of 0.75–1 g for the isometric measurement of contractions. The bathing Krebs solution contained bacitracin (3 mg l^{-1}), bovine serum albumin (50 mg l^{-1}), indomethacin (5×10^{-6} M), thiorphan (10^{-6} M), captopril (10^{-6} M) and bestatin (10^{-6} M) (Maggi *et al.*, 1989)

[1] Author for correspondence.

to protect the peptides and was gassed with 95% O_2:5% CO_2 at a temperature of 37 °C. After an equilibration period of 60–90 min the tissues were electrically stimulated (ES) (Grass S48 Stimulator connected to a Med-Lab Stimu-Splitter II) via platinum electrodes positioned for transmural stimulation of the GPI (0.1 Hz, 0.5 ms, 80% of current for maximum response) or field stimulation of the RVD (0.1 Hz, 1 ms duration, 0.3 mA). When stable reproducible contractions of the tissues were obtained (approx. 10 min), BQ-123 (10^{-5} M), PD 142893 (10^{-5} M) or vehicle were added before the addition of cumulative concentrations of ET-1, ET-3, SX6b or SX6c (10^{-11} to 3×10^{-7} M). Changes in twitch tension were calculated as a percentage of the initial stable levels. Each tissue was used for only one curve.

Materials

The Krebs buffer used for the GPI had the following composition (mM): NaCl 118, KCl 4.7, KH_2PO_4 1.2, $MgSO_4.7H_2O$ 1.17, $CaCl_2.6H_2O$ 2.5, $NaHCO_3$ 25, glucose 5.6. Krebs buffer without $MgSO_4.7H_2O$ was used for the RVD. BQ-123 and PD 142893 were synthesized by Parke-Davis, MI, U.S.A. ET-1, ET-3, SX6b and SX6c were purchased from Peptide Institute (Osaka, Japan). BQ-123 and the endothelin/sarafotoxin peptides were reconstituted in 0.9% w/v saline containing 1% w/v bovine serum albumin and 10 mM sodium bicarbonate. PD 142893 was reconstituted in dimethylsulphoxide (10^{-3} M) and added directly to the organ baths. All other compounds were obtained from Sigma Chemical Co. (Poole, Dorset) and dissolved in either distilled water or saline.

Statistics

Statistical differences between curves were determined by two-way analysis of variance and a $P<0.01$ was taken as significant. Statistical differences between points were determined by unpaired two-tailed Student's t test, and between points and basal by a one sample test. For both tests a $P<0.05$ was taken as significant.

Results

Rat vas deferens

ET-1 (10^{-11} to 3×10^{-7} M) potentiated twitches of the RVD induced by nerve stimulation in a concentration-dependent manner (threshold of 10^{-10} M, Figure 1). ET-3 also potentiated the responses (Figures 1 and 2) but with a higher threshold concentration (3×10^{-9} M). SX6b had a similar threshold to ET-1 but at concentrations of 3×10^{-9} M or greater was significantly ($P<0.05$) more active than ET-1 (Figure 1). The concentration-response curve for ET-3 also crossed that for ET-1 and at a concentration of 10^{-7} M ET-3 produced a greater increase in twitch size than did ET-1 at the same concentration ($P<0.05$). SX6c at concentrations of up to 3×10^{-8} M was without effect. Thus, at threshold the rank order of peptides was ET-1 = SX6b > ET-3 >>> SX6c, and at concentrations of 3×10^{-8} M and higher, SX6b > ET-3 > ET-1 >>> SX6c. The endothelin/sarafotoxin peptides were without significant effect on the basal tone of the RVD.

In the presence of BQ-123 (10^{-5} M) or PD 142893 (10^{-5} M) SX6b (Figure 3) and ET-3 (Figure 2) no longer potentiated the responses to nerve stimulation. In the presence of either antagonist the concentration-response curve for ET-1 was shifted to the same degree such that the new thresholds were both approx. 3×10^{-9} M (Figure 4). In addition, in the presence of PD 142893, but not BQ-123, the responses to concentrations of ET-1 of 3×10^{-8} M and 10^{-7} M were significantly greater than control ($P<0.05$, Figure 4).

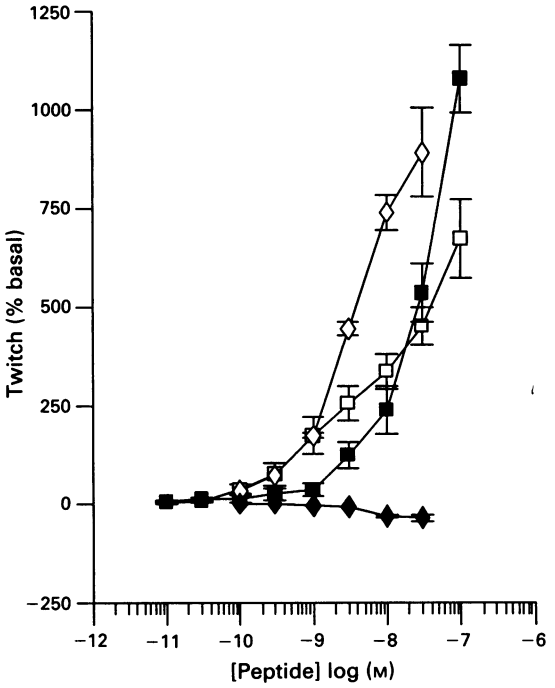

Figure 1 Comparison of the potentiating effects of the endothelin/sarafotoxin peptides on the twitch responses of the rat vas deferens to electrical field stimulation. Endothelin-1 (ET-1; □); ET-3, (■); sarafotoxin 6b (SX6b; ◇); SX6c (◆). Results are calculated as the mean (± s.e. mean, vertical bars) ($n \geqslant 6$).

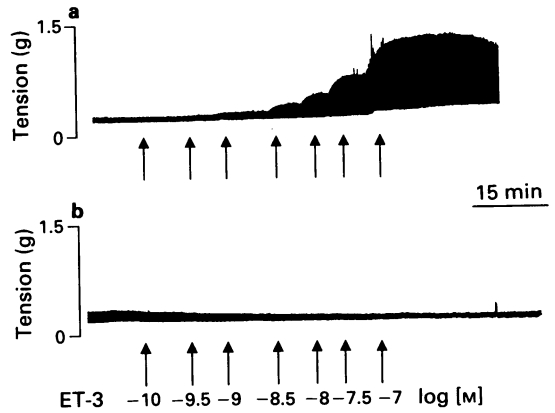

Figure 2 Effect of BQ-123 on the potentiation of twitch response in the rat vas deferens (RVD) induced by endothelin-3 (ET-3). (a) Cumulative concentrations of ET-3 (10^{-10} to 10^{-7} M) produced concentration-dependent increases in the twitch responses of the RVD in response to field stimulation. (b) In the presence of BQ-123 (10^{-5} M), ET-3 (up to 10^{-7} M) failed to potentiate the twitch responses of the RVD. Traces are from original experiments and are typical of at least 5 other preparations.

Guinea-pig ileum

ET-1, ET-3, SX6b and SX6c were equipotent in inhibiting twitches of the GPI in response to transmural stimulation (EC_{50}s 2×10^{-10}, 1.5×10^{-10}, 8×10^{-11}, 1.2×10^{-11} M, respectively, Figures 5, 6a and b). In addition, ET-1 and SX6b, but to a much lesser extent ET-3 and SX6c, increased the basal tension of the GPI (Figure 7). The increases induced by ET-1 (Figure 8) or SX6b (data not shown) were strongly antagonized by either BQ-123 or PD 142893. For instance, the EC_{50} for ET-1 increased from 10^{-9} M in control to 4×10^{-8} M in the presence of BQ-123 (10^{-5} M) or PD 142893 (10^{-5} M).

In the presence of PD 142893 (10^{-5} M) the inhibitory effects of all the endothelin/sarafotoxin peptides were unaffected (e.g. Figure 9a, $P>0.01$, $n=3-7$ for each). BQ-123 (10^{-1} M) caused small, but significant ($P<0.01$) shifts in the concentration-response curves for ET-3 (Figure 9b) and SX6c (Figure 9c).

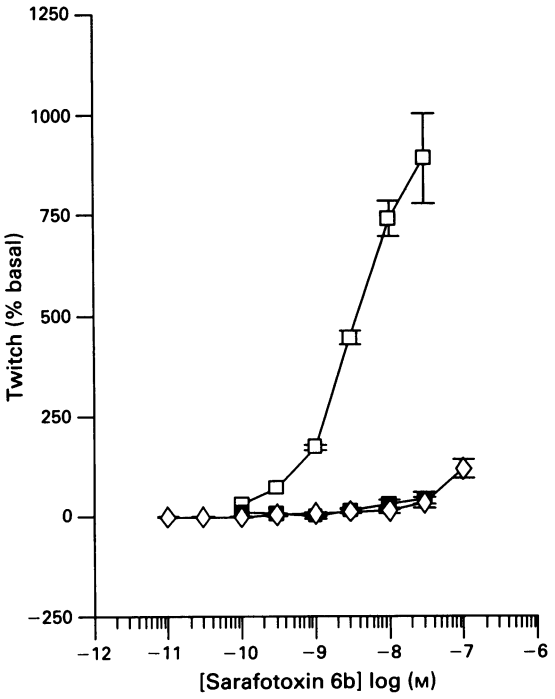

Figure 3 Effects of BQ-123 and PD 142893 on the potentiating effects of sarafotoxin 6b on the twitch responses of the rat vas deferens. Control, (□); +BQ-123 (10^{-5} M), (■); +PD 142893 (10^{-5} M), (◇). Results are calculated as the mean (± s.e. mean, vertical bars) ($n \geq 6$).

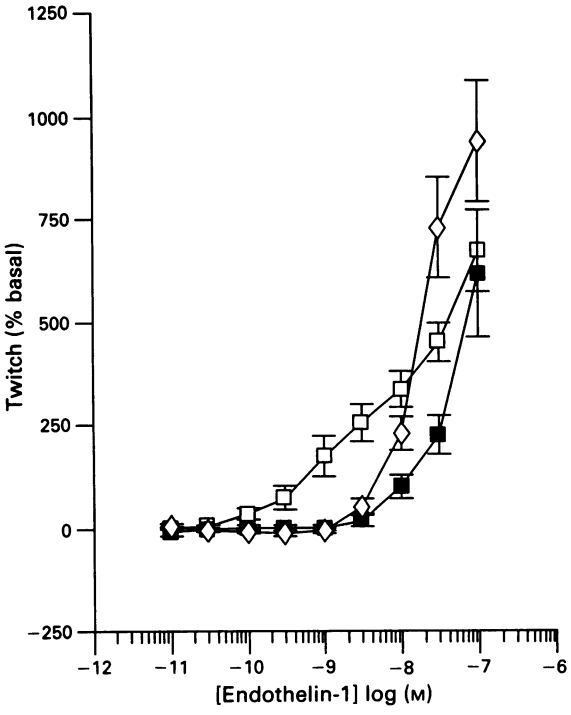

Figure 4 Effects of BQ-123 and PD 142893 on the potentiating effects of endothelin-1 on the twitch responses of the rat vas deferens Control, (□); +BQ-123 (10^{-5} M), (■); +PD 142893 (10^{-5} M), (◇). Results are calculated as the mean (± s.e. mean, vertical bars)($n \geq 6$).

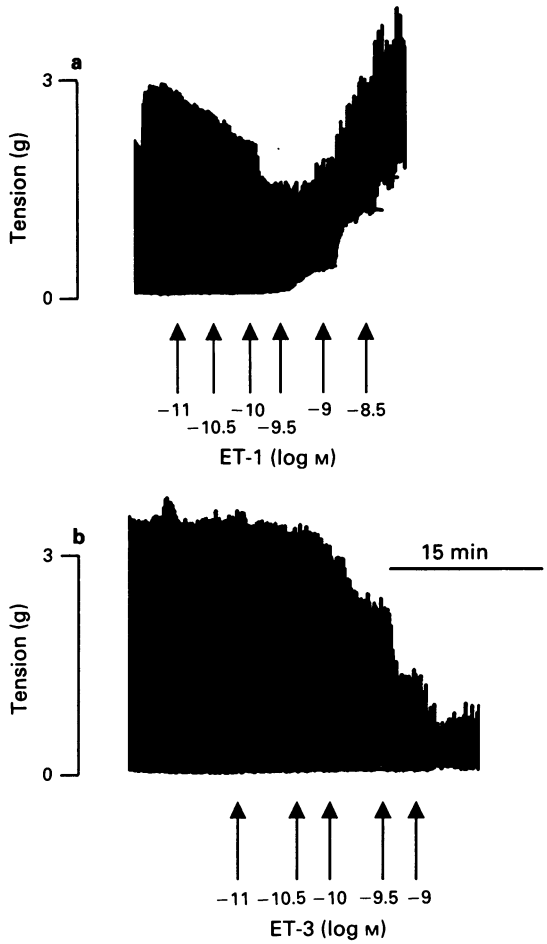

Figure 5 Effects of endothelin-1 (ET-1) and ET-3 on the responses of the transmurally stimulated guinea-pig ileum (GPI). (a) In the GPI cumulative concentrations of ET-1 (10^{-11} to 3×10^{-9} M) caused concentration-dependent reductions in twitch size and an elevation in the basal tone of the tissue. (b) In similar experiments ET-3 (10^{-11} to 10^{-9} M) caused only reductions in twitch size. Traces are from original experiments and are typical of 3-8 other preparations.

Discussion

We have compared the abilities of BQ-123 and PD 142893 to antagonize the effects of the endothelin/sarafotoxin peptides on autonomic nerve transmission in the RVD and GPI. Our data show that different endothelin-receptors mediate the effects of the endothelin/sarafotoxin peptides in these two preparations.

In the RVD the relative potencies of the peptides, SX6b $\geq$ ET-1 > ET-3, and the lack of effect of SX6c correspond with an action on the ET_A receptor. The strong antagonism by BQ-123 or PD 142893 of the potentiating effects of SX6b, ET-3 or ET-1 gives extra weight to this conclusion. This receptor would correlate with that present, for instance, in the rat thoracic aorta, on which ET-3 is less than one tenth as potent as ET-1, SX6c is inactive (Maggi *et al.*, 1989; Panek *et al.*, 1992; Warner *et al.*, 1993), and BQ-123 strongly antagonizes the effects of ET-1 (Sumner *et al.*, 1992). This conclusion is at odds with that of Télémaque & D'Orléans-Juste (1991), who suggested that ET_B receptors mediate the potentiation of twitches in the RVD. However, the observation that SX6c is without effect clearly points to mediation by non-ET_B receptors. On the other hand the relative resistance of the ET-1 response to BQ-123 and PD142893, and the closeness of the ET-1 and ET-3 concentration-response curves may suggest that this non-ET_B receptor is not identical to the ET_A receptor present on the

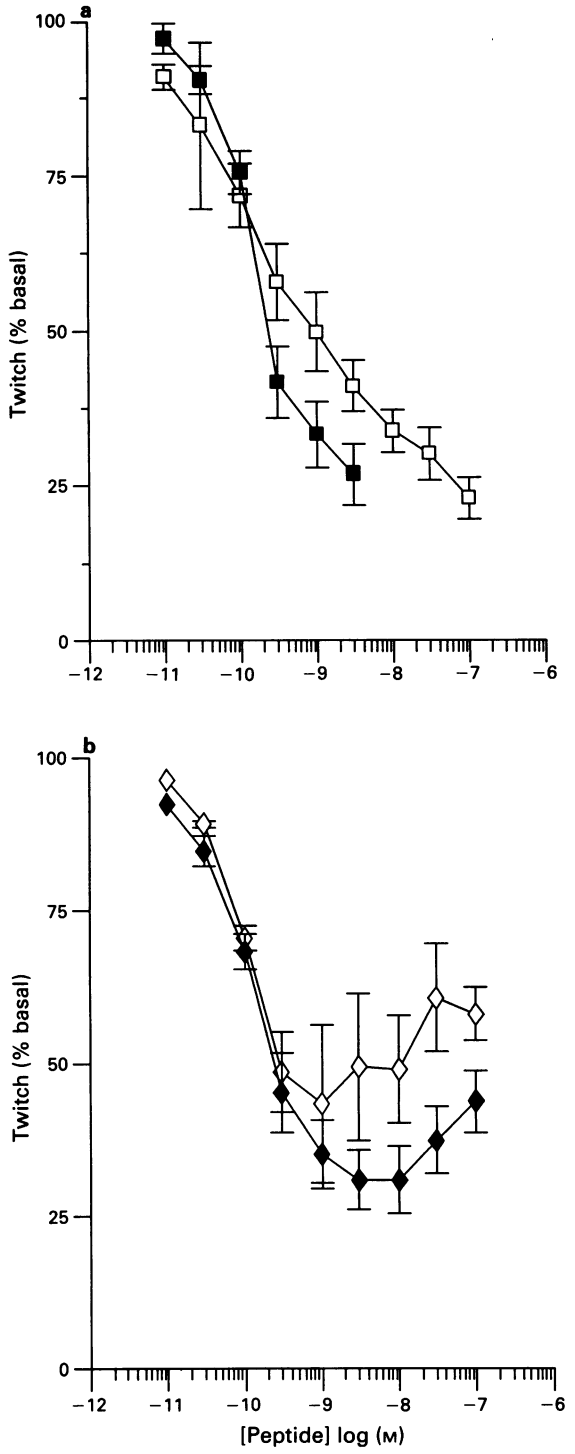

Figure 6 Comparison of the inhibitory effects of the endothelin/sarafotoxin peptides on the twitch responses of the guinea-pig ileum (GPI) to electrical field stimulation. (a) Comparison of the inhibitory effects of endothelin (ET-1) and ET-3 on the twitch responses of the GPI to electrical field stimulation. ET-1, (□); ET-3, (■). (b) Comparison of the inhibitory effects of sarafotoxin 6b (SX6b) and SX6c in the same tissue. SX6b, (◇); SX6c, (◆). Results are calculated as the mean (± s.e. mean, vertical bars) ($n = 3-9$).

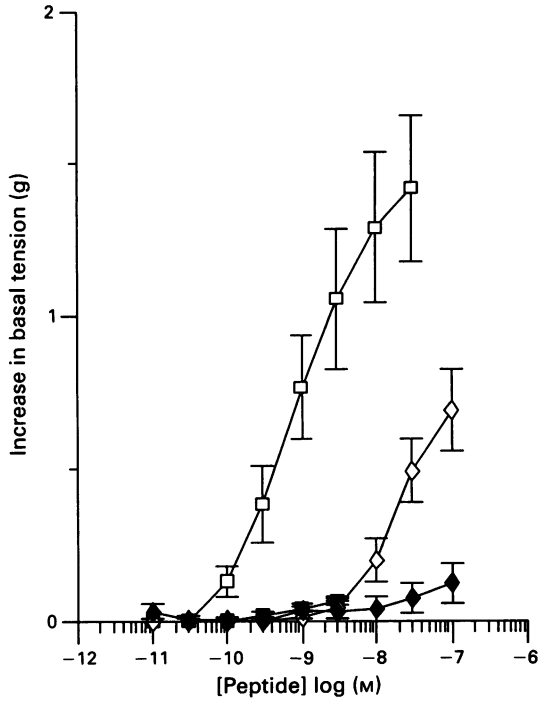

Figure 7 Comparison of the increases in basal tone of the guinea-pig ileum induced by the endothelin/sarafotoxin peptides. Endothelin-1 (ET-1; □); ET-3, (■); sarafotoxin 6b (SX6b; ◇); SX6c, (◆). Results are calculated as the mean (± s.e. mean, vertical bars) ($n \geqslant 6$).

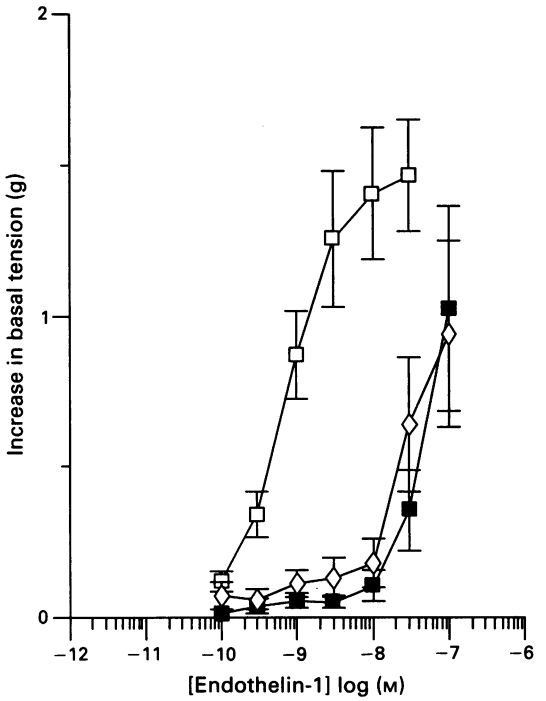

Figure 8 Effects of BQ-123 and PD 142893 on elevations of the basal tone of the guinea-pig ileum induced by endothelin-1 (ET-1). Control, (□); +BQ-123 (10^{-5} M), (■); +PD 142893 (10^{-5} M), (◇). Results are calculated as the mean (± s.e. mean, vertical bars) ($n \geqslant 6$).

rat thoracic aorta. We also found that at the highest concentrations used ET-3 produced a greater potentiation in the twitch response than ET-1 (Télémaque & D'Orléans-Juste, 1991). One explanation for this lack of parallelism between the concentration-response curves for ET-1 and ET-3/SX6b is provided by the presence of endothelin receptors both pre- and postsynaptically in the RVD. Activation of the presynaptic receptors inhibits noradrenaline release, whereas the postsynaptic ones mediate an increased responsiveness to nerve stimulation (Wiklund *et al.*, 1991). Thus, at low concentrations ET-1 potentiates transmission by a postsynaptic effect that becomes limited at higher concentrations due to presynaptic inhibition. The net result is a flattened ET-1 concentration-response curve. The subtype of this presynap-

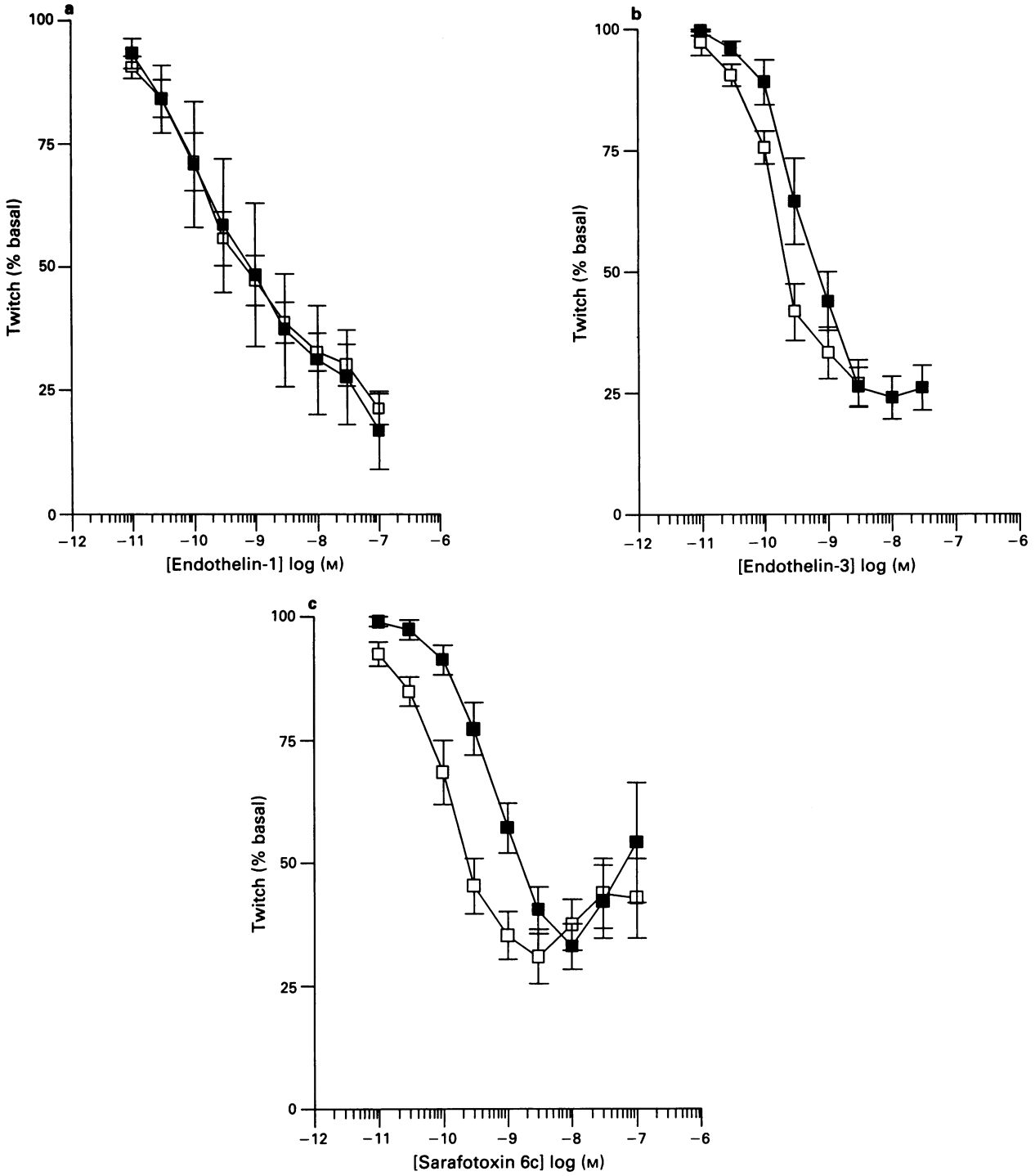

Figure 9 Effect of BQ-123 or PD 142893 on the inhibitory effects of the endothelin/sarafotoxin peptides on the twitch responses of the guinea-pig ileum to electrical field stimulation. (a) Endothelin-1 (ET-1): control, (□); +PD 142893 (10^{-5} M), (■). (b) ET-3: control, (□), + BQ-123 (10^{-5} M) (■). (c) Sarafotoxin 6c: control, (□); + BQ-123 (10^{-5}), (■) Results are calculated as the mean (± s.e. mean, vertical bars) ($n \geqslant 6$).

tic receptor is unclear, but may most closely resemble the ET_A receptor. For instance, ET-1 in relatively high concentrations, reduces transmitter release, whereas ET-3 does not (Wiklund *et al.*, 1991). On the other hand PD 142893, but not BQ-123 appears to antagonize the effects of ET-1 on this receptor, producing a potentiation of the responses to higher concentrations of ET-1. In addition, SX6b appears to be without effect, for its concentration-response curve is parallel to that of ET-3. Thus, this receptor may represent a subtype of the ET_A receptor. An alternative explanation of the non-parallelism between the concentration-response curves for ET-1 and ET-3/SX6b may be that different receptors mediate the effects of the former and latter peptides. The receptor mediating the effects of ET-3/SX6b may also be more sensitive to antagonism by BQ-123 and PD 142893, explaining why the two antagonists were less effective against ET-1. However, this model does not include a role for those receptors that influence neurotransmitter release presynaptically (Wiklund *et al.*, 1991). The true reasons for these disparities in the endothelin/sarafotoxin peptide con-centration-response curves may finally be provided by experiments examining the effects of a full range of endothelin/sarafotoxin receptor agonists and antagonists on neurotransmitter release in conjunction with studies of mechanical responsiveness. However,

the results presented here suggest that multiple receptor types may be involved in mediating the effects of the endothelin/sarafotoxin peptides within this tissue.

In the GPI the four endothelin/sarafotoxin peptides were approximately equipotent at inhibiting the twitches induced by field stimulation, as has been partly demonstrated before (Maggi *et al.*, 1989; Guimarães & Rae, 1992) whereas ET-1 and SX6b were considerably more active than ET-3 or SX6c in directly contracting the preparations. Coupled together with our observations that both BQ-123 and PD 142893 strongly antagonized the contractions induced by the endothelin/sarafotoxin peptides, as is the case in the rat thoracic aorta (Warner *et al.*, 1993), this clearly suggests that this latter effect is mediated by ET_A receptors. Conversely, the inhibitory effects of ET-1 on twitches were not influenced by either antagonist. Taken together with the similar potencies of the endothelin/sarafotoxin peptides this suggests mediation by ET_B receptors, but different from those present on the endothelium, which are antagonized by PD 142893 (Warner *et al.*, 1993). However, we did observe that BQ-123 caused small, approximately three fold rightward shifts in the inhibitory concentration-response curves to ET-3 or SX6c. Thus, there may possibly be an involvement of a receptor mediating these responses that is not identical to that ET_B receptor present, for instance, on the guinea-pig bronchus (Hay, 1992) or rabbit jugular vein (Sumner *et al.*, 1992) which is insensitive to the effects of BQ-123.

Thus, at least two receptor populations must be present in the GPI, one mediating the neuromodulatory effects of the endothelin/sarafotoxin peptides and one their direct effects on the intestinal smooth muscle. Interestingly, binding studies (Wollberg *et al.*, 1991) have indicated only one population of non-discriminating, i.e. ET_B receptors, that presumably represents those mediating the effects of the endothelin/sarafotoxin peptides on neurotransmission. Possibly, therefore, the ET-1/SX6b-selective receptors represent only a fraction of those present within the tissue. However, as ET-1 was approximately 10 fold more potent at inhibiting the twitch response than increasing the basal tone, and ET-3, which is abundantly expressed in the intestine (Matsumoto *et al.*, 1989), selectively inhibited the twitch responses, the non-selective ET receptors mediating the neuromodulatory effects of the endothelins are likely to be the more important in regard to ileum motility.

Thus, the effects of the endothelins on neurotransmission are mediated by both pre- and postsynaptic receptors. In the RVD and GPI the postsynaptic ET receptor appears to be an ET_A receptor, which produces potentiation of the twitch response of the RVD and an increase in the basal tone of the GPI. Activation of the presynaptic receptors leads to a reduction in transmitter release (Wiklund *et al.*, 1991). In the RVD this presynaptic receptor is acted upon by ET-1, but apparently not by ET-3. However, it appears to be antagonised by PD 142893. In the GPI the presynaptic receptor is more clearly of the ET_B subtype. However, the complexity of the nervous system in this latter preparation may be the explanation for the presence of additional receptors, as indicated by the effects of BQ-123 on the responses to ET-3 and SX6c.

This work was supported by the Parke-Davis Pharmaceutical Research Division of Warner-Lambert Co. We thank Drs A. Doherty and W. Cody of the Chemistry Department for providing the endothelin antagonists BQ-123 and PD 142893 (Ac-(3,3-d-diphenylalanyl)-L-Leu-L-Asp-L-Ile-L-Trp trifluoroacetate) for these studies.

References

ALLCOCK, G.H., WARNER, T.D. & VANE, J.R. (1993). Different effects of endothelins and sarafotoxins on neurotransmission in the guinea-pig ileum and rat vas deferens are mediated by different receptors. *Br. J. Pharmacol.*, **108**, 165P.

AMBAR, I., KLOOG, Y., SCHVARTZ, I., HAZUM, E. & SOKOLOVSKY, M. (1989). Competitive interaction between endothelin and sarafotoxin: binding and phosphoinositides hydrolysis in rat atria and brain. *Biochem. Biophys. Res. Commun*, **158**, 195–201.

ARAI, H., HORI, S., ARAMORI, I., OHKUBO, H. & NAKANISHI, S. (1990). Cloning and expression of a cDNA encoding an endothelin receptor. *Nature*, **348**, 730 – 732.

CLOZEL, M., GRAY, G.A., BREU, W., LÖFFLER, B.-M. & OSTERWALDER, R. (1992). The endothelin ET_B receptor mediates both vasodilation and vasoconstriction *in vivo*. *Biochem. Biophys. Res. Commun.*, **186**, 867 – 873.

CODY, W.L., DOHERTY, A.M., HE, J.X., DEPUE, P.L., RAPUNDALO, S.T., HINGORANI, G.A., MAJOR, T.C., PANEK, R.L., DUDLEY, D.T., HALEEN, S.J., LADOUCEUR, D., HILL, K.E., FLYNN, M.A. & REYNOLDS, E.E. (1992). Design of a functional hexapeptide antagonist of endothelin. *J. Med. Chem.*, **35**, 3301 – 3303.

GUIMARÃES, C. & RAE, G. (1992). Dual effects of endothelins -1, -2 and -3 on guinea-pig field stimulated ileum: possible mediation by two receptors coupled to pertussis toxin-insensitive mechanisms. *J. Pharmacol. Exp. Ther.*, **261**, 1253 – 1259.

HAY, D.W.P. (1992). Pharmacological evidence for distinct endothelin receptors in guinea-pig bronchus and aorta. *Br. J. Pharmacol.*, **106**, 759-761.

HILEY, C.R., PELTON, J.T. & MILLER R.C. (1989). Effects of endothelin on field stimulated rat vas deferens and guinea-pig ileum. *Br. J. Pharmacol.*, **96**, 104P

IHARA, M., NOGUCHI, K., SAEKI, T., FUKURODA, T., TSUCHIDA, S., KIMURA, S., FUKAMI, T., ISHIKAWA, K., NISHIKIBE, M. & YANO, M. (1992). Biological profiles of highly potent endothelin antagonists selective for the ET_A receptor. *Life Sci.*, **50**, 247 – 255.

MAGGI, C.A., GIULIANI, S., PATACCHINI, R., ROVERO, P., GIACHETTI, A. & MELI, A. (1989). The activity of peptides of the endothelin family in various mammalian smooth muscle preparations. *Eur. J. Pharmacol.*, **174**, 23 – 31.

MATSUMOTO, H., SUZUKI, N., ONDA, H. & FUJINO, M. (1989). Abundance of endothelin-3 in rat intestine, pituitary gland and brain. *Biochem. Biophys. Res. Commun.*, **164**, 74 – 80

PANEK, R.L., MAJOR, T.C., HINGORANI, G.P., DOHERTY, A.M., TAYLOR, D.G. & RAPUNDALO, S.T. (1992). Endothelin and structurally related analogs distinguish between endothelin receptor subtypes. *Biochem. Biophys. Res. Commun.*, **183**, 566 – 571.

RAE, G.A. & CALIXTO, J.B. (1990). Effects of endothelins on nerve-mediated contractions of the mouse vas deferens. *Life Sci.*, **47**, PL83-PL89.

SAKURAI, T., YANAGISAWA, M., TAKUWA, Y., MIYAZAKI, H., KIMURA, S., GOTO, K. & MASAKI, T. (1990). Cloning of a cDNA encoding a non-isopeptide-selective subtype of the endothelin receptor. *Nature*, **348**, 732 – 735.

SAEKI, T., IHARA, M., FUKURODA, T., YAMAGIWA, M. & YANO, M. (1991). [$Ala^{1,3,11,15}$]Endothelin-1 analogs with ET_B agonistic activity. *Biochem. Biophys. Res. Commun.*, **179**, 286-292.

SUMNER, M.J., CANNON, T.R., MUNDIN, J.W., WHITE, D.G. & WATTS, I.S. (1992). Endothelin ET_A and ET_B receptors mediate vascular smooth muscle contraction. *Br. J. Pharmacol.*, **107**, 858 – 860.

TABUCHI, Y., NAKAMURA, M., RAKUGI, H., NAGANO, M., MIKAMI, H. & OGIHARA, T. (1989). Endothelin inhibits presynaptic adrenergic transmission in the rat mesenteric artery. *Biochem. Biophys. Res. Commun.*, **161**, 803 – 808.

TÉLÉMAQUE, S. & D'ORLÉANS-JUSTE, P. (1991). Presence of a phosphoramidon-sensitive endothelin-converting enzyme which converts big-endothelin-1, but not big-endothelin-3, in the rat vas deferens. *Naunyn-Schmied. Arch. Pharmacol.*, **344**, 505-507.

WARNER, T.D., ALLCOCK, G.H., CORDER, R. & VANE, J.R. (1993) Use of the endothelin antagonists BQ-123 and PD142893 to reveal three receptors mediating smooth muscle contraction and the release of EDRF. *Br. J. Pharmacol.*, (in press).

WIKLUND, N.P., OHLEN, A. & CEDERQVIST, B. (1988). Inhibition of neuroeffector transmission by endothelin in the guinea-pig femoral artery. *Acta Physiol. Scand.*, **134**, 311 – 312.

WIKLUND, N.P., WIKLUND, C.U., OHLEN, A. & GUSTAFSSON, L.E. (1989). Cholinergic modulation by endothelin in guinea-pig ileum. *Neurosci. Lett.*, **101**, 342 – 346.

WIKLUND N.P., OHLEN, A., WIKLUND, C.U., HEDQVIST, P. & GUSTAFFSON, L.E. (1990). Endothelin modulation of neuroeffector transmission in rat and guinea-pig vas deferens. *Eur. J. Pharmacol.*, **185**, 25 – 33

WIKLUND, N.P., WIKLUND, C.U., CEDERQVIST, B., OHLEN, A., HEDQVIST, P. & GUSTAFSSON, L.E. (1991). Endothelin modulation of neuroeffector transmission in smooth muscle. *J. Cardiovasc. Pharmacol.*, 17(Suppl. 7), S335–339.

WILLIAMS, D.L., JR., JONES, K.L., PETTIBONE, D.J., LIS, E.V. & CLINESCHMIDT, B.V. (1991). Sarafotoxin S6c: an agonist which distinguishes between endothelin receptor subtypes. *Biochem. Biophys. Res. Commun.*, **175**, 556 – 561.

WOLLBERG, Z., BDOLAH, A., GALRON, R., SOKOLOVSKY, M. & KOCHVA, E. ((1991). Contractile effects and binding properties of endothelins/sarafotoxins in the guinea-pig ileum. *Eur. J. Pharmacol*, **198**, 31 – 36

(Received April 2, 1993
Revised June 8, 1993
Accepted June 10, 1993)

Br. J. Pharmacol. (1993), **110**, 790–794

Structural features important for the biological activity of the potassium channel blocking dendrotoxins

Michelle Hollecker, [1]*David L. Marshall & [2]*Alan L. Harvey

Centre de Biophysique Moléculaire, CNRS, 1A Avenue de la Recherche Scientifique, F-45071 Orleans Cedex 2, France, and *Department of Physiology and Pharmacology, University of Strathclyde, Glasgow G1 1XW

1 Dendrotoxins from mamba snake venoms are small proteins that block neuronal K^+ channels. In order to investigate structural features associated with their biological activity, partially folded versions of dendrotoxins I and K from black mamba (*Dendroaspis polylepis*) were prepared by selectively reducing one or more of their three S-S bonds.

2 The modified toxins were tested for ability to compete with ^{125}I-labelled native toxin I to high affinity binding sites on rat brain synaptosomal membranes and for the ability to increase acetylcholine release in a neuromuscular preparation.

3 Binding affinity increased progressively as the toxins folded to the native conformation and the most biologically active of the modified species were those in which only the disulphide bond between residues 14 and 38 was not formed. These intermediates had native-like conformations as determined by circular dichroism but still had about 5–10 times lower affinity than native toxins.

4 Addition of negatively charged groups to block the free sulphydryls at positions 14 and 38 caused a further, marked loss of activity.

5 The results are consistent with the existence of two important regions in the dendrotoxin molecules. The region containing two of the disulphide bonds (around Cys5-Cys55 and Cys30-Cys51) and much of the secondary structure is essential for the binding affinity of the toxins, while the region around Cys14 and Cys38, equivalent to part of the antiprotease site of the homologous protease inhibitor from bovine pancreas (BPTI), plays an important role in the potency of dendrotoxins.

Keywords: Dendrotoxins; mamba snakes; neurotoxin; potassium channel; synaptosomes; neuromuscular junction; structure-activity relationship; acetylcholine release

Introduction

Dendrotoxins are small globular proteins isolated from the venom of mamba snakes (*Dendroaspis* species) (Harvey & Karlsson, 1980; 1982). Their overall structures, as determined by nuclear magnetic resonance (n.m.r.) and X-ray crystallography (Keller *et al.*, 1983; Skarzynski, 1992; Foray *et al.*, 1992), are similar to those of Kunitz-type protease inhibitors, such as the well-characterized bovine pancreatic trypsin inhibitor (BPTI) (Creighton, 1975; Dufton, 1985; Pardi *et al.*, 1983) (for structure, see Figure 1). The dendrotoxins enhance the evoked release of neurotransmitters by reducing certain K^+ conductances of nerve membranes (for review, see Harvey & Anderson, 1991). Although several studies have been undertaken in order to characterize the membranal acceptor sites for dendrotoxins, little has been done to elucidate the structure-activity relationships of the toxins. As highly homologous dendrotoxins show selective actions on different subtypes of neuronal K^+ channels (Benishin *et al.*, 1988; Awan & Dolly, 1991), understanding the structural features of the dendrotoxins that are important for activity may throw light on how molecules interact with different types of K^+ channels.

Previously, the folding pattern of dendrotoxins I and K from the black mamba *Dendroaspis polylepis polylepis* was studied using the redox properties of the disulphide bridges linking cysteines 30 to 51, 5 to 55 and 14 to 38 (numbered according to BPTI) (Hollecker & Creighton, 1983), in a similar way as had been done for BPTI (Creighton, 1978). The kinetic intermediates were trapped in a stable form by blocking the free thiols either with iodoacetate or with iodoacetamide (intermediates are named after the disulphide bonds they contain). The role of the intermediate species in the kinetics of folding was elucidated: toxin I and toxin K refold via the formation of the first disulphide 30–51. Intermediate (30–51) is a disordered form of the molecule with some elements of secondary structures. Then, the protein can take two different pathways to attain its final native conformation. The simple one consists of making a second disulphide 5–55, followed by formation of disulphide 14–38. Alternatively, the second disulphide to be formed can be 14–38, giving intermediate (30–51, 14–38). This intermediate has elements of the native secondary structures, the antiprotease site around disulphide 14–38 is complete, but the other end of the molecule is open because of the lack of the disulphide bond 5–55. This species cannot complete its refolding by simply forming the 5–55 disulphide bond and it must undertake an internal rearrangement to intermediate (30–51, 5–55). In both pathways, intermediate (30–51, 5–55) is the last step before complete refolding. This intermediate has all the secondary structures found in the native protein, which are localized around disulphides 30–51 and 5–55, but the two loops constituting the equivalent of the antiprotease site in BPTI are not linked together by the disulphide bond 14–38. Hence, the cleft between them is open. Nevertheless, this intermediate has been shown by crystallography, 2D-n.m.r. and circular dichroism to have an overall conformation that is native-like. The very last step in the refolding of the two toxins is the linkage of the disulphide bond 14–38, making the equivalent of the antiprotease site of BPTI complete.

In order to define the structural features of the dendrotoxins that are important for their activity, we tested the main intermediate forms of toxins I and K by using a competition binding assay with ^{125}I-labelled toxin I and neuronal membranes, and a functional assay for the facilitation of acetyl-

[1] Present address: Department of Brain and Cognitive Sciences, Massachusetts Institute of Technology, Cambridge, MA 02139, U.S.A.
[2] Author for correspondence.

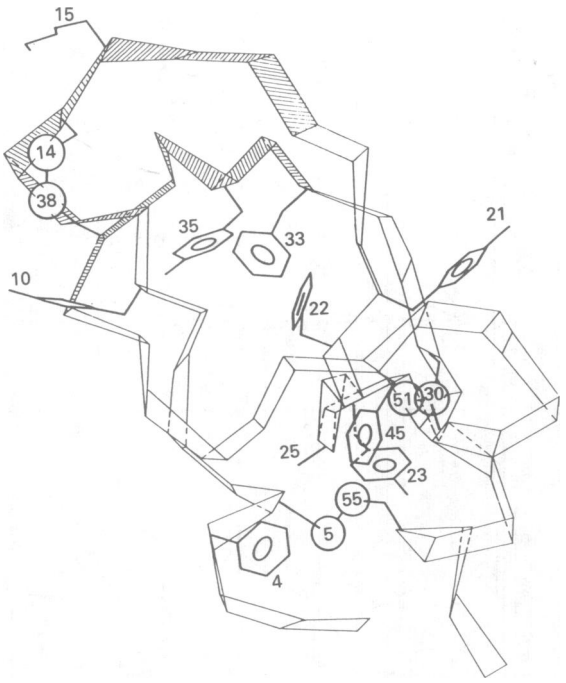

Figure 1 Backbone structure of bovine pancreatic trypsin inhibitor (BPTI) showing the disulphide bonds between residues 5 and 55, 30 and 51, and 14 and 38. The hatched region corresponds to the antiprotease site of BPTI.

choline release, using the chick biventer cervicis nerve-muscle preparation *in vitro*. For these experiments, the purity of the intermediate forms was essential. The various folded species were separated by ion-exchange chromatography on CM52 cellulose where they eluted very far apart from each other due to their differences in shape and charge. Hence, contamination by native proteins was practically impossible, but this was carefully checked by electrophoresis on native acrylamide gels.

A preliminary account of these results was presented to the British Pharmacological Society (Marshall *et al.*, 1991).

Methods

Isolation and preparation of toxin derivatives

Dendrotoxins I and K from black mamba *Dendroaspis polylepis polylepis* venom (Jabria BV, The Netherlands) were isolated and purified by ion exchange chromatography on a CM-cellulose column, as described previously (Hollecker & Creighton, 1983). The primary intermediates that accumulated transiently during both refolding and unfolding of reduced and native proteins I and K were trapped in a stable form with either iodoacetic acid or iodoacetamide, and then isolated and purified by ion-exchange chromatography (Hollecker & Creighton, 1983). The purity of the toxin species was checked by gel electrophoresis and was confirmed by ^{2}D-n.m.r.; no contamination by native toxins was detected.

Circular dichroism measurements

Circular dichroism measurements were performed in the spectral range from 190 to 350 nm with a Jobin-Yvon Mark IIIS dichrograph under the same conditions as described previously (Hollecker & Larcher, 1989).

Binding of ^{125}I-labelled toxin to synaptosomal membranes

Native toxin I was radioiodinated (specific activity 100–250 Ci mmol^{-1}), and binding assays using rat brain synaptosomal membranes were performed as previously described (Harvey *et al.*, 1989). ^{125}I-labelled toxin I bound in a saturable manner to synaptosomal membranes with a K_D of 5×10^{-10} M. Nonspecific binding was about 15% of total at 1.0 nM [^{125}I]-toxin I. Iodination of dendrotoxins has been reported to have no effect on their biological activities (Black *et al.*, 1986). Binding data were analysed by the Equilibrium Binding Data Analysis (EBDA) programme (Elsevier-Biosoft).

Chick biventer cervicis preparations

Experiments were performed on biventer cervicis nerve-muscle preparations as described by Harvey & Karlsson (1980). Twitches were evoked by stimulating the motor nerve every 10 s with pulses of 0.2 ms duration and a voltage greater than that which produced a maximal twitch. There was no change in twitch height in control preparations maintained for the duration of the experiment, and, in the presence of dendrotoxins, the increase in twitch height reflected the facilitation of acetylcholine release (Harvey & Karlsson, 1980). Contractions to exogenously applied acetylcholine (10^{-3} M), carbachol (2×10^{-5} M) and KCl (4×10^{-2} M) were obtained prior to the addition of the toxin and at the end of the experiment to test for additional effects of the modified toxins on cholinoceptor sensitivity or muscle contractility. None of the native or modified toxins affected postjunctional responses. Because of the small quantities of modified toxins that could be prepared, each toxin species was tested routinely at 7.1×10^{-7} M (5 μg ml^{-1}) on 4–8 preparations. With some of the less active species, 3.0 μM was also tested.

Results

Correlation of activity and binding affinity with folding state

In these experiments, the free sulphydryl groups of the partly refolded species were irreversibly blocked with iodoacetate.

As expected, there was very little displacement of radiolabelled toxin I from its binding site on rat brain synaptosomal membranes by completely unfolded toxins I and K, even at concentrations of 10^{-5} M. With both toxins, the one disulphide intermediates (30–51) and the two disulphide forms (30–51, 14–38) were also weak at displacing radiolabelled toxin I. Table 1 summarizes the apparent K_i values for native and modified toxins. Although the displacement curves were parallel to those with native toxin, considerably more modified toxin was needed: IC_{50}s were around 10^{-5} M compared with 10^{-9} M for native toxin I and 10^{-8} M for native toxin K (Figure 2). Nevertheless, the binding affinity of these two partly folded forms was already higher than that of a fully folded, structurally homologous molecule

Table 1 Inhibition of ^{125}I-labelled toxin I binding to synaptosomal membranes by native and modified dendrotoxins

Derivative	*Apparent* K_i (M) Toxin I	Toxin K
Native	$1.2 \pm 0.3 \times 10^{-10}$	$3.4 \pm 0.9 \times 10^{-9}$
(30–51, 5–55) acetamide	$6.4 \pm 1.0 \times 10^{-10}$	$5.1 \pm 3.4 \times 10^{-8}$
(30–51, 5–55) acetate	$2.0 \pm 0.6 \times 10^{-8}$	$1.3 \pm 0.5 \times 10^{-7}$
(30–51, 14–38)	$4.6 \pm 2.3 \times 10^{-7}$	2.0×10^{-7}
(30–51)	3.2×10^{-7}	2.0×10^{-7}
Reduced	$> 10^{-5}$	$> 2.4 \times 10^{-6}$

Values are means ± s.e.mean of 10 separate determinations for toxin I, 7 for toxin K, and 4 for the other species, except where no s.e.mean is given (mean of duplicate determinations).

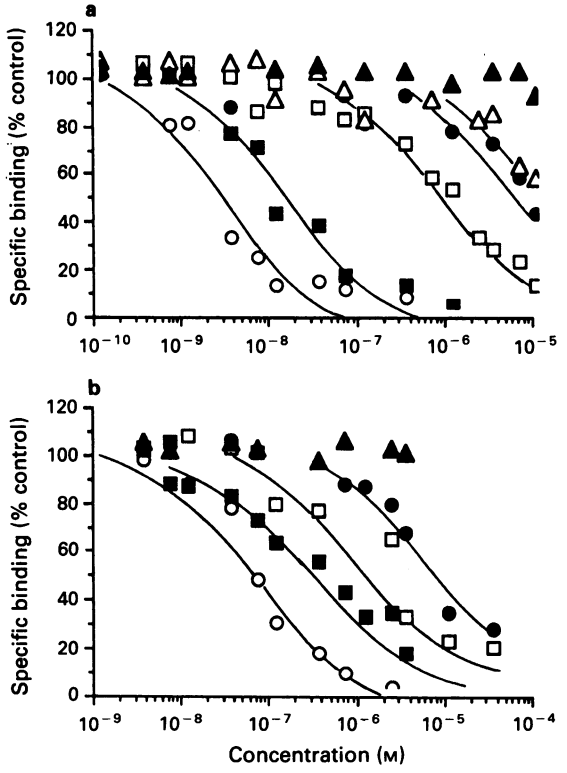

Figure 2 Displacement of radiolabelled toxin I binding to rat brain synaptosomal membranes of modified derivatives of (a) toxin I and (b) toxin K: (○) native toxin; (■) iodoacetamide form of intermediate (30–51, 5–55); (□) iodoacetate form of intermediate (30–51, 5–55); (●) intermediate (30–51, 14–38); (△) intermediate (30–51); (▲) reduced toxin. Each point represents the average of duplicate determinations. Specific binding in the absence of competing ligands was 620 fmol mg^{-1} protein.

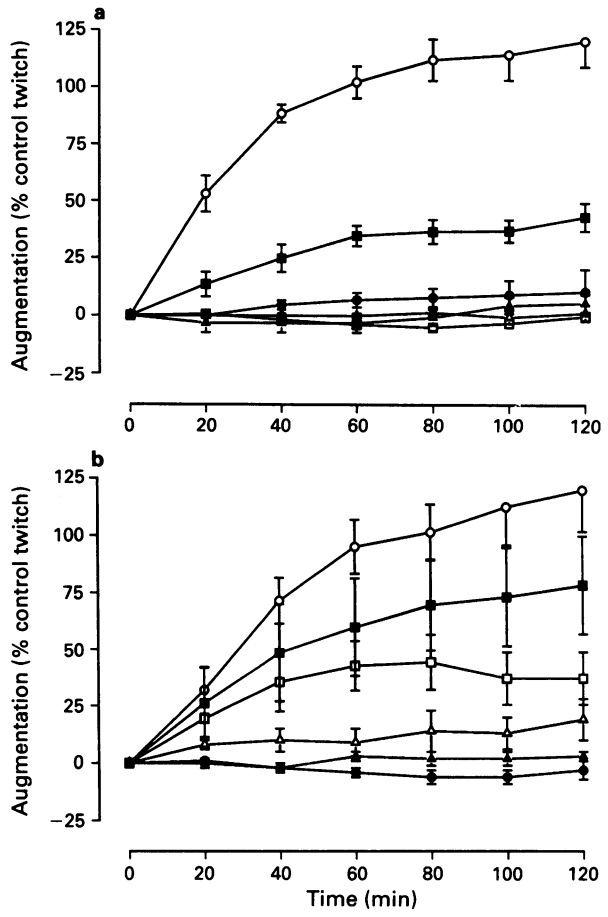

Figure 3 Augmentation of indirectly stimulated muscle twitches of chick biventer cervicis nerve-muscle preparations by (a) toxin I and (b) toxin K derivatives: (○) native toxin; (■) iodoacetamide form of intermediate (30–51, 5–55); (□) iodoacetate form of intermediate (30–51, 5–55); (●) intermediate (30–51, 14–38); (△) intermediate (30–51); (▲) reduced toxin (all tested at 7.14×10^{-7} M). Each point represents the mean (± s.e.mean) of 4–9 preparations.

like BPTI, which caused no displacement at concentrations up to 1.4×10^{-5} M (data not shown). When tested in chick biventer cervicis preparations at 7.1×10^{-7} M, these forms of the toxins produced little or no augmentation of twitch height (Figure 3). Toxin I (30–51) and toxin I (30–51, 14–38) also failed to augment twitch height when tested at 3.0×10^{-6} M.

With both toxin I and toxin K, the iodoacetate intermediates (30–51, 5–55) competed more effectively than the other modified species with radiolabelled toxin I for its binding sites (Figure 2). Compared to the native forms, toxin I (30–51, 5–55) showed relatively less activity than toxin K (30–51, 5–55) (Figure 2), with the toxin I species having less than 0.6% of the affinity of native toxin I, while the toxin K derivative had about 3% of the affinity of native toxin K (Table 1). Similarly, on chick biventer cervicis preparations, these two variants were more active than the other partly folded forms. Toxin K (30–51, 5–55) produced about 40% increase in twitch height after 120 min, whereas toxin I (30–51, 5–55) produced 6% increase (Figure 3). Increasing the concentration of toxin I (30–51, 5–55) from 5 to 7.5 μg ml^{-1} caused a 30% augmentation in twitch height (data not shown).

Effects of selective modification of the charge of residues 14 and 38

In the previous experiments, the binding affinity of the two toxins was found to increase in line with the progressive acquisition of secondary structure and globally native conformation. However, no significant functional activity was detected until the last step before complete refolding. This activity was still weak compared to that of native toxins, although the difference in conformation between native proteins and their intermediate forms (30–51, 5–55) is known to be very small (Hollecker & Larcher, 1989). The region of the molecules where disulphides 30–51 and 5–55 and all the secondary structures are localized is already identical, the only conformational difference observed being at the part of the molecule corresponding to the antiprotease site of BPTI, where the two loops formed by the segments 10 to 17 and 33 to 39 are not linked by the disulphide bond 14–38. This leaves the cleft (containing Trp 35 in toxin I) slightly open. Added to that conformational change, there is a difference of two negative charges that are introduced by blocking thiols 14 and 38 with iodoacetate.

That such local modifications can have a large impact on the activity of the two toxins pinpoints this region of the molecule as being a potentially important site for the activity of the dendrotoxins. The effect of the two negative charges introduced can be examined by blocking thiols 14 and 38 with iodoacetamide instead of iodoacetate. The steric hindrance of the two additional groups is the same, but the groups are neutral instead of negative. This did not introduce further differences in the backbone conformation of intermediate (30–51, 5–55), as checked by CD measurements on toxin I in the far-u.v. region (Figure 4). In the near u.v. region, nevertheless, some differences could be seen in the contributions of residues Trp 35 and Tyr 15 to the spectra, probably due to interactions between these two residues and the two different blocking groups.

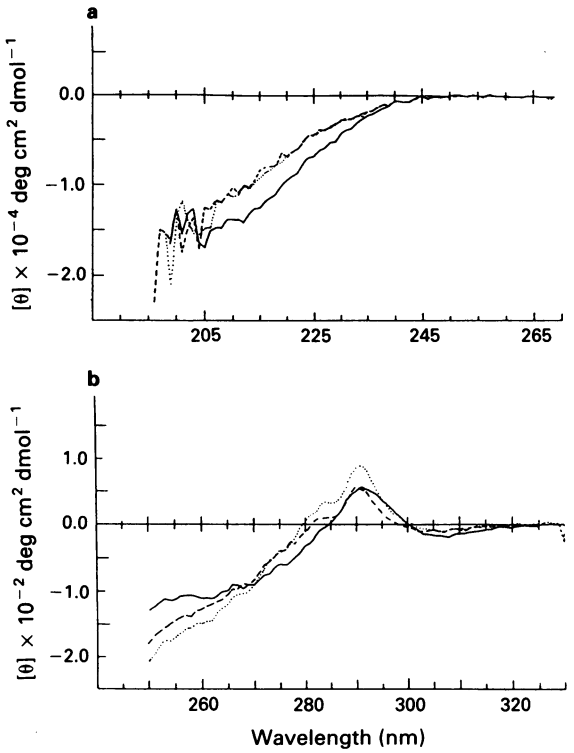

Figure 4 Circular dichroism spectra in the (a) far u.v. and (b) near u.v. regions of the following species: native toxin I (———), and intermediates I (30–51, 5–55) and Cys 14 and Cys 38 blocked with either iodoacetate (– – – –) or iodoacetamide (. . . .).

Removal of the two negative charges had a large effect on biological activity: there was a 60 fold increase in affinity with toxin I and a five fold increase with toxin K (Figure 2 and Table 1). The iodoacetamide forms were more active on the chick biventer cervicis preparation than the iodoacetate forms. With the iodoacetamide form of toxin K (30–51, 5–55), there was a maximum augmentation of 70% compared with 40% for the iodoacetate form and with the iodoacetamide form of toxin I (30–51, 5–55) 30% compared with 6% (Figure 3).

Discussion

During refolding of reduced forms of dendrotoxins I and K, the binding affinity of the toxins increased as the toxins acquired more of their final secondary structures and 3D conformation. Biological activity detectable in the functional assay appeared only in the last step before complete refolding. Although the subtypes of K^+ channels sensitive to dendrotoxins at motor nerve terminals are not known with certainty, it is expected that they will be represented in the total binding sites found on brain synaptosomal membranes. Consequently, some correlation between binding assays and functional assays on chick biventer preparations would also be expected, although differences in potency are usually seen in terms of rate of augmentation, rather than height of maximum augmentation (Harvey & Karlsson, 1982).

The present results indicate that the overall conformation of the molecule is necessary for binding affinity of the toxin to its acceptor sites. This must be primarily because the final conformation brings the residues responsible for the binding into the right spatial arrangement, as native BPTI, which has a virtually identical conformation to toxin I and toxin K, has even less binding affinity than the reduced forms of the two toxins. As the binding affinity increases with the acquisition of secondary structures, one can infer that the residues important for binding of the toxin to its acceptor sites are localized in the region of disulphides 30–51 and 5–55.

The iodoacetate form of intermediate (30–51, 5–55) has a native-like conformation and shows weak biological activity but relatively high binding affinity. Cysteines 14 and 38 are at the extreme of the molecule in a region which is not highly structured. Changing the ionic charges on these two residues has a major effect on the biological activity, indicating that this region (called the 'antiprotease site' in BPTI) is involved in the K^+ channel blocking activity of the two toxins.

The selective breaking of cystine 14–38 in toxins I and K, and blocking of the two thiols with neutral charges reveals the direct effect of the local conformational changes introduced around cystine 14–38 on biological activity. The loss of functional activity observed is far higher than could be expected from the slight decrease in binding affinity. This is particularly clear with toxin I, and suggests the probable existence of two important sites on the protein for blocking K^+ channels.

Previous investigations of the amino acid sequences of dendrotoxins and homologous protease inhibitors predicted two possible functionally important sites, one involving conserved Lys residues at positions 3, 26 and 28 (Harvey *et al.*, 1984), and the other one being the BPTI-like antiprotease site, i.e. the region around the 14–38 disulphide bond (Dufton, 1985). Our results indicate that both sites are involved.

Among the dendrotoxins, α-dendrotoxin, from green mamba venom, differs from toxin I in only 5 residues. Two of them are at the N and C terminals, and should not play a very important role in binding interactions. The three other modifications are localized in the region corresponding to the antiprotease site in BPTI, at positions 16, 32 and 34. In toxin I, these positions are occupied by three uncharged polar groups, namely Gln, Gly and Thr, which are replaced in α-dendrotoxin by two negatively charged residues, Asp, and one positively charged residue, Arg. α-Dendrotoxin is five fold less active than toxin I. As there cannot be any modification of conformation between the two toxins, the loss of binding affinity and toxin activity measured in them can be directly correlated to the charged residues added. In the case of α-dendrotoxin, the negative charges probably exert a repulsive effect on the membrane, making the binding, and hence the activity, weaker.

Toxin I and toxin K are small compact molecules with a pear shape and a length of about 2.9 nm. These molecules are highly basic, with a very asymmetrical distribution of the positive charges. These are concentrated at the broad base of the molecule, where our experiments indicate that the site responsible for binding affinity is localized. The other important site is at the other extremity of the molecule. This gives an idea of the way the toxin interacts with the K^+ channel. From studies of α-dendrotoxin and cloned K^+ channels expressed in oocytes, there is evidence that negatively charged residues in an extracellular part of the channel protein are important for toxin binding (Hurst *et al.*, 1991). However, the activity of the toxin is not strongly voltage-dependent, suggesting that it is not being driven into the pore of open channels. Our results suggest that there is an ionic interaction between some of the Lys residues in the 'base' of the toxin with negatively charged residues on the surface of the K^+ channels. However, the toxin must have a conformation close to native for it to interact fully with the channel to cause efficient blockade. The precise details of the molecule interaction remain to be elucidated. Studies with selectively mutated K^+ channels confirm that multi-point attachments are required to explain the high potency and selectivity of the dendrotoxins (Hurst *et al.*, 1991; Stocker *et al.*, 1991).

We thank Dr P.N. Strong, Royal Postgraduate Medical School, London, for help with radiolabelling, and Dr F. Culard, C.B.M., Orleans, France for use of the circular dichroism equipment.

References

AWAN, K.A. & DOLLY, J.O. (1991). K^+ Channel sub-types in rat brain: characteristic locations revealed using β-bungarotoxin, α- and δ-dendrotoxins. *Neuroscience*, **40**, 29–39.

BENISHIN, C.G., SORENSEN, R.G., BROWN, W.E., KRUEGER, B.K. & BLAUSTEIN, M.P. (1988). Four polypeptide components of green mamba venom selectively block certain potassium channels in rat brain synaptosomes. *Mol. Pharmacol.*, **34**, 152–159.

BLACK, A.R., BREEZE, A.L., OTHMAN, I.B. & DOLLY, J.O. (1986). Involvement of neuronal acceptors for dendrotoxin in its convulsive action in rat brain. *Biochem. J.*, **237**, 397–404.

CREIGHTON, T.E. (1975). Homology of protein structures: proteinase inhibitors. *Nature*, **255**, 743–745.

CREIGHTON, T.E. (1978). Experimental studies of protein folding and unfolding. *Prog. Biophys. Mol. Biol.*, **33**, 231–297.

DUFTON, M.J. (1985). Proteinase inhibitors and dendrotoxins. Sequence classification, structural prediction and structure/activity. *Eur. J. Biochem.*, **153**, 647–654.

FORAY, M.-F., LANCELIN, J.-M., HOLLECKER, M. & MARION, D. (1992). Sequence-specific ^{1}H-NMR assignment and secondary structure of black mamba dendrotoxin I, a highly selective blocker of voltage-gated potassium channels. *Eur. J. Biochem.*, **211**, 813–820.

HARVEY, A.L. & ANDERSON, A.J. (1991). Dendrotoxins: snake toxins that block potassium channels and facilitate neurotransmitter release. In *Snake Toxins*, ed. Harvey, A.L. pp. 131–164, New York: Pergamon.

HARVEY, A.L. & KARLSSON, E. (1980). Dendrotoxin from the venom of the green mamba, *Dendroaspis angusticeps*. A neurotoxin that enhances acetylcholine release at neuromuscular junctions. *Naunyn-Schmied. Arch. Pharmacol.*, **312**, 1–6.

HARVEY, A.L. & KARLSSON, E. (1982). Protease inhibitor homologues from mamba venoms: facilitation of acetylcholine release and interactions with prejunctional blocking toxins. *Br. J. Pharmacol.*, **77**, 153–161.

HARVEY, A.L., ANDERSON, A.J. & KARLSSON, E. (1984). Facilitation of transmitter release by neurotoxins from snake venoms. *J. Physiol. (Paris)*, **79**, 222–227.

HARVEY, A.L., MARSHALL, D.L., DE-ALLIE, F.A. & STRONG, P.N. (1989). Interactions between dendrotoxin, a blocker of voltage-dependent potassium channels, and charybdotoxin, a blocker of calcium-activated potassium channels at binding sites on neuronal membranes. *Biochem. Biophys. Res. Commun.*, **163**, 394–397.

HOLLECKER, M. & CREIGHTON, T.E. (1983). Evolutionary conservation and variation of protein folding pathways – two protease inhibitor homologues from black mamba venom. *J. Mol. Biol.*, **168**, 409–437.

HOLLECKER, M. & LARCHER, D. (1989). Conformational forces affecting the folding pathways of dendrotoxins I and K from black mamba venom. *Eur. J. Biochem.*, **179**, 87–94.

HURST, R.S., BUSCH, A.E., KAVANAUGH, M.P., OSBORNE, P.B., NORTH, R.A. & ADELMAN, J.P. (1991). Identification of amino acid residues involved in dendrotoxin block of rat voltage-dependent potassium channels. *Mol. Pharmacol.*, **40**, 572–576.

KELLER, R.M., BAUMANN, R., HUNZIKER-KWIK, E.-H., JOUBERT, F.J. & WÜTHRICH, K. (1983). Assignment of the ^{1}H nuclear magnetic resonance spectrum of the trypsin inhibitor homologue K from *Dendroaspis polylepis polylepis*. Two-dimensional nuclear magnetic resonance at 360 and 500 MHz. *J. Mol. Biol.*, **163**, 623–646.

MARSHALL, D.L., HARVEY, A.L. & HOLLECKER, M. (1991). Structure/activity relationships in the facilitatory actions of the dendrotoxins. *Br. J. Pharmacol.*, **104**, 190P.

PARDI, A., WAGNER, G. & WÜTHRICH, K. (1983). Protein conformation and proton nuclear magnetic resonance chemical shifts. *Eur. J. Biochem.*, **137**, 445–454.

SKARZYNSKI, T. (1992). Crystal structure of α-dendrotoxin from the green mamba venom and its comparison with the structure of bovine pancreatic trypsin inhibitor. *J. Mol. Biol.*, **224**, 671–683.

STOCKER, M., PONGS, O., HOTH, M., HEINEMANN, S.H., STUHMER, W., SCHROTER, K.-H. & RUPPERSBERG, J.P. (1991). Swapping of functional domains in voltage-gated K^+ channels. *Proc. R. Soc. B.*, **245**, 101–107.

(Received October 6, 1992
Revised May 5, 1993
Accepted May 21, 1993)

Br. J. Pharmacol. (1993), **110**, 795–803

Tachykinin NK_1 but not NK_2 receptors mediate non-cholinergic excitatory junction potentials in the circular muscle of guinea-pig colon

*Vladimir Zagorodnyuk, Paolo Santicioli & [1]Carlo Alberto Maggi

Pharmacology Department, A. Menarini Pharmaceuticals, Via Sette Santi 3, Florence, Italy and *Department Neuro-muscular Physiology, Bogomoletz Institute of Physiology, Bogomoletz Str. 4, Kiev, Ukraine

1 The effect of tachykinin NK_1 and NK_2 receptor antagonists on noncholinergic excitatory junction potentials (e.j.ps) evoked by electric field stimulation (EFS) in the circular muscle of the guinea-pig proximal colon was investigated by means of a sucrose-gap technique.

2 In the presence of 1 μM atropine, submaximal EFS (10 Hz, 20–30 V, 0.5 ms pulse width, 1 s train duration) evoked an inhibitory junction potential (i.j.p.) followed by e.j.p. with superimposed action potentials (APs) and contraction. Addition of either N^G-nitro-L-arginine (L-NOARG, 0.1 mM) or apamin (0.1 μM) inhibited the evoked i.j.p. and the combined administration of the two agents almost abolished it. In the presence of both L-NOARG and apamin, an atropine-resistant e.j.p. was the only electrical response evoked by EFS in 50% of cases and a small i.j.p. (10% of original amplitude) followed by e.j.p. was evident in the remainder.

3 In the presence of L-NOARG and apamin, the tachykinin NK_1 receptor antagonists, (±)-CP 96,345 and GR 82,334 (10 nM–3 μM) concentration-dependently inhibited the atropine-resistant e.j.p. and accompanying contraction evoked by EFS. EC_{50} values were: 0.77 μM (e.j.p. inhibition) and 0.22 μM (inhibition of contraction) for (±)-CP 96,345; 0.61 μM (e.j.p. inhibition) and 0.20 μM (inhibition of contraction) for GR 82,334. The tachykinin NK_2 receptor antagonists, MEN 10,376 (up to 3 μM) and SR 48,968 (up to 1 μM) had no effect on the atropine-resistant e.j.p. MEN 10,376 (3 μM) but not SR 48,968 produced a slight inhibition of the evoked contraction.

4 (±)-CP 96,345 (3 μM) and GR 82,334 (3 μM) markedly reduced (81 and 89% inhibition, respectively) the atropine-resistant e.j.p. in the absence of L-NOARG and apamin, without affecting the i.j.p. MEN 10,376 (3 μM) and SR 48,968 (1 μM) had no significant effect on noncholinergic i.j.p. and e.j.p. evoked in the absence of apamin and L-NOARG.

5 The electrical and mechanical responses to the NK_1 receptor agonist [Sar^9]substance P (SP) sulfone were blocked by (±)-CP 96,345 (3 μM) or GR 82,334 (3 μM) which, at the same concentration, failed to affect the responses to the NK_2 receptor agonist [βAla^8] neurokinin A (NKA) (4-10). In contrast, MEN 10,376 (3 μM) or SR 48,968 (1 μM) blocked the response to [βAla^8]NKA(4-10) without affecting the response to [Sar^9]SP sulfone.

6 In the presence of L-NOARG and apamin, and in the absence of atropine, EFS of low pulse width (0.02–0.03 ms, other parameters as above) produced cholinergic e.j.ps and contraction which were unaffected by GR 82,334 (3 μM). (±)-CP 96,345 (3 μM) produced 24% reduction in the area of the atropine-sensitive e.j.p. without affecting the peak amplitude of e.j.p. or contraction.

7 These findings demonstrate that the noncholinergic e.j.ps and accompanying contraction of the circular muscle of the guinea-pig colon are produced through activation of intramural tachykininergic nerves and that the resultant smooth muscle response is almost entirely mediated through NK_1 receptors.

Keywords: Tachykinins; tachykinin receptors; guinea-pig proximal colon; NK_1 receptor; tachykinin receptor antagonists; noncholinergic excitatory junction potentials

Introduction

Anatomical, neurochemical and pharmacological evidence implies a major role for tachykinins (TKs) as excitatory neuromuscular transmitters in the mammalian gut (Franco *et al.*, 1979; Bartho *et al.*, 1982; Costa *et al.*, 1985; Bartho & Holzer, 1985 for review). Substance P (SP) and neurokinin A (NKA) are synthesized by enteric neurones projecting to the circular and longitudinal muscle layers of the mammalian gut (Costa *et al.*, 1987; Sternini *et al.*, 1989; Too *et al.*, 1989; Shuttleworth *et al.*, 1991) and the release of endogenous tachykinins in response to depolarizing and physiological stimuli (peristalsis) has been demonstrated (e.g. Donnerer *et al.*, 1984; Theodorsson *et al.*, 1991). SP and NKA are powerful spasmogens in the mammalian gut: the direct contractile activity of tachykinins on smooth muscle cells is mediated, in many instances, through NK_1 (SP-preferring) and NK_2 (NKA-preferring) receptors (e.g. Maggi *et al.*, 1990; 1992; Giuliani *et al.*, 1993). Since both SP and NKA are synthesized by enteric neurones through the expression of the preprotachykinin I gene (Sternini *et al.*, 1989), the concomitant release of the two mediators during nerve activity in the gut, and the simultaneous presence of NK_1 and NK_2 receptors on target smooth muscle cells represents a putative example of tachykininergic co-transmission. This raises the question of the relative contribution of the two mediators to the final response and the mechanisms governing this event (e.g. Bartho *et al.*, 1992).

Non-cholinergic excitatory junction potentials (e.j.ps) have been recorded in the circular (Shuba & Vladimirova, 1980; Bywater & Taylor, 1983; 1986; Crist *et al.*, 1991) and longitudinal (Bauer & Kuriyama, 1982) muscle of the guinea-pig gut. It has been proposed that atropine-resistant e.j.ps in the guinea-pig ileum are caused by the release of SP (Bauer & Kuriyama, 1982; Niel *et al.*, 1983; Crist *et al.*, 1991). Evidence for this was obtained in two ways: (i) by studying

[1] Author for correspondence.

the effect of SP receptor desensitization on the atropine-resistant e.j.ps; (ii) by using non-selective tachykinins antagonists such as [D-Arg[1],D-Pro[2],D-Trp[7,9],Leu[11]]SP or spantide. The use of spantide and other TK receptor antagonists of first generation (Maggi et al., 1993 for review) poses important limits to the final demonstration of a neurotransmitter role for TKs, for the following reasons: (1) spantide and its congeners possess, at certain concentrations, local anaesthetic activity and inhibit the action of mediators (for e.g. bombesin) unrelated to TKs; (2) owing to their low potency, spantide and its congeners do not discriminate between NK_1 and NK_2 receptors (e.g. Buck & Shatzer, 1988).

Previously, we showed that both NK_1 and NK_2 receptors are present in the circular muscle of the guinea-pig colon to mediate the direct contractile response to TKs (Giuliani et al., 1993). The aim of this study was to investigate the effect of novel potent antagonists selective for the NK_1 receptor, (±)-CP 96,345 (Snider et al., 1991) and GR 82,334 (Hagan et al., 1991) or for the NK_2 receptor MEN 10,376 (Maggi et al., 1991) and SR 48,968 (Emonds-Alt et al., 1992), on the atropine-resistant e.j.p. and following contraction produced by electrical field stimulation (EFS) in the circular muscle of the guinea-pig proximal colon. To study noncholinergic e.j.ps in detail it would be necessary to block inhibitory junction potentials (i.j.ps) because EFS excites all nerve fibres within the smooth muscle strip. It appears possible that more than one transmitter determines nonadrenergic noncholinergic relaxation in the gut (Costa et al., 1986; Manzini et al., 1986). As shown in a previous functional study (Maggi & Giuliani, 1993), the combined administration of apamin and N^G-nitro-L-arginine (L-NOARG) was most effective in inhibiting the mechanical nonadrenergic noncholinergic relaxation in the circular muscle of the guinea-pig proximal colon. From this, the effect of selective NK_1 and NK_2 receptor antagonists was studied in the presence of apamin and L-NOARG.

Methods

Male albino guinea-pigs (250–300 g) were stunned and bled. A ring of proximal colon (1–2 cm from the caecum-colonic junction) was excised and placed in oxygenated (96% O_2 and 4% CO_2) Krebs solution of the following composition ($mmol^{-1}$): NaCl 119, $NaHCO_3$ 25, KH_2PO_4 1.2, $MgSO_4$ 1.5, KCl 4.7, $CaCl_2$ 2.5 and glucose 11. The pH of the solutions was 7.4. The ring was opened and pinned flat in a Petri dish and mucosa-free circular muscle strips were dissected. Strips approximately 0.5–0.8 mm wide and 10 mm long were cut in parallel to the circular muscle of the guinea-pig proximal colon. The strips were superfused with oxygenated Krebs solution at a rate of 1 ml min^{-1}. The temperature of Krebs solution was kept constant at 35 ± 0.5°C.

A single sucrose-gap, modified as described in details by Artemenko et al. (1982) and Hoyle (1987) was used to investigate changes in membrane potential and mechanical activity in response to electrical field stimulation. The modifications were made to a rubber membrane type of single sucrose gap apparatus to facilitate the recording of isometric tension in smooth muscle strips and enable the simultaneous recording of electrotonic potentials and junction potentials. Junction potentials were evoked by electrical field stimulation (EFS) of intramural nerves. Unless otherwise stated, atropine (1 μM) was present in the Krebs solution from the beginning of the experiments.

In a preliminary study it was found that submaximal parameters of stimulation were required to demonstrate an atropine-resistant excitatory junction potential (e.j.p.) in response to EFS (see results). For this purpose trains of pulses (pulse width 0.5 ms) were delivered for 1 s at a frequency of 10 Hz at submaximal voltage (20–30 V). In these conditions an inhibitory junction potential (i.j.p.) and e.j.p. were evoked by EFS. The effect of TK receptor antagonists was investigated in the presence of L-NOARG (0.1 mM) and apamin (0.1 μM) to eliminate or inhibit (see results) i.j.ps evoked by EFS. In some experiments, cholinergic e.j.ps were evoked in the presence of L-NOARG and apamin, but in the absence of atropine by using low pulse width (0.02–0.03 ms) EFS (other parameters as above).

GR 82,334, MEN 10,376 and SR 48,968 were applied to the circular muscle for 15 min while (±)-CP 96,345 was applied for at least 20 min. In some experiments, the electrical and mechanical responses produced by the NK_1 receptor selective agonist [Sar[9]]SP sulfone and the NK_2 receptor selective agonist [βAla[8]]NKA(4-10) were recorded in the absence and presence of the various TK receptor antagonists. For each agonist a concentration of 0.3 μM was applied for 10 s through the superfusion system: this concentration was chosen from preliminary experiments showing that it produces a reproducible contractile response of comparable size to [Sar[9]]SP sulfone and [βAla[8]]NKA(4-10). These experiments were performed in the presence of 1 μM atropine.

In preliminary experiments phentolamine (3.1 μM) and propranolol (3.4 μM) did not significantly affect the i.j.ps produced by EFS. For this reason adrenoceptor blockers were not routinely used in the experiments.

For i.j.p. and e.j.p., the following parameters were evaluated: latency, amplitude, duration, time to peak ($t1$) and time of recovery from peak to baseline ($t2$). To evaluate the effect of TK receptor antagonists on e.j.p. the area of depolarization was calculated by use of a MiniMop apparatus (Kontron, Germany).

Statistical analysis

All data in the text are mean ± standard error of the mean (s.e.mean). Statistical analysis was performed by means of Student's t test for paired or unpaired data, or by means of analysis of variance, when applicable.

Drugs

Drugs used were: atropine HCl (Serva, Heidelberg, Germany), phentolamine mesylate (Ciba-Geigy), propranolol HCl, N^G-nitro-L-arginine (L-NOARG) and apamin (Sigma).

MEN 10,376 or [Tyr[5],D-Trp[6,8,9],Lys[10]]NKA(4-10); [βAla[8]]-NKA(4-10) and (±) CP 96,345 ((±)-*cis*-2-(diphenylmethyl)-*N*-[(2-methoxyphenyl)-methyl]-1-azabicyclo[2.2.2.]octan-3-amine) were synthesized at Chemistry Department, A. Menarini Pharmaceuticals, Florence, Italy. [Sar[9]]SP sulfone was from Peninsula. GR 82,334 or [D-Pro[9][Spiro-γ-lactam]Leu[10],Trp[11]] physalaemin(1-11) from Neosystem, Strasbourg, France. SR 48,968 ((S)-N-methyl-*N*[4-(4-acetylamino-4-phenylpiperidino)-2-(3,4-dichlorophenyl) butyl] benzamide) was a kind gift of Drs Emonds-Alt & Le Fur (Sanofi, Montpellier, France).

Results

General

In the presence of atropine (Figure 1) a single pulse of EFS (0.5 ms, 20–60 V) evoked i.j.p. but not e.j.p. or contraction. A train of stimuli at a frequency of 10 Hz (1 s duration) evoked i.j.p., an atropine-resistant e.j.p. and contraction when using submaximal voltage (20–30 V) (Figure 1). Supramaximal (60 V) train stimulation caused i.j.p., hyperpolarization (after the first nonadrenergic i.j.p.) and relaxation but no e.j.p. or contraction. After this stimulation the e.j.p. and contraction evoked by submaximal train stimulation were depressed: 10–15 min were required for recovery of the original response to submaximal EFS (Figure 1). Because of these results all junction potentials were evoked by using submaximal parameters of EFS.

In the presence of atropine (1 μM), EFS (10 Hz, 20–30 V, 0.5 ms for 1 s) induced i.j.ps followed by noncholinergic e.j.ps

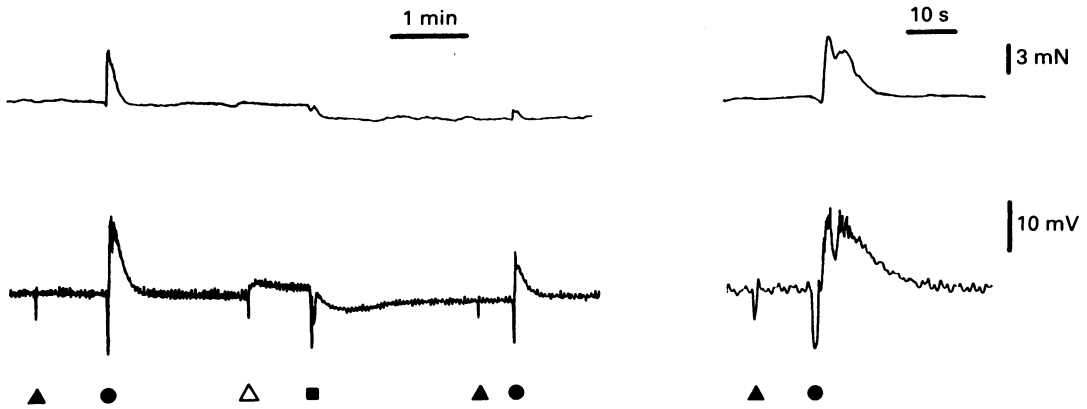

Figure 1 Electrical (lower tracing) and mechanical (upper tracing) response of the circular muscle of the guinea-pig proximal colon to EFS in the presence of atropine (1 μM). Triangles mark the response to single pulse EFS (▲, 20 V; △, 60 V, pulse width was 0.5 ms in both cases). Submaximal (20 V, ●) but not supramaximal (60 V, ■) train EFS (10 Hz for 1 s, 0.5 ms pulse width) evoked an e.j.p. and contraction. After application of a supramaximal (■) train EFS, e.j.p. and contraction produced by submaximal (●) train EFS were depressed and recovered 15 min later (expanded time scale at the right).

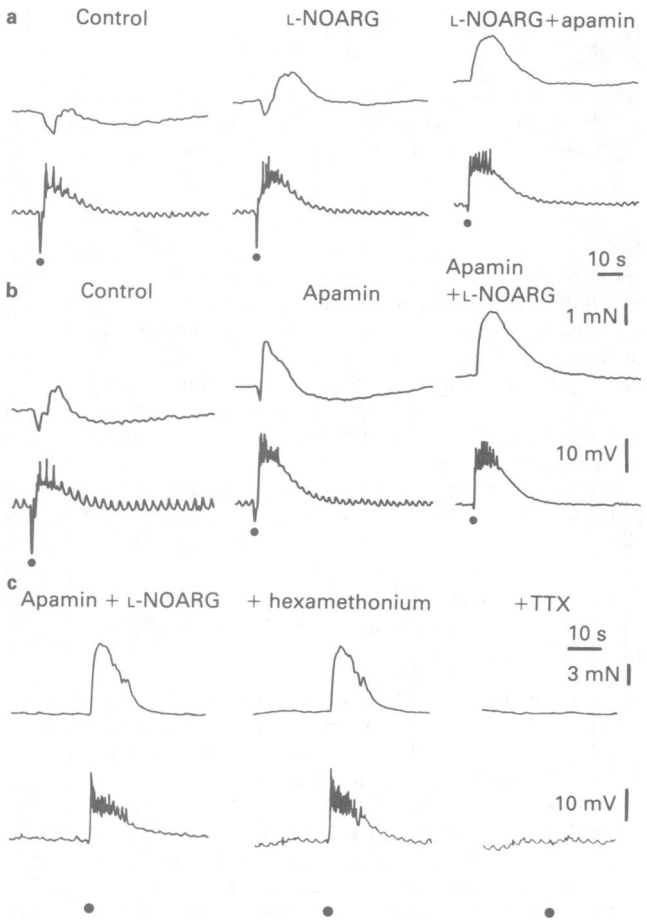

Figure 2 Typical tracings showing the effects of N^G-nitro-L-arginine (L-NOARG) (a) and apamin (b) on junction potentials and changes in tension evoked by EFS (10 Hz, 1 s, 20 V, 0.5 ms, applied at ●) in the circular muscle from guinea-pig proximal colon. Experiments performed in the presence of atropine (1 μM). The effect of L-NOARG (0.1 mM) and apamin (0.1 μM) are shown after 15 min; effect of combined administration of apamin and L-NOARG after 30 min of action. (c) Shows the effect of hexamethonium and tetrodotoxin (TTX) on e.j.p. and contraction of the circular muscle of the guinea-pig colon produced by EFS (10 Hz, 1 s, 20 V, 0.5 ms, applied at ●) in the presence of apamin and L-NOARG (applied 30 min beforehand); the effect of hexamethonium (10 μM) is shown after 20 min and the effect of TTX (0.3 μM) after 15 min of action. Top tracing is muscle tension, lower tracing is change in membrane potential.

(rebound excitation, off-response) and action potentials (APs) (Figure 2a). The mechanical response was dependent on the tone of the smooth muscle strip; when tone was high (Figure 2a) the response was triphasic: (i) a primary relaxation, (ii) a rebound contraction and (iii) a secondary relaxation.

Effects of L-NOARG and apamin on i.j.p.

L-NOARG (0.1 mM) produced an increase in tone of the muscle strips with maximum at 5–10 min from its administration, followed by a decline to baseline. Resting membrane potential and the latency of i.j.ps were not significantly affected by L-NOARG ($n = 5$). The amplitude of i.j.ps was slightly (12%) but significantly ($P < 0.05$, $n = 6$) reduced by L-NOARG. L-NOARG also reduced the duration (37%, $P < 0.01$, $n = 6$) and time of decay of i.j.ps ($t2$, 38%, $P < 0.05$, $n = 6$) (Table 1 and Figure 2a).

Apamin (0.1 μM) caused a small depolarization of cell membrane by 1.96 ± 0.3 mV ($n = 5$) followed by an increase in tone of the muscle strip, which declined (after 15–30 min) to baseline. Apamin markedly reduced the amplitude (56% inhibition, $P < 0.01$, $n = 6$) and increased both latency (51%, $P < 0.01$, $n = 5$) and time to peak ($t1$, 31%, $P < 0.01$, $n = 6$) of i.j.ps (Table 1 and Figure 2b).

The combined application of apamin (0.1 μM) and L-NOARG (0.1 mM) caused depolarization of cell membrane by 1.8 ± 0.3 mV ($n = 17$) followed by an increase of tone of muscle strip. The maximum depolarization and increase of tone was achieved in 10–15 min and with time (30–45 min) both declined to basal values. The i.j.p. was almost abolished by the combined administration of apamin and L-NOARG. After application of apamin and L-NOARG, alone or in combination, a clear enhancement/unmasking of EFS-evoked e.j.p./APs and accompanying contraction was evident (Figure 2). Owing to the preceding i.j.p. and relaxation, these effects were not quantitated nor it is possible to decide whether this is due to removal of inhibition or may also involve prejunctional enhancement of noncholinergic excitation.

In the presence of apamin and L-NOARG, submaximal EFS evoked only noncholinergic e.j.ps in 50% of cases; in the remainder EFS evoked a small nonadrenergic i.j.p. (10% of control) followed by non-cholinergic e.j.p. (Figures 2 and 3). If present, the amplitude and total duration of i.j.ps (were 1.3 ± 0.3 mV ($n = 17$) and 703 ± 70 ms ($n = 7$), respectively. The electrophysiological parameters of non-cholinergic e.j.p. evoked in the presence of apamin and L-NOARG are summarized in Table 2.

The non-cholinergic e.j.p. and APs evoked in the presence of L-NOARG and apamin were not affected by hex-

Table 1 Effect of apamin (0.1 μM) or N^G-nitro-L-arginine (0.1 mM, L-NOARG) on parameters of the inhibitory junction potential (i.j.p.) evoked by electrical field stimulation (10 Hz, 20–30 V, 0.5 ms pulse width for 1 s) in the circular muscle of the guinea-pig proximal colon

	Latency (ms)	*Amplitude* (mV)	*Duration* (ms)	t*1* (ms)	t*2* (ms)
Control	140 ± 6.3 ($n = 5$)	13.8 ± 0.8 ($n = 6$)	1913 ± 130 ($n = 6$)	613 ± 26 ($n = 6$)	1300 ± 122 ($n = 12$)
+ Apamin	212 ± 12** ($n = 5$)	6.1 ± 0.8** ($n = 6$)	1813 ± 123 ($n = 6$)	806 ± 54** ($n = 6$)	940 ± 96 ($n = 6$)
Control	148 ± 4.8 ($n = 7$)	13.8 ± 0.8 ($n = 6$)	2260 ± 97 ($n = 6$)	573 ± 59 ($n = 6$)	1660 ± 93 ($n = 6$)
+ L-NOARG	153 ± 8.4 ($n = 7$)	12.1 ± 0.7* ($n = 6$)	1520 ± 217** ($n = 6$)	486 ± 24 ($n = 6$)	1033 ± 216* ($n = 6$)

Atropine (1 μM) was present throughout the experiment.
*$P < 0.05$; **$P < 0.01$.

Table 2 Electrophysiological parameters of the atropine-resistant and atropine-sensitive excitatory junction potential (e.j.p.) evoked by electrical field stimulation in the circular muscle of the guinea-pig proximal colon

	Latency (ms)	*Amplitude* (mV)	*Duration* (s)	t*1* (s)	t*2* (s)
Atropine-resistant e.j.p.	736 ± 31 ($n = 24$)	12 ± 0.6 ($n = 70$)	31 ± 0.8 ($n = 43$)	3.1 ± 0.3 ($n = 40$)	27.5 ± 0.9 ($n = 40$)
Atropine-sensitive e.j.p.	147 ± 6.7 ($n = 3$)	9.5 ± 0.6 ($n = 9$)	11.3 ± 0.8 ($n = 9$)	1.2 ± 0.1 ($n = 9$)	10.1 ± 0.8 ($n = 9$)

Parameters of EFS were 10 Hz, 20–30 V for 1 s, pulse width was 0.5 ms for atropine-resistant e.j.p. and 0.02–0.03 ms for atropine-sensitive e.j.p. Atropine-resistant e.j.p. was recorded in the presence of atropine (1 μM), apamin (0.1 μM) and N^G-nitro-L-arginine (L-NOARG, 0.1 mM), atropine-sensitive e.j.p. was recorded in the presence of apamin (0.1 μM) and L-NOARG (0.1 mM).

amethonium (10 μM, $n = 3$) but were blocked by tetrodotoxin (TTX, 0.3 μM, $n = 3$) (Figure 2c).

Effects of selective NK_1 and NK_2 receptor antagonists on noncholinergic e.j.ps and contractions evoked by EFS in the presence of L-NOARG and apamin

GR 82,334 (up to 3 μM), MEN 10,376 (up to 3 μM) and SR 48,968 (up to 1 μM) had no agonist effect on mechanical or electrical activity of the circular muscle. (±)-CP 96,345 (3 μM) caused a small but significant depolarization of the cell membrane by 1.0 ± 0.4 mV ($n = 7$, $P < 0.05$).

The non-peptide NK_1 receptor antagonist, (±)-CP 96,345 concentration-dependently (Figures 3 and 4) inhibited the non-cholinergic e.j.p. and contractions, EC_{50} (95% c.l. in parentheses) being 0.77 μM (0.31–1.91 μM) and 0.22 μM (0.17–0.29 μM), respectively.

The peptide NK_1 receptor antagonist GR 82,334 concentration-dependently inhibited the non-cholinergic e.j.p. and contractions (Figures 3 and 4), EC_{50} being 0.61 μM (0.43–0.87 μM) and 0.20 μM (0.09–0.44 μM), respectively. Typical tracings showing the inhibitory effect of NK_1 receptor antagonists on the non-cholinergic e.j.p. and contraction are shown in Figure 3. The effect of GR 82,334 (3 μM) developed faster (more than 50% block occurred within 3–5 min from application) than that of (±)-CP 96,345 (more than 50% block occurred at 10–15 min after application). Data on the concentration-dependent inhibition of e.j.p. and contraction are shown in Figure 4.

The non-peptide NK_2 receptor antagonist SR 48,968 (up to 1 μM) and the peptide NK_2 receptor antagonist MEN 10,376 (up to 3 μM) had no marked effects on non-cholinergic e.j.p. and contractions evoked by EFS (Figures 3 and 4). At the highest concentration tested, MEN 10,376 (3 μM) and SR 48,968 (1 μM) caused a small but significant (against control responses of the same strips) inhibition of non-cholinergic contractions of 32 ± 5% ($n = 6$, $P < 0.01$) and 13 ± 5% ($n = 11$, $P < 0.05$), respectively (Figure 4).

In control experiments, a small spontaneous decay in amplitude of non-cholinergic contractions during 20 min perfusion with Krebs solution was observed. The amplitude of spontaneous decay of contraction was 16 ± 4% ($n = 6$, $P < 0.05$). The inhibitory effect of MEN 10,376 (3 μM) was significantly larger than that of spontaneous decay (measured on different preparations), while the effect of SR 48,968 was not significantly different from spontaneous decay.

The amplitude of non-cholinergic e.j.ps evoked by EFS did not significantly change (1 ± 4%, $n = 6$, NS) during 20 min perfusion with Krebs solution.

Summarizing this section the non-cholinergic e.j.ps were not affected by NK_2 receptor antagonists and a small reduction of contraction was only evident for 3 μM MEN 10,376.

Effects of NK_1 and NK_2 receptor antagonists on the response to EFS in the absence of apamin and L-NOARG

In atropine-containing Krebs solution, GR 82,334 (3 μM) and (±)-CP 96,345 (3 μM) markedly reduced the non-cholinergic e.j.ps by 89 ± 2% ($n = 6$, $P < 0.001$) and 81 ± 4% ($n = 5$, $P < 0.001$) while the amplitude of non-adrenergic i.j.ps was unaffected (Figure 5).

SR 48,968 (1 μM) and MEN 10,376 (3 μM) had no marked effect on e.j.ps or i.j.ps (Figure 5). SR 48,968 (1 μM) slightly reduced the amplitude of non-adrenergic i.j.ps by 8 ± 2% ($n = 6$, $P < 0.01$) while leaving non-cholinergic e.j.ps unaffected. MEN 10,376 (3 μM) caused a small reduction in the amplitude of both e.j.ps and i.j.ps by 17 ± 4 ($n = 7$, $P < 0.01$) and by 8 ± 2% ($n = 9$, $P < 0.01$).

None of these antagonist displayed any significant agonist effect on contractile and electrical activity of the circular muscle under these conditions.

Effect of selective NK_1 and NK_2 receptor antagonists on electrical and mechanical response to [Sar^9]SP sulfone and [βAla^8]NKA(4-10)

Application of the NK_1 receptor selective agonist, [Sar^9]SP sulfone (0.3 μM for 10 s) and of the NK_2 receptor selective agonist, [βAla^8]NKA(4-10) (0.3 μM for 10 s) both produced

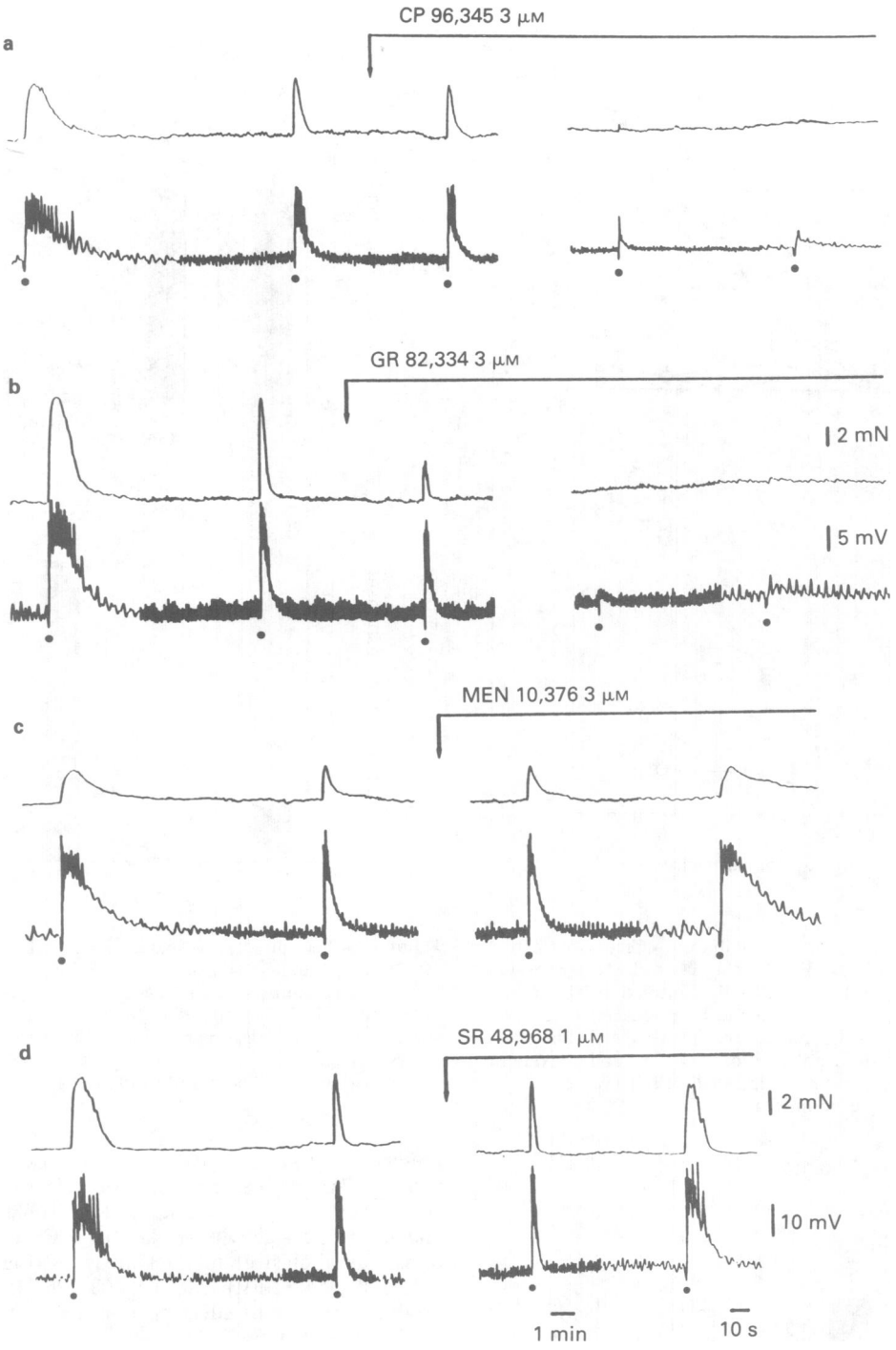

Figure 3 Typical tracings illustrating the effects of (±)-CP 96,345 (a), GR 82,334 (b), MEN 10,376 (c) and SR 48,968 (d) on the non-cholinergic e.j.ps and contractions in the circular muscle from guinea-pig proximal colon in the presence of atropine (1 μM), apamin (0.1 μM) and N^G-nitro-L-arginine (L-NOARG, 0.1 mM). The effect of (±)-CP 96,345 (3 μM) is shown after 23 min of application. The effects of GR 82,334 (3 μM) MEN 10,376 (3 μM) and SR 48,968 (1 μM) are shown at 15 min after application. Upper tracing is muscle tension, lower tracing is change in membrane potential.

depolarization of the membrane by 10.2 ± 0.9 ($n = 17$) and 4.6 ± 0.4 mV ($n = 24$), respectively, and accompanying contraction of the circular muscle of the colon (range 2–5 mN).

The NK_1 receptor antagonist, GR 82,334 (3 μM) inhibited the amplitude of [Sar^9]SP sulfone (0.3 μM)-induced contraction and depolarization by 80 and 75%, respectively ($P < 0.05$). (±)-CP 96,345 (3 μM) inhibited [Sar^9]SP sulfone-induced contraction and depolarization by 95 and 97%, respectively ($P < 0.05$, Figure 6). Neither GR 82,334 nor (±)-CP 96,345 inhibited depolarization and contraction observed in response to [βAla^8]NKA(4-10) (Figure 6).

The NK_2 receptor antagonist, MEN 10,376 (3 μM) inhibited the amplitude of the [βAla^8]NKA(4-10)-induced contraction and depolarization by 75 and 80%, respectively ($P < 0.05$). SR 48,968 (1 μM) inhibited the amplitude of [βAla^8]NKA(4-10)-induced contractions and depolarization by 90 and 88%, respectively ($P < 0.05$, Figure 6). The responses to [Sar^9]SP sulfone were not significantly affected by MEN 10,376 or SR 48,968 (Figure 6).

Effects of NK_1 receptor antagonists on cholinergic e.j.ps and contractions evoked by EFS

A frequency of stimulation of 10 Hz for 1 s, 20–30 V and pulse width of 0.02–0.03 ms was selected to obtain consistent cholinergic e.j.ps followed by APs and contractions in the

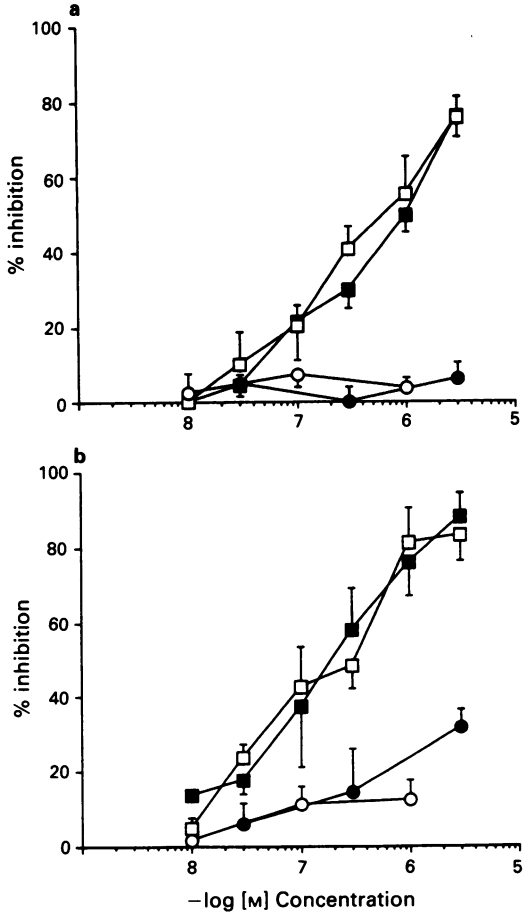

Figure 4 Concentration-dependent inhibitory effect of (±)-CP 96,345 (■), GR 82,334 (□), MEN 10,376 (●) and SR 48,968 (○) on non-cholinergic e.j.ps (a) and following contractions (b) in circular muscle of the guinea-pig colon in the presence of atropine (1 μM), apamin (0.1 μM) and N^G-nitro-L-arginine (0.1 mM). The effect of antagonists on area of depolarization of e.j.p. and maximum amplitude of contraction were calculated. Each value is the mean ± s.e.mean of 4–12 experiments.

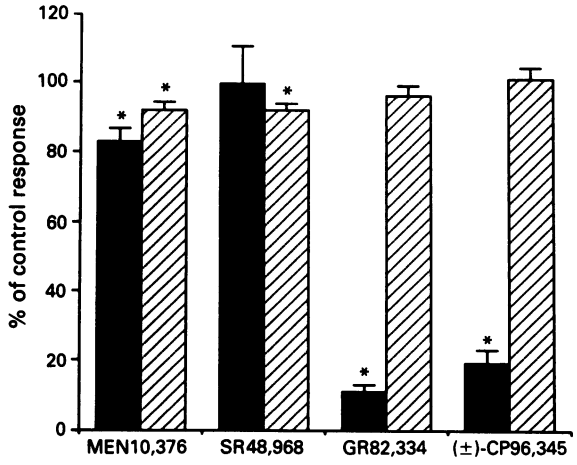

Figure 5 Effect of MEN 10,376 (3 μM), SR 48,968 (1 μM), GR 82,334 (3 μM) and (±)-CP 96,345 (3 μM) on atropine (1 μM)-resistant i.j.p. (hatched columns) and e.j.p. (solid columns) evoked by submaximal train EFS in the circular muscle of the guinea-pig colon in the absence of apamin and N^G-nitro-L-arginine. Each value is mean ± s.e.mean of 5–9 experiments. *Significantly different from controls: $P<0.05$.

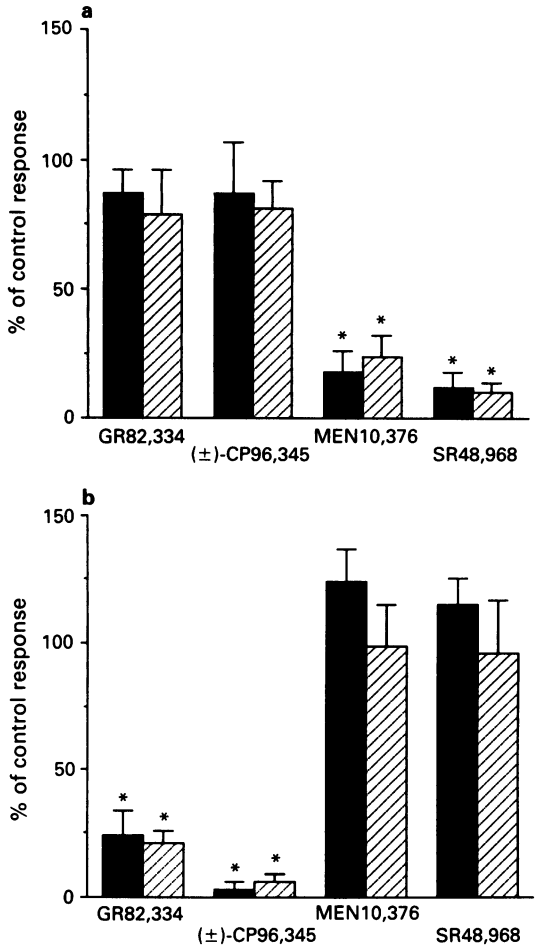

Figure 6 Effect of (±)-CP 96,345 (3 μM), GR 82,334 (3 μM), MEN 10,376 (3 μM) and SR 48,968 (1 μM) on the amplitude of depolarization (solid columns) and contraction (hatched columns) induced by [βAla^8]NKA(4-10) (a) and [Sar^9]SP sulfone (b) in circular muscle strips from guinea-pig proximal colon. Experiments performed in the presence of atropine (1 μM). Each value is the mean ± s.e.mean of 3–6 experiments. *Significantly different from control: $P<0.05$.

presence of apamin (0.1 μM) and L-NOARG (0.1 mM) (Figure 7a,c). The electrophysiological characteristics of cholinergic e.j.ps are summarized in Table 2. The electrical and mechanical activity evoked by EFS under these conditions was abolished by 1 μM atropine (Figure 7).

GR 82,334 (3 μM) and (±)-CP 96,345 (3 μM) did not produce any agonist effect on contractile or electrical activity of the smooth muscle.

GR 82,334 (3 μM) had no effect either on cholinergic e.j.ps or contractions (Figure 7a and b). (±)-CP 96,345 (3 μM) slightly reduced by 24 ± 5% the cholinergic e.j.ps (calculated as area of depolarization), but did not affect the peak amplitude of e.j.ps or contractions evoked by EFS (Figure 7c and d).

Discussion

Recent studies on the role of TKs as enteric excitatory transmitters have taken advantage of novel receptor antagonists of both peptide (second generation) and non-peptide (third generation) nature (Maggi *et al.*, 1993 for review) which are more potent than spantide and also possess remarkable selectivity for either NK_1 or NK_2 receptors. By use of these novel ligands, evidence has been obtained that the NK_1 receptor is the main mediator of atropine-resistant neuromuscular transmission in the longitudinal muscle of the guinea-pig ileum (Taylor & Kilpatrick, 1992), while the NK_2

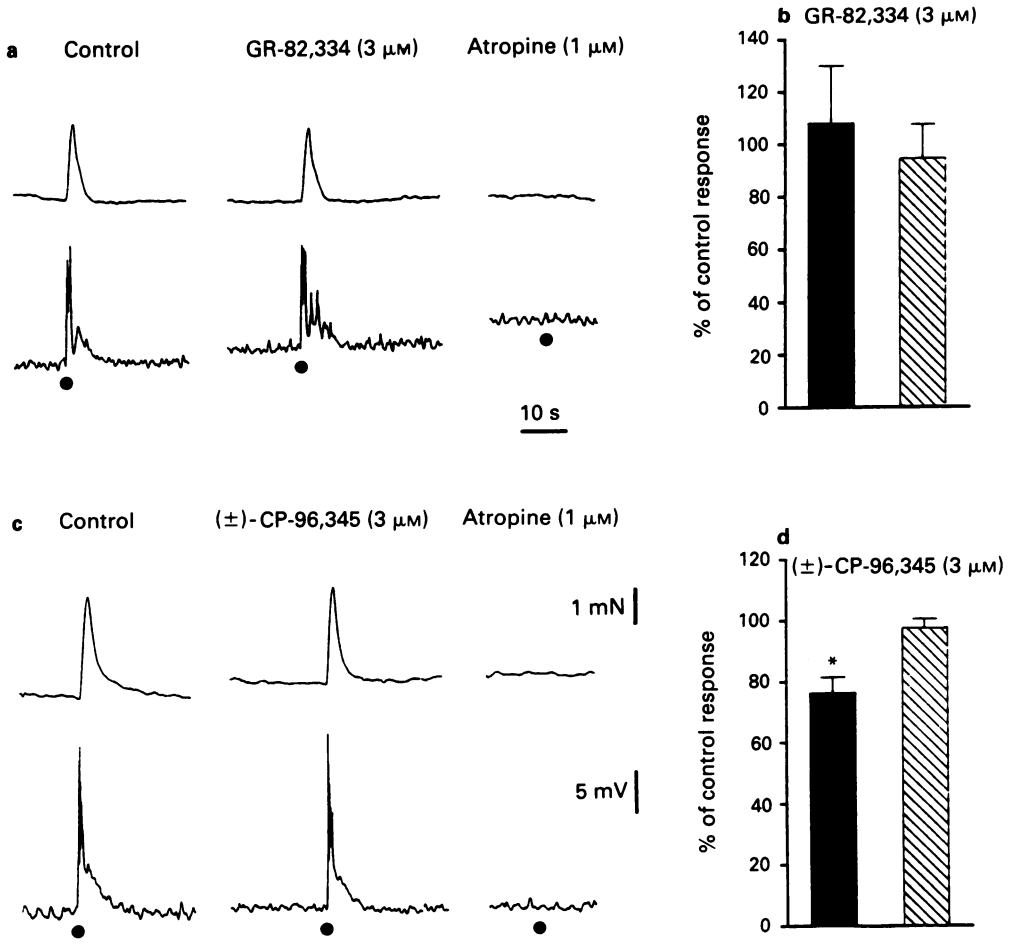

Figure 7 Effects of GR 82,334 (a and b) and (±)-CP 96,345 (c and d) on the atropine-sensitive e.j.ps and contractions evoked by train EFS (10 Hz, 20 V for 1 s, pulse width 0.02 ms) in the presence of apamin (0.1 μM) and N^G-nitro-L-arginine (0.1 mM). In (a) and (c) the effect of GR 82,334 (3 μM) and (±)-CP 96,345 (3 μM) are shown at 15 and 25 min from application, respectively. Upper tracing is muscle tension, lower tracing is change in membrane potential. The area of depolarization of cholinergic e.j.ps (solid columns) and amplitude of contraction (hatched columns) were calculated and are shown in (b) and (d), respectively. Each value is mean ± s.e.mean of 5 experiments. *Significantly different from control: $P<0.05$.

receptor predominates in the circular muscle of the guinea-pig and human ileum (Bartho *et al.*, 1992; Maggi *et al.*, 1992; Holzer *et al.*, 1993).

Because a previous functional study (Giuliani *et al.*, 1993) indicated that functional NK_1 and NK_2 receptors mediate contraction of the circular muscle of the guinea-pig proximal colon, we have used selective NK_1 and NK_2 receptor antagonists to gain information as to whether TK receptors are involved in the generation of noncholinergic e.j.ps in this preparation. GR 82,334 (Hagan *et al.*, 1991) and CP 96,345 (Snider *et al.*, 1991) have been characterized as highly selective NK_1 receptor antagonists, while MEN 10,376 (Maggi *et al.*, 1991) and SR 48,968 (Emonds-Alt *et al.*, 1992) are highly selective NK_2 receptor antagonists. For each one of these ligands, evidence for effective blockade of the respective preferred receptor and selectivity was established by using the selective NK_1 receptor agonist, [Sar^9]SP sulfone (Dion *et al.*, 1987) and the NK_2 receptor selective agonist [βAla^8]NKA(4-10) (Rovero *et al.*, 1989).

The present results indicate that NK_1 but not NK_2 receptor antagonists concentration-dependently inhibit the non-cholinergic e.j.ps and accompanying contraction in response to EFS. The NK_1 receptor antagonists (±)-CP 96,345 (Snider *et al.*, 1991) and GR 82,334 (Hagan *et al.*, 1991) inhibited the atropine-resistant e.j.ps both in the presence and absence of apamin and L-NOARG. This provides strong evidence for predominant involvement of NK_1 receptors in non-cholinergic excitatory neurotransmission to the circular muscle of the guinea-pig proximal colon, where this response is evident either as primary contraction (in the presence of atropine, apamin and L-NOARG) or as a 'rebound' contraction (in the presence of atropine alone).

The EC_{50}s of CP 96,345 and GR 82,334 in inhibiting the atropine resistant e.j.p. and contraction produced by EFS are higher than one would expect on the basis of the affinities of these ligands for the NK_1 receptor in this preparation: thus, when tested against [Sar^9]SP sulfone in the circular muscle of the colon, both (±)-CP 96,345 and GR 82,334 act as competitive antagonists with pK_B values of 8.41 and 7.49, respectively (Maggi, unpublished data). On the other hand, the EC_{50} values of (±)-CP 96,345 and GR 82,334 in blocking the noncholinergic contraction were 0.22 and 0.20 μM, respectively. The reason why higher concentrations of NK_1 receptors antagonists are needed to block endogenous TKs than those which are sufficient to inhibit effectively the action of exogenous TKs is unclear: this may involve a difference in the accessibility of antagonist to NK_1 receptors stimulated by the endogenous agonist vs those stimulated by exogenous agonists and/or a high local concentration of the agonist released during nerve activity. Nevertheless, the EC_{50} of GR 82,334 for inhibiting the atropine-resistant contraction in guinea-pig colon is in good agreement with the EC_{50}, of this antagonist in blocking the atropine-resistant contraction in the longitudinal muscle of the ileum (Taylor & Kilpatrick, 1992; EC_{50} 0.56 μM) vs a pK_B value of 7.64 at the NK_1 receptor in the same preparation (Hagan *et al.*, 1991).

The present results show that the time course of inhibition by GR 82,334 is approximately three times faster than for (±)-CP 96,345. Furthermore, unlike (±)-CP 96,345, the inhibitory effect of GR 82,334 on noncholinergic e.j.p. can be rapidly reversed by washing (unpublished data) The explanation for the difference in time course of action of the two antagonists is not known.

Because of the relatively high concentrations of NK_1 receptor antagonists required to block the atropine-resistant e.j.p., it was important to assess their selectivity. The highest concentration tested of both antagonists is selective at the postjunctional level because the excitatory responses to NK_2 receptor stimulation were unchanged. The present findings also indicate that 3 μM GR 82,334 does not exert nonspecific effects at prejunctional level because neither the nonadrenergic i.j.p. nor the atropine-sensitive e.j.p and contraction were modified by this antagonist. Likewise, 3 μM (±)-CP 96,345 did not inhibit the nonadrenergic i.j.p. and peak amplitude of the atropine-sensitive e.j.p. or contraction: only a minor reduction of the atropine-sensitive e.j.p. was observed, if measured as total area of depolarization. This is probably a nonspecific effect of (±)-CP 96,345 which, at high concentrations, can inhibit voltage-dependent calcium channels (e.g. Schmidt *et al.*, 1992). Although we cannot exclude the possibility that nonspecific effects of (±)-CP 96,345 may have contributed to inhibition of the atropine-resistant e.j.p. and contraction, the extent of the inhibitory effect on the area of the atropine-sensitive e.j.p. is certainly minor as compared to the almost total suppression of atropine-resistant e.j.p. We conclude that the major part of the inhibitory effect of this nonpeptide antagonist on the atropine-resistant e.j.p. and accompanying contraction is due to blockade of the action of endogenous TKs at NK_1 receptors.

At 3 μM, MEN 10,376 produced a minor inhibitory effect on the atropine-resistant mechanical response to EFS which is statistically significant as compared to the spontaneous decay observed in control strips. Since this concentration of MEN 10,376 does not affect the electrical and mechanical response to selective NK_1 receptor stimulation, this may indicate a minor contribution of NK_2 receptors to noncholinergic excitation of the circular muscle. However, SR 48,968 which is more potent than MEN 10,376 in blocking NK_2 receptors in the colon (Giuliani *et al.*, 1993), did not significantly affect the atropine-resistant e.j.p.

After intravenous administration to anaesthetized guinea-pigs, both NK_1 (CP 96,345) and NK_2 (MEN 10,376 and SR 48,968) receptor antagonists produce long-lasting inhibition of atropine-resistant but hexamethonium-sensitive phasic pressure waves produced by radial stretch (balloon distension) in the guinea-pig proximal colon (Giuliani *et al.*, 1993). On the basis of the present findings, it appears that the activity of CP 96,345 could involve blockade on neuromuscular excitatory transmission from enteric tachykininergic nerves to the circular muscle. The activity of NK_2 receptor antagonists in the *in vivo* model (Giuliani *et al.*, 1993) remains unexplained. Since the present study was performed using only one frequency of stimulation to evoke the noncholinergic e.j.p. and accompanying contraction, we cannot exclude the possibility that enteric tachykininergic nerves were activated by balloon distension *in vivo* to a sufficient extent to produce NK_2 receptor stimulation.

In the major part of the present experiments, the effect of NK_1 and NK_2 receptor antagonists was investigated in the presence of apamin and L-NOARG to block the non-adrenergic i.j.ps. Non-adrenergic i.j.ps have a multiple nature in the guinea-pig colon (Vladimirova & Shuba, 1984). Both apamin and L-NOARG effectively but partially inhibited the nonadrenergic i.j.p. and a residual small i.j.p. was observed in about 50% of cases in the presence of both drugs. The identity of the mediators of i.j.ps has not been conclusively demonstrated: for the first, apamin-sensitive, phase of i.j.p., adenosine triphosphate (ATP) was suggested as a likely mediator (Vladimirova & Shuba, 1984). The second, apamin-resistant, phase of i.j.ps was inhibited by the nitric oxide (NO)-synthase blocker, L-NOARG. Thus NO could be responsible for part of the apamin-resistant i.j.ps in the circular muscle of the guinea-pig proximal colon.

In conclusion, the present findings indicate a major role for SP and NK_1 receptors in mediating non-cholinergic e.j.ps and contractions evoked by EFS in the circular muscle of the guinea-pig proximal colon. Since NK_2 receptors mediate tachykininergic neuromuscular transmission to the circular muscle of the guinea-pig ileum (Bartho *et al.*, 1992; Holzer *et al.*, 1993), the use of receptor selective antagonists reveals a remarkable regional specialization in the TK receptor types which mediate neuromuscular transmission to endogenous TKs in the gut.

References

ARTEMENKO, D.P., BURY, V.A., VLADIMIROVA, I.A. & SHUBA, M.F. (1982). Modification of the single sucrose-gap method. *Physiol. Zhurn.*, **28**, 374–380.

BARTHO, L. & HOLZER, P. (1985). Search for a physiological role of substance P in gastrointestinal motility. *Neuroscience*, **16**, 1–32.

BARTHO, L., HOLZER, P., DONNERER, J. & LEMBECK, F. (1982). Evidence for the involvement of substance P in the atropine-resistant peristalsis of guinea-pig ileum. *Neurosci. Lett.*, **32**, 69–74.

BARTHO, L., SANTICIOLI, P., PATACCHINI, R. & MAGGI, C.A. (1992). Tachykininergic transmission to the circular muscle of the guinea-pig ileum: evidence of the involvement of NK_2 receptors. *Br. J. Pharmacol.*, **105**, 805–810.

BAUER, V. & KURIYAMA, H. (1982). The nature of non-cholinergic, non-adrenergic transmission in longitudinal and circular muscle of the guinea-pig ileum. *J. Physiol.*, **330**, 375–391.

BUCK, S.H. & SHATZER, S.A. (1988). Agonist and antagonist binding to tachykinin peptide NK-2 receptors. *Life Sci.*, **42**, 2701–2708.

BYWATER, R.A.R. & TAYLOR, G.S. (1983). Non-cholinergic fast and slow post-stimulus depolarization in the guinea-pig ileum. *J. Physiol.*, **340**, 47–56.

BYWATER, R.A.R. & TAYLOR, G.S. (1986). Noncholinergic excitatory and inhibitory junction potentials in the circular smooth muscle of the guinea-pig ileum. *J. Physiol.*, **374**, 153–164.

COSTA, M., FURNESS, J.B. & LLEWELLYN-SMITH, I.J. (1987). Histochemistry of the enteric nervous system. In *Physiology of the Gastrointestinal Tract*, 2nd Edition, ed. Johnson, L.R. pp. 1–40. New York: Raven Press.

COSTA, M., FURNESS, J.B., PULLIN, C.O. & BORNSTEIN, J. (1985). Substance P enteric neurons mediate non-cholinergic transmission to the circular muscle of the guinea-pig intestine. *Naunyn Schmied. Arch. Pharmacol.*, **328**, 446–453.

COSTA, M., FURNESS, J.B. & HUMPHREYS, C.M.S. (1986). Apamin distinguishes two types of relaxation mediated by enteric nerves in the guinea-pig gastrointestinal tract. *Naunyn Schmied. Arch. Pharmacol.*, **332**, 79–88.

CRIST, J.R., HE, X.D. & GOYAL, R.K. (1991). The nature of non-cholinergic membrane potential responses to transmural stimulation in guinea-pig ileum. *Gastroenterology*, **100**, 1006–1015.

DION, S., D'ORLEANS-JUSTE, P., DRAPEAU, G., RHALEB, N.E., ROUSSI, N., TOUSIGNANT, C. & REGOLI, D. (1987). Characterization of neurokinin receptors in various isolated organs by the use of selective agonists. *Life Sci.*, **41**, 2269–2278.

DONNERER, J., BARTHO, L., HOLZER, P. & LEMBECK, F. (1984). Intestinal peristalsis associated with release of immunoreactive substance P. *Neuroscience*, **11**, 913–918.

EMONDS ALT, X., VILAIN, P., GOULAOUIC, P., PROIETTO, V., VAN BROECK, D., ADVENIER, C., NALINE, E., NELIAT, G., LE FUR, G. & BRELIERE, J.C. (1992). A potent and selective nonpeptide antagonist of the neurokinin A (NK-2) receptor. *Life Sci.-Pharmacol. Lett.*, **50** PL101–106.

FRANCO, R., COSTA, M. & FURNESS, J.B. (1979). Evidence for the release of endogenous substance P from intestinal nerves. *Naunyn Schmied. Arch. Pharmacol.*, **306**, 195–201.

GIULIANI, S., LECCI, A. & MAGGI, C.A. (1993). Tachykinins and reflexly-evoked atropine-resistant motility in the guinea-pig colon in vivo. *J. Pharmacol. Exp. Ther.*, (in press).

HAGAN, R.M., IRELAND, S.J., BAILEY, F., MCBRIDE, C., JORDAN, C.A. & WARD, P. (1991). A spirolactam conformationally-constrained analogue of physalaemin which is a peptidase resistant, selective NK-1 receptor antagonist. *Br. J. Pharmacol.*, **102,** 168P.

HOLZER, P., SCHLUET, W. & MAGGI, C.A. (1993). Ascending enteric reflex contraction: roles of acetylcholine and tachykinins in relation to distension and propagation of excitation. *J. Pharmacol. Exp. Ther.*, **264,** 391–396.

HOYLE, C.H.V. (1987). A modified single sucrose gap – junction potentials and electrotonic potentials in gastrointestinal smooth muscle. *J. Pharmacol. Methods*, **18,** 219–226.

MAGGI, C.A. & GIULIANI, S. (1993). Multiple inhibitory mechanisms mediate non-adrenergic non-cholinergic relaxation in the circular muscle of the guinea-pig ileum. *Naunyn-Schmied. Arch. Pharmacol.*, (in press).

MAGGI, C.A., GIULIANI, S., BALLATI, L., LECCI, A., MANZINI, S., PATACCHINI, R., RENZETTI, A.R., ROVERO, P., QUARTARA, L. & GIACHETTI, A. (1991). In vivo evidence for tachykininergic transmission using a new NK-2 receptor selective antagonist, MEN 10376. *J. Pharmacol. Exp. Ther.*, **257,** 1172–1178.

MAGGI, C.A., GIULIANI, S., PATACCHINI, R., SANTICIOLI, P., THEODORSSON, E., BARBANTI, G., TURINI, D. & GIACHETTI, A. (1992). Tachykinin antagonists inhibit nerve-mediated contractions in the circular muscle of the human ileum. *Gastroenterology*, **102,** 88–96.

MAGGI, C.A., PATACCHINI, R., GIACHETTI, A. & MELI, A. (1990). Tachykinin receptors in the circular muscle of the guinea-pig ileum. *Br. J. Pharmacol.*, **101,** 996–1000.

MAGGI, C.A., PATACCHINI, R., ROVERO, P. & GIACHETTI, A. (1993). Tachykinin receptors and tachykinin receptor antagonists. *J. Autonom. Pharmacol.*, **13,** 23–93.

MANZINI, S., MAGGI, C.A. & MELI, A. (1986). Pharmacological evidence that at least two different nonadrenergic noncholinergic inhibitory systems are present in the rat small intestine. *Eur. J. Pharmacol.*, **123,** 229–236.

NIEL, J.P., BYWATER, R.A.R. & TAYLOR, G.S. (1983). Effect of substance-P on non-cholinergic fast and slow post-stimulus depolarization in the guinea-pig ileum. *J. Autonom. Nerv. Syst.*, **9,** 573–584.

ROVERO, P., PESTELLINI, V., RHALEB, N.E., DION, S., ROUSSI, N., TOUSIGNANT, C., TELEMAQUE, S., DRAPEAU, G. & REDOLI, D. (1989). Structure-activity studies of neurokinin A. *Neuropeptides*, **13,** 263–270.

SCHMIDT, A.W., MCLEAN, S. & HEYM, J. (1992). The substance P receptor antagonist CP 96,345 interacts with calcium channels. *Eur. J. Pharmacol.*, **219,** 491–492.

SHUBA, M.F. & VLADIMIROVA, I.A. (1980). Effect of apamin on the electrical responses of smooth muscle to adenosine 5'-triphosphate and to non-adrenergic, non-cholinergic nerve stimulation. *Neuroscience*, **5,** 853–859.

SHUTTLEWORTH, C.W.R., MURPHY, R., FURNESS, J.B. & POMPOLO, S. (1991). Comparison of the presence and actions of substance P and neurokinin A in guinea-pig taenia coli. *Neuropeptides*, **19,** 23–34.

SNIDER, R.M., CONSTANTINE, J.W., LOWER III, J.A., LONGO, K.P., LEBEL, W.S., WOODY, H.A., DROZDA, S.E., DESAI, M.C., VINICK, F.J., SPENCER, R.W. & HESS, H.J. (1991). A potent nonpeptide antagonist of the substance P (NK-1) receptor. *Science*, **251,** 435–437.

STERNINI, C., ANDERSON, K., FRANTZ, G., KRAUSE, J.E. & BRECHA, N.S. (1989). Expression of substance P/neurokinin A-encoding preprotachykinin messenger RNA in the rat enteric nervous system. *Gastroenterology*, **97,** 348–356.

TAYLOR, S.J. & KILPATRICK, C.J. (1992). Characterization of histamine H_3 receptors controlling nonadrenergic noncholinergic contractions of the guinea-pig isolated ileum. *Br. J. Pharmacol.*, **105,** 667–674.

THEODORSSON, E., SMEDFORS, B., HELLSTROM, P., SODER, O., ALY, A., MUSAT, A., PANJA, A.B. & JOHANSSON, C. (1991). Aspects on the role of tachykinins and VIP in control of secretion, motility and blood flow in the gut. *Adv. Exp. Med. Biol.*, **298,** 233–240.

TOO, H.P., CORDOVA, J.L. & MAGGIO, J.E. (1989). A novel radioimmunoassay for neuromedin K. I. Absence of neurmedin K-like immunoreactivity in guinea-pig ileum and urinary bladder. II. Heterogeneity of tachykinins in guinea-pig tissues. *Regul. Pept.*, **26,** 93–105.

VLADIMIROVA, I.A. & SHUBA, M.F. (1984). Synaptic processes in smooth muscle. *Neurophysiology*, **16,** 307–319.

(Received January 20, 1993
Revised May 13, 1993
Accepted June 1, 1993)

Br. J. Pharmacol. (1993), **110**, 804–808

Muscarinic effect of atrial natriuretic peptide on rabbit airways

*†A. Robichaud, ‡C. Saunier, †M.C. Michoud & *†[1]P. du Souich

*Dépt. de pharmacologie, Faculté de Médecine, Université de Montréal, †Hôtel-Dieu de Montréal, Québec, Canada and ‡INSERM U14, Vandoeuvre-Les-Nancy, France

1 The aim of the present work was to investigate under which circumstances atrial natriuretic peptide (ANP) modulates airway resistance.

2 Of the six groups of rabbits ($n = 5$) studied, three received an infusion of ANP (80 ng min^{-1} kg^{-1} i.v.) for a period of 100 min, while the other three were infused with the vehicle. Before receiving the infusion of ANP or the vehicle, the animals were pretreated with atropine (0.5 mg kg^{-1} i.v.), propranolol (2 mg kg^{-1} i.v.) or not pretreated. After 75 min of infusion of ANP, bronchoconstriction was induced by inhalation of histamine. Respiratory resistance (Rrs) was measured before and 3, 5, 10, 15 and 20 min post-histamine challenge.

3 Following 75 min of ANP infusion, plasma ANP concentration increased from 153 ± 52 (mean ± s.e.mean) to 1441 ± 203 pg ml^{-1} ($P<0.05$) without affecting baseline Rrs. Control Rrs values (12.5–20.4 cmH_2O l^{-1} s) were significantly increased following the inhalation of histamine ($P<0.001$). By themselves, atropine, propranolol or ANP did not modify the histamine-induced increase in Rrs. However, when the animals were pretreated with atropine, ANP infusion significantly reduced the increase in Rrs induced by histamine (30 ± 2 vs 51 ± 6 cmH_2O l^{-1} s; $P<0.05$).

4 These data suggest that ANP has an indirect modulating effect on the airway smooth muscle and will decrease Rrs when muscarinic receptors are blocked.

Keywords: Atrial natriuretic peptide; respiratory resistance; airway smooth muscle; rabbit; histamine; atropine; propranolol

Introduction

There is growing evidence that the atrial natriuretic peptide (ANP), first known for its role in the regulation of vascular capacitance and of intravascular blood volume (Goetz, 1988, Cantin & Genest, 1986), also has extravascular effects. In addition to the cardiovascular system and the kidney, the central and automonic nervous systems, the lungs, the adrenal glands, the digestive and reproductive system and lymph nodes have been suggested to be target organs for ANP (Vollmar, 1990; Gutkowska & Nemer, 1989).

In the lung, ANP has been demonstrated to be a powerful relaxant of guinea-pig and bovine isolated tracheal smooth muscle (O'Donnell *et al.*, 1985; Hamel & Ford-Hutchinson, 1986; Watanabe *et al.*, 1988; Potvin & Varma, 1989; Ishii & Murad, 1989). However, it has also been shown that ANP elicits no effect on rabbit and human airway smooth muscle *in vitro*, despite the fact that it can induce a bronchodilatation *in vivo* (Labat *et al.*, 1988; Candenas *et al.*, 1991; Hulks *et al.*, 1989; Chanez *et al.*, 1990; Robichaud *et al.*, 1993).

It has been suggested that the vaso- and bronchodilating actions of ANP are mediated by the guanosine 3':5'-cyclic monophosphate (cyclic GMP) intracellular messenger that induces the relaxation of smooth muscle (Hamet *et al.*, 1984; Winquist *et al.*, 1984; Cornwell & Lincoln, 1989; Watanabe *et al.*, 1990). However, there is growing evidence suggesting that these effects may be mediated by the autonomic nervous system (Kuchel *et al.*, 1987; Debinski *et al.*, 1990; Menard, 1991). Supporting a neuromodulatory function of ANP is the fact that it has been identified in peripheral parasympathetic (sensory nodose ganglia) and sympathetic (superior and inferior cervical, superior mesenteric and celiac) ganglia (Debinski *et al.*, 1986; 1987a). In addition, several studies suggest that ANP stimulates vagal activity leading to a fall in arterial pressure and to a decrease in renal sympathetic nerve activity (Ackermann *et al.*, 1984; Thoren *et al.*, 1986; Volpe *et al.*, 1987; Imaizumi *et al.*, 1987; Schultz *et al.*, 1988; Zeuzem *et al.*, 1990).

To further understand the contradictory results concerning the modulatory effect of ANP on respiratory resistance, we investigated the action of ANP on airway smooth muscle tone during histamine-induced bronchoconstriction in rabbits pretreated with parasympathetic or sympathetic blockers.

Methods

Animal preparation

Experiments were conducted on 30 male, New Zealand rabbits (2.0–3.3 kg; CEGAV, St Mars d'Egrenne, France), divided into 6 groups of 5 animals each. The animals were anaesthetized with sodium thiopentone (Rhône-Poulenc, Paris, France) with an initial dose of 14–20 mg kg^{-1} i.v. Additional anaesthetic was added as needed during the experiment. A tracheotomy was performed, but the animals breathed spontaneously. The left jugular vein and carotid artery were catheterized (PE 60, Clay Adams, Parsippany, NJ, U.S.A.) to permit the infusion of ANP and the determination of arterial blood pressure. Blood pressure was assessed by use of a Bell and Howell transducer (0–750 mmHg, type 4-327 I) coupled to a chart recorder (Brush 2400 Gould).

Experimental protocol

Three groups received an infusion of ANP (80 ng min^{-1} kg^{-1} i.v.) (ANP [99–126]; IAF Biochem, Montreal, Canada), and three groups received an infusion of the vehicle, i.e. a solution of saline 0.9%:glucose 5% (50:50 v/v) containing 0.2% heat inactivated (50°C, 30 min) bovine serum albumin. Immediately before the beginning of the infusion of ANP or its vehicle, the animals were pretreated with atropine 0.5 mg kg^{-1} i.v. (groups AT-ANP or AT, respectively), (±)-propranolol 2 mg kg^{-1} i.v. (groups PR-ANP or PR, respectively), or not pretreated (groups ANP or sham, respectively) (Szarek *et al.*, 1986).

After surgical preparation of the animals, ANP was in-

[1] Author for correspondence.

fused for 75 min, in order to raise ANP plasma concentrations to a steady-state level (Marleau *et al.*, 1989). Following this, bronchoconstriction was induced by inhalation of a nebulized solution of histamine (1%) for 3 min, (Aerosoliseur Gauchard, Paris, France; flow rate: 0.12 ml min^{-1}); a dose producing approximately 50% response in rabbits (Berend *et al.*, 1986; Quan *et al.*, 1986). The infusion of ANP was continued during the entire experiment, resulting in a total infusion time of 100 min. Respiratory resistance, ventilation and respiratory frequency were measured before and 75 min after the beginning of ANP or vehicle infusion as well as 3, 5, 10, 15 and 20 min post-histamine inhalation. Measurements of blood gases and mean arterial blood pressure and blood sampling for plasma ANP determinations were made before and 75 min after the beginning of ANP infusion and 20 min post-histamine challenge.

Respiratory parameters

Respiratory resistance was measured by the forced oscillation method (Peslin, 1986) as described previously (Robichaud *et al.*, 1993). Briefly, sinusoidal pressure oscillations (amplitude 2 cmH_2O peak to peak, frequency 20 Hz) were applied to the airway opening. The applied pressure and airway flow signal, measured with a Celesco^R LCVR transducer (Canoga Park, CA, U.S.A.; range ± 2 cmH_2O) and a Fleish n°0 pneumotachograph (Metabo, Epalinges, Switzerland), respectively, were recorded for a period of 6.4 s at a sample frequency of 160 Hz by an Apple 2 microcomputer. Respiratory resistance was computed on a cycle-per-cycle basis from the pressure signal in phase with flow. Ventilation and respiratory frequency were obtained from the flow signal.

Analytical method

Plasma ANP was determined by radioimmunoassay (RIA) after extraction on Sep-pak cartridges according to the method described by Larose *et al.* (1985).

Statistical analysis

Results are presented as mean ± s.e.mean. Statistically significant differences between group means were calculated using a two-way analysis of variance for repeated measures combined with multiple procedures (Tuckey B) for each significant interaction (Winer, 1971). The alpha error was fixed at 5%.

Results

Arterial blood gases

In the sham group, arterial oxygen pressure (Pa_{O_2}) and arterial partial pressure of CO_2 (Pa_{CO_2}) were respectively 81.2 ± 1.6 and 27.1 ± 0.7 mmHg during the control period, 88.4 ± 3.4 and 25.0 ± 1.1 mmHg after 75 min of vehicle infusion, and 87.8 ± 3.5 and 21.2 ± 1.8 mmHg 20 min following histamine inhalation. Arterial pH of the sham animals was 7.43 ± 0.03 and 7.45 ± 0.02 at baseline and following 75 min of vehicle infusion, respectively. It increased significantly to 7.51 ± 0.02 after the inhalation of histamine. Mean values of Pa_{O_2}, Pa_{CO_2}, and pH were comparable between experimental groups.

Plasma ANP

Mean values of plasma ANP concentrations determined in the six experimental groups studied are shown in Figure 1. During the control period, baseline ANP plasma concentrations were similar in all groups. Compared to the baseline, the infusion of the vehicle, the inhalation of histamine, and parasympathetic (atropine) or sympathetic (propranolol) blockade did not affect the levels of endogenous ANP. In the groups receiving the infusion of ANP (i.e. ANP, AT-ANP, PR-ANP), plasma ANP concentrations increased approximately ten fold; the concentrations generated by the infusion of ANP were comparable between the groups.

Mean arterial pressure

In the control period, mean arterial pressure was comparable between groups (Figure 2). Compared to baseline values, the infusion of the vehicle did not affect mean arterial pressure, whether histamine was present or not. The infusion of ANP

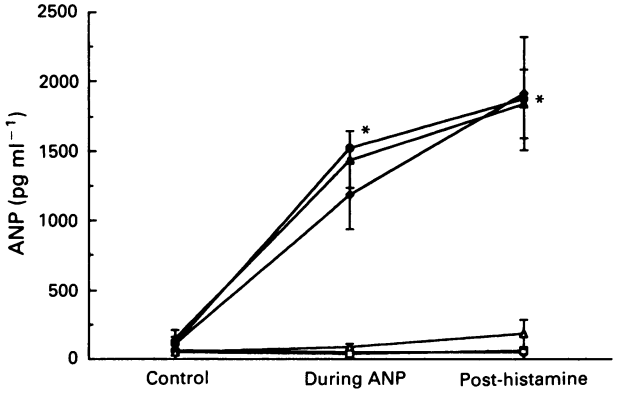

Figure 1 Atrial natriuretic peptide (ANP) plasma concentrations were determined before (baseline), 75 min after the beginning of the infusion of ANP (during ANP), and 20 min post-histamine challenge (post-histamine). *Significant difference from baseline at $P<0.05$. (○) Sham = group receiving an infusion of the vehicle (saline 0.9%: glucose 5% [50:50 v/v] + inactivated bovine serum albumin 0.2%) ($n=5$); (□) AT = group pretreated with atropine (0.5 mg kg^{-1} i.v.) + infusion of the vehicle ($n=5$); (△) PR = group pretreated with propranolol (2 mg kg^{-1} i.v.) + infusion of the vehicle ($n=5$); (▲) ANP = group receiving an infusion of ANP (80 ng min^{-1} kg^{-1} i.v.) ($n=5$): (◆) AT-ANP = group pretreated with atropine + infusion of ANP ($n=5$); (●) PR-ANP = group pretreated with propranolol + infusion of ANP ($n=5$).

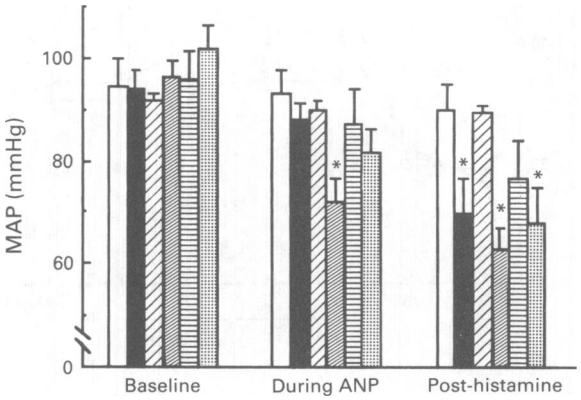

Figure 2 Mean arterial pressure (MAP) was determined before (baseline), 75 min after the beginning of the infusion of atrial natriuretic peptide (ANP) (during ANP), and 20 min post-histamine challenge (post-histamine). *Significant difference from baseline at $P<0.05$. (□) Sham = group receiving an infusion of the vehicle (saline 0.9%: glucose 5% 50:50 v/v] + inactivated bovine serum albumin 0.2%) ($n=5$); (▨) AT = group pretreated with atropine (0.5 mg kg^{-1} i.v.) + infusion of the vehicle ($n=5$); (▤) PR = group pretreated with propranolol (2 mg kg^{-1} i.v.) + infusion of the vehicle ($n=5$); (■) ANP = group receiving an infusion of ANP (80 ng min^{-1} kg^{-1} i.v.) ($n=5$); (▨) AT-ANP = group pretreated with atropine + infusion of ANP ($n=5$); (▩) PR-ANP = group pretreated with propranolol + infusion of ANP ($n=5$).

Table 1 Respiratory parameters ($\dot{V}_E$ is ventilation, f is respiratory frequency) were determined prior to (baseline), 75 min after the beginning of the infusion of atrial natriuretic peptide (ANP) (during ANP), and 20 min post-histamine challenge (post-histamine)

Parameters	*Groups*	*Baseline*	*During ANP*	*Post-histamine*
$\dot{V}_E$	Sham	1.0 ± 0.1	0.8 ± 0.1	1.0 ± 0.1
(l min^{-1})	ANP	1.1 ± 0.1	1.0 ± 0.1	1.2 ± 0.1
	AT	1.3 ± 0.1	1.2 ± 0.2	1.3 ± 0.3
	AT-ANP	1.1 ± 0.1	1.5 ± 0.3	1.3 ± 0.4
	PR	1.1 ± 0.1	0.9 ± 0.1	1.1 ± 0.1
	PR-ANP	1.2 ± 0.2	1.2 ± 0.2	1.2 ± 0.1
f	Sham	72 ± 7	65 ± 7	68 ± 13
(breaths per min)	ANP	66 ± 10	80 ± 15	77 ± 8
	AT	89 ± 5	65 ± 9	79 ± 13
	AT-PR	63 ± 5	82 ± 11	83 ± 16
	PR	93 ± 10	76 ± 5	75 ± 4
	PR-ANP	88 ± 16	75 ± 3	86 ± 5

Sham = group receiving an infusion of the vehicle (saline 0.9%: glucose 5% [50:50 v/v] + inactivated bovine serum albumin 0.2%) ($n = 5$); AT = group pretreated with atropine (0.5 mg kg^{-1} i.v.) + infusion of the vehicle ($n = 5$); PR = group pretreated with propranolol (2 mg kg^{-1} i.v.) + infusion of the vehicle ($n = 5$); ANP = group receiving an infusion of ANP (80 ng min^{-1} kg^{-1} i.v.) ($n = 5$); AT-ANP = group pretreated with atropine + infusion of ANP ($n = 5$); PR-ANP = group pretreated with propranolol + infusion of ANP ($n = 5$).

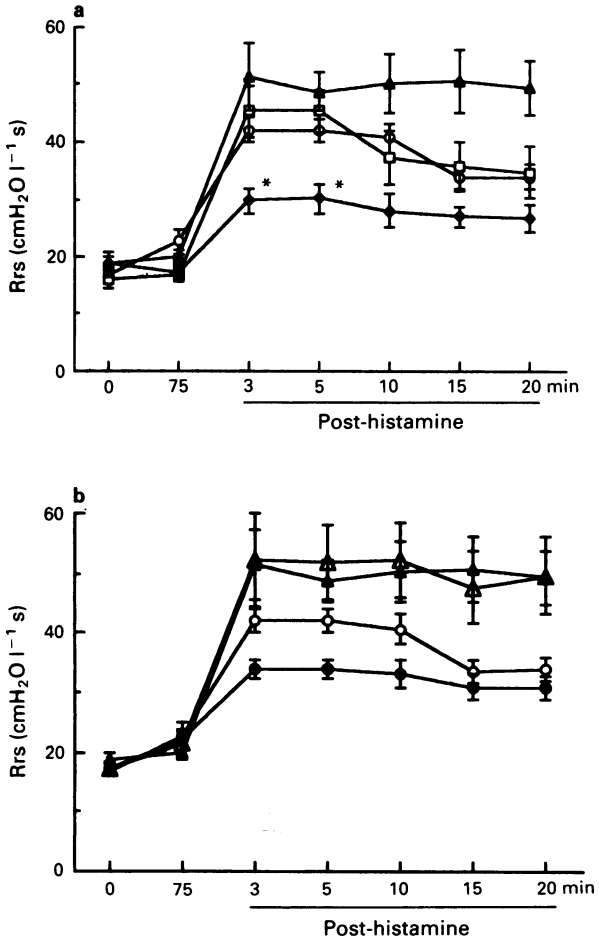

Figure 3 Mean respiratory resistance (Rrs) values during control (t = 0) and atrial natriuretic peptide (ANP) infusion periods (t = 75) and after histamine challenge (a) in the sham, ANP, AT and AT-ANP groups; (b) in the sham, ANP, PR and PR-ANP groups. *Significant difference at $P < 0.05$ compared to sham and ANP groups. (○) Sham = group receiving an infusion of the vehicle (saline 0.9%: glucose 5% [50:50 v/v] + inactivated bovine serum albumin 0.2%) ($n = 5$); (□) AT = group pretreated with atropine (0.5 mg kg^{-1} i.v.) + infusion of the vehicle ($n = 5$); (△) PR = group pretreated with propranolol (2 mg kg^{-1} i.v.) + infusion of the vehicle ($n = 5$); (▲) ANP = group receiving an infusion of ANP (80 ng min^{-1} kg^{-1} i.v.) ($n = 5$); (◆) AT-ANP = group pretreated with atropine + infusion of ANP ($n = 5$); (●) PR-ANP = group pretreated with propranolol + infusion of ANP ($n = 5$).

by itself also did not modify the mean arterial pressure; however, following histamine inhalation, blood pressure was significantly lower than baseline values. Atropine did not alter mean arterial pressure, but the combination of atropine and ANP infusion (i.e. AT-ANP group) produced a significant drop in blood pressure, a decrease that was slightly potentiated by the inhalation of histamine. Sympathetic blockade with propranolol did not significantly modify mean arterial pressure of animals receiving the vehicle. In animals receiving the infusion of ANP and pretreated with propranolol (i.e. group PR-ANP), mean arterial pressure remained stable during the infusion period. However, following the inhalation of histamine a significant fall in blood pressure was noted.

Ventilatory parameters

Mean values for ventilation and respiratory frequency of the different groups are shown in Table 1. These parameters were not affected by the infusion of ANP or its vehicle, or by the inhalation of histamine. The administration of parasympathetic or sympathetic blockers did not alter these respiratory characteristics of the animals.

Respiratory resistance

During the control period (t = 0), as well as after 75 min of ANP infusion, respiratory resistance remained stable in each group studied (Figure 3). In the sham group, the values of respiratory resistance increased significantly following the inhalation of histamine (from 16.9 ± 1.3 to 40.6 ± 2.7 cmH$_2$O l^{-1} s) ($P < 0.001$). The infusion of ANP tended to increase the respiratory resistance, although the difference was not statistically significant.

Parasympathetic blockade

Compared to the sham group, the histamine-induced increase in respiratory resistance was not modified by atropine (i.e. AT group) (Figure 3a). However, in the animals pretreated with atropine and receiving an infusion of ANP (i.e. AT-ANP group), the increase in respiratory resistance induced by histamine was significantly lower 3 and 5 min after the challenge, compared to animals receiving only the infusion of ANP or of the vehicle.

Sympathetic blockade

Compared to the sham group, the administration of propranolol induced a slight, but not significant, increase in res-

piratory resistance following the inhalation of histamine (Figure 3b). The animals receiving the infusion of ANP (i.e. PR-ANP group) tended to show a decrease in the degree of histamine-induced bronchoconstriction; however, this did not reach statistical significance.

Discussion

Histamine is known to induce bronchoconstriction both by a direct effect on H_1 receptors and by cholinergic reflex activation (Shore *et al.*, 1983; Sheppard *et al.*, 1984). Since atropine did not influence the degree of histamine-induced bronchoconstriction under the present experimental conditions, we might assume that the cholinergic component of the action of histamine did not contribute much to the increase in respiratory resistance.

It has been demonstrated that rabbit airway smooth muscle is devoid of sympathetic innervation; however, catecholamine-containing cells have been identified in the ganglia of the bronchi (Mann, 1971), although their role in modulating bronchial tone does not appear important. In the present study, blockade of sympathetic β-adrenoceptors with propranolol tended to increase histamine-induced bronchoconstriction beyond the level observed in the sham group. Although it did not reach statistical significance, this action of propranolol is probably attributable to an increased cholinergic outflow as a result of withdrawal of the sympathetic activity. Alternatively, by treating the animals with a β-blocking drug, the α-adrenoceptors, being left unopposed, can induce a contraction of the airway smooth muscle (Kneussl & Richardson, 1978; Simonsson *et al.*, 1972), that is potentiated by the administration of histamine (Kneussl & Richardson, 1978). Therefore, it appears that the sympathetic nervous system may indirectly modulate rabbit airways and may partially blunt the response to histamine.

Following histamine inhalation, ANP tended to potentiate the bronchoconstriction. Since respiratory resistance was significantly decreased when ANP was infused to atropine-pretreated rabbits, we can assume that ANP elicits a parasympathomimetic effect in the respiratory system, as has already been described for the cardiovascular system. In addition, ANP appears to increase cholinergic activation by histamine, since atropine reduces ANP-induced changes in respiratory resistance below the values observed following the inhalation of histamine alone.

Several studies have demonstrated a direct sympatho-inhibitory effect of ANP *in vitro* as well as *in vivo* (Drewett *et al.*, 1988; 1989; Zukowska-Grojec *et al.*, 1986; Debinski *et al.*, 1987b; Bergey *et al.*, 1989; Floras, 1990). Therefore, in addition to a direct parasympathomimetic effect, we may speculate that ANP enhanced cholinergic outflow through sympathetic inhibition and induced a small bronchoconstriction that is reduced by atropine.

A slight decrease in the degree of histamine-induced bronchoconstriction (although not statistically significant) was also noted when ANP was infused in the presence of propranolol. Since, ANP exerts sympatho-inhibitory effects in the lung, it is possible that it exerts an α-adrenoceptor inhibition; this may explain why the combination of ANP and propranolol decreases histamine-induced increase in respiratory resistance. Supporting such speculation, Haass *et al.* (1985) have shown in vagotomized pithed rats that ANP can block blood pressure responses to α-adrenoceptor agonists.

In another study, we found that ANP decreased respiratory resistance following histamine inhalation (Robichaud *et al.*, 1993). The discrepancy with the results of the present investigation may be explained by differences in the experimental conditions. In the other study, the animals had a higher ventilation and tidal volume immediately before the histamine challenge, as well as a higher level of histamine-induced bronchoconstriction. Since lung irritant receptors associated with vagal reflex activation are more active in rabbits breathing more deeply (Mills *et al.*, 1969), it is possible that histamine triggered a more important cholinergic reflex activation in the previous study. Another difference between the two investigations, is the reduction in mean arterial pressure after ANP infusion. As a consequence, we may speculate that homeostatic reactions (activation of sympathetic, renin-angiotensin systems, etc.) were more important in the present study and that they may have changed bronchial reactivity to histamine in the presence of ANP, either directly or indirectly.

In summary, it appears that ANP may influence airway smooth muscle tone by affecting the pulmonary autonomic nervous system, and that the effect of ANP on airway smooth muscle tone depends upon the baseline conditions of the animal.

The authors wish to thank C. Duvivier and C. Gallina (INSERM U. 14, France) for technical advice. This work was supported by grant MA 10324 from the Medical Research Council, by the Quebec Lung Association and by the Hôtel-Dieu Foundation. A.R. is recipient of a studentship from MRC.

References

ACKERMANN, U., IRIZAWA, T.G., MILOJEVIC, S. & SONNENBERG, H. (1984). Cardiovascular effects of atrial extracts in anesthetized rats. *Can. J. Physiol. Pharmacol.*, **62**, 819–826.

BEREND, N., ARMOUR, C.L. & BLACK, J.L. (1986). Indomethacin inhibits the increased airway responsiveness to histamine following inhalation of C5a des Arg in rabbits. *Agents & Actions*, **18**, 468–472.

BERGEY, J.L., MUCH, D.R., KRATUNIS, V. & ASAAD, M. (1989). Effect of human ANF(99-126) on sympathetic nerve function, hemodynamic parameters and plasma cGMP levels in anesthetized, ganglion-blocked dogs. *Eur. J. Pharmacol.*, **159**, 103–112.

CANDENAS, M.-L., NACINE, E., PUYBASSET, L., DEVILLIER, P. & ADVENIER, C. (1991). Effect of atrial natriuretic peptide and of atriopeptins on the human isolated bronchus. Comparison with the reaction of guinea-pig isolated trachea. *Pulmonary Pharmacol.*, **4**, 120–125.

CANTIN, M. & GENEST, J. (1986). The heart as an endocrine gland. *Sci. Amer.*, **254**, 76–81.

CHANEZ, P., MANN, C., BOUSQUET, J., CHABRIER, P.E., GODARD, P., BRAQUET, P. & MICHEL, F.B. (1990). Atrial natriuretic factor (ANF) is a potent bronchodilator in asthma. *J. Allerg. Clin. Immunol.*, **86**, 321–324.

CORNWELL, T.L. & LINCOLN, T.M. (1989). Regulation of intracellular Ca^{2+} levels in cultured vascular smooth muscle cells. Reduction of Ca^{2+} by atriopeptin and 8-bromo-cyclic GMP is mediated by cyclic GMP-dependent protein kinase. *J. Biol. Chem.*, **264**, 1146–1155.

DEBINSKI, W., GUTKOWSKA, J., KUCHEL, O., RACZ, K., BUU, N.T., CANTIN, M. & GENEST, J. (1986). ANF-like peptide(s) in the peripheral autonomic nervous system. *Biochem. Biophys. Res. Commun.*, **134**, 279–284.

DEBINSKI, W., GUTKOWSKA, J., KUCHEL, O., RACZ, K., BUU, N.T., CANTIN, M. & GENEST, J. (1987a). Presence of an atrial natriuretic factor-like peptide in the rat superior cervical ganglia. *Neuroendocrinology*, **46**, 236–240.

DEBINSKI, W., KUCHEL, O. & BUU, N.T. (1990). Atrial natriuretic factor is a new neuromodulatory peptide. *Neuroscience*, **36**, 15–20.

DEBINSKI, W., KUCHEL, O., BUU, N.T., CANTIN, M. & GENEST, J. (1987b). Atrial natriuretic factor partially inhibits the stimulated catecholamine synthesis in superior cervical ganglia of the rat. *Neurosci. Lett.*, **77**, 92–96.

DREWETT, J., MARCHAND, G., ZIEGLER, R. & TRACHTE, G. (1988). Atrial natriuretic factor inhibits norepinephrine release in an adrenergic clonal cell line (PC12). *Eur. J. Pharmacol.*, **150,** 175–179.

DREWETT, J.G., TRACHTE, G.J. & MARCHAND, G.R. (1989). Atrial natriuretic factor inhibits adrenergic and purinergic neurotransmission in the rabbit isolated vas deferens. *J. Pharmacol. Exp. Ther.*, **248,** 135–142.

FLORAS, J.S. (1990). Sympathoinhibitory effects of atrial natriuretic factor in normal human. *Circulation*, **81,** 1860–1863.

GOETZ, K.L. (1988). Physiology and pathophysiology of atrial peptides. *Am. J. Physiol.*, **254,** E1–E15.

GUTKOWSKA, J. & NEMER, M. (1989). Structure, expression and function of atrial natriuretic factor in extraatrial tissues. *Endocrine Rev.*, **10,** 519–536.

HAASS, M., KOPIN, I.J., GOLDSTEIN, D.S. & ZUKOWSKA-GROJEC, Z. (1985). Differential inhibition of alpha adrenoceptor-mediated pressor responses by rat atrial natriuretic peptide in the pithed rat. *J. Pharmacol. Exp. Ther.*, **235,** 122–127.

HAMEL, R. & FORD-HUTCHINSON, A.W. (1986). Relaxant profile of synthetic atrial natriuretic factor on guinea pig pulmonary tissues. *Eur. J. Pharmacol.*, **121,** 151–155.

HAMET, P., TREMBLAY, J., PANG, S.C., GARCIA, R., THIBAULT, G., GUTKOWSKA, J., CANTIN, M. & GENEST, J. (1984). Effect of native and synthetic atrial natriuretic factor in cyclic GMP. *Biochem. Biophys. Res. Commun.*, **123,** 515–527.

HULKS, G., JARDINE, A., CONNELL, J.M. & THOMSON, N.C. (1989). Bronchodilator effect of atrial natriuretic factor on bronchomotor tone in the normal human airway. *Br. Med. J.*, **299,** 1081–1082.

IMAIZUMI, T., TAKESHITA, A., HIGASHI, H. & NAKAMURA, M. (1987). Alpha-ANP alters reflex control of lumbar and renal sympathetic nerve activity and heart rate. *Am. J. Physiol.*, **253,** H1136–H1140.

ISHII, K. & MURAD, F. (1989). ANP relaxes bovine tracheal smooth muscle and increases cGMP. *Am. J. Physiol.*, **256,** C495–C500.

KNEUSSL, M.P. & RICHARDSON, J.B. (1978). Alpha-adrenergic receptors in human and canine tracheal bronchial smooth muscle. *J. Appl. Physiol.*, **45,** 307–311.

KUCHEL, O., DEBINSKI, W., RACZ, K., BUU, N.T., GARCIA, R., CUSSON, J.R., LAROCHELLE, P., CANTIN, M. & GENEST, J. (1987). An emerging relationship between peripheral sympathetic nervous activity and atrial natriuretic factors. *Life Sci.*, **40,** 1545–1551.

LABAT, C., NOREL, X., BENVENISTE, J. & BRINK, C. (1988). Vasorelaxant effects of atrial peptide II on isolated human pulmonary muscle preparations. *Eur. J. Pharmacol.*, **150,** 397–400.

LAROSE, P., MELOCHE, S., SOUICH, P. DU., LÉAN, A. DE. & ONG, H. (1985). Radioimmunoassay of atrial natriuretic factor: human plasma levels. *Biochem. Biophys. Res. Commun.*, **130,** 553–558.

MANN, S.P. (1971). The innervation of mammalian bronchial smooth muscle: the localization of catecholamines and cholinesterases. *Histochem. J.*, **3,** 319–331.

MARLEAU, S., ONG, H, LÉAN, A. DE. & SOUICH, P. DU. (1989). Disposition and dynamics of atrial natriuretic factor in conscious rabbits. *J. Pharmacol. Exp. Ther.*, **251,** 328–333.

MENARD, O. (1991). Facteur atrial natriurétique et poumon. *Rev. Mal. Respir.*, **8,** 153–167.

MILLS, J.E., SELLICK, H. & WIDDICOMBE, J.G. (1969). Activity of lung irritant receptors in pulmonary microembolism, anaphylaxis and drug-induced bronchoconstrictions. *J. Physiol.*, **203,** 337–357.

O'DONNELL, M., GARIPPA, R. & WELTON, A.F. (1985). Relaxant activity of atriopeptins in isolated guinea pig airway and vascular smooth muscle. *Peptides*, **6,** 597–601.

PESLIN, R. (1986). Methods for measuring total respiratory impedance by forced oscillations. *Bull. Eur. Physiopath. Respir.*, **22,** 621–631.

POTVIN, W. & VARMA, D.R. (1989). Bronchodilator activity of atrial natriuretic peptide in guinea pigs. *Can. J. Physiol. Pharmacol.*, **67,** 1213–1218.

QUAN, S.F., WITTEN, M.L., STEVENSON, J.L. & ROSEBERRY, H.R. (1986). Variability of pulmonary responsiveness to aerosolized histamine in normal rabbits. *Respiration*, **50,** 108–116.

ROBICHAUD, A., SAUNIER, C., MICHOUD, M.C., DUVIVIER, C., PESLIN, R. & SOUICH, P. DU. (1993). Effect of atrial natriuretic factor on histamine-induced bronchoconstriction in anesthetized rabbits. *Peptides*, (in press).

SCHULTZ, H.D., GARDNER, D.G., DESCHEPPER, C.F., COLERIDGE, H.M. & COLERIDGE, J.C.G. (1988). Vagal C-fibers blockade abolishes sympathetic inhibition by atrial natriuretic factor. *Am. J. Physiol.*, **255,** R6–R13.

SHEPPARD, D., EPSTEIN, J., SKOOGH, B.E., BETHEL, R.A., NADEL, J.A. & BOUSHEY, H.A. (1984). Variable inhibition of histamine-induced bronchoconstriction by atropine in subjects with asthma. *J. Allergy Clin. Immunol.*, **73,** 82–87.

SHORE, S., IRVIN, C.G., SHENKIER, T. & MARTIN, J.G. (1983). Mechanism of histamine-induced contraction of canine airway smooth muscle. *J. Appl. Physiol.*, **255,** 22–26.

SIMONSSON, B.G., SVEDMYR, N., SKOOGH, B.-E., ANDERSSON, R. & BERGH, N.P. (1972). In vivo and in vitro studies on alpha-receptors in human airways. Potentiation with bacterial endotoxin. *Scand. J. Respir. Dis.*, **53,** 227–236.

SZAREK, J.L., GILLESPIE, M.N., ALTIERE, R.J. & DIAMOND, L. (1986). Reflex activation of nonadrenergic noncholinergic inhibitory nervous system in feline airways. *Am. Rev. Respir. Dis.*, **133,** 1159–1162.

THOREN, P., MARK, A.L., MORGAN, D.A., O'NEIL, T.P., NEEDLEMAN, P. & BRODY, M.J. (1986). Activation of vagal depressor reflexes by atriopeptins inhibits renal sympathetic nerve activity. *Am. J. Physiol.*, **251,** H1252–H1259.

VOLLMAR, A.M. (1990). Atrial natriuretic peptide in peripheral organs other than the heart. *Klin. Wochenschr.*, **68,** 699–708.

VOLPE, M., CUOCOLO, A., VECCHINONE, F., MELE, A.F., CONDORELLI, M. & TRIMARCO, B. (1987). Vagal mediation of the effects of atrial natriuretic factor on blood pressure and arterial baroreflexes in the rabbits. *Circ. Res.*, **60,** 747–755.

WATANABE, H., SUZUKI, K., TAKAGI, K. & SATAKE, T. (1990). Mechanism of atrial natriuretic polypeptide and sodium nitroprusside-induced relaxation in guinea-pig tracheal smooth muscle. *Arzneim. Forsch./Drug Res.*, **40**(II), 771–776.

WATANABE, H., TAKAGI, K. & SATAKE, T. (1988). Relaxant effect of atrial natriuretic polypeptide on guinea-pig tracheal smooth muscle. *Prog. Biochem. Pharmacol.*, **23,** 136–141.

WINER, B.J. (1971). *Statistical Principals in Experimental Design.* New York: McGraw-Hill.

WINQUIST, R.J., FAISON, E.P., WALDMAN, S.A., SCHWARTZ, K., MURAD, F. & RAPOPORT, R.M. (1984). Atrial natriuretic factor elicits an endothelium-independent relaxation and activates guanylate cyclase in vascular smooth muscle. *Proc. Natl. Acad. Sci. U.S.A.*, **81,** 7661–7664.

ZEUZEM, S., OLBRICH, H.G., HAAK, T. & JUNGMANN (1990). In vivo evidence that human atrial natriuretic factor (99-126) (hANP) stimulates parasympathetic activity in man. *Eur. J. Clin. Pharmacol.*, **39,** 77–79.

ZUKOWSKA-GROJEC, Z, HAASS, M., KOPIN, I.J. & ZAMIR, N. (1986). Interactions of atrial natriuretic peptide with the sympathetic and endocrine system in the pithed rat. *J. Pharmacol. Exp. Ther.*, **239,** 480–487.

(Received November 23, 1992
Revised May 11, 1993
Accepted June 10, 1993)

Br. J. Pharmacol. (1993), **110**, 809–815

Characterization of the effects of lithium on phosphatidylinositol (PI) cycle activity in human muscarinic m1 receptor-transfected CHO cells

[1]John R. Atack, Angela M. Prior, Douglas Griffith & C. Ian Ragan

Merck Sharp & Dohme Research Laboratories, Neuroscience Research Centre, Terlings Park, Eastwick Road, Harlow, Essex CM20 2QR

1 The effects of lithium on [^{3}H]-inositol and [^{3}H]-cytidine incorporation into [^{3}H]-inositol monophosphates ([^{3}H]-$InsP_1$) and [^{3}H]-cytidine monophosphorylphosphatidate ([^{3}H]-CMP-PA), respectively, and inositol 1,4,5-trisphosphate ($InsP_3$) and inositol 1,3,4,5-tetrakisphosphate ($InsP_4$) mass were studied in carbachol-stimulated human m1 muscarinic receptor-transfected Chinese hamster ovary cells (m1 CHO cells).

2 Lithium alone (10 mM) had no appreciable effects on any of the four parameters measured; it was only in carbachol-stimulated cells that the effects of lithium became apparent.

3 In the presence of carbachol (1 mM), lithium (10 mM) caused a relatively rapid (within 5 min) accumulation of [^{3}H]-$InsP_1$ and [^{3}H]-CMP-PA which continued up to about 20–30 min, after which accumulation slowed down. On the other hand, the elevation in $InsP_3$ and $InsP_4$ levels produced by carbachol was not altered by lithium in the short-term and only at later times (>20–30 min) was the response attenuated, with $InsP_3$ and $InsP_4$ levels approaching basal.

4 The effects of lithium on carbachol-stimulated [^{3}H]-$InsP_1$ and [^{3}H]-CMP-PA accumulation and the attenuation of the carbachol-induced elevation of $InsP_3$ and $InsP_4$ were all dose-dependent, with EC_{50}s in the region of 1 mM.

5 The lithium-induced effects on [^{3}H]-CMP-PA and $InsP_3$ and $InsP_4$ in carbachol-stimulated cells could be reversed, in a dose-dependent manner, by preincubation with exogenous *myo*-inositol (EC_{50} = 2–3 mM) but not by the inactive analogue *scyllo*-inositol, indicating that these effects occur as a consequence of depletion of inositol.

6 The temporal effects of lithium are consistent with lithium inhibiting inositol monophosphatase, causing accumulation of $InsP_1$, resulting in lower free inositol levels. This leads to accumulation of CMP-PA and reduced PI synthesis which, once agonist-linked membrane inositol phospholipids are depleted, produces attenuated $InsP_3$ and $InsP_4$ responses.

7 These results in m1 CHO cells support the hypothesis that lithium affects the PI cycle cell signalling pathway by depletion of inositol due to inhibition of inositol monophosphatase.

Keywords: Lithium; phosphatidylinositol; inositol monophosphate; inositol monophosphatase; cytidine monophosphorylphosphatidate; inositol 1,4,5-trisphosphate; inositol 1,3,4,5-tetrakisphosphate; m1 CHO cells; carbachol

Introduction

It is over 40 years since the original description of the use of lithium in the treatment of manic depression (Cade, 1949), yet the mechanism by which lithium exerts its therapeutic effects remains uncertain. It has been proposed, however, that manic depression may be associated with hyperactivity of certain transmitter systems linked to the phosphatidylinositol (PI) signal transduction pathway and that lithium may act by inhibiting the PI cycle as a consequence of depletion of intracellular inositol, thereby reducing the hyperactivity in these transmitter systems (Berridge *et al.*, 1982; 1989; Nahorski *et al.*, 1991).

According to this hypothesis, lithium inhibits inositol monophosphatase (IMPase), which is a key enzyme in the PI cycle in that it dephosphorylates inositol monophosphates ($InsP_1$) producing inositol that can combine with cytidine monophosphorylphosphatidate (CMP-PA) to produce PI in a reaction catalysed by the enzyme PI synthase (Berridge & Irvine, 1989; Ragan, 1990). Intracellular inositol originates either from transport into the cell via a low- or high-affinity mechanism or from dephosphorylation of $InsP_1$, which are derived from the inositol 1,4,5-trisphosphate ($InsP_3$) and inositol 1,3,4,5-tetrakisphosphate ($InsP_4$) second messengers or as an intermediate in the *de novo* synthesis of inositol from glucose 6-phosphate. In cells where inositol is derived primarily from the dephosphorylation of $InsP_1$ by IMPase rather than by transport mechanisms, inhibition of IMPase effectively depletes intracellular inositol and results in reduced membrane inositol phospholipids available for signal transduction, ultimately resulting in reduced levels of $InsP_3$ and $InsP_4$ following stimulation.

Evidence in support of this hypothesis originates primarily from work in rat or mouse cortical slice preparations in which, under stimulated conditions, lithium results in an accumulation of $InsP_1$ (Batty & Nahorski, 1985; Kennedy *et al.*, 1989). There is a concomitant accumulation of CMP-PA, presumably as a result of decreased inositol concentrations (Godfrey, 1989; Kennedy *et al.*, 1989; Nahorski *et al.*, 1991) and an attenuation of the stimulus-dependent increase in $InsP_3$ and $InsP_4$ (Kennedy *et al.*, 1989; 1990; Varney *et al.*, 1992).

Clearly, the effects of lithium on [^{3}H]-$InsP_1$ and [^{3}H]-CMP-PA, which accumulate as a direct effect of the inhibition of IMPase, should occur prior to any effects on the second messengers $InsP_3$ and $InsP_4$, which should occur not in parallel with the effects on [^{3}H]-$InsP_1$ and [^{3}H]-CMP-PA, but only after a lag interval that corresponds to the finite time required to deplete existing agonist-linked membrane inositol phospholipids. To examine the temporal effects of lithium on

[1] Author for correspondence.

the PI cycle, we have measured, in Chinese hamster ovary cells transfected with the PI-linked (Fisher *et al.*, 1992) human muscarinic m1 cholinoceptor (m1 CHO cells), the incorporation of [^{3}H]-inositol into [^{3}H]-$InsP_1$ and [^{3}H]-cytidine into [^{3}H]-CMP-PA and, using radioreceptor binding assays, the mass of $InsP_3$ and $InsP_4$ second messengers. The results show that in carbachol-stimulated cells, lithium produced a relatively rapid (i.e. within 5 min) accumulation of [^{3}H]-$InsP_1$ and [^{3}H]-CMP-PA but that the attenuation of the carbachol-induced increase in $InsP_3$ and $InsP_4$ occurred only after 20–30 min. These effects were all dose-dependent and their reversal by *myo-* but not *scyllo*-inositol is consistent with them being due to a depletion of inositol secondary to inhibition of IMPase.

Methods

[^{3}H]-inositol incorporation into [^{3}H]-$InsP_1$

The method for the incorporation of [^{3}H]-inositol into [^{3}H]-$InsP_1$ was a modification of methods used in the rat cortical slice preparation (Batty & Nahorski, 1985) as described in more detail elsewhere (Atack *et al.*, 1993). Briefly, cells were grown to confluence for 2 days in Eagles minimal essential medium (inositol concentration = 11 μM) containing 10% foetal bovine serum and 0.5 μCi ml^{-1} [^{3}H]-inositol (80 Ci mmol^{-1}). Cells were harvested (2×10^6 cells ml^{-1}) into Krebs Henseleit buffer plus 0.5 μCi ml^{-1} [^{3}H]-inositol. Cells (280 μl) were then incubated at 37°C in the presence of LiCl for 30 min followed by, as required, carbachol (assay concentration = 1 mM), to give a final assay volume of 300 μl. Incubations were stopped by addition of 1 M trichloroacetic acid and samples were centrifuged, washed with diethyl ether and neutralised. Finally, [^{3}H]-$InsP_1$ were separated from [^{3}H]-inositol by Dowex-formate anion exchange chromatography (Berridge *et al.*, 1983).

[^{3}H]-cytidine incorporation into [^{3}H]-CMP-PA

The method employed was modified from that of Downes & Stone (1986). Cells were grown to confluence in 24-well plates (2×10^5 cells/well) and the medium replaced with 200 μl/well of fresh Dulbecco's minimal essential medium (inositol concentration = 40 μM) containing 3 μCi [^{3}H]-cytidine, lithium, *myo-* or *scyllo*-inositol as appropriate and were incubated at 37°C for 30 min followed by stimulation with carbachol (1 mM). Incubations were stopped with 1 ml chloroform:methanol (1:2 v/v) and a further 500 μl chloroform and 500 μl water added to each sample. Samples were aspirated from the wells and centrifuged at 1000 r.p.m. for 10 min and the upper phase removed. The lower phase was washed with 1 ml methanol:1 M HCl (1:1 v/v). Finally, 200 μl of lower phase was transferred to scintillation vials for counting.

Measurement of $InsP_3$ and $InsP_4$

Cells were grown, harvested, incubated and extracted as for the incorporation of [^{3}H]-inositol into [^{3}H]-$InsP_1$ except that no [^{3}H]-inositol was included. The concentrations of $InsP_3$ and $InsP_4$ were measured in separate triplicate 30 μl aliquots (total assay volume of 120 μl) of the same sample using previously published radioreceptor binding assays employing bovine adrenal and rat cerebellar membranes for $InsP_3$ and $InsP_4$ measurements, respectively (Challiss *et al.*, 1988; 1990; Challiss & Nahorski, 1990). Protein concentrations were determined on aliquots of harvested cells by the method of Lowry *et al.* (1951).

Materials

[^{3}H]-inositol and unlabelled $InsP_3$ and $InsP_4$ were obtained from Amersham International plc, [^{3}H]-$InsP_3$ and [^{32}P]-$InsP_4$ were from Du Pont (UK) Ltd, Dowex formate anion exchange resin from Bio-Rad, cell culture media from Gibco and organic solvents from Fisons plc. [^{3}H]-cytidine, carbachol, lithium chloride, *myo*-inositol, *scyllo*-inositol and all other reagents were purchased from Sigma.

Results

Time course of effects of lithium on [^{3}H]-$InsP_1$ and [^{3}H]-CMP-PA accumulation

[^{3}H]-$InsP_1$ In the presence of lithium alone (10 mM) or carbachol alone (1 mM) there was a slight elevation in $InsP_1$ levels, by about 20%, even at the earliest time points studied. This degree of increase in $InsP_1$ was maintained throughout the 60 min duration of the experiment with lithium alone whereas with carbachol alone $InsP_1$ levels increased to about 40% above basal at times greater than 20 min (Figure 1a).

In the presence of both lithium and carbachol, there was a pronounced increase in [^{3}H]-$InsP_1$ levels over and above levels in control (i.e. lithium-alone or carbachol-alone) by 5 min after which [^{3}H]-$InsP_1$ continued to accumulate linearly

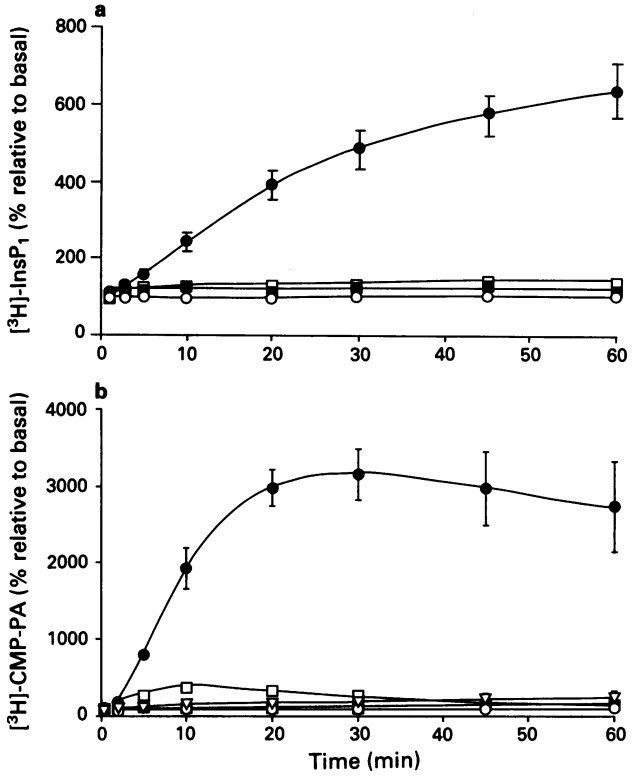

Figure 1 Levels of [^{3}H]-inositol monophosphates ([^{3}H]-$InsP_1$) (a) and [^{3}H]-cytidine monophosphorylphosphatidate ([^{3}H]-CMP-PA) (b) in m1 CHO cells as a function of time after addition of carbachol or buffer under a variety of experimental conditions: (○) basal (no lithium and no carbachol); □ plus carbachol (no lithium plus stimulation with 1 mM carbachol for varying times); (■) plus lithium (preincubation for 30 min with 10 mM lithium followed by addition of buffer); (●) plus lithium and carbachol (preincubation for 30 min with 10 mM lithium and stimulation with 1 mM carbachol); (▽) plus lithium, carbachol and inositol (preincubation for 30 min with 10 mM lithium and 10 mM *myo*-inositol and stimulation with 1 mM carbachol). Values are expressed as a percentage of basal and are presented as mean ± s.e.mean ($n = 7$ and $n = 4$ for [^{3}H]-$InsP_1$ and [^{3}H]-CMP-PA, respectively). Note that in carbachol-stimulated cells, accumulation of both [^{3}H]-$InsP_1$ and [^{3}H]-CMP-PA occurred within 5 min and that 10 mM *myo*-inositol reversed the lithium-induced accumulation of [^{3}H]-CMP-PA.

until after 20–30 min of stimulation. After 30 min the rate of accumulation slowed down considerably. Maximum levels of [^{3}H]-InsP$_1$ levels reached about 600% of basal levels (Figure 1a).

[^{3}H]-CMP-PA Generally, the effects of lithium on the accumulation of [^{3}H]-CMP-PA (Figure 1b) were similar to those seen with [^{3}H]-InsP$_1$. Thus, lithium alone (10 mM) elevated [^{3}H]-CMP-PA levels by about 20% and carbachol alone (1 mM) also stimulated accumulation but to a greater extent than seen for [^{3}H]-InsP$_1$, with [^{3}H]-CMP-PA achieving levels after 10 min of cholinoceptor stimulation about 4 fold of basal. With lithium plus carbachol there was a 70% increase in levels at 2 min which became pronounced after 5 min. As with [^{3}H]-InsP$_1$, there was a linear accumulation of [^{3}H]-CMP-PA up to about 20 min after which levels plateaued, with maximum [^{3}H]-CMP-PA levels reaching about 30 fold higher than basal.

When cells were preincubated with *myo*-inositol (10 mM) in addition to lithium and then stimulated with carbachol, the effects were dramatic with the large increase in [^{3}H]-CMP-PA seen with lithium and carbachol in the absence of *myo*-inositol being abolished. However, although [^{3}H]-CMP-PA levels were initially (up to about 2 min) around 40% lower than basal, at later time points there was a slight, progressive increase in levels to about 250% of basal by 60 min, suggesting that the reversal of the effects of lithium was about 95%.

Time course of effects of lithium on InsP$_3$ and InsP$_4$

InsP$_3$ Lithium alone (10 mM) had essentially no effect on InsP$_3$ concentrations whereas carbachol alone (1 mM) rapidly produced, within 10 s, a large increase in InsP$_3$ levels to about 300% of basal (Figure 2a). Thereafter, InsP$_3$ concentrations were maintained at between 200–300% of basal throughout the duration of the experiment. In the presence of lithium and carbachol, the short-term (< 10 min) effects (i.e. large increase in InsP$_3$ levels) were essentially the same as in the absence of lithium. However, by 30 min lithium had clearly attenuated the increase in InsP$_3$ caused by carbachol, with InsP$_3$ concentrations reaching basal (Figure 2a). The attenuation of the carbachol-induced elevation of InsP$_3$ by lithium could be reversed by the addition of exogenous *myo*-inositol (10 mM) with the response in lithium/carbachol/*myo*-inositol-treated cells being the same as in cells stimulated by carbachol alone (i.e. *myo*-inositol cancels out the effects of lithium). Indeed, if anything, InsP$_3$ levels were enhanced in the presence of exogenous *myo*-inositol (see also Lee *et al.*, 1992).

InsP$_4$ The effects of lithium on InsP$_4$ (Figure 2b) were qualitatively the same as seen with InsP$_3$. Hence, lithium alone (10 mM) had no effect on InsP$_4$ levels whereas carbachol alone (1 mM) produced a rapid increase in InsP$_4$ levels to about 500% of basal within the first minute. The

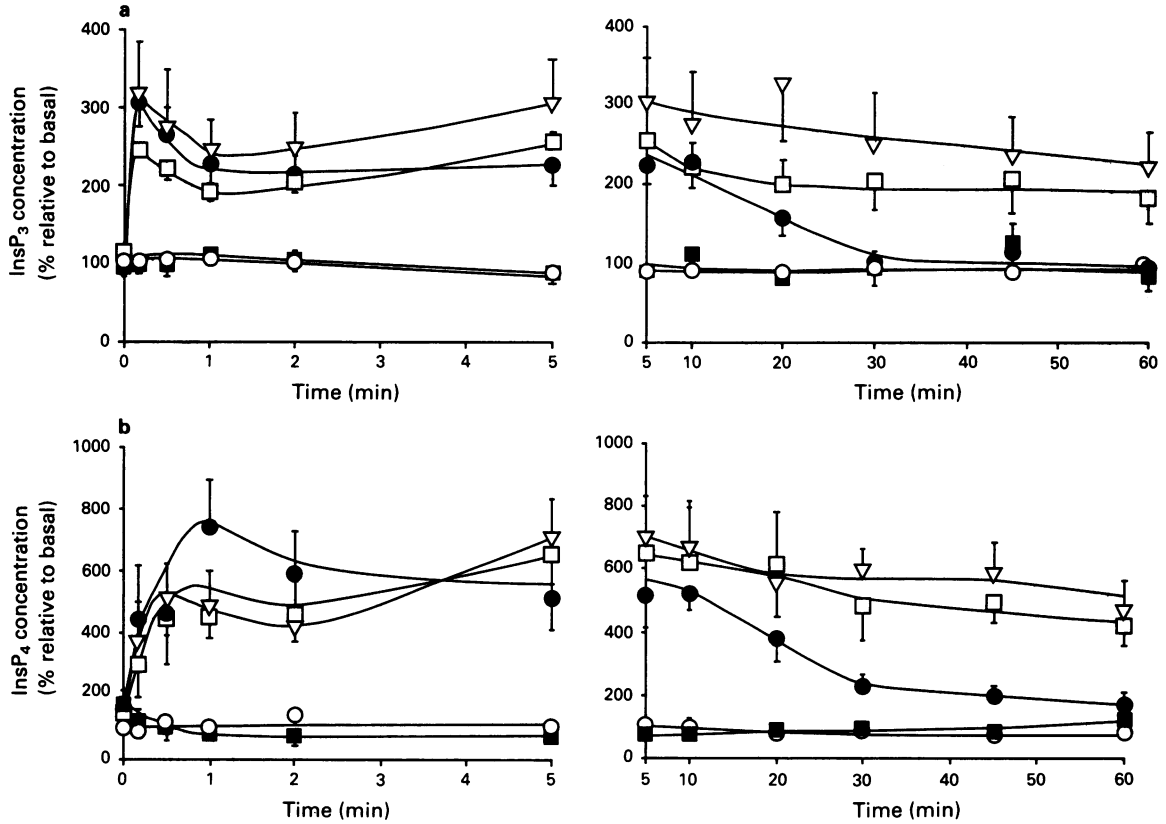

Figure 2 Levels of inositol 1,4,5-trisphosphate (InsP$_3$) (a) and inositol 1,3,4,5-tetrakisphosphate (InsP$_4$) (b) in m1 CHO cells as a function of time after addition of carbachol or buffer under a variety of experimental conditions (figures on left show 0–5 min, figures on right show 5–60 min): (○) basal (no lithium and no carbachol); (□) plus carbachol (no lithium plus stimulation with 1 mM carbachol for varying times); (■) plus lithium (preincubation for 30 min with 10 mM lithium followed by addition of buffer); (●) plus lithium and carbachol (preincubation for 30 min with 10 mM lithium and stimulation with 1 mM carbachol for varying times); (▽) plus Li, carbachol and inositol (preincubation for 30 min with 10 mM lithium and 10 mM *myo*-inositol plus stimulation with 1 mM carbachol). Values are expressed as a percentage of basal values (averaged across the various time points) and are presented as mean ± s.e.mean ($n = 7$ and $n = 4$ for InsP$_3$ and InsP$_4$, respectively). Basal InsP$_3$ and InsP$_4$ concentrations were in the region of 30 and 10 pmol mg^{-1} protein, respectively. Note that lithium only started to attenuate the carbachol-induced elevation of InsP$_3$ and InsP$_4$ after 20–30 min and that this attenuation was reversed by the addition of exogenous *myo*-inositol (10 mM).

carbachol-induced elevation of $InsP_4$ was sustained throughout the experiment, with values varying between about 500–600% of basal. The short-term (< 10 min) effects of lithium on the carbachol-stimulated increase in $InsP_4$ were essentially negligible, but by 20 min the response to carbachol became attenuated. However, this attenuation was not as marked as with $InsP_3$ (which reached basal levels by 30 min) with $InsP_4$ levels approaching basal only by 60 min. Again as with $InsP_3$, the lithium attenuation of the carbachol-induced increase in $InsP_4$ could be reversed by *myo*-inositol, with the lithium/carbachol/*myo*-inositol time course being the same as seen with carbachol alone.

Lithium dose-response curves

Figure 3 shows that the effects of lithium on [^{3}H]-$InsP_1$ and [^{3}H]-CMP-PA accumulation and on the attenuation of the carbachol-induced elevation of $InsP_3$ and $InsP_4$ levels were all dose-dependent. Moreover, the mean EC_{50}s (± s.e.mean) for these various effects were all comparable: 1.2 ± 0.4 mM ([^{3}H]-$InsP_1$ response); 0.8 ± 0.2 mM ([^{3}H]-CMP-PA); 0.9 ± 0.2 mM ($InsP_3$); and 0.9 ± 0.2 mM ($InsP_4$).

Reversal of effects of lithium by myo- *but not* scyllo-*inositol*

Figure 4 shows that the effects of lithium on [^{3}H]-CMP-PA accumulation and on the attenuation of the carbachol-induced elevation of $InsP_3$ and $InsP_4$ levels could all be reversed, in a dose-dependent manner, by *myo*- but not *scyllo*-inositol. The mean EC_{50}s (± s.e.mean) for reversal by *myo*-inositol were: 1.4 ± 0.2 mM for prevention of lithium-induced [^{3}H]-CMP-PA accumulation and 2.7 ± 0.3 mM and 3.3 ± 0.4 mM for the reversal of the lithium-induced attenuation of the $InsP_3$ and $InsP_4$ responses, respectively.

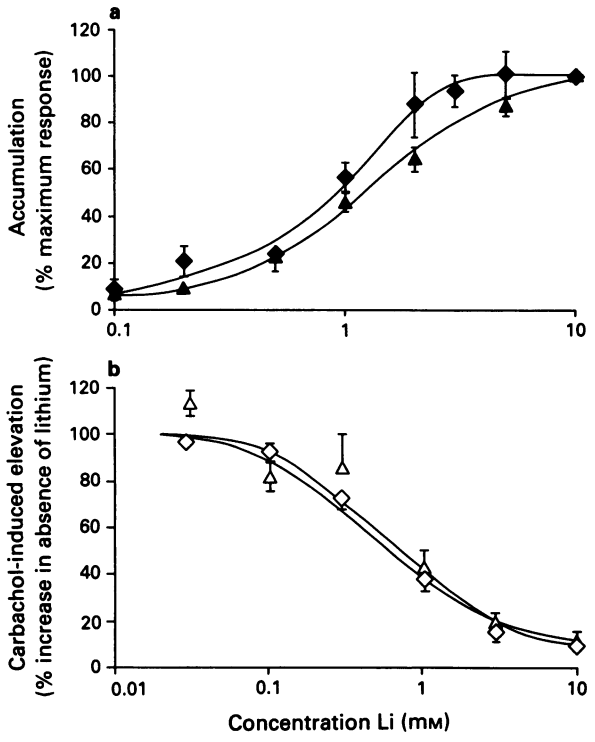

Figure 3 Effects of various concentrations of lithium (preincubation = 30 min) in carbachol-stimulated (1 mM; duration = 60 min) m1 CHO cells on accumulation of [^{3}H]-inositol monophosphates ([^{3}H]-$InsP_1$) (◆) and [^{3}H]-cytidine monophosphorylphosphatidate ([^{3}H]-CMP-PA) (▲) (a) and attenuation of carbachol-induced increase in inositol 1,4,5-trisphosphate ($InsP_3$) (◇) and inositol 1,3,4,5-tetrakisphosphate ($InsP_4$) (△) (b). Mean (± s.e.mean) EC_{50} values were 1.2 ± 0.4 mM (n = 7) for [^{3}H]-$InsP_1$; 0.8 ± 0.2 mM (n = 6) for [^{3}H]-CMP-PA; 0.9 ± 0.2 mM (n = 6) for $InsP_3$; and 0.9 ± 0.2 mM (n = 5) for $InsP_4$.

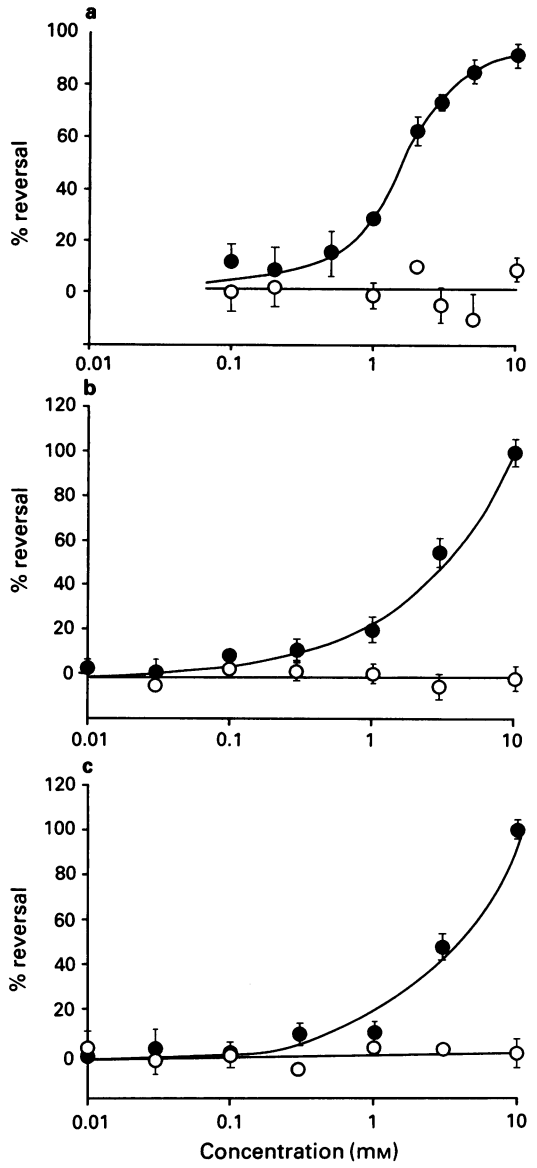

Figure 4 Reversal of the effects of lithium (10 mM, preincubation = 30 min) on carbachol-stimulated (1 mM; duration = 60 min) [^{3}H]-cytidine monophosphorylphosphatidate ([^{3}H]-CMP-PA) accumulation (a) and inositol 1,4,5-trisphosphate ($InsP_3$) (b) and inositol 1,3,4,5-tetrakisphosphate ($InsP_4$) (c) levels by *myo*-inositol (●) but not *scyllo*-inositol (○) (i.e. experimental conditions plus lithium, carbachol, and [various] *myo*- or *scyllo*-inositol). Mean (± s.e.mean) EC_{50} values for *myo*-inositol reversal for [^{3}H]-CMPA-PA, $InsP_3$ and $InsP_4$ were 1.4 ± 0.2 mM (n = 6), 2.7 ± 0.3 mM (n = 4) and 3.3 ± 0.4 mM (n = 3), respectively.

Discussion

The linearity of [^{3}H]-$InsP_1$ accumulation over the first 20–30 min in carbachol-stimulated m1 CHO cells is comparable to that seen in the rat cortical slice preparation (Gonzales & Crews, 1984; Kennedy *et al.*, 1989) and the EC_{50} for this lithium-induced effect in m1 CHO cells (1.2 mM, Figure 3; in agreement with a previous report of 1 mM; Atack *et al.*, 1993) was equivalent to that in cortical slices (1–2 mM for total inositol phosphates i.e. inositol mono- plus polyphosphates [Berridge *et al.*, 1982; Brown *et al.*,

1984] and 0.5 and 0.3 mM for $InsP_1$ [Batty & Nahorski, 1985; Kennedy *et al.*, 1989]). However, the EC_{50} for lithium in mouse cortical slices was much lower (ca. 0.1 mM; Whitworth & Kendall, 1988). The reduced rate of [^{3}H]-$InsP_1$ accumulation after about 20–30 min was also very similar to that seen in rat cortical slices (Gonzales & Crews, 1984) and in thyrotropin-releasing hormone-stimulated GH_3 pituitary tumour cells (Drummond *et al.*, 1984; Hughes & Drummond, 1987) and is consistent with reduced PI cycle activity, presumably as a consequence of inositol depletion. Unfortunately, using the present method involving [^{3}H]-inositol prelabelling, it is not possible to address the issue of whether exogenous *myo*-inositol can reverse this effect (i.e. can exogenous inositol maintain stimulated PI cycle turnover resulting in a continued, linear $InsP_1$ accumulation?) since exogenous inositol would upset the established isotopic equilibrium. However, this issue could be addressed by mass measurements of $InsP_1$ isomers (Atack *et al.*, 1992).

The dramatic accumulation of [^{3}H]-CMP-PA seen in m1 CHO cells resembled that seen following cholinoceptor stimulation in parotid gland slices (Downes & Stone, 1986) and rat cerebral cortex slices (Godfrey, 1989; Kennedy *et al.*, 1990; Nahorski *et al.*, 1991). However, whereas in rat cortical slices (Godfrey, 1989; Kennedy *et al.*, 1990) accumulation was immediate, there was a 2–5 min lag period in m1 CHO cells whilst in parotid gland there was a slightly longer lag (Downes & Stone, 1986). These differences are presumably due to the different tissue preparations employed. The dose-dependency of the effect of lithium on [^{3}H]-CMP-PA accumulation in m1 CHO cells (0.8 mM; Figure 3) was similar to that seen in the rat cortical slice preparation (0.6 mM: Godfrey, 1989; Kennedy *et al.*, 1990). A striking feature of the response in both m1 CHO cells and the rat cortical slice preparation is the similarity between the [^{3}H]-CMP-PA accumulation and the [^{3}H]-$InsP_1$ accumulation i.e. 2–5 min lag in m1 CHO cells and immediate response in rat cortical slices (Figure 1 and Kennedy *et al.*, 1989; 1990). These data confirm that [^{3}H]-CMP-PA accumulation is a sensitive indicator of inositol depletion caused by accumulation of [^{3}H]-$InsP_1$ due to inhibition of IMPase (Downes & Stone, 1986; Kennedy *et al.*, 1990; Nahorski *et al.*, 1991).

With respect to $InsP_3$ and $InsP_4$, the greater increase in $InsP_4$ compared to $InsP_3$ following cholinoceptor stimulation in the absence of lithium is similar to that reported in rat, mouse and guinea-pig cortical slices (Whitworth & Kendall, 1988; Kennedy *et al.*, 1990; Nahorski *et al.*, 1991; Lee *et al.*, 1992). As regards the time course of carbachol-stimulated increases in $InsP_3$ and $InsP_4$, there was an initial spike of $InsP_3$ within the first min, whereas $InsP_4$ levels rose less dramatically with no evidence of a peak within the first min. These results are in agreement with previous observations using m1 CHO cells (Lambert *et al.*, 1991b) or the human neuroblastoma cell line SH-SY5Y, which express endogenous m3 muscarinic receptors (Lambert & Nahorski, 1990; Lambert *et al.*, 1991a). In the presence of lithium, there was a definite lag time of about 20–30 min before lithium started to attenuate the carbachol-induced elevation in $InsP_3$ and $InsP_4$; at early time points, carbachol-stimulated $InsP_3$ and $InsP_4$ concentrations were essentially the same in the presence and absence of lithium. A similar lag period of about 10–20 min has been reported for reductions in $InsP_3$ and $InsP_4$ in the rat (Kennedy *et al.*, 1989; 1990; Nahorski *et al.*, 1991; Varney *et al.*, 1992) and mouse (Whitworth & Kendall, 1988) cortical slice preparations. Furthermore, in electrophysiological studies, the ability of muscarinic stimulation to block the inhibitory actions of adenosine in a hippocampal preparation was inhibited by lithium only after a 10–15 min lag (Worley *et al.*, 1988) and the densitization of carbachol-induced hippocampal cell firing was attenuated by lithium (an effect that could be reversed with 1 mM *myo*-inositol) only after an appreciable delay (Pontzer & Crews, 1990). This lag period presumably represents the time required for depletion of agonist-linked membrane inositol phospholipids after which the response to stimulation becomes reduced. The EC_{50} of lithium's effect on $InsP_3$ and $InsP_4$ levels in m1 CHO cells were the same, 0.9 mM (Figure 3), which is higher than seen in the rat cortical slice preparation for $InsP_3$ and $InsP_4$ (0.3 and 0.1 mM, respectively: Kennedy *et al.*, 1989).

The various time course data are consistent with lithium exerting its effect on the PI cycle via inhibition of IMPase, resulting in accumulation of [^{3}H]-$InsP_1$ and reduced free inositol available for PI synthesis, thereby causing a concomitant increase in [^{3}H]-CMP-PA levels. Although [^{3}H]-CMP-PA accumulation and therefore reduced PI synthesis occurred within the initial 5 min after carbachol stimulation, PI signal transduction presumably continues as normal as judged by the linearity of $InsP_1$ accumulation (suggesting that the rate of $InsP_1$ production is constant) and the lack of effect of lithium on carbachol-stimulated increases in $InsP_3$ and $InsP_4$. However, after about 20–30 min, membrane inositol phospholipids become depleted due to continued stimulation of the cells such that carbachol-induced increases in $InsP_3$ and $InsP_4$ become attenuated. At this point flux through the PI cycle becomes reduced resulting in reduced $InsP_1$ production, and hence the decreased rate of [^{3}H]-$InsP_1$ and [^{3}H]-CMP-PA accumulation (Figure 1).

The key aspect of this sequence of events is the reduction in free inositol available for PI synthesis as a consequence of inhibition of IMPase. If this is correct then replenishment by exogenous *myo*-inositol should reverse all these features (i.e. accumulation of [^{3}H]-$InsP_1$ and [^{3}H]-CMP-PA and attenuation of the carbachol-induced increases in $InsP_3$ and $InsP_4$). Although it was not possible to study the effects of *myo*-inositol on reversal of $InsP_1$ accumulation (see above), *myo*-inositol was able to abolish the effect of lithium on [^{3}H]-CMP-PA and $InsP_3$ and $InsP_4$. Hence, lithium-induced accumulation of [^{3}H]-CMP-PA following cholinoceptor stimulation in m1 CHO cells was almost completely reversed by addition of 10 mM *myo*- but not *scyllo*-inositol with an EC_{50} of 1.4 mM and the attenuation of $InsP_3$ and $InsP_4$ responses by lithium were reversed by *myo*-inositol with respective EC_{50}s of 2.7 and 3.3 mM (Figure 4). These results are similar to those seen in parotid gland where [^{3}H]-CMP-PA accumulation could be restored to levels seen in the absence of lithium by 10–30 mM *myo*-inositol (Downes & Stones, 1986). In cholinoceptor-stimulated rat brain slices, Godfrey (1989) observed complete reversal of lithium-induced [^{3}H]-CMP-PA accumulation by 10 mM *myo*-inositol, with an EC_{50} of 0.8 mM and in an autoradiographic study of [^{3}H]-cytidine incorporation into membrane [^{3}H]-CMP-PA, Hwang *et al.* (1990) reported a reversal of the effects of lithium by *myo*-inositol at a concentration of 20 mM. However, also in rat brain slices, Nahorski and colleagues (Kennedy *et al.*, 1990; Nahorski *et al.*, 1991) reported only partial reversal of lithium-induced [^{3}H]-CMP-PA accumulation and attenuation of $InsP_3$ and $InsP_4$ responses by 10 and 30 mM *myo*-inositol (but no effect of *scyllo*-inositol), presumably due in these particular preparations to relatively poor transport of exogenous *myo*-inositol into inositol-depleted cells. The differences in responses of different tissues may, as suggested by Nahorski *et al.* (1991), reflect differences in inositol reserves, inositol transport systems, resting inositol monophosphates and differences in the kinetic properties of PI synthase between tissues (e.g. different EC_{50} values for *myo*-inositol for the reversal of [^{3}H]-CMP-PA accumulation in rat, mouse and guinea-pig cortical slice preparations: Lee *et al.*, 1992).

It should be emphasised that in the present study, the effects of lithium were readily observed in cells grown in low inositol concentration medium. Indeed, the validity of the hypothesis that lithium may exert its effects *in vivo* via its actions on PI cycle activity due to inositol depletion has recently been challenged by observations that although lithium does indeed attenuate agonist-induced increases in $InsP_3$ and $InsP_4$ in rat and mouse cortical slices, there is no comparable effect in guinea-pig or monkey brain cortical slices (Dixon *et al.*, 1992; Lee *et al.*, 1992). These species

differences were ascribed to differences in endogenous inositol levels in the different cortical slice preparations.

Clearly, in tissues in which inositol depletion can be easily achieved (e.g. rat or mouse cortical slices or m1 CHO cells), the effects of lithium on PI cycle activity are readily observed. However, the key issue, highlighted by the studies of Hokin and colleagues (Dixon *et al.*, 1992; Lee *et al.*, 1992), is whether sufficient inositol depletion to impair PI cycle functioning occurs *in vivo*. Thus, it is possible that in the brain *in vivo*, although free inositol levels fall after lithium administration, the decrement of about 35% (Allison & Stewart, 1971; Sherman *et al.*, 1986) may not be sufficient to be rate-limiting in the synthesis of PI and consequently the levels of brain $InsP_3$ and $InsP_4$ may not be altered *in vivo* by lithium-treatment. However, it has recently been reported that lithium can attenuate pilocarpine-induced elevations in rat cortical $InsP_3$ levels (Jope *et al.*, 1992). Moreover, this effect was observed at 60 min but not 20 min, a time course consistent with the effects seen in m1 CHO cells (Figure 2). It therefore seems that the reduced levels of inositol in the rat cortex *in vivo* are indeed sufficient to impair PI-linked intracellular signalling (or at least $InsP_3$), presumably as a consequence of reduced PI synthesis caused by inositol depletion.

In summary, we have characterized the effects of lithium on [^{3}H]-$InsP_1$ and [^{3}H]-CMP-PA accumulation and $InsP_3$ and $InsP_4$ concentrations in cholinoceptor-stimulated m1 CHO cells. The effects of lithium were all dose-dependent with EC_{50}s in the region of 1 mM, which is approximately equivalent to therapeutic plasma levels of lithium (Drummond, 1987) and also comparable to the K_i for lithium vs inositol monophosphatase (Hallcher & Sherman, 1980; Gee *et al.*, 1988; McAllister *et al.*, 1992). The effects of lithium on [^{3}H]-CMP-PA and $InsP_3$ and $InsP_4$ were all consistent with being due to inositol depletion since exogenous *myo-* but not *scyllo*-inositol were able to reverse these effects. These data support the hypothesis that lithium can modulate PI cycle activity due to inositol depletion as a consequence of inhibition of IMPase.

References

ALLISON, J.H. & STEWART, M.A. (1971). Reduced brain inositol in lithium-treated rats. *Nature (New Biol.)*, **233**, 267–268.

ATACK, J.R., COOK, S.M., WATT, A.P. & RAGAN, C.I. (1992). Measurement of lithium-induced changes in mouse inositol(1) phosphate levels *in vivo*. *J. Neurochem.*, **59**, 1946–1954.

ATACK, J.R., COOK, S.M., WATT, A.P., FLETCHER, S.R. & RAGAN, C.I. (1993). *In vitro* and *in vivo* inhibition of inositol monophosphatase by the bisphosphonate L-690,330. *J. Neurochem.*, **60**, 652–658.

BATTY, I. & NAHORSKI, S.R. (1985). Differential effects of lithium on muscarinic receptor stimulation of inositol phosphates in rat cerebral cortex slices. *J. Neurochem.*, **45**, 1514–1521.

BERRIDGE, M.J., DAWSON, R.M.C., DOWNES, C.P., HESLOP, J.P. & IRVINE, R.F. (1983). Changes in the levels of inositol phosphates after agonist-dependent hydrolysis of membrane phosphoinositides. *Biochem. J.*, **212**, 473–482.

BERRIDGE, M.J., DOWNES, C.P. & HANLEY, M.R. (1982). Lithium amplifies agonist-dependent phosphatidylinositol responses in brain and salivary glands. *Biochem. J.*, **206**, 587–595.

BERRIDGE, M.J., DOWNES, C.P. & HANLEY, M.R. (1989). Neural and developmental actions of lithium: a unifying hypothesis. *Cell*, **59**, 411–419.

BERRIDGE, M.J. & IRVINE, R.F. (1989). Inositol phosphates and cell signalling. *Nature*, **341**, 197–205.

BROWN, E., KENDALL, D.A. & NAHORSKI, S.R. (1984). Inositol phospholipid hydrolysis in rat cerebral cortical slices: I. Receptor characterisation. *J. Neurochem.*, **42**, 1379–1387.

CADE, J.F.J. (1949). Lithium salts in the treatment of psychotic excitement. *Med. J. Aust.*, **2**, 349–352.

CHALLISS, R.A.J., BATTY, I.H. & NAHORSKI, S.R. (1988). Mass measurements of inositol (1,4,5)trisphosphate in rat cerebral cortex slices using a radioreceptor assay: effects of neurotransmitters and depolarization. *Biochem. Biophys. Res. Commun.*, **157**, 684–691.

CHALLISS, R.A.J., CHILVERS, E.R., WILLCOCKS, A.L. & NAHORSKI, S.R. (1990). Heterogeneity of [^{3}H]inositol 1,4,5-trisphosphate binding sites in adrenal-cortical membranes – characterization and validation of a radioreceptor assay. *Biochem. J.*, **265**, 421–427.

CHALLISS, R.A.J. & NAHORSKI, S.R. (1990). Neurotransmitter and depolarization-stimulated accumulation of inositol 1,3,4,5-tetrakisphosphate mass in rat cerebral cortex slices. *J. Neurochem.*, **54**, 2138–2141.

DIXON, J.F., LEE, C.H., LOS, G.V. & HOKIN, L.E. (1992). Lithium enhances accumulation of [^{3}H]inositol radioactivity and mass of second messenger inositol 1,4,5-trisphosphate in monkey cerebral cortex slices. *J. Neurochem.*, **59**, 2332–2335.

DOWNES, C.P. & STONE, M.A. (1986). Lithium-induced reduction in intracellular inositol supply in cholinergically stimulated parotid gland. *Biochem. J.*, **234**, 199–204.

DRUMMOND, A.H. (1987). Lithium and inositol lipid-linked signalling mechanisms. *Trends Pharmacol. Sci.*, **8**, 129–133.

DRUMMOND, A.H., BUSHFIELD, M. & MACPHEE, C.H. (1984). Thyrotropin-releasing hormone-stimulated [^{3}H]inositol metabolism in GH3 pituitary tumor cells – studies with lithium. *Mol. Pharmacol.*, **25**, 201–208.

FISHER, S.K., HEACOCK, A.M. & AGRANOFF, B.W. (1992). Inositol lipids and signal transduction in the nervous system: an update. *J. Neurochem.*, **58**, 18–38.

GEE, N.S., RAGAN, C.I., WATLING, K.J., ASPLEY, S., JACKSON, R.G., REID, G.G., GANI, D. & SHUTE, J.K. (1988). The purification and properties of *myo*-inositol monophosphatase from bovine brain. *Biochem. J.*, **249**, 883–889.

GODFREY, P.P. (1989). Potentiation by lithium of CMP-phosphatidate formation in carbachol-stimulated rat cerebral-cortical slices and its reversal by *myo*-inositol. *Biochem. J.*, **258**, 621–624.

GONZALES, R.A. & CREWS, F.T. (1984). Characterization of the cholinergic stimulation of phosphoinositide hydrolysis in rat brain slices. *J. Neurosci.*, **4**, 3120–3127.

HALLCHER, L.M. & SHERMAN, W.R. (1980). The effects of lithium ion and other agents on the activity of *myo*-inositol-1-phosphatase from bovine brain. *J. Biol. Chem.*, **255**, 10896–10901.

HUGHES, P.J. & DRUMMOND, A.H. (1987). Formation of inositol phosphate isomers in GH3 pituitary tumour cells stimulated with thyrotropin-releasing hormone – acute effects of lithium ions. *Biochem. J.*, **248**, 463–470.

HWANG, P.M., BREDT, D.S. & SNYDER, S.H. (1990). Autoradiographic imaging of phosphoinositide turnover in the brain. *Science*, **249**, 802–804.

JOPE, R.S., SONG, L. & KOLASA, K. (1992). Inositol trisphosphate, cyclic AMP, and cyclic GMP in rat brain regions after lithium and seizures. *Biol. Psychiatry*, **31**, 505–514.

KENNEDY, E.D., CHALLISS, R.A.J. & NAHORSKI, S.R. (1989). Lithium reduces the accumulation of inositol polyphosphate second messengers following cholinergic stimulation of cerebral cortex slices. *J. Neurochem.*, **53**, 1652–1655.

KENNEDY, E.D., CHALLISS, R.A.J., RAGAN, C.I. & NAHORSKI, S.R. (1990). Reduced inositol polyphosphate accumulation and inositol supply induced by lithium in stimulated cerebral cortex slices. *Biochem. J.*, **267**, 781–786.

LAMBERT, D.G., CHALLISS, R.A.J. & NAHORSKI, S.R. (1991a). Accumulation and metabolism of Ins(1,4,5)P_3 and Ins(1,3,4,5)P_4 in muscarinic-receptor-stimulated SH-SY5Y neuroblastoma cells. *Biochem. J.*, **273**, 791–794.

LAMBERT, D.G., FREEDMAN, S.B., HARLEY, E.A., CHALLISS, R.A.J. & NAHORSKI, S.R. (1991b). Inositol polyphosphate accumulation and intracellular calcium responses in chinese hamster ovary cells expressing cloned human m1 muscarinic receptors. *Mol. Neuropharmacol.*, **1**, 135–140.

LAMBERT, D.G. & NAHORSKI, S.R. (1990). Muscarinic-receptor-mediated changes in intracellular Ca^{2+} and inositol 1,4,5-trisphosphate mass in a human neuroblastoma cell line, SH-SY5Y. *Biochem. J.*, **265**, 555–562.

LEE, C.H., DIXON, J.F., REICHMAN, M., MOUMMI, C., LOS, G. & HOKIN, L.E. (1992). Li^+ increases accumulation of inositol 1,4,5-trisphosphate and inositol 1,3,4,5-tetrakisphosphate in cholinergically stimulated brain cortex slices in guinea pig, mouse and rat – the increases require inositol supplementation in mouse and rat but not in guinea pig. *Biochem J.*, **282,** 377–385.

LOWRY, O.H., ROSEBROUGH, N.J., FARR, A.L. & RANDALL, R.J. (1951). Protein measurement with the Folin phenol reagent. *J. Biol. Chem.*, **193,** 265–275.

MCALLISTER, G., WHITING, P., HAMMOND, E.A., KNOWLES, M.R., ATACK, J.R., BAILEY, F.J., MAIGETTER, R. & RAGAN, C.I. (1992). cDNA cloning of human and rat brain *myo*-inositol monophosphatase: expression and characterization of the human recombinant enzyme. *Biochem J.*, **284,** 749–754.

NAHORSKI, S.R., RAGAN, C.I. & CHALLISS, R.A.J. (1991). Lithium and the phosphoinositide cycle: an example of uncompetitive inhibition and its pharmacological consequences. *Trends Pharmacol. Sci.*, **12,** 297–303.

PONTZER, N.J. & CREWS, F.T. (1990). Desensitization of muscarinic stimulated hippocampal cell firing is related to phosphoinositide hydrolysis and inhibited by lithium. *J. Pharmacol. Exp. Ther.*, **253,** 921–929.

RAGAN, C.I. (1990). The effect of lithium on inositol phosphate metabolism. In *Lithium and Cell Physiology*. ed. Bach R.O. & Gallicchio V.S. pp. 102–120. New York: Springer-Verlag.

SHERMAN, W.R., GISH, B.G., HONCHAR, M.P. & MUNSELL, L.Y. (1986). Effects of lithium on phosphoinositide metabolism in vivo. *Fed. Proc.*, **45,** 2639–2646.

VARNEY, M.A., GODFREY, P.P., DRUMMOND, A.H. & WATSON, S.P. (1992). Chronic lithium treatment inhibits basal and agonist-stimulated responses in rat cerebral cortex and GH_3 pituitary cells. *Mol. Pharmacol.*, **42,** 671–678.

WHITWORTH, P. & KENDALL, D.A. (1988). Lithium selectively inhibits muscarinic receptor-stimulated inositol tetrakisphosphate accumulation in mouse cerebral cortex slices. *J. Neurochem.*, **51,** 258–265.

WORLEY, P.F., HELLER, W.A., SNYDER, S.H. & BARABAN, J.M. (1988). Lithium blocks a phosphoinositide-mediated cholinergic response in hippocampal slices. *Science*, **239,** 1428–1429.

(Received March 1, 1993
Revised May 16, 1993
Accepted May 19, 1993)

Br. J. Pharmacol. (1993), **110**, 816–820

The role of nitric oxide in cholinergic neurotransmission in rat trachea

Kiyohisa Sekizawa, Takeyasu Fukushima, *Yasushi Ikarashi, *Yuji Maruyama & [1]Hidetada Sasaki

Department of Geriatric Medicine, Tohoku University School of Medicine, Sendai 980 and *Department of Neuropsychopharmacology (Tsumura), Gunma University School of Medicine, Maebashi 371, Japan

1 We have investigated the role of nitric oxide (NO) in cholinergic contraction in rat trachea.

2 Methylene blue (10 nM to 30 μM) potentiated cholinergic contraction induced by electrical field stimulation (EFS) at 5 Hz in a concentration-dependent fashion. At a concentration of 30 μM, methylene blue decreased responses to log EFS frequency, producing 50% of maximum contraction from a control value of 0.74 ± 0.09 Hz to 0.30 ± 0.05 Hz without a significant effect on concentration-response curves to acetylcholine (ACh).

3 N^G-monomethyl-L-arginine (L-NMMA; 100 μM) also potentiated cholinergic contraction induced by EFS at 5 Hz (131.5 ± 4.6% of control) without having any effect against ACh (3 μM)-induced contractions. Likewise, L-NMMA (100 μM) significantly increased EFS (5 Hz)-evoked release of ACh from tracheal segments into the bath solution (51.4 ± 4.0 pmol ml^{-1} in the presence of L-NMMA and 35.0 ± 1.8 pmol ml^{-1} in the absence of L-NMMA, respectively).

4 Administration of NO (present in acidified soluton of $NaNO_2$) (1 nM to 10 μM) and sodium nitroprusside (100 nM to 10 μM) concentration-dependently reduced EFS (5 Hz)-induced cholinergic contractions without having a significant effect on ACh (3 μM)-induced contractions. These results were unaffected by prior exposure of the tissues to L-NMMA (100 μM).

5 Dibutyryl cyclic GMP (3 mM) also reduced cholinergic contractions induced by EFS at 5 Hz (70.1 ± 3.6% of control) without any significant effect on ACh (3 μM)-induced contractions.

6 Pretreatment of tissues with capsaicin (30 μM) or α-chymotrypsin (1 u ml^{-1}) failed to inhibit methylene blue (30 μM)-induced potentiation of responses to EFS at 5 Hz.

7 These results suggest that an endogenous NO-like factor may mediate prejunctional inhibition of cholinergic contraction through a cyclic GMP-dependent mechanism in rat trachea.

Keywords: Nitric oxide; vasoactive intestinal peptide; non-adrenergic inhibitory nerve; acetylcholine release

Introduction

There is evidence that nitric oxide (NO) is a mediator of non-adrenergic non-cholinergic (NANC) stimulation-induced relaxations of the anococcygeus muscle of the rat (Li & Rand, 1989; Gillespie *et al.*, 1989) and mouse (Gibson *et al.*, 1990) and of rat gastric fundus strips (Li & Rand, 1990). In the airway, NO plays a role in NANC relaxation of tracheal smooth muscle in guinea-pigs (Tucker *et al.*, 1990; Li & Rand, 1991).

Vasoactive intestinal polypeptide (VIP), another candidate for NANC inhibitory neurotransmitters, has been shown to inhibit cholinergic neurotransmission in ferret (Sekizawa *et al.*, 1988), cat (Aikawa *et al.*, 1990; Hakoda & Ito, 1990; Xie *et al.*, 1991) and dog (Hakoda & Ito, 1990; Xie *et al.*, 1991) trachea as well as relaxing airway smooth muscle (Altiere & Diamond, 1984; Palmer *et al.*, 1986). However, the modulatory effect of NO on cholinergic neurotransmission is not known.

We have therefore investigated the effects of N^G-monomethyl-L-arginine (L-NMMA), an inhibitor of NO synthesis and methylene blue, an inhibitior of NO-activated guanylate cyclase (Ignarro, 1989), on cholinergic contractions evoked by electrical field stimulation (EFS), to determine whether endogenous NO has a modulatory action on cholinergic neurones. We have also investigated the effects of the agonist NO and sodium nitroprusside (SNP) which is known to release NO (Moncada, 1992) on EFS-induced cholinergic contraction.

[1] Author for correspondence.

Methods

Male Sprague-Dawley rats (Funabashi Farm, Shizuoka, Japan), weighing 250 to 300 g, were anaesthetized with sodium pentobarbitone (50 mg, i.p.). The trachea was removed rapidly and transverse rings (3 mm long) were cut from it. These rings were mounted in organ baths containing 5 ml Krebs-Henseleit solution maintained at 37°C. Isometric tension was continuously measured with a force transducer (TB 612-T, Nihon Koden, Japan) connected to a pen recorder (HORIZ-8K, San-ei Co., Japan). Tracheal rings were placed between two rectangular platinum electrodes (6 × 40 mm) for EFS. These tissues were stretched initially to a tension of 1 g for 30 s and thereafter maintained for 60 min under a resting tension of 0.5 g, which was found to be optimal for measuring changes in tension. EFS (supramaximal voltage of 50 V and 0.5 ms duration) was applied for 30 s. All experiments were carried out in the presence of indomethaciin (1 μM), propranolol (1 μM) and phentolamine (10 μM). The contractile responses induced under these conditions were completely abolished by tetrodotoxin (1 μM) or by atropine (1 μM), confirming the neural and cholinergic nature of the response.

Experimental protocol

To determine the baseline responses, tissues were stimulated electrically five times at 5 Hz at 5 min intervals. We then added increasing concentrations of methylene blue (from 10 nM to 30 μM) and repeated the stimulation 10 min after the administration of each concentration of methylene blue, when the effect of methylene blue on the response to EFS reached its maximum. Methylene blue was administered after the preceding contraction had returned to the baseline. In

preliminary studies, we found that methylene blue caused a concentration-dependent increase in contractions induced by EFS at 5 Hz. However, because methylene blue itself changed the baseline tension at concentrations higher than 100 μM, we studied the effect of 30 μM methylene blue on stimulus frequency-response curves to EFS. To determine the effects of methylene blue on stimulus frequency-response curves we stimulated tissues by varying the stimulus frequencies from 1 Hz to 50 Hz. After the first frequency-response curve was completed, we performed the second one 10 min after the administration of methylene blue at a concentration of 30 μM. To determine whether the effects of methylene blue are mediated by postjunctional cholinergic mechanisms, we studied the effects of methylene blue (30 μM) on the cumulative concentration-response curves to acetylcholine (ACh) (from 1 nM to 1 mM). Likewise, we tested the effects of L-NMMA on the contractile response to EFS at 5 Hz and ACh (3 μM), which produced a contractile response equivalent to that produced by EFS at 5 Hz. L-NMMA (100 μM) was added 20 min before the response to EFS or ACh was elicited.

Effects of the agonists NO (from 1 nM to 1 mM), SNP (from 100 nM to 0.1 mM) and dibutyryl guanosine 3':5'-cyclic monophosphate (db cyclic GMP, 3 mM) on the contractile responses to EFS at 5 Hz and ACh (3 μM) were also studied. Because ACh (3 μM)-induced contractions required 2 min to reach maximum, NO was added immediately before ACh, but 2 min before the more rapidly developing response to EFS. Other agonists were added 10 min before stimulation with either EFS or ACh. To evaluate further whether endogenous NO released during EFS modified the agonist-induced effects on the contractile response to EFS, we tested NO (10 μM), sodium nitroprusside (SNP) (10 μM) and db cyclic GMP (3 mM) on contractions induced by EFS at 5 Hz in the presence of L-NMMA (100 μM).

To examine the effect of endogenously released VIP and sensory neuropeptides such as substance P and neurokinin A on EFS-induced contractions, we tested the effects of α-chymotrypsin (1 u ml^{-1}) and capsaicin (30 μM) on methylene blue (30 μM)-induced potentiating actions on contractions induced by EFS at 5 Hz. Tissues were pretreated with α-chymotrypsin for 15 min before the study. In the case of capsaicin, tissues were pretreated for 20 min and were washed out before the study.

Measurement of ACh release

To examine whether endogenous NO inhibits ACh release from rat trachea, we performed parallel studies on paired rings of the same length (3 mm) from the same animal. One randomly chosen tracheal ring was pretreated with L-NMMA (100 μM) and the other was pretreated with the vehicle of L-NMMA. The tracheal rings were mounted in the 2 ml organ bath and maintained for 60 min in the same condition as in the case of tension measurement. Then, the contents of the bath were emptied, the bath was refilled with buffer (same contents), and either L-NMMA (100 μM) or the vehicle of L-NMMA was added into the bath. Twenty minutes after the addition of L-NMMA, EFS at 5 Hz (50 V and 0.5 ms duration) was applied for 30 min. All experiments were carried out in the presence of indomethacin (10 μM), propranolol (1 μM), phentolamine (1 μM) and neostigmine (1 μM) (Baker *et al.*, 1992). Neostigmine was present to prevent hydrolysis of ACh by endogenous acetylcholinesterase activity. After the end of EFS, the incubation solution was stored at − 80°C until analysis. We also examined the release of ACh from tracheal rings (3 mm long) during 30 min incubation without EFS. In the analysis, 10 μl of a 20 pM solution of ethylhomocholine (EHC), as an internal standard for ACh, was added to 1 ml of the incubation solution and mixed. The mixture was filtered with a 0.45 μm-millipore filter and 100 μl aliquots were subjected to analysis by liquid chromatography according to the procedure previously described (Ikarashi *et al.*, 1984; 1992). The system consisted of a pump, an injector with a 100 μl sample loop and a work station for the data processing used in conjunction with an amperometric detector with a platinum electrode (IRICA Instrument Inc., Kyoto, Japan). The analytical column was a Bioanalytical Systems Acetylcholine Separation Column (60 mm × 4 mm i.d., 3 μm, polystyrene-based packing materials, Bioanalytical Systems, BAS, West Lafayette, IN, U.S.A.). An immobilized column (5 mm × 4 mm i.d., BAS) containing acetylcholinesterase (AChE) and choline oxidase (ChO) was used for post-column reaction. A glassy carbon pre-column (IRICA) was used for removing interfering peaks except for targeted compounds. The column temperatures were maintained at 35°C by means of a temperature controller (IRICA). The mobile phase comprised a 0.05 M phosphate buffer, pH 8.4 containing 1 mM EDTA-2Na and 0.4 mM sodium octanesulphonate. The flow rate was 0.7 ml min^{-1}. The electrode potential was set at + 0.5 V relative to a Ag/AgCl reference electrode. The principle of the technique is based upon the separation of EHC and ACh in the separation column, followed by their enzymatic conversion through post-column reaction with AChE and ChO to hydrogen peroxide, which is detectable electrochemically by platinum electrode. Under the chromatographic conditions, the retention times of EHC and ACh were 5.75 and 10.64 min, respectively. A calibration curve for the determination of ACh is linear between 0 and 80 pmol ml^{-1}. The minimum detection limit in the injected sample was at least 0.25 pmol for ACh. In preliminary experiments, the addition of indomethacin (10 μM), propranolol (1 μM), phentolamine (1 μM), neostigmine (1 μM) or L-NMMA (100 μM) to the Krebs-Henseleit buffer did not create retention peaks.

The following drugs were used: tetrodotoxin, atropine sulphate, indomethacin, methylene blue, capsaicin, α-chymotrypsin, vasoactive intestinal peptide, N^2, 2'-O-dibutyryl guanosine 3':5'-cyclic monophosphate, ACh iodide (Sigma), (±)-propranolol hydrochloride, sodium nitroprusside dehydrate (Wako Pure Chemicals), phentolamine (Ciba Geigy). N^G-monomethyl-L-arginine was kindly given by Dr K. Aisaka (Suntory Limited, Osaka, Japan). EHC iodide as IS was synthesized from iodoethane and 3-dimethylamino-1-propanol.

Values are expressed as mean ± s.e.mean. Statistical analysis was performed by one way analysis of variance. Significance was accepted at $P<0.05$.

Results

Methylene blue up to concentrations of 30 μM did not change the baseline tension. However, methylene blue (from 10 nM to 30 μM) caused a concentration-dependent increase in the contractile response to EFS at 5 z (Figure 1). EFS frequency-response curves were evaluated by mean (± s.e.mean) log frequency of the stimulation producing 50% of maximal contraction to EFS (ES_{50}). EFS frequency-response curves were reproducible and ES_{50} did not differ significantly between the first and second frequency-response curves in the absence of methylene blue (0.74 ± 0.07 Hz vs. 0.75 ± 0.10 Hz; $P<0.50$, $n=5$). However, methylene blue (30 μM) shifted the mean frequency-response curve to the left and significantly reduced ES_{50} (0.74 ± 0.09 Hz vs. 0.30 ± 0.05 Hz; $P<0.01$, $n=7$) (Figure 2a). In contrast to EFS-induced contractions, ACh-induced contractions were not affected by methylene blue (30 μM) (− log EC_{50} = 5.45 ± 0.49 M vs. 5.45 ± 0.38 M; $P<0.50$, $n=7$) (Figure 2b).

L-NNMA (100 μM) significantly increased the contractile response to EFS at 5 Hz (131.5 ± 4.6% of control, $P<0.01$, $n=7$) but it had no significant effect on the contractile response to exogenously administered ACh (3 μM) (98.2 ± 5.4% of control, $P>0.30$, $n=7$). The amount of acetylcholine in the bath solution was below the detection limit without EFS. However, EFS at 5 Hz caused a significant

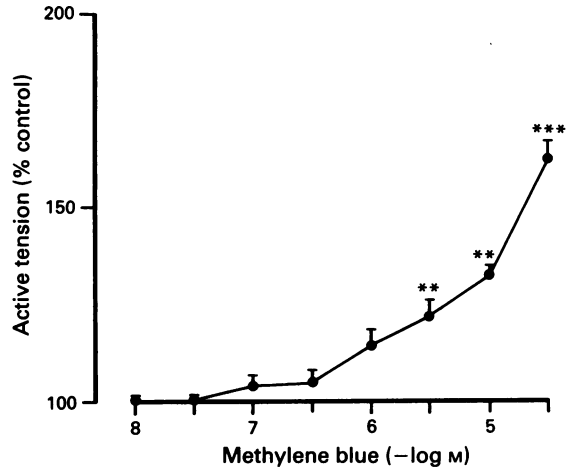

Figure 1 Concentration-response curves to methylene blue in the contractile response to electrical field stimulation (EFS) at 5 Hz. Data are shown as mean ± s.e.mean of values from 7 rats. Significant differences from control values are indicated by $^{**}P<0.01$ and $^{***}P<0.001$.

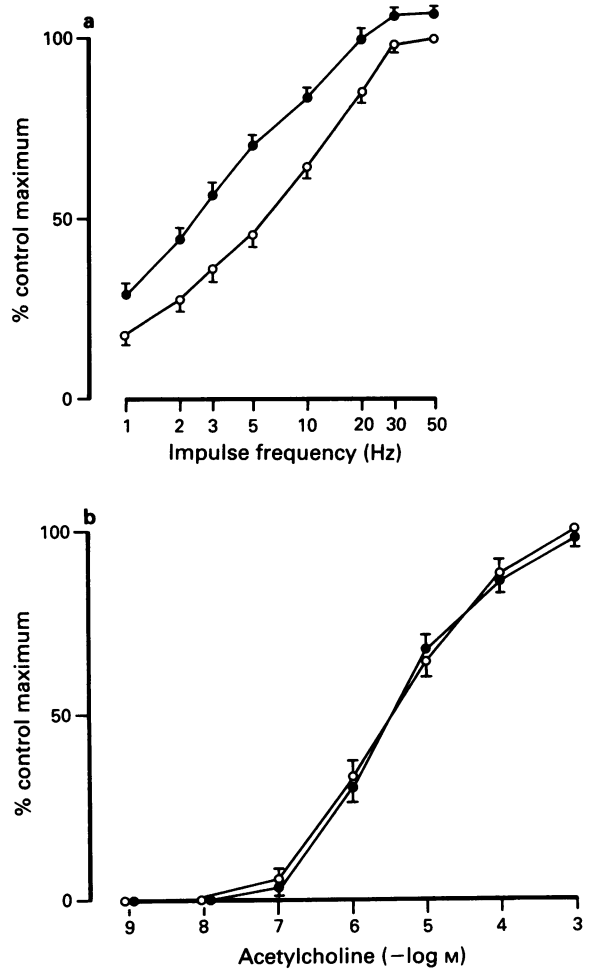

Figure 2 (a) Effects of methylene blue on the frequency-response curve to electrical field stimulation (EFS). Data are shown as mean ± s.e.mean of values from 7 rats. EFS at 50 Hz caused contractions of 1.2 ± 0.4 g in control conditions. Methylene blue (30 μM; ●) shifted the control frequency-response curve (○) to the left. (b) Concentration-response curves to acetylcholine (ACh) in the presence (●) and absence (○) of methylene blue (30 μM). Data are shown as mean ± s.e.mean of values from 7 rats. Maximal contraction induced by ACh was 1.1 ± 0.3 g in control conditions.

release of ACh from tracheal segments into the bath solution and this release of ACh was significantly enhanced by L-NMMA (100 μM) (51.4 ± 4.0 pmol ml^{-1} in the presence of L-NMMA vs. 35.0 ± 1.8 pmol ml^{-1} in the absence of L-NMMA; $P<0.01$, $n=7$) (Figure 3).

Administration of NO (present in acidified solution of $NaNO_2$) and SNP decreased the amplitude of the contractile responses to both EFS at 5 Hz and ACh (3 μM) (Figure 4a,b). The inhibition of each was concentration-dependent. NO and SNP at 10 μM inhibited EFS-induced contractions (67.0 ± 4.8% of control and 72.0 ± 3.6% of control respectively; $P<0.01$) but did not significantly alter the contractile response of exogenously administered ACh (3 μM) (95.1 ± 4.7% of control and 96.1 ± 3.2% of control, respectively; $P>0.20$). Likewise, inhibitory effects of NO (10 μM) and SNP (10 μM) on EFS-induced contractions did not differ significantly in the presence or absence of L-NMMA (100 μM) (71.0 ± 5.2% of control in the presence of L-NMMA vs. 67.0 ± 4.8% of control in the absence of L-NMMA and 69.3 ± 4.1% of control in the presence of L-NMMA vs. 72.0 ± 3.6% of control in the absence of L-NMMA, respectively; $P>0.20$). NO at 1 mM and SNP at 0.1 mM inhibited EFS-induced cholinergic contractions (14.6 ± 3.0% of control and 51.2 ± 3.1% of control, respectively; $P<0.001$) and ACh-induced contractions (56.8 ± 5.0% of control and 79.0 ± 4.0% of control, respectively; $P<0.01$).

Db cyclic GMP (3 mM) significantly inhibited the contractile response to EFS at 5 Hz both in the presence and absence of L-NMMA (100 μM) (67.2 ± 4.3% of control and 70.1 ± 3.6% of control, respectively; $P<0.01$, $n=5$) without affecting ACh (3 μM)-induced contractions (101.8 ± 4.9% of control; $P>0.50$, $n=5$).

Pretreatment of tissues with either capsaicin (30 μM) or α-chymotrypsin (1 u ml^{-1}) failed to inhibit methylene blue (30 μM)-induced potentiating responses to EFS at 5 Hz (168.2 ± 5.0% of control in the absence of treatment, 164.8 ± 4.9% of control in the presence of capsaicin and 171.3 ± 7.2% of control in the presence of α-chymotrypsin, respectively, $P>0.20$, $n=5$).

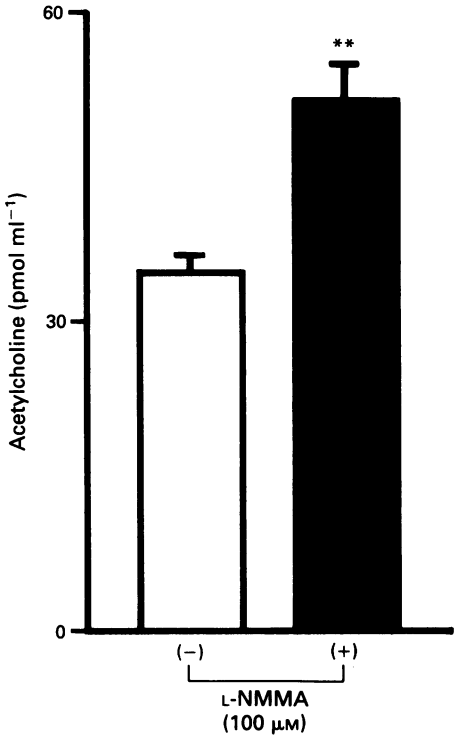

Figure 3 Electrical field stimulation (5 Hz)-evoked release of acetylcholine in the presence of N^G-monomethyl-L-arginine (L-NMMA, 100 μM; solid column) and the vehicle of L-NMMA (open column). Data are shown as mean ± s.e.mean of values from 7 rats. Significant difference between columns is indicated by $^{**}P<0.01$.

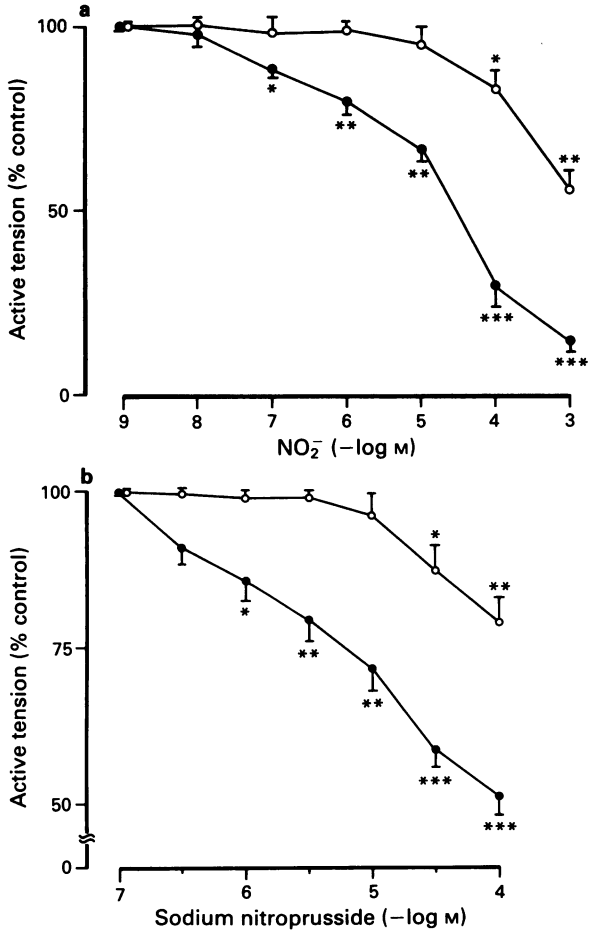

Figure 4 (a) Concentration-response curves to nitric oxide (NO, present in acidified solution of $NaNO_2$) in the contractile responses to electrical field stimulation (EFS) at 5 Hz (●) and acetylcholine (3 μM; ○). Data are shown as mean ± s.e.mean of values from 7 rats. Significant differences from control values are indicated by $*P<0.05$, $**P<0.01$ and $***P<0.001$. (b) Concentration-response curves to sodium nitroprusside (SNP) in the contractile responses to electrical field stimulation (EFS) at 5 Hz (●) and acetylcholine (3 μM; ○). Data are shown as mean ± s.e.mean of values from 7 rats. Significant differences from control values are indicated by $*P<0.05$, $**P<0.01$ and $***P<0.001$.

Discussion

In the presence of adrenoceptor antagonists and indomethacin, EFS caused contractions which were abolished by atropine and tetrodotoxin, suggesting that these responses resulted from cholinergic nerve stimulation. Since these contractions were significantly potentiated by L-NMMA, a specific inhibitor of NO production (Palmer *et al.*, 1988; Moncada *et al.*, 1989: Johns *et al.*, 1990), inhibition of these contractions was mediated by an NO-like factor. In addition, exogenous administration of NO and SNP, an agent releasing NO (Moncada, 1992) reduced the cholinergic contraction induced by EFS. Furthermore, methylene blue, an agent believed to inhibit the activation of NO-activated guanylate cyclase (Martin *et al.*, 1985; Ignarro *et al.*, 1989) potentiated the cholinergic contraction induced by EFS, an opposite effect observed to that with the stable cyclic GMP analogue, db cyclic GMP. These results indicate the endogenous NO-like factor modulates cholinergic contraction through a cyclic GMP-dependent mechanism.

In order to establish whether NO elicits its inhibitory effects prejunctionally on neuronal terminals or postjunctionally on the acetylcholine receptors of the airway smooth muscle, we compared the effects of L-NMMA and methylene blue on the contractile response to EFS with the effects that they had on the contractile response to ACh. Both L-NMMA and methylene blue potentiated contractions induced by EFS without a significant effect on contractions induced by ACh. Likewise, exogenous NO and SNP in concentrations that did not alter the contractile response to ACh inhibited similar contractions induced by EFS. Furthermore, L-NMMA enhanced release of ACh from tracheal segments induced by EFS. These results indicate that an endogenous NO-like factor inhibits the release of ACh from cholinergic nerves. Brave *et al.* (1991) showed that L-N^G-nitro-arginine potentiates contractions induced by EFS but has no effect on ACh release in the guinea-pig trachea. They suggested that NO released along with ACh during EFS acts directly on smooth muscle to produce effects opposite to those of ACh. In the present study, we used the rat trachea and therefore a species difference may explain the difference between the present study and that of Brave *et al.* (1991). However, the present study cannot rule out the contribution of a postsynaptic relaxant effect of endogenously released NO on EFS-induced contractions.

Although the precise nature of the NANC inhibitory neurotransmitter in the airway is still debated, VIP is believed to be the most likely candidate. VIP has been shown to inhibit prejunctionally cholinergic contractions in the airway (Sekizawa *et al.*, 1988: Aikawa *et al.*, 1990; Hakoda & Ito, 1990; Xie *et al.*, 1991). However, α-chymotrypsin which inhibits the relaxant action of VIP in the airway (Li & Rand, 1991) did not alter methylene blue-induced potentiating responses to EFS, suggesting that prejunctional inhibition of cholinergic contractions is not mediated via VIP in rat trachea. Likewise, sensory neuropeptides such as substance P and neurokinin A are unlikely to be the mechanism for prejunctional inhibition of cholinergic contractions because pretreatment of tissues with capsaicin failed to alter methylene blue-induced potentiating effects on cholinergic contractions.

The source of NO released during EFS is unknown in the present study. However, it is possible that NO could be released from nerves, endothelial cells lining blood vessels or other cell types that express NO synthase (Moncada *et al.*, 1991). NO causes relaxation of airway smooth muscle (Tucker *et al.*, 1990; Li & Rand, 1991) and pulmonary artery (Liu *et al.*, 1991). The receptor for NO in several tissues and cells including nerves appears to be soluble guanylate cyclase (Rapoport & Murad, 1983; Moncada, 1992). Cyclic GMP is reported to inhibit noradrenaline release from sympathetic nerve endings in canine vascular smooth muscle (Greenberg *et al.*, 1990). Our data suggest that the effects of NO on cholinergic nerve endings are also mediated via a cyclic GMP-dependent mechanism.

In conclusion, our study suggests that an endogenous NO-like factor released during EFS may mediate prejunctional inhibition of cholinergic contraction through a cyclic GMP-dependent mechanism.

The authors thank Dr K. Aisaka for gifts of L-NMMA and Mr G. Crittenden for correcting the manuscript.

References

AIKAWA, T., SEKIZAWA, K., ITABASHI, S., SASAKI, H. & TAKISHIMA, T. (1990). Nonadrenergic inhibitory nerves attenuate neurally mediated contraction in cat bronchi. *J. Appl. Physiol.*, **69**, 1594–1598.

ALTIERE, R.J. & DIAMOND, L. (1984). Comparison of vasoactive intestinal peptide and isoproterenol relaxant effects in isolated cat airways. *J. Appl. Physiol.*, **56**, 986–992.

BAKER, D.G., DON, H.F. & BROWN, J.K. (1992). Direct measurement of acetylcholine release in guinea pig trachea. *Am. J. Physiol.*, **263,** L142–L147.

BRAVE, S.R., HOBBS, A.J., GIBSON, A. & TUCKER, J.F. (1991). The influence of L-N^G-nitro-arginine on field stimulation induced contractions and acetylcholine release in guinea pig isolated tracheal smooth muscle. *Biochem. Biophys. Res. Commun.*, **179,** 1017–1022.

GIBSON, A., MIRZAZADEH, S., HOBBS, A.J. & MOORE, P.K. (1990). L-N^G-monomethyl arginine and L-N^G-nitro arginine inhibit non-adrenergic, non-cholinergic relaxation of the mouse anococcygeus muscle. *Br. J. Pharmacol.*, **99,** 602–606.

GILLESPIE, J.S., LIU, X. & MARTIN, W. (1989). The effects of L-arginine and N^G-monomethyl L-arginine on the response of the rat anococcygeus muscle to NANC nerve stimulation. *Br. J. Pharmacol.*, **98,** 1080–1082.

GREENBERG, S.S., DIECKE, F.P.J., CANTOR, E., PEEVY, K. & TANAKA, T.P. (1990). Inhibition of sympathetic neurotransmitter release by modulators of cyclic GMP in canine vascular smooth muscle. *Eur. J. Pharmacol.*, **187,** 409–423.

HAKODA, H. & ITO, Y. (1990). Modulation of cholinergic neurotransmission by the peptide VIP, VIP antiserum and VIP antagonists in dog and cat trachea. *J. Physiol.*, **428,** 133–154.

IGNARRO, L.J. (1989). Heme-dependent activation of soluble guanylate cyclase by nitric oxide: regulation of enzyme activity by porphyrins and metalloporphyrins. *Semi. Hematol.*, **26,** 63–76.

IKARASHI, Y., IWATSUKI, H., BLANK, C.L. & MARUYAMA, Y. (1992). Glassy carbon pre-column for direct determination of acetylcholine and choline in biological samples using liquid chromatography with electrochemical detection. *J. Chromatogr.*, **575,** 29–37.

IKARASHI, Y., SASAHARA, T. & MARUYAMA, Y. (1984). A simple method for determination of choline (Ch) and acetylcholine (ACh) in rat brain regions using high-performance liquid chromatography with electrochemical detection (HPLC-ED). *Folia Pharmacol. Japan.*, **84,** 529–536.

JOHNS, R.A., PEACH, M.J., LINDEN, J. & TICHOTSKY, A. (1990). N^G-monomethyl L-arginine inhibits endothelium-derived relaxing factor-stimulated cyclic GMP accumulation in cocultures of the endothelial and vascular smooth muscle cells by an action specific to the endothelial cell. *Circ. Res.*, **67,** 979–985.

LI, C.G. & RAND, M.J. (1989). Evidence for a role of nitric oxide in the neurotransmitter system mediating relaxation of the rat anococcygeus muscle. *Clin. Exp. Pharmacol. Physiol.*, **16,** 933–938.

LI, C.G. & RAND, M.J. (1990). Evidence suggesting that nitric oxide (NO) mediates NANC neurotransmission in rat gastric fundus and anococcygeus muscle. *Clin. Exp. Pharmacol. Physiol.*, **16** (Suppl.), 184.

LI, C.G. & RAND, M.J. (1991). Evidence that part of the NANC relaxant response of guinea-pig trachea to electric field stimulation is mediated by nitric oxide. *Br. J. Pharmacol.*, **102,** 91–94.

LIU, S.F., CRAWLEY, D.E., EVANS, T.W. & BARNES, P.J. (1991). Endogenous nitric oxide modulates adrenergic neural vasoconstriction in guinea-pig pulmonary artery. *Br. J. Pharmacol.*, **104,** 565–569

MARTIN, W., VILLANI, G.M., JOTHIANANDAN, D. & FURCHGOTT, R.F. (1985). Selective blockade of endothelium-dependent and glyceryl trinitrate-induced relaxation by hemoglobin and methylene blue in the rabbit aorta. *J. Pharmacol. Exp. Ther.*, **232,** 708–716.

MONCADA, S. (1992). The L-arginine; nitric oxide pathway. *Acta Physiol. Scand.*, **145,** 201–227.

MONCADA, S., PALMER, R.M.J. & HIGGS, E.A. (1989). Biosynthesis of nitric oxide from L-arginine. A pathway for the regulation of cell function and communication. *Biochem. Pharmacol.*, **38,** 1709–1715.

MONCADA, S., PALMER, R.M.J. & HIGGS, E.A. (1991). Nitric oxide: Physiology, Pathophysiology, and Pharmacology. *Pharmacol. Rev.*, **43,** 109–142.

PALMER, J.B.D., CUSS, F.M.C. & BARNES, P.J. (1986). VIP and PHM and their role in nonadrenergic inhibitory responses in isolated human airways. *J. Appl. Physiol.*, **61,** 1322–1328.

PALMER, R.M.J., REES, D.D., ASHTON, D.S. & MONCADA, S. (1988). L-arginine is the physiological precursor for the formation of nitric oxide in endothelium-dependent relaxation. *Biochem. Biophys. Res. Commun.*, **153,** 1251–1256.

RAPPORT, R.M. & MURAD, F. (1983). Agonist-induced endothelium-dependent relaxation in rat thoracic aorta may be mediated through cGMP. *Circ. Res.*, **52,** 352–357.

SEKIZAWA, K., TAMAOKI, J., GRAF, P.D. & NADEL, J.A. (1988). Modulation of cholinergic neurotransmission by vasoactive intestinal peptide in ferret trachea. *J. Appl. Physiol.*, **64,** 2433–2437.

TUCKER, J.F., BRAVE, S.R., CHARALAMBOUS, L., HOBBS, A.J. & GIBSON, A. (1990). L-N^G-nitro arginine inhibits non-adrenergic, non-cholinergic relaxations of guinea-pig isolated tracheal smooth muscle. *Br. J. Pharmacol.*, **100,** 663–664.

XIE, Z., HIROSE, T., HAKODA, H. & ITO, Y. (1991). Effects of vasoactive intestinal polypeptide antagonists on cholinergic neurotransmission in dog and cat trachea. *Br. J. Pharmacol.*, **104,** 938–944.

(Received March 10, 1993
Revised June 8, 1993
Accepted June 15, 1993)

Br. J. Pharmacol. (1993), **110**, 821–827

The effects of a converting enzyme inhibitor (captopril) and angiotensin II on fetal renal function

[1]E.R. Lumbers, J.H. Burrell, R.I. Menzies & A.D. Stevens

School of Physiology and Pharmacology, University of NSW, PO Box 1, Kensington, Sydney, NSW 2033, Australia

1 Renal function was studied in chronically catheterized fetal sheep (119–128 days gestation), before and during treatment of the ewe with the angiotensin converting enzyme (ACE) inhibitor, captopril, which crosses the placenta and blocks the fetal renin angiotensin system.

2 An i.v. dose of 15 mg (about 319 $\mu g\ kg^{-1}$) of captopril to salt-replete ewes followed by an infusion to the ewe of 6 $mg\ h^{-1}$ (about 128 $\mu g\ kg^{-1}\ h^{-1}$) caused a fall in fetal arterial pressure ($P<0.01$), and a rise in fetal renal blood flow (RBF) from 67.9 ± 5.6 to 84.9 ± 8.3 ml min^{-1} (mean ± s.e.mean) ($P<0.05$). Renal vascular resistance and glomerular filtration rate (GFR) fell ($P<0.01$); fetal urine flow ($P<0.01$) and sodium excretion declined ($P<0.05$).

3 Ewes were treated for the next 2 days with 15 mg captopril twice daily. On the 4th day, 15 mg was given to the ewe and fetal renal function studied for 2 h during the infusion of captopril (6 $mg\ h^{-1}$) to the ewe. Of the 9 surviving fetuses, 3 were anuric and 3 had low urine flow rates. When 6 $\mu g\ kg^{-1}\ h^{-1}$ of angiotensin II was infused directly into the fetus RBF fell from 69 ± 10.1 ml min^{-1} to 31 ± 13.9 ml min^{-1}, GFR rose ($P<0.05$) and urine flow ($P<0.01$) and sodium excretion increased in all fetuses.

4 It is concluded that the small fall in fetal arterial pressure partly contributed to the fall in fetal GFR but in addition, efferent arteriolar tone fell so that the filtration pressure fell further. Thus maintenance of fetal renal function depends on the integrity of the fetal renin angiotensin system. These findings explain why use of ACE inhibitors in human pregnancy is associated with neonatal anuria.

Keywords: Captopril; glomerular filtration rate; angiotensin II; sodium excretion

Introduction

It has been claimed that angiotensin converting enzyme inhibitors (ACE inhibitors) are fetotoxic (Broughton Pipkin *et al.*, 1982) possibly because of their effects on maternal and fetal cardiovascular function (Lumbers *et al.*, 1992). When captopril was given to the pregnant ewe, maternal and fetal hypotension occurred; uteroplacental and umbilicoplacental blood flows both fell and there was a small but significant decline in fetal arterial Po_2. In addition, fetal urine flow rate decreased (Lumbers *et al.*, 1992). Clinically, treatment of pregnancy associated hypertension with ACE inhibitors has been associated with neonatal anuria (Editorial, Lancet 1989; Shubiger *et al.*, 1988). Furthermore, recent reports of oligohydramnios and pulmonary hypoplasia (see Brent & Beckman, 1991) may result from a fall in the rate of production of amniotic fluid due to reduced production of fetal urine. However, previous studies in which captopril was administered directly to fetal sheep failed to show any marked effects of the drug on fetal renal function, although it was noted that in an older group, glomerular filtration rate (GFR) tended to fall as did renal vascular resistance (Robillard *et al.*, 1983). Captopril given to the ewe rapidly crosses the placenta and blocks the formation of fetal angiotensin II (AII) (Lumbers *et al.*, 1992). Thus it is likely that captopril given directly to the fetus (Robillard *et al.*, 1983) would cross back into the maternal circulation so lowering the concentration of captopril in fetal blood.

To test the hypothesis that repeated administration of captopril to the mother (a more likely clinical regimen) would adversely affect fetal renal function, and to determine the role (if any) of the fetal renin-AII system in maintenance of fetal renal function, experiments were carried out in pregnant ewes and their fetuses. In these experiments the acute effects of maternally administered captopril on fetal renal function were studied; the ewes were treated with captopril for a further 2 days and fetal renal function measured on the 4th day of captopril treatment, after which AII was infused into the fetus. In an attempt to minimize the maternal and fetal cardiovascular effects of converting enzyme blockade described in an earlier study (Lumbers *et al.*, 1992), ewes were given an excess of salt as a supplement in their diet.

[1] Author for correspondence.

Methods

Experimental protocols were approved by the Animal Care and Ethics Committee, University of NSW.

Surgery

Thirteen pregnant ewes (119–128 days gestation) were anaesthetized with an i.v. dose of 1 g sodium thiopentone and maintained with 2–3% halothane in oxygen. As these agents cross the placenta, each fetus was also anaesthetized (Lumbers, E.R., unpublished observations).

Under aseptic conditions polyvinyl catheters (1.5 mm o.d., 1.0 mm i.d.) were inserted into one fetal femoral artery, and both tarsal veins and a suprapubic catheter was inserted in the bladder (Lumbers & Stevens, 1983). A polyvinyl catheter (2.7 mm o.d., 1.5 mm i.d.) was inserted into the right maternal carotid artery, and a Swann-Ganz catheter passed into the maternal pulmonary artery by the right jugular vein. At the end of surgery and for the next 2 days, procaine penicillin (600 mg) and dihydrostreptomycin sulphate mixture (750 mg) were given i.m. to the ewe and into the amniotic cavity.

The ewes were housed in metabolic cages in a laboratory maintained at 18–20°C. The average weight of pregnant ewes in this laboratory is 46.8 ± 0.8 (mean ± s.e., $n = 47$). They had free access to water and a diet of lucerne chaff and oats. An excess of salt, 16.5 g/day of sodium chloride (BDH Chemicals), was added to the ewe's diet. Lucerne chaff contains about 33 mmol kg^{-1} of salt and the ewes eat 1–1.5 kg/day (Gibson & Lumbers, 1992). The excess salt was added to

suppress maternal plasma renin activity and minimize the effects of captopril on maternal and fetal cardiovascular function (see Lumbers *et al.*, 1992). Maternal food and water intake and urine output were recorded daily. No experiments were carried out for at least 5 days after surgery.

Experimental protocol

Thirteen fetuses (123–133 days gestation) were studied on the first day of the experiment.

Day 1 On the first day, the fetal bladder was drained for 45 min; 30 min before the first urine collection, the fetus was given 1.8 μCi kg^{-1} estimated body weight of sodium [^{125}I]-iothalamte (Amersham) and 250 μmol kg^{-1} of lithium. These injections were followed by continuous i.v. infusions of sodium iothalamate (0.3 μCi kg^{-1} h^{-1}) and lithium (10 μmol kg^{-1} h^{-1}). The ewe was given an i.v. dose of 150 μmol kg^{-1} of lithium chloride (BDH Chemical Ltd).

Urine was collected under anaerobic conditions (i.e. into a glass burette under a 1 cm layer of mineral oil) at 30 min intervals for 4 h. During the first 2 h, control observations were made. Then an i.v. dose of 15 mg captopril (about 319 μg kg^{-1}) was given to the ewe, followed by a continuous infusion of captopril (6 mg h^{-1}, about 128 μg kg^{-1} h^{-1}) for the next 2 h. These doses of captopril given to the ewe block the formation of AII in the fetus (Lumbers *et al.*, 1992).

Arterial blood samples (4 ml) were collected from ewe and fetus halfway through the 2nd and 4th control collection periods and halfway through the 2nd and 4th 30 min periods of captopril treatment. At the end of the experiment, the maternal captopril infusion was stopped and catheters were flushed with 0.15 M saline containing 100 i.u. of heparin ml^{-1}.

Days 2 and 3 On days 2 and 3, 15 mg (about 319 μg kg^{-1}) of captopril was given i.v., twice daily to the ewe. To determine if the fetus was alive, 1–2 ml of fetal arterial blood was taken; the bladder catheter was opened and drained for 0.5 h and urine collected for another 0.5 h immediately after the ewe had been given the first of her 2 daily injections of captopril.

Day 4 On day 4, the ewe was given an i.v. injection of 15 mg (about 319 μg kg^{-1}) captopril in the period during which the fetal bladder was drained, i.e. 30 min before urine collections began. An infusion of 6 mg h^{-1} (about 128 μg kg^{-1} h^{-1}) of captopril for 2 h was also started. After 2 h, the infusion of captopril was stopped and 6 μg kg^{-1} h^{-1} of AII was infused i.v. into the fetus for the next 3 h. This high dose of AII was chosen to ensure that there was sufficient AII in the fetal circulation. Fetal plasma AII levels measured during infusion of a similar dose of AII (5.8 μg kg^{-1} h^{-1}) were about 400 pg ml^{-1} (Robillard *et al.*, 1992). Arterial blood samples (4 ml) were collected from both ewe and fetus halfway through the 2nd and 4th periods during which captopril was given to the ewe and halfway through the 2nd, 4th and 6th periods during which AII was infused into the fetus.

Measurements

On days 1 and 4 maternal and fetal arterial blood pressures, intra-amniotic pressure and heart rates were recorded continuously throughout the experiment, with Bell and Howell pressure transducers connected to a Grass Polygraph recorder and an IBM compatible PC. Fetal pressures were corrected for intra-amniotic pressure.

In 9 sheep on day 1 and 6 sheep on day 4, 5 measurements of maternal cardiac output were made in each hour and the 5 values were averaged. An Edwards Model COM-1 cardiac computer was used. Injections of 10 ml of ice-cold saline were given (for methods, see Caine *et al.*, 1985; Lumbers *et al.*, 1992).

Blood gases and pH were measured with a CIBA-Corning Blood Gas System (model 288). Fetal urinary and fetal and maternal plasma sodium and potassium levels were measured on a Radiometer Flame Photometer (model FLM3). Fetal urinary and fetal and maternal plasma osmolality were measured with a Fiske One-Ten Osmometer (model 3D11). Plasma and urinary lithium levels were measured in a Perkins-Elmer absorption spectrophotometer (model 272). Maternal and fetal plasma renin activity (PRA) were measured as the rate of formation of angiotensin I at pH 7.5 and at 37°C. Angiotensin I was measured by radioimmunoassay (Lumbers & Lee Lewes, 1979). Urinary bicarbonate, titratable acid and ammonium excretion rates were measured by methods of Gyory & Edwards (1967) and Gyory *et al.* (1974).

It is not possible to use clearance of *p*-aminohippurate to measure fetal renal plasma flow (Elbourne *et al.*, 1990), therefore, renal blood flows were measured with radiolabelled microspheres. On day 1, measurements were made 10–15 min before captopril was given to the ewe and 2 h after it was first given. On day 4, blood flows were measured 10–15 min before the infusion of AII began (i.e. during infusion of captopril to the ewe), and at the end of the AII infusion. The 15 μm microspheres were labelled with one of the following isotopes: ^{141}Ce, ^{103}Ru, ^{46}Sc, ^{95}Nb, ^{51}Cr, ^{113}Sn (Nentrac, DuPont), and suspended in saline and Tween 80. Tween 80 was added approximately 30 min before injection of the first dose of microspheres to make a final concentration of 0.1% (v/v). The injections of particular isotopes were randomized. Approximately 2.4×10^6 microspheres were injected into the fetus via a tarsal vein catheter, and flushed with 5 ml saline. A reference sample of fetal arterial blood was withdrawn into pre-weighed, heparinised syringes. Sampling began before the injection and continued for a further 3 min at a rate of 2 ml min^{-1}. The total withdrawal time was monitored with a stopwatch and the syringes full of blood were weighed. The volume of the fetal catheters was approximately 1 ml (see also Lumbers *et al.*, 1992).

It is unlikely that these injections affected the fetal circulation or fetal renal function as there were no acute circulatory effects in fetuses given 5 injections of more than 1 million spheres (Heymann *et al.*, 1977) and no effects of 2 injections of 4 million spheres on fetal renal function (Robillard *et al.*, 1981).

At the end of the experiment ewe and fetus were killed by i.v. injection of sodium pentobarbitone (6 g). Left and right fetal kidneys were removed and counted. The activities of the isotopes in tissues and reference samples were measured in a Packard gamma counter (Model 5650). The activity of pure samples of each isotope was measured in each channel and the degree of overlap of each isotope into other channels was calculated. A matrix set up on a Microsoft Excell spreadsheet on an IBM compatible PC was used to solve the simultaneous equations required to calculate flows. Since the fetal kidneys were weighed, total renal blood flow (ml min^{-1}) and renal blood flow g^{-1} (ml min^{-1} g^{-1}) were both measured (see Lumbers *et al.*, 1992).

Data analysis

Maternal and fetal arterial blood pressures and pulse interval measurements were collected for 10 s periods every 2.5 min; the average for each 30 min period was then calculated. Heart rate was measured from the blood pressure record.

Fetal renal vascular resistance (R, arbitrary units) was calculated from the formula

$$R = \text{arterial pressure(mmHg)/flow(ml min}^{-1}\text{)}$$

Fetal glomerular filtration rate (GFR) was calculated as the clearance of [^{125}I]-sodium iothalamate (Lumbers *et al.*, 1985). Fetal total fractional sodium reabsorption was calculated from the formula

$$1 - CNa/GFR$$

(where CNa is the clearance of sodium).

If the major site of reabsorption of lithium is the proximal tubule (Thomsen *et al.*, 1981), then the fractional reabsorption of sodium in the proximal tubule will be the same as that of lithium, and can be calculated from the formula

$$1 - \text{CLi/GFR}$$

(where CLi is the clearance of lithium).

Distal fractional sodium reabsorption is therefore

$$\text{CLi/GFR} - \text{CNa/GFR}$$

(see Lumbers *et al.*, 1988).

Plasma bicarbonate levels (mmol l^{-1}) were calculated from the formula

$$HCO_3^- = 0.0294 \times PCO_2 \times 10^{(-4.9911 + 0.6576pH + 0.0262pH^2)}$$

(Armentrout *et al.*, 1977).

Statistical analyses were performed by use of an IBM compatible PC and SPSS (Statistical Package for the Social Sciences, Nie *et al.*, 1982). Values are expressed as mean ± s.e.mean. The number *n* refers to the number of animals in which values for a given variable were obtained at a particular time. Data were analysed by analysis of variance of repeated measures and Dunnett's 2-tailed multiple comparison test (Zar, 1984). The data were analysed as follows.

Day 1 An analysis of the acute effects of captopril on the fetus was made by comparing data collected during infusion of captopril for 2 h (PC_1-PC_4) with the mean of the 4 × 30 min control (Con) values.

Day 4 An analysis of the effect of stopping captopril treatment and infusing AII on renal function in fetuses whose mothers had received 3 days of treatment with captopril was made by comparing the data obtained during the 3 h infusion of AII (A_1-A_6) with the mean of the 4 × 30 min values obtained during the preceding 2 h period (D_4) during which captopril was infused into the ewe.

Drugs

Sodium thiopentone (Pentothal, Abbott) and halothane (Fluothane, ICI) were used as anaesthetic agents. Procaine pencillin and dihydrostreptomycin mixture (Hydropen, Bomac) was administered post operatively. Captopril (ER Squibb & Sons Inc.) and angiotensin II (Hypertensin, Ciba) were dissolved in 0.15 M saline on the day of use. Sodium pentobarbitone (Valobarb, Coopers Animal Health Australia Ltd.) was used to kill the ewe and foetus.

Results

Effect of captopril on the survival of the fetus

One fetus died within an hour of captopril being given to the ewe (results from this animal are not included). Three died on the second or third day of the experiment, but were considered healthy on the first day and their results are included in the analysis of the acute effects of captopril on fetal renal function. There was no obvious abnormality in any of the animals which died, although one of them which died on the second day may have developed an infection. In another fetus, the venous and arterial catheters became blocked so that the effects of stopping captopril treatment and infusing AII to the fetus could not be measured.

Acute effects of captopril on ewe and fetus (Day 1)

Ewe Within the first 30 min period of captopril treatment maternal mean arterial pressure fell from 89 ± 3.2 to 83 ± 3.1 mmHg and remained low ($P<0.01$). Cardiac output increased from 9.0 ± 0.8 l min^{-1} to 10.2 ± 0.9 l min^{-1} ($P<0.01$) but later was unchanged (9.6 ± 0.8 l min^{-1}). Initially heart rate was unchanged from control values of 139 ± 5.9 beats min^{-1} ($n = 9$), but in the third 30 min period of treatment there was a transient rise to 149 ± 5 beats min^{-1} ($n = 7$, $P<0.05$). Maternal PRA rose ($P = 0.05$, Table 1). There were no changes in 12 ewes in arterial PO_2 (101 ± 1.5 mmHg), PCO_2 (36.7 ± 1.1 mmHg), pH (7.48 ± 0.01), plasma osmolality (292 ± 3.3 mosm kg^{-1}) and plasma sodium levels (147 ± 2.0 mmol l^{-1}). Potassium levels rose by the end of the infusion and the plasma sodium:potassium ratio increased ($P<0.01$; Table 1). Bicarbonate levels fell initially ($P<0.05$), but were not different from control at the end of the experiment. Maternal haematocrit rose and remained elevated ($P<0.01$; Table 1).

Fetus Fetal arterial pressure fell slightly ($P = 0.01$; Table 1) but heart rate did not change from control values of 169 ± 3.5 beats min^{-1}. Fetal PRA increased ($P<0.01$; Table 1) and fetal PO_2 fell ($P = 0.01$; Table 1). In 12 fetuses arterial PCO_2 (52.5 ± 1.0 mmHg) and haematocrit (32.1 ± 0.35%) did not change, neither did fetal arterial pH (7.38 ± 0.007), plasma sodium (146 ± 2.1 mmol l^{-1}), potassium (3.6 ± 0.15 mmol l^{-1}), sodium:potassium ratio (41.1 ± 1.9), osmolality (284 ± 2.9 mosm kg^{-1}) and bicarbonate levels (29.7 ± 0.48 mmol l^{-1}).

Fetal renal blood flow rose from 67.9 ± 5.6 to 84.9 ± 8.3 ml min^{-1} ($P<0.05$, $n = 10$) and renal vascular resistance fell from control values of 0.85 ± 0.09 units to 0.67 ± 0.01 units ($P<0.01$, $n = 10$). Fetal GFR fell within 1 h from 4.2 ± 0.4 ml min^{-1} to 2.7 ± 0.4 ml min^{-1} ($P<0.01$, $n = 11$; Figure 1b) and remained low. Thus filtration fraction (FF, GFR/RBF) decreased from 0.07 ± 0.006 to 0.04 ± 0.006 ($P<0.01$, $n = 10$).

Fetal urine flow rate and free water clearance fell after captopril had been given for 1 h and reached a nadir in the last period of the experiment ($P<0.01$; Figure 1a, Table 1). Osmolar excretion and urinary sodium excretion decreased during captopril treatment ($P<0.05$; Table 1). Potassium excretion did not change, neither did the urinary sodium: potassium ratio (Table 1). Although the total amount of sodium and the amounts of sodium reabsorbed by both proximal and distal tubules decreased ($P<0.05$ or $P<0.01$; Table 2) neither total nor proximal and distal fractional sodium reabsorptions were altered (Table 2). The rates of excretion of ammonium and titratable acid did not change, but bicarbonate excretion fell ($P<0.05$; Table 1).

Effects of chronic captopril treatment on ewe and fetus

On the next 2 days 15 mg (about 319 μg kg^{-1} h^{-1}) of captopril was given i.v. twice daily to the ewe. Fetal arterial blood gases and pH were also measured. Fetal arterial PO_2 remained low (18.7 ± 1.1, $n = 7$; 19.0 ± 1.0, $n = 8$); fetal PCO_2 and pH were 54 ± 2.0 mmHg ($n = 7$), 53 ± 2.2 mmHg ($n = 8$) and 7.36 ± 0.03 and 7.35 ± 0.008 respectively. Urine flow rate was low (Figure 1a). In 3 fetuses on the 4th day following i.v. administration of captopril to the ewe and during i.v. infusion of 6 mg h^{-1} (about 128 μg kg^{-1} h^{-1}) of captopril into the ewe there was either no urine flow or intermittent very low flow. If no urine flow occurred in a 30 min period a value of zero flow was recorded. The values for the 4 × 30 min periods were averaged and this mean value was used. In another 3 fetuses, urine flow was very low at this time while the remaining 3 fetuses produced urine at rates that were within the normal range. The infusion of captopril was stopped after 2 h and an i.v. infusion of 6 μg kg^{-1} h^{-1} of AII was given to the fetus to see if fetal urine flow would resume or increase.

Effects of stopping captopril infusion and infusing AII in 8 ewes and their fetuses

Ewe Maternal arterial pressure started to rise from 80.5 ± 4.1 mmHg ($n = 8$); within 30 min of stopping captopril treat-

Table 1 Acute effects of captopril on maternal and fetal renal function

Ewe	*Con*		PC_2		PC_4	
PRA	0.2 ± 0	(8)	6.1 ± 2.4*	(8)	5.8 ± 1.8*	(7)
HCT (12)	27.2 ± 0.8		29.3 ± 0.9**		29.1 ± 0.9**	
P_{HCO_3} (12)	25.9 ± 0.5		24.6 ± 0.6*		25 ± 0.5	
P_K (12)	3.9 ± 0.11		4.0 ± 0.1		4.2 ± 0.1**	
P_{NaK} (12)	38 ± 0.82		36.9 ± 1.0		35.0 ± 1.1**	
Fetus	*Con*		PC_2		PC_4	
PRA	3.7 ± 1.2	(11)	12.5 ± 2.7**	(11)	12.2 ± 2.6**	(10)
MAPF (12)	53.8 ± 1.1		50.2 ± 1.4**		50.3 ± 1.6**	
Po_2F	21.4 ± 0.8	(12)	19.6 ± 0.7**	(12)	20.3 ± 0.8*	(11)
UV_{Na}	11.9 ± 1.7	(12)	8.0 ± 1.6**	(11)	7.5 ± 1.0**	(11)
C_{H_2O}	0.29 ± 0.06	(11)	0.16 ± 0.04**	(10)	0.13 ± 0.04**	(9)
UV_{OSM} (12)	56.3 ± 4.8		37.1 ± 5.2**		36.7 ± 5.2**	
U_{OSM} (12)	152 ± 32		168 ± 30		185 ± 29	
UV_K	1.5 ± 0.4	(12)	1.3 ± 0.4	(11)	1.2 ± 0.3	(11)
U_{NaK}	17.1 ± 4.8	(12)	14.8 ± 4.4	(11)	14.0 ± 4.1	(11)
UV_{HCO_3}	3 ± 0.06	(8)	2.1 ± 0.5	(6)	1.4 ± 0.2*	(4)
UV_{tit}	1.4 ± 0.4	(8)	1.5 ± 0.3	(6)	1.4 ± 0.5	(4)
UV_{NH_4}	2.5 ± 0.5	(8)	1.9 ± 0.5	(6)	1.9 ± 0.8	(4)

Values are mean ± s.e.mean.

Acute effects of captopril (PC_2 to PC_4) on maternal and fetal plasma renin activity (PRA; ng ml^{-1} h^{-1}), maternal haematocrit (HCT, %), plasma bicarbonate and potassium levels ($PHCO_3$, PK; mmol l^{-1}), sodium:potassium ratio (PNaK) and fetal mean arterial pressure (MAPF; mmHg), arterial oxygen tension (Po_2F; mmHg), urinary sodium excretion (UV_{Na}; μmol min^{-1}), free water clearance (C_{H_2O}; ml min^{-1}), urinary osmolar excretion (UV_{OSM}; μosm min^{-1}), osmolality (U_{OSM}; mosm kg^{-1}), potassium (UV_K; μmol min^{-1}) and bicarbonate (UV_{HCO_3}; μmol min^{-1}) excretions, urinary sodium:potassium ratio (U_{NaK}), titratable acid (UV_{tit}; μmol min^{-1}) and ammonium excretion rates (UV_{NH_4}; μmol min^{-1}).

*$P<0.05$, **$P<0.01$ for differences from control (Dunnett's test). Con = mean of values collected 2 h prior to administration of 15 mg (about 319 μg kg^{-1}) of captopril intravenously to the ewe followed by an infusion to the ewe of 6 mg h^{-1} (about 128 μg kg^{-1} h^{-1}) on Day 1 of the experiment. PC_2 and PC_4 are the 2nd and 4th 30 min collection periods during which captopril was infused into the ewe. Numbers in parentheses = number of animals from which data were obtained.

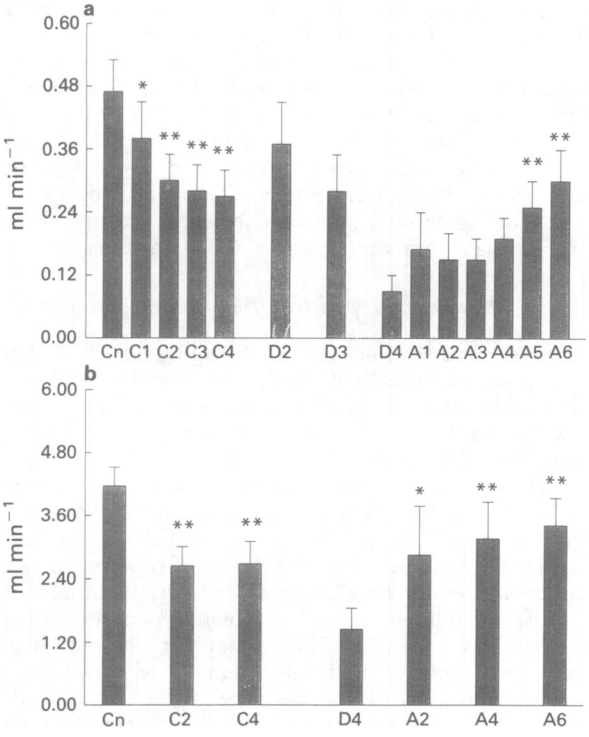

Figure 1 Acute effects (C_1-C_4) and chronic effects (D_4) of captopril (15 mg [about 319 μg kg^{-1}] i.v. followed by an infusion of 6 mg h^{-1} [about 128 μg kg^{-1} h^{-1}] for 2 h given to the pregnant ewe), and the effects of an infusion of angiotensin II (AII, 6 μg kg^{-1} h^{-1}, A_1-A_6) to the fetus on the 4th day on mean ± s.e.mean (a) fetal urine flow, and (b) fetal glomerular filtration rate (ml min^{-1}). Cn = control values. D_2, D_3 = days 2 and 3 of the experiment. A_{1-6} = 6 × 30 min period after captopril treatment of the ewe was stopped and during which the fetus was given 6 μg kg^{-1} h^{-1} of AII. *$P<0.05$; **$P<0.01$. C_1 to C_4 were compared with Cn on Day 1 and A_1 to A_6 were compared with D_4 on Day 4.

ment it was 85.3 ± 14.3 mmHg ($P<0.01$); it continued to increase over the next 2.5 h so that it was 89.4 ± 4.1 mmHg ($P<0.01$) at the end of the experiment. Cardiac output did not change (control values were 10.9 ± 0.1 l min^{-1}, $n = 6$); maternal PRA tended to fall, and haematocrit fell as did maternal plasma sodium:potassium ratio ($P<0.05$, $P<0.01$ respectively; Table 3). In the 9 ewes there were no changes in maternal arterial Po_2 (103 ± 1.3 mmHg), Pco_2 (36.4 ± 1.2 mmHg), pH (7.46 ± 0.009) nor in plasma sodium (146 ± 1.3 mmol l^{-1}), osmolality (294 ± 2.8 mmol l^{-1}) and potassium (4.2 ± 0.1 mmol l^{-1}), but the sodium:potassium ratio declined initially ($P<0.05$; Table 3).

Fetus Fetal arterial pressure increased when the infusion of AII to the fetus began, and captopril treatment of the ewe stopped (Table 3). Heart rate also increased from 161 ± 5.5 beats min^{-1} to 198 ± 11 in the 4th period after captopril treatment finished ($P<0.05$); fetal PRA fell ($P<0.01$; Table 3).

By the end of the 3 h infusion of AII, fetal arterial Po_2 was elevated compared with values obtained during captopril treatment ($P<0.05$; Table 3). Arterial Pco_2 (54.7 ± 1.4 mmHg, $n = 9$), pH (7.34 ± 0.005), plasma sodium (144 ± 1.7 mmol l^{-1}), potassium (3.8 ± 0.13 mmol l^{-1}), sodium:potassium ratio (38 ± 1.5), osmolality (284 ± 2.0 mosm kg^{-1}), bicarbonate (28.2 ± 0.8 mmol l^{-1}) levels and haematocrit (32.4 ± 0.8%) were unchanged in the 8 fetuses given AII.

After captopril treatment of the ewe was stopped and an infusion of AII into the fetus begun, urine flow rate increased within 60 min as did urinary sodium and osmolar excretion in all the animals in which it was measured (Table 3). Free water clearance and the excretion of potassium were unchanged as was the urinary sodium:potassium ratio. The total amount of sodium reabsorbed and the fractional reabsorption of sodium did not change, neither did the amounts and fractions of the filtered sodium load reabsorbed by the proximal and distal tubules (Table 2).

During captopril, mean fetal renal blood flow was 69 ± 10.1 ml min^{-1} ($n = 6$, D_4). At the end of the infusion of AII,

it was 31 ± 13.9 ml min^{-1} ($n = 5$); it decreased in 4 of the 5 fetuses in which both blood flows were measured. Renal vascular resistance also increased from 0.8 ± 0.09 ($n = 6$) to 2.9 ± 0.8 ($n = 5$) units during AII infusion. GFR increased from a mean value of 1.45 ± 0.4 ml min^{-1} measured during captopril treatment to 3.42 ± 0.5 ml min^{-1} measured during A_6 ($P < 0.01$, $n = 8$, Figure 1b). Thus filtration fractions (FF) increased from a mean value of 0.02 ± 0.01 to 0.17 ± 0.06 ($n = 5$). This increase occurred in 4 of the 5 fetuses in which matched values were obtained.

There were no relationships between changes in fetal arterial pressure caused by captopril treatment and changes

Table 2 Effects of captopril alone (Day 1) and together with i.v. infusion of angiotensin II (Day 4) on handling of sodium by the fetal kidney

	Day 1			*Day 4*			
	Con	*PC_2*	*PC_4*	*D_4*	*A_2*	*A_4*	*A_6*
RNa	609 ± 56.8	376 ± 156**	400 ± 175**	355 ± 62.2	395 ± 123.3	437 ± 110	489 ± 83.5
FRNa	97.9 ± 0.3	97.7 ± 0.4	97.4 ± 0.8	97.1 ± 1.0	96.4 ± 1.6	93.4 ± 3.7	96.8 ± 1.4
	(11)	(9)	(10)	(5)	(4)	(6)	(7)
RNaP	427 ± 48.6	269 ± 42**	293 ± 49*	168 ± 67.5	172 ± 105	311 ± 140	373 ± 96.1
FRNaP	63.3 ± 2.7	69.4 ± 2.6	70.1 ± 4.3	76.3 ± 14.6	81.7 ± 7.9	77.9 ± 3.4	76.9 ± 3.2
	(7)	(7)	(7)	(4)	(3)	(5)	(6)
RNaD	212 ± 35	123 ± 15**	112 ± 28**	62.3 ± 12	39.4 ± 12.1	54.2 ± 21	95.2 ± 24.1
FRNaD	34.3 ± 2.7	28.7 ± 2.7	27 ± 3.5	22.8 ± 4.8	21.4 ± 5.9	14.4 ± 3.2	19.6 ± 3.1
	(7)	(6)	(7)	(3)	(2)	(4)	(5)

Day 1: effect of captopril treatment on the handling of sodium by the fetal kidney. Con = control period. PC_2 and PC_4 are the 30 min periods 0.5–1 h and 1.5–2 h after treatment with captopril (15 mg intravenously and 6 μg kg^{-1} h^{-1} captopril) began.
Day 4: data were collected on the 4th day during captopril treatment (D_4) and then during an i.v. infusion of 6 μg kg^{-1} h^{-1} of angiotensin II (AII) to the fetus. A_2, A_4 and A_6 are the 2nd, 4th and 6th 30 min period of infusion of AII into the fetus.
RNa = total reabsorbed sodium (μmol min^{-1}), FRNa = % of filtered sodium load that is reabsorbed, RNaP, FRNaP are the amounts of and % of the filtered sodium reabsorbed by those segments of the nephron that reabsorb lithium (i.e. proximal) and RNaD and FRNaD are the amounts and % of the filtered sodium load reabsorbed at those tubular sites from which lithium is not reabsorbed (i.e. distal).
*$P < 0.05$; **$P < 0.01$ by Dunnett's test. Numbers in parentheses = number of animals from which data were obtained.

Table 3 Values obtained during captopril treatment of ewe and during an i.v. infusion of angiotensin II to the fetus

Ewe	*D_4*	*A_2*	*A_4*	*A_6*
PRA	5.7 ± 1.6	2.7 ± 0.7	1.7 ± 0.6	
	(9)	(8)	(7)	
HCT	28.5 ± 1.1	28.8 ± 1.3	28.3 ± 1.3	27.4 ± 1.1*
	(9)	(8)	(8)	(8)
P_{HCO_3}	25 ± 0.5	25.3 ± 0.6	25.1 ± 0.7	25.4 ± 0.6
	(9)	(8)	(8)	(8)
P_K	4.2 ± 0.1	4.5 ± 0.13	4.3 ± 0.1	4.1 ± 0.1
	(9)	(8)	(8)	(8)
P_{NaK}	35.2 ± 1.0	33 ± 0.9*	33.8 ± 0.9*	35.5 ± 0.8
	(9)	(8)	(8)	(8)
Fetus				
HR	161 ± 5.5	171 ± 8	198 ± 11*	180 ± 5
	(9)	(8)	(8)	(8)
PRA	9.3 ± 2.2	7.2 ± 1.3*	5.7 ± 1.2**	
	(9)	(6)	(7)	
MAPF (8)	47.8 ± 3.5	54.2 ± 3.4**	58.6 ± 3.3**	58.6 ± 3.4**
Po_2	18.1 ± 0.7	18.6 ± 0.6	19 ± 0.5	19.8 ± 0.7*
	(8)	(7)	(7)	(8)
UV_{Na} (8)	5.3 ± 2.2	11.4 ± 6.1	12.2 ± 5	16 ± 8.3
C_{H_2O}	0.03 ± 0.01	−0.01 ± 0.03	0.001 ± 0.03	0.1 ± 0.06
	(8)	(5)	(7)	(7)
U_{OSM}	228 ± 31.2	267 ± 32.9	276 ± 30	222 ± 38.9
	(8)	(7)	(8)	(8)
UV_{OSM}	21.8 ± 6.9	41 ± 17.0	52.1 ± 14.3	63.5 ± 21.5**
	(9)	(8)	(8)	(8)
UV_K	1.1 ± 0.5	1.9 ± 1.2	1.9 ± 0.8	2.7 ± 1.2
	(9)	(8)	(8)	(8)
U_{NaK}	5.4 ± 1.1	7.0 ± 1.3	9.4 ± 2.2	7.3 ± 1.6
	(6)	(7)	(8)	(8)

Mean ± s.e.mean values obtained during captopril treatment of the ewe (i.v. 15 mg [about 319 μg kg^{-1}], followed by an infusion of 6 mg h^{-1} [about 128 μg kg^{-1} h^{-1}] for 2 h) on the 4th day (D_4), and during an i.v. infusion of angiotensin II (AII, 6 μg kg^{-1} h^{-1}) to the fetus for 3 h. A_2, A_4 and A_6 refer to the 2nd, 4th and last 30 min periods of infusion of AII. Maternal and fetal plasma renin activity (PRA; ng ml^{-1} h^{-1}), maternal haematocrit (HCT; %), plasma bicarbonate and potassium levels ($PHCO_3$, PK; mmol l^{-1}), fetal mean arterial pressure (MAPF), oxygen tension (Po_2; mmHg), urinary sodium excretion (UV_{Na}; μmol min^{-1}), fetal free water clearance (C_{H_2O}; ml min^{-1}), urinary osmolality (U_{OSM}; mosm kg^{-1}), urinary osmolar (UV_{OSM}; μosm min^{-1}) and potassium (UV_K; μmol min^{-1}) excretion rates, and plasma and urinary sodium:potassium ratios (P_{NaK}, U_{NaK}).
*$P < 0.05$; **$P < 0.01$ for differences obtained during infusion of angiotensin II (AII, 6 μg kg^{-1} h^{-1}; A_2, A_4 and A_6) from mean values in 2 h period of captopril treatment. Numbers in parentheses = number of animals from which data were obtained.

in fetal renal blood flow or GFR. There was however a direct relationship between the rise in fetal mean arterial pressure and the change in renal blood flow induced by AII infusion ($r = -0.93$, $P < 0.02$, $n = 5$).

Discussion

The ewes were given access to 16–20 g of salt, to reduce the effects of ACE inhibition on maternal blood pressure. These doses of captopril given to the ewe block the pressor response to AI in both ewe and fetus (Lumbers *et al.*, 1992). Maternal pressure still fell, although the effects of captopril on maternal BP were rapidly reversed when captopril treatment was stopped (Table 3). Treatment with captopril was also associated with a fall in maternal plasma sodium:potassium ratio, a rise in plasma potassium and haematocrit (Table 1). This rise in haematocrit suggests that a fall in maternal blood volume occurred; this effect was reversed when captopril treatment was stopped (Table 3). Lack of AII may have led to a fall in maternal plasma aldosterone levels which could account for the changes in potassium, sodium: potassium ratio and haematocrit.

Maternal hypotension due to ACE inhibition is associated with reduced placental blood flow (Lumbers *et al.*, 1992); this probably caused the fall in fetal arterial P_{O_2} that was observed (Tables 1 and 3; see also Lumbers *et al.*, 1992). The fall in fetal arterial P_{O_2} may partly account for the 4 unexplained fetal deaths that occurred within 2 days of beginning treatment. Broughton Pipkin *et al.* (1982) first described the fetotoxic effects of captopril in the fetal sheep and rabbit; the present findings confirm that this drug is toxic for the sheep fetus.

A major reason for carrying out this experiment was to find out why fetal urine flow fell when captopril was given to the pregnant ewe (see Lumbers *et al.*, 1992), and why there have been a number of case reports which show an association between oligohydramnios and/or neonatal anuria during treatment of women with ACE inhibitors during pregnancy (Editorial, Lancet, 1989; Hanssens *et al.*, 1991). In the present study in the sheep in which the ACE inhibitor used, i.e. captopril, crossed the placenta, there was an initial acute fall in urine flow. Significantly by the 4th day of treatment 6 of the 9 remaining fetuses were oliguric or anuric, although this was rapidly reversed when maternal captopril treatment was stopped and AII infused directly into the fetus. These changes in urine flow (Figure 1a) and sodium excretion (Table 2 and 3) were due to changes in fetal GFR. There were no changes in tubular handling of sodium except those that were dependent on the concomitant changes in GFR, i.e. glomerulotubular balance was maintained (Table 2).

Kleinman & Lubbe (1972) concluded that the arterial pressures of very young animals were below the autoregulatory range. Blockade of the fetal renin angiotensin system produces falls in fetal arterial pressure that are variable (see Broughton Pipkin & O'Brien, 1978; Iwamoto & Rudolph, 1979; Lumbers *et al.*, 1992). In a previous study, i.v. infusion of the AII antagonist, saralasin, had minimal effects on fetal arterial pressure, yet GFR fell by about 0.9 ml min^{-1}, a fall similar to the fall in GFR that occurred (0.87 ml min^{-1}) when fetal arterial pressure was lowered by 14/9 mmHg (Lumbers & Stevens, 1987). A contribution to the fall in GFR of the small fall in fetal arterial pressure (ca. 3 mmHg) due to captopril treatment cannot be completely excluded. In sick infants treated with captopril, oliguria in association with severe hypotension has been reported (Tack & Perlman, 1988). However, it is likely that in fetuses, saralasin and captopril reduced GFR through effects other than their effects on arterial pressure. Since RBF increased, and renal vascular resistance and GFR fell, GFR probably failed because post glomerular (efferent arteriolar) resistance fell. When AII levels were increased renal vascular resistance rose as did GFR. Only a post glomerular action of AII could cause these changes to occur simultaneously. Therefore, in the fetus, normal fetal renal function depends on the integrity of the fetal RAS. This is not the case in the normal adult, although in the adult underperfused kidney (e.g. in renal artery stenosis) AII does play an essential role in maintenance of GFR (Hall *et al.*, 1979; Anderson *et al.*, 1990). The fetal kidney is underperfused, i.e. fetal sheep renal plasma flow is low (about 1.0 ± 0.2 ml min^{-1} g^{-1} kidney). In adult nonpregnant sheep it is 4.7 ± 0.5 ml min^{-1} g^{-1} (Hill, 1985; Hill & Lumbers, 1988). Fetal and adult GFRs are 0.14 ± 0.01 and 0.66 ml min^{-1} g^{-1} kidney respectively (Hill, 1985; Hill & Lumbers, 1988). Thus the filtration fractions (FF) are the same (ca. 0.14), yet the renal perfusion pressure is 35 mmHg less in the fetus (see Table 1 and Figure 1a). To maintain a similar FF at this lower perfusion pressure, fetal post glomerular resistance (efferent arteriolar tone) must normally be high. Since lack of AII was associated with failure of GFR and renal vasodilatation, and infusion of AII restored GFR while renal vascular resistance increased, it would seem that the endogenous fetal RAS plays an essential role in maintenance of post glomerular vascular resistance and therefore GFR.

In summary, inhibition of the activities of fetal and maternal RAS were associated with maternal hypotension, a fall in fetal arterial P_{O_2}, preliminary evidence of reduced maternal blood volume and unexpected fetal death. All these, except for the haemoconcentration, have been reported previously under acute conditions (Broughton Pipkin *et al.*, 1982; Lumbers *et al.*, 1992). In addition, blockade of the fetal RAS caused oliguria/anuria due to failure of glomerular ultrafiltration in 6 of the 9 surviving fetuses. It is not clear why there was a variability in the sensitivity of individual fetuses to this effect of captopril. It should be noted, that this is also seen in clinical case reports, e.g. Kreft Jais *et al.* (1987) reported no cases of neonatal anuria among 22 women who had received captopril, whilst the editorial in Lancet (1989) cites 10 case reports of oliguria/anuria. Since fetal urine is the major substrate of amniotic fluid, oliguria and anuria will cause oligohydramnios and pulmonary hypoplasia (see Brent & Beckman, 1991). The effects of fetal ACE inhibition on fetal renal function were rapidly reversed by stopping captopril treatment and infusing AII.

This work was supported by grants from the National Health and Medical Research Council (Australia) and the Australian Kidney Foundation. We would like to thank Ms R. Enriquez and Ms R. Zucca for their technical assistance.

References

ANDERSON, W.P., DENTON, K.M., WOODS, R.L. & ALCORN, D. (1990). Angiotensin II and the maintenance of GFR and renal blood flow during renal artery narrowing. *Kidney Int.*, **38**, S109–S113.

ARMENTROUT, T., KATZ, S., THORNBURG, K.L. & FABER, J.J. (1977). Osmotic flow through the placental barrier of chronically prepared sheep. *Am. J. Physiol.*, **233**, H466–H474.

BRENT, R.L. & BECKMAN, D.A. (1991). Angiotensin-converting enzyme inhibitors, an embryopathic class of drugs with unique properties: information for chemical teratology counselors. *Teratology*, **43**, 543–546.

BROUGHTON PIPKIN, F. & O'BRIEN, P.M.S. (1978). Effect of the specific angiotensin antagonist (Sar^1) (Ala^8) angiotensin II on blood pressure and the renin-angiotensin system in the conscious pregnant ewe and fetus. *Am. J. Obstet. Gynecol.*, **132,** 7–15.

BROUGHTON PIPKIN, F., SYMONDS, E.M. & TURNER, S.R. (1982). The effect of captopril (SQ 14,225) upon mother and fetus in the chronically cannulated ewe and in the pregnant rabbit. *J. Physiol.*, **323,** 415–422.

CAINE, A.C., LUMBERS, E.R. & REID, I.A. (1985). The effects and interactions of angiotensin and vasopressin on the heart of unanaesthetized sheep. *J. Physiol.*, **367,** 1–11.

EDITORIAL (1989). Are ACE inhibitors safe in pregnancy? *Lancet*, **ii,** 482–483.

ELBOURNE, I., LUMBERS, E.R. & HILL, K.J. (1990). The secretion of organic acids and bases by the ovine fetal kidney. *Q. J. Exp. Physiol.*, **75,** 211–221.

GIBSON, K.J. & LUMBERS, E.R. (1992). Mechanisms by which the pregnant ewe can sustain increased salt and water supply to the fetus. *J. Physiol.*, **445,** 569–579.

GYORY, A.Z. & EDWARDS, K.D.G. (1967). Simultaneous determination of bicarbonate and titratable acid in urine. *Aust. J. Exp. Biol. Med. Sci.*, **45,** 141–147.

GYORY, A.Z., EDWARDS, K.D.G., STEWART, J.H. & WHYTE, H.M. (1974). Comprehensive one-day renal function testing in man. *J. Clin. Pathol. (Lond.)*, **27,** 382–391.

HALL, J.E., COLEMAN, T.O., GUYTON, A.C., BALFE, J.W. & SALGADO, H.C. (1979). Intrarenal role of angiotensin II and (des-Asp) angiotensin II. *Am. J. Physiol.*, **236,** F252–F259.

HANSSENS, M., KEIRSE, M.J., VANKELECOM, F. & ANDRÉ VAN ASSCHE, F. (1991). Fetal and neonatal effects of treatment with angiotensin-converting enzyme inhibitors in pregnancy. *Obstet. Gynecol.*, **78,** 128–135.

HEYMANN, M.A., PAYNE, B.D., HOFFMAN, J.I.E. & RUDOLF, A.M. (1977). Blood flow measurements with radionuclide labelled particles. *Prog. Cardiovasc. Dis.*, **20,** 55–79.

HILL, K.J. (1985). Renal function: endocrine and developmental aspects. *Br. Med. Sci. Thesis*, University of NSW, pp. 89–90.

HILL, K.J. & LUMBERS, E.R. (1988). Renal function in adult and fetal sheep. *J. Develop. Physiol.*, **10,** 149–159.

IWAMOTO, H.S. & RUDOLPH, A.M. (1979). Effect of endogenous angiotensin II on the fetal circulation. *J. Develop. Physiol.*, **1,** 283–293.

KLEINMAN, L.I. & LUBBE, R.J. (1972). Factors affecting the maturation of glomerular filtration rate and renal plasma flow in the new-born dog. *J. Physiol.*, **223,** 395–409.

KREFT-JAIS, C., PLOUIN, P.-F. & TCHBROUTSKY, C. (1987). Angiotensin converting enzyme inhibition with captopril in human pregnancy. *J. Hypert.*, **5** (Suppl. 5), S553–S554.

LUMBERS, E.R., HILL, K.J. & BENNETT, V.J. (1988). Proximal and distal tubular activity in chronically catheterized fetal sheep compared with the adult. *Can. J. Physiol. Pharmacol.*, **66,** 697–702.

LUMBERS, E.R., KINGSFORD, N.M., MENZIES, R.I. & STEVENS, A.D. (1992). The acute effects of captopril, an angiotensin converting enzyme inhibitor, on the pregnant ewe and her fetus. *Am. J. Physiol.*, **262,** R754–R760.

LUMBERS, E.R. & LEE LEWIS, J. (1979). The actions of vasoactive drugs on fetal and maternal plasma renin activity. *Biol. Neonate*, **35,** 23–32.

LUMBERS, E.R., SMITH, F.G. & STEVENS, A.D. (1985). Measurement of net transplacental transfer of fluid to the fetal sheep. *J. Physiol.*, **364,** 289–299.

LUMBERS, E.R. & STEVENS, A.D. (1983). Changes in fetal renal function in response to infusions of a hyperosmotic solution of mannitol to the ewe. *J. Physiol.*, **343,** 439–446.

LUMBERS, E.R. & STEVENS, A.D. (1987). The effects of frusemide, saralasin and hypotension on fetal plasma renin activity and on fetal renal function. *J. Physiol.*, **393,** 479–490.

NIE, N.H., HULL, C.H., STEINBRENNER, K. & BENT, D.H. (1982). *Statistical Package for the Social Sciences* (2nd ed.). London: McGraw-Hill.

ROBILLARD, J.E., GOMEZ, R.A., VAN ORDEN, D. & SMITH, F.G. JR. (1982). Comparison of the adrenal and renal responses to angiotensin II in fetal lambs and adult sheep. *Circ. Res.*, **50,** 140–147.

ROBILLARD, J.E., WEISMANN, D.N., GOMEZ, A., AYRES, N.A., LAWTON, W.J. & VAN ORDEN, D.E. (1983). Renal and adrenal responses to converting enzyme inhibition in fetal and newborn life. *Am. J. Physiol.*, **244,** R249–R256.

ROBILLARD, J.E., WEISMAN, D.N. & HERIN, P. (1981). Ontogeny of single glomerular perfusion rate in fetal and newborn lambs. *Pediatr. Res.*, **15,** 1248–1255.

SHUBIGER, G., FLURY, G. & NUSSBERGER, J. (1988). Enalapril for pregnancy-induced hypertension: acute renal failure in a neonate. *Ann. Int. Med.*, **108,** 215–216.

TACK, E.D. & PERLMAN, J.M. (1988). Renal failure in sick hypertensive premature infants receiving captopril therapy. *J. Pediatr.*, **112,** 805–810.

THOMSEN, K., HOLSTEIN-RATHLOU, N.H. & LEYSSAC, P.P. (1981). Comparison of three measures of proximal reabsorption: lithium clearance, occlusion time, and micropuncture. *Am. J. Physiol.*, **241,** F348–F355.

ZAR, J.H. (1984). *Biostatistical Analysis* (2nd ed.). Englewood Cliffs, N.J.: Prentice-Hall Inc.

(Received March 29, 1993
Revised May 20, 1993
Accepted May 21, 1993)

Br. J. Pharmacol. (1993), **110**, 828–832

Ionomycin-induced acetylcholine release and its inhibition by adenosine at frog motor nerve endings

[1]James M. Hunt & [2]Eugene M. Silinsky

Department of Pharmacology, Northwestern University Medical School, 303 East Chicago Avenue, Chicago, IL 60611, U.S.A.

1 Acetylcholine (ACh) evoked secretion by the calcium ionophore, ionomycin, was studied at frog motor nerve endings.

2 Bath application of ionomycin stimulated an irreversible increase in the rate of spontaneous, quantal ACh release in the presence of extracellular Ca^{2+}. In contrast, local application of ionomycin stimulated a rapid, reversible acceleration of spontaneous ACh release.

3 The magnitude of the secretory response to ionomycin was dependent both upon the concentration of ionophore and the concentration of extracellular Ca^{2+}.

4 Adenosine or 2-chloroadenosine inhibited ionomycin-stimulated ACh release with the same potency and efficacy observed previously for these adenosine analogues as inhibitors of ACh secretion evoked by nerve impulses.

5 These results support the conclusion that adenosine receptor activation inhibits quantal ACh secretion at a site distal to that of Ca^{2+} entry at frog motor nerve endings.

Keywords: Neurotransmitter release; frog neuromuscular junction; adenosine; ionomycin; calcium

Introduction

Adenosine inhibits the release of neurotransmitter substances in both the central and peripheral nervous systems of many vertebrate species (Phillis, 1985; Ribeiro & Sebastiao, 1986; Silinsky, 1989). At vertebrate motor nerve endings, exogenous adenosine has been shown to reduce both the synchronized release of acetycholine (ACh) by nerve impulses and the rate of spontaneous secretion of discrete acetylcholine quanta (Ginsborg & Hirst, 1972; Silinsky, 1984). Studies in hippocampal slices (Fredholm *et al.*, 1990), rat brain synaptosomes (Ribeiro *et al.*, 1979), and rat neuromuscular junction (Hamilton & Smith, 1991) have suggested that adenosine reduces depolarization-induced Ca^{2+} entry into the nerve terminals, thus reducing the amount of Ca^{2+} available to trigger neurotransmitter release. However, studies in rat brain synaptosomes (Barr *et al.*, 1985), and at neuromuscular junctions of frog (Silinsky, 1984; Silinsky & Solsona, 1992), *Torpedo* (Muller *et al.*, 1987), and rat (Ginsborg & Hirst, 1972) have suggested that adenosine might be acting at a site distal to Ca^{2+} entry, thus reducing the amount of neurotransmitter released by a given amount of Ca^{2+}.

Although physiological neurotransmitter release is triggered by a depolarization-induced Ca^{2+} influx through voltage-dependent calcium channels, Ca^{2+} from other sources is also able to trigger neurotransmitter secretion. For example, calcium-containing lipid vesicles (liposomes) have been found to deliver their entrapped Ca^{2+} to the nerve terminal cytoplasm and induce ACh release by a method that bypasses active Ca^{2+} channels. ACh release evoked by calcium-containing liposomes is also inhibited by adenosine (Silinsky, 1984), thus implying that adenosine is acting at a site distal to Ca^{2+} entry in the frog.

With regard to the liposome experiments, it has been suggested that adenosine could be inhibiting the fusion of liposomes with the nerve terminal plasma membrane, thus reducing neurotransmitter release by reducing the rate at which Ca^{2+} is delivered to the nerve terminal (see comment by J.W. Phillis in discussion to Silinsky *et al.*, 1987). To address this possibility, we have used the Ca^{2+} ionophore ionomycin (Beeler *et al.*, 1979) to deliver Ca^{2+} to the nerve terminal cytoplasm as an alternative method of bypassing Ca^{2+} channels. Ionomycin is an anionic polyether antibiotic ionophore which has been shown to be highly selective for Ca^{2+}. In this paper we describe the characteristics of ionomycin-induced ACh release at frog neuromuscular junction and its inhibition by adenosine. Some of these results have been presented previously as an abstract (Hunt *et al.*, 1992).

Methods

General

Cutaneous pectoris nerve-muscle preparations of the frog *Rana pipiens* were dissected and superfused with flowing Ringer solution. Supramaximal stimulation pulses were delivered to the nerve supply through a suction electrode. Intracellular recordings were made at endplate regions by use of glass microelectrodes filled with 3 M KCl and with resistances of 8–25 Mohms. Signals from the microelectrode were fed into a conventional high input impedance preamplifier, the output of which was delivered to an oscilloscope, an AT-compatible microcomputer (via a TL-1 DMA interface purchased from Axon Instruments Inc. for on line data collection), and an Indec IR-2 Instrumentation Recorder (in the event that further data analysis was required).

Miniature endplate potentials (m.e.p.ps) were recorded on line and later analysed with the Axotape software package (Axon Instruments). In a few experiments, endplate potentials (e.p.ps) were recorded on line and later analysed using the pClamp software package (Axon Instruments).

Measurements of quantal ACh release

The rate of spontaneous, quantal ACh release (m.e.p.p. frequency) was determined by continuously monitoring membrane potential and counting the number of m.e.p.ps per second. Reported me.p.p. frequencies are the average of at least 30 s of continuous recording unless otherwise noted in the text. The plots of m.e.p.p. frequency over time were constructed using a 10 s bin of m.e.p.p. frequency shifted by

[1] Present address: Department of Neurobiology, Dook University, Durham, NC, U.S.A.
[2] Author for correspondence.

5 s (Rahamimoff & Yaari, 1973). This method tends to minimize the effects of small bursts of m.e.p.ps and allows for a more accurate determination of the time lag between addition of calcium to the superfusion fluid and a rise in m.e.p.p. frequency. In a few experiments, the mean number of ACh quanta released synchronously by a nerve impulse was calculated by conventional methods (del Castillo & Katz, 1954; see Discussion).

The statistical procedures are identical to those described previously (see Silinsky, 1984, pp. 244–245). In most instances, appropriate averaging techniques were used to make statistically significant differences at $P<<0.01$ (see Silinsky, 1984). In instances where significance was at the $P<0.05$ level, this is stated within the text.

Solutions and drug application

Normal frog Ringer contained (mM): NaCl 115, KCl 2, $CaCl_2$ 1.8, HEPES 2 (to buffer the pH of the Ringer to 7.2–7.4) and was used in the majority of experiments during electrode impalement. In many experiments Ca^{2+}-free or low Ca^{2+} Ringer was used to control the level of ACh release. The Ca^{2+}-free Ringer contained no added $CaCl_2$, 1.8 mM $MgCl_2$ and 1 mg l^{-1} neostigmine methyl sulphate to increase m.e.p.p. amplitudes. The low Ca^{2+} Ringer contained 1.8 mM $MgCl_2$, 1 mg l^{-1} neostigmine methylsulphate and the indicated concentration of $CaCl_2$. Chemicals were purchased from Sigma Chemicals (St. Louis, MO, U.S.A.) with the exception of ionomycin which was obtained from Cal-Biochem (La Jolla, CA, U.S.A.). Stock solutions of ionomycin were prepared by injecting 470 µl of dimethylsulphoxide (DMSO) into a 5 mg vial of ionomycin. Dilution of 10 µl of this stock solution to 10 ml with Ringer gave a final concentration of 15 µM ionomycin and 0.1% v/v DMSO. When lower concentrations of ionomycin were used, DMSO was added to maintain a final concentration of 0.1% v/v.

Ionomycin and adenosine were dissolved in Ringer solution and administered by one of two methods of superfusion. For the first method, bath administration, indicated concentrations of drug were superfused over the entire preparation. Solutions were changed by transferring the inlet tube of the roller pump from one solution to another. For the second method, local fast-flow application, solutions were gravity fed through one of a series of glass barrels (300 µm inside diameter, Garner glass), positioned in such a way that the solution bathed only the area surrounding the site of microelectrode impalement (Yellen, 1982). With this rapid superfusion system, the latency between the opening of a fast-flow barrel and the beginning of a depolarization evoked by ACh (100 µM) was 50–100 ms.

Results

General observations on the effects of ionomycin on spontaneous ACh release

Ionomycin (15 µM) increased the rate of spontaneous quantal acetylcholine release (m.e.p.p. frequency) and required extracellular Ca^{2+} to do so. Figure 1 illustrates a typical experiment with bath application of ionomycin. Note that extracellular Ca^{2+} was present at the beginning and end of the experiment but was absent during the period indicated by the lower bar (Figure 1, Ca^{2+}-free). As Figure 1 shows, before the additon of ionomycin, when the Ringer was changed from the Ca^{2+}-containing solution to Ca^{2+}-free Ringer (lower bar), no changes in m.e.p.p. frequency were observed. Similarly, addition of ionomycin (upper bar) in the absence of extracellular Ca^{2+} also had no significant effect on m.e.p.p. frequency. However, re-introducing Ca^{2+} in the presence of ionomycin (Figure 1, end of lower bar) increased m.e.p.p. frequency by more than ten fold before a spontaneous muscle contracture dislodged the electrode. In the

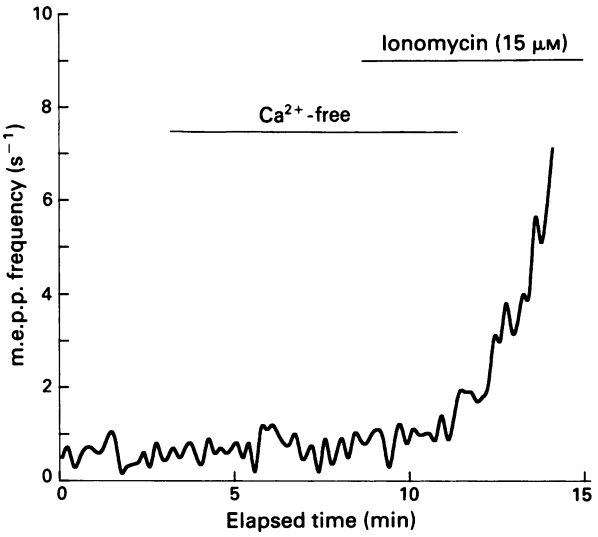

Figure 1 Increases in quantal acetylcholine (ACh) release produced by bath application of ionomycin (15 µM). Preparation was superfused with calcium Ringer containing 0.9 mM $Ca^{2+}$and 1.8 mM Mg^{2+} except during time indicated by the lower bar (Ca^{2+}-free) during which the preparation was superfused with Ringer containing no added Ca^{2+} and 1.8 mM Mg^{2+}. Upper bar indicates addition of ionomycin in Ringer. Note m.e.p.p. frequency only began to increase significantly after Ca^{2+} was returned to the bath.

majority of experiments, muscle contractures occurred within 5–10 min following exposure to ionomycin and Ca^{2+}. However, in several experiments the impalements were maintained as long as 45 min following the withdrawal of ionomycin with no decrease in m.e.p.p. frequency (data not shown).

The extent to which ionomycin increased m.e.p.p. frequency was quite variable. In one preparation, following a 5–10 min exposure to 15 µM ionomycin, m.e.p.p. frequencies ranging from 2–3 s^{-1} to >40 s^{-1} were seen in 25 impalements. The m.e.p.p. frequencies remained high after ionomycin superfusion was stopped but declined in the absence of extracellular Ca^{2+}. This variability may reflect a heterogeneity in the ability of nerve terminals to extrude Ca^{2+} that had been transported into the cytoplasm via ionophore (Rasgado-Flores *et al.*, 1987).

Local application of 15 µM ionomycin by fast flow superfusion (Yellen, 1982) also produced increases in m.e.p.p. frequency, but these were rapidly reversible. Figure 2 shows an example of a nerve terminal responding strongly to local application of 15 µM ionomycin (bar) in the presence of extracellular Ca^{2+}. As with bath application, the response to ionomycin was quite variable between nerve terminals. However, the speed with which it is possible to change solutions with the fast flow superfusion system (see Methods) allowed us to examine dose-response relationships between ionomycin or external Ca^{2+} concentration and m.e.p.p. frequency in single impalements.

Dependency of ionomycin-induced ACh released on the concentrations of ionomycin and extracellular Ca^{2+}

Figures 3 and 4 illustrate experiments made using fast-flow superfusion methods to evaluate the dependency of ACh release upon the concentrations of ionomycin (Figure 3) and Ca^{2+} (Figure 4). Figure 3 shows that larger increases in m.e.p.p. frequency were observed with increasing concentrations of ionomycin. Note that the external Ca^{2+} concentration was held constant throughout the experiment, suggesting that the rate of Ca^{2+} transport increased with the concentration of ionomycin. Figure 4 shows that a constant concentration of ionomycin stimulated larger increases in m.e.p.p. frequencies as the extracellular Ca^{2+} concentration was in-

creased. These results suggest that ionomycin is an efficient transporter of Ca^{2+} from the extracellular fluid to the strategic regions of the nerve terminal that promote ACh release.

Inhibition of ionomycin-stimulated ACh secretion by adenosine

Maximal concentrations of adenosine receptor agonists generally reduce spontaneous ACh release (m.e.p.p. frequency) and evoked ACh release (e.p.p. amplitude) by approximately 50% (Silinsky, 1984). In a total of 13 experiments, 50 μM adenosine or 25 μM 2-chloroadenosine reduced m.e.p.p. frequency 50.4 ± 1.9% (range 38–63%) in the presence of ionomycin and extracellular Ca^{2+}. This implies the maximal effect of adenosine receptor activation is unchanged in the presence of ionomycin. With regards to the potency of adenosine, Figure 5 summarizes the dose-response relationship for adenosine as an inhibitor of ionomycin-stimulated ACh secretion in two cells. Of the two cells, one responded strongly to ionomycin (m.e.p.p. frequency ≈21 s^{-1}), while the other did not (m.e.p.p. frequency ≈2.5 s^{-1}). In both of these cells the concentration of adenosine needed to produce maximal inhibition was 20–30 μM. Thus the

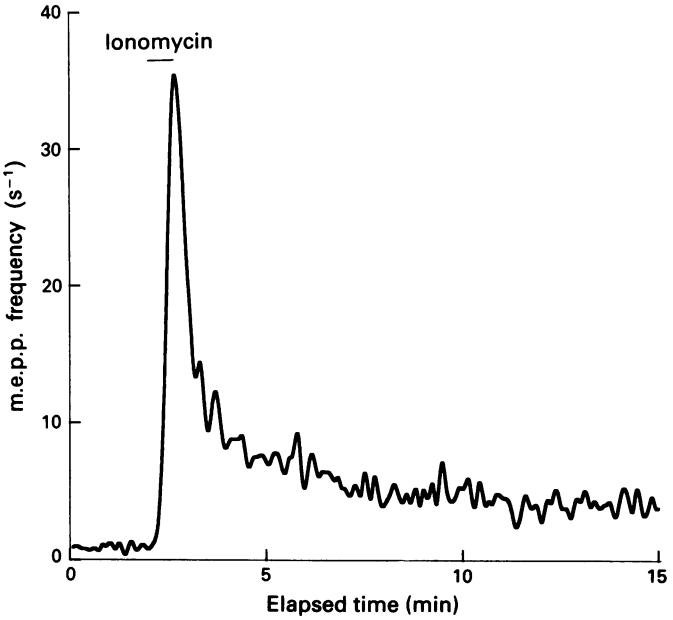

Figure 2 Increases in acetylcholine (ACh) release produced by local fast-flow application of ionomycin. Preparation was superfused in the bath with low Ca^{2+} Ringer containing 1 mM Ca^{2+} and 1.8 mM Mg^{2+} for the duration of the experiment. During the time indicated by the bar 15 μM ionomycin was superfused locally.

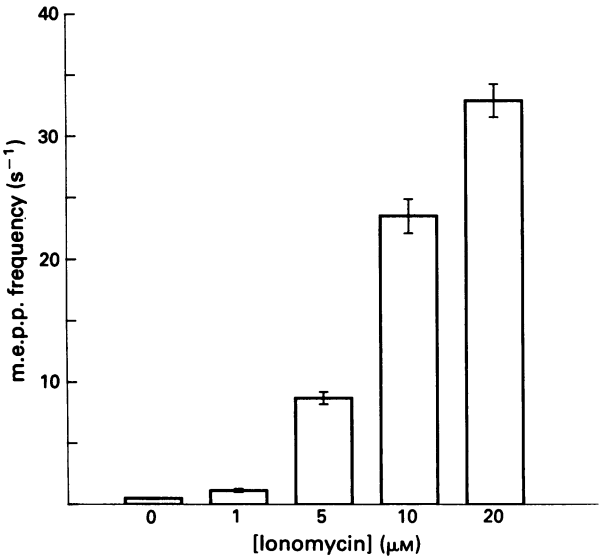

Figure 3 Concentration-dependence of ionomycin-induced acetylcholine (ACh) release. Preparation was bathed in low Ca^{2+} Ringer containing 0.5 mM Ca^{2+} and 1.8 mM Mg^{2+}. The indicated concentration of ionomycin was applied via the fast-flow superfusion system. Similar results were seen in 4 experiments.

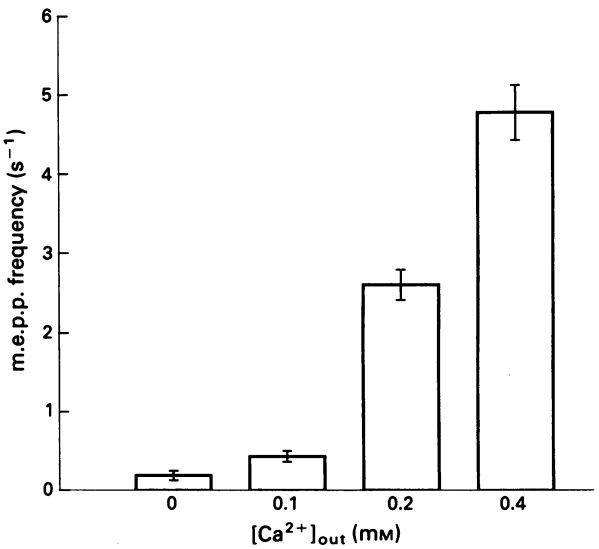

Figure 4 Calcium-dependence of ionomycin-stimulated increases in m.e.p.p. frequency. Preparation was bathed in Ca^{2+}-free Ringer with 5 μM ionomycin added. The indicated concentration of Ca^{2+} was applied via the fast-flow superfusion system. Similar results were seen in 3 experiments.

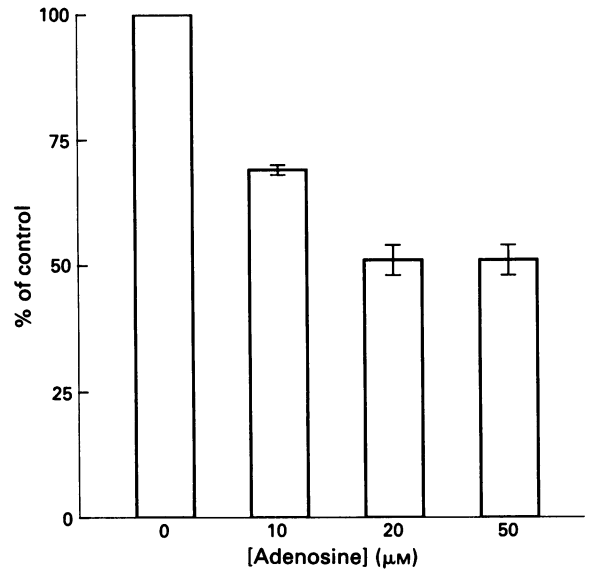

Figure 5 Concentration-dependent inhibition of ionomycin-stimulated acetylcholine (ACh) secretion by adenosine. Preparation was bathed in low Ca^{2+} Ringer containing 0.5 mM Ca^{2+}, 1.8 mM Mg^{2+}, and 5 μM ionomycin. The indicated concentration of adenosine was applied via the fast-flow superfusion system. The results show the averaged dose-response data from two experiments. Control m.e.p.p. frequencies were 2.63 s^{-1} and 21.15 s^{-1}. For details of other experiments, see text.

potency and efficacy of adenosine is unchanged in the presence of a Ca^{2+} influx stimulated by ionomycin (see Silinsky, 1984, for example).

Discussion

These results are consistent with ionomycin acting as a rapid, selective ionophore for translocating extracellular Ca^{2+} into the nerve terminal cytoplasm. Once in the cytoplasm, the Ca^{2+} delivered by this ionophore reaches strategic regions of the nerve terminal that control neurotransmitter release and accelerates the rate of quantal ACh release.

X-537A, a less specific ionophore, also increases ACh release (Kita & Van der Kloot, 1976). However, X537A also admits Na^+ and hence causes membrane depolarization as well as producing a profound decrease in postjunctional ACh sensitivity. Such effects were not observed with ionomycin in these experiments. Furthermore, in PC12 cells, X-537A induced the secretion of catecholamines (Pozzan *et al.*, 1984) but this effect was accompanied by disruption of cell morphology and lysis of secretory vesicles. In the same study ionomycin did not induce any morphological changes during secretion from PC12 cells. A23187, a less selective Ca^{2+} ionophore (Liu *et al.*, 1978), has also been used to study secretion. However, at frog neuromuscular junction, A23187 produced irreversible ultra-structural changes both at nerve endings (Llados *et al.*, 1984) and at post-junctional loci (Statham *et al.*, 1976). Thus, our present results, when viewed in the light of these previous studies, suggest that ionomycin is a kinder, gentler ionophore, which can be a very useful tool for bypassing voltage-dependent Ca^{2+} channels while studying the properties of calcium-dependent neurosecretion.

It should be noted that X-537A was also reported to increase e.p.p. amplitude (Kita & Van der Kloot, 1976). In several experiments (data not shown) ionomycin increased e.p.p. amplitude by increasing the mean number of quanta released. Increases in evoked ACh release produced by ionomycin were also antagonized by adenosine (data not shown).

Both bath application and fast flow superfusion of ionomycin increased m.e.p.p. frequency in the presence of extracellular calcium. However, with fast-flow superfusion, ionomycin increased m.e.p.p. frequency more rapidly and in a largely reversible manner. This suggests that the kinetics of the ionomycin response are strongly influenced by tissue loading, as might be expected for such a lipophilic compound. Indeed, a similar phenomenon has been seen when phorbol esters are used to activate protein kinase C. Specifically, initial experiments in hippocampal slices suggested that phorbol esters produced an irreversible potentiation of neurotransmitter release (Akers *et al.*, 1986; Malenka *et al.*, 1986). In contrast, later experiments using more extensive washing revealed the phorbol-induced potentiation to be reversible (Muller *et al.*, 1988). Thus, the use of local superfusion techniques for the administration of lipophilic compounds may help to avoid experimental artefacts due to tissue loading.

If voltage-dependent Ca^{2+} channels are the target sites for the inhibitory effects of adenosine, then ACh secretion induced by ionomycin should be insensitive to adenosine. In fact, this is *not* the case. Adenosine inhibited ACh release from frog motor nerve endings regardless of whether the trigger Ca^{2+} emanated from voltage-dependent Ca^{2+} channels, Ca^{2+}-filled liposomes (Silinsky, 1984), or Ca^{2+} ionophores (this paper). Furthermore, recent evidence suggests that Ca^{2+} currents responsible for initiating evoked ACh release at frog motor nerve endings are not blocked by adenosine (Silinsky & Solsona, 1992). Thus, at frog neuromuscular junctions, adenosine must be acting at a site distal to Ca^{2+} entry.

It is not known whether Ca^{2+}-dependent ACh release evoked by methods which avoid active membrane Ca^{2+} channels can be inhibited by adenosine at motor nerve endings in species other than frog. Some evidence in favour of an intracellular target site for the effect of adenosine has been found in studies on rat neuromuscular junctions (Ginsborg & Hirst, 1972). However, in rat motor nerve, adenosine (50 μM) reduces Ca^{2+} currents measured in solutions containing high concentrations of K^+ channel blockers by 29% (Hamilton & Smith, 1991). As Ca^{2+} currents in mammalian motor nerve endings are not blocked by ω-conotoxin (Anderson & Harvey, 1987) and are thus not of the N-type found in frog (Silinsky & Solsona, 1992), it is possible that adenosine receptors in different species could be coupled to different transduction mechanisms. For example mammalian motor nerve endings may possess P channels (Llinas *et al.*, 1989; Hamilton & Smith, 1991; Silinsky & Solsona, 1992) which could be inhibited by adenosine either by a direct coupling between pertussis toxin-sensitive G-proteins (Hamilton & Smith, 1991) or indirectly via soluble second messengers (Chen *et al.*, 1989). It is also possible that moderate effects of neuromodulatory substances can be observed on Ca^{2+} entry under conditions in which the principal inhibitory action is at the secretory apparatus (see Man-Son-Hing *et al.*, 1989; see below).

Results of experiments on hippocampus (Dunwiddie, 1984; Klapstein & Colmers, 1992) and rat cultured hippocampal neurones (Scholz & Miller, 1992) are consistent with a mechanism by which adenosine inhibits neurotransmitter release downstream of Ca^{2+} entry. Furthermore, in cultured snail neurones, the predominant mechanism by which FRMF-amide inhibits ACh release is also independent of Ca^{2+} entry (Man-Son-Hing *et al.*, 1989). Finally, in non-neural cells, it has been suggested that somatostatin inhibits both ACTH secretion from anterior pituitary (AtT-20) cells (Luini & de Matteis, 1990) and insulin secretion from HIY-T15 insuloma cells (Ullrich *et al.*, 1990) independently of Ca^{2+} entry. These results suggest that the process by which adenosine inhibits ACh release at frog motor nerve endings may not be unique to the neuromuscular junction or even to adenosine, but may represent a common mechanism by which the release of a prepackaged secretory product is modulated.

This work was supported by a research grant (NS 12782) and a training grant from the National Institutes of Health (T32 NS 07140).

References

AKERS, R.F., LOVEINGER, D.M., COLLEY, P.A., LINDEN, D.J. & ROUTTENBERG, A. (1986). Translocation of protein kinase C activity may mediate hippocampal long-term potentiation. *Science*, **231**, 587–589.

ANDERSON, A.J. & HARVEY, A.L. (1987). ω-Conotoxin does not block the verapamil-sensitive calcium channels at mouse motor nerve terminals. *Neurosci. Lett.*, **82**, 177–180.

BARR, E., DANIEL, L.C. & LESLIE, S.W. (1985). Synaptosomal calcium uptake unaltered by adenosine and 2-chloroadenosine. *Biochem. Pharmacol.*, **34**, 713–715.

BEELER, T.J., JONA, I. & MARTONOSI, A. (1979). The effect of ionomycin on calcium fluxes in sarcoplasmic reticulum vesicles and liposomes. *J. Biol. Chem.*, **254**, 6229–6231.

CHEN, H., SINGH, Y.N. & DRYDEN, W.F. (1989). Transduction mechanism involving the presynaptic adenosine receptor at mouse motor nerve terminals. *Neurosci. Lett.*, **96**, 318–322.

DEL CASTILLO, J. & KATZ, B. (1954). Quantal components of the end-plate potential. *J. Physiol.*, **124**, 560–573.

DUNWIDDIE, T.V. (1984). Interactions between the effects of adenosine and calcium on synaptic responses in rat hippocampus *in vitro*. *J. Physiol.*, **350**, 545–559.

FREDHOLM, B.B., DUNER-ENGSTROM, M., FASTBOM, J., HU, P.S. & VAN DER PLOEG, I. (1990). Role of G proteins, cyclic AMP, and ion channels in the inhibition of transmitter release by adenosine. *Ann. NY Acad. Sci.*, **604**, 276–288.

GINSBORG, B.L. & HIRST, G.D.S. (1972). The effect of adenosine on the release of the transmitter from the phrenic nerve of the rat. *J. Physiol.*, **224**, 629–645.

HAMILTON, B.R. & SMITH, D.O. (1991). Autoreceptor-mediated purinergic and cholinergic inhibition of motor nerve terminal calcium currents in the rat. *J. Physiol.*, **432**, 327–341.

HUNT, J.M., WILFERHT, H.M. & SILINSKY, E.M. (1992). Adenosine inhibits the calcium-dependent acetylcholine secretion induced by ionomycin. *Soc. Neurosci. Abs.*, **18**, 636.

KITA, H. & VAN DER KLOOT, W. (1976). Effects of the ionophore X537A on acetylcholine release at the frog neuromuscular junction. *J. Physiol.*, **259**, 177–198.

KLAPSTEIN, G.J. & COLMERS, W.F. (1992). 4-Aminopyridine and low Ca^{2+} differentiate presynaptic inhibition mediated by neuropeptide Y, baclofen, and 2-chloroadenosine in rat hippocampal CA1 *in vitro*. *Br. J. Pharmacol.*, **105**, 470–474.

LIU, W.C., SLUSARCHYK, D.S., ASTLE, G., TREJO, W.H., BROWN, W.E. & MEYERS, E. (1978). Ionomycin, a new polyether antibiotic. *J. Antibiotics (Tokyo)*, **31**, 815–819.

LLADOS, F.T., ROSS-CANADA, J. & PAPPAS, G.D. (1984). Ultrastructural and physiological effects of the ionophore A23187 at identified frog neuromuscular junctions. *Neurosci.*, **13**, 237–247.

LLINAS, R., SUGIMORA, M., LIN, J.W. & CHERKSEY, B. (1989). Blocking and isolation of a calcium channel from neurons in mammalians and cephalopods using a toxin fraction (FTX) from funnel web spider poison. *Proc. Natl. Acad. Sci. U.S.A.*, **86**, 1689–1693.

LUINI, A. & DE MATTEIS, M.A. (1990). Evidence that receptor-linked G protein inhibits exocytosis by a post-second-messenger mechanism in AtT-20 cells. *J. Neurochem.*, **54**, 30–38.

MALENKA, R.C., MADISON, D.V. & NICOLL, R.A. (1986). Potentiation of synaptic transmission in the hippocampus by phorbol esters. *Nature*, **321**, 175–177.

MAN-SON-HING, H., ZORAN, M.J., LUKOWIAK, K. & HAYDON, P.G. (1989). A neuromodulator of synaptic transmission acts on the secretory apparatus as well as on ion channels. *Nature*, **341**, 237–239.

MULLER, D., LOCTIN, F., & DUNANT, Y. (1987). Inhibition of evoked acetylcholine release: two different mechanisms in the *Torpedo* electric organ. *Eur. J. Pharmacol.*, **133**, 225–224.

MULLER, D., TURNBULL, J., BAUDRY, M. & LYNCH, G. (1988). Phorbol ester-induced synaptic facilitation is different than long-term potentiation. *Proc. Natl. Acad. Sci. U.S.A.*, **85**, 6997–7000.

PHILLIS, J.W. (1985). The pharmacology of purines in the CNS: interactions with psychoactive agents. In *Purines: Pharmacology and Physiological Roles*. ed. Stone, T.W. pp. 45–56. London: MacMillan Press.

POZZAN, T., GATTI, G., DOZIO, N., VICENTINI, L.M. & MELDOLESI, J. (1984). Ca^{2+}-dependent and -independent release of neurotransmitters from PC12 cells: a role for protein kinase C activation. *J. Cell Biol.*, **99**, 628–638.

RAHAMIMOFF, R. & YAARI, Y. (1973). Delayed release of transmitter at the frog neuromuscular junction. *J. Physiol.*, **228**, 241–257.

RASGADO-FLORES, H., SANCHEZ-ARMASS, S., BLAUSTEIN, M.P. & NACHSHEN, D.A. (1987). Strontium, barium, and manganese metabolism in isolated presynaptic nerve terminals. *Am. J. Physiol.*, **252**, C604–C610.

RIBEIRO, J.A., SA-ALMEIDA, A.M. & NAMORADO, J.M. (1979). Adenosine and adenosine triphosphate decrease ^{45}Ca uptake by synaptosomes stimulated by potassium. *Biochem. Pharmacol.*, **28**, 1297–1300.

RIBEIRO, J.A. & SEBASTIAO, A.M. (1986). Adenosine receptors and calcium: basis for proposing a third (A3) type of adenosine receptor. *Prog. Neurobiol.*, **26**, 179–209.

SCHOLZ, K.P. & MILLER, R.J. (1992). Inhibition of quantal transmitter release in the absence of calcium influx by a G protein-linked adenosine receptor at hippocampal synapses. *Neuron*, **8**, 1139–1150.

SILINSKY, E.M. (1984). On the mechanism by which adenosine receptor activation inhibits the release of acetylcholine from frog motor nerve endings. *J. Physiol.*, **346**, 243–256.

SILINSKY, E.M. (1989). Adenosine derivatives and neuronal function. *Seminars Neurosci.*, **1**, 155–165.

SILINSKY, E.M., HIRSH, J.K. & VOGEL, S.M. (1987). Intracellular calcium mediating adenosine effects at neuromuscular junctions. In *Topics and Perspectives in Adenosine Research*. ed. Gerlach, E. & Becker, B.F. pp. 537–548. Berlin: Springer-Verlag.

SILINSKY, E.M. & SOLSONA, C.S. (1992). Calcium currents at motor nerve endings: absence of effects of adenosine receptor agonists in the frog. *J. Physiol.*, **457**, 315–328.

STATHAM, H.E., DUNCAN, C.J. & SMITH, J.L. (1976). The effect of the ionophore A23187 on the ultrastructural and electrophysiological properties of frog skeletal muscle. *Cell Tissue Res.*, **173**, 193–209.

ULLRICH, S., PRENTKI, M. & WOLLHEIM, C.B. (1990). Somatostatin inhibition of Ca^{2+}-induced insulin secretion in permeabilized HIY-T15 cells. *Biochem. J.*, **270**, 273–276.

YELLEN, G. (1982). Single Ca^{2+}-activated non-selective cation channels in neuroblastoma. *Nature*, **296**, 357–359.

(Received February 4, 1993
Revised May 20, 1993
Accepted May 28, 1993)

Br. J. Pharmacol. (1993), **110**, 833–839

Modulation of cholinergic and substance P-like neurotransmission by nitric oxide in the guinea-pig ileum

[1]*†Claes U. Wiklund, *Caroline Olgart, *,**N. Peter Wiklund & *†Lars E. Gustafsson

*Department of Physiology, †Institute of Environmental Medicine, **Department of Urology at the Karolinska Hospital, Karolinska Institute, Box 60 400, S-104 01 Stockholm, Sweden

1 The role of endogenous nitric oxide (NO) as a modulator of enteric neurotransmission was investigated in longitudinal muscle myenteric plexus (LMMP) preparations of guinea-pig isolated ileum.

2 In tissues previously incubated with [^{3}H]-choline, exogenous NO inhibited electrically-evoked [^{3}H]-choline overflow as well as responses to exogenous agonists, indicating that NO has the potential of neuromodulation both pre- and postjunctionally.

3 A series of NO synthase inhibitors enhanced contractile responses to nerve stimulation indicating inhibitory neuromodulation by endogenous NO.

4 The potency order of the NO synthase inhibitors and their consistent effects after dexamethasone, on responses to nerve stimulation, indicate action on a constitutive NO synthase.

5 Responses enhanced by NO synthase inhibitors were inhibited by the substance P receptor antagonist, spantide, suggesting a neuromodulatory influence on substance P-like neurotransmission by the endogenous NO.

6 NO synthase inhibition did not modify contractile responses to application of acetylcholine or substance P, or [^{3}H]-choline overflow, indicating that endogenous NO mainly has a prejunctional inhibitory action on substance P-like neurotransmission. Nor did it modify responses to direct electrical muscle stimulation in the presence of tetrodotoxin. This suggests a prejunctional enhancing effect by NO synthesis inhibition.

7 Evidence for endogenous NO modulation of acetylcholine release was obtained when NO synthase inhibition modified atropine-sensitive, nerve-mediated contractile responses. However, [^{3}H]-choline overflow was unaltered by NO synthase inhibition.

8 NO synthase inhibition did not modify responses to inhibitory neurotransmission.

9 The findings suggest that endogenous NO inhibits substance P-like motor neurotransmission, probably via prejunctional mechanisms. Cholinergic transmission may also be reduced by endogenous NO, acting prejunctionally.

Keywords: Nitric oxide; neuromodulation; cholinergic; tachykinin; smooth muscle; transmitter release

Introduction

Endothelial cells can release nitric oxide (NO) in response to various stimuli such as bradykinin and acetylcholine (Palmer *et al.*, 1987). NO is enzymatically formed from the amino acid, L-arginine (Palmer *et al.*, 1988), through oxidation with molecular oxygen (Leone *et al.*, 1991, Stuehr *et al.*, 1991). Derivatives or arginine with modified substituents at the guanidino terminus, such as N^G-monomethyl-L-arginine (L-NMMA) have been shown to inhibit stereospecifically the NO synthases, responsible for NO synthesis (Hibbs *et al.*, 1987; Palmer *et al.*, 1988; Rees *et al.*, 1990b). NO is also formed in other tissues such as the central nervous system (Garthwaite *et al.*, 1988; Knowles *et al.*, 1989; Bredt & Snyder, 1990) and in neutrophils (Rimele *et al.*, 1988; McCall *et al.*, 1989).

It has been proposed that NO is an inhibitory neurotransmitter (Martin *et al.*, 1988; Gillespie & Sheng, 1988; Li & Rand, 1989; Gibson *et al.*, 1990) and a NO synthase has been found in enteric nerves (Bredt *et al.*, 1990). Furthermore, it has been suggested that endogenous NO can inhibit substance P-like motor neurotransmission in the guinea-pig ileum (Gustafsson *et al.*, 1990a,b) since L-NMMA enhances tachykinin-mediated nerve-evoked contractions.

We have now studied the neuromodulatory effects of a series of L-arginine analogues and the putative presence of endotoxin-dependent NO synthase, in guinea-pig ileum. This was investigated since, at least in vascular *in vitro* preparations, activation of an endotoxin-inducible NO synthase can modify responses to agonist application (Rees *et al.*, 1990a). NO was applied exogenously to evaluate possible neuromodulatory actions at increased concentrations of NO.

[1] Author for correspondence at: Department of Physiology, Karolinska Institute, Box 60 400, S-104 01 Stockholm, Sweden.

Methods

General procedure

Guinea-pigs (300–500 g) of either sex were stunned and bled. Longitudinal muscle myenteric plexus (LMMP) preparations of isolated ileum were prepared and suspended vertically in 3 or 6 ml tissue baths, made of Perspex and equipped with platinum electrodes 10 mm in length and 10 mm apart. Motor activity was recorded isometrically (release experiments), or isotonically (muscle response experiments). Tyrode solution (mM: Na 149, K 2.9, Ca 1.8, Mg 0.5, Cl 144, HCO_3 23.8, H_2PO_4 0.4 and glucose 5.5) was continuously aerated with 5% CO_2 in O_2 before and throughout the experiments. After 20 min at room temperature the tissue bath temperature was raised to and maintained at 37°C. Preparation weights (wet weight) were 10–15 mg in contraction experiments and 60–180 mg in release experiments.

Contractile responses to nerve stimulation

LMMP preparations of the guinea-pig ileum were transmurally stimulated (3 Hz, 0.2 ms, 180 pulses at 5 min inter-

vals) at an isotonic load of 2 mN and with an initial 20 min period at room temperature as mentioned above.

Relaxations to nerve stimulation

LMMP preparations were treated with histamine (10^{-6} M) and atropine (3×10^{-7} M) and stimulated transmurally (3 Hz, 0.2 ms, 15 pulses at 4 min intervals). The relaxation to nerve stimulation was followed by a rebound contraction. Tetrodotoxin (3×10^{-7} M) abolished both the relaxation and the contraction induced by transmural stimulation.

Application of NO by means of acid nitrite

To study neuromodulatory effects of exogenous NO, acid solutions of nitrite were added to LMMP preparations. Sodium nitrite ($NaNO_2$) in 0.1 M hydrochloric acid emits NO, and had been used successfully to mimic NO (Furchgott *et al.*, 1987; Khan & Furchgott, 1987; Furchgott, 1988).

Acetylcholine release

Large (60–180 mg wet wt.) LMMP preparations were obtained as above, and were incubated for 1 h with 15 μCi ml^{-1} [methyl-^{3}H]-choline during continuous transmural stimulation (0.2 Hz, 0.2 ms) in the presence of 10^{-6} M choline. After a 30 min rinsing period, [^{3}H]-choline overflow was monitored during constant perfusion (1 ml min^{-1}) of the tissue bath with Tyrode containing 10^{-5} M hemicholinium-3, and was taken as a quantitative measurement of acetylcholine release (Szerb, 1976; Kilbinger, 1977).

Drugs

N^G-monomethyl-L-arginine (L-NMMA) and N^G-monomethyl-D-arginine (D-NMMA), synthesized according to Patthy *et al.* (1977), were gifts from Dr S. Moncada, Wellcome Research Labs, Beckenham, Kent, UK. L-arginine, D-arginine, N^ω-nitro-L-arginine methyl ester (L-NAME), N^ω-nitro-L-arginine benzyl ester (L-NABE), N^ω-nitro-L-arginine (L-NOARG), N^G, N'^G-dimethyl-L-arginine (L-NDMA), Myelin basic protein (MBP) from rabbit brain, 8-methyl-N-vanillyl-6-nonenamide (capsaicin), tetrodotoxin, guanethidine sulphate, acetylcholine chloride and atropine sulphate were purchased from Sigma Chemical Co (St. Louis, U.S.A.). For molecular structures of the L-arginine analogues see Figure 1. N^ω-nitro-D-arginine (D-NARG), N^ω-nitro-D-arginine methyl ester (D-NAME) and L-NO_2-arginine phenylalanine-methyl ester (NOARG-PHE) were from BACHEM Feinchemikalien AG, Budendorf, Switzerland. Substance P and spantide were gifts from the Wellcome Foundation Ltd, Beckenham, U.K. [Methyl-^{3}H]-choline (15 Ci $mmol^{-1}$) was from Amersham, UK. Hemicholinium-3 was from Aldrich-Europe, Belgium. Dexamethasone phosphate was from Merck Sharp & Dohme, Rahway, N.J., U.S.A. Capsaicin was dissolved in ethanol (95% v/v). Added amounts of ethanol did not affect the LMMP preparations in control experiments. All other drugs were dissolved in distilled water.

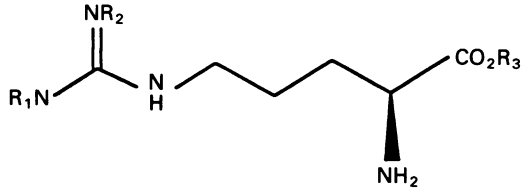

	R_1	R_2	R_3
L-Arginine	H_2	H	H
L-NMMA	CH_3	H	H
L-NOARG	NO_2	H	H
L-NAME	NO_2	H	CH_3
L-NABE	NO_2	H	$CH_2C_6H_5$
L-NDMA	CH_3	CH_3	H

Figure 1 Molecular structures of L-arginine analogues. L-Arginine, N^G-monomethyl-L-arginine (L-NMMA), N^ω-nitro-L-arginine (L-NOARG), N^ω-nitro-L-arginine methyl ester (L-NAME), N^ω-nitro-L-arginine benzyl ester (L-NABE) and N^G, N'^G-dimethyl-L-arginine (L-NDMA).

Statistics

Experimental data are expressed as mean values ± s.e.mean. Statistical significance was analysed by Student's *t* test for paired or unpaired variables.

Results

Characterization of responses to nerve stimulation

In response to transmural stimulation, LMMP preparations of guinea-pig ileum exhibited biphasic contractile responses (Figure 2), which were abolished by tetrodotoxin (3×10^{-7} M). The contractions consisted of a fast twitch and a slow tonic ('hump') response. The tonic contraction was more well-developed in preparations preoxygenated at room temperature (80.1 ± 5.7% of control twitch contraction), than in preparations studied after immediate mounting at 37°C (47.6 ± 6.4% of control twitch contraction; $P < 0.01$, $n = 6$). The twitch contraction was antagonized by atropine (Figure 2). The tonic contraction was antagonized by the substance P-receptor antagonist, spantide (Figure 2). The substance P-like nerve-mediated tonic contraction was not affected by 1 h preincubation with capsaicin at 10^{-5} M.

Effects of NO synthase inhibitors on nerve responses in drug-naïve preparations

L-NOARG, at 2×10^{-5} M, increased the tonic contraction but did not affect the twitch contraction (Figure 2a, 3a). Both the tonic and the twitch contractions were enhanced during L-NMMA (10^{-4} M) treatment (Figure 3b). In the presence of spantide at a concentration that completely abolished atropine-resistant contractions, L-NOARG enhanced the cholinergic tonic phase of the contraction (Figure 4).

NO synthase inhibitors on atropine-resistant contractile responses

In the presence of 10^{-6} M atropine, the atropine-resistant response to transmural nerve stimulation was markedly enhanced by NO synthase inhibitors. All had the same maximal effect although they had variable potency (Figure 2, 5a). The enhancement by the NO-synthase inhibitors was evident also in the presence of guanethidine, 10^{-4} M. Atropine-resistant contractions in the absence or presence of NO-synthase inhibitors were abolished by the substance P-receptor antagonist, spantide (3×10^{-5} M) (Figure 2c and data not shown). The effects of the L-arginine analogues at maximally effective concentrations were reversible on washing and did not show any marked tachyphylaxis. At supramaximal concentrations (10^{-4} and 5×10^{-4} M for the nitro- and methyl-derivatives respectively), the effects were only slowly reversible, and showed distinct tachyphylaxis. The enhancing effects on atropine-resistant contractions by L-NMMA (10^{-4} M), L-NOARG, L-NAME and L-NABE (10^{-5} M) were stereospecifically reversed by L-arginine (10^{-3} M) but not by the enantiomer D-arginine (10^{-3} M) (Figure 6). The D-arginine analogues N^G-monomethyl-D-

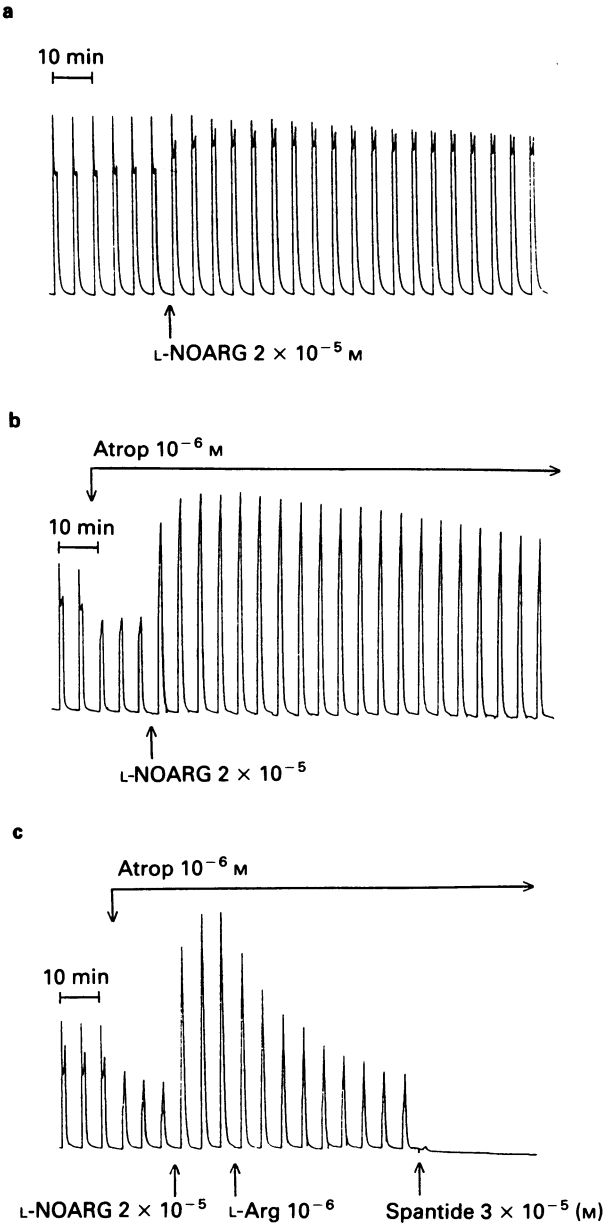

Figure 2 Three preparations of guinea-pig ileum LMMP. Contractile responses to transmural nerve stimulation, 3 Hz, 0.2 ms, 180 pulses at 5 min intervals. (a) N^{ω}-nitro-L-arginine (L-NOARG) (2×10^{-5} M) enhanced the tonic 'hump' phase of nerve-mediated contractions. (b) Atropine (Atrop, 10^{-6} M) abolished the twitch contraction. After pretreatment with atropine the enhancement by L-NOARG was pronounced. (c) The enhancement by L-NOARG was reversed by L-arginine. The atropine-resistant contractions were abolished by the substance P-receptor antagonist, spantide.

arginine (D-NMMA), N^{ω}-nitro-D-arginine methyl ester (D-NAME) and N^{ω}-nitro-D-arginine (D-NOARG) did not affect the atropine-resistant contractions (Figure 5b).

Another naturally occurring (McDermott, 1976; Patthy *et al.*, 1977) arginine analogue, N^{G}, N'^{G}-dimethyl-L-arginine (symmetric dimethyl arginine, L-NDMA) was examined for effects on neurotransmission. After purification from its counter-ion 2-(4'-hydroxyazobenzene) benzoic acid (HABA) on Sep-Pak C_{18} columns, L-NDMA did not affect contractile responses to nerve stimulation, regardless of the presence or absence of atropine (Figure 5a). The commercially available preparation of L-NDMA inhibited nerve-mediated contractions, but this effect could be mimicked with HABA. In contrast to L-NDMA, L-NMMA similarly eluted through

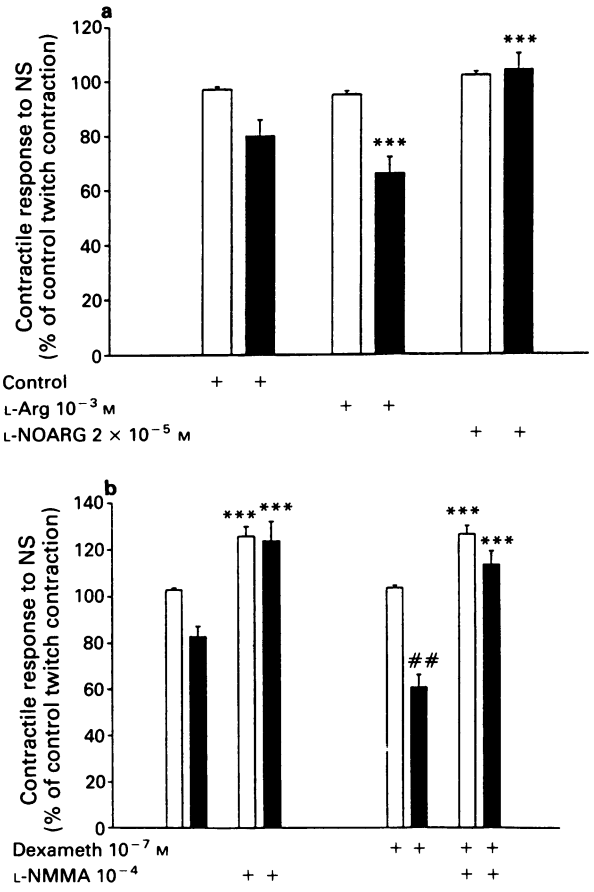

Figure 3 Contractile responses to nerve stimulation, 3 Hz, 0.2 ms, 180 pulses at 5 min intervals in guinea-pig ileum LMMP. Twitch contractions (open columns) and tonic 'hump' contractions (solid columns) to nerve stimulation (tonic 'hump' contractions expressed as a % of control twitch contractions). (a) L-Arginine (10^{-3} M) inhibited ($P<0.001$) and N^{ω}-nitro-L-arginine (L-NOARG, 2×10^{-5} M) enhanced the tonic contraction ($P<0.001$) and did not affect the twitch contraction ($n = 6$). (b) The tonic contraction in preparations pretreated with dexamethasone had a lower amplitude compared with drug-naïve preparations ($P<0.01$, $n = 12$). However, L-NMMA (10^{-4} M) enhanced both the twitch and the hump contraction to nerve stimulation ($P<0.001$) in the absence and after pretreatment with dexamethasone (10^{-7} M). ***$P<0.001$; ##$P<0.01$ (hump contraction: dexamethasone vs control).

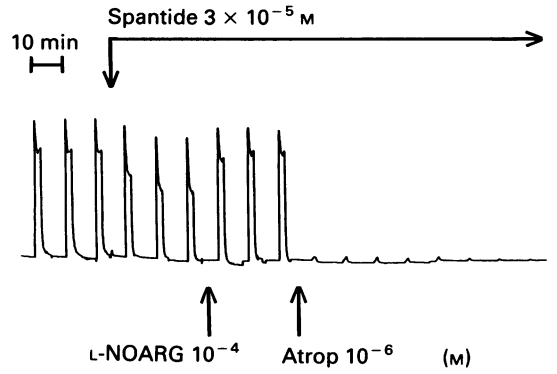

Figure 4 Contractile responses to nerve stimulation (3 Hz, 0.2 ms, 180 pulses at 5 min intervals) in guinea-pig ileum LMMP. The substance P-receptor antagonist, spantide, at a concentration that abolishes atropine-resistant contractions, (see Figure 2) inhibited both the twitch and the tonic contractile response. N^{ω}-nitro-L-arginine (L-NOARG, 10^{-4} M) enhanced both phases of nerve-mediated contractions after pretreatment with spantide. The enhanced responses were abolished by atropine.

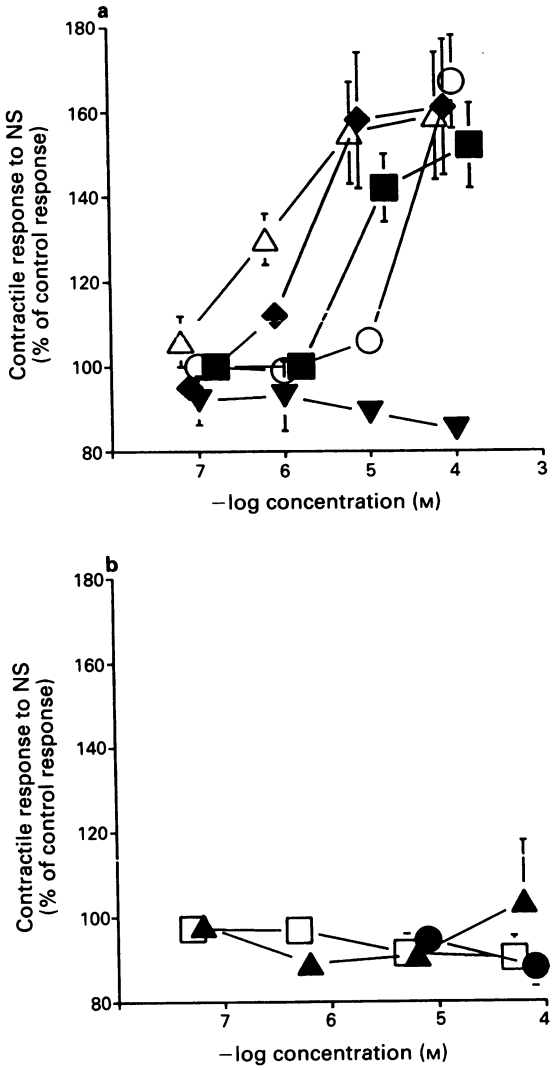

Figure 5 Atropine-resistant (10^{-6} M) tonic contractions to nerve stimulation (NS, 3 Hz, 0.2 ms, 180 pulses at 5 min intervals) in guinea-pig ileum LMMP. (a) Enhancement of contractions to nerve stimulation by L-arginine analogues: N^G-monomethyl-L-arginine (L-NMMA) (○); N^ω-nitro-L-arginine (L-NOARG) (△); N^ω-nitro-L-arginine methyl ester (L-NAME) (■) and N^ω-nitro-L-arginine benzyl ester (L-NABE) (◆); N^G, N'^G-dimethyl-L-arginine (L-NDMA) (▼) did not modify the contractions. (b) The D-arginine analogues N^G-monomethyl-D-arginine (D-NMMA) (●), N^ω-nitro-D-arginine (D-NOARG) (▲), N^ω-nitro-D-arginine methyl ester (D-NAME) (□) did not modify the contractions to nerve stimulation ($n = 6$).

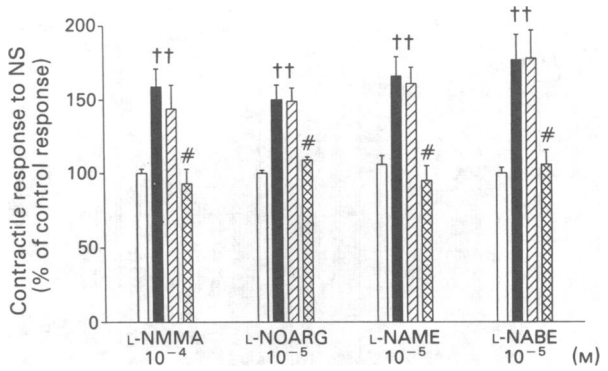

Figure 6 Atropine-resistant (10^{-6} M) tonic contractions to nerve stimulation, (3 Hz, 0.2 ms, 180 pulses at 5 min intervals) in guinea-pig ileum LMMP. (Controls, in the presence of atropine = open columns). Enhancement by the NO synthase inhibitors (solid columns) L-NMMA (10^{-4} M), L-NOARG (10^{-5} M), L-NAME (10^{-5} M) and L-NABE (10^{-5} M). The enhancement by the NO synthase inhibitors was reversed by L-arginine (L-Arg 10^{-3} M) (cross-hatched columns) whereas D-arginine (D-Arg, 10^{-3} M) (hatched columns) did not modify the responses. $^{\dagger}P < 0.01$ compared with control; # $P < 0.01$ compared with responses enhanced by NO synthase inhibitors; $n = 6$. L-NMMA = N^G-monomethyl-L-arginine; L-NOARG = N^ω-nitro-L-arginine; L-NAME = N^ω-nitro-L-arginine methyl ester; L-NABE = N^ω-nitro-L-arginine benzyl ester.

Sep-Pak columns retained its stimulatory activity. Myelin basic protein, of which L-NMMA is a constituent (McDermott, 1976; Patthy *et al.*, 1977; Rawal *et al.*, 1992), did not affect contractions to nerve stimulation at 10 μg ml^{-1} regardless of the presence or absence of atropine. This corresponds to 5×10^{-7} M concentration of myelin basic protein, and 0.96×10^{-7} M of protein bound L-NMMA and asymmetric dimethyl arginine, both compounds having nearly similar NO synthase inhibitory capacity (Vallance *et al.*, 1992). The dipeptide L-NO_2-arginine-phenylalanine methyl ester (NOARG-Phe methyl ester) enhanced nerve-mediated contractions by 56 ± 10% at 10^{-4} M in atropine-treated tissues, and its effect was reversed by L-arginine.

L-Arginine on drug-naïve preparations

L-Arginine, the substrate for NO synthesis, at 10^{-3} M, inhibited the tonic contraction by 18 ± 2% whereas the twitch contraction was not affected (Figure 3a). In preparations stimulated for 5 s at 1 min intervals, L-arginine did not affect the twitch contractions to nerve stimulation as previously reported (Gustafsson *et al.*, 1990a).

NO synthase inhibition after dexamethasone

To study whether endotoxin-inducible NO synthase was involved in the neuromodulation in guinea-pig ileum, 8 μmol kg^{-1} dexamethasone was given intraperitoneally to a group of animals 1 h before they were killed. The small intestine and the muscle preparations were then kept in dexamethasone-containing (10^{-7} M) solution before and throughout the experiments. Although dexamethasone inhibited contractile responses slightly, L-NMMA (10^{-4} M) enhanced nerve-mediated contractions in the dexamethasone-treated preparations to a similar degree as in untreated controls (Figure 3b).

NO synthase inhibitors on inhibitory nerve responses

Transmural stimulation in the presence of atropine and histamine elicited biphasic responses, relaxations followed by contractions before stimulation ceased, and showing maximum contraction after stimulation ('rebound contraction') (Figure 7). The amplitude of the relaxations was small, only amounting to 1.0 ± 0.6% of control contractions to nerve stimulation in drug-naïve preparations. The rebound contractions were enhanced by L-NOARG and abolished or greatly reduced by the substance P-receptor antagonist, spantide (Figure 7). L-NOARG did not significantly affect relaxations to nerve stimulation in the absence or presence of spantide (3×10^{-5} M) ($n = 7$).

NO synthase inhibitors on responses to exogenous agonists

L-NOARG 10^{-4} M did not enhance contractile responses to acetylcholine (10^{-7} M), substance P (10^{-9} M) or direct muscle stimulation in the presence of tetrodotoxin (3×10^{-7} M) (3 Hz, 2.0 ms, 15 pulses at 1 min intervals) ($n = 5$ for each group). The contractile responses to these agonists were submaximal (50–75% of responses to transmural nerve stimulation).

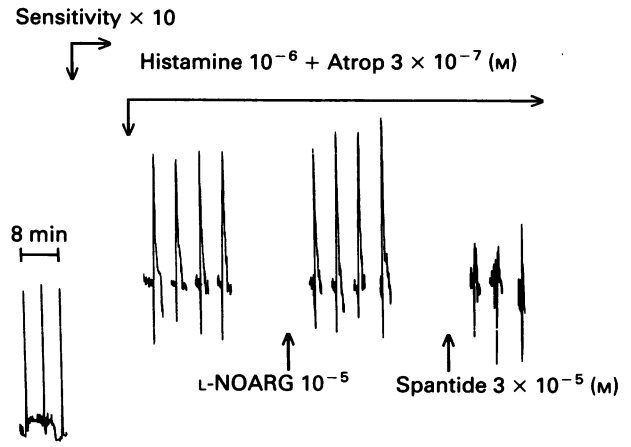

Figure 7 Relaxations and rebound contractions to nerve stimulation (3 Hz, 0.2 ms, 15 pulses at 4 min intervals) in guinea-pig ileum LMMP, in the presence of histamine (3×10^{-7} M) and atropine (Atrop 10^{-6} M). N^{ω}-nitro-L-arginine (L-NOARG, 10^{-5} M) enhanced the rebound contractions but did not modify the relaxations. Spantide (3×10^{-5} M) abolished the enhanced contractile responses.

Exogenous NO on responses to nerve stimulation and exogenous agonists

NO application by administration of acidified sodium nitrite (10^{-9}–10^{-3} M) dose-dependently and reversibly inhibited contractile responses to nerve stimulation (data not shown and Figure 8). The threshold concentration for the inhibitory effect was 10^{-7} M. At 10^{-6} M both the twitch and the tonic phase were inhibited by approximately 50%. Higher concentrations of sodium nitrite had only minor additional effects, and HCl controls lacked effects.

Acid nitrite (10^{-6}–10^{-4} M) dose-dependently inhibited contractile responses to acetylcholine, substance P or neurokinin A at concentrations submaximally effective when compared to electrical stimulation (data not shown). At 10^{-5} M acid nitrite the responses were inhibited by approximately 30–60%.

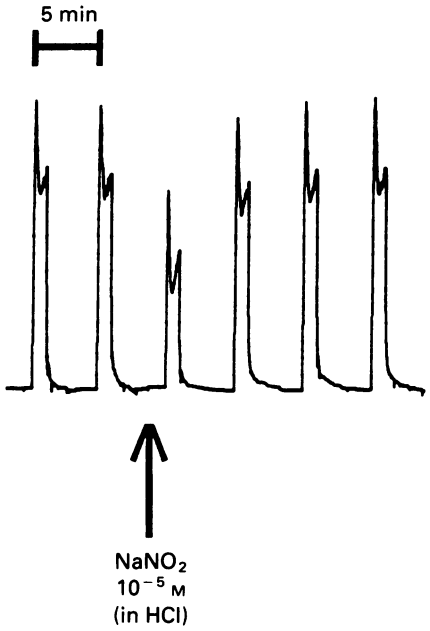

Figure 8 Contractile responses to nerve stimulation, (3 Hz, 0.2 ms, 180 pulses at 5 min intervals) in guinea-pig ileum LMMP. Acid nitrite ($NaNO_2$ in HCl) reversibly inhibited nerve-mediated contractions. The acid that was used (10^{-1} M HCl), when added to the tissue bath, corresponded at most to a 10^{-4} M theoretical addition, and was effectively buffered by the 23.8×10^{-3} M bicarbonate. Thus, it did not affect the pH of the bath fluid or the nerve-mediated contractions in parallel control experiments (not shown).

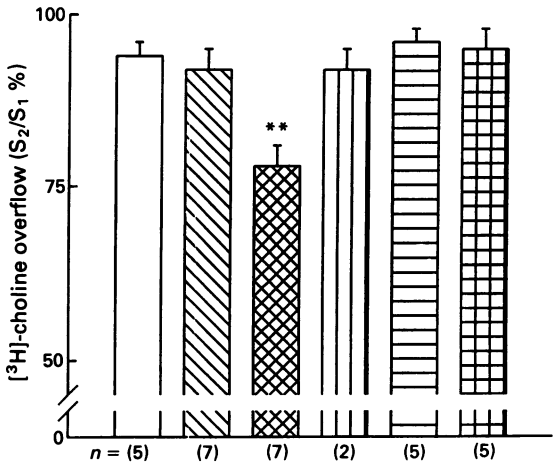

Figure 9 Stimulation-evoked (3 Hz, 0.2 ms, 180 pulses at 12 min intervals) $[^3H]$-choline overflow in guinea-pig ileum LMMP preparations prelabelled with $[^3H]$-choline. The overflow of ^3H is expressed as quotients between two sequential stimulation periods (S_2/S_1). (Control = open column). Sodium nitrite ($NaNO_2$) in 10^{-1} hydrochloric acid (▩) inhibited $[^3H]$-choline overflow ($P<0.01$), whereas $NaNO_2$ in distilled water (▨) was without effect. Hydrochloric acid (▥) at the concentration used with $NaNO_2$ (theoretically reaching 10^{-4} M in the tissue bath), did not modify the $[^3H]$-choline overflow. Included are also previous data (Gustafsson *et al.*, 1990b) showing that N^G-monomethyl-L-arginine (L-NMMA, ▤) or L-arginine (▦) did not modify $[^3H]$-choline overflow. Number of experiments indicated in parentheses; s.e.mean is shown except for the effect of HCl where range is denoted. $^{**}P<0.01$.

Effects of NO and NO synthase inhibition on $[^3H]$-choline overflow

Multistranded preparations of guinea-pig ileum LMMP were preincubated with $[^3H]$-choline for 1 h and subsequently stimulated transmurally (3 Hz, 0.2 ms, 180 pulses at 12 min intervals) giving reproducible release of $[^3H]$-choline. Sodium nitrite (10^{-4} M) in 0.1 M hydrochloric acid inhibited stimulation-evoked release of $[^3H]$-choline by 17 ± 3% (Figure 9), whereas non-acidified nitrite lacked effect. As previously shown, L-NMMA or L-arginine did not affect $[^3H]$-choline overflow (Gustafsson *et al.*, 1990b, and Figure 9).

Discussion

The present study clearly indicates that endogenous NO modulates autonomic neurotransmission in guinea-pig isolated ileum. The main function observed is an inhibition of substance P-like neurotransmission, probably at a prejunctional site. There is also a smaller inhibitory influence on cholinergic transmission, by endogenous NO.

The main evidence for neuromodulation by endogenous NO was the enhancement of nerve-mediated contractions by NO synthase inhibitors. Furthermore, exogenous NO inhibited $[^3H]$-choline overflow and responses to exogenous agonists, clearly indicating that NO is capable of both pre- and postjunctional modulation of neurotransmission. NO synthase inhibitors did not modify responses to exogenous agonists, either of the peptide or the acetylcholine type, lending further support for a prejunctional action of endogenous NO. The finding that NO synthase inhibition enhanced responses to nerve stimulation in the presence of atropine, and that such responses could be abolished by

substance P receptor antagonism, shows that the neuromodulatory influence of endogenous NO was exerted on the substance P-like neurotransmission. Accordingly, NO synthase inhibition lacked effect on acetylcholine release, as determined by the [^{3}H]-choline method. Definitive evidence for prejunctional modulation of substance P-like neurotransmission will have to await determinations of the release of substance P or its homologues in tissue bath fluid.

NO as a mediator of inhibitory neurotransmission is not a likely explanation for the enhancement by NO synthase inhibitors of responses to excitatory neurotransmission. Firstly, exogenous NO inhibited [^{3}H]-choline overflow, showing that NO is able to inhibit neurotransmitter release. Secondly, NO synthase inhibition did not modify nerve-mediated relaxations. This contrasts with a role for NO as a mediator of inhibitory neurotransmission in other locations in the gastrointestinal tract, e.g. in the circular muscle layer of the intestine or in the stomach; or in genital tissue (Desai *et al.*, 1991; Ignarro *et al.*, 1990a,b).

All the substituted L-arginine analogues except L-NDMA enhanced contractile responses to nerve stimulation indicating the presence of endogenous neuromodulatory NO in guinea-pig ileum, in accordance with previous studies with L-NMMA (Gustafsson *et al.*, 1990b). The effects of the L-arginine analogues were not mimicked by their D-counterparts, and were antagonized by L-arginine but not by D-arginine, indicating stereoselective inhibition of NO synthase (Palmer *et al.*, 1988; Palacios *et al.*, 1989).

L-Arginine inhibited the tonic phase of contractions to nerve stimulation suggesting that when substrate for NO synthase is added, the endogenous NO production is stimulated.

The potency order of the NO synthase inhibitors is compatible with a constitutive, calcium- and NADPH-dependent NO synthase (Palacios *et al.*, 1989). This is further corroborated by the lack of effect of dexamethasone-pretreatment in the ileum preparations, making a contribution of an endotoxin-stimulated inducible NO synthase in endogenous neuromodulation by NO in the guinea-pig ileum unlikely. Further support for the involvement of a constitutive enzyme would be gained from demonstration of calcium-dependence (cf. Moncada *et al.*, 1991), and preliminary data which show that guinea-pig LMMP is capable of NO release support such a relationship (Wiklund *et al.*, 1993).

The effect of the dipeptide L-NOARG-PHE and the lack of neuromodulating effect by symmetric dimethylarginine (L-NDMA) or by myelin basic protein, which contains both mono- and dimethylated arginines (McDermott, 1976; Patthy *et al.*, 1977), indicate that not all methylated arginines are active as NO synthase inhibitors. For L-NDMA, this is in agreement with recent data which also demonstrate that the unsymmetric dimethyl analogue is a synthase inhibitor (Vallance *et al.*, 1992). These results also show that dipeptides are, in intact or hydrolysed form, capable of NO synthase inhibition in the ileum, whereas larger proteins like myelin basic protein seem inactive, at least *in vitro*. The size limit for enzyme inhibition by polypeptides in this system remains to be determined.

The site of production of endogenous NO in the ileum can also only be a matter of speculation. However, neuronal localization for one type of NO synthase has been demonstrated in the small intestine (Bredt *et al.*, 1990). In support, nerve stimulation in intestine can release NO-like bioactivity (Bult *et al.*, 1990), and chemiluminescence determination of NO release also indicates a dependence on neuronal activity in the intestine (Wiklund *et al.*, 1993).

In conclusion, exogenous NO can inhibit transmitter release, as evident from the [^{3}H]-choline overflow experiments. In the guinea-pig isolated ileum, endogenous NO mainly exerts a tonic prejunctional inhibition on substance P-like motor neurotransmission, although a slight effect on cholinergic transmission may also occur. Regardless of the site of NO action, a modulation by NO of non-adrenergic non-cholinergic (NANC) excitatory neurotransmission would be in agreement with observations of NANC neuromodulation by NO in other tissues (Gustafsson *et al.*, 1990a; Cederqvist *et al.*, 1991).

Supported by the Swedish MRC (7919), the Swedish National Environment Protection Board (31207), the Karolinska Institute, the Institute of Environmental Medicine and Tore and Ragnar Söderberg's foundations.

References

BREDT, D.S., HWANG, P.M. & SNYDER, S.H. (1990). Localization of nitric oxide synthase indicating a neural role for nitric oxide. *Nature*, **347**, 768–770.

BREDT, D.S. & SNYDER, S.H. (1990). Isolation of nitric oxide synthetase, a calmodulin-requiring enzyme. *Proc. Natl. Acad. Sci. U.S.A.*, **87**, 682–685.

BULT, H., BOECKXSTAENS, G.E., PELCKMANS, P.A., JORDAENS, F.H., VAN MAERCKE, Y.M. & HERMAN, A.G. (1990). Nitric oxide as an inhibitory non-adrenergic non-cholinergic neurotransmitter. *Nature*, **345**, 346–347.

CEDERQVIST, B., WIKLUND, N.P., PERSSON, M.G. & GUSTAFSSON, L.E. (1991). Modulation of neuroeffector transmission in the guinea pig pulmonary artery by endogenous nitric oxide. *Neurosci. Lett.*, **127**, 67–69.

DESAI, K.M., SESSA, W.C. & VANE, J.R. (1991). Involvement of nitric oxide in the reflex relaxation of the stomach to accommodate food or fluid. *Nature*, **351**, 477–479.

FURCHGOTT, R.F. (1988). Studies on relaxation of rabbit aorta by sodium nitrite: the basis for the proposal that the acid-activatable inhibitory factor from bovine retractor penis is inorganic nitrite and the endothelium-derived relaxing factor is nitric oxide. In *Vasodilation: Vascular Smooth Muscle, Peptides, Autonomic Nerves and Endothelium*. ed. Vanhoutte, P.M., pp. 401–414. New York: Raven Press.

FURCHGOTT, R.F., KHAN, M.T. & JOTHIANANDAN, D. (1987). Comparison of endothelium-dependent relaxation and nitric oxide-induced relaxation in rabbit aorta. *Fed. Proc.*, **46**, 385 (abstract).

GARTHWAITE, J., CHARLES, S.L. & CHESS-WILLIAMS, R. (1988). Endothelium-derived relaxing factor release on activation of NMDA receptors suggests a role as intercellular messenger in the brain. *Nature*, **336**, 385–388.

GIBSON, A., MIRZAZADEH, S., HOBBS, A.J. & MOORE, P.K. (1990). L-N^G-monomethyl arginine and L-N^G-nitro arginine inhibit non-adrenergic, non-cholinergic relaxation of the mouse anococcygeus muscle. *Br. J. Pharmacol.*, **99**, 602–606.

GILLESPIE, J.S. & SHENG, H. (1988). Influence of haemoglobin and erythrocytes on the effects of EDRF, a smooth muscle inhibitory factor, and nitric oxide on vascular and non-vascular smooth muscle. *Br. J. Pharmacol.*, **95**, 1151–1156.

GUSTAFSSON, L.E., WIKLUND, N.P., WIKLUND, C.U., CEDERQVIST, B., PERSSON, M.G. & MONCADA, S. (1990a). Modulation of autonomic neuroeffector transmission by nitric oxide-like activity in guinea-pig smooth muscle. In *Nitric Oxide from L-Arginine: a Bioregulatory System*. ed. Moncada, S. & Higgs, E.A. pp. 177–181. Amsterdam: Elsevier Science Publishers B.V. (Biomedical Division).

GUSTAFSSON, L.E., WIKLUND, C.U., WIKLUND, N.P., PERSSON, M.G. & MONCADA, S. (1990b). Modulation of autonomic neuroeffector transmission by nitric oxide in guinea pig ileum. *Biochem. Biophys. Res. Commun.*, **173**, 106–110.

HIBBS, J.B. Jr., TAINTOR, R.R. & VAVRIN, Z. (1987). Macrophage cytotoxicity: role for L-arginine deiminase activity and imino nitrogen oxidation to nitrite. *Science*, **235**, 473–476.

IGNARRO, L.J., BUSH, P.A., BUGA, G.M. & RAJFER, J. (1990a). Neurotransmitter identity doubt. *Nature*, **347**, 131–132.

IGNARRO, L.J., BUSH, P.A., BUGA, G.M., WOOD, K.S., FUKUTO, J.M. & RAJFER, J. (1990b). Nitric oxide and cyclic GMP formation upon electrical field stimulation cause relaxation of corpus cavernosum smooth muscle. *Biochem. Biophys. Res. Commun.*, **170,** 843–850.

KHAN, M.T., FURCHGOTT, R.F. (1987). Additional evidence that endothelium-derived relaxing factor in nitric oxide. In *Pharmacology*. ed. Randä, M.J., Roper, C. pp. 341–344. Elsevier: Amsterdam.

KILBINGER, H. (1977). Modulation by oxotremorine and atropine of acetylcholine release evoked by electrical stimulation of the myenteric plexus of the guinea-pig ileum. *Naunyn-Schmied. Arch. Pharmacol.*, **300,** 145–151.

KNOWLES, R.G., PALACIOS, M., PALMER, R.M.J. & MONCADA, S. (1989). Formation of nitric oxide from L-arginine in the central nervous system: a transduction mechanism for stimulation of the soluble guanylate cyclase. *Proc. Natl. Acad. Sci. U.S.A.*, **86,** 5159–5162.

LEONE, A.M., PALMER, R.M.J., KNOWLES, R.G., FRANCIS, P.L., ASHTON, D.S. & MONCADA, S. (1991). Constitutive and inducible nitric oxide synthases incorporate molecular oxygen into both nitric oxide and citrulline. *J. Biol. Chem.*, **266,** 23790–23795.

LI, C.G. & RAND, M.J. (1989). Evidence for a role of nitric oxide in the neurotransmitter system mediating relaxation of the rat anococcygeus muscle. *Clin. Exp. Pharmacol. Physiol.*, **16,** 933–938.

MARTIN, W., SMITH, J.A., LEWIS, M.J. & HENDERSON, A.H. (1988). Evidence that inhibitory factor extracted from bovine retractor penis is nitrite, whose acid-activated derivative is stabilized nitric oxide. *Br. J. Pharmacol.*, **93,** 579–586.

MCCALL, T.B., BOUGHTON-SMITH, N.K., PALMER, R.M.J., WHITTLE, B.J.R. & MONCADA, S. (1989). Synthesis of nitric oxide from L-arginine by neutrophils. Release and interaction with superoxide anion. *Biochem. J.*, **261,** 293–296.

MCDERMOTT, J.R. (1976). Studies on the catabolism of N^G-methylarginine, N^G, N'^G-dimethylarginine and N^G,N^G-dimethylarginine in the rabbit. *Biochem. J.*, **154,** 179–184.

MONCADA, S., PALMER, R.M.J. & HIGGS, E.A. (1991). Nitric oxide: physiology, pathophysiology, and pharmacology. *Pharmacol. Rev.*, **43,** 109–142.

PALACIOS, M., KNOWLES, R.G., PALMER, R.M.J. & MONCADA, S. (1989). Nitric oxide from L-arginine stimulates the soluble guanylate cyclase in adrenal glands. *Biochem. Biophys. Res. Commun.*, **165,** 802–809.

PALMER, R.M.J., FERRIDGE, A.G. & MONCADA, S. (1987). Nitric oxide release accounts for the biological activity of endothelium-derived relaxing factor. *Nature*, **327,** 524–526.

PALMER, R.M.J., REES, D.D., ASHTON, D.S. & MONCADA, S. (1988). L-arginine is the physiological precursor for the formation of nitric oxide in endothelium-dependent relaxation. *Biochem. Biophys. Res. Commun.*, **153,** 1251–1256.

PATTHY, A., BAJUSZ, S. & PATTHY, L. (1977). Preparation and characterization of N^G-mono-, di- and trimethylated arginines. *Acta Biochim. Biophys. Acad. Sci. Hung.*, **12,** 191–196.

RAWAL, N., LEE, Y.-J., PAIK, W.K. & KIM, S. (1992). Studies on N^G-methylarginine derivatives in myelin basic protein from developing and mutant mouse brain. *Biochem. J.*, **287,** 929–935.

REES, D.D., CELLEK, S., PALMER, R.M.J. & MONCADA, S. (1990a). Dexamethasone prevents the induction by endotoxin of a nitric oxide synthase and the associated effects on vascular tone: an insight into endotoxin shock. *Biochem. Biophys. Res. Commun.*, **173,** 541–547.

REES, D.D., PALMER, R.M.J., SCHULZ, R., HODSON, H.F. & MONCADA, S. (1990b). Characterization of three inhibitors of endothelial nitric oxide synthase *in vitro* and *in vivo*. *Br. J. Pharmacol.*, **101,** 746–752.

RIMELE, T.J., STURM, R.J., ADAMS, L.M., HENRY, D.E., HEASLIP, R.J., WEICHMAN, B.M. & GRIMES, D. (1988). Interaction of neutrophils with vascular smooth muscle: identification of a neutrophil-derived relaxing factor. *J. Pharmacol. Exp. Ther.*, **245,** 102–111.

STUEHR, D.J., CHO, H.J. SOO KWON, N., WEISE, M.F. & NATHAN, C.F. (1991). Purification and characterization of the cytokine-induced macrophage nitric oxide synthase: An FAD and FMN-containing flavoprotein. *Proc. Natl. Acad. Sci. U.S.A.*, **88,** 7773–7777.

SZERB, J.C. (1976). Storage and release of labelled acetylcholine in the myenteric plexus of the guinea-pig ileum. *Can. J. Physiol. Pharmacol.*, **54,** 12–22.

VALLANCE, P., LEONE, A., CALVER, A., COLLIER, J. & MONCADA, S. (1992). Accumulation of an endogenous inhibitor of nitric oxide synthesis in chronic renal failure. *Lancet*, **339,** 572–575.

WIKLUND, C.U., WIKLUND, N.P. & GUSTAFSSON, L.E. (1993). Modulation of neuroeffector transmission by endogenous nitric oxide: a role for acetylcholine-receptor activated NO formation, as indicated by measurements of NO/nitrite release. *Eur. J. Pharmacol.*, (in press).

(Received July 20, 1992
Revised April 18, 1993
Accepted May 24, 1993)

Br. J. Pharmacol. (1993), **110**, 840–846

Stimulated eosinophils and proteinases augment the transepithelial flux of albumin in bovine bronchial mucosa

Carolyn A. Herbert, *David Edwards, *John R. Boot & [1]Clive Robinson

Department of Pharmacology & Clinical Pharmacology, St George's Hospital Medical School, Cranmer Terrace, London SW17 0RE and *Lilly Research Centre Ltd, Eli Lilly & Co., Erl Wood Manor, Windlesham, Surrey GU20 6PH

1 The apical to basolateral transmucosal flux of albumin has been measured in isolated sheets of bovine bronchial and tracheal mucosa. Under resting conditions the net unidirectional flux in the bronchial mucosa was not significantly different from that measured previously for the basolateral to apical vector. In contrast, the apical to basolateral flux in the tracheal mucosa was significantly lower than that measured in the opposite direction.

2 Addition of guinea-pig peritoneal eosinophils to the apical side of the tissues had no significant effect on the transmucosal flux of albumin in either the bronchial or tracheal mucosa.

3 When eosinophils were stimulated with the ionophore A23187 or by opsonic adherence to tissues treated with a guinea-pig anti-bovine airway epithelium antibody, the bronchial mucosal sheets that had been exposed showed a significant increase in the transmucosal flux of albumin. However, tissues from the tracheal mucosa were resistant to the effects of stimulated eosinophils.

4 Histologically, sheets of mucosa from bovine main bronchi that had been exposed to stimulated eosinophils were characterized by epithelial injury consisting of loss of columnar epithelium from the underlying basal cell layer and biomatrix. Much less evidence of cellular injury was observed in tracheal tissues.

5 Bacterial collagenases applied to the apical side of the sheets were shown to increase the permeability of the bronchial mucosa to albumin and to produce histological changes that had similarities with the pattern of damage produced by stimulated eosinophils.

6 These observations demonstrate that the ability of eosinophils to injure the bronchial mucosa is independent of the side of the tissue on which they are present. Furthermore, key aspects of the injury process may be reproduced, at least in part, by metalloproteinases.

Keywords: Airway mucosa; trachea; bronchus; proteinases; tissue injury; eosinophil; albumin; matrix metalloproteinase

Introduction

Detachment of airway epithelial cells from their anchorage to basal cells and the biomatrix sub-stratum is a hallmark feature of the pathology of bronchial asthma (Naylor *et al.*, 1962; Laitinen *et al.*, 1985; Elia *et al.*, 1988; Jeffery *et al.*, 1989; Montefort *et al.*, 1992). Although there is compelling circumstantial evidence for the involvement of cytotoxic proteins, oxidants and other mediators in this process (Hastie *et al.*, 1987; Agosti *et al.*, 1987; Ayars *et al.*, 1989; Motojima *et al.*, 1989) there is little appreciation of the mechanistic events that occur to cause the phenomenon.

Current evidence suggests that a key event in the chronic inflammatory progression of asthma involves the priming and activation of eosinophils that have infiltrated into the bronchial sub-mucosa and airway lumen (Djukanović *et al.*, 1990; Aalbers *et al.*, 1993). Through their ability to express injury-promoting mediators, in particular the arginine-rich proteins of the eosinophil specific granule, eosinophils could play an important role in both the amplification and attenuation of airway inflammation (for review see Montefort *et al.*, 1992).

We have previously shown that these events can be modelled *in vitro* in a manner that allows the mechanism of the interaction of eosinophils with the airway mucosa to be studied under carefully controlled conditions (Herbert *et al.*, 1991a). Using modified Ussing Chambers which permit the separate bathing of the apical and basolateral faces of sheets of bovine bronchial epithelium, we have demonstrated that stimulated eosinophils or neutrophils from guinea-pigs are able to elicit tissue damage that is rapid in onset. This damage is characterized functionally by an increase in the permeability to macromolecules such as serum albumin, and morphologically by loss of epithelial cells in a manner that is strikingly reminiscent of the asthmatic airway (Laitinen *et al.*, 1985; Herbert *et al.*, 1991a; Montefort *et al.*, 1992). To avoid misunderstanding with terminology that has been used in a less precise and undefined way, we will refer to this combination of functional and structural changes as epithelial or mucosal injury.

Our previous experiments have been confined to an examination of the effects of eosinophils added to the basolateral side of the epithelium. An interesting feature of these results was the ability of the broad-spectrum anti-proteinase α_2-macroglobulin to inhibit these eosinophil-dependent changes (Herbert *et al.*, 1991a). We have subsequently shown that the interaction between eosinophils and the airway mucosa results in the expression and activation of latent metalloproteinases which could be involved in the detachment of epithelial cells (Herbert *et al.*, unpublished).

The present study had two components. In the first, our intention was to establish whether the ability of eosinophils to cause mucosal injury was restricted to their being on the basolateral side of the tissue. We reasoned that their activation on the apical side would provide information about whether eosinophils are capable of producing epithelial shedding when they are present in the airway lumen. In the second series of studies, we investigated the ability of an exogenous metalloproteinase to mimic the effect of stimulated eosinophils in this model. Together, these two components provide further mechanistic information about the interaction between eosinophils and the airway mucosa. A preliminary account of aspects of this work has been presented to The British Pharmacological Society (Herbert *et al.*, 1991b).

[1] Author for correspondence.

Methods

Tissue chambers

The methods used in these experiments have been described in detail elsewhere. In brief, fresh bovine lungs were obtained from a local abattoir and used within 1 h *post mortem*. A mid length section of trachea and main bronchi were identified, opened by incision and carefully removed by dissection. Dissected tissues were placed in Eagle's Minimum Essential Medium (MEM) buffered with 10 mM HEPES and washed extensively. The tissues were then cut into 1–2 cm^2 sized pieces and mounted between two acrylic plates each of which had a central aperture (0.8 cm and 0.5 cm diameter for the tracheal and bronchial tissues respectively). The tissues were sandwiched between the two plates by means of a circular array of pins and a leakproof seal obtained by means of a concentrically positioned rubber O-ring. Each assembled tissue 'sandwich' was then mounted between two water-jacketed half chambers which allowed the independent bathing of the apical and basolateral faces of the tissue.

Both sides of the apparatus were initially filled with MEM (2 ml per half chamber) and the tissue allowed to equilibrate at 37°C for 30 min. After equilibration, the chambers were orientated vertically and the bathing solution on the apical side replaced with medium containing cells (1 ml) or enzyme solution (200 µl). After predetermined exposure periods these solutions were removed, the chambers placed horizontally and then refilled with fresh cell- or enzyme-free medium prior to the measurement of albumin flux.

Measurement of albumin flux

The half-chambers on the apical side of the tissue were loaded with 2 ml MEM containing 2 µCi ^{125}I-labelled bovine serum albumin (BSA, sp. act. 2.1–3.5 µCi μg^{-1}). After addition of tracer the chambers were agitated gently throughout the rest of the experiment. At 0, 15, 30, 60, 90, 120, 150 and 180 min after addition, 25 µl samples of MEM were withdrawn by microsyringe from the half-chamber on the basolateral side of the tissue. Radioactivity was determined by gamma counting or scintillation analysis using, respectively, a Canberra-Packard Cobra B5003 or Packard 2000CA instrument. The net unidirectional rate of albumin movement was calculated as described elsewhere (Herbert *et al.*, 1991a). For comparative purposes, data are also included for studies where basolateral to apical fluxes were measured.

Purification and use of eosinophils

A peritoneal eosinophilia was established in male Dunkin-Hartley strain guinea-pigs by use of polymyxin B (Herbert *et al.*, 1991a). Peritoneal lavage was performed and the eosinophils enriched by centrifugation on discontinuous gradients of metrizamide (Herbert *et al.*, 1991a). Eosinophil purity was determined by staining with eosin/pontamine sky blue and cell viability measured by trypan blue exclusion. Preparations of $<80\%$ purity and $<90\%$ viability were discarded.

Eosinophils were stimulated with the calcium ionophore A23187 and also by initiating an antibody-dependent cytotoxicity reaction in mucosal sheets that had been opsonized by guinea-pig anti-bovine airway epithelium heat-inactivated serum (Herbert *et al.*, 1991a). For use in experiments the A23187 was maintained as a stock solution in dimethyl sulphoxide (DMSO) and diluted in MEM to produce the final concentration required (5 µM). Appropriate controls were employed to establish the effect of the 1% DMSO vehicle. For immunological activation, appropriate controls using heat-inactivated non-immune serum (sham treatment) were incorporated into the experimental design.

Treatment of tissues with enzymes

Solutions of bacterial collagenase were prepared in MEM and added as 200 µl aliquots to the apical side of the tissue when the chambers were mounted vertically. For comparison, in some experiments the enzymes were applied to the basolateral side of the tissue. After predetermined exposure periods, the enzyme solution was removed from each chamber and the chambers rinsed with MEM prior to measurement of albumin flux.

LDH assay

Lactate dehydrogenase (LDH) activity was measured in chamber fluid samples and expressed as a percentage of the total tissue LDH determined in homogenates of airway mucosa. The activity of LDH was quantified with a colourimetric assay involving the NADH-dependent reduction of pyruvic acid to lactic acid. Unreacted pyruvic acid was treated with 2,4-dinitrophenylhydrazine, the absorbance of the coloured product formed being inversely proportional to the LDH activity in the sample.

Processing of tissue samples

Sheets of bronchial or tracheal mucosa were fixed in 10% formalin (phosphate buffered at pH 7.4) whilst still mounted in the acrylic plates. After 10 min the exposed tissue was dissected free and fixed for a further 2–7 days prior to automated processing. The tissues were dehydrated through 70–100% alcohol, placed into xylene and then wax embedded. Sections (2–4 µm) were cut with a microtome. The strips were dried for at least 60 min, dewaxed and hydrated prior to staining. This was achieved by sequential treatment with xylene, alcohol (100–70%) and finally into water. Sections were stained with Ehrlich's haematoxylin (45 min room temperature) washed with water and briefly dipped into 70% alcohol/1% hydrochloric acid. Haematoxylin staining was repeated, and after washing with water the sections were counterstained for 5 min with 1% aqueous eosin (yellowish) and washed. Specimens were then dehydrated through 70–100% alcohol, equilibrated with xylene and mounted in distrine dibutylphalite xylene (DPX).

Materials

The following were purchased as indicated: radiolabelled albumin (NEN Du Pont Research Products, Stevenage, Herts.); Opti-Fluor scintillant (Canberra-Packard, Caversham, Berks.); metrizamide (Nycomed, Birmingham); ionophore A23187; reagents for assay of LDH; DMSO; Eagle's MEM (Sigma, Poole, Dorset). Collagenase (Clostridiopeptidase A, E.C. 3.4.24.3) from *Clostridium histolyticum* was also obtained from Sigma. In the present paper we describe experiments performed with two types of bacterial collagenase (Sigma type I and Sigma type IV). Both of these preparations are ammonium sulphate fractionations of bacterial culture supernatants and consequently contain small quantities of other enzyme activities. It should also be noted that the Sigma 'type' designations do not refer to the type of collagen preferentially degraded by the enzymes and to avoid such confusion in this manuscript we shall refer to them by their respective catalogue numbers as collagenase C0130 and collagenase C5138. Collagenase C0130 contained 300 collagen digestion units per mg solid and also contained 0.6, 99 and 0.6 units mg^{-1} of clostripain, caseinase and tryptic activity as determined by spectrophotometric assay. Collagenase C5138 had >650 collagen digestion units per mg solid and contained the same enzymes as impurities at specific activities of 0.29, 60 and 0.05 units mg^{-1}. For reference, the definitions of the individual enzyme units are as listed below: collagenase-one unit releases peptides from native interstitial collagen equivalent to 1 µmol L-leucine in 5 h at pH 7.4 and 37°C in the presence of calcium; clostripain-one unit hydrolyses 1 µmol N-α-benzoyl-L-arginine ethyl ester (BAEE) per min at pH 7.6 at 25°C in the presence

of 2.5 mM dithiothreitol; caseinase-one unit hydrolyses casein to produce colouration of Folin-Ciocalteau reagent equivalent to 1 μmol of L-tyrosine in 5 h at pH 7.5 and 37°C; tryptic activity-one unit hydrolyses 1 μmol BAEE per min at pH 7.6 and 25°C.

All other reagents were obtained as described previously (Herbert *et al.*, 1991a).

Statistics

Data are presented as the mean ± s.e.mean of n separate experiments. Statistical comparisons were made using the Mann-Whitney two sample test. Probability values (P) $\leqslant 0.05$ were considered statistically significant.

Results

Under control conditions in the absence of added eosinophils, the net unidirectional flux of albumin in the bronchial mucosa was 2.42 ± 0.13 fmol cm^{-2} min^{-1} for the basolateral to apical vector, whilst the corresponding value for the apical to basolateral vector was 2.39 ± 0.08 fmol cm^{-2} min^{-1} ($n = 32$ for each). In contrast, there was a significant difference between the vectorial rates in the tracheal preparation. For the basolateral to apical vector the net unidirectional flux was 1.00 ± 0.06 fmol cm^{-2} min^{-1} compared to 0.60 ± 0.04 fmol cm^{-2} min^{-1} in the reverse direction ($P \leqslant 0.001$, $n = 21$ and $n = 9$ respectively).

Eosinophils obtained by peritoneal lavage were enriched to an average of $86.9 \pm 2.8\%$ purity. The remaining cells consisted of $7.4 \pm 1.3\%$ macrophages, $3.8 \pm 1.7\%$ lymphocytes and $1.9 \pm 0.5\%$ neutrophils. Viability was $97.7 \pm 0.5\%$. We have shown elsewhere that eosinophils obtained in this way may be activated by 5 μM A23187 to produce a maximal release of leukotrienes (Herbert *et al.*, 1991a). In the presence of unstimulated eosinophils the net apical to basolateral (i.e. inward) flux of albumin was 0.64 ± 0.08 and 1.88 ± 0.15 fmol cm^{-2} min^{-1} in sheets of tracheal and bronchial mucosa respectively (data derived by compilation of information from Table 1). When compared with the corresponding basolateral to apical (i.e. outward) fluxes in the presence of unstimulated cells, there was no difference between the values in the bronchi (2.13 ± 0.19 outward, versus 1.88 ± 0.15 fmol cm^{-2} min^{-1} inward) whereas the inward flux was significantly lower than the outward in the trachea (0.96 ± 0.10 versus 0.64 ± 0.08). Data for the basolateral to apical direction ($n = 9$ and 11 experiments in trachea and bronchus) are derived from Herbert *et al.* (1991a).

Stimulation of eosinophils with 5 μM A23187 resulted in a significant augmentation of albumin flux after incubation of the cells with the bronchial mucosa (Table 1). In contrast, there was no significant effect in tracheal tissues (Table 1).

Opsonization of the apical side of the bronchial mucosa with a guinea-pig antibody which binds to epithelial cells had no significant effect on the resting transmucosal flux of albumin. Furthermore, addition of eosinophils to the apical side of these sham-treated tissues did not produce a significant change in the flux of albumin (data not shown). However, bronchial tissues that had been actively opsonized exhibited a significantly increased net rate of albumin flux when exposed to eosinophils for 60 min (Table 1). In contrast to this effect in the bronchial tissues, the net unidirectional flux of albumin in the tracheal tissues was unchanged by this manoeuvre (Table 1), and it was similarly unaffected by the process of tissue opsonization.

Histologically, bronchial tissues that had been exposed to stimulated eosinophils were characterized by gross disruption of the normal architecture of the epithelium (Figure 1). Extensive loss of columnar epithelium was noted with, in most of these cases, retention of attachments between basal cells and the underlying biomatrix. In areas where columnar epithelium was still present, there was visual evidence of cell shrinkage, vacuolation and loss of focal intercellular contact on the apical side of the epithelium. In contrast to these striking changes evident in the bronchial mucosa, at this resolution there was little evidence of disruption of the tracheal tissues.

In further experiments we examined the effects of exposing either the apical or the basolateral sides of airway mucosal tissue to collagenase preparations derived from *C. histolyticum*. The majority of experiments were performed with collagenase C5138, although comparative studies were made with the C0130 preparation. When added to the basolateral surface of bronchi and incubated for 3 h, 0.1 and 0.5 mg ml^{-1} concentrations of collagenase C5318 produced a significant increase in the basolateral to apical flux of albumin (Figure 2). Lower concentrations were ineffective, however. In some cases we also took the opportunity to investigate the changes in the net flux of mannitol using dual isotope liquid scintillation counting. Under control conditions the net flux of mannitol was, as expected for a solute of smaller mass and molecular radius, greater than that of albumin, and it was significantly increased by the highest concentration (0.1 mg ml^{-1}) of collagenase tested in that particular series of experiments (Figure 2). At concentrations of collagenase in the range 0.1–0.5 mg ml^{-1} damage to the mucosal sheet was sometimes evident at the macroscopic level and this possibly explains the heterogeneity of response depicted in Figure 2. At the single 0.5 mg ml^{-1} concentration tested, collagenase preparation C0130 was significantly less active than C5138 ($P \leqslant 0.05$), although this is most probably due to the fact that its collagenolytic specific activity was only half that of the C5138 preparation (see Methods). Nevertheless it still produced a significant augmentation of the net flux of albumin when compared to enzyme-free controls (Figure 2).

When added to the apical surface of the tissue, 0.1 and 0.5 mg ml^{-1} concentrations of collagenase C5138 produced significant increases in the net apical to basolateral flux of albumin when compared to the control (Figure 2). These changes were smaller in magnitude than those produced by exposure of the basolateral surface to the enzyme, but there was only a statistically significant difference for the 0.1 mg ml^{-1} concentration ($P \leqslant 0.01$). In the absence of enzyme, there was no significant differences between the control net

Table 1 Effect of lumenally applied eosinophils (3.3×10^6 ml^{-1}, contact time with mucosa 60 min) on the net apical to basolateral flux of bovine serum albumin in mucosal tissues from the trachea and main bronchus

Conditions	*Net unidirectional flux* (fmol cm^{-2} min^{-1}) *Tracheal mucosa*	*Bronchial mucosa*
Eosinophils plus 1% DMSO	0.72 ± 0.15	1.78 ± 0.20
Eosinophils plus 5 μM A23187	0.65 ± 0.09	5.95 ± 1.50*
Eosinophils plus sham opsonization	0.57 ± 0.07	2.02 ± 0.26
Eosinophils plus active opsonization	0.67 ± 0.07	3.70 ± 0.41*

Data are mean ± s.e.mean from 4–5 separate donor tissues.
*Significantly ($P \leqslant 0.05$) different from the appropriate control.

unidirectional fluxes in this particular series of experiments, with net rates of 2.92 ± 0.27 and 2.32 ± 0.10 fmol cm^{-2} min^{-1} for the basolateral to apical and apical to basolateral vectors respectively.

The exposure of the basolateral side of the bronchial mucosa to 0.1 mg ml^{-1} collagenase C5138 was not associated with a significant increase in the net amount of LDH released from the tissues over the 180 min incubation period (Figure 3), although the data indicate that there appeared to be a trend to slightly elevated release of LDH after collagenase exposure.

Both collagenase preparations also produced a significant

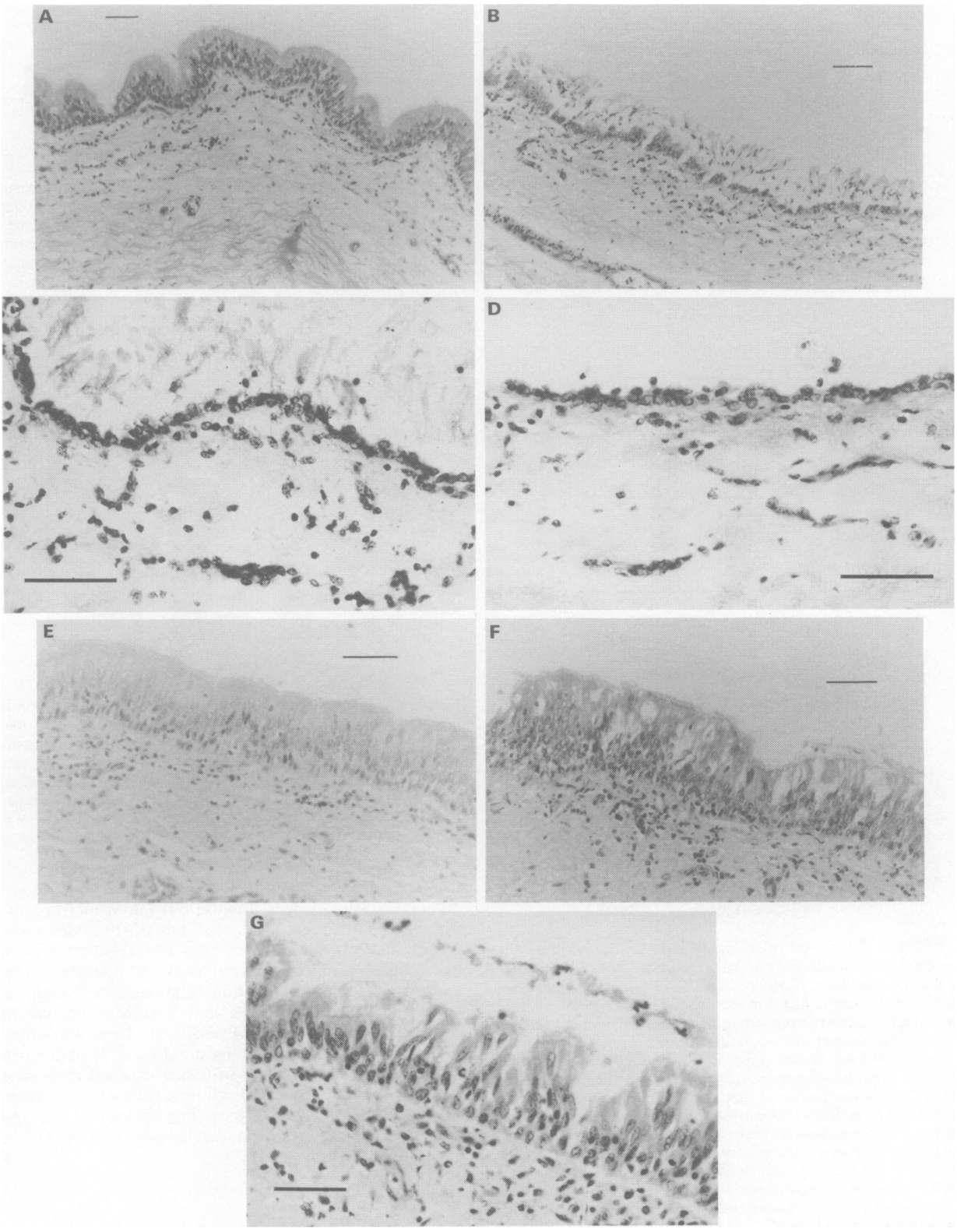

Figure 1 Panels (A-D) depict photomicrographs of haematoxylin and eosin-stained sections of bovine bronchial mucosa under (A) normal conditions, (B) following 180 min exposure of the basolateral side to 0.5 mg ml^{-1} C5318 collagenase, (C) after exposure of the apical surface to ionophore stimulated eosinophils for 60 min and (D) after exposure of the opsonized apical surface to eosinophils in an antibody-dependent cytotoxicity reaction. Panels (E-G) depict sections of tracheal mucosa under (E) control conditions, (F-G) following 180 min exposure of the basolateral side to 0.5 mg ml^{-1} C5318 collagenase. Scale bars depict 50 μm.

increase in the outward flux of albumin in the tracheal mucosa when added to the basolateral side at 0.5 mg ml^{-1} for 180 min (Figure 4). Apical addition of collagenase and inward flux of albumin was not tested.

Bronchial tissues that had been exposed to bacterial collagenase exhibited a pattern of injury that was broadly similar to that seen with eosinophils, although some differences were evident. Intense disruption or frank exfoliation of columnar cells was noted, but where evidence of these cells remained, the mucosa was characterized by loss of intercellular contacts between adjacent epithelial cells and their shrinkage or vacuolation (Figure 1). Although contact between basal cells and the matrix substratum was apparently normal at this level of resolution, there was occasional evidence of basal cell denudation (Figure 1), a finding that was not generally observed in tissues exposed to eosinophils. With the exception of basal cell loss, the metalloenzymes also produced changes in the gross morphology of the tracheal mucosa similar to those in the bronchi (Figure 1).

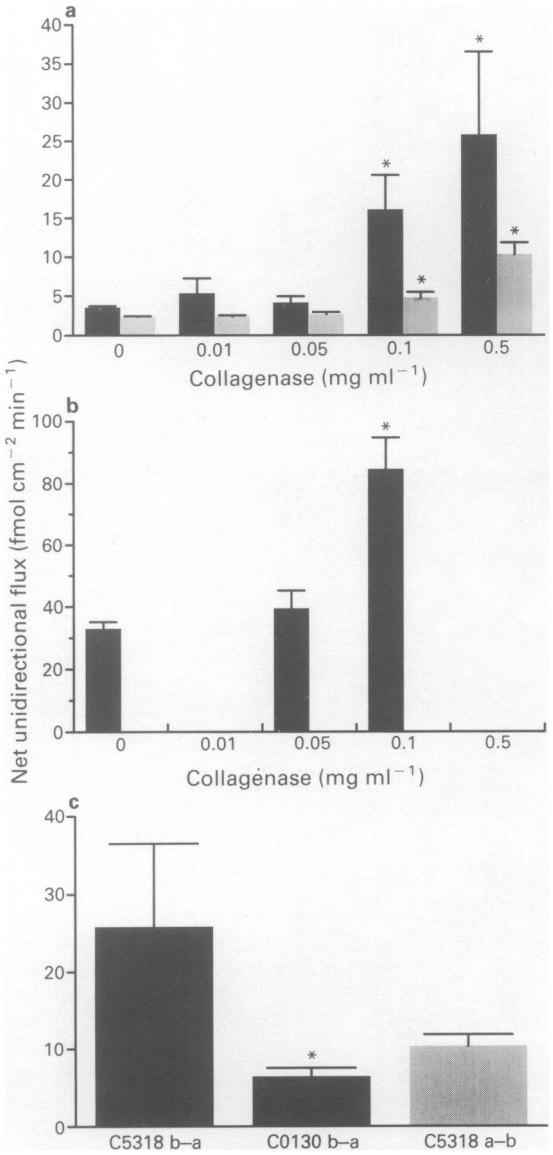

Figure 2 Effect of bacterial collagenase C5318 on the resulting net unidirectional flux of albumin when applied to bovine bronchial mucosa for 180 min. In (a) solid columns show basolateral addition of enzyme and albumin flux for the basolateral to apical vector. Stippled columns show corresponding addition to the apical surface and apical to basolateral flux. Data are mean ± s.e.mean from 4–8 experiments. Asterisks indicate significant differences ($P \leqslant 0.05$) with respect to the appropriate enzyme-free control. In (b) corresponding changes in the net unidirectional flux of [^{3}H]-mannitol produced by collagenase C5138 added to the basolateral side of the tissues. Data are from 3–5 experiments. Asterisks indicate significant differences ($P \leqslant 0.05$) with respect to the appropriate enzyme-free control. (c) Comparison of the effect of collagenases C5318 and C0130 added to the basolateral surface of bovine bronchial mucosa. The albumin flux vector was measured in the basolateral to apical (b-a) direction after 180 min exposure to 0.5 mg ml^{-1} solutions of the enzymes. For comparison, the stippled column illustrates the effect of the same concentration of C5138 applied to the apical side and where the flux vector was apical to basolateral (a-b). Data from 4–6 experiments. All treatments produced albumin fluxes that were significantly greater than enzyme-free controls. Asterisk indicates a significant ($P \leqslant 0.05$) difference between the C5318 and C0130 preparations.

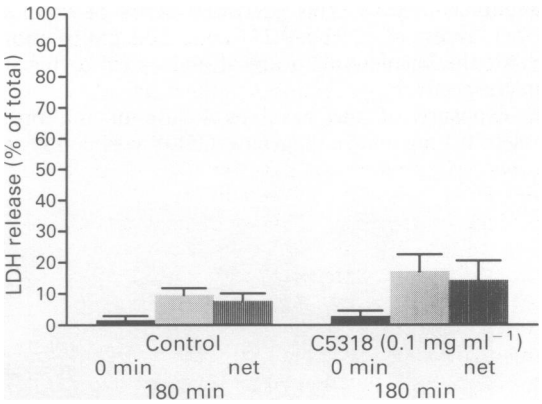

Figure 3 Release of lactic dehydrogenase (LDH) from bovine bronchial mucosa following treatment with 0.1 mg ml^{-1} collagenase C5318 for 180 min added to the basolateral side of the tissue. LDH activity was measured in pooled medium from the apical and basolateral sides of the chambers in order to obtain a measurement of all the LDH that had been released. Medium was sampled at 0 min (start of incubation) and after 180 min (end of enzyme incubation). The third column in each section of the figure illustrates the net release. Data from 5 experiments. There was no significant difference between the control (no enzyme) and enzyme treatments.

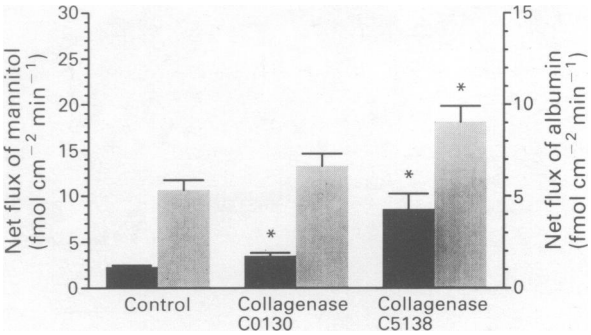

Figure 4 Effect of bacterial collagenases C0130 and C5138 on the net unidirectional flux of albumin (solid columns) and mannitol (shaded columns) after application of the enzymes to the basolateral side of tracheal mucosa of 0.5 mg ml^{-1} for 180 min. The vector of solute flow was basolateral to apical for this series of studies. Asterisks indicate significant differences ($P < 0.01$–0.05) with respect to the appropriate enzyme-free control value, data from 4–9 experiments in each case.

Discussion

In this study we have provided a further demonstration that guinea-pig eosinophils stimulated either by the calcium ionophore A23187 or by adherence to an opsonized bronchial mucosa are capable of augmenting the rate of flux of albumin across the tissue. This increase in permeability is accompanied by histological evidence of the loss of columnar

epithelium. Unlike the bronchial mucosa, the tissue dissected from the trachea was, under the conditions employed here, resistant to being exposed to stimulated eosinophils.

Previously, we have used eosinophils added to the basolateral side of tissues in order to mimic the infiltration of these cells into the airway sub-mucosa during an inflammatory reaction. We have now shown that the ability of stimulated eosinophils to initiate mucosal injury is independent of the side of the bronchial mucosa to which they are added. The magnitude of the changes in net flux produced under the present conditions are broadly comparable with those reported in our earlier work (Herbert *et al.*, 1991a). This suggests that whatever the mechanism(s) of this mucosal injury it is not impeded by the presence of interepithelial tight junctions at the apical side of the tissue.

From a theoretical viewpoint, our findings are consistent with the mediator(s) of this effect being able to act directly on epithelial cells, or being of sufficiently small molecular radius to negotiate intercellular junctions and act upon other cell types present in the tissue preparations. Amongst the many putative mediators released by eosinophils there are numerous contenders for either of these roles. Thus the arginine-rich proteins of the eosinophil granules are attractive candidates as macromolecular mediators that exert effects directly on epithelial cells, whilst oxidants (superoxide anion, hydrogen peroxide and hydroxyl radicals) are pervasive, tissue injury promoting species that might act at sites in addition to epithelial cells themselves. Further experiments will be necessary to establish the relative importance of different routes to epithelial injury.

Our previous studies have highlighted the possible involvement of proteinases in eosinophil-mediated epithelial injury in this model (Herbert *et al.*, 1991a). Little is known about proteolytic activities released by eosinophils, but one study has suggested that they contain collagenolytic activity directed toward type I and type III collagen (Davis *et al.*, 1984). In support of our initial pharmacological studies we have found that the interaction between eosinophils and the airway epithelium is associated with expression and activation of metalloproteinases (our unpublished data) that appear to be derived from the airway mucosa and not the eosinophils themselves. This series of observations suggested to us that matrix metalloenzymes may become activated by eosinophils and contribute to the detachment of columnar epithelial cells, particularly if structural components of the biomatrix are already damaged by oxidants (Thomas *et al.*, 1982; Grisham *et al.*, 1984; Vissers & Winterbourn, 1991).

Using collagenases derived from a bacterial source we have confirmed that metalloenzymes do have the potential to elicit a striking pattern of injury when added to either the basolateral or apical side of the bronchial mucosa. This loss of cells was not predominantly a cytolytic process as judged by the modest release of LDH. Addition of the enzyme to the apical side of the bronchial mucosa produced a marginal decrease in its effectiveness, most likely because its diffusion was initially restricted by epithelial tight junctions. In contrast to basolateral addition in the bronchial mucosa, the trachea was more resistant to the effects of both enzyme preparations tested, possibly as a result of the greater thickness of the tracheal mucosa e.g. compare Figure 2a with Figure 4. Damage of the airway mucosa by proteinases, basic proteins or other factors is known to have functional consequences by increasing tissue penetration of agonists (Jeppsson *et al.*, 1991; Takubo *et al.*, 1991; Yang *et al.*, 1991; Sparrow & Mitchell, 1991; Omari & Sparrow, 1992; Omari *et al.*, 1993a,b).

Morphologically, although the pattern of injury caused by eosinophils and bacterial collagenase exhibited some similarities, there were also some differences. The most significant of these was the failure of eosinophils but not collagenase (under the conditions used) to injure the tracheal mucosa. In the bronchial mucosa, outright detachment of columnar epithelium occurred with both enzyme and eosinophil treatment, although it was a more notable feature of tissues exposed to stimulated eosinophils. Where columnar cells were still visible, their gross morphology was abnormal, with evidence of vacuolation, shrinkage and disruption of contacts between adjacent epithelial cells. Bronchial mucosa that had been exposed to eosinophils usually retained a layer of basal cells attached to the biomatrix, whereas foci of basal cell loss were evident in enzyme-treated bronchi. The reasons for the apparent resilience of basal cells to detachment in the injury process is not known, although it has been speculated that this may arise because of differences in cellular adhesion mechanisms present in columnar and basal cells (see Montefort *et al.*, 1992 for review). However, it is likely that other explanations account for at least some of this resilience, either as a result of biochemical differences in the composition of lipid membranes, or a differential distribution of antioxidant and antiproteinase defences between the two cell types. Indeed, under *in vitro* culture, cell types exhibit differential sensitivities to eosinophil cytotoxicity in conditions that are not easily explicable by differences in cellular adhesion (Davis *et al.*, 1984).

The passage of serum albumin across the airway mucosa itself deserves some comment. In the present study we have provided evidence that both under resting conditions in the absence of any external manipulations, and in the presence of unstimulated eosinophils, there was a significantly greater outward flux of albumin. This difference was not observed in the bronchial mucosa, although it was noteworthy that the presence of unstimulated eosinophils caused a downward trend in the unidirectional fluxes measured in the bronchial tissues. We have observed this tendency previously (Herbert *et al.*, 1991a) and it may be related to the coating of the bronchial mucosa by adherent eosinophils leading to a reduction in the opportunities for macromolecular solute flow.

The precise routes by which albumin crosses the airway mucosa are not known. In addition to paracellular diffusion, previous studies in the airway epithelium have presented preliminary evidence for active basolateral to apical transport of albumin (Webber & Widdicombe, 1989; Price *et al.*, 1990), or its carrier-facilitated movement in the apical to basolateral direction in other species (Kwang-Jin *et al.*, 1985; Johnson *et al.*, 1989). We have observed saturability of the apical to basolateral flux of albumin in bovine bronchial mucosa, also consistent with the existence of carrier-mediated events (Herbert *et al.*, 1990 and unpublished data). Because virtually nothing is known about how these poorly characterized processes may be regulated by both physiological and pathophysiological events, it is possible that the presence of inflammatory cells and their mediators may exert an influence on the permeability of solutes. Current information suggests that, at least for platelet activating factor, this is likely to be the case (Rogers *et al.*, 1990). Clearly, the physiological control of mucosal permeability to macromolecules warrants further investigation given the likely importance of the protein load of epithelial lining fluid to its microviscosity and biochemical properties.

In summary, we have demonstrated that interaction of stimulated eosinophils with the apical side of the bronchial epithelium results in a rapid disorganization of its architecture and a significant increase in the permeability of the mucosa to albumin. Although it is probable that many different mediators contribute to these complex events, they can be reproduced, in part, by treatment of tissues with collagenase. This suggests that metalloproteinases deserve consideration as putative mediators of the eosinophil-dependent exfoliation of epithelial cells.

Aspects of this work have been supported by the SERC, The Medical Research Council and The British Lung Foundation. We thank Don Brandon for expert assistance.

References

AALBERS, R., KAUFFMAN, H.F., VRUGT, B., SMITH, M., KOËTER, G.H., TIMENS, W. & DE MONCHY, J.G.R. (1993). Bronchial lavage and bronchoalveolar lavage in allergen-induced single early and dual asthmatic responders. *Am. Rev. Respir Dis.*, **147,** 76–81.

AGOSTI, J.M., ALTMAN, L.C., AYARS, G.H., LOEGERING, D.A., GLEICH, G.J. & KLEBANOFF, S.J. (1987). The injurious effects of eosinophil peroxidase, hydrogen peroxide and halides on pneumocytes *in vitro*. *J. Allergy Clin. Immunol.*, **79,** 496–504.

AYARS, G.H., ALTMAN, L.C., MCMANUS, M.M., AGOSTI, J.M., BAKER, C., LUCHTEL, D.L., LOEGERING, D.A. & GLEICH, G.J. (1989). Injurious effect of the eosinophil peroxide-hydrogen peroxide-halide system and major basic protein on human nasal epithelium *in vitro*. *Am. Rev. Respir. Dis.*, **140,** 125–131.

DAVIS, W.B., FELLS, G.A., SUN, X.-H., GADEK, J.E., VENET, A. & CRYSTAL, R.G. (1984). Eosinophil-mediated injury to lung parenchymal cells and interstitial matrix. A possible role for eosinophils in chronic inflammatory disorders of the lower respiratory tract. *J. Clin. Invest.*, **74,** 269–278.

DJUKANOVIĆ, R., WILSON, J.W., BRITTEN, K.M., WILSON, S.J., WALLS, A.F., ROCHE, W.R., HOWARTH, P.H. & HOLGATE, S.T. (1990). Mast cells and eosinophils in the bronchial mucosa of symptomatic atopic asthmatics and healthy controls and their relationship to disease activity. *Am. Rev. Respir. Dis.*, **142,** 434–457.

ELIA, C., BUCCA, C., ROLLA, G., SCAPPATICCI, E.& CANTINO, D. (1988). Freeze fracture study of human bronchial epithelium in normal, bronchitic and asthmatic subjects. *J. Submicrosc. Cytol.*, **20,** 509–517.

GRISHAM, M.B., JEFFERSON, M.M., MELTON, D.F. & THOMAS, E.L. (1984). Chlorination of endogenous amines by isolated neutrophils. Ammonia-dependent bactericidal, cytotoxic and cytolytic activities of chloramines. *J. Biol. Chem.*, **259,** 10404–10413.

HASTIE, A.T., LOEGERING, D.A., GLEICH, G.J. & KUEPPERS, F. (1987). The effect of purified eosinophilic major basic protein on mammalian ciliary activity. *Am. Rev. Respir. Dis.*, **135,** 848–853.

HERBERT, C.A., EDWARDS, D., BOOT, J.R. & ROBINSON, C. (1991a). In vitro modulation of the eosinophil-dependent enhancement of the permeability of the bronchial mucosa. *Br. J. Pharmacol.*, **104,** 391–398.

HERBERT, C.A., EDWARDS, D., BOOT, J.R. & ROBINSON, C. (1991b). Further studies of the eosinophil-dependent enhancement of the permeability of the bronchial mucosa to albumin. *Br. J. Pharmacol.*, **102,** 27P.

HERBERT, C.A., SUMMERS, J.A. & ROBINSON, C. (1990). In vitro techniques for the study of transepithelial protein flux in the airways and its modulation by inflammatory cells and mediators. *Br. J. Pharmacol.*, **100,** 477P.

JEFFERY, P.K., WARDLAW, A.J., NELSON, F.C., COLLINS, J.V. & KAY, A.B. (1989). Bronchial biopsies in asthma. An ultrastructural quantitative study and correlation with hyperreactivity. *Am. Rev. Respir. Dis.*, **140,** 1745–1753.

JEPPSSON, A.B., SUNDLER, F., LUTS, A., WALDECK, B. & WIDMARK, E. (1991). Hydrogen peroxide-induced epithelial damage increases terbutaline transport in guinea pig trachea wall: implications for drug delivery. *Pulm. Pharmacol.*, **4,** 73–79.

JOHNSON, L.G., CHENG, P.W. & BOUCHER, R.C. (1989). Albumin absorption by canine bronchial epithelium. *J. Appl. Physiol.*, **66,** 2772–2777.

KWANG-JIN, K., LEBON, T.R., SHINBANE, J.S. & CRANDALL, E.D. (1985). Asymmetric albumin transport across bullfrog alveolar epithelium. *J. Appl. Physiol.*, **59,** 1290–1297.

LAITINEN, L.A., HEINO, M., LAITINEN, A., KAVA, T. & HAAHTELA, T. (1985). Damage of the airway epithelium and bronchial reactivity in patients with asthma. *Am. Rev. Respir. Dis.*, **131,** 599–606.

MONTEFORT, S., HERBERT, C.A., ROBINSON, C. & HOLGATE, S.T. (1992). The bronchial epithelium as a target for inflammatory attack in asthma. *Clin. Exp. Allergy*, **22,** 511–520.

MOTOJIMA, S., FRIGAS, E., LOEGERING, D.A. & GLEICH, G.J. (1989). Toxicity of eosinophil cationic proteins for guinea pig tracheal epithelium in vitro. *Am. Rev. Respir. Dis.*, **139,** 801–805.

NAYLOR, B.M. (1962). The shedding of the mucosa of the bronchial tree in asthma. *Thorax*, **17,** 69–72.

OMARI, T.I. & SPARROW, M.P. (1992). Epithelial disruption by proteases augments the responsiveness of porcine bronchial segments. *Clin. Exp. Pharmacol. Physiol.*, **19,** 785–794.

OMARI, T.I., SPARROW, M.P., CHURCH, M.K., HOLGATE, S.T. & ROBINSON, C. (1993a). A comparison of the effects of polyarginine and stimulated eosinophils on the responsiveness of the bovine isovolumic bronchial segment preparation. *Br. J. Pharmacol.*, **109,** 553–561.

OMARI, T.I., SPARROW, M.A. & MITCHELL, H.W. (1993b). Responsiveness of human isolated bronchial segments and its relationship to epithelial loss. *Br. J. Clin. Pharmacol.*, **35,** 357–365.

PRICE, A.M., WEBBER, S.E. & WIDDICOMBE, J.G. (1990). Transport of albumin by the rabbit trachea in vitro. *J. Appl. Physiol.*, **68,** 726–730.

ROGERS, D.F., ALTON, E.W.F.W., AURSUDKIJ, B., BOSCHETTO, P., DEWAR, A. & BARNES, P.J. (1990). Effect of platelet activating factor on formation and composition of airway fluid in the guinea-pig trachea. *J. Physiol.*, **431,** 643–658.

SPARROW, M.P. & MITCHELL, H.W. (1991). Modulation by the epithelium of the extent of bronchial narrowing produced by substances perfused through the lumen. *Br. J. Pharmacol.*, **103,** 1160–1164.

TAKUBO, T., BANKS, K. & MARTIN, J.G. (1991). Epithelium modulates the potency of vasoactive intestinal peptide in the guinea pig. *J. Appl. Physiol.*, **65,** 721–727.

THOMAS, E.L., JEFFERSON, M.M. & GRISHAM, M.B. (1982). Myeloperoxidase-catalyzed incorporation of amines into proteins: role of hypochlorous acid and dichloramines. *Biochemistry*, **21,** 6299–6308.

VISSERS, M.C.M. & WINTERBOURN, C.C. (1991). Oxidative damage to fibronectin. I. The effects of the neutrophil myeloperoxidase system and HOCl. *Arch. Biochem. Biophys.*, **285,** 53–59.

WEBBER, S.E. & WIDDICOMBE, J.G. (1989). The transport of albumin across the ferret in vitro whole trachea. *J. Physiol.*, **408,** 457–472.

YANG, J., MITZNER, W. & HIRSCHMAN, C. (1991). Role of the epithelium in airway smooth muscle responses to relaxant agonists. *J. Appl. Physiol.*, **71,** 1434–1440.

(Received March 9, 1993
Accepted May 24, 1993)

Br. J. Pharmacol. (1993), **110**, 847–853

Extracellular ATP and UTP activation of phospholipase D is mediated by protein kinase C-ε in rat renal mesangial cells

[1]Josef Pfeilschifter & Claire Merriweather

Department of Pharmacology, Biocenter, University of Basel, Klingelbergstrasse 70, CH-4056 Basel, Switzerland

1 We have studied whether a nucleotide receptor mediates the effects of extracellular ATP and UTP on phosphatidylcholine metabolism in rat cultured glomerular mesangial cells.

2 ATP and UTP stimulated a biphasic 1,2-diacylglycerol (DAG) formation in [^{3}H]-arachidonic acid-labelled mesangial cells. In contrast, in cells labelled with [^{3}H]-myristic acid, a tracer that preferentially marks phosphatidylcholine, both nucleotides induced a delayed monophasic production of DAG with a concomitant increase in phosphatidic acid and choline formation.

3 A phospholipase D-mediated phosphatidylcholine hydrolysis was further suggested by the observation that ATP and UTP stimulate the accumulation of phosphatidylethanol, when ethanol was added to mesangial cells.

4 The rank order of potency of a series of nucleotide analogues for stimulation of phosphatidylethanol formation was UTP = ATP > ITP > ATPγS > βγ-imido-ATP = ADP > 2-methylthio-ATP = βγ-methylene-ATP = ADPβS, while AMP, adenosine, CTP and GTP were inactive, indicating the presence of a nucleotide receptor.

5 Elevation of cytosolic free Ca^{2+} by the calcium ionophore A23187 (1 μM) or the Ca^{2+}-ATPase inhibitor, thapsigargin (200 nM) slightly increased phosphatidylethanol formation. However, chelation of cytosolic Ca^{2+} with high concentrations of Quin 2 did not attenuate ATP- and UTP-induced phosphatidylethanol production, thus suggesting that Ca^{2+} is not crucially involved in agonist-stimulated phospholipase D activation.

6 The protein kinase C (PKC) activator, phorbol 12-myristate 13-acetate (PMA), but not the biologically inactive 4α-phorbol 12,13-didecanoate, increased phospholipase D activity in mesangial cells, suggesting that PKC may mediate nucleotide-induced phosphatidylcholine hydrolysis.

7 Down-regulation of PKC-α and -δ isoenzymes by 8 h PMA treatment still resulted in full phospholipase D activation. In contrast, a 24 h treatment of mesangial cells with PMA, a regimen that also causes depletion of PKC-ε, markedly attenuated nucleotide-evoked phosphatidylethanol formation. In addition, the selective PKC inhibitor, calphostin C attenuated ATP- and UTP-induced phosphatidylethanol production.

8 In summary, these data suggest that extracellular ATP and UTP use a common nucleotide receptor to activate phospholipase D-mediated phosphatidylcholine hydrolysis. Stimulation of phospholipase D appears to involve the PKC-ε isoenzyme, activated by DAG derived from phosphoinositide hydrolysis by phospholipase C.

Keywords: Phospholipase D; nucleotide receptors; renal mesangial cells; protein kinase C

Introduction

Extracellular adenine nucleotides have an important impact on a wide range of physiological responses of cells (Gordon, 1986). These effects of extracellular adenosine 5'-triphosphate (ATP) on cells appear to be mediated through specific P_2-type purinoceptors (Burnstock, 1978). In 1985, Burnstock & Kennedy proposed a further subclassification of P_2-purinoceptors into P_{2x} and P_{2y} subtypes on the basis of agonist potency order and functional responses. Later, additional subtypes of P_2-purinoceptors have been described on platelets (P_{2T}-type) and on mast cells (P_{2Z}-type) (Gordon, 1986). Extracellular ATP has been demonstrated to couple via P_2-purinoceptor to polyphosphoinositide degrading phospholipase C in hepatocytes (Charest *et al.*, 1985), endothelial cells (Pirotton *et al.*, 1987), HL-60 cells (Cockcroft & Stutchfield, 1989), macrophages (Pfeilschifter *et al.*, 1989) and various other cell types (for review see El-Moatassim *et al.*, 1992). In the kidney, ATP has been reported to stimulate the inositol lipid signalling cascade and subsequent Ca^{2+} mobilization in mesangial cells (Pfeilschifter, 1990a,b; Schulze-Lohoff *et al.*, 1992; Pavenstädt *et al.*, 1993), glomerular epithelial cells (Pavenstädt *et al.*, 1992) and MDCK cells (Paulmichl *et al.*, 1991).

More recently another nucleotide, UTP, was shown to be involved in the regulation of diverse cell functions (for review see Seifert & Schulz, 1989). Häussinger *et al.* (1987) and von Kügelgen *et al.* (1987) were the first to suggest that the action of UTP could involve a receptor distinct from the P_2-purinoceptor in rat liver. However, in certain other tissues, ATP and UTP may use a common nucleotide receptor for triggering their biological responses (Pfeilschifter, 1990b; Davidson *et al.*, 1990; for review see O'Connor, 1992). This latter receptor type appears to be distinct from previously described P_2-purinoceptor subtypes. Using rat mesangial cells, we have previously demonstrated that UTP and ATP stimulated phosphoinositide turnover, and that responses to both agonists were affected equally well by pertussis toxin and phorbol ester, non-additive at maximal concentrations, similarly attenuated by reactive blue 2 and displayed cross-desensitization. These features are all consistent with the hypothesis that ATP and UTP activate a common nucleotide receptor (Pfeilschifter, 1990b).

Another important signalling pathway appears to act exclusively on phosphatidylcholine in response to a wide variety of agonists and thus generates phosphatidic acid and

[1] Author for correspondence.

1,2-diacylglycerol (DAG) from lipid sources other than phosphoinositides (for review see Billah & Anthes, 1990). In mesangial cells, platelet-derived growth factor (Pfeilschifter & Hosang, 1991), angiotensin II (Pfeilschifter *et al.*, 1992), endothelin (Kester *et al.*, 1992) and vasopressin (Troyer *et al.*, 1992) have been reported to stimulate phosphatidylcholine hydrolysis by phospholipase D activity. In the present study we have investigated the effects of ATP and UTP on phosphatidylcholine hydrolysis. We present evidence that ATP and UTP activate with similar potencies and characteristics phospholipase D-mediated phosphatidylcholine turnover, thus suggesting that a common nucleotide receptor not only triggers phosphoinositide, but also phosphatidylcholine signalling cascades in rat mesangial cells.

Methods

Cell culture

Rat glomerular mesangial cells were cultured as described previously (Pfeilschifter *et al.*, 1984). In a second step, single cells were cloned by limited dilution using 96-micro-well plates. Clones with apparent mesangial cell morphology were used for further processing. The cells exhibited the typical stellate morphology. Moreover, there was positive staining for the intermediate filaments desmin and vimentin, which are considered to be specific for myogenic cells (Travo *et al.*, 1982), positive staining for Thy 1.1 antigen, negative staining for factor VIII-related antigen and cytokeratin excluded endothelial and epithelial contaminations, respectively. The generation of inositol trisphosphate upon activation of the angiotensin II AT_1 receptor was used as a functional criterion for characterizing the cloned cell line (Pfeilschifter, 1990c). The cells were grown in RPMI 1640 supplemented with 10% fetal calf serum, penicillin (100 u ml^{-1}), streptomycin (100 $\mu g\ ml^{-1}$) and bovine insulin at 0.66 u ml^{-1} (Sigma).

Extraction and separation of diacylglycerol

Mesangial cells were labelled for 24 h with [^{3}H]-arachidonic acid (1.0 $\mu Ci\ ml^{-1}$; specific activity 240 Ci $mmol^{-1}$) or [^{3}H]-myristic acid (2.0 $\mu Ci\ ml^{-1}$; specific activity 54 Ci $mmol^{-1}$) in RPMI 1640 containing 10% fetal calf serum. The lipid extraction was performed according to Bligh & Dyer (1959). For separation of DAG the lipid extracts were dissolved in chloroform/methanol and spotted onto thin layer chromatography (t.l.c.) plates (precoated silica gel 60 with concentration zone, 0.25 mm thick). The chromatographs were developed in one dimension using n-heptane/diethyl ether/acetic acid (75:25:4, by vol.) as described by Pfeilschifter *et al.* (1984).

Assay of phospholipase D-catalyzed phosphatidylcholine hydrolysis

Nucleotide stimulated phosphatidylcholine hydrolysis was measured in cells prelabelled for 40 h with [methyl-^{3}H]-choline (5 $\mu Ci\ ml^{-1}$; specific activity 76 Ci $mmol^{-1}$) or for 24 h with [^{3}H]-myristic acid (2.0 $\mu Ci\ ml^{-1}$; specific activity 54 Ci $mmol^{-1}$). Prelabelled confluent cells were washed several times with medium to remove unincorporated label. The cells were incubated for a further 1 h. Ethanol was added to cell monolayers prelabelled with [^{3}H]-myristic acid 5 min prior to the addition of ATP or UTP. Incubations were terminated by collecting the medium and adding ice-cold methanol to the cells. After harvesting the cells from the dishes with a rubber policeman, lipids were extracted according to Bligh & Dyer (1959). Radioactivity in aliquots of medium, aqueous phase and chloroform phase was determined. Lipid extracts were separated by t.l.c., developed with either the top phase of ethyl acetate /2,2,4-trimethyl pentane/acetic acid/water (13:2:3:10, by vol.) for separation of phosphatidylethanol and phosphatidic acid or with chloroform/methanol/acetic acid/water (100:30:35:3, by vol.), for separation of phospholipids. Aqueous cell extracts and media were separated by ion-exchange chromatography on Dowex 50-WH^+ columns exactly as described by Cook & Wakelam (1989). Separation of aqueous extracts was cross-checked by a t.l.c. procedure modified from that described by Pritchard & Vance (1981) on silica gel G plates, developed with 0.5% NaCl/methanol/concentrated NH_4OH (10:10:1, by vol).

Statistical analysis

Statistical analysis was performed by one way analysis of variance (ANOVA). For multiple comparisons with the same control group, the limit of significance was divided by the number of comparisons according to Bonferroni.

Chemicals

[^{3}H]-choline and [^{3}H]-myristic acid were purchased from Amersham International, UK; [^{3}H]-arachidonic acid was from Du Pont de Nemours International, Regensdorf, Switzerland; ATP ATPγS, ADP, AMP, UTP, GTP, CTP, ITP, adenosine, cell culture media and nutrients were from Boehringer-Mannheim, Rotkreuz, Switzerland; βγ-imido-ATP, βγ-methylene-ATP and ADPβS were from Fluka Chemie, Buchs, Switzerland; 2-methylthio-ATP and calphostin C were from Ciba-Geigy Ltd., Basel, Switzerland; suramin was from Sigma Chemicals, Buchs, Switzerland; and phorbol 12-myristate 13-acetate (PMA), 4α-phorbol 12,13-didecanoate were from Calbiochem, Lucerne, Switzerland.

T.l.c. plates and all other chemicals used were from Merck, Darmstadt, Germany.

Results

ATP and UTP stimulate a biphasic DAG formation

Previously we have shown that [^{3}H]-myristic acid is selectively incorporated into phosphatidylcholine, whereas [^{3}H]-archidonic acid is equally distributed in phosphatidylcholine, phosphatidylethanolamine and phosphoinositides (Pfeilschifter *et al.*, 1992). Stimulation of mesangial cells with ATP (100 μM) or UTP (100 μM) increased the labelling of DAG, irrespective of the tracer used. The production of DAG was biphasic in [^{3}H]-arachidonic acid-labelled cells, with a first peak occurring at 20 s after the exposure to either ATP or UTP and a second peak at 5 min (Figure 1a). The first peak corresponds to the formation of inositol 1,4,5-trisphosphate (Pfeilschifter 1990a,b). DAG formation, therefore, may derive from phospholipase C-induced phosphoinositide hydrolysis. The second DAG peak occurred after inositol 1,4,5-trisphosphate levels had returned to control values. The time course of ATP- and UTP-stimulated DAG production in [^{3}H]-myristic acid-labelled cells is depicted in Figure 1b. DAG formation started to increase at 1 min and reached a maximum at 10 min. ATP- and UTP-induced production of DAG was dose-dependent as shown in Figure 2. There was no significant difference in the DAG response to ATP and UTP stimulation as regards the time-course and potency of both nucleotides, although UTP tended to be slightly more potent than ATP. In parallel to the nucleotide-triggered DAG formation there was a marked stimulation of phosphatidic acid generation (Figure 3).

ATP and UTP activate phospholipase D

Mesangial cells were labelled with [^{3}H]-choline and phosphatidylcholine hydrolysis was studied by analysis of the hydrophilic degradation products. Exposure of the cells to ATP (100 μM) or UTP (100 μM) caused a strong increase in choline production (Figure 4). There was no significant in-

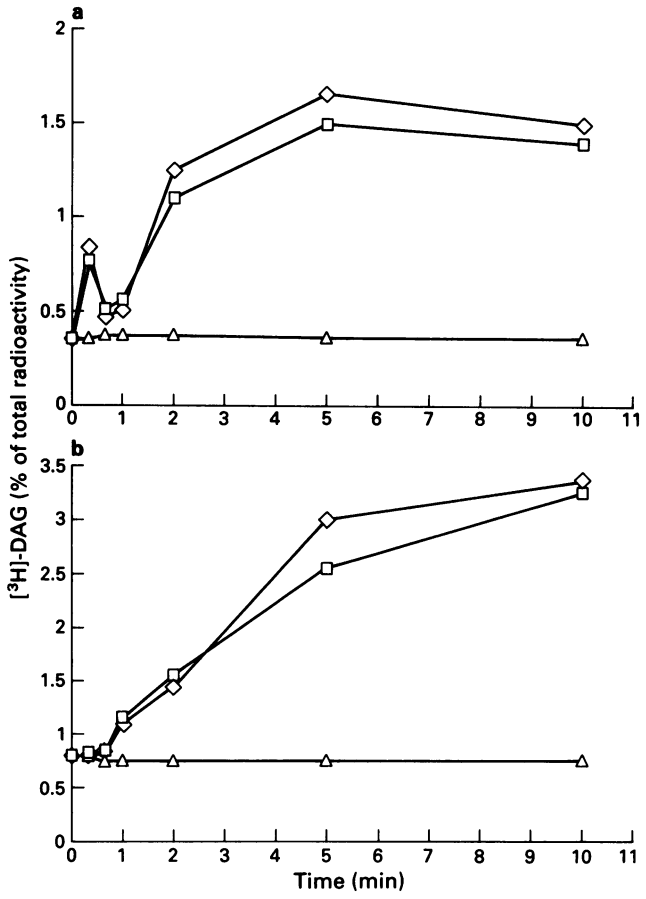

Figure 1 Time course of ATP and UTP-stimulated 1,2-diacylglycerol (DAG) formation in mesangial cells. Confluent cells were labelled with either [^{3}H]-arachidonic acid (a) or [^{3}H]-myristic acid (b) for 24 h. Cultures were then stimulated with ATP (100 μM, □), UTP (100 μM, ◇) or vehicle (△) for the indicated time periods. [^{3}H]-DAG formation was determined as described in Methods. Data are expressed as percentage of total incorporated radioactivity and are means of four experiments; the s.d. ranged from 5–12%.

crease in [^{3}H]-choline phosphate or in [^{3}H]-glycerophosphocholine upon stimulation of cells with ATP or UTP (data not shown). These data suggest that extracellular nucleotides activate a phospholipase D in mesangial cells, which degrades phosphatidylcholine. Phospholipase D can be more specifically assessed by its ability to catalyze a phosphatidyl transfer reaction in which ethanol or other primary alcohols act as the phosphatidyl moiety acceptor, thus generating phosphatidylethanol (Billah & Anthes, 1990). In the absence of ethanol, ATP and UTP stimulated the formation of phosphatidic acid and DAG (Figure 5). In the presence of 1% ethanol, ATP and UTP triggered the production of phosphatidylethanol, paralleled by a concomitant decline in phosphatidic acid and DAG accumulation (Figure 5). Obviously, both nucleotides triggered phospholipase D activation to a comparable extent. Preincubation of the cells with the putative P_2-receptor antagonist, suramin, dose-dependently attenuated both ATP- and UTP-induced phosphatidylethanol formation (Figure 6).

Table 1 shows the specificity for nucleotides and one nucleoside (100 μM each) in stimulating the production of phosphatidylethanol in mesangial cells. ITP, ATPγS, ADP and βγ-imido-ATP potently stimulated phosphatidylethanol production. βγ-Methylene-ATP, 2-methylthio-ATP and ADPβS had only a weak effect on phosphatidylethanol formation, while AMP, CTP, GTP and adenosine were completely ineffective in this capacity. The rank order of potency of the nucleotide analogues is compatible with a (common)

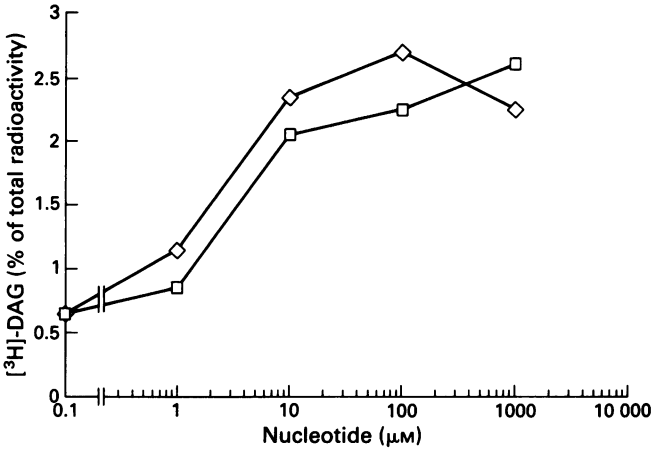

Figure 2 Dose-response curve of ATP- and UTP-stimulated 1,2-diacylglycerol (DAG) formation in mesangial cells. Confluent cells were labelled with [^{3}H]-myristic acid for 24 h and then stimulated with the indicated concentrations of ATP (□) or UTP (◇) for 10 min. [^{3}H]-DAG formation was determined as described in Methods. Data are expressed as percentage of total incorporated radioactivity and are means of four experiments; the s.d. ranged from 4–18%.

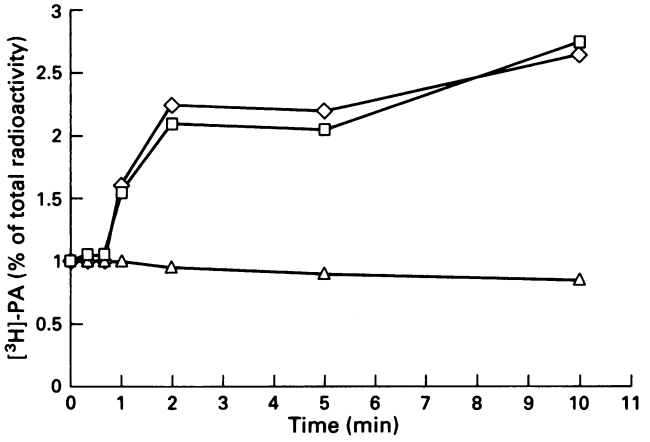

Figure 3 Time course of ATP- and UTP- stimulated phosphatidic acid (PA) formation in mesangial cells. Confluent cells were labelled with [^{3}H]-myristic acid for 24 h and then stimulated with ATP (100 μM, □), UTP (100 μM, ◇) or vehicle (△) for the indicated time periods. [^{3}H]-PA formation was determined as described in Methods. Data are expressed as percentage of total incorporated radioactivity and are means of four experiments; the s.d. ranged from 6–17%.

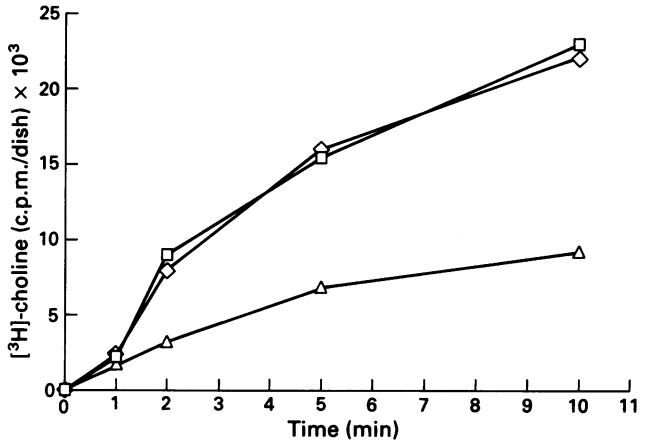

Figure 4 Time course of ATP- and UTP-stimulated choline formation in mesangial cells. Confluent cells were labelled for 40 h with [^{3}H]-choline. Cultures were then stimulated with ATP (100 μM, □), UTP (100 μM, ◇), or vehicle (△) for the indicated time periods. [^{3}H]-choline formation was determined in the culture supernatant. Results are means of four experiments, the s.d. ranged from 6–17%.

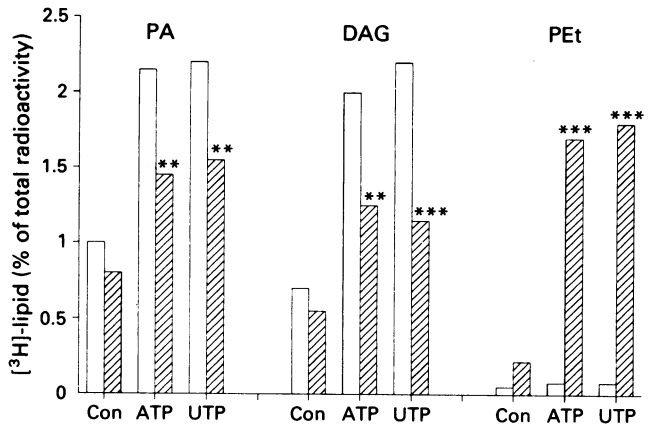

Figure 5 Effect of ATP and UTP on phosphatidic acid (PA), 1,2-diacylglycerol (DAG) and phosphatidylethanol (PEt) formation in mesangial cells. Confluent cells were labelled with [^{3}H]-myristic acid and then exposed to ATP (100 μM), UTP (100 μM) or vehicle (Con) for 10 min, either in the presence (hatched columns) or absence (open columns) of 1% ethanol. [^{3}H]-phosphatidic acid (PA), [^{3}H]-phosphatidylethanol (PEt) and [^{3}H]-DAG formation was determined as described in Methods. Data are expressed as percentage of total incorporated radioactivity and are means of four experiments; the s.d. ranged from 3–13%. Significant differences from corresponding control (without ethanol): $^{**}P<0.01$ and $^{***}P<0.001$, ANOVA.

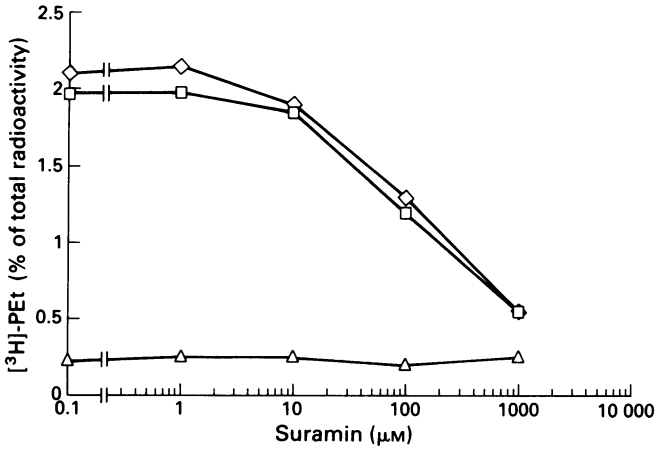

Figure 6 Effect of suramin on ATP- and UTP-stimulated phosphatidylethanol (PEt) formation in mesangial cells. Confluent cells were labelled for 24 h with [^{3}H]-myristic acid and pretreated for 30 min with the indicated concentrations of suramin. Cultures were then stimulated with ATP (100 μM, □), UTP (100 μM, ◇) or vehicle (△) for 10 min in the presence of 1% ethanol. Lipid extraction and separation was performed as described in Methods. Results are means of four experiments; s.d. ranged from 5–18%.

nucleotide receptor-mediated phospholipase D activation. Further evidence for this suggestion was provided by the lack of additivity of maximal doses of ATP and UTP on phosphatidylethanol formation (Table 1).

Roles of calcium and protein kinase C (PKC) in ATP and UTP-stimulated phospholipase D activation

It has been previously demonstrated that ATP and UTP evoke an increased inositol 1,4,5-trisphosphate and DAG generation from phosphatidylinositol 4,5-bisphosphate which trigger Ca^{2+} mobilization and PKC activation, respectively (Pfeilschifter, 1990a,b). We were, therefore, interested to investigate what role, if any, the increased intracellular Ca^{2+} and PKC play in ATP- and UTP-stimulated phospholipase D-mediated phosphatidylcholine hydrolysis. The requirement of Ca^{2+} for phospholipase D activity was examined using the

Table 1 Effects of different nucleotides and one nucleoside on phosphatidylethanol (PEt) formation in mesangial cells

Addition	*PEt* (% of total radioactivity)
Control	0.21 ± 0.05
ATP	1.85 ± 0.19***
UTP	1.97 ± 0.21***
ITP	1.64 ± 0.09***
CTP	0.30 ± 0.07
GTP	0.30 ± 0.06
ADP	1.14 ± 0.11***
AMP	0.24 ± 0.03
Adenosine	0.19 ± 0.05
ATPγS	1.42 ± 0.14***
βγ-imido-ATP	1.12 ± 0.10***
βγ-methylene-ATP	0.57 ± 0.09
2-methylthio-ATP	0.64 ± 0.08*
ADPβS	0.53 ± 0.07
ATP + UTP	1.98 ± 0.22***

Confluent mesangial cells were incubated for 24 h with [^{3}H]-myristic acid and then exposed to the different nucleotides or one nucleoside (100 μM each) for 10 min in the presence of 1% ethanol. Lipid extraction and separation was performed as described in Methods. Results are means ± s.d. of four experiments.
Significant differences from control: $^{*}P<0.05$ and $^{***}P<0.001$; ANOVA.

Ca^{2+} ionophore, A23187, the Ca^{2+} ATPase inhibitor, thapsigargin and by chelation of intracellular Ca^{2+} with high concentrations of Quin 2. As shown in Figure 7, A23187 (1 μM) and thapsigargin (200 nM) slightly increased phophatidylethanol formation. However, chelation of cytosolic Ca^{2+} with high doses of the Ca^{2+} buffer, Quin 2, did not attenuate ATP- or UTP-stimulated phosphatidylethanol formation, thus suggesting that an increase in cytosolic free Ca^{2+} is not essential for phospholipase D activation by nucleotides in mesangial cells.

The possible involvement of PKC in the nucleotide stimulation of phospholipase D activity was examined using phorbol esters, PKC down-regulation experiments, as well as a specific inhibitor of PKC. As shown in Figure 8, the PKC activator PMA caused a dose-dependent increase in phosphatidylethanol production. In contrast, the biologically inactive phorbol ester, 4α-phorbol 12,13-didecanoate, did not

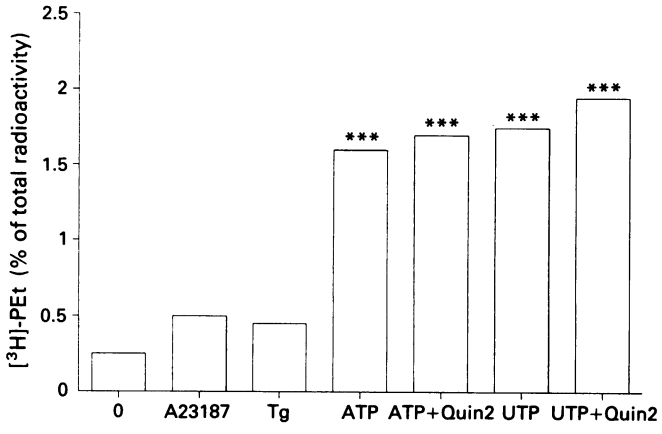

Figure 7 Effects of Ca^{2+} on phosphatidylethanol (PEt) formation in mesangial cells. Confluent cells were labelled for 24 h with [^{3}H]-myristic acid and pretreated for 60 min with 100 μM Quin 2/AM where indicated. Cultures were then stimulated with ATP (100 μM), UTP (100 μM), the Ca^{2+} ionophore A23187 (1 μM) or the Ca^{2+}-ATPase inhibitor, thapsigargin (Tg, 200 nM) for 10 min in the presence of 1% ethanol. Lipid extraction and separation was performed as described in Methods. Results are means of four experiments; s.d. ranged from 4–11%. Significant differences from control: $^{***}P<0.001$; ANOVA.

activate phospholipase D (Figure 8). Furthermore, PKC down-regulation by prolonged PMA treatment (24 h) blocked ATP- and UTP-stimulated phosphatidylethanol synthesis (Figure 9). However, a 8 h treatment with PMA that causes depletion of α- and δ-isoenzymes of PKC in mesangial cells (Huwiler *et al.*, 1991; 1992) was not sufficient to eliminate nucleotide-induced phospholipase D activation (Figure 9). It was necessary to preincubate the cells for 24 h with PMA, a regimen that also causes depletion of PKC-ε (Huwiler *et al.*, 1991), to prevent completely the responses to ATP and UTP (Figure 9). Moreover, the selective PKC inhibitor, calphostin C (1 μM) (Kobayashi *et al.*, 1989) attenuated ATP- and UTP-stimulated phosphatidylethanol formation (Figure 10).

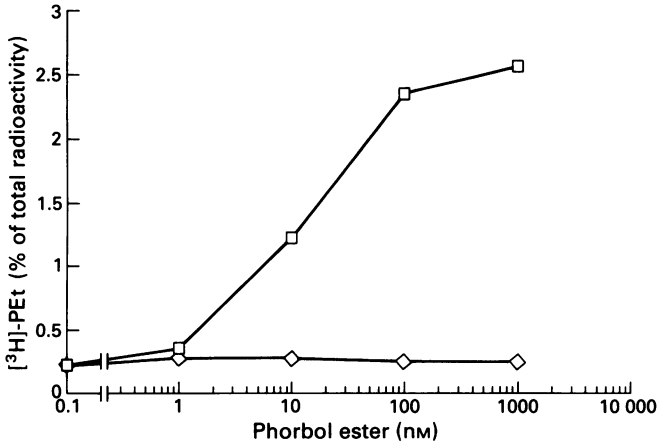

Figure 8 Dose-response curve of phorbol ester-stimulated phosphatidylethanol (PEt) formation in mesangial cells. Confluent cells were labelled for 24 h with [^{3}H]-myristic acid and then stimulated with the indicated concentrations of phorbol 12-myristate 13-acetate (PMA, □), or 4α-phorbol 12,13-didecanoate (◇) for 10 min in the presence of 1% ethanol. Lipid extraction and separation was performed as described in Methods. Results are means of four experiments; s.d. ranged from 3–9%.

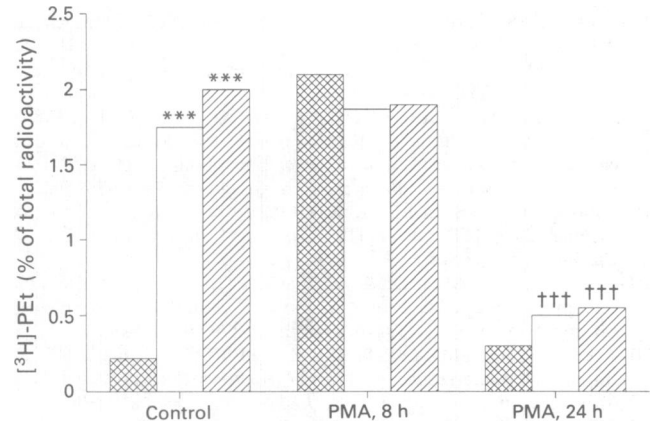

Figure 9 Effects of protein kinase C (PKC) down-regulation on ATP- and UTP-stimulated phosphatidylethanol (PEt) formation in mesangial cells. Confluent cells were labelled for 24 h with [^{3}H]-myristic acid and either non-pretreated (control) or pretreated for 8 h or 24 h with phorbol 12-myristate 13-acetate (PMA, 500 nM) as indicated. Cultures were then washed and stimulated with ATP (100 μM, open columns), UTP (100 μM, hatched columns) or vehicle (cross-hatched columns) for 10 min in the presence of 1% ethanol. Lipid extraction and separation was performed as described in Methods. Results are means of four experiments; s.d. ranged from 5–19%. Significant differences from corresponding control (without stimulation): ***$P<0.001$; ANOVA. Significant differences from corresponding control ATP and UTP stimulation (without PMA pretreatment): †††$P<0.001$; ANOVA.

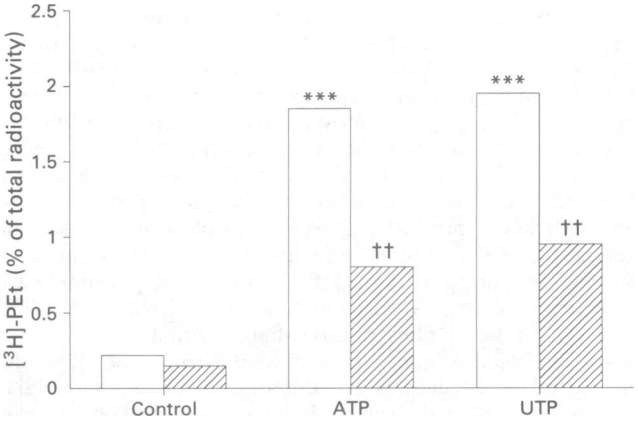

Figure 10 Effect of calphostin C on ATP- and UTP-stimulated phosphatidylethanol (PEt) formation in mesangial cells. Confluent cells were labelled for 24 h with [^{3}H]-myristic acid and pretreated for 30 min with calphosin C (1 μM, hatched columns) or vehicle (open columns). Cultures were then stimulated with ATP (100 μM), UTP (100 μM) or vehicle for 10 min in the presence of 1% ethanol. Lipid extraction and separation was performed as described in Methods. Results are means of four experiments; s.d. ranged from 7–14%. Significant differences from corresponding control: ***$P<0.001$; ANOVA. Significant differences from corresponding ATP or UTP stimulation in the absence of inhibitor. ††$P<0.01$, ANOVA.

Discussion

The presence of a nucleotide receptor with pharmacological characteristics different from those classically reported for a P_2-purinoceptor have been described first for sheep pituitary cells (Davidson *et al.*, 1990) and rat renal mesangial cells (Pfeilschifter, 1990b). ATP and UTP display similar potencies in activating the inositol lipid signalling cascade and subsequent Ca^{2+} mobilization whereas classical P_{2y} agonists (2-methylthio-ATP, ADPβS) and P_{2x} agonists (α,β-methylene-ATP; β,γ-methylene-ATP) were either inactive or showed only minor activity (Pfeilschifter, 1990b; Davidson *et al.*, 1990). The presence of this putative nucleotide receptor has also been described for human airway epithelial cells (Brown *et al.*, 1991), rat hepatocytes (Keppens *et al.*, 1992), the neuronal cell line N1E-115 (Iredale *et al.*, 1992), PC-12 phaeochromocytoma cells (Murrin & Boarder, 1992; Raha *et al.*, 1993) and a variety of other cell types (for review see O'Connor, 1992).

In the present study we have shown that ATP and UTP activate a phosphatidylcholine degrading phospholipase D in mesangial cells. Again, ATP and UTP displayed comparable potencies and characteristics in triggering this important signalling cascade, consistent with the hypothesis that ATP and UTP act via a common nucleotide receptor.

Phosphatidylcholine hydrolysis stimulated by ATP and UTP has also been demonstrated in endothelial cells (Purkiss & Boarder, 1992). Ultimate proof of a common nucleotide receptor mediating the described functional cell responses requires the development of convincing antagonists for either P_2-purinoceptors or the proposed nucleotide and pyrimidinoceptors.

We also have addressed the question concerning the pathways leading to activation of phospholipase D. There is substantial evidence for a role of Ca^{2+} and PKC in the activation of phospholipase D, indicating that activation of this enzyme is secondary to phosphoinositide hydrolysis (Billah & Anthes, 1990). In mesangial cells Ca^{2+} mobilization by the Ca^{2+} ionophore, A23187, and the Ca^{2+}-ATPase inhibitor, thapsigagrin, is able to trigger a small increase in phospholipase D activity. However, chelation of intracellular Ca^{2+} with high concentrations of Quin 2 did not affect ATP- and UTP-induced phospholipase D activation, indicating that agonist stimulation of the enzyme does not crucially

depend on Ca^{2+}. In this connection it is noteworthy that endothelin-stimulated phospholipase D was found to be Ca^{2+}-independent in mesangial cells (Kester *et al.*, 1992). In contrast, several lines of evidence indicate that PKC plays a major role in regulating phospholipase D activity in mesangial cells. First, the tumour promoting phorbol ester, PMA, activated phosphatidylcholine metabolism, whereas a biological inactive phorbol ester did not increase phosphatidylethanol production. Second, calphostin C, a specific inhibitor of PKC, interacting with the regulatory domain of the enzyme, attenuated nucleotide-stimulated phospholipase D activity. Third, down-regulation of PKC blocked ATP- and UTP-induced phosphatidylethanol formation.

PKC exists as a family of at least 10 isoenzymes, all having closely related structures but differing in tissue and cellular distribution and in their individual enzymological characteristics (Nishizuka, 1992). By immunoblot analysis we have shown previously that mesangial cells express four PKC isoenzymes, PKC-α, -δ, -ε and -ζ (Huwiler *et al.*, 1991; 1992; 1993). No PKC-β, -γ and -η isoforms were detected. On exposure to PMA, these isoenzymes displayed distinctly different down-regulation kinetics. An 8 h treatment with PMA was sufficient to deplete mesangial cells completely of PKC-α and -δ isotypes and a 24 h incubation with PMA was necessary to down-regulate PKC-ε. In contrast, PMA treatment for 24 h did not induce any depletion of PKC-ζ (Huwiler *et al.*, 1991; 1992; 1993). By comparing the down-regulation kinetics of the mesangial cell PKC isoenzymes with the time course of removal of the specific cellular functions, we have suggested that PKC-α and -δ may negatively regulate phosphoinositide turnover in response to angiotensin II (Huwiler *et al.*, 1991; 1992; Ochsner *et al.*, 1993) whereas PKC-ε is a candidate for regulation of phospholipase A_2 and prostaglandin synthesis in mesangial cells (Huwiler *et al.*, 1991). The data in Figure 9 show that an 8 h treatment with PMA still caused full activation of phospholipase D in mesangial cells, thus clearly ruling out a contribution of PKC-α or -δ isoenzymes to this cell response. In order to prevent ATP- and UTP-stimulated phosphatidylethanol formation, a 24 h incubation with PMA was required, suggesting that PKC-ε may not only trigger phospholipase A_2, but also phosphatidylcholine-specific phospholiase D. PKC-ε is a typical representative of the Ca^{2+}-independent group B isoenzymes (Stabel & Parker, 1991). In this connection it is worth noting that inhibitors of PKC which display a selectivity for the Ca^{2+}-dependent group A isoenzymes as compared to the Ca^{2+}-independent group B isotypes, such as staurosporine (McGlynn *et al.*, 1992), K-252a (Gschwendt *et al.*, 1989) or the specific PKC inhibitor CGP 41251 (Mate, B.M., Meyer, T., Stabel, S., Jaken, S., Fabbro, D. & Hynes, N.E., personal communication), did not inhibit ATP- or UTP-induced phospholipase D activation (Pfeilschifter & Merriweather, unpublished observations). Failure to achieve inhibition of phospholipase D with PKC inhibitors has led to the suggestion that phorbol ester may act in part through a PKC-independent mechanism (for review, see Billah & Anthes, 1990). Our observations could provide an alternative explanation for some of these reports. However, one should be aware that there may be a cell type-specific link between certain PKC isoenzymes and phosphilipase D activation. Overexpression of $PKC\beta_1$ in fibroblasts has been reported to enhance phospholipase D activity after PMA or endothelin-1 stimulation (Pai *et al.*, 1991a,b). On the other hand, DAG derived from phospholipase D-mediated phosphatidylcholine hydrolysis has been shown to activate selectively PKC-β in interferon-α-activated leucocytes (Pfeffer *et al.*, 1990) and PKC-ζ in activated *Xenopus* oocytes (Dominguez *et al.*, 1992). Thus, PKC-mediated activation of phospholipase D and the subsequent generation of DAG may provide a positive feedback loop to sustain PKC activation in cells.

In summary, our data suggest that ATP and UTP use a common nucleotide receptor to activate a phophatidylcholine-specific phospholipase D in mesangial cells. Furthermore, we provide evidence for a role of PKC-ε in mediating this nucleotide-induced cell response.

This work was supported by a grant from Ciba-Geigy Ltd. to C.M.

References

BILLAH, M.M. & ANTHES, J.C. (1990). The regulation and cellular functions of phosphatidylcholine hydrolysis. *Biochem. J.*, **269**, 281–291.

BLIGH, E.G. & DYER, W.J. (1959). A rapid method of total lipid extraction and purification. *Can. J. Biochem. Physiol.*, **37**, 911–917.

BROWN, H.A., LAZAROWSKI, E.R., BOUCHER, R.C. & HARDEN, T.K. (1991). Evidence that UTP and ATP regulate phospholipase C through a common extracellular 5'-nucleotide receptor in human airway epithelial cells. *Mol. Pharmacol.*, **40**, 648–655.

BURNSTOCK, G. (1978). A basis for distinguishing two types of purinergic receptors. In *Cell Membrane Receptors for Drugs and Hormones: A Multidisciplinary Approach*. ed. Straub, R.W. & Bolis, L. pp. 107–118. New York: Raven Press.

BURNSTOCK, G. & KENNEDY, C. (1985). Is there a basis for distinguishing two types of P_2-purinoceptor? *Gen. Pharmacol.*, **16**, 433–440.

CHAREST, R., BLACKMORE, P.F. & EXTON, J.H. (1985). Characterization of responses of isolated rat hepatocytes of ATP and ADP. *J. Biol. Chem.*, **260**, 15789–15794.

COCKCROFT, S. & STUTCHFIELD, J. (1989). ATP stimulates secretion in human neutrophils and HL60 cells via a pertussis toxin-sensitive guanine nucleotide-binding protein coupled to phospholipase C. *FEBS Lett.*, **245**, 25–29.

DAVIDSON, J.S., WAKEFIELD, I.K., SOHNIUS, U., VAN DER MERWE, P.A. & MILLAR, R.P. (1990). A novel extracellular nucleotide receptor coupled to phosphoinositidase-C in pituitary cells. *Endocrinology*, **126**, 80–87.

DOMINGUEZ, I., DIAZ-MECO, M.T., MUNICIO, M.M., BERRA, E., GARCIA DE HERREROS, A., CORNET, M.E., SANZ, L. & MOSCAT, J. (1992). Evidence for a role of protein kinase C ζ subspecies in maturation of *Xenopus laevis* oocytes. *Mol. Cell. Biol.*, **12**, 3776–3783.

EL-MOATASSIM, C., DORNAND, J. & MANI, J.C. (1992). Extracellular ATP and cell signalling. *Biochim. Biophys. Acta*, **1134**, 31–45.

GORDON, J.L. (1986). Extracellular ATP: effects, sources and fate. *Biochem. J.*, **233**, 309–319.

GSCHWENDT, M., LEIBERSPERGER, H. & MARKS, F. (1989). Differentiative action of K252a on protein kinase C and a calcium-unresponsive, phorbol ester/phospholipid-activated protein kinase. *Biochem. Biophys. Res. Commun.*, **164**, 974–982.

HÄUSSINGER, D., STEHLE, T. & GEROK, W. (1987). Actions of extracellular UTP and ATP in perfused in rat liver. *Eur. J. Biochem.*, **167**, 65–71.

HUWILER, A., FABBRO, D. & PFEILSCHIFTER, J. (1991). Possible regulatory functions of protein kinas C-α and -ε isoenzymes in rat renal mesangial cells. *Biochem. J.*, **279**, 441–445.

HUWILER, A., FABBRO, D., STABEL, S. & PFEILSCHIFTER, J. (1992). Immunocharacterization of δ- and ζ-isoenzymes of protein kinase C in rat renal mesangial cells. *FEBS Lett.*, **300**, 259–262.

HUWILER, A., SCHULZE-LOHOFF, E., FABBRO, D. & PFEILSCHIFTER, J. (1993). Immunocharacterization of protein kinase C isoenzymes in rat kidney glomeruli, and cultured glomerular epithelial and mesangial cells. *Exp. Nephrol.*, **1**, 19–25.

IREDALE, P.A., MARTIN, K.F., ALEXANDER, S.P.H., HILL, S.J. & KENDALL, D.A. (1992). Inositol 1,4,5-trisphosphate generation and calcium mobilization via activation of an atypical P_2 receptor in the neuronal cell line, N1E-115. *Br. J. Pharmacol.*, **107**, 1083–1087.

KEPPENS, S., VANDEKERCKHOVE, A. & DE WULF, H. (1992). Extracellular ATP and UTP exert similar effects on rat isolated hepatocytes. *Br. J. Pharmacol.*, **105**, 475–479.

KESTER, M., SIMONSON, M.S., MCDERMOTT, R.G., BALDI, E. & DUNN, M.J. (1992). Endothelium stimulates phosphatidic acid formation in cultured rat mesangial cells: role of a protein kinase C-regulated phospholipase D. *J. Cell. Physiol.*, **150**, 578–585.

KOBAYASHI, E., NAKANO, H., MORIMOTO, M., TAMAOKI, T. (1989). Calphostin C (UCN-1028C), a novel microbial compound, is a highly potent and specific inhibitor of protein kinase C. *Biochem. Biophys. Res. Commun.*, **156**, 548–553.

MCGLYNN, E., LIEBETANZ, J., REUTENER, S., WOOD, J., LYDON, N.B., HOFSTETTER, H., VANEK, M., MEYER, T. & FABBRO, D. (1992). Expression and partial characterization of rat protein kinase C-δ and protein kinase C-ζ in insect cells using recombinant baculovirus. *J. Cell Biochem.*, **49**, 239–250.

MURRIN, R.J.A. & BOARDER, M.R. (1991). Neuronal 'nucleotide' receptor linked to phospholipase C and phospholipase D? Stimulation of PC12 cells by ATP analogues and UTP. *Mol. Pharmacol.*, **41**, 561–568.

NISHIZUKA, Y. (1992). Intracellular signaling by hydrolysis of phospholipids and activation of protein kinase C. *Science*, **258**, 607–614.

OCHSNER, M., HUWILER, A., FLECK, T. & PFEILSCHIFTER, J. (1993). Protein kinase C inhibitors potentiate angiotensin II-induced phosphoinositide hydrolysis and intracellular Ca^{2+} mobilization in renal mesangial cells. *Eur. J. Pharmacol., Mol. Pharmacol.* (in press).

O'CONNOR, S.E. (1992). Recent development in the classification and functional significance of receptors for ATP and UTP, evidence for nucleotide receptors. *Life Sci.*, **50**, 1657–1664.

PAI, J.-K., DOBEK, E.A. & BISHOP, W.R. (1991a). Endothelin-1 activates phospholipase D and thymidine incorporation in fibroblasts overexpressing protein kinase. $C_{\beta 1}$. *Cell Reg.*, **2**, 897–903.

PAI, J.-K., PACHTER, J.A., WEINSTEIN, I.B. & BISHOP, W.R. (1991b). Overexpression of protein kinase Cβ1 enhances phospholipase D activity and diacylglycerol formation in phorbol ester-stimulated rat fibroblasts. *Proc. Natl. Acad. Sci. U.S.A.*, **88**, 598–602.

PAULMICHL, M., PFEILSCHIFTER, J. WÖLL, E. & LANG, F. (1991). Cellular mechanisms of ATP-induced hyperpolarization in renal epitheloid MDCK-cells. *J. Cell. Physiol.*, **147**, 68–75.

PAVENSTÄDT, H., SPÄTH, M. SCHLUNCK, G., NAUCK, M., FISCHER, R., WANNER, C. & SCHOLLMEYER, P. (1992). Effect of nucleotides on the cytosolic free calcium activity and inositol phosphate formation in human glomerular epithelial cells. *Br. J. Pharmacol.*, **107**, 189–195.

PAVENSTÄDT, H., GLOY, J., LEIPZIGER, J. KLÄR, B., PFEILSCHIFTER, J., SCHOLLMEYER, P. & GREGER, R. (1993). Effects of extracellular ATP on contraction, cytosolic calcium activity, membrane voltage and ion currents of rat mesangial cells in primary culture. *Br. J. Pharmacol.*, (in press).

PFEFFER, L.M., STRULOVICI, B. & SALTIEL, A.R. (1990). Interferon-α selectively activates the β isoform of protein kinase C through phosphatidylcholine hydrolysis. *Proc. Natl. Acad. Sci. U.S.A.*, **87**, 6537–6541.

PFEILSCHIFTER, J. (1990a). Extracellular ATP stimulates polyphosphoinositide hydrolysis and prostaglandin synthesis in rat mesangial cells. *Cell. Signal.*, **2**, 129–138.

PFEILSCHIFTER, J. (1990b). Comparison of extracellular ATP and UTP signalling in rat mesangial cells. *Biochem. J.*, **272**, 469–472.

PFEILSCHIFTER, J. (1990c). Angiotensin II B-type receptor mediates phosphoinositide hydrolysis in mesangial cells. *Eur. J. Pharmacol.*, **184**, 201–202.

PFEILSCHIFTER, J. & HOSANG, M. (1991). Effects of homo- and heterodimeric isoforms of PDGF on signalling events in rat renal mesangial cells. *Cell. Signal.*, **3**, 413–424.

PFEILSCHIFTER, J., KURTZ, A. & BAUER, C. (1984). Activation of phospholipase C and prostaglandin synthesis by (arginine) vasopressin in cultures of rat renal mesangial cells. *Biochem. J.*, **223**, 855–859.

PFEILSCHIFTER, J., THÜRING, B. & FESTA, F. (1989). Extracellular ATP stimulates poly (inositol phospholipid) hydrolysis and eicosanoid synthesis in mouse peritoneal macrophages in culture. *Eur. J. Biochem.*, **186**, 509–513.

PFEILSCHIFTER, J., HUWILER, A., MERRIWEATHER, C. & BRINER, V.A. (1992). Angiotensin II stimulation of phospholipase D in rat renal mesangial cells is mediated by the AT_1 receptor subtype. *Eur. J. Pharmacol. Mol. Pharmacol.*, **225**, 57–62.

PIROTTON, S., RASPE, E., DEMOLLE, D., ERNEUX, C. & BOEYNAEMS, J.-M. (1987). Involvement of inositol 1,4,5-trisphosphate and calcium in the action of adenine nucleotides on aortic endothelial cells. *J. Biol. Chem.*, **262**, 17461–17466.

PRITCHARD, P.H. & VANCE, D.E. (1981). Choline metabolism and phosphatidylcholine biosynthesis in cultured rat hepatocytes. *Biochem. J.*, **196**, 261–267.

PURKISS, J.R. & BOARDER, M.R. (1992). Stimulation of phosphatidate synthesis in endothelial cells in response to P_2-receptor activation. *Biochem. J.*, **287**, 31–36.

RAHA, S., DE SOUZA, L.R. & REED, J.K. (1993). Intracellular signalling by nucleotide receptors in PC12 pheochromocytoma cells. *J. Cell. Physiol.*, **154**, 623–630.

SCHULZE-LOHOFF, E., ZANNER, S., OGILVIE, A. & STERZEL, R.B. (1992). Extracellular ATP stimulates proliferation of cultured mesangial cells via P_2-purinergic receptors. *Am. J. Physiol.*, **263**, F374–F383.

SEIFERT, R. & SCHULTZ, G. (1989). Involvement of pyrimidine receptors in the regulation of cell functions by uridine and by uracil nucleotides. *Trends Pharmacol. Sci.*, **10**, 365–369.

STABEL, S. & PARKER, P.J. (1991). Protein kinase C. *Pharmacol. Ther.*, **51**, 712–795.

TRAVO, P., WEBER, K. & OSBORN, M. (1982). Co-existence of vimentin and desmin type intermediate filaments in a subpopulation of adult rat vascular smooth muscle cells growing in primary culture. *Exp. Cell. Res.*, **139**, 87–94.

TROYER, D.A., GONZALEZ, O.F. PADILLA, R.M. & KREISBERG, J.I. (1992). Vasopressin and phorbol ester-stimulated phosphatidylcholine metabolism in mesangial cells. *Am. J. Physiol.*, **262**, F185–F191.

VON KÜGELGEN, I., HÄUSSINGER, D. & STARKE, K. (1987). Evidence for a vasonconstriction-mediating receptor for UTP, distinct from the P_2 purine receptor, in rabbit ear artery. *Arch. Pharmacol.*, **336**, 556–560.

(Received April 5, 1993
Revised May 25, 1993
Accepted June 1, 1993)

Br. J. Pharmacol. (1993), **110**, 854–860

Characterization of the adenosine receptors of the rat superior cervical ganglion

[1]G.P. Connolly, T.W. Stone & *F. Brown

Department of Pharmacology, Glasgow University, Glasgow, G12 8QQ and *SmithKline Beecham Pharmaceuticals Research and Development, Harlow, Essex CM19 5AD

1 Adenosine analogues caused hyperpolarization and inhibition of the depolarizing response to muscarine of the rat isolated superior cervical ganglion (SCG) measured by a 'grease gap' recording technique. The receptors mediating these responses have been characterized by use of a range of selective adenosine analogues and adenosine receptor antagonists.

2 In decreasing order of potency N^6-cyclopentyladenosine (CPA), 2-chloroadenosine (2CA), adenosine, 2-phenylaminoadenosine (PAA), caused concentration-dependent hyperpolarizations whilst N^6-(9-fluorenylmethyl)adenosine (PD 117,413) was inactive at up to 100 μM.

3 The order of potency of adenosine analogues in depressing depolarization caused by a submaximal concentration of muscarine (100 nM) was: CPA > **R**-PIA = 2CA > NECA > **S**-PIA > BZA > adenosine > PAA, where **R**- and **S**-PIA = **R**(−)- and **S**(+)-N^6-(2-phenylisopropyl)adenosine, NECA = 5'N-ethylcarboxamidoadenosine and BZA = N^6-benzyladenosine. PD 117,413 was inactive at concentrations up to 100 μM. The maximum inhibitions of the muscarine-induced depolarization by CPA, 2CA, NECA and BZA were similar. **R**-PIA, **S**-PIA and PAA produced similar maximal inhibitions which were significantly smaller than those produced by CPA.

4 Hyperpolarizations caused by adenosine were antagonized by the P_1-purinoceptor selective antagonist 1,3-dimethyl-8-phenylxanthine (8PT) and by the selective A_1-adenosine receptor antagonist, 1,3-dipropyl-8-(4-((2aminoethyl)amino)carbonylmethyloxyphenyl)xanthine (XAC). Hyperpolarizations caused by CPA, adenosine and PAA were antagonized by the A_1-selective antagonist, 8-cyclopentyl-1,3-dipropylxanthine (DPCPX) but not by the A_2-selective antagonist, 3,7-dimethyl-1-propargylxanthine (DMPX).

5 Inhibition of the muscarinic-induced depolarization by CPA was antagonized by 8PT and DPCPX but not by DMPX.

6 It is concluded that the neurones of the rat SCG possess P_1-purinoceptors of the A_1-adenosine receptor subtype which mediate hyperpolarization and inhibition of depolarization caused by muscarine.

Keywords: Purines; adenosine; A_1-purinoceptors; A_2-purinoceptors; rat superior cervical ganglion; methylxanthines

Introduction

Adenosine hyperpolarizes the rat superior cervical ganglion (SCG) (Brown *et al.*, 1979; Connolly, 1991) and selectively depresses the depolarization by muscarinic agonists (Connolly & Stone, 1988; Connolly, 1991). We have investigated the receptors involved in mediating these effects using a range of adenosine analogues and some selective adenosine receptor antagonists.

The classification of purine receptors (purinoceptors) into P_1- and P_2-purinoceptors is based upon the selectivity of adenosine and nucleoside analogues of adenosine that show preference for P_1-purinoceptors and whose actions are antagonized by methylxanthines. By contrast P_2-purinoceptors show a greater selectivity for adenosine 5'-triphosphate and nucleotide analogues of adenosine 5'-triphosphate and their actions are not antagonized by methylxanthines (Burnstock, 1978; Stone, 1989). Further classification of P_1-purinoceptors into A_1- and A_2-adenosine receptor subtypes has been achieved by the use of 5'- and N^6-substituted analogues of adenosine (Van Calker *et al.*, 1979; Londos *et al.*, 1980). More recently the relative affinity of N^6-substituted adenosine analogues in binding studies has been examined by Daly *et al.* (1986) and Ukena *et al.* (1987) and it was proposed that the adenosine receptor analogues 5'-N-ethylcarboxamidoadenosine (NECA), N^6-cyclohexyladenosine (CHA), N^6-cyclopentyladenosine (CPA), **R**(+)- and **S**(−)-N^6-phenyl-isopropyladenosine (**R**-PIA and **S**-PIA), 2-chloroadenosine (2CA) and 2-phenylaminoadenosine (PAA) would be useful in functional studies for defining receptor subtypes. In both functional studies and binding studies a potency order of adenosine analogues for A_1-adenosine receptors was CPA > **R**-PIA ≥ 2CA ≥ NECA > **S**-PIA > PAA and for A_2-adenosine receptors was NECA > 2CA > PAA = **R**-PIA > CPA > **S**-PIA (Williams, 1989).

One antagonist that has proved useful in intact tissue studies is 1,3-dimethyl-8-phenylxanthine (8PT) which is a selective P_1-purinoceptor antagonist that is non-selective for A_1- and A_2-adenosine receptors (Collis, 1985). Some antagonists that have been found to exhibit useful selectivity between A_1- and A_2-adenosine receptors include the A_1-receptor selective 1,3-dipropyl-8-(4-((2-aminoethyl)amino)carbonylmethyloxyphenyl) xanthine (XAC) (Daly *et al.*, 1986; Fredholm *et al.*, 1987) and the more potent 8-cyclopentyl-1,3-dipropylxanthine (DPCPX) (Bruns *et al.*, 1987) and the A_2-receptor selective antagonist 3,7-dimethyl-1-propargylxanthine (DMPX) (Ukena *et al.*, 1986; Seale *et al.*, 1988).

Here we describe the effects of adenosine analogues on the basal d.c. potential and depolarization caused by muscarine, and the effects on these responses of selective A_1- and A_2-adenosine receptor antagonists, recorded by a grease gap technique from the rat isolated SCG. A preliminary report of this study has been presented elsewhere (Connolly & Brown, 1992).

[1] Author for correspondence, present address: Department of Physiology, University College London, Gower Street, London WC1E 6BT.

Methods

Ganglia were isolated, desheathed, and set up for recording of the d.c. potential between the ganglion body and the internal carotid nerve (ICN) as described before (Connolly, 1991; Connolly & Stone, 1993a). In brief, male Wistar rats (120 to 390 g) were terminally anaesthetized with urethane. The ganglion and an attached length of ICN were removed, desheathed and placed in a perfusion bath where a central chamber contained the ganglion body separated by a grease seal from the chamber containing the ICN. The potential difference between the ganglion and ICN was detected via electrodes in each chamber and after amplification was recorded with a pen recorder. The submerged body of the ganglion was perfused with either a standard physiological salt solution (referred to as PSS) or a low potassium and calcium PSS (low K^+/Ca^{2+} PSS). PSSs were continuously gassed with 5% CO_2/95% O_2 and maintained at pH 7.4 and 25 ± 1°C. The composition of PSS (expressed in mM) was: NaCl 125, $NaHCO_3$ 25, KCl 5, KH_2PO_4 1, $MgSO_4$ 1, glucose 10, $CaCl_2$ 2.5 and for low K^+/Ca^{2+} PSS, KCl and $CaCl_2$ were reduced to 1 and 0.1 mM respectively.

Muscarinic and adenosine agonists were dissolved in PSS as 10 or 100 mM stock solutions and frozen (−20°C) as aliquots. New aliquots of stock solutions were used for each experiment. To avoid precipitation of insoluble 8PT, 5–10 mg of 8PT was dissolved in up to 100 µl of alkali (1 M NaOH) and made up in PSS as a 10 mM stock solution which was diluted to a final concentration of 10 µM in PSS and the pH adjusted to 7.4 with dilute HCl.

Experimental protocols were derived from initial experiments. Drugs were applied for times that were found to be sufficient for potential changes to reach a plateau and allow repeated applications without desensitization. Ganglia were perfused for 2 to 3 h with PSS, during which time responses to muscarine (100 nM) and potassium (3 mM) stabilized and repeated applications of muscarine and analogues of adenosine produced reproducible responses and concentration-response curves could be obtained. Application of 100 nM muscarine produced submaximal depolarizations of ganglia of about 57% of the maximum response obtained with 1 µM muscarine (EC_{50} 84 nM for muscarine in PSS, $n = 15$). The depolarization evoked by muscarine was measured by extrapolation of the resting basal d.c. potential from the start of the application of muscarine to the finish of the depolarization, i.e. return to the basal level, and measuring the peak response during this time.

For hyperpolarizing responses, adenosine analogues were applied for 2 min periods at 20 min intervals and concentration-response curves were constructed by applying single concentrations of an analogue. Responses to adenosine and its analogues were measured by extrapolation of the resting basal d.c. potential from the start of the application of an analogue to the finish of the hyperpolarization, i.e. return to the basal level and measuring the peak response during this time.

For antagonism of hyperpolarizations caused by adenosine analogues, low K^+/Ca^{2+} PSS was used because hyperpolarizations evoked by adenosine, CPA, NECA and PAA were enhanced in low K^+/Ca^{2+} containing PSS compared to responses obtained in PSS, and could be more accurately assessed in the former solution (see Results, cf. Figure 1 and Table 1). Two concentration-response curves to a single adenosine analogue were made on each ganglion, the first being the control responses followed by the response to the same adenosine analogue after a minimum of 30 min incubation in the presence of an antagonist. In the absence of an adenosine-receptor antagonist the first and second concentration-response curves to adenosine and CPA (in PSS or low Ca^{2+}/K^+ PSS) were reproducible (results not shown, see Connolly, 1991). Occasionally a third concentration-response curve to an adenosine analogue was obtained after increasing the concentration of the antagonist in the bathing medium and allowing an additional 40 min incubation with the antagonist. Responses caused by a given concentration of an analogue of adenosine in the absence and presence of an adenosine-receptor antagonist were compared for statistically significant difference by a paired Student's t test.

During perfusion with PSS, muscarine (100 nM) was applied for 1 min at 20 min intervals. After obtaining two or three reproducible depolarizing responses to muscarine (the last response being used as a control response) the inhibition by adenosine analogues of the depolarization was determined by applying an adenosine analogue for a period of 5 min starting 1 min before the addition of muscarine. The concentration and sequence of adenosine analogues tested on each ganglia was randomized so that at least 4 ganglia from 3 different animals were used. The depolarizing response caused by muscarine after washing out the adenosine analogue returned to the control level within one or two applications of muscarine. Each ganglion was used as its own control and statistical differences between the response caused by muscarine before (control) and in the presence of an adenosine analogue were determine by a paired t test, and are expressed as the percentage inhibition of the control response caused by muscarine. When studying the effect of adenosine receptor antagonists (minimum 30 min incubation) on the inhibition caused by an adenosine analogue of the depolarization caused by muscarine, each concentration-response curve took at least 3 h and made it impractical to study more than one concentration of antagonist per experiment.

In all cases responses are expressed as mean ± s.e.mean (n), where n is the number of ganglia studied, and are derived from a minimum of three experiments with ganglia from three or more rats. Differences between responses (paired Student's t test, two-tailed) were considered significant if P values less than 0.05 were obtained. A non-statistically significant difference between responses is indicated by NS.

Drugs

Adenosine analogues N^6-cyclopentyladenosine (CPA), 2-chloroadenosine (2CA), N^6-benzyladenosine (BZA), 5'-(N-ethylcarboxamido)adenosine (NECA), 2-phenylaminoadenosine (PAA), and **R**(−)- and **S**(+)-N^6-(2-phenylisopropyl)-adenosine were bought from Research Biochemicals Inc (RBI). N^6-(9-fluorenylmethyl)adenosine (PD 117,413) was a gift of Warner-Lambert/Park Davis, Ann Arbour, U.S.A. Adenosine hemisulphate (AD) was bought from Sigma Chemical Co. Ltd. U.K.

Adenosine receptor antagonists 1,3-Dipropyl-8-(4-((2-aminoethyl)amino)carbonylmethyloxyphenyl)xanthine (XAC), 8-cyclopentyl-1,3-dipropylxanthine (DPCPX), and 1,3-dimethyl-8-phenylxanthine (8PT) were bought from RBI. 3,7-Dimethyl-1-(2-propynyl)xanthine (DMPX) was a most kind gift supplied by Dr John Daly (NIDDK, NIH, Bethesda, Maryland, U.S.A.).

(±)-Muscarine was bought from RBI. Salts used for PSS were of Analar grade.

Results

The effect of adenosine analogues on the d.c. potential

In order of decreasing potency, CPA, 2CA, adenosine and PAA caused reproducible, concentration-dependent, hyperpolarizations of ganglia (Figure 1). Adenosine elicited its maximal response more rapidly than did some of its analogues; however, all adenosine analogues elicited their maximum response within 2 min. Responses to supramaximal concentrations of adenosine (> 100 µM) were not altered by increasing the contact time from 2 to 5 min or by prolonging the interval between applications from 20 to 60 min. PAA,

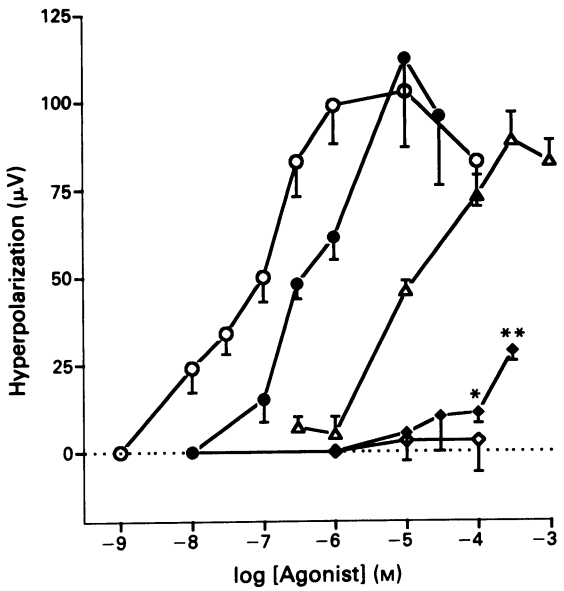

Figure 1 Effect of adenosine analogues on the d.c. potential of the rat superior cervical ganglion (SCG). Each point represents the mean response recorded in standard PSS, from three ganglia (six for 2CA) where (○) = CPA, (●) = 2CA, (△) = adenosine, (◆) = PAA and (◇) PD 117,413. In this and subsequent figures the symbol indicates the mean response and the bar the s.e.mean of the response. Statistically significant difference between responses in the absence and presence of antagonist (paired, 2-tailed, Student's t test) in this and in subsequent figures is indicated by $*P<0.05$; $**P<0.01$ and $***P<0.001$. For list of abbreviations see drugs.

up to the limits of solubility, caused concentration-dependent hyperpolarizations which at 100 and 300 μM were significantly different from the basal d.c. potential ($P<0.05$ ($n=6$) and $P<0.01$ ($n=4$) respectively) (Figure 1). The maximal response caused by PAA was considerably smaller than that observed for other adenosine analogues and the response evoked by 100 μM PAA was unaltered by increasing the contact time to 5 min. PD 117,413 at 10 μM and 100 μM did not significantly change the d.c. potential (-3 ± 2 μV, $n=7$ and -3 ± 9 μV, $n=10$ respectively). The potency order for hyperpolarization and EC_{50}s (μM) were: CPA (0.12) > 2CA (0.6) > adenosine (10) >> PAA (17) >> PD 117,413 (inactive).

The effect of adenosine analogues on the response to muscarine

All the adenosine analogues tested, except PD 117,413 caused concentration-dependent reduction of the depolarization caused by mucarine (Table 1). The changes obtained with PD 117.413 at 10 μM and 100 μM were insignificant (-6 ± 3%, $n=6$ and $+8\pm7$%, $n=5$ respectively). In order of decreasing potency CPA, 2CA, NECA and BZA produced similar (and not significantly different) maximal % inhibitions of the depolarization caused by muscarine. In contrast, in decreasing potency order **R**-PIA, S-PIA, adenosine and PAA produced smaller maximal % inhibitions of the depolarization caused by muscarine which were not significantly different from each other, but were significantly different when compared to the maximal % inhibition caused by CPA (Table 1).

The overall potency order for the inhibition of responses caused by muscarine by adenosine analogues was: CPA > 2CA = **R**-PIA > NECA > S-PIA > BZA > adenosine > PAA >> PD 117,413 (inactive).

Effect of adenosine receptor antagonists on the hyperpolarization caused by adenosine analogues

The effects of adenosine-receptor antagonists on the hyperpolarizing responses caused by adenosine and CPA were studied in low K^+/Ca^{2+} PSS as responses caused by these compounds were significantly enhanced, e.g. compare responses evoked by CPA in PSS to those in low K^+/Ca^{2+} (Figures 1 and 3a) and responses evoked by adenosine in PSS and low K^+/Ca^{2+} (Figures 1 and 2).

Adenosine-induced hyperpolarizations were antagonized by the P_1-purinoceptor selective antagonist 8PT (1 and 10 μM) (Figure 2) and by the selective A_1-adenosine receptor antagonist XAC (3, 10 and 100 nM) (illustrated for 3 and 100 nM XAC in Figure 3b).

The selective A_1-adenosine receptor antagonist DPCPX (0.3 nM or 1 nM) antagonized hyperpolarizations caused by CPA or adenosine (Figure 3a). DPCPX (1 nM) significantly reduced hyperpolarizations caused by NECA and CPA and reversed hyperpolarizations caused by PAA into small depolarizations (PAA control response = -94 ± 23 μV and in presence of DPCPX (1 nM) 43 ± 5 μV, $n=4$, $P<0.05$) (Figure 4). The selective A_2-adenosine receptor antagonist, DMPX, at 10 μM did not significantly affect hyperpolarizations caused by adenosine (control responses caused by 10 and 100 μM adenosine were -198 ± 7 μV, -258 ± 43 μV and in the presence of DMPX, -168 ± 17 μV and -308 ± 91 μV, respectively, $n=4$), CPA (control response caused by 0.1 μM CPA -272 ± 64 μV and in the presence of DMPX, -262 ± 70 μV, $n=4$) and hyperpolarizations caused by PAA (control responses caused by 10 and 100 μM PAA were -47 ± 17 μV, -112 ± 20 μV and in the presence of DMPX, -33 ± 15 μV and -83 ± 24 μV, respectively, $n=4$). DMPX at 50 μM did not affect hyperpolarizations caused by adenosine (Figure 3c). The antagonism of responses evoked by adenosine by 8PT, XAC and DPCPX all appeared to show non-parallel rightward shifts of the concentration res-

Table 1 The effect of adenosine analogues on the depolarizing response of the rat superior cervical ganglion (SCG) to muscarine

Adenosine analogue	*IC_{50}* (μM)	*Maximum % inhibition of response to muscarine*[a]	*Relative efficacy*[b]	*Con*[c] *for maximum inhibition* (μM)	*Potency relative to CPA*
CPA	0.02	39 ± 3*** (10)	1.0 ± 0.08[NS]	0.3	1
R-PIA	0.07	25 ± 3** (7)	0.6 ± 0.12**	1	0.29
2CA	0.07	36 ± 5*** (7)	0.9 ± 0.14[NS]	0.3	0.28
NECA	0.12	28 ± 5*** (8)	0.7 ± 0.18[NS]	1	0.17
S-PIA	0.34	21 ± 2** (4)	0.5 ± 0.10**	3	0.06
BZA	10	36 ± 2*** (6)	0.9 ± 0.06[NS]	30	0.002
Adenosine	15	27 ± 2*** (62)	0.7 ± 0.08**	100	0.001
PAA	⩾ 15	⩾ 19 ± 4** (4)	⩾ 0.5 ± 0.21**	⩾ 300	⩽ 0.001

Responses are the mean ± s.e.mean (n).

[a]Statistically significant differences in responses to muscarine in the absence and presence of adenosine or its analogues are indicated. $*P<0.05$; $**P<0.01$ and $***P<0.001$.

[b]Relative efficacy = % maximum inhibition caused by an adenosine analogue/% maximum inhibition caused by CPA. The % maximum inhibition caused by CPA was compared to the % maximum inhibition caused by other adenosine analogues and statistically significant differences (using an unpaired t test to compare individual % maximal inhibitions for each group of analogues to the % maximal inhibitions caused by CPA) is indicated by $**P<0.01$ and NS (not significant).

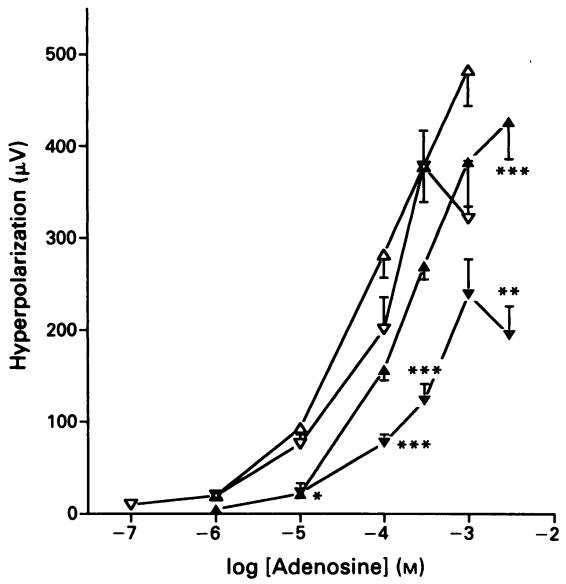

Figure 2 Effect of 1,3-dimethyl-8-phenylxanthine (8PT) on the adenosine-induced hyperpolarization of the rat superior cervical ganglion. Responses in low K^+/Ca^{2+} PSS evoked by adenosine in the absence (Δ), (∇) and presence of 1 μM (▲) and 10 μM (▼) 8PT respectively ($n = 4$ to 7). Statistical significance as for Figure 1.

ponse curves with a reduction in the maximum response (Figures 2, 3a,b).

Effect of adenosine receptor antagonists on the inhibition of the depolarization to muscarine by adenosine analogues

The inhibition of muscarine-induced depolarization by adenosine and CPA was reproducible and consistent within a single ganglion, e.g. CPA at 0.1 μM inhibited the depolarization caused by muscarine (100 nM) in three ganglia by 28 ± 3% and 27 ± 5% upon repetition (NS). 8PT (1 μM (not shown) and 10 μM) antagonized the effect of CPA in inhibiting the depolarization caused by muscarine (rightward shift of the concentration-response curve, Figure 5). 8PT (1 and 10 μM) significantly antagonized the inhibition by 10 and 100 μM adenosine (data not shown) and at 10 μM, 8PT antagonized the inhibition by 0.3 μM 2CA, from 38 ± 2% to 11 ± 5% ($n = 3$, $P < 0.05$). DPCPX at 0.5 nM or 1 nM antagonized the inhibitory effect of CPA, causing a reduction of the maximal inhibition of the muscarine-induced depolarization (as illustrated for 0.5 nM DPCPX in Figure 5) and at 10 nM DPCPX abolished the inhibition caused by 0.1 and 0.3 μM CPA (control % inhibitions of muscarine-induced depolarization caused by 0.1 and 0.3 μM CPA were 25 ± 3% and 35 ± 3% and in the presence of DPCPX (10 nM), 3 ± 3% and 3 ± 7%, respectively, both significantly different from controls, $P < 0.05$, $n = 5$). In contrast, DMPX (10 μM) was without effect on the inhibition caused by 0.1 μM CPA (control response 27 ± 4% and in the presence of DMPX (10 μM) 29 ± 5%, respectively).

Discussion

The potency order of adenosine analogues in hyperpolarizing the SCG and inhibiting the depolarization caused by muscarine was characteristic of that generally observed for A_1-adenosine receptor agonists and differed markedly from the order characteristic of A_2-adenosine receptor agonists as outlined in the Introduction and as described and reviewed by Williams (1989). Both the absolute potency and relative order of potency of adenosine analogues in hyperpolarizing

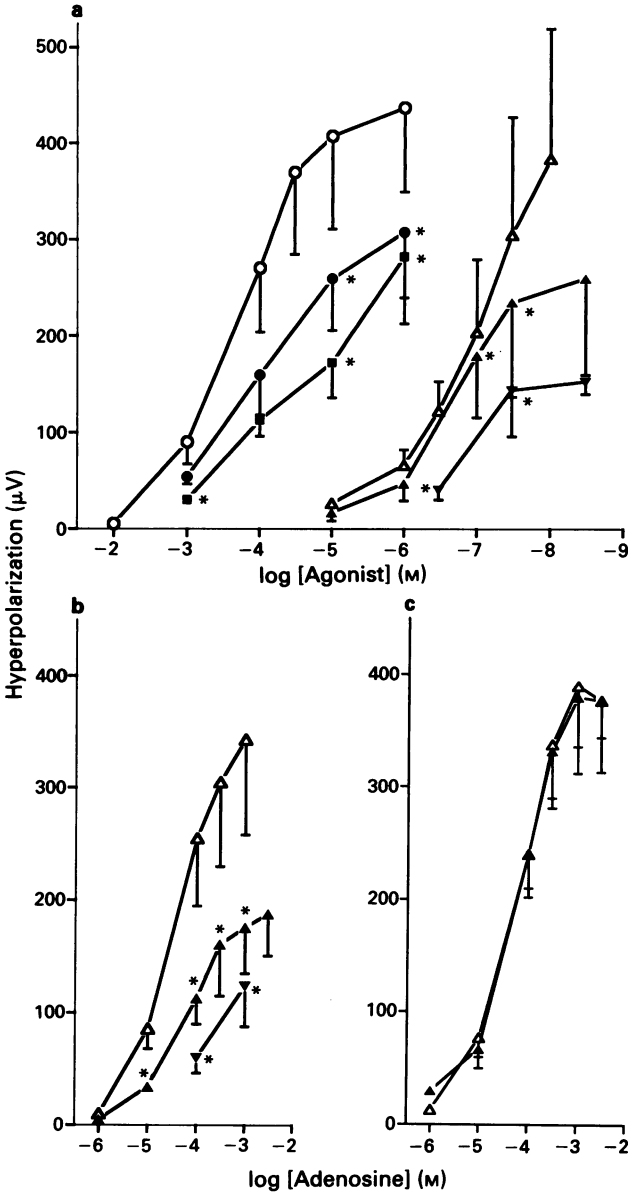

Figure 3 The effect of DPCPX on the hyperpolarization evoked by CPA and the effect of DPCPX, XAC or DMPX on the adenosine-induced hyperpolarization of the rat superior cervical ganglion (SCG). (a) Response evoked by CPA in the absence (○) and presence of DPCPX at 0.3 nM (●) and 0.9 nM (■) and the response evoked by adenosine in the absence (Δ) and presence of DPCPX at 0.3 nM (▲) and 1 nM (▼). (b) Response evoked by adenosine in the absence (Δ) and presence of 3 nM (▲) and 100 nM (▼) XAC. (c) Responses evoked by adenosine in the absence (Δ) and presence of 50 μM DMPX (▲). Responses were recorded in low Ca^{2+}/K^+ PSS from 3 or 4 ganglia. Statistical significance as for Figure 1. Abbreviations are given under Drugs.

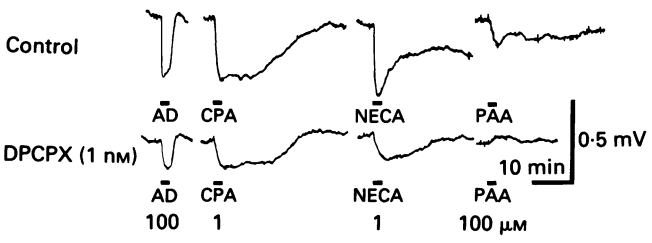

Figure 4 The effect of DPCPX on the response of a single rat superior cervical ganglion to adenosine analogues. Responses observed in low Ca^{2+}/K^+ PSS in the absence (control) and presence of 1 nM DPCPX. For list of abbreviations see Drugs.

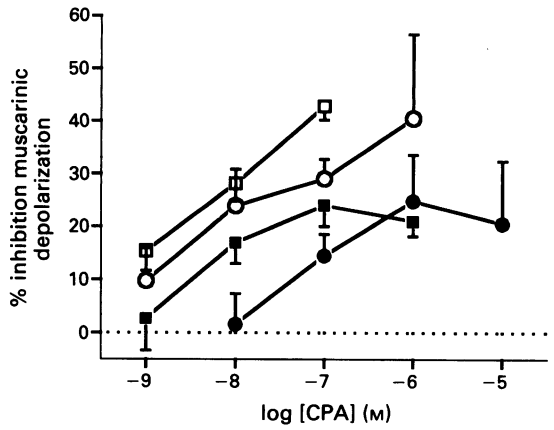

Figure 5 Effect of 8PT and DPCPX on the inhibition by CPA of the depolarizing response evoked by muscarine on the rat superior cervical ganglion. Inhibition by CPA of the response evoked by muscarine in the absence (□), (○) and presence of 10 μM 8PT (■) or 0.5 nM DPCPX (●) respectively. $n = 4$ to 8 ganglia in PSS.

ganglia are similar to values reported for tissues containing A_1-adenosine receptors (Daly, 1982). However, for effects on the SCG, adenosine was an exception in being lower in rank order and absolute potency than expected. This probably occurred as a result of extensive uptake and metabolism of adenosine (Connolly & Stone, 1993a). The very potent effects of the selective A_1-adenosine receptor analogue, CPA (Williams *et al.*, 1986; Williams, 1989) and the low potency and inactivity of the selective A_2-adenosine receptor analogues, PAA (Williams, 1989) and PD 117,413 (Trivedi *et al.*, 1988) supported the view that A_1- and not A_2-adenosine receptors were involved in both the hyperpolarization and inhibition of the muscarinic depolarization. BZA, a non-selective A_1/A_2-adenosine receptor analogue (Bruns *et al.*, 1986), with similar physico-chemical properties to CPA, produced comparable maximal inhibitions of the response caused by muscarine to those obtained with CPA. A concentration-ratio of 500 for the EC_{50}s for the inhibition of muscarine-induced depolarizations by CPA and BZA, strongly indicates this effect is mediated by A_1-adenosine receptors. Additional support for an A_1-adenosine receptor mediated effect is shown by the good correlation between the ability of adenosine analogues to inhibit muscarinic depolarizations and their affinities in inhibiting [^{3}H]-CHA binding to rat brain membranes (A_1-adenosine receptors) (correlation coefficient, $r = 0.93$), but poor correlation with inhibition of binding of [^{3}H]-NECA to striatal brain membranes (A_2-adenosine receptors) ($r = 0.33$) (binding data from Bruns *et al.*, 1986).

The antagonism of the concentration-response curve for adenosine-induced hyperpolarization by 8PT was similar to that obtained for the purinoceptors of many tissues such as the guinea-pig atrium and aorta (Collis *et al.*, 1986), and rat vas deferens (Stone, 1985), and is consistent with the presence of P_1-purinoceptors on the rat SCG. However it is not possible to define the adenosine receptor subtype by using 8PT as it is nonselective for A_1- and A_2-adenosine receptor subtypes (Collis *et al.*, 1986). 1,3-Dimethyl-4-sulphophenyl-8-phenylxanthine, a non-membrane-permeating analogue of 8PT also effectively antagonized both the CPA-induced hyperpolarization and inhibition of muscarinic depolarization (data not shown; Connolly, 1991) and indicated that these responses were mediated via externally located adenosine receptors. 8PT did not alter the basal d.c. potential of the SCG or its response to muscarine (data not shown) and this suggested that there was little endogenously released adenosine.

The indications for adenosine receptor involvement were fully borne out by the results of the studies with selective antagonists. In this respect, DPCPX, a potent and selective A_1-adenosine receptor antagonist (Bruns *et al.*, 1987), antagonized adenosine analogue-induced hyperpolarizations and inhibition of muscarinic depolarization at sub to low nanomolar concentrations whereas XAC, a less potent selective A_1-adenosine receptor antagonist (Williams, 1989) antagonized adenosine-induced hyperpolarizations at low nanomolar concentrations. However, the non-parallel nature of the antagonism of the effects of adenosine and CPA by DPCPX and XAC obscured further analysis of the data in terms of relative affinities. It is worthy of comment, that DPCPX at the subnanomolar concentrations tested produced a significant antagonism of the adenosine- and CPA-induced responses. Interestingly, recent studies have reported pA_2 values for DPCPX at A_1-adenosine receptors on guinea-pig isolated atria which are less than 9 (Collis *et al.*, 1989). The reason for the apparently unsurmountable inhibition and higher potency of DPCPX for adenosine receptors of the rat SCG is unclear.

It is unlikely that the potentiation of the responses to adenosine analogues in low Ca^{2+}/K^+ PSS was due to a reduction in uptake by nucleoside transporters because hyperpolarizations evoked by 2CA (which is not a substrate for the adenosine transporter of the rat SCG (Connolly & Stone, 1993a)) and hyperpolarizations evoked by adenosine were doubled in size when the extracellular Ca^{2+} concentration ($[Ca^{2+}]_e$) was reduced from 2.5 to 0.1 mM in the presence of 6 mM K^+ (Connolly & Stone, 1993b). Reduced $[Ca^{2+}]_e$ is known to facilitate the effects of drugs on sympathetic ganglia, e.g. enhancing depolarizations evoked by 5-hydroxytryptamine on rabbit SCG (Nash & Wallis, 1981) and enhances hyperpolarizations evoked by either α-adrenoceptor agonists (Brown & Caulfield, 1979) or muscarine (Brown *et al.*, 1980) on rat SCG. The omission of Ca^{2+} was found to enhance muscarine-induced hyperpolarizations of the rat SCG and this effect was reversed by increasing the concentration of extracellular magnesium ($[Mg^{2+}]_e$) (Brown *et al.*, 1980). A similar observation was reported by Connolly & Stone (1993b), who found that increasing the $[Mg^{2+}]_e$ in solutions containing low $[Ca^{2+}]_e$ abolished the potentiation of both adenosine-induced hyperpolarizations and K^+-induced depolarization of the rat SCG. We also observed that a reduction or an increase in $[K^+]_e$ potentiated or reduced adenosine-induced hyperpolarizations respectively, indicating that the hyperpolarizing action of adenosine may result from an increase in K^+ efflux (Connolly & Stone, 1993b). Thus the ability of low Ca^{2+}/K^+ PSS to potentiate hyperpolarizations evoked by adenosine and its analogues, as reported here, probably results from a combination of the two potentiating effects described above i.e. due to a reduction in both $[Ca^{2+}]_e$ and K^+ concentration.

In other studies on isolated tissues it has been suggested that variations in $[Ca^{2+}]_e$ are a useful procedure for converting weakly-effective agonists into more strongly effective ones, with the caveat that low $[Ca^{2+}]_e$ may alter agonist efficacy and alter the shape of the transducer relationship (Dougall & Leff, 1987). Similarly it was reported that Ca^{2+} ions are involved in receptor activation by agonists such as acetylcholine or histamine in the taenia of the guinea-pig and α-adrenoceptor agonists in vas deferens of the rat, but are not involved in the interactions of competitive antagonists with the same receptors (Takagi *et al.*, 1972). Thus low K^+/Ca^{2+} PSS, may have altered adenosine-receptor-effector coupling. However, although low K^+/Ca^{2+} PSS enhanced the size of CPA-evoked hyperpolarizations it did not alter the EC_{50} value for CPA-induced hyperpolarizations (cf. Figures 1 and 3a). Furthermore the order of potency of adenosine analogues reported here was similar in PSS or low K^+/Ca^{2+} PSS (e.g. cf. Figures 1 and 3a for CPA and adenosine) suggesting adenosine and its analogues may be altered in a similar manner by low K^+/Ca^{2+} PSS. It seems unlikely that a reduction in the K^+ and Ca^{2+} content of the PSS was responsible for the apparently unsurmountable antagonism

produced by DPCPX because a similar apparent unsurmountable antagonism and potency was found for the effect of DPCPX (0.6 nM) on the concentration-response curve for adenosine-induced hyperpolarizations in PSS containing 2.5 or 0.1 mM Ca^{2+} (Connolly, 1991).

Other factors, such as a low receptor reserve and the slow dissociation of DPCPX from its receptor or an action of high concentrations of adenosine analogues at adenosine receptors other than A_1-adenosine receptors may explain the apparently unsurmountable action of DPCPX. There are reports of some substituted xanthines exhibiting unsurmountable and competitive antagonism at adenosine receptors depending upon the tissue or receptor subtype examined (Burnstock & Hoyle, 1985; Williams *et al.*, 1987; Bailey *et al.*, 1992). Unsurmountable antagonism by DPCPX could have occurred if high concentrations of adenosine analogues had activated a second receptor with unusual characteristics. In this respect it is interesting that antagonism of PAA-induced hyperpolarization by DPCPX apparently revealed a depolarizing (possibly A_2-adenosine receptor mediated) effect of PAA. The complete lack of antagonism obtained with the selective A_2-adenosine receptor antagonist DMPX (Ukena *et al.*, 1986; Seale *et al.*, 1988) at 10 or 50 μM argues against any involvement of A_2-adenosine receptor-mediated effects in either the hyperpolarization or inhibition of muscarinic depolarizations. The similar maximal inhibitions of the depolarization to muscarine by the non-selective A_1/A_2-adenosine receptor analogues, 2CA, NECA and BZA (Bruns *et al.*, 1986) to those obtained with CPA also indicates that A_2-adenosine receptors may not be responsible for mediating the noncompetitive antagonism exhibited by DPCPX.

In conclusion, the results presented here show that the rat isolated SCG possesses external P_1-purinoceptors of the A_1-adenosine receptor subtype which hyperpolarize and inhibit the depolarizing response caused by muscarine.

G.P.C. was the recipient of an S.E.R.C. studentship. Part of this work was performed at SmithKline Beecham (SB) Pharmaceuticals Research and Development (Harlow). G.P.C. wishes to thank SB for the provision of laboratory and other facilities, and SB employees for their help.

References

BAILEY, S.J., HICKMAN, D. & HOURANI, S.M.O. (1992). Characterization of the P_1-purinoceptors mediating contraction of the rat colon muscularis mucosae. *Br. J. Pharmacol.*, **105**, 400–404.

BROWN, D.A. & CAULFIELD, M.P. (1979). Hyperpolarizing α_2-adrenoceptors in rat sympathetic ganglia. *Br. J. Pharmacol.*, **65**, 435–446.

BROWN, D.A., CAULFIELD, M.P. & KIRBY, P.J. (1979). Relation between catecholamine-induced cyclic AMP changes and hyperpolarisation in isolated rat sympathetic ganglia. *J. Physiol.*, **290**, 441–451.

BROWN, D.A., FATHERAZI, S., GARTHWAITE, J.G. & WHITE, R.D. (1980). Muscarinic receptors in rat sympathetic ganglia. *Br. J. Pharmacol.*, **70**, 577–592.

BRUNS, R.F., FERGUS, J.H., BADGER, E.W., BRISTOL, J.A., SANTAY, L.A., HARTMAN, J.D., HAYS, S.J. & HUANG, C.C. (1987). Binding of the A1-selective adenosine antagonist 8-cyclopentyl-1,3-dipropylxanthine to rat brain membranes. *Naunyn Schmied. Arch. Pharmacol.*, **335**, 59–63.

BRUNS, R.F., LU, G.H. & PUGSLEY, T.A. (1986). Characterization of the A_2-adenosine receptor labelled by [^{3}H]-NECA in rat striatal membranes. *Mol. Pharmacol.*, **29**, 331–346.

BURNSTOCK, G. (1978). A basis for distinguishing two types of purinergic receptor. In *Cell Membrane Receptors for Drugs and Hormones: A Multidisciplinary Approach*. Straub, R.W. & Bolis, L. pp. 107–118. New York: Raven Press.

BURNSTOCK, G. & HOYLE, C.H.V. (1985). PACPX – a substituted xanthine-antagonizes both the A_1 and A_2 subclasses of the P_1-purinceptor: antagonism of the A_2 subclass is competitive but antagonism of the A_1 subclass is not. *Br. J. Pharmacol.*, **85**, 291–296.

COLLIS, M.G. (1985). Are there two types of adenosine receptor in peripheral tissues? In *Purines: Pharmacology and Physiological Roles*. Stone, T.W. pp. 75–84. London: Macmillan.

COLLIS, M.G., PALMER, D.B. & SAVILLE, V.L. (1986). Comparison of the potency of 8-phenyltheophylline as an antagonist at A_1 and A_2 adenosine receptors in atria and aorta from the guines-pig. *J. Pharm. Pharmacol.*, **37**, 278–280.

COLLIS, M.G., STOGGALL, S.M. & MARTIN, F.M. (1989). Apparent affinity of 1,3-dipropyl-8-cyclopentlyxanthine for adenosine A_1 and A_2 receptors in isolated tissues from guinea-pigs. *Br. J. Pharmacol.*, **97**, 1274–1278.

CONNOLLY, G.P. (1991). Pharmacology of adenosine receptors of the rat isolated superior cervical ganglion. *Ph. D. Thesis, University of Glasgow.*

CONNOLLY, G.P. & BROWN, F. (1992). Characterisation of the adenosine receptors of the rat superior cervical ganglion. *Int. J. Purine. Pyrimidine Res.*, **3**, 74 P69

CONNOLLY, G.P. & STONE, T.W. (1988). Adenosine antagonises depolarisation to muscarine but not GABA on rat superior ganglia. *Br. J. Pharmacol.*, **95**, 841P.

CONNOLLY, G.P. & STONE, T.W. (1993a). On the site of action and inactivation of adenosine by the rat superior cervical ganglion. *J. Auton. Pharmacol.*, **13**, 213–224.

CONNOLLY, G.P. & STONE, T.W. (1993b). The ionic mechanism of action of adenosine on the rat superior cervical ganglion. *J. Auton. Pharmacol.*, **13**, 253–266.

DALY, J.W. (1982). Adenosine receptors: targets for future drugs. *J. Med. Chem.*, **25**, 197–207.

DALY, J.W., PADGETT, W., THOMPSON, R.D., KUSACHI, S., BUGNI, W.J. & OLSSON, R.A. (1986). Structure-activity relationships for N^6-substituted adenosines at a brain A_1-adenosine receptor with a comparison to an A_2-adenosine receptor regulating coronary blood flow. *Biochem. Pharmacol.*, **35**, 2467–2481.

DOUGALL, I.G. & LEFF, P. (1987). Pharmacological analysis of the calcium-dependence of μ-receptor agonism. *Br. J. Pharmacol.*, **92**, 723–731.

FREDHOLM, B.B., JACOBSON, K.A., JONZON, B., KIRK, K.L., LI, Y.O. & DALY, J.W. (1987). Evidence that a novel 8-phenyl-substituted xanthine derivative is a cardioselective adenosine receptor antagonist in vivo. *J. Cardiovasc. Pharmacol.*, **9**, 396–400.

LONDOS, C., COOPER, D.M.F & WOLFF, J. (1980). Subclasses of external adenosine receptors. *Proc. Natl. Acad. Sci. U.S.A.*, **77**, 2551–2554.

NASH, H.L. & WALLIS, D.I. (1981). Effects of divalent cations on responses of a sympathetic ganglion to and 1,1-dimethyl-4-phenyl piperazinium. *Br. J. Pharmacol.*, **73**, 759–772.

SEALE, T.W., ABLA, K.A., SHAMIN, M.T., CARNEY, J.W. & DALY, J.W. (1988). 3,7-Dimethyl-1-propargylxanthine: a potent and selective in vivo antagonist of adenosine analogs. *Life Sci.*, **43**, 1671–1684.

STONE, T.W. (1985). Classification of adenosine-receptors in the CNS. In *Methods in Pharmacology*, Vol. 6, ed. Paton, D.M. pp. 305–316. London: Plenum Press.

STONE, T.W. (1989). Purine receptors and their pharmacological roles. *Adv. Drug Res.*, **18**, 292–429.

TAKAGI, K., TAKAYANAGI, I. & LIAO, C.S. (1972). The effects of calcium and magnesium ions on drug-receptor interactions. *Eur. J. Pharmacol.*, **19**, 330–342.

TRIVEDI, B.K., BRISTOL, J.A., BRUNS, R.F., HALEEN, S.J. & STEFFEN, R.P. (1988). N^6(Arylalkyl)adenosines. Identification of N^6-(9-fluorenyl-methyl)adenosine as a highly potent analogue for the adenosine A_2 receptor. *J. Med. Chem.*, **31**, 271–273.

UKENA, D., OLSSON, R.A. & DALY, J.W. (1987). Definition of subclasses of adenosine receptors associated with adenylate cyclase: interaction of adenosine analogues with inhibitory A_1 receptors and stimulatory A_2 receptors. *Can. J. Physiol. Pharmacol.*, **65**, 365–376.

UKENA, D., SHAMIM, M.T., PADGETT, W. & DALY, J.W. (1986). Analogs of caffeine: antagonists with selectivity for A_2 adenosine receptors. *Life Sci.*, **39**, 743–750.

VAN CALKER, D., MULLER, M. & HAMPRECHT, B. (1979). Adenosine regulates via two different types of receptors the accumulation of cyclic AMP in cultured brain cells. *J. Neurochem.*, **33**, 999–1005.

WILLIAMS, M. (1989). Adenosine antagonists. *Med. Res. Rev.*, **9**, 219–243.

WILLIAMS, M., BRAUNVALDER, A. & ERICKSON, T.S. (1986). Evaluation of binding of the A-1 selective adenosine radioligand, cyclopentyladenosine (CPA), to rat brain tissue. *Naunyn Schmied. Arch. Pharmacol.*, **332**, 179–183.

WILLIAMS, M., JARVIS, M.F., STILLS, M.A., FERKANY, J.W. & BRAUNWALDER, A. (1987). Biochemical characterisation of the antagonist actions of the xanthines, PACPX (1,3-dipropyl-8(2-amino-4-chloro)phenylxanthine) and 8-PT (8-phenyltheophylline) at A_1 and A_2 receptors in rat brain tissue. *Biochem. Pharmacol.*, **36**, 4024–4027.

(Received April 27, 1993
Revised May 25, 1993
Accepted June 2, 1993)

Br. J. Pharmacol. (1993), **110**, 861–867

Evidence that depletion of internal calcium stores sensitive to noradrenaline elicits a contractile response dependent on extracellular calcium in rat aorta

M. Antonia Noguera & [1]M. Pilar D'Ocon

Laboratorio de Farmacognosia y Farmacodinamia, Departamento de Farmacología, Facultad de Farmacia, Universidad de Valencia, C/Vicent Andrés Estellés s/n, 46100 Burjassot, Valencia, Spain

1 Noradrenaline 1 μM induced a contractile response in rat isolated aorta in the presence or in the absence of extracellular Ca^{2+} with depletion of intracellular Ca^{2+} stores. Thereafter, during incubation in the presence of Ca^{2+}, an increase in the resting tone was observed. Such a contractile response did not occur after exposure to caffeine or 5-hydroxytryptamine.

2 This increase in tension was inhibited in a concentration-dependent manner by α-adrenoceptor antagonists (prazosin, phentolamine and yohimbine), the non-specific relaxing compound, papaverine and by the Ca^{2+}-entry blocker, nifedipine. Therefore, this contractile process is related to depletion of Ca^{2+} stores sensitive to noradrenaline and is linked to Ca^{2+} entry through voltage-operated Ca^{2+} channels and α-adrenoceptors.

3 Phentolamine and yohimbine did not block the Ca^{2+} refill pathway; prazosin and nifedipine inhibited the reuptake of Ca^{2+} by an internal store sensitive only to noradrenaline; papaverine inhibited the refilling of caffeine- and noradrenaline-sensitive Ca^{2+}-stores.

Keywords: Intracellular Ca^{2+}; rat aorta; noradrenaline; receptor-regulated Ca^{2+} entry; papaverine; α-adrenoceptors

Introduction

The characteristics of noradrenaline-induced contractions in smooth muscle have been widely studied and it is currently believed that the increase in tension in Ca^{2+}-containing solution comprises two distinct phases. The initial phasic contraction results from intracellular Ca^{2+} release following an increase in the turnover of phosphatidylinositol and the production of inositol 1,4,5-trisphosphate. In the continuing presence of noradrenaline, contraction is maintained and this phase is associated with Ca^{2+}-influx via a specific pathway (Bolton, 1979; Bray *et al.*, 1991). However, the results of electrophysiological studies of Ca^{2+} currents in smooth muscle are still confusing: noradrenaline increases the L-type Ca^{2+} current (Benham & Tsien, 1988; Fukumitsu *et al.*, 1990), but produces either no effect on voltage-activated inward currents (Yatani *et al.*, 1987) or reduces them (Imaizumi *et al.*, 1991) in different experimental procedures or in different smooth muscles.

In rat aorta, different authors (Morel & Godfraind, 1991; Nishimura *et al.*, 1991) have shown that noradrenaline activates voltage-operated Ca^{2+} channels that contain specific, voltage-sensitive binding sites for Ca^{2+} channel blocking dihydropyridines, but the existence of a fraction of noradrenaline-stimulated Ca^{2+}-entry that is resistant to nisoldipine blockade suggests that another Ca^{2+} entry pathway is also activated by the agonist. Whereas the role of endoplasmic reticulum in agonist-induced Ca^{2+}-release which involves the generation of inositol 1,4,5-trisphosphate is reasonably well established, the route, or routes, of Ca^{2+} entry into the agonist-sensitive internal Ca^{2+} stores remains an interesting dispute. Putney (1986, 1990) has postulated that depletion of the intracellular Ca^{2+} pools, even in the absence of receptor activation or increases in inositol polyphosphates, should activate the same Ca^{2+} entry mechanism that is normally activated, so long as the intracellular Ca^{2+} pools are not permitted to refill. We have found that after depleting noradrenaline releasable Ca^{2+} pools in Ca^{2+}-free medium, exposure to Ca^{2+}-containing solution, in the absence of the agonist, to allow the refilling of these intracellular Ca^{2+} stores, induces a considerable increase in the resting tone (IRT) of rat aorta.

The present work analyzes the pathways for this Ca^{2+} entry into the cell that are responsible for generating an increase in the resting tone of rat aorta during the refilling of Ca^{2+} pools, and their relation to voltage-operated Ca^{2+} channels and α-adrenoceptor activation. In order to do so, we have elicited this increase in tension in the presence of different concentrations of nifedipine, an organic Ca^{2+} entry blocker, and prazosin, phentolamine and yohimbine, α-adrenoceptor antagonists. Papaverine was also tested as a non-specific relaxing compound that prevents contractile responses in different smooth muscles (Lugnier *et al.*, 1986; Iino *et al.*, 1988; Sato *et al.*, 1988).

Methods

Helically cut strips of the thoracic aorta of male Wistar rats (200–220 g) were prepared and mounted as described by Furchgott & Zawadzki (1980). In some experiments, thoracic aortic strips were bisected and the halves were used to perform parallel experiments. Each preparation was suspended in a 10 ml organ bath containing physiological solution, maintained at 37°C and gassed with 95% O_2 and 5% CO_2. An initial load of 1 g was applied to each preparation and maintained throughout a 75–90 min equilibration period. Tension was recorded isometrically on a Philips recorder (PM 8222) coupled to a Hewlett Packard amplifier (8805D) using force-displacement transducers (Gould Statham UC2).

Endothelium-denuded aortic strips were prepared by rubbing the entire intimal surface. The absence of relaxant response (100%) after acetylcholine (10^{-4} M) addition to preparations contracted with noradrenaline (1 μM) indicated the absence of a functional endothelium in all strips (Furchgott & Zawadzki, 1980).

Experimental procedures

Concentration-response curves of relaxation to prazosin, yohimbine, phentolamine, nifedipine and papaverine were

[1] Author for correspondence.

obtained by addition of cumulative concentrations of the compounds to tissues in which sustained contractions had been induced by 1 μM noradrenaline or by exposure to a solution containing 80 mM KCl (prepared by equimolar substitution of KCl for NaCl in the physiological solution). Relaxations were expressed as a percentage of the maximum increment of tension obtained by agonist addition. E_{max} represents the maximal relaxation (100%) obtained after addition of the highest concentration of each compound. The concentration needed to produce 50% inhibition (IC_{50}) was obtained from a linear regression plot of all points between 20% and 80% of the maximal response.

Figure 1 shows the different experimental procedures designed to study the increase in the resting tone of aorta obtained at 37°C by exposure to physiological solution during the refilling of the intracellular Ca^{2+} stores sensitive to noradrenaline.

A separate series of experiments assessed the effects of prazosin, yohimbine, phentolamine, nifedipine and papaverine on the increase in tension. Noradrenaline (1 μM) was added in Ca-containing solution at 37°C and then the tissue was treated with Ca^{2+}-free, EDTA-containing solution for 15 min. After this time noradrenaline was applied until no contraction was induced, indicating complete depletion of internal Ca^{2+} stores sensitive to noradrenaline. The aorta was then pretreated with different concentrations of prazosin, yohimbine, phentolamine nifedipine and papaverine 15 min before an increase in the resting tone of aorta was induced (Figure 2). The magnitude of this increase in the presence of different concentrations of each compound was expressed as a percentage of the reference increase in resting tone obtained in the absence of any agent. In order to determine the IC_{50} values for each compound relative to the inhibition of the increase in tension, a linear regression analysis of all points obtained was performed; IC_{50} was calculated from this linear regression plot, but it was impossible to calculate s.e.mean. Each point was the mean of 4–7 experiments.

Another series of experiments was done to clarify the possible action of these compounds on the refilling of the intracellular Ca^{2+} stores. In this experimental procedure noradrenaline (NA2; Figure 2) or caffeine (Caf1; Figure 3) was added in Ca^{2+}-free medium after the incubation period in the presence of Ca^{2+} and of the highest concentrations of the compounds that completely inhibited the increase in resting tone. When caffeine was added to the organ bath, noradrenaline was also applied later (NA2; Figure 3). These experiments were carried out at 25°C because the contractile activity of caffeine in Ca^{2+}-free medium has only been observed at this temperature (Sato *et al.*, 1988; Noguera & D'Ocon, 1992). Subsequently, the tissue was incubated again in the presence of Ca^{2+}, and noradrenaline (NA3; Figure 3) was applied in physiological solution.

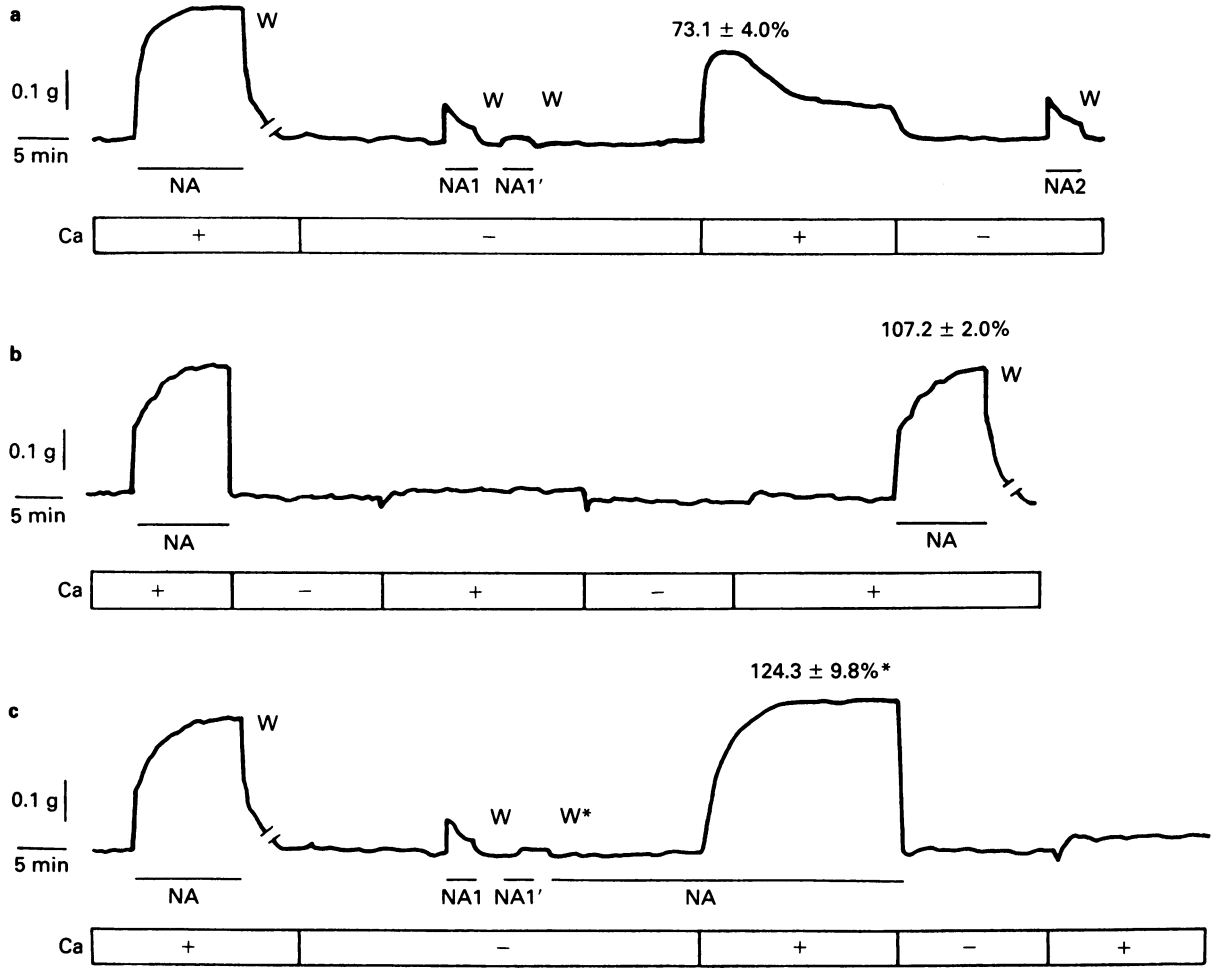

Figure 1 Schematic representation of different experimental procedures used to analyze the increases in tone observed after noradrenaline (NA)-induced depletion of intracellular Ca^{2+} stores. The increase in the resting tone and contractions in Ca^{2+}-free medium are expressed as a percentage of the noradrenaline-induced contraction in physiological solution. All values represent mean ± s.e.mean. Each value is the mean of 5–10 experiments. Preincubation time in Ca^{2+}-free medium: 15 min. W = washing; W* = washing with Ca^{2+} and EDTA-free solution. $^*P < 0.001$, significantly different from the noradrenaline-induced contraction in physiological solution.

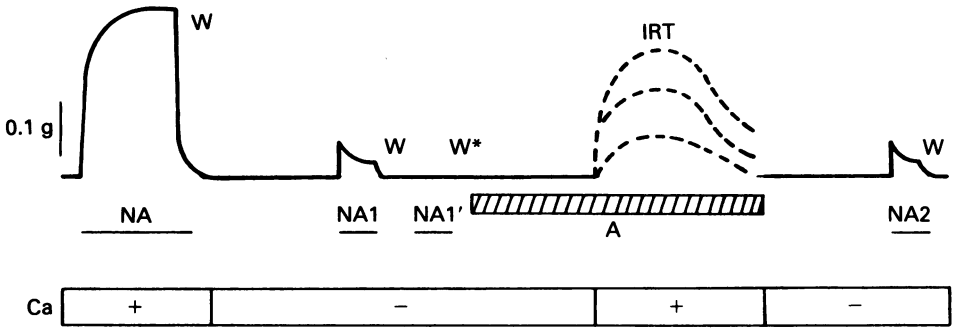

Figure 2 Experimental procedure used to analyze the modification of the increase in the resting tone of aorta obtained in the presence of different concentrations of the testing agents (A). Preincubation time in Ca^{2+}-free medium: 15 min. W = washing, W* = washing with Ca^{2+} and EDTA-free solution. NA1: addition of the agonist after 15 min of incubation in Ca^{2+}-free medium. NA1': addition of the agonist after washing (W) in Ca^{2+}-free medium. NA2: addition of the agonist after a 20 min resting period in physiological solution and 15 min in Ca^{2+}-free medium.

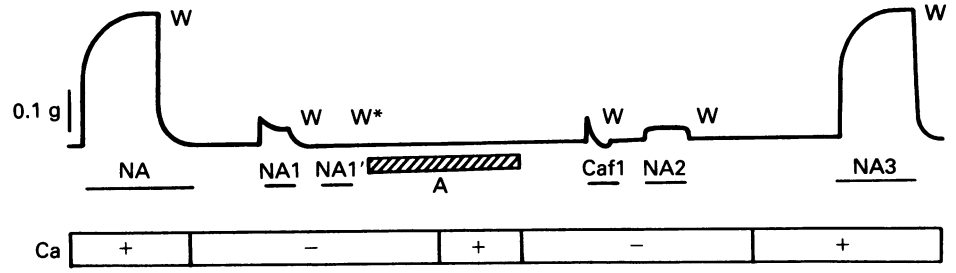

Figure 3 Experimental procedure used to analyze the refilling of internal Ca^{2+} storage sites in the presence of the testing agents (A) after depletion of noradrenaline-sensitive intracellular Ca^{2+} pools. The experiments were carried out at 25°C. Preincubation time in Ca^{2+}-free medium = 15 min. W = washing. W* = washing with Ca^{2+} and EDTA-free solution. NA1': first addition of noradrenaline after 15 min of incubation in Ca^{2+}-free medium. NA1': addition of the agonist after washing (W) in Ca^{2+}-free medium. Caf1: addition of caffeine after an incubation for 20 min in the presence of Ca^{2+} and 15 min in Ca^{2+}-free medium. NA2: addition of noradrenaline in Ca^{2+}-free medium after removing caffeine from the organ bath. NA3: addition of noradrenaline in physiological solution after 20 min exposure to Ca^{2+}-containing solution.

Drugs and solutions

The following drugs were obtained from Sigma (St. Louis MO, U.S.A.): anhydrous caffeine, 5-hydroxytryptamine creatinine sulphate complex, acetylcholine, phentolamine, yohimbine, prazosin, nifedipine and papaverine; (−)-noradrenaline L-tartrate was from Merck (Darmstadt, FRG). Other reagents were of analytical grade. All compounds were dissolved in distilled water with the exception of caffeine, which was dissolved in Ca^{2+}-free physiological solution (prepared by omission of $CaCl_2$). Nifedipine was dissolved in ethanol (10^{-2} M) before being diluted in distilled water and stored in the dark.

Composition of the physiological solution was (mM): NaCl 118, KCl 4.75, $CaCl_2$ 1.8, $MgCl_2$ 1.2, KH_2PO_4 1.2, $NaHCO_3$ 25, and glucose 11. Ca^{2+}-free solution had the same composition except that $CaCl_2$ was omitted and EDTA (0.1 mM) was added.

Analysis of results

Contractions in physiological solution were expressed in mg of developed tension and, when elicited in Ca^{2+}-free medium, as a percentage of the noradrenaline-, caffeine- or 5-hydroxytryptamine-induced contractions obtained in normal physiological solution, respectively. Increases in resting tone were also expressed as a percentage of the noradrenaline-induced contraction in normal physiological solution.

Results are presented as the mean ± s.e.mean for n determinations obtained from different animals. Statistical significance was evaluated by Student's t test for unpaired data. Differences were considered significant when $P<0.05$.

To determine IC_{50} values a linear regression analysis was performed (Graph Pad Software; San Diego, California, U.S.A).

Results

Analysis of the increase in the resting tone of rat aorta in different experimental conditions

In the presence of 1 μM noradrenaline, a concentration sufficient to evoke a maximal contraction, the magnitude of the contractile response of rat aortic tissues was 358.0 ± 55.3 mg ($n = 6$). The tissues were then exposed to Ca^{2+}-free solution for 15 min (Figure 4a) when addition of noradrenaline induced a biphasic contraction (NA1). The magnitude of these contractions after 15 min in Ca^{2+}-free medium is described in Table 1a. A contraction was not evoked upon a second application of 1 μM noradrenaline in Ca^{2+}-free solution (NA1'; Figure 4a). Upon re-exposure of the tissues to a Ca^{2+}-containing solution for 20 min, an increase in the resting tone was observed. This increase was 73.1 ± 4.0% ($n = 6$) relative to noradrenaline-induced contractions in physiological solution. Returning the tissues to a Ca^{2+}-free solution reduced the tension to baseline and further application of noradrenaline (NA2) 15 min later induced a contraction similar in size to that of the first contraction elicited in Ca^{2+}-free solution (NA1; Figure 4a; Table 1).

Caffeine (10 mM) elicited a rapid transient contraction in Ca^{2+}-containing solution at 37°C (113.1 ± 12.2 mg; $n = 9$),

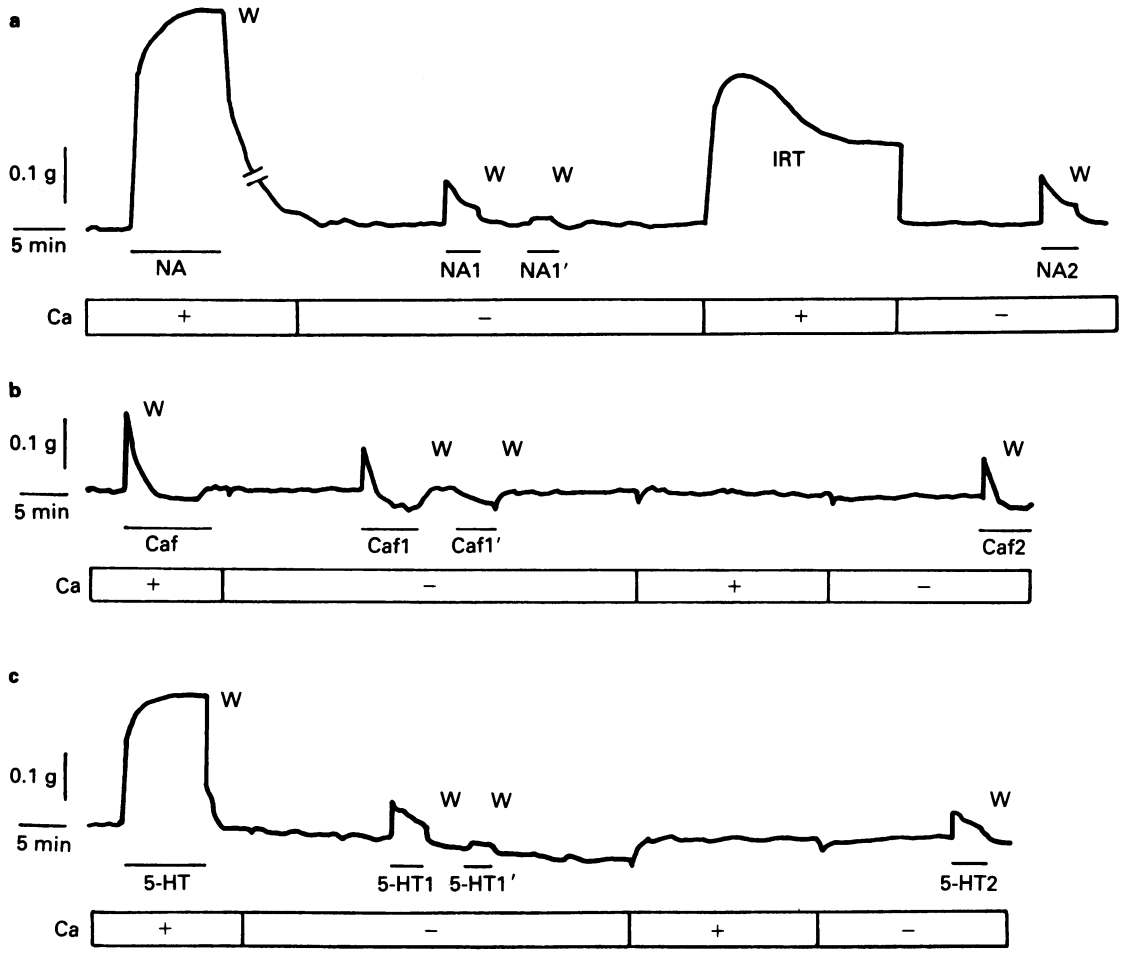

Figure 4 Schematic representation of (a) the increase in the resting tone of aorta obtained after depletion of noradrenaline (NA)-sensitive intracellular Ca^{2+} stores by exposure to noradrenaline in the absence of Ca^{2+}, (b) the effect of caffeine (Caf) and (c) the effect of 5-hydroxytryptamine (5-HT). Preincubation time in Ca^{2+}-free medium: 15 min. W = washing. NA1, Caf1, 5-HT_1: addition of the agonist after 15 min incubation in Ca^{2+}-free medium. NA1', Caf1', 5-HT_1': addition of the agonist after washing (W) in Ca^{2+}-free medium. NA2, Caf2, 5-HT_2: addition of the agonist after 20 min resting period in physiological solution and 15 min in Ca^{2+}-free medium.

Table 1 Increase in the resting tone of rat aortic segments elicited by 1 μM noradrenaline (NA), 10 mM caffeine (Caf) and 1 μM 5-hydroxytryptamine (5-HT)

	n	T (°C)	Ca^{2+}-containing Agonist (mg)	Ca^{2+}-free Agonist 1 (%) phasic	tonic	Ca^{2+}-containing 20 min Increasing tone (%) (IRT)	Ca^{2+}-free Agonist 2 (%) phasic	tonic
NA	6	37	358.0 ± 55.3	22.8 ± 1.4	15.2 ± 1.5	73.1 ± 4.0	21.0 ± 0.8	12.8 ± 1.5
Caf	4	25	123.1 ± 9.3	42.2 ± 9.7		NR	46.1 ± 10.1	
5-HT	6	37	215.3 ± 11.4	19.7 ± 1.5		NR	14.0 ± 1.2	

Increases in tone and contractions in Ca^{2+}-free medium are expressed as a percentage of the noradrenaline-, caffeine- or 5-hydroxytryptamine-induced contractions in physiological solution respectively.
All values represent mean ± s.e.mean, n = number of experiments.
Agonist1: first addition of the agonist after 15 min of incubation in Ca^{2+}-free medium.
Agonist2: second addition of the agonist after 20 min in Ca^{2+}-containing and 15 min in Ca^{2+}-free medium.
NR: no response.

but in Ca^{2+}-free medium no contractile response was observed. At 25°C, exposure to caffeine induced a transient contraction both in Ca^{2+}-containing solution and after 15 min in Ca^{2+}-free medium (CAF1). The size of these contractile responses are shown in Table 1. During the 20 min exposure to physiological solution, refilling of the intracellular Ca^{2+} stores was observed (since a contraction was obtained at CAF2) but there was no increase in the resting tone of the tissues (Figure 4b).

Similar results were obtained when 1 μM 5-hydroxytryptamine was added to the organ bath at 37°C, eliciting a sustained contraction in physiological solution of smaller magnitude than that elicited by noradrenaline (215.3 ± 11.4 mg; n = 6). In Ca^{2+}-free medium, 5-hydroxytryptamine induced a transient phasic contraction (5-HT_1) (Figure 4, Table 1). Subsequent exposure to Ca^{2+}-containing physiological solution (20 min) produced no increase in the resting tone of the aorta (Figure 4c), but after returning to a Ca^{2+}-free

medium 5-hydroxytryptamine again induced a contraction (5-HT_2), similar in size to that first obtained in Ca^{2+}-free medium.

As shown in Figure 1, when tissues had not been exposed to noradrenaline in the absence of extracellular Ca^{2+}, exposure to Ca^{2+}-containing solution (after an exposure to Ca^{2+}-free solution) did not result in the development of a contraction and subsequent contractile responses to noradrenaline in Ca^{2+}-containing solution were unaffected ($n = 5$; Figure 1b). Conversely, if noradrenaline was included during exposure to Ca^{2+} 1.8 mM, the result was a sustained and significantly higher contraction than that obtained in the presence of Ca^{2+} at the beginning of the experiment ($n = 6$; $P < 0.001$; Figure 1c).

Modification of the increase in the resting tone of aorta by preincubation with different concentrations of the testing agents

To investigate the possible relation between the increase in the resting tone of aorta and α-adrenoceptors or voltage-dependent Ca^{2+} channels, we studied the actions of prazosin, phentolamine, yohimbine, nifedipine and papaverine on this increase in tension. In physiological solution, contractile responses to noradrenaline or KCl (408.8 ± 57.4 mg and 340.0 ± 26.8 mg respectively) were relaxed in a concentration-dependent manner by exposure to prazosin (10^{-13}–10^{-4} M), phentolamine (10^{-12}–10^{-4} M), yohimbine (10^{-11}–10^{-3} M), nifedipine (10^{-12}–10^{-6} M) or papaverine (10^{-8}–5×10^{-5} M).

Table 2 pIC_{50} values of compounds on the increase in the resting tone of aorta (IRT) and on KCl- and noradrenaline (NA)-induced contractions

		KCl	*NA*	*IRT*
Prazosin	pIC_{50}	4.42 ± 0.19	9.70 ± 0.09*	10.20
		$n = 4$	$n = 5$	
	E_{max} (%)	67.1 ± 7.7	106.4 ± 5.2	
Phentolamine	pIC_{50}	5.19 ± 0.05	7.01 ± 0.20*	8.53
		$n = 4$	$n = 7$	
	E_{max} (%)	83.3 ± 16.5	107.4 ± 4.8	
Yohimbine	pIC_{50}	4.26 ± 0.06	6.80 ± 0.09*	9.09
		$n = 4$	$n = 6$	
	E_{max} (%)	101.9 ± 2.1	108.0 ± 4.3	
Nifedipine	pIC_{50}	9.16 ± 0.10	8.07 ± 0.11*	10.23
		$n = 5$	$n = 5$	
	E_{max} (%)	98.1 ± 12.6	93.2 ± 8.7	
Papaverine	pIC_{50}	5.51 ± 0.10	5.29 ± 0.07	5.24
		$n = 8$	$n = 6$	
	E_{max} (%)	104.8 ± 8.5	111.5 ± 8.3	

All values represent mean ± s.e.mean, n = number of experiments, except the values of pIC_{50} (IRT), which are presented as mean.
*$P < 0.001$, significantly different from pIC_{50} (KCl).

IC_{50} values for each compound are summarized in Table 2.

The experimental procedure shown in Figure 2 was used in order to determine how the increase in tone was modified by preincubation (15 min) in the presence of different concentrations of prazosin (10^{-13}–10^{-8} M), phentolamine (10^{-11}–10^{-7} M), yohimbine (10^{-12}–10^{-7} M), nifedipine (10^{-13}–10^{-6} M) or papaverine (10^{-7}–10^{-4} M). All of these compounds concentration-dependently inhibited the contractile process. The calculated IC_{50} values for each compound to inhibit the increase in the resting tone are summarized in Table 2. A complete inhibition (100%) of the contractile response was obtained in the presence of 10^{-8} M prazosin, 10^{-7} M phentolamine or yohimbine, 10^{-6} M nifedipine or 10^{-4} M papaverine.

Influence of agents on the refilling of intracellular Ca stores sensitive to noradrenaline

After a 20 min incubation period in physiological solution in the presence of concentrations of phentolamine and yohimbine that completely inhibited the increase in the resting tone (10^{-7} M), the α-adrenoceptor antagonists were washed out and a recovery of the noradrenaline-induced contraction in Ca^{2+}-free medium (NA2; Figure 2) was observed: 21.8 ± 4.0% ($n = 6$) after phentolamine treatment and 19.9 ± 4.9% ($n = 5$) after yohimbine treatment, relative to noradrenaline-induced contractions in physiological solution. Therefore, this concentration of the α-adrenoceptor antagonists does not seem to modify the repletion of intracellular Ca^{2+} stores sensitive to noradrenaline. On the other hand, when the refilling of Ca^{2+} stores was performed in the presence of 10^{-8} M prazosin, 10^{-6} M nifedipine or 10^{-4} M papaverine, later addition of noradrenaline in Ca^{2+}-free medium (NA2) did not promote any contractile response.

Influence of inhibitors on the refilling of intracellular Ca-stores sensitive to caffeine or noradrenaline

In order to clarify the possible action of these compounds on the repletion of intracellular Ca^{2+} stores, another series of experiments were carried out at 25°C in which caffeine (10 mM), instead of noradrenaline, was added to Ca^{2+}-free medium after the refilling period in the presence of Ca^{2+} (Figure 3). The magnitude of the caffeine-induced contraction (CAF1) in Ca^{2+}-free medium was 21.0 ± 3.1%, $n = 3$; relative to the noradrenaline-induced contraction in Ca^{2+}-containing medium. After washing in Ca^{2+}-free solution, addition of noradrenaline (NA2) elicited a small contractile response (6.5 ± 0.6%, $n = 3$; relative to the contraction induced by noradrenaline in physiological solution; Table 3). This response is due to the release of Ca^{2+} from a store sensitive only to noradrenaline (Noguera & D'Ocon, 1992). After 20 min exposure to Ca^{2+}-containing solution, complete recovery of the noradrenaline-induced contraction (NA3) was obtained.

Table 3 Contractile responses to caffeine (Caf1) and noradrenaline (NA2) in Ca^{2+}-free medium after an incubation period in the presence of testing agents in Ca^{2+}-containing solution (see Figure 2) and recovery of noradrenaline-elicited response in Ca^{2+}-containing solution (NA3)

Agent	(M)	n	*Caf1*	*NA2*	*NA3*
–	–	3	21.0 ± 3.1	6.5 ± 0.6	114.0 ± 5.0
Prazosin	10^{-8}	4	17.2 ± 4.2	–	92.6 ± 12.7
Phentolamine	10^{-7}	5	22.7 ± 3.7	10.1 ± 1.9	96.3 ± 15.4
Yohimbine	10^{-7}	5	19.6 ± 2.8	8.0 ± 0.8	81.5 ± 9.3
Nifedipine	10^{-6}	3	19.3 ± 4.1	–	38.4 ± 7.2 *
Papaverine	10^{-4}	3	–	–	7.3 ± 0.2*

Contractions are expressed as a percentage of the noradrenaline-induced contraction in physiological solution. All values represent mean ± s.e.mean, n = number of experiments.
*$P < 0.001$, significantly different from control.
Caf1: Addition of caffeine after 20 min in the presence of Ca^{2+} and 15 min in Ca^{2+}-free medium.
NA2: Addition of noradrenaline in Ca^{2+}-free medium after removing caffeine from the organ bath.
NA3: Addition of noradrenaline in physiological solution after 20 min of exposure to Ca^{2+}-containing solution.

Using the same experimental procedure, except that either phentolamine or yohimbine (10^{-7} M) were added during the refilling of the stores in the presence of Ca^{2+}, washout of the α-adrenoceptor antagonists in Ca^{2+}-free medium and addition of caffeine elicited a phasic contraction (CAF1). Subsequent addition of noradrenaline in Ca^{2+}-free solution produced a small tonic contraction (NA2) that was not modified by previous exposure of tissues to phentolamine or yohimbine (Table 3). After a further incubation period of 20 min in physiological solution the size of the contractile response to noradrenaline was restored (NA3).

When the stores were refilled in the presence of either 10^{-8} M prazosin or 10^{-6} M nifedipine, addition of caffeine in Ca^{2+}-free medium (Caf1) yielded a contractile response similar in magnitude to that obtained in the absence of the antagonists (Table 3). Later addition of noradrenaline (NA2) in Ca^{2+}-free medium did not induce any response. After 20 min in the presence of Ca^{2+}, the response to noradrenaline (NA3) after tissue exposure to nifedipine was significantly smaller than that obtained in the absence of nifedipine, but recovery of the response to noradrenaline was complete after prazosin treatment (Table 3).

When 10^{-4} M papaverine was present during the repletion of the internal Ca^{2+} stores neither caffeine nor noradrenaline elicited any contractile response when they were added in Ca^{2+}-free medium in the absence of papaverine (CAF1, NA2; Table 3). Furthermore, noradrenaline induced a significantly smaller contraction ($P<0.001$) when applied after 20 min exposure to Ca^{2+}-containing solution (NA3; Table 3).

Discussion

The results show that in rat aorta, noradrenaline-, 5-hydroxytryptamine- or caffeine-induced contractions in Ca^{2+}-free medium are associated with the emptying of intracellular Ca^{2+} stores of limited capacity and that further addition of the agonists evokes no mechanical response. These intracellular Ca^{2+} pools, when emptied, can be rapidly replenished from the extracellular space by incubation in Ca^{2+}-containing solution. The rapid refilling of the pools with extracellular Ca^{2+} occurs in the absence of the contractile agonist. It might be assumed that any means of depleting the intracellular Ca^{2+} pool, even in the absence of receptor activation or increases in inositol polyphosphates, activates the same Ca^{2+} entry mechanism normally activated by agonists (Putney, 1986; 1990; Rowena *et al.*, 1992).

A question arises from these results about the pathway for Ca^{2+} entry because there are at least two possible routes. Ca^{2+} may enter the cytoplasm directly on its way to the internal compartments sensitive to the agonists (Putney, 1990; Rowena *et al.*, 1992) or Ca^{2+} entry may involve direct replenishment of the intracellular pool in the absence of the agonist and its continuous discharge to the cytoplasm when the agonist is present (Itoh *et al.*, 1981; 1985; Hisayama & Takayanagi, 1988; Low *et al.*, 1991).

The observation that exposure of the tissues to Ca^{2+} after emptying of intracellular Ca^{2+} stores by exposure to caffeine or 5-hydroxytryptamine did not result in a contractile response suggests that the pathway for refilling could be a relatively direct one that does not involve transfer of Ca^{2+} through the cytosol to the intracellular storage sites. However, after depletion of noradrenaline-sensitive Ca^{2+} stores, there was an increase in the resting tone of aorta on re-exposure to Ca^{2+}. This Ca^{2+}-dependent contraction has been described in previous studies carried out in rabbit aorta (Deth & Lynch, 1981), although no explanation for the observation was advanced.

This increase in the resting tone of aorta therefore seems to be strictly related to adrenoceptors and not just to the emptying of intracellular Ca^{2+} pools sensitive to an agonist. This increase in tone takes place in the absence of the agonist, indicating that it is a consequence of the previous activation of adrenoceptors. Removal of the endothelium rules out possible involvement of endothelium-derived factors in this mechanical response.

When a contractile response to noradrenaline was elicited in the presence of Ca^{2+} and the tissue was washed in Ca^{2+}-free medium and then in a Ca^{2+}-containing solution, without attempting to deplete intracellular Ca^{2+} stores in the absence of Ca^{2+}, there was no increase in the resting tone of the tissue in Ca-containing solution (Figure 1b), suggesting that depletion of intracellular Ca^{2+} pools was required for an increased permeability of the plasma membrane permitting Ca^{2+} entry. This could explain the fact that noradrenaline-induced contractions in Ca^{2+}-containing solution after depletion of intracellular stores were of a significantly greater magnitude than the standard response (Figure 1c). On this basis, it can be assumed that the depletion of noradrenaline-sensitive Ca^{2+} stores are the signal for the entry of extracellular Ca^{2+} not only to refill organelles, but also to activate contractile proteins. The magnitude of the mechanical response decreases proportionally with the time of exposure to Ca^{2+}-containing medium, which means that the accelerated entry of Ca^{2+} to replenish the intracellular pools inactivates the entry mechanism.

According to Sato *et al.* (1988), noradrenaline has the ability to augment the efficacy of contraction (i.e. the response to a given concentration of intracellular Ca^{2+}) in vascular smooth muscle, and this may be responsible for the increase in the resting tone if it continues when the agonist is removed from the incubating medium.

We assessed the influence of three α-adrenoceptor antagonists (prazosin, phentolamine and yohimbine) on the magnitude of this increase in the resting tone. Treatment with α-adrenoceptor antagonists induced a concentration-dependent inhibition of the response and it was completely abolished in the presence of the highest concentrations tested. This seems to indicate that α-adrenoceptors are involved in the increase in resting tone. An explanation for this effect in the absence of an α-adrenoceptor agonist may be that mobilization of an intracellular Ca^{2+} pool sensitive to noradrenaline could determine the fixing of the α-adrenoceptor in an activated state until the intracellular Ca^{2+} pool is refilled and that these antagonists bind to the α-adrenoceptor in the absence of Ca^{2+} and fix it in an inactivated state, in a manner similar to that of Ca^{2+}-channel blockers on the voltage-dependent Ca^{2+} channels (Trautwein & Pelzer, 1985; Godfraind *et al.*, 1986). This hypothesis requires further investigation, but Schütz & Freissmuth (1992) have suggested that antagonists not only bind to G protein-coupled receptors, but also induce a conformation change unfavourable to the coupling of the receptor to its G protein.

The inhibition of this increase in tension in a concentration-dependent manner by nifedipine would seem to relate this mechanical response to Ca^{2+}-entry via voltage-operated Ca^{2+} channels. The great sensitivity of the increase in the resting tone to nifedipine suggests that a change in membrane potential might be involved.

According to previous work (Noguera & D'Ocon, 1992; Low *et al.*, 1991; present results) noradrenaline induces a biphasic contractile response in Ca^{2+}-free medium. The present study provides the novel observation that this biphasic response is mediated by two different intracellular Ca^{2+} pools with different refilling processes: compartment 1 is sensitive to noradrenaline and caffeine, nifedipine and prazosin do not modify its refilling process; compartment 2 is sensitive only to noradrenaline; nifedipine and prazosin completely inhibit its repletion. Papaverine blocks the repletion of both compartments and the presence of phentolamine or yohimbine affects neither.

In view of the above findings, we propose a model for Ca^{2+} entry into intracellular stores sensitive to noradrenaline (one of them common to caffeine). The first component of the noradrenaline-induced contraction in Ca^{2+}-free medium indicates Ca^{2+} release from the endoplasmic reticulum (com-

partment 1) (Low *et al.*, 1991). The second component of the biphasic response to noradrenaline in the absence of extracellular Ca^{2+} might be represented by compartment 2. This Ca^{2+} storage compartment lies close to, and may be directly connected to, the plasma membrane (Devine *et al.*, 1972; Van Breemen & Saida, 1989; Noguera & D'Ocon, 1992). This second component is susceptible to modulation by nifedipine and prazosin and includes the passage of Ca^{2+} through L-type Ca^{2+}-channels for the refilling of the internal Ca^{2+} pool. The gate at this passage may be voltage-operated, although the α_{1a}-adrenoceptor subtype is directly related to it (Minneman, 1988). There is some evidence (Saida & Van Breemen, 1983; Leijten *et al.*, 1985; Wakui *et al.*, 1990) that the intracellular Ca^{2+} pool specific to noradrenaline can be released by receptor activation and the release of this small pool might trigger Ca^{2+} release from the internal store common to noradrenaline and caffeine. Thus, the fact that prazosin and nifedipine block the uptake of Ca^{2+} into the small pool specific to noradrenaline (compartment 2) explains the lack of response to noradrenaline in Ca^{2+}-free medium: the first component of the biphasic response is abolished because the release of the internal Ca^{2+} pool common to noradrenaline and caffeine (compartment 1) depends on the previous release of Ca^{2+} from the pool specific to noradrenaline (compartment 2) when this agonist is employed. However, complete recovery of the contractile response induced by caffeine in Ca^{2+}-free medium is observed, indicating that the refilling and release of compartment 1 may, in fact, be independent of the presence of the antagonists.

Phentolamine and yohimbine did not block these Ca^{2+} refill pathways but the fact that the increase in the resting tone related to α-adrenoceptors activation was abolished may suggest that the entry of Ca^{2+} in the presence of these antagonists is not able to activate the contractile proteins because of the blockade of the process of sensitization mediated by α-adrenoceptors.

In summary, the present study shows that incubation in Ca^{2+}-containing solution after depletion of noradrenaline-sensitive intracellular Ca^{2+} stores increases the resting tone of rat aorta. This increase in tension was inhibited by α-adrenoceptor antagonists such as prazosin, phentolamine and yohimbine, and by Ca^{2+} channel blockers such as nifedipine. Papaverine also inhibited the increase. During this contractile process, the intracellular Ca^{2+} stores sensitive to noradrenaline refill, but the repletion of these internal pools is differentially modulated by the agents tested.

References

BENHAM, C.D. & TSIEN, R.W. (1988). Noradrenaline modulations of calcium channels in single smooth muscle cells from rabbit ear artery. *J. Physiol.*, **404**, 767–784.

BOLTON, T.B. (1979). Mechanisms of action of transmitters and other substances on smooth muscle. *Physiol. Rev.*, **59**, 606–718.

BRAY, K.M., WESTON, A.H., DUTY, S., NEWGREEN, D.T., LONGMORE, J., EDWARDS, G. & BROWN, T.J. (1991). Differences between the effects of cromakalim and nifedipine on agonist-induced responses in rabbit aorta. *Br. J. Pharmacol.*, **102**, 337–344.

DETH, R.C. & LYNCH, C.J. (1981). Relative contributions of Ca influx and cellular Ca release during drug-induced activation of the rabbit aorta. *Am. J. Physiol.*, **240**, C239–C247.

DEVINE, C.E., SOMLYO, A.V., SOMLYO, A.P. (1972). Sarcoplasmic reticulum and excitation-contraction coupling in mammalian smooth muscle. *J. Cell. Biol.*, **52**, 690–718.

FUKUMITSU, T., HAYASHI, H., TOKUNO, H. & TOMITA, T. (1990). Increase in calcium channel current by β-adrenoceptor agonists in single smooth muscle cells isolated from porcine coronary artery. *Br. J. Pharmacol.*, **100**, 593–599.

FURCHGOTT, R.F. & ZAWADZKI, J.V. (1980). The obligatory role of endothelial cells in the relaxation of arterial smooth muscle by acetylcholine. *Nature*, **288**, 373–376.

GODFRAIND, T., MILLER, R. & WIBO, M. (1986). Ca antagonism and Ca entry blockade. *Am. Soc. Pharmacol. Exp. Ther.*, **38**, 312–415.

HISAYAMA, T. & TAKAYANAGI, I. (1988). Ryanodine: its possible mechanism of action in the caffeine-sensitive Ca-store of smooth muscle. *Pflügers Arch.*, **412**, 376–381.

IINO, M., KOBAYASHI, T. & ENDO, M. (1988). Use of ryanodine for functional removal of the calcium store in smooth muscle cells of the guinea-pig. *Biochem. Biophys. Res. Commun.*, **152**, 417–422.

IMAIZUMI, Y., TAKEDA, M., MURAKI, K. & WATANABE, M. (1991). Mechanisms of NE-induced reduction of Ca current in single smooth muscle cells from guinea-pig vas deferens. *Am. J. Physiol.*, **260**, C17–C25.

ITOH, T., KURIYAMA, H. & SUZUKI, H. (1981). Excitation-contraction coupling in smooth muscle cells of the guinea-pig mesenteric artery. *J. Physiol.*, **321**, 513.

ITOH, T., UENO, H. & KURIYAMA, H. (1985). Calcium-induced calcium release mechanism in vascular smooth muscles-assessments based on contractions evoked in intact and saponin-treated skinned muscles. *Experientia*, **41**, 989.

LEIJTEN, P., CAUVIN, C., LODGE, N., SAIDA, K. & VAN BREEMEN, C. (1985). Ca^{2+} sources mobilized by α1-receptor activation in vascular smooth muscle. *Clin. Sci.*, **68**, 47–50.

LOW, A.M., GASPAR, V., KWAN, C.Y., DARBY, P.J., BOURREAU, J.P. & DANIEL, E.E. (1991). Thapsigargin inhibits repletion of phenylephrine-sensitive intracellular Ca pool in vascular smooth muscles. *J. Pharmacol. Exp. Ther.*, **258**, 1105–1113.

LUGNIER, C., SHOEFFTER, P., LE BEC, A., STROUTHON, E. & STOCLET, J.C. (1986). Selective inhibition of cyclic nucleotide phosphodiesterase on human bovine and rat aorta. *Biochem. Pharmacol.*, **35**, 1743–1751.

MINNEMAN, K.P. (1988). α1-adrenergic receptor subtypes, inositol phosphates, and sources of cell calcium. *Pharmacol. Rev.*, **40**, 87–119.

MOREL, N. & GODFRAIND, T. (1991). Characterization in rat aorta of the binding sites responsible for blockade of noradrenaline-evoked calcium entry by nisoldipine. *Br. J. Pharmacol.*, **102**, 467–477.

NISHIMURA, K., OTA, M. & ITO, K. (1991). Existence of two components in the tonic contraction of rat aorta mediated by α_1-adrenoceptor activation. *Br. J. Pharmacol.*, **102**, 215–221.

NOGUERA, M.A. & D'OCON, M.P. (1992). Different and common intracellular calcium-stores mobilized by noradrenaline and caffeine in vascular smooth muscle. *Naunyn Schmied Arch. Pharmacol.*, **345**, 333–341.

PUTNEY, J.W. (1986). A model for receptor-regulated calcium entry. *Cell Calcium*, **7**, 1–12.

PUTNEY, J.W. (1990). Capacitative calcium revisited. *Cell Calcium*, **11**, 611–634.

ROWENA, J.D., HURWITZ, L.M., MIRZA, Z., STRAUSS, H.C. & WHORTON, A.R. (1992). Regulation of extracellular calcium entry in endothelial cells: role of intracellular Ca pool. *Am. J. Physiol.*, **262**, C171–C181.

SAIDA, K. & VAN BREEMEN, C. (1983). A possible Ca^{2+}-induced Ca^{2+}-release mechanism mediated by norepinephrine in vascular smooth muscle. *Pflügers Arch.*, **397**, 166–167.

SATO, K., OZAKI, H. & KARAKI, H. (1988). Changes in cytosolic calcium levels in vascular smooth muscle strip measured simultaneously with contraction using fluorescent calcium indicator fura 2^1. *J. Pharmacol. Exp. Ther.*, **246**, 294–300.

SCHUTZ, W. & FREISSMUTH, M. (1992). Reverse intrinsic activity of antagonists on G protein-coupled receptors. *Trends Pharmacol. Sci.*, **13**, 376–380.

TRAUTWEIN, W. & PELZER, D. (1985). Voltage-dependent gating of single calcium channels in the cardiac cell membrane and its modulation by drugs. In *Calcium and Cell Physiology*. ed. Marmé, D. pp. 53–93. Berlin Heildelberg: Springer-Verlag.

VAN BREEMEN, C. & SAIDA, K. (1989). Cellular mechanisms regulating Cai smooth muscle. *Annu. Rev. Physiol.*, **51**, 315–329.

WAKUI, M., OSIPCHUK, Y.V. & PETERSEN, O.H. (1990). Receptor-activated cytoplasmic Ca spiking mediated by inositol trisphosphate is due to Ca-induced Ca release. *Cell*, **63**, 1025–1032.

YATANI, A., SEIDEL, C.L., ALLEN, J. & BROWN, A.M. (1987). Whole cell and single-channel calcium currents of isolated smooth muscle cells from saphenous vein. *Circ. Res.*, **60**, 523–533.

(Received June 22, 1992
Revised March 5, 1993
Accepted June 4, 1993)

Br. J. Pharmacol. (1993), **110**, 868–874

Serum corticosterone, interleukin-1 and tumour necrosis factor in rat experimental endotoxaemia: comparison between Lewis and Wistar strains

M. Perretti, G.S. Duncan, R.J. Flower & [1]S.H. Peers

Department of Biochemical Pharmacology, The William Harvey Research Institute, Medical College of St Bartholomew's Hospital, Charterhouse Square, London EC1M 6BQ

1 Circulating corticosterone, interleukin-1 (IL-1) and tumour necrosis factor-α (TNFα) activities in serum of Lewis and Wistar rats were measured following injection of lipopolysaccharide (LPS). IL-1 was measured as 'lymphocyte activation factor' (LAF) activity following precipitation of inhibitory activity with polyethylene glycol. TNFα activity was measured as cytotoxic activity.

2 Compared to the Wistar, the Lewis rat had higher circulating LAF and TNF activities following LPS, and release of both cytokines was prolonged in this strain.

3 Corticosterone increases in response to LPS were less in the Lewis than in the Wistar rat following the initial peak at 1 h; basal corticosterone was lower in the Lewis rat.

4 Adrenalectomized Lewis rats had even greater amounts of circulating LAF and TNF activities following LPS than did intact animals; the effect of adrenalectomy was not however mimicked by acute treatment with the steroid receptor antagonist, RU486, suggesting that endogenous corticosteroids did not acutely control cytokine release.

5 Although *in vivo* administration of anti-murine IL-1α antiserum significantly lowered LAF activity of serum, circulating corticosterone in response to LPS was not affected. Similarly, treatment with anti-murine TNFα monoclonal antibody (mAb) abrogated TNF activity without affecting corticosterone, suggesting that other mediators may be responsible for corticosterone release following LPS.

6 This 'overproduction' of inflammatory cytokines together with lower circulating corticosterone may contribute to the susceptibility of the Lewis rat to diseases such as adjuvant arthritis or experimental allergic encephalomyelitis.

Keywords: Endotoxaemia; interleukin-1; tumour necrosis factor-α (TNFα); glucocorticosteroids

Introduction

Interleukin-1 (IL-1) and tumour necrosis factor-α (TNFα) are pluripotent cytokines with a central role in the onset and maintenance of chronic inflammatory conditions in both man and experimental animals (Miller & Dinarello, 1987; Arend & Dayer, 1990). Synthesis of these cytokines must be finely regulated and as with other inflammatory mediators, glucocorticoid hormones have the capacity to inhibit their generation, down-regulating transcription and translation of both IL-1 and TNFα (Beutler *et al.*, 1986; Knudsen *et al.*, 1987; Lee *et al.*, 1988). Moreover, IL-1 and TNFα are potent stimulators of the hypothalamo-pituitary-adrenal (HPA) axis leading to increased circulating corticosteroids (Besedovsky *et al.*, 1991). The importance of this immunoregulatory feedback is indicated by enhanced cytokine release in adrenalectomized (ADX) animals (Perretti *et al.*, 1989; Zuckerman *et al.*, 1989) which show exaggerated inflammatory responses (Flower *et al.*, 1986; Perretti *et al.*, 1991). The Lewis strain of rat is particularly susceptible to such chronic inflammatory models as cell-wall arthritis and experimental allergic encephalomyelitis (EAE): this susceptibility has been attributed to a defect in the HPA axis in this strain which results in lower corticosterone (CCS) responses following challenge with various stimuli including IL-1 (Sternberg *et al.*, 1989a; Mason, 1991). Additionally, under normal conditions, Lewis rats have lower basal CCS than other strains (Griffin & Whitacre, 1991; Villas *et al.*, 1991).

Amongst the many activities of IL-1 and TNFα, their roles as mediators of septic shock are well established, and cytokine levels are transiently elevated in animal models of shock and gram-negative sepsis (Dinarello, 1991). Lipopolysaccharide (LPS) is frequently used to induce release of IL-1 and TNFα, and this is associated with an increase in circulating corticosteroids. This latter effect partially explains the rapidly-induced tolerance to subsequent LPS challenge (Beutler *et al.*, 1986; Zuckerman *et al.*, 1991).

Most studies concerning LPS-induced cytokine release have been performed in the mouse. Here, using a recently-described method to remove inhibitory activity present in serum (Hopkins & Humphreys, 1990), we have been able to measure circulating lymphocyte activation factor (LAF) activity in the rat. Therefore, in the present study, we have compared the release of IL-1 and TNFα following LPS administration in Lewis and Wistar rats, and investigated the relationship between these cytokines and CCS. Furthermore, the effect of acute or prolonged ablation of corticosteroids by use of the steroid receptor antagonist, mifepristone (RU486) and adrenalectomy respectively were examined. A preliminary account of some of these results was presented to the British Pharmacological Society (Peers *et al.*, 1992).

Methods

Animals

Male Wistar and Lewis rats (200–250 g) were obtained from Harlan-Olac, (Bicester, Oxon) and kept in the Animal Unit for at least 7 days before use. Animals received food and water *ad libitum*, and lighting was maintained on a 12 h cycle. ADX rats were obtained from the same source, and received saline drinking water. Adrenalectomy was confirmed

[1] Author for correspondence at present address: Allelix Biopharmaceuticals, 6850 Goreway Drive, Mississauga, Ontario L4V 1P1, Canada.

by measurement of CCS. To minimise undue stress, animals were maintained in established groups, handled repeatedly and moved to the experimental room at least 16 h before the start of the experiment.

Experimental protocol

LPS (*E. coli* 055:B5) was administered i.p. in 1 ml sterile saline between 09 h 00 min and 11 h 00 min. After the indicated interval, animals were anaesthetized with CO_2, and a blood sample taken by cardiac puncture. Previous experiments indicated that this minimized stress to the animals and allowed measurement of basal CCS. Blood was allowed to clot at 4° for 2–3 h and centrifuged (600 *g*, 4°C, 30 min) to obtain sera which was stored in aliquots at − 20°C before assay for CCS or TNF activity, or at − 70°C before assay for LAF activity. All assays were performed within 4 weeks of serum collection. Dexamethasone (as phosphate) was administered s.c. and RU486 (mifepristone) was administered orally at the indicated time before LPS. Antiserum or antibodies were injected s.c. 16 h before LPS administration (Perretti *et al.*, 1992).

TNF bioassay

Serum TNF was assayed as cytotoxic activity against murine L-929 fibroblasts (Meager *et al.*, 1989). Briefly, L-M cells were seeded at $1-2 \times 10^5$ per well in flat-bottomed 96-well plates in RPMI-1640 medium containing 5% foetal calf serum (FCS) and incubated for 16 h, after which non-adherent cells were removed by washing in warmed balanced salt solution. Sterile filtered sera were diluted in RPMI-1640 (+ 5% FCS) containing 3 $\mu g\ ml^{-1}$ actinomycin D and serial five-fold dilutions added (volume 0.2 ml). After 20 h incubation, supernatants were discarded, the monolayer washed and adherent cells stained with crystal violet solution (0.5% in 20% methanol) for 10 min. Plates were rinsed with tap water and allowed to dry, after which the stained cells were lysed with 33% acetic acid, and optical density read at 570 nm. Standard curves were constructed using human recombinant TNFα; the limit of detection was approximately 10 $pg\ ml^{-1}$. Data are shown as TNF 'units', being 1/serum dilution giving 50% cytotoxicity (equivalent of approximately 100 $pg\ ml^{-1}$ human TNFα). Data are shown as values for individual sera, unless otherwise stated.

In experiments to confirm cytotoxic activity as being TNFα, filtered serum samples were preincubated for 2 h at 4°C with a monoclonal antibody (mAb) against murine TNFα at twice the final concentration before addition to cells as described above. In other experiments, sera were heated to 56°C for 30 min, centrifuged to remove precipitate then filtered and used as described above.

IL-1 bioassay

Sera were thawed and extensively dialysed ($1:1000 \times 3$) against phosphate buffered saline (PBS) and sterile filtered. IL-1 was assessed as LAF activity using the murine thymocyte co-stimulation assay as previously described (Perretti *et al.*, 1989) following incubation of dialysed, filtered sera with 12% polyethylene glycol (PEG; Hopkins & Humphreys, 1990): equal volumes of sera and 24% PEG were incubated for 30 min on ice then centrifuged and supernatants diluted with RPMI-1640 medium to obtain a starting dilution of 1/40. Incubations were performed in 96-well plates under the following conditions: 0.6×10^6 thymocytes from C3/HeJ mice aged 6–8 weeks (Harlan-Olac) were incubated in RPMI-1640 medium containing 5% FCS with 1.5 $\mu g\ ml^{-1}$ phytohaemagglutinin (PHA), 0.6% PEG and five fold serial dilutions of sera (prepared as above) for 72 h before pulsing with 1 μCi per well [^{3}H]-thymidine. After a further 16 h, the cells were harvested, and filters counted by liquid scintillation. Standard curves were run using recombinant human IL-1α. LAF activity is presented as ng ml^{-1} IL-1 activity calculated from the standard curve for a dilution of serum which gave approximately 50% maximum incorporation. The limit of detection was 5–10 $pg\ ml^{-1}$. All data shown are representative of at least two separate experiments conducted in triplicate with sera pooled from 2–4 rats.

In experiments to confirm the identity of LAF activity as IL-1, sera were dialysed and then incubated with specific antisera or pre-immune serum overnight at 4°C before incubation with PEG as described above, with antiserum at a final dilution of 1:720. In experiments using the IL-1 receptor antagonist protein (IL-1ra; McIntyre *et al.*, 1991), thymocytes were preincubated for 1 h with the protein at double the final concentration before addition of serum samples and incubation as above.

Assay of serum CCS

Serum CCS was assayed with a commercially available radioimmunoassay according to the manufacturer's instructions (ICN-Flow).

Materials

Mifepristone (RU486) was the kind gift of Roussel-Uclaf, Roumainville, France; recombinant human IL-1α was from National Institute for Biological Standards Control, South Mimms, Herts., batch 86.632 (sp. act. 5×10^6 u ml^{-1}); recombinant human TNFα and anti-murine TNFα mAb the kind gifts of Celltech, Slough, Berks.; anti-murine IL-1β antiserum the gift of Dr R.C. Newton, DuPont-Merck, Wilmington, DE, U.S.A. IL1-ra was the generous gift of Upjohn, Kalamazoo, MI, U.S.A. Anti-murine IL-1α antiserum was from Genzyme, Maidstone, Kent. L-M cells, balanced salts solutions and media were from ICN-Flow, High Wycombe, Bucks.; heat-treated FCS was from Difco, East Molesley, Surrey. [^{3}H]-thymidine (sp. act. 5 Ci $mmol^{-1}$) was from Amersham International, Aylesbury, Bucks. Dexamethasone phosphate was from Evans, Greenford, UK; PHA was from Wellcome Diagnostics, Beckenham, Kent; all other reagents were from Sigma, Poole, Dorset.

Statistics

Statistical differences were calculated by using Student's unpaired *t* test, regarding $P < 0.05$ as significant.

Results

Validation of bioassays

LAF activity was confirmed as predominantly IL-1 by the use of IL-1ra. Pre-incubation of the thymocytes for 1 h with IL-1ra before addition of samples significantly inhibited LAF activity of authentic IL-1α (0.5–50 ng ml^{-1} inhibited essentially by 100% by 5 $\mu g\ ml^{-1}$ IL-1ra) and of serum samples (Figure 1a). The precise nature of circulating LAF activity was determined using anti-murine IL-1α and anti-murine IL-1β antisera which significantly reduced LAF activity of serum samples (Figure 1a), and suggested that the majority of this activity in serum following LPS consists of IL-1α. With all these procedures, a maximal inhibition of approximately 75% was achieved.

Cytotoxic activity in serum was stable to heating to 56°C for 30 min (Figure 1b), indicating that complement did not account for significant amounts of TNF-like activity. Preincubation of serum samples (2 h, 4°C) with a mAb against murine TNFα completely removed cytotoxic activity, confirming its identity as TNFα (Figure 1b).

Figure 1 shows data with serum from Wistar rats: essentially the same results were obtained with Lewis serum i.e. maximum 75% reduction of LAF activity with IL-1ra and complete inhibition of cytotoxic activity with anti-TNFα.

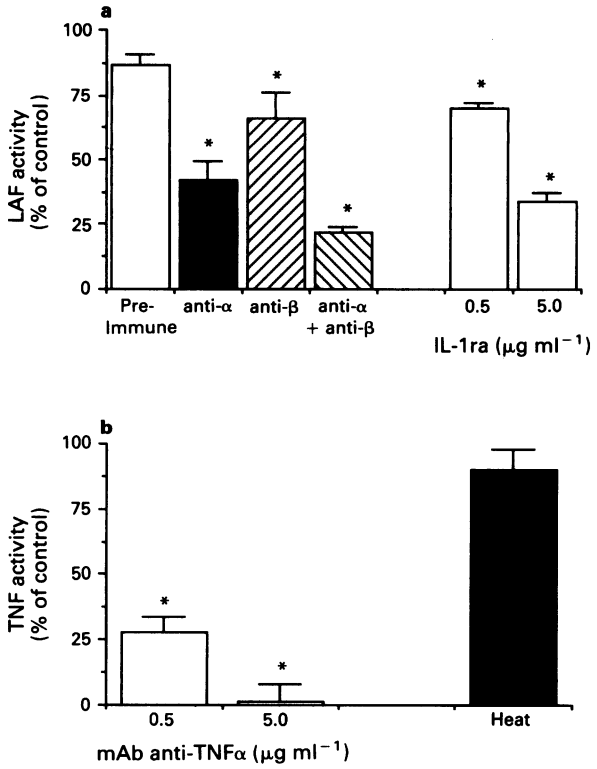

Figure 1 Validation of bioassays: (a) Effect of incubation with pre-immune serum of specific anti-sera raised against murine interleukin-1α (IL-1α) or IL-1β or IL-1ra upon lymphocyte activation factor (LAF) activity; (b) effect of preincubation with anti-murine tumour necrosis factor α-monoclonal antibody (TNFα mAb) or heating to 56°C for 30 min ('heat') upon cytotoxic activity. Data are shown as percentage of control, mean ± s.e.mean for triplicate measurements from serum pooled from 3 Wistar rats (a) 3 h and (b) 1 h following 1 mg kg^{-1} LPS i.p. *$P<0.05$ vs control response.

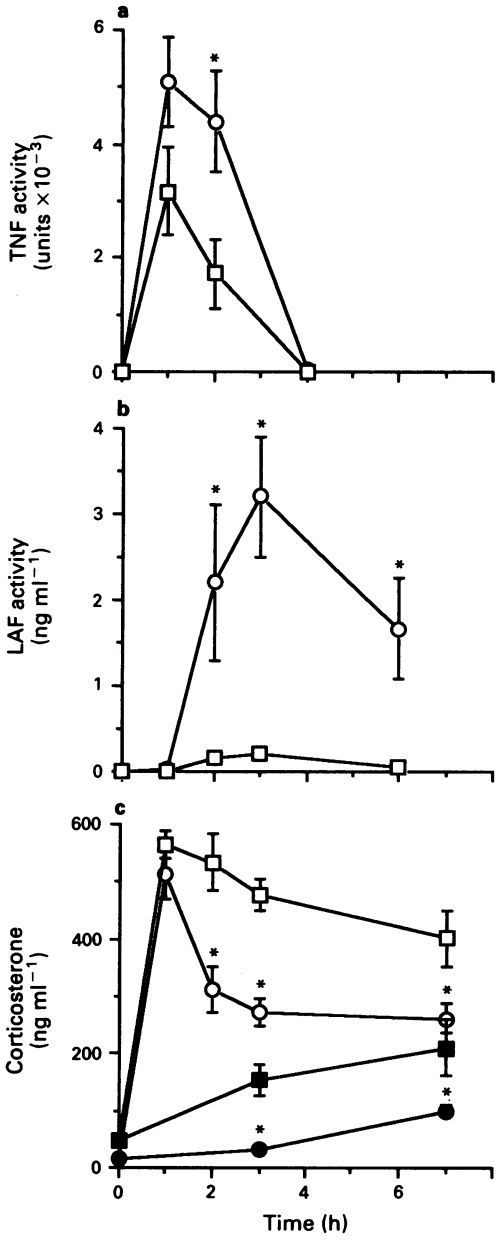

Figure 2 Time course of release of (a) tumour necrosis factor (TNF) activity (units), (b) lymphocyte activation factor (LAF) activity (ng ml^{-1}) and (c) corticosterone (CCS, ng ml^{-1}) following 1 mg kg^{-1} lipopolysaccharide (LPS) i.p. at T = 0 in (○) Lewis and (□) Wistar rats. CCS following saline injection is shown as solid symbols (●, ■). Data are shown as mean ± s.e.mean for at least 4 rats (a and c) or for 2 separate experiments performed in triplicate (b). *$P<0.05$, Lewis vs Wistar strain.

Effect of LPS upon serum IL-1, TNFα and CCS

No LAF or TNF activity was detectable in sera from untreated or saline-treated animals from either strain.

Administration of LPS 1 mg kg^{-1} i.p. caused the sequential appearance of TNFα and IL-1 in serum (Figure 2), accompanied by an increase in circulating CCS. TNF activity was detectable in sera from both strains 1 h after LPS, declining thereafter in the Wistar, but maintained at similar level in the Lewis for 2 h such that at this time there was significantly more TNF activity in Lewis serum (Figure 2a). TNF activity was no longer detectable in serum from either strain 4 h after LPS. In Wistar rats, LAF activity was detectable 2 h following LPS (0.17 ± 0.01 ng ml^{-1}), peaked at 3 h (0.22 ± 0.04 ng ml^{-1}), and then slowly declined (Figure 2b); no IL-1 activity was detectable 24 h after LPS (data not shown). Serum from Lewis rats consistently (3 experiments) contained significantly more IL-1 activity (5–10 fold) than did that from Wistar; the time-course of release was similar in both strains.

CCS was significantly elevated by LPS 1 h after injection in both strains (Figure 2c) and remained significantly elevated compared with saline-treated animals for at least 24 h, although by this time levels were only slightly higher than basal levels (90 ± 33 and 148 ± 12 ng ml^{-1} for Lewis and Wistar respectively). In the Wistar rats, the initial peak level was maintained for at least 3 h and declined slowly; in the Lewis rats, levels were equal to those in the Wistar rats at 1 h, but thereafter dropped, although still remaining significantly higher than basal CCS in this strain. It is noticeable that the Wistar rats had higher basal CCS, so that at 7 h post injection, CCS in LPS-treated Lewis rats was similar to that in saline-treated Wistar rats at the same time, although approximately double the Lewis basal levels. CCS levels in saline-treated Wistar rats were significantly higher than in Lewis rats as the rise in circadian CCS occurred during the afternoon (i.e. 3–7 h post injection).

The effect of LPS was dose-dependent (0.01–1 mg kg^{-1}, Figure 3). TNF data (Figure 3a) are shown 1 h following LPS when activity peaked in both strains; similarly LAF activity is given at 3 h post LPS (Figure 3b). In both cases, activity was detectable following 0.1 mg kg^{-1}, with significant difference in IL-1 between Lewis and Wistar rats at 1 mg kg^{-1}. There is no significant difference between strains in TNF release, although a trend is apparent; it is probable that at 2 h post-LPS, a significantly greater response would be seen in Lewis rats (see Figure 2). CCS data are shown at 3 h (Figure 3c), when levels in the Lewis rats are significantly

Table 1 Effect of pretreatment with dexamethasone (Dex, 0.5 mg kg^{-1}, s.c.) or RU486 (RU, 20 mg kg^{-1}, p.o.) upon serum lymphocyte activation factor (LAF) activity and tumour necrosis factor-α (TNFα) activity at the indicated time following 1 mg kg^{-1} lipopolysaccharide (LPS) in Lewis and Wistar rats

	TNF activity		*LAF activity*	
	Lewis	Wistar	Lewis	Wistar
Control (1 h)	4483 ± 1202	772 ± 122	ND	ND
+ Dex	912 ± 24*	264 ± 110*	ND	ND
+ RU	4154 ± 1291	1552 ± 668	ND	ND
Control (3 h)	42 ± 19	30 ± 6	3.97 ± 0.89	0.87 ± 0.04
+ Dex	NT	NT	0.29 ± 0.05*	0.14 ± 0.06*
+ RU	34 ± 10	18 ± 3	2.87 ± 1.58	1.10 ± 0.15

LAF activity is shown as ng ml^{-1} interleukin-1α (IL-1α) equivalents, mean ± s.e.mean for replicates from one experiment using serum pooled from 3 rats and TNF activity as units ml^{-1}, mean ± s.e.mean for 4–5 rats. ND: not detectable; NT: not tested. *$P<0.05$ vs appropriate controls.

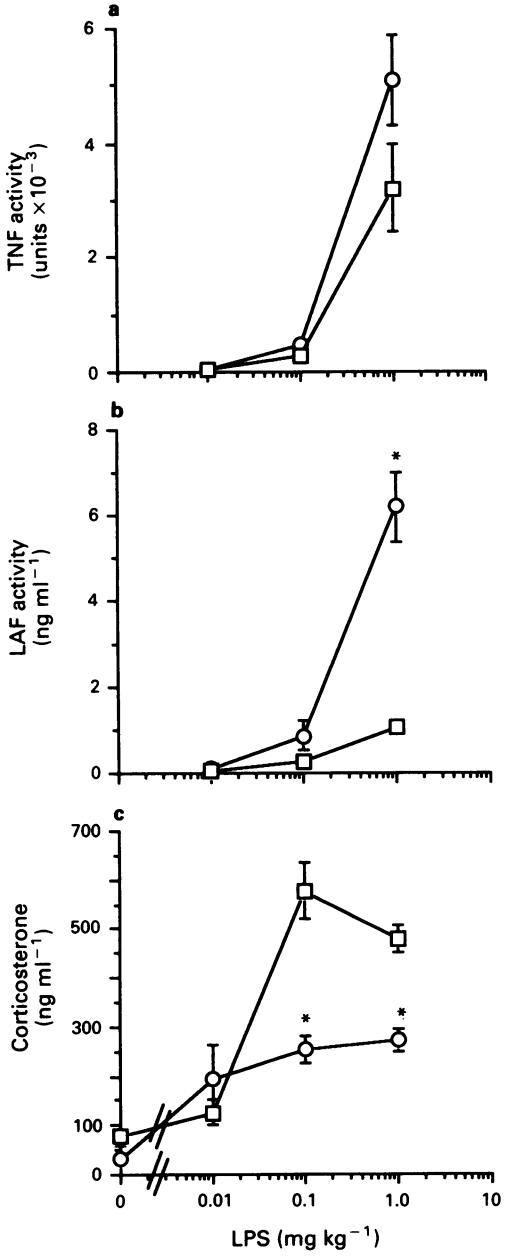

Figure 3 Dose-response to lipopolysaccharide (LPS): (a) tumour necrosis factor (TNF) activity (units), (b) lymphocyte activation factor (LAF) activity (ng ml^{-1}) and (c) corticosterone (CCS, ng ml^{-1}) in response to i.p. LPS in (○) Lewis and (□) Wistar rats. Data are shown as mean ± s.e.mean for at least 4 rats (a and c) or for 3 separate experiments performed in triplicate (b). *$P<0.05$ Lewis vs Wistar strain.

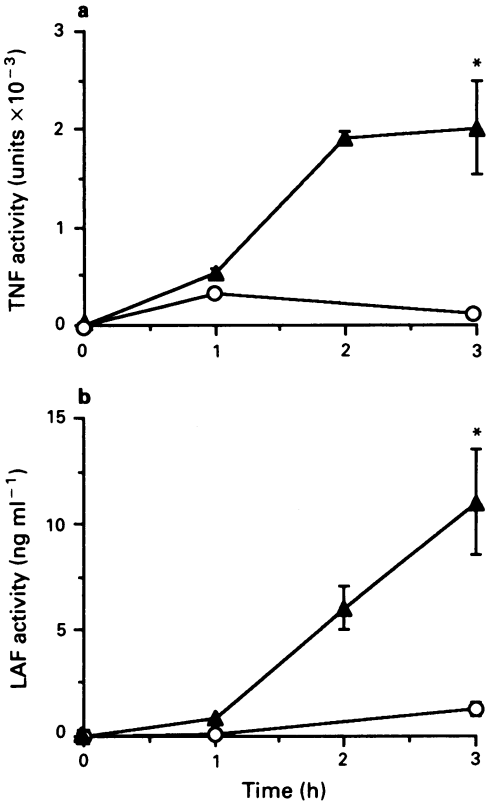

Figure 4 Effect of adrenalectomy upon release of (a) tumour necrosis factor (TNF) activity (units) and (b) lymphocyte activation factor (LAF) activity (ng ml^{-1}) in control (○) and adrenalectomized (ADX) (▲) Lewis rats following 1 mg kg^{-1} lipopolysaccharide (LPS) i.p. Data are shown as mean ± s.e.mean for 4 rats. *$P<0.05$ ADX vs control rats.

lower than those in the Wistar rats; 1 h following LPS however there is no significant difference in CCS at any of the doses used (data not shown) indicating the importance of the time of measurement. An increase in CCS was seen at all doses of LPS tested.

Modulation of cytokine release by exogenous and endogenous corticosteroids

Dexamethasone (0.5 mg kg^{-1}, s.c.) 1 h before injection of LPS significantly inhibited release of both IL-1 and TNF in both strains (Table 1). To discover whether endogenous CCS chronically affected cytokine release, ADX Lewis rats were injected with 1 mg kg^{-1} LPS. These animals appeared markedly ill following LPS injection, and were destroyed at 3 h since it was believed that they would not survive to 6 h.

Table 2 Effect of *in vivo* pretreatment with anti-murine tumour necrosis factor-α monoclonal antibody (TNFα mAb) or anti-murine interleukin-1α (IL-1α) antiserum upon corticosterone (CCS), TNF and lymphocyte activation factor (LAF) activity

Treatment	*CCS*	*TNF activity*	*LAF activity*
Control 1 h	385 ± 20	2338 ± 1092	ND
+ anti-TNFα	329 ± 16	< 10	ND
Control 3 h	222 ± 28	ND	0.95 ± 0.18
+ anti-TNFα	200 ± 26	ND	0.57 ± 0.14
+ anti-IL-α	223 ± 63	ND	0.46 ± 0.17*

Lewis rats were pretreated with mAb (20 mg kg^{-1}) or antiserum (20 mg kg^{-1}) s.c. 16 h before i.p. injection of 1 mg kg^{-1} LPS. CCS is shown as ng ml^{-1}, TNF activity as units and LAF activity as ng ml^{-1} IL-1α, mean ± s.e.mean for at least 4 rats. ND: not detectable.
*$P < 0.05$ vs appropriate controls.

Figure 4 shows that ADX Lewis rats released significantly more TNF than did intact animals (Figure 4a): at 1 h, there was no significant difference between ADX and intact animals, but in ADX rats, TNF release was prolonged, with high levels of activity detectable at 3 h. Similarly, LAF activity was significantly more elevated in serum from ADX rats at 3 h after LPS injection (Figure 4b), and unlike intact animals, was just detectable 1 h post LPS.

In order to investigate the acute role of endogenous corticosteroids released as part of the response to LPS in control of cytokine release, animals were pretreated with the steroid receptor antagonist, RU486 (20 mg kg^{-1}, p.o.) 1 h before injection of LPS. This dose did not significantly affect serum TNF in either rat strain 1 h or 3 h following LPS (Table 1). RU486 pretreatment did not affect serum IL-1 measured at 3 h in either strain, and in one experiment, had no effect upon serum IL-1 measured 6 h after LPS in the Wistar rats (data not shown).

Interaction between cytokines and CCS release

The mechanism by which LPS stimulates the HPA axis remains unclear, although many cytokines including IL-1 and TNFα are able to cause corticosteroid release. In order to investigate the involvement of IL-1 and TNFα in the elevation of CCS, Lewis rats were injected with anti-murine TNFα mAb (20 mg kg^{-1}) or with anti-murine IL-1α antiserum (20 mg kg^{-1}) or with pre-immune serum s.c. Table 2 shows that although anti-TNFα mAb effectively neutralised serum cytotoxic activity at 1 h, there was no significant effect of the antibody upon CCS at this time, suggesting that TNFα was not vital for HPA axis stimulation. Three hours after LPS, although the anti-IL-1α antiserum significantly reduced LAF activity, there was no significant effect upon circulating CCS. Moreover, anti-TNFα mAb did not significantly affect either CCS or LAF activity measured at 3 h.

Discussion

These data confirm in two strains of rat the sequential release of TNF and IL-1 activity accompanied by increased CCS following LPS *in vivo* described in other species (Dinarello, 1991). The CCS response appears to be more sensitive to LPS than is cytokine release, as seen with responses to 0.01 mg kg^{-1} (Figure 3): this may be a genuine phenomenon, since for example, the CCS increase occurs at lower doses of LPS than does pyresis (Derijk *et al.*, 1991) rather than a lack of sensitivity of our cytokine assays. We have measured serum IL-1 activity using bioassay following the removal of inhibitory activity, a problem which has confounded such measurements until recently; we believe that this is the first account of serum IL-1 activity following LPS in the rat. Although specific inhibitory activity may be present in serum (Shaw, 1990) it has been suggested that PEG precipitation is likely to remove non-specific inhibitory activity (Hopkins & Humphreys, 1990) and the assay may therefore reflect biologically available IL-1. The identity of LAF activity as predominantly IL-1 has been confirmed by the use of IL-1ra and by specific antisera; the remaining LAF activity not neutralised by these procedures may be due to other cytokines released during endotoxaemia such as IL-2 or IL-6. Serum cytotoxic activity has been identified as entirely TNFα by use of specific mAb against murine TNFα.

One important observation reported here is the apparent 'over-production' of cytokines in the Lewis compared with the Wistar rat, seen predominantly as a sustained release of TNF, and as an increased and sustained release of LAF activity. The pattern of the CCS response is also different, with a transient peak in the Lewis compared to maintained elevation in the Wistar rat. It has been suggested that the Lewis strain has a defect in HPA axis responses to a variety of stimuli including IL-1 (MacPhee *et al.*, 1989; Sternberg *et al.*, 1989a,b), and this appears also to be the case for the maintained response to LPS, although the immediate response is identical in both strains. We also confirmed the observations of others (Griffin & Whitacre, 1991; Villas *et al.*, 1991) that circadian CCS is lower in the Lewis rat. Since IL-1 and TNF are down-regulated by corticosteroids (Beutler *et al.*, 1986; Knudsen *et al.*, 1987; Lee *et al.*, 1988) and ADX animals show increased cytokine release (Perretti *et al.*, 1989; Zuckerman *et al.*, 1989) the over-production of cytokines in the Lewis rat may be a consequence of lower circulating CCS in this strain.

Endogenous corticosteroids have important anti-inflammatory roles even in the Lewis strain however (MacPhee *et al.*, 1989), and adrenalectomized Lewis rats show significantly increased levels of both IL-1 and TNF activity following LPS, confirming previous observations in adrenalectomized rats and mice (Perretti *et al.*, 1989; Zuckerman *et al.*, 1989; Parant *et al.*, 1991). Interestingly, the steroid antagonist, RU486, failed to affect cytokine release (confirming the observations of Hawes *et al.* (1992) upon TNFα) suggesting that it is the preceding level of corticosteroids that may determine the size of acute response to LPS; CCS released as part of the response may have a role in the 'switching off' of the gene following the response (Evans & Zuckerman, 1991), although this was not apparent over the short-term. Others have shown that RU486 reduces survival over several days in models of septic shock (Hawes *et al.*, 1992; Lazar *et al.*, 1992). It seems unlikely that break-through of CCS occurred in our experiments; the dose of RU486 used effectively blocks the anti-inflammatory actions of dexamethasone (Peers *et al.*, 1988; and unpublished observations), and in addition, circulating CCS were elevated in these animals (unpublished observations), indicating effective block of CCS negative feedback on the HPA axis. It should be noted that dexamethasone administered 1 h before LPS (albeit at a moderate-to-high anti-inflammatory dose) significantly inhibited TNF and LAF activities at 1 and 3 h respectively, suggesting that the 'lag phase' for inhibition of synthesis is not necessarily long, and a response to endogenous CCS could have been observed. *In vitro* evidence indicates that glucocorticoids have significant actions upon cytokine gene activation when applied before, but are much less effective when applied after the stimulus (Lee *et al.*, 1988). Taken together, these observations suggest that endogenous corticosteroids released in response to LPS may help to protect against the effects of released cytokines, rather than affecting their release in the short-term: glucocorticoids protect ADX animals against IL-1 as well as adjuvant-induced death (Perretti *et al.*, 1991). Corticosteroids are involved in the development of tolerance to LPS (Beutler *et al.*, 1986; Evans & Zuckerman, 1991), although LPS-tolerant mice release reduced TNFα but normal amounts of IL-1 in response to LPS, again suggesting that corticosteroid control of TNFα

and IL-1 *in vivo* may differ. Another possibility for the discrepancy between ADX animals and those treated acutely with RU486 is the possible involvement of adrenaline in control of cytokine release (Severn *et al.*, 1992). Clearly ADX animals will not show increases in circulating adrenaline following LPS, although RU486 treatment should not affect this response in intact animals. It would be interesting to investigate combined treatment with RU486 and β-adrenoceptor blockers upon cytokine release following LPS.

The mechanism by which inflammatory stimuli activate the HPS axis is a subject of much debate, with IL-1 a major candidate (Rivier *et al.*, 1989) and other cytokines including TNFα and IL-6 are able to increase CCS (Besedovsky *et al.*, 1991). Given the time-course of cytokine release, it is tempting to speculate that the initial rise in CCS following LPS may be due to TNFα, with the subsequent plateau phase due to IL-1 and possibly IL-6. Our observations with anti-TNFα and anti-IL1 do not support this suggestion however. The anti-TNFα mAb completely blocked *in vitro* cytotoxic activity, yet did not affect CCS levels at 1 h. LAF activity measured at 3 h was not significantly reduced by anti-TNFα suggesting that TNFα alone is not responsible for IL-1 release by LPS (Dinarello *et al.*, 1986; Zuckerman *et al.*, 1991). Similarly, the polyclonal anti-murine IL1α significantly reduced serum LAF activity without affecting CCS measured at 3 h; it is possible that sufficient IL-1 remained (either remaining IL-1α or IL-1β which is also present, Figure 1) to stimulate the CCS response. From our data, neither TNFα nor IL-1α appear fully to account for HPA axis activation by LPS. Alternative mechanisms by which LPS activates the HPS axis have been suggested, and the ability of pyrogenic doses of LPS to bypass the macrophage, a likely source of cytokines, has been observed (Derijk *et al.*, 1991). Interestingly, LPS has been shown to increase CCS in rats with lesions of the paraventricular nuclei (Elenkov *et al.*, 1992), suggesting a direct effect on the pituitary. Given that the lesion in the Lewis rat is believed to be globally-defective CRF release (Calogero *et al.*, 1992), such a mechanism may explain the pattern of CCS response in the Lewis strain.

In conclusion, our data show that while release of the cytokines IL-1 and TNF in response to LPS is tonically controlled by endogenous corticosteroids, corticosteroids released during the response do not acutely control cytokine generation. Moreover, TNFα and possible also IL-1 are not responsible for HPA axis activation during the early part of the response. Overproduction of cytokines in the Lewis rat may have implications concerning their susceptibility to models of experimental diseases such as adjuvant arthritis or EAE, where these cytokines appear to be involved (Jacobs *et al.*, 1991; Bromberg *et al.*, 1992): it has been suggested that imbalances in the cytokine network may contribute to immune dysregulation in the certain strains of mouse (Levine *et al.*, 1991).

This work was funded by the Ono Pharmaceutical Co, Osaka, Japan. R.J.F. is supported by an endowment from Lilly, UK. We thank Roussel-Uclarf, Celltech, National Institute for Biological Standards Control and DuPont-Merck for generous gifts of reagents.

References

AREND, W.P. & DAYER, J.-M. (1990). Cytokines and cytokine inhibitors are antagonists in rheumatoid arthritis. *Arthritis Rheum.*, **33**, 305–315.

BESEDOVSKY, H., DEL REY, A., KLUSMAN, I., FURUKAWA, H., MONGE ARDITI, G. & KABIERSCH, A. (1991). Cytokines as modulators of the hypothalamus-pituitary-adrenal axis. *J. Steroid Biochem. Mol. Biol.*, **40**, 613–618.

BEUTLER, B., KROCHIN, N., MILSARK, I.W., LUEDKE, C. & CERAMI, A. (1986). Control of cachectin (tumour necrosis factor) synthesis: mechanisms of endotoxin resistance. *Science*, **232**, 977–980.

BROMBERG, J.S., CHAVIN, K.D. & KUNKEL, S.L. (1992). Anti-tumour necrosis factor antibodies suppress cell-mediated immunity in vivo. *J. Immunol.*, **148**, 3412–3417.

CALOGERO, A.E., STERNBERG, E.M., BAGDY, G., SMITH, C., BERNARDINI, R., AKSENTIJEVICH, S., WILDER, R.L., GOLD, P.W. & CHROUSOS, G.P. (1992). Neurotransmitter-induced hypothalamic-pituitary-adrenal axis responsiveness is defective in inflammatory disease-susceptible Lewis rats. *Neuroendocrinol.*, **55**, 600– 608.

DERIJK, R., VAN ROOIJEN, N,. TILDERS, F.J.H., BESEDOVSKY, H.O., DEL REY, A. & BERKENBOSCH, F. (1991). Selective depletion of macrophages prevents pituitary-adrenal activation in response to subpyrogenic, but not pyrogenic, doses of bacterial endotoxin in rats. *Endocrinol.*, **128**, 330–338.

DINARELLO, C.A. (1991). The pro-inflammatory cytokines interleukin-1 and tumour necrosis factor and treatment of the septic shock syndrome. *J. Infect. Dis.*, **63**, 1177–1184.

DINARELLO, C.A., CANNON, J.G., WOLLFF, S.M., BERNHEIM, H.A., BEUTLER, B., CERAMI, A., FIGARI, I.S., PALLADINO, M.A. & O'CONNOR, J.V. (1986). Tumour necrosis factor(cachectin) is an endogenous pyrogen and induces production of interleukin-1. *J. Exp. Med.*, **163**, 1433–1450.

ELENKOV, I.J., KOVACS, K., KISS, J., BERTOK, I.L. & VISSI, E.S. (1992). Lipopolysaccharide is able to bypass corticotrophin-releasing factor in affecting plasma ACTH and corticosterone levels: evidence from rats with lesions of the paraventricular nucleus. *J. Endocrinol.*, **133**, 231–236.

EVANS, G.F. & ZUCKERMAN, S.H. (1991). Glucocorticoid-dependent and -independent mechanisms involved in lipopolysaccharide tolerance. *Eur. J. Immunol.*, **21**, 1973–1979.

FLOWER, R.J., PARENTE, L., PERSICO, P. & SALMON, J.A. (1986). A comparison of the acute inflammatory response in adrenalectomised and sham-operated rats. *Br. J. Pharmacol.*, **87**, 57–62.

GRIFFIN, A.C. & WHITACRE, C.C. (1991). Sex and strain differences in the circadian rhythm fluctuation of endocrine and immune function in the rat: implications for rodent models of autoimmune disease. *J. Neuroimmunol.*, **35**, 53–64.

HAWES, A.S., ROCK, C.S., KEOGH, C.V., LOWRY, S.F. & CALVANO, S.E. (1992). In vivo effects of the antiglucocorticoid RU486 on glucocorticoid and cytokine responses to Escerichia coli endotoxin. *Infect. Immun.*, **60**, 2641–2647.

HOPKINS, S.J. & HUMPHREYS, M. (1990). Bioassay of interleukin-1 in serum and plasma following removal of inhibitory activity with polyethylene glycol. *J. Immunol. Methods*, **133**, 127–131.

JACOBS, C.A., BAKER, P.E., ROUX, E.R., PICHA, K.S., TOIVOLA, B., WAUGH, S. & KENNEDY, M.K. (1991). Experimental autoimmune encephalomyelitis is exacerbated by IL-1α and suppressed by soluble IL-1 receptor. *J. Immunol.*, **146**, 2983–2989.

KNUDSEN, P.J., DINARELLO, C.A. & STROM, T.B. (1987). Glucocorticoids inhibit transcriptional and post-transcriptional expression of interleukin-1 in U937 cells. *J. Immunol.*, **139**, 4129–4134.

LAZAR, G., LAZAR, G. & AGARWAL, M.K. (1992). Modification of septic shock in mice by the antiglucocorticoid RU38486. *Circ. Shock*, **32**, 180–184.

LEE, W., OPPENHEIM, J.J. & MATSUSHIMA, K. (1988). Glucocorticoids selectively inhibit the transcription of the interleukin-1β gene and decrease the stability of the interleukin-1β mRNA. *J. Immunol.*, **140**, 1204–1208.

LEVINE, J., HARTWELL, D. & BELLER, D.I. (1991). Imbalanced cytokine production by macrophages from autoimmune-prone mice. *Immunol. Lett.*, **30**, 183–192.

MACPHEE, I.A.M., ANTONI, F.A. & MASON, D.W. (1989). Spontaneous recovery of rats from experimental allergic encephalomyelitis is dependent upon regulation of the immune system by endogenous adrenal corticosteroids. *J. Exp. Med.*, **169**, 431–444.

MASON, D. (1991). Genetic variation in the stress response: susceptibility to experimental allergic encephalomyelitis and implications for human inflammatory disease. *Immunol. Today*, **57**, 57–60.

McINTYRE, K.W., STEPAN, G.J., KOLINSKY, K.D., BENJAMIN, W.R., PLOCINSKI, J.M., KAFFKA, K.L., CAMPDEN, C.A., CHIZZONITE, R.A. & KILIAN, P.L. (1991). Inhibition of interleukin-1 (IL1) binding and bioactivity *in vitro* and modulation of acute inflammation in vivo by IL-1 receptor antagonist and anti-IL-1 receptor monoclonal antibody. *J. Exp. Med.*, **173,** 931–939.

MEAGER, A., LEUNG, H. & WOOLLEY, J. (1989). Assays for tumour necrosis factor and related cytokines. *J. Immunol. Methods.*, **116,** 1–17.

MILLER, L.C. & DINARELLO, C.A. (1987). Biologic activities of interleukin-1 relevant to rheumatic diseases. *Pathol. Immunopathol. Res.*, **6,** 22–36.

PARANT, M, LE CONTEL, C., PARANT, F. & CHEDID, L. (1991). Influence of endogenous glucocorticoid on endotoxin-induced production of circulating TNFα. *Lymphokine & Cytokine Res.*, **10,** 265–271.

PEERS, S.H., MOON, D. & FLOWER, R.J. (1988). Reversal of the anti-inflammatory effects of dexamethasone by the glucocorticoid antagonist RU38486. *Biochem. Pharmacol.*, **37,** 556–557.

PEERS, S.H., DUNCAN, G.S., FLOWER, R.J. & PERRETTI, M. (1992). Release of interleukin-1 (IL-1), tumour necrosis factor-α (TNFα) activity and corticosterone in experimental endotoxaemia in Lewis and Wistar rats. *Br. J. Pharmacol.*, **107,** 258P.

PERRETTI, M., BECHERUCCI, C., SCAPIGLIATI, G. & PARENTE, L. (1989). The effect of adrenalectomy on interleukin-1 release *in vitro* and *in vivo*. *Br. J. Pharmacol.*, **98,** 1137–1142.

PERRETTI, M., MUGRIDGE, K.G., BECHERUCCI, C. & PARENTE, L. (1991). Evidence that interleukin-1 and lipoxygenase metabolites mediate the lethal effect of complete Freund's adjuvant in adrenalectomised rats. *Lymphokine Cytokine Res.*, **10,** 239–243.

PERRETTI, M., SOLITO, E. & PARENTE, L. (1992). Evidence that endogenous interleukin-1 is involved in leukocyte migration in acute experimental inflammation in rats and mice. *Agents Actions*, **35,** 71–78.

RIVIER, C., CHIZZONITE, R. & VALE, W. (1989). In the mouse, the activation of the hypothalamic-pituitary-adrenal axis by lipolysaccharide (endotoxin) is mediated through interleukin-1. *Endocrinol.*, **125,** 2800–2805.

SEVERN, A., RAPSON, N.T., HUNTER, C.A., LIEW, F.Y. (1992). Regulation of tumour necrosis factor production by adrenaline and β-adrenergic agonists. *J. Immunol.*, **148,** 3441–3445.

SHAW, A. (1990). Naturally occurring inhibitors of cytokines. In *Cytokines and Inflammation.* ed. Kinball, E.S. pp. 35–57. Ann Arbor: CRC Press.

STERNBERG, E.M., HILL, J.M., CHROUSOS, G.P., KAMILARIS, T., LISTWAK, S.J., GOLD, P.W. & WILDER, R.L. (1989a). Inflammatory mediator-induced hypothalamic-pituitary-adrenal axis activation is defective in streptococcal cell wall arthritis-susceptible Lewis rats. *Proc. Natl. Acad. Sci. U.S.A.*, **86,** 2374–2378.

STERNBERG, E.M., YOUNG, W.S., BERNARDINI, R., CALOGERO, A.E., CHROUSOS, G.P., GOLD, P.W. & WILDER, R.L. (1989b). A central nervous system defect in biosynthesis of corticotropin-releasing hormone is associated with susceptibility to streptococcal cell wall arthritis in Lewis rats. *Proc. Natl. Acad. Sci. U.S.A.*, **86,** 4771–4775.

VILLAS, P.A., DRONSFIELD, M.J. & BLANKENHORN, E.P. (1991). Experimental allergic encephalomyelitis and corticosterone. Studies in resistant and susceptible rat strains. *Clin. Immunol. Immunopathol.*, **61,** 29–40.

ZUCKERMAN, S.H., SHELLJAUS, J. & BUTLER, L.D. (1989). Differential regulation of lipopolysaccharide-induced interleukin-1 and tumour necrosis factor synthesis: effects of endogenous and exogenous glucocorticoids and the role of the pituitary-adrenal axis. *Eur. J. Immunol.*, **19,** 301–305.

ZUCKERMAN, S.H., EVANS, G.F. & BUTLER, L.D. (1991). Endotoxin tolerance: independent regulation of interleukin-1 and tumour necrosis factor expression. *Infection & Immunity*, **59,** 2774–2780.

(Received February 22, 1993
Revised May 12, 1993
Accepted June 4, 1993)

Br. J. Pharmacol. (1993), **110**, 875–881

Eicosanoid-induced Ca^{2+} release and sustained contraction in Ca^{2+}-free media are mediated by different signal transduction pathways in rat aorta

Ryuichi Kurata, [1]Issei Takayanagi & [2]Tetsuhiro Hisayama

Department of Chemical Pharmacology, Toho University School of Pharmaceutical Sciences, 2-2-1, Miyama, Funabashi, Chiba 274, Japan

1 The effects of 12-*O*-tetradecanoyl 4β-phorbol 13-acetate (β-TPA) on the inositol 1,4,5-trisphosphate (IP_3) production, Ca^{2+} release from the intracellular Ca^{2+} stores and sensitization of contractile apparatus, induced by prostaglandin $F_{2\alpha}$ ($PGF_{2\alpha}$) and U46619, a thromboxane A_2-mimetic, were studied, using fura-2-loaded and -unloaded rat thoracic aortic strips.

2 Both eicosanoids had characteristic patterns of responses in Ca^{2+}-free, 2 mM EGTA-containing solution (Ca^{2+}-free solution). They induced transient increases in intracellular Ca^{2+} concentration ($[Ca^{2+}]_i$) without corresponding transient contraction, but produced delayed, sustained contraction, where $[Ca^{2+}]_i$ was returned to the basal level.

3 Treatment with β-TPA for 60 min reduced the eicosanoids-induced IP_3 production, suggesting that the treatment inhibits PIP_2 breakdown.

4 The treatment also attenuated $[Ca^{2+}]_i$ transient induced by the eicosanoids, but not by caffeine (an IP_3-independent releaser of stored Ca^{2+}), in fura-2-loaded preparations incubated in Ca^{2+}-free solution.

5 In contrast in the presence of β-TPA, the sustained contractions evoked by the eicosanoids in Ca^{2+}-free solution were potentiated, suggesting that the sites of actions of β-TPA and the eicosanoids may differ from each other.

6 $PGF_{2\alpha}$ and U46619 utilize different and parallel signal transduction pathways to release Ca^{2+} by IP_3 produced by PIP_2 breakdown (β-TPA-sensitive), and to increase the sensitivity of contractile apparatus, in which protein kinase C may not be involved (β-TPA-insensitive).

Keywords: Vascular smooth muscle; prostaglandin $F_{2\alpha}$; U46619; calcium; fura-2; Ca stores; protein kinase C; phorbol ester; inositol trisphosphate

Introduction

Activation of Ca^{2+}-mobilizing receptors, has been shown to stimulate PIP_2 breakdown, catalyzed by phospholipase C. This reaction results in an increased formation of inositol 1,4,5-trisphosphate (IP_3) and diacylglycerol (DG), which it has been suggested, contributes to vascular smooth muscle contraction by releasing Ca^{2+} from the sarcoplasmic reticulum (SR; Berridge, 1989), stimulating Ca^{2+} entry (Litten *et al.*, 1987) and sensitizing contractile apparatus by activating protein kinase C (PKC; Rasmussen *et al.*, 1987; Ruzycky & Morgan, 1989; Karaki, 1989). One approach to monitor the IP_3-induced intracellular Ca^{2+} release and the PKC-mediated increased sensitivity of contractile elements is to study the muscle responses to receptor agonists under Ca^{2+}-free conditions. For example, transient and sustained contractions in Ca^{2+}-free media have been assumed to be due to the released Ca^{2+} and changes in Ca^{2+}-sensitivity of the contractile apparatus (Bradley & Morgan, 1987; Karaki, 1989).

We previously reported that under Ca^{2+}-free conditions, prostaglandins $F_{2\alpha}$ ($PGF_{2\alpha}$) elicited an immediate transient increase in $[Ca^{2+}]_i$ without any corresponding contraction. On the other hand, the large size of the sustained contraction which follows occurred without any increase in $[Ca^{2+}]_i$ (Hisayama *et al.*, 1990). Similar observation has been reported by other researchers (Bradley & Morgan, 1987; Heaslip & Sickels, 1989; Ozaki *et al.*, 1990). However, the α_1-adrenoceptor stimulant, phenylephrine caused a transient increase in $[Ca^{2+}]_i$ accompanied by a corresponding transient contraction. This was followed by a small, sustained contraction where $[Ca^{2+}]_i$ was reduced to the basal level (Hisayama *et al.*, 1990). The $PGF_{2\alpha}$-like actions are shared by endothelin-1 (Huang *et al.*, 1990a). These results seem to point to three issues intimately involved in receptor-mediated signal transduction, Ca^{2+}-mobilization and contractile mechanisms: (1) the $[Ca^{2+}]_i$ transient does not necessarily produce a transient contraction; (2) in contrast, contraction that is sustained in nature can be produced without any appreciable increase in $[Ca^{2+}]_i$; (3) the relative predominance between induction of the transient contraction by released Ca^{2+} from the SR and the sustained contraction brought about by increased responsiveness of contractile apparatus to Ca^{2+}, depends on the type of the receptor stimulated. The third case seems to be important, because it suggests that the signal transduction utilized by Ca^{2+} mobilizing receptors could not be accounted for by a unitary system, such as PIP_2 breakdown.

The present work was undertaken to obtain insight mainly into the third point. It is well known that short-term treatment with phorbol esters results in inhibition of receptor-mediated PIP_2 breakdown (Orellana *et al.*, 1985; Leeb-Lundberg *et al.*, 1985; Roth *et al.*, 1986; Litten *et al.*, 1987; Slivka & Insel, 1988; Kaya *et al.*, 1989; Araki *et al.*, 1989). This providues us with a possible method of addressing this point, i.e., to learn which of the functional response(s) could be induced by the PIP_2 breakdown reaction. Thus, the effects of 12-*O*-tetradecanoyl 4β-phorbol 13-acetate (β-TPA) on IP_3 production, $[Ca^{2+}]_i$ transient and sustained contraction in response to thromboxane A_2 receptor agonists (U46619 and $PGF_{2\alpha}$) were investigated. In addition, regarding the second point, we also studied the relationship of the sustained contraction induced by the eicosanoids with PKC.

[1] Author for correspondence.

[2] Present address: Department of Chemical Pharmacology, Faculty of Pharmaceutical Sciences, University of Tokushima, 1-78-1, Shomachi, Tokushima 770, Japan.

Methods

Tissue preparation

Male 8 to 12-week-old Wistar rats weighing 200–300 g were stunned and bled. The thoracic aorta was dissected out and spiral strips, 2–3 mm wide and 7–10 mm long, were prepared. The endothelium was removed by gently rubbing the intimal surface with filter paper moistened with normal physiological saline solution (PSS).

Measurement of muscle tension

The aortic strips were suspended in siliconized organ baths filled with a normal PSS which contained (mM): NaCl 145, KCl 45, $CaCl_2$ 2.5, $MgCl_2$ 1.2, N-2-hydroxyethylpiperazine *N'* -2-ethanesulphonic acid (HEPES) 20, N,N'-tetrakis(2-pyridylmethyl)ethylenedeiamine (TPEN) 10, glucose 11 and ethylenediamine-N,N'-tetraacetic acid (EDTA) Na_2 10 μM (pH 7.4 at 37°C). The solution was gassed with 100% O_2 and maintained at 37°C. Isometric tension development was recorded under an initial tension of 0.5 g. After equilibration in normal PSS for 60 min, the strips were challenged with 1 μM phenylephrine three times. Tension generated by the last challenge was used as a reference value to normalize the size of the response of the eicosanoids. In some experiments, we used Ca^{2+}-free PSS (made by omitting Ca^{2+} from normal PSS and adding 2 mM [ethylene *bis*(oxyethylenenitrilo)] N,N'-tetraacetic acid (EGTA) or high K^+ PSS (made by replacing NaCl with an equimolar amount of KCl).

Measurement of endogenous IP_3 content

Segments of aorta were equilibrated in normal PSS at 37°C bubbled with 100% O_2 for 2 h. After treatment with appropriate drugs and/or solutions, if necessary, U46619 (1 μM) and $PGF_{2\alpha}$ (10 μM) were added at timed intervals. The preparations were quickly frozen in liquid nitrogen and homogenized in ice-cold 6% trichloroacetic acid (TCA). The homogenate was centrifuged, and the resulting supernatant used for determination of IP_3 levels. TCA was extracted with water-saturated ethyl ether and the solution was then neutralized by addition of $NaHCO_3$. After concentration of the samples by lyophilization, IP_3 was measured by protein binding assay with commercially available [^{3}H]-IP_3 assay system. Each experimental group consisted of 4 to 5 preparations from different animals.

Measurement of $[Ca^{2+}]_i$ in fura-2-loaded preparation

The experiment was carried out as described previously (Sato *et al.*, 1988; Hisayama *et al.*, 1990). The strips were incubated with 5 μM fura-2/AM in normal PSS for 3–4 h at room temperature in the presence of 0.2% Cremophor EL, then rinsed with the solution for 15 min. Thereafter, experiments were performed with a double wavelength excitation fluorimeter (CAF 100, Japan spectroscopic Co., Tokyo, Japan) where the fura-2-loaded strips was fixed horizontally in a bath that was bubbled with 100% O_2 at 37°C. The mechanical activity was monitored isometrically. Simultaneously, 500 nm fluorescence emitted by 340 nm and 380 nm excitation (F_{340} and F_{380}, respectively) were measured by successive alternating illuminations (48 Hz), and the ratio ($R_{340/380}$) of F_{340} to F_{380} was automatically calculated. In the muscle strips that were successfully loaded with fura-2, the increase in $[Ca^{2+}]_i$ resulted in a symmetrical increase in F_{340} and decrease in F_{380}, and an increase in $R_{340/380}$. Relative changes of $[Ca^{2+}]_i$ were determined by measuring the $R_{340/380}$. (Himpens & Somlyo, 1988; Sato *et al.*, 1988; Hisayama *et al.*, 1990). Changes in $R_{340/380}$ and muscle tension were expressed as a percentage of those seen with caffeine (30 mM) and phenylephrine (1 μM) in normal PSS, respectively.

Treatment with β-TPA

IP_3 determination After equilibration in normal PSS for 2–3 h, the preparations were treated with β-TPA (5 μM) for 60 min in the same buffer, followed by incubation with U46619 (1 μM) or $PGF_{2\alpha}$ (10 μM) for 15 and 45 s, respectively.

$[Ca^{2+}]_i$ determination The fura-2 loaded aortae were treated with β-TPA (5 μM) first in the normal PSS for 55 min, followed by incubation in the Ca^{2+}-free PSS for 5 min. After incubation in the Ca^{2+}-free medium in the continuing presence of β-TPA for 5 min, the prostanoids were applied and the change in $[Ca^{2+}]_i$ level was monitored.

Muscle tension measurement As shown in Figure 4b, the Ca^{2+} released from the intracellular Ca^{2+} store sites is unlikely to contribute to the development of the sustained contraction induced in Ca^{2+}-free PSS by the eicosanoids. However, to determine the effect of β-TPA on the sustained contractions, we carried out the experiment according to the following protocol which was somewhat different from that used in the $[Ca^{2+}]_i$ determination experiment, so that any interference in the contractions by the released Ca^{2+}, or by a possible buffering action of fura-2 for Ca^{2+} was excluded completely. The fura-2-*unloaded* preparations were incubated in Ca^{2+}-free PSS before and during treatment with β-TPA (5 μM), if necessary, for 5 min and 60 min, respectively, for the contraction to reach a steady-state level and for the stored Ca^{2+} to be depleted. The prostanoids were then added and the size of the resulting contractions measured.

Statistics

Numerical results are presented as the mean ± s.e. with the number of the observations in parentheses. Tests for significance were made by Student's two-tailed, unpaired *t* test or Duncan's new multiple range test, a *P* value less than 0.05 being considered significant.

Drugs

The following drugs were used: U46619 ((15)S-hydroxy-11α,9α-(epoxymethano)-prosta-5Z,13E-dienoic acid) (Cayman Chemical Co., Ann Arbor, MI, U.S.A.), prostaglandin $F_{2\alpha}$ (Ono Pharmaceutical Co., Ltd., Osaka, Japan), 1-phenylephrine hydrochloride, caffeine, flurbiprofen (Sigma Chemical Co., St. Louis, MO, U.S.A.), fura-2/AM, EDTA Na_2, TPEN, HEPES, EGTA (Dojindo Laboratories, Kumamoto, Japan), Cremophor EL (Nacalai Tesque, Kyoto, Japan), 4α and 4β isomers of 12-*O*-tetradecanoylphorbol 13-acetate (α- and β-TPA; Funakoshi Co. Ltd., Tokyo, Japan). The [^{3}H]-IP_3 assay system was purchased from Amersham Japan (Tokyo, Japan). Other chemicals used were of analytical grade.

Results

Effect of short-term treatment with β-TPA on endogenous IP_3 formation by U46619 and $PGF_{2\alpha}$

Figure 1 shows the endogenous IP_3 levels between 0 (= unstimulated) and 15 min following incubation of rat aortic segments with U46619 and $PGF_{2\alpha}$ at concentrations of 1 and 10 μM, which produced maximum contractions, respectively (for example, see Figure 3 and Table 2). Both eicosanoids induced transient increases in IP_3 production, which were observed 15 and 45 s after incubation with U46619 and $PGF_{2\alpha}$, respectively. Thereafter, the IP_3 levels declined rapidly to the basal values.

The IP_3 levels, which were increased by U46619 and $PGF_{2\alpha}$ from the basal values of 34.1 ± 4.1 to 69.1 ± 4.7 and 66.3 ± 4.3 pmol mg^{-1} wet wt., were significantly reduced by the

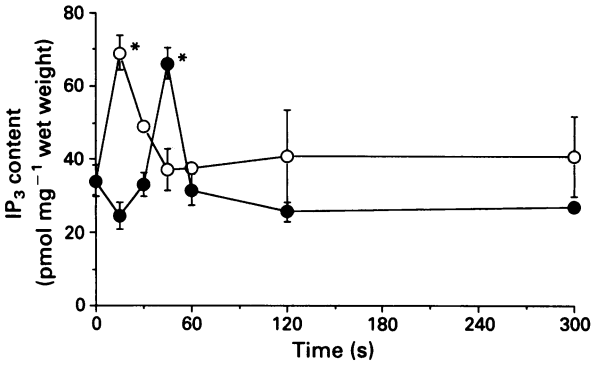

Figure 1 Time course of changes in the contents of endogenous IP_3 in the presence of $PGF_{2\alpha}$ and U46619 in rat aortic strips. The concentrations of $PGF_{2\alpha}$ (●) and U46619 (○) applied were 10 and 1 μM, respectively. Abscissa scale: time after addition of each eicosanoid; ordinate: IP_3 contents. Values are the means ± s.e. of 4–8 preparations. *$P<0.05$ versus the control value (= 0 time point).

Table 1 Effect of prior treatment with β-TPA on the IP_3 content determined in the presence of $PGF_{2\alpha}$ and U46619 in rat aortic strips

	IP_3 content (pmol mg^{-1} wet weight)	n
Basal	34.1 ± 4.1	8
β-TPA	30.1 ± 1.0	4
$PGF_{2\alpha}$	66.3 ± 4.3*	7
U46619	69.1 ± 4.7*	8
$PGF_{2\alpha}$ + β-TPA	48.7 ± 6.0†	5
U46619 + β-TPA	48.5 ± 2.8†	4

After the 60 min treatment with β-TPA (5 μM), the preparations were incubated with $PGF_{2\alpha}$ (10 μM) and U46619 (1 μM) for 45 and 15 s, respectively. Figures are the means of 4–8 preparations with s.e.
*$P<0.05$ versus the basal value (= 0 time point); †$P<0.05$ versus the values obtained with each eicosanoid alone.

60-min treatment with β-TPA (5 μM) to 48.5 ± 2.8 and 48.7 ± 6.0 ($n = 4-5$; $P<0.05$), respectively (Table 1). The inactive isomer, α-TPA had no effect on the IP_3 formation induced by these eicosanoids (data not shown).

Contractile responses to U46619 and $PGF_{2\alpha}$ under Ca^{2+}-free conditions

In the absence of external Ca^{2+}, U46619 (Figure 2) and $PGF_{2\alpha}$ induced only relatively large sustained contractions which were not accompanied by any transient contraction. When the amplitude of the phenylephrine (1 μM)-induced contraction in the normal PSS was taken as the reference (= 100%), the maximum contractions induced by U46619 (1 μM) and $PGF_{2\alpha}$ (10 μM) were 154.4 ± 2.1 ($n = 8$) and 127.8 ± 4.7% ($n = 5$) in the normal PSS, and 30.8 ± 2.9 ($n = 8$) and 25.4 ± 1.6% ($n = 5$) in the Ca^{2+}-free PSS, respectively (Figure 3 and Table 2).

Changes in intracellular Ca^{2+} level induced by U46619 and $PGF_{2\alpha}$ under Ca^{2+}-free conditions

As shown in Figure 4a, in the fura-2-loaded preparations, deprivation of extracellular Ca^{2+} resulted in a rapid decrease in $[Ca^{2+}]_i$, which reached the steady-state level in about 5 min. At this point, U46619 (1 μM) and $PGF_{2\alpha}$ (10 μM) evoked transient increases in $[Ca^{2+}]_i$, which were 23.6 ± 1.0 ($n = 5$) and 21.1 ± 2.1% ($n = 5$) respectively of that induced by 30 mM caffeine in the normal PSS. However, the $[Ca^{2+}]_i$ transients were not accompanied by any corresponding contractions, as shown in Figure 2 with the fura-2-unloaded preparations. In the falling phase of the transient increases in $[Ca^{2+}]_i$, the contractions began to develop, and were well sustained where the $[Ca^{2+}]_i$ was returned to the resting level. U46619, added 40 min after Ca^{2+} depletion, induced only the sustained contractions and not the $[Ca^{2+}]_i$ transient (Figure 4b).

Effect of short-term treatment with β-TPA on Ca^{2+} release and sustained contraction induced by U46619 and $PGF_{2\alpha}$

β-TPA, applied at 5 μM in the normal PSS, produced a slowly developing large contraction, which reached a plateau in about 60 min, with a slight increase in $[Ca^{2+}]_i$: the amplitude of the contraction was 117.4 ± 10.2% ($n = 5$) of that induced by phenylephrine (1 μM), and the increase in $[Ca^{2+}]_i$

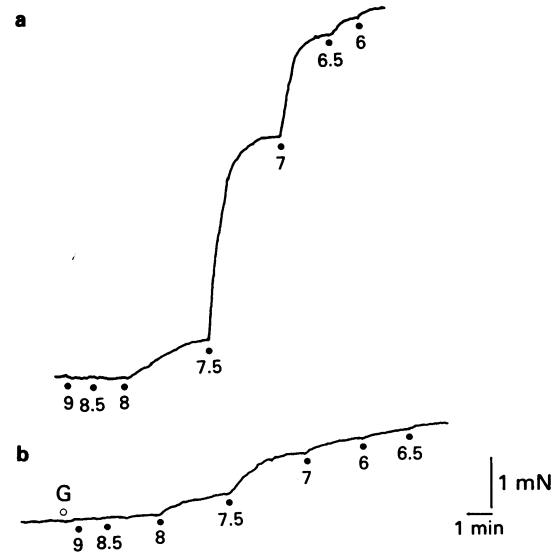

Figure 2 Typical tracing of contractions of rat aortic strips induced by cumulative application of U46619 in normal (a) and Ca^{2+}-free, 2 mM EGTA-containing (Ca^{2+}-free; b) solutions. G marks the change from normal solution to Ca^{2+}-free solution. Numbers show the negative logarithm of molar concentration of U46619 in the muscle bath. Vertical and horizontal bars show 1 mN and 1 min, respectively.

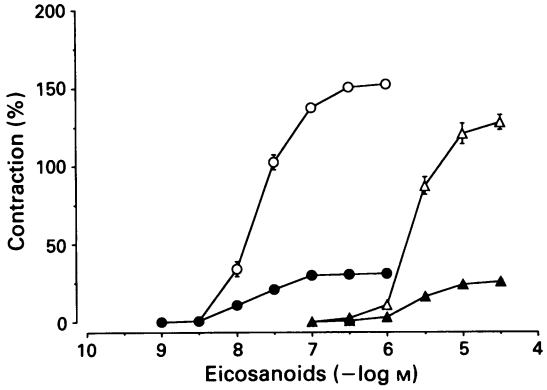

Figure 3 Concentration-response curves for $PGF_{2\alpha}$ and U46619 in normal and Ca^{2+}-free, 2 mM EGTA-containing solutions in rat aortic strips. The contractions induced by $PGF_{2\alpha}$ (△, ▲) and U46619 (○, ●) in the absence (closed symbols) and presence (open symbols) of extracellular Ca^{2+}, are shown in relation to the phenylephrine (1 μM)-evoked contraction in normal solution which was taken as 100%. Abscissa scale; concentrations of eicosanoids; ordinate scale; contraction. Values are the means ± s.e. of 6 preparations.

Table 2 Values of $-\log EC_{50}$ and intrinsic activities of $PGF_{2\alpha}$ and U46619 in normal and Ca^{2+}-free, 2 mM EGTA-containing solutions

	$-\log EC_{50}$	*Intrinsic activity*	n
In normal solution			
$PGF_{2\alpha}$	5.65 ± 0.02	1.28 ± 0.05	5
U46619	7.70 ± 0.07	1.54 ± 0.02	8
In Ca^{2+}-free solution			
$PGF_{2\alpha}$	5.64 ± 0.02	0.25 ± 0.02	5
U46619	7.77 ± 0.03	0.31 ± 0.03	8

Figures are the means of 5–8 preparations with s.e.

Table 3 Effect of prior treatment with β-TPA on $[Ca^{2+}]_i$ transients induced by $PGF_{2\alpha}$, U46619 and caffeine in Ca^{2+}-free, 2 mM EGTA-containing solution in fura-2-loaded rat aortic strips

	$[Ca^{2+}]_i$ transient	n
$PGF_{2\alpha}$	20.1 ± 1.1	5
U46619	19.8 ± 2.6	5
$PGF_{2\alpha}$ + β-TPA	11.3 ± 0.9*	6
U46619 + β-TPA	12.6 ± 1.9*	6

The preparations were incubated with and without β-TPA (5 μM) for 55 min in normal solution. $PGF_{2\alpha}$ (10 μM) and U46619 (1 μM) were then applied 5 min after changing medium to Ca^{2+}-free, 2 mM EGTA-containing solution. Experimental details are as for Figure 5. Values were normalized in relation to the $[Ca^{2+}]_i$ transient evoked by caffeine (30 mM) in normal solution which was taken to be 100%. Figures are the means of 5–6 preparations with s.e. *$P < 0.05$ versus the values obtained with the corresponding eicosanoid alone.

was 10.7 ± 3.0% ($n = 5$) of that by caffeine (30 mM). Neither stress nor $[Ca^{2+}]_i$ was changed by the same concentration of α-TPA.

To study the effect of β-TPA on the Ca^{2+} release and contractions induced by the eicosanoids, the fura-2-loaded preparations were treated for 60 min. Ca^{2+} deprivation resulted in a rapid decrease in the $[Ca^{2+}]_i$ level below the resting one observed in the normal PSS with a slight reduction of the β-TPA-induced contraction. Five minutes later, application of $PGF_{2\alpha}$ or U46619 resulted in the development of a larger contraction than that produced by either eicosanoid alone, while inducing the attenuated amplitude of the $[Ca^{2+}]_i$ transient (Figure 5). As shown in Table 3, the increases in $[Ca^{2+}]_i$ level by U46619 and $PGF_{2\alpha}$ were significantly reduced by prior treatment with β-TPA ($P < 0.05$). On the other hand, there was no difference between the caffeine (30 mM)-induced $[Ca^{2+}]_i$ transients in the absence of $[Ca^{2+}]_o$ observed with the control and β-TPA-treated preparations [24.1 ± 1.8 ($n = 6$) and 20.3 ± 2.9% ($n = 6$) of that evoked by caffeine (30 mM) in normal PSS, respectively]. The $[Ca^{2+}]_i$ transient induced by the eicosanoids was not affected by the same concentration of α-TPA (data not shown).

In contrast, Figure 5b shows that β-TPA had no antagonizing effect on the sustained contraction. After changing the medium to Ca^{2+}-free PSS, the (fura-2-unloaded) preparation was treated for 60 min with β-TPA, if necessary, and then U46619 or $PGF_{2\alpha}$ was applied. The size of contraction induced by β-TPA, U46619 or $PGF_{2\alpha}$ applied alone was 43.1 ± 2.0 ($n = 4$), 31.9 ± 1.7 ($n = 6$) or 12.9 ± 1.0% ($n = 4$) of that induced by 1 μM phenylephrine in normal PSS (the reference contraction), respectively. After treatment with β-TPA, additional contractions by U46619 and $PGF_{2\alpha}$ [= (the total size of contraction by each eicosanoid with β-TPA) − (the size of the β-TPA-induced contraction just before addition of the eicosanoid)] were 50.2 ± 5.1 ($n = 4$) and 25.5 ± 2.7% ($n = 5$) of the reference contraction, respectively. These values were significantly larger than that induced by the corresponding eicosanoid alone ($P < 0.05$; Table 4).

Effects of flurbiprofen and quinacrine on Ca^{2+} release and the sustained contraction induced by U46619 and $PGF_{2\alpha}$

Prior treatment with a potent cyclo-oxygenase inhibitor, flurbiprofen (3 μM) or quinacrine (100 μM) for 30 min had no effect on the Ca^{2+} transients or sustained contractions by EC_{50} concentrations of U46619 (0.03 μM) and $PGF_{2\alpha}$ (3 μM) (Table 5).

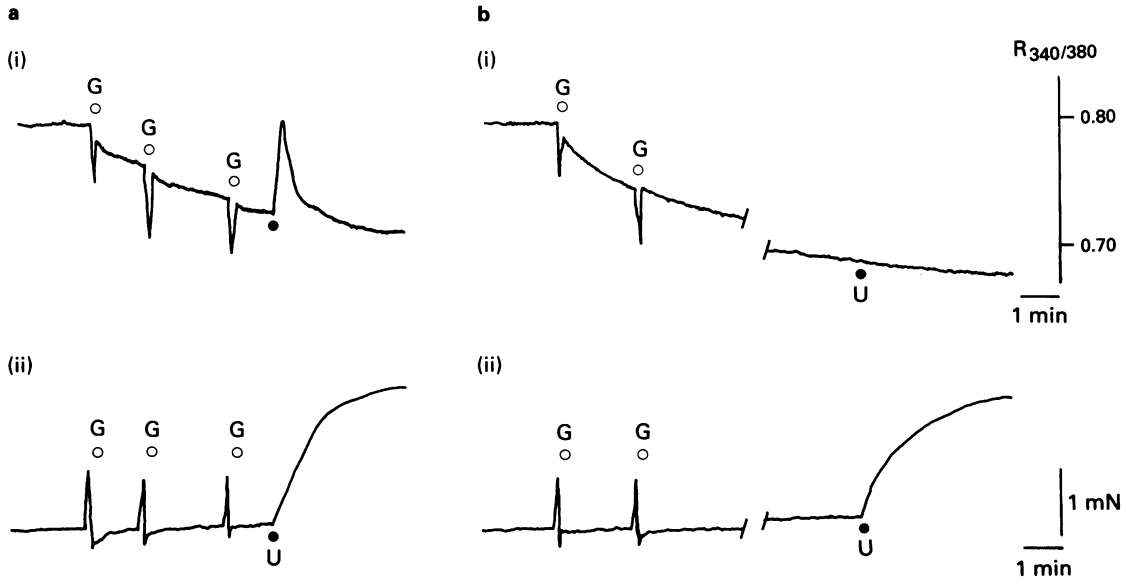

Figure 4 Typical tracings of U46619-induced $[Ca^{2+}]_i$ transients (i) and contractions (ii) obtained 5 (a) and 40 min (b) after incubation of fura-2-loaded rat aortic strips in Ca^{2+}-free, 2 mM EGTA-containing solution (Ca^{2+}-free solution). G, change of the medium from normal to Ca^{2+}-free solution; U, addition of U46619 (1 μM). Vertical and horizontal bars show $R_{340/380}$ (i) and 1 mN (ii), and 1 min, respectively.

Table 4 Effect of prior treatment with β-TPA on sustained contractions induced by $PGF_{2\alpha}$, U46619 in Ca^{2+}-free, 2 mM EGTA-containing solution in rat aortic strips

	Δ *Contraction*	n
$PGF_{2\alpha}$	12.9 ± 1.0	4
U46619	31.9 ± 1.7	6
$PGF_{2\alpha}$ + β-TPA	25.5 ± 2.7*	5
U46619 + β-TPA	50.2 ± 5.1*	4

Five minutes after deprivation of extracellular Ca^{2+}, the preparation was incubated in the absence and presence of β-TPA (5 μM) for 1 h, and $PGF_{2\alpha}$ (10 μM) or U46619 (1 μM) was then applied. Values are shown according to the following formula: (the amplitude of contraction by each eicosanoid) − (the tension level obtained just before addition of the eicosanoid), and normalized in relation to the phenylephrine (1 μM)-induced contraction (100%). Figures are the means of 4–6 preparations with s.e.
*$P<0.05$ versus the values obtained with the corresponding eicosanoid alone.

Table 5 Effect of flurbiprofen and quinacrine on the $PGF_{2\alpha}$- and U46619-induced sustained contractions in Ca^{2+}-free, 2 mM EGTA-containing solution in rat aortic strips

	Contraction	n
$PGF_{2\alpha}$ + flurbiprofen	7.6 ± 0.4	4
U46619 + flurbiprofen	20.6 ± 1.2	4
$PGF_{2\alpha}$ + quinacrine	8.6 ± 1.5	6
U46619 + quinacrine	23.7 ± 3.8	4

The preparations were incubated with and without flurbiprofen (1 μM) or quinacrine (100 μM) for 25 min in normal solution. $PGF_{2\alpha}$ (3 μM) and U46619 (30 nM) were then applied 5 min after changing medium to Ca^{2+}-free, 2 mM EGTA-containing solution with and without flurbiprofen or quinacrine. Figures are normalized for the contraction by each eicosanoid alone to be 100%, and are the means of 4–6 preparations with s.e.

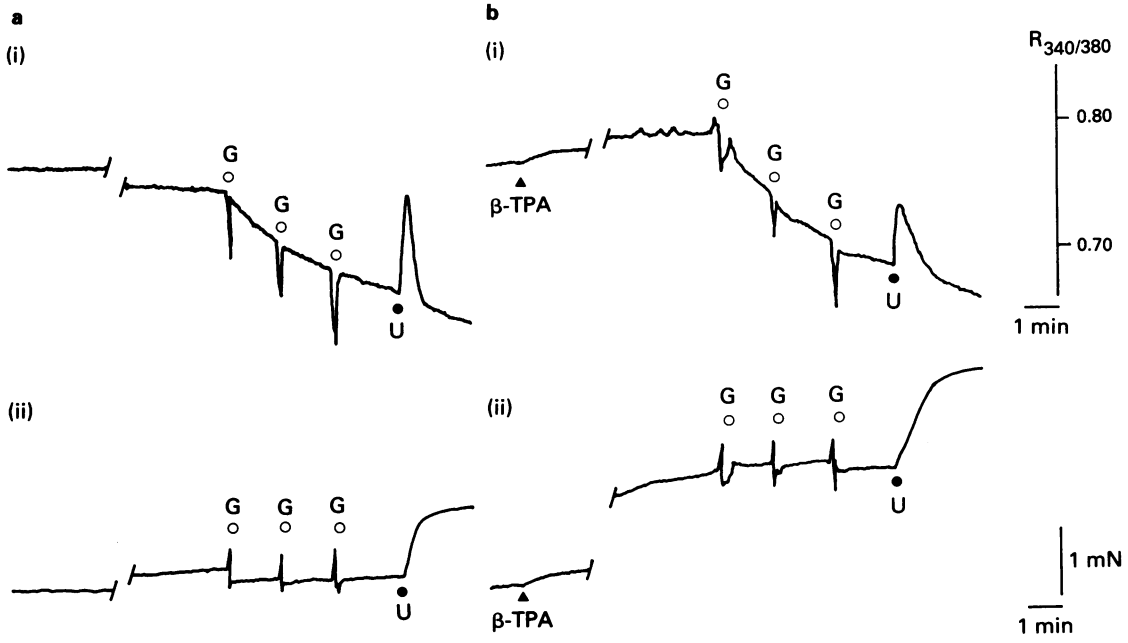

Figure 5 Typical tracings of $[Ca^{2+}]_i$ transients (a) and contractions (b) induced by U46619 observed 5 min after incubation in Ca^{2+}-free, 2 mM EGTA-containing solution (Ca^{2+}-free solution) in fura-2-loaded rat aortic strips which had been incubated in the absence (a) and presence (b) of β-TPA. β-TPA (5 μM) was added 55 min before change of the medium from normal solution to Ca^{2+}-free solution, and present throughout. β-TPA, start of incubation with β-TPA; G, change of the medium from normal to Ca^{2+}-free solution; U, addition of U46619 (1 μM). Vertical and horizontal bars show $R_{340/380}$ (i) and 1 mN (ii), and 1 min, respectively.

Discussion

In the present study, we monitored PIP_2 breakdown by measuring the content of IP_3, which is one of the products of the reaction. The rat aortic strips responded to $PGF_{2\alpha}$ and U46619, both of which act on the thromboxane A_2 receptor in this tissue (Kennedy *et al.*, 1982; Hanasaki *et al.*, 1988), with an increased production of endogenous IP_3. The response was transient in nature, as observed with α_1-adrenoceptor agonists (Langlands & Diamond, 1990; Huang *et al.*, 1990b). Prior short-term treatment with β-TPA greatly reduced the eicosanoid-induced production of IP_3. The effect of β-TPA seems to be specific, since α-TPA, the biologically-inactive isomer, did not affect the IP_3 contents.

It is well known that stimulated PIP_2 breakdown mediated by activation of Ca^{2+} mobilizing receptors is inhibited by short-term treatment with active phorbol esters in many cell types (Orellana *et al.*, 1985; Leeb-Lundberg *et al.*, 1985; Litten *et al.*, 1987; Slivka & Insel, 1988; Kaya *et al.*, 1989; Chardonnens *et al.*, 1990), including vascular smooth muscle cells (Roth *et al.*, 1986; Reynolds *et al.*, 1989; Araki *et al.*, 1989). Our results showing that the 60-min treatment with β-TPA reduced the increased production of IP_3 by $PGF_{2\alpha}$ and U46619 are consistent with these reports, and suggest that the IP_3-and DG-mediated responses to these eicosanoids should be diminished by prior treatment with the phorbol ester. The experiments were carried out under Ca^{2+}-free conditions, since the transient and sustained contractions under such conditions have been assumed to be due to the Ca^{2+} released by IP_3 and changes in Ca^{2+}-sensitivity of contractile apparatus by PKC, respectively (Bradley & Morgan, 1987; Karaki, 1989; Huang *et al.*, 1990b; Hisayama *et al.*, 1990).

In the absence of extracellular Ca^{2+}, both eicosanoids produced transient increases in $[Ca^{2+}]_i$, most probably by releasing Ca^{2+} from the intracellular Ca^{2+} stores or the SR. However, the transients were not accompanied by corresponding transient contractions. In the falling phase of the transient increases in $[Ca^{2+}]_i$, the contractions began to develop

and were well sustained, even though the $[Ca^{2+}]_i$ had then returned to the resting level. Prior short-term treatment with β-TPA, while having no significant effect on the $[Ca^{2+}]_i$ transient induced by caffeine which releases Ca^{2+} through an IP_3-independent mechanism (Endo, 1977), significantly reduced the amplitude of the $[Ca^{2+}]_i$ transient evoked by $PGF_{2\alpha}$ and U46619, as it did on IP_3 production, suggesting that the Ca^{2+} release is triggered by IP_3 produced by PIP_2 breakdown. The reduction of $[Ca^{2+}]_i$ transient by the phorbol ester was, however, smaller than that of IP_3 production. We have no explanation about this point, but it might be that other than IP_3-independent Ca^{2+} release is induced by the eicosanoids.

In contrast, the sustained contractions induced in Ca^{2+}-free media were not inhibited but augmented by the prior short-term treatment with β-TPA. This suggests that the signal-transducing pathway utilized for development of the sustained contraction is different from that for the intracellular Ca^{2+} release, and further that at least DG derived from PIP_2 is not involved in the sustained contraction. Rather, the extra contraction of the β-TPA-treated preparations by the eicosanoid [(the total size of contraction by each eicosanoid with β-TPA) − (the size of the β-TPA-induced contraction just before addition of the eicosanoid)] was larger in size than that of the sustained contraction by either eicosanoid alone: synergism between β-TPA and the eicosanoids was observed in inducing the sustained contraction under Ca^{2+}-free conditions. This would raise the possibility that the mechanism involved in the eicosanoid-induced sustained contractions is unrelated to the PKC that is activated by application of β-TPA. Similar synergism with β-TPA was obtained with urotensin II (Itoh *et al.*, 1991).

On the other hand, the prior short-term treatment with β-TPA resulted in attenuation of IP_3 production and Ca^{2+} release, but no effect on the sustained contraction in response to endothelin-1 (Huang *et al.*, 1990a,b). Although the pathway used by endothelin-1 for Ca^{2+} release also differs from that for sustained contraction, the mechanism involved in the latter is somewhat different from that in the eicosanoid-induced contraction, because the effects of β-TPA and endothelin-1 were additive in inducing the sustained contraction. This result was recently confirmed (Itoh *et al.*, 1991). Therefore, mechanistically, the receptor-mediated sustained contraction obtained under Ca^{2+}-free conditions may be of at least two types.

It has been reported that the prior short-term treatment with phorbol esters, while inhibiting PIP_2 breakdown, potentiates the phospholipase A_2 activity which is stimulated by some drugs, such as endothelin-1 (Reynolds *et al.*, 1989), vasopressin (Chardonnens *et al.*, 1990), and bradykinin (Slivka & Insel, 1988). One might consider whether or not the synergistic effect of β-TPA on the eicosanoid-induced sustained contraction shown in the present study is the result of potentiated phospholipase A_2 activity by the phorbol ester, which resulted in the increase in the effective concentration of constrictor eicosanoids due to their accumulation in the organ bath during prolonged incubation with $PGF_{2\alpha}$ or U46619. This situation has been demonstrated with endothelin-1 (Reynolds & Mok, 1990). However, in our case, this possibility can be excluded, since quinacrine and flurbiprofen had no inhibitory effect on the contraction induced by the eicosanoids, the concentrations of which were around their EC_{50} values to make it easier to detect any inhibition.

The present study strongly suggests that in the rat aorta, $PGF_{2\alpha}$ and U46619 utilize different and parallel signal transduction pathways to release Ca^{2+} by IP_3 produced by PIP_2 breakdown, and to increase the sensitivity of contractile apparatus in which PKC may not be involved. Work is in progress to determine whether the two independent pathways derive from different receptor types or coupling of one type of receptor with different effector systems.

This study was supported by a Grant-in-Aid for Scientific Research from the Ministry of Education, Science and Culture, Japan (No. 04304030).

References

ARAKI, S., KAWAHARA, Y., KARIYA, K., SUNAKO, M., FUKUZAKI, H. & TAKAI, Y. (1989). Stimulation of phospholipase C-mediated hydrolysis of phosphoinositides by endothelin in cultured rabbit aorta smooth muscle cells. *Biochem. Biophys. Res. Commun.*, **159**, 1072–1079.

BERRIDGE, M.J. (1989). Inositol phosphates and cell signalling. *Nature*, **341**, 197–205.

BRADLEY, A.B. & MORGAN, K. (1987). Alterations in cytoplasmic calcium sensitivity during porcine coronary artery contractions as detected by aequorin. *J. Physiol,*. **385**, 437–448.

CHARDONNENS, D., LANG, U,. ROSSIER, M.F., CAPPONI, A.M. & VALLOTTON, M.B. (1990). Inhibitory and stimulatory effects of phorbol ester on vasopressin-induced cellular responses in cultured rat aortic smooth muscle cells. *J. Biol. Chem.*, **265**, 10451–10457.

ENDO, M. (1977). Calcium release from the sarcoplasmic reticulum. *Physiol. Rev.*, **57**, 71–108.

HANASAKI, K., NAKANO, K., KASAI, H., ARITA, H., OHTANI, K. & DOTEUCHI, M. (1988). Specific receptors for thromboxane A_2 in cultured vascular smooth muscle cells of rat aorta. *Biochem. Biophys. Res. Commun.*, **150**, 1170–1175.

HEASLIP, R.J. & SICKELS, B.D. (1989). Evidence that prostaglandins can contract the rat aorta *via* a novel protein kinase C-dependent mechanism. *J. Pharmacol. Exp. Ther.*, **250**, 44–51.

HIMPENS, B. & SOMLYO, A.P. (1988). Free-calcium and force transients during depolarization and pharmacomechanical coupling in guinea-pig smooth muscle. *J. Physiol.*, **395**, 507–530.

HISAYAMA, T., TAKAYANAGI, I. & OKAMOTO, Y. (1990). Ryanodine reveals multiple contractile and relaxant mechanisms in vascular smooth muscle: simultaneous measurements of mechanical activity and of cytoplasmic free Ca^{2+} level with fura-2. *Br. J. Pharmacol.*, **100**, 677–684.

HUANG, X.-N., HISAYAMA, T. & TAKAYANAGI, I. (1990a). Endothelin-1 induced contraction of rat aorta: contributions made by Ca^{2+} influx and activation of contractile apparatus associated with no change in cytoplasmic Ca^{2+} level. *Naunyn-Schmied Arch. Pharmacol.*, **341**, 80–87.

HUANG, X.-N., TAKAYANAGI, I. & HISAYAMA, T. (1990b). Endothelin-1 induced contraction of rat aorta in Ca^{2+}-free medium independent of phosphatidylinositol 4, 5-bisphosphate (PIP_2) breakdown. *Gen. Pharmacol.*, **21**, 893–898.

ITOH, H., HIGUCHI, H., HIRAOKA, N., ITO, M., KONISHI, T., NAKANO, T. & LEDERIS, K. (1991). Contraction of rat thoracic aorta strips by endothelin-1 in the absence of extracellular Ca^{2+}. *Br. J. Pharmacol.*, **104**, 847–852.

KARAKI, H. (1989). Ca^{2+} localization and sensitivity in vascular smooth muscle. *Trends Pharmacol. Sci.*, **10**, 320–325.

KAYA, H., PATTON, G.M. & HONG, S.L. (1989). Bradykinin-induced activation of phospholipase A_2 is independent of the activation of phosphoinositide-hydrolyzing phospholipase C. *J. Biol. Chem.*, **264**, 4972–4977.

KENNEDY, I., COLEMAN, R.A., HUMPHREY, P.P.A., LEVY, G.P. & LUMLEY, P. (1982). Studies on the characterization of prostanoid receptors: a proposed classification. *Prostaglandins*, **24**, 667–689.

LANGLANDS, J.M. & DIAMOND, J. (1990). The effect of phenylephrine on inositol 1,4,5-trisphosphate levels in vascular smooth muscle measured using a protein binding assay system. *Biochem. Biophys. Res. Commun.*, **173**, 1258–1265.

LEEB-LUNDBERG, L.M.F., COTECCHIA, S., LOMASNEY, J.W., DEBERNARDIS, J.F., LEFKOWITZ, R.J. & CARON, M.G. (1985). Phorbol esters promote α_1-adrenergic receptor phosphorylation and receptor uncoupling from inositol phospholipid metabolism. *Proc. Natl. Acad. Sci. U.S.A.*, **82**, 5651–5655.

LITTEN, R.Z., SUBA, E.A. & ROTH, B.L. (1987). Effects of a phorbol ester on rat aortic contraction and calcium influx in the presence and absence of BAY k 8644. *Eur. J. Pharmacol.*, **144,** 185–191.

ORELLANA, S.A., SOLSKI, P.A. & BROWN, J.H. (1985). Phorbol ester inhibits phosphoinositide hydrolysis and calcium mobilization in cultured astrocytoma cells. *J. Biol. Chem.*, **260,** 5236–5239.

OZAKI, H., OHYAMA, T., SATO, K. & KARAKI, H. (1990). Ca^{2+}-dependent and independent mechanisms of sustained contraction in vascular smooth muscle of rat aorta. *Jpn. J. Pharmacol.*, **52,** 509–512.

RASMUSSEN, H., TAKUWA, Y. & PARK, S. (1987). Protein kinase C in the regulation of smooth muscle contraction. *FASEB J.*, **1,** 177–185.

REYNOLDS, E.E. & MOK, L.L.S. (1990). Role of thromboxane A_2/prostaglandin H_2 receptor in the vasoconstrictor response of rat aorta to endothelin. *J. Pharmacol. Exp. Ther.*, **252,** 915–921.

REYNOLDS, E.E., MOK, L.L.S. & KUROKAWA, S. (1989). Phorbol ester dissociates endothelin-stimulated phosphoinositide hydrolysis and arachidonic acid release in vascular smooth muscle cells. *Biochem. Biophys. Res. Commun.*, **160,** 868–873.

ROTH, B.L., NAKAKI, T., CHUANG, D.-M. & COSTA, E. (1986). 5-Hydroxytryptamine$_2$ receptors coupled to phospholipase C in rat aorta: modulation of phosphoinositide turnover by phorbol ester. *J. Pharmacol. Exp. Ther.*, **238,** 480–485.

RUZYCKY, A.L. & MORGAN, K.G. (1989). Involvement of the protein kinase C system in calcium-force relationships in ferret aorta. *Br. J. Pharmacol.*, **97,** 391–400.

SATO, K., OZAKI, H. & KARAKI, H. (1988). Changes in cytosolic calcium level in vascular smooth muscle strip measured simultaneously with contraction using fluorescent calcium indicator fura 2. *J. Pharmacol. Exp. Ther.*, **246,** 294–300.

SLIVKA, S.R. & INSEL, P.A. (1988). Phorbol ester and neomycin dissociate bradykinin receptor-mediated arachidonic acid release and polyphosphoinositide hydrolysis in Madin-Darby canine kidney cells. Evidence that bradykinin mediates noninterdependent activation of phospholipases A_2 and C. *J. Biol. Chem.*, **263,** 14640–14647.

(Received January 21, 1993
Revised May 25, 1993
Accepted June 7, 1993)

Br. J. Pharmacol. (1993), **110**, 882–888

Pharmacological activity of (−)-discretamine, a novel vascular α-adrenoceptor and 5-hydroxytryptamine receptor antagonist, isolated from *Fissistigma glaucescens*

[1]Feng-Nien Ko, †Sheu-Meei Yu, Ming-Jai Su, *Yang-Chang Wu & Che-Ming Teng

Pharmacological Institute, College of Medicine, National Taiwan University, Taipei, †Department of Pharmacology, Chang Gung Medical College, Tao-Yuan and *School of Pharmacy, Kaohsiung Medical College, Kaohsiung, Taiwan

1 The pharmacological activity of (−)-discretamine, isolated from *Fissistigma glaucescens*, was determined in rat isolated thoracic aorta, cardiac tissues and ventricular myocytes and guinea-pig isolated trachea.

2 (−)-Discretamine was found to be an α_1-adrenoceptor blocking agent in rat thoracic aorta as revealed by its competitive antagonism of noradrenaline ($pA_2 = 7.20 \pm 0.10$)- or phenylephrine ($pA_2 = 7.60 \pm 0.09$)-induced vasoconstriction. It was as potent as phentolamine ($pA_2 = 7.51 \pm 0.10$), but was more potent than yohimbine ($pA_2 = 6.18 \pm 0.06$). Removal of endothelium significantly increased the antagonistic potency of (−)-discretamine on noradrenaline ($pA_2 = 7.52 \pm 0.09$)- or phenylephrine ($pA_2 = 7.90 \pm 0.09$)-induced vasoconstriction.

3 (−)-Discretamine was also an α_2-adrenoceptor blocking agent ($pA_2 = 6.30 \pm 0.15$) and a 5-hydroxytryptamine antagonist ($pA_2 = 6.87 \pm 0.06$), both in rat aorta denuded of endothelium.

4 (−)-Discretamine protected α-adrenoceptors from alkylation by the irreversible blocking agent, phenoxybenzamine.

5 [^{3}H]-inositol monophosphate formation caused by noradrenaline (3 μM) in rat thoracic aorta was suppressed by (−)-discretamine (10 and 30 μM) and prazosin (3 μM).

6 A high concentration of (−)-discretamine (30 μM) did not affect the contraction induced by the thromboxane receptor agonist U-46619, prostaglandin $F_{2\alpha}$ ($PGF_{2\alpha}$), angiotensin II, high K^+ or endothelin in rat aorta denuded of endothelium. Neither cyclic AMP nor cyclic GMP content of rat thoracic aorta was changed by (−)-discretamine.

7 Contraction of guinea-pig trachea caused by histamine, leukotriene C_4 or carbachol was not affected by (−)-discretamine (30 μM). (−)-Discretamine also did not block β_1- or β_2-adrenoceptor-mediated responses induced by isoprenaline in rat right atria and guinea-pig trachea.

8 A voltage clamp study in rat ventricular single myocytes revealed that sodium inward current, slow inward Ca^{2+} current or transient (I_{to}) and steady state (I_{800}) outward current was not affected by (−)-discretamine (30 μM).

9 It is concluded that (−)-discretamine is a selective α-adrenoceptor and 5-HT receptor antagonist in vascular smooth muscle.

Keywords: α-Adrenoceptor antagonist; 5-hydroxytryptamine receptor antagonist; (−)-discretamine; rat thoracic aorta; *Fissistigma glaucescens*

Introduction

α-Adrenoceptors are involved in a variety of physiological processes, including regulation of blood pressure (Minneman, 1988). Although the role played by α-adrenoceptors in hypertensive disease remains unclear, the blockade of α-adrenoceptors by appropriate antagonistic drugs is effective in lowering blood pressure, particularly with the selective α_1-antagonists such as prazosin (Cavero & Roach, 1980; Stanaszek *et al.*, 1983; Titmarsch & Monk, 1987). The chemical structures of α-adrenoceptor antagonists may be of pharmaceutical interest and/or useful for pharmacological study. However, the chemical structure of α-adrenoceptor antagonists is strikingly unrelated to their pharmacological activity. Phenoxybenzamine is a phenylethylamine derivative which is chemically related to endogenous catecholamines. Phentolamine is an imidazoline derivative. Prazosin is a piperazinyl quinazoline derivative, which shows some resemblance both to papaverine and to the aminopyrimidine moiety of adenosine 3′:5′-cyclic monophosphate (cyclic AMP) and guanosine 3′:5′-cyclic monophosphate (cyclic GMP). Yohimbine is an indolealkylamine alkaloid and its structure resemblance to reserpine is apparent.

Medicinal plants have been used as traditional remedies in oriental countries over hundreds of years. In a large scale screening test, we have found many biologically active compounds isolated from plant sources. Among them, (−)-discretamine (Figure 1), a tetrahydroprotoberberine alkaloid isolated from *Fissistigma glaucescens* (Lu *et al.*, 1985), inhibited noradrenaline-induced contraction of rat thoracic aorta. In the present study, we have determined the selectivity of this agent for several receptor types and ion channels.

Methods

Rat aortic contraction

Wistar rats of either sex, 250–300 g, were killed by a blow to the head. The thoracic aorta was isolated and excess fat and connective tissue were removed. The vessels were cut into rings of about 5 mm in length and mounted in organ baths

[1] Author for correspondence at: Pharmacological Institute, College of Medicine, National Taiwan University, No. 1, Jen-Ai Rd., 1st Section, Taipei, 10018 Taiwan.

containing 5 ml Krebs solution of the following composition (mM): NaCl 118.4, KCl 4.7, $MgSO_4$ 1.2, KH_2PO_4 1.2, glucose 11.7, $CaCl_2$ 1.9 and $NaHCO_3$ 25.0. The tissue bath solution was maintained at 37°C and gassed with 95% O_2-5% CO_2. Two stainless steel hooks were inserted into the aortic lumen, one was fixed while the other was connected to a transducer. Aortae were equilibrated in the medium for 90 min with three changes of Krebs solution and maintained under an optimal tension of 1 g before specific experimental protocols were initiated. Contractions were recorded isometrically via a force-displacement transducer connected to a Grass polygraph. In some experiments, the endothelium was removed by rubbing with a cotton ball and the absence of acetylcholine-induced relaxation was taken as an indicator that vessels were denuded successfully. Aortae were allowed to equilibrate for 15 min with (−)-discretamine before the generation of a cumulative concentration-response curve with each agonist for 15–30 min at 3 min intervals. Results are expressed as percentage of the maximal control response for each agonist before the addition of (−)-discretamine.

The contractile effects of calcium were studied in rings stabilized in K^+ (60 mM) solution without Ca^{2+}. Calcium was then added from stock dilutions to obtain the desired concentrations, and the effect of each Ca^{2+} concentration was recorded. The maximal tension attained at 3 mM Ca^{2+} was considered as 100%. The high-K^+ solution was prepared by substituting NaCl with KCl in an equimolar amount.

Cyclic AMP and cylic GMP assay of rat aorta

The content of cyclic AMP or cyclic GMP was assayed on aortic rings as previously described (Itoh *et al.*, 1982; Kauffman *et al.*, 1987). After incubation of aortic rings with dimethylsulphoxide (DMSO, 0.1%), forskolin, sodium nitroprusside or (−)-discretamine for 2 min, the aortic rings were rapidly frozen in liquid nitrogen and stored at −80°C until homogenized in 0.5 ml 10% trichloroacetic acid and 4 mM EDTA using a Potter glass/glass homogenizer. The homogenate was centrifuged at 10,000 × *g* for 5 min and the supernatant was removed and extracted with 4 × 3 vol of ether, and the cyclic AMP or cyclic GMP content was then assayed using RIA kits. The precipitate was used for protein assay (Lowry *et al.*, 1951). Cyclic AMP and cyclic GMP levels were expressed as pmol mg^{-1} protein.

Measurement of [^{3}H]-inositol monophosphate

The same procedure as described by Hirata *et al.* (1990) was used. Briefly, rat thoracic aorta were exposed to Krebs solution containing 10 μCi ml^{-1} of [^{3}H]-myo-inositol for 3 h and gassed with 95% O_2-5% CO_2 mixture. The tissues were then transferred to tubes containing fresh Krebs solution with DMSO (0.1%), (−)-discretamine or prazosin for 15 min, and saline or noradrenaline (3 μM) was added and the tubes incubated for another 15 min. LiCl (10 mM) was added 5 min before noradrenaline to inhibit metabolism of inositol monophosphate (Berridge *et al.*, 1982). Aortae were then frozen in liquid nitrogen and homogenized in 1.3 ml of 10% trichloroacetic acid. After centrifugation, 1 ml of supernatant was collected and trichloroacetic acid was removed by washing with 4 × 3 vol of ether. The inositol monophosphate in the aqueous phase was analysed by application of the sample to a column of 1 ml Dowex-1 ion-exchange resin according to the method of Neylon & Summers (1987). The pellets of the tissues were resuspended in 1.0 N NaOH and assayed for protein according to the method of Lowry *et al.* (1951).

Guinea-pig tracheal contraction

Tracheae from guinea-pigs were dissected out, transferred to a dish containing Krebs solution and cut transversely between the segments of cartilage. Several of these, usually about 5, were tied together so as to form a chain, which was then mounted in Krebs solution at 37°C, gassed with 95% O_2-5% CO_2. One end of the chain was attached to a fixed pin in the bath and the other to a force-displacement transducer connected to a Grass polygraph. Resting tension on each tissue was set at 1 g. Tracheae were allowed to equilibrate for at least 1 h and washed periodically. Cumulative concentration-response curves were obtained by application of various concentrations of spasmogens for 15–18 min at 3 min intervals. Responses were found to be reproducible with this procedure. Tracheal rings were preincubated with DMSO (0.1%) or (−)-discretamine for 15 min, then various concentrations of spasmogens were added at 3 min intervals. Results are expressed as percentage of the maximal control response for each agonist.

Rat right and left atria

Right and left atria strips (4 × 6 mm) were quickly dissected from the hearts of male WKY rats (weighing 250–300 g) and placed in an organ bath containing 10 ml Tyrode solution gassed with 95% O_2-5% CO_2 kept at 36.0 ± 0.2°C. The composition of Tyrode solution was (mM): NaCl 137, KCl 5.4, $MgCl_2$ 1.1, $NaHCO_3$ 11.9, NaH_2PO_4 0.33, dextrose 11 and $CaCl_2$ 2. Contractions of spontaneously beating right atria and electrically driven left atria strips were measured by connecting one end of the preparation using a fine silk thread to a force displacement transducer (Type BG 25, Gould) and tension was recorded on a Gould 2200S recorder. A preload of 500 mg was used. The left atria strips were stimulated at a frequency of 2 Hz by rectangular pulses of 1 ms duration at supramaximal intensity via an isolated Grass SD9 stimulator.

Single myocyte isolation

Single myocytes were isolated from adult rats by enzymatic dissociation as described by Mitra & Morad (1985). Briefly, the heart was rapidly excised from pentobarbitone anaesthetized rats. The aorta was cannulated and retrogradly perfused with Ca^{2+}-free Tyrode solution containing (mM): NaCl 137, KCl 5.4, $MgCl_2$ 1.1, dextrose 11, and HEPES-NaOH buffer (pH 7.4) 10. The perfusate was oxygenated and maintained at 37 ± 0.2°C. After 5 min, the perfusate was changed to the same solution containing 1 mg ml^{-1} collagenase (Type I) and 0.3 mg ml^{-1} protease (Type XIV). After 20–30 min digestion, the residual enzyme-containing solution was cleaned by 5 min perfusion with 0.2 mM Ca^{2+} Tyrode solution. Thereafter, the left and right ventricules were separated from atria, dispersed and stored in 0.2 mM Ca^{2+} Tyrode solution for later use. Only rod-like relaxed ventricular myocytes showing clear striations were used for the experiments.

Whole-cell recording of rat single myocytes

Transmembrane currents were recorded by use of the single-pipette whole-cell patch clamp technique (Hamill *et al.*, 1981). Rat ventricular cells were transferred to a chamber mounted on an inverted microscope (Nikon Diaphot, Nikon Co., Tokyo, Japan) for electrophysiological recording and were bathed in Tyrode solution containing (mM): NaCl 137, KCl 5.4, $CaCl_2$ 2, $MgCl_2$ 1.1, dextrose 11 and HEPES-NaOH buffer (pH 7.0) 10. All experiments were performed at room temperature (23–25°C). Electrode junction potentials (5 to 10 mV) were measured and nulled before impalement of the cell. The formation of a high resistance seal was monitored by applying 1 nA current from a digital pulse generator. A high resistance seal (5 to 10 gigaohm) was obtained before disruption of the membrane patch. The cells were dialyzed with the electrode solution for 3 to 5 min to reach equilibrium state after disruption of the membrane patch. In voltage clamp experiments series resistance compensation was used to offset the series resistance due to the pipette tip resistance. During measurement of potassium outward currents, the

contamination of calcium inward current (I_{Ca}) was prevented by adding 1 mM Co^{2+} to the bathing medium. Under this condition, 800 ms depolarization of membrane potential to a level positive to −40 mV usually results in a generation of fast sodium inward current (I_{Na}) followed by a transient and steady-state outward potassium current. In order to eliminate the contamination of inward current completely, 30 μM tetrodotoxin (TTX) was added to inhibit the I_{Na}. The magnitude of transient and steady-state outward current was measured at 10 ms after the start and the end of the 800 ms depolarizing pulses, respectively.

During measurement of I_{Na} and I_{Ca}, the potassium currents were prevented by adding 2–4 mM Cs^+ to the bathing medium and internal dialysis of the cells with Cs^+-containing internal solution of the following composition (mM): CsCl 130, EGTA 5, tetraethylammonium (TEA) chloride 15, cyclic AMP 0.03, dextrose 5, HEPES-CsOH buffer (pH 7.4) 10. Under such circumstances inward and outward K^+ currents were almost abolished within 4 to 6 min (Iijima *et al.*, 1985). In cells bathed in normal Tyrode solution, I_{Na} elicited by depolarization to −40 mV was larger than 20 nA. In this condition, the spatial and voltage control of membrane potential was not satisfactory. To improve the clamp efficiency, the I_{Na} was reduced by bathing the cells in low Na^+ Tyrode solution (122 mM NaCl was substituted with choline chloride) and internal dialysis of the cell with Na^+ containing (5 mM) Cs^+ pipette solution. In measurement of I_{Ca}, the I_{Na} was inactivated by the first step depolarizing of membrane potential to −40 mV, the I_{Ca} could then be activated by the second step depolarization to levels positive to −20 mV.

Data analysis

In each experiment, agonist dose-response curves in the presence of (−)-discretamine were related to the control dose-response curve, of which the maximum response was taken as 100%. In most experiments, three to four concentrations of (−)-discretamine were tested and the slopes of the resulting Schild plots were used to assess competitive antagonism. The pA_2 values were calculated for each concentration of (−)-discretamine according to: $pA_2 = -\log$ ([antagonist]/dose-ratio − 1]) (Mackay, 1978).

The experimental results are expressed as the mean ± s.e.mean and accompanied by the number of observations. Statistical significance was assessed by Student's *t* test and *P* values less than 0.05 were considered significant.

Drugs

(−)-Discretamine (Figure 1) was isolated from the plant *Fissistigma glaucescens* as previously described (Lu *et al.*, 1985). The following drugs were used: noradrenaline HCl, isoprenaline HCl, yohimbine HCl, prazosin HCl, phentolamine HCl, phenoxybenzamine HCl, clonidine HCl, U-46619 (9,11-dideoxy-9α, 11α,-methanoepoxy prostaglandin $F_{2\alpha}$), angiotensin II acetate, endothelin, carbachol, acetylcholine HCl, myo-inositol, histamine dihydrochloride, 5-hydroxytryptamine creatinine sulphate (5-HT), collagenase (Type I), protease (Type XIV), trichloroacetic acid and Dowex-1 resin (100-200 mesh: × 8, chloride) were obtained

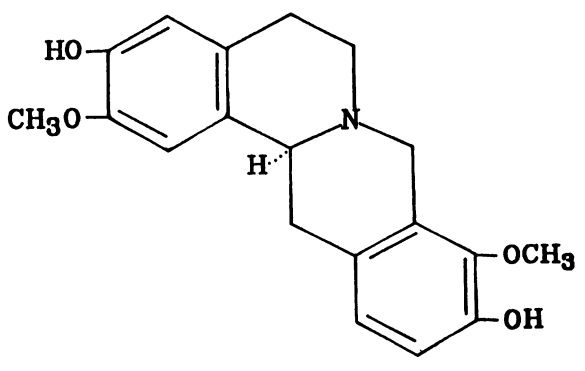

Figure 1 Chemical structure of (−)-discretamine.

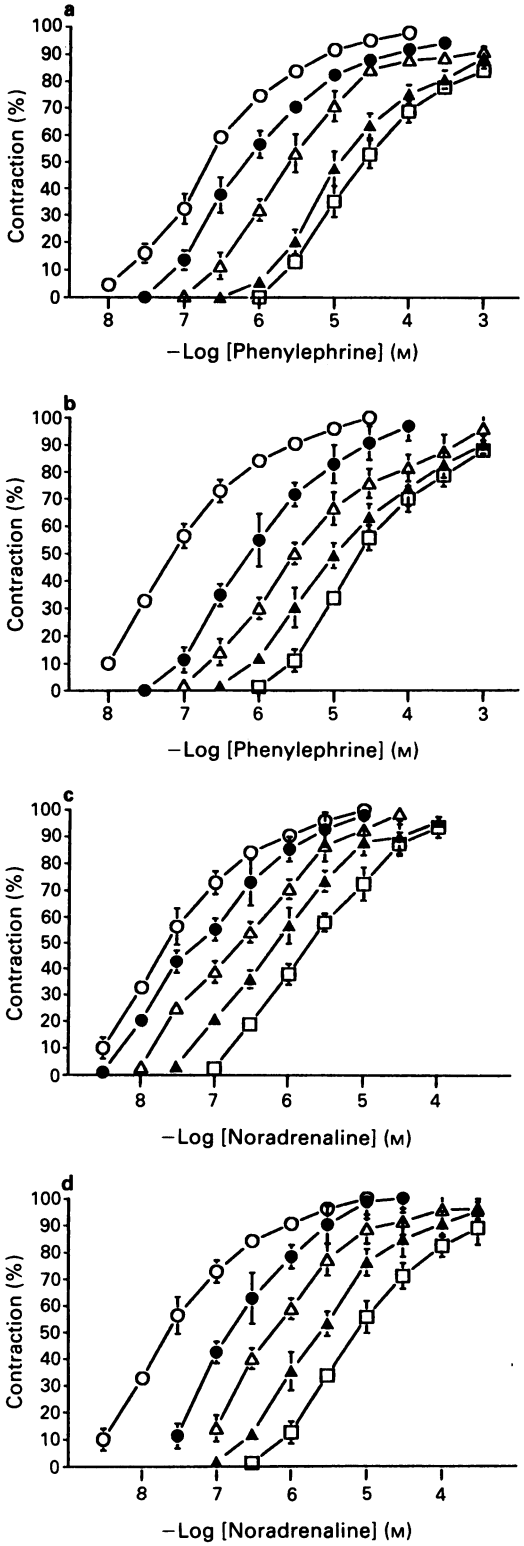

Figure 2 Cumulative concentration-response curves to phenylephrine and noradrenaline in rat thoracic aorta with intact (a and c) or without (b and d) endothelium. Dimethylsulphoxide (0.1%, control) (○) or (−)-discretamine, 0.1 μM (●), 0.3 μM (△), 1.0 μM (▲) and 3 μM (□) were preincubated with aorta for 15 min. Each point represents the mean and vertical bars show s.e.mean ($n = 6$–8).

from Sigma Chemical Co.; phenylephrine HCl was from Denmarks Apotekerforening; leukotriene C_4 and prostaglandin $F_{2\alpha}$ ($PGF_{2\alpha}$) were from Biomol Research Lab.; cyclic AMP and cyclic GMP RIA kits and myo-[2-^{3}H]inositol was purchased from Amersham. (−)-Discretamine was dissolved in DMSO and the final concentration of DMSO in the bathing solution did not exceed 0.1% and had no effect on the muscle contraction.

Results

α-Adrenoceptor antagonism in rat aorta

α-Adrenoceptor antagonistic properties of (−)-discretamine were evaluated against concentration-response curves to phenylephrine and noradrenaline in rat thoracic aorta. (−)-Discretamine (0.1–3 μM) produced a parallel, rightward shift of the curve consistent with competitive blockade (Figure 2a and c). The pA_2 values of (−)-discretamine against phenylephrine and noradrenaline were 7.60 ± 0.09 (slope range 0.83–1.17) and 7.20 ± 0.10 (slope range 0.92–1.21), respectively. This concentration-related shift by (−)-discretamine was significantly pronounced in rat thoracic aorta in which the endothelium had been removed (Figure 2b and d). The pA_2 values of (−)-discretamine against phenylephrine and noradrenaline in rat aortae denuded of endothelium were 7.90 ± 0.09 (slope range 0.78–1.23) and 7.52 ± 0.09 (slope range 0.85–1.18), respectively. Concentration-response curve analysis of phenylephrine-induced contraction of intact rat aortae were performed for the α_1-adrenoceptor antagonism by (−)-discretamine in comparison with phentolamine and yohimbine. (−)-Discretamine was equi-potent to phentolamine (pA_2 = 7.51 ± 0.10) but was more potent than yohimbine (pA_2 = 6.18 ± 0.06). In all cases the Schild slopes were not significantly different from 1.0.

(−)-Discretamine protected α-adrenoceptors from alkylation by the irreversible blocking agents, phenoxybenzamine (Figure 3). Phenoxybenzamine alone (50 nM) produced an insurmountable blockade, shown as a non-parallel, rightward shift of the concentration-response curve with a depressed maximum response. Prior addition of (−)-discretamine (30 μM) prevented this insurmountable blockade.

To see if signal transduction after α_1-adrenoceptor activation was blocked by (−)-discretamine, rat thoracic aortae were labelled with [^{3}H]-myo-inositol. The accumulation of [^{3}H]-inositol monophosphate in rat aortae was increased in the presence of noradrenaline (3 μM). This increase was significantly suppressed by prazosin (3 μM) or (−)-discretamine (10 or 30 μM) (Table 1).

(−)-Discretamine also produced a concentration-related shift in the concentration-response curves for clonidine and 5-HT in rat aorta denuded of endothelium (Figure 4). An unconstrained Schild plot was derived from shifts in concentration-response curves in individual tissues. The pA_2 against α_2-adrenoceptor and 5-HT receptor were 6.30 ± 0.15 and 6.87 ± 0.06 and the slopes of the Schild plots were 1.35 (range 1.04–1.66) and 0.61 (range 0.49–0.73), respectively.

A high concentration of (−)-discretamine (30 μM) did not block the increase in tension produced by Ca^{2+} (60 mM K^+

Table 1 Effects of prazosin and (−)-discretamine on the accumulation of [^{3}H]-inositol monophosphate in rat thoracic aortae by noradrenaline

Treatment	*[^{3}H]-inositol monophosphate* (c.p.m. mg^{-1} protein)
Resting	1568 ± 109
Noradrenaline (3 μM)	3187 ± 214
Prazosin (3 μM)	1692 ± 175*
(−)-Discretamine (10 μM)	2112 ± 126*
(30 μM)	1664 ± 115*

Rat aortic segments were preincubated with dimethylsulphoxide (0.1%, for resting and control), prazosin (3 μM) or (−)-discretamine for 15 min, then saline (for resting) or noradrenaline (3 μM) was added for another 15 min. Data are presented as total [^{3}H]-inositol monophosphate accumulated (c.p.m. mg^{-1} protein) and expressed as means ± s.e.mean (n = 4). *P < 0.001 as compared with the control value.

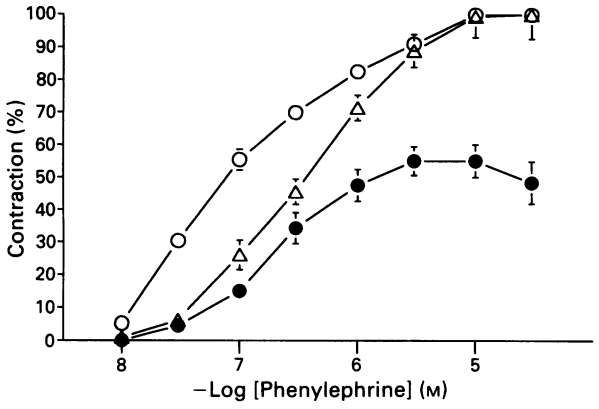

Figure 3 Protection by (−)-discretamine against irreversible, non-competitive inhibition by phenoxybenzamine in rat thoracic aorta. (○) Phenylephrine control curve (n = 8). Aortae were subsequently exposed to either dimethylsulphoxide (0.1%, 15 min) and phenoxybenzamine (50 nM, 10 min) (●, n = 4) or (−)-discretamine (30 μM, 15 min) and phenoxybenzamine (50 nM, 10 min) (△, n = 4) before thorough washing and subsequent generation of the concentration-response curves. Each point represents the mean and vertical bars show s.e.mean.

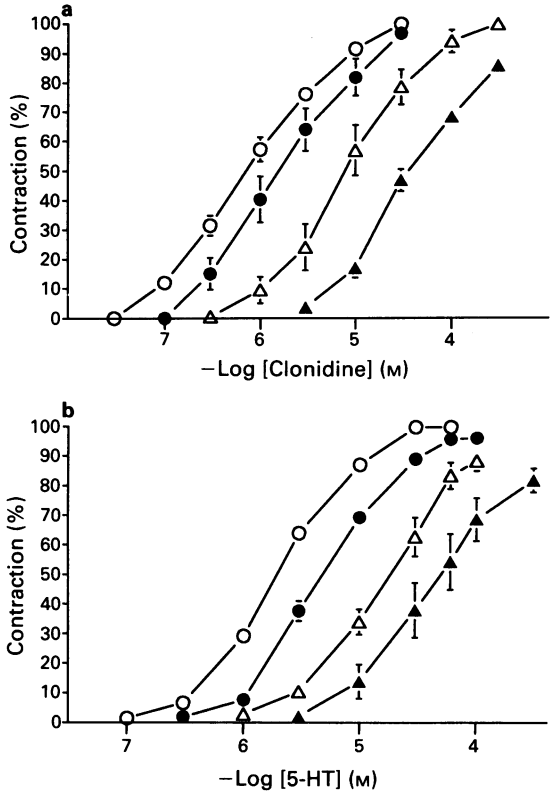

Figure 4 Cumulative concentration-response curves to clonidine (a) and 5-hydroxytryptamine (5-HT) (b) in denuded rat thoracic aorta. Dimethylsulphoxide (0.1%, control) (○) and (−)-discretamine were preincubated with aorta for 15 min. (a) (−)-discretamine, 1.0 μM (●), 3.0 μM (△) and 10 μM (▲); (b) (−)-discretamine, 0.3 μM (●), 3.0 μM (△) and 30 μM (▲). Each point represents the mean and vertical bars show s.e.mean (n = 6–7).

depolarization), angiotensin II, U-46619 and $PGF_{2\alpha}$ in rat aorta denuded of endothelium (Table 2). The slowly developed tension caused by endothelium (3 nM, 1.13 ± 0.08 g after 20 min challenge, $n = 6$) was also not inhibited by a high concentration of (−)-discretamine (1.12 ± 0.06 g, $n = 6$).

Effects of (−)-discretamine on the cyclic GMP and cyclic AMP formation in rat aorta

The cyclic nucleotide content of the aorta was measured by radioimmunoassay. As shown in Table 3, sodium nitroprusside and forskolin markedly elevated cyclic GMP and cyclic AMP levels in rat aorta, respectively. (−)-Discretamine (30 μM) did not exert any effect on the contents of these cyclic nucleotides.

Antagonism against histamine, leukotriene C_4, carbachol and isoprenaline in guinea-pig trachea

In guinea-pig trachea, histamine, leukotriene C_4 and carbachol caused contraction of tracheal smooth muscle. (−)-Discretamine (30 μM) did not depress all these concentration-response curves. (−)-Discretamine (30 μM) also had no effect on the isoprenaline-induced relaxation of guinea-pig trachea precontracted by carbachol (1 μM) (Table 2).

β_1-Adrenoceptor blockade in rat right and left atria

(−)-Discretamine (30 μM) did not affect the sinus nodal rate and contractility in isolated right and left atria from the rat. It also did not affect the inotropic and chronotropic concentration-response curve for isoprenaline in rat right and left atria (Table 2 for right atria).

Effects of (−)-discretamine on Na^+ (I_{Na}), Ca^{2+} (I_{Ca}) and K^+ current

The I_{Na} and I_{Ca} were examined with a whole cell voltage clamp technique. The cells were depolarized from a holding potential of −80 mV to −40 mV for 10 ms to inactivate the I_{Na} (Weidmann, 1955; Lee *et al.*, 1981), and then to 0 mV for 30 ms to evoke the I_{Ca}. (−)-Discretamine (30 μM) did not affect either I_{Na} or I_{Ca} current (data not shown). The effect of

Table 2 Activity of (−)-discretamine at receptors other than α-adrenoceptors and 5-HT receptors

Tissue (response)	*Competing drug*	*Concentration-ratio*	n
Rat aorta (contraction)	U-46619	1.55 ± 0.12	7
	$PGF_{2\alpha}$	1.15 ± 0.06	7
	Angiotensin II	1.07 ± 0.06	7
	Calcium	1.00 ± 0.04	7
Guinea-pig trachea (contraction)	Histamine	1.20 ± 0.10	5
	Carbachol	1.59 ± 0.21	5
	Leukotriene C_4	1.15 ± 0.13	6
Guinea-pig trachea (relaxation)	Isoprenaline	0.78 ± 0.10	5
Rat right atria (rate)	Isoprenaline	0.95 ± 0.11	6
(force of contraction)	Isoprenaline	1.04 ± 0.08	6

Concentration-ratio was calculated from EC_{50} values in the presence or absence of (−)-discretamine (30 μM) and presented as means ± s.e.mean. n = number of estimates.

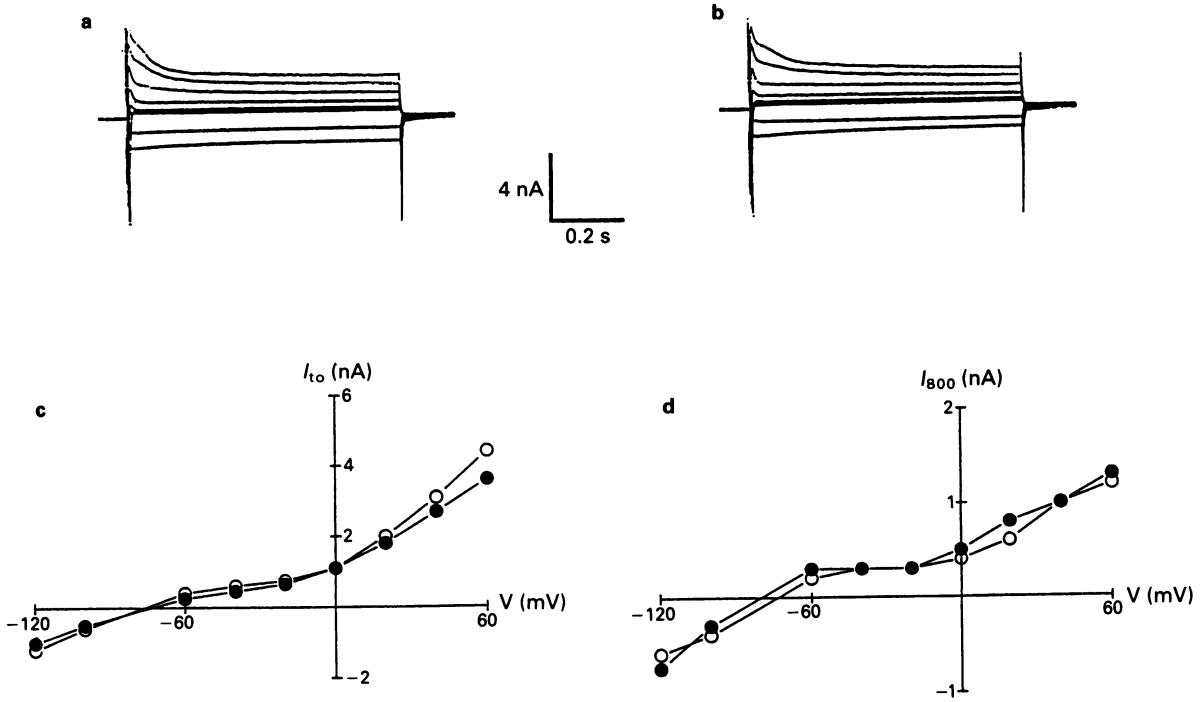

Figure 5 Voltage-dependence of transient (I_{to}) and steady state (I_{800}) currents in the absence (○) and presence (●) of (−)-discretamine. (a) and (b) Typical current traces induced by 800 ms depolarization or hyperpolarization pulses in 20 mV increments between −120 and +60 mV from a holding potential of −80 mV. Horizontal line indicates zero-current level. Tetrodotoxin 30 μM and Co^{2+} 1 mM were added to the external solution to block I_{Na} and I_{Ca}, respectively. (c) and (d) I-V curves of I_{to} and I_{800}.

Table 3 Effects of (−)-discretamine on the cyclic GMP and cyclic AMP formation of rat thoracic aorta

	Cyclic GMP	*Cyclic AMP*
	(pmol mg^{-1} protein)	
Control	2.10 ± 0.10	2.85 ± 0.21
Sodium nitroprusside (1 μM)	5.60 ± 0.60*	–
Forskolin (1 μM)	–	5.37 ± 0.19*
(−)-Discretamine (30 μM)	2.26 ± 0.41	3.06 ± 0.31

After preincubation of aortic rings in Krebs solution for 5 min, dimethylsulphoxide (0.1%, control), sodium nitroprusside, forskolin or discretamine was added for another 2 min and the reaction was stopped by immersing the tissue into liquid nitrogen. Cyclic GMP and cyclic AMP content in rat aortae were measured. Results are expressed as the means ± s.e.mean ($n = 4$). *$P < 0.001$ as compared with the respective control.

(−)-discretamine (30 μM) on the K^+ outward currents were examined in the absence of the inward Na^+ and Ca^{2+} currents which were abolished by TTX (30 μM) and Co^{2+} (1 mM), respectively. As shown in Figure 5, both the current-voltage relationships of transient outward (I_{to}) and steady state outward (I_{800}) currents were not affected by (−)-discretamine.

Discussion

The present studies have demonstrated that (−)-discretamine, a tetrahydroprotoberberine alkaloid isolated from *Fissistigma glaucescens*, inhibited the contractile responses of rat aorta to the adrenoceptor agonists, noradrenaline, phenylephrine and clonidine. It also protected α-adrenoceptors against irreversible blockade by phenoxybenzamine, and inhibited [^{3}H]-inositol monophosphate formation caused by noradrenaline. It acts as a selective α-adrenoceptor antagonist without affecting the contraction of rat aorta caused by high-potassium depolarization, the thromboxane receptor agonist (U-46619), $PGF_{2\alpha}$, angiotensin II or endothelin. In addition, it also had no apparent effects on the leukotriene C_4 receptor, β_2-adrenoceptor and histamine and muscarinic receptors in guinea-pig trachea. β_1-Adrenoceptors of rat right and left atria and sodium, potassium and calcium channels of rat ventricular single myocytes were not affected by (−)-discretamine. All these data indicate that (−)-discretamine is a selective α-adrenoceptor blocking drug.

(−)-Discretamine also possessed 5-HT receptor blocking activity in a non-competitive manner, since the Schild plot slope was far from 1 (range 0.49–0.73). Its potency for blocking 5-HT receptors is about 10 times less than its potency for blocking α_1-adrenoceptors. The activity profile of (−)-discretamine resembles that of the structurally dissimilar agent ketanserin in possessing both α-adrenoceptor and 5-HT receptor blocking properties (Van Nueten *et al.*, 1981; Kalkman *et al.*, 1982). Quantitatively these agents differ in that (−)-discretamine is more selective for α_1-adrenoceptors while ketanserin shows about a 10 fold selectivity for 5-HT receptors. Furthermore, (−)-discretamine has a non-competitive while ketanserin has a competitive blocking action at 5-HT receptors (Van Nueten *et al.*, 1981). It has been shown that there is a high degree of cross reactivity between compounds interacting at α-adrenoceptors and 5-HT receptors (Apperley *et al.*, 1976; Black *et al.*, 1981; Purdy *et al.*, 1987). Zifa & Fillion (1992) demonstrated that the α_1-adrenoceptor in the rat has a 70% homology with the 5-HT_2 receptor. The efficiency of (−)-discretamine at 5-HT receptors can be explained by the close homology of these two receptors.

Cyclic nucleotides are very important for relaxing vascular smooth muscles (Murad, 1986). Forskolin and sodium nitroprusside have been shown to be potent relaxing agents in vascular smooth muscles. Forskolin increases cyclic AMP levels via activation of adenylate cyclase (Ousterhout & Sperelakis, 1987); sodium nitroprusside produces prompt, dose-dependent increases in the cyclic GMP level by directly activating guanylate cyclase (Gruetter *et al.*, 1979). Neither the cyclic AMP nor the cyclic GMP content was changed by (−)-discretamine (Table 3). This indicates that α-adrenoceptor and 5-HT receptor antagonistic effects of (−)-discretamine are not mediated by increase of cellular cyclic nucleotide concentrations.

The vascular endothelium plays an important role in controlling vascular tone via the secretion of both relaxant and contractile factors (Jaffe, 1985; Vanhoutte *et al.*, 1986). Endothelial cells respond to a variety of neurochemical and physical stimuli to release endothelium-derived relaxing factor (EDRF) and prostacyclin (PGI_2). Endothelium modulates the vasoconstrictor responses to many agonists, and EDRF is mainly responsible for these effects (Egleme *et al.*, 1984; Palmer *et al.*, 1987). The α-adrenoceptor antagonistic action of (−)-discretamine persisted in aorta denuded of endothelium. Thus, the α-adrenoceptor antagonism by (−)-discretamine was independent of the endothelium and was not mediated by either EDRF or PGI_2. Analysis of the concentration-response curves of (−)-discretamine revealed that competitive antagonism against noradrenaline and phenylephrine occurred in aorta in the presence or absence of endothelium. It has been reported that vascular endothelium modifies the mode of antagonism by prazosin and doxazosin but not those by phentolamine and yohimbine of the noradrenaline and phenylephrine concentration-response curves (Alosachie & Godfraind, 1986). Prazosin and doxazosin act as non-competitive antagonists against noradrenaline and phenylephrine in the presence of endothelium and as competitive antagonists after removal of endothelium. Thus, vascular endothelium modifies the mode of antagonism of prazosin and doxazosin but not those of (−)-discretamine, phentolamine and yohimbine. However, removal of endothelium did significantly increase the antagonistic potency of (−)-discretamine on noradrenaline- or phenylephrine-induced vasoconstriction.

In conclusion, (−)-discretamine is a novel vascular α-adrenoceptor and 5-HT receptor antagonist with rank order of $\alpha_1 > 5\text{-HT} > \alpha_2$. Its structural novelty may provide an original chemical basis for the development of new α-adrenoceptor blockers.

This work was supported by Research Grant from the National Science Council of the Republic of China (NSC81-0412-B002-543).

References

ALOSACHIE, I. & GODFRAIND, T. (1986). Role of cyclic GMP in the modulation by endothelium of the adrenolytic action of prazosin in the rat isolated aorta. *Br. J. Pharmacol.*, **89**, 525–532.

APPERLEY, E., HUMPHREY, P.P.A. & LEVY, G.P. (1976). Receptors for 5-hydroxytryptamine and noradrenaline in rabbit isolated ear artery and aorta. *Br. J. Pharmacol.*, **58**, 211–221.

BERRIDGE, M.J., DOWNES, C.P. & HANLEY, M.R. (1982). Lithium amplifies agonist-dependent phosphoinositol response in brain and salivary glands. *Biochem. J.*, **206**, 587–595.

BLACK, J.L., FRENCH, R.J. & MYLECHARANE, E.J. (1981). Receptor mechanisms for 5-hydroxytryptamine in rabbit arteries. *Br. J. Pharmacol.*, **74**, 619–626.

CAVERO, I. & ROACH, A.G. (1980). The pharmacology of prazosin, a novel antihypertensive agent. *Life Sci.*, **27**, 1525–1540.

EGLEME, C., GODFRAIND, T. & MILLER, R.C. (1984). Enhanced responsiveness of rat isolated aorta to clonidine after removal of endothelial cells. *Br. J. Pharmacol.*, **81**, 16–18.

GRUETTER, C.A., BARRY, B.K., MCNAMARA, D.B., GRUETTER, D.Y., KADOWITZ, P.J. & IGNARRO, L.J. (1979). Relaxation of bovine coronary artery and activation of coronary arterial guanylate cyclase by nitric oxide, nitroprusside and a carcinogenic nitrosamine. *J. Cycl. Nucleotide Res.*, **5**, 211–224.

HAMILL, O.P., MARTY, A., NEHER, E., SAKMANN, B. & SIGWORTH, F.J. (1981). Improved patch-clamp techniques for high resolution current recording from cells and cell-free membrane patches. *Pflügers Arch.*, **391**, 85–100.

HIRATA, M., KOHSE, K.P., CHANG, C.H., IKEBE, T. & MURAD, F. (1990). Mechanism of cyclic GMP inhibition of inositol phosphate formation in rat aorta segments and cultured bovine aortic smooth muscle cells. *J. Biol. Chem.*, **265**, 1268–1273.

IIJIMA, T., IRISAWA, H. & KAMEYAMA, M. (1985). Membrane currents and their modification by acetylcholine in isolated single atrial cells of the guinea-pig. *J. Physiol.*, **359**, 485–501.

ITOH, T., IZUMI, H. & KURIYAMA, H. (1982). Mechanisms of relaxation induced by activation of β-adrenoceptors in muscle cells of guinea-pig mesenteric artery. *J. Physiol.*, **326**, 475–493.

JAFFE, E.A. (1985). Physiological functions of normal endothelial cells. *Ann. N.Y. Acad. Sci.*, **454**, 279–291.

KALKMAN, H.O., TIMMERMANS, P.B.M.W.M. & VAN ZWIETEN, P.A. (1982). Characterization of the antihypertensive properties of ketanserin (R41 468) in rats. *J. Pharmacol. Exp. Ther.*, **222**, 227–231.

KAUFFMAN, R.F., SCHENCK, K.W., UTTERBACK, B.G., CROWE, V.G. & COHEN, M.L. (1987). In vitro vascular relaxation by new inotropic agents: relationship to phosphodiesterase inhibition and cyclic nucleotides. *J. Pharmacol. Exp. Ther.*, **242**, 864–871.

LEE, K.S., HUME, J.R., GILES, W. & BROWN, A.M. (1981). Sodium current depression by lidocaine and quinidine in isolated ventricular cells. *Nature*, **291**, 325–327.

LOWRY, D.H., ROSEBROUGH, N.J., FARR, A.L. & RANDALL, R.J. (1951). Protein measurement with the Folin phenol reagent. *J. Biol. Chem.*, **193**, 265–275.

LU, S.T., WU, Y.C. & LEOU, S.P. (1985). Alkaloids of Formosan Fissistigma and Goniothalamus species. *Phytochemistry*, **24**, 1829–1834.

MACKAY, D. (1978). How should values of pA_2 and affinity constants for pharmacological competitive antagonists be estimated? *J. Pharm. Pharmacol.*, **30**, 312–313.

MINNEMAN, K.P. (1988). α_1-Adrenergic receptor subtypes, inositol phosphates, and sources of cell Ca^{2+}. *Pharmacol. Rev.*, **40**, 87–119.

MITRA, R. & MORAD, M. (1985). A uniform enzymatic method for the dissociation of myocytes from heart and stomach of vertebrates. *Am. J. Physiol.*, **249**, H1056–H1060.

MURAD, F. (1986). Cyclic guanosine monophosphate as a mediator of vasodilation. *J. Clin. Invest.*, **78**, 1–5.

NEYLON, C.B. & SUMMERS, R.J. (1987). Stimulation of α_1-adrenoceptors in rat kidney mediates increased inositol phospholipid hydrolysis. *Br. J. Pharmacol.*, **91**, 367–376.

OUSTERHOUT, J.M. & SPERELAKIS, N. (1987). Cyclic nucleotides depress action potentials in cultured aortic smooth muscle cells. *Eur. J. Pharmacol.*, **144**, 7–14.

PALMER, R.J.M., FERRIGE, A.G. & MONCADA, S. (1987). Nitric oxide release accounts for the biological activity of endothelium derived relaxing factor. *Nature*, **327**, 524–526.

PURDY, R.E., MURRAY, D.L. & STUPECKY, G.L. (1987). Receptors for 5-hydroxytryptamine in rabbit blood vessels: activation of alpha adrenoceptors in rabbit thoracic aorta. *J. Pharmacol. Exp. Ther.*, **240**, 535–541.

STANASZEK, W.F., KELLERMAN, D. & BROGDEN, R.N. (1983). Prazosin update. A review of its pharmacological properties and therapeutic use in hypertension and congestive heart failure. *Drugs*, **25**, 339–384.

TITMARSCH, S. & MONK, J.P. (1987). Terazosin. A review of its pharmacodynamic and pharmacokinetic properties, and therapeutic efficacy in essential hypertension. *Drugs*, **33**, 461–477.

VANHOUTTE, P.M., RUBANY, G.M., MILLER, V.M. & HOUSTON, D.S. (1986). Modulation of vascular smooth muscle contraction by endothelium. *Annu. Rev. Physiol.*, **48**, 307–320.

VAN NUETEN, T.M., JANSSEN, P.A.J., VAN BEEK, J., XHONNEUX, R., VERBEUREN, T.J. & VANHOUTTE, P.M. (1981). Vascular effects of ketanserin (R41 468), a novel antagonist of 5-HT_2 serotonergic receptors. *J. Pharmacol. Exp. Ther.*, **218**, 217–230.

WEIDMAN, S. (1955). Effects of calcium ions and local anesthetics on electrical properties of purkinje fibers. *J. Physiol.*, **129**, 568–582.

ZIFA, E. & FILLION, G. (1992). 5-Hydroxytryptamine receptors. *Pharmacol. Rev.*, **44**, 401–458.

(Received April 2, 1993
Revised June 2, 1993
Accepted June 8, 1993)

Br. J. Pharmacol. (1993), **110**, 889–895

Necessity of divalent cations for recovery from carbachol-induced nicotinic acetylcholine receptor inactivation at snake twitch fibre endplates

[1]Jean C. Hardwick & Rodney L. Parsons

Department of Anatomy and Neurobiology, College of Medicine, University of Vermont, Burlington, Vt 05405, U.S.A.

1 Previous studies demonstrated that elevation of the extracellular calcium concentration during a prolonged exposure to a high concentration of carbachol reverses the staurosporine-induced decrease in the extent of endplate resensitization in voltage-clamped snake twitch fibres. The present studies were designed to establish the site, specificity and potential mechanisms by which calcium could reverse the effects of staurosporine on acetylcholine receptor recovery.

2 Pretreatment of potassium-depolarized muscle preparations with 0.5 μM staurosporine, followed by a 10 min incubation with 540 μM carbachol, produced a significant decrease in the recovery of miniature endplate current (m.e.p.c.) amplitudes. Raising the extracellular calcium concentration from 1 mM to 10 mM during the agonist application reversed this inhibition. In addition, a brief (3 min) incubation in an elevated calcium (10 mM) solution in staurosporine-treated preparations previously exposed to 540 μM carbachol also reversed the reduction in m.e.p.c. amplitude.

3 Substitution of calcium with 10 mM strontium had no effect on the staurosporine-induced decrease in m.e.p.c. amplitude, whereas 10 mM magnesium partially substituted for calcium. Inclusion of (+)-tubocurarine (13 μM) in the 10 mM calcium solution to prevent the influx of calcium through agonist-activated channels did not prevent the reversal of the staurosporine-induced decrease in m.e.p.c. amplitudes. This suggested that the site of action of calcium on endplate resensitization was extracellular.

4 Analysis of acetylcholine (ACh)-induced single channel currents demonstrated that a population of small conductance channels seen only in the staurosporine-treated preparations following carbachol exposure, was still present in staurosporine-treated preparations incubated in 540 μM carbachol solution containing 10 mM calcium. Thus the effect of calcium on ACh receptor recovery was not due to the conversion of the small conductance channels to the normal, large conductance channels.

5 Removal of calcium from the extracellular solution with the magnesium concentration unchanged, resulted in no change in the extent of m.e.p.c. amplitude recovery, nor did it alter the ability of staurosporine to inhibit recovery. Removal of both calcium and magnesium resulted in a significant decrease in the extent of recovery and staurosporine produced no additional decrease. This decrease in m.e.p.c. recovery in the divalent cation-free solution was not associated with a change in mean channel conductance as determined by noise analysis.

6 Based on the results from these experiments, we suggest that, with prolonged exposure to agonist, some ACh receptors at the endplate become irreversibly inactivated. For full recovery of endplate sensitivity to occur, inactivated ACh receptors must be replaced. Part of the replacement ACh receptors appear to be recruited from a readily available but not previously activated pool and this process is dependent on extracellular calcium and/or magnesium. Thus, elevation of extracellular calcium may be able to reverse the apparent decrease in endplate sensitivity in staurosporine-treated fibres following carbachol exposure by increasing the number of functional receptors at the endplate.

Keywords: Acetylcholine receptors; staurosporine; protein phosphorylation; miniature endplate currents; single channel recordings

Introduction

Previously, we demonstrated that the broad acting protein kinase inhibitor, staurosporine, decreased the extent of acetylcholine receptor (ACh receptor) recovery from carbachol-induced desensitization (Hardwick *et al.*, 1991). This decrease in sensitivity was seen as a decrease in both the amplitude of carbachol-induced currents and averaged miniature endplate currents (m.e.p.cs). We suggested that the staurosporine-induced decrease in recovery resulted from an inhibition of phosphorylation of the ACh receptor or a closely related protein which was required for resensitization to occur. More recently, we showed that following recovery from a prolonged carbachol exposure, a population of small conductance ACh-activated channels is present only in staurosporine-treated preparations (Hardwick & Parsons, 1993). We postulated that, in staurosporine-pretreated preparations, the reduced amplitude of m.e.p.cs following prolonged carbachol application was the result of the activation by ACh of a mixture of small and large conductance channels. In our initial study, we also found that elevation of the extracellular calcium concentration during the exposure to carbachol antagonized the decrease in recovery produced by staurosporine (Hardwick *et al.*, 1991). The present study was done to examine the effect of calcium on the staurosporine-induced decrease in recovery in more detail. Experiments were designed to establish the site and specificity of the action of calcium as well as the mechanism by which calcium reversed the staurosporine-induced decrease in ACh receptor recovery.

[1] Author for correspondence.

Methods

General methods

All experiments were done at room temperature on potassium-depolarized twitch fibre endplates of costocutaneous muscles isolated from garter snakes (*Thamnophis*) following procedures described previously (Hardwick *et al.*, 1991; Hardwick & Parsons, 1993). Snakes were killed by rapid decapitation and the muscles, with portions of the rib and skin, were pinned out on Sylgard-coated petri dishes in a physiological solution containing in mM: NaCl 159, KCl 2.5, $MgCl_2$ 4.2, $CaCl_2$ 1.0, HEPES 1.0, pH 7.3 (Dionne & Parsons, 1981). Experiments were done after muscle preparations had been bathed for 20–30 min in an isotonic potassium propionate (KP) solution. In a number of experiments, the divalent cation concentration was altered during the course of the experiment as summarized in Table 1.

Carbachol (540 μM, Sigma Chemical Co., St. Louis, MO, U.S.A.) and staurosporine (0.5 μM in 0.05% dimethylsulphoxide, Calbiochem, San Diego, CA, U.S.A.) were added directly to the solution bathing the muscle preparations. In the case of staurosporine, the preparations were exposed for 10–15 min to the drug and then washed several times with drug-free solution before starting the experiments. Our previous studies had demonstrated that staurosporine alone had no effect on either the activation or the gating kinetics of the m.e.p.cs (Hardwick *et al.*, 1991). The concentration of 0.5 μM staurosporine was chosen based on results from our previous studies (Hardwick *et al.*, 1991).

Electrophysiological methods

M.e.p.cs were recorded by standard two electrode voltage clamp techniques similar to those employed in previous studies (Dionne & Parsons, 1981; Connor *et al.*, 1984; Fiekers *et al.*, 1987). The endplate region of individual fibres was voltage-clamped to − 100 mV and a 20–30 s record containing m.e.p.cs was stored on a PCM recorder (Vetter) for later analysis. Mean m.e.p.c. amplitude was determined from an average of 50–100 m.e.p.cs by use of the programme SCAN, provided by Dr John Dempster for the University of Strathclyde.

The protocol used to assess endplate sensitivity was identical to that employed in earlier studies (Hardwick & Parsons, 1993). Average m.e.p.c. amplitude was determined from 2–3 individual endplates in a given preparation voltage clamped to − 100 mV prior to carbachol application and again in different fibres from the same preparation following removal of carbachol. Previous studies demonstrated that there was no change in mean m.e.p.c. amplitude or amplitude distribution in the isotonic potassium solution over the time frame of these experiments (Hardwick *et al.*, 1991). For noise analysis, the endplates, held at − 100 mV, were initially perfused with agonist-free solution to record the background noise and then perfused with the same solution containing 30 μM carbachol. Mean channel conductance was determined by use of a computer programme, SPAN, written by Dr John Dempster of the University of Strathclyde. Records of single channel activity were made on cell-attached patches with an Axopatch voltage clamp system as described previously (Hamill *et al.*, 1981; Hardwick & Parsons, 1993). Nerve terminals were removed by enzymatic treatment to expose the endplate as described previously (Betz & Sakmann, 1973; Hardwick & Parsons, 1993). The patch pipette contained Ca/Mg-KP with the magnesium chloride concentration raised to 8.2 mM to facilitate seal formation and 1 μM ACh to activate ACh receptors. The current output signal was low-pass filtered at 5 kHz (4-pole Bessel) and stored on a PCM recorder for later analysis. The current signal was sampled at 33 kHz for analysis using the programme pClamp (version 5.5.1, Axon Instruments).

Statistics

Statistical significance was determined by analysis of variance or Student's t test with $P<0.05$ considered significant. Values shown represent the mean ± s.e.mean of n different fibres from at least 3 different animals.

Results

Elevated calcium can antagonize the staurosporine-induced decrease in recovery following a prolonged carbachol application

In our initial study, we found that raising the external calcium concentration from 1 mM to 10 mM during a 2–3 min local perfusion of the endplate with carbachol reversed the staurosporine-induced decrease in m.e.p.c. amplitude following the recovery from desensitization (Hardwick *et al.*, 1991). The first experiments in the present study were done to test whether elevating calcium could also effectively antagonize the staurosporine-induced decrease in recovery when the duration of carbachol application was increased to 10 min. M.e.p.cs were recorded from endplates voltage clamped to − 100 mV in control and staurosporine-pretreated preparations prior to and 5–15 min after a 10 min bath exposure to 540 μM carbachol. In the first group of preparations, the calcium concentration in the KP solution was maintained at 1 mM (Ca/Mg-KP, see Table 1) throughout the experiment. In the second group of preparations, the calcium concentration before and after carbachol application was 1 mM, but was elevated to 10 mM (KP-10Ca, see Table 1) during the carbachol exposure. At control endplates, there was no significant difference in the extent of m.e.p.c. amplitude recovery when the calcium concentration was either 1 mM or 10 mM during the carbachol exposure. At staurosporine-pretreated endplates, elevation of the calcium concentration during the carbachol exposure resulted in a significant increase in the extent of m.e.p.c. amplitude recovery (Table 2). As was seen in previous studies (Hardwick *et al.*, 1991; Hardwick & Parsons, 1993), there was no change in the time constant of m.e.p.c. decay following carbachol exposure in control or staurosporine-treated preparations (data not shown).

Large and small conductance channels are present following ACh receptor recovery in staurosporine-pretreated preparations exposed to 10 mM calcium during the 540 μM carbachol application

We showed in our previous study that, following recovery from carbachol exposure, a small conductance ACh-activated channel was observed in staurosporine-treated preparations which was not seen following recovery in control preparations (Hardwick & Parsons, 1993). Here, we tested whether exposure to elevated calcium reversed the staurosporine-induced decrease in m.e.p.c. amplitude by converting the small conductance channels to the large conductance type. Cell-attached recordings of single channel activity were made in Ca/Mg-KP on endplates from control and staurosporine-pretreated fibres 10–25 min after a 10 min exposure to KP-10Ca containing 540 μM carbachol. All recordings were made with the patch held at − 100 mV.

Channel activity was recorded in 6 patches made on control fibres and 8 patches made on staurosporine-pretreated preparations. Only the large conductance channel was observed at control endplates, following recovery from the 10 min exposure to carbachol in KP-10Ca (Figure 1a). Further, the mean amplitude (− 4.58 ± 0.34 pA) of the ACh-activated currents recorded at − 100 mV was identical to those determined previously for control endplates in Ca/Mg-KP either prior to or following exposure to carbachol (Hardwick &

Table 1 Composition of the different isotonic potassium propionate (KP) solutions used in this study

	Concentration [mM]						
	K propionate	$CaCl_2$	$MgCl_2$	$SrCl_2$	$CsCl_2$	EGTA	HEPES
Ca/Mg-KP	161	1.0	4.2	0	5.0	0	1.0
KP-10Ca	161	10	4.2	0	5.0	0	1.0
KP-10Mg	161	0	10	0	5.0	0	1.0
KP-10Sr	161	0	4.2	10	5.0	0	1.0
Ca-deficient KP	161	0	4.2	0	5.0	0.5	1.0
Ca/Mg-deficient KP	161	0	0	0	5.0	0	1.0

Table 2 Elevation of the calcium concentration during the carbachol application reverses the staurosporine-induced decrease in recovery.

	M.e.p.c. amplitude following carbachol exposure			
	1 mM Ca^{2+}		10 mM Ca^{2+}	
Treatment	nA	% recovery	nA	% recovery
Control	-5.62 ± 0.20 (16)	85%	-5.77 ± 0.24 (16)	87%
Staurosporine	-4.93 ± 0.13* (33)	75%	-5.45 ± 0.15 (23)	82%

The average m.e.p.c. amplitude was determined at control and staurosporine-treated endplates following a 10 min exposure to 540 μM carbachol. The concentration of extracellular calcium was either 1 mM or 10 mM during the agonist application. Staurosporine pretreatment produced a significant decrease ($P<0.05$) in m.e.p.c. amplitude following agonist exposure with 1 mM calcium whereas there was no significant decrease in the m.e.p.c. amplitude when the calcium concentration was 10 mM. Values represent the mean ± s.e.mean from *n* fibres (given in parentheses). The percentage recovery is the amplitude following carbachol exposure versus the m.e.p.c. amplitude prior to carbachol exposure. Average m.e.p.c. amplitude prior to carbachol exposure was -6.61 ± 0.26 nA ($n = 7$).

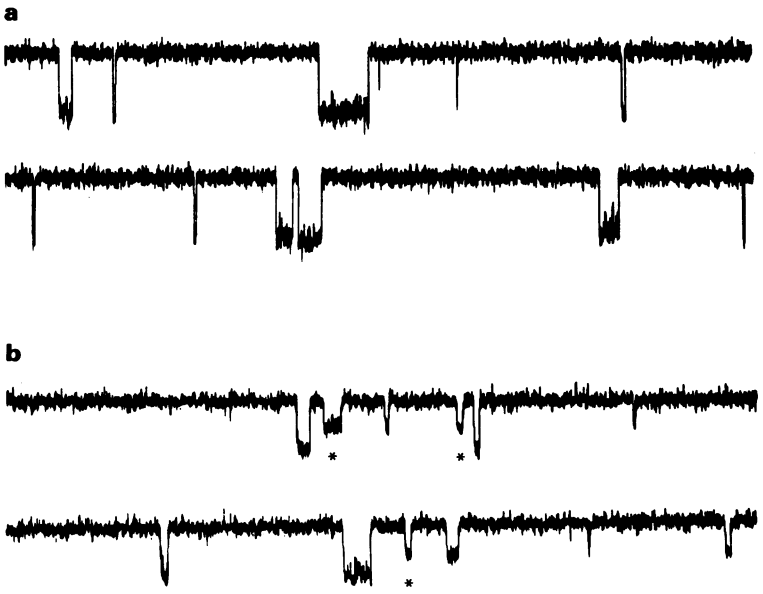

Figure 1 Acetylcholine (ACh)-induced currents were recorded from cell-attached patches held at − 100 mV from control (a) and staurosporine-treated (b) endplates following a 10 min incubation with 540 μM carbachol containing 10 mM Ca^{2+}. A population of small amplitude channels was observed only in the staurosporine-treated preparations (asterisk). Calibration bars x axis = 5 pA, y axis = 20 ms.

Parsons, 1993). In contrast, of the 11 channels observed in the 8 patches made in Ca/Mg-KP on staurosporine-pretreated fibres following exposure to 540 μM carbachol in KP-10Ca, 4 were small conductance channels and 7 were large conductance channels (Figure 1b). The mean amplitudes (-2.89 ± 0.19 pA and -4.87 ± 0.10 pA) of the two populations of the ACh-activated currents recorded at − 100 mV from patches on the staurosporine-pretreated fibres were similar to those reported previously for staurosporine-pretreated preparations exposed to 540 μM carbachol in Ca/Mg-KP (Hardwick & Parsons, 1993).

Elevated calcium concentrations can antagonize the staurosporine-induced decrease in m.e.p.c. recovery when applied following the carbachol application and in the presence of the ACh-receptor inhibitor, (+)-tubocurarine

We also tested whether elevating the calcium concentration after the period of carbachol exposure could effectively reverse the staurosporine-induced decrease in recovery of m.e.p.c. amplitudes. For these experiments, m.e.p.cs were recorded from endplates of different fibres in control and

staurosporine-pretreated preparations prior and following a 10 min exposure to 540 μM carbachol. The calcium concentration was maintained at 1 mM before and during the carbachol exposure. After removing the carbachol, the preparations were washed for 5 min in agonist-free Ca/Mg-KP and m.e.p.cs recorded. These same preparations were then exposed to KP-10Ca (see Table 1) for 3 min, returned to Ca/Mg-KP for approximately 5 additional minutes and m.e.p.cs recorded from another group of fibres. In control preparations, the m.e.p.c. amplitude recovered to approximately 85% of the pre-carbachol values following the recovery period in Ca/Mg-KP and did not change significantly following the 3 min exposure to KP-10Ca (Table 3). In contrast, in staurosporine-pretreated preparations, the m.e.p.c. amplitude recovered to only 75% of the pre-carbachol value following the recovery period in Ca/Mg-KP, but increased significantly to approximately 90% of the pre-carbachol value after the 3 min exposure to KP-10Ca (Table 3).

Previously, we proposed that calcium influx through nicotinic receptor channels was a critical step in the calcium-induced reversal of the staurosporine-induced decrease in resensitization (Hardwick *et al.*, 1991). However, the observation that elevation of calcium after the carbachol exposure effectively reversed the staurosporine-induced decrease in m.e.p.c. amplitude suggested that influx of calcium through activated ACh receptors may not be required. M.e.p.c. frequency increases substantially during exposure to KP-10Ca (Hardwick *et al.*, 1991). Therefore, during the period of increased m.e.p.c. frequency, sufficient ACh receptors might be activated to promote calcium influx at the endplate. This possibility was tested in another series of experiments in which 13 μM (+)-tubocurarine was included in the KP-10Ca solution. In control fibres, no m.e.p.cs were discernible from the background noise when 13 μM (+)-tubocurarine was present. The addition of (+)-tubocurarine to KP-10Ca did not reduce the ability of a 3 min exposure to 10 mM calcium to antagonize the staurosporine-induced decrease in resensitization (Table 3).

To determine the specificity of this effect for calcium, the ability of other divalent cations, specifically strontium and magnesium, to antagonize the staurosporine-induced decrease in m.e.p.c. recovery was also tested. M.e.p.c.s were recorded from a series of control and staurosporine-pretreated fibres in Ca/Mg-KP 5–15 min after a 10 min exposure to 540 μM carbachol (in Ca/Mg-KP) and again in Ca/Mg-KP after a 3 min exposure to either 10 mM strontium (KP-10Sr) or 10 mM magnesium (KP-10Mg, see Table 1). At both control and staurosporine-pretreated preparations, the 3 min exposure to KP-10Sr produced no significant effect on m.e.p.c. amplitude during recovery from the 10 min carbachol exposure (Table 4). At control endplates, exposure to KP-10Mg did not significantly affect the m.e.p.c. amplitude (Table 4). In contrast, at staurosporine-pretreated endplates, m.e.p.c. amplitude was consistently increased following the 3 min exposure to KP-10Mg such that there was no longer a significant difference between staurosporine and untreated endplates. However, the total extent of recovery in the KP-10Mg was still less than that of elevated calcium (compare Tables 3 and 4).

M.e.p.c. amplitude recovery requires divalent cations in the extracellular solution

The results of the single channel studies indicated that exposure to KP-10Ca along with carbachol did not reverse the staurosporine-induced decrease in m.e.p.c. recovery by converting small conductance ACh-activated channels to large conductance channels. Therefore, exposure to 10 mM calcium must have antagonized the staurosporine action by another mechanism such as increasing the number of functional ACh receptors. If this proposal is correct, then calcium could be another factor regulating the recruitment of new receptors to replace those irreversibly inactivated during the carbachol application (Hardwick & Parsons, 1993). Therefore, we tested the dependence of m.e.p.c. recovery on extracellular calcium. Initally, we determined the extent of m.e.p.c. amplitude recovery following a 10 min exposure to 540 μM carbachol in preparations maintained in a Ca-deficient-KP solution (see Table 1). The muscle preparations were first incubated in Ca/Mg-KP for approximately 15 min. The preparations were then equilibrated in Ca-deficient-KP for an additional 15 min, incubated for 10 min in Ca-deficient-KP containing 540 μM carbachol and washed well with agonist-free Ca-deficient-KP prior to recording m.e.p.cs. M.e.p.cs also were recorded from other fibres in preparations which were not exposed to carbachol, but maintained in Ca-deficient-KP for similar durations. We found that for endplates voltage-clamped to − 100 mV, m.e.p.c. amplitudes decreased when the solution bathing the preparations was changed from Ca/Mg-KP (− 5.59 ± 0.25 nA, $n = 11$) to Ca-deficient-KP (− 4.86 ± 0.18 nA, $n = 21$). M.e.p.c. amplitudes were decreased by 15% in fibres recovering from a 10 min exposure to Ca-deficient-KP containing carbachol as compared to fibres maintained in Ca-deficient-KP for the same length of time. However, a 15% reduction in m.e.p.c. amplitudes also occurs in control fibres kept in Ca/Mg-KP following a 10 min exposure to 540 μM carbachol (Figure 2). Consequently, the extent of m.e.p.c. amplitude recovery following the exposure to carbachol was similar for preparations kept in Ca/Mg-KP and Ca-deficient-KP.

Staurosporine-pretreatment significantly decreased the extent of m.e.p.c. amplitude recovery in preparations kept in Ca-deficient-KP (Figure 2). For these experiments, the muscle preparations were pretreated with staurosporine during the initial 15 min equilibration in Ca-deficient-KP. The staurosporine-induced decrease in the extent of recovery was

Table 3 Elevation of the extracellular calcium concentration in the absence of receptor activation reverses the effects of staurosporine on m.e.p.c. amplitudes

	M.e.p.c. amplitude					
	Following 10 min 540 μM CCh		*3 min 10 mM Ca^{2+} KP*		*3 min 10 mM Ca^{2+}/(+)-TC*	
Treatment	*nA*	*% recovery*	*nA*	*% recovery*	*nA*	*% recovery*
Control	− 5.86 ± 0.21 (19)	88%	− 6.40 ± 0.27 (13)	96%	− 6.72 ± 0.27 (8)	100%
Staurosporine	− 5.00 ± 0.10* (35)	75%	− 5.83 ± 0.20 (35)	87%	− 6.32 ± 0.24 (15)	94%

M.e.p.c. amplitudes were measured in control and staurosporine-treated fibres prior to agonist application, following a 10 min exposure to 540 μM carbachol (CCh) and again following an additional 3 min in either KP containing 10 mM Ca^{2+} alone or KP containinig 10 mM Ca^{2+} + 13 μM (+)-tubocurarine ((+)-TC). M.e.p.c. amplitudes were significantly reduced in staurosporine-treated preparations following carbachol exposure ($P < 0.05$) but this reduction in amplitude was reversed following a brief incubation in either elevated calcium solution. The values shown are the means ± s.e.mean of n fibres (shown in parentheses). Percentage recovery is the amplitude following the treatment indicated versus the m.e.p.c. amplitude prior to carbachol exposure. Average m.e.p.c. amplitude prior to exposure to carbachol was − 6.69 ± 0.26 nA ($n = 7$).

Table 4 The effects of other divalent cations on m.e.p.c. amplitudes following carbachol exposure

	M.e.p.c. amplitude (nA)					
	Following 10 min 540 μM *CCh*		*3 min* 10 mM Sr^{2+} *KP*		*3 min* 10 mM Mg^{2+} *KP*	
Treatment	*nA*	*% recovery*	*nA*	*% recovery*	*nA*	*% recovery*
Control	− 5.42 ± 0.13 (17)	92%	− 5.15 ± 0.15 (15)	87%	− 5.59 ± 0.27 (14)	94%
Staurosporine	− 4.58 ± 0.23*,† (18)	77%	− 4.76 ± 0.13† (15)	80%	− 5.03 ± 0.18 (13)	85%

*$P < 0.05$ vs control fibres under the same conditions
†$P < 0.001$ vs amplitudes before agonist application
M.e.p.c. amplitudes were measured in control and staurosporine-treated fibres prior to agonist exposure, following a 10 min exposure to 540 μM carbachol, and following an additional exposure to either KP containing 10 mM Sr^{2+} or KP containinig 10 mM Mg^{2+}. Staurosporine-treated fibres showed a significant reduction in m.e.p.c. amplitude versus control fibres following carbachol exposure. Following the 3 min incubation in KP with either 10 mM Sr^{2+} or 10 mM Mg^{2+}, there was no significant difference between staurosporine-treated and control fibres. However, the m.e.p.c. amplitude in staurosporine-treated fibres incubated in 10 mM Mg^{2+} was no longer significantly different from the untreated values. The values shown are the means ± s.e.mean of *n* fibres (shown in parentheses). Percentage recovery was the amplitude following the indicated treatment versus the m.e.p.c. amplitude prior to carbachol exposure. Average m.e.p.c. amplitude prior to carbachol exposure was − 5.92 ± 0.28 nA ($n = 5$).

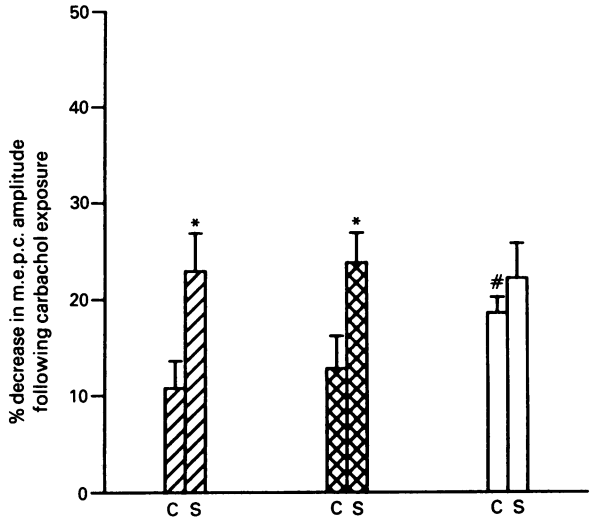

Figure 2 Average m.e.p.c. amplitudes were measured prior to agonist exposure and following a 10 min incubation with 540 μM carbachol in control (C) and staurosporine-treated (S) fibres in three different isotonic potassium solutions. In the normal Ca/Mg-KP (hatched columns) and the Ca-deficient-KP, (cross-hatched columns), staurosporine treatment resulted in a significantly greater inhibition of m.e.p.c. amplitude. In the Ca/Mg-deficient-KP (open columns), there was no difference between control and staurosporine-treated fibres following carbachol exposure. In addition, the percentage decrease in m.e.p.c. amplitude in those fibres maintained in Ca/Mg-deficient-KP was significantly greater than that seen in fibres maintained in Ca/Mg-KP.

essentially the same for preparations bathed in either Ca/Mg-KP or Ca-deficient-KP.

The results from the preceding experiments indicated that removal of external calcium, without also eliminating magnesium, did not significantly alter m.e.p.c. amplitude recovery following a 10 min carbachol exposure, nor did it alter the ability of staurosporine to decrease the extent of recovery (Figure 2). This suggested that magnesium, in the absence of calcium, must sustain the resensitization process. To test this possibility, we measured the extent of m.e.p.c. amplitude recovery in preparations kept in Ca/Mg-deficient-KP (see Table 1).

Initially, we found that the mean m.e.p.c. amplitude recorded at endplates voltage-clamped to − 100 mV was similar in preparations kept in Ca/Mg-deficient-KP (− 4.56 ± 0.13 nA, $n = 32$) to that obtained for endplates maintained in Ca-deficient-KP (− 4.86 ± 0.18 nA, $n = 21$). Next, we determined the extent of m.e.p.c. amplitude recovery following a 10 min exposure to 540 μM carbachol in Ca/Mg-deficient-KP. We found that m.e.p.c. amplitude recovered significantly less, after carbachol exposure, at endplates in preparations kept in Ca/Mg-deficient-KP than at endplates in preparations bathed in either Ca-deficient-KP or Ca/Mg-KP (Figure 2). In a separate series of experiments, we also tested whether staurosporine-pretreatment would decrease the extent of m.e.p.c. amplitude recovery in preparations maintained in Ca/Mg-deficient-KP. We found that staurosporine-pretreatment did not further decrease the extent of m.e.p.c. amplitude recovery in these preparations (Figure 2).

Mean channel conductance following recovery is unchanged in staurosporine-treated preparations maintained in Ca/Mg-deficient-KP

We felt that the decrease in extent of m.e.p.c. amplitude recovery observed in preparations maintained in Ca/Mg-deficient-KP could result from either a decrease in the number of activatable ACh receptors or a decrease in the single channel conductance of individual activated ACh receptors. The latter mechanism appears to be responsible, at least in part, for the staurosporine-induced decrease in m.e.p.c. amplitude recovery (Hardwick & Parsons, 1993). To test whether the latter mechanism might be involved, single channel recordings were attempted in preparations kept in Ca/Mg-deficient-KP. Out of over a dozen muscle preparations, only one successful patch was obtained. This patch, from a control fibre maintained in Ca/Mg-deficient-KP, demonstrated a single population of channels, however, we were unable to record channels at sufficient voltages to estimate the slope conductance. It was also necessary to add 8 mM magnesium to the patch solution to obtain this single seal, making the interpretation of the results difficult since the channels would no longer be exposed to a divalent cation-free solution. In general, we found that, following the enzymatic cleaning, the muscle fibres were too delicate to withstand incubation in a divalent cation-free solution. Therefore, we abandoned the patch clamp experiments and initiated experiments to estimate mean channel conductance using noise measurements made on intact endplates in preparations kept in Ca/Mg-deficient-KP. Previously, we showed in staurosporine-pretreated preparations with noise measurements that, after recovery from carbachol exposure, mean channel conductance was reduced (Hardwick & Parsons, 1993). Therefore, we felt that this was an adequate means to test whether the conductance of the ACh-activated channels

Table 5 Comparison of mean channel conductance (γ) and m.e.p.c. amplitudes in Ca/Mg-deficient-KP in control and staurosporine-treated preparations

	γ		M.e.p.c.	
	pS	*% untreated*	*nA*	*% untreated*
Before	24 ± 3 (4)	100%	− 4.52 ± 0.34 (5)	100%
Control recovery	24 ± 2^{NS} (5)	100%	− 3.47 ± 0.16* (7)	77%
Stauro recovery	19 ± 2^{NS} (4)	79%	− 3.45 ± 0.17* (8)	76%

*$P < 0.05$ versus untreated preparations
NS, not significantly different from untreated preparations.
Mean channel conductance (γ) estimated from the response to 30 μM carbachol was determined at endplates prior to carbachol exposure in control and staurosporine (Stauro)-treated fibres following a 10 min incubation with 540 μM carbachol. Average m.e.p.c. amplitudes were measured in the same preparation. The results are expressed as the mean ± s.e.mean of *n* fibres (shown in parentheses). The values are also shown as a percentage of those in the untreated preparations. There was no significant change in the mean channel conductance following agonist application in either control or staurosporine-treated fibres whereas there was a significant decrease in the m.e.p.c. amplitude in these same preparations.

was changed following recovery from carbachol exposure at endplates bathed in Ca/Mg-deficient-KP.

To record agonist-induced membrane noise, noise measurements were made before and during microperfusion of 30 μM carbachol onto an individual endplate. Results were obtained from muscle preparations maintained in Ca/Mg-deficient-KP. Both untreated preparations and preparations which had been pretreated with 0.5 μM staurosporine were studied. For both groups of muscle preparations, membrane noise measurements was recorded prior to and following a 10 min incubation in Ca/Mg-deficient-KP containing 540 μM carbachol. We found that for preparations maintained in Ca/Mg-deficient-KP and not exposed to agonist, the mean channel conductance was approximately 50% lower than that reported previously for fibres maintained in KP (24 pS versus 41 pS, Hardwick & Parsons, 1993). This finding is consistent with the decrease in m.e.p.c. amplitude noted in Ca/Mg-deficient-KP which was described above. In addition, we found that, following exposure to 540 μM carbachol, there was no significant decrease in mean channel conductance at either untreated or staurosporine-treated fibres (Table 5).

M.e.p.c. amplitude recovery was also measured in these same preparations. We found that although the mean channel conductance was not decreased following recovery from carbachol application, there was a significant decrease in the m.e.p.c. amplitude after carbachol exposure of both the untreated and staurosporine-pretreated preparations. A comparison of the decrease in mean channel conductance and m.e.p.c. amplitude is presented in Table 5.

Discussion

We reported previously that elevating the extracellular calcium concentration reversed the staurosporine-induced decrease in extent of m.e.p.c. amplitude recovery (Hardwick *et al.*, 1991). This observation was confirmed in the present study. Also, we had proposed that calcium, acting at an intracellular site, reversed the staurosporine-induced decrease in m.e.p.c. amplitude recovery by stimulating additional kinase activity (Hardwick *et al.*, 1991). The results obtained in this study do not support our initial hypothesis. The fact that exposure to 10 mM calcium after the carbachol application was as effective as raising extracellular calcium during the agonist exposure suggested that calcium is acting at an extracellular site. In chronically depolarized muscle fibres, calcium permeability is very limited at the endplate except when ACh channels are activated (Jenkinson & Nicholls, 1961; Parsons & Nastuk, 1969; Manthey, 1974). Even if calcium were able to enter through ACh-activated channels, the observation that elevated calcium still reversed the staurosporine-induced decrease in recovery when (+)-tubocurarine was present also indicated that influx through ACh-activated channels was not required. Assuming that the site of calcium action is indeed extracellular, then the change in the staurosporine-induced decrease in extent of recovery with calcium is probably not due to the stimulation or reactivation of intracellular protein kinases which phosphorylate the ACh receptor or a related protein. In fact, in staurosporine-pretreated preparations, elevated calcium effectively increased the extent of m.e.p.c. recovery even though many small conductance channels were still present. Therefore, we conclude that the calcium-induced increase in the extent of m.e.p.c. amplitude recovery is not due to the conversion of small conductance ACh channels to large conductance channels and that stimulation of phosphorylation is not the mechanism by which calcium increases endplate sensitivity at the staurosporine-treated endplates.

If the site of calcium action is extracellular, not intracellular and not related to protein phosphorylation, what is a plausible alternative mechanism? We suggest that extracellular calcium plays a critical role in the accumulation and stabilization of newly recruited ACh receptors in the endplate membrane. This suggestion is consistent with previous studies which show that extracellular calcium is essential for the agrin-induced accumulation and stabilization of ACh receptors on myotubes (Wallace, 1988; Nastuk *et al.*, 1991). Interestingly, in cultured muscle cells, other divalent cations including magnesium do not substitute for calcium as promoters of ACh receptor clustering (Bloch, 1983). In contrast, at snake twitch fibre endplates, magnesium appeared to be able to substitute partially for calcium so that m.e.p.c. recovery occurred to essentially the same extent in Ca/Mg-KP as in Ca-deficient-KP. Exposure to 10 mM magnesium resulted in a partial increase in the extent of m.e.p.c. recovery at staurosporine-treated fibres. The difference in results could be due to differences in species studied or conditions of the experiments. For instance, the concentrations of magnesium used in the present study were higher than those tested previously. Although magnesium could replace calcium, strontium was an ineffective substitute. M.e.p.cs recorded in Ca-deficient-KP and Ca/Mg-deficient-KP were significantly smaller than those recorded from fibres kept in Ca/Mg-KP. Previously, Lambert & Parsons (1970) demonstrated at potassium-depolarized frog endplates that post-junctional sensitivity to cholinoceptor agonists decreased markedly in calcium-deficient solutions. These authors showed that magnesium was able to replace calcium, but higher concentrations were required. We suggest that the decrease in m.e.p.c. amplitude we noted in the Ca-deficient-KP and Ca/Mg-deficient-KP is caused by a similar decrease in responsiveness of the postsynaptic membrane rather than to a decreased quantal size.

Based on the observations made in the present study, we propose that calcium and magnesium are key extracellular factors determining the density of functional ACh receptor-channel complexes at the endplate. This view is consistent with the observation that the extent of m.e.p.c amplitude recovery following exposure to carbachol was much less when the preparations were kept in a divalent cation deficient solution than when calcium and/or magnesium were present. Further, after exposure to 10 mM calcium, the mean m.e.p.c. amplitude was actually greater than the control values both with and without carbachol exposure (see Tables 2 and 3) even though the single channel conductance was not affected. Lastly, even though m.e.p.c. amplitude recovery was enhanced in staurosporine-pretreated preparations by exposure to 10 mM calcium, many small conductance channels were still present. Thus, the simplest explanation of the observed increase in endplate sensitivity in staurosporine-treated fibres is that brief exposure to 10 mM calcium stimulated an increase in the density of functional ACh receptors.

We propose the following scheme as a working model for the role of extracellular divalent cations, especially calcium, and intracellular phosphorylation in the regulation of endplate sensitivity following a prolonged exposure to carbachol. When the endplate is exposed to high doses of agonist, many of the activated ACh receptors become desensitized (Katz & Thesleff, 1957; Connor *et al.*, 1984). If agonist concentration is sufficiently high and exposure prolonged, then some of the ACh receptors become irreversibly inactivated. This would explain why m.e.p.c. amplitudes do not recover fully even after a long period of recovery (Hardwick *et al.*, 1991). To maintain the 'normal density' of ACh receptors at the endplate, new receptors must replace those inactivated. Partial resensitization occurs rapidly so that the synthesis of new receptors is not involved over the time frame of these experiments (Hardwick *et al.*, 1991). Therefore, we suggest that some replacement ACh receptors are derived from a pool of previously synthesized, recruitable, but nonactivatible ACh receptors. Based on the results of our previous studies and the present study, we propose that the recruitment and conversion of these ACh receptors from a nonactivatable to an activatable state is a two step process. The first step, which requires extracellular calcium or magnesium, involves the recruitment and anchoring of new receptors in the membrane. These newly recruited ACh receptors are then rapidly phosphorylated by a staurosporine-sensitive protein kinase. The phosphorylated ACh receptor is the prevalent ACh receptor at twitch fibre endplates and when activated produces the large conductance response. With staurosporine treatment, this second step is inhibited and results in an intermediate form of the receptor which is activatible but has a smaller conductance value. Therefore, small conductance channels were still observed in the staurosporine-treated preparations, even with exposure to elevated calcium.

In conclusion, in the present study, as in our earlier work, a sustained agonist application was used to activate repetitively ACh receptors and cause a significant number to become irreversibly inactivated in a short time period. We suggest that this procedure provides a good model system for studying the mechanisms regulating the normal 'use dependent' turnover of ACh receptor-channel complexes in the endplate membrane of adult muscle fibres.

We would like to thank Dr John Dempster for the generous gifts of the programme SCAN. We would also like to thank Mr Dean Melen for expert technical assistance and Dr Cynthia Forehand for critical review of the manuscript. This work was supported by NIH grants NS 08580 to J.C.H. and NS 23978 to R.L.P.

References

BETZ, W. & SAKMANN, B. (1973). Effects of proteolytic enzymes on function and structure of frog neuromuscular junctions. *J. Physiol.*, **230**, 673–688.

BLOCH, R.J. (1983). Actylcholine receptor clustering in rat myotubes: requirements for Ca^{2+} and effects of drugs which depolymerize microtubules. *J. Neurosci.*, **3**, 2670–2680.

CONNOR, E.A., FIEKERS, J.F., NEEL, D.S., PARSONS, R.L. & SCHNITZLER, R.M. (1984). Comparison of cholinergic activation and desensitization at snake twitch and slow muscle fibre end-plates. *J. Physiol.*, **351**, 657–674.

DIONNE, V.E. & PARSONS, R.L. (1981). Characteristics of the acetylcholine-operated channel at twitch and slow fibre neuromuscular junctions of the garter snake. *J. Physiol.*, **310**, 145–158.

FIEKERS, J.F., NEEL, D.S. & PARSONS, R.L. (1987). Acceleration of desensitization by agonist pretreatment in the snake. *J. Physiol.*, **391**, 109–124.

HAMILL, O.P., MARTY, A., NEHER, E., SAKMANN, B. & SIGWORTH, F. (1981). Improved patch-clamp techniques for high resolution current recording from cells and cell-free membrane platelets. *Pflügers Arch.*, **391**, 85–100.

HARDWICK, J.C., CONIGLIO, L.M. & PARSONS, R.L. (1991). Staurosporine inhibits the extent of acetylcholine receptor recovery from carbachol-induced desensitization in snake twitch fibres. *Br. J. Pharmacol.*, **104**, 879–886.

HARDWICK, J.C. & PARSONS, R.L. (1993). Mechanism of staurosporine-induced decrease in acetylcholine receptor recovery from desensitization. *Br. J. Pharmacol.*, **108**, 741–748.

JENKINSON, D.H. & NICHOLLS, J.G. (1961). Contractures and permeability changes produced by acetylcholine in depolarized denervated muscle. *J. Gen. Physiol.*, **159**, 111–127.

KATZ, B. & THESLEFF, S. (1957). A study of the 'desensitization' produced by acetylcholine at the motor end-plate. *J. Physiol.*, **138**, 63–80.

LAMBERT, D.H. & PARSONS, R.L. (1970). Influence of polyvalent cations on the activation of muscle end-plate receptors. *J. Gen. Physiol.*, **56**, 309–321.

MANTHEY, A.A. (1974). Changes in Ca permeability of muscle fibers during desensitization in carbamylcholine. *Am. J. Physiol.*, **226**, 481–489

NASTUK, M.A., LIETH, E., MA, J., CARDASIS, C.A., MOYNIHAN, E.B., MCKECHNIE, B.A. & FALLON, J.R. (1991). The putative agrin receptor binds ligand in a calcium-dependent manner and aggregates during agrin-induced acetylcholine receptor clustering. *Neuron*, **7**, 807–818.

PARSONS, R.L. & NASTUK, W.L. (1969). Activation of contractile system in depolarized skeletal muscle fibres. *Am. J. Physiol.*, **217**, 364–369.

WALLACE, B.G. (1988). Regulation of agrin-induced acetylcholine receptor aggregation by Ca^{++} and phorbol ester. *J. Cell Biol.*, **107**, 267–278.

(Received April 5, 1993
Revised June 9, 1993
Accepted June 11, 1993)

Br. J. Pharmacol. (1993), **110**, 896–902

Role of oxygen radicals and arachidonic acid metabolites in the reverse passive Arthus reaction and carrageenin paw oedema in the rat

[1]N.K. Boughton-Smith, A.M. Deakin, R.L. Follenfant, B.J.R. Whittle & *L.G. Garland

Department of Pharmacology and *Research Directorate, Wellcome Research Laboratories, Beckenham, Kent, BR3 3BS

1 The role of arachidonic acid metabolites and oxygen radicals in carrageenin-induced rat paw oedema and dermal reverse passive Arthus reaction (RPA) have been investigated.

2 Indomethacin (10 mg kg^{-1}, p.o.) inhibited carrageenin paw oedema when administered 30 min before, but not 2 h after carrageenin. BWB70C (10 mg kg^{-1}, p.o.), a selective inhibitor of 5-lipoxygenase, had no effect whether administered before or after carrageenin. Administration of both indomethacin and BWB70C had no greater anti-inflammatory effect than indomethacin alone.

3 BW755C (20 mg kg^{-1}, p.o.), which inhibits the cyclo-oxygenase and lipoxygenase pathways of arachidonic acid metabolism, or superoxide dismutase-polyethylene glycol conjugate (SOD-PEG, 3000 u, i.v.) inhibited carrageenin paw oedema whether administered either 30 min before, or 2 h after carrageenin.

4 Pretreatment with dexamethasone (0.1 mg kg^{-1}) or colchicine (2 mg kg^{-1}), likewise suppressed carrageenin paw oedema.

5 BW755C (25–100 mg kg^{-1}, p.o.) dose-dependently reduced plasma leakage in the RPA, whereas indomethacin (5 mg kg^{-1}, p.o.) or BWB70C either alone or in combination, did not.

6 SOD-PEG (300–3000 u, i.v.) dose-dependently inhibited plasma leakage in the RPA. In addition, the iron chelator and peroxyl radical scavenger, desferrioxamine (200 mg kg^{-1}, s.c.) also inhibited plasma leakage.

7 Pretreatment with dexamethasone (0.1 mg kg^{-1}) or colchicine (1 mg kg^{-1}) reduced the plasma leakage in RPA, whereas MK-886 (10 mg kg^{-1}) had no effect.

8 These results indicate an important role for oxygen radicals but not arachidonic acid metabolites in the maintenance of carrageenin paw oedema and the plasma leakage in RPA. Furthermore, the results suggest that the anti-inflammatory actions of BW755C can be dissociated from its effects on arachidonic acid metabolism and are attributed to its anti-oxidant activity.

Keywords: Carrageenin oedema; reverse passive Arthus reaction; neutrophil-dependent plasma leakage; cyclo-oxygenase; lipoxygenase; 5-lipoxygenase inhibitor; BW755C; oxygen radicals

Introduction

There is considerable evidence from both *in vitro* and *in vivo* studies that oxygen-derived radicals play a role in acute inflammation. Reactive oxygen molecules generated enzymically or from activated phagocytes, damage mammalian cells, including endothelial cells (for review, Fantone & Ward, 1982; Ward, 1991). Administration of oxygen radical generating systems into the lung, knee joint or foot of experimental animals leads to increases in vascular permeability, cellular infiltration and tissue damage (for review, Schraufstatter *et al.*, 1987). Furthermore, the anti-oxidant enzyme, superoxide dismutase (SOD) has anti-inflammatory activity in models of acute inflammation (Oyanagui, 1976).

Arachidonic acid metabolites of the cyclo-oxygenase and lipoxygenase enzymes have also been implicated as mediators of acute inflammation. The vasodilator prostaglandins produce erythema and hyperalgesia (for review, see Higgs *et al.*, 1984), while the potent actions of the 5-lipoxygenase product, leukotriene B_4 (LTB_4) on polymorphonuclear leucocytes (PMN's) may contribute to their accumulation and activation at sites of inflammation (for review, see Lewis *et al.*, 1990). Furthermore, in the presence of vasodilator prostaglandins, LTB_4 produces a neutrophil-dependent increase in vascular permeability (Wedmore & Williams, 1981).

The role of arachidonic acid metabolites has been investigated in a number of models of acute inflammation. Thus carrageenin-induced paw oedema in the rat has been used extensively to determine the activity of non-steroid anti-inflammatory or aspirin-like drugs which inhibit prostaglandin synthesis (Higgs *et al.*, 1983). The experimental anti-inflammatory compound BW755C, a dual cyclo-oxygenase/lipoxygenase inhibitor, also inhibits carrageenin-induced paw oedema (Higgs *et al.*, 1979). Oxygen radicals have also been implicated in models of acute inflammation in which there is a neutrophil-dependent increase in vascular permeability (for review, see Fantone & Ward, 1982). However, the role of oxygen radicals in acute inflammation in relation to the activity of arachidonic acid metabolites remains unclear. In the present study the role of both oxygen radicals and arachidonate metabolites have been investigated in carrageenin-induced paw oedema and in the dermal reverse passive Arthus reaction (RPA) in the rat.

Methods

Carrageenin paw oedema

Male Wistar rats (140–190 g) which had been fasted overnight (18 h) received a subplantar injection in the right hind paw of carrageenin (100 µl of 1% suspension in 0.85% saline). Paw thickness was measured from ventral to dorsal

[1] Author for correspondence at present address: Department of Pharmacology, Fisons Pharmaceuticals, Loughborough, Leicestershire, LE11 0RH.

surfaces, with dial callipers (Mitutoyo), immediately prior to carrageenin injection and then at hourly intervals from 1–6 h afterwards. Oedema was expressed as the increase in paw thickness (in mm) measured after carrageenin injection compared to the pre-injection value for individual animals.

Drugs were administered orally in 0.25% methyl cellulose (celacol) or intravenously (dose volume of 5 ml kg^{-1}), either 30 min before or 2 h after carrageenin, unless otherwise stated. Doses were selected from previous studies (indomethacin, Higgs *et al.*, 1983; BWB70C, Salmon *et al.*, 1989 and unpublished data; BW755C, Higgs *et al.*, 1979; Salmon, 1986; MK-886, Gillard *et al.*, 1989).

Reverse passive Arthus reaction

Male Wistar rats (225–275 g) which had been fasted overnight were anaesthetized with halothane (2%, 3 l – oxygen min^{-1}). Antigen (3 mg rabbit IgG), mixed with ^{125}I-labelled human serum albumin (HSA; 0.5 μCi) and Evans blue (2.5% in saline), was injected via the tail vein (1 ml). Immediately afterwards, either antibody (50 μg goat anti-rabbit IgG) or saline was injected intra-dermally (50 μl, 12 × 0.4 mm needle), in triplicate according to a random plan, to a previously shaved area of dorsal skin. The rats were allowed to recover from the anaesthesia.

Rats were re-anaesthetized with halothane 90 min after challenge and, following laparotomy, blood (1 ml) was drawn from the abdominal aorta into tri-sodium citrate (0.315% final concentration). Plasma was separated by centrifugation (10,000 *g*; 2 min). The rats were killed by cervical dislocation, the dorsal skin removed and injection sites (blue areas) and two untreated sites punched out with a cork borer (17 mm). Radioactivity in skin samples and duplicate plasma samples (100 μl) was counted (Nuclear Enterprises – NE1600 gamma counter). Plasma leakage was calculated as μl of plasma.

BW755C, BWB70C and indomethacin were administered orally 1 h before and MK-886, 4 h before induction of the RPA response, (suspended in 0.5% methyl cellulose, dosing volume of 1 ml kg^{-1}). Colchicine and dexamethasone were administered subcutaneously 2 h before and desferrioxamine 1 h before induction of the RPA reaction. Superoxide dismutase-polyethylene glycol conjugate (SOD-PEG) was injected i.v. (in saline, 2 ml kg^{-1}) via the tail vein 1 min before initiation of RPA. Control animals received the vehicle via the relevant route of administration.

Myeloperoxidase activity

Myeloperoxidase (MPO), a haemoprotein which is located in azurophil granules of neutrophils where it plays a role in bacterial killing, has been used as an enzyme marker of neutrophil infiltration in various tissues (Bradley *et al.*, 1982). In the present study, MPO was measured by a method similar to that described by Bradley *et al.* (1982).

Skin sites were finely chopped with scissors and homogenized (Ultra turrax 45 s) in 3 ml of 0.5% hexadecyltrimethyl-ammonium bromide (HTAB) in 50 mM potassium phosphate buffer (pH 6). Aliquots (1 ml) were frozen (on cardice) and thawed (immersion in warm water, 37°C) three times. Following centrifugation (10,000 *g* for 20 min) the supernatant (200 μl) was mixed in a cuvette with 2.8 ml of 50 mM phosphate buffer (pH 6) containing 0.167 mg ml^{-1} O-dianisidine dihydrochloride and 0.0005% hydrogen peroxide at 37°C and the change in absorbance at 460 nm measured immediately (Guildford Response spectrophotometer). The MPO activity is expressed as the number of rat peritoneal neutrophils (glycogen elicited and purified as described by McCall *et al.*, 1989) containing an equivalent amount of MPO.

Plasma SOD activity

SOD activity was measured spectrophotometrically in diluted plasma (1:2) as inhibition of ferricytochrome C reduction by O_2^-. Ferricytochrome C (20 mM) was incubated (37°C) with an O_2^- generating system (5 mu xanthine oxidase and 100 μM hypoxanthine, 37°C) and increases in absorbance at 550 nm measured (Guildford Response spectrophotometer). The amount of O_2^--scavenging activity in the plasma was expressed as units of SOD activity.

Statistical analysis

Results are expressed as mean ± s.e.mean of (*n*) rats. Where appropriate, statistical significance was calculated by Student's *t* test for unpaired data (two tailed) or one way analysis of variance (ANOVA) and Bonferroni corrected *P* value for multiple comparisons. The level of statistical significance was taken as $P<0.05$. In time course experiments (Figures 1–5) analysis by Student's *t* test was made at one time point (3 h), being representative of the drug-induced change.

Materials

BWB70C ((E)-N-3-[3-(4-fluorophenoxy)phenyl]-1(**R,S**)-methyl-prop-2-en-l-yl-*N*-hydroxyurea), (Salmon *et al.*, 1989) and BW755C (3-amino-l-[*m*-(trifluoromethyl)phenyl]-2-pyrazoline) (Higgs *et al.*, 1979), MK-886(3-[1-(4-chlorobenzyl)-3-*t*-butylthio-5-isopropylindol-2-yl]-2,2-dimethylpropanoic acid) (Gillard *et al.*, 1989) were synthesized by Wellcome Research Laboratories (Beckenham). Dexamethasone (Decadron) was obtained from Merk, Sharpe and Dohme (Hertfordshire) and desferrioxamine (Desferal) from Ciba Laboratories (Horsham). Methyl cellulose was obtained from Courtaulds Fine Chemicals (Derby), O-dianisidine di-hydrochloride and hexadecyltrimethyl-ammonium bromide from Aldrich Chemical Co. Ltd., (Dorset), Halothane BP from RPM Animal Health Ltd., and ^{125}I-labelled human serum albumin (2.5 μCi mg^{-1} protein) from Amersham International plc (Amersham). All other reagents and antibodies were obtained from Sigma Chemical Co. Ltd. (Poole, Dorset).

Results

Carrageenin paw oedema

Cyclo-oxygenase and 5-lipoxygenase inhibitors A subplantar injection of carrageenin in control rats induced an increase in paw thickness over 6 h (Figure 1). Pretreatment with indomethacin (10 mg kg^{-1}, p.o.) 30 min before carrageenin prevented the increase in paw thickness between 2 and 6 h ($P<0.001$ at 3 h, $n=5$, Figure 1a), while treatment with indomethacin (10 mg kg^{-1}, p.o.) 2 h after carrageenin had no effect on paw oedema (Figure 1b). The selective 5-lipoxygenase inhibitor, BWB70C (10 mg kg^{-1}, p.o.) had no effect on paw thickness whether administered 30 min before or 2 h after carrageenin (Figures 1a and b). Pretreatment with a combination of indomethacin (10 mg kg^{-1}, p.o.) and BWB70-C (10 mg kg^{-1}, p.o.) inhibited the increase in paw thickness produced between 1 and 6 h ($P<0.01$ at 3 h, $n=5$, Figure 1a) but had no inhibitory effect when administered 2 h after carrageenin (Figure 1b).

BW755C Pretreatment (30 min) with BW755C (20 mg kg^{-1}, p.o.) inhibited oedema formation produced between 2 and 6 h after carrageenin (Figure 2a). Furthermore, treatment with BW755C (20 mg kg^{-1}, p.o.) 2 h after injection of carrageenin also inhibited the increases in paw thickness over the subsequent 4 h, while producing an apparent reversal of oedema formation (Figure 2b).

SOD-PEG SOD-PEG (3000 u, i.v.) inhibited the increase in paw thickness when given either before (30 min) or 2 h after carrageenin (Figure 3). The inhibition produced by SOD-PEG when given after carrageenin was dose-dependent with

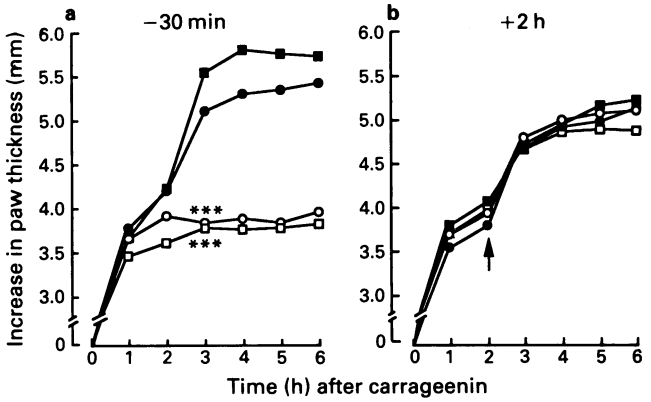

Figure 1 Effect of indomethacin and BWB70C on carrageenin-induced paw oedema administered either (a) 30 min before or (b) 2 h after carrageenin, as indicated by an arrow: (■) celacol; (□) indomethacin (10 mg kg^{-1}, p.o.); (●) BWB70C (10 mg kg^{-1}, p.o.); (○) indomethacin + BWB70C. Results are shown as the mean increase in paw thickness (mm) of 5 rats, statistical significance from the celacol group was determined after 3 h (***$P<0.001$). For clarity s.e.mean are not included, but are less than 5% of the mean for all points.

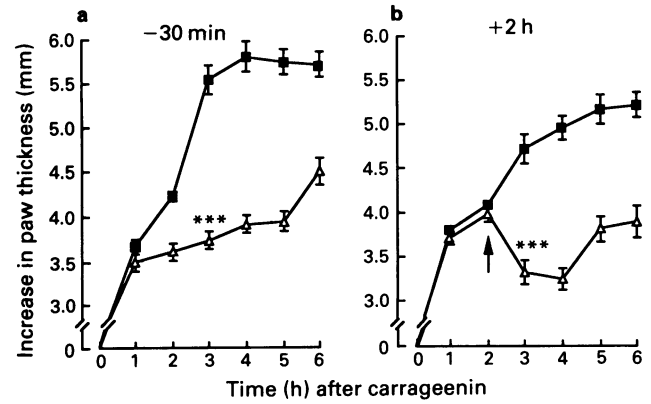

Figure 2 Inhibition of carrageenin-induced paw oedema by BW755C, administered either (a) 30 min before or (b) 2 h after carrageenin, as indicated by an arrow; (■) celacol; (△) BW755C (20 mg kg^{-1}, p.o.). Results expressed as the increase in paw thickness (mm) are shown as mean ± s.e.mean of 5 rats; statistical significance from the celacol group was determined after 3 h (***$P<0.001$).

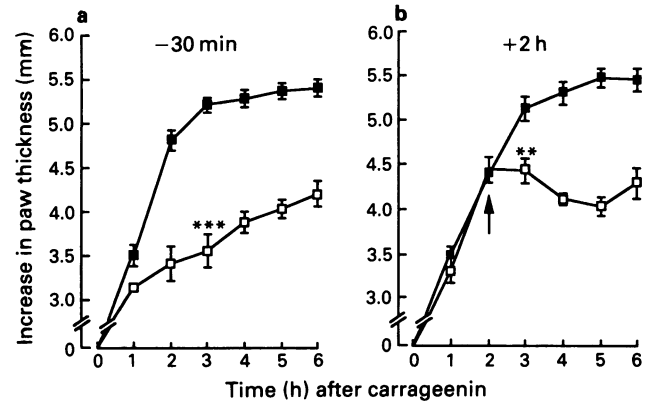

Figure 3 Inhibition of carrageenin-induced paw oedema by superoxide dismutase-polyethylene glycol conjugate (SOD-PEG) administered either (a) 30 min before or (b) 2 h after carrageenin, as indicated by an arrow; (■) saline; (□) SOD-PEG (3 000 u, i.v.). Results expressed as the increase in paw thickness (mm) are shown as mean ± s.e.mean of 6 rats; statistical significance from the saline group was determined after 3 h (***$P<0.001$).

a reduction in paw thickness between 1 and 4 h at doses of 300, 1 000 and 3 000 u of 47 ± 8%, 59 ± 7% and 83 ± 7% respectively ($n = 6$). Furthermore, the high dose of SOD-PEG (3 000 u) caused an apparent reversal of the oedema (Figure 3b).

Plasma SOD-like activity from untreated rats was equivalent to 24 u ml^{-1} SOD ($n = 2$). Immediately after an intravenous bolus injection of SOD-PEG (1 500 u) the activity in plasma rose to 195 ± 10 u ml^{-1} of SOD-like activity which decreased to 137 ± 6 u ml^{-1} after 3 h and 140 ± 5 u ml^{-1} after 6 h ($n = 3$).

Dexamethasone Preatment with dexamethasone (0.1 mg kg^{-1}, i.v.) completely suppressed the increase in paw thickness between 2 and 6 h after carrageenin (Figure 4a). Given 2 h after carrageenin, the glucocorticoid also reduced oedema in a time-dependent manner (Figure 4b).

Colchicine The inhibitor of microtubule activity, colchicine, was used to determine the role of leucocytes in the oedema response to carrageenin. Colchicine (2 mg kg^{-1}, s.c.) inhibited the increase in paw thickness induced by carrageenin. The degree of inhibition was dependent upon the time of pretreatment prior to challenge (Figure 5).

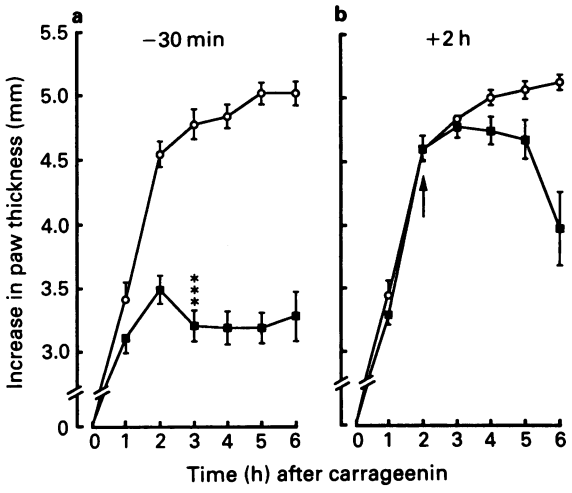

Figure 4 Effect of dexamethasone on carrageenin-induced paw oedema, administered either (a) 30 min before or (b) 2 h after carregeenin, as indicated by an arrow; (○) saline; (■) dexamethasone (0.1 mg kg^{-1}, i.m.). Results expressed as the increase in paw thickness (mm) are shown as mean ± s.e.mean of 6 rats; statistical significance from the saline group was determined after 3 h (***$P<0.001$).

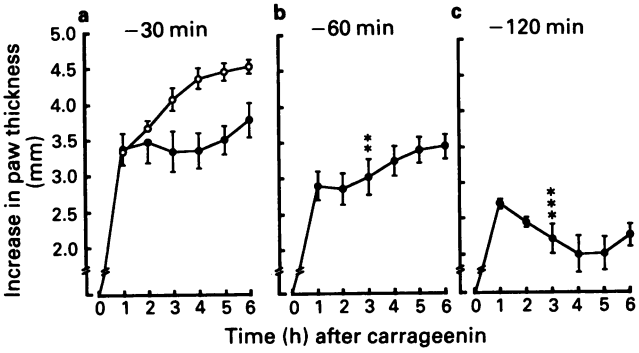

Figure 5 Effect of colchicine on carrageenin-induced paw oedema, administered (a) 30 min, (b) 60 min and (c) 120 min before carrageenin; (○) saline; (●) colchicine 2 mg kg^{-1}, s.c. Results expressed as the increase in paw thickness (mm) are shown as mean ± s.e.mean of 6 rats; statistical significance from the saline group was determined after 3 h (**$P<0.01$, ***$P<0.001$).

Dermal reverse passive Arthus reaction

The induction of the RPA response, by intravenous antigen and intradermal antibody, resulted in a substantial increase in plasma leakage within 90 min (68 ± 6 μl plasma/site, $n = 30$, $P < 0.001$ compared to saline-injected sites). Dermal administration of antibody (50 μg) in the absence of antigen ($n = 3$) or saline injection (50 μl) produced minimal plasma leakage (< 10 μl, $n = 20$).

Table 1 The effect of inhibitors of arachidonic acid metabolism on plasma leakage in the rat dermal reverse passive Arthus (RPA) reaction

Compound	Dose (mg kg^{-1})	Route	Pretreatment time	% control plasma leakage	n
Indomethacin	5	p.o.	1 h	103 ± 17	(8)
BWB70C	10	p.o.	1 h	149 ± 10	(8)
	100	p.o.	1 h	105 ± 24	(3)
Indomethacin + BWB70C	5 10	p.o.	1 h	106 ± 11	(5)
MK-886	10	p.o.	4 h	136 ± 11	(4)
Dexamethasone	0.1	s.c.	2 h	9 ± 1**	(4)

Drugs were administered prior to induction of the RPA reaction as shown by the pretreatment time. Results are expressed as percentage of the plasma leakage in RPA sites from control rats as mean ± s.e.mean of (n) rats. The data are from three separate experiments and statistical significance of inhibition was calculated by comparison with the appropriate control group before normalization to percentage control (**$P < 0.01$).

Cyclo-oxygenase and 5-lipoxygenase inhibition Pretreatment (1 h) with indomethacin (5 mg kg^{-1}, p.o.) or BWB70C (10 mg kg^{-1}, p.o.), either alone or in combination, did not reduce the plasma leakage in the RPA sites (Table 1). A higher dose of BWB70C (100 mg kg^{-1}, p.o.) or MK-886 (10 mg kg^{-1}, p.o., 4 h prior to challenge) also failed to inhibit plasma leakage (Table 1).

BW755C Pretreatment (1 h) with BW755C (25–100 mg kg^{-1}, p.o.) produced a dose-dependent reduction in plasma leakage in RPA sites (Figure 6a). At the highest dose (100 mg kg^{-1}, p.o.) the plasma leakage in RPA sites was not significantly different from that produced by the saline injected sites ($P < 0.001$; $n = 5$).

SOD-PEG and desferrioxamine SOD-PEG (300–3 000 u, i.v. 1 min prior to challenge) dose-dependently reduced plasma leakage in RPA sites (Figure 6b), producing a 53 ± 9% inhibition ($P < 0.01$; $n = 4$–8) of plasma leakage at the highest dose (3 000 u, i.v.) The vehicle (PEG 200 nmol, i.v.) had no significant effect on plasma leakage in RPA sites (73 ± 10 μl; $n = 7$) compared to RPA sites in rats receiving only saline (64 ± 9 μl; $n = 4$). The iron chelator and peroxyl radical scavenger, desferrioxamine (200 mg kg^{-1}, s.c. 1 h prior to challenge) also significantly inhibited plasma leakage (44 ± 12% inhibition, $n = 6$, $P < 0.01$).

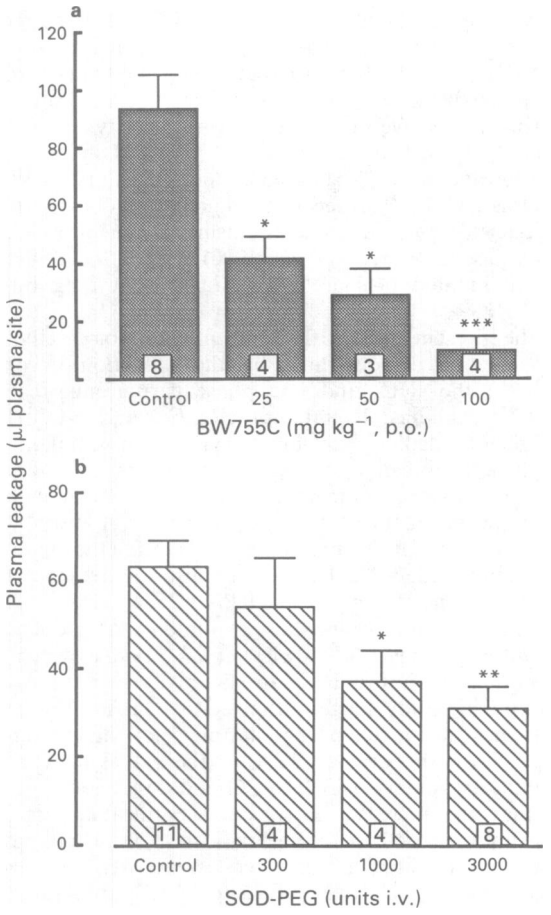

Figure 6 Dose-dependent inhibition of plasma leakage in the rat dermal reverse passive Arthus (RPA) reaction by (a) BW755C (25–100 mg kg^{-1}) and (b) superoxide dismutase-polyethylene glycol conjugate (SOD-PEG, 300–3 000 u). Results expressed as μl plasma leakage per site are shown as mean ± s.e.mean of n (number in column) rats, where statistically significant difference from control animals is shown as *$P < 0.05$; **$P < 0.01$; ***$P < 0.001$.

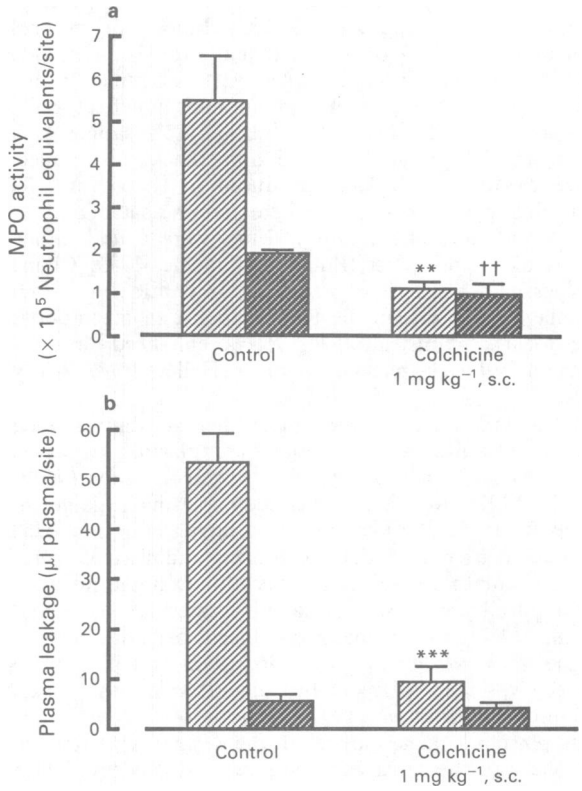

Figure 7 Effect of colchicine (1 mg kg^{-1}, s.c.) on (a) neutrophil infiltration, measured by myeloperoxidase (MPO) activity, (b) plasma leakage, in reverse passive Arthus reaction (RPA) (light columns) and saline (dark columns) injected sites. MPO levels were expressed as neutrophil equivalents, from values obtained from a standard curve constructed with known numbers of rat peritoneal neutrophils. Results are shown as mean ± s.e.mean of 7–8 rats. Statistical significance compared to the RPA response in control rats is shown as **$P < 0.01$, ***$P < 0.001$ and compared to the saline injected site in control rats as ††$P < 0.01$.

Dexamethasone Administration of dexamethasone (0.1 mg kg^{-1}, s.c.) 2 h before induction of the RPA reaction significantly reduced plasma leakage (91 ± 1% inhibition, $n = 4$; $P < 0.01$; Table 1).

Colchicine Colchicine (1 mg kg^{-1}, s.c. 2 h prior to challenge) inhibited neutrophil accumulation in the RPA reaction by 80 ± 4% ($P < 0.01$; $n = 7-8$), as measured by MPO activity (Figure 7a). The MPO activity in the saline-injected sites was also lower in the colchicine-treated group than in the controls. The decreased MPO activity in colchicine-treated animals is unlikely to be due to a direct inhibitory activity of colchicine on the enzyme or assay system, as colchicine (10 μg ml^{-1}) had no effect on MPO activity from rat peritoneal neutrophils *in vitro* (data not shown). In a parallel experiment (Figure 7b) colchicine administration significantly inhibited plasma leakage in RPA sites by 83 ± 5% ($P < 0.001$; $n = 7$).

Discussion

The present study provides strong evidence for an important role of oxygen radicals in the plasma leakage produced during the dermal reverse passive Arthus reaction (RPA) and in the oedema induced by carrageenin in the rat paw. Furthermore, the data suggest that arachidonic acid cyclo-oxygenase (CO) and 5-lipoxygenase (5-LO) products do not contribute to the increases in plasma leakage in the dermal RPA or the later phase of the carrageenin paw oedema.

Carrageenin paw oedema has been used extensively to evaluate non-steroid anti-inflammatory drugs and the activity of these compounds is closely related to their potency as inhibitors of CO (Higgs *et al.*, 1983). Indeed, in the present study pretreatment with indomethacin abolished the oedema induced by carrageenin. However, administration of indomethacin 2 h after carrageenin had no effect on paw oedema, confirming previous studies by Holsapple & Yim (1984). In the present study, indomethacin also failed to reduce the plasma leakage produced in the dermal RPA, confirming previous studies where indomethacin and other non steroid anti-inflammatory drugs were found either to have weak or no effect (Pflum & Graeme, 1979; Chang & Otterness, 1981; Carter *et al.*, 1982). In contrast, prostaglandins may play a role in the RPA response in the rabbit skin since local administration of PGE_2 enhanced, and indomethacin reduced, plasma leakage (Hellewell & Williams, 1987).

At the inflammatory site where there is damaged endothelium, vasodilators may potentiate plasma leakage and hence oedema formation by increasing blood flow (Williams & Peck, 1977). In the present study, plasma leakage in rat dermal RPA and the later phase of carrageenin paw oedema appeared to be independent of prostaglandins, and therefore other vasodilators may be involved, for example nitric oxide (NO). Indeed, recent studies have indicated a role for NO in substance P- and carrageenin-induced oedema in the rat (Hughes *et al.*, 1990; Ialenti *et al.*, 1992) and in endotoxin-induced vascular permeability changes in the intestine (Boughton-Smith *et al.*, 1992).

The plasma leakage induced in the dermal RPA and in the later phase of the carrageenin-induced paw oedema has been proposed to be neutrophil-dependent (Humphrey, 1955). This mechanism of action is supported in the present study by the inhibition with colchicine (an inhibitor of microtubule activity that prevents leucocyte motility) of neutrophil infiltration and plasma leakage in dermal RPA and carrageenin-induced paw oedema. Although LTB_4 is thought to be a major mediator of neutrophil accumulation and plasma leakage in man and rabbit (for review, see Higgs *et al.*, 1984), both the selective 5-LO inhibitor BWB70C and the 5-lipoxygenase activating protein (FLAP) inhibitor MK-886 failed to reduce the plasma leakage in the dermal RPA at doses that markedly inhibit leukotriene synthesis *in vivo* (Salmon *et al.*, 1989; Gillard *et al.*, 1989). BWB70C was also without effect on the carrageenin-induced paw oedema, confirming previous studies with other selective 5-LO inhibitors (Higgs *et al.*, 1988). Although Namiki *et al.* (1986) reported that LTB_4 was chemotactic for rat neutrophils *in vitro*, others have failed to demonstrate such an effect (Kreisle *et al.*, 1985, Kopp *et al.*, 1985). Moreover, binding studies suggest that rat neutrophils lack the low affinity LTB_4 receptor which is thought to mediate chemotaxis (Kreisle *et al.*, 1985), which therefore may explain the lack of activity of 5-LO inhibitors in these neutrophil-dependent models of inflammation.

The 'dual inhibitor' of CO and LO, BW755C, reduced paw oedema when administered either before or after carrageenin. In addition, BW755C produced a dose-dependent inhibition of plasma exudation in the dermal RPA. The effect of BW755C given before carrageenin may be mediated via CO inhibition since pretreatment with indomethacin was also effective. However, the anti-inflammatory effect of BW755C when given after carrageenin and in the RPA was independent of 5-LO and CO as the combination of BWB70C and indomethacin failed to inhibit these responses. BW755C also inhibits the 12-LO and 15-LO pathways of arachidonic acid metabolism (Randall *et al.*, 1980). Since these enzymes would not be inhibited by the combination of BWB70C and indomethacin at the doses used, the anti-inflammatory activity of BW755C may have been due to inhibition of 12-LO or 15-LO. However, the anti-inflammatory activity of BW755C may also be mediated by its anti-oxidant activity (Marnett *et al.*, 1982; Pekoe *et al.*, 1982). This mechanism is supported by the ability of both SOD-PEG, and desferrioxamine to attenuate vascular leakage in dermal RPA. Also, SOD-PEG, like BW755C, reduced oedema when administered either before or after carrageenin. SOD has previously been shown to have anti-inflammatory activity in both carrageenin paw oedema (Oyanagui, 1976) and in rat dermal RPA (Petrone *et al.*, 1980; McCormick *et al.*, 1981; Warren *et al.*, 1987; 1990). Furthermore, Fligiel *et al.* (1984) reported that desferrioxamine attenuated plasma leakage in rat dermal RPA, although Warren *et al.* (1990) found that desferrioxamine attenuated plasma leakage in the rat lung but not dermal RPA.

In the present study, the anti-inflammatory activity of dexamethasone demonstrated by the reduction in plasma leakage in the RPA and late phase carrageenin reactions cannot be explained by inhibition of CO and 5-LO. However, glucocorticoids, via inhibition of phospholipase A_2 through induction of lipocortin, will also inhibit 12-LO and 15-LO pathways of arachidonic acid metabolism and also prevent the production of PAF (for review, Flower, 1989), which may account for the activity of dexamethasone in the present study. Indeed a PAF antagonist suppressed oedema formation in the rabbit dermal RPA (Hellewell & Williams, 1986). In addition, dexamethasone inhibits the induction of NO synthase *in vivo* (Knowles *et al.*, 1990), which may contribute to its anti-inflammatory activity in these models.

The present study suggests that neither prostaglandins nor leukotrienes have a role in the later phase of carrageenin paw oedema or in the dermal RPA in the rat skin. The anti-inflammatory activity of SOD-PEG and desferrioxamine suggests that the increases in vascular permeability in these models are mediated by oxygen radicals. The results presented illustrate qualitative differences in activity between the combination of selective CO and 5-LO inhibitors and BW755C, a so-called dual inhibitor of CO and 5-LO. Indeed, the activity of BW755C in the present study is best explained as being due to CO inhibition, for the initial suppression of carrageenin paw oedema, while activity as a scavenger of oxygen radicals may account for inhibition of the subsequent phases, as well as its activity in dermal RPA. Previous studies on the prevention of gastric mucosal injury in the rat by

BW755C have also indicated that this action is independent of CO and 5-LO inhibition (Boughton-Smith & Whittle, 1988). These observations illustrate clearly that the use of BW755C to evaluate the role of leukotrienes in models of inflammation is potentially misleading, and therefore should be discontinued. These findings also suggest that the rat dermal RPA and the later phases of the carrageenin paw oedema may be suitable models for the *in vivo* assessment of the anti-inflammatory actions of novel anti-oxidants and inhibitors of oxygen radical generation.

References

BOUGHTON-SMITH, N.K., BERRY, S., EVANS, S.M., WHITTLE, B.J.R. & MONCADA, S. (1992). Intestinal damage and the induction of nitric oxide synthase by endotoxin in the rat. *Br. J. Pharmacol.*, **107**, 79P.

BOUGHTON-SMITH, N.K. & WHITTLE, B.J.R. (1988). Failure of the inhibition of rat gastric mucosal 5-lipoxygenase by novel acetohydroxamic acids to prevent ethanol-induced damage. *Br. J. Pharmacol.*, **95**, 155–162.

BRADLEY, P.P., PRIEBAT, D.A., CHRISTENSEN, R.D. & ROTHSTEIN, G. (1982). Measurement of cutaneous inflammation. Estimation of neutrophil content with an enzyme marker. *J. Invest. Dermatol.*, **78**, 206–209.

CARTER, G.W., MARTIN, M.K., KRAUSE, R.A. & YOUNG, P.R. (1982). The effects of anti-inflammatory and other agents on the rat dermal arthus reaction. *Res. Commun. Chem. Pathol. Pharmacol.*, **35**, 189–207.

CHANG, Y.-H. & OTTERNESS, I.G. (1981). Effects of pharmacological agents on the reversed passive Arthus reaction in the rat. *Eur. J. Pharmacol.*, **69**, 155–164.

FANTONE, J.C. & WARD, P.A. (1982). Role of oxygen-derived free radicals and metabolites in leukocyte-dependent inflammatory reactions. *Am. J. Pathol.*, **107**, 397–418.

FLOWER, R.J. (1989). Lipocortin. *Biochem. Soc. Trans.*, **17**, 276–278.

FLIGIEL, S.E.G., WARD, P.A., JOHNSON, K.J. & TILL, G.O. (1984). Evidence for a role of hydroxyl radical in immune-complex-induced vasculitis. *Am. J. Pathol.*, **115**, 375–382.

GILLARD, J., FORD-HUTCHINSON, A.W., CHAN, C., CHARLESON, S., DENIS, D., FOSTER, A., FORTIN, R., LEGER, S., MCFARLANE, C.S., MORTON, H., PIECHUTA, H., RIENDEAU, D., ROUZER, C.A., ROKACH, J., YOUNG, R., MACINTYRE, D.E., PETERSON, L., BACH, T., EIERMANN, G., HOPPLE, S., HUMES, J., HUPE, L., LUELL, S., METZGER, J., MEURER, R., MILLER, D.K., OPAS, E. & PACHOLOK, S. (1989). L-663,536 (MK-886) (3-(1-(4-chlorobenzyl)-3-t-butyl-thio-5-isopropylindol-2-yl)-2,2-dimethylpropanoic acid), a novel, orally active leukotriene biosynthesis inhibitor. *Can. J. Physiol. Pharmacol.*, **67**, 456–464.

HELLEWELL, P.G. & WILLIAMS, T.J. (1986). A specific antagonist of platelet-activating factor suppresses oedema formation in an arthus reaction but not oedema induced by leukocyte chemoattractants in rabbit skin. *J. Immunol.*, **137**, 302–307.

HELLEWELL, P.G. & WILLIAMS, T.J. (1987). Interaction between eicosanoids and other mediators of inflammation. In *Eicosanoids in Inflammatory Conditions of the Lung, Skin and Joints*. ed. Church, M. & Robinson, C. pp. 43–65. *Adv. Eicosanoid Res.*, Lancester: MTP Press.

HIGGS, G.A., FLOWER, R.J. & VANE, J.R. (1979). A new approach to anti-inflammatory drugs. *Biochem. Pharmacol.*, **28**, 1959–1961.

HIGGS, G.A., FOLLENFANT, R.L. & GARLAND, L.G. (1988). Selective inhibitors of arachidonate 5-lipoxygenase by novel acetohydroxamic acids: effects on acute inflammatory responses. *Br. J. Pharmacol.*, **94**, 547–551.

HIGGS, G.A., MONCADA, S. & VANE, J.R. (1983). The mode of action of anti-inflammatory drugs which prevent the peroxidation of arachidonic acid. In *Anti-rheumatic Drugs*. pp. 11–36. ed. Huskisson, E.C. Praeger: Praeger Publishers.

HIGGS, G.A., MONCADA, S. & VANE, J.R. (1984). Eicosanoids and inflammation. *Ann. Clin. Res.*, **16**, 287–299.

HOLSAPPLE, M.P. & YIM, G.K.W. (1984). Therapeutic reduction of ongoing carrageenin-induced inflammation by lipoxygenase, but not cyclooxygenase inhibitors. *Inflammation*, **8**, 223–229.

HUGHES, S.R., WILLIAMS, T.J. & BRAIN, S.D. (1990). Evidence that endogenous nitric oxide modulates oedema formation induced by substance P. *Eur. J. Pharmacol.*, **191**, 481–484.

HUMPHREY, J.H. (1955). The mechanism of Arthus Reactions II. The role of PMN leukocytes and platelets in reversed passive Arthus reaction in the guinea-pig. *Br. J. Exp. Pathol.*, **36**, 283–289.

IALENTI, A., IANARO, A., MONCADA, S. & DI ROSA, M. (1992). Modulation of acute inflammation by endogenous nitric oxide. *Eur. J. Pharmacol.*, **211**, 177–182.

KNOWLES, R.G., SALTER, M., BROOKS, S.L. & MONCADA, S. (1990). Anti-inflammatory glucocorticoids inhibit the induction by endotoxin of nitric oxide synthase in the lung, liver and aorta of the rat. *Biochem. Biophys. Res. Commun.*, **172**, 1042–1048.

KOPP, D.E., ESSER, B., TASHOFF, T., GOLDMAN, D.W., GOETZL, E.J. & LEMANSKE, R.F. (1986). *In vivo* and *in vitro* assessment of the role of leukotriene B_4 as a mediator of rat cutaneous late-phase reactions. *J. Allergy Clin. Immunol.*, **77**, 302–308.

KREISLE, R.A., PARKER, C.W., GRIFFIN, G.L., SENIOR, R.M. & STENSON, W. (1985). Studies of leukotriene B_4-specific binding and function in rat polymorphonuclear leucocytes: absence of a chemotactic response. *J. Immunol.*, **134**, 3356–3363.

LEWIS, R.A., AUSTEN, K.F. & SOBERMAN, R.J. (1990). Leukotrienes and other products of the 5-lipoxygenase pathway – biochemistry and relation to pathobiology in human diseases. *N. Engl. J. Med.*, **323**, 645–655.

MARNETT, L.J., SIEDLIK, P.H. & FUNG, W.M. (1982). Oxidation of phenidone and BW755C by prostaglandin endoperoxide synthase. *J. Biol. Chem.*, **257**, 6957–6964.

MCCALL, T.B., BOUGHTON-SMITH, N.K., PALMER, R.M.J., WHITTLE, B.J.R. & MONCADA, S. (1989). Synthesis of nitric oxide from L-arginine by neutrophils. Release and interaction with superoxide anion. *Biochem. J.*, **261**, 293–296.

MCCORMICK, J.R., HARKIN, M.M., JOHNSON, K.J. & WARD, P.A. (1981). Suppression by superoxide dismutase of immune-complex induced pulmonary alveolitis and dermal inflammation. *Am. J. Pathol.*, **102**, 55–61.

NAMIKI, M., IGARASHI, Y., SAKAMOTO, K., NAKAMURA, T. & KOGA, Y. (1986). Pharmacological profiles of a potential LTB_4 antagonist, SM-9064. *Biochem. Biophys. Res. Commun.*, **138**, 540–546.

OYANAGUI, Y. (1976). Participation of superoxide anions at the prostaglandin phase of carrageenin foot-oedema. *Biochem. Pharmacol.*, **25**, 1465–1472.

PEKOE, G., VAN-DYKE, K., PEDEN, D., MENGOLI, H. & ENGLISH, D. (1982). Antioxidant theory of non-steroidal anti-inflammatory drugs based upon the inhibition of luminol-enhanced chemiluminescence from the myeloperoxidase reaction. *Agents Actions*, **12**, 371–376.

PETRONE, W.F., ENGLISH, D.K., WONG, K. & MCCORD, J.M. (1980). Free radicals and inflammation: superoxide-dependent activation of a neutrophil chemotactic factor in plasma. *Proc. Natl. Acad. Sci. U.S.A.*, **77**, 1159–1163.

PFLUM, L. & GRAEME, M.L. (1979). The Arthus reaction in rats, a possible test for anti-inflammatory and antirheumatic drugs. *Agents Actions*, **9**, 184–189.

RANDALL, R.W., EAKINS, K.E., HIGGS, G.A., SALMON, J.A. & TATESON, J.E. (1980). Inhibition of arachidonic acid cyclooxygenase and lipoxygenase activities by indomethacin and compound BW755C. *Agents Actions*, **10**, 553–555.

SALMON, J.A. (1986). Inhibition of prostaglandin, thromboxane and leukotriene biosynthesis. *Adv. Drug Res.*, **15**, 111–167.

SALMON, J.A., JACKSON, W.P. & GARLAND, L.G. (1989). Inhibition of 5-lipoxygenase: development of hydroxamic acids and hydroxyureas as potential therapeutic agents. *Adv. Prostaglandin Thromboxane Leukot. Res.*, **21A**, 109–112.

SCHRAUFSTATTER, I.U., HYSLOP, P.A., JACKSON, J. & COCHRANE, C.C. (1987). Oxidant injury of cells. *Int. J. Tissue React.*, **9**, 317–324.

WARD, P.A. (1991). Mechanisms of endothelial cell injury. *J. Lab. Clin. Med.*, **118**, 421–425.

WARREN, J.S., WARD, P.A., JOHNSON, K.J. & GINGSBERG, I. (1987). Modulation of acute immune complex-mediated tissue injury in the presence of polyionic substances. *Am. J. Pathol.*, **128**, 67–77.

WARREN, J.S., YABROFF, K.R., MANDEL, D.M., JOHNSON, K.J. & WARD, P.A. (1990). Role of O_2^- in neutrophil recruitment into sites of dermal and pulmonary vasculitis. *Free Rad. Biol. Med.*, **8**, 163–172.

WEDMORE, C.V. & WILLIAMS, T.J. (1981). Control of vascular permeability by polymorphonuclear leukocytes in inflammation. *Nature*, **289**, 646–650.

WILLIAMS, T.J. & PECK, M.J. (1977). Role of prostaglandin-mediated vasodilatation in inflammation. *Nature*, **270**, 530–532.

(Received March 17, 1993
Revised June 1, 1993
Accepted June 15, 1993)

Br. J. Pharmacol. (1993), **110**, 903–909

Electrophysiological actions of alfentanil: intracellular studies in the rat locus coeruleus neurones

[1]T.H. Chiu, M.H. Yeh, *S.K. Tsai & †M.S. Mok

Departments of Physiology & *Anaesthesiology, National Yang-Ming Medical College, Shih-Pai, Taipei, Taiwan and Department of †Anaesthesiology, USC School of Medicine, LAC-USC Medical Center, Los Angeles, California 90033, U.S.A.

1 The electrophysiological effects of alfentanil on 156 neurones of the rat locus coeruleus were investigated by use of intracellular recordings from the *in vitro* brain slice preparation.

2 Bath application of alfentanil (5–100 nM) reversibly decreased the firing rate of all neurones tested in a dose-dependent manner, with an IC_{50} 4.1 nM.

3 Based on inhibition of the spontaneous firing rate, alfentanil was 22 times more potent than morphine.

4 At 100 nM, alfentanil produced a complete inhibition of firing of all neurones tested ($n = 62$); the inhibition was accompanied by a membrane hyperpolarization 17.0 ± 0.8 mV (range 6.1–30.3 mV, $n = 62$) and a reduction in input resistance $26.4 \pm 1.7\%$ (range 6.5–53%, $n = 51$).

5 The effects of alfentanil were antagonized by naloxone, with a dissociation equilibrium constant of 2.7 ± 0.4 nM ($n = 6$).

6 The reversal potential for the alfentanil-induced hyperpolarization was -110 ± 2 mV ($n = 9$), which is approximately the potassium equilibrium potential.

7 The alfentanil-induced hyperpolarization was blocked by caesium chloride and barium chloride.

8 These results indicate that alfentanil binds to μ-opioid receptors on the cell membrane of neurones of the locus coeruleus. This leads to opening of the inward-going rectification potassium channels, resulting in the observed hyperpolarization of the membrane.

Keywords: Alfentanil; locus coeruleus; brain slice; intracellular recording; μ-opioid receptors; potassium channels

Introduction

The 4-anilinopiperidine series of analgesic/anaesthetics are potent, synthetic opioids which are structurally and physicochemically dissimilar from morphine. Of this series alfentanil, fentanyl and sufentanil are representative compounds (Cookson *et al.*, 1983). In recent years, agents of this novel class have become extremely popular in clinical anaesthesia because of the superior analgesic potency and cardiovascular stability that they provide (Sebel *et al.*, 1982). According to animal studies, the analgesic potency of alfentanil is 30 to 73 times greater than morphine, one fourth as great as fentanyl, and one sixty-sixth as great as sufentanil (Niemegeer & Janssen, 1981; Janssen, 1984). Studies of *in vitro* receptor binding have shown that these 4-anilinopiperidine derivatives possess high opiate receptor affinities, primarily at the μ-receptor site (Leysen *et al.*, 1983). Little is known about the mechanism of action of anilinopiperidine derivatives in the central nervous system.

The hippocampal formation is the most commonly used brain structure for the study of anaesthetic effects, which have been extensively described both *in vivo* and *in vitro* (for a review, see Pocock & Richards, 1991). We have conducted a detailed assessment of the actions of alfentanil on neurones of locus coeruleus (LC) using intracellular recording analysis techniques. The LC brain slice was the subject of the present investigation for three reasons. First, the LC contains the greatest concentration of noradrenergic cell bodies in the central nervous system (CNS), with projections from this small pontine nucleus responsible for more than half the noradrenaline in the brain (Amaral & Sinnamon, 1977). Since the LC has extensive projections to many CNS areas, alterations of the activity of LC neurones would be expected to cause widespread effects in CNS. Second, immunocytochemical and immunofluorescent studies showed that nerve terminals that contain opioid peptides innervate neurones of the LC (Finley *et al.*, 1981; Léger *et al.*, 1983). Electrophysiological studies also indicate that opioid receptors in the LC are of the μ type (Williams & North, 1984; North, 1986). Third, the LC is the primary origin of descending noradrenergic analgesic fibres (for reviews see Proudfit, 1988; Lipp, 1991; Jones, 1991). Electrophysiological studies have provided strong evidence for a role of LC in modulating analgesia. Lesions of the LC impair the ability of morphine to suppress responses to electrical stimuli of the rat fore paw (Sasa *et al.*, 1977), and analgesia induced by electrical stimulation of LC neurones has been demonstrated in several studies (see Proudfit, 1988 for references). Furthermore, microinjection studies have identified several brain regions as important in mediating opiate analgesia, including the periaqueductal gray, LC, nucleus raphe magnus and nucleus reticularis gigantocellularis (see Bodnar *et al.*, 1988 for references). Bodnar *et al.* (1988) also observed profound analgesia following the microinjection of morphine into these four brain regions and further claimed that morphine analgesia was more potent in the LC than in the periaqueductal gray. Recently, synergistic analgesic interactions between these supraspinal analgesic systems have been reported and nucleus raphe magnus is suggested to form a relay or the final common pathway for opioid-induced supraspinal analgesia (Bodnar *et al.*, 1991; Lipp, 1991; Rossi *et al.*, 1992).

Methods

Preparation and maintenance of slices of locus coeruleus

The methods used to prepare and maintain slices of locus coeruleus of the rat were similar to those previously described (Shefner & Chiu, 1986; Chiu *et al.*, 1990). In brief,

[1] Author for correspondence at: Department of Physiology, National Yang-Ming Medical College, Shih-Pai, Taipei, Taiwan.

male Sprague-Dawley rats (120–200 g) were anaesthetized with ether and their brains were rapidly removed. A block of tissue containing the pons was excised and attached to a small Plexiglass stage with cyanoacrylate glue; an agar block, next to the tissue, served to support it during sectioning. The tissue was then submerged in oxygenated artificial cerebrospinal fluid (artificial CSF), maintained at 3–5°C, in the well of a Lancer 1000 vibratome and coronal slices of pons (300–350 μm thick) were cut. A slice containing a cross-section through the caudal end of the locus coeruleus was mounted in the recording chamber and allowed to equilibrate for 1 h. The recording chamber consisted of a Plexiglass bath (0.3 ml) with a nylon net stretched tightly across it. The slice was placed on a square of lens paper on top of the net and an electron microscopy grid, held down by platinum wires, was placed over the locus coeruleus to keep the slice from floating. The slice was completely submerged in artificial CSF of the following composition (mM): NaCl 126, KCl 2.5, NaH_2PO_4 1.2, $NaHCO_3$ 26.2, $MgCl_2$ 1.3, $CaCl_2$ 2.4, glucose 11.1 (saturated with 95% O_2/5% CO_2, pH = 7.4). The temperature of the artificial CSF was 33–34°C and the flow rate was 2.3 ml min^{-1}.

Intracellular recording

The slice was viewed from above through a dissection microscope. In the trans-illuminated slice, the locus coeruleus is seen as a translucent area lying on the lateral aspect of the periventricular gray, below the fourth ventricle. Recording microelectrodes, filled with KCl (2 M) and having d.c. tip resistance 40–70 MΩ, were used. They were inserted into the locus coeruleus under visual control. Intracellular potentials were recorded by an amplifier with an active bridge circuit, allowing the injection of current through the recording electrode (WPI M707). Current and voltage traces were displayed on a storage oscilloscope (Textronix 5113) and a rectilinear pen recorder (Gould 2400). Input resistance was measured by passing pulses of hyperpolarizing current of varied amplitudes; the resulting alterations of voltage were measured and voltage-current (V/I) curves were constructed. Current pulses were of sufficient duration (250–300 ms) to charge fully the membrane capacitance and to reach a steady-state voltage deflection.

Perfusion of solutions and drugs

A valve system was used to switch solutions, superfusing the preparation, from control artificial CSF to CSF which contained drugs. The period required for test solutions to reach the chamber was known and was in the range 25–35 s. Equilibration to the full concentration of the drug in the chamber took approximately 2.5 min. Drugs were administered for a sufficient period to reach a steady-state response and the effects were observed at 5 min or longer, after the beginning of infusion of the drug.

Drugs

The following drugs were used: alfentanil hydrochloride (Janssen), morphine sulphate (Narcotics Bureau, Taiwan), naloxone hydrochloride, caesium chloride and barium chloride (Sigma). Numerical data are expressed as mean ± standard error of the mean (s.e..mean).

Results

The present results are based on recordings made from 156 locus coeruleus neurones in total, with stable intracellular impalements. These cells had resting membrane potentials of − 50– − 71.7 mV (− 60.7 ± 0.4 mV, $n = 156$) and apparent input resistance of 101–362 MΩ (161 ± 5 MΩ, $n = 141$). They fired spontaneously from 0.4 to 3.8 Hz (2.2 ± 0.1 Hz, $n = 156$), with a regular interspike interval characteristic of neurones of the locus coeruleus in the slice preparation (Williams *et al.*, 1984).

Alfentanil responses

Alfentanil (5–100 nM) reversibly decreased the firing rate of all neurones of the locus coeruleus tested. Although neurones varied in their sensitivity to alfentanil, the inhibition of firing rate, hyperpolarization of the membrane potential and reduction in input resistance depended on concentration (Figure 1). The most sensitive of these effects, which caused a remarkable change even at small alfentanil concentrations, was decrease of the firing rate. At 5 and 10 nM alfentanil, which respectively gave 58% ($n = 14$, including 3 cells in which firing was completely suppressed) and 76% ($n = 29$, including 12 cells in which firing was completely suppressed) inhibition of the neuronal firing rate, little hyperpolarization and small reduction of input resistance of the neurones were seen. Larger concentrations of alfentanil (30 and 50 nM) caused not only greater inhibition of firing but also hyperpolarization of the membrane potential and decreased input resistance. There was considerable variation of the size of hyperpolarizations and reductions of input resistance induced by the same concentration of alfentanil in different neurones. For instance, the amplitudes of hyperpolarization and reduction of input resistance in response to 30 nM alfentanil were in the range 0–18 mV (9.1 ± 0.7 mV, $n = 47$) and from 0 to 37% (12.7 ± 1.4%, $n = 40$), respectively. At 100 nM, alfentanil produced complete inhibition of firing of all neurones tested ($n = 62$); the inhibition was associated with a 17 mV hyperpolarization (range 6.1–30.3 mV, $n = 62$) and a 26% reduction in input resistance (range 6.5–53%, $n = 51$). Because locus coeruleus neurones have a pronounced inward rectification, we demonstrated that the decrease of input resistance observed as an effect of alfentanil was not due to membrane rectification induced by the hyperpolarization. The resistance decrease persisted when the membrane potential was manually clamped back to its predrug value during the peak of the effect (e.g. Figure 5b).

Comparison of potencies of alfentanil and morphine

Dose-response curves for alfentanil and morphine for the inhibition of firing rate were compared in 5 neurones of the locus coeruleus. The neurones were perfused individually with one of the two drugs at varied concentrations and then with those of the other. Figure 2 shows the results from one cell, in which alfentanil was 21 times more potent than morphine. A comparison of the IC_{50} between alfentanil and morphine in these 5 neurones is listed in Table 1. On average, alfentanil was 22 times more potent than morphine. In three

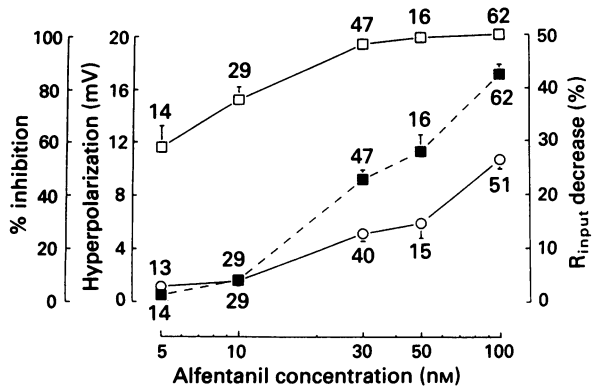

Figure 1 Dose-dependent effects of alfentanil on the firing rate (□), membrane potential (■) and input resistance (○) of neurones of the locus coeruleus. Mean ± s.e.mean is shown for the number of neurones indicated.

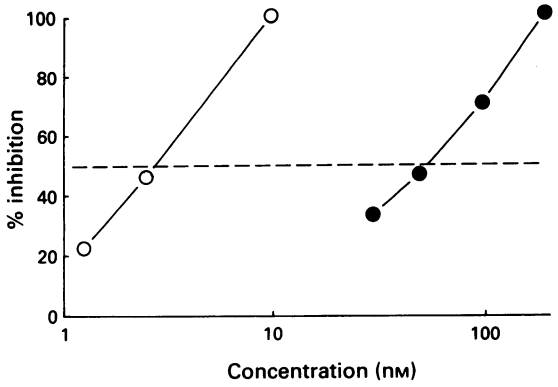

Figure 2 The dose-response curves for alfentanil (○) and morphine (●) were compared on the inhibition of neuronal firing in the locus coeruleus. The IC_{50} is defined as the concentration which gave 50% inhibition of neuronal firing. The calculated IC_{50} of alfentanil, obtained from this figure, was 2.6 nM; that of morphine was 55.2 nM. In this cell, alfentanil was 21 times more potent than morphine.

Table 1 IC_{50} of morphine and alfentanil for inhibition of spontaneous firing of neurones of the locus coeruleus

Cell no.	*IC_{50} of morphine* (nM)	*IC_{50} of alfentanil* (nM)	*IC_{50} ratio* (Morph/Alf)
1	72.9	2.7	27.2
2	59.2	2.3	25.8
3	55.2	2.6	21.0
4	52.1	2.5	20.9
5	32.2	2.6	12.6
Mean ± s.e.mean	54.3 ± 6.6	2.5 ± 0.1	21.5

The dose-response curve of cell 3 is shown in Figure 2.

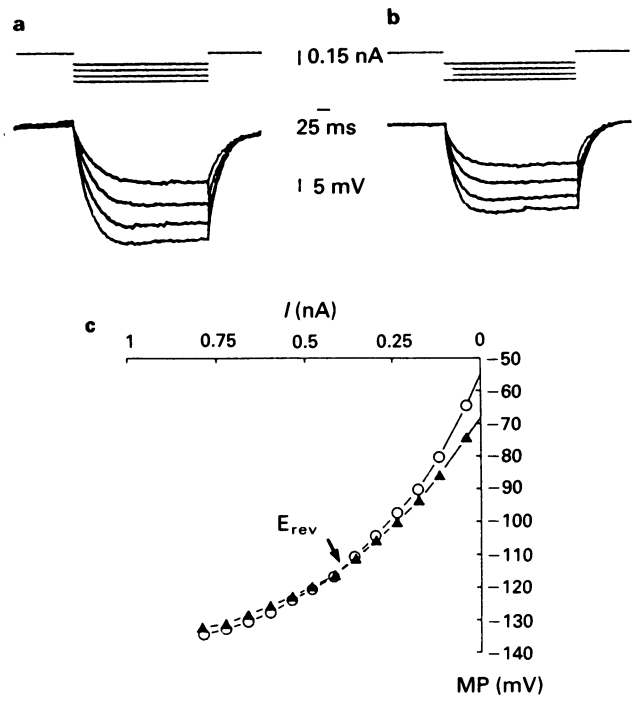

Figure 3 Effect of alfentanil on the current-voltage relationship of a neurone in the locus coeruleus. (a) The injected hyperpolarizing current pulses and the generated electrotonic potentials of the neurone, perfused with normal artificial CSF. (b) The current pulses and electrotonic potentials of the same neurone, perfused with alfentanil (100 nM). (c) Current-voltage curves for this neurone, perfused with (○) control artificial CSF and (▲) alfentanil (100 nM). The arrow indicates the reversal potential, which was − 115 mV in this neurone.

other neurones, alfentanil and morphine at greater concentrations were applied to induce stronger hyperpolarization in the LC neurones. These concentration-dependent hyperpolarizations were used to construct dose-response curves. However, it was generally impracticable to construct full concentration-hyperpolarization sigmoidal curves for both alfentanil and morphine during the course of a recording from a single cell. The rank order of potency of alfentanil and morphine was, therefore, determined by comparing their equieffective concentrations that produced a 15-mV hyperpolarization (the half-maximal response caused by 100 μM normorphine; see Williams & North, 1984). The equieffective concentration of morphine was 25 times greater than that for alfentanil.

Current-voltage relationship before and after perfusion of alfentanil

The current-voltage relationship of the locus coeruleus neurones revealed an anomalous rectification that has been described previously (Andrade & Aghajanian, 1984; Osmanovic & Shefner, 1987; Williams *et al.*, 1988). That the value of the alfentanil reversal potential was so negative made it difficult to reverse alfentanil responses by hyperpolarizing the membrane with d.c. current injection. Instead, the reversal potential for alfentanil-induced hyperpolarization was calculated from the intersection of the control current-voltage curve and the curve obtained in the presence of alfentanil. The relationship between injected current pulses and steady-state membrane potentials is shown in Figure 3c.

After alfentanil administration the slope of the current-voltage curve was reduced throughout the voltage range examined; hence the decreased input resistance elicited by alfentanil resulted not simply from anomalous rectification by the cell membrane. The alfentanil reversal potential ranged from − 101 to − 117 mV; the average was − 110 ± 2 mV ($n = 9$).

Effect of naloxone on reversing the hyperpolarization caused by alfentanil

Perfusion of naloxone (100 nM) produced no significant change of membrane potential or input resistance in neurones of the locus coeruleus. However, a small increase in firing rate was occasionally observed. Pretreatment with naloxone (100 nM) and then changing the perfusate to alfentanil (100 nM), mixed with naloxone (100 nM), eliminated the effects of alfentanil on these neurones. Neither firing rate, membrane potential nor input resistance was altered, compared with the pre-alfentanil state ($n = 4$). In another six neurones, the duration of recording was sufficient to construct concentration-response curves for alfentanil, in the absence and presence of naloxone; an example is presented in Figure 4. Naloxone produced a parallel, dose-related shift to the right of the concentration-response curve for alfentanil. To determine the dissociation equilibrium constants (K_D) for naloxone, we calculated the dose-ratio by dividing the concentration of alfentanil, required to produce a given hyperpolarization in the presence of naloxone, by the concentration of alfentanil, required to give an equal hyperpolarization in the absence of naloxone. These dose-ratios were then used to construct the Schild plots, described by Williams & North (1984). These experiments yielded a K_D value of 2.7 ± 0.4 nM ($n = 6$) for the antagonism of alfentanil-induced hyperpolarizations by naloxone.

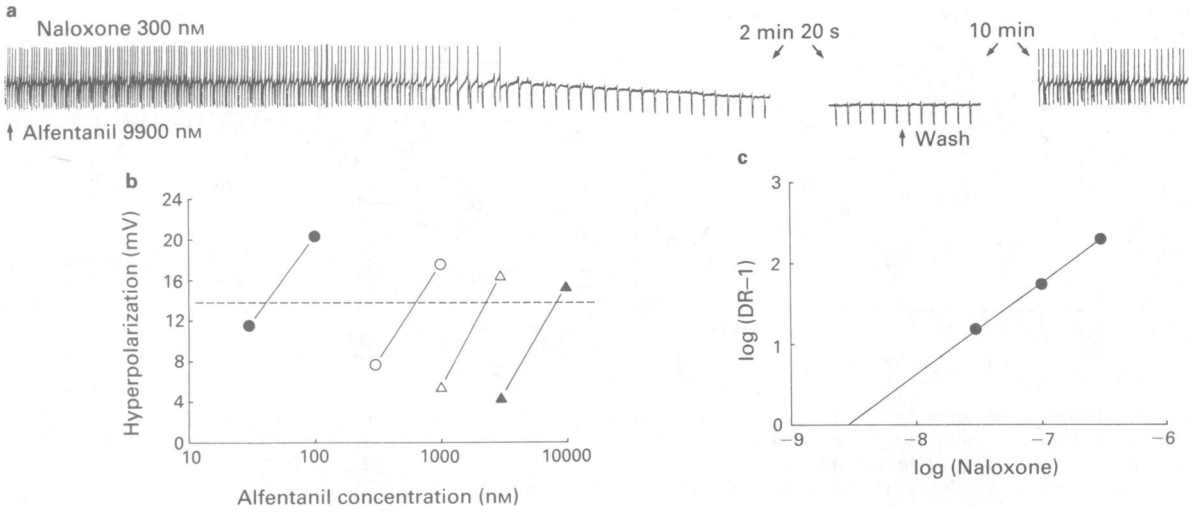

Figure 4 Antagonism by naloxone of alfentanil-induced hyperpolarization. (a) Shows hyperpolarization induced by superfusion of alfentanil (9900 nM) in the presence of naloxone (300 nM). (b) Dose-response curves for alfentanil in the presence of different concentrations of naloxone: control (●); naloxone 30 nM (○); 100 nM (△) and 300 nM (▲). (c) Schild plot of data shown in (b), at a response level 14 mV. The dissociation equilibrium constant was 2.9 nM in this neurone.

Effect of $BaCl_2$ and CsCl on blocking hyperpolarization caused by alfentanil

The blocking effects of barium (0.3 mM) and caesium (3 mM) on alfentanil-induced hyperpolarization were tested in 8 and 5 neurones of the locus coeruleus, respectively. Barium depolarized the membrane and increased the amplitude and duration of the action potential. Caesium also increased the peak amplitude, duration and afterhyperpolarization of the neuronal action potential. As shown in Figure 5b, superfusion with alfentanil (100 nM) for 4.5 min produced complete inhibition of spontaneous firing, hyperpolarization of the membrane potential (16.5 mV) and decreased input resistance (25%). After superfusion with caesium chloride (3 mM) for 25 min, or barium chloride (0.3 mM) for 15 min, the same neurone was challenged with alfentanil (100 nM), again in the presence of caesium (Figure 5c) or barium (Figure 5d). During caesium treatment, alfentanil-induced hyperpolarization still occurred, though to a lesser degree (67% reduction). Barium, on the other hand, completely prevented alfentanil-induced hyperpolarization, but inhibition of spontaneous firing remained (a 37% reduction). In eight neurones tested, barium completely blocked the hyperpolarization caused by alfentanil, but a partial suppression of the baseline firing rate was still observed ($48 \pm 10\%$, $n = 8$). In the caesium-treated neurones, caesium reduced but did not eliminate hyperpolarization of alfentanil. On the average, caesium reduced the alfentanil-induced hyperpolarization by 44% of these five cells.

Discussion

Our investigation provides evidence that alfentanil is able to inhibit the spontaneous firing rate, cause hyperpolarization of the membrane potential and reduce the input resistance of neurones of the locus coeruleus. These findings are consistent with those of previous studies that indicate that many anaesthetic agents reduce the neuronal excitability of central neurones by increasing membrane conductance and producing hyperpolarization (Nicoll & Madison, 1982; Berg-Johnsen & Langmoen, 1987; O'Beirne *et al.*, 1987). The functional significance of this hyperpolarization would be to increase the threshold of impulse initiation and thus to decrease the probability that a cell discharges in response to a given excitatory synaptic input. By use of extracellular single neurone recording, it has been demonstrated that alfentanil inhibited both the spontaneous activity of medullary respiratory neurones in rats (Hewson & Bradley, 1982) and the noxiously evoked activity of cells in the nucleus reticularis gigantocellularis in cats (Yuge *et al.*, 1985). The present results on the spontaneous neuronal activity are compatible with the extracellular findings. We also found that the depressant effects of alfentanil on neurones of the locus coeruleus were more potent than those of morphine. Comparison of the ability of alfentanil and morphine to inhibit neuronal firing in the locus coeruleus showed that alfentanil was 22 times as potent as morphine. Although in some studies no evidence was found of alteration of membrane potential with anaesthetic agent treatment (Weakly, 1969; Zorychta & Capek, 1978; Sawada & Yamamoto, 1985; Richards & Strupinski, 1986), the present results that alfentanil is 25 times as potent as morphine in causing hyperpolarization confirm previous observations that there is a clear correlation between the anaesthetic (or analgesic) potency and the hyperpolarization potency (Nicoll & Madison, 1982, see Figure 1).

The observation that naloxone was able to counteract the inhibitory effect of alfentanil on neurones of the locus coeruleus is consistent with previous reports, which demonstrated that naloxone competitively reversed the effects of opioid substances ([D-Ala^2,*N*-methyl-Phe^4,Gly^5-ol]enkephalin), with a dissociation equilibrium constant in the range 1.5–2 nM (Williams & North, 1984; McFadzean *et al.*, 1987). Our work showed that naloxone antagonized the actions of alfentanil, with a dissociation equilibrium constant about 2.7 nM, which is within the range used to define the μ-opiate receptor (0.5–3 nM, North, 1986) and appears to be much smaller than the antagonistic K_D values for naloxone on δ- and κ-receptors (30 and 15 nM, respectively; North, 1986, Table 1). North *et al.* (1987) also demonstrated that the μ-agonist, and not the δ-agonist, caused hyperpolarization of neurones of the locus coeruleus. Extrapolating from these results, we suggest that hyperpolarization caused by alfentanil was also mediated by μ-opiate receptors (Leysen *et al.*, 1983).

Hyperpolarization of neurones of the locus coeruleus, caused by alfentanil, appears to be due to the opening of potassium channels, that display anomalous rectification, for the following reasons: (1) alfentanil enhanced anomalous rectification; (2) caesium and barium suppressed alfentanil-induced hyperpolarization, and (3) the reversal potential of the hyperpolarization was about −110 mV, approximately the potassium equilibrium potential (Williams *et al.*, 1988).

This evidence is consistent with previous studies that indicated that the opioid-induced potassium conductances in neurones of the submucous plexus (North *et al.*, 1987), the arcuate nucleus (Loose & Kelly, 1990) and locus coeruleus (North *et al.*,1987; Williams *et al.*, 1988) are characterized by inward rectification. Caesium chloride, however, can only partially suppress alfentanil-induced hyperpolarization in the neurones tested (see also North & Williams, 1985; Chiu *et al.*, 1990). In contrast, hyperpolarization induced by alfentanil was completely suppressed by barium in the neurones tested. These data indicate that barium was more effective than caesium in suppressing alfentanil-induced hyperpolarization. Extracellular barium and caesium block inward-rectifying potassium channels in the LC (Osmanovic & Shefner, 1987; Williams *et al.*, 1988) but the behaviour of caesium blocking differs from that of barium blocking. Externally applied caesium appeared to cause only a voltage-dependent block of the inward potassium current through the inward rectifier but had no effect on the outward potassium current induced by opioids (North *et al.*, 1987) or somatostatin (Mihara *et al.*, 1987). External barium, in contrast, can block both inward and outward potassium currents (see Constanti & Galvan, 1983 for references). Furthermore, barium carries charge through calcium channels more effectively than calcium itself in the LC (Williams *et al.*, 1984) and in several other kinds of excitable membrane (see Schwindt & Crill,

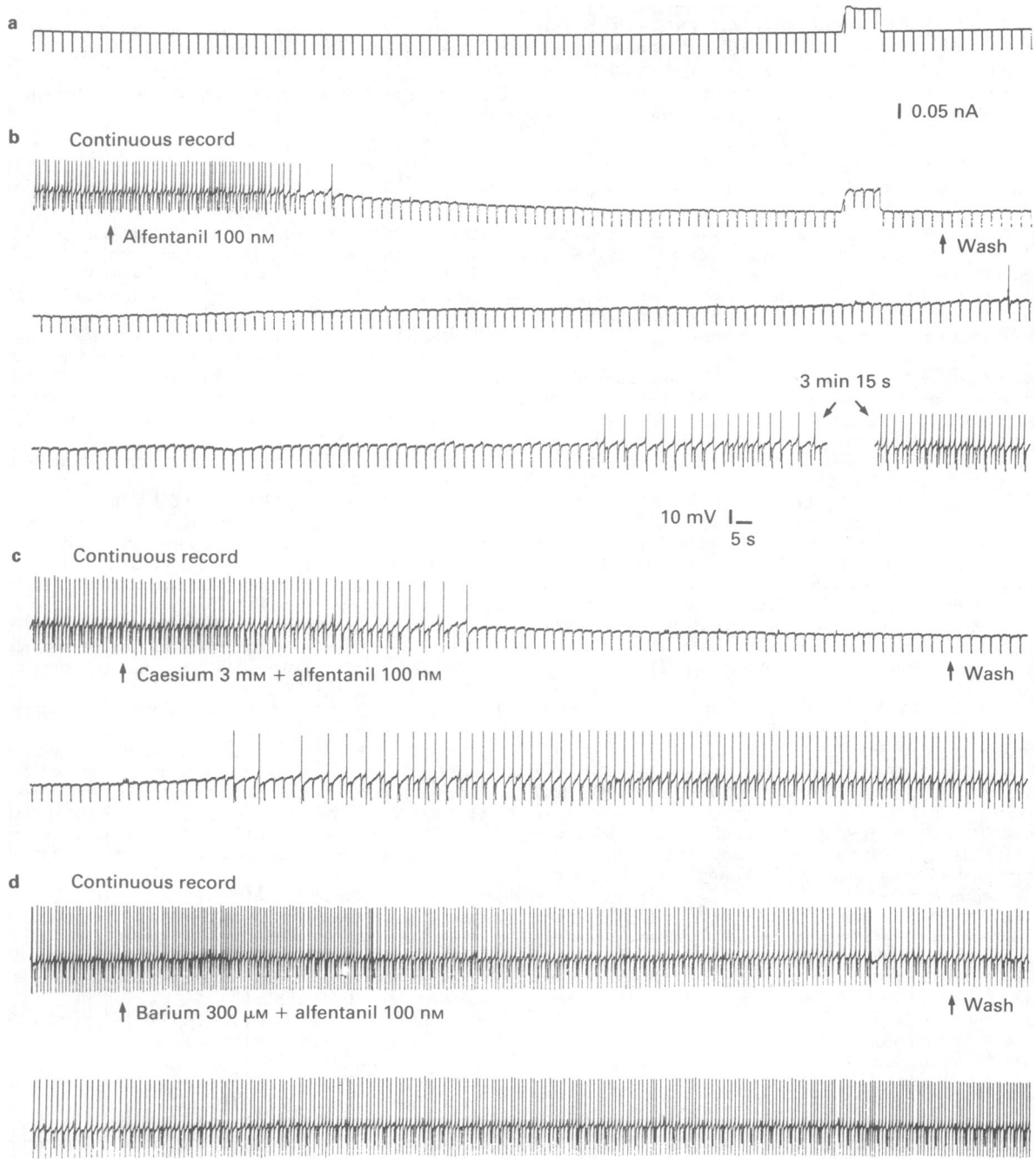

Figure 5 Effects of caesium and barium on alfentanil-induced hyperpolarization in a neurone in the locus coeruleus. (a) Shows the injected current with amplitude 0.065 nA, duration 300 ms and frequency 0.3 Hz. (b) Superfusion with alfentanil (100 nM) caused complete inhibition of the firing rate, hyperpolarization of the membrane potential (16.5 mV) and a decrease in input resistance (25%). During the steady state of hyperpolarization, a d.c. depolarizing current was injected to return the membrane potential of this cell to its predrug level (see curent trace in a). When this was done, the input resistance was still decreased, as compared with the predrug state. (c) In the presence of caesium (3 mM), alfentanil-induced hyperpolarization still occurred, though to a lesser degree (a 67% reduction). (d) In the presence of barium (0.3 mM), alfentanil (100 nM) produced no hyperpolarization. However, inhibition of spontaneous firing still occurred, although it was not complete (37% inhibition).

1980, for references), which in turn would generate a depolarizing current. In combination, these effects of barium would contribute to its actions in opposing the alfentanil-induced hyperpolarization.

The mechanisms by which the LC involved in the mediation of opioid analgesia are complicated as there appears to be interaction between the supraspinal systems. A review of the literature indicates that participation of the LC in modulating morphine-induced antinociception is mediated indirectly through the nucleus raphe magnus (Lipp, 1991). Neurones in two classes are identified in the nucleus raphe magnus, termed off- and on-cells (Fields *et al.*, 1988; see also Pan *et al.*, 1990). Several lines of evidence indicate that on-cells function primarily as intrinsic GABAergic interneurones that inhibit off-cells and that disinhibition (activation) of off-cells results in antinociception (Pan *et al.*, 1990; Fields *et al.*, 1991; Heinricher *et al.*, 1992). Pharmacological investigations have shown that on-cells but not off-cells were consistently and selectively excited by noradrenaline, and this facilitatory effect was reversed by the α_1-antagonist, prazosin (Heinricher *et al.*, 1988). Since the nucleus raphe magnus receives noradrenergic innervation from the LC (Chu & Bloom, 1974; Amaral & Sinnamon, 1977; Sakai *et al.*, 1979; Westlund & Coulter, 1980; Dong & Shen, 1986), then direct inhibition of LC neurones by opioid substances (e.g. alfentanil) results in decreased release of noradrenaline within the nucleus raphe magnus. Consequently, lifting of the tonic excitatory influence of noradrenaline on the on-cells disrupts GABA inhibition of the off-cells. This disinhibition allows the descending inhibitory influence of off-cells on the spinal pain-transmission to be facilitated and could be the possible mechanism by which the LC mediates opioid (alfentanil) supraspinal analgesia (Lipp, 1991; Field *et al.*, 1991; Heinricher *et al.*, 1992; Heinricher & Tortorici, 1992).

This work was supported in part by NSC78-0412-B010-30 (to T.H.C.) from the National Science Council, and a Tjing-Ling Medical Foundation Professorship (to T.H.C.), Taiwan. We appreciate the help given to us by Miss M.J. Chen in preparing this manuscript.

References

AMARAL, O.G. & SINNAMON, H.M. (1977). The locus coeruleus: neurobiology of a central noradrenergic nucleus. *Prog. Neurobiol.*, **9**, 147–196.

ANDRADE, R. & AGHAJANIAN, G.K. (1984). Locus coeruleus activity in vitro: intrinsic regulation by a calcium-dependent potassium conductance but not α_2-adrenoceptors. *J. Neurosci.*, **4**, 161–170.

BERG-JOHNSEN, J. & LANGMOEN, I.A. (1987). Isoflurane hyperpolarizes neurones in rat and human cerebral cortex. *Acta Physiol. Scand.*, **130**, 679–685.

BODNAR, R., PAUL, D. & PASTERNAK, G.W. (1991). Synergistic analgesic interactions between the periaqueductal gray and the locus coeruleus. *Brain Res.*, **558**, 224–230.

BODNAR, R.J., WILLIAMS, C.L., LEE, S.J. & PASTERNAK, G.W. (1988). Role of μ_1-opiate receptors in supraspinal opiate analgesia: a microinjection study. *Brain Res.*, **447**, 25–34.

CHIU, T.H., CHEN, T.Y., HO, C.L. & CHIANG, S.T. (1990). Electrophysiological effects of dermorphin on locus coeruleus neurones of rat. *Neuropharmacol.*, **29**, 747–755.

CHU, N.S. & BLOOM, F.E. (1974). The catecholamine-containing neurones in the cat dorsolateral pontine tegmentum: distribution of the cell bodies and some axonal projections. *Brain Res.*, **66**, 1–21.

CONSTANTI, A. & GALVAN, M. (1983). Fast inward-rectifying current accounts for anomalous rectification in olfactory cortex neurones. *J. Physiol.*, **335**, 153–178.

COOKSON, R.F., NIEMEGEERS, C.J.E. & VANDEN BUSSCHE, G. (1983). The development of alfentanil. *Br. J. Anaesth.*, **55**, 147s–155s.

DONG, X. & SHEN, E. (1986). Origin of monoaminergic innervation of the nucleus raphe magnus – a combined monoamine histochemistry and fluorescent retrograde tracing study in the rat. *Scientia Sinica*, **6**, 599–608.

FIELDS, H.L., BARBARO, N.M. & HEINRICHER, M.M. (1988). Brainstem neuronal circuitry underlying the antinociceptive action of opiates. *Progr. Brain Res.*, **77**, 245–257.

FIELDS, H.L., HEINRICHER, M.M. & MASON, P. (1991). Neurotransmitters in nociceptive modulatory circuits. *Annu. Rev. Neurosci.*, **14**, 219–245.

FINLEY, J.C.W., LINDSTRÖM, P. & PETRUSZ, P. (1981). Immunocytochemical localization of β-endorphin-containing neurones in the rat brain. *Neuroendocrinol.*, **33**, 28–42.

HEINRICHER, M.M., HAWS, C.M. & FIELDS, H.L. (1988). Opposing actions of norepinephrine and clonidine on single pain-modulating neurones in rostral ventromedial medulla. In *Pain Research and Clinical Management*. ed. Dubner, R., Gebhart, G.F. & Bond, M.R. pp. 590–594. Amsterdam: Elsevier.

HEINRICHER, M.M., MORGAN, M.M. & FIELDS, H.L. (1992). Direct and indirect actions of morphine on medullary neurones that modulate nociception. *Neurosci.*, **48**, 533–543.

HEINRICHER, M.M. & TORTORICI, V. (1992). Activation of off-cells is a common element in the antinociception produced by direct local application of both opioids and $GABA_A$ receptor antagonists in the rat rostral ventromedial medulla (RVM). *Soc. Neurosci. Abstr.*, **18**, p835.

HEWSON, G. & BRADLEY, P.B. (1982). The effects of anilidopiperidine analgesics on single respiratory and non-respiratory neurones in the brain stem of the rat. *Life Sci.*, **31**, 2335–2338.

JANSSEN, P.A. (1984). The development of new synthetic narcotics. In *Opioids in Anaesthesia*. ed. Estafanous, F.G. pp. 37–44. Boston: Butterworth.

JONES, S.L. (1991). Descending noradrenergic influences on pain. *Progr. Brain Res.*, **88**, 381–394.

LÉGER, L., CHARNAY, Y., CHAYVIALLE, J.A., BÉROD, A., DRAY, F., PUJOL, J.F., JOUVET, M. & DUBOIS, P.M. (1983). Localization of substance P- and enkephalin-like immunoreactivity in relation to catecholamine-containing cell bodies in the cat dorsolateral pontine tegmentum: an immunofluorescence study. *Neurosci.*, **8**, 525–546.

LEYSEN, J.E., GOMMEREN, W. & NIEMEGEERS, C.J.E. (1983). [^{3}H]-sufentanil, a superior ligand for μ-opiate receptors: binding properties and regional distribution in rat brain and spinal cord. *Eur. J. Pharmacol.*, **87**, 209–225.

LIPP, J. (1991). Possible mechanisms of morphine analgesia. *Clin. Neuropharmacol.*, **14**, 131–147.

LOOSE, M.D. & KELLY, M.J. (1990). Opioids act at μ-receptors to hyperpolarize arcuate neurones via an inwardly rectifying potassium conductance. *Brain Res.*, **513**, 15–23.

MCFADZEAN, I., LACEY, M.G., HILL, R.G. & HENDERSON, G. (1987). Kappa opioid receptor activation depresses excitatory synaptic input to rat locus coeruleus neurones in vitro. *Neurosci.*, **20**, 231–239.

MIHARA, S., NORTH, R.A. & SURPRENANT, A. (1987). Somatostatin increases an inwardly rectifying potassium conductance in guinea-pig submucous plexus neurones. *J. Physiol.*, **390**, 335–355.

NICOLL, R.A. & MADISON, D.V. (1982). General anaesthetics hyperpolarize neurones in the vertebrate central nervous system. *Science*, **217**, 1055–1057.

NIEMEGEER, C.J.E. & JANSSEN, P.A.J. (1981). Alfentanil (R39209), a particularly short-acting intravenous narcotic analgesic in rats. *Drug Dev. Res.*, **1**, 83–88.

NORTH, R.A. (1986). Opioid receptor types and membrane ion channels. *Trends. Neurosci.*, **9**, 114–117.

NORTH, R.A. & WILLIAMS, J.T. (1985). On the potassium conductance increased by opioids in rat locus coeruleus neurones. *J. Physiol.*, **364**, 265–280.

NORTH, R.A., WILLIAMS, J.T., SURPRENANT, A. & CHRISTIE, M.J. (1987). μ and δ receptors belong to a family of receptors that are coupled to potassium channels. *Proc. Natl. Acad. Sci. U.S.A.*, **84**, 5487–5491.

O'BEIRNE, M., GUREVICH, N. & CARLEN, P.L. (1987). Pentobarbital inhibits hippocampal neurones by increasing potassium conductance. *Can. J. Physiol. Pharmacol.*, **65**, 36–41.

OSMANOVIC, S.S. & SHEFNER, S.A. (1987). Anomalous rectification in rat locus coeruleus neurones. *Brain Res.*, **417**, 161–166.

PAN, Z.Z., WILLIAMS, J.T. & OSBORNE, P.B. (1990). Opioid actions on single nucleus raphe magnus neurones from rat and guinea-pig in vitro. *J. Physiol.*, **427**, 519–532.

POCOCK, G. & RICHARDS, C.D. (1991). Cellular mechanisms in general anaesthesia. *Br. J. Anaesth.*, **66**, 116–128.

PROUDFIT, H.K. (1988). Pharmacologic evidence for the modulation of nociception by noradrenergic neurones. *Progr. Brain Res.*, **77**, 357–370.

RICHARDS, C.D. & STRUPINSKI, K. (1986). An analysis of the action of pentobarbitone on the excitatory postsynaptic potentials and membrane properties of neurones in the guinea-pig olfactory cortex. *Br. J. Pharmacol.*, **89**, 321–325.

ROSSI, G.C., PASTERNAK, G.W., KIEFEL, J.M. & BODNAR, R.J. (1992). Supraspinal morphine analgesia: synergy between mesencephalic, pontine and medullary sites in rats. *Soc. Neurosci. Abstr.*, **18**, p 834.

SAKAI, K., SASTRE, J.P., SALVERT, D., TOURET, M., TOHYAMA, M. & JOUVET, M. (1979). Tegmentoreticular projections with special reference to the muscular atonia during paradoxical sleep in the cat: an HRP study. *Brain Res.*, **176**, 233–254.

SASA, M., HUNEKIYO, K., OSUMI, Y. & TAKOARI, S. (1977). Attenuation of morphine analgesia in rats with lesions of the locus coeruleus and dorsal raphe nucleus. *Eur. J. Pharmacol.*, **42**, 53–62.

SAWADA, S. & YAMAMOTO, C. (1985). Blocking action of pentobarbital on receptors for excitatory amino acids in the guinea-pig hippocampus. *Exp. Brain Res.*, **59**, 226–231.

SCHWINDT, P.C. & CRILL, W.E. (1980). Effects of barium on cat spinal motoneurones studied by voltage clamp. *J. Neurophysiol.*, **44**, 827–846.

SEBEL, P.S., BOVILL, J.G. & VAN DER HAVEN, A. (1982). Cardiovascular effects of alfentanil anaesthesia. *Br. J. Anaesth.*, **54**, 1185–1190.

SHEFNER, S.A. & CHIU, T.H. (1986). Adenosine inhibits locus coeruleus neurones: an intracellular study in a rat brain slice preparation. *Brain Res.*, **366**, 364–368.

WEAKLY, J.N. (1969). Effect of barbiturates on quantal synaptic transmission in spinal motoneurones. *J. Physiol.*, **204**, 63–77.

WESTLUND, K.N. & COULTER, J.D. (1980). Descending projections of the locus coeruleus and subcoeruleus/medial parabrachial nuclei in monkey: axonal transport studies and dopamine-β-hydroxylase immunocytochemistry. *Brain Res. Rev.*, **2**, 235–264.

WILLIAMS, J.T. & NORTH, R.A. (1984). Opiate-receptor interactions on single locus coeruleus neurones. *Mol. Pharmacol.*, **26**, 489–497.

WILLIAMS, J.T., NORTH, R.A., SHEFNER, S.A., NISHI, S. & EGAN, T.M. (1984). Membrane properties of rat locus coeruleus neurones. *Neurosci.*, **13**, 137–156.

WILLIAMS, J.T., NORTH, R.A. & TOKIMASA, T. (1988). Inward rectification of resting and opiate-activated potassium currents in rat locus coeruleus neurones. *J. Neurosci.*, **8**, 4299–4306.

YUGE, O., KITAHATA, L.M., COLLINS, J.G., MATSUMOTO, M. TABATABAI, M., SUZUKAWA, M. & TANAKA, A. (1985). Fentanyl and alfentanil suppress brainstem pain transmission. *Anesth. Analg.*, **64**, 597–600.

ZORYCHTA, E. & CAPEK, R. (1978). Depression of spinal monosynaptic transmission by diethyl ether: quantal analysis of unitary synaptic potential. *J. Pharmacol. Exp. Ther.*, **207**, 825–836.

(Received July 13, 1992
Revised May 17, 1993
Accepted May 18, 1993)

Br. J. Pharmacol. (1993), **110**, 910–916

Evidence that M_1 muscarinic receptors enhance noradrenaline release in mouse atria by activating protein kinase C

Mary Costa, Michelle Barrington & [1]Henryk Majewski

Prince Henry's Institute of Medical Research, PO Box 152, Clayton, Victoria, Australia 3168

1 The M_1 selective muscarinic agonist, McNeil A 343, enhanced the electrically evoked release of noradrenaline from postganglionic sympathetic nerves in mouse atria. This has been found previously to be due to activation of muscarinic receptors of the M_1 subtype, probably located on sympathetic nerve terminals. The present study investigated the signal transduction mechanisms involved in the release-enhancing effects of McNeil A 343. The release of noradrenaline from mouse atria was assessed by measuring the electrically-induced (3 Hz, 60 s) outflow of radioactivity from atria which had been pre-incubated with [^{3}H]-noradrenaline.

2 8-Bromo cyclic AMP in the presence of IBMX was used to enhance maximally S-I noradrenaline release through cyclic AMP-dependent mechanisms. However, the facilitatory effect of McNeil A 343 (10 μM) was not different from the effect in the absence of these drugs, suggesting that McNeil A 343 enhances noradrenaline release independently of the cyclic AMP system. Furthermore, the release-enhancing effect of McNeil A 343 (10 μM) on noradrenaline release was also not altered by the 5-lipoxygenase inhibitor, BW A4C.

3 The facilitatory effect of McNeil A 343 was not altered in the presence of drugs (trifluoperazine, W7, and calmidazolium) which inhibit calmodulin-dependent processes, suggesting that the mechanisms of action of McNeil A 343 does not depend on calmodulin.

4 It was considered likely that the facilitatory effect of McNeil A 343 on noradrenaline release may be due to activation of protein kinase C, since activators of protein kinase C enhance noradrenaline release. The facilitatory effect of McNeil A 343 was abolished by the non-selective protein kinase C inhibitor, K-252a. To investigate further the involvement of protein kinase C, mouse atria were chronically incubated (9–10 h) with the protein kinase C activator, 4β-phorbol dibutyrate (1.0 μM) in order to down-regulate protein kinase C activity. In protein kinase C-down-regulated atria, the facilitatory effect of McNeil A 343 (30 μM) was abolished. Incubation with 4α-phorbol dibutyrate which does not affect protein kinase C did not reduce the facilitatory effect of McNeil A 343. This provides evidence that activation of protein kinase C is involved in the signal transduction process of McNeil A 343.

Keywords: Noradrenaline release; M_1 muscarinic receptors; McNeil A 343; calmodulin antagonists; protein kinase C

Introduction

It is well established that postganglionic sympathetic nerve terminals are endowed with release-inhibiting muscarinic receptors (see Muscholl, 1980; Mitchelson, 1988). However, the muscarinic agonist, McNeil A 343, enhances action-potential evoked release of noradrenaline from sympathetically innervated tissues (Allen *et al.*, 1972; 1974; Fozard & Muscholl, 1974; Nedergaard, 1980; Arbilla *et al.*, 1986; Vizi *et al.*, 1989). In the past this effect was thought not to involve muscarinic receptors as it was resistant to blockade by atropine (Allen *et al.*, 1972; 1974; Fozard & Muscholl, 1974; Nedergaard, 1980; Arbilla *et al.*, 1986; Vizi *et al.*, 1989). However, in a recent study in mouse atria (Costa & Majewski, 1991) it was found that the facilitatory effect of low concentrations of McNeil A 343 on stimulation-induced release of noradrenaline was blocked by the muscarinic receptor antagonists, atropine, pirenzepine, dicyclomine and methoctramine, with the rank order of antagonism (pirenzepine > methoctramine) suggesting that an M_1 receptor was involved. On the other hand, the inhibitory effect of carbachol on noradrenaline release was blocked with a rank order of antagonism methoctramine > pirenzepine, suggesting that this was mediated through M_2 muscarinic receptors. Thus it may be that noradrenaline release from sympathetic nerves is under dual M_1 and M_2 modulation. In field stimulated mouse atria, the facilitatory M_1 receptors on sympathetic nerves were not activated by endogenously released acetylcholine since pirenzepine did not inhibit noradrenaline release (Costa & Majewski, 1991). However, in rabbit atria, pirenzepine did inhibit noradrenaline release during concomitant parasympathetic/sympathetic nerve stimulation (Muscholl *et al.*, 1989; Altes *et al.*, 1990; Harbermeier-Muth *et al.*, 1990), suggesting physiological activation of M_1-receptors by neuronally released acetylcholine.

The aim of the present study was to characterize further the M_1 facilitatory mechanism on sympathetic nerves by investigating the signal transduction pathway through which it operates. Candidate pathways include the adenosine 3':5'-cyclic monophosphate (cyclic AMP) system since activation of this system results in enhanced release of noradrenaline (see Majewski *et al.*, 1988); arachidonic acid metabolites since activation of muscarinic receptors releases arachidonic acid metabolites in many tissue and cell types (see Nathanson, 1987); and the phospholipase C pathway since in many systems M_1 receptors transduce their effect through this system (see Fisher & Agranoff, 1987). Two important second messengers are formed as a result of phospholipase C activity; inositol trisphosphate and diacylglycerol (see Berridge, 1987). The major action of inositol trisphosphate is to release calcium from intracellular stores (Berridge & Irvine, 1984), and this may influence neurotransmitter release since calcium binds to calmodulin which may then activate calcium-calmodulin protein kinases thought to be involved in the neurotransmitter release process (see Greengard, 1987). Diacylglycerol, on the other hand, activates protein kinase C, a process which enhances noradrenaline release from many tissues both in the central nervous system and periphery (see Majewski *et al.*, 1990). In this study all of these mechanisms

[1] Author for correspondence.

were investigated to determine the signal transduction pathway utilized by release-enhancing M_1 receptors in sympathetic nerves.

Methods

[^{3}H]-noradrenaline release

Mice of either sex (15–25 g) were decapitated and the heart was rapidly removed and placed in Krebs-Henseleit solution which was bubbled with a mixture of 5% CO_2, 95% O_2. The atria were dissected free of the surrounding tissue and placed in an organ bath with Krebs-Henseleit solution which was maintained at 37°C and constantly gassed with 5% CO_2, 95% O_2. The atria were incubated with [^{3}H]-noradrenaline (15 μCi ml^{-1}; 0.37 μM) for 20 min to label transmitter noradrenaline stores. Following incubation the atria were tied loosely to a disc and transferred to individual flow cells. The tissues were washed by superfusing them at a rate of 2 ml min^{-1} for 60 min with Krebs-Henseleit solution which was maintained at 37°C and constantly gassed with 5% CO_2, 95% O_2. A priming stimulation was delivered to the atria 45 min after the beginning of the washing period. The priming stimulation consisted of square wave pulses, 1 ms duration, 15 V cm^{-1} field gradient, and was delivered at 3 Hz for 60 s through two platinum electrodes which were fixed into the flow cell and situated either side of the tissue. The washing procedure and the priming stimulation were designed to remove unbound and loosely bound radioactive compounds from the atria. After the washing period, 3 min fractions of the solution superfusing the atria were collected for the next 54 min. There were two test stimulation periods (S1 and S2), delivered at 6 and 42 min from the onset of sample collection. The stimulation parameters for the test stimulations were the same as those for the priming stimulations (15 V cm^{-1}, 3 Hz, 60 s). The effects of drugs were assessed by superfusing them only during the second stimulation period. In most experiments drugs were present from either 24 min or 15 min prior to the second stimulation period.

At the end of all experiments the atria were dissolved overnight in 2 ml Soluene 350 (Packard Instruments, Wilmington, U.S.A.). The samples of the superfusion solution and the dissolved atria were added to 6–12 ml Picofluor 40 (Packard), and the radioactive content of the samples and the atria was estimated with a liquid scintillation counter. Corrections for counting efficiency were determined by automatic external standardization, and all measurements were expressed as disintegrations per min (d.p.m.).

Chronic experiments with phorbol dibutyrate

Mouse isolated atria were dissected free and placed in 25–50 ml of tissue culture medium to which either vehicle (dimethylsulphoxide, DMSO, 0.05% v/v) or phorbol ester (1.0 μM) had been added. The solution containing the atria was placed in an incubator which had a 95% O_2, 5% CO_2 environment and was maintained at 37°C, for 9–10 h. The culture medium had been equilibrated in the incubator for 20 min before the atria were added. Following the preincubation the atria were removed, rinsed in Krebs-Henseleit solution and then a [^{3}H]-noradrenaline release experiment was conducted as described by Foucart *et al.* (1991), where instead of flow cells, the atria was placed in an organ bath and the outflow of radioactivity measured in 3 min samples of the bathing fluid. Some experiments on non-preincubated atria were also performed in organ baths as indicated in the results.

Calculation of radioactive outflow

The fractional radioactive outflow of a sample was calculated as the radioactive content of the sample expressed as a percentage of the total tissue radioactivity at the time the sample was collected. The spontaneous (resting) outflow of radioactivity was calculated as the mean value of the fractional radioactive content of the sample taken immediately before the stimulation and of the sample taken 9 min following the onset of stimulation. The fractional stimulation-induced outflow of radioactivity was calculated by adding the fractional radioactive content of the sample during which stimulation occurred and the sample immediately following, and then subtracting twice the mean fractional resting outflow of radioactivity.

Statistical analysis of results

All data are expressed as mean and standard error of the mean (s.e.mean). The data were analysed by Student's *t* tests. Where multiple comparisons against a single control were made, one way analysis of variance (ANOVA) followed by Dunnett's tests were done. Where appropriate, two-way ANOVA were also carried out to determine whether effects of McNeil A 343 in relation to drug-free control experiments (A) were affected by a particular treatment (B). In this case the significance was determined from the interaction term A*B in the analysis of variance table, where variable A comprised McNeil A 343 and control experiments and variable B comprised McNeil A 343 and control experiments after the treatment. Probability levels (P) of less than 0.05 were taken to indicate statistical significance in all cases.

Materials

The following drugs were used: (−)-2,5,6-[^{3}H]-noradrenaline (specific activity 40.8 Ci mmol^{-1}; NEN, Boston, U.S.A.), 3-isobutyl-1-methylxanthine (IBMX), W-7 (N-(6-aminohexyl-5-chloro-1-napthalenesulphonamide), 4β-phorbol dibutyrate, calmidazolium (R 24 571) and trifluoperazine (Sigma, St Louis, U.S.A.); 8-bromoadenosine 3′,5′-cyclic monophosphate (Boehringer-Mannheim, Mannheim, FRG); 4α-phorbol dibutyrate (LC Services, Woburn, U.S.A.); McNeil A 343 (4-(*m*-chlorophenylcarbamoyloxy)-2-butynyltrimethylammonium chloride; McNeil Laboratories, Australia). BW A4C (N-(3-phenoxycinnamyl) acetohydroxamic acid) was a gift from Wellcome, UK. K-252a ((8**R***,9**S***,11**S***)-(−)-9-hydroxy-9-methoxycarbonyl-8-methyl-2,3,9,10-tetrahydro-8-11-epoxy-1H, 8H,11H-2,7b,11a-triazadi benz[a,g]cycloocta[c,d,e,]trinden-1-one) was a generous gift from Dr H. Kase, Kyowa Hakko Kogyo, Japan.

Trifluoperazine, W-7, calmidazolium, BW A4C, phorbol dibutyrate and K-252a were dissolved in DMSO before being further diluted in Krebs-Henseleit. All other drugs were dissolved directly in Krebs-Henseleit solution.

The modified Krebs-Henseleit solution had the following composition (mM): NaCl 118, KCl 4.7, $CaCl_2$ 2.5, $NaHCO_3$ 25.0, KH_2PO_4 1.03, $MgSO_4$ 0.45, D-(+)-glucose 11.1, disodium edetate 0.067, and ascorbic acid 0.14.

The tissue culture medium used was Medium 199 with Hank's salt without glutamine (Commonwealth Serum Laboratories, Parkville, Australia) to which bovine serum albumin (5 g l^{-1}) and sodium pyruvate (0.5 mM) were added.

Results

Cyclic AMP and McNeil A 343

Mouse atria were incubated with [^{3}H]-noradrenaline and two stimulations were delivered (S1 and S2). The absolute fractional stimulation-induced (S-I) outflow of radioactivity for all experimental groups in the first stimulation period (FR1) is given in Table 1.

The M_1 selective agonist, McNeil A 343 (10 μM), significantly enhanced the fractional S-I outflow of radioactivity from mouse atria when it was present during the second

Table 1 The baseline parameters for the outflow of radioactivity corresponding to the first stimulation period (S1) from mouse atria pre-incubated with [^{3}H]-noradrenaline

Treatment	n	*S1 × 100*	*R1 × 100*
		Flow cell experiments	
No pre-incubation	80	0.43 ± 0.02	0.43 ± 0.01
		Organ bath experiments	
		Series 1	
No pre-incubation	10	1.37 ± 0.28	1.19 ± 0.12
DMSO incubation	8	1.22 ± 0.09	1.92 ± 0.11
4α-PDB incubation	8	1.43 ± 0.24	1.86 ± 0.15
		Series 2	
DMSO incubation	13	1.14 ± 0.13	2.00 ± 0.23
4β-PDB incubation	12	1.60 ± 0.13	2.52 ± 0.21

Mouse atria were incubated with [^{3}H]-noradrenaline, washed for 60 min and the outflow of radioactivity was measured. There were two test stimulation periods and the fractional stimulation-induced outflow of radioactivity in the first stimulation period (S1) multiplied by 100 is shown as is the corresponding fractional resting (spontaneous) outflow (R1). Mean ± s.e.mean values are given, and n is the number of experiments. Some atria were chronically incubated for 9–10 h with either DMSO or 4α- or 4β-phorbol dibutyrate (PDB) prior to the experiment. There were two series of these experiments. Both the fractional S-I outflow in S1 and the corresponding resting outflow of radioactivity were higher in organ bath experiments compared to the flow cells ($P<0.05$, two way analysis of variance). However there were no significant differences in the fractional S-I outflow within the organ bath groups ($P>0.05$, two way analysis of variance) but the resting outflow of radioactivity was significantly higher in all the pre-incubated atria compared to non-pre-incubated atria within the organ bath groups ($P<0.05$, two way analysis of variance, followed by Dunnett's test).

stimulation period (Figure 1). The combination of 3-isobutyl-1-methyl-xanthine (IBMX; 100 μM) and 8-bromo cyclic AMP (270 μM) enhanced the fractional S-I outflow of radioactivity (Figure 1), and it has been shown previously that this concentration of 8-bromo cyclic AMP in the presence of IBMX is maximally effective for enhancing noradrenaline release from mouse atria (Costa & Majewski, 1990). In the presence of 8-bromo cyclic AMP (270 μM) and IBMX (100 μM), the facilitatory effect of McNeil A 343 (10 μM) on the fractional S-I outflow of radioactivity was not significantly different from the effect of McNeil A 343 in the absence of these drugs (Figure 1).

5-Lipoxygenase and McNeil A 343

The 5-lipoxygenase inhibitor BW A4C (1.0 μM), present in the second stimulation period, did not alter the fractional S-I outflow of radioactivity ($P>0.05$, Students's t test; Figure 1). When McNeil A 343 was present with BW A4C, the increase in the fractional S-I outflow of radioactivity was not different from that produced by McNeil A 343 alone (Figure 1).

Calmodulin antagonists and McNeil A 343

By itself, the calmodulin antagonist calmidazolium (1.0 μM) did not alter the fractional S-I outflow of radioactivity when it was present only during the second stimulation period ($P>0.05$, Dunnett's test after one-way ANOVA; Figure 2). However, two other compounds which inhibit calmodulin effects, trifluoperazine (1.0 μM) and W-7 (10 μM), significantly increased the fractional S-I outflow of radioactivity from mouse atria (Figure 2). The enhancing effect of McNeil A 343 (10 μM) in the presence of calmidazolium (1.0 μM), trifluoperazine (1.0 μM) or W-7 (10 μM) was not significantly different from the effect of McNeil A 343 in the absence of these calmodulin antagonists (Figure 2).

DMSO at a final concentration of 0.1% (solvent for BW A4C and calmodulin inhibitors) did not alter either the

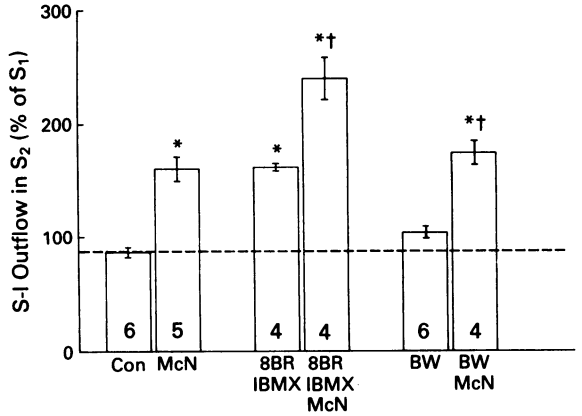

Figure 1 The influence of 8-bromo cyclic AMP (8BR; 270 μM) plus 3-isobutyl-1-methylxanthine (IBMX, 100 μM) and BWA4C (BW; 1.0 μM) on the facilitatory effect of McNeil A 343 (McN; 10 μM) on the fractional stimulation-induced (S-I) outflow of radioactivity from mouse atria pre-incubated with [^{3}H]-noradrenaline. There were two stimulation periods (3 Hz, 60 s) 36 min apart. All drugs were present from 15 min before the second stimulation period. The mean fractional S-I outflow in the second stimulation period (S2) expressed as a percentage of that in the first (S1) is shown. The columns represent the mean ± s.e.mean. The number of experiments is at the base of each column. *Represents a significant difference from control (Con; $P<0.05$, Dunnett's test after one-way ANOVA), and †represents a significant difference from 8-bromo cyclic AMP plus IBMX or BW A4C as appropriate ($P<0.05$, Student's t test). The enhancing effect of McNeil A 343 was not altered by 8-bromo cyclic AMP and IBMX, or BW A4C ($P<0.05$, two-way ANOVA).

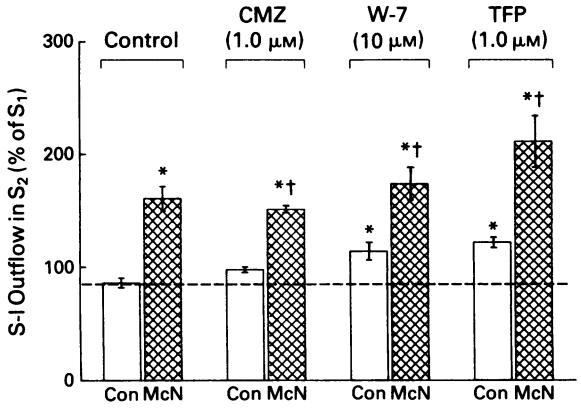

Figure 2 The influence of calmidazolium (CMZ; 1.0 μM), W-7 (10 μM) and trifluoperazine (TFP; 1.0 μM) on the facilitatory effect of McNeil A 343 (McN; 10 μM) on the fractional stimulation-induced (S-I) outflow of radioactivity from mouse atria pre-incubated with [^{3}H]-noradrenaline. There were two stimulation periods (3 Hz, 60 s) 36 min apart. McNeil A 343 was present from 15 min before the second stimulation period. All other drugs were present from 24 min before the second stimulation period. The mean fractional S-I outflow in the second stimulation period (S2) expressed as a percentage of that in the first (S1) is shown. The columns represent the mean ± s.e.mean. The number of experiments in each series was 4–6. *Represents a significant difference from the drug free control (Con; $P<0.05$, Dunnett's test after one-way ANOVA), and †represents a significant difference from the respective drug control experiment ($P<0.05$, Student's t test). The enhancing effect of McNeil A 343 was not altered by either calmidazolium, W-7 or trifluoperazine ($P>0.05$, two-way ANOVA).

radioactive outflow from the tissue, or the effects of the drugs on the fractional S-I outflow of radioactivity (not shown).

Protein kinase C and McNeil A 343

The protein kinase C inhibitor K-252a (1.0 μM), present by itself in the second stimulation period did not alter the fractional S-I outflow of radioactivity ($P > 0.05$, Student's t test; Figure 3). In the presence of K-252a, McNeil A 343 (10 μM) did not facilitate the fractional S-I outflow of radioactivity from mouse atria (Figure 3).

Further experiments were conducted in organ baths instead of flow cells. In flow cells the atria are superfused with Krebs-Henseleit solution at 1 ml min^{-1} whereas in organ bath experiments the atria were bathed in solution which was replaced every 3 min. The spontaneous and stimulation-induced outflow of radioactivity was less in flow cell experiments compared to organ bath experiments (Table 1). It is unclear why this was observed but it may be related to the more extensive washing by the superfusion in flow cells after incubation with [^{3}H]-noradrenaline and/or different electrode geometry between the two systems. In atria which had been pre-incubated with either vehicle (0.05% DMSO) for 9–10 h or the phorbol ester which does not activate protein kinase C, 4α-phorbol dibutyrate (1.0 μM), McNeil A 343 (30 μM) enhanced the S-I outflow of radioactivity to a similar extent (Figure 4). In a separate series of experiments (series 2), both 4β-phorbol dibutyrate (1.0 μM) and McNeil A 343 (30 μM) added before the second stimulation significantly enhanced the S-I outflow of radioactivity from mouse atria which had been chronically (9–10 h) incubated with vehicle (0.05% DMSO; Figure 4). However, after pre-incubation with 4β-phorbol dibutyrate (1.0 μM) for 9–10 h to down-regulate protein kinase C, subsequent addition of 4β-phorbol dibutyrate (1.0 μM) did not alter the fractional S-I outflow of radioactivity indicating down-regulation of protein kinase C (Figure 4). In 4β-phorbol dibutyrate pre-incubated atria, McNeil A 343 (30 μM) also did not alter the S-I outflow of radioactivity (Figure 4). In the pre-incubated atria, the fractional S-I outflow of radioactivity in the first stimulation period was not significantly different from non-pre-incubated atria in organ baths for any of the pre-incubated groups (DMSO, 4α-phorbol dibutyrate, 4β-phorbol dibutyrate, series 1 and series 2) (Table 1). The spontaneous (resting) outflow of radioactivity was significantly increased in pre-incubated atria over non-pre-incubated atria (Table 1).

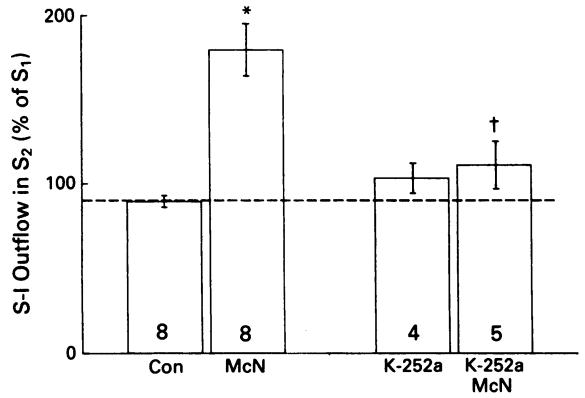

Figure 3 The influence of K-252a (1.0 μM) on the facilitatory effect of McNeil A 343 (McN; 10 μM) on the fractional stimulation-induced (S-I) outflow of radioactivity from mouse atria pre-incubated with [^{3}H]-noradrenaline. There were two stimulation periods (3 Hz, 60 s) 36 min apart. McNeil A 343 was present from 15 min before the second stimulation period, and K-252a was present from 24 min before the second stimulation period. The mean fractional S-I outflow in the second stimulation period (S2) expressed as a percentage of that in the first (S1) is shown. The columns represent the mean ± s.e.mean. The number of experiments is at the base of each column. *Represents a significant difference from control (Con; $P < 0.05$, Dunnett's test after one way ANOVA); †indicates that the enhancing effect of McNeil A 343 was significantly inhibited by K-252a ($P < 0.05$, two-way ANOVA).

Spontaneous outflow of radioactivity

McNeil A 343 (10 μM), either by itself or in the presence of other drugs, inhibited the spontaneous outflow of radioactivity by about 10% from mouse isolated atria which had been incubated with [^{3}H]-noradrenaline and this was not affected by any of the other treatments used in combination with McNeil A 343 (not shown). Other drugs used in the present study had minor or no effect on the spontaneous outflow (not shown).

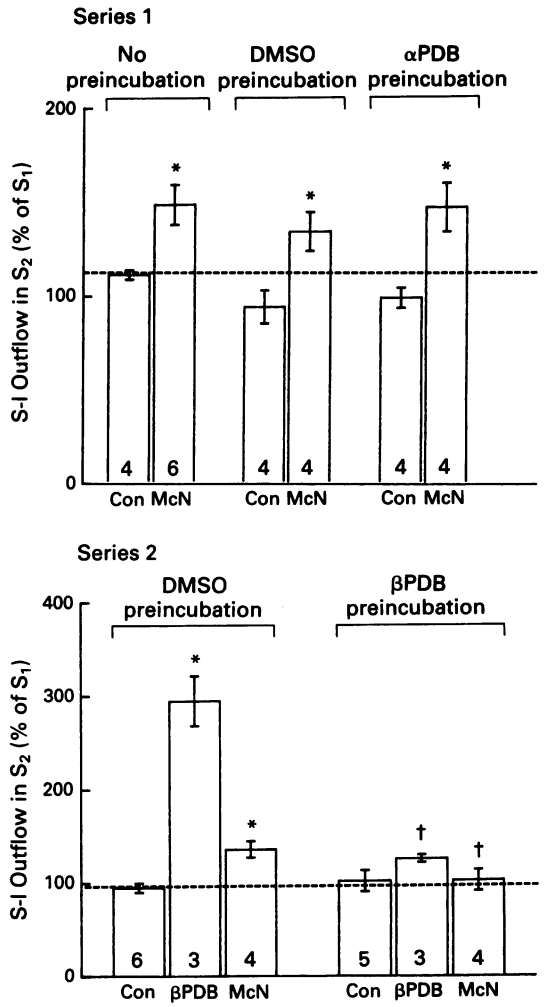

Figure 4 The effect of prolonged incubation (9–10 h) with 4α- or 4β-phorbol dibutyrate (αPDB, βPDB, 1.0 μM) on the facilitatory effect of subsequently applied 4β-phorbol dibutyrate (1.0 μM) and McNeil A 343 (McN; 30 μM) on the fractional stimulation-induced (S-I) outflow of radioactivity from mouse atria pre-incubated with [^{3}H]-noradrenaline. Mouse isolated atria were incubated with tissue culture medium containing 4α- and 4β-phorbol dibutyrate (1.0 μM) or DMSO (vehicle) for 9–10 h prior to being incubated with [^{3}H]-noradrenaline. There were two series of experiments: series 1 and series 2 done at different times. In some experiments the atria were used without prior incubation. In all experiments there were two stimulation periods (3 Hz, 60 s) 36 min apart. McNeil A 343 was present from 15 min before the second stimulation period, and 4β-phorbol dibutyrate was present from 24 min prior to the second stimulation period. The mean fractional S-I outflow in the second stimulation period (S2) expressed as a percentage of that in the first (S1) is shown. The columns represent the mean ± s.e.mean. The number of experiments is at the base of each column. *Represents a significant difference from the vehicle control (Con) ($P < 0.05$, Student's t test); †indicates that the enhancing effects of 4β-phorbol dibutyrate or McNeil A 343 were significantly reduced in 4β-phorbol dibutyrate pre-incubated atria ($P < 0.05$, two-way ANOVA).

Discussion

The present study was designed to elucidate possible transduction pathways associated with enhancement of noradrenaline release from sympathetic nerves through muscarinic receptors. In the present study, as previously observed (Costa & Majewski, 1991), the muscarinic agonist McNeil A 343 enhanced the stimulation-induced (S-I) release of noradrenaline from mouse atria. This effect was found most likely to be due to activation of M_1 muscarinic receptors at postganglionic sympathetic nerve varicosities (Costa & Majewski, 1991).

One intraneuronal pathway involved in the enhancement of noradrenaline release from nerve terminals is the adenylate cyclase-cyclic AMP system (see Majewski *et al.*, 1988). There have been reports that cyclic AMP levels in some neurones are raised following activation of muscarinic receptors (Hanley & Iversen, 1978; Lenox *et al.*, 1980; Briggs *et al.*, 1982), and a recent report indicates that muscarinic receptors in the rat olfactory bulb are linked directly to stimulation of adenylate cyclase activity (Onali & Olianas, 1990). In the present study the combination of 8-bromo cyclic AMP and the phosphodiesterase inhibitor, IBMX, enhanced the S-I release of noradrenaline. This has been shown previously in mouse atria (Costa & Majewski, 1988) where the cyclic AMP-dependent pathway for enhancing noradrenaline release was saturated using the same concentrations of these agents. Under these conditions the release-enhancing effects of prejunctional β-adrenoceptors and prejunctional ACTH receptors were abolished (Costa & Majewski, 1988), which is consistent with the linking of these receptors to adenylate cyclase (Göthert & Hentrich, 1984; Johnston *et al.*, 1987; Costa & Majewski, 1988; 1990). However, in the present study the release-enhancing effect of McNeil A 343 was maintained in the presence of 8-bromo cyclic AMP and IBMX, ruling out the possibility of a cyclic AMP-mediated mechanism in this case.

Activation of muscarinic receptors releases arachidonic acid from many tissues including the heart (Junstad & Wennmalm, 1974), and metabolites of arachidonic acid, particularly the prostaglandins, have been found to modulate noradrenaline release (see Hedqvist, 1977; Malik & Sehic, 1990). In a previous study in rabbit pulmonary artery it was found that cyclo-oxygenase metabolites of arachidonic acid did not mediate the facilitatory effect of McNeil A 343 on noradrenaline release (Nedergaard, 1980) although this was not directly tested in the present study. In the present study we have extended these findings to suggest that certain lipoxygenase metabolites of arachidonic acid are also not involved since BW A4C, which is a relatively selective 5-lipoxygenase inhibitor (Tateson *et al.*, 1988), did not alter the facilitatory effect of McNeil A 343 on noradrenaline release.

Muscarinic receptors of the M_1 subtype have been closely associated with the phospholipase C-inositol trisphosphate/diacylglycerol signal transduction mechanism in many systems (see Eglen & Whiting, 1986; Nathanson, 1987; Mitchelson, 1988). The second messenger inositol trisphosphate releases Ca^{2+} from intracellular stores, which by binding to calmodulin may activate calmodulin-dependent enzymes thought to have a role in neurotransmitter release (see Greengard, 1987). However, in the present study the facilitatory effect of McNeil A 343 on noradrenaline release was not altered in the presence of the calmodulin antagonists, calmidazolium (Van Belle, 1981), W-7 (Hidaka *et al.*, 1981) or trifluoperazine (Levin & Weiss, 1979), suggesting that this pathway was not involved.

None of the calmodulin antagonists by themselves decreased the S-I release of noradrenaline. This is in marked contrast to the release-inhibiting effects of these agents (W7 and trifluoperazine) in brain synaptosomes (DeLorenzo, 1985), which has been interpreted as evidence for a role for calmodulin in the process of neurotransmitter release (DeLorenzo, 1981; 1985; see also Llinàs *et al.*, 1985). However, other studies have also failed to observe inhibition of neurotransmitter release in various systems (Publicover, 1985; Jinnai *et al.*, 1986; Reimann *et al.*, 1988) using W7, trifluoperazine and calmidazolium. Thus, there may not be a universal role for calcium-calmodulin kinases in neurotransmitter release processes.

The other metabolite formed by the action of phospholipase C is diacylglycerol, which can activate protein kinase C to phosphorylate proteins associated with the process of neurotransmitter release (Nishizuka, 1984; 1986). Indeed, protein kinase C activators such as phorbol esters enhance the release of noradrenaline from many tissues including mouse atria (see Musgrave & Majewski, 1989). In the present study the protein kinase C inhibitor K-252a (Kase *et al.*, 1987) abolished the facilitatory effect of McNeil A 343 on noradrenaline release. Similar results have been observed with other protein kinase C inhibitors on muscarinic enhancement of neurotransmitter release in the central nervous system (Diamant *et al.*, 1988; Xu *et al.*, 1990), where a role for protein kinase C was assumed. However, some caution must be used since protein kinase C inhibitors are in general relatively non-selective. For example, K-252a has inhibitory effects on a wide range of other intracellular systems including cyclic AMP-dependent protein kinase, cyclic GMP-dependent protein kinase, myosin light chain kinase, as well as calmodulin and some calmodulin-dependent enzymes (Kase *et al.*, 1987; Nakanishi *et al.*, 1988; see Rüegg & Burgess, 1989). In the present study it is unlikely that K-252a inhibited the effect of McNeil A 343 by altering cyclic AMP- or calmodulin-dependent transduction systems since the experiments described above rule out their involvement.

Another approach taken to test whether protein kinase C was involved was to down-regulate protein kinase C by long-term exposure (9–10 h) to protein kinase C activating phorbol esters such as 4β-phorbol dibutyrate (Mathies *et al.*, 1987; Young *et al.*, 1987). In the present study, after 4β-phorbol dibutyrate pretreatment the facilitatory effect of subsequently applied phorbol esters on noradrenaline release was abolished, indicating functional protein kinase C down-regulation. Similar results were obtained previously in mouse atria by Foucart *et al.* (1991) who also showed that 4α-phorbol dibutyrate, which does not activate protein kinase C but has the other chemical characteristics of 4β-phorbol dibutyrate (Niedel & Blackshear, 1986), did not produce down-regulation of protein kinase C. Using 4β-phorbol dibutyrate treatment in the present study, the facilitatory effect of McNeil A 343 on noradrenaline release was abolished, strongly suggesting that a functional protein kinase C mechanism was necessary for enhancement of noradrenaline release through M_1 receptors. After 4α-phorbol dibutyrate treatment the facilitatory effect of McNeil A 343 on noradrenaline release was still observed indicating that the inhibition of this effect of McNeil A 343 produced by 4β-phorbol dibutyrate was probably a specific protein kinase C effect.

There are two possible roles for protein kinase C. The first is that it is part of a final common pathway in the release process, necessary for the full manifestation of enhanced transmitter release. For example, the ability of many drugs (such as 8-bromo cyclic AMP, isoprenaline, idazoxan, tetraethylammonium and angiotensin II, as well as high frequency electrical stimulation) to enhance noradrenaline release in mouse atria is reduced but not abolished by protein kinase C inhibitors and protein kinase C down-regulation (Foucart *et al.*, 1991; Musgrave *et al.*, 1991). Thus, a partially reduced effect of McNeil A 343 by anti-protein kinase C measures may be expected. However, given the direct linking of M_1 receptors to protein kinase C in other systems (see above), a second alternative is that protein kinase C may directly transduce M_1-facilitation on noradrenaline release especially since the PKC inhibitor and PKC down regulation completely inhibited the facilitatory effect of McNeil A 343. A similar

observation was made with angiotensin II (Musgrave *et al.*, 1991; Foucart *et al.*, 1991) where it was also suggested that protein kinase C directly transduces the facilitatory effect on noradrenaline release.

It is not clear whether these facilitatory M_1 receptors are of physiological significance, particularly for the tonic modulation of noradrenaline release *in vivo*, since in a previous study the M_1 antagonist, pirenzepine, by itself did not inhibit noradrenaline receptors from field stimulated mouse atria (Costa & Majewski, 1991), suggesting that they were not activated by endogenously released acetylcholine. However, another possibility is that modulation of neurotransmitter release is not the only function of M_1 receptors especially since protein kinase C is involved in a number of cell functions such as neurotransmitter synthesis, as well as growth and development (Nishizuka, 1986). A physiological role for M_1 receptors in this arena remains to be investigated.

M.C. was in receipt of an Australian Government Postgraduate Research Award. The work was supported by grants from the National Health and Medical Research Council of Australia.

References

ALLEN, G.S., RAND, M.J. & STORY, D.F. (1972). Effects of McN-A-343 and DMPP on the uptake and release of ^{3}H-noradrenaline by guinea-pig atria. *Br. J. Pharmacol.*, **45**, 480–489.

ALLEN, G.S., RAND, M.J. & STORY, D.F. (1974). Effects of the muscarinic agonist McN-A-343 on the release by sympathetic nerve stimulation of [^{3}H]-noradrenaline from rabbit isolated ear arteries and guinea-pig atria. *Br. J. Pharmacol.*, **51**, 29–34.

ALTES, U., HABERMEIER-MUTH, A. & MUSCHOLL, E. (1990). Further evidence of a presynaptic excitatory M1 muscarinic receptor at postganglionic cardiac adrenergic nerves. *Naunyn-Schmied. Arch. Pharmacol.*, **341**, R86.

ARBILLA, S., LANGER, S.Z. & NIDDAM, R. (1986). Modulation of (^{3}H)-NA and (^{3}H)-ACH release by muscarinic receptors in the rat, differences between occipital cortical, striatal and atrial slices. *Br. J. Pharmacol.*, **87**, 30P.

BERRIDGE, M.J. (1987). Inositol trisphosphate and diacylglycerol: two interacting second messengers. *Annu. Rev. Biochem.*, **56**, 159–193.

BERRIDGE, M.J. & IRVINE, R.F. (1984). Inositol trisphosphate, a novel second messenger in cellular signal transduction. *Nature*, **312**, 315–321.

BRIGGS, C.A., WHITING, G.J., ARIANO, M.A. & MCAFEE, D.A. (1982). Cyclic nucleotide metabolism in the sympathetic ganglion. *Cell. Mol. Neurobiol.*, **2**, 129–141.

COSTA, M. & MAJEWSKI, H. (1988). Facilitation of noradrenaline release from sympathetic nerves through activation of ACTH receptors, β-adrenoceptors and angiotensin II receptors. *Br. J. Pharmacol.*, **95**, 993–1001.

COSTA, M. & MAJEWSKI, H. (1990). Inhibitory prejunctional muscarinic receptors at sympathetic nerves do not function through a cyclic AMP dependent pathway. *Naunyn-Schmied. Arch. Pharmacol.*, **342**, 630–639.

COSTA, M. & MAJEWSKI, H. (1991). Evidence for facilitatory and inhibitory muscarinic receptors on postganglionic sympathetic nerves in mouse isolated atria. *Br. J. Pharmacol.*, **102**, 855–860.

DELORENZO, R.J. (1981). The calmodulin hypothesis of neurotransmission. *Cell Calcium*, **2**, 365–385.

DELORENZO, R.J. (1985). Calcium and calmodulin control of neurotransmitter synthesis and release. In *Calcium and Cell Physiology*. ed. Marmé, D. pp. 265–284. Berlin, Heidelberg: Springer-Verlag.

DIAMANT, S., LEV-ARI, I., UZIELLI, I. & ATLAS, D. (1988). Muscarinic agonists evoke neurotransmitter release: possible roles for phosphatidyl inositol bisphosphate breakdown products in neuromodulation. *J. Neurochem.*, **51**, 795–802.

EGLEN, R.M. & WHITING, R.L. (1986). Muscarinic receptor subtypes: a critique of the current classification and a proposal for a working nomenclature. *J. Autonom. Pharmacol.*, **5**, 323–346.

FISHER, S.K. & AGRANOFF, B.W. (1987). Receptor activation and inositol lipid hydrolysis and neural tissues. *J. Neurochem.*, **48**, 999–1017.

FOUCART, S., MUSGRAVE, I.F. & MAJEWSKI, H. (1991). Long term treatment with phorbol esters and the modulation of noradrenaline release. *Mol. Neuropharmacol.*, **1**, 95–101.

FOZARD, J.R. & MUSCHOLL, E. (1974). Atropine-resistant effects of the muscarinic agonists McN-A-343 and AHR 602 on cardiac performance and the release of noradrenaline from sympathetic nerves of the perfused rabbit heart. *Br. J. Pharmacol.*, **50**, 531–541.

GÖTHERT, M. & HENTRICH, F. (1984). Role of cAMP for regulation of impulse-evoked noradrenaline release from the rabbit pulmonary artery and its possible relationship to presynaptic ACTH receptors. *Naunyn-Schmied. Arch. Pharmacol.*, **328**, 127–134.

GREENGARD, P. (1987). Neuronal phosphoproteins. Mediators of signal transduction. *Mol. Neurobiol.*, **1**, 81–119.

HABERMEIER-MUTH, A., ALTES, U., FORSYTH, K.M. & MUSCHOLL, E. (1990). A presynaptic excitatory M1 muscarine receptor at postganglionic cardiac noradrenergic nerve fibres that is activated by endogenous acetylcholine. *Naunyn-Schmied. Arch. Pharmacol.*, **342**, 483–489.

HANLEY, M.R. & IVERSEN, L.L. (1978). Muscarinic cholinergic receptors in rat corpus striatum and regulation of guanosine cyclic 3',5' monophosphate. *Mol. Pharmacol.*, **14**, 246–255.

HEDQVIST, P. (1977). Basic mechanisms of prostaglandin action on autonomic neurotransmission. *Annu. Rev. Pharmacol. Toxicol.*, **17**, 259–279.

HIDAKA, H., ASANO, M. & TANAKA, T. (1981). Activity-structure relationship of calmodulin antagonists. Naphthalenesulfonamide derivatives. *Mol. Pharmacol.*, **20**, 571–578.

JINNAI, K., TAKAHASHI, K. & FUJITA, T. (1986). Enhancement of spontaneous acetylcholine release from motor nerve terminal by calmodulin inhibitors. *Eur. J. Pharmacol.*, **130**, 197–201.

JOHNSTON, H., MAJEWSKI, H. & MUSGRAVE, I.F. (1987). Involvement of cyclic nucleotides in prejunctional modulation of noradrenaline release in mouse atria. *Br. J. Pharmacol.*, **91**, 773–781.

JUNSTAD, M. & WENNMALM, Å. (1974). Release of prostaglandin from the rabbit isolated heart followng vagal nerve stimulation or acetylcholine infusion. *Br. J. Pharmacol.*, **52**, 375–379.

KASE, H., IWAHASHI, K., NAKANISHI, S., MATSUDA, Y., YAMADA, K., TAKAHASHI, M., MURAKATA, C., SATO, A. & KANEKO, M. (1987). K-252 compounds, novel and potent inhibitors of protein kinase C and cyclic nucleotide-dependent protein kinases. *Biochem. Biophys. Res. Commun.*, **142**, 436–440.

LENOX, R.H., KANT, G.J. & MEYERHOFF, J.L. (1980). Regional sensitivity of cyclic AMP and cyclic GMP in rat brain to central cholinergic stimulation. *Life Sci.*, **26**, 2201–2209.

LEVIN, R.M. & WEISS, B. (1979). Selective binding of antipsychotics and other psychoactive agents to the calcium-dependent activator of cyclic nucleotide phosphodiesterase. *J Pharmacol. Exp. Ther.*, **208**, 454–459.

LLINAS, R., MCGUINNESS, T.L., LEONARD, C.S., SUGIMORI, M. & GREENGARD, P. (1985). Intraterminal injection of synapsin I or calcium/calmodulin-dependent protein kianse II alters neurotransmitter release at the squid giant synapse. *Proc. Natl. Acad. Sci. U.S.A.*, **82**, 3035–3039.

MAJEWSKI, H., COSTA, M. FOUCART, S., MURPHY, T.V. & MUSGRAVE, I.F. (1990). Second messengers are involved in facilitatory but not inhibitory receptor actions at sympathetic nerve endings. *Ann. N.Y. Acad. Sci.*, **604**, 266–275.

MAJEWSKI, H., ISHAC, E.J.N. & MUSGRAVE, I.F. (1988). Intraneuronal mechanisms involved in the modulation of noradrenaline release through prejunctional receptors. In *Vascular Neuroeffector Mechanisms*. ed. Bevan, J.A., Majewski, H., Maxwell, R.A. & Story, D.F. pp. 243–250. New York: ICSU Press.

MALIK, K.U. & SEHIC, E. (1990). Prostaglandins and the release of the adrenergic transmitter. *Ann. N.Y. Acad. Sci.*, **604**, 222–236.

MATHIES, H.J.G., PALFREY, H.C., HIRNING, L.D. & MILLER, R.J. (1987). Down regulation of protein kinase C in neuronal cells: effects on neurotransmitter release. *J. Neurosci.*, **7**, 1198–1206.

MITCHELSON, F. (1988). Muscarinic receptor differentiation. *Pharmacol. Ther.*, **37**, 357–423.

MUSCHOLL, E. (1980). Peripheral muscarinic control of norepinephrine release in the cardiovascular system. *Am. J. Physiol.*, **239**, H713–H720.

MUSCHOLL, E., FORSYTH, K.M. & HABERMEIER-MUTH, A. (1989). A presynaptic excitatory M1 muscarinic receptor at postganglionic cardiac adrenergic fibers that is activated by endogenous acetylcholine. *Naunyn-Schmied. Arch. Pharmacol.*, **339,** R88.

MUSGRAVE, I.F., FOUCART, S. & MAJEWSKI, H. (1991). Evidence that angiotensin II enhances noradrenaline release from sympathetic nerves in mouse atria by activating protein kinase C. *J. Auton. Pharmacol.*, **11,** 211–220.

MUSGRAVE, I.F. & MAJEWSKI, H. (1989). Effect of phorbol esters and polymyxin B on modulation of noradrenaline release in mouse atria. *Naunyn-Schmied. Arch. Pharmacol.*, **339,** 48–53.

NAKANISHI, S., YAMADA, K., KASE, H., NAKAMURA, S. & NONOMURA, Y. (1988). K-252a, a novel microbial product, inhibits smooth muscle myosin light chain kinase. *J. Biol. Chem.*, **263,** 6215–6219.

NATHANSON, N.M. (1987). Molecular properties of the muscarinic acetylcholine receptor. *Annu. Rev. Neurosci.*, **10,** 195–236.

NEDERGAARD, O.A. (1980). Modulation by the muscarinic agonist McN-A-343 of noradrenaline release from vascular sympathetic neurones. *J. Cardiovasc. Pharmacol.*, **2,** 629–643.

NIEDEL, J.E. & BLACKSHEAR, P.J. (1986). Protein kinase C. In *Phosphoinositides and Receptor Mechanisms.* ed. Putney, J. pp. 47–88. New York: A.R. Liss.

NISHIZUKA, Y. (1984). Turnover of inositol phospholipids and signal transduction. *Science*, **225,** 1365–1370.

NISHIZUKA, Y. (1986). Studies and perspectives of protein kinase C. *Science*, **233,** 305–312.

ONALI, P. & OLIANAS, M.C. (1990). Stimulation of adenylate cyclase activity as a novel signal transduction mechanism for central muscarinic receptors. *Proceedings of the XI International Congress of Pharmacol., Eur. J. Pharmacol.*, **183,** 2159.

PUBLICOVER, S.J. (1985). Calmodulin, synchronous and asynchronous release of neurotransmitter. *Comp. Biochem. Physiol.*, **82A,** 7–11.

REIMANN, W., KÖLLHOFER, U. & WAGNER, B. (1988). W-7 at calmodulin-antagonistic concentrations facilitates noradrenaline release from rat brain cortex slices. *Eur. J. Pharmacol.*, **147,** 481–485.

RÜEGG, U.T. & BURGESS, G.M. (1989). Staurosporine, K-252 and UCN-01: potent but nonspecific inhibitors of protein kinases. *Trends Pharmacol. Sci.*, **10,** 218–220.

TATESON, J.E., RANDALL, R.W., REYNOLDS, C.H., JACKSON, W.P., BHATTACHERJEE, P., SALMON, J.A. & GARLAND, L.G. (1988). Selective inhibition of arachidonate 5-lipoxygenase by novel acetohydroxamic acids: biochemical assessment *in vitro* and *ex vivo*. *Br. J. Pharmacol.*, **94,** 528–539.

VAN BELLE, H. (1981). R 24 571: a potent inhibitor of calmodulin-activated enzymes. *Cell Calcium*, **2,** 483–494.

VIZI, E.S., KOBAYASHI, O., TÖRÖCSIK, A., KINJO, M., NAGASHIMA, H., MANABE, N., GOLDINER, P.L., POTTER, P.E. & FOLDES, F.F. (1989). Heterogeneity of presynaptic muscarinic receptors involved in modulation of transmitter release. *Neurosci.*, **31,** 259–267.

XU, M., YAMAMOTO, T. & KATO, T. (1990). In vivo striatal dopamine release by M1 muscarinic receptors is induced by activation of protein kinase C. *J. Neurochem.*, **54,** 1917–1919.

YOUNG, S., PARKER, P.J., ULLRICH, A. & STABEL, S. (1987). Down-regulation of protein kinase C is due to an increased rate of degradation. *Biochem. J.*, **244,** 775–779.

(Received May 10, 1993
Revised June 4, 1993
Accepted June 16, 1993)

Br. J. Pharmacol. (1993), **110**, 917–924

Characterization and pharmacological modulation of antigen-induced peritonitis in actively sensitized mice

*Cláudia Zuany-Amorim, Dominique Leduc, B. Boris Vargaftig & [1]Marina Pretolani

Unité de Pharmacologie Cellulaire, Unité Associée Institut Pasteur, INSERM n° 285, 25, rue du Dr. Roux, 75015, Paris, France and *Fundação Oswaldo Cruz, IOC, Departamento de Fisiologia e Farmacodinâmica, Rio de Janeiro, Brazil

1 The intraperitoneal (i.p.) injection of 1 or 10 μg ovalbumin to sensitized Balb/c mice led to an acute histamine release, firstly evidenced 1 min after the challenge and returning to basal levels 30 min thereafter. This phenomenon was unaccompanied by protein extravasation. A dose-dependent increase in the amounts of immunoreactive leukotriene (LT) C_4 and LTB_4 was observed in the peritoneal washing from sensitized mice 6 h after 1 or 10 μg ovalbumin administration. In separate experiments, the i.p. administration of 1 mg activated zymosan to non-immunized mice was followed by a marked protein extravasation, and by immunoreactive LTC_4 and LTB_4, but not histamine, release in mouse peritoneum 1 h after its injection.

2 Mediator release in the mice peritoneal cavity was concomitant with a transient neutrophil infiltration, which peaked at 6 h and returned to basal levels thereafter. An intense eosinophil accumulation starting at 24 h, peaking at 48 h and returning to basal values at 164 h, was also observed.

3 Ovalbumin (1 μg)-induced eosinophilia, observed at 24 h, was reduced by the pretreatment of the animals with dexamethasone (1 mg kg^{-1}, s.c.) or with the 5-lipoxygenase inhibitor, BWA4C (20 mg kg^{-1}, s.c.), whereas indomethacin (2 mg kg^{-1}, s.c.) and the platelet-activating factor (PAF)-antagonist SR 27417 (10 mg kg^{-1}, s.c.) were ineffective. These results indicate that metabolites of arachidonic acid of lipoxygenase pathway, but not cyclo-oxygenase derivatives or PAF, mediate antigen-induced eosinophil accumulation in the mouse peritoneum.

4 The histamine H_1 receptor antagonist drug, cetirizine (15–30 mg kg^{-1}, s.c.) markedly reduced ovalbumin-induced eosinophil accumulation under conditions where terfenadine was ineffective, suggesting that the effect of cetirizine was not related to the inhibition of the H_1 receptor effects of histamine.

5 The immunosuppressive agent, FK-506 (1–2 mg kg^{-1}, s.c.) and the protein synthesis inhibitor, cylcoheximide, when administered either *in situ* (0.06 ng/cavity) or systemically (5 mg kg^{-1}, s.c.), prevented antigen-induced eosinophil accumulation in the mouse peritoneum, contributing to the concept that substances (probably cytokines) originating from lymphocytes may be involved in the modulation of the eosinophilotactic response in this model.

6 The results of the present study indicate that the i.p. administration of ovalbumin to actively sensitized mice induced late eosinophil accumulation in the peritoneal cavity. This phenomenon, which may be in part mediated by the release of lipoxygenase metabolites and/or by newly generated factors, such as T-lymphocytes-derived eosinophilotactic cytokines, offers an interesting tool to investigate the mechanism of action of anti-allergic and anti-inflammatory drugs.

Keywords: Eosinophils; allergic response; zymosan; leukotrienes

Introduction

The participation of eosinophils in allergic reactions is suggested by the presence of specific receptors for anaphylactic immunoglobulins, adhesion molecules and pro-inflammatory mediators at their surface (Capron, 1992). Eosinophils are prominent inflammatory cells involved with allergic disorders, which are recruited in elevated numbers into the airways and the pleural cavity of several species, including guinea-pigs, mice and rats, following antigen challenge (Lellouch-Tubiana *et al.*, 1988; Gulbenkian *et al.*, 1990; Lima *et al.*, 1991; Okudara *et al.*, 1991). The ability of activated eosinophils to release eosinophil-derived cytotoxic proteins, such as major basic protein and eosinophil-derived neurotoxin (Gleich, 1990), has associated these cells with epithelial damage and tissue injury. In addition, the number of eosinophils in the airways correlates with the severity of the late phase asthma (Bousquet *et al.*, 1990), suggesting that their presence in inflamed tissues contributes to the perpetuation and the amplification of the disease. However, the mechanisms responsible for the attraction and the localisation of eosinophils at the site of allergic reactions remain, to be elucidated fully. Lipid mediators, such as platelet-activating factor (PAF), or leukotriene (LT) B_4 are potent chemotactic agents for eosinophils from different species (Ford-Hutchinson *et al.*, 1980; Lellouch-Tubiana *et al.*, 1988; Martins *et al.*, 1991; Coëffier *et al.*, 1991). Furthermore, it has been suggested recently that cytokines released by activated T-lymphocytes, such as interleukin-5 (IL-5), IL-3 or granulocyte-macrophage colony stimulating factor (GM-CSF), may play a role in eosinophil accumulation at the site of the allergic reactions (Owen *et al.*, 1987; Rothenberg *et al.*, 1988; Sanderson, 1992). This phenomenon may depend on the ability of those cytokines to induce eosinophil proliferation from their bone-marrow precursors and to enhance their survival. Thus, drugs inhibiting the pro-inflammatory activities of lipid mediators on one hand and those interfering with the activation of T-lymphocytes, on the other, are potentially useful in the treatment of allergic disorders.

The mechanisms of inflammatory reactions have been largely investigated in mice (Colorado *et al.*, 1991; Amorim *et al.*, 1992a,b; Perretti *et al.*, 1992), with particular emphasis on the role of eosinophil infiltration which accompanies helminthic infections (Sher *et al.*, 1990; Secor *et al.*, 1990). However, only few studies have focused on the effects of antigen challenge in sensitised mice in terms of cell migration and activation. In particular, Spicer *et al.* (1986) described

[1] Author for correspondence.

the kinetics of cell infiltration in the peritoneal cavity of sensitized mice following antigen administration. Using a limited number of anti-inflammatory and anti-allergic drugs, they have also shown that metabolites of arachidonic acid or vasoactive amines are not involved in antigen-induced eosinophilia. However, the interactions between cell mobilisation and other inflammatory parameters, such as local mediator release, were not investigated. Consequently, the mechanisms responsible for the cell attraction and, particularly, those involved in the maintenance of eosinophils at the site of hypersensitivity reaction remain to be determined.

In an attempt to define better the role of different mediators and inflammatory cells in antigen-induced peritonitis in sensitized mice, we investigated the changes in cell distribution and mediator release in the peritoneal washing following ovalbumin administration to sensitized Balb/c mice. Changes in eosinophil distribution were modulated by different inhibitors of synthesis and antagonists of receptors for inflammatory mediators, and by drugs effective on the T-lymphocyte function.

Methods

Animals and sensitization procedure

Male Balb/C mice aged 8 weeks, weighing approximately 25–30 g raised at the Pasteur Institute (Paris, France), were actively sensitized by a subcutaneous (s.c.) injection of 0.4 ml 0.9% w/v NaCl (saline) containing 100 μg ovalbumin adsorbed in 1.6 mg aluminium hydroxide (Andersson & Brattsand, 1982). Seven days later, the animals received the same dose of ovalbumin in the presence of $Al(OH)_3$ and were used 7 days thereafter.

Antigen-induced peritonitis

Peritonitis was induced by the intraperitoneal (i.p.) injection of 0.4 ml of a solution containing 2.5 or 25 μg ml^{-1} ovalbumin diluted in sterile saline (1 or 10 μg of ovalbumin, as final doses injected per cavity). Control animals received the same volume of sterile saline. At various time intervals after antigen challenge (30 min–164 h), animals were killed by an overdose of ether and the peritoneal cavity was opened and washed with 3 ml of heparinised saline (10 U ml^{-1}). Approximately 90% of the initial volume was recovered. In rare cases, when haemorrhages were noted in the peritoneal cavity, the animals were discarded.

Zymosan-induced peritonitis

Non-immunized mice (25–30 g) were injected i.p. with 0.4 ml of a solution containing 2.5 mg ml^{-1} activated zymosan (AZ) (1 mg, as final dose injected) prepared according to Bruijnzeel *et al.* (1985). The peritoneal cavity was washed 1 or 4 h after the stimulation, as described above.

Leucocyte analysis

Total leucocytes present in the peritoneal lavages were counted in a Coulter counter ZM (Coultronics, Margency, France) and expressed as numbers of cells ml^{-1}. Differential cell counts were performed after cytocentrifugation (Hettich-Universal) and staining with Diff-Quik stain (Baxter Dade AG, Dudingen). At least 300 cells were counted and results were expressed as number of each cell population ml^{-1}.

Drug treatment

The dose of 1 μg of ovalbumin and the time of 24 h after challenge were selected to study the pharmacological modulation of ovalbumin-induced peritonitis.

The steroidal anti-inflammatory agent, dexamethasone (1 mg kg^{-1}), the non-steroidal anti-inflammatory drug, indomethacin (2 mg kg^{-1}) and the selective 5-lipoxygenase inhibitor, BWA4C (20 mg kg^{-1}) (Payne *et al.*, 1988) were injected s.c. 1 h before antigen challenge. The PAF antagonist, SR 27417 (10 mg kg^{-1}) (Herbert *et al.*, 1991) and the histamine H_1-antagonists, terfenadine (10 mg or 30 mg kg^{-1}, s.c.), or cetirizine (7.5–30 mg kg^{-1}) were administered s.c., 1 h before and 6 h after antigen challenge. The protein synthesis inhibitor cycloheximide was injected either i.p. at a dose of 0.06 ng/cavity 5 min before, or s.c. at 5 mg kg^{-1} 5 h before antigen challenge. The immunosuppressive compound FK-506 (0.5–2.0 mg kg^{-1}) (Yamamoto *et al.*, 1990) was injected s.c. 6 h and 5 min before ovalbumin provocation. All drugs were dissolved in sterile saline, except SR 27417, which was dissolved in 0.1 N HCl and saline (0.1:1, v/v), BWA4C, which was first dissolved in dimethylsulphoxide (DMSO) and further diluted in saline (0.1:1, v/v) and FK-506 which was dissolved in a mixture of ethanol, Tween 80 and saline (1:0.2:8.8; v/v/v). The appropriate vehicles were injected in control experiments.

Measurement of immunoreactive LTC_4-like material, LTB_4 and histamine in the peritoneal washing

Immunoreactive LTC_4-like material was measured in the supernatant from peritoneal washings (centrifuged at 1,200 *g* for 15 min at 4°C) by radioimmunoassay according to Aehringhaus *et al.* (1982) and to Young *et al.* (1991). Briefly, dextran-coated charcoal was used to separate unbound ligand by centrifugation at 1,200 *g* for 10 min at 4°C. The monoclonal anti-LTC_4 antibody employed (kindly provided by Dr U. Zor and Dr F. Kohen, Weizmann Institut, Rehovot, Israel) was 10% crossreactive with LTD_4 and less than 0.1% with LTA_4 and LTB_4. The sensitivity of the assay was approximately 15 pg of immunoreactive LTC_4 in 0.1 ml sample.

Immunoreactive LTB_4 in the supernatants from peritoneal washings (centrifuged at 1,200 *g* for 15 min at 4°C) was determined by enzyme-linked-immunosorbent assay (Laboratoire des Stallergenes, Fresnes, France) according to Pradelles *et al.* (1985). The monoclonal antibody anti-LTB_4 was $<$ 0.1% crossreactive with LTC_4, LTD_4 and LTE_4. The sensitivity of the assay was 2 pg of LTB_4/0.1 sample.

For the histamine assay, 0.5 ml of the supernatant from peritoneal washings (centrifuged for 2 min at 12,000 *g* and at 4°C) were mixed with 0.5 ml of 0.8 N perchloric acid. After centrifugation for 10 min at 1,200 *g* and at 4°C, the supernatants were stored at 4°C. An automatic spectrofluorometric assay for histamine was performed, according to a previously published method (Lebel, 1983).

Protein assay

The fluids recovered from the peritoneal cavities were centrifuged for 2 min at 12,000 *g* at room temperature and the protein contents were measured in the supernatants by a standard dye-binding technique, as described by Bradford (1976).

Materials

Ovalbumin (5x crystallized) was from Immunobiological (Costa Mesa; U.S.A.); zymosan type A, cycloheximide, dexamethasone phosphate and indomethacin were purchased from Sigma Chemical Co. (St. Louis, MO. U.S.A.). Aluminium hydroxide (Andersson & Brattsand, 1982) was from Merck (Darmstadt, Germany). Heparin was from Choay (Paris, France) and the dye reagent for the protein assay (Bio-Rad Protein assay) was from Gmbh Laboratory (Ivry-Sur-Seine, France). Tween-80 was from Fluka Chemika (Buchs, Switzerland). Radiolabelled LTC_4 was from Amersham (Buckinghamshire); LTC_4 was from PRIMED-CNRS (Paris, France) and LTB_4 was from Cascade, Euromedex

(Strasbourg, France). BWA4C (N-(3-benzylcinnamyl)acetohydroxamic acid) was a gift from Dr S. Moncada (Wellcome Research Laboratories, Beckenham UK). SR 27417 [N-(2-dimethylaminoethyl)-N-(3-pyridinyl methyl) [4-(2,4,6-triisopropylphenyl)tetrahydrofuran] was kindly provided by Dr J.M. Herbert (Sanofi; France). Terfenadine was a gift from Dr M. Bloom (Merrell Dow; Paris, France). Cetirizine was kindly supplied by Dr J.P. Rihoux (UCB; Braine L'Alleud, Belgium). FK-506 (17-allyl-1,14-dihydroxy-12-(2-(4-hydroxy-3-methoxy-cyclohexyl)1-methylvinyl)-23,25-dimethoxy-13,19,21,27-tetramethyl-11,28-dioxa-4-azatricyclo(22,3,10)4,9)octacos-18-ene-2,3,10,16-tetraone) was a gift from Dr K. Murato (Fujisawa Pharmaceutical; Osaka, Japan).

Statistical analysis

Data were analysed by standard statistical packages for one way analysis of variance (ANOVA) followed by Student's t test for unpaired values. P values of 0.05 or less were considered significant. Results are expressed as means ± standard error of the mean (s.e.mean).

Results

Kinetics of cellular distribution in peritoneal lavage from ovalbumin-challenged mice

The i.p. injection of 1 or 10 μg ovalbumin to sensitized mice did not modify the number of total cells in the peritoneal washing at 6 h, as compared to sensitized saline-challenged animals. In contrast, a significant increase in the number of total cells was noted at 24 and 48 h, but only for the higher dose of antigen (10 μg) (Figure 1). Ovalbumin induced a marked and dose-dependent increase in the number of neutrophils, which peaked at 6 h and returned to basal values thereafter (Figure 1). Challenge with either 1 or 10 μg ovalbumin also induced a dose-dependent eosinophil infiltration, starting at 24 h, and reaching a maximum at 48 h. At 164 h, the eosinophil counts returned to basal levels (Figure 1). No significant changes in the numbers of mononuclear cells were observed at any time-point considered (Figure 1). When non-immunized mice were injected with 10 μg ovalbumin, no changes in cellular distribution were detected at 24 h (data not shown).

Effect of antigen challenge and of AZ on protein extravasation in mouse peritoneal cavity

The i.p. administration of ovalbumin to sensitized mice failed to trigger protein extravasation above values measured in saline-challenged animals at any time considered (Table 1). In contrast, AZ (1 mg/cavity) was highly effective in promoting protein extravasation in the peritoneal cavity of non-immunized mice 1 h after stimulation. Indeed, 45.1 ± 9.2 μg ml^{-1} and 417.6 ± 41 μg ml^{-1} proteins were detected in the peritoneal washing from saline- and AZ-injected mice, respectively ($n = 6$; $P < 0.001$). Four hours after AZ administration, the levels of proteins were markedly decreased, but values were still significantly different, as compared to those measured in saline-injected animals (28.5 ± 9.8 μg ml^{-1} and 209.7 ± 21.7 μg ml^{-1} proteins for saline and AZ-injected mice, respectively, $n = 6$; $P < 0.001$).

Effect of antigen challenge and of AZ on histamine, immunoreactive LTC_4-like material and LTB_4 release in mouse peritoneal washing

Histamine release was detected in the peritoneal washing of sensitized mice 1 min after antigen challenge. The levels of histamine progressively decreased and returned to basal levels at 30 min (Table 1). In contrast, the i.p. injection of 1 mg AZ was not followed by histamine secretion at any time point considered (data not shown). A dose-dependent release of immunoreactive LTC_4-like material in the peritoneal washing was observed 6 h after antigen challenge, but values reached statistical significance, as compared to saline-injected mice, only for 1 μg ovalbumin (Table 1). The i.p. administration of 1 mg AZ to non-sensitized mice triggered the release of high amounts of immunoreactive LTC_4-like material, which peaked 1 h after its injection (saline-injected mice = 0.05 ± 0.04 ng ml^{-1}; AZ-injected mice = 10.1 ± 0.8 ng ml^{-1}; $n = 6$; $P < 0.001$) and returned to basal levels at 4 h. Higher concentrations of immunoreactive LTB_4 were measured in the peritoneal washing from sensitized mice after the i.p. injection of 1 or 10 μg ovalbumin, as compared to saline-challenged

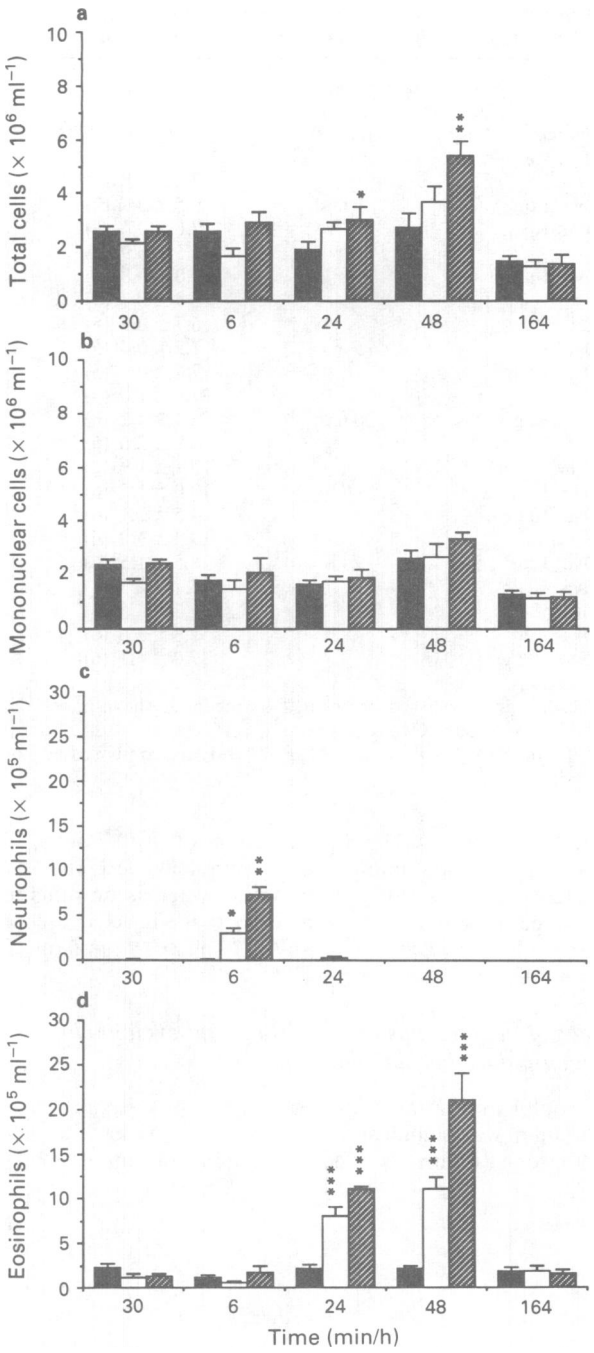

Figure 1 Kinetics of total cell (a), mononuclear cell (b), neutrophil (c) and eosinophil (d) distribution in the peritoneal cavity of sensitized mice. Cells were counted and differentiated at various time-intervals (30 min–164 h) after the injection of either saline (■), or 1 (□), or 10 μg (▨) ovalbumin. Results are expressed as mean ± s.e.mean of 5–11 experiments. $*P < 0.05$, $**P < 0.01$ and $***P < 0.001$, as compared to saline-injected animals.

Table 1 Kinetics of antigen-induced protein extravasation, histamine, immunoreactive leukotriene C_4 (LTC_4)-like material and LTB_4 release in the peritoneal washing from sensitized Balb/C mice

		Parameters			
Stimulus	*Time* (min-h)	*Proteins* ($\mu g\ ml^{-1}$)	*Histamine* ($ng\ ml^{-1}$)	*LTC_4* ($ng\ ml^{-1}$)	*LTB_4* ($pg\ ml^{-1}$)
Saline		7.8 ± 0.9 (5)	9.1 ± 1.9 (6)	0.2 ± 0.1 (6)	ND
Ova 1 μg	1 min	9.5 ± 0.7 (7)	26.6 ± 5.7 (6)*	0.4 ± 0.2 (6)	ND
Ova 10 μg		7.6 ± 0.6 (6)	30.3 ± 1.9 (6)***	0.2 ± 0.0 (6)	ND
Saline		8.5 ± 0.9 (6)	6.0 ± 1.5 (6)	0.2 ± 0.1 (6)	ND
Ova 1 μg	5 min	10.0 ± 0.8 (6)	13.1 ± 2.3 (6)*	0.2 ± 0.0 (6)	ND
Ova 10 μg		8.9 ± 0.7 (7)	17.9 ± 3.9 (6)*	0.2 ± 0.2 (6)	ND
Saline		6.7 ± 0.5 (5)	5.0 ± 1.4 (6)	0.2 ± 0.2 (4)	ND
Ova 1 μg	15 min	7.2 ± 0.4 (5)	4.5 ± 0.4 (6)	0.2 ± 0.0 (5)	ND
Ova 10 μg		7.7 ± 0.6 (5)	11.3 ± 1.2 (6)***	0.3 ± 0.1 (5)	ND
Saline		21.0 ± 1.0 (6)	3.4 ± 0.4 (6)	0.8 ± 0.5 (6)	54.0 ± 5.0 (5)
Ova 1 μg	30 min	26.1 ± 4.2 (6)	1.9 ± 0.4 (6)	1.4 ± 0.2 (6)	63.0 ± 16.0 (5)
Ova 10 μg		21.9 ± 2.6 (6)	3.2 ± 0.7 (6)	1.1 ± 0.7 (6)	49.0 ± 6.0 (5)
Saline		15.1 ± 1.9 (6)	7.5 ± 0.8 (6)	1.9 ± 0.6 (6)	5.0 ± 1.0 (5)
Ova 1 μg	6 h	18.0 ± 1.5 (6)	4.8 ± 0.5 (6)	4.4 ± 0.6 (12)**	156.0 ± 40.0 (11)*
Ova 10 μg		14.5 ± 2.1 (6)	4.6 ± 0.4 (6)	2.6 ± 0.1 (6)	162.0 ± 70.0 (6)*
Saline		19.4 ± 4.0 (6)	6.1 ± 0.3 (6)	1.8 ± 0.7 (6)	5.0 ± 0.8 (4)
Ova 1 μg	24 h	18.5 ± 1.5 (6)	5.3 ± 0.5 (6)	0.5 ± 0.2 (6)	5.0 ± 1.0 (12)
Ova 10 μg		23.1 ± 2.5 (4)	4.0 ± 0.3 (5)	1.9 ± 0.9 (5)	18.0 ± 7.0 (6)
Saline		31.7 ± 8.5 (5)	6.6 ± 0.8 (6)	2.2 ± 0.2 (5)	5.0 ± 0.8 (5)
Ova 1 μg	48 h	32.6 ± 3.6 (6)	7.3 ± 0.8 (6)	2.5 ± 0.7 (5)	4.0 ± 0.9 (5)
Ova 10 μg		37.0 ± 4.1 (6)	3.5 ± 0.3 (6)	2.2 ± 0.5 (4)	9.0 ± 3.0 (5)

Results are expressed as mean ± s.e.mean of the number of experiments indicated in parentheses.
ND = not done; Ova = ovalbumin.
*$P<0.05$; **$P<0.01$ and ***$P<0.001$, as compared to saline-injected mice.

animals (Table 1). The i.p. injection of AZ induced the release of increased amounts of immunoreactive LTB_4 above the basal values 1 h after its injection, whereas no difference was noted after 4 h, as compared to saline-injected preparations (saline-injected mice = 77 ± 14 $pg\ ml^{-1}$; AZ-injected mice = 349 ± 65 $pg\ ml^{-1}$, $n = 5-6$; $P<0.01$).

Effect of dexamethasone, BWA4C and cycloheximide on antigen-induced eosinophilia

Eosinophil infiltration triggered by the i.p. injection of 1 μg ovalbumin was significantly reduced by 1 $mg\ kg^{-1}$ s.c. dexamethasone (Figure 2). The s.c. administration of BWA4C (20 $mg\ kg^{-1}$) significantly inhibited eosinophil accumulation in the mice peritoneal cavity at 24 h (Figure 2). The dose of BWA4C selected suppressed ovalbumin (1 μg)-induced LTC_4-like material generation, as measured at 6 h in the peritoneal fluid. Indeed, 4.5 ± 0.6 and 1.3 ± 0.4 $ng\ ml^{-1}$ LTC_4 were measured in the peritoneal washings from antigen-challenged vehicle- or BWA4C-treated mice, respectively ($n = 6$, $P<0.01$).

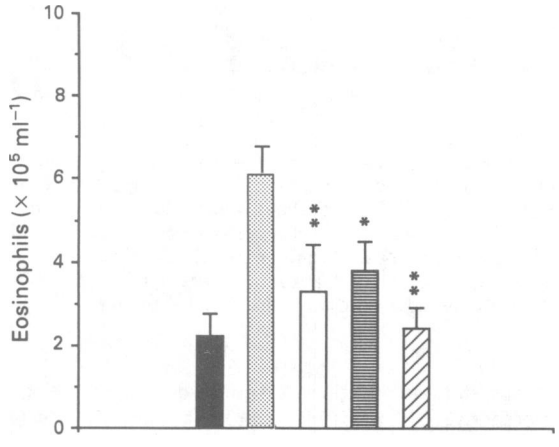

Figure 2 Eosinophil distribution in the peritoneal washing from sensitized mice challenged i.p. 24 h before with either saline (■), or with 1 μg ovalbumin and pretreated by a single s.c. injection of 0.1:1 v/v DMSO-saline (▩), or of dexamethasone (□, 1 $mg\ kg^{-1}$,) or of BWA4C (▤, 20 $mg\ kg^{-1}$) 1 h before the challenge; (▨) represents the number of eosinophils measured in the peritoneal washing from ovalbumin-challenged mice which had received an i.p. injection of 0.06 ng cycloheximide 5 min before antigen provocation. Data are presented as mean ± s.e.mean of 6 experiments. *$P<0.05$ and **$P<0.01$, as compared to antigen-challenged vehicle-injected animals.

Antigen-induced eosinophilia was also suppressed by the *in situ* administration of 0.06 ng cycloheximide 5 min before ovalbumin injection (Figure 2). A significant reduction in the number of eosinophils was also observed when cycloheximide was administered by the s.c. route at 5 $mg\ kg^{-1}$, 5 h before antigen challenge. Indeed, 9.6 ± 1.9 and 4.1 ± 0.4 × $10^5\ ml^{-1}$ eosinophils were found in the peritoneal washing from saline- and cycloheximide-treated mice, respectively ($n = 6$, $P<0.001$).

Effect of indomethacin and SR 27417 on antigen-induced eosinophilia

Pretreatment of sensitized mice with indomethacin (2 mg kg^{-1}, s.c.) 1 h before ovalbumin administration, was ineffective against eosinophilia (Figure 3). The s.c. treatment with the PAF-antagonist SR 27417 (10 $mg\ kg^{-1}$) 1 h before and 6 h after antigen challenge led to a slight, but not statistically significant, reduction of eosinophil accumulation in the peritoneal washing (Figure 3).

Effect of terfenadine and cetirizine on antigen-induced eosinophilia

The s.c. treatment with cetirizine (15–30 $mg\ kg^{-1}$, 1 h and 6 h after the challenge) dose-dependently reduced the eosinophilia induced by 1 μg ovalbumin (Figure 4). The administration of 10 or 30 $mg\ kg^{-1}$ terfenadine under the same conditions was ineffective. Indeed, 5.6 ± 0.1 × $10^5\ ml^{-1}$, 3.6 ± 0.1 × $10^5\ ml^{-1}$ and 6.2 ± 0.1 × $10^5\ ml^{-1}$ eosinophils were counted in the peritoneal lavage from ovalbumin untreated or terfenadine (10 or 30 $mg\ kg^{-1}$)-treated mice, respectively ($n = 5-6$, difference not statistically significant). In separate experiments, non-immunized mice were treated s.c.

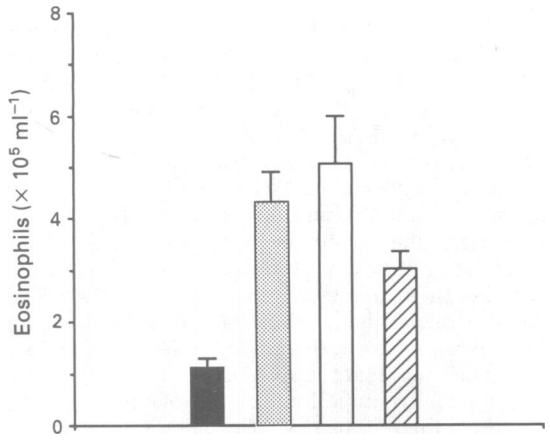

Figure 3 Effect of indomethacin and of the PAF antagonist, SR 24417, on antigen-induced eosinophil accumulation in the peritoneal cavity of sensitized mice. Animals were challenged with i.p. saline (■), or with 1 μg ovalbumin and pretreated either with a s.c. injection of 0.1 N HCl-saline (0.3:1; v/v) 1 h before and 6 h after the challenge (▩), or with 2 mg kg^{-1} indomethacin 1 h before the challenge (□), or with SR 27417, injected s.c. twice, 1 h before and 6 h after the challenge (▨). Each point represents the mean ± s.e.mean of 6 experiments.

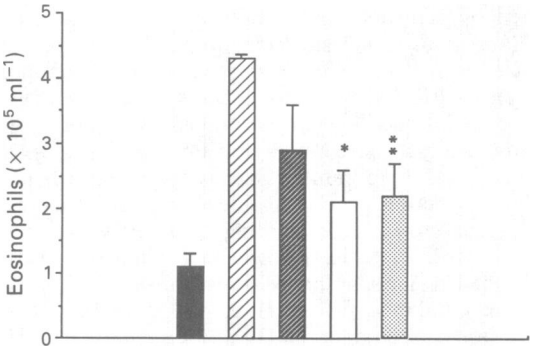

Figure 4 Eosinophil counts in the peritoneal washing from sensitized mice challenged i.p. 24 h before either saline (■), or with 1 μg ovalbumin (▨). Ovalbumin-challenged animals were treated by two s.c. injections of saline (▨), or of cetirizine (▨, □, ▩, 7.5, 15 or 30 mg kg^{-1}, respectively) 1 h before and 6 h after the challenge. Results are expressed as mean ± s.e.mean of 5–6 experiments. *$P<0.05$ and **$P<0.01$, as compared to ovalbumin-challenged vehicle-injected animals.

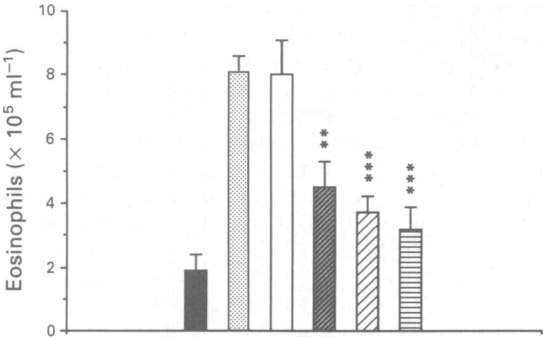

Figure 5 Effect of FK-506 on antigen-induced eosinophil accumulation in the peritoneal washing from sensitized mice killed 24 h after the challenge. Animals were injected i.p. either with saline (■), or with 1 μg ovalbumin (▩) and they were treated s.c. with the vehicle (ethanol, Tween 80 and saline, 1:0.2:8.8; v/v/v; □), or with 0.5 mg kg^{-1} (▨), 1 mg kg^{-1} (▨) or 2 mg kg^{-1} (▤) FK-506, injected twice, 6 h and 5 min before the challenge. Results are expressed as mean ± s.e.mean of 5–11 experiments. *$P<0.05$, **$P<0.01$ and ***$P<0.001$, as compared to antigen-challenged untreated mice.

with 30 mg kg^{-1} of cetirizine or terfenadine and challenged with 1 mg/cavity histamine 18 or 24 h later. Protein extravasation, as measured by Evans blue dye technique 30 min after the stimulation, was inhibited to a similar extent in cetirizine or terfenadine-treated animals (data not shown).

Effect of FK-506 on antigen-induced eosinophilia

Eosinophilia induced by the i.p. injection of 1 μg ovalbumin was inhibited by the s.c. administration of 0.5–2.0 mg kg^{-1} FK-506 6 h and 5 min before the challenge (Figure 5). Indeed, a significant reduction (50%) in the number of eosinophils was observed even with the lower dose of FK-506 (0.5 mg kg^{-1}). Pretreatment with 1 or 2 mg kg^{-1} FK-506 decreased by 54% and 60%, respectively the numbers of eosinophils measured in the peritoneal washing 24 h after antigen challenge.

Discussion

The i.p. injection of ovalbumin to sensitized Balb/C mice induced a transient neutrophil infiltration in the peritoneal cavity, which peaked at 6 h and was not accompanied by an increase in the total number of cells. At 24 h, when the number of neutrophils had returned to basal levels, a dramatic eosinophil augmentation, which peaked at 48 h and resolved at 164 h, was observed. The mechanism explaining the early recruitment of neutrophils to the site of inflammatory reaction secondary to antigen challenge is not fully elucidated. However, similar kinetics for cell infiltration induced by antigen challenge have been described in other species. Hutson *et al.* (1988) and Tarayre *et al.* (1992) reported that antigen provocation of sensitized guinea-pigs and rats respectively, is followed by an early rise in the number of neutrophils in the bronchoalveolar lavage fluid, followed by late eosinophil infiltration.

Eosinophil numbers are augmented in several diseases, such as pollen-sensitive rhinitis (Bentley *et al.*, 1992), asthma (Azzawi *et al.*, 1992), parasite infection (Secor *et al.*, 1990) and rheumatoid arthritis (Venge, 1990). One of the intriguing aspects of eosinophilia is its biological specificity, since an increase in the number of eosinophils may occur in the absence of a rise in other leucocyte populations (Strath & Sanderson, 1986; Maxwel *et al.*, 1987). In confirmation, no changes in the other cell types accompanied antigen-induced eosinophil accumulation in our experiments. In fact, eosinophil increment triggered by 10 μg ovalbumin reflected an augmentation in the number of total cells, as evaluated at 24 and 48 h. Our present findings are partly in conflict with those of Spicer *et al.* (1986), who showed that the injection of ragweed pollen extract into the peritoneal cavity of actively sensitized mice induced eosinophil accumulation, which was accompanied by mononuclear cell increase.

The mechanisms underlying hypersensitivity reactions involve the immune activation of antibody-bound cells, followed by the release of vasoactive amines, such as histamine and 5-hydroxytryptamine, and of newly generated mediators, such as PAF and leukotrienes (Drews, 1990). In the present study, we demonstrated a very early histamine secretion in the peritoneal cavity following antigen challenge, resulting most likely from mast cell degranulation (Prouvost-Danon *et al.*, 1972). In contrast, antigen challenge was followed by a late release of immunoreactive LTC_4 and LTB_4 in the peritoneal washing, which peaked at 6 h. Even though the ability of sensitized mast cells to generate peptido – leukotrienes following antigen stimulation is well-established (Mencia-Huerta *et al.*, 1983), the different kinetics for histamine and for immunoreactive LTC_4 and LTB_4 release presently reported suggests that a cell type other than the mast cell accounts for leukotriene production. Indeed, it has been reported that mononuclear cells and eosinophils are capable of generating

peptido-leukotrienes following antigen challenge (Rankin *et al.*, 1982; Shaw *et al.*, 1985).

Although the injection of ovalbumin triggered cell accumulation in the mouse peritoneal cavity, no protein extravasation was detected at any time point considered. This phenomenon is not due to a low immune response induced by immunization, since the intraplantar injection of ovalbumin to mice sensitized by the same procedure as used in this study elicited a marked paw oedema (unpublished results). Furthermore, the ability of AZ to increase the protein content in the peritoneal cavity suggests that the model described here, as others reported recently (Perretti *et al.*, 1992), allows the evaluation of protein extravasation and mediator release induced by pro-inflammatory stimuli. Taken together, these results suggest that antigen-induced cell migration into the peritoneal cavity of sensitized mice is unrelated to an increase in the vascular permeability. This concept has already been proposed by Griswold *et al.* (1991), who demonstrated that the i.p. injection of LTC_4 to the mouse induced protein leakage but not polymorphonuclear leucocyte infiltration, whereas the i.p. administration of LTB_4 led to polymorphonuclear infiltration without protein extravasation.

In order to investigate the mechanisms responsible for antigen-induced late eosinophil accumulation in the mouse peritoneum, different pharmacological tools were used in the present study. Our results showing that ovalbumin-induced eosinophilia observed at 24 h was suppressed by the steroidal anti-inflammatory agent, dexamethasone, are in agreement with those of Spicer *et al.* (1986). Since dexamethasone is a drug with a large spectrum of effects, it is difficult to determine which of its activities is involved with inhibition. In fact, inhibition by dexamethasone of eosinophil recruitment during late allergic reactions may result from decreased circulating numbers, from the inhibition of the local production of chemo-attractant factors and from an interference with their chemotaxis and diapedesis (Zweiman *et al.*, 1976; Dunsky *et al.*, 1977). In addition, glucocorticoids are very effective in inhibiting cytokine production by activated T-lymphocytes (Schleimer, 1990). In our experimental conditions, it can be speculated that, at least in part, dexamethasone may act via the inhibition of phospholipase A_2 (Flower *et al.*, 1988) and, consequently, of the arachidonic acid metabolism, since pretreatment with the selective 5-lipoxygenase inhibitor, BWA4C, reduced antigen-induced eosinophil infiltration in the peritoneal cavity. Our findings differ from those of Spicer *et al.* (1986), who claimed that the effect of dexamethasone did not involve the inhibition of the arachidonic acid metabolism. In this model, the participation of lipoxygenase derivatives is also suggested by our findings of increased amounts of LTB_4 in the peritoneal washing 6 h after antigen challenge. Since LTB_4 is chemotactic for guinea-pig (Coëffier *et al.*, 1991) and human (Bruijnzeel *et al.*, 1990) eosinophils, it can be hypothesized that eosinophil accumulation induced by antigen provocation is in part related to *in situ* LTB_4 production. Conversely, neither indomethacin nor the PAF antagonist, SR 27417, significantly modified the eosinophil accumulation in the peritoneal cavity following antigen challenge, indicating that neither cyclo-oxygenase derivatives nor PAF mediate antigen-induced eosinophil infiltration in the mouse peritoneum.

The histamine H_1-receptor antagonist, cetirizine, markedly reduced eosinophil accumulation under conditions where terfenadine was ineffective. Since both drugs were equally effective in inhibiting histamine-induced vascular leakage, the effects of cetirizine on eosinophil infiltration secondary to antigen challenge are probably not related to the antagonism of the H_1 receptor for histamine. Similar findings were described by Leprevost *et al.* (1988), who demonstrated that cetirizine, but not polaramine, another histamine H_1 receptor antagonist, inhibited the *in vitro* guinea-pig eosinophil migration triggered by PAF. More recently, Kyan-Aung *et al.* (1992) demonstrated that cetirizine impairs N-formyl-methionyl-leucyl-phenylalanine (fMLP)- or IL-1-induced adhesion of eosinophils, but not neutrophils, to endothelial cells. These results suggest that inhibition by cetirizine of antigen-induced eosinophil recruitment may result from its ability to act on the expression of adhesion molecules on endothelial cells.

The systemic administration of cycloheximide suppressed the late eosinophil accumulation induced by antigen challenge, suggesting that newly-generated material(s) may be responsible for eosinophil infiltration observed in the present study. Interestingly, when cycloheximide was injected i.p. at a very low dose, a similar degree of inhibition was observed. These results suggest that cycloheximide may act via the inhibition of the local expression of adhesion molecules and/or by suppressing the production of chemotactic factor(s) for eosinophils.

Recent studies indicate that some cytokines promote eosinophil chemotaxis in various species, including mice. These cytokines are IL-3 and GM-CSF, which are involved in monocyte-macrophage and eosinophil proliferation (Lopez *et al.*, 1986; 1987; 1988) and IL-5, which acts specifically on the eosinophil lineage (Lopez *et al.*, 1988). IL-5 is primarily produced by activated Th2 lymphocytes, even though mast cells (Plaut *et al.*, 1989) and eosinophils (Desreumaux *et al.*, 1992) are also a source for this cytokine. The immunosuppressive agent FK-506 was also effective in decreasing eosinophil accumulation triggered by antigen challenge, a marked inhibition being achieved with the dose of $2\,mg\,kg^{-1}$. The ability of FK-506 to inhibit selectively the *in vitro* T cell cytokine production has been widely described (Kino *et al.*, 1987; Sawada *et al.*, 1987; Harding *et al.*, 1989; Sierkierka *et al.*, 1989). More recently, Hatfield & Roehm (1992) demonstrated that FK-506 also blocked *in vitro* production of mast cell-derived cytokines, such as IL-2, IL-3, IL-4 and GM-CSF, at concentrations comparable to those effective on T cells. Our results suggest that the inhibitory effect of FK-506 may result from its ability to prevent the formation of eosinophilotactic cytokines responsible for eosinophil accumulation triggered by antigen challenge. The concept that IL-5 may be involved in *in vivo* eosinophil recruitment has been already supported by Kaneto *et al.* (1991), who showed that pretreatment of sensitized mice with a specific antibody against IL-5 decreased the antigen-induced eosinophil influx in the peritoneal cavity. In addition, the same authors demonstrated that peritoneal cells from immunized mice were able to produce IL-5, when cultured in the presence of the specific antigen. In conclusion, the present study demonstrates that the i.p. administration of ovalbumin to actively sensitized mice induces late eosinophil accumulation in the peritoneal cavity. This phenomenon, which may be in part mediated by the release of lipoxygenase metabolites and/or by newly generated factors, such as T-lymphocyte-derived eosinophilotactic cytokines, offers an interesting tool to investigate the mechanism of action of anti-allergic and anti-inflammatory drugs.

The authors wish to thank Prof. B. David and Ms A. Leroy (Unité d'Immunoallergie, Institut Pasteur, Paris, France) for histamine determinations. C.Z.-A. is supported by the Brazilian funding agency CNPq.

References

AEHRINGHAUS, U., WOLBLING, R.H., KONIG, W., PATRONO, C., PESKAR, B.M. & PESKAR, B.A. (1982). Release of Leukotriene C_4 from human polymorphonuclear leucocytes as determined by radioimmunoassay. *FEBS Letts.*, **146**, 111–114.

AMORIM, C.Z., CORDEIRO, R.S.B. & VARGAFTIG, B.B. (1992a). Interference of antihistamines and anti-allergic drugs with antigen-induced paw edema in boosted and unboosted mice. *Eur. J. Pharmacol.*, **216**, 429–434.

AMORIM, C.Z., MARTINS, M.A., CORDEIRO, R.S.B. & VARGAFTIG, B.B. (1992b). Differential inhibition by the PAF receptor antagonist, WEB 2170, of allergic inflammation in single sensitized and boosted mice. *Eur. J. Pharmacol.*, **211**, 29–34.

ANDERSSON, P. & BRATTSAND, R. (1982). Protective effects of the glucocorticoid, budesonide on lung anaphylaxis in actively sensitized guinea-pigs: inhibition of IgE but not of IgG mediate anaphylaxis. *Br. J. Pharmacol.*, **76**, 139–147.

AZZAWI, M., JOHNSTON, S., MAJUMDAR, KAY, A.B. & JEFFERY, P.K. (1992). T lymphocytes and activated eosinophils in airway mucosa in fatal asthma and cystic fibrosis. *Am. Rev. Respir. Dis.*, **145**, 1477–1482.

BENTLEY, A.M., CUMBERWORTH, V., VARNEY, V.A., JACOBSON, M.R., SUDDERICK, R.M., KAY, A.B. & DURHAM, S.R. (1992). Studies during the pollen season in understanding allergic rhinitis. In *Advances in Allergology and Clinical Immunology*, ed. Godard, Ph., Bousquet, J. & Michel, F.B. pp. 457–464. Carnforth, England: Parthenon Publishing.

BOUSQUET, J., CHANEZ, P., LACOSTE, J.Y., BARNEON, G., GHAVANIAN, N., ENANDER, I., VENGE, P., AHLSTEDT, S., SIMONY, L.J., GODARD, P. & MICHEL, F.B. (1990). Eosinophilic inflammation in asthma. *N. Engl. J. Med.*, **323**, 1033–1045.

BRADFORD, M.M. (1976). A rapid and sensitive method for the quantification of microgram quantities of protein utilizing the principle of protein-dye binding. *Analyt. Biochem.*, **72**, 248–254.

BRUIJNZEEL, P.L.B., KOK, P.T.M., HAMELINK, M.L., KIJNE, A.M. & VERHAGEN, J. (1985). Exclusive leukotriene C_4 synthesis by purified human eosinophils induced by opsonized zymosan. *FEBS Letts.*, **189**, 350–354.

BRUIJNZEEL, P.L.B., WARRINGA, R.A.J., KOK, P.T.M. & KREUKNIET, J. (1990). Inhibition of neutrophil and eosinophil-induced chemotaxis by nedocromil sodium and sodium cromoglycate. *Br. J. Pharmacol.*, **99**, 798–802.

CAPRON, M. (1992). Receptors and mechanisms of activation of eosinophils. In *Advances in Allergology and Clinical Immunology*. ed. Godard, Ph., Bousquet, J. & Michel, F.B. pp. 187–194. Carnforth, England: Parthenon Publishing.

COËFFIER, E., JOSEPH, D. & VARGAFTIG, B.B. (1991). LTB_4 a potent chemotactic factor for purified guinea-pig eosinophils: interference of PAF-acether antagonists. *Int. J. Immunopharmacol.*, **13**, 273–282.

COLORADO, A., SLAMA, J.T. & STAVINOHA, W.B. (1991). A new method for measuring auricular inflammation in the mouse. *J. Pharmacol. Methods*, **26**, 73–77.

DESREUMAUX, P., JANIN, A., COLOMBEL, J.F., PRIN, L., PLUMAS, J., EMILE, D., TORPIER, G., CAPRON, A. & CAPRON, M. (1992). Interleukin 5 messenger RNA expression by eosinophils in the intestinal mucosa of patients with coeliac disease. *J. Exp. Med.*, **175**, 293–296.

DREWS, J. (1990). Substances with an antiallergic effect. In *Immunopharmacology – Principles and Perspectives*. pp. 165–172. Berlin, Heidelberg: Springer-Verlag.

DUNSKY, E.H., ATKINS, P.C. & ZWEIMAN, B. (1977). Histologic responses in human skin test reactions to ragweed. IV. Effects of a single intravenous injection of steroids. *J. Allergy Clin. Immunol.*, **59**, 142–146.

FLOWER, R.J. (1988). Lipocortin and the mechanism of action of the glucocorticoids. *Br. J. Pharmacol.*, **94**, 987–1015.

FORD-HUTCHINSON, A.W., BRAY, M.A. & DOIG, M.V. (1980). Leukotriene B_4 a potent chemotactic and aggregating substance released from polymorphonuclear leucocytes. *Nature*, **286**, 264–265.

GLEICH, G.J. (1990). The eosinophil and bronchial asthma: current understanding. *J. Allergy Clin. Immunol.*, **85**, 422–436.

GRISWOLD, D.E., WEBB, E.F. & HILLEGASS, L.M. (1991). Induction of plasma exudation and inflammatory cell infiltration by leukotriene C_4 and leukotriene B_4 in mouse peritonitis. *Inflammation*, **15**, 251–258.

GULBENKIAN, R.A., FERNANDEZ, X., KREUTNER, W., MINNICOZZI, M., WATNICK, A.S., KUNG, T. & EGAN, R. (1990). Anaphylactic challenge causes eosinophil accumulation in bronchoalveolar lavage fluid of guinea pigs. Modulation by betamethasone, phenidone, indomethacin, WEB 2086, and a novel anti-allergy agent, SCH 37224. *Am. Rev. Respir. Dis.*, **142**, 630–635.

HARDING, M.W., GALAT, A., UEHLING, D.E. & SCHREIBER, S.L. (1989). A receptor for immunosuppressant FK-506 is a cis-trans peptidyl-prolyl isomerase. *Nature*, **341**, 758–760.

HATFIELD, S.M. & ROEHM, N.W. (1992). Cyclosporine and FK-506 inhibition of murine mast cell cytokine production. *J. Pharmacol. Exp. Ther.*, **260**, 680–688.

HERBERT, J.M., BERNAT, A., VALETTE, V.G., LALE, A., LAPLACE, M.C., LESPY, L., SAVI, P., MAFFRAND, J.P. & LE FUR, G. (1991). Biochemical and pharmacological activities of SR 27417, a highly potent, long-acting platelet-activating factor receptor antagonist. *J. Pharmacol. Exp. Ther.*, **258**, 44–51.

HUTSON, P.A., CHURCH, M.K., CLAY, T.P., TIMOTHY, P.C., MILLER, P. & HOLGATE, S.T. (1988). Early and late-phase bronchoconstriction after allergen challenge of nonanesthetized guinea pigs. I. The association of disordered airway physiology of leucocyte infiltration. *Am. Rev. Respir. Dis.*, **137**, 548–557.

KANETO, M., HITOSHI, Y., TAKATSU, K. & MATSUMOTO, S. (1991). Role of interleukin-5 in local accumulation of eosinophils in mouse allergic peritonitis. *Int. Arch. Allergy Appl. Immunol.*, **96**, 41–45.

KINO, T., HATANAKA, H., HASHIMOTO, M., NISHIYAMA, M., GOTO, T., OKUHARA, M., KOHSAKA, M., AOKI, H. & IMANAKA, H. (1987). FK-506, a novel immunosupressant isolated from a Streptomyces I. Fermentation, isolation, and physiochemical and biological characteristics. *J. Antibiotics*, **40**, 1249–1255.

KYAN-AUNG, U., HALLSWORTH, M., HASKARD, D., DE VOS, C. & LEE, T.H. (1992). The effects of cetirizine on the adhesion of human eosinophils and neutrophils to cultured human umbilical vein endothelial cells. *J. Allergy Clin. Immunol.*, **90**, 270–272.

LEBEL, B. (1983). A high-sampling rate automated continuous-flow fluorimetric technique for the analysis of nanogram levels of histamine in biological samples. *Analyt. Biochem.*, **133**, 16–29.

LELLOUCH-TUBIANA, A., LEFORT, J., SIMON, M-T., PFISTER, A. & VARGAFTIG, B.B. (1988). Eosinophil recruitment into guinea-pig lungs after PAF-acether and allergen administration. *Am. Rev. Respir. Dis.*, **137**, 948–954.

LEPREVOST, C., CAPRON, M., DE VOS, C., TOMASSINI, M. & CAPRON, A. (1988). Inhibition of eosinophil chemotaxis by a new antiallergic compound (cetirizine). *Int. Arch. Allergy Appl. Immunol.*, **87**, 9–13.

LIMA, M.C.R., MARTINS, M.A., PEREZ, S.A.C., SILVA, P.M.R., CORDEIRO, R.S.B. & VARGAFTIG, B.B. (1991). Effect of azelastine on PAF-acether and antigen-induced pleurisy in rats. *Eur. J. Pharmacol.*, **197**, 201–207.

LOPEZ, A.F., SANDERSON, C.J., GAMBLE, J.R., CAMPBELL, H.D., YOUNG, I. & VADAS, M.A. (1988). Recombinant human interleukin-5 is a selective activator of human eosinophil function. *J. Exp. Med.*, **167**, 219–224.

LOPEZ, A.F., TO, L.B., YANG, Y., GAMBLE, J.R., SHANNON, M.F., BURNS, G.F., DYSON, P.G., JUTTNER, C.A., CLARK, S. & VADAS, M.A. (1987). Stimulation of proliferation, differentiation and function of human cells by primate interleukin 3. *Proc. Natl. Acad. Sci. U.S.A.*, **84**, 2761–2765.

LOPEZ, A.F., WILLIAMSON, D.J., GAMBLE, J.R., BEGLEY, C.G., HARLAN, J.M., KLEBANOFF, S.J., WALTERSDORPH, A., WONG, G., CLARK, S.C. & VADAS, M.A. (1986). Recombinant human granulocyte-macrophage colony stimulating factor stimulates in vitro mature human neutrophil and eosinophil functions, surface receptor expression, and survival. *J. Clin. Invest.*, **78**, 1220–1228.

MARTINS, M.A., ETIENNE, A., SOULARD, C., DOMINGO, M.T. & BRAQUET, P. (1991). Chemotactic effect of PAF-acether on eosinophils from normal rats. *Braz. J. Med. Biol. Res.*, **22**, 1151–1154.

MAXWEL, C., HUSSIAN, R., NUTMAN, T.B., POINDEXTER, R.W., LITTLE, M.D., SCHAD, G.A. & OTTESEN, E.A. (1987). The clinical and immunologic responses of normal human volunteers to low dose hookworm (*Necator americanus*) infection. *Am. J. Trop. Med. Hyg.*, **37**, 126–131.

MENCIA-HUERTA, J.M., RAZIN, E., RINGEL, E.W., COREY, E.J., HOOVER, D., AUSTEN, K.F. & LEWIS, R.A. (1983). Immunologic and Ionophore – induced generation of leukotriene B_4 from mouse bone marrow-derived mast cells. *J. Immunol.*, **130**, 1885–1890.

OKUDARA, H.M., MATSUZAKI, G., DOHL, M., SUKO, M., KASUYA, S. & TAKATSU, K. (1991). T-Cell-dependent accumulation of eosinophils in the lung and its inhibition by monoclonal anti-interleukin-5. *Int. Arch. Allergy Appl. Immunol.*, **199**, 171–173.

OWEN, W.F. Jr., ROTHENBERG, M.E., SILBERSTEIN, D.S., GASSON, J.C., STEVENS, R.L., AUSTEN, K.F. & SOBERMAN, R.J. (1987). Regulation of human eosinophil viability, density and function by granulocyte/macrophage colony-stimulating factor in the presence of 3T3 fibroblasts. *J. Exp. Med.*, **166**, 129–141.

PAYNE, A.N., GARLAND, L.G., LEES, I.W. & SALMON, J.A. (1988). Selective inhibition of arachidonate 5-lipoxygenase by a novel anti-hydroxamic acid: effects on bronchial anaphylaxis in anaesthetized guinea-pigs. *Br. J. Pharmacol.*, **94**, 540–546.

PERRETTI, M., SOLITO, E. & PARENTE, L. (1992). Evidence that endogeneous interleukin-1 is involved in leucocyte migration in acute experimental inflammation in rats and mice. *Agents Actions*, **35**, 71–78.

PLAUT, M., PIERCE, J.H., WATSON, C.J., HAMLEY-HYDE, J., NORDAN, R.P. & PAUL, W.E. (1989). Mast cell lines produce lymphokines in response to cross-linkage of Fcε RI or to calcium ionophores. *Nature*, **339**, 64–67.

PRADELLES, P., GRASSI, J. & MACLOUF, J. (1985). Enzyme immunoassays of eicosanoids using acetylcholine esterase as label: an alternative to radioimmunoassay. *Analyt. Chem.*, **57**, 1170–1173.

PROUVOST-DANON, A., BINAGHI, R., ROCHAS, S. & BOUSSACARON, Y. (1972). Immunochemical identification of mouse IgE. *Immunology*, **23**, 481–491.

RANKIN, J.A., HITCHCOCK, M. & MERRIL, W.W. (1982). IgE-dependent release of leukotriene C_4 from alveolar macrophages. *Nature*, **297**, 329–331.

ROTHENBERG, M.E., OWENS, W.F., SILBERSTEIN, D.S., WOODS, J., SOBERMAN, R.J., AUSTEN, K.F. & STEVENS, R.L. (1988). Human eosinophils have prolonged survival, enhanced functional properties, and become hypodense when exposed to human interleukin 3. *J. Clin. Invest.*, **81**, 1986–1992.

SANDERSON, C.J. (1992). Interleukin-5, eosinophils, and disease. *Blood*, **79**, 3101–3109.

SAWADA, S., SUZUKI, G., KAWASE, Y. & TAKAKU, F. (1987). Novel immunosuppressive agent, FK-506. In vitro effects on the cloned T cell activation. *J. Immunol.*, **139**, 1797–1803.

SCHLEIMER, R.P. (1990). Effects of glucocorticosteroids on inflammatory cells relevant to their therapeutic applications in asthma. *Am. Rev. Respir. Dis.*, **141**, S59–S69.

SECOR, W.E., STEWART, S.J. & COLLEY, D.G. (1990). Eosinophils and immune mechanisms. VI. The synergistic combination of granulocyte-macrophage colony-stimulating factor and IL-5 accounts for eosinophil-stimulation promoter activity in Schistosoma mansoni-infected mice. *J. Immunol.*, **144**, 1484–1489.

SHAW, R.J., WALSH, G.M. & CROMWELL, O. (1985). Activated human eosinophils generate SRS-A leukotrienes following IgG-dependent stimulation. *Nature*, **316**, 150–152.

SHER, A., COFFMAN, R.L., HIENY, S., SCOTT, P. & CHEEVER, A.W. (1990). Interleukin 5 is required for the blood and tissue eosinophilia but not granuloma formation induced by injection with Schistosoma mansoni. *Proc. Natl. Acad. Sci. U.S.A.*, **87**, 61–65.

SIERKIERKA, J.J.,HUNG, S.H.Y., POE, M., LIN, C.S. & SIGAL, N.H. (1989). A cytosolic binding protein for the immunosuppressant FK-506 had peptidylpropyl isomerase activity but is distinct from cyclophilin. *Nature*, **341**, 755–757.

SPICER, B.A., HATT, P.A., LACOCK, S.M. & SMITH, H. (1986). Effect of drugs on the increase in cell numbers in the peritoneal cavity of the actively sensitized mouse after intraperitoneal challenge with antigen. *Int. Arch. Allergy Appl. Immunol.*, **81**, 81–84.

STRATH, M. & SANDERSON, C.J. (1986). Detection of eosinophil differentiation factor and its relationship to eosinophilia in *Mesocestoides corti*-infected mice. *Exp. Hematol.*, **14**, 16–20.

TARAYRE, J.P., ALIAGA, M., BARBARA, M., TIIISSEYRE, N., VIEU, S. & TISNE-VERSAILLES, J. (1992). Model of bronchial allergic inflammation in the brown norway rat. Pharmacological modulation. *Int. J. Immunopharmacol.*, **14**, 847–855.

VENGE, P. (1990). The human eosinophil in inflammation. *Agents Actions*, **29**, 122–126.

YAMAMOTO, K., MORI, A., NAKAHAMA, T., ITO, M., OKUDAIRA, H. & MIYAMOTO, T. (1990). Experimental treatment of autoimmune MRL-LPR-LPR mice with immunosuppressive compound FK-506. *Immunology*, **69**, 222–227.

YOUNG, P.R., RANDLY, L.B., LANNI, C., SUMMERS, J.B., BROOK, D.W. & CARTER, G.W. (1991). Inhibition of leukotriene biosynthesis in the rat peritoneal cavity. *Eur. J. Pharmacol.*, **205**, 259–266.

ZWEIMAN, B., SLOTT, R.I. & ATKINS, P.C. (1976). Histologic studies of human skin test responses to ragweed and compound 48/80. *J. Allergy Clin. Immunol.*, **58**, 657–663.

(Received January 4, 1993
Revised June 9, 1993
Accepted June 15, 1993)

British Journal of Pharmacology

VOLUME 110 (2) OCTOBER 1993

BRITISH JOURNAL OF PHARMACOLOGY

The *British Journal of Pharmacology* welcomes contributions in all fields of experimental pharmacology including neuroscience, biochemical, cellular and molecular pharmacology. The Board of Editors represents a wide range of expertise and ensures that well-presented work is published as promptly as possible, consistent with maintaining the overall quality of the journal.

Edited for the British Pharmacological Society by

A.T. Birmingham
(Chairman)

R.W. Horton **W.A. Large**
(Secretaries)

Submission of manuscripts: Manuscripts (two copies) should be sent to The Editorial Office, British Journal of Pharmacology, St. George's Hospital Medical School, Cranmer Terrace, London SW17 0RE.

Authors should consult the Instructions to Authors and the Nomenclature Guidelines for Authors in Vol. **108,** 275–284. These Instructions and Guidelines also appear with the journal Index for Volumes 105–107, 1992. A checklist of the essential requirements is summarised in each issue of the journal on the inside of the back cover.

The *British Journal of Pharmacology* is published monthly by the Scientific & Medical Division, Macmillan Press Ltd.

The journal is covered by *Current Contents*, *Excerpta Medica* and *Index Medicus*.

All business correspondence and reprint requests should be addressed to the Scientific & Medical Division, Macmillan Press Ltd., Houndmills, Basingstoke, Hampshire RG21 2XS, UK. Telephone: (0256) 29242; Fax: (0256) 810526.

Enquiries concerning advertising space or rates should be addressed to: Michael Rowley, Advertisement Manager, Macmillan Press Ltd., 4 Little Essex Street, London WC2R 3LF. Telephone: 071 836 6633; Fax: 071 379 0820.

Annual subscription prices for 1993 EC £455, elsewhere £499/US$923 (sterling rate is definitive). Orders must be accompanied by remittance. Cheques should be made payable to Macmillan Press, and sent to: Macmillan Press Ltd., Subscription Department, Brunel Road, Houndmills, Basingstoke, Hampshire RG21 2XS, UK.
Overseas subscribers may make payments into UK Post Office Giro Account No. 5192455. Full details must accompany the payment.

British Journal of Pharmacology (ISSN 0007–1188) is published monthly by Macmillan Publishers Ltd, c/o Mercury Airfreight International Ltd, 2323 Randolph Avenue, Avenel, NJ 07001, USA. Subscription price is $923.00 per annum. 2nd class postage is paid at Rahway NJ. *Postmaster*: send address corrections to Macmillan Publishers, c/o Mercury Airfreight International Ltd, 2323 Randolph Avenue, Avenel NJ 07001.

ISSN 0007–1188
0007–1188/93 $9.00 + $0.00

PREPARATION OF MANUSCRIPTS

Authors are strongly recommended to read the full *Instructions to Authors* and *Nomenclature Guidelines for Authors* (*Br. J. Pharmacol.* 1993, **108,** 275–284) before submitting a manuscript for publication in the *British Journal of Pharmacology*. The manuscript and cover letter should be checked against the following list before mailing.

The original and one copy of the manuscript must be supplied. Manuscripts must be typed in double-line spacing on one side of A4 paper, in type not smaller than 12 characters per inch or 10 point. Both copies to include Tables and a set of labelled Figures. One set of Figures without numbers or letters is also to be included. The text to be arranged in the following subsections:

1. **Title**—To have no more than 150 characters on a separate page, which should also include a Short Title (50 characters maximum) and the name and address of the author for correspondence.
2. **Summary**—To be arranged in numbered paragraphs (Full Papers) or a single paragraph (Special Reports).
   —to include aims, principal results and conclusions.
   —to include Key words (10 maximum) at end of summary.
3. **Introduction**—To contain concise statements of the problem and the aims of the investigation.
4. **Methods**—To have brief but adequate account of the procedures; *full names of drugs* (*including those referred to by manufacturer's code*), sources of drugs and statistical tests to be stated.
5. **Results**—To have no repetition of data in Figures, Tables and text.
6. **Discussion**—Findings and conclusions to be placed in context of other relevant work.
   NB Simple repetition of results and unwarranted speculation are not acceptable.
7. **Acknowledgments**—Sources of support. Sources of drugs not widely available commercially.
8. **References**—All references in the text to be included in the Reference List and *vice versa*. References in alphabetical order with complete citations; Journals publishing 'in press' papers identified.
   References to manuscripts submitted to other journals but not yet accepted are not allowed.
9. **Tables**—Each on a separate page and prepared in accordance with current requirements of the Journal.
10. **Figures**—Both labelled and non-labelled Figures to be prepared in accordance with current requirements of the Journal (see *Instructions to Authors*, 1993, **108,** 275–281) and provided with Figure Number and Authors' names on back (*in pencil*).
    —each legend to be typed on a separate page and carrying keys to symbols.
    —keys to symbols and histograms must not appear on the figures themselves, but in the respective legends.
    —'box style' figures are not in keeping with the Journal style; line drawings etc must have only left-hand and bottom axes.
11. **Manuscripts**—To be accompanied by a declaration signed by each author that
    (a) results are original
    (b) approval of all persons concerned has been given to submit manuscripts for consideration (see also 12b)
    (c) the same material is neither 'in press' (i.e. is in proof or has definitely been accepted for publication) nor under consideration elsewhere. Furthermore it will not be submitted or published elsewhere before a decision has been reached by the Editorial Board of the *British Journal of Pharmacology* and will not be submitted elsewhere if accepted by the *British Journal of Pharmacology*.
    (d) Copyright assignment is included.
12. **Cover letter**—To state clearly
    (a) Corresponding author's full postal address, telephone, telex or Fax number
    (b) where appropriate, that *either* ethical approval has been given for investigation *or* Company or Institutional permission to publish work has been received.
13. **Reminder**—Packaging to be sufficiently robust to protect Figures and to withstand mailing.

Failure to comply with *Instructions to Authors* may lead to substantial delays in processing, review and publication and may even jeopardize acceptance of the manuscript.

NOMENCLATURE

Authors are reminded that accepted receptor and associated terminology is laid out in *Nomenclature Guidelines for Authors*, as published in the *British Journal of Pharmacology*, *Br. J. Pharmacol.*, 1993, **108,** 282–284.

SPECIAL REPORTS

The purpose of *Special Reports* is to provide rapid publication for **new** and **important** results which the Editorial Board considers are likely to be of special pharmacological significance. *Special Reports* will have publication priority over all other material and so authors are asked to consider carefully the status of their work before submission.

In order to speed publication there is normally no revision allowed beyond very minor typographical or grammatical corrections. If significant revision is required, the Board may either invite rapid re-submission or, more probably, propose that it be re-written as a Full Paper and be re-submitted for consideration. In order to reduce delays, proofs of *Special Reports* will be sent to authors but **essential corrections must reach the Production Office within 48 hours of receipt.** Authors should ensure that their submitted material conforms exactly to the following requirements.

Special Reports should normally occupy no more than two printed pages of the Journal; two illustrations (Figures or Tables, with legends) are permitted. As a guideline, with type face of 12 pitch and double-line spacing, a page of A4 paper could contain about 400 words. The absolute maximum length of the *Special Report* is 1700 words. For each Figure or Table, please deduct 200 words. The manuscript should comprise a Title page with key words (maximum of 10), a Summary consisting of a single short paragraph, followed by Introduction, Methods, Results, Discussion and References (maximum of 10). In all other respects, the requirements are the same as for Full Papers (see current 'Instructions to Authors').

BRITISH JOURNAL OF PHARMACOLOGY VOLUME 110 (2) 1993

Contents continue inside back cover

Typeset by Elite Typesetting Techniques, Southampton, Hampshire
and printed in Great Britain by Unwin Brothers Ltd., The Gresham Press, Old Woking, Surrey

See last page of issue for PREPARATION OF MANUSCRIPTS